VOLUME 28 / NUMBER 14
JULY 23, 1990
ACC. NOS. N90-20920 TO N90-21721

STAR
AN ABSTRACT JOURNAL

Scientific and Technical Aerospace Reports

PRODUCED BY THE
SCIENTIFIC AND TECHNICAL
INFORMATION
DIVISION

NASA

NATIONAL AERONAUTICS AND SPACE ADMINISTRATION

WHAT YOU CAN DO FOR *STAR*

All users of this abstract service are urged to forward reports to be considered for announcement in *STAR*. This will aid NASA in its efforts to provide the fullest possible coverage of all scientific and technical publications that might support aeronautics and space research and development. If you have prepared relevant reports (other than those that you will transmit to NASA, DOD, or DOE through the usual contract- or grant-reporting channels), please send them for consideration to the NASA Scientific and Technical Information Facility, P.O. Box 8757, BWI Airport, MD 21240.

Reprints of journal articles, book chapters, and conference papers are also welcome. These will be considered for announcement in *STAR's* companion journal, *International Aerospace Abstracts*.

You may specify a particular source to be included in a report announcement if you wish; otherwise the report will be placed on public sale at the National Technical Information Service. Copyrighted publications will be announced but not distributed or sold.

PURCHASE OF *STAR*

The semimonthly issues are available to registered users on annual subscription from the NASA Scientific and Technical Information Facility, ATTN: Registration Services, P.O. Box 8757, BWI Airport, MD 21240. *STAR* is publicly available on annual subscription from the Superintendent of Documents, U.S. Government Printing Office, Washington, DC 20402.

PUBLISHED BY:

UNITED STATES GOVERNMENT
NATIONAL AERONAUTICS AND SPACE ADMINISTRATION
SCIENTIFIC AND TECHNICAL INFORMATION DIVISION
Scientific and Technical Aerospace Reports, Volume 28, is prepared by the NASA Scientific and Technical Information Facility operated for the National Aeronautics and Space Administration by RMS Associates.

The Administrator of the National Aeronautics and Space Administration has determined that the publication of this periodical is necessary in the transaction of the public business required by law of this agency. Use of funds for printing this periodical has been approved by the Director of the Office of Management and Budget through March 22, 1991.

US ISSN 0036-8741

Scientific and Technical Aerospace Reports (STAR) is issued twice a month and contains abstracts and indexes of meeting papers, conference proceedings, and unlimited distribution reports that have been added to the NASA Scientific and Technical Information Database during the preceding period. These citations may also be accessed online via NASA/RECON or via AIAA's Aerospace Database (File 108) through Dialog Information Services, Inc.

STAR subject coverage includes all aerospace-related areas that will help NASA achieve its mission. Material is gathered from all over the world and includes significant input from many countries under exchange and access agreements.

Consult the indexes at the back of this volume to help zero in on what you are looking for. These include:

Subject Index
Personal Author Index
Corporate Source Index
Contract Number Index
Report/Accession Number Index

STAR's companion abstract journal *International Aerospace Abstracts* should be used if you are looking for references to periodicals, books, and published meeting papers or conference proceedings.

Questions and comments should be addressed to:

NASA Scientific and Technical Information Facility
User Services
P.O. Box 8757
BWI Airport, MD 21240
301-621-0150

VOLUME 28 NUMBER 14 / JULY 23, 1990

TABLE OF CONTENTS

AERONAUTICS

Includes aeronautics (general); aerodynamics; air transportation and safety; aircraft communications and navigation; aircraft design, testing and performance; aircraft instrumentation; aircraft propulsion and power; aircraft stability and control; and research and support facilities (air).

For related information see also *Astronautics.*

01 AERONAUTICS (GENERAL) 1905

02 AERODYNAMICS 1909

Includes aerodynamics of bodies, combinations, wings, rotors, and control surfaces; and internal flow in ducts and turbomachinery.

For related information see also *34 Fluid Mechanics and Heat Transfer.*

03 AIR TRANSPORTATION AND SAFETY 1913

Includes passenger and cargo air transport operations; and aircraft accidents.

For related information see also *16 Space Transportation* and *85 Urban Technology and Transportation.*

04 AIRCRAFT COMMUNICATIONS AND NAVIGATION 1914

Includes digital and voice communication with aircraft; air navigation systems (satellite and ground based); and air traffic control.

For related information see also *17 Space Communications, Spacecraft Communications, Command and Tracking* and *32 Communications and Radar.*

05 AIRCRAFT DESIGN, TESTING AND PERFORMANCE 1915

Includes aircraft simulation technology.

For related information see also *18 Spacecraft Design, Testing and Performance* and *39 Structural Mechanics.* For land transportation vehicles see *85 Urban Technology and Transportation.*

06 AIRCRAFT INSTRUMENTATION 1921

Includes cockpit and cabin display devices; and flight instruments.

For related information see also *19 Spacecraft Instrumentation* and *35 Instrumentation and Photography.*

07 AIRCRAFT PROPULSION AND POWER 1922

Includes prime propulsion systems and systems components, e.g., gas turbine engines and compressors; and onboard auxiliary power plants for aircraft.

For related information see also *20 Spacecraft Propulsion and Power, 28 Propellants and Fuels,* and *44 Energy Production and Conversion.*

08 AIRCRAFT STABILITY AND CONTROL 1928

Includes aircraft handling qualities; piloting; flight controls; and autopilots.

For related information see also *05 Aircraft Design, Testing and Performance.*

09 RESEARCH AND SUPPORT FACILITIES (AIR) 1929

Includes airports, hangars and runways; aircraft repair and overhaul facilities; wind tunnels; shock tubes; and aircraft engine test stands.

For related information see also *14 Ground Support Systems and Facilities (Space).*

ASTRONAUTICS

Includes astronautics (general); astrodynamics; ground support systems and facilities (space); launch vehicles and space vehicles; space transportation; space communications, spacecraft communications, command and tracking; spacecraft design, testing and performance; spacecraft instrumentation; and spacecraft propulsion and power.

For related information see also *Aeronautics.*

12 ASTRONAUTICS (GENERAL) 1930

For extraterrestrial exploration see *91 Lunar and Planetary Exploration.*

13 ASTRODYNAMICS 1930

Includes powered and free-flight trajectories; and orbital and launching dynamics.

14 GROUND SUPPORT SYSTEMS AND FACILITIES (SPACE) 1931

Includes launch complexes, research and production facilities; ground support equipment, e.g., mobile transporters; and simulators.

For related information see also *09 Research and Support Facilities (Air).*

15 LAUNCH VEHICLES AND SPACE VEHICLES N.A.

Includes boosters; operating problems of launch/space vehicle systems; and reusable vehicles.

For related information see also *20 Spacecraft Propulsion and Power.*

16 SPACE TRANSPORTATION 1932

Includes passenger and cargo space transportation, e.g., shuttle operations; and space rescue techniques.

For related information see also *03 Air Transportation and Safety* and *18 Spacecraft Design, Testing and Performance.* For space suits see *54 Man/System Technology and Life Support.*

17 SPACE COMMUNICATIONS, SPACECRAFT COMMUNICATIONS, COMMAND AND TRACKING 1933

Includes telemetry; space communications networks; astronavigation and guidance; and radio blackout.

For related information see also *04 Aircraft Communications and Navigation* and *32 Communications and Radar.*

18 SPACECRAFT DESIGN, TESTING AND PERFORMANCE 1933

Includes satellites; space platforms; space stations; spacecraft systems and components such as thermal and environmental controls; and attitude controls.

For life support systems see *54 Man/System Technology and Life Support.* For related information see also *05 Aircraft Design, Testing and Performance, 39 Structural Mechanics,* and *16 Space Transportation.*

19 SPACECRAFT INSTRUMENTATION 1940

For related information see also *06 Aircraft Instrumentation* and *35 Instrumentation and Photography.*

20 SPACECRAFT PROPULSION AND POWER 1941

Includes main propulsion systems and components, e.g. rocket engines; and spacecraft auxiliary power sources.

For related information see also *07 Aircraft Propulsion and Power, 28 Propellants and Fuels, 44 Energy Production and Conversion,* and *15 Launch Vehicles and Space Vehicles.*

CHEMISTRY AND MATERIALS

Includes chemistry and materials (general); composite materials; inorganic and physical chemistry; metallic materials; nonmetallic materials; propellants and fuels; and materials processing.

23 CHEMISTRY AND MATERIALS (GENERAL) 1942

24 COMPOSITE MATERIALS 1943

Includes physical, chemical, and mechanical properties of laminates and other composite materials.

For ceramic materials see *27 Nonmetallic Materials.*

25 INORGANIC AND PHYSICAL CHEMISTRY 1947

Includes chemical analysis, e.g., chromatography; combustion theory; electrochemistry; and photochemistry.

For related information see also *77 Thermodynamics and Statistical Physics.*

26 METALLIC MATERIALS 1949

Includes physical, chemical, and mechanical properties of metals, e.g., corrosion; and metallurgy.

27 NONMETALLIC MATERIALS 1952

Includes physical, chemical, and mechanical properties of plastics, elastomers, lubricants, polymers, textiles, adhesives, and ceramic materials.

For composite materials see *24 Composite Materials.*

28 PROPELLANTS AND FUELS 1956

Includes rocket propellants, igniters and oxidizers; their storage and handling procedures; and aircraft fuels.

For related information see also *07 Aircraft Propulsion and Power, 20 Spacecraft Propulsion and Power,* and *44 Energy Production and Conversion.*

29 MATERIALS PROCESSING 1957

Includes space-based development of products and processes for commercial application.

For biological materials see *55 Space Biology.*

ENGINEERING

Includes engineering (general); communications and radar; electronics and electrical engineering; fluid mechanics and heat transfer; instrumentation and photography; lasers and masers; mechanical engineering; quality assurance and reliability; and structural mechanics.

For related information see also *Physics.*

31 ENGINEERING (GENERAL) 1958

Includes vacuum technology; control engineering; display engineering; cryogenics; and fire prevention.

32 COMMUNICATIONS AND RADAR 1960

Includes radar; land and global communications; communications theory; and optical communications.

For related information see also *04 Aircraft Communications and Navigation* and *17 Space Communications, Spacecraft Communications, Command and Tracking.* For search and rescue see *03 Air Transportation and Safety,* and *16 Space Transportation.*

33 ELECTRONICS AND ELECTRICAL ENGINEERING 1968

Includes test equipment and maintainability; components, e.g., tunnel diodes and transistors; microminiaturization; and integrated circuitry.

For related information see also *60 Computer Operations and Hardware* and *76 Solid-State Physics.*

34 FLUID MECHANICS AND HEAT TRANSFER 1970

Includes boundary layers; hydrodynamics; fluidics; mass transfer and ablation cooling.

For related information see also *02 Aerodynamics* and *77 Thermodynamics and Statistical Physics.*

35 INSTRUMENTATION AND PHOTOGRAPHY 1975

Includes remote sensors; measuring instruments and gauges; detectors; cameras and photographic supplies; and holography.

For aerial photography see *43 Earth Resources and Remote Sensing.* For related information see also *06 Aircraft Instrumentation* and *19 Spacecraft Instrumentation.*

36 LASERS AND MASERS 1984

Includes parametric amplifiers.

For related information see also *76 Solid-State Physics.*

37 MECHANICAL ENGINEERING 1986

Includes auxiliary systems (nonpower); machine elements and processes; and mechanical equipment.

38 QUALITY ASSURANCE AND RELIABILITY 1989

Includes product sampling procedures and techniques; and quality control.

39 STRUCTURAL MECHANICS 1990

Includes structural element design and weight analysis; fatigue; and thermal stress.

For applications see *05 Aircraft Design, Testing and Performance* and *18 Spacecraft Design, Testing and Performance.*

GEOSCIENCES

Includes geosciences (general); earth resources and remote sensing; energy production and conversion; environment pollution; geophysics; meteorology and climatology; and oceanography.

For related information see also *Space Sciences.*

42 GEOSCIENCES (GENERAL) N.A.

43 EARTH RESOURCES AND REMOTE SENSING 1995

Includes remote sensing of earth resources by aircraft and spacecraft; photogrammetry; and aerial photography.

For instrumentation see *35 Instrumentation and Photography.*

44 ENERGY PRODUCTION AND CONVERSION 2001

Includes specific energy conversion systems, e.g., fuel cells; global sources of energy; geophysical conversion; and windpower.

For related information see also *07 Aircraft Propulsion and Power, 20 Spacecraft Propulsion and Power,* and *28 Propellants and Fuels.*

45 ENVIRONMENT POLLUTION 2003

Includes atmospheric, noise, thermal, and water pollution.

46 GEOPHYSICS 2005

Includes aeronomy; upper and lower atmosphere studies; ionospheric and magnetospheric physics; and geomagnetism.

For space radiation see *93 Space Radiation.*

47 METEOROLOGY AND CLIMATOLOGY 2006

Includes weather forecasting and modification.

48 OCEANOGRAPHY 2008

Includes biological, dynamic, and physical oceanography; and marine resources.

For related information see also *43 Earth Resources and Remote Sensing.*

LIFE SCIENCES

Includes life sciences (general); aerospace medicine; behavioral sciences; man/system technology and life support; and space biology.

51 LIFE SCIENCES (GENERAL) 2009

52 AEROSPACE MEDICINE 2010

Includes physiological factors; biological effects of radiation; and effects of weightlessness on man and animals.

53 BEHAVIORAL SCIENCES 2010

Includes psychological factors; individual and group behavior; crew training and evaluation; and psychiatric research.

54 MAN/SYSTEM TECHNOLOGY AND LIFE SUPPORT 2011

Includes human engineering; biotechnology; and space suits and protective clothing.

For related information see also *16 Space Transportation.*

55 SPACE BIOLOGY N.A.

Includes exobiology; planetary biology; and extraterrestrial life.

MATHEMATICAL AND COMPUTER SCIENCES

Includes mathematical and computer sciences (general); computer operations and hardware; computer programming and software; computer systems; cybernetics; numerical analysis; statistics and probability; systems analysis; and theoretical mathematics.

59 MATHEMATICAL AND COMPUTER SCIENCES (GENERAL) 2011

60 COMPUTER OPERATIONS AND HARDWARE 2011

Includes hardware for computer graphics, firmware, and data processing.

For components see *33 Electronics and Electrical Engineering.*

61 COMPUTER PROGRAMMING AND SOFTWARE 2012

Includes computer programs, routines, algorithms, and specific applications, e.g., CAD/CAM.

62 COMPUTER SYSTEMS 2016

Includes computer networks and special application computer systems.

63 CYBERNETICS 2017

Includes feedback and control theory, artificial intelligence, robotics and expert systems.

For related information see also *54 Man/System Technology and Life Support.*

64 NUMERICAL ANALYSIS 2018

Includes iteration, difference equations, and numerical approximation.

65 STATISTICS AND PROBABILITY N.A.

Includes data sampling and smoothing; Monte Carlo method; and stochastic processes.

66 SYSTEMS ANALYSIS N.A.

Includes mathematical modeling; network analysis; and operations research.

67 THEORETICAL MATHEMATICS 2022

Includes topology and number theory.

PHYSICS

Includes physics (general); acoustics; atomic and molecular physics; nuclear and high-energy physics; optics; plasma physics; solid-state physics; and thermodynamics and statistical physics.

For related information see also *Engineering.*

70 PHYSICS (GENERAL) 2022

For precision time and time interval (PTTI) see *35 Instrumentation and Photography;* for geophysics, astrophysics or solar physics see *46 Geophysics, 90 Astrophysics,* or *92 Solar Physics.*

71 ACOUSTICS 2022
Includes sound generation, transmission, and attenuation.
For noise pollution see *45 Environment Pollution.*

72 ATOMIC AND MOLECULAR PHYSICS 2024
Includes atomic structure, electron properties, and molecular spectra.

73 NUCLEAR AND HIGH-ENERGY PHYSICS 2026
Includes elementary and nuclear particles; and reactor theory.
For space radiation see *93 Space Radiation.*

74 OPTICS 2026
Includes light phenomena and optical devices.
For lasers see *36 Lasers and Masers.*

75 PLASMA PHYSICS 2027
Includes magnetohydrodynamics and plasma fusion.
For ionospheric plasmas see *46 Geophysics.* For space plasmas see *90 Astrophysics.*

76 SOLID-STATE PHYSICS 2030
Includes superconductivity.
For related information see also *33 Electronics and Electrical Engineering* and *36 Lasers and Masers.*

77 THERMODYNAMICS AND STATISTICAL PHYSICS 2034
Includes quantum mechanics; theoretical physics; and Bose and Fermi statistics.
For related information see also *25 Inorganic and Physical Chemistry* and *34 Fluid Mechanics and Heat Transfer.*

SOCIAL SCIENCES

Includes social sciences (general); administration and management; documentation and information science; economics and cost analysis; law, political science, and space policy; and urban technology and transportation.

80 SOCIAL SCIENCES (GENERAL) N.A.
Includes educational matters.

81 ADMINISTRATION AND MANAGEMENT 2036
Includes management planning and research.

82 DOCUMENTATION AND INFORMATION SCIENCE 2036
Includes information management; information storage and retrieval technology; technical writing; graphic arts; and micrography.
For computer documentation see *61 Computer Programming and Software.*

83 ECONOMICS AND COST ANALYSIS N.A.
Includes cost effectiveness studies.

84 LAW, POLITICAL SCIENCE AND SPACE POLICY N.A.
Includes NASA appropriation hearings; aviation law; space law and policy; international law; international cooperation; and patent policy.

85 URBAN TECHNOLOGY AND TRANSPORTATION 2037
Includes applications of space technology to urban problems; technology transfer; technology assessment; and surface and mass transportation.
For related information see *03 Air Transportation and Safety, 16 Space Transportation,* and *44 Energy Production and Conversion.*

SPACE SCIENCES

Includes space sciences (general); astronomy; astrophysics; lunar and planetary exploration; solar physics; and space radiation.
For related information see also *Geosciences.*

88 SPACE SCIENCES (GENERAL) N.A.

89 ASTRONOMY 2037
Includes radio, gamma-ray, and infrared astronomy; and astrometry.

90 ASTROPHYSICS 2039
Includes cosmology; celestial mechanics; space plasmas; and interstellar and interplanetary gases and dust.
For related information see also *75 Plasma Physics.*

91 LUNAR AND PLANETARY EXPLORATION 2042
Includes planetology; and manned and unmanned flights.
For spacecraft design or space stations see *18 Spacecraft Design, Testing and Performance.*

92 SOLAR PHYSICS 2042
Includes solar activity, solar flares, solar radiation and sunspots.
For related information see *93 Space Radiation.*

93 SPACE RADIATION 2043
Includes cosmic radiation; and inner and outer earth's radiation belts.
For biological effects of radiation see *52 Aerospace Medicine.* For theory see *73 Nuclear and High-Energy Physics.*

GENERAL

Includes aeronautical, astronautical, and space science related histories, biographies, and pertinent reports too broad for categorization; histories or broad overviews of NASA programs.

99 GENERAL 2044

Note: N.A. means that no abstracts were assigned to this category for this issue.

SUBJECT INDEX I-1
PERSONAL AUTHOR INDEX I-55
CORPORATE SOURCE INDEX I-63
CONTRACT NUMBER INDEX I-73
REPORT/ACCESSION NUMBER INDEX .. I-75
APPENDIX—ABOUT STAR A-1

TYPICAL CITATION AND ABSTRACT

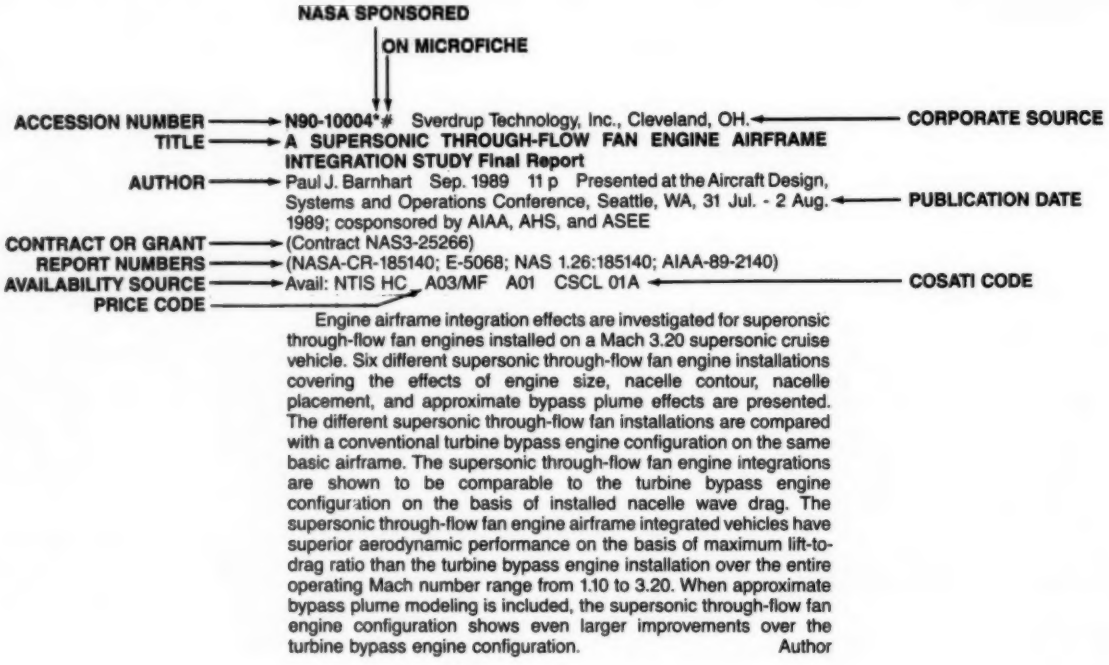
NASA SPONSORED
ON MICROFICHE
ACCESSION NUMBER
N90-10004*# Sverdrup Technology, Inc., Cleveland, OH.
CORPORATE SOURCE
TITLE
A SUPERSONIC THROUGH-FLOW FAN ENGINE AIRFRAME INTEGRATION STUDY Final Report
AUTHOR
Paul J. Barnhart Sep. 1989 11 p Presented at the Aircraft Design, Systems and Operations Conference, Seattle, WA, 31 Jul. - 2 Aug. 1989; cosponsored by AIAA, AHS, and ASEE
PUBLICATION DATE
CONTRACT OR GRANT
(Contract NAS3-25266)
REPORT NUMBERS
(NASA-CR-185140; E-5068; NAS 1.26:185140; AIAA-89-2140)
AVAILABILITY SOURCE
Avail: NTIS HC A03/MF A01 CSCL 01A
COSATI CODE
PRICE CODE
Engine airframe integration effects are investigated for superonsic through-flow fan engines installed on a Mach 3.20 supersonic cruise vehicle. Six different supersonic through-flow fan engine installations covering the effects of engine size, nacelle contour, nacelle placement, and approximate bypass plume effects are presented. The different supersonic through-flow fan installations are compared with a conventional turbine bypass engine configuration on the same basic airframe. The supersonic through-flow fan engine integrations are shown to be comparable to the turbine bypass engine configuration on the basis of installed nacelle wave drag. The supersonic through-flow fan engine airframe integrated vehicles have superior aerodynamic performance on the basis of maximum lift-to-drag ratio than the turbine bypass engine installation over the entire operating Mach number range from 1.10 to 3.20. When approximate bypass plume modeling is included, the supersonic through-flow fan engine configuration shows even larger improvements over the turbine bypass engine configuration. Author

VOLUME 28 NUMBER 14 / JULY 23, 1990

Scientific and Technical Aerospace Reports

A Semimonthly Publication of the National Aeronautics and Space Administration

01 AERONAUTICS (GENERAL)

N90-20920# Federal Aviation Administration, Washington, DC. Office of Management Systems.
CENSUS OF US CIVIL AIRCRAFT Annual Report, 1988
31 Dec. 1988 365 p
(PB90-120296; AMS-420) Avail: NTIS HC A16/MF A02; SOD HC $17.00 as 050-007-00839-2 CSCL 01B

Information about the U.S. civil aircraft fleet is presented. Detailed tables of air carrier aircraft and an inventory of registered aircraft by manufacturer and model are included and general aviation aircraft by state and county of the owner. Author

N90-20921*# National Aeronautics and Space Administration. Langley Research Center, Hampton, VA.
JOINT UNIVERSITY PROGRAM FOR AIR TRANSPORTATION RESEARCH, 1988-1989
Frederick R. Morrell, comp. Mar. 1990 202 p Research program held during 1988-1989; sponsored by NASA, Langley Research Center and FAA
(NASA-CP-3063; L-16740; NAS 1.55:3063) Avail: NTIS HC A10/MF A02 CSCL 01C

The research conducted during 1988 to 1989 under the NASA/FAA-sponsored Joint University Program for Air Transportation Research is summarized. The Joint University Program is a coordinated set of three grants sponsored by NASA Langley Research Center and the Federal Aviation Administration, one each with the Massachusetts Institute of Technology, Ohio University, and Princeton University. Completed works, status reports, and annotated bibliographies are presented for research topics, which include computer science, guidance and control theory and practice, aircraft performance, flight dynamics, and applied experimental psychology. An overview of the year's activities for each university is also presented. For individual titles, see N90-20922 through N90-20941.

N90-20922*# Massachusetts Inst. of Tech., Cambridge. Flight Transportation Lab.
INVESTIGATION OF AIR TRANSPORTATION TECHNOLOGY AT THE MASSACHUSETTS INSTITUTE OF TECHNOLOGY, 1988-1989 **c03**
Robert W. Simpson *In* NASA, Langley Research Center, Joint University Program for Air Transportation Research, 1988-1989 Mar. 1990 p 1-5 (For primary document see N90-20921 14-01)
Avail: NTIS HC A10/MF A02 CSCL 01C

There are four areas of research being pursued in 1988 under sponsorship of the FAA/NASA Joint University Research Program, and one area which has been completed. The four active areas were: (1) Automatic Speech Recognition (ASR) in Air Traffic Control. The purpose of this research effort is to demonstrate the feasibility of using ASR technology within the ATC environment and to address the problems involved, especially the relevant human factors issues. (2) A Rule-Based Planning and Scheduling System. Planning denotes the formulation of a detailed scheme, program, or method worked out beforehand for the accomplishment of a goal. It involves the analysis of the desired goal and its division into sub-goals which are subsequently treated in the same way until a set of primitive objectives is obtained. (3) Modeling of Ice Accretion on Aircraft in Glaze Icing Conditions. The work in aircraft icing over the past year has focused on the fundamental aspects of glaze ice accretion, with the goal of improving analytical ice accretion models. Over the past year, studies have been conducted on the generation of surface roughness on accreting ice surfaces with the goal of providing a deterministic surface roughness in the ice accretion models. (4) Cockpit Display of Hazardous Weather Information. Information transfer and display issues associated with the dissemination of hazardous weather warnings are studied in the context of windshear alerts. Author

N90-20923*# Massachusetts Inst. of Tech., Cambridge. Flight Transportation Lab.
AUTOMATIC SPEECH RECOGNITION IN AIR TRAFFIC CONTROL **c04**
Joakim Karlsson *In* NASA, Langley Research Center, Joint University Program for Air Transportation Research, 1988-1989 Mar. 1990 p 7-15 (For primary document see N90-20921 14-01)
Avail: NTIS HC A10/MF A02 CSCL 01C

Automatic Speech Recognition (ASR) technology and its application to the Air Traffic Control system are described. The advantages of applying ASR to Air Traffic Control, as well as criteria for choosing a suitable ASR system are presented. Results from previous research and directions for future work at the Flight Transportation Laboratory are outlined. Author

N90-20924*# Massachusetts Inst. of Tech., Cambridge.
COCKPIT DISPLAY OF HAZARDOUS WIND SHEAR INFORMATION **c03**
Craig Wanke and R. John Hansman, Jr. *In* NASA, Langley Research Center, Joint University Program for Air Transportation Research, 1988-1989 Mar. 1990 p 17-34 (For primary document see N90-20921 14-01)
Avail: NTIS HC A10/MF A02 CSCL 01C

Information on cockpit display of wind shear information is given in viewgraph form. Based on the current status of windshear sensors and candidate data dissemination systems, the near-term capabilities for windshear avoidance will most likely include: (1) Ground-based detection: TDWR (Terminal Doppler Weather Radar), LLWAS (Low-Level Windshear Alert System), Automated PIREPS; (2) Ground-Air datalinks: Air traffic control voice channels, Mode-S digital datalink, ACARS alphanumeric datalink. The possible datapaths for integration of these systems are illustrated in a diagram. In the future, airborne windshear detection systems such as lidars, passive IR detectors, or airborne Doppler radars may also become available. Possible future datalinks include satellite downlink and specialized en route weather channels. Author

N90-20925*# National Aeronautics and Space Administration. Lewis Research Center, Cleveland, OH.
MODELING OF SURFACE ROUGHNESS EFFECTS ON GLAZE ICE ACCRETION **c03**
R. John Hansman, Jr., Keiko Yamaguchi, Brian M. Berkowitz (Sverdrup Technology, Inc., Middleburg Heights, OH.), and Mark Potapczuk *In* NASA, Langley Research Center, Joint University Program for Air Transportation Research, 1988-1989 Mar. 1990 p 35-42 (For primary document see N90-20921 14-01)

(Grants NAG3-666; NGL-22-009-640; NSF 85-52702)
Avail: NTIS HC A10/MF A02 CSCL 01C

A series of experimental investigations focused on studying the cause and effect of roughness on accreting glaze ice surfaces were conducted. Detailed microvideo observations were made of glaze ice accretions on 1 to 4 inch diameter cylinders in three icing wind tunnels (the Data Products of New England six inch test facility, the NASA Lewis Icing Research Tunnel, and the B. F. Goodrich Ice Protection Research Facility). Infrared thermal video recordings were made of accreting ice surfaces in the Goodrich facility. Distinct zones of surface water behavior were observed; a smooth wet zone in the stagnation region with a uniform water film; a rough zone where surface tension effects caused coalescence of surface water into stationary beads; a horn zone where roughness elements grow into horn shapes; a runback zone where surface water ran back as rivulets; and a dry zone where rime feathers formed. The location of the transition from the smooth to the rough zone was found to migrate with time towards the stagnation point. The behavior of the transition appeared to be controlled by boundary layer transition and bead formation mechanisms at the interface between the smooth and rough zones. Regions of wet ice growth and enhanced heat transfer were clearly visible in the infrared video recordings of glaze ice surfaces. A simple multi-zone modification to the current glaze ice accretion model was proposed to include spatial variability in surface roughness. Author

N90-20926*# Massachusetts Inst. of Tech., Cambridge. Dept. of Aeronautics and Astronautics.

ULTRASONIC TECHNIQUES FOR AIRCRAFT ICE ACCRETION MEASUREMENT **c03**

R. John Hansman, Jr., Mark S. Kirby, and Fred Lichtenfelts (Simmonds Precision Products, Inc., Vergennes, VT.) *In* NASA, Langley Research Center, Joint University Program for Air Transportation Research, 1988-1989 Mar. 1990 p 43-53 Sponsored by NSF (For primary document see N90-20921 14-01)
(Grants NAG3-666; NGL-22-009-640)
Avail: NTIS HC A10/MF A02 CSCL 01C

Results of tests to measure ice growth in natural (flight) and artificial (icing wind tunnel) icing conditions are presented. Ice thickness is measured using an ultrasonic pulse-echo technique. Two icing regimes, wet and dry ice growth, are identified and the unique ultrasonic signal characteristics associated with these different types of ice growth are described. Ultrasonic measurements of ice growth on cylinders and airfoils exposed to artificial and natural icing conditions are presented. An accuracy of plus or minus 0.5 mm is achieved for ice thickness measurement using the pulse-echo technique. The performance of two-probe type ice detectors is compared to the surface mounted ultrasonic system. The ultrasonically measured ice accretion rates and ice surface condition (wet or dry) are used to compare the heat transfer characteristics for flight and icing wind tunnel environments. In general the heat transfer coefficient is inferred to be higher in the wind tunnel environment, not likely due to higher freestream turbulence levels. Finally, preliminary results of tests to measure ice growth on airfoil using an array of ultrasonic transducers are described. Ice profiles obtained during flight in natural icing conditions are shown and compared with mechanical and stereo image measurements. Author

N90-20927*# Massachusetts Inst. of Tech., Cambridge.

INVESTIGATION OF SURFACE WATER BEHAVIOR DURING GLAZE ICE ACCRETION **c03**

R. John Hansman, Jr. and Stephen R. Turnock (Southampton Univ., England) *In* NASA, Langley Research Center, Joint University Program for Air Transportation Research, 1988-1989 Mar. 1990 p 55-62 (For primary document see N90-20921 14-01)
(Grants NAG3-666; NGL-22-009-640; NSF 85-52702)
Avail: NTIS HC A10/MF A02 CSCL 01C

A series of experimental investigations that focused on isolating the primary factors that control the behavior of unfrozen surface water during glaze ice accretion were conducted. Detailed microvideo observations were made of glaze ice accretions on 2.54 cm diam cylinders in a closed-loop refrigerated wind tunnel. Distinct zones of surface water behavior were observed; a smooth wet zone in the stagnation region with a uniform water film, a rough zone where surface tension effects caused coalescence of surface water into stationary beads, and a zone where surface water ran back as rivulets. The location of the transition from the smooth to the rough zone was found to migrate towards the stagnation point with time. Comparative tests were conducted to study the effect of the substrate thermal and roughness properties on ice accretion. The importance of surface water behavior was evaluated by the addition of a surface tension reducing agent to the icing tunnel water supply, which significantly altered the accreted glaze ice shape. Measurements were made to determine the contact angle behavior of water droplets on ice. A simple multizone modification to current glaze ice accretion models was proposed to include the observed surface roughness behavior. Author

N90-20928*# Massachusetts Inst. of Tech., Cambridge. Dept. of Aeronautics and Astronautics.

THE INFLUENCE OF ICE ACCRETION PHYSICS ON THE FORECASTING OF AIRCRAFT ICING CONDITIONS **c03**

R. John Hansman, Jr. *In* NASA, Langley Research Center, Joint University Program for Air Transportation Research, 1988-1989 Mar. 1990 p 63-67 Sponsored by NSF (For primary document see N90-20921 14-01)
(Grants NAG3-666; NGL-22-009-640)
Avail: NTIS HC A10/MF A02 CSCL 01C

The physics which control aircraft ice accretion are reviewed in the context of identifying and forecasting hazardous icing conditions. The severity of aircraft icing is found to be extremely sensitive to temperature, liquid water content and droplet size distribution particularly near the transition between rime and mixed icing. The difficulty in measurement and the variability of these factors with altitude, position and time coupled with variable aircraft sensitivity make forecasting and identifying icing conditions difficult. Automated Pilot Reports (PIREPS) are suggested as one mechanism for improving the data base necessary to forecast icing conditions. Author

N90-20929*# Massachusetts Inst. of Tech., Cambridge. Dept. of Aeronautics and Astronautics.

COCKPIT DISPLAY OF HAZARDOUS WEATHER INFORMATION **c03**

R. John Hansman, Jr. and Craig Wanke *In* NASA, Langley Research Center, Joint University Program for Air Transportation Research, 1988-1989 Mar. 1990 p 69-76 (For primary document see N90-20921 14-01)
(Contract NAG1-690; NGL-22-009-640; BARR-10-119)
Avail: NTIS HC A10/MF A02 CSCL 01C

Information transfer and display issues associated with the dissemination of hazardous weather warnings are studied in the context of windshear alerts. Operational and developmental windshear detection systems are briefly reviewed. The July 11, 1988 microburst events observed as part of the Denver Terminal Doppler Weather Radar (TDWR) operational evaluation are analyzed in terms of information transfer and the effectiveness of the microburst alerts. Information transfer, message content and display issues associated with microburst alerts generated from ground based sources are evaluated by means of pilot opinion surveys and part task simulator studies. Author

N90-20930*# Massachusetts Inst. of Tech., Cambridge. Flight Transportation Lab.

TIME AND TRUTH IN PLANS **c81**

Lyman R. Hazelton, Jr. *In* NASA, Langley Research Center, Joint University Program for Air Transportation Research, 1988-1989 Mar. 1990 p 77-91 (For primary document see N90-20921 14-01)
(Grant NGL-22-009-640)
Avail: NTIS HC A10/MF A02 CSCL 01C

Some of the logical components of a rule based planning and scheduling system are described. The researcher points out a deficiency in the conventional truth maintenance approach to this class of problems and suggests a new mechanism which overcomes the problem. This extension of the idea of justification truth maintenance may seem at first to be a small philosophical step. However, it embodies a process of basic human reasoning which is so common and automatic as to escape conscious detection without careful introspection. It is vital to any successful implementation of a rule based planning reasoner. Author

N90-20931*# Ohio Univ., Athens.
RIDGE REGRESSION PROCESSING **c04**
Mark R. Kuhl *In* NASA, Langley Research Center, Joint University Program for Air Transportation Research, 1988-1989 Mar. 1990 p 99-104 (For primary document see N90-20921 14-01)
Avail: NTIS HC A10/MF A02 CSCL 01C

Current navigation requirements depend on a geometric dilution of precision (GDOP) criterion. As long as the GDOP stays below a specific value, navigation requirements are met. The GDOP will exceed the specified value when the measurement geometry becomes too collinear. A new signal processing technique, called Ridge Regression Processing, can reduce the effects of nearly collinear measurement geometry; thereby reducing the inflation of the measurement errors. It is shown that the Ridge signal processor gives a consistently better mean squared error (MSE) in position than the Ordinary Least Mean Squares (OLS) estimator. The applicability of this technique is currently being investigated to improve the following areas: receiver autonomous integrity monitoring (RAIM), coverage requirements, availability requirements, and precision approaches. Author

N90-20932*# Ohio Univ., Athens.
OPTIMIZATION OF THE EFFECTIVE GPS DATA RATE **c04**
David S. McIntyre *In* NASA, Langley Research Center, Joint University Program for Air Transportation Research, 1988-1989 Mar. 1990 p 105-109 (For primary document see N90-20921 14-01)
Avail: NTIS HC A10/MF A02 CSCL 01C

Ohio University's Avionics Engineering Center is performing research directed towards the integration of the NAVSTAR Global Positioning System (GPS) and the Inertial Navigation System (INS) for attitude and heading determination. The integration of GPS/INS offers synergistic benefits. INS gyro drift error can be compensated by the long-term stability of GPS by means of an in-flight data monitoring algorithm. Using GPS data as a reference is more advantageous than implementing an additional INS since GPS offers a dissimilar redundancy to the attitude and heading determination configuration. In converse, the short-term stability of the INS can be used to correct or substitute for faulty GPS data due to tracking loop phase lag or data gaps because of satellite shielding. The optimization of the effective GPS data rate is essential for the proper execution of an integrated GPS/INS in-flight algorithm. GPS attitude and heading information must be consistently available during INS outages. Present research efforts involve the development of an in-flight algorithm that maximizes the potential of integrated GPS/INS. This algorithm determines the acceptable limits of phase lag that the GPS tracking loop introduces to the flight control system (FCS) during the transmission of information. Once these calculated limits are exceeded, INS data are used to insure the continuous availability of attitude and heading information to the flight control system. Author

N90-20933*# Ohio Univ., Athens. Avionics Engineering Center.
SOLE MEANS NAVIGATION AND INTEGRITY THROUGH HYBRID LORAN-C AND NAVSTAR GPS **c04**
Frank vanGraas *In* NASA, Langley Research Center, Joint University Program for Air Transportation Research, 1988-1989 Mar. 1990 p 111-118 (For primary document see N90-20921 14-01)
(Grant NGR-009-017)
Avail: NTIS HC A10/MF A02 CSCL 01C

A sole means navigation system does not only call for integrity, but also for coverage, reliability, availability and accuracy. Even though ground monitored GPS will provide integrity, availability is still not sufficient. One satellite outage can affect a large service area for several hours per day. The same holds for differential GPS; a total satellite outage cannot be corrected for. To obtain sufficient coverage, extra measurements are needed, either in the form of extra GPS satellites (expensive) or through redundant measurements from other systems. LORAN-C is available and will, hybridized with GPS, result in a system that has the potential to satisfy the requirements for a sole means navigation system for use in the continental United States. Assumptions are made about the qualification sole means, mainly based on current sole means systems such as VOR/DME. In order to allow for system design that will satisfy sole means requirements, it is recommended that a definition of a sole means navigation system be established. This definition must include requirements for availability, reliability, and integrity currently not specified. In addition to the definition of a sole means navigation system, certification requirements must be established for hybrid navigation systems. This will allow for design and production of a new generation of airborne navigation systems that will reduce overall system costs and simplify training procedures. Author

N90-20934*# Ohio Univ., Athens. Avionics Engineering Center.
WEATHER DATA DISSEMINATION TO AIRCRAFT **c03**
Richard H. McFarland and Craig B. Parker *In* NASA, Langley Research Center, Joint University Program for Air Transportation Research, 1988-1989 Mar. 1990 p 119-127 (For primary document see N90-20921 14-01)
Avail: NTIS HC A10/MF A02 CSCL 01C

Documentation exists that shows weather to be responsible for approximately 40 percent of all general aviation accidents with fatalities. Weather data products available on the ground are becoming more sophisticated and greater in number. Although many of these data are critical to aircraft safety, they currently must be transmitted verbally to the aircraft. This process is labor intensive and provides a low rate of information transfer. Consequently, the pilot is often forced to make life-critical decisions based on incomplete and outdated information. Automated transmission of weather data from the ground to the aircraft can provide the aircrew with accurate data in near-real time. The current National Airspace System Plan calls for such an uplink capability to be provided by the Mode S Beacon System data link. Although this system has a very advanced data link capability, it will not be capable of providing adequate weather data to all airspace users in its planned configuration. This paper delineates some of the important weather data uplink system requirements, and describes a system which is capable of meeting these requirements. The proposed system utilizes a run-length coding technique for image data compression and a hybrid phase and amplitude modulation technique for the transmission of both voice and weather data on existing aeronautical Very High Frequency (VHF) voice communication channels. Author

N90-20935*# Princeton Univ., NJ. Dept. of Mechanical and Aerospace Engineering.
INVESTIGATION OF AIR TRANSPORTATION TECHNOLOGY AT PRINCETON UNIVERSITY, 1988-1989 **c03**
Robert F. Stengel *In* NASA, Langley Research Center, Joint University Program for Air Transportation Research, 1988-1989 Mar. 1990 p 131-144 (For primary document see N90-20921 14-01)
Avail: NTIS HC A10/MF A02 CSCL 01C

The Air Transportation Technology Program at Princeton University, a program emphasizing graduate and undergraduate student research, proceeded along several avenues during the past year. A study of optimal trajectories for penetration of microbursts when encounter is unavoidable was conducted. The emphasis of current wind shear research is on developing an expert system for wind shear avoidance. A knowledge-based reconfigurable flight control system that is implemented with the Pascal programming language using parallel microprocessors was developed. This expert system could be considered a prototype

for a failure-tolerant control system that can be constructed using existing hardware. Development of a real-time cockpit simulator continued during the year. The simulator provides a single-person crew station with both conventional and advanced control devices; it currently is programmed to simulate the Navion single-engine general aviation airplane. Alternatives for the air traffic control system giving particular attention to the institutional structure of the FAA are analyzed. A simple numerical procedure for estimating the stochastic robustness of control systems is being investigated. The revitalization of the general aviation industry is also discussed. Author

N90-20936*# Princeton Univ., NJ. Dept. of Mechanical and Aerospace Engineering.
APPLICATION OF STOCHASTIC ROBUSTNESS TO AIRCRAFT CONTROL SYSTEMS **c08**
Laura E. Ryan *In* NASA, Langley Research Center, Joint University Program for Air Transportation Research, 1988-1989 Mar. 1990 p 145-166 (For primary document see N90-20921 14-01)
Avail: NTIS HC A10/MF A02 CSCL 01C

Guaranteeing robustness has long been an important design objective of control system analysis. Stochastic robustness is a simple numerical procedure that can be used to measure and gain insight into robustness properties associated with linear control systems. In the realm of aircraft control systems, problems such as the effects of flight condition perturbations and model-order uncertainties on robustness are easily and effectively analyzed using stochastic robustness. The concept of stochastic robustness is reviewed and examples are presented demonstrating its use in flight control system analysis. Author

N90-20937*# Princeton Univ., NJ. Dept. of Mechanical and Aerospace Engineering.
NEURAL NETWORKS FOR AIRCRAFT CONTROL **c08**
Dennis Linse *In* NASA, Langley Research Center, Joint University Program for Air Transportation Research, 1988-1989 Mar. 1990 p 167-181 (For primary document see N90-20921 14-01)
Avail: NTIS HC A10/MF A02 CSCL 01C

Current research in Artificial Neural Networks indicates that networks offer some potential advantages in adaptation and fault tolerance. This research is directed at determining the possible applicability of neural networks to aircraft control. The first application will be to aircraft trim. Neural network node characteristics, network topology and operation, neural network learning and example histories using neighboring optimal control with a neural net are discussed. Author

N90-20938*# Princeton Univ., NJ. Dept. of Mechanical and Aerospace Engineering.
AN EXPERT SYSTEM FOR WIND SHEAR AVOIDANCE **c03**
Robert F. Stengel and D. Alexander Stratton *In* NASA, Langley Research Center, Joint University Program for Air Transportation Research, 1988-1989 Mar. 1990 p 183-188 (For primary document see N90-20921 14-01)
(Grant NAG1-834)
Avail: NTIS HC A10/MF A02 CSCL 01C

A study of intelligent guidance and control concepts for protecting against the adverse effects of wind shear during aircraft takeoffs and landings is being conducted, with current emphasis on developing an expert system for wind shear avoidance. Principal objectives are to develop methods for assessing the likelihood of wind shear encounter (based on real-time information in the cockpit), for deciding what flight path to pursue (e.g., takeoff abort, landing go-around, or normal climbout or glide slope), and for using the aircraft's full potential for combating wind shear. This study requires the definition of both deterministic and statistical techniques for fusing internal and external information , for making go/no-go decisions, and for generating commands to the manually controlled flight. The program has begun with the development of the WindShear Safety Advisor, an expert system for pilot aiding that is based on the FAA Windshear Training Aid; a two-volume manual that presents an overview , pilot guide, training program, and substantiating data provides guidelines for this initial development. The WindShear Safety Advisor expert system currently contains over 200 rules and is coded in the LISP programming language. Author

N90-20939*# Princeton Univ., NJ. Dept. of Mechanical and Aerospace Engineering.
RULE-BASED MECHANISMS OF LEARNING FOR INTELLIGENT ADAPTIVE FLIGHT CONTROL **c08**
David A. Handelman and Robert F. Stengel *In* NASA, Langley Research Center, Joint University Program for Air Transportation Research, 1988-1989 Mar. 1990 p 189-194 (For primary document see N90-20921 14-01)
(Contract DAAG29-84-K-0048)
Avail: NTIS HC A10/MF A02 CSCL 01C

How certain aspects of human learning can be used to characterize learning in intelligent adaptive control systems is investigated. Reflexive and declarative memory and learning are described. It is shown that model-based systems-theoretic adaptive control methods exhibit attributes of reflexive learning, whereas the problem-solving capabilities of knowledge-based systems of artificial intelligence are naturally suited for implementing declarative learning. Issues related to learning in knowledge-based control systems are addressed, with particular attention given to rule-based systems. A mechanism for real-time rule-based knowledge acquisition is suggested, and utilization of this mechanism within the context of failure diagnosis for fault-tolerant flight control is demonstrated. Author

N90-20940*# Princeton Univ., NJ. Dept. of Mechanical and Aerospace Engineering.
PERSPECTIVES ON THE USE OF RULE-BASED CONTROL **c08**
David A. Handelman and Robert F. Stengel *In* NASA, Langley Research Center, Joint University Program for Air Transportation Research, 1988-1989 Mar. 1990 p 195-200 (For primary document see N90-20921 14-01)
(Contract DAAG29-84-K-0048)
Avail: NTIS HC A10/MF A02 CSCL 01C

Issues regarding the application of artificial intelligence techniques to real-time control are discussed. Advantages associated with knowledge-based programming are discussed. A proposed rule-based control technique is summarized and applied to the problem of automated aircraft emergency procedure execution. Although emergency procedures are by definition predominately procedural, their numerous evaluation and decision points make a declarative representation of the knowledge they encode highly attractive, resulting in an organized and easily maintained software hierarchy. Simulation results demonstrate that real-time performance can be obtained using a microprocessor-based controller. It is concluded that a rule-based control system design approach may prove more useful than conventional methods under certain circumstances, and that declarative rules with embedded procedural code provide a sound basis for the construction of complex, yet economical, control systems. Author

N90-20941*# Princeton Univ., NJ. Dept. of Mechanical and Aerospace Engineering.
STOCHASTIC ROBUSTNESS OF LINEAR CONTROL SYSTEMS **c08**
Robert F. Stengel and Laura E. Ryan *In* NASA, Langley Research Center, Joint University Program for Air Transportation Research, 1988-1989 Mar. 1990 p 201-206 (For primary document see N90-20921 14-01)
(Grant NGL-31-001-252)
Avail: NTIS HC A10/MF A02 CSCL 01C

A simple numerical procedure for estimating the stochastic robustness of a linear, time-invariant system is described. Monte Carlo evaluation of the system's eigenvalues allows the probability of instability and the related stochastic root locus to be estimated. This definition of robustness is an alternative to existing deterministic definitions that address both structured and unstructured parameter variations directly. This analysis approach

treats not only Gaussian parameter uncertainties but non-Gaussian cases, including uncertain-but-bounded variations. Trivial extensions of the procedure admit alternate discriminants to be considered. Thus, the probabilities that stipulated degrees of instability will be exceeded or that closed-loop roots will leave desirable regions also can be estimated. Results are particularly amenable to graphical presentation. Author

N90-20942*# National Aeronautics and Space Administration. Lewis Research Center, Cleveland, OH.
LASER-VELOCIMETER-MEASURED FLOW FIELD AROUND AN ADVANCED, SWEPT, EIGHT-BLADE PROPELLER AT MACH 0.8
Harvey E. Neuman, John A. Serafini, Daniel Y. Whipple, and Brian T. Howard May 1985 100 p
(NASA-TP-2462; E-2429; NAS 1.60:2462) Avail: Issuing Activity CSCL 01B

A laser velocimeter has been used to measure velocities in the flow field around an advanced, eight-blade, high-speed propeller in the NASA Lewis 8- by 6-Foot Supersonic Wind Tunnel. The propeller was nominally 62.23 cm (24.5 in.) in diameter and was operated both at windmill and near the design power condition at a free-stream Mach number of 0.8. The detailed three-dimensional velocity data obtained are being made available here to enable researchers to verify emerging advanced propeller design and analysis codes. Data were obtained at two axial positions ahead of the propeller, at two axial positions downstream of the propeller, and at seven radial positions within the bladed passages extending from the inlet of the blades to downstream of the blade exit. A four-beam laser velocimeter system was configured to measure two velocity components simultaneously. Author

N90-20943*# Sverdrup Technology, Inc., Cleveland, OH.
USERS MANUAL FOR THE NASA LEWIS ICE ACCRETION PREDICTION CODE (LEWICE) Final Report
Gary A. Ruff and Brian M. Berkowitz May 1990 240 p
(Contract NAS3-25266)
(NASA-CR-185129; NAS 1.26:185129) Avail: NTIS HC A11/MF A02 CSCL 01B

LEWICE is an ice accretion prediction code that applies a time-stepping procedure to calculate the shape of an ice accretion. The potential flow field is calculated in LEWICE using the Douglas Hess-Smith 2-D panel code (S24Y). This potential flow field is then used to calculate the trajectories of particles and the impingement points on the body. These calculations are performed to determine the distribution of liquid water impinging on the body, which then serves as input to the icing thermodynamic code. The icing thermodynamic model is based on the work of Messinger, but contains several major modifications and improvements. This model is used to calculate the ice growth rate at each point on the surface of the geometry. By specifying an icing time increment, the ice growth rate can be interpreted as an ice thickness which is added to the body, resulting in the generation of new coordinates. This procedure is repeated, beginning with the potential flow calculations, until the desired icing time is reached. The operation of LEWICE is illustrated through the use of five examples. These examples are representative of the types of applications expected for LEWICE. All input and output is discussed, along with many of the diagnostic messages contained in the code. Several error conditions that may occur in the code for certain icing conditions are identified, and a course of action is recommended. LEWICE has been used to calculate a variety of ice shapes, but should still be considered a research code. The code should be exercised further to identify any shortcomings and inadequacies. Any modifications identified as a result of these cases, or of additional experimental results, should be incorporated into the model. Using it as a test bed for improvements to the ice accretion model is one important application of LEWICE. Author

02 AERODYNAMICS

Includes aerodynamics of bodies, combinations, wings, rotors, and control surfaces; and internal flow in ducts and turbomachinery.

For related information see also *34 Fluid Mechanics and Heat Transfer.*

N90-20944 North Carolina State Univ., Raleigh.
RELATING FLOW BETWEEN COUNTER-ROTATING PROPELLERS TO AERODYNAMIC INTERACTION NOISE Ph.D. Thesis
Howard Van Liew Patrick 1989 199 p
Avail: Univ. Microfilms Order No. DA8918129

Axial and circumferential flow velocity components were measured at discrete points between 28 cm diameter straight bladed, hobby-craft model aircraft counter-rotating propellers using a single sensor hot-film anemometer. Coherence analysis was used to determine a relationship between the far-field radiated noise and the measured flow velocity components at the primary aerodynamic interaction tones. Tests were performed in an open-jet anechoic wind tunnel with a 0.6 m square nozzle at a free-stream speed of 0.08 Mach number. The forward propeller had three blades and the abaft propeller consisted of four blades. Primary test variables were radical and axial positions of the hot-film sensor and rotor-to-rotor spacing. The major conclusions were based upon the concept that if the relationship between the fluid flow velocity and the radiated noise was linear, the coherence function would be expected to be unity. At the primary aerodynamic interaction frequencies, it was determined that the degree of linearity varied radially along the propeller blade span, i.e., nonlinearities were found to exist. This partial linearity was composed of three distinct regions. Near the motor housing, there existed a small region of appreciable linearity, for both flow components, which decreased dramatically a short distance out from the housing. This phenomenon was associated with the viscous boundary layer flow from the motor housing. Dissert. Abstr.

N90-20945 Florida Univ., Gainesville.
ON TOTAL VARIATION DIMINISHING SCHEMES FOR TRANSONIC TURBULENT FLOW COMPUTATION Ph.D. Thesis
Ming-Hsiung Chen 1988 151 p
Avail: Univ. Microfilms Order No. DA8923945

Recently a number of techniques for constructing nonlinear, second-order accurate, high-resolution shock capturing schemes for systems of hyperbolic conservation laws were developed in order to simulate complex flow fields more accurately and efficiently. These schemes, called total variation diminishing (TVD), are free from generating spurious oscillations across the shocks and contact discontinuities, and can converge to physically realizable solution with the aid of entropy correction. The TVD schemes developed for two-dimensional planar flows were extended to three-dimensional flows. On the application side, a thin-layer Navier-Stokes flow code based on the conventional Beam-Warming scheme was modified to incorporate the TVD schemes in the solution process. A variable time step procedure was also implemented into the code for more efficient computation of the steady state flows. The transonic turbulent flow over an axisymmetric projectile is adopted as the test problem to assess the performance of three variants of the TVD scheme, two upwind schemes with flux limiters proposed by Van Leer and Roe and one symmetric scheme. The combinations of the high accuracy, good robustness, and improving computational efficiency offered by the TVD schemes make them extremely attractive for computing flow with shocks. Among the three variants, it is found that the convergence rate of the flux limiter proposed by Van Leer for the upwind TVD scheme is least affected by the incoming flow Mach numbers. Dissert. Abstr.

N90-20946*# National Aeronautics and Space Administration. Langley Research Center, Hampton, VA.
DISCRETE-VORTEX MODEL FOR THE SYMMETRIC-VORTEX FLOW ON CONES

Thomas G. Gainer Washington May 1990 29 p
(NASA-TP-2989; L-16586; NAS 1.60:2989) Avail: NTIS HC A03/MF A01 CSCL 01A

A relatively simple but accurate potential flow model was developed for studying the symmetric vortex flow on cones. The model is a modified version of the model first developed by Bryson, in which discrete vortices and straight-line feeding sheets were used to represent the flow field. It differs, however, in the zero-force condition used to position the vortices and determine their circulation strengths. The Bryson model imposed the condition that the net force on the feeding sheets and discrete vortices must be zero. The proposed model satisfies this zero-force condition by having the vortices move as free vortices, at a velocity equal to at the local crossflow velocity at their centers. When the free-vortex assumption is made, a solution is obtained in the form of two nonlinear algebraic equations that relate the vortex center coordinates and vortex strengths to the cone angle and angle of attack. The vortex center locations calculated using the model are in good agreement with experimental values. The cone normal forces as well as center locations are in good agreement with the vortex cloud method of calculating symmetric flow fields. Author

N90-20947 North Carolina State Univ., Raleigh.
AN APPROXIMATE VISCOUS SHOCK LAYER METHOD FOR CALCULATING THE HYPERSONIC FLOW OVER BLUNT-NOSED BODIES Ph.D. Thesis
Arthur Christian Grantz 1989 154 p
Avail: Univ. Microfilms Order No. DA8926329

An approximate method is presented which can calculate the surface and flow-field properties for the fully viscous hypersonic flow over blunt-nosed bodies at an angle of attack. Using the second order pressure equation of Maslen and incorporating viscous terms into the streamwise momentum and energy equations, a simple method is obtained which can calculate both the subsonic and supersonic regions of the shock layer and does not require a starting solution for the shock shape. Surface heat transfer and pressure predictions from the present method compare very well with the more accurate viscous shock layer method, flight and wind tunnel data at zero degrees angle of attack. Equilibrium air and turbulence models are also incorporated into the approximate method. Surface pressure results compare well with theory and experiment for 15 and 25 degree sphere cones, at small to moderate angles of attack. Comparisons with experiment and a viscous shock layer method indicate that the approximate method does not calculate surface streamlines accurately, however. Consequently, surface heat transfer rate predictions which are accurate for small angles of attack, deteriorate for larger angles of attack where the calculated surface streamlines are less accurate. Surface pressures are well predicted since the accuracy of surface streamlines has only a small effect on the pressure.
Dissert. Abstr.

N90-20948# Air Force Inst. of Tech., Wright-Patterson AFB, OH. School of Engineering.
COMPARISON OF C- AND O-GRID GENERATION METHODS USING A NACA 0012 AIRFOIL M.S. Thesis
Mark J. Lutton Dec. 1989 128 p
(AD-A216375; AFIT/GAE/ENY/89D-21) Avail: NTIS HC A07/MF A01 CSCL 20/4

An investigation is undertaken to compare the performance of C- and O-grid generation methods as applied to numerically predicting the flow about a NACA 0012 airfoil. Both types of grid were generated using a hyperbolic grid generation code. The solution of the flow field was numerically calculated using the Beam and Warming algorithm to solve the two-dimensional Navier-Stokes equations for viscous, compressible flow. Numerical solutions are obtained for Mach number ranging from 0.3 to 1.1, angle of attack ranging from 0 to 13 degress, and Reynolds numbers between 2 and 6 million. The numerical results obtained from both C- and O-grids are compared to experimental data. Results indicate a weakness is the method of applying the boundary conditions in the wake or the C-grid, while the overall resolution in the wake is poor for the O-grid due to inadequate control of grid spacing in that region. The transformation metrics are examined to explain differences observed in grid performance. GRA

N90-20949*# Rockwell International Science Center, Thousand Oaks, CA.
SOME ASPECTS OF ESSENTIALLY NONOSCILLATORY (ENO) FORMULATIONS FOR THE EULER EQUATIONS, PART 3 Final Report
Sukumar R. Chakravarthy Washington May 1990 69 p
(Contract NAS1-17492)
(NASA-CR-4285; NAS 1.26:4285) Avail: NTIS HC A04/MF A01 CSCL 01A

An essentially nonoscillatory (ENO) formulation is described for hyperbolic systems of conservation laws. ENO approaches are based on smart interpolation to avoid spurious numerical oscillations. ENO schemes are a superset of Total Variation Diminishing (TVD) schemes. In the recent past, TVD formulations were used to construct shock capturing finite difference methods. At extremum points of the solution, TVD schemes automatically reduce to being first-order accurate discretizations locally, while away from extrema they can be constructed to be of higher order accuracy. The new framework helps construct essentially non-oscillatory finite difference methods without recourse to local reductions of accuracy to first order. Thus arbitrarily high orders of accuracy can be obtained. The basic general ideas of the new approach can be specialized in several ways and one specific implementation is described based on: (1) the integral form of the conservation laws; (2) reconstruction based on the primitive functions; (3) extension to multiple dimensions in a tensor product fashion; and (4) Runge-Kutta time integration. The resulting method is fourth-order accurate in time and space and is applicable to uniform Cartesian grids. The construction of such schemes for scalar equations and systems in one and two space dimensions is described along with several examples which illustrate interesting aspects of the new approach. Author

N90-20950*# Old Dominion Univ., Norfolk, VA. Dept. of Mechanical Engineering and Mechanics.
EFFECTS OF NOSE BLUNTNESS AND SHOCK-SHOCK INTERACTIONS ON BLUNT BODIES IN VISCOUS HYPERSONIC FLOWS Progress Report, period ending 31 Dec. 1989
D. J. Singh and S. N. Tiwari Jan. 1990 187 p
(Grant NAG1-423)
(NASA-CR-186451; NAS 1.26:186451) Avail: NTIS HC A09/MF A01 CSCL 01A

A numerical study was conducted to investigate the effects of blunt leading edges on the viscous flow field around a hypersonic vehicle such as the proposed National Aero-Space Plane. Attention is focused on two specific regions of the flow field. In the first region, effects of nose bluntness on the forebody flow field are investigated. The second region of the flow considered is around the leading edges of the scramjet inlet. In this region, the interaction of the forebody shock with the shock produced by the blunt leading edges of the inlet compression surfaces is analyzed. Analysis of these flow regions is required to accurately predict the overall flow field as well as to get necessary information on localized zones of high pressure and intense heating. The results for the forebody flow field are discussed first, followed by the results for the shock interaction in the inlet leading edge region. Author

N90-20951# National Aeronautical Lab., Bangalore (India). Computational and Theoretical Fluid Dynamics Div.
MULTIGRID ACCELERATED RELAXATION SOLUTION OF TRANSONIC FULL POTENTIAL FLOW EQUATION
J. P. Singh Dec. 1989 30 p
(PD-CF-8942) Avail: NTIS HC A03/MF A01

The multigrid method has been incorporated in the Garabedian-Korn inviscid code, as adapted at N.A.L., to accelerate its convergence. The results show a large CPU time saving in achieving converged solution with a residue tolerance level of

10(exp -4). The demonstrations include both subcritical and supercritical Mach numbers. Author

N90-20952*# Cessna Aircraft Co., Wichita, KS.
FLIGHT TEST INVESTIGATION OF CERTIFICATION ISSUES PERTAINING TO GENERAL-AVIATION-TYPE AIRCRAFT WITH NATURAL LAMINAR FLOW
Wayne A. Doty Apr. 1990 49 p
(Contract NAS1-18561)
(NASA-CR-181967; NAS 1.26:181967) Avail: NTIS HC A03/MF A01 CSCL 01A

Development of Natural Laminar Flow (NLF) technology for application to general aviation-type aircraft has raised some question as to the adequacy of FAR Part 23 for certification of aircraft with significant NLF. A series of flight tests were conducted with a modified Cessna T210R to allow quantitative comparison of the aircraft's ability to meet certification requirements with significant NLF and with boundary layer transition fixed near the leading edge. There were no significant differences between the two conditions except an increasing in drag, which resulted in longer takeoff distances and reduced climb performance. Author

N90-20953*# Old Dominion Univ., Norfolk, VA. Research Foundation
AN OVERLAPPED GRID METHOD FOR MULTIGRID, FINITE VOLUME/DIFFERENCE FLOW SOLVERS: MaGGIE Report, 1987 - 1989
Oktay Baysal and Victor R. Lessard Feb. 1990 111 p
(Grant NAG1-664)
(NASA-CR-182008; NAS 1.26:182008) Avail: NTIS HC A06/MF A01 CSCL 01A

The objective is to develop a domain decomposition method via overlapping/embedding the component grids, which is to be used by upwind, multi-grid, finite volume solution algorithms. A computer code, given the name MaGGiE (Multi-Geometry Grid Embedder) is developed to meet this objective. MaGGiE takes independently generated component grids as input, and automatically constructs the composite mesh and interpolation data, which can be used by the finite volume solution methods with or without multigrid convergence acceleration. Six demonstrative examples showing various aspects of the overlap technique are presented and discussed. These cases are used for developing the procedure for overlapping grids of different topologies, and to evaluate the grid connection and interpolation data for finite volume calculations on a composite mesh. Time fluxes are transferred between mesh interfaces using a trilinear interpolation procedure. Conservation losses are minimal at the interfaces using this method. The multi-grid solution algorithm, using the coaser grid connections, improves the convergence time history as compared to the solution on composite mesh without multi-gridding. Author

N90-20954 Texas Univ., Austin.
COMPUTATION OF NONEQUILIBRIUM CHEMICALLY REACTING FLOWS IN HYPERSONIC FLOW FIELD Ph.D. Thesis
Ting-Lung Chiang 1989 186 p
Avail: Univ. Microfilms Order No. DA8920677

In recent years a renewed interest in the design of various hypersonic vehicles has necessitated the inclusion of chemically reacting flows for the solution of hypersonic flowfields. From the physical point of view, all chemical reactions take some time to reach equilibrium state. Therefore, finite-rate (nonequilibrium) chemistry models must be utilized for hypersonic flowfield computations. A compelling difficulty in the numerical simulation of chemically reacting flow is the selection of the marching time step. Usually, the characteristic time scale of the gas dynamic equations is different from that of the chemistry equations. A numerical algorithm that determines the chemistry marching time step is developed. Von Neumann stability analysis is applied to the chemistry equations to provide a criteria for the selection of time step for a stable solution. Both the quasi one-dimensional nozzle problem and the 2-D/axisymmetric blunt body problem are used for numerical validation. Unsteady Euler equations and chemistry equations are written in the conservative form so that the shock capturing scheme can be applied. A five species model is selected for the air compositions. The governing equations are discretized by an implicit, flux-splitting finite difference formulation to provide a better stability characteristic and faster convergence. The gas dynamic equations and chemistry equations are solved interactively and communicated by the loosely-coupled scheme. Author

N90-20955 Purdue Univ., West Lafayette, IN.
A TWO-DIMENSIONAL UNSTEADY ANALYSIS FOR TRANSONIC AND SUPERSONIC CASCADE FLOWS Ph.D. Thesis
Yung-Fu Kao 1989 162 p
Avail: Univ. Microfilms Order No. DA9003914

A mathematical model based on the 2-D unsteady full potential equation was developed to predict the unsteady response of cascade flows at subsonic, transonic, and supersonic speeds. A time marching algorithm based on a quasi-Newton iteration technique is employed. A time sheared scheme is used to calculate non-Zero interblade phase angle oscillation cases. Multiple passage calculations are needed if the interblade time lag is large. Contrary to the classical linear theory, the effects of blade shape, flow incidence angle, cascade geometries, and presence of shock wave are fully considered. The validity and accuracy was demonstrated by comparison to available experimental data and other theoretical analyses over wide flow ranges for various cascade configurations. The mathematical model and procedures adopted can be applied to turbomachinery flutter analysis. Dissert. Abstr.

N90-20956 Purdue Univ., West Lafayette, IN.
MEASUREMENT OF LIFT DEVELOPMENT ON RAPIDLY-ACCELERATED WINGS Ph.D. Thesis
Richard Steven Sawyer 1989 198 p
Avail: Univ. Microfilms Order No. DA9003954

Current analyses for treating the response of wings in unsteady flow fields are either extremely costly or involve major simplifications to allow calculation. Such simplifications normally include neglecting the effects of viscosity and assuming a simple wake model. Situations are explored wheresuch analyses were expected to fail, as well as work. For one set of tests, a large bore, short stroke air cylinder was used to give models a rapid acceleration to a constant speed. Other tests were performed using models under constant accelerations from rest. Lift as a function of time for various planforms was gathered using combinations of piezoelectric force tranducers. The result of the Fast Start test was that the analytical indicial response function, derived for a finite wing, does manifest itself in a real test. Constant Acceleration tests furnished numerous conclusions. Response of a rectangular wing was much higher than expected, due to a finite development time for a laminar separation. Delta wing studies showed lower response than expected for pre-stall tests, possibly as a result of leading edge vortex burst movement under acceleration. Post-stall delta wing tests featured a nonmonotonic response with acceleration. This was attributed to a reformation or destruction of large scale structures in an otherwise bluff body wake. Dissert. Abstr.

N90-20957 California Univ., Davis.
CONVERGENCE ACCELERATION OF HYPERSONIC FLOW CALCULATIONS: A NONLINEAR RELAXATION FACTOR Ph.D. Thesis
Samson Hok-Chi Cheung 1989 120 p
Avail: Univ. Microfilms Order No. DA9002725

In computational fluid dynamics (CFD), steady-flow solutions are typically obtained from computer codes in which a large number of iterations are performed. The iterations are required to evolve the solution from initial conditions. In order to capture meaningful physical features of the flow field, such as boundary layers, separation points, and vortices in two or three-dimensional problems, very fine grids are needed. Also, it was noticed that a code which runs fast in subsonic and transonic flow simulations is not necessarily fast in hypersonic simulations. Thus, in order to

resolve any of these realistic features, a large amount of computer time (CPU time) is required. The objective is to speed up the rates of convergence for hypersonic flow calculations and explore the underlining mathematical theory. The rates of convergence of viscous and inviscid hypersonic flow calculations computed using the Steger-Warming flux vector splitting scheme are analyzed and accelerated. Techniques such as Wynn's epsilon-algorithm and overrelaxation methods are applied to accelerate the rate of convergence. A relaxation factor for the nonlinear iterative scheme is found analytically and confirmed numerically. The effect of the relaxation factor on the spectrum of the iterative matrix is studied. It is shown that such an overrelaxation factor produces a favorable preconditioning for Wynn's epsilon-algorithm. A net savings of 40 to 60 percent in computer time is demonstrated for many cases in two and three-dimensional calculations. Author

N90-20958 Iowa Univ., Iowa City.
COMPUTATION OF VISCOUS FLOW AROUND A PROPELLER-SHAFT CONFIGURATION WITH INFINITE-PITCH RECTANGULAR BLADES Ph.D. Thesis
Hyoung-Tae Kim 1989 278 p
Avail: Univ. Microfilms Order No. DA9004919

A viscous-solution method is set forth for calculating marine propeller flow fields. The overall computational method is described, and results for both laminar and turbulent flow are presented and discussed with regard to the flow physics, for the idealized geometry of a propeller-shaft configuration with infinite pitch rectangular blades. It is shown that the flow exhibits many of the distinctive features of interest, including the development and evolution of the shaft and blade boundary layers and wakes, and tip, passage, and hub vortices. Also considered are the influences of a thick-inlet boundary layer, the propeller angular velocity, and the blade number. Comparisons are made with some relevant experimental and computational studies, including results from a lifting-surface propeller-performance program, to aid in evaluating the present method. Close similarity and consistency are demonstrated. The latter case shows that the present method accurately predicts the blade loading, including viscous effects, and clearly displays the ability to resolve the viscous regions in distinction from the inviscid flow approach. Dissert. Abstr.

N90-20959 Council for National Academic Awards (England).
FLOW IN A FORWARD SWEPT CENTRIFUGAL FAN, VOLUMES 1 AND 2 Ph.D. Thesis
B. E. Mealing 1988 583 p
Avail: Univ. Microfilms Order No. BRDX86775

The original objective, to improve the efficiency of a forward curved centrifugal fan, was redirected to the urgent solution of a serious impeller life problem arising under certain service conditions. Using a variety of techniques, the flow pattern within the blade passage was analyzed and the cause of the problem diagnosed. A new impeller was designed and was found to solve the service life problem while also yielding an improvement in efficiency. Because the project was carried out under the Total Technology program, the scope was widened to include consideration of the fan application in a suction roadsweeper: as a result of the wider technical and commercial study, an opportunity was identified for a new product offering benefits much greater than those sought within the scope of the original objective. Dissert. Abstr.

N90-20960 Rensselaer Polytechnic Inst., Troy, NY.
OPTIMUM HYPERSONIC AIRFOILS WITH ATTACHED SHOCKS Ph.D. Thesis
Barbara Agnes Wagner 1989 112 p
Avail: Univ. Microfilms Order No. DA9011319

In the framework of Hypersonic Small Disturbance Theory the self-similar flow generated by power law bodies F(x) = x sup k is studied. A body shape which is optimum with respect to (C (sup 3/2) sub L)(C sub D) is found. Furthermore a wider class of shapes is constructed using the streamlines of the known flow field and an optimum is found within this wider class. Use is made of the solution of this problem for a generalization of Nonweiler's idea leading to the design of the caret wing and here leading to the design of a wide class of 3-D hypersonic wings. Also Cole and Aroesty's solution for the flow field of a class of bodies supporting exponential shock shapes is used to design 3-D wings. Finally, a 3-D perturbation of the basic caret wing is formulated and solved. Here, the off-design condition consists of a small deviation of the cross section shape from the inverted V cross section sha.e. Dissert. Abstr.

N90-20961 Southampton Univ. (England).
MEASUREMENT AND PREDICTION OF PROPELLER BLADE SURFACE PRESSURE DISTRIBUTIONS Ph.D. Thesis
David Tudor Owen 1989 202 p
Avail: Univ. Microfilms Order No. BRDX87364

The development of an advanced method for the aerodynamic testing of model propellers is described. The technique involves the measurement of the time averaged surface pressure distributions on rotating model propeller blades, thereby giving access to more detailed information than was previously possible. This information may be used both to improve the fundamental understanding of propeller aerodynamics, and to provide high quality detailed validation data for theoretical predictive techniques. The experimental system is described, and results showing the effects of changes in advance ratio, blade setting angle, number of blades, and nacelle geometry are discussed. Flow phenomena unrepresentative of full scale flight conditions were identified and removed, thus ensuring the realistic testing of propellers at model scale. In addition, the development of a potential flow theoretical method for the prediction of the flowfield around propeller/axisymmetric nacelle combinations is described. The technique uses a vortex lattice representation for the propeller blades, together with a surface source distribution for the non-lifting surfaces (spinner, hub, and nacelle). The method is found to predict all the trends experimentally observed and to give good numerical agreement for the blade surface pressures over the outboard half of the propeller radius. Author

N90-20962 Southampton Univ. (England).
PARAMETRIC RESONANCE IN HORIZONTAL AXIS WIND TURBINES Ph.D. Thesis
Everaldo Alencar doNascimentoFeitosa 1989 197 p
Avail: Univ. Microfilms Order No. BRDX87354

Regions of parametric resonance are predicted for the flexible blades or horizontal axis wind turbines subjected to periodic parametric loading due to gravity. The mathematical model consists of rigid blade flapping, rigid blade lagging, and shaft torsion degrees of freedom. A hypothetical hinge offset, flapping, and lagging stiffnesses, and aerodynamic loading are considered in the model. Also, hinge inclination which induces stiffness coupling is included in the analysis. The equations of motion (Mathieu/Hill's equation) are investigated using the Harmonic Balance Method for the determination of the main parametric resonance. The analysis was carried out with the support of the computer algebra system REDUCE. Particular attention is given to: the importance of aerodynamic terms; the influence of coning angle; the influence of the flapping and lagging stiffnesses, and the influence of the hinge inclination. The size and position of these regions of instability are significantly affected by these factors. Experimental results are presented from wind tunnel tests in which a horizontal axis wind turbine model of 1.82 m diameter with flexible blades was investigated. The experimental results show clearly some regions of parametric resonance. Dissert. Abstr.

N90-20963# Helsinki Univ. of Technology, Espoo (Finland). Lab. of Aerodynamics.
AN EVALUATION OF THE TWO-DIMENSIONAL EULER AND NAVIER-STOKES CALCULATIONS BASED ON A FLUX-VECTOR SPLITTING
Timo Siikonen and Jaakko Hoffren 28 Sep. 1989 38 p
(PB90-166778; SER-B-89-B18; ISBN-951-22-0040-6; ISSN-0358-2620) Avail: NTIS HC A03/MF A01 CSCL 01A

A method involving a flux vector splitting with a multigrid acceleration for the solution of the Euler equations, and for the

solution of the thin-layer Navier-Stokes equations was applied. The performance of the Euler thin-layer Navier-Stokes code is evaluated. Emphasis is laid on the accuracy of the calculated force coefficients, as well as on the computational efficiency with different computers. Computational results are presented for inviscid and viscous flows over a NACA 0012 airfoil. Author

N90-20964# Technische Hogeschool, Delft (Netherlands). Dept. of Aerospace Engineering.
EXPERIMENTAL AND NUMERICAL INVESTIGATION OF THE VORTEX FLOW OVER A SHARP EDGED DELTA WING; WITH AND WITHOUT SIDESLIP
S. H. J. Naarding and N. G. Verhaagen Dec. 1988 227 p
(PB90-167131; LR-573) Avail: NTIS HC A11/MF A02 CSCL 01A

Wind tunnel experiments were performed on a sharp edged biconvex delta wing of unit aspect ratio, with and without sideslip. Laserlight sheet and oil flow visualization, as well as total pressure traverses served to establish the evolution of the primary and secondary vortex systems with sideslip. In addition, surface pressure distribution and force balance measurements were performed. Author

N90-20965*# Missouri Univ., Rolla. Dept. of Mechanical Engineering and Aerospace Engineering and Engineering Mechanics.
AN AERODYNAMIC TRADEOFF STUDY OF THE SCISSOR WING CONFIGURATION Final Report
Bruce P. Selberg, Kamran Rokhsaz, and Clinton S. Housh May 1990 63 p
(Grant NAG1-975)
(NASA-CR-186576; NAS 1.26:186576) Avail: NTIS HC A04/MF A01 CSCL 01A

A scissor wing configuration, consisting of two independently sweeping wings was numerically studied. This configuration was also compared with an equivalent fixed wing baseline. Aerodynamic and stability and control characteristics of these geometries were investigated over a wide range of flight Mach numbers. It is demonstrated that in the purely subsonic flight regime, the scissor wing can achieve higher aerodynamic efficiency as the result of slightly higher aspect ratio. In the transonic regime, the lift to drag ratio of the scissor wing is shown to be higher than that of the baseline, for higer values of the lift coefficient. This tends to make the scissor wing more efficient during transonic cruise at high altitudes as well as during air combat at all altitudes. In supersonic flight, where the wings are maintained at maximum sweep angle, the scissor wing is shown to have a decided advantage in terms of reduced wave drag. From the view point of stability and control, the scissor wing is shown to have distinct advantages. It is shown that this geometry can maintain a constant static margin in supersonic as well as subsonic flight, by proper sweep scheduling. Furthermore, it is demonstrated that addition of wing mounted elevons can greatly enhance control authority in pitch and roll. Author

N90-20977# Deutsche Forschungs- und Versuchsanstalt fuer Luft- und Raumfahrt, Goettingen (Germany, F.R.). Inst. for Theoretical Fluid Mechanics.
PROGRESS IN INVERSE DESIGN AND OPTIMIZATION IN AERODYNAMICS
Helmut Sobieczky *In* AGARD, Computational Methods for Aerodynamic Design (Inverse) and Optimization Mar. 1990 10 p (For primary document see N90-20976 14-05)
Copyright Avail: NTIS HC A15/MF A02; Non-NATO Nationals requests available only from AGARD/Scientific Publications Executive

N90-21013# Centre National de la Recherche Scientifique, Ecully (France).
PARABOLIZED CALCULATIONS OF TURBULENT THREE DIMENSIONAL FLOWS IN A TURBINE DUCT
P. Ferrand, F. Leboeuf, F. Pommel, and E. Parkinson *In* AGARD, Secondary Flows in Turbomachines Feb. 1990 9 p Sponsored by Direction des Recherches et Etudes Techniques, France (For primary document see N90-21009 14-07)
Copyright Avail: NTIS HC A15/MF A02; Non-NATO Nationals requests available only from AGARD/Scientific Publications Executive

03 AIR TRANSPORTATION AND SAFETY

Includes passenger and cargo air transport operations; and aircraft accidents.

For related information see also *16 Space Transportation* and *85 Urban Technology and Transportation.*

N90-20966# National Transportation Safety Board, Washington, DC.
ANNUAL REVIEW OF AIRCRAFT ACCIDENT DATA: US GENERAL AVIATION CALENDAR YEAR 1987
12 Dec. 1989 87 p
(PB90-138066; NTSB/ARG-89/01) Avail: NTIS HC A05/MF A01 CSCL 01C

A statistical compilation and review is presented of general aviation accidents which occurred in 1987 in the United States, its territories and possessions, and in international waters. The accidents reported are all those involving U.S. registered aircraft not conducting operations under 14 CFR 121, 14 CFR 125, 14 CFR 127, or 14 CFR 135. There are five sections: (1) All Accidents; (2) Fatal Accidents; (3) Serious Injury Accidents; (4) Property Damage Accidents; and (5) Midair Collision Accidents. Several tables present accident parameters for 1987 accidents only, and each section includes tabulations which present comparative statistics for 1987 and for the five-year period 1982 to 1986. Author

N90-20967# Federal Aviation Administration, Atlantic City, NJ.
FULL-SCALE AIR TRANSPORT CATEGORY FUSELAGE BURNTHROUGH TESTS
Harry Webster, George Geyer, Dung Do, Joseph Wright, John Collins, and Lawrence Hampton Feb. 1990 33 p
(DOT/FAA/CT-TN89/65) Avail: NTIS HC A03/MF A01

The observations, test data, and conclusions obtained during the course of six full-scale fuselage burnthrough tests are presented. A comprehensive data base was developed which represented the flammability resistance of an intact fuselage when exposed to an exterior fuel fire. Three tests were conducted with the fuselage on the ground simulating a wheels-up condition, and three tests were conducted with the wheels down. Test results: (1) the aluminum skin provides protection from a fully developed fuel fire for 30 to 60 seconds; (2) the fiberglass acoustical insulation is an effective thermal barrier; (3) flame penetration into the cheek area provides a fire path into the cabin through the floor air return grills; (4) the aircraft with its gear extended is more vulnerable to burnthrough from a pool fire than an aircraft resting on its belly; and (5) areas, such as the empennage crawlthrough, that are not acoustically insulated are more vulnerable to burnthrough than other parts of the insulated fuselage. Author

N90-20922*# Massachusetts Inst. of Tech., Cambridge. Flight Transportation Lab.
INVESTIGATION OF AIR TRANSPORTATION TECHNOLOGY AT THE MASSACHUSETTS INSTITUTE OF TECHNOLOGY, 1988-1989
Robert W. Simpson *In* NASA, Langley Research Center, Joint University Program for Air Transportation Research, 1988-1989 Mar. 1990 p 1-5 (For primary document see N90-20921 14-01)
Avail: NTIS HC A10/MF A02 CSCL 01C

N90-20924*# Massachusetts Inst. of Tech., Cambridge.
COCKPIT DISPLAY OF HAZARDOUS WIND SHEAR INFORMATION
Craig Wanke and R. John Hansman, Jr. *In* NASA, Langley

Research Center, Joint University Program for Air Transportation Research, 1988-1989 Mar. 1990 p 17-34 (For primary document see N90-20921 14-01)
Avail: NTIS HC A10/MF A02 CSCL 01C

N90-20925*# National Aeronautics and Space Administration. Lewis Research Center, Cleveland, OH.
MODELING OF SURFACE ROUGHNESS EFFECTS ON GLAZE ICE ACCRETION
R. John Hansman, Jr., Keiko Yamaguchi, Brian M. Berkowitz (Sverdrup Technology, Inc., Middleburg Heights, OH.), and Mark Potapczuk *In* NASA, Langley Research Center, Joint University Program for Air Transportation Research, 1988-1989 Mar. 1990 p 35-42 (For primary document see N90-20921 14-01)
(Grants NAG3-666; NGL-22-009-640; NSF 85-52702)
Avail: NTIS HC A10/MF A02 CSCL 01C

N90-20926*# Massachusetts Inst. of Tech., Cambridge. Dept. of Aeronautics and Astronautics.
ULTRASONIC TECHNIQUES FOR AIRCRAFT ICE ACCRETION MEASUREMENT
R. John Hansman, Jr., Mark S. Kirby, and Fred Lichtenfelts (Simmonds Precision Products, Inc., Vergennes, VT.) *In* NASA, Langley Research Center, Joint University Program for Air Transportation Research, 1988-1989 Mar. 1990 p 43-53 Sponsored by NSF (For primary document see N90-20921 14-01)
(Grants NAG3-666; NGL-22-009-640)
Avail: NTIS HC A10/MF A02 CSCL 01C

N90-20927*# Massachusetts Inst. of Tech., Cambridge.
INVESTIGATION OF SURFACE WATER BEHAVIOR DURING GLAZE ICE ACCRETION
R. John Hansman, Jr. and Stephen R. Turnock (Southampton Univ., England) *In* NASA, Langley Research Center, Joint University Program for Air Transportation Research, 1988-1989 Mar. 1990 p 55-62 (For primary document see N90-20921 14-01)
(Grants NAG3-666; NGL-22-009-640; NSF 85-52702)
Avail: NTIS HC A10/MF A02 CSCL 01C

N90-20928*# Massachusetts Inst. of Tech., Cambridge. Dept. of Aeronautics and Astronautics.
THE INFLUENCE OF ICE ACCRETION PHYSICS ON THE FORECASTING OF AIRCRAFT ICING CONDITIONS
R. John Hansman, Jr. *In* NASA, Langley Research Center, Joint University Program for Air Transportation Research, 1988-1989 Mar. 1990 p 63-67 Sponsored by NSF (For primary document see N90-20921 14-01)
(Grants NAG3-666; NGL-22-009-640)
Avail: NTIS HC A10/MF A02 CSCL 01C

N90-20929*# Massachusetts Inst. of Tech., Cambridge. Dept. of Aeronautics and Astronautics.
COCKPIT DISPLAY OF HAZARDOUS WEATHER INFORMATION
R. John Hansman, Jr. and Craig Wanke *In* NASA, Langley Research Center, Joint University Program for Air Transportation Research, 1988-1989 Mar. 1990 p 69-76 (For primary document see N90-20921 14-01)
(Contract NAG1-690; NGL-22-009-640; BARR-10-119)
Avail: NTIS HC A10/MF A02 CSCL 01C

N90-20934*# Ohio Univ., Athens. Avionics Engineering Center.
WEATHER DATA DISSEMINATION TO AIRCRAFT
Richard H. McFarland and Craig B. Parker *In* NASA, Langley Research Center, Joint University Program for Air Transportation Research, 1988-1989 Mar. 1990 p 119-127 (For primary document see N90-20921 14-01)
Avail: NTIS HC A10/MF A02 CSCL 01C

N90-20935*# Princeton Univ., NJ. Dept. of Mechanical and Aerospace Engineering.
INVESTIGATION OF AIR TRANSPORTATION TECHNOLOGY AT PRINCETON UNIVERSITY, 1988-1989
Robert F. Stengel *In* NASA, Langley Research Center, Joint University Program for Air Transportation Research, 1988-1989 Mar. 1990 p 131-144 (For primary document see N90-20921 14-01)
Avail: NTIS HC A10/MF A02 CSCL 01C

N90-20938*# Princeton Univ., NJ. Dept. of Mechanical and Aerospace Engineering.
AN EXPERT SYSTEM FOR WIND SHEAR AVOIDANCE
Robert F. Stengel and D. Alexander Stratton *In* NASA, Langley Research Center, Joint University Program for Air Transportation Research, 1988-1989 Mar. 1990 p 183-188 (For primary document see N90-20921 14-01)
(Grant NAG1-834)
Avail: NTIS HC A10/MF A02 CSCL 01C

04 AIRCRAFT COMMUNICATIONS AND NAVIGATION

Includes digital and voice communication with aircraft; air navigation systems (satellite and ground based); and air traffic control.

For related information see also *17 Space Communications, Spacecraft Communications, Command and Tracking* and *Communications and Radar.*

N90-20968# Federal Aviation Administration, Atlantic City, NJ. Technical Center.
PLAN FOR THE FAA AIR TRAFFIC OPERATIONAL EVALUATION OF THE AUTOMATED SURFACE OBSERVING SYSTEM (ASOS)
Elizabeth Turcich and Bruce E. Ware (Data Transformation Corp., Houston, TX.) Nov. 1989 26 p
(DOT/FAA/CT-TN89/56) Avail: NTIS HC A03/MF A01

The Automated Surface Observing System (ASOS) is a weather collection and display system that will be installed in Air Traffic Control Towers (ATCT). The system will be procured, installed, operated, and maintained by the National Weather Service (NWS) for the Federal Aviation Administration (FAA) under a Memorandum of Agreement (MOA). This plan outlines the FAA's operational evaluation of the preproduction ASOS systems. Two companies, Magnavox and AAI Corporation, are under contract to develop the ASOS. The FAA will evaluate the Magnavox system at the Wichita ATCT and AAI's system at the Tulsa ATCT. The 6-week evaluations of each system will be the only FAA operational test of the ASOS. Data will be collected via questionnaires completed by Air Traffic Control Specialists (ATCS) at both sites and ATCSs brought in from other sites to assess the system. The results of the evaluation will be used for consideration in the production contract award and for making any necessary changes to the system. Author

N90-20969*# Mayflower Communications Co., Inc., Reading, MA.
AUTONOMOUS INTEGRATED GPS/INS NAVIGATION EXPERIMENT FOR OMV. PHASE 1: FEASIBILITY STUDY
Triveni N. Upadhyay, George J. Priovolos, and Harley Rhodehamel Washington NASA Jan. 1990 93 p
(Contract NAS8-38031)
(NASA-CR-4267; NAS 1.26:4267) Avail: NTIS HC A05/MF A01 CSCL 17G

The phase 1 research focused on the experiment definition. A tightly integrated Global Positioning System/Inertial Navigation System (GPS/INS) navigation filter design was analyzed and was shown, via detailed computer simulation, to provide precise position, velocity, and attitude (alignment) data to support navigation and attitude control requirements of future NASA missions. The application of the integrated filter was also shown to provide the

opportunity to calibrate inertial instrument errors which is particularly useful in reducing INS error growth during times of GPS outages. While the Orbital Maneuvering Vehicle (OMV) provides a good target platform for demonstration and for possible flight implementation to provide improved capability, a successful proof-of-concept ground demonstration can be obtained using any simulated mission scenario data, such as Space Transfer Vehicle, Shuttle-C, Space Station. Author

N90-20970# National Aeronautical Lab., Bangalore (India). Flight Mechanics and Controls Div.
FLIGHT PATH RECONSTRUCTION USING EXTENDED KALMAN FILTERING TECHNIQUES
V. Parameswaran and E. Plaetschke Jan. 1990 76 p
(PD-FC-9001) Avail: NTIS HC A05/MF A01

An algorithm for the flight path reconstruction of state variables and for estimation of unknown constant bias and scale factor errors in measured data using extended Kalman filter and fixed interval smoother was developed. The models are based on the six-degree-of freedom kinematic equations relating measured aircraft responses. The technique is demonstrated with the aid of typical examples using flight test data. Also some sensitivity studies on the variation of noise covariance matrices were performed. The results of FPR using extended Kalman filter and maximum likelihood methods are presented. Finally aerodynamic estimation was carried out with a simple linear model on different data sets names: (1) flight measured data not corrected for bias and scale factor errors; (2) using EKF corrected data; and (3) using ML corrected data. Author

N90-20923*# Massachusetts Inst. of Tech., Cambridge. Flight Transportation Lab.
AUTOMATIC SPEECH RECOGNITION IN AIR TRAFFIC CONTROL
Joakim Karlsson *In* NASA, Langley Research Center, Joint University Program for Air Transportation Research, 1988-1989 Mar. 1990 p 7-15 (For primary document see N90-20921 14-01)
Avail: NTIS HC A10/MF A02 CSCL 01C

N90-20931*# Ohio Univ., Athens.
RIDGE REGRESSION PROCESSING
Mark R. Kuhl *In* NASA, Langley Research Center, Joint University Program for Air Transportation Research, 1988-1989 Mar. 1990 p 99-104 (For primary document see N90-20921 14-01)
Avail: NTIS HC A10/MF A02 CSCL 01C

N90-20932*# Ohio Univ., Athens.
OPTIMIZATION OF THE EFFECTIVE GPS DATA RATE
David S. McIntyre *In* NASA, Langley Research Center, Joint University Program for Air Transportation Research, 1988-1989 Mar. 1990 p 105-109 (For primary document see N90-20921 14-01)
Avail: NTIS HC A10/MF A02 CSCL 01C

N90-20933*# Ohio Univ., Athens. Avionics Engineering Center.
SOLE MEANS NAVIGATION AND INTEGRITY THROUGH HYBRID LORAN-C AND NAVSTAR GPS
Frank vanGraas *In* NASA, Langley Research Center, Joint University Program for Air Transportation Research, 1988-1989 Mar. 1990 p 111-118 (For primary document see N90-20921 14-01)
(Grant NGR-009-017)
Avail: NTIS HC A10/MF A02 CSCL 01C

05 AIRCRAFT DESIGN, TESTING AND PERFORMANCE

Includes aircraft simulation technology.

For related information see also *18 Spacecraft Design, Testing and Performance* and *39 Structural Mechanics.*For land transportation vehicles see *85 Urban Technology and Transportation.*

N90-20971*# Notre Dame Univ., IN. Dept. of Aerospace and Mechanical Engineering.
THE MANTA: AN RPV DESIGN TO INVESTIGATE FORCES AND MOMENTS ON A LIFTING SURFACE Final Design Proposal
Kevin Bryan, John Soutar, Peter Witty, Bruno Mediate, Thomas Quast, Dan Combs, Martin Schubert, David Condron, Scott Taylor, and Ed Garino et al 1989 91 p
(Contract NASw-4435)
(NASA-CR-186227; NAS 1.26:186227) Avail: NTIS HC A05/MF A01 CSCL 01C

The overall goal was to investigate and exploit the advantages of using remotely powered vehicles (RPV's) for in-flight data collection at low Reynold's numbers. The data to be collected is on actual flight loads for any type of rectangular or tapered airfoil section, including vertical and horizontal stabilizers. The data will be on a test specimen using a force-balance system which is located forward of the aircraft to insure an undisturbed air flow over the test section. The collected data of the lift, drag and moment of the test specimen is to be radioed to a grand receiver, thus providing real-time data acquisition. The design of the mission profile and the selection of the instrumentation to satisfy aerodynamic requirements are studied and tested. A half-size demonstrator was constructed and flown to test the flight worthiness of the system. Author

N90-20972# Royal Aircraft Establishment, Farnborough (England).
THE ROLE OF STRUCTURAL ANALYSIS IN AIRWORTHINESS CERTIFICATION
P. Bartholomew Apr. 1989 21 p
(BR112064; RAE-TM-MS-1129) Copyright Avail: NTIS HC A03/MF A01

Those uses of structural analysis which have a bearing on airworthiness are reviewed. In particular the extent to which finite element analysis is already implicitly relied on in the context of clearance by test is considered, and factors which may be expected to lead to an increased reliance are discussed. One such factor is the increased use of the computer aided engineering (CAE) approach which changes the design process itself. An assessment is made of actions required to ensure that results of analysis provide a consistent and reliable basis for airworthiness judgement. Author

N90-20973# Royal Aircraft Establishment, Farnborough (England).
COMPUTER-AIDED STRUCTURAL OPTIMISATION OF AIRCRAFT STRUCTURES
P. Bartholomew and H. Wellen Sep. 1989 19 p
(BR112837; RAE-TM-MAT-STR-1138) Copyright Avail: NTIS HC A03/MF A01

The principal methods used within the computer program STARS for the computer-aided design of optimum structures subject to a variety of contraints are described. Based on the foundations set forth regarding both structural and optimization aspects, a description is given of the Newton method as applied in STARS. Likewise, the shape optimization developed in the form of a hierarchical approach is described. Test problems connected with this are presented. Practical examples are given that show how research originated at RAE has been continued and applied at MBB. This includes various components which are typical in aircraft construction and also a description of the manner in which flutter optimization is being accomplished with STARS at MBB in combination with the in-house aeroelastic program. Author

N90-20974*# National Aeronautics and Space Administration. Langley Research Center, Hampton, VA.
PERFORMANCE DATA FROM A WIND-TUNNEL TEST OF TWO MAIN-ROTOR BLADE DESIGNS FOR A UTILITY-CLASS HELICOPTER
Jeffrey D. Singleton, William T. Yeager, Jr., and Matthew L. Wilbur Washington Jun. 1990 82 p Prepared in cooperation with Army Aviation Systems Command, Hampton, VA
(NASA-TM-4183; L-16736; NAS 1.15:4183; AVSCOM-TM-90-B-004) Avail: NTIS HC A05/MF A01 CSCL 01C

An investigation was conducted in the NASA Langley Transonic Dynamics Tunnel to evaluate an advanced main rotor designed for use on a utility class helicopter, specifically the U.S. Army UH-60A Blackhawk. This rotor design incorporated advanced twist, airfoil cross sections, and geometric planform. For evaluation purposes, the current UH-60A main rotor was also tested and is referred to as the baseline blade set. A total of four blade sets were tested. One set of both the baseline and the advanced rotors were dynamically scaled to represent a full scale helicopter rotor blade design. The remaining advanced and baseline blade sets were not dynamically scaled so as to isolate the effects of structural elasticity. The investigation was conducted in hover and at rotor advance ratios ranging from 0.15 to 0.4 at a range of nominal test medium densities from 0.00238 to 0.009 slugs/cu ft. This range of densities, coupled with varying rotor lift and propulsive force, allowed for the simulation of several vehicle gross weight and density altitude combinations. Performance data are presented for all blade sets without analysis; however, cross referencing of data with flight condition may be useful to the analyst for validating aeroelastic theories and design methodologies as well as for evaluating advanced design parameters. Author

N90-20975# National Aeronautical Lab., Bangalore (India). Computational and Theoretical Fluid Dynamics Div.
DESIGN OF A NATURAL LAMINAR FLOW AIRFOIL FOR AN UNMANNED AIRCRAFT
K. R. Srilatha and P. Ramamoorthy Mar. 1990 9 p
(PD-CF-9004) Avail: NTIS HC A02/MF A01

A 12 percent thick natural laminar flow (NLF) airfoil is designed for an unmanned aircraft for reconnaissance and target acquisition roles. This airfoil is compared with NACA 64, -612 airfoil of same thickness. NAL airfoil, designated as NAL-NLF-120, has given better performance than NACA airfoil at the design conditions. For that matter in the entire range 0.4 less than or = C sub L less than or = 0.8 NAL airfoil performs better than the NACA airfoil. Author

N90-20976# Advisory Group for Aerospace Research and Development, Neuilly-Sur-Seine (France). Fluid Dynamics Panel.
COMPUTATIONAL METHODS FOR AERODYNAMIC DESIGN (INVERSE) AND OPTIMIZATION
Mar. 1990 331 p In ENGLISH and FRENCH Meeting held in Loen, Norway, 22-23 May 1989
(AGARD-CP-463; ISBN-92-835-0542-5) Copyright Avail: NTIS HC A15/MF A02; Non-NATO Nationals requests available only from AGARD/Scientific Publications Executive

Computational Fluid Dynamics (CFD) play an increasingly important role in the aerodynamic design of flight vehicles. The main reasons for this are the rapid developments in computer hardware and solution algorithms in combination with the increasing requirements (and potential) for improving aerodynamic quality and reducing design cycle time and cost. This meeting focused on those CFD-based methods which address the problem of design for given aerodynamic characteristics in a direct sense. Examples are inverse methods which provide the detailed geometry required to generate a given pressure distribution and methods utilizing numerical optimization techniques to obtain the geometry that minimizes, subject to constraints, a given aerodynamic objective function. For individual titles, see N90-20977 through N90-20999.

N90-20977# Deutsche Forschungs- und Versuchsanstalt fuer Luft- und Raumfahrt, Goettingen (Germany, F.R.). Inst. for Theoretical Fluid Mechanics.
PROGRESS IN INVERSE DESIGN AND OPTIMIZATION IN AERODYNAMICS **c02**
Helmut Sobieczky *In* AGARD, Computational Methods for Aerodynamic Design (Inverse) and Optimization Mar. 1990 10 p (For primary document see N90-20976 14-05)
Copyright Avail: NTIS HC A15/MF A02; Non-NATO Nationals requests available only from AGARD/Scientific Publications Executive

Aerodynamic design was developed to an advanced state of the art: inverse methods allow for strong control of aerodynamic airfoil or wing performance so that optimization strategies are no longer beyond practical use and knowledge bases can be established for the implementation in aerodynamic expert systems. Some recent steps into this direction are reviewed. Author

N90-20978# Aircraft Research Association Ltd., Bedford (England).
AEROFOIL DESIGN TECHNIQUES
A. J. Bocci *In* AGARD, Computational Methods for Aerodynamic Design (Inverse) and Optimization Mar. 1990 18 p Sponsored in part by Procurement Executive, Ministry of Defence; British Aerospace Aircraft Group, Hatfield, England; Dowty Rotol Ltd.; and Dept. of Trade and Industry (For primary document see N90-20976 14-05)
Copyright Avail: NTIS HC A15/MF A02; Non-NATO Nationals requests available only from AGARD/Scientific Publications Executive

Various airfoil design exercises carried out at ARA over the years are described, concentrating on the part played by the inverse methods. The design of an airfoil suitable for the wing of a combat aircraft research model was successful in meeting a number of performance requirements but the inverse supercritical method used gave an unsatisfactory intermediate profile and off-design calculations were necessary to resolve the problem. In a research exercise involving the design of an airfoil suitable for the wing of a transport aircraft to take advantage of full-scale Reynolds number, the inverse supercritical method used produced changes to the geometry in an opposite sense to those finally required. It is suggested that the difficulties with the inverse supercritical methods arose because appropriate design target pressures were not known and because viscous effects were not included in the methods. Subsequent designs of laminar flow airfoils and high-speed propeller blade airfoils are described. For these cases, a technique was used involving a subcritical method, with progressive adjustment of target pressures until a geometry arose with suitable flow development according to a viscous supercritical method, with little use of supercritical inverse methods. Author

N90-20979# Deutsche Forschungs- und Versuchsanstalt fuer Luft- und Raumfahrt, Brunswick (Germany, F.R.). Inst. fuer Entwurfsaerodynamik.
AERODYNAMIC DESIGN TECHNIQUES AT DLR INSTITUTE FOR DESIGN AERODYNAMICS
H. Koester, C.-H. Rohardt, K.-H. Horstmann, and R. Radespiel *In* AGARD, Computational Methods for Aerodynamic Design (Inverse) and Optimization Mar. 1990 15 p (For primary document see N90-20976 14-05)
Copyright Avail: NTIS HC A15/MF A02; Non-NATO Nationals requests available only from AGARD/Scientific Publications Executive

Some general remarks about aerodynamic design are given first. Then, a short survey of the design methods used here including the basic ideas and, particularly, an improvement of the design method of McFadden for supercritical airfoils are presented. Also, an overview is given of the analysis methods in use at the DLR institute for design aerodynamics. Design procedures, which use the forementioned design and analysis methods, are explained in detail. With these procedures, several designs of airfoils and nacelles were performed. Results of selected design examples are discussed. Author

N90-20980# Grumman Aerospace Corp., Bethpage, NY.
INVERSE DESIGN OF AIRFOIL CONTOURS: CONSTRAINTS, NUMERICAL METHOD, AND APPLICATIONS
G. Volpe *In* AGARD, Computational Methods for Aerodynamic Design (Inverse) and Optimization Mar. 1990 18 p (For primary document see N90-20976 14-05)
Copyright Avail: NTIS HC A15/MF A02; Non-NATO Nationals requests available only from AGARD/Scientific Publications Executive

The classical problem of constructing an airfoil profile that corresponds to an arbitrarily prescribed speed distribution is discussed and recast in a form suitable for transonic applications. The problem, in general, is not well posed unless the specified speed distribution satisfies certain constraints. Thus, a solution exists only if the speed distribution contains a sufficient number of free parameters with values that can be adjusted in order to satisfy the constraints. The nature of the constraints are discussed and several strategies proposed for introducing the necessary freedom in the speed distribution. The computational method described determines the values of the parameters as part of the solution. It is based on the numerical solution of the full potential equation in conservation form with Dirichlet-type boundary conditions by a multigrid-ADI scheme. The general applicability and the accuracy of the numerical method are illustrated by several examples. Author

N90-20981# Textron Bell Helicopter, Fort Worth, TX.
AN EFFICIENT AIRFOIL DESIGN METHOD USING THE NAVIER-STOKES EQUATIONS
J. B. Malone, J. C. Narramore, and L. N. Sankar (Georgia Inst. of Tech., Atlanta.) *In* AGARD, Computational Methods for Aerodynamic Design (Inverse) and Optimization Mar. 1990 18 p (For primary document see N90-20976 14-05)
Copyright Avail: NTIS HC A15/MF A02; Non-NATO Nationals requests available only from AGARD/Scientific Publications Executive

An airfoil design procedure is described that was incorporated into an existing 2-D Navier-Stokes airfoil analysis method. The resulting design method, an iterative procedure based on a residual-correction algorithm, permits the automated design of airfoil sections with prescribed surface pressure distributions. The inverse design method and the technique used to specify target pressure distributions are described. It presents several example problems to demonstrate application of the design procedure. It shows that this inverse design method develops useful airfoil configurations with a reasonable expenditure of computer resources. Author

N90-20982# Messerschmitt-Boelkow-Blohm G.m.b.H., Munich (Germany, F.R.). Dept. of Theoretical Aerodynamic.
AN INTENSIVE PROCEDURE FOR THE DESIGN OF PRESSURE-SPECIFIED THREE-DIMENSIONAL CONFIGURATIONS AT SUBSONIC AND SUPERSONIC SPEEDS BY MEANS OF A HIGHER-ORDER PANEL METHOD
L. Fornasier *In* AGARD, Computational Methods for Aerodynamic Design (Inverse) and Optimization Mar. 1990 10 p (For primary document see N90-20976 14-05)
(Contract T/RF-41/E0010/E14)
Copyright Avail: NTIS HC A15/MF A02; Non-NATO Nationals requests available only from AGARD/Scientific Publications Executive

An advanced panel method employing singularity distributions of higher order and based on mixed boundary conditions of Dirichlet- and Neumann-type was recently developed for the potential flow analysis of arbitrary airplane configurations at subsonic and supersonic speeds. Some work is in progress to provide this method with a design option capable of relofting the surface of a given configuration from prescribed pressure distributions. The purpose is to present the mathematical background of the inverse algorithm and to account on some examples of application. Author

N90-20983# National Aerospace Lab., Amsterdam (Netherlands).
A SYSTEM FOR TRANSONIC WING DESIGN WITH GEOMETRIC CONSTRAINTS BASED ON AN INVERSE METHOD
F. J. Brandsma and J. M. J. Fray *In* AGARD, Computational Methods for Aerodynamic Design (Inverse) and Optimization Mar. 1990 9 p (For primary document see N90-20976 14-05)
Copyright Avail: NTIS HC A15/MF A02; Non-NATO Nationals requests available only from AGARD/Scientific Publications Executive

A new system was described for transonic wing design with prescribed pressure distribution in the presence of a fixed body. The residual correction method, on which the design system is based, combines a complex direct flow solver with simple correction rules (inverse supersonic wavy-wall plus inverse 3-D panel method). It is possible to define geometric constraints for the wing to be designed, which is an essential part of the method. Weight factors on the pressure defect corrections and on the corrections associated with the geometric constraints can be adjusted during the iteration process, allowing a maximal control over the design procedure, in order to reach the design goals in the best possible way. The practical applicability of the transonic wing design system was demonstrated by an example. Author

N90-20984# Politecnico di Milano (Italy). Dipartimento di Ingegneria Aerospaziale.
A FAST COLLOCATION METHOD FOR TRANSONIC AIRFOIL DESIGN
Sergio DePonte, Maurizio Boffadossi, and Claudio Mantegazza (Aeronautica Macchi S.p.A., Varese, Italy) *In* AGARD, Computational Methods for Aerodynamic Design (Inverse) and Optimization Mar. 1990 7 p (For primary document see N90-20976 14-05)
Copyright Avail: NTIS HC A15/MF A02; Non-NATO Nationals requests available only from AGARD/Scientific Publications Executive

In the method of ficticious gas for transonic airfoil modification, an attempt was made to introduce a fully elliptic calculation code by the use of compressibility sources. This is done both with the idea of overcoming some of the finite-difference limitations and in order to reduce the computational time. Taking as reference the standard Hess-Smith panel method in two dimensions, compressibility effects are taken into account by means of source panels into the flowfield. The panels form a grid which is limited in extension only where Mach number gradients are expected and much more limited compared to usual computational domains. The system is fast and in general does not present convergence problems from the practical point of use, although large numbers of iterations may have some convergence problems. The final result is always a very strong reduction in wave drag of the airfoil, as it is the aim of the method. Author

N90-20985# Von Karman Inst. for Fluid Dynamics, Rhode-Saint-Genese (Belgium).
SUBSONIC AND TRANSONIC BLADE DESIGN BY MEANS OF ANALYSIS CODES **c07**
R. A. VandeBraembussche, O. Leonard, and L. Nekmouche *In* AGARD, Computational Methods for Aerodynamic Design (Inverse) and Optimization Mar. 1990 11 p (For primary document see N90-20976 14-05)
Copyright Avail: NTIS HC A15/MF A02; Non-NATO Nationals requests available only from AGARD/Scientific Publications Executive

An iterative procedure for cascade blade design, using a direct flow solver and a blade geometry modification algorithm is presented. The procedure starts with the analysis of a given cascade geometry using an existing flow solver. The difference between the calculated velocity distribution and the required one is used as an input for the modification algorithm. This procedure results in the definition of a new blade shape for which the calculated velocity distribution is closer to the desired one. Examples for both subsonic and transonic flow are presented and

show a rapid convergence to the geometry required for the desired velocity distribution. The main advantage of the proposed method is that existing analysis codes can be used, for the design and for the off-design analysis. Some restrictions which have to be imposed on the required velocity distribution are also discussed.
Author

N90-20986# Middle East Technical Univ., Ankara (Turkey).
A COMPUTATIONAL DESIGN METHOD FOR SHOCK FREE TRANSONIC CASCADES AND AIRFOILS
T. A. Cetinkaya, I. S. Akmandor, and Ahmet S. Ucer *In* AGARD, Computational Methods for Aerodynamic Design (Inverse) and Optimization Mar. 1990 10 p (For primary document see N90-20976 14-05)
Copyright Avail: NTIS HC A15/MF A02; Non-NATO Nationals requests available only from AGARD/Scientific Publications Executive

A computational method was formulated for efficient inverse design of blading. The surface pressure distribution is specified and, as a result, the geometric shape of an airfoil or cascade blade is obtained. A steady, two-dimensional Euler code for transonic flow was implemented. The code uses a finite volume technique on a computational grid which is based on assumed streamlines. The grid is being updated during the solution procedure. The blade contour, being a streamline, corresponds to a part of the solution domain boundary where the desired pressure distribution is given. Free parameters are introduced into the prescribed pressure distribution and this satisfies the closure constraints. Examples based on redesign of known shapes are presented.
Author

N90-20987# Stuttgart Univ. (Germany, F.R.). Inst. fuer Aero- und Gasdynamik.
INVERSE COMPUTATION OF TRANSONIC INTERNAL FLOWS WITH APPLICATION FOR MULTI-POINT-DESIGN OF SUPERCRITICAL COMPRESSOR BLADES
E. Schmidt and F. Klimetzek (Daimler-Benz A.G., Stuttgart, Germany, F.R.) *In* AGARD, Computational Methods for Aerodynamic Design (Inverse) and Optimization Mar. 1990 13 p Sponsored by Deutsche Forschungsgemeinschaft and Forschungsvereinigung Verbrennungskraftmaschinen (For primary document see N90-20976 14-05)
Copyright Avail: NTIS HC A15/MF A02; Non-NATO Nationals requests available only from AGARD/Scientific Publications Executive

The method solves the inverse problem for supercritical blade-to-blade flow on stream surfaces of revolution with variable radius and variable stream surface thickness in a relative system. Some provisions for the treatment of the ill-posed design problem in local supersonic regions are discussed. A procedure for the design of cascades with improved off-design behavior is described and compared with experimental results. Comparisons with other numerical methods and experimental results are also included.
Author

N90-20988# Office National d'Etudes et de Recherches Aerospatiales, Paris (France). Direction de l'Aerodynamique.
AN INVERSE METHOD FOR THE DESIGN OF TURBOMACHINE BLADES [UNE METHODE INVERSE POUR LA DETERMINATION D'AUBES DE TURBOMACHINES] **c07**
Olivier-Pierre Jacquotte *In* AGARD, Computational Methods for Aerodynamic Design (Inverse) and Optimization Mar. 1990 16 p In FRENCH Sponsored by SNECMA (For primary document see N90-20976 14-05)
Copyright Avail: NTIS HC A15/MF A02; Non-NATO Nationals requests available only from AGARD/Scientific Publications Executive

An inverse method for the determination of turbomachinery cascade profiles, which can be applied to transonic flow, is described. The method is related to quasi-three-dimensional flow around the blade cascade and is based on the solution of the inverse form of the potential scalar equation associated with the absolute speed in reference to the relative bounds of the blade. The correct mathematical definition of the inverse formula for compressible cascade is examined. The desired profile is obtained after a eries of iterations resulting in parameter adjustments permitted by the convergence. The finite element method is used as the solution technique. The most immediate concern is the preliminary validation of the method and the possibility of restoration of a known profile starting from a gross initialization is shown. Finally, some test cases are shown.
Transl. by E.J.R.

N90-20989# Instituto Superior Tecnico, Lisbon (Portugal). Dept. of Mechanical Engineering.
APPLICATION OF AN INVERSE METHOD TO THE DESIGN OF A RADIAL INFLOW TURBINE **c07**
Joao Eduardo Borges *In* AGARD, Computational Methods for Aerodynamic Design (Inverse) and Optimization Mar. 1990 16 p Sponsored in part by Holset Engineering Co., England; Churchill Coll., Cambridge, England; and Junta Nacional de Investigacao Cientifica e Tecnologica, Portugal (For primary document see N90-20976 14-05)
Copyright Avail: NTIS HC A15/MF A02; Non-NATO Nationals requests available only from AGARD/Scientific Publications Executive

A truly three-dimensional inverse method is described and applied to the design of the rotor of a radial inflow turbine with a specific speed equal to 0.6. The described indirect method uses a mean swirl (i.e. radius times mean tangential velocity) specification and applies to inviscid and incompressible fluid. In addition, it is assumed that the inlet flow is uniform and that the blades are infinitely thin. The action of the blades is modelled by surface vorticity, using the Clebsch formulation for the calculation of the velocity field. The blade shape is evaluated by requiring it to be aligned with the local velocity vectors throughout its entire length. Since the vorticity depends on the blade shape, the problem must be solved iteratively. As the mean swirl specification is not a familiar input design, its physical significance is discussed and some advice is given on the best way of choosing it. Finally, the results of some experimental tests are briefly discussed. In these tests the performance of a rotor designed using the present indirect method was compared with that achieved by an impeller designed using conventional techniques. It is shown that the rotor designed using the inverse method is more efficient than the conventional impeller.
Author

N90-20990# Politecnico di Torino (Italy).
NUMERICAL METHOD FOR DESIGNING 3D TURBOMACHINERY BLADE ROWS **c07**
L. Zannetti, F. Larocca (Fiat Aviazione S.p.A., Turin, Italy), and R. Marsilio *In* AGARD, Computational Methods for Aerodynamic Design (Inverse) and Optimization Mar. 1990 9 p (For primary document see N90-20976 14-05)
Copyright Avail: NTIS HC A15/MF A02; Non-NATO Nationals requests available only from AGARD/Scientific Publications Executive

The aim is to present a newly improved method to solve inverse problems for inviscid, compressible, rotational flows in 3-D ducts or 3-D rows of blades. A finite-difference time-dependent computation is performed in a channel whose walls are deformable and that adjust themselves to the design data. In the present 3-D formulation the ideas outlined are followed, a mathematical model based on the contravariant components of the flow velocity and a second-order accurated finite-difference scheme are used. A new procedure is used at the boundaries, which is simpler and more rigorous than the previous one.
Author

N90-20991*# Sverdrup Technology, Inc., Eglin AFB, FL.
AERODYNAMIC OPTIMIZATION BY SIMULTANEOUSLY UPDATING FLOW VARIABLES AND DESIGN PARAMETERS
M. H. Rizk *In* AGARD, Computational Methods for Aerodynamic Design (Inverse) and Optimization Mar. 1990 18 p (For primary document see N90-20976 14-05)
(Contracts NAS3-24855; NAS2-12157)
Copyright Avail: NTIS HC A15/MF A02; Non-NATO Nationals

requests available only from AGARD/Scientific Publications Executive CSCL 01C

The application of conventional optimization schemes to aerodynamic design problems leads to inner-outer iterative procedures that are very costly. An alternative approach is presented based on the idea of updating the flow variable iterative solutions and the design parameter iterative solutions simultaneously. Two schemes based on this idea are applied to problems of correcting wind tunnel wall interference and optimizing advanced propeller designs. The first of these schemes is applicable to a limited class of two-design-parameter problems with an equality constraint. It requires the computation of a single flow solution. The second scheme is suitable for application to general aerodynamic problems. It requires the computation of several flow solutions in parallel. In both schemes, the design parameters are updated as the iterative flow solutions evolve. Computations are performed to test the schemes' efficiency, accuracy, and sensitivity to variations in the computational parameters. Author

N90-20992# National Aerospace Lab., Amsterdam (Netherlands).

CONSTRAINED SPANLOAD OPTIMIZATION FOR MINIMUM DRAG OF MULTI-LIFTING-SURFACE CONFIGURATIONS

R. F. vandeDam *In* AGARD, Computational Methods for Aerodynamic Design (Inverse) and Optimization Mar. 1990 14 p Sponsored by Netherlands Agency for Aerospace Programs (For primary document see N90-20976 14-05)

Copyright Avail: NTIS HC A15/MF A02; Non-NATO Nationals requests available only from AGARD/Scientific Publications Executive

An interactive computer program system was developed that can be used in aircraft drag minimization studies. It comprises algorithms for choosing the spanwise distributions of lift, pitching moment, chord, and thickness-to-chord ratio of lifting elements. The choices are optimal in that they minimize induced plus viscous drag while satisfying constraints of aerodynamic, flight-mechanical and structural nature. The configurations that can be dealt with, may consist of a number of segments representing, for instance, wings or parts of wings, horizontal tails or canards, winglets or flaprail-fairings. Also the interaction between propellers and lifting elements may be included in the procedure. The induced drag is computed using the Trefftz-plane integral (farfield analysis), while the viscous drag follows from form factor methods. Mathematical formulations of the constrained optimization problems are used, that are based on the calculus of variations. The method was integrated in an infrastructure that allows the capabilities of the method to be efficiently exploited in a multidisciplinary environment. The theoretical models and methods underlying the analysis and optimization capability, comparisons with other theories, information aspects, and some examples of applications, are presented. Author

N90-20993# National Aerospace Lab., Amsterdam (Netherlands).

NUMERICAL OPTIMIZATION OF TARGET PRESSURE DISTRIBUTIONS FOR SUBSONIC AND TRANSONIC AIRFOIL DESIGN

J. A. vanEgmond *In* AGARD, Computational Methods for Aerodynamic Design (Inverse) and Optimization Mar. 1990 11 p (For primary document see N90-20976 14-05)

Copyright Avail: NTIS HC A15/MF A02; Non-NATO Nationals requests available only from AGARD/Scientific Publications Executive

Inverse aerodynamic design, calculating the geometry from prescribed pressure distributions, leaves the designer with the problem to define proper target pressure distributions. Numerical optimization techniques are employed to support the aerodynamic designer in the definition of target pressure distributions for subsonic and transonic airfoil design. A general parametric representation of airfoil pressure distributions is given, taking into account the physical characteristics of the airfoil flow. This parametric representation enables the designer to define optimum target pressure distributions through numerical optimization techniques. Worked out examples show that a large class of airfoils can be described by the proposed procedure, a simple line search method. In general, a large number of iterations is needed to arrive at the final (optimal) solution. However the requirement of a large number of iterations is not a serious drawback of the approach described. Finally, it is concluded that application of numerical optimization techniques is not (yet) to be considered as a routine job but considerable possibilities are offered to improve design results. Author

N90-20994# Aeronautica Macchi S.p.A., Varese (Italy). Dept. of Advanced Studies.

A TOOL FOR AUTOMATIC DESIGN OF AIRFOILS IN DIFFERENT OPERATING CONDITIONS

L. Ghielmi, R. Marazzi, and A. Baron (Politecnico di Milano, Italy) *In* AGARD, Computational Methods for Aerodynamic Design (Inverse) and Optimization Mar. 1990 12 p (For primary document see N90-20976 14-05)

Copyright Avail: NTIS HC A15/MF A02; Non-NATO Nationals requests available only from AGARD/Scientific Publications Executive

An optimization procedure is described which applies to the design of airfoils able to satisfy requirements essentially set for transonic flight. Suitable airfoils are obtained through radical changes of the starting geometry with little time consumption. One of the main features of the design methodology is an extensive use of constraints; it proved to be very efficient both to obtain a good quality of the design and to reduce the time needed. Another feature is the use of effective shape functions, which are not aerofunctions obtained through inverse methods. The results show airfoils designed to satisfy both a maneuver and a dash performance requirement. A comparison of different design approaches is also presented; this is made possible by the short times required for the design, which includes the optimized deflections of the leading edge and trailing edge flaps. Suggestions are given for further developments of a smart system for airfoil design. Author

N90-20995# Office National d'Etudes et de Recherches Aerospatiales, Paris (France).

THE USE OF NUMERICAL OPTIMIZATION FOR HELICOPTER AIRFOIL AND BLADE DESIGN

J. Reneaux and M. Allongue (Aerospatiale, Marignane, France) *In* AGARD, Computational Methods for Aerodynamic Design (Inverse) and Optimization Mar. 1990 12 p In FRENCH, ENGLISH summary (For primary document see N90-20976 14-05)

Copyright Avail: NTIS HC A15/MF A02; Non-NATO Nationals requests available only from AGARD/Scientific Publications Executive

The numerical optimization methods were successfully applied to airfoil design at ONERA, and to helicpter blade design at the Aerospatiale Helicopter Department. The constrained minimization method chosen is the one developed by Vanderplaats. For the design of helicopter airfoils, the minimization algorithms and transonic viscous flow analysis method are linked together. The design of a 12 percent thick airfoil and a 9 percent thick airfoil for helicopter blades were carried out with two design points, one corresponding to the advancing blade conditions and the other to the retreating blade conditions in forward flight. Two-dimensional tests performed in the ONERA S3MA wind tunnel confirmed the theoretical predicted gains. The design of helicopter blades is achieved through the association of the minimization method and a rotor performance analysis method using the blade element theory. The optimization of the spanwise locations of the airfoils of different thickness-to-chord ratios were carried out with one or two design points corresponding to different flight conditions. The method was applied to the rotor design for a helicopter of the 8 to 10 tons gross weight class. The applications discussed show the interest of the numerical optimization techniques for the helicopter rotor design particularly when several flight conditions

and many parameters and constraints have to be taken into account. Author

N90-20996# · Dornier-Werke G.m.b.H., Friedrichshafen (Germany, F.R.).
AERODYNAMIC DESIGN BY OPTIMIZATION
K.-W. Bock *In* AGARD, Computational Methods for Aerodynamic Design (Inverse) and Optimization Mar. 1990 12 p (For primary document see N90-20976 14-05)
Copyright Avail: NTIS HC A15/MF A02; Non-NATO Nationals requests available only from AGARD/Scientific Publications Executive

The experience gained when coupling different aerodynamic analysis codes and optimization procedures is described. First a simple problem is considered (airfoil of minimum wave drag, analysis by shock expansion theory) in order to compare the usability of a random search procedure to that of a gradient method (COPES by G. N. Vanderplaats). The second one shows a superior performance. Then three aerodynamic programs are coupled with COPES and tested: Euler space-marching program for bodies of revolution at supersonic; transonic airfoil redesign method (fictitious gas concept); and multiple airfoil analysis code for flap position optimization. It can be demonstrated that COPES is a very universal optimization tool which can be easily combined even with complex aerodynamic codes. Its convergence is good even under constraints. This is important because the number of analysis calculations is most important for typical aerodynamic problems of high numerical expense. Author

N90-20997# Office National d'Etudes et de Recherches Aerospatiales, Paris (France).
NUMERICAL OPTIMIZATION OF WINGS IN TRANSONIC FLOW
D. Destarac, J. Reneaux, and D. Gisquet (Aerospatiale, Toulouse, France) *In* AGARD, Computational Methods for Aerodynamic Design (Inverse) and Optimization Mar. 1990 12 p In FRENCH; ENGLISH summary (For primary document see N90-20976 14-05)
Copyright Avail: NTIS HC A15/MF A02; Non-NATO Nationals requests available only from AGARD/Scientific Publications Executive

The numerical optimization method for wings in transonic flow presented associates a constrained minimization program, a fast direct aerodynamic code, and a shape modification technique. Possibilities of optimization with regard to the total aerodynamic coefficients of a wing are shown. A method for estimating inviscid drag is recommended. Two application cases of the optimization method in the quasi inverse mode, by aiming at a given pressure distribution, are described. One is the adaptation of the inner part of a transport aircraft wing, a problem to which optimization is a well suited approach, considering the highly three-dimensional phenomena involved, and the necessity of respecting constraints related to the aircraft design. Another example, the modification of a four-engined jet aircraft in order to reduce perturbations created by the propulsive system, shows that interference problems between the wing and other components of the aircraft can also be approached by numerical optimization. Author

N90-20998# Princeton Univ., NJ.
AERODYNAMIC DESIGN VIA CONTROL THEORY **c61**
Antony Jameson *In* AGARD, Computational Methods for Aerodynamic Design (Inverse) and Optimization Mar. 1990 32 p (For primary document see N90-20976 14-05)
Copyright Avail: NTIS HC A15/MF A02; Non-NATO Nationals requests available only from AGARD/Scientific Publications Executive

The purpose is to demonstrate by representative examples that control theory can be used to formulate computationally feasible procedures for aerodynamic design. The cost of each iteration is of the same order as two flow solutions, since the adjoint equation is of comparable complexity to the flow equation, and the remaining auxiliary equations could be solved quite inexpensively. Provided, therefore, that one can afford the cost of a moderate number of flow solutions, procedures of this type can be used to derive improved designs. The approach is quite general, not limited to particular choices of the coordinate transformation or cost function, which might in fact contain measures of other criteria of performance such as lift and drag. For the sake of simplicity certain complicating factors, such as the need to include a special term in the mapping function to generate a corner at the trailing edge, have been suppressed from the present analysis. Also it remains to explore the numerical implementation of the design procedures proposed. Author

N90-20999# Arnold Engineering Development Center, Arnold Air Force Station, TN.
OPTIMIZATION OF AERODYNAMIC DESIGNS USING COMPUTATIONAL FLUID DYNAMICS **c34**
D. H. Huddleston and C. W. Mastin (Mississippi State Univ., Mississippi State.) *In* AGARD, Computational Methods for Aerodynamic Design (Inverse) and Optimization Mar. 1990 10 p Prepared in cooperation with Sverdrup Technology, Inc., Arnold AFS, TN (For primary document see N90-20976 14-05)
Copyright Avail: NTIS HC A15/MF A02; Non-NATO Nationals requests available only from AGARD/Scientific Publications Executive

An aerodynamic design optimization technique which couples direct optimization algorithms with the analysis capability provided by appropriate computational fluid dynamics (CFD) programs is presented. This technique is intended to be an aid in designing the aerodynamic shapes and test conditions required for the successful simulation of aircraft engine inlet conditions in a ground test environment. However, the method is applicable to other aerodynamic design problems. The approach minimizes a nonlinear least-squares objective function which may be defined in a region remote to the geometric surface being optimized. In this study finite-difference Euler and Navier-Stokes codes were applied to obtain the objective function evaluations, although the optimization method could be coupled with any CFD analysis technique. Results are presented for a NACA0012 airfoil, convergent/divergent nozzles, and a planar, supersonic forebody simulator design. Author

N90-21000# National Transportation Safety Board, Washington, DC.
BRAKE PERFORMANCE OF THE MCDONNELL DOUGLAS DC-10-30/40 DURING HIGH SPEED, HIGH ENERGY REJECTED TAKEOFFS Special Investigation Report, 1988 - 1989
27 Feb. 1990 38 p
(PB90-917004; NTSB/SIR-90/01) Avail: NTIS HC A03/MF A01 CSCL 01C

On May 21, 1988, a McDonnell Douglas Corporation DC-10-30 overran the runway during a rejected takeoff (RTO) at the Dallas-Fort Worth International Airport, Texas. The airplane was damaged beyond economical repair, and 8 occupants were injured. The brakes had been certified to FAA-approved procedures, yet failed at only 36 percent of the design requirement. As a result of this accident, the Safety Board conducted a special investigation of DC-10-30/40 brakes. The investigation found that the testing requirements and procedures for certifying DC-10-30/40 brakes were inadequate, that only new brakes were used for the certification tests, and that worn brakes do not have the energy capacity or stopping capability of new brakes. The Safety Board also examined the potential decrease of the accelerate-stop safety margin for RTOs provided in the FAA Approved Airplane Flight Manual. The Safety Board believes that the concerns expressed about the adequacy of the certification process for the DC-10-30/40 may apply to the certification of all transport category airplanes. Recommendations were issued to the Federal Aviation Administration and focus on the following safety issues: certification tests and procedures related to the brakes of the DC-10-30/40; brake wear replacement limits; and airplane stopping distance. Author

N90-21001# European Office of Aerospace Research and Development, London (England). Structures/Structural Materials.
HOTOL STRUCTURES AND MATERIALS AT BRITISH AEROSPACE, WARTON, UK
James G. R. Hansen 11 Oct. 1989 14 p
(EOARD-LR-90-001) Avail: NTIS HC A03/MF A01

HOTOL is British Aerospace's concept for a single-stage-to-orbit, horizontal take-off and landing aerospace plane. Categories of advanced structural materials for HOTOL are summarized and where on the structure these materials would be utilized is shown. Author

N90-21002 Department of the Navy, Washington, DC.
INFLATABLE FUEL TANK BUFFER Patent
Jack R. Bates, inventor (to Navy) 12 Dec. 1989 5 p Filed 6 Jun. 1983
(AD-D014446; US-Patent-Appl-SN-501667;
US-Patent-Class-244-135) Avail: US Patent and Trademark Office CSCL 01/3

An inflatable bladder is placed between the wall of an aircraft inlet duct and the liquid fuel to reduce the potential damage caused by hydrodynamic ram effects from a projectile penetrating the fuel tank. The inflatable bladder is inflated by a regulated gas source prior to combat. The inflatable bladder may be formed as a double layered section of a rubber bladder fuel cell type fuel tank, or an inflatable bladder may be bonded to the inner surface of an integral fuel tank wall. GRA

N90-21003# Starmark Corp., Arlington, VA.
AN EARLY OVERVIEW OF TILTROTOR AIRCRAFT CHARACTERISTICS AND PILOT PROCEDURES IN CIVIL TRANSPORT APPLICATIONS Final Report
David L. Green, Harold Andrews, and Michael Saraniero Dec. 1989 77 p Prepared in cooperation with Federal Aviation Administration, Washington, DC
(Contract DTFA01-89-P-01074)
(DOT/FAA/DS-89/37) Avail: NTIS HC A05/MF A01

A brief description is provided of tiltrotor aircraft, and some of their projected operating characteristics are identified. Two operations are of particular interest: steep approaches into a confined metropolitan vertiport; and approaches into a vertiport without sufficient clear airspace for a conventional missed approach from a low decision height. Both operations are of interest in order to minimize the airspace needed to conduct such operations. A brief simulation was conducted to support the analysis using a fixed base simulator. The flight simulation involved a quick look at innovative and tiltrotor unique maneuvers to identify and evaluate operations at or near the operational limits. The tiltrotor shows promise of permitting much steeper approach and departure maneuvers than what can be done with either an airplane or a helicopter. Author

06 AIRCRAFT INSTRUMENTATION

Includes cockpit and cabin display devices; and flight instruments.

For related information see also *19 Spacecraft Instrumentation* and *35 Instrumentation and Photography.*

N90-21004*# National Aeronautics and Space Administration. Langley Research Center, Hampton, VA.
STEREOPSIS CUEING EFFECTS ON HOVER-IN-TURBULENCE PERFORMANCE IN A SIMULATED ROTORCRAFT
Russell V. Parrish and Steven P. Williams (Army Aviation Systems Command, Hampton, VA.) Washington May 1990 62 p
(DA Proj. 1L1-61102-AH-45)
(NASA-TP-2980; L-16652; NAS 1.60:2980;
AVSCOM-TR-90-B-002) Avail: NTIS HC A04/MF A01 CSCL 01D

The efficacy of stereopsis cueing in pictorial displays was assessed in a real-time piloted simulation experiment of a rotorcraft precision hover-in-turbulence task. Seven pilots endeavored to maintain a hover by visually aligning a set of inner and outer wickets (major elements of a real-world pictorial display, thus attaining the desired hover position, in a full factorial experimental design. The display conditions examined included the presence or absence of a velocity display element (a velocity head-up display) as well as the stereopsis cueing conditions, which included non-stereo (binoptic or monoscopic - no depth cues other than those provided by a perspective, real-world display), stereo 3-D, and hyper stereo (telestereoscopic). Subjective and objective results indicated that the depth cues provided by the stereo displays enhanced the situational awareness of the pilot and enabled improved hover performance to be achieved. The velocity display element also improved the hover performance, with the best hover performance being achieved with the combined use of stereo and the velocity display element. Pilot control input data revealed that less control action was required to attain the improved hover performance with the stereo displays. Author

N90-21005*# National Aeronautics and Space Administration. Langley Research Center, Hampton, VA.
SIMULATOR COMPARISON OF THUMBALL, THUMB SWITCH, AND TOUCH SCREEN INPUT CONCEPTS FOR INTERACTION WITH A LARGE SCREEN COCKPIT DISPLAY FORMAT
Denise R. Jones and Russell V. Parrish Apr. 1990 31 p
(NASA-TM-102587; NAS 1.15:102587) Avail: NTIS HC A03/MF A01 CSCL 01D

A piloted simulation study was conducted comparing three different input methods for interfacing to a large screen, multiwindow, whole flight deck display for management of transport aircraft systems. The thumball concept utilized a miniature trackball embedded in a conventional side arm controller. The multifunction control throttle and stick (MCTAS) concept employed a thumb switch located in the throttle handle. The touch screen concept provided data entry through a capacitive touch screen installed on the display surface. The objective and subjective results obtained indicate that, with present implementations, the thumball concept was the most appropriate for interfacing with aircraft systems/subsystems presented on a large screen display. Not unexpectedly, the completion time differences between the three concepts varied with the task being performed, although the thumball implementation consistently outperformed the other two concepts. However, pilot suggestions for improved implementations of the MCTAS and touch screen concepts could reduce some of these differences. Author

N90-21006*# Aerometrics, Inc., Sunnyvale, CA.
ADVANCED INSTRUMENTATION FOR AIRCRAFT ICING RESEARCH Final Report
W. Bachalo, J. Smith, and R. Rudoff Apr. 1990 103 p
(Contract NAS3-25317)
(NASA-CR-185225; NAS 1.26:185225) Avail: NTIS HC A06/MF A01 CSCL 01D

A compact and rugged probe based on the phase Doppler method was evaluated as a means for characterizing icing clouds using airborne platforms and for advancing aircraft icing research in large scale wind tunnels. The Phase Doppler Particle Analyzer (PDPA) upon which the new probe was based is now widely recognized as an accurate method for the complete characterization of sprays. The prototype fiber optic-based probe was evaluated in simulated aircraft icing clouds and found to have the qualities essential to providing information that will advance aircraft icing research. Measurement comparisons of the size and velocity distributions made with the standard PDPA and the fiber optic probe were in excellent agreement as were the measurements of number density and liquid water content. Preliminary testing in the NASA Lewis Icing Research Tunnel (IRT) produced reasonable results but revealed some problems with vibration and signal quality at high speeds. The cause of these problems were identified and design changes were proposed to eliminate the shortcomings of the probe. Author

07 AIRCRAFT PROPULSION AND POWER

Includes prime propulsion systems and systems components, e.g., gas turbine engines and compressors; and onboard auxilliary power plants for aircraft.

For related information see also *20 Spacecraft Propulsion and Power, 28 Propellants and Fuels,* and *44 Energy Production and Conversion.*

N90-21007 Cincinnati Univ., OH.
LDV MEASUREMENTS AND THE FLOW ANALYSIS IN THE VORTEX REGION OF A RADIAL INFLOW TURBINE Ph.D. Thesis
A. N. Lakshminarasimha 1989 192 p
Avail: Univ. Microfilms Order No. DA9003252

Detailed measurements were performed in the vortex (vaneless) region of a radial inflow turbine using a three component LDV. First, an error and uncertainty analysis based on a large sample size measurements taken at the inlet and the exit of the vortex region are presented. The flow in the vortex region is then described by contour plots of velocity, flow angle, and whirl velocity contours in the vortex region. In addition pitch averaged mean and turbulence quantities in the vaneless region are also presented. These results indicate that the flow in the vortex region is characterized by a rapid mixing region. Unlike in axial machines, the wake region of the nozzle guide vanes were found to diffuse faster. The non-uniformities in the flow in the circumferential direction were attributed to both the scroll and the nozzle performance. In order to evaluate the degree of non-uniformity in the vortex region, the mass averaged velocity for the sector at different radii from the entrance to the exit was calculated. The percentage difference between the measured actual velocity at a point and the mass averaged velocity at that radii was used to calculate the degree of non-uniformity in the vortex region. The degree of non-uniformity was higher near the plexglass (endwall region) than in a plane near the midchannel. The degree of non-uniformity decreased repidly in the downstream direction. In addition detailed pressure measurements were carried out in the vortex region. Using the measured surface static pressure and velocity total pressure loss was estimated. Total pressure loss was found to be high at the entrance to the vortex zone and near guide vane wake region.
Dissert. Abstr.

N90-21008# Federal Aviation Administration, Atlantic City, NJ.
STATISTICS ON AIRCRAFT GAS TURBINE ENGINE ROTOR FAILURES THAT OCCURRED IN US COMMERCIAL AVIATION DURING 1986 Final Report
R. A. DeLucia, J. T. Salvino (Naval Air Propulsion Test Center, Trenton, NJ.), and B. C. Fenton Jan. 1990 27 p
(DOT/FAA/CT-89/30; NAPC-PE-188) Avail: NTIS HC A03/MF A01

Statistical information relating to gas turbine engine rotor failures which occurred during 1986 in U.S. commercial aviation service use is presented. Two hundred forty-nine failures occurred in 1986. Rotor fragments were generated in 140 of the failures, and of these 16 were uncontained. The predominant failure involved blade fragments, 93 percent of which were contained. Two disk failures occurred and all were uncontained. Sixty-five percent of the 249 failures occurred during the takeoff and climb stages of flight.
Author

N90-21009# Advisory Group for Aerospace Research and Development, Neuilly-Sur-Seine (France). Propulsion and Energetics Panel.
SECONDARY FLOWS IN TURBOMACHINES
Feb. 1990 342 p In ENGLISH and FRENCH Meeting held in Luxembourg, 30 Aug. - 1 Sep. 1989
(AGARD-CP-469; ISBN-92-835-0544-1) Copyright Avail: NTIS HC A15/MF A02; Non-NATO Nationals requests available only from AGARD/Scientific Publications Executive

The Specialists' Meeting was arranged in the following sessions: Basic Flow Phenomena; Experimental Results; Three-Dimensional Computation and Comparison with Experiments; Tip Clearance Flows; and Secondary Flow Effects on Heat Transfer. The Technical Evaluation Report is included at the beginning of the proceedings. Questions and answers of the discussions follow each report. A forum was offered for experts to discuss computational and experimental methods and results of secondary flow in cascades, compressors, and turbines. Computational fluid dynamics was found to be an adequate tool to represent qualitative phenomena, but on the accuracy of predicting losses and exit angles there was some disagreement. Many papers dealt with experimental investigations which are obviously essentiai for evaluating secondary flow models. For individual titles, see N90-21010 through N90-21033.

N90-21010# Vrije Univ., Amsterdam (Netherlands). Dept. of Fluid Mechanics.
SECONDARY FLOWS AND RADIAL MIXING PREDICTIONS IN AXIAL COMPRESSORS
J. DeRuyck, Ch. Hirsch, and P. Segaert *In* AGARD, Secondary Flows in Turbomachines Feb. 1990 19 p Sponsored in part by AFOSR, Bolling AFB, Washington, DC and IWONL, Brussels, Belgium (For primary document see N90-21009 14-07)
Copyright Avail: NTIS HC A15/MF A02; Non-NATO Nationals requests available only from AGARD/Scientific Publications Executive

A radial mixing computation method is presented in the framework of an integrated quasi-3D approximation method for turbomachinery flow computations. The radial mixing computation is performed on a transverse surface S3, the only type of stream surface hitherto not considered in the quasi-3D computation. Both convective and diffusive mixing mechanisms are taken into account: the convective mixing due to secondary flows is computed explicitly, while the diffusive mixing due to the random effects of turbulence is modeled by empirical coefficients. The flow field on the S3-surface is reconstructed from the knowledge of axial vorticity contributions for different flow regions, which are added to constitute the right-hand side of a quasi-harmonic Poisson-type stream function equation. These axial vorticity components are obtained through vorticity equations for the inviscid flow region, combined with integral methods for the 3D end-wall boundary layers, 3D profile boundary layers, and 3D asymmetric wakes. The validity of the secondary flow computation is assessed through comparisons between computational results and experimental data. The method is applied to predict the redistribution of radial temperature profiles for three axial turbomachines: a linear cascade and two single-stage compressor rotors.
Author

N90-21011# United Technologies Research Center, East Hartford, CT.
THE EFFECTS OF COMPRESSOR ENDWALL FLOW ON AIRFOIL INCIDENCE AND DEVIATION
Robert P. Dring and H. David Joslyn *In* AGARD, Secondary Flows in Turbomachines Feb. 1990 9 p (For primary document see N90-21009 14-07)
Copyright Avail: NTIS HC A15/MF A02; Non-NATO Nationals requests available only from AGARD/Scientific Publications Executive

A previous examination of through flow theory in compressors has demonstrated that while there are many ways to define the average flow angle at a particular span location downstream of an airfoil, only one definition is consistent with the formulation of through flow theory. It was also demonstrated that the flow in the endwall regions is especially sensitive to this question due to the strong secondary flows and the hub corner separations that commonly occur. The question of how these observations may be extended to the airfoil-to-airfoil flow analysis is examined. It is demonstrated that the question of the correct average can have a strong impact on both airfoil incidence and deviation. Differences of up to 13 degrees are demonstrated. It is also suggested that one specific angle definition results in better predictions of airfoil pressure distributions.
Author

N90-21012# Middle East Technical Univ., Ankara (Turkey). Dept. of Mechanical Engineering.

A STUDY ON SECONDARY FLOW AND SPANWISE MIXING IN AXIAL FLOW COMPRESSORS

Murat Erkilet and Ahmet S. Ucer *In* AGARD, Secondary Flows in Turbomachines Feb. 1990 10 p (For primary document see N90-21009 14-07)

Copyright Avail: NTIS HC A15/MF A02; Non-NATO Nationals requests available only from AGARD/Scientific Publications Executive

Axisymmetric throughflow equations are reformulated in order to introduce the effect of spanwise mixing in axial flow compressors. The spanwise mixing model used in this investigation assumes that turbulent diffusion is the dominant physical mechanism for the onset of spanwise mixing rather than the deterministic nature of secondary flow model. Two-dimensional loss and deviation correlations available in the open literature are used together with the 3-D, secondary flow loss models for middle stages. End-wall boundary layer blockage is either introduced from experimental data if available or calculated using simple models. Finite element method is used for the solution of the equation of motion.

Author

N90-21013# Centre National de la Recherche Scientifique, Ecully (France).

PARABOLIZED CALCULATIONS OF TURBULENT THREE DIMENSIONAL FLOWS IN A TURBINE DUCT **c02**

P. Ferrand, F. Leboeuf, F. Pommel, and E. Parkinson *In* AGARD, Secondary Flows in Turbomachines Feb. 1990 9 p Sponsored by Direction des Recherches et Etudes Techniques, France (For primary document see N90-21009 14-07)

Copyright Avail: NTIS HC A15/MF A02; Non-NATO Nationals requests available only from AGARD/Scientific Publications Executive

For a number of practical flows with a dominating convective direction, it is often possible to neglect the diffusive phenomenona in this direction. This hypothesis is particularly true in turbomachinery ducts where the Reynolds numbers are usually very high. In this case, the diffusive terms in the main convective direction are eliminated. Concerning the velocity, the problem described by the Navier-Stokes equations becomes parabolic. However, in all the subsonic zones, the pressure tends to transfer the downstream information in the upstream direction, which is typical of an elliptical behavior. As a consequence, eliminating those diffusive terms in the Navier-Stokes equations is not sufficient to obtain a pure problem. The momentum equations have a parabolic nature and can be treated by a space marching resolution. On the opposite, the elliptic nature of the pressure equation has to be taken into account. In a subsonic flow, with highly curved ducts, it is then necessary to define an hybrid parabolic-elliptical method called quasi-elliptical. The idea, based on parabolized methods recognizing the elliptical pressure effect, was already used successfully by Kulisa-Belloir for local reverse flows. In this case, a boundary-layer model is used in strong interaction with a pressure calculation based on a small potential perturbation method generated by the viscous wall flow. The integral equation obtained with Green's theorem restores properly the elliptical effect on the wall, if the elliptical pressure is to be restored in a supersonic boundary-layer. A new method calculating three dimensional flows in turbomachinery ducts with a quasi-ellipticity hypothesis for the velocity field is presented. The main ideas of the method are presented; then its specific aspects are detailed. At last, its capacity is viewed on a representative test case typical of a turbine duct.

Author

N90-21014# Motoren- und Turbinen-Union Muenchen G.m.b.H. (Germany, F.R.).

EXPERIMENTAL AND NUMERICAL STUDY ON BASIC PHENOMENA OF SECONDARY FLOWS IN TURBINES

R. Niehuis, P. Luecking, and B. Stubert *In* AGARD, Secondary Flows in Turbomachines Feb. 1990 17 p Sponsored by the Germany Ministry for Research and Technology (For primary document see N90-21009 14-07)

Copyright Avail: NTIS HC A15/MF A02; Non-NATO Nationals requests available only from AGARD/Scientific Publications Executive

The recent understanding and the basic principles of secondary flow development in turbines, such as the formation of a horseshoe vortex and a passage vortex, are illustrated. Results are obtained for an experimental investigation of the three-dimensional flow within an annular cascade rig of an inlet guide vane of a low pressure turbine. Flow calculations with a three dimensional Euler and a partially parabolized Navier-Stokes code were performed, and the numerical results are discussed and compared with the experiment. Additionally, the computer codes were applied to calculate the three dimensional flow within two different model configurations designed to expose the influence and the contribution of different secondary flow phenomena in the end wall region.

Author

N90-21015# Brescia Univ. (Italy). Dept. di Meccanica.

SECONDARY FLOWS AND REYNOLDS STRESS DISTRIBUTIONS DOWNSTREAM OF A TURBINE CASCADE AT DIFFERENT EXPANSION RATIOS

Antonio Perdichizzi, Marina Ubaldi, and Pietro Zunino (Genoa Univ., Italy) *In* AGARD, Secondary Flows in Turbomachines Feb. 1990 13 p (For primary document see N90-21009 14-07)

Copyright Avail: NTIS HC A15/MF A02; Non-NATO Nationals requests available only from AGARD/Scientific Publications Executive

The results are presented for an experimental investigation on secondary flows and turbulence in a plane located 30 percent of an axial chord downstream of a turbine cascade. Mean velocity field, energy loss, and Reynolds stress distributions were measured with pressure and hot-wire probes at different expansion ratios for three isentropic outlet Mach numbers M(sub 2is) = 0.3, 0.5, and 0.7. High levels of turbulence kinetic energy are found in the passage-shed vortex interaction region and in the corner vortex, while lower values are present in the wake. The turbulent shear stress distributions, analyzed in detail, are consistent with the mean strain field. As the Mach number increases, the turbulence kinetic energy level is significantly reduced. The bar UV and bar vw shear stresses show a similar trend, while the bar uw component remains the same magnitude, revealing different contributions to the dissipation rate.

Author

N90-21016# Durham Univ. (England). School of Engineering and Applied Science.

AN INVESTIGATION OF SECONDARY FLOWS IN NOZZLE GUIDE VANES

R. G. Dominy and S. C. Harding (Rolls-Royce Ltd., Bristol, England) *In* AGARD, Secondary Flows in Turbomachines Feb. 1990 15 p Sponsored by the British Science and Engineering Research Council (For primary document see N90-21009 14-07)

Copyright Avail: NTIS HC A15/MF A02; Non-NATO Nationals requests available only from AGARD/Scientific Publications Executive

Much of the energy loss that occurs in turbine nozzles is associated with the strongly three dimensional secondary flows that result from the interaction between the surface boundary layers and the nozzle row with its associated pressure field. Three alternative nozzles, each performing the same duty, with different degrees of three dimensionality in their designs to control secondary flow are studied. The chosen nozzle guide vanes are fully representative of the current generation of high hub-tip ratio aero engine nozzles in which the proportion of the overall loss that is attributable to secondary flows is high. A computational analysis of all three nozzles is presented including predictions from three alternative viscous, three dimensional methods. These detailed measurements and predictions demonstrate the significant influence of the vane geometries on the magnitude and the distribution of the secondary losses.

Author

N90-21017# Royal Aerospace Establishment, Farnborough (England). Propulsion Dept.

SECONDARY FLOW PREDICTIONS FOR A TRANSONIC NOZZLE GUIDE VANE

G. C. Horton *In* AGARD, Secondary Flows in Turbomachines Feb. 1990 12 p (For primary document see N90-21009 14-07)

Copyright Avail: NTIS HC A15/MF A02; Non-NATO Nationals requests available only from AGARD/Scientific Publications Executive

To improve turbine efficiency it is necessary to design the blading to control the flow, including the secondary flow, and hence reduce the losses. A method is therefore required to predict the three-dimensional flow, with losses, within turbine geometries. Three-dimensional viscous flow programs offer the capability of doing this. Such a program (as developed by Dawes) is available at the Royal Aerospace Establishment, Pyestock. It was used to analyze the flow through a transonic turbine nozzle guide vane which was tested in cascade at Pyestock. The predictions are compared with surface pressure and downstream traverse results to assess the ability of the program to predict secondary flows and losses in a highly loaded nozzle guide vane operating at representative engine conditions. Author

N90-21018# Deutsche Forschungsanstalt fuer Luft- und Raumfahrt, Cologne (Germany, F.R.). Inst. fuer Antriebstechnik.

SECONDARY FLOW IN A TURBINE GUIDE VANE WITH LOW ASPECT RATIO

D. Wegener, J. Quest, and W. Hoffmann *In* AGARD, Secondary Flows in Turbomachines Feb. 1990 9 p (For primary document see N90-21009 14-07)

Copyright Avail: NTIS HC A15/MF A02; Non-NATO Nationals requests available only from AGARD/Scientific Publications Executive

The flow field of an annular turbine cascade with low aspect ratio (0.6) is investigated by means of experiments and numerical calculations. An advanced computer code was applied to solve the three dimensional Reynolds averaged Navier-Stokes equations. Detailed measurements with 5-hole probes and an advanced Laser-Two-Focus velocimeter (L2F) were carried out to evaluate the numerical solution of the flow field. Flow visualization on the endwalls and on the blade surfaces complement the experimental data and help to understand the secondary flow phenomena. The results show that this 3D-NS calculation is an efficient tool to predict complex secondary flow phenomena. Author

N90-21019# Deutsche Forschungsanstalt fuer Luft- und Raumfahrt, Goettingen (Germany, F.R.). Inst. fuer Experimentelle Stroemungsmechanik.

MEASUREMENT OF THE FLOW FIELD IN THE BLADE PASSAGE AND SIDE-WALL REGION OF A PLANE TURBINE CASCADE

E. Detemple-Laake *In* AGARD, Secondary Flows in Turbomachines Feb. 1990 13 p (For primary document see N90-21009 14-07)

Copyright Avail: NTIS HC A15/MF A02; Non-NATO Nationals requests available only from AGARD/Scientific Publications Executive

The transonic flow through a plane cascade consisting of profiles designed for a highly loaded gas turbine rotor of a high pressure stage is investigated. The experiments presented are part of an entire test program performed in a special wind tunnel at the DLR. The measurements of the side-wall pressure distribution in a blade passage are described. The parameters varied are the inlet flow angle and the downstream isentropic Mach number. Based on the results of Schlieren photographs of the flow field and suface oil flow patterns on the blades and the side-wall, the experimental results are interpreted. Author

N90-21020# Deutsche Forschungsanstalt fuer Luft- und Raumfahrt, Cologne (Germany, F.R.). Inst. fuer Antriebstechnik.

CENTRIFUGAL IMPELLER GEOMETRY AND ITS INFLUENCE ON SECONDARY FLOWS

H. Krain and W. Hoffmann *In* AGARD, Secondary Flows in Turbomachines Feb. 1990 17 p (For primary document see N90-21009 14-07)

Copyright Avail: NTIS HC A15/MF A02; Non-NATO Nationals requests available only from AGARD/Scientific Publications Executive

Detailed experimental and theoretical flow field studies are carried out for two 30 degree, high pressure ratio impellers having the same blade geometry but different shroud contours. An advanced Laser-Two-Focus Velocimeter is used to obtain experimental data. The theoretical investigations are performed with a 3D-viscous code that was coupled with a postprocessor primarily suitable for turbomachinery flow field studies. Comparisons between measured and calculated data are carried out and the influence of the flow channel variation on the through flow velocity patterns and secondary flow structures are discussed. Author

N90-21021# Office National d'Etudes et de Recherches Aerospatiales, Paris (France).

CALCULATION OF THE THREE DIMENSIONAL TURBULENT FLOW IN A LINEAR TURBINE BLADE [CALCUL DE L'ECOULEMENT TRIDIMENSIONNEL TURBULENT DANS UN AUBAGE RECTILIGNE DE TURBINE]

L. Cambier and B. Escande *In* AGARD, Secondary Flows in Turbomachines Feb. 1990 15 p In FRENCH; ENGLISH summary (For primary document see N90-21009 14-07)

Copyright Avail: NTIS HC A15/MF A02; Non-NATO Nationals requests available only from AGARD/Scientific Publications Executive

The numerical simulation of a three-dimensional turbulent flow in a linear turbine cascade, is examined by solution of the Reynolds-averaged compressible Navier-Stokes equations with an algebraic turbulence model. The numerical method is characterized by an explicit centered finite difference scheme, associated with a multigrid convergence acceleration. The splitting of the computational domain in an O-type subdomain around the blade and two H-type subdomains upstream and downstream allows an accurate description of the round leading edges and trailing edges, while setting the upstream and downstream boundaries of the domain sufficiently far from the blade. The results obtained in a mesh containing more than 300,000 points (in a domain bounded by a symmetry plane) show complex phenomena of secondary flows, qualitatively similar to the phenomena observed in an experiment carried out at a lower flow velocity. Author

N90-21022# Societe Nationale d'Etude et de Construction de Moteurs d'Aviation, Moissy-Cramayel (France).

CALCULATION OF THE SECONDARY FLOW IN AN AXIAL TURBINE [CALCUL DES ECOULEMENTS SECONDAIRES DANS UNE TURBINE AXIALE]

J. Bernard and F. Falchetti *In* AGARD, Secondary Flows in Turbomachines Feb. 1990 12 p In FRENCH; ENGLISH summary (For primary document see N90-21009 14-07)

Copyright Avail: NTIS HC A15/MF A02; Non-NATO Nationals requests available only from AGARD/Scientific Publications Executive

Satisfactory prediction of secondary flow effects can be considered a major objective in the design and analysis of turbine blades. A method, initially developed for the computation of secondary flows in multi-stage compressors, is briefly presented together with results obtained on a turbine nozzle cascade and on a low pressure turbine stage. Satisfactory results are obtained for the secondary vorticity as well as for the local variations in the velocity triangles. However, secondary losses and blockage are not well predicted due to the integral character of the wall boundary layer calculation used in the model. However, use of the method together with current correlations can yield interesting results especially as far as successive blade row adaptation is concerned. For detailed predictions of blade row performance, in particular secondary flow effects, the turbine designer must implement more complex methods developed for the resolution of the three-dimensional Navier-Stokes equations. Author

N90-21023# General Electric Co., Schenectady, NY. Corporate Research and Development.
GENERATION AND DECAY OF SECONDARY FLOWS AND THEIR IMPACT ON AERODYNAMIC PERFORMANCE OF MODERN TURBOMACHINERY COMPONENTS
C. Hah *In* AGARD, Secondary Flows in Turbomachines Feb. 1990 13 p (For primary document see N90-21009 14-07)
Copyright Avail: NTIS HC A15/MF A02; Non-NATO Nationals requests available only from AGARD/Scientific Publications Executive

A three-dimensional viscous flow code is used to distinguish aerodynamic performance of different designs of turbomachinery components. Two designs of a high-pressure-ratio turbine nozzle and a centrifugal compressor impeller are numerically studied to investigate detailed flow development and overall aerodynamic performance. It is indicated that the current viscous code can differentiate aerodynamic performance of various designs of turbomachinery components. Author

N90-21024# National Technical Univ., Athens (Greece). Lab. of Thermal Turbomachines.
SECONDARY FLOW CALCULATIONS FOR AXIAL AND RADIAL COMPRESSORS
D. Douvikas, J. Kaldellis, and K. D. Papailiou *In* AGARD, Secondary Flows in Turbomachines Feb. 1990 17 p (For primary document see N90-21009 14-07)
Copyright Avail: NTIS HC A15/MF A02; Non-NATO Nationals requests available only from AGARD/Scientific Publications Executive

A secondary flow calculation method is presented, the development of which was recently completed in the Thermal Turbomachinery Laboratory of the National Technical University of Athens. This method makes use of the meridional vorticity transport equation, the momentum integral equation, and the mean kinetic energy integral equation. Emphasis is placed upon the use of a coherent two-zone model and care is taken to describe adequately the flow inside an unbounded (external), semi-bounded (annulus), and fully-bounded (bladed) space. The hub and tip secondary flow development is calculated simultaneously, so that, the use of an approximate model for the interaction between the viscous shear layer and the external flow, permits this last flow field to be adapted to the growth of the wall shear layers during the computational procedure. Not only the meridional but also the peripheral blockage is taken into account during this procedure. An additional approximate viscous-inviscid interaction model is used, when shocks are present in the passage. An attempt is made to place the method in historical perspective. Then, after its brief discription, comparisons with experimental results are presented along with the appropriate discussion in order to evaluate the capabilities of the method. Author

N90-21025*# National Aeronautics and Space Administration. Lewis Research Center, Cleveland, OH.
THE NUMERICAL SIMULATION OF MULTISTAGE TURBOMACHINERY FLOWS
J. J. Adamczyk, T. A. Beach, M. L. Celestina, R. A. Mulac, and W. M. To (Sverdrup Technology, Inc., Cleveland, OH.) *In* AGARD, Secondary Flows in Turbomachines Feb. 1990 13 p (For primary document see N90-21009 14-07)
Copyright Avail: NTIS HC A15/MF A02; Non-NATO Nationals requests available only from AGARD/Scientific Publications Executive CSCL 21E

The need to account for momentum and energy transport by the unsteady deterministic flow field in modeling the time-averaged flow state within a blade row passage embedded in a multistage compressor is assessed. It was found that, within the endwall regions, large-scale three-dimensional unsteady structures existed which caused significant transport of momentum and energy across the time-averaged stream surface of a stator flow field. These experiments confirmed that the tranport process is dominated by turbulent diffusion in the midspan region. A model was then proposed for simulating this transport process, and a limited study was undertaken to assess its validity. Author

N90-21026# Connecticut Univ., Storrs. Dept. of Mechanical Engineering.
RESEARCH ON CASCADE SECONDARY AND TIP-LEAKAGE FLOWS: PERIODICITY AND SURFACE FLOW VISUALIZATION
L. S. Langston *In* AGARD, Secondary Flows in Turbomachines Feb. 1990 15 p (For primary document see N90-21009 14-07)
Copyright Avail: NTIS HC A15/MF A02; Non-NATO Nationals requests available only from AGARD/Scientific Publications Executive

Large scale planar cascade experimental studies were used for some years now to sort out and measure three-dimensional flows in axial flow turbines. In particular, these planar cascades were and are used for secondary flow studies and more recently for tip clearance studies. Cascade periodicity and the use of surface flow visualization in planar turbine cascades, in these studies are the topics of focus. Since results from these cascade experimental studies are based on a planar casade that usually has few airfoils, the topic of how periodicity is achieved in a finite cascade is an important one. One method of achieving periodicity in a 4-airfoil cascade is discussed. The use of surface flow visualization in these cascade studies has benn prominent. A commetary is given on three techniques that were used, and on the interpretation of the results from each technique. Author

N90-21027# Carleton Univ., Ottawa (Ontario). Dept. of Mechanical and Aerospace Engineering.
LOSSES IN THE TIP-LEAKAGE FLOW OF A PLANAR CASCADE OF TURBINE BLADES
M. I. Yaras and S. A. Sjolander *In* AGARD, Secondary Flows in Turbomachines Feb. 1990 13 p Sponsored in part by Pratt and Whitney Canada, Inc. (For primary document see N90-21009 14-07)
(Grant NSERC-A1671)
Copyright Avail: NTIS HC A15/MF A02; Non-NATO Nationals requests available only from AGARD/Scientific Publications Executive

The total pressure losses in the tip-leakage flow of a planar cascade of turbine blades are examined. The objective is to clarify the loss mechanisms which affect the tip gap flow as well as to provide additional data on tip-leakage losses for use in correlations. Clearances of 1.5 to 5.5 percent of the blade chord are considered. The flow was measured also for zero clearance to identify the conventional secondary flow component of the loss. The data presented clarify the role played in the evolution of the tip-leakage losses by: the viscous stresses and separation bubbles inside the tip gap; the sudden expansion as the flow emerges from the gap; and the mixing out process as the tip-leakage vortex develops downstream of the trailing edge. The direct loss within the clearance gap is found to be relatively unimportant for the full range of clearances. The measurements are compared with commonly-used correlations for the tip-leakage losses. Author

N90-21028# Technische Hochschule, Aachen (Germany, F.R.). Inst. fuer Strahlantriebe und Turboarbeitsmaschinen.
COMPUTATIONAL PREDICTION AND MEASUREMENT OF THE FLOW IN AXIAL TURBINE CASCADES AND STAGES
H. E. Gallus, K. Weskamp, and J. Zeschky *In* AGARD, Secondary Flows in Turbomachines Feb. 1990 10 p (For primary document see N90-21009 14-07)
Copyright Avail: NTIS HC A15/MF A02; Non-NATO Nationals requests available only from AGARD/Scientific Publications Executive

A partially-parabolic program was developed to calculate the three-dimensional, viscous flow through subsonic axial turbine guide vanes and rotor blades. To provide test cases for the calculations, a detailed experimental study of the flow in an axial turbine stage as well as in an axial-flow turbine cascade was performed. The obtained results and the comparison of the theoretical and experimental data are discussed. Author

N90-21029# Technische Hochschule, Aachen (Germany, F.R.). Inst. for Jet Propulsion and Turbomachinery.
ANALYSIS OF THE ROTOR TIP LEAKAGE FLOW WITH TIP COOLING AIR EJECTION
W. Koschel, H. Schmidt, and A. Vornberger *In* AGARD, Secondary Flows in Turbomachines Feb. 1990 14 p Sponsored by Deutsche Forschungsgemeinschaft (For primary document see N90-21009 14-07)
Copyright Avail: NTIS HC A15/MF A02; Non-NATO Nationals requests available only from AGARD/Scientific Publications Executive

A numerical simulation of turbine rotor tip leakage flow was carried out taking into account tip coolant flow injection. The numerical scheme is based on a finite element method for the integration of the Navier-Stokes equations in the conservative form using an explicit two-step Taylor-Galerkin algorithm. The application of unstructured grids together with local refinement strategies allows a detailed resolution of viscous flow phenomena in the clearance gap. The analysis is performed for an HP turbine blade with a tip groove without and with tip coolant flow injection. The effect of varying clearance height and of wall motion is also considered. Results on 2D-flow computations are presented and discussed in regard to viscous flow effects and to the relative mass flow discharge in the tip clearance for the different investigated configurations. Author

N90-21030# Rolls-Royce Ltd., Derby (England).
DETAILED HEAT TRANSFER MEASUREMENTS IN NOZZLE GUIDE VANE PASSAGES IN LINEAR AND ANNULAR CASCADES IN THE PRESENCE OF SECONDARY FLOWS c34
N. W. Harvey, Z. Wang, P. T. Ireland, and T. V. Jones (Oxford Univ., England) *In* AGARD, Secondary Flows in Turbomachines Feb. 1990 13 p Sponsored in part by the Ministry of Defence and Rolls-Royce Plc., England (For primary document see N90-21009 14-07)
Copyright Avail: NTIS HC A15/MF A02; Non-NATO Nationals requests available only from AGARD/Scientific Publications Executive

Two transient techniques are used to measure the heat transfer coefficient distributions in nozzle guide vane passages. The first employs liquid crystal methods in a Cold Heat Transfer Tunnel and examines the flow in a two-dimensional cascade. The second uses localized thin film heat transfer gauges within an annular cascade at engine representative Mach numbers and Reynolds numbers. The techniques are described and the resulting heat transfer coefficient distributions are discussed and interpreted in terms of the secondary flows and vortex structures. Typical heat transfer distributions are presented over the endwalls and blade surfaces. An analysis of the endwall heat transfer results is presented for the annular cascade. Author

N90-21031# Virginia Polytechnic Inst. and State Univ., Blacksburg. Dept. of Mechanical Engineering.
EFFECTS OF SECONDARY FLOW ON HEAT TRANSFER IN ROTATING PASSAGES c34
Joan G. Moore and John Moore *In* AGARD, Secondary Flows in Turbomachines Feb. 1990 13 p Sponsored by Rolls-Royce Plc. (For primary document see N90-21009 14-07)
Copyright Avail: NTIS HC A15/MF A02; Non-NATO Nationals requests available only from AGARD/Scientific Publications Executive

Secondary flow in rotating cooling passages of jet engine turbine rotors is considered. A Navier-Stokes calculation procedure for turbulent flow is used to compute flow development in a radially outward flow channel, round a sharp 180 degree bend, and in the radially inward flow channel downstream. Areas of high and low heat transfer are explained by secondary flow development and quantitative results show regions of design interest. Author

N90-21032# Office National d'Etudes et de Recherches Aerospatiales, Paris (France).
THEORETICAL STUDY OF THE FLOW IN A ROTATING CHANNEL. EXPERIMENTAL STUDY THROUGH FLOW VISUALIZATION IN A CURVED CHANNEL c34
Joel Guidez, Pierre-Jacques Michard, and Denis Dutoya *In* AGARD, Secondary Flows in Turbomachines Feb. 1990 14 p Sponsored by Direction des Recherches et Etudes Techniques (For primary document see N90-21009 14-07)
Copyright Avail: NTIS HC A15/MF A02; Non-NATO Nationals requests available only from AGARD/Scientific Publications Executive

An experimental and theoretical study of the heat transfer and flow in rotating channels is in development at ONERA. These channels simulate some simple internal cavities of turbine blades. It was experimentally demonstrated that the rotation speed induces a global enhancement of the heat transfer coefficient. The phenomenon can be explained by the secondary flows connected to the Coriolis force. Theoretically, the Navier-Stokes equations that govern this problem are numerically solved in 3D (time marching, ADI method). For laminar and turbulent flows, the results obtained point out the secondary structures (two and four vortices). In addition, by means of rotation-curvature analogy, the visualization of the streamlines in a water-channel flow with air or hydrogen bubbles shows the same flow structures. Author

N90-21033# National Research Council of Canada, Ottawa (Ontario). Gas Dynamics Lab.
THE EFFECT OF SECONDARY FLOW ON THE REDISTRIBUTION OF THE TOTAL TEMPERATURE FIELD DOWNSTREAM OF A STATIONARY TURBINE CASCADE
W. E. Carscallen and P. H. Oosthuizen (Queens Univ., Kingston, Ontario) *In* AGARD, Secondary Flows in Turbomachines Feb. 1990 18 p (For primary document see N90-21009 14-07)
Copyright Avail: NTIS HC A15/MF A02; Non-NATO Nationals requests available only from AGARD/Scientific Publications Executive

Early testing at the National Research Council of Canada's (NRCC) Highly Loaded Turbine Test Rig revealed that the total temperature downstream of a turbine nozzle was redistributed relative to the nozzle inlet total temperature distribution and furthermore there was an apparent change in area averaged total temperature across the stator row. In order to examine these observations a transonic planar cascade of the exhauster type was constructed at NRCC. Tests were carried out at pressure ratios giving nozzle isentropic exit Mach numbers ranging from low subsonic to low supersonic. Wedge probes were used to measure total pressure, total temperature, and flow angles downstream of the nozzle blade. Test results indicated that the exit total temperature distributions are highly redistributed and possible reasons for this phenomena are discussed. Results of area averaged aerodynamic losses are also given and their relation to the change in total temperature across the nozzle blades are discussed. Author

N90-21034 Oklahoma Univ., Norman.
PERFORMANCE OF AN AERO-SPACE PLANE PROPULSION NOZZLE Ph.D. Thesis
Yoon-Yeong Bae 1989 135 p Previously announced in IAA as A89-42103
Avail: Univ. Microfilms Order No. DA9003663

An inviscid and viscous analysis is provided for an exposed half nozzle that is used with a scramjet for thrust generation. The analysis is based on the inviscid theory of a 2-D, minimum length nozzle with a curved inlet surface, where the flow may be sonic or supersonic. Inlet conditions are prescribed and the gas is assumed to be perfect. Viscous, and when appropriate inviscid, nondimensional parametric results are provided for the thrust, lift, heat transfer, pitching moment, and a variety of boundary layer thicknesses. In addition to global results, wall distributions of pressure, heat transfer, etc., are provided. The analysis demonstrates that the nozzle produced a considerable lift force whose magnitude may exceed the thrust and a significant pitching

moment. The thrust is quite sensitive to the inlet Mach number; it rapidly decreases as the inlet Mach number increases. There is little loss in the thrust as the nozzle's downstream wall is truncated. The corresponding decrease in lift and the pitching moment is moderate. Dissert. Abstr.

N90-21035 Council for National Academic Awards (England).
SUPERSONIC NOZZLE DESIGN OF ARBITRARY CROSS-SECTION Ph.D. Thesis
A. Haddad 1988 201 p
Avail: Univ. Microfilms Order No. BRDX86766

An investigation, both theoretical and experimental in nature, was undertaken to develop a simple method for the design of supersonic nozzles and, indeed, inlets of quite complex shapes from known or calculated axisymmetric flowfields. The axisymmetric flowfield is determined using a computer program based on the method of characteristics. Streamlines are calculated by direct integration of the axisymmetric stream function. The desired shape is chosen at the exit of the computed axisymmetric nozzle having the desired length and Mach number. Its describing points are then traced along the corresponding streamlines back to the throat. Streamsheets formed by these streamlines define the new shape. Following this approach, two three-dimensional nozzles were designed: one of elliptical cross-section and a two-dimensional wedge. Flows within the two configurations were further simulated using a general purpose three-dimensional CFD code, 'PHOENICS' (Parabolic, hyperbolic, or elliptic numerical integration code series), while the elliptical nozzle was subsequently manufactured and submitted to experimental tests. Results from the experimental tests and three-dimensional numerical simulation, as well as predictions of the performance of the nonaxisymmetric nozzles and their axisymmetric counterparts were obtained and compared. Good agreement was achieved between the several components of the study demonstrating that it is possible, using this relatively simple method, to design satisfactory three-dimensional nozzles. Author

N90-21036*# National Aeronautics and Space Administration. Lewis Research Center, Cleveland, OH.
PROBABILISTIC MODELING FOR SIMULATION OF AERODYNAMIC UNCERTAINTIES IN PROPULSION SYSTEMS
Awatef Hamed (Cincinnati Univ., OH.) Dec. 1989 28 p
(NASA Order C-99066-G)
(NASA-TM-102472; ICOMP-89-32; E-5260; NAS 1.15:102472)
Avail: NTIS HC A03/MF A01 CSCL 21E

The numerical simulation of the probabilistic aerothermodynamic response of propulsion system components to randomness in their environment was explored. The reusable rocket engine turbopumps were selected as an example because of the severe cryogenic environment in which they operate. The thermal and combustion instabilities, coupled with the engine thrust requirements from start up to shut down, lead to randomness in the flow variables and uncertainties in the aerodynamic loading. The probabilistic modeling of the turbopumps aerodynamic response was accomplished using the panel method coupled with fast probability integration methods. The aerodynamic response in the form of probabilistic rotor blades and splitter loading were predicted and the results presented for specified flow coefficient and rotor preswirl variance. Possible future applications of the aerothermodynamic probabilistic modeling in engine transient simulation, condition monitoring and engine life prediction are briefly discussed. Author

N90-21037*# Sverdrup Technology, Inc., Cleveland, OH.
EXHAUST NOZZLES FOR PROPULSION SYSTEMS WITH EMPHASIS ON SUPERSONIC CRUISE AIRCRAFT
Leonard E. Stitt May 1990 107 p
(Contract NAS3-25266)
(NASA-RP-1235; E-4789; NAS 1.61:1235) Avail: NTIS HC A06/MF A01 CSCL 21E

This compendium summarizes the contributions of the NASA-Lewis and its contractors to supersonic exhaust nozzle research from 1963 to 1985. Two major research and technology efforts sponsored this nozzle research work; the U.S. Supersonic Transport (SST) Program and the follow-on Supersonic Cruise Research (SCR) Program. They account for two generations of nozzle technology: the first from 1963 to 1971, and the second from 1971 to 1985. First, the equations used to calculate nozzle thrust are introduced. Then the general types of nozzles are presented, followed by a discussion of those types proposed for supersonic aircraft. Next, the first-generation nozzles designed specifically for the Boeing SST and the second-generation nozzles designed under the SCR program are separately reviewed and then compared. A chapter on throttle-dependent afterbody drag is included, since drag has a major effect on the off-design performance of supersonic nozzles. A chapter on the performance of supersonic dash nozzles follows, since these nozzles have similar design problems, Finally, the nozzle test facilities used at NASA-Lewis during this nozzle research effort are identified and discussed. These facilities include static test stands, a transonic wind tunnel, and a flying testbed aircraft. A concluding section points to the future: a third generation of nozzles designed for a new era of high speed civil transports to produce even greater advances in performance, to meet new noise rules, and to ensure the continuity of over two decades of NASA research. Author

N90-21038*# National Aeronautics and Space Administration. Lewis Research Center, Cleveland, OH.
SUPERSONIC THROUGH-FLOW FAN ENGINE AND AIRCRAFT MISSION PERFORMANCE
Leo C. Franciscus and Jaime J. Maldonado (Puerto Rico Univ., Mayaguez.) 1989 15 p Presented at the Aircraft Design, Systems, and Operations Conference, Seattle, WA, 31 Jul. - 2 Aug. 1989; cosponsored by AIAA, AHS, and ASEE
(NASA-TM-102304; E-4991; NAS 1.15:102304; AIAA-89-2139)
Avail: NTIS HC A03/MF A01 CSCL 21E

A study was made to evaluate potential improvement to a commercial supersonic transport by powering it with supersonic through-flow fan turbofan engines. A Mach 3.2 mission was considered. The three supersonic fan engines considered were designed to operate at bypass ratios of 0.25, 0.5, and 0.75 at supersonic cruise. For comparison a turbine bypass turbojet was included in the study. The engines were evaluated on the basis of aircraft takeoff gross weight with a payload of 250 passengers for a fixed range of 5000 N.MI. The installed specific fuel consumption of the supersonic fan engines was 7 to 8 percent lower than that of the turbine bypass engine. The aircraft powered by the supersonic fan engines had takeoff gross weights 9 to 13 percent lower than aircraft powered by turbine bypass engines. Author

N90-20985# Von Karman Inst. for Fluid Dynamics, Rhode-Saint-Genese (Belgium).
SUBSONIC AND TRANSONIC BLADE DESIGN BY MEANS OF ANALYSIS CODES
R. A. VandeBraembussche, O. Leonard, and L. Nekmouche *In* AGARD, Computational Methods for Aerodynamic Design (Inverse) and Optimization Mar. 1990 11 p (For primary document see N90-20976 14-05)
Copyright Avail: NTIS HC A15/MF A02; Non-NATO Nationals requests available only from AGARD/Scientific Publications Executive

N90-20988# Office National d'Etudes et de Recherches Aerospatiales, Paris (France). Direction de l'Aerodynamique.
AN INVERSE METHOD FOR THE DESIGN OF TURBOMACHINE BLADES [UNE METHODE INVERSE POUR LA DETERMINATION D'AUBES DE TURBOMACHINES]
Olivier-Pierre Jacquotte *In* AGARD, Computational Methods for Aerodynamic Design (Inverse) and Optimization Mar. 1990 16 p In FRENCH Sponsored by SNECMA (For primary document see N90-20976 14-05)
Copyright Avail: NTIS HC A15/MF A02; Non-NATO Nationals requests available only from AGARD/Scientific Publications Executive

N90-20989# Instituto Superior Tecnico, Lisbon (Portugal). Dept. of Mechanical Engineering.
APPLICATION OF AN INVERSE METHOD TO THE DESIGN OF A RADIAL INFLOW TURBINE
Joao Eduardo Borges *In* AGARD, Computational Methods for Aerodynamic Design (Inverse) and Optimization Mar. 1990 16 p Sponsored in part by Holset Engineering Co., England; Churchill Coll., Cambridge, England; and Junta Nacional de Investigacao Cientifica e Tecnologica, Portugal (For primary document see N90-20976 14-05)
Copyright Avail: NTIS HC A15/MF A02; Non-NATO Nationals requests available only from AGARD/Scientific Publications Executive

N90-20990# Politecnico di Torino (Italy).
NUMERICAL METHOD FOR DESIGNING 3D TURBOMACHINERY BLADE ROWS
L. Zannetti, F. Larocca (Fiat Aviazione S.p.A., Turin, Italy), and R. Marsilio *In* AGARD, Computational Methods for Aerodynamic Design (Inverse) and Optimization Mar. 1990 9 p (For primary document see N90-20976 14-05)
Copyright Avail: NTIS HC A15/MF A02; Non-NATO Nationals requests available only from AGARD/Scientific Publications Executive

08 AIRCRAFT STABILITY AND CONTROL

Includes aircraft handling qualities; piloting; flight controls; and autopilots.

For related information see also *05 Aircraft Design, Testing and Performance.*

N90-21039 Virginia Polytechnic Inst. and State Univ., Blacksburg.
EXPERIMENTAL AND THEORETICAL INVESTIGATION OF OPTIMAL CONTROL METHODS WITH MODEL REDUCTION Ph.D. Thesis
George Cushen Schamel, II 1989 140 p
Avail: Univ. Microfilms Order No. DA9003608

Three types of optimized controllers are developed and tested on two laboratory structures. The two structures represented a progression in complexity and challenge to the controllers. The first structure was simple enough to be accurately modeled so the analytical frequencies and mode shapes agreed with the experimental measurements. The second structure, being more complex, was more difficult to model so differences between the analytical results and experiment measurements were present. These differences required the application of a correction method to the reduced models developed for the second structure. The correction method was shown to work with good results on one reduced model and with poor results on the second reduced model. Two direct rate feedback control laws and a linear quadratic regulator with state estimation (LQG controller) were designed and implemented on both structures. It was shown that the performance of the LQG controller can be approached with a much simpler direct rate feedback controller with better analytical-experimental agreement. The best analytical-experimental agreement occurred with the simplest controller applied analytically to the corrected reduced model, demonstrating the validity of the correction method as well as giving a strong reason to use simpler controller designs. Dissert. Abstr.

N90-21040 Georgia Inst. of Tech., Atlanta.
DESIGN OF A HELICOPTER AUTOMATIC FLIGHT CONTROL SYSTEM USING ADAPTIVE CONTROL Ph.D. Thesis
Philip Matthew FitzSimons 1989 198 p
Avail: Univ. Microfilms Order No. DA9005476

Due to the complexity of the equations of motion governing the dynamics of the helicopter, the design of automatic flight control systems has proven to be a difficult, time consuming task, often employing ad hoc methods to reach a solution. There is a need for a systematic control system design procedure. Since handling quality specifications are often given in terms easily interpreted for linear time invariant system design, it is convenient to construct a reference model that exhibits satisfactory performance and design the control system such that the actual helicopter behaves like this reference model. One method of control system design that follows this approach is known as adaptive model following control. There is an established theory for the stability of adaptive model following control systems. However, this theory has the restriction that the helicopter (plant) dynamics are linear time invariant. The effects of considering nonlinearities (due to kinematics and aerodynamics) and unmodeled high frequency dynamics (due to the rotor dynamics) are considered. Two different mathematical models of the helicopter are used. One model calculates the aerodynamic forces and moments as functions of the control positions and vehicle velocities and uses Euler's equations. The other model uses the same structure except that it includes a transfer function approximation to the rotor dynamics at the inputs to assess the impact of unmodeled high frequency rotor dynamics on the performance of the control system. The helicopter models are based on the McDonnell Douglas Helicopter Company's Apache AH-64. Author

N90-21041# Helsinki Univ. of Technology, Espoo (Finland). Lab. of Aerodynamics.
SUBSONIC FLUTTER ANALYSIS USING MSC/NASTRAN
Kari Renko 10 Jul. 1989 158 p Sponsored by Finnish Air Force
(PB90-166786; SER-B-89-B16; ISBN-951-754-951-2) Avail: NTIS HC A08/MF A01 CSCL 01A

Standard practices to perform flutter analyses on complex aircraft configurations in subsonic flow are presented. Flutter solution is performed using the MSC/NASTRAN program. Modifications to MSC/NASTRAN's flutter solution are devised to allow the calculation of unsteady pressure distribution on lifting surfaces and the use of ground vibration test results to represent the dynamic properties of the structure. Several supplementary programs are included which transfer model geometry and analysis results into the SDRC I-DEAS program package's database. The I-DEAS package is then used to visualize the data. Several output routines were written to generate two dimensional xy-plots of analysis results. Author

N90-20936*# Princeton Univ., NJ. Dept. of Mechanical and Aerospace Engineering.
APPLICATION OF STOCHASTIC ROBUSTNESS TO AIRCRAFT CONTROL SYSTEMS
Laura E. Ryan *In* NASA, Langley Research Center, Joint University Program for Air Transportation Research, 1988-1989 Mar. 1990 p 145-166 (For primary document see N90-20921 14-01)
Avail: NTIS HC A10/MF A02 CSCL 01C

N90-20937*# Princeton Univ., NJ. Dept. of Mechanical and Aerospace Engineering.
NEURAL NETWORKS FOR AIRCRAFT CONTROL
Dennis Linse *In* NASA, Langley Research Center, Joint University Program for Air Transportation Research, 1988-1989 Mar. 1990 p 167-181 (For primary document see N90-20921 14-01)
Avail: NTIS HC A10/MF A02 CSCL 01C

N90-20939*# Princeton Univ., NJ. Dept. of Mechanical and Aerospace Engineering.
RULE-BASED MECHANISMS OF LEARNING FOR INTELLIGENT ADAPTIVE FLIGHT CONTROL
David A. Handelman and Robert F. Stengel *In* NASA, Langley Research Center, Joint University Program for Air Transportation Research, 1988-1989 Mar. 1990 p 189-194 (For primary document see N90-20921 14-01)
(Contract DAAG29-84-K-0048)
Avail: NTIS HC A10/MF A02 CSCL 01C

N90-20940*# Princeton Univ., NJ. Dept. of Mechanical and Aerospace Engineering.
PERSPECTIVES ON THE USE OF RULE-BASED CONTROL
David A. Handelman and Robert F. Stengel *In* NASA, Langley Research Center, Joint University Program for Air Transportation Research, 1988-1989 Mar. 1990 p 195-200 (For primary document see N90-20921 14-01)
(Contract DAAG29-84-K-0048)
Avail: NTIS HC A10/MF A02 CSCL 01C

N90-20941*# Princeton Univ., NJ. Dept. of Mechanical and Aerospace Engineering.
STOCHASTIC ROBUSTNESS OF LINEAR CONTROL SYSTEMS
Robert F. Stengel and Laura E. Ryan *In* NASA, Langley Research Center, Joint University Program for Air Transportation Research, 1988-1989 Mar. 1990 p 201-206 (For primary document see N90-20921 14-01)
(Grant NGL-31-001-252)
Avail: NTIS HC A10/MF A02 CSCL 01C

09 RESEARCH AND SUPPORT FACILITIES (AIR)

Includes airports, hangars and runways; aircraft repair and overhaul facilities; wind tunnels; shock tubes; and aircraft engine test stands.

For related information see also *14 Ground Support Systems and Facilities (Space).*

N90-21042# Federal Aviation Administration, Atlantic City, NJ.
MODIFIED TOUCHDOWN ZONE LIGHTING
Paul H. Jones Jan. 1990 15 p
(DOT/FAA/CT-TN89/70) Avail: NTIS HC A03/MF A01

A simulator evaluation was conducted to determine the adequacy of the standard touchdown zone (TDZ) lighting system under extremely low visibility conditions and to develop, if necessary, a modified TDZ lighting system. All testing was conducted using the Federal Aviation Administration (FAA) B-727 simulator at the Mike Monroney Aeronautical Center, Oklahoma City. The adequacy of the lighting system guidance was determined through pilot comments and by noting the aircraft track during the rollout. A post-flight questionnaire was completed by the test pilots. Only 10 out of 14 (71 percent) pilots were able to determine their location relative to centerline at 300 feet Runway Visual Range (RVR) with the standard TDZ lighting system. Some of the pilots could only determine their location down to 500 feet RVR, so a modified system was developed. With the modified system all pilots were able to achieve adequate centerline orientation at 300 feet RVR. From the results of this simulator evaluation we must conclude that, given a true reduced visibility condition of 300 to 500 feet RVR and with an automatic landing (auto-land) system malfunction which delivered the aircraft to a touchdown point immediately over the TDZ lighting system, a pilot would not have sufficient lateral guidance to achieve adequate centerline orientation during rollout. Author

N90-21043# National Aeronautical Lab., Bangalore (India). Systems Engineering Div.
HUMAN CENTRIFUGE CONTROLLER
T. V. S. Rao, Vijayalaxmi Shankar, and C. Aswath Feb. 1989 24 p
(NAL-TM-SE-8901) Avail: NTIS HC A03/MF A01

The aging electronic control desk for the Human Centrifuge System (HCS) at the Institute of Aviation Medicine (IAM), Bangalore was upgraded and rebuilt. HCS existence at IAM, its work and use are outlined. The NAL designed, personal computer (PC) based electron control desk used with the HCS to control the rotational speed of the Human Centrifuge (HC) is described. The control desk is used for running the HC to produce various g(acceleration) patterns such as normal g profiles and combat g profiles which are generally experienced by pilots. The PC is used for speed reference signal generation, supervision of the sequence of operations to be carried out at the start of the centrifuge and continuous checking of the correct operation of the overall HCS. The NAL designed control desk functionally replaces the original control desk and all the safety features that existed earlier have been retained in the new controller. Use of PC has resulted in a flexible programming environment and use of the latest available solid state components employed in building the controller has resulted in a reliable system. Author

N90-21044# Materials Research Labs., Maribyrnong (Australia).
A CORROSION FATIGUE/STRESS CORROSION TESTING FACILITY AT MATERIALS RESEARCH LABORATORY
M. Z. Shah Khan, I. A. Burch, and B. J. Baxter 1989 28 p
(MRL-TN-568; AR-006-288) Avail: NTIS HC A03/MF A01

The mechanical testing facility at Materials Research Laboratory was employed for conducting corrosion fatigue and stress-corrosion cracking investigations. Attention is focussed on adapting two servo-hydraulic testing machines (MTS) for corrosion fatigue endurance tests on smooth specimens, and the development of an electro-mechanical testing rig for corrosion fatigue crack growth and stress-corrosion cracking tests on notched specimens. Emphasis is placed on specimen design and experimental techniques in conjunction with relatively inexpensive and simple command generation devices. The method of measuring crack growth is reported. Fracture mechanics relations for the determination of crack tip stress-intensity and critical material properties are described. Author

N90-21045# Federal Aviation Administration, Washington, DC. Advanced System Design Service.
CRITERIA FOR POLYMER CONCRETE ON AIRPORT PAVEMENTS Final Report
Krish Pandalai Jul. 1989 175 p
(Contract DTFA-01-86-Y-01015)
(DOT/FAA/DS-89/18) Avail: NTIS HC A08/MF A01

The subject of polymer concrete (PC) has generated a lot of interest among researchers during the past decade. This is due to the many advantages that polymer concrete pavement offers compared to regular portland cement concrete. The advantages of polymer concrete, when compared to portland cement concrete include, quick curing and setting, reduced moisture sensitivity and permeability and improved mechanical properties resulting in reduced pavement thickness to support the same load. These advantages will lead to attractive life cycle cost benefits. Material properties and mix designs for PC with epoxy, methylmethacrylate (MMA) and polyester as the binder material were investigated and presented. Pavement thickness design charts, developed for various aircraft, quality control methods, construction procedures and cost analysis are also presented. It was shown that increased material cost of PC can be offset by the reduced thickness of pavement. In order to develop life cycle cost information, it is necessary to obtain field performance data of PC pavement, especially in the composite design mode. Author

N90-21046# European Office of Aerospace Research and Development, London (England).
PROCEEDINGS OF THE 13TH INTERNATIONAL CONGRESS ON INSTRUMENTATION IN AEROSPACE SIMULATION FACILITIES
Fred T. Gilliam Sep. 1989 10 p Congress held in Goettingen, Federal Republic of Germany, 18-21 Sep. 1989
(EOARD-LR-89-069) Avail: NTIS HC A02/MF A01

The technical program of the 13th International Congress on Instrumentation in Aerospace Simulation Facilities (ICIASF) is summarized. Important developments in instrumentation application, instrumentation system enhancements, and new systems being developed are briefly described here. Specific instrumentation systems discussed include laser Doppler velocimetry (LDV), particle image velocimetry (PIV), laser induced fluorescence (LIF), liquid crystals, infrared (IR) imaging, and several other techniques. Author

N90-21047*# National Aeronautics and Space Administration. Langley Research Center, Hampton, VA.
EXPERIMENTAL AEROELASTICITY HISTORY, STATUS AND FUTURE IN BRIEF
Rodney H. Ricketts Apr. 1990 14 p Presented at the AIAA/ASME/ASCE/AHS/ASC 31st Structures, Structural Dynamics, and Materials Conference, Long Beach, CA, 2-4 Apr. 1990 Previously announced in IAA as A90-29598
(NASA-TM-102651; NAS 1.15:102651; AIAA-90-0978) Avail: NTIS HC A03/MF A01 CSCL 14B

NASA conducts wind tunnel experiments to determine and understand the aeroelastic characteristics of new and advanced flight vehicles, including fixed-wing, rotary-wing and space-launch configurations. Review and assessments are made of the state-of-the-art in experimental aeroelasticity regarding available facilities, measurement techniques, and other means and devices useful in testing. In addition, some past experimental programs are described which assisted in the development of new technology, validated new analysis codes, or provided needed information for clearing flight envelopes of unwanted aeroelastic response. Finally, needs and requirements for advances and improvements in testing capabilities for future experimental research and development programs are described. Author

N90-21048# Australian National Committee for Crystallography, Canberra.
A REQUIREMENT FOR AUSTRALIAN RESEARCH: ACCESS TO BIG SCIENCE FACILITIES, A REPORT BY THE AUSTRALIAN NATIONAL COMMITTEE FOR CRYSTALLOGRAPHY
Mar. 1989 49 p
(DE90-614784; INIS-mf-11589) Avail: NTIS (US Sales Only) HC A03/MF A01

Two types of Big Science research facility - synchrotron radiation sources and intense neutron beams - are now recognized as essential resources for a wide range of research activities in chemistry, physics, and biology. The cost of such facilities and the lack of a sufficiently large user base will probably preclude their construction in Australia in the foreseeable future. The needs of Australian crystallographers for access to such facilities are assessed. In relation to synchrotron radiation sources, the Committee considered only the question of access to such facilities overseas. In relation to neutron beam sources, the Committee's inquiries included not only the question of access to powerful facilities overseas but also the special problems which confront Australian crystallographers as a result of the obsolescence of the HIFAR reactor. The arguments about, and options for, funding Australian use of facilities overseas are presented. The Committee concluded there is a strong case for the purchase of a beam-line at an overseas synchrotron radiation facility and a strong, though less urgent, case for substantial Australian involvement in an overseas neutron beam facility. The Committee recommended that the Australian HIFAR reactor be refurbished in its present shell, retaining the present flux and power levels, and that in the upgrading of the neutron scattering instrumentation at HIFAR special consideration be given to including items which are sufficiently specialized to attract the international neutron scattering community. DOE

N90-21049# Systems Control Technology, Inc., Arlington, VA.
INDIANAPOLIS DOWNTOWN HELIPORT: OPERATIONS ANALYSIS AND MARKETING HISTORY Final Report
Deborah J. Peisen and Robert B. Newman Mar. 1990 91 p
(Contract DTFA01-87-C-00014)
(Rept-90RR-13; DOT/FAA/DS-89/32) Avail: NTIS HC A05/MF A01

In response to increasing helicopter demand, the FAA initiated the FAA/Industry National Prototype Heliport Demonstration and Development Program. Four cities were selected for the demonstration program. These were: New York, New Orleans, Los Angeles, and Indianapolis. In January 1985, the Indianapolis Downtown Heliport was the first of the demonstration heliports to open. The operational characteristics are analyzed of the Indianapolis Downtown Heliport from its opening in 1985 through March 1989, and the marketing techniques used during the planning and development stages of the heliport as well as the continuing marketing effort used to retain and increase business are studied. An analysis of operations at the heliport is performed using data collected by the heliport operators. The parameters examined concentrate on the types of missions, the variations and trends in the number of operations, the geographic distribution of the helicopters that use the facility, and the types of services required by the helicopter operators using the heliport. Due to limitations in the amount and accuracy of data available, only generalized trends rather than detailed statistical conclusions could be developed. Author

12 ASTRONAUTICS (GENERAL)

For extraterrestrial exploration see *91 Lunar and Planetary Exploration.*

N90-21050*# National Aeronautics and Space Administration, Washington, DC.
THE PARTNERSHIP: SPACE SHUTTLE, SPACE SCIENCE, AND SPACE STATION
Philip E. Culbertson and Robert F. Freitag [1989] 15 p
(NASA-TM-102900; NAS 1.15:102900) Avail: NTIS HC A03/MF A01 CSCL 22A

An overview of the NASA Space Station Program functions, design, and planned implementation is presented. The discussed functions for the permanently manned space facility include: (1) development of new technologies and related commercial products; (2) observations of the Earth and the universe; (3) provision of service facilities for resupply, maintenance, upgrade and repair of payloads and spacecraft; (4) provision of a transportation node for stationing, processing and dispatching payloads and vehicles; (5) provision of manufacturing and assembly facilities; (6) provision of a storage depot for parts and payloads; and (7) provision of a staging base for future space endeavors. The fundamental concept for the Space Station, as given, is that it be designed, operated, and evolved in response to a broad variety of scientific, technological, and commercial user interests. The Space Shuttle's role as the principal transportation system for the construction and maintenance of the Space Station and the servicing and support of the station crew is also discussed. Author

13 ASTRODYNAMICS

Includes powered and free-flight trajectories; and orbital and launching dynamics.

N90-21051*# Rice Univ., Houston, TX. Aero-Astronautics Group.
OPTIMAL TRAJECTORIES FOR THE AEROASSISTED FLIGHT EXPERIMENT. PART 3: FORMULATION, RESULTS, AND ANALYSIS
A. Miele, T. Wang, W. Y. Lee, and Z. G. Zhao 1989 59 p Sponsored in part by Boeing Military Airplane Co., Seattle, WA
(Contract JPL-956415; NAG8-755)
(NASA-CR-186165; NAS 1.26:186165;
AERO-ASTRONAUTICS-242-Pt-3) Avail: NTIS HC A04/MF A01 CSCL 22A

The determination of optimal trajectories for the aero-assisted flight experiment (AFE) is investigated. The intent of this experiment is to simulate a GEO-to-LEO transfer, where GEO denotes a geosynchronous Earth orbit and LEO denotes a low Earth orbit. The trajectories of an AFE spacecraft are analyzed in a 3D-space, employing the full system of 6 ODEs describing the atmospheric pass. The atmospheric entry conditions are given, and the atmospheric exit conditions are adjusted in such a way that the following conditions are satisfied: (1) the atmospheric velocity depletion is such that, after exiting, the AFE spacecraft first ascends to a specified apogee and then descends to a specified perigee;

and (2) the exit orbital plane is identical with the entry orbital plane. The final maneuver, not analyzed here, includes the rendezvous with and the capture by the space shuttle. Author

N90-21052# Massachusetts Inst. of Tech., Cambridge. Dept. of Earth, Atmospheric, and Planetary Sciences.
AMBIGUITY BOOTSTRAPPING TO DETERMINE GPS ORBITS AND BASELINES Scientific Report No. 6
Charles C. Counselman, III 10 Oct. 1989 14 p Presented at the 2nd Symposium on GPS Applications in Space, MA, 10 Oct. 1989
(Contract F19628-86-K-0009)
(AD-A218206; GL-TR-89-0278) Avail: NTIS HC A03/MF A01 CSCL 22/3

For GPS satellite orbit and interstation baseline determination, the most accurate observable available is carrier phase, differenced between observing stations and between satellites to cancel both transmitter and receiver related errors. For maximum accuracy, the integer cycle ambiguities of the doubly differenced observations must be resolved. To perform this ambiguity resolution, the author proposed a bootstrapping strategy. This strategy requires the tracking stations to have a wide ranging progression of spacings. By conventional Integrated Doppler processing of the observations from the most widely space stations, the orbits are determined well enough to permit resolution of the ambiguities for the most closely spaced stations. The resolution of these ambiguities reduces the uncertainty of the orbit determination enough to enable ambiguity resolution for more widely spaced stations, which further reduces the orbital uncertainty. Further details of the strategy are presented. Author

N90-21053 Virginia Polytechnic Inst. and State Univ., Blacksburg.
A HOMOTOPY APPROACH TO THE SOLUTIONS OF MINIMUM-FUEL SPACE-FLIGHT RENDEZVOUS PROBLEMS Ph.D. Thesis
Gopal Vasudevan 1989 148 p
Avail: Univ. Microfilms Order No. DA9003613

A homotopy approach for solving constrained parameter optimization problems is examined. The first order necessary conditions, with the complementarity conditions represented using a technique due to Mangasarian, are solved. The equations are augmented to avoid singularities which occur when the active constraint set changes. The Chow-Yorke algorithm is used to track the homotopy path leading to the solution to the desired problem at the terminal point. Since the Chow-Yorke algorithm requires a fairly accurate computation of the Jacobian matrix, analytical representation of the system of equations is desired. Consequently, equations obtained using the true anomaly regularization of the governing equations were employed for the above purpose. A homotopy map suited for the space flight rendezvous problem including a minimum radius constraint is developed, which can naturally deform any initial problem into some other valid desired problem. Several coplanar and non-coplanar solutions for circular and elliptic cases are presented for the restricted time problem with a minimum radius constraint. Dissert. Abstr.

N90-21054# Instituto de Pesquisas Espaciais, Sao Jose dos Campos (Brazil).
SUBOPTIMAL AND HYBRID NUMERICAL SOLUTION SCHEMES FOR ORBIT TRANSFER MANOEUVRES
Antonio Fernando BertachinideAlmeidaPrado and Atair RiosNeto Oct. 1989 14 p Presented at the International Symposium on Space Dynamics, Toulouse, France, 6-10 Nov. 1989; sponsored by CNES
(INPE-4991-PRE/1556) Avail: NTIS HC A03/MF A01

The problem of spacecraft orbit transfer with minimum fuel consumption is considered, in terms of selecting, implementing, and testing numerical optimal and suboptimal solutions. After a search in the literature and analysis of results available, two schemes of solution to the problem were selected. In the first one the associated optimal control problem is numerically treated by using a direct search approach together with suboptimal parameterized control. In the second one, a hybrid approach is used where the determination of the initial values of lagrange multipliers (to solve the equations given by the maximum principle) is transformed in a direct search problem. In both schemes, the numerical solution of the problem in each iteration is reduced to one of nonlinear programming, which is then solved with the gradient projection method. The spacecraft is supposed to be in keplerian motion controlled by the thrusters that are assumed to be of fixed magnitude (either low or high) and operating in an on-off mode. Author

14 GROUND SUPPORT SYSTEMS AND FACILITIES (SPACE)

Includes launch complexes, research and production facilities; ground support equipment, e.g., mobile transporters; and simulators.

For related information see also *09 Research and Support Facilities (Air).*

N90-21055# Army Communications-Electronics Command, Fort Monmouth, NJ.
LASER CONTROLLED SEMICONDUCTOR ARMATURE FOR ELECTROMAGNETIC LAUNCHERS Patent Application
Louis J. Jasper, Jr., inventor (to Army), Maurice Weiner, inventor (to Army), and Lawrence J. Bovino, inventor (to Army) 16 Jan. 1990 13 p
(AD-D014435; US-Patent-Appl-SN-466142) Avail: NTIS HC A03/MF A01 CSCL 09/7

An electromagnetic launcher or railgun includes a projectile or armature which is comprised of an optically activated semiconductor switch device including a body of bulk semiconductor material, such as gallium arsenide (GaAs) or gallium arsenide doped with chromium (Cr:GaAs), located between a pair of rails across which is connected a relatively high current source. A source of optical energy, such as a pulsed laser, directs optical energy to at least one surface of the semiconductor switch device where the conductivity of the semiconductor body, is thereby increased and current from the source is transformed between the rails through the semiconductor body, causing an electromagnetic Lorentz type drive force to be built up behind the armature, which is set into motion and rapidly accelerated along the rails. GRA

N90-21056# Oak Ridge National Lab., TN.
SIMPLE LIGHT GAS GUNS FOR HYPERVELOCITY STUDIES
S. K. Combs, H. H. Haselton, and S. L. Milora 1990 22 p Presented at the Special Operations Expo '90, Idaho Falls, ID, 20-22 Mar. 1990
(Contract DE-AC05-84OR-21400)
(DE90-008907; CONF-9003122-1) Avail: NTIS HC A03/MF A01

Two-stage light guns are used extensively in hypervelocity research. The applications of this technology include impact studies and special materials development. Oak Ridge National Laboratory (ORNL) has developed two-stage guns that accelerate small projectiles (4-mm nominal diameter) to velocities of up to approximately 5 km/s. These guns are relatively small and simple (thus, easy to operate), allowing a significant number of test shots to be carried out and data accumulated in a short time. Materials that have been used for projectiles include plastics, frozen isotopes of hydrogen, and lithium hydride. One gun has been used to demonstrate repetitive operation at a rate of 0.7 Hz; and, with a few design improvements, it appears capable of performing at firing frequencies of 1 to 2 Hz. A schematic of ORNL two-stage device is shown below. Unlike most such devices, no rupture disks are used. Instead, a fast valve (high-flow type) initiates the acceleration process in the first stage. Projectiles can be loaded into the gun breech via the slide mechanism; this action was automated which allows repetitive firing. Alternatively, the device is equipped with pipe gun apparatus in which gas can be frozen

in-situ in the gun barrel to form the projectile. This equipment operates with high reliability and is well suited for small-scale testing at high velocity. DOE

N90-21057# Lawrence Livermore National Lab., CA.
RAILGUN PERFORMANCE WITH A TWO-STAGE LIGHT-GAS GUN INJECTOR
R. S. Hawke, A. R. Susoeff, J. R. Asay, C. A. Hall, C. H. Konrad, G. W. Wellman, R. J. Hickman, W. A. Heath, J. R. Martinez, and J. L. Sauve (Edgerton, Germeshausen and Grier, Inc., Albuquerque, NM.) et al 1990 6 p Presented at the 5th IEEE Symposium on Electromagnetic Launch Technology, Destin, FL, 1-5 Apr. 1990
(Contract W-7405-eng-48)
(DE90-009183; UCRL--101932; CONF-9004136-8) Avail: NTIS HC A02/MF A01

This paper summarizes the results obtained with the HELEOS railgun which uses a two-stage light-gas gun (2SLGG) as an (pi)injector. The high velocity 2SLGG injector preaccelerates projectiles up to approximately 8 km/s. The high injector velocity reduces the exposure duration of the railgun barrel to the passing high temperature plasma armature, thereby reducing the ablation subsequent armature growth. The 2SLGG also provides a column of cool, high pressure hydrogen gas to insulate the rails behind the projectile, thereby eliminating restrike. A means to form an armature behind the injected projectile has been developed. In preliminary tests, the third stage railgun has successfully increased the projectile velocity by 1.35 km/s. Extensive diagnostics have been used to determine the behavior of the armature and track the launcher's performance. In some cases, velocity increase in the railgun section has been achieved, which is in close agreement with theoretical predictions, whereas in other experiments deviations from theoretical have been observed. The reasons for and implications of these results will be addressed. Recent tests are reported. DOE

N90-21058*# Martin Marietta Corp., Denver, CO. Near-Field Test Lab.
MILLIMETER WAVE NEAR-FIELD STUDY Final Report
Neill Kefauver Apr. 1990 51 p
(Contract NAS1-18455)
(NASA-CR-182014; NAS 1.26:182014; MCR-89-575) Avail: NTIS HC A04/MF A01 CSCL 20N

The possibility is evaluated of current technology measuring large aperture millimeter wave antennas. Included are a mathematical modeling of system errors, experimental data supporting error model, predictions of system accuracy at millimeter wavelengths, advantage of near-field measurements, and a cost estimate for a facility upgrade. The use is emphasized of software compensation and other inexpensive alternatives to develop a near optimum solution to near-field measurement problems at millimeter wavelengths. Author

N90-21089*# Jet Propulsion Lab., California Inst. of Tech., Pasadena.
CSI TECHNOLOGY VALIDATION ON AN LSS GROUND EXPERIMENT FACILITY
S. J. Wang and D. B. Eldred *In* NASA, Langley Research Center, NASA/DOD Controls-Structures Interaction Technology 1989 Aug. 1989 p 475-49 (For primary document see N90-21062 14-18)
Avail: NTIS HC A23/MF A03 CSCL 14B

15 LAUNCH VEHICLES AND SPACE VEHICLES

Includes boosters; operating problems of launch/space vehicle systems; and reusable vehicles.

For related information see also *20 Spacecraft Propulsion and Power.*

No abstracts in this category.

16 SPACE TRANSPORTATION

Includes passenger and cargo space transportation, e.g., shuttle operations; and space rescue techniques.

For related information see also *03 Air Transportation and Safety* and *18 Spacecraft Design, Testing and Performance.* For space suits see *54 Man/System Technology and Life Support.*

N90-21059*# Northeastern Univ., Boston, MA. Dept. of Chemical Engineering.
MECHANISTIC MODEL FOR CATALYTIC RECOMBINATION DURING AEROBRAKING MANEUVERS Final Report
Ronald J. Willey 30 Nov. 1989 88 p
(Grant NAG9-314)
(NASA-CR-185611; NAS 1.26:185611) Avail: NTIS HC A05/MF A01 CSCL 22B

Several mechanistic models are developed to predict recombination coefficients for use in heat shield design for reusable surface insulation (RSI) on aerobraking vehicles such as space shuttles. The models are applied over a temperature range of 300 to 1800 K and a stagnation pressure range of 0 to 3,000 Pa. A four parameter model in temperature was found to work best; however, several models (including those with atom concentrations at the surface) were also investigated. Mechanistic models developed with atom concentration terms may be applicable when sufficient data becomes available. The requirement is shown for recombination experiments in the 300 to 1000 K and 1500 to 1850 K temperature range, with deliberate concentration variations. Author

N90-21060*# Thiokol Corp., Brigham City, UT. Space Operations.
TRANSPORTATION MONITORING UNIT QUALIFICATION Final Report
M. Cook 8 Mar. 1990 227 p
(Contract NAS8-30490)
(NASA-CR-183930; NAS 1.26:183930; TWR-18782) Avail: NTIS HC A11/MF A02 CSCL 22B

Transportation monitoring unit (TMU) qualification testing was performed between 3 Mar. and 14 Dec. 1989. The purpose of the testing was to qualify the TMUs to monitor and store temperature and acceleration data on redesigned solid rocket motor segments and exit cones while they are being shipped from Utah's Thiokol Corporation, Space Operations, to Kennedy Space Center. TMUs were subjected to transportation tests that concerned the structural integrity of the TMUs only, and did not involve TMU measuring capability. This testing was terminated prior to completion due to mounting plate failures, high and low temperature shutdown failures, and data collection errors. Corrective actions taken by the vendor to eliminate high temperature shutdowns were ineffective. An evaluation was performed on the TMUs to determine the TMU vibration and temperature measuring accuracy at a variety of temperatures. This test demonstrated that TMU measured shock levels are high, and that TMUs are temperature sensitive because of decreased accuracy at high and low temperatures. It was determined that modifications to the current TMU system, such that it could be qualified for use, would require a complete redesign and remanufacture. Because the cost of redesigning and remanufacturing the present TMU system exceeds the cost of

procuring a new system that could be qualified without modification, it is recommended that an alternate transportation monitoring system be qualified. Author

17 SPACE COMM., SPACECRAFT COMM., COMMAND & TRACKING

Includes telemetry; space communications networks; astronavigation and guidance; and radio blackout.

For related information see also *04 Aircraft Communications and Navigation* and *32 Communications and Radar.*

N90-21061* National Aeronautics and Space Administration. Pasadena Office, CA.
VLSI SINGLE-CHIP (255,223) REED-SOLOMON ENCODER WITH INTERLEAVER Patent
In-Shek Hsu, inventor (to NASA), Leslie J. Deutsch, inventor (to NASA), Trieu-Kie Truong, inventor (to NASA), and Irving S. Reed, inventor (to NASA) (Jet Propulsion Lab., California Inst. of Tech., Pasadena.) 6 Mar. 1990 15 p Filed 18 May 1988 Supersedes N88-27220 (26 - 21, p 2902)
(Contract NAS7-918)
(NASA-Case-NPO-17280-1-CU; US-Patent-4,907,233; US-Patent-Appl-SN-195226; US-Patent-Class-371-37.4; US-Patent-Class-371-38.1; US-Patent-Class-371-041; US-Patent-Class-371-043) Avail: US Patent and Trademark Office CSCL 09F

The invention relates to a concatenated Reed-Solomon/convolutional encoding system consisting of a Reed-Solomon outer code and a convolutional inner code for downlink telemetry in space mission, and more particularly to a Reed-Solomon encoder with programmable interleaving of the information symbols and code correction symbols to combat error bursts in the Viberbi decoder. NASA

18 SPACECRAFT DESIGN, TESTING AND PERFORMANCE

Includes satellites; space platforms; space stations; spacecraft systems and components such as thermal and environmental controls; and attitude controls.

For life support systems see *54 Man/System Technology and Life Support.* For related information see also *05 Aircraft Design, Testing and Performance, 39 Structural Mechanics,* and *16 Space Transportation.*

N90-21062*# National Aeronautics and Space Administration. Langley Research Center, Hampton, VA.
NASA/DOD CONTROLS-STRUCTURES INTERACTION TECHNOLOGY 1989
Jerry R. Newsom, comp. Washington Aug. 1989 543 p Conference held in San Diego, CA, 29 Jan. - 2 Feb. 1989; sponsored by NASA Langley Research Center, Hampton, VA and Wright Research Development Center, Wright-Patterson AFB, OH (NASA-CP-3041; L-16602; NAS 1.55:3041) Avail: NTIS HC A23/MF A03 CSCL 22B

The purpose of this conference was to report to industry, academia, and government agencies on the current status of controls-structures interaction technology. The agenda covered ground testing, integrated design, analysis, flight experiments, and concepts. For individual titles, see N90-21063 through N90-21092.

N90-21063*# Jet Propulsion Lab., California Inst. of Tech., Pasadena.
A SPACEBORNE OPTICAL INTERFEROMETER: THE JPL CSI MISSION FOCUS **c19**
R. A. Laskin *In* NASA, Langley Research Center, NASA/DOD Controls-Structures Interaction Technology 1989 Aug. 1989 p 1-15 (For primary document see N90-21062 14-18)
Avail: NTIS HC A23/MF A03 CSCL 14B

The JPL Control Structure Interaction (CSI) program is part of the larger NASA-wide CSI program. Within this larger context, the JPL CSI program will emphasize technology for systems that demand micron or sub-micron level control, so-called Micro-Precision Controlled Structures (u-PCS). The development of such technology will make it practical to fly missions with large optical or large precision antenna systems. In keeping with the focused nature of the desired technology, the JPL approach is to identify a focus mission, develop the focus mission CSI system design to a preliminary level, and then use this design to drive out requirements for CSI technology development in the design and analysis, ground test bed, and flight experiment areas. Author

N90-21064*# Martin Marietta Aerospace, Denver, CO.
ZENITH STAR: A STRUCTURAL CONTROL CHALLENGE
L. A. Morine *In* NASA, Langley Research Center, NASA/DOD Control-Structures Interaction Technology 1989 Aug. 1989 p 17-29 (For primary document see N90-21062 14-18)
Avail: NTIS HC A23/MF A03 CSCL 22B

The Zenith Star Experiment is designed to demonstrate and evaluate the performance of a laser in space to answer critical issues relevant to SDI. The spacecraft design, control system architecture, and vehicle control are discussed. B.G.

N90-21065*# Martin Marietta Aerospace, Denver, CO.
PACOSS PROGRAM STATUS AND RESULTS
K. E. Richards, Jr. *In* NASA, Langley Research Center, NASA/DOD Controls-Structure Interaction Technology 1989 Aug. 1989 p 31-65 (For primary document see N90-21062 14-18)
Avail: NTIS HC A23/MF A03 CSCL 22B

Future large space systems (LSS), both civilian and military, will have performance objectives which require stringent pointing accuracies, relatively fast retargeting times, short settling times, accurate dynamic shape requirements, or combinations thereof. Many of these structures will be large but lightweight and will exhibit a dense, low-frequency modal spectrum with significant content within the control bandwidth. Although it is possible in principle to achieve structural vibration control with purely active means, experience with complex structures has shown that the realities of plant model inaccuracies and real sensor and actuator dynamics frequently combine to produce disappointing results. It was shown that a combination of passive and active control will result in a simpler system which can be expected to be more reliable and less expensive than a corresponding system utilizing active control exclusively. The goals of the Passive and Active Control of Space Structures (PACOSS) program consist of a thorough investigation of the relative roles of passive active vibration control, and the development of validated means of vibration control. The program approach, representative system article, dynamic test article, and test status and results are outlined. Author

N90-21066*# Jet Propulsion Lab., California Inst. of Tech., Pasadena.
VIBRATION ISOLATION VERSUS VIBRATION COMPENSATION ON MULTIPLE PAYLOAD PLATFORMS
S. W. Sirlin *In* NASA, Langley Research Center, NASA/DOD Controls-Structures Interaction Technology 1989 Aug. 1989 p 67-81 (For primary document see N90-21062 14-18)
Avail: NTIS HC A23/MF A03 CSCL 22B

There are many future science instruments with high performance pointing (sub microradian) requirements. To build a separate spacecraft for each payload is prohibitively expensive, especially as not all instruments need to be in space for a long duration. Putting multiple payloads on a single basebody that supplies power, communications, and orbit maintenance is cheaper, easier to service, and allows for the spacecraft bus to be reused as new instruments become available to replace old instruments. Once several payloads are mounted together, the articulation of one may disturb another. The situation is even more extreme

when the basebody serves multiple purposes, such as space station which has construction, satellite servicing, and man motion adding to the disturbance environment. The challenge then is to maintain high performance at low cost in a multiple payload environment. The goal is to supply many future science instruments with high performance pointing (sub microradian). The options are independent spacecraft for each payload (expensive); or multiple payloads on a single basebody (cheaper, easier to service, basebody reusable for several short duration payloads). The problems are one payload can disturb another, and other activities create large disturbances (construction, satellite servicing, and man motion). Author

N90-21067*# National Aeronautics and Space Administration. Goddard Space Flight Center, Greenbelt, MD.
GOES I-M AND BEYOND: SCIENCE REQUIREMENTS AND TECHNOLOGY CHALLENGES
William E. Shenk *In* NASA, Langley Research Center, NASA/DOD Controls-Structures Interaction Technology 1989 Aug. 1989 p 83-90 (For primary document see N90-21062 14-18)
Avail: NTIS HC A23/MF A03 CSCL 22B

Measurement of Earth observation parameters from geosynchronous satellites; severe local storm observational guidelines; major instrument requirements; rapid convective cell growth; geosynchronous satellite requirements; and major technological challenges for the next 25 years are discussed. B.G.

N90-21068*# National Aeronautics and Space Administration. Langley Research Center, Hampton, VA.
CONTROLLED MULTIBODY DYNAMICS SIMULATION FOR LARGE SPACE STRUCTURES
J. M. Housner, S. C. Wu, and C. W. Chang (Comtek Co., Yorktown, VA.) *In its* NASA/DOD Controls-Structures Interaction Technology 1989 Aug. 1989 p 91-109 (For primary document see N90-21062 14-18)
Avail: NTIS HC A23/MF A03 CSCL 22B

Multibody dynamics discipline, and dynamic simulation in control structure interaction (CSI) design are discussed. The use, capabilities, and architecture of the Large Angle Transient Dynamics (LATDYN) code as a simulation tool are explained. A generic joint body with various types of hinge connections; finite element and element coordinate systems; results of a flexible beam spin-up on a plane; mini-mast deployment; space crane and robotic slewing manipulations; a potential CSI test article; and multibody benchmark experiments are also described. B.G.

N90-21069*# Mechanical Dynamics, Inc., Ann Arbor, MI.
ELEMENT-SPECIFIC MODAL FORMULATIONS FOR LARGE-DISPLACEMENT MULTIBODY DYNAMICS
R. R. Ryan and H. H. Yoo (Michigan Univ., Ann Arbor.) *In* NASA, Langley Research Center, NASA/DOD Controls-Structures Interaction Technology 1989 Aug. 1989 p 111-12 (For primary document see N90-21062 14-18)
Avail: NTIS HC A23/MF A03 CSCL 22B

Large dispacement assumed-mode modeling techniques are examined in the context of multibody elastodynamics. The range of both general and element-specific approaches are studied with the aid of examples involving beams, plates, and shells. For systems undergoing primarily structural bending and twisting with little or no membrane distortion, it is found that fully-linear, element-specific, modal formulations provide the most accurate time history solutions at the least expense. When membrane effects become dominant in structural problems due to loading and boundary conditions, one must naturally resort to a formulation involving a nonlinear stress-strain relationship in addition to nonlinear terms associated with large overall system motion. Such nonlinear models were investigated using assumed modes and found to lead to modal convergence difficulties when standard free-free structural modes are employed. A constrained mode formulation aimed at addressing the convergence problem is proposed. Author

N90-21070*# National Aeronautics and Space Administration. Langley Research Center, Hampton, VA.
NONLINEAR AND DISTRIBUTED PARAMETER MODELS OF THE MINI-MAST TRUSS
Lawrence W. Taylor, Jr. *In its* NASA/DOD Controls-Structures Interaction Technology 1989 Aug. 1989 p 131-150 (For primary document see N90-21062 14-18)
Avail: NTIS HC A23/MF A03 CSCL 22B

Large spacecraft such as Space Station Freedom employ large trusses in their construction. The structural dynamics of such trusses often exhibit nonlinear behavior and little damping which can impact significantly the performance of control systems. The Mini-MAST truss was constructed to research such structural dynamics and control systems. The Mini-MAST truss is an object of study for the guest investigator program as part of NASA's controls-structures interaction program. The Mini-MAST truss is deployable and about 65 ft long. Although the bending characteristics of the Mini-MAST truss are essentially linear, the angular deflection under torsional loading has exhibited significant hysteresis and nonlinear stiffness. It is the purpose to develop nonlinear and distributed parameter models of the truss and to compare the model dynamics with actual measurements. Distributed parameter models have the advantage of requiring fewer model parameters. A tangent function is used to describe the nonlinear stiffness in torsion, partly because of the convenience of its easily expressed inverse. Hysteretic slip elements are introduced and extended to a continuum to account for the observed hysteresis in torsion. The contribution of slipping to the structural damping is analyzed and found to be strongly dependent on the applied loads. Because of the many factors which affect the damping and stiffness in a truss, it is risky to assume linearity. Author

N90-21071*# Lawrence Livermore National Lab., CA.
A DISTRIBUTED FINITE-ELEMENT MODELING AND CONTROL APPROACH FOR LARGE FLEXIBLE STRUCTURES
K. D. Young *In* NASA, Langley Research Center, NASA/DOD Controls-Structures Interaction Technology 1989 Aug. 1989 p 151-16 (For primary document see N90-21062 14-18)
Avail: NTIS HC A23/MF A03 CSCL 22B

An unconventional framework is described for the design of decentralized controllers for large flexible structures. In contrast to conventional control system design practice which begins with a model of the open loop plant, the controlled plant is assembled from controlled components in which the modeling phase and the control design phase are integrated at the component level. The developed framework is called controlled component synthesis (CCS) to reflect that it is motivated by the well developed Component Mode Synthesis (CMS) methods which were demonstrated to be effective for solving large complex structural analysis problems for almost three decades. The design philosophy behind CCS is also closely related to that of the subsystem decomposition approach in decentralized control. Author

N90-21072*# Alabama Univ., Huntsville. Dept. of Electrical and Computer Engineering.
EFFECTIVE TECHNIQUES FOR THE IDENTIFICATION AND ACCOMMODATION OF DISTURBANCES
C. D. Johnson *In* NASA, Langley Research Center, NASA/DOD Controls-Structures Interaction Technology 1989 Aug. 1989 p 163-18 (For primary document see N90-21062 14-18)
Avail: NTIS HC A23/MF A03 CSCL 22B

The successful control of dynamic systems such as space stations, or launch vehicles, requires a controller design methodology that acknowledges and addresses the disruptive effects caused by external and internal disturbances that inevitably act on such systems. These disturbances, technically defined as uncontrollable inputs, typically vary with time in an uncertain manner and usually cannot be directly measured in real time. A relatively new non-statistical technique for modeling, and (on-line) identification, of those complex uncertain disturbances that are not as erratic and capricious as random noise is described. This technique applies to multi-input cases and to many of the practical

disturbances associated with the control of space stations, or launch vehicles. Then, a collection of smart controller design techniques that allow controlled dynamic systems, with possible multi-input controls, to accommodate (cope with) such disturbances with extraordinary effectiveness are associated. These new smart controllers are designed by non-statistical techniques and typically turn out to be unconventional forms of dynamic linear controllers (compensators) with constant coefficients. The simplicity and reliability of linear, constant coefficient controllers is well-known in the aerospace field. Author

N90-21073*# National Aeronautics and Space Administration. Langley Research Center, Hampton, VA.
MODELING AND CONTROL OF FLEXIBLE SPACE PLATFORMS WITH ARTICULATED PAYLOADS
Philip C. Graves (Vigyan Research Associates, Inc., Hampton, VA.) and Suresh M. Joshi *In its* NASA/DOD Controls-Structures Interaction Technology 1989 Aug. 1989 p 181-210 (For primary document see N90-21062 14-18)
Avail: NTIS HC A23/MF A03 CSCL 22B

The first steps in developing a methodology for spacecraft control-structure interaction (CSI) optimization are identification and classification of anticipated missions, and the development of tractable mathematical models in each mission class. A mathematical model of a generic large flexible space platform (LFSP) with multiple independently pointed rigid payloads is considered. The objective is not to develop a general purpose numerical simulation, but rather to develop an analytically tractable mathematical model of such composite systems. The equations of motion for a single payload case are derived, and are linearized about zero steady-state. The resulting model is then extended to include multiple rigid payloads, yielding the desired analytical form. The mathematical models developed clearly show the internal inertial/elastic couplings, and are therefore suitable for analytical and numerical studies. A simple decentralized control law is proposed for fine pointing the payloads and LFSP attitude control, and simulation results are presented for an example problem. The decentralized controller is shown to be adequate for the example problem chosen, but does not, in general, guarantee stability. A centralized dissipative controller is then proposed, requiring a symmetric form of the composite system equations. Such a controller guarantees robust closed loop stability despite unmodeled elastic dynamics and parameter uncertainties. Author

N90-21074*# National Aeronautics and Space Administration. Lewis Research Center, Cleveland, OH.
DETECTION OF POTENTIAL SPACE STATION CONTROL/STRUCTURE INTERACTION WITH CO-ST-IN
Kelly Carney, Ron Graham, Doug Kyr, and Paul Andrew Bielloch (SDRC, Inc., San Diego, CA.) *In* NASA, Langley Research Center, NASA/DOD Controls-Structures Interaction Technology 1989 Aug. 1989 p 211-22 (For primary document see N90-21062 14-18)
Avail: NTIS HC A23/MF A03 CSCL 22B

The NASA Lewis Research Center is concerned with the potential of interaction between space station controllers and the solar PV array structures. The models required to handle this problem are very large, and automated methods were developed for the transfer of data between structural dynamic and control system analysis software. These methods emphasize the need to achieve accurate coupled analysis results while using as small a model as possible. Specific tools which help the analyst in this regard include modal order techniques, the use of mode acceleration to calculate internal loads and stresses and the transfer of Craig-Bampton components to reduce problems associated with modal sufficiency. These techniques were applied to a space station model with 366 modes below 1 Hz. Attitude control, and alpha and beta joint control were simulated. The inclusion of alpha and beta joint controllers is important when examining overall space station dynamics. An initial choice of control parameters does indicate a potential for control/structure interaction during reboost. As expected this is exacerbated by increasing the rate gain and decreasing the hysteresis of the reaction control system (RCS) in order to improve rigid body performance. Author

N90-21075*# Air Force Wright Aeronautical Labs., Wright-Patterson AFB, OH.
OPTIMIZATION OF THE STRUCTURAL AND CONTROL SYSTEM FOR LSS WITH REDUCED-ORDER MODEL
N. S. Khot *In* NASA, Langley Research Center, NASA/DOD Controls-Structures Interaction Technology 1989 Aug. 1989 p 229-23 (For primary document see N90-21062 14-18)
Avail: NTIS HC A23/MF A03 CSCL 22B

The objective is the simultaneous design of the structural and control system for space structures. The minimum weight of the structure is the objective function, and the constraints are placed on the closed loop distribution of the frequencies and the damping parameters. The controls approach used is linear quadratic regulator with constant feedback. A reduced-order control system is used. The effect of uncontrolled modes is taken into consideration by the model error sensitivity suppression (MESS) technique which modified the weighting parameters for the control forces. For illustration, an ACOSS-FOUR structure is designed for a different number of controlled modes with specified values for the closed loop damping parameters and frequencies. The dynamic response of the optimum designs for an initial disturbance is compared. Author

N90-21076*# National Aeronautics and Space Administration. Langley Research Center, Hampton, VA.
COMPUTATIONAL ARCHITECTURE FOR INTEGRATED CONTROLS AND STRUCTURES DESIGN
W. Keith Belvin and K. C. Park (Colorado Univ., Boulder.) *In its* NASA/DOD Controls-Structures Interaction Technology 1989 Aug. 1989 p 241-260 (For primary document see N90-21062 14-18)
Avail: NTIS HC A23/MF A03 CSCL 22B

To facilitate the development of control structure interaction (CSI) design methodology, a computational architecture for interdisciplinary design of active structures is presented. The emphasis of the computational procedure is to exploit existing sparse matrix structural analysis techniques, in-core data transfer with control synthesis programs, and versatility in the optimization methodology to avoid unnecessary structural or control calculations. The architecture is designed such that all required structure, control and optimization analyses are performed within one program. Hence, the optimization strategy is not unduly constrained by cold starts of existing structural analysis and control synthesis packages. Author

N90-21077*# Colorado Univ., Boulder. Dept. of Aerospace Engineering Sciences.
CONTROLLER REDUCTION FOR EFFECTIVE INTERDISCIPLINARY DESIGN OF ACTIVE STRUCTURES
Mark J. Balas and Ralph Quan *In* NASA, Langley Research Center, NASA/DOD Controls-Structures Interaction Technology 1989 Aug. 1989 p 261-27 (For primary document see N90-21062 14-18)
Avail: NTIS HC A23/MF A03 CSCL 22B

Control problems of large aerospace structures are intrinsically interdisciplinary and require strategies which address the complete interaction between flexible structures, electromechanical actuators and sensors, and feedback control algorithms. Current research and future directions which will require an interdisciplinary team effort in dynamics, control and optimization of such structures are being surveyed. It is generally agreed that the dynamics of space structures require large scale discrete modeling, resulting in thousands of discrete unknowns. Proven control strategies, on the other hand, employ a low order controller that is based on a reduced order model of structures. Integration of such low order controllers and large scale dynamics models often leads to serious deterioration of the closed loop stability margin and even instability. To alleviate this stability deterioration while low order controllers remain effective, the following approach was investigated: (1) retain

low order controllers based on reduced order models of structures as the basic control strategy; (2) introduce a compensator that will directly account for the deterioration of stability margin due to controller-structure integration; and (3) assess overall performance of the integrated control structure system by developing measures of suboptimality in the combination of (1) and (2). The benefits include: simplicity in the design of basic controllers, thus facilitating the optimization of structure control interactions; increased understanding of the roles of the compensator so as to modify the structure as well as the basic controller, if necessary, for improved performance; and adaptability to localize controllers by viewing the compensator as a systems integration filter. Author

N90-21078*# Jet Propulsion Lab., California Inst. of Tech., Pasadena.
RECENT EXPERIENCE IN SIMULTANEOUS CONTROL-STRUCTURE OPTIMIZATION
M. Salama, R. Ramaker, and M. Milman *In* NASA, Langley Research Center, NASA/DOD Controls-Structures Interaction Technology 1989 Aug. 1989 p 271-28 (For primary document see N90-21062 14-18)
Avail: NTIS HC A23/MF A03 CSCL 22B

To show the feasibility of simultaneous optimization as design procedure, low order problems were used in conjunction with simple control formulations. The numerical results indicate that simultaneous optimization is not only feasible, but also advantageous. Such advantages come at the expense of introducing complexities beyond those encountered in structure optimization alone, or control optimization alone. Examples include: larger design parameter space, optimization may combine continuous and combinatoric variables, and the combined objective function may be nonconvex. Future extensions to include large order problems, more complex objective functions and constraints, and more sophisticated control formulations will require further research to ensure that the additional complexities do not outweigh the advantages of simultaneous optimization. Some areas requiring more efficient tools than currently available include: multiobjective criteria and nonconvex optimization. Efficient techniques to deal with optimization over combinatoric and continuous variables, and with truncation issues for structure and control parameters of both the model space as well as the design space need to be developed. Author

N90-21079*# National Aeronautics and Space Administration. Langley Research Center, Hampton, VA.
A SURVEY OF EXPERIMENTS AND EXPERIMENTAL FACILITIES FOR ACTIVE CONTROL OF FLEXIBLE STRUCTURES
Dean W. Sparks, Jr., Garnett C. Horner, Jer-Nan Juang, and Gerhard Klose (Jet Propulsion Lab., California Inst. of Tech., Pasadena.) *In its* NASA/DOD Controls-Structures Interaction Technology 1989 Aug. 1989 p 285-315 (For primary document see N90-21062 14-18)
Avail: NTIS HC A23/MF A03 CSCL 22B

A brief survey of large space structure control related experiments and facilities was presented. This survey covered experiments performed before and up to 1982, and those of the present period (1982-...). Finally, the future planned experiments and facilities in support of the control-structure interaction (CSI) program were reported. It was stated that new, improved ground test facilities are needed to verify the new CSI design techniques that will allow future space structures to perform planned NASA missions. Author

N90-21080*# National Aeronautics and Space Administration. Langley Research Center, Hampton, VA.
NASA CSI SUSPENSION METHODS OVERVIEW
Stanley E. Woodard and Victor M. Cooley *In its* NASA/DOD Controls-Structures Interaction Technology 1989 Aug. 1989 p 317-333 (For primary document see N90-21062 14-18)
Avail: NTIS HC A23/MF A03 CSCL 22B

New suspension techniques will be necesary for ground testing the flexible spacecraft anticipated in NASA's future space activity. The most complex spacecraft involve nonlinear maneuvering (i.e., large angle slewing) with articulating substructures such as remote manipulating systems. The NASA control-structure interaction (CSI) ground test method team has begun researching and developing methodology to suspend the future class of spacecraft. This overview describes the work completed thus far. The research objective and technical approach will be presented first. Second, will be a suspension device overview followed by an assessment of existing hardware. Two different mechanical zero-spring-rate mechanisms will be compared for optimal performance. Next, will be a description of how existing hardware can be evolved to meet more general suspension requirements. A comparison of suspending articulating structures overhead vs underneath will follow. After a few experimental results from the zero-spring-rate mechanism/air suspension cart will be concluding remarks and future work. Author

N90-21081*# Martin Marietta Aerospace, Denver, CO.
AN AIR-BEARING WEIGHT OFFLOAD SYSTEM FOR GROUND TEST OF HEAVY LSS STRUCTURES
R. B. Rice *In* NASA, Langley Research Center, NASA/DOD Controls-Structures Interaction Technology 1989 Aug. 1989 p 335-34 (For primary document see N90-21062 14-18)
Avail: NTIS HC A23/MF A03 CSCL 22B

The capability and use of the Gravity Offload Facility (GOF) are discussed. Briefly explained are the: truss and base casting; carriage assembly; carriage weldment; vertical lift axis control; lifting cylinder; payload gimbal; motion base layout; and control processor. B.G.

N90-21082*# Lockheed Missiles and Space Co., Palo Alto, CA.
ASCIE: AN INTEGRATED EXPERIMENT TO STUDY CSI IN LARGE SEGMENTED OPTICAL SYSTEMS **c74**
Jean-Noel Aubrun and Kenneth R. Lorell *In* NASA, Langley Research Center, NASA/DOD Controls-Structures Interaction Technology 1989 Aug. 1989 p 349-36 (For primary document see N90-21062 14-18)
Avail: NTIS HC A23/MF A03 CSCL 20F

A description of the advanced structures/control integrated experiment (ASCIE) experimental setup, a generic test bed for several essential technologies was presented. In particular its multi-input, multi-output, non-collocated control system and its complex structural dynamics, characteristic of large segmented systems make it an ideal test bed for Control-Structure Interaction (CSI) experiments. The high accuracy of its measurement system will make it possible to investigate the dynamics of microvibrations and its implication for the CSI phenomenon. Author

N90-21083*# Texas A&M Univ., College Station.
CSI SENSING AND CONTROL: ANALYTICAL AND EXPERIMENTAL RESULTS
J. L. Junkins, T. C. Pollock, and Z. H. Rahman *In* NASA, Langley Research Center, NASA/DOD Controls-Structures Interaction Technology 1989 Aug. 1989 p 363-38 (For primary document see N90-21062 14-18)
Avail: NTIS HC A23/MF A03 CSCL 22B

Recent work on structural identification and large-angle maneuvers with vibration suppression was presented. The recent work has sought to balance structural and controls analysis activities by involving the analysts directly in the validation and experimental aspects of the research. Some new sensing, actuation, system identification, and control concepts were successfully implemented. An overview of these results is given. Author

N90-21084*# Jet Propulsion Lab., California Inst. of Tech., Pasadena.
EXPERIMENTAL EVALUATION OF ACTIVE-MEMBER CONTROL OF PRECISION STRUCTURES
James Fanson, Gary Blackwood, and Cheng-Chih Chu *In* NASA, Langley Research Center, NASA/DOD Controls-Structures Interaction Technology 1989 Aug. 1989 p 387-41 (For primary

document see N90-21062 14-18)
Avail: NTIS HC A23/MF A03 CSCL 22B

The results of closed loop experiments that use piezoelectric active-members to control the flexible motion of a precision truss structure are described. These experiments are directed toward the development of high-performance structural systems as part of the Control/Structure Interaction (CSI) program at JPL. The focus of CSI activity at JPL is to develop the technology necessary to accurately control both the shape and vibration levels in the precision structures from which proposed large space-based observatories will be built. Structural error budgets for these types of structures will likely be in the sub-micron regime; optical tolerances will be even tighter. In order to achieve system level stability and local positioning at this level, it is generally expected that some form of active control will be required. Author

N90-21085*# National Aeronautics and Space Administration. Marshall Space Flight Center, Huntsville, AL.
CONTROLS, ASTROPHYSICS, AND STRUCTURES EXPERIMENT IN SPACE (CASES)
Henry B. Waites and John P. Sharkey *In* NASA, Langley Research Center, NASA/DOD Controls-Structures Interaction Technology 1989 Aug. 1989 p 411-42 (For primary document see N90-21062 14-18)
Avail: NTIS HC A23/MF A03 CSCL 22B

As the size and performance requirements of future NASA and DOD spacecrafts and payloads tend to increase, the associated control systems that must effect these requirements tend to interact with the vehicle's structural dynamics. Some of the Control Structure Interaction (CSI) issues are being addressed in a flight experiment which is entitled CASES (Controls, Astrophysics and Structures Experiment in Space). As one of the first CSI flight experiments, the main emphasis for CASES is to provide a test bed for validating CSI developments and simultaneously, to pave the way for subsequent CSI experiments and science missions by establishing precedents for flight qualifying Large Space Structures (LSS)-class spacecraft. In addition, CASES provides an opportunity to obtain data bases for in-space controls and structures experiments and, at the same time, to gather hard x ray data from pertinent galactic sources. Author

N90-21086*# Naval Research Lab., Washington, DC.
LACE FLIGHT DYNAMICS EXPERIMENT
Shalom Fisher *In* NASA, Langley Research Center, NASA/DOD Controls-Structures Interaction Technology 1989 Aug. 1989 p 427-44 (For primary document see N90-21062 14-18)
Avail: NTIS HC A23/MF A03 CSCL 22B

The Low Power Atmospheric Compensation Experiment (LACE) is scheduled for launch in late 1989 into a 556 km altitude circular orbit of 43 deg inclination. The LACE flight dynamics experiment is an experiment secondary to the primary LACE mission. The purpose of the experiment is to provide on-orbit systems identification of the LACE spacecraft. The structure of the LACE spacecraft is of special interest to the CSI community. It incorporates 3 deployable/retractable booms of maximum length 45.72 m (150 ft) mounted on a rectangular parallelepiped bus of mass 1,200 kg. The zenith directed gravity gradient boom is mounted on the top of the bus; the retroreflector boom is mounted forward and deployed along the velocity vector, the balance boom is mounted and pointed aft. Attitude stabilization is accomplished by means of gravity gradient torques and by a momentum wheel. The LACE flight dynamics experiment is designed to measure modal frequencies, damping ratios, and oscillation amplitudes of the LACE spacecraft, as well as the vibration intensity generated by boom deployments and retractions. It is anticipated that this experiment will provide an opportunity for improvements in the accuracy of computer simulations of flexible structures and multibody dynamics. Author

N90-21087*# Air Force Wright Aeronautical Labs., Wright-Patterson AFB, OH.
SPACE TRUSS ZERO GRAVITY DYNAMICS
Andy Swanson *In* NASA, Langley Research Center, NASA/DOD Controls-Structures Interaction Technology 1989 Aug. 1989 p 445-45 (For primary document see N90-21062 14-18)
Avail: NTIS HC A23/MF A03 CSCL 22B

The Structural Dynamics Branch of the Air Force Flight Dynamics Laboratory in cooperation with the Reduced Gravity Office of the NASA Lyndon B. Johnson Space Center (JSC) plans to perform zero-gravity dynamic tests of a 12-meter truss structure. This presentation describes the program and presents all results obtained to date. Author

N90-21088*# Air Force Academy, CO.
UNITED STATES AIR FORCE ACADEMY GET-AWAY-SPECIAL FLEXIBLE BEAM EXPERIMENT
Keith W. Bubb, Steven E. Lamberson, and Thomas A. Lash *In* NASA, Langley Research Center, NASA/DOD Controls-Structures Interaction Technology 1989 Aug. 1989 p 459-47 (For primary document see N90-21062 14-18)
Avail: NTIS HC A23/MF A03 CSCL 22B

The Department of Astronautics at the United States Air Force Academy is currently planning to fly an experiment in a NASA Get-Away-Special (GAS) canister. The experiment was named the flex beam experiment. The primary technical objective of the flex beam experiment is to measure the damping of a thin beam in the vacuum and zero G environment of space. By measuring the damping in space, it is hoped to determine the amount of damping the beam normally experiences due to the gravitational forces present on Earth. This will allow validation of models which predict the dynamics of thin beams in the space environment. The experiment will also allow the Academy to develop and improve its ability to perform experiments within the confines of a NASA GAS canister. Several experiments, of limited technical difficulty, were flown by the Academy. More complex experiments are currently planned and it is hoped to learn techniques with each space shuttle flight. Author

N90-21089*# Jet Propulsion Lab., California Inst. of Tech., Pasadena.
CSI TECHNOLOGY VALIDATION ON AN LSS GROUND EXPERIMENT FACILITY **c14**
S. J. Wang and D. B. Eldred *In* NASA, Langley Research Center, NASA/DOD Controls-Structures Interaction Technology 1989 Aug. 1989 p 475-49 (For primary document see N90-21062 14-18)
Avail: NTIS HC A23/MF A03 CSCL 14B

The test bed developed at JPL for experimental evaluation of new technologies for the control of large flexible space structures is described. The experiment consists of a flexible spacecraft dynamic simulator, sensors, actuators, a microcomputer, and an advanced programming environment. The test bed has been operational for over a year, and thus far nine experiments were completed or are currently in progress. Several of these experiments were reported at the 1987 CSI conference, and several recent ones are documented in this paper, including high order adaptive control, non-parametric system identification, and mu-synthesis robust control. An aggressive program of experiments is planned for the forseeable future. Author

N90-21090*# National Aeronautics and Space Administration. Langley Research Center, Hampton, VA.
STRAIN AND DYNAMIC MEASUREMENTS USING FIBER OPTIC SENSORS EMBEDDED INTO GRAPHITE/EPOXY TUBES **c74**
D. W. DeHart, T. Doederlein, J. Koury (Air Force Astronautics Lab., Edwards AFB, CA.), R. S. Rogowski, J. S. Heyman, and M. S. Holben, Jr. *In its* NASA/DOD Controls-Structures Interaction Technology 1989 Aug. 1989 p 497-506 (For primary document see N90-21062 14-18)
Avail: NTIS HC A23/MF A03 CSCL 20F

Graphite/epoxy tubes were fabricated with embedded optical fibers to evaluate the feasibility of monitoring strains with a fiber optic technique. Resistance strain gauges were attached to the tubes to measure strain at four locations along the tube for comparison with the fiber optic sensors. Both static and dynamic

strain measurements were made with excellent agreement between the embedded fiber optic strain sensor and the strain gauges. Strain measurements of 10(exp -7) can be detected with the optical phase locked loop (OPLL) system using optical fiber. Because of their light weight, compatibility with composites, immunity to electromagnetic interference, and based on the static and dynamic results obtained, fiber optic sensors embedded in composites may be useful as the sensing component of smart structures. Author

N90-21091*# Air Force Astronautics Lab., Edwards AFB, CA.
INITIAL OPERATIONAL CAPABILITY OF THE ASTREX LARGE SPACE STRUCTURES TEST BED
G. A. Norris *In* NASA, Langley Research Center, NASA/DOD Controls-Structures Interaction Technology 1989 Aug. 1989 p 507-52 (For primary document see N90-21062 14-18)
Avail: NTIS HC A23/MF A03 CSCL 22B

Future DOD, NASA, and SDI space systems will be larger than any spacecraft flown before. The economics of placing these large space systems (LSS) into orbit dictates that they be as low in mass as possible. The combination of very large size and relatively low mass produces systems which possess little structural rigidity. This flexibility causes severe technical problems when combined with the precise shape and pointing requirements associated with many future LSS missions. Development of new control technologies which can solve these problems and enable future LSS missions is under way, but a test bed is needed for demonstration and evaluation of the emerging control hardware (sensors and actuators) and methodologies. In particular, the need exists for a facility which enables both large angle slewing and subsequent pointing/shape control of a variety of flexible bodies. The Air Force Astronautics Laboratory (AFAL) has conceived the Advanced Space Structures Technology Research Experiments (ASTREX) facility to fill this need. An overview of the ASTREX facility is given. Author

N90-21092*# Air Force Wright Aeronautical Labs., Wright-Patterson AFB, OH.
IN-HOUSE EXPERIMENTS IN LARGE SPACE STRUCTURES AT THE AIR FORCE WRIGHT AERONAUTICAL LABORATORIES FLIGHT DYNAMICS LABORATORY
Robert W. Gordon, Umit Ozguner, and Steven Yurkovich (Ohio State Univ., Columbus.) *In* NASA, Langley Research Center, NASA/DOD Controls-Structures Interaction Technology 1989 Aug. 1989 p 523-54 (For primary document see N90-21062 14-18)
Avail: NTIS HC A23/MF A03 CSCL 22B

The Flight Dynamics Laboratory is committed to an in-house, experimental investigation of several technical areas critical to the dynamic performance of future Air Force large space structures. The advanced beam experiment was successfully completed and provided much experience in the implementation of active control approaches on real hardware. A series of experiments is under way in evaluating ground test methods on the 12 meter trusses with significant passive damping. Ground simulated zero-g response data from the undamped truss will be compared directly with true zero-g flight test data. The performance of several leading active control approaches will be measured and compared on one of the trusses in the presence of significant passive damping. In the future, the PACOSS dynamic test article will be set up as a test bed for the evaluation of system identification and control techniques on a complex, representative structure with high modal density and significant passive damping. Author

N90-21093# Instituto de Pesquisas Espaciais, Sao Jose dos Campos (Brazil).
DESIGN OF A DIGITAL MODEL FOLLOWING CONTROLLER OF REACTION WHEEL TORQUES
Gilberto daCunhaTrivelato and Marcelo LopesdeOliveiraeSouza Dec. 1988 9 p In PORTUGUESE; ENGLISH summary Presented at the 7th SBA Congresso Brasileiro de Automatica, Sao Jose dos Campos, Brazil, 15-19 Aug. 1988
(INPE-4753-PRE/1425) Avail: NTIS HC A02/MF A01

The design of a digital model following controller of reaction wheel torques (used in attitude control of artificial satellites) is presented. This controller is intended to reduce the effects of wheel disturbing torques, and wheel sensor noises on the wheel torque. The controller structure used, the criteria for choosing the wheel sampling time, the controller gain, the sensor quantization level, and the current quantization level is summarized while considering the wheel torque requirements. Finally, the digitally simulated system response to zero and step reference torques, and the corresponding hardware implemented responses are discussed. These tests show that such a controller reduces considerably those effects and satisfies those requirements, and the design criteria used are satisfactory. Author

N90-21094# Instituto de Pesquisas Espaciais, Sao Jose dos Campos (Brazil).
ATTITUDE CONTROL MODES FOR THE MECB REMOTE SENSING SATELLITES
Danton Nunes Dec. 1988 8 p Presented at the 6th Japan-Brazil Symposium on Science and Technology, Space Science and Technology Workshop, Sao Jose dos Campos, Brazil, 10-12 Aug. 1988 Submitted for publication
(INPE-4755-PRE/1427) Avail: NTIS HC A02/MF A01

The MECB (Brazilian Complete Space Mission) remote sensing satellites (RSS) will operate from a circular polar heliosynchronous orbit to take pictures from the Earth in the visible and near infrared bands, with global coverage of 4 days. These satellites will be three axis stabilized with active attitude control. The operating modes of the attitude and orbit control subsystem (AOCS) and the several maneuvers necessary to lead from unknown attitude and angular rate, after separation, to nominal Earth pointing for photography are presented. Author

N90-21095*# National Aeronautics and Space Administration. Marshall Space Flight Center, Huntsville, AL.
GLOBAL NONLINEAR OPTIMIZATION OF SPACECRAFT PROTECTIVE STRUCTURES DESIGN
R. A. Mog, J. N. Lovett, Jr. (Alabama Univ., Huntsville.), and S. L. Avans Jan. 1990 29 p
(NASA-TM-100387; NAS 1.15:100387) Avail: NTIS HC A03/MF A01 CSCL 22B

The global optimization of protective structural designs for spacecraft subject to hypervelocity meteoroid and space debris impacts is presented. This nonlinear problem is first formulated for weight minimization of the space station core module configuration using the Nysmith impact predictor. Next, the equivalence and uniqueness of local and global optima is shown using properties of convexity. This analysis results in a new feasibility condition for this problem. The solution existence is then shown, followed by a comparison of optimization techniques. Finally, a sensitivity analysis is presented to determine the effects of variations in the systemic parameters on optimal design. The results show that global optimization of this problem is unique and may be achieved by a number of methods, provided the feasibility condition is satisfied. Furthermore, module structural design thicknesses and weight increase with increasing projectile velocity and diameter and decrease with increasing separation between bumper and wall for the Nysmith predictor. Author

N90-21096*# National Aeronautics and Space Administration. Langley Research Center, Hampton, VA.
PRELIMINARY DESIGN APPROACH FOR LARGE HIGH PRECISION SEGMENTED REFLECTORS
Martin M. Mikulas, Jr., Timothy J. Collins, and John M. Hedgepeth (Astro Aerospace Corp., Carpinteria, CA.) Feb. 1990 51 p
(NASA-TM-102605; NAS 1.15:102605) Avail: NTIS HC A04/MF A01 CSCL 22B

A simplified preliminary design capability for erectable precision segmented reflectors is presented. This design capability permits a rapid assessment of a wide range of reflector parameters as well as new structural concepts and materials. The preliminary design approach was applied to a range of precision reflectors from 10 meters to 100 meters in diameter while considering standard design drivers. The design drivers considered were: weight, fundamental frequency, launch packaging volume, part

count, and on-orbit assembly time. For the range of parameters considered, on-orbit assembly time was identified as the major design driver. A family of modular panels is introduced which can significantly reduce the number of reflector parts and the on-orbit assembly time. Author

N90-21097*# Ball Aerospace Systems Div., Boulder, CO.
BASG THERMOMECHANICAL PUMP HELIUM 2 TRANSFER TESTS
G. L. Mills, D. A. Newell, and A. R. Urbach Mar. 1990 72 p
(Contract NAS2-11979)
(NASA-CR-177541; A-90127; NAS 1.26:177541) Avail: NTIS HC A04/MF A01 CSCL 22B

The purpose of the effort described was to perform experiments and calculations related to using a thermomechanical pump in the space-based resupply of the Space Infrared Telescope Facility (SIRTF) with Helium 2. Thermomechanical (fountain effect) pumps have long been suggested as a means for pumping large quantities of Helium 2. The unique properties of Helium 2 have made it useful for cooling space instruments. Several space science missions, including SIRTF, are now being planned which would benefit greatly from on-orbit resupply of Helium 2. A series of experiments were performed to demonstrate that large volumes of Helium 2 can be transferred with a thermomechanical pump at high flow rates and at high efficiency from one dewar to another through valves and lines that are similar to the plumbing arrangement that would be necessary to accomplish such a transfer on-orbit. In addition, temperature, pressure, and flow rate data taken during the tests were used to verify and refine a computer model which was developed. Author

N90-21098*# National Aeronautics and Space Administration. Lyndon B. Johnson Space Center, Houston, TX.
COSMIC DUST COLLECTION FACILITY: SCIENTIFIC OBJECTIVES AND PROGRAMMATIC RELATIONS
Fred Hoerz, ed., D. E. Brownlee, T. E. Bunch, D. Grounds, E. Grun, Y. Rummel, W. L. Quaide, and R. M. Walker Mar. 1990 32 p
(NASA-TM-102160; S-602; NAS 1.15:102160) Avail: NTIS HC A03/MF A01 CSCL 22B

The science objectives are summarized for the Cosmic Dust Collection Facility (CDCF) on Space Station Freedom and these objectives are related to ongoing science programs and mission planning within NASA. The purpose is to illustrate the potential of the CDCF project within the broad context of early solar system sciences that emphasize the study of primitive objects in state-of-the-art analytical and experimental laboratories on Earth. Current knowledge about the sources of cosmic dust and their associated orbital dynamics is examined, and the results are reviewed of modern microanalytical investigations of extraterrestrial dust particles collected on Earth. Major areas of scientific inquiry and uncertainty are identified and it is shown how CDCF will contribute to their solution. General facility and instrument concepts that need to be pursued are introduced, and the major development tasks that are needed to attain the scientific objectives of the CDCF project are identified. Author

N90-21099*# DRC Consultants, Inc., Flushing, NY.
HEAVILY LOADED JOINTS FOR ASSEMBLING AEROBRAKE SUPPORT TRUSSES
Hannskarl Bandel, Nils Olsson, and Boris Levintov Mar. 1990 111 p Prepared for Boeing Co., Seattle, WA
(Contract NAS1-18224)
(NASA-CR-181992; NAS 1.26:181992) Avail: NTIS HC A06/MF A01 CSCL 22B

The major emphasis was to develop erectable joints for large aerobrake support trusses. The truss joints must be able to withstand the large forces experienced by the truss during the aero-pass, as well as be easily assembled and disassembled on orbit by astronauts or robots. Other important design considerations include; strength, stiffness, and allowable error in strut length. Six mechanical joint designs, as well as a seventh joint design, where a high strength epoxy is injected to make the connection rigid, are presented. Author

N90-21100# Air Force Inst. of Tech., Wright-Patterson AFB, OH.
NASA'S ADVANCED COMMUNICATIONS TECHNOLOGY SATELLITE (ACTS): WILL IT BENEFIT COMMERCIAL/MILITARY SATELLITES M.S. Thesis
Colin B. Cosgrove, Jr. 1988 104 p
(AD-A217710; AFIT/CI/CIA-88-242) Avail: NTIS HC A06/MF A01 CSCL 22/2

In 1978 NASA began research and development activities to determine needed technological advancements for the next generation or satellite communications systems. From this beginning evolved the Advanced Communications Technology Satellite (ACTS) program. The purpose of the ACTS is to develop and flight-test high-risk technologies necessary for the United States' continued communications. NASA identified the key technologies of onboard baseband processor, microwave switch matrix, multiple beam antennas with electronically hopping narrow spot beams, automatic rain fade compensation, and Ka band (20/30 GHz) components for inclusion in the ACTS program. With the ACTS scheduled for launch in 1992, whether or not the program will provide the desired benefits to commercial and military satellites is determined. This determination is reached by first reviewing the technologies of the ACTS as well as those of present and planned communications satellites in commercial and military sectors. By comparing the reviewed technologies, a conclusion about the ACTS' ability to fulfill NASA's goal is reached. GRA

N90-21101# Nuclear Utility Services, Inc., Gaithersburg, MD.
FINAL SAFETY ANALYSIS REPORT FOR THE ULYSSES MISSION. VOLUME 3 (BOOK 1): NUCLEAR RISK ANALYSIS DOCUMENT
Mar. 1990 39 p
(Contract DE-AC01-87NE-32134)
(DE90-008691; NUS-5250-Vol-3-Bk-1; ULS-FSAR-005) Avail: NTIS HC A03/MF A01

The purpose of the Nuclear Risk Analysis Document (NRAD) is to provide an analysis of the range of potential consequences of accidents which have been identified during the launching and deployment of the Ulysses mission spacecraft. The specific consequences analyzed are those associated with the possible release of radioactive material (fuel) of the Radioisotope Thermoelectric Generator (RTG). They are in terms of radiation doses to people and areas of deposition of radioactive material. These consequence analyses can be used in several ways. One way is to identify the potential range of consequences which might have to be dealt with if there were to be an accident with a release of fuel to assure that, given such an accident, the health and safety of the public will be reasonably protected. Another use of the information, along with accident and release probabilities, is to estimate the risks associated with the mission. That is, most space launches occur without incident. Given an accident, the most probable result relative to the RTGs is complete containment of the radioactive material. Only a small fraction of accidents might result in a release of fuel and subsequent radiological consequences. The combination of probability with consequence is risk, which can be compared to other human and societal risks to assure that no undue risks are implied by undertaking the mission. DOE

N90-21102# Nuclear Utility Services, Inc., Gaithersburg, MD.
FINAL SAFETY ANALYSIS REPORT FOR THE ULYSSES MISSION. VOLUME 3 (BOOK 2): NUCLEAR RISK ANALYSIS DOCUMENT-APPENDICES
Mar. 1990 194 p
(Contract DE-AC01-87NE-32134)
(DE90-008692; NUS-5250-Vol-3-Bk-2; ULS-FSAR-006) Avail: NTIS HC A09/MF A02

This appendix describes the methods used in evaluating the radiological consequences and the integrated mission risks presented in the Nuclear Risk Analysis Document (NRAD), Book

1. Since the location of an accident having a release is important to the type of accidents that are possible, the amount of release, and to the consequences of that release, each mission phase is analyzed separately. Mission Phases 0 and 1 are on the launch pad or during early ascent in the Cape Canaveral area. Consequence analyses during these phases make use of meteorological, demographic, and land use data for the Kennedy Space Center (KSC) and environs. Phase 2 involves the possibility of a failure during later ascent with a reentry and impact along an African ground track. An accident during Phases 3 and 4 can result in a reentry anywhere within the 28 deg north 28 deg south latitude bands. A worldwide data base has been used for the accident consequence analyses for mission Phases 2, 3, and 4. The specific data used for these analyses are contained in Appendices C, E, F, and G. DOE

N90-21103# General Electric Co., Philadelphia, PA. Astro Space Div.
FINAL SAFETY ANALYSIS REPORT FOR THE ULYSSES MISSION. VOLUME 2 (BOOK 1): ACCIDENT MODEL DOCUMENT
Mar. 1990 121 p
(Contract DE-AC01-79ET-32043)
(DE90-008694; DOE/ET-32043/T31-Vol-2-Bk-1; ULS-FSAR-003)
Avail: NTIS HC A06/MF A02

The status of the accident analysis for the Ulysses outer planetary space science mission is presented in this Final Safety Analysis Report (FSAR). This mission employs a Radioisotope Thermoelectric Generator (RTG) as the prime electrical power source for the spacecraft. Ulysses will be launched into Earth orbit using the Space Shuttle and will use the Inertial Upper Stage (IUS)/Payload Assist Module - Special (PAM-S) boosters to place the spacecraft into an Earth escape trajectory. The RTG employs silicon-germanium thermoelectric couples to produce electricity from the heat energy that results from the decay of the radioisotope fuel, Plutonium-238, used in the RTG heat source. The heat source configuration used in the RTG is termed General Purpose Heat Source (GPHS), and the RTG is designated GPHS-RTG. The use of radioactive material in these missions necessitates evaluations of the radiological risks that may be encountered by launch complex personnel as well as by the Earth's general population resulting from postulated malfunctions or failures occurring in the mission operations. The FSAR presents the results of a rigorous safety assessment, including substantial analyses and testing, of the launch and deployment of the RTG for the Ulysses mission. DOE

N90-21104# General Electric Co., Philadelphia, PA. Astro Space Div.
FINAL SAFETY ANALYSIS REPORT FOR THE ULYSSES MISSION. VOLUME 2: ACCIDENT MODEL DOCUMENT-APPENDICES
Mar. 1990 673 p
(Contract DE-AC01-79ET-32043)
(DE90-008695; DOE/ET-32043/T31-Vol-2-Bk-2; ULS-FSAR-004)
Avail: NTIS HC A99/MF A04

This section of the Accident Model document presents the appendices which describe the various analyses that have been conducted for use in the Ulysses Final Safety Analysis Report. Included in these appendices are the approaches, techniques, conditions and assumptions used in the development of the analytical models plus the detailed results of the analyses. Also included in these appendices are summaries of the accidents and their associated probabilities and environment models taken from the Shuttle Data Book (NSTS-08116), plus summaries of the several segments of a recent safety test program. Accident Definition and Probabilities; Accident Environments; Hydrocode Analysis of Radioisotope Thermionic Generator (RTG) Response to Accident Environments; Launch Accident Scenario Evaluation Program (LASEP); JPL Reentry Breakup Analysis; Safety Test Program Summary and Result; and Vaporization of PuO2 in a Space Shuttle Fireball are among the appendices includes. DOE

N90-21105# Instituto de Pesquisas Espaciais, Sao Jose dos Campos (Brazil).
SPACE ENVIRONMENT SIMULATION OF THE SCD-01 SATELLITE THROUGH HEATING PLATES [SIMULACAO DO AMBIENTE ESPACIAL DO SATELITE SCD-01 POR PLACAS AQUECEDORAS]
Humberto PontesCardoso and Ezio CastejonGarcia Aug. 1989 6 p In PORTUGUESE; ENGLISH summary Presented at the 10th Brazilian Conference on Mechanical Engineering, COBEM, Rio de Janeiro, Brazil, 5-8 Dec. 1989
(INPE-4988-PRE/1550) Avail: NTIS HC A02/MF A01

The space simulation model was developed for the realization of thermal vacuum tests acceptance of the SCD-01 Brazilian satellite. The adopted method is based in the simulation by infrared heater plates. The results confirmed the technic suitability. Author

N90-21106# Nuclear Utility Services, Inc., Gaithersburg, MD.
FINAL SAFETY ANALYSIS REPORT FOR THE ULYSSES MISSION Executive Summary
Mar. 1990 25 p
(Contract DE-AC01-87NE-32134)
(DE90-008690; NUS-5249-Exec-Summ;
ULS-FSAR-001-Exec-Summ) Avail: NTIS HC A03/MF A01

This document is a condensed version of the information presented in the Ulysses Mission Final Safety Analysis Report (FSAR). An earlier Safety Status Report (January 31, 1990) presented interim information to support NASA's Environmental Impact Statement for the mission. It was the best information available at the time the National Environmental Policy Act (NEPA) process required for timely support of NASA's decision making process. Section 1 of this Summary Report is a brief description of the Ulysses Mission. Section 2 contains descriptions of the Ulysses spacecraft, the Radioisotope Thermoelectric Generator that provides electrical power to the scientific instruments, radios, and control systems, and a description of the launch vehicle. Section 3 is a summary description of the Ulysses mission accident analyses and risk assessment and their results. DOE

N90-21107# General Electric Co., Philadelphia, PA. Astro Space Div.
FINAL SAFETY ANALYSIS REPORT FOR THE ULYSSES MISSION. VOLUME 1: REFERENCE DESIGN DOCUMENT
Mar. 1990 160 p
(Contract DE-AC01-79ET-32043)
(DE90-008693; DOE/ET-32043/T31-Vol-1; ULS-FSAR-002-Vol-1)
Avail: NTIS HC A08/MF A01

The Final Safety Analysis Report (FSAR) 2 consists of three volumes which are related to the safety analysis of the Ulysses mission: Volume 1, Reference Design Document (RDD); Volume 2, Accident Model Document (AMD); and Volume 3, Nuclear Risk Analysis Document (NRAD). An Executive Summary pertaining to Volumes 1 and 2 is also provided. Volume 1, this document, provides the background design information required to understand the analyses presented in Volumes 2 and 3. It contains descriptions of the Radioisotope Thermionic Generator (RTG), the Ulysses spacecraft, the Space Shuttle, the Inertial Upper Stage (IUS), the Payload Assist Module --- Special (PAM-S), the trajectory and flight characteristics including flight contingency modes, and the launch site. There are two appendices in Volume 1 which provide detailed material properties for the RTG. DOE

19 SPACECRAFT INSTRUMENTATION

For related information see also *06 Aircraft Instrumentation* and *35 Instrumentation and Photography.*

N90-21063*# Jet Propulsion Lab., California Inst. of Tech., Pasadena.
A SPACEBORNE OPTICAL INTERFEROMETER: THE JPL CSI MISSION FOCUS
R. A. Laskin *In* NASA, Langley Research Center, NASA/DOD

Controls-Structures Interaction Technology 1989 Aug. 1989 p 1-15 (For primary document see N90-21062 14-18)
Avail: NTIS HC A23/MF A03 CSCL 14B

20 SPACECRAFT PROPULSION AND POWER

Includes main propulsion systems and components, e.g., rocket engines; and spacecraft auxilliary power sources.

For related information see also *07 Aircraft Propulsion and Power, 28 Propellants and Fuels, 44 Energy Production and Conversion,* and *15 Launch Vehicles and Space Vehicles.*

N90-21108*# Texas A&M Univ., College Station. Dept. of Nuclear Engineering.
A RADIOLOGICAL ASSESSMENT OF NUCLEAR POWER AND PROPULSION OPERATIONS NEAR SPACE STATION FREEDOM Contract Report, Jan. 1988 - Jan. 1990
Wesley E. Bolch, J. Kelly Thomas, K. Lee Peddicord, Paul Nelson, David T. Marshall, and Donna M. Busche Mar. 1990 115 p
(Grant NAG3-944)
(NASA-CR-185185; NAS 1.26:185185) Avail: NTIS HC A06/MF A01 CSCL 10B

Scenarios were identified which involve the use of nuclear power systems in the vicinity of Space Station Freedom (SSF) and their radiological impact on the SSF crew was quantified. Several of the developed scenarios relate to the use of SSF as an evolutionary transportation node for lunar and Mars missions. In particular, radiation doses delivered to SSF crew were calculated for both the launch and subsequent return of a Nuclear Electric Propulsion (NEP) cargo vehicle and a Nuclear Thermal Rocket (NTR) personnel vehicle to low earth orbit. The use of nuclear power on co-orbiting platforms and the storage and handling issues associated with radioisotope power systems were also explored as they relate to SSF. A central philosophy in these analyses was the utilization of a radiation dose budget, defined as the difference between recommended dose limits from all radiation sources and estimated doses received by crew members from natural space radiations. Consequently, for each scenario examined, the dose budget concept was used to identify and quantify constraints on operational parameters such as launch separation distances, returned vehicle parking distances, and reactor shutdown times prior to vehicle approach. The results indicate that realistic scenarios do not exist which would preclude the use of nuclear power sources in the vicinity of SSF. The radiation dose to the SSF crew can be maintained at safe levels solely by implementing proper and reasonable operating procedures. Author

N90-21109*# Ohio State Univ., Columbus. Dept. of Aeronautical and Astronautical Engineering.
THE EFFECTS OF MAGNETIC NOZZLE CONFIGURATIONS ON PLASMA THRUSTERS Semiannual Progress Report, 1 Jul. - 31 Dec. 1989
Thomas M. York Feb. 1990 71 p
(Grant NAG3-843)
(NASA-CR-186465; NAS 1.26:186465; AARL-P-90-1) Avail: NTIS HC A04/MF A01 CSCL 21C

Plasma thrusters have been operated at power levels from 10 kw to 0.1 MW. When these devices have had magnetic fields applied to them which form a nozzle configuration for the expanding plasma, they have shown marked increases in exhaust velocity which is in direct proportion to the magnitude of the applied field. Further, recent results have shown that electrode erosion may be influenced by applied magnetic fields. This research effort is directed to the experimental and computational study of the effects of applied magnetic field nozzles in the acceleration of plasma flows. Plasma source devices which eliminate the plasma interaction in normal thrusters are studied as most basic. Normal thruster configurations were studied without applied fields and with applied magnetic nozzle fields. Unique computational studies utilize existing codes which accurately include transport processes. Unique diagnostic studies supported the experimental studies to generate new data. Both computation and diagnostics were combined to indicate the physical mechanisms and transport properties that are operative in order to allow scaling and accurate prediction of thruster performance. Author

N90-21110*# National Aeronautics and Space Administration. Lewis Research Center, Cleveland, OH.
THE EFFECT OF LEVELING COATINGS ON THE ATOMIC OXYGEN DURABILITY OF SOLAR CONCENTRATOR SURFACES
Kim K. deGroh, Therese M. Dever, and William F. Quinn (Cleveland State Univ., OH.) Apr. 1990 18 p Presented at the 8th International Conference on Thin Films, and the 17th International Conference on Metallurgical Coatings, San Diego, CA, 2-6 Apr. 1990; spons. in part by Intern. Union for Vacuum Sci., Tech., and Appl. and the Amer. Vacuum Society
(NASA-TM-102557; E-5375; NAS 1.15:102557) Avail: NTIS HC A03/MF A01 CSCL 10A

Space power systems for Space Station Freedom will be exposed to the harsh environment of low earth orbit (LEO). Neutral atomic oxygen is the major constituent in LEO and has the potential of severely reducing the efficiency of solar dynamic power systems through degradation of the concentrator surfaces. Several transparent dielectric thin films have been found to provide atomic oxygen protection, but atomic oxygen undercutting at inherent defect sites is still a threat to solar dynamic power system survivability. Leveling coatings smooth microscopically rough surfaces, thus eliminating potential defect sites prone to oxidation attack on concentrator surfaces. The ability of leveling coatings to improve the atomic oxygen durability of concentrator surfaces was investigated. The application of a EPO-TEK 377 epoxy leveling coating on a graphite epoxy substrate resulted in an increase in solar specular reflectance, a decrease in the atomic oxygen defect density by an order of magnitude and a corresponding order of magnitude decrease in the percent loss of specular reflectance during atomic oxygen plasma ashing. Author

N90-21111 Department of the Navy, Washington, DC.
CONCENTRIC LAYER RAMJET FUEL Patent
George W. Burdette, inventor (to Navy) and John P. Francis, inventor (to Navy) 8 Mar. 1988 5 p Filed 8 Dec. 1986
(AD-D014443; US-Patent-4,729,317; US-Patent-Appl-SN-938922; US-Patent-Class-102-287) Avail: US Patent and Trademark Office CSCL 21/5

An air-breathing solid fuel rocket motor containing a solid fuel ramjet grain having a plurality of concentric layers of solid fuel which provide a means of controlling the thrust of the motor is disclosed. GRA

N90-21112 Virginia Polytechnic Inst. and State Univ., Blacksburg.
STRESS ANALYSIS OF ROCKET MOTORS WITH VISCOELASTIC PROPELLANT BY A MIXED FINITE ELEMENT MODEL Ph.D. Thesis
Yung Tun Lin 1989 195 p
Avail: Univ. Microfilms Order No. DA9005012

A mixed variational statement and corresponding finite element model are developed for an axisymmetric solid body under external symmetric loads using the updated Lagrangian formulation. The mixed finite element formulation treats the nodal displacements and stresses as the variables that can be approximated independently. The method of static condensation is used to keep some stresses across interfaces of a solid of revolution discontinuous. The stiffness matrix is transformed from semi-positive definite to positive definite. A rocket motor is composed of case, propellant, and hollow air core and is modeled as an axisymmetric solid. The propellant of a rocket motor is treated as a viscoelastic material. Static and dynamic analyses are performed under two opposite line loads, two opposite patch loads and one line and one patch load combination. The modified Newton-Raphson method is used in the solutions of nonlinear algebraic equations. The analysis of free vibration is executed

first and then the Newmark direct integration method is used in a transient analysis. Results of these analyses are compared with solutions obtained from different methods that are independent of the finite element method. Author

N90-21113*# Toledo Univ., OH. Dept. of Electrical Engineering.
A COMPARATIVE STUDY OF ELECTRIC POWER DISTRIBUTION SYSTEMS FOR SPACECRAFT Final Report, 19 Jun. - 31 Dec. 1989
Thomas A. Stuart and Roger J. King Jan. 1990 134 p
(Grant NAG3-708)
(NASA-CR-186531; NAS 1.26:186531) Avail: NTIS HC A07/MF A01 CSCL 22B

The electric power distribution systems for spacecraft are compared concentrating on two interrelated issues: the choice between dc and high frequency ac, and the converter/inverter topology to be used at the power source. The relative merits of dc and ac distribution are discussed. Specific converter and inverter topologies are identified and analyzed in detail for the purpose of detailed comparison. Finally, specific topologies are recommended for use in dc and ac systems. Author

N90-21114*# National Aeronautics and Space Administration. Lewis Research Center, Cleveland, OH.
RECENT STIRLING ENGINE LOSS-UNDERSTANDING RESULTS
Roy C. Tew, Lanny G. Thieme, and James E. Dudenhoefer 1990 11 p Prepared for presentation at the 25th Intersociety Energy Conversion Engineering Conference, Reno, NV, 12-17 Aug. 1990; sponsored in part by AIChE, SAE, ACS, AIAA, ASME, and IEEE
(NASA-TM-103122; E-5450; NAS 1.15:103122) Avail: NTIS HC A03/MF A01 CSCL 10B

For several years, NASA and other U.S. government agencies have been funding experimental and analytical efforts to improve the understanding of Stirling thermodynamic losses. NASA's objective is to improve Stirling engine design capability to support the development of new engines for space power. An overview of these efforts was last given at the 1988 IECEC. Recent results of this research are reviewed. Author

N90-21115# Instituto de Pesquisas Espaciais, Sao Jose dos Campos (Brazil).
NUMERICAL SIMULATION MODEL FOR HYDRAZINE ATTITUDE CONTROL THRUSTERS. PART 1: MODEL DESCRIPTION
Sonia Maria GomesdeGonzalezVillalobos and Philippe Remy Bernar Devloo [1989] 46 p
(INPE-4952-RPE/601) Avail: NTIS HC A03/MF A01

A sufficiently detailed model was developed of the operation of catalytic reactors as those used in monopropellant hydrazine thrusters. Transient continuous operation of a plug flow reactor with heat and mass transfer between gas and solid phases was considered. By employing appropriate conservation equations for the two phases, reactor operation can be described in terms of a system of nonlinear differential equations. A finite element algorithm was derived from the SUPG method and a computer program was designed in order to simulate the transient numerical model. Steady-state temperature and concentration profiles are shown for a typical reactor configuration. Author

N90-21116*# National Aeronautics and Space Administration. Lewis Research Center, Cleveland, OH.
EFFECT OF KOH CONCENTRATION ON LEO CYCLE LIFE OF IPV NICKEL-HYDROGEN FLIGHT BATTERY CELLS
John J. Smithrick and Stephen W. Hall (Naval Weapons Support Center, Crane, IN.) 1990 8 p Proposed for presentation at the 25th Intersociety Energy Conversion Engineering Conference, Reno, NV, 12-17 Aug. 1990; cosponsored by AIChE, SAE, ACS, AIAA, ASME, IEEE
(NASA-TM-103127; E-5457; NAS 1.15:103127) Avail: NTIS HC A02/MF A01 CSCL 10C

A breakthrough in low earth orbit (LEO) cycle life of individual pressure vessel (IPV) nickel hydrogen battery cells was reported. The cycle life of boiler plate cells containing 26 percent potassium hydroxide (KOH) electrolyte was about 40,000 LEO cycles compared to 3500 cycles for cells containing 31 percent KOH. The effect of KOH concentration on cycle life was studied. The cycle regime was a stressful accelerated LEO, which consisted of a 27.5 min charge followed by a 17.5 min charge (2 x normal rate). The depth of discharge (DOD) was 80 percent. The cell temperature was maintained at 23 C. The next step is to validate these results using flight hardware and a real time LEO test. NASA Lewis has a contract with the Naval Weapons Support Center (NWSC), Crane, Indiana, to validate the boiler plate test results. Six 48 A-hr Hughes recirculation design IPV nickel-hydrogen flight battery cells are being evaluated. Three of the cells contain 26 percent KOH (test cells) and three contain 31 percent KOH (control cells). They are undergoing real time LEO cycle life testing. The cycle regime is a 90-min LEO orbit consisting of a 54-min charge followed by a 36-min discharge. The depth-of-discharge is 80 percent. The cell temperature is maintained at 10 C. The cells were cycled for over 8000 cycles in the continuing test. There were no failures for the cells containing 26 percent KOH. There was two failures, however, for the cells containing 31 percent KOH. Author

N90-21117*# Thiokol Corp., Brigham City, UT. Space Operations.
TECHNICAL EVALUATION MOTOR NO. 5 (TEM-5) Final Report
M. Cook 19 Mar. 1990 195 p
(Contract NAS8-30490)
(NASA-CR-183932; NAS 1.26:183932; TWR-17649) Avail: NTIS HC A09/MF A02 CSCL 21H

Technical Evaluation Motor No. 5 (TEM-5) was static test fired at the Thiokol Corporation Static Test Bay T-97. TEM-5 was a full scale, full duration static test fire of a high performance motor (HPM) configuration solid rocket motor (SRM). The primary purpose of TEM static tests is to recover SRM case and nozzle hardware for use in the redesigned solid rocket motor (RSRM) flight program. Inspection and instrumentation data indicate that the TEM-5 static test firing was successful. The ambient temperature during the test was 41 F and the propellant mean bulk temperature (PMBT) was 72 F. Ballistics performance values were within the specified requirements. The overall performance of the TEM-5 components and test equipment was nominal. Dissembly inspection revealed that joint putty was in contact with the inner groove of the inner primary seal of the ignitor adapter-to-forward dome (inner) joint gasket; this condition had not occurred on any previous static test motor or flight RSRM. While no qualification issues were addressed on TEM-5, two significant component changes were evaluated. Those changes were a new vented assembly process for the case-to-nozzle joint and the installation of two redesigned field joint protection systems. Performance of the vented case-to-nozzle joint assembly was successful, and the assembly/performance differences between the two field joint protection system (FJPS) configurations were compared. Author

23 CHEMISTRY AND MATERIALS (GENERAL)

N90-21118* National Aeronautics and Space Administration. Langley Research Center, Hampton, VA.
BIS(4-(3,4-DIMETHYLENEPYRROLIDYL)-PHENYL) METHANE Patent
Raphael M. Ottenbrite, inventor (to NASA) (Virginia Commonwealth Univ., Richmond.) 25 Jul. 1989 6 p Filed 19 Jul. 1988
(Grant NAG1-672)
(NASA-Case-LAR-13965-1-CU; US-Patent-4,851,544; US-Patent-Appl-SN-221386; US-Patent-Class-548-524;

US-Patent-Class-526-262; US-Patent-Class-528-322; US-Patent-Class-548-400) Avail: US Patent and Trademark Office CSCL 07A

It is the primary object of the present invention to prepare high temperature polymeric materials, especially linear aromatic polyimides, which maintain their integrity and toughness during long exposure times at elevated temperatures. According to the present invention, this object is achieved, and the attending benefits are obtained, by first providing the bis(exocyclodiene) bis(4-(3,4-dinethylene pyrrolidyl) phenyl) methane, which is formed from the monomer N-phenyl 3,4-dimethylene pyrrolidine. This bis-(exocyclodiene) undergoes Diels-Alder reaction with a bismaleimide without the evolution of gaseous by-products, to form the aromatic polyimide.

Official Gazette of the U.S. Patent and Trademark Office

24 COMPOSITE MATERIALS

Includes physical, chemical, and mechanical properties of laminates and other composite materials.

For ceramic materials see *27 Nonmetallic Materials*.

N90-21119 Stanford Univ., CA.
FILAMENT WINDING OF COMPOSITE CYLINDERS Ph.D. Thesis
Emilio P. Calius 1989 206 p
Avail: Univ. Microfilms Order No. DA8925840

A model was developed for the analysis of the effects of the manufacturing process upon filament-wound cylinders made of a thermoset matrix composite. The model relates the process variables (winding speed, fiber tension, applied temperature) to the parameters characterizing the composite cylinder and the mandrel. The model is applicable to cylinders for which the diameter is large compared to the wall thickness. The model was implemented in a user-friendly computer code suitable for generating numerical results. During the winding and the subsequent oven curing the model and the corresponding code provide: the temperature throughout the cylinder and mandrel, the degree of cure throughout the cylinder, the viscosity throughout the cylinder, the fiber positions, the fiber tensions, the stresses and strains throughout the cylinder and mandrel, and the porosity throughout the cylinder. Tests were performed to validate the model. In these tests 3, 4, and 6 inch internal diameter cylinders were wound using Hercules and Fiberite graphite-epoxy tows. The temperatures and strains inside these cylinders were measured. The measured temperatures and strains were compared to those computed by the computer simulation. Good agreements were found between the data and the results of this model, indicating that the model is a useful representation of the process. A sample problem is also presented which demonstrates what information can be generated by the model. The use of the model in the selection of the proper process variable values is also briefly discussed. Dissert. Abstr.

N90-21120# Materials Research Labs., Maribyrnong (Australia).
REINFORCEMENT-MATRIX INTERFACE EFFECTS IN METAL MATRIX COMPOSITES
P. J. C. Chappell 1989 15 p
(MRL-TN-562; AR-006-282) Avail: NTIS HC A03/MF A01

Many properties of metal matrix composites are strongly influenced by the nature of the reinforcement-matrix interface. This in turn depends upon factors such as pretreatment of the fibers and composite fabrication techniques. The nature of the reinforcement-matrix interface is most commonly studied by electron spectroscopic techniques, which can give information about the degree of bonding between the reinforcement and matrix, and the formation of additional phases in the matrix material or at the interface. The use of these techniques to investigate the inter-relationship between fabrication techniques, interface properties and mechanical properties is described, and a number of specific examples are given. Author

N90-21121# United Kingdom Atomic Energy Authority, Harwell (England). National Nondestructive Testing Centre.
ACOUSTIC CHARACTERISATION OF AN ALUMINIUM SILICON CARBIDE METAL MATRIX COMPOSITE
D. J. Buttle and C. B. Scruby Oct. 1988 27 p
(AERE-R-13273) Avail: NTIS HC A03/MF A01

Many of the new metal matrix composite materials (MMC's) have not been fully characterized in terms of their modes of fracture. Acoustic emission (AE) techniques are well established for characterization of fracture in metals and are proposed for the study of MMC's. For AE to be successful, the acoustic properties of the material must be known. It is also important for the ultrasonic attenuation to be low enough to permit the propagation of broad-band pulses. The acoustic properties of an aluminum silicon carbide MMC using laser generated ultrasound are investigated. The observed bulk and surface AE signals compared well with theoretical waveforms calculated using a Green's function analysis, indicating that elastic waves propagate with little distortion in MMC's. The acoustic wave velocities were found to be higher in the MMC material than in the aluminum base alloy which was believed to be due to the bulk effect of SiC particles. Fourier analysis of the AE signals also indicated higher attenuation particularly for the higher frequencies within the 6 MHz bandwidth. Elastic constants were calculated from the wave velocities and these confirmed that the MMC was stiffer than the base material. The attenuation was only slightly higher in the MMC material. Therefore, there appears to be no technical reasons why a high fidelity AE technique could not be applied to MMC materials for acoustic source location, characterization, and general fracture studies. Author

N90-21122*# National Aeronautics and Space Administration. Langley Research Center, Hampton, VA.
RELEVANCE OF IMPACTER SHAPE TO NONVISIBLE DAMAGE AND RESIDUAL TENSILE STRENGTH OF A THICK GRAPHITE/EPOXY LAMINATE
C. C. Poe, Jr. Jan. 1990 50 p Presented at the ASTM 3rd Symposium on Composite Materials: Fatigue and Fracture, Orlando, FL, 6-9 Nov. 1989
(NASA-TM-102599; NAS 1.15:102599) Avail: NTIS HC A03/MF A01 CSCL 11D

A study was made to determine the relevance of impacter shape to nonvisible damage and tensile residual strength of a 36 mm (1.4 in.) thick graphite/epoxy motor case. The shapes of the impacters were as follows: 12.7 mm (0.5 in.) and 25.4 mm (1.0 in.) diameter hemispheres, a sharp corner, and a 6.3 mm (0.25 in.) diameter bolt-like rod. The investigation revealed that damage initiated when the contact pressure exceeded a critical level. However, the damage was not visible on the surface until an even higher pressure was exceeded. The damage on the surface consisted of a crater shaped like the impacter, and the damage below the surface consisted of broken fibers. The impact energy to initiate damage or cause visible damage on the surface increased approximately with impacter diameter to the third power. The reduction in strength for nonvisible damage increased with increasing diameter, 9 and 30 percent for the 12.7 mm (0.5 in.) and 25.4 mm (1.0 in.) diameter hemispheres, respectively. The corner impacter made visible damage on the surface for even the smallest impact energy. The rod impacter acted like a punch and sliced through the composite. Even so, the critical level of pressure to initiate damage was the same for the rod and hemispherical impacters. Factors of safety for nonvisible damage increased with increasing kinetic energy of impact. The effects of impacter shape on impact force, damage size, damage visibility, and residual tensile strength were predicted quite well assuming Hertzian contact and using maximum stress criteria and a surface crack analysis. Author

N90-21123*# National Aeronautics and Space Administration. Lewis Research Center, Cleveland, OH.
CHARACTERIZATION OF FAILURE PROCESSES IN TUNGSTEN COPPER COMPOSITES UNDER FATIGUE LOADING CONDITIONS

Yong-Suk Kim (National Academy of Sciences - National Research Council, Washington, DC.), Michael J. Verrilli, and Timothy P. Gabb 1989 22 p Presented at the International Symposium for Testing and Failure Analysis (ISTFA '89), Los Angeles, CA, 6-10 Nov. 1989; sponsored by ASM International
(NASA-TM-102371; E-5090; NAS 1.15:102371) Avail: NTIS HC A03/MF A01 CSCL 11D

A fractographic and metallographic investigation was performed on specimens of a tungsten fiber reinforced copper matrix composite (9 vol percent), which had experienced fatigue failures at elevated temperatures. Major failure modes and possible failure mechanisms, with an emphasis placed on characterizing fatigue damage accumulation, were determined. Metallography of specimens fatigued under isothermal cyclic loading suggested that fatigue damage initiates in the matrix. Cracks nucleated within the copper matrix at grain boundaries, and they propagated through cavity coalescence. The growing cracks subsequently interacted with the reinforcing tungsten fibers, producing a localized ductile fiber failure. Examinations of interrupted tests before final failure confirmed the suggested fatigue damage processes. Author

N90-21124*# National Aeronautics and Space Administration. Lewis Research Center, Cleveland, OH.
USE OF UNBALANCED LAMINATES AS A SCREENING METHOD FOR MICROCRACKING
Demetrios S. Papadopoulos (Case Western Reserve Univ., Cleveland, OH.) and Kenneth J. Bowles 1990 17 p Presented at the 35th International SAMPE Symposium, Anaheim, CA, 2-5 Apr. 1990
(NASA-TM-102517; E-5214; NAS 1.15:102517) Avail: NTIS HC A03/MF A01 CSCL 11D

State-of-the-art, high temperature polyimide matrix composites, reinforced with continuous graphite fibers are known to be susceptible to intraply cracking when thermally cycled over their useful service temperature range. It is believed that the transply cracking, in part, results from residual stresses caused by differences in coefficients of thermal expansion (CTE) between the polymer matrix and the reinforcement. Thermal cycling tests to investigate this phenomenon involve expensive time and energy consuming programs which are not economically feasible for use as a part of a materials screening process. As an alternative to thermal cycling studies, a study of unbalanced crossply graphite fiber reinforcement composites was conducted to assess the effect of the composite ply layup and surface condition on the residual stresses that remain after the processing of these materials. The residual stresses were assessed by measuring the radii of curvature of the types of laminates that were studied. The temperature at which stress-free conditions existed were determined and a dye penetrant method was used to observe surface damage resulting from excessive residual stress buildup. These results are compared with some published results of thermal cycling tests that were previously conducted on balanced polyimide composites. Author

N90-21125*# National Aeronautics and Space Administration. Marshall Space Flight Center, Huntsville, AL.
CROSS-SECTIONAL EXAMINATION OF THE DAMAGE ZONE IN IMPACTED SPECIMENS OF CARBON/EPOXY AND CARBON/PEEK COMPOSITES
A. T. Nettles and N. J. Magold Feb. 1990 21 p
(NASA-TM-100391; NAS 1.15:100391) Avail: NTIS HC A03/MF A01 CSCL 11D

Drop weight impact testing was utilized to inflict damage on eight-ply bidirectional and unidirectional samples of carbon/epoxy and carbon/PEEK (polyetheretherketone) test specimens with impact energies ranging from 0.80 J to 1.76 J. The impacting tip was of a smaller diameter (4.2-mm) than those used in most previous studies, and the specimens were placed with a diamond wheel wafering saw through the impacted area perpendicular to the outer fibers. Photographs at 12 x magnification were taken of these cross-sections and examined. The results on the bidirectional samples show little damage until 1.13 J, at which point delaminations were seen in the epoxy specimens. The PEEK specimens showed less delamination than the epoxy specimens for a given impact energy level. The unidirectional specimens displayed more damage than the bidirectional samples for a given impact energy, with the PEEK specimens showing much less damage than the epoxy material. Author

N90-21126*# National Aeronautics and Space Administration. Langley Research Center, Hampton, VA.
COMBINED EFFECT OF MATRIX CRACKING AND STRESS-FREE EDGE ON DELAMINATION
S. A. Salpekar and T. K. OBrien (Army Aerostructures Directorate, Hampton, VA.) Mar. 1990 66 p
(NASA-TM-102591; NAS 1.15:102591; AVSCOM-TM-90-B-002)
Avail: NTIS HC A04/MF A01 CSCL 11D

The effect of the stress-free edge on the growth of local delaminations initiating from a matrix crack in (0 sub 2/90 sub 4) sub s and (+ or - 45.90 sub 4) sub s glass epoxy laminates is investigated using 3-D finite element analysis. The presence of high interlaminar normal stresses at the intersection (corner) of the matrix crack with the stress-free edge, suggests that a mode I delamination may initiate at the corners. The strain energy release rates (G) were calculated by modeling a uniform through-width delamination and two inclined delaminations at 10.6 deg and 45 deg to the matrix crack. All components of G have high values near the free edges. The mode I component of G is high at small delamination length and becomes zero for a delamination length of one-ply thickness. The total G values near the free edge agreed well with previously derived closed form solution. The quasi-3D solutions agreed well with the 3-D interior solutions. Author

N90-21127# Massachusetts Inst. of Tech., Cambridge. Lab. for Advanced Composites.
FRACTURE AND LONGEVITY OF COMPOSITE STRUCTURES
Final Report, 15 Jun. 1985 - 14 Jun. 1987
Paul A. Lagace Jun. 1988 125 p
(Grant AF-AFOSR-0206-85; AF Proj. 2302)
(AD-A217827; TELAC-88-14; AFOSR-90-0082TR) Avail: NTIS HC A06/MF A01 CSCL 11/4

The results of several investigations into the fracture and longevity of composite structures are reported. During this year, the work has concentrated on the phenomena of delamination and final failure. Work is reported on the initiation of delamination under tensile and compressive loading. Work on the growth of delamination and the final failure of the specimen under tensile load is also reported. The primary objective of this ongoing research continues to be to gain understanding of the fundamental mechanisms involved in the failure of filamentary composite materials so that the methodologies for predicting fracture and longevity can be developed and enhanced. In addition, via this research, needed data bases can be identified and partially provided. This latter objective does not imply the establishment of the data base within the scope of this effort. Rather, through both analysis and directed experimentation, the critical parameters can be identified and studied in order to gain an understanding of the fundamental fracture and damage mechanisms of composites so that proper engineering data bases and methodologies can be established. Delamination plays an important role in the failure of composite structures. Interlaminar stresses which arise in gradient fields can trigger the failure of the interply resin layer. Author

N90-21128# Materials Research Labs., Maribyrnong (Australia).
A COMPUTATIONAL MODEL OF THE PERFORATION OF MULTI-LAYER METALLIC LAMINATES
Ray L. Woodward and Ian G. Crouch 1989 34 p
(MRL-RR-9-89) Copyright Avail: NTIS HC A03/MF A01

A model for the deformation of multi-layer metallic laminate targets during ballistic impact is described. The model divides the process into a stage of plug acceleration followed by dishing of the rear of the target, and allows for the effects of variable interlamellar bend strength. A computational procedure is described, as well as the mechanical test procedures to generate the input data for the program. Examples of the application of the model are described to illustrate the interpretation of results, the

limitations of the model, and the use of the model's parametric studies for laminate design. The computer program is listed with typical input and output data. Author

N90-21129*# Lockheed Engineering and Sciences Co., Hampton, VA. Polymeric Materials Section.
LaRC TPI 1500 SERIES POLYMERS Final Report
Tan-Hung Hou and Jia-Mo Bai (Old Dominion Univ., Norfolk, VA.) Apr. 1990 41 p Presented at the 35th International SAMPE Symposium and Exhibition, Anaheim, CA, 2-5 Apr. 1990
(Contract NAS1-19000)
(NASA-CR-181899; NAS 1.26:181899) Avail: NTIS HC A03/MF A01 CSCL 11D

The crystallization behavior and the melt flow properties of two batches of 1500 series LaRC-TPI polymers from Mitsui Toatsu Chemicals (MTC) were investigated. The characterization methods include Differential Scanning Calorimetry, the x ray diffractography and the melt rheology. The as-received materials possess initial crystalline melting peak temperatures of 295 and 305 C, respectively. These materials are less readily recrystallizable at elevated temperatures when compared to other semicrystalline thermoplastics. For the samples annealed at temperatures below 330 C, a semicrystalline polymer can be obtained. On the other hand, a purely amorphous structure is realized in the samples annealed at temperatures above 330 C. Isothermal crystallization kinetics were studied by means of the simple Avrami equation. The viscoelastic properties at elevated temperatures below and above glass transition temperature of the polymers were measured. Information with regard to the molecule sizes and distributions in these polymers were also extracted from melt rheology. Author

N90-21130*# National Aeronautics and Space Administration. Langley Research Center, Hampton, VA.
THREE-DIMENSIONAL ELASTIC-PLASTIC ANALYSIS OF SHALLOW CRACKS IN SINGLE-EDGE-CRACK-TENSION SPECIMENS
Kunigal N. Shivakumar (Analytical Services and Materials, Inc., Hampton, VA.) and James C. Newman, Jr. Apr. 1990 32 p
(NASA-TM-102636; NAS 1.15:102636) Avail: NTIS HC A03/MF A01 CSCL 11D

Three dimensional, elastic-plastic, finite element results are presented for single-edge crack-tension specimens with several shallow crack-length-to-width ratios (0.05 less than or equal to a/W less than or equal to 0.5). Results showed the need to model the initial yield plateau in the stress-strain behavior to accurately model deformation of the A36 steel specimens. The crack-tip-opening-displacement was found to be linearly proportional to the crack-mouth-opening displacement. A new deformation dependent plastic-eta factor equation is presented for calculating the J-integral from test load-displacement records. This equation was shown to be accurate for all crack lengths considered. Author

N90-21131*# National Aeronautics and Space Administration. Lewis Research Center, Cleveland, OH.
FIBER PUSHOUT TEST: A THREE-DIMENSIONAL FINITE ELEMENT COMPUTATIONAL SIMULATION
Subodh K. Mital and Christos C. Chamis Apr. 1990 18 p
(NASA Order C-99066-G)
(NASA-TM-102565; ICOMP-90-11; E-5389; NAS 1.15:102565)
Avail: NTIS HC A03/MF A01 CSCL 11D

A fiber pushthrough process was computationally simulated using three-dimensional finite element method. The interface material is replaced by an anisotropic material with greatly reduced shear modulus in order to simulate the fiber pushthrough process using a linear analysis. Such a procedure is easily implemented and is computationally very effective. It can be used to predict fiber pushthrough load for a composite system at any temperature. The average interface shear strength obtained from pushthrough load can easily be separated into its two components: one that comes from frictional stresses and the other that comes from chemical adhesion between fiber and the matrix and mechanical interlocking that develops due to shrinkage of the composite because of phase change during the processing. Step-by-step procedures are described to perform the computational simulation, to establish bounds on interfacial bond strength and to interpret interfacial bond quality. Author

N90-21132*# National Aeronautics and Space Administration. Lewis Research Center, Cleveland, OH.
MULTI-OBJECTIVE SHAPE AND MATERIAL OPTIMIZATION OF COMPOSITE STRUCTURES INCLUDING DAMPING
D. A. Saravanos (Case Western Reserve Univ., Cleveland, OH.) and Christos C. Chamis 1990 19 p Presented at the 31st Structures, Structural Dynamics, and Materials Conference, Long Beach, CA, 2-4 Apr. 1990; cosponsored by AIAA, ASME, ASCE, AHS, and ASC Previously announced in IAA as A90-29262
(NASA-TM-102579; E-5410; NAS 1.15:102579) Avail: NTIS HC A03/MF A01 CSCL 11D

A multi-objective optimal design methodology is developed for light-weight, low cost composite structures of improved dynamic performance. The design objectives include minimization of resonance amplitudes (or maximization of modal damping), weight, and material cost. The design vector includes micromechanics, laminate, and structural shape parameters. Performance constraints are imposed on static displacements, dynamic amplitudes, and natural frequencies. The effects of damping on the dynamics of composite structures are incorporated. Preliminary applications on a cantilever composite beam illustrated that only the proposed multi-objective optimization, as opposed to single objective functions, simultaneously improved all objectives. The significance of composite damping in the design of advanced composite structures was also demonstrated, indicating the design methods based on undamped dynamics may fail to improve the dynamic performance near resonances. Author

N90-21133*# National Aeronautics and Space Administration. Lewis Research Center, Cleveland, OH.
NICALON/SILICONOXYCARBIDE CERAMIC COMPOSITES
Frances I. Hurwitz, John Z. Gyekenyesi, Paula J. Conroy, and Ann L. Rivera (Case Western Reserve Univ., Cleveland, OH.) 1990 21 p Presented at the 14th Annual Conference on Composites and Advanced Ceramics, Cocoa Beach, FL, 14-17 Jan. 1990; sponsored by American Ceramic Society
(NASA-TM-102563; E-5383; NAS 1.15:102563) Avail: NTIS HC A03/MF A01 CSCL 11D

A series of silsesquioxane copolymers was synthesized by acid hydrolysis and condensation of trimethoxysilanes of the form RSi(OCH3)3, where R = methyl or phenyl. By varying pH, water/methoxy and methyl/phenyl ratios, the molecular structure, polymer rheology and ceramic composition can be controlled. The polymers form an amorphous siliconoxycarbide on pyrolysis. Composites of Nicalon/siliconoxycarbide were fractured in four-point flexure and in tension to evaluate the influence of matrix composition, final fabrication temperature and use of filler on composite mode of failure, modulus, strain capability and strength. Incorporation of filler was found to increase matrix compressive strength. Employment of processing temperatures of 1375 to 1400 C enhanced strain to failure and reduced the tendency toward brittle fracture. Mixed mode (compression/shear and tension/shear) failures were observed in flexural samples processed to the higher temperatures, giving rise to nonlinear stress-strain curves. Tensile samples pyrolyzed to 1400 C showed linear-elastic behavior and failed by fracture of fiber bundles. Matrix material was found to be adherent to the fiber surface after failure. These results demonstrate the need for tensile testing to establish composite behavior. Author

N90-21134 Nebraska Univ., Lincoln.
COMPRESSIVE BEHAVIOR OF LAMINATED COMPOSITE STRUCTURES Ph.D. Thesis
Siu-Ping Ko 1989 146 p
Avail: Univ. Microfilms Order No. DA9004684

Physical testing of laminated structures has indicated that the compressive strength is often considerably lower than that predicted by analytical methods. Poor testing techniques and poorly

constructed materials seem to be possible reasons for the premature failure. However, since many of the failures are characterized by delamination of the structures, the cause of the failure may be due to local buckling of the composite plies. A ply buckling model is studied to assist in the understanding of the failure mechanisms. In order to find the failure envelope, inplane fracture and overall buckling are assumed as the failure modes of these structures. The classical theory of elasticity for thin shells, including transverse shear deformation, is used in the derivation. Then the relations between the predicted failure stresses and laminate orientations can be obtained. A simple optimum design procedure for laminate orientation and hoop/helical ply thickness ratio is proposed by using the previous two failure theories. The optimal point may be defined as the highest intersection of the various failure criteria. Results are presented in the form of a parametric study for three stacking sequences. Finally, the comparison of the failure stresses between the laminate with and without an inside hoop layer is discussed. Dissert. Abstr.

N90-21135 California Univ., Los Angeles.
TWO-DIMENSIONAL DAMAGE MODELS OF FIBER-REINFORCED COMPOSITES Ph.D. Thesis
Vagarshak Vardanyan 1989 119 p
Avail: Univ. Microfilms Order No. DA9005209

The fracture mechanics of fiber reinforced composites is investigated at the micromechanical level within the framework of linear 2-D elastostatics. Damage models of a broken fiber, fiber-matrix interface debonding, matrix cracking and their interaction are examined for arrays of both finite and infinite length fibers embedded in an elastic matrix. These general problems are preceded by the corresponding single fiber problems which permit the investigation of the local damage in detail. It was determined that the failure mechanism of a unidirectionally fiber-reinforced ply--the propagation of debonding or matrix cracking in a stable or unstable manner continues until the next fiber breaks. The quantitative analysis of the damage propagation was accomplished by determining the dependence of damage propagation on material and geometrical characteristics of the composite, in particular upon the initial damage configuration. Dissert. Abstr.

N90-21136 Iowa State Univ. of Science and Technology, Ames.
FRACTURE OF SANDWICHED COMPOSITES Ph.D. Thesis
Weh-Huei Lin 1989 108 p
Avail: Univ. Microfilms Order No. DA9003548

Fracture of a pair of collinear cracks in various materials, such as an isotropic strip, an orthotropic strip, a bonded isotropic adhesive layer, and sandwiched orthotropic layers, is investigated. The crack surfaces are subjected to an arbitrary opening pressure p(x). The problems are formulated in terms of Fredholm integral equation of the second kind by making use of the techniques of Fourier transform and finite Hilbert transform. In case of uniform opening pressure p(x) = sigma, exact expressions for the stress intensity factors and the shape of deformed cracks are obtained. Numerical calculations are carried out to study the effects of various boundary geometries and material properties on the fracture of the chosen materials. Dissert. Abstr.

N90-21137*# National Aeronautics and Space Administration. Lewis Research Center, Cleveland, OH.
STRUCTURAL TAILORING OF SELECT FIBER COMPOSITE STRUCTURES
Christos C. Chamis and Robert I. Rubinstein (Sverdrup Technology, Inc., Cleveland, OH.) Feb. 1990 14 p Presented at the 45th Annual Conference on the Society of Plastics Industry Reinforced Plastics/Composites Inst., Washington, DC, 12-16 Feb. 1990
(NASA-TM-102484; E-5273; NAS 1.15:102484) Avail: NTIS HC A03/MF A01 CSCL 11D

A multidisciplinary design process for aerospace propulsion composite structures was formalized and embedded into computer codes. These computer codes are streamlined to obtain tailored designs for select composite structures. The codes available are briefly described with sample cases to illustrate their applications. The sample cases include aircraft engine blades, propfans (turboprops), flat, and cylindrical panels. Typical results illustrate that the use of these codes enable the designer to obtain designs which meet all the design requirements with maximum benefits in efficiency, noise, weight or thermal distortions. Author

N90-21138*# National Aeronautics and Space Administration. Lewis Research Center, Cleveland, OH.
HIGH TEMPERATURE FATIGUE BEHAVIOR OF TUNGSTEN COPPER COMPOSITES
Michael J. Verrilli, Yong-Suk Kim, and Timothy P. Gabb Oct. 1989 18 p Presented at the Symposium on Fundamental Relationships Between Microstructure and Mechanical Properties of Metal-Matrix Composites, Indianapolis, IN, 1-5 Oct. 1989; sponsored in part by the Metallurgical Society and the American Society for Metals
(NASA-TM-102404; E-5156; NAS 1.15:102404) Avail: NTIS HC A03/MF A01 CSCL 11D

The high temperature fatigue behavior of a 9 vol percent, tungsten fiber reinforced copper matrix composite was investigated. Load-controlled isothermal fatigue experiments at 260 and 560 C and thermomechanical fatigue (TMF) experiments, both in phase and out of phase between 260 and 560 C, were performed. The stress-strain response displayed considerable inelasticity under all conditions. Also, strain ratcheting was observed during all the fatigue experiments. For the isothermal fatigue and in-phase TMF tests, the ratcheting was always in a tensile direction, continuing until failure. The ratcheting during the out-of-phase TMF test shifted from a tensile direction to a compressive direction. This behavior was thought to be associated with the observed bulging and the extensive cracking of the out-of-phase specimen. For all cases, the fatigue lives were found to be controlled by damage to the copper matrix. Grain boundary cavitation was the dominant damage mechanism of the matrix. On a stress basis, TMF loading reduced lives substantially, relative to isothermal cycling. In-phase cycling resulted in the shortest lives, and isothermal fatigue at 260 C, the longest. Author

N90-21139# Lawrence Livermore National Lab., CA. Chemistry and Materials Science Dept.
DIRECT SUBLIMATION OF NaCl SALT FROM CARBON MATRIXES
Yury Zundelevich Jan. 1990 65 p
(Contract W-7405-eng-48)
(DE90-007927; UCID-21955) Avail: NTIS HC A04/MF A01

This report provides the theoretical groundwork for the design and operation of a system for sublimation of NaCl from carbon matrixes. The findings and recommendations summarized below are based on the results of computer modeling of momentum, heat and mass transport occurring in a sublimator, condenser and the vacuum system that comprise a complete sublimation system. Three major sublimation modes have been considered: in the absence of inert gas, in stagnant inert gas and in flowing inert gas. In the absence of inert gas sublimation is most rapid (typically under 2 days for the base case of 12 bars with 12 micron pore size at 800 C in sublimator). At the beginning of the process (before pronounced porous layer is formed) the sublimation rate tends to be explosive so that condenser could be easily overcome unless the sublimator temperature is gradually ramped over few hours to the final 800 C from a much lower level. DOE

N90-21140*# National Aeronautics and Space Administration. Langley Research Center, Hampton, VA.
MICROMECHANICS ANALYSIS OF SPACE SIMULATED THERMAL DEFORMATIONS AND STRESSES IN CONTINUOUS FIBER REINFORCED COMPOSITES
David E. Bowles Mar. 1990 119 p
(NASA-TM-102633; NAS 1.15:102633) Avail: NTIS HC A06/MF A01 CSCL 11D

Space simulated thermally induced deformations and stresses in continuous fiber reinforced composites were investigated with a micromechanics analysis. The investigation focused on two primary areas. First, available explicit expressions for predicting the effective coefficients of thermal expansion (CTEs) for a composite were

compared with each other, and with a finite element (FE) analysis, developed specifically for this study. Analytical comparisons were made for a wide range of fiber/matrix systems, and predicted values were compared with experimental data. The second area of investigation focused on the determination of thermally induced stress fields in the individual constituents. Stresses predicted from the FE analysis were compared to those predicted from a closed-form solution to the composite cylinder (CC) model, for two carbon fiber/epoxy composites. A global-local formulation, combining laminated plate theory and FE analysis, was used to determine the stresses in multidirectional laminates. Thermally induced damage initiation predictions were also made. Author

N90-21141# Instituto de Pesquisas Espaciais, Sao Jose dos Campos (Brazil).
RESISTANCE MECHANICS FOR LAMINATED COMPOSITE MATERIALS [RESISTENCIA MECANICA DE LAMINADOS EM MATERIAIS COMPOSTOS]
Thomas Leomil Shaw 1990 41 p In PORTUGUESE; ENGLISH summary
(INPE-4919-RPE/594) Avail: NTIS HC A03/MF A01

The computational implementation of the classical theory for laminated composite materials is presented in terms of tensors, deformation, equivalent models, and fault criteria. Author

N90-21142# Technische Hogeschool, Delft (Netherlands). Dept. of Aerospace Engineering.
CRACK STOPPERS AND ARALL LAMINATES
J. Schijve Mar. 1989 26 p
(PB90-166588; LR-589) Avail: NTIS HC A03/MF A01 CSCL 11D

Tests were carried out on fatigue crack growth in 2024-T3 Alclad sheet specimens reinforced with strips. Strip materials were 2024-T3, 7075-T6, Ti-6Al-4V and ARALL. Adhesive bonded and riveted strips were used. Integral strips were tested for 2024-T3 only. Several observations were made on crack growth retardation caused by the strips. Adhesive bonding gives better results than riveting. The best strip materials were ARALL and the Ti-alloy. ARALL with advanced glass fibers are the most effective solution for crack stopper bands in a pressurized fuselage. Moreover, they offer less production problems. Author

N90-21143*# National Aeronautics and Space Administration. Lewis Research Center, Cleveland, OH.
OPTIMAL FABRICATION PROCESSES FOR UNIDIRECTIONAL METAL-MATRIX COMPOSITES: A COMPUTATIONAL SIMULATION
D. A. Saravanos, P. L. N. Murthy, and M. Morel (Sverdrup Technology, Inc., Cleveland, OH.) 1990 19 p Presented at the 35th International SAMPE Symposium and Exhibition, Anaheim, CA, 2-5 Apr. 1990
(NASA-TM-102559; E-5379; NAS 1.15:102559) Avail: NTIS HC A03/MF A01 CSCL 11D

A method is proposed for optimizing the fabrication process of unidirectional metal matrix composites. The temperature and pressure histories are optimized such that the residual microstresses of the composite at the end of the fabrication process are minimized and the material integrity throughout the process is ensured. The response of the composite during the fabrication is simulated based on a nonlinear micromechanics theory. The optimal fabrication problem is formulated and solved with non-linear programming. Application cases regarding the optimization of the fabrication cool-down phases of unidirectional ultra-high modulus graphite/copper and silicon carbide/titanium composites are presented. Author

N90-21144# Los Alamos National Lab., NM.
STRENGTHENING MECHANISMS OF TUNGSTEN POWDER REINFORCED URANIUM M.S. Thesis- MIT, Boston
Melissa Ann Krawizcki Apr. 1990 64 p
(Contract W-7405-eng-36)
(DE90-009331; LA-11558-T) Copyright Avail: NTIS HC A04/MF A01

Tungsten powder reinforced uranium composites exhibit a three-fold increase in yield strength due to precipitation hardening. The tungsten-rich interphase precipitates form at the moving beta to alpha phase boundary during slow cooling. Further increases in yield strength, attained with increasing tungsten content, are due to composite strengthening. The composite strengthening is verified by increasing elastic modulus with increasing tungsten content. Age hardening behavior is observed, with strengthening occurring at aging temperatures low, in the alpha phase. Temperatures higher in alpha give initial strengthening followed by rapid overaging. Beta phase aging temperatures result in a very soft structure with interphase precipitates observable optically. Wrought material exhibits significant strain hardening as well as composite strengthening due to elongation of the tungsten particles. DOE

25 INORGANIC AND PHYSICAL CHEMISTRY

Includes chemical analysis, e.g., chromatography; combustion theory; electrochemistry; and photochemistry.

For related information see also *77 Thermodynamics and Statistical Physics.*.

N90-21145# Societe Francaise de Chimie-Physique, Paris. Div. de Chimie Physique.
MODELLING OF MOLECULAR STRUCTURES AND PROPERTIES IN PHYSICAL CHEMISTRY AND BIOPHYSICS
Sep. 1989 101 p In ENGLISH and FRENCH Meeting held in Nancy, France, 11-15 Sep. 1989
(Contract DAJA89-M-0063)
(AD-A214561; R/D-6178-CH-02) Avail: NTIS HC A06/MF A01 CSCL 07/4

A collection of abstracts are presented from the papers presented at the conference. Some representative topics are: General theory of intermolecular forces; A vibrational molecular force field for macromolecular modeling; Modeling of biomolecular properties by molecular dynamics simulation; Theoretical study of a conformational change in an enzyme (methodology and first results on citrate synthase); Design and synthesis of a new bifunctional microprotein by interactive modeling; Force field calculations of siderophores; Stability and conformations of Fe-III chelates with novel iron related parameters; and Effects of structure and charge on phthalocyanine dimers. E.R.

N90-21146# Illinois Univ., Chicago. Dept. of Chemical Engineering.
PHASE EQUILIBRIUM OF MIXTURES CONSISTING OF MOLECULES WITH LARGE SIZE AND SHAPE DIFFERENCES (THERMODYNAMIC MODELING OF SUPERCRITICAL FLUID EXTRACTION AND RETROGRADE CONDENSATION, SFE/RC) Annual Report, 15 Apr. 1988 - 15 Apr. 1989
G. Ali Mansoori Jun. 1989 121 p
(Contract GRI-5086-260-1244)
(PB90-131285; GRI-89/0159) Avail: NTIS HC A06/MF A01 CSCL 07D

Initial success was achieved in the development accurate techniques for calculation of thermodynamic properties of asymmetric mixtures and application of the techniques for industrial modeling of supercritical fluid extraction and retrograde condensation (SFE/RC). By using equations of state it is possible to accurately calculate the minimum miscibility conditions and solubility of heavy and intermediate hydrocarbons in miscible solvents and phase behavior of complex reservoir fluids. The research is based on statistical mechanical mixing rules and the conformal solution theory of polar fluid mixtures. Author

N90-21147# Pontificia Univ. Catolica, Rio de Janeiro (Brazil). Dept. de Quimica.
STUDY OF NEW TECHNIQUE OF SOLID COMBUSTIBLE MATERIALS TO DETERMINATION OF VOLATILE ELEMENTS BY FLAME ATOMIC ABSORPTION SPECTROPHOTOMETRY Ph.D. Thesis

15 Sep. 1988 254 p In PORTUGUESE; ENGLISH summary (DE90-612907; INIS-BR-1801) Avail: NTIS (US Sales Only) HC A12/MF A02

A new technique for direct trace element analysis of solid combustible materials is described. The samples (up to 10 mg) are weighed on a graphite platform which is then placed in a quartz tube at the focal point of three infrared lamps. When the lamps are turned on, the sample burns in a stream of air, and the resulting dry aerosol containing volatile elements such as Hg, Cd, Bi, Tl, Zn, Pb, and Cu is carried into the mixing chamber and thence into the flame, where the atomic absorption measurement is carried out. This technique overcomes chemical sample preparation steps, avoiding contaminations of losses associated with these steps. A furnace in flame system, where the aerosol is transported to a flame heated T-tube, is also described. The influence of flame stoichiometry, observation height, platform material and air flux intensity was studied in order to determine optimal analytical conditions. DOE

N90-21148# Joint Inst. for Nuclear Research, Dubna (USSR). Lab. of Nuclear Reactions.

NEUTRON AUTORADIOGRAPHY OF HYDROGEN

Yu. G. Teterev 1988 8 p In RUSSIAN; ENGLISH summary (DE90-612930; JINR-18-88-815) Avail: NTIS (US Sales Only) HC A02/MF A01

The physical principle of the neutron autoradiography method consists in the registration of the distribution number of neutrons, which are scattered isotopically on nuclei of a tested element, whereas in conventional autoradiography the isotropic radiation of nuclei investigated is recorded. The experimental investigation of the main features of the method of neutron autoradiography for hydrogen was done by using a-resonance filter and a resonance detector made of metallic indium. To demonstrate the possibilities of the proposed method, it was compared with the traditional methods of autoradiography and neutron radiography. The method of neutron autoradiography for thin objects given an object contrast about 20 times higher than in the case of neutron radiography. The minimum detectable content of hydrogen in an object is 3x10(exp -5) gxcm(exp -2). The proposed method has a very high selectivity of hydrogen determination in any object. The sharpness of image has not been studied but it seems that the obtained degree of sharpness is good enough for solving quite a number of problems. The practical use of the method is no more complicated than conventional autoradiography and is substantially easier than that of neutron radiography. The high contrast and selectivity of the method enable one to investigate geological problems. DOE

N90-21149# International Centre for Theoretical Physics, Trieste (Italy).

ON THE DYNAMICS OF POLYMER MIXTURES IN SOLUTION USING THE RPA

Mustapha Benmouna Sep. 1989 8 p Submitted for publication

(DE90-613689; IC-89/236) Avail: NTIS (US Sales Only) HC A02/MF A01

The dynamics of polymer mixtures and copolymers in solution is investigated using the Random Phase Approximation (RPA). It is shown that the known results for the intermediate scattering functions are recovered in the Rouse limit only. If hydrodynamic interaction is not negligible, a discrepancy appears. This discrepancy can be observed by combining static and dynamic scattering experiments. DOE

N90-21150# International Centre for Theoretical Physics, Trieste (Italy).

IONIC EQUILIBRIUM BETWEEN OCTAHEDRAL AND TETRAHEDRAL COMPLEXES IN LIQUID ALUMINIUM-SODIUM FLUORIDE MIXTURES

Z. Akdeniz (Istanbul Univ., Turkey) and M. P. Tosi Sep. 1989 14 p

(DE90-613690; IC-89/249) Avail: NTIS (US Sales Only) HC A03/MF A01

An earlier statistical mechanical theory of complexing in molten mixtures of polyvalent metal halides and alkali halides is extended to situations in which an ionic equilibrium is established between two different types of complexes. The specific systems of interest are the mixtures of aluminium fluoride and sodium fluoride, in which early Raman scattering experiments by Gilbert, Mamantov and Begun have demonstrated coexistence of octahedral (AlF 6 (exp 3-) units and tetrahedral (AlF sub 4 (exp -) units in the concentration range between 0.25 and 0.5 of AlF sub 3. Our treatment is based on a simple ionic model and involves an evaluation of binding free energies for the two units in vacuo, showing that AlF sub 6 exp 3- is strongly unstable against dissociation in this state; and a statistical mechanical theory of the liquid mixture, in which AlF sub 6 exp 3- is stabilized by ionic screening interactions. The resulting ionic equilibrium in the liquid involves, in excellent agreement with the Raman data, strong suppression of dissociation for AlF sub 6 exp 3-, except near the composition corresponding to criolite AlF exp 3.3NaF. The temperature dependence of the ionic equilibrium is also evaluated, with special attention to molten criolite. Analogous calculations on aluminium-sodium chloride mixtures show that in these systems the equilibrium is completely shifted in favor of the AlCl sub 4 exp - species, as a consequence of its stabilization by halogen polarizability. DOE

N90-21151# Allied-Signal Aerospace Co., Kansas City, MO.

A SOLUTION LEVEL INDICATOR SYSTEM Final Report

C. L. Barben Apr. 1990 92 p

(Contract DE-AC04-76DP-00613)

(DE90-007939; KCP-613-4266) Avail: NTIS HC A05/MF A01

A computer-based system was developed and built to monitor liquid volumes used for chemical analyses on a laboratory robot. The robot performs dilutions and titrations for production solutions to analyze inherent component concentrations. For successful testing, sufficient analytical chemicals (titrants) and water must exist to perform each analysis. This system provides a quick and convenient display of volumes for the operator to maintain an adequate supply of chemicals and water for proper robot operation. In addition, the system monitors liquid volume of post-analysis waste mixtures in the effluent barrel to preclude overfilling the container. DOE

N90-21152# Allied-Signal Aerospace Co., Kansas City, MO.

ANALYTICAL SCIENCES

T. Hickman 1990 72 p

(Contract DE-AC04-76DP-00613)

(DE90-007965; KCP-613-4074) Avail: NTIS HC A04/MF A01

The mission of the Analytical Sciences Department of the Kansas City Division of Allied-Signal Inc. is to provide chemical, physical, mechanical, and metallurgical analyses. Materials, processes, and products are tested both within the laboratory area and on-site. The laboratory area has over 38,600 square feet and over $8 million in equipment, most of which is research grade. The Analytical Sciences Department is composed of 78 people committed to providing quality results on schedule with optimum cost management. The department is organized onto four sections: Mechanical Analysis, Organic Chemistry, Inorganic Chemistry, and Product Diagnostics. For failure analysis, customers have found the stress analysis in the Mechanical Analysis section and the chemical/electron optical/surface analysis in the Product Diagnostics section particularly helpful. The purpose of this directory is to assist those who use the services provided by the Analytical Sciences Department. Several reference tables are given which provide analysis term definitions and show interrelationships and limits of analytical techniques. A special section has been added on sample preparation and preservation so that the customer can help ensure sample integrity. DOE

N90-21153# Lawrence Livermore National Lab., CA.

MAGNETRON SPUTTERED BORON FILMS AND Ti/B MULTILAYER STRUCTURES

D. M. Makowiecki, A. F. Jankowski, M. A. McKernan, and R. J. Foreman Mar. 1990 18 p Presented at the Integrated

Contractors Meeting and SUBWOG 12A Meeting on Coatings, Livermore, CA, 8-9 May 1990
(Contract W-7405-eng-48)
(DE90-009190; UCRL-JC-103223; CONF-9005148-1) Avail: NTIS HC A03/MF A01

Boron and Ti/B films have been magnetron sputter deposited and characterized using x ray diffraction, Auger-depth profiling, and electron microscopy. The amorphous boron films contain no morphological growth features, unlike those characteristically found in thin films prepared by various PVD processes. The use of a high density boron sputtered target prepared by hot isostatic pressing was a major factor in controlling the deposition process. Consequently, the RF sputter deposited boron proves feasible for ultra-thin band pass filters as well as the low Z element in high Z/low Z mirrors which enhance reflectivity from grazing to normal incidence. DOE

N90-21154# Oak Ridge National Lab., TN. Metals and Ceramics Div.
MODELING THE TEMPERATURE DEPENDENCE OF THE THERMAL CONDUCTIVITY OF ALUMINUM NITRIDE
Ralph B. Dinwiddie and David G. Onn (Delaware Univ., Newark.) 1989 12 p Presented at the 21st International Thermal Conductivity Conference, Lexington, MA, 15-18 Oct. 1989
(Contract DE-AC05-84OR-21400)
(DE90-009428; CONF-8910319-3) Avail: NTIS HC A03/MF A01

Data on the thermal conductivity of commercially available aluminum nitride substrates, over the temperature range of 20 to 500 K, is analyzed using the Klemens-Callaway model. Parameters in this model which include crystallite size and impurity concentration, are determined through a nonlinear least squares fitting routine. The resulting parameters are compared with values obtained from other experimental techniques such as scanning electron microscopy (SEM) and proton induced x ray emission (PIXE). A graphical method was developed for the estimation of impurity concentration and crystallite size from low temperature thermal conductivity data. DOE

N90-21155# SRI International Corp., Menlo Park, CA. Molecular Physics Lab.
HIGH-RESOLUTION BRILLOUIN GAIN SPECTROSCOPY IN SOLIDS
Gregory W. Faris, Leonard E. Jusinski, Mark J. Dyer, William K. Bischel, and Albert Peet Hickman 18 Dec. 1989 14 p Prepared for LLNL, CA
(Contract W-7405-eng-48)
(DE90-009475; UCRL-CR-103295; MP-89-224) Avail: NTIS HC A03/MF A01

The first high-resolution Brillouin gain spectroscopy in solids is reported. Resonances corresponding to longitudinal (compressional) and transverse (shear) acoustic waves in fused silica are observed with good resolution and high signal to noise. Absolute gain coefficients, linewidths, and Brillouin frequency shifts are measured. Agreement with previously measured values is good. DOE

26 METALLIC MATERIALS

Includes physical, chemical, and mechanical properties of metals, e.g., corrosion; and metallurgy.

N90-21156# Lawrence Livermore National Lab., CA.
ORDERING MECHANISM IN SUBSTITUTIONAL NI-Cr ALLOYS: THEORY AND EXPERIMENT
P. E. A. Turchi, R. H. Howell, A. L. Wachs, M. J. Fluss, F. J. Pinski, D. D. Johnson, G. M. Stocks, D. M. Nicholson, and W. Schweika (IFKJ G.m.b.H., Julich, Germany, F.R.) 28 Nov. 1989 8 p Presented at the Materials Research Society Fall Meeting, Boston, MA, 27 Nov. - 2 Dec. 1989
(Contracts W-7405-eng-48; DE-AC05-84OR-21400; DE-AC04-76DP-00789)
(DE90-006268; UCRL-101106; CONF-891119-82) Avail: NTIS HC A02/MF A01

Previously, the short range order (SRO) had been extracted from the neutron diffuse scattering intensities on Ni--Cr alloys with 11 to 25 at. pct. chromium. These data were analyzed using inverse-Monte Carlo simulations to extract atomic interactions and the results suggested the existence of a well defined, flat sheet of Fermi e (110) direction. This suggestion suggestion is investigated with a series of calculations which are based on the first-principles Korringa-Kohn-Rostoker coherent potential approximation (KKRCPA). The electronic structure was calculated along with the Block spectral function at the Fermi energy. The effective cluster interactions using the generalized perturbation method (GPM) is then calculated and then they are compared with the above mentioned experimentally deduced interactions. In addition, preliminary results are presented of 2-D angular correlation of positron annihilation radiation (2D-ACPAR) measurements, which probe the Fermiology of this alloy system. The positron experiments demonstrate the existence of well-defined features in the Fermi surface of Cr11Ni89 but the calculations still have not yet established the origin of SRO in this system. DOE

N90-21157# United Kingdom Atomic Energy Authority, Harwell (England). Materials Physics and Metallurgy Div.
A STEM STUDY OF CHANGING GRAIN BOUNDARY CHEMISTRY DURING THE SENSITISATION OF AISI 304 STAINLESS STEEL
S. R. Ortner May 1989 43 p
(AERE-R-13418) Avail: NTIS HC A03/MF A01

The compositions of grain boundaries and the regions around them were analyzed in specimens of AISI 304 stainless steel after solution treatment, and after aging for 3 hours and 24 hours at 650 C. These aging treatments produce materials unsensitized, lightly sensitized and heavily sensitized to intergranular stress corrosion cracking (IGSCC) respectively. Cr, Mo, and P segregate to solution treated boundaries; Fe and Ni desegregate; Mn, Cu, and Si interact only slightly with the boundary. The amounts of segregation vary from boundary to boundary, even among general, high angle boundaries. After 3 hours at 650 C, Cr depletion profiles, offset by Fe and Ni enhancement, develop around the boundaries. The profiles are usually asymmetric due to boundary migration, and their width and depth vary from boundary to boundary. Diffusion profiles do not form along the boundaries. Segregation of P is increased, while Cr and Mo is decreased. The Cr depletion profiles deepen, broaden and become less variable in shape after extended aging, and are sometimes offset by Mn enhancement. Even after 24 hours however, facets may be found which do not show Cr depletion. CR and Mo segregation are lost from facets showing Cr depletion. The loss of segregation shows that the boundary moves away from equilibrium with the matrix during aging. The causes of variability between boundaries, and the effect on IGSCC of segregation, and changes in segregation levels, are considered. Author

N90-21158# United Kingdom Atomic Energy Authority, Harwell (England). Materials Physics and Metallurgy Div.
TITANIUM ALUMINIDES: PROCESSING, PROPERTIES AND POTENTIAL
M. Strangwood and A. Vassel (Office National d'Etudes et de Recherches Aerospatiales, Paris, France) Apr. 1989 92 p
(AERE-R-13198) Avail: NTIS HC A05/MF A01

A review of published literature on titanium aluminides (concentrating on TiAl, Ti3Al, and TiAl3) was carried out to assess the current development of these materials for engineering applications. Advantageous high temperature properties are highlighted as are limitations in low temperature performance. Proposed mechanisms and causes for aluminide behavior are considered and where possible, related to processing route and potential applications. On the basis of the review, possible routes for development of these materials with properties suitable for high temperature engineering applications are suggested. Author

N90-21159# United Kingdom Atomic Energy Authority, Harwell (England). Materials Development Div.
CURRENT FLUCTUATIONS ASSOCIATED WITH LOCALISED CORROSION: MECHANISTIC STUDIES OF THE EARLY STAGES OF PITTING AND STRESS CORROSION CRACKING OF STAINLESS STEEL
P. Balkwill, J. Stewart, D. B. Wells (Oxford Univ., England), C. Westcott, and D. E. Williams Jun. 1989 11 p
(AERE-R-13531) Avail: NTIS HC A03/MF A01

The applicability of a feedback model for the initiation of pitting corrosion of stainless steel is discussed on the basis of measurements of current fluctuations associated with the initiation and temporary propagation of unstable micropits. The frequency of such fluctuations varies with the potential, potential scan rate, and film thickness, but all such variations appear to reduce to a common curve if the passive current density is plotted as the independent variable. The effects of laminar and turbulent flow on the initiation of pitting corrosion were also discussed and it is shown that turbulent flow exerts its effect by affecting the solution concentration field around the pit mouth and hence the resistance to current flow to the developing pit. Finally, it is shown that current fluctuations occur during the early stages of stress corrosion cracking of a sensitized stainless steel, and that each pulse corresponds approximately to the movement of a crack across a single grain boundary facet. Author

N90-21160# United Kingdom Atomic Energy Authority, Harwell (England). Theoretical Physics Div.
MATHEMATICAL MODELLING OF INTERGRANULAR ATTACK IN STAINLESS STEELS: A PRELIMINARY STUDY
A. W. Herbert Jun. 1988 23 p
(AERE-M-3698) Avail: NTIS HC A03/MF A01

Intergranular attack in stainless steels is modeled using a percolation theory approach. It is assumed that intergranular attack occurs only on sensitized grain boundaries which are depleted of chromium. The percolation of these randomly distributed, sensitized grain boundary facets are considered. Relevant results from percolation theory are collected and a simple two-dimensional numerical model is developed. Ways in which this approach could be pursued, and eventually extended to realistic systems, are discussed. Author

N90-21161# United Kingdom Atomic Energy Authority, Harwell (England). Materials Physics and Metallurgy Div.
GRAIN BOUNDARY PRECIPITATION IN NI3AI BASED ALLOYS
M. Strangwood, R. James (Cambridge Univ., England), and C. A. Hippsley Jan. 1989 27 p
(AERE-R-13362) Avail: NTIS HC A03/MF A01

Three Ni3Al based alloys, all containing boron, but varying in substitutional alloying elements, were examined using transmission electron microscopy (TEM) and scanning transmission electron microscopy (STEM). The addition of Cr resulted in grain boundary (Cr, Ni)xB precipitate formation. In the presence of Ti and Zr with a complex thermomechanical treatment sub-grain boundary precipitates of Cr-rich borides, carbides and possibly oxides were formed in addition to the grain boundary precipitates. Author

N90-21162# National Inst. of Standards and Technology, Gaithersburg, MD. Metallurgy Div.
CORROSION BEHAVIOR OF MILD STEEL IH HIGH pH AQUEOUS MEDIA
Anna C. Fraker and Jonice S. Harris Sep. 1989 20 p Sponsored by Nuclear Regulatory Commission, Washington, DC
(PB90-131152; NISTIR-89/4173) Avail: NTIS HC A03/MF A01 CSCL 11F

A study of the corrosion behavior and localized corrosion susceptibility of mild steel in a simulated ground water with a pH of 9.75 and a temperature of 95 C is presented. The steel used was A27, ASTM Grade 60-30. The steel did not passivate in the aqueous environment used. The corrosion rate decreased with exposure time. Corrosion occurred in an uneven form over the surface, and although some pitting may have been present, no deep pits were observed. The amount and distribution of the areas of ferrite and pearlite as well as the impurities were determined to be important as related to uneven corrosion and to localized attack. Author

N90-21163# Helsinki Univ. of Technology, Espoo (Finland). Lab. of Materials Processing and Powder Metallurgy.
PHASE EQUILIBRIA AND SOLUTION THERMODYNAMICS OF BISMUTH-LEAD ALLOYS
Pekka Taskinen 1989 14 p Sponsored by Jernkontorets Forskning, Stockholm, Sweden
(PB90-138421; TKK-V-B46; ISBN-951-754-969-5) Avail: NTIS HC A03/MF A01 CSCL 11F

Solution thermodynamics of solid and liquid bismuth-lead alloys were assessed critically by least squares methods using simultaneously experimental phase diagrams and thermodynamic measurements on the system. The available excessive literature data were searched through 1989 and the optimization of the thermodynamic model parameters was carried out by using the Lukas program. The alloy phases were treated as substitutional solutions. Orthogonal Legendre polynomials with (XPb-XBi) as the concentration variable were used for the optimization of the excess Gibbs energy terms. The integral excess Gibbs energies of the alloy phases were calculated to have the given temperature and composition dependencies. Author

N90-21164*# National Aeronautics and Space Administration. Langley Research Center, Hampton, VA.
A COMPENDIUM OF SOURCES OF FRACTURE TOUGHNESS AND FATIGUE CRACK GROWTH DATA FOR METALLIC ALLOYS, PART 4
C. Michael Hudson and John J. Ferrainolo May 1990 38 p
(NASA-TM-102646; NAS 1.15:102646) Avail: NTIS HC A03/MF A01 CSCL 11F

A collection of sources is presented of fracture toughness and fatigue crack growth data for metallic alloys. Author

N90-21165*# Aerojet Technical Systems Co., Sacramento, CA.
HYDROCARBON-FUEL/COMBUSTION-CHAMBER-LINER MATERIALS COMPATIBILITY Interim Final Report, 7 Nov. 1986 - 31 Oct. 1989
Mark L. Gage Apr. 1990 249 p
(Contract NAS3-25070)
(NASA-CR-185203; NAS 1.26:185203; KBQ-FR-1; RPT/D0406-54) Avail: NTIS HC A11/MF A02 CSCL 11F

Results of material compatibility experiments using hydrocarbon fuels in contact with copper-based combustion chamber liner materials are presented. Mil-Spec RP-1, n- dodecane, propane, and methane fuels were tested in contact with OFHC, NASA-Z, and ZrCu coppers. Two distinct test methods were employed. Static tests, in which copper coupons were exposed to fuel for long durations at constant temperature and pressure, provided compatibility data in a precisely controlled environment. Dynamic tests, using the Aerojet Carbothermal Test Facility, provided fuel and copper compatibility data under realistic booster engine service conditions. Tests were conducted using very pure grades of each fuel and fuels to which a contaminant, e.g., ethylene or methyl mercaptan, was added to define the role played by fuel impurities. Conclusions are reached as to degradation mechanisms and effects, methods for the elimination of these mechanisms, selection of copper alloy combustion chamber liners, and hydrocarbon fuel purchase specifications. Author

N90-21166# International Centre for Theoretical Physics, Trieste (Italy).
MODIFIED TIGHT-BINDING APPROXIMATION AND ELECTRON-PHONON SPECTRAL FUNCTION FOR TRANSITION METALS
A. L. Kuzensky and A. P. Zhernov (Kurchatov, I. V. Inst. of Atomic Energy, Moscow, USSR) Sep. 1989 18 p Submitted for publication
(DE90-614022; IC-89/245) Avail: NTIS (US Sales Only) HC A03/MF A01

The modified tight-binding approximation has been analyzed in

detail and is applied to the derivation of an expression for electron-phonon spectral function (EPSF) which enters the strong coupling equations of superconductivity. Numerical calculations of the EPSF and the electron phonon coupling parameter for five transition metals, V, Nb, Mo, W and Ta have been performed.
DOE

N90-21167# Pacific Northwest Lab., Richland, WA.
GRAIN BOUNDARY CHEMISTRY EFFECTS ON IRRADIATION-ASSISTED STRESS CORROSION CRACKING
S. M. Bruemmer, L. A. Charlot, and E. P. Simonen Mar. 1990 12 p Presented at Corrosion '90, Las Vegas, NV, 23-27 Apr. 1990
(Contract DE-AC06-76RL-01830)
(DE90-008623; PNL-SA-17601; CONF-900403-9) Avail: NTIS HC A03/MF A01

Radiation-induced segregation (RIS) to grain boundaries and interfacial microchemistry effects on intergranular stress corrosion cracking (IGSCC) was investigated in 304 and 316 stainless steels (SS). Irradiation dose effects on RIS to grain boundaries were studied using nickel ion bombardment of fine-grained, sputter-deposited SS. Grain boundary chemistry effects on the intergranular (IG) corrosion and stress corrosion cracking (SCC) were examined by varying phosphorus segregation and chromium depletion through controlled thermal treatments. Grain boundary enrichment of phosphorus was found to promote IG corrosion, but not SCC, of 316 SS in low-temperature, sulfuric acid solutions at transpassive potentials. DOE

N90-21168# Argonne National Lab., IL. Materials and Components Technology Div.
HIGH-TEMPERATURE OXIDATION AND SULFIDATION OF Fe-20Cr-16Ni-4Al-1Y2O3 OXIDE-DISPERSION-STRENGTHENED ALLOY
A. U. Malik and K. Natesan Oct. 1989 41 p
(Contract W-31-109-eng-38)
(DE90-007897; ANL/FE-89-7) Avail: NTIS HC A03/MF A01

High-temperature oxidation and sulfidation studies were conducted on an oxide dispersion strengthened alloy of composition Fe--20Cr--16Ni--4Al--1Y2 O3. The oxidation studies were conducted in air and low-pO2 environments over a temperature range of 650 to 1200 C. Results are also reported on the sulfidation resistance of preformed oxide scales and the influence of reoxidation of preformed sulfide scales. Detailed microstructural results and x ray diffraction analysis data are presented to substantiate the corrosion behavior of the alloy over the wide range of conditions anticipated in fossil-energy systems. Data are also presented on the corrosion behavior of the alloy in oxygen/sulfur mixed gas atmospheres, and the results are used to compare the corrosion behavior of the present alloy with other chromia- and alumina-forming alloys. DOE

N90-21169# Oak Ridge National Lab., TN. Metals and Ceramics Div.
LECTURE ON ORDERED INTERMETALLIC ALLOYS
C. T. Liu 20 Mar. 1990 6 p Presented at a Conference on Ordered Intermetallic Alloys, Sao Paulo, Brazil, 4-9 Mar. 1990
(Contract DE-AC05-84OR-21400)
(DE90-009011; ORNL/FTR-3566) Avail: NTIS HC A02/MF A01

The author gave a week-long lecture on Ordered Intermetallic Alloys --- Physical Metallurgy, Mechanical Behavior and Alloy Design at the Instituto de Pesquisas Energeticas e Nucleares, National Commission for Nuclear Energy, Brazil. While in Brazil, the author learned about recent research on Ni3Al alloys and industrial interest in ordered intermetallics. DOE

N90-21170* National Aeronautics and Space Administration. Langley Research Center, Hampton, VA.
MAGNETO ACOUSTIC EMISSION APPARATUS FOR TESTING MATERIALS FOR EMBRITTLEMENT Patent
Sidney G. Allison, inventor (to NASA), Namkung Min, inventor (to NASA), William T. Yost, inventor (to NASA), and John H. Cantrell, inventor (to NASA) 27 Mar. 1990 10 p Filed 23 Jun. 1988 Supersedes N88-29012 (26 - 23, p 3195)
(NASA-Case-LAR-13817-1; US-Patent-4,912,411; US-Patent-Appl-SN-210486; US-Patent-Class-324-235; US-Patent-Class-073-801; US-Patent-Class-324-209; US-Patent-Class-324-226; US-Patent-Class-324-227; US-Patent-Class-324-239) Avail: US Patent and Trademark Office CSCL 11F

A method and apparatus for testing steel components for temper embrittlement uses magneto-acoustic emission to nondestructively evaluate the component. Acoustic emission signals occur more frequently at higher levels in embrittled components. A pair of electromagnets are used to create magnetic induction in the test component. Magneto-acoustic emission signals may be generated by applying an ac current to the electromagnets. The acoustic emission signals are analyzed to provide a comparison between a component known to be unembrittled and a test component. Magnetic remanence is determined by applying a dc current to the electromagnets, then turning the magnets off and observing the residual magnetic induction.
Official Gazette of the U.S. Patent and Trademark Office

N90-21171*# California Univ., Santa Barbara.
SURFACE CHARACTERIZATION OF HYDROGEN CHARGED AND UNCHARGED ALPHA-2 AND GAMMA TITANIUM ALUMINIDE ALLOYS USING AES AND REELS
M. R. Shanabarger [1990] 12 p
(Contract NCC2-63)
(NASA-CR-186561; NAS 1.26:186561) Avail: NTIS HC A03/MF A01 CSCL 11F

The surfaces of selected uncharged and hydrogen charged alpha-2 and gamma titanium aluminide alloys with Nb additions were characterized by Auger electron (AES) and reflected electron energy loss (REELS) spectroscopy. The alloy surfaces were cleaned before analysis at room temperature by ion sputtering. The low energy (500 eV) ion sputtering process preferentially sputtered the surface concentration. The surface concentrations were determined by comparing AES data from the alloys with corresponding data from elemental references. No differences were observed in the Ti or Nb Auger spectra for the uncharged and hydrogen charged alloys, even though the alpha-2 alloy had 33.4 atomic percent dissolved hydrogen. Also, no differences were observed in the AES spectra when hydrogen was adsorbed from the gas phase. Bulk plasmon energy shifts were observed in all alloys. The energy shifts were induced either by dissolved hydrogen (alpha-2 alloy) or hydrogen adsorbed from the gas phase (alpha-2 and gamma alloys). The adsorption induced plasmon energy shifts were greatest for the gamma alloy and cp-Ti metal. Author

N90-21172# Lawrence Livermore National Lab., CA.
FORMATION OF SUBSURFACE ALUMINUM LAYERS IN BERYLLIUM BY ION IMPLANTATION AND POST-IMPLANT ANNEALING Ph.D. Thesis
David Ward Brown Jan. 1990 196 p
(Contract W-7405-eng-48)
(DE90-007975; UCRL-53947) Avail: NTIS HC A10/MF A01

Subsurface layers of aluminum were formed in both monocrystalline and polycrystalline beryllium by implanting high doses of 200 keV Al(sup +) ions into beryllium and subsequently annealing the implanted material. Contrary to conventional wisdom on ion implantation, such layers demonstrate that ion implantation can in fact, be used, to form an essentially pure layer of an implanted species in a target material. In single crystal targets implanted at approximately 50 C, aluminum layer formation was critically dependent on the implanted dose. Cross-sectional transmission electron microscopy showed the aluminium layers were monocrystalline and had abrupt interfaces with the beryllium bulk and overlayer. Scanning electron microscopy revealed defects in the layers consisting of beryllium columns extending through the aluminum from the beryllium overlayer to the bulk. Study of implanted polycrystalline material showed that layer formation occurred for all grain orientations present, but that the defect density was grain dependent. An explanation of layer formation is

developed based on the observed lamellar precipitate morphology in the as-implanted state and on predicted coarsening behavior of this morphology during annealing. DOE

N90-21173# Sandia National Labs., Albuquerque, NM. Wind Energy Research Div.
FATIGUE CRACK GROWTH FROM NARROW-BAND GAUSSIAN SPECTRUM LOADING IN 6063 ALUMINUM ALLOY
Paul S. Veers and James A. VanDenAvyle 1990 42 p Presented at the 1st Symposium on Advances in Fatigue Lifetime Predictive Techniques, San Francisco, CA, 25 Apr. 1990; sponsored by ASTM Committee E-9 on Fatigue
(Contract DE-AC04-76DP-00789)
(DE90-008957; SAND-89-1576C; CONF-9004164-1) Avail: NTIS HC A03/MF A01

Constant amplitude and narrow band Gaussian loadings are applied to extruded 6063 aluminum crack growth specimens in an effort to characterize the effective stress intensity levels during random loading. Crack growth rates are determined for constant amplitude loadings at stress ratios (R) of 0.09, 0.3 and 0.5, and for a variable amplitude loading simulated to match a narrow band Gaussian spectrum. Crack opening stress levels measured by the compliance method during the constant amplitude loading are found to differ substantially for -T5 and -T6 heat treatments due to a change from intergranular to transgranular crack growth. Crack opening load ratios correlate well with the maximum applied stress intensity factor, K(sub max), for the -T5 material. The K(sub max) dependence leads to an effective halving of the crack growth exponent. Calculated variable amplitude lives are much shorter when this correlation is taken into account (an acceleration effect) and show a greater difference between loading blocks condensed by racetrack filtering at threshold levels of two and four standard deviations, similar to what was observed in the tests. Crack-opening-load measurements in one specimen with the narrow-band Gaussian (variable amplitude) loading failed to detect any closure. A substantial difference in the closure behavior of nominally identical R = .3 tests indicates that closure may occur irregularly in the extruded aluminum. Calculated crack-growth lives, assuming no closure in the variable amplitude tests, are much shorter than the test results. Including closure in the variable amplitude loadings greatly improves the predictions. DOE

N90-21174# Westinghouse Savannah River Co., Aiken, SC.
DETERMINATION OF LI-AI ALLOY EXTENT IN TUBULAR ALUMINUM ELEMENTS BY SMALL SOURCE NEUTRON RADIOLOGY
S. R. Salaymeh, T. P. Varallo, J. J. Antal, and A. S. Marotta (Army Materials Technology Lab., Watertown, MA.) 1989 26 p Presented at the 3rd World Conference on Neutron Radiography, Osaka, Japan, 14-18 May 1989
(Contract DE-AC09-89SR-18035)
(DE90-009142; DP-MS-88-225; CONF-890554-4) Avail: NTIS HC A03/MF A01

Eddy current is the only nondestructive technique used to determine the extent of the Li--Al alloy in tubular aluminum target tubes. It was desired to have an independent nondestructive method to confirm the extent of the alloy at the tube ends. The method explored and described in this paper is to provide a neutron radioscopic image of 25 cm sections of each tube end. Two small-source neutron radiologic systems were used in this study, a mobile accelerator neutron radiography system and a californium-252 system. These two systems have been shown to provide an accurate alternative method for the determination of the extent of Li--Al alloy in target elements. DOE

N90-21175# Sandia National Labs., Albuquerque, NM. Physical Metallurgy Div.
COMPATIBILITY OF Au BASE THICK FILMS WITH SOLDER ALLOYS: SOLID STATE GROWTH OF INTERMETALLICS
J. J. Stephens and A. D. Romig, Jr. 1990 4 p Presented at the 16th DOE Compatibility, Aging andService Life Conference, Livermore, CA, 24-26 Apr. 1990
(Contract DE-AC04-76DP-00078)
(DE90-009285; SAND-90-0782C; CONF-9004146-4) Avail: NTIS HC A01/MF A01

Long term reliability of solder joints in thick film Au hybrid microcircuits require either minimization of the solid state growth of intermetallics or verification that if present, they do not compromise component performance. Intermetallic compounds such as AuIn2 or AuSn4 arise from the solid state reaction between Au thick films and 50Pb-50In or 63Sn-37Pb solder alloys, respectively; they are undesirable due to their brittle mechanical behavior caused by lack of a sufficient number of independent slip systems for plastic deformation. In addition, they may alter the resistivity of a circuit and thereby alter electronic performance. A brief overview is present on the Au thick film inks/solder alloy systems whose intermetallic growth kinetics were characterized at SNL, Albuquerque for hybrid microcircuit electronic applications. DOE

N90-21176# Washington Univ., Seattle. Dept. of Materials Science and Engineering.
CONTROLLED PRODUCTION AND CHARACTERIZATION OF METASTABLE INTERMETALLICS Final Report, 1 Aug. 1987 - 31 Dec. 1989
M. J. Kaufman Mar. 1990 13 p
(Contract DE-FG06-87ER-45327)
(DE90-009384; DOE/ER-45327/2) Avail: NTIS HC A03/MF A01

The purpose was to establish whether or not it is possible to produce metastable intermetallics as bulk single phase materials and, if possible, to characterize the properties of these phases accordingly. The Al-Ge system was selected as the prototype for this study because of the relative ease with which metastable phases are formed in this system. In addition, the Ti-Al and Ti-Al-Nb systems were also studied based on the controversial nature of their stable and metastable phase equilibria as well as the greater technological significance. The results from all three systems will be described below. Finally, a brief examination of the Al3X compounds (X = Ti, Hf and Zr) was initiated but discontinued when the preliminary results, and those of other investigators, indicated that these materials were not responding favorably to either stable or metastable processing. DOE

27 NONMETALLIC MATERIALS

Includes physical, chemical, and mechanical properties of plastics, elastomers, lubricants, polymers, textiles, adhesives, and ceramic materials.

For composite materials see *24 Composite Materials.*

N90-21177* National Aeronautics and Space Administration. Ames Research Center, Moffett Field, CA.
BORON-CONTAINING ORGANOSILANE POLYMERS AND CERAMIC MATERIALS THEREOF Patent
Salvatore R. Riccitiello, inventor (to NASA), Ming-Ta S. Hsu, inventor (to NASA), and Timothy S. Chen, inventor (to NASA) (Information General Corp., Palo Alto, CA.) 25 Jul. 1989 10 p Filed 11 Aug. 1988 Continuation-in-part of US-Patent-4,767,728; US-Patent-Appl-SN-890577, dated 30 Jul. 1986
(NASA-Case-ARC-11649-2-SB; US-Patent-4,851,491; US-Patent-Appl-SN-231027; US-Patent-Class-528-4; US-Patent-Class-528-10; US-Patent-Class-528-30; US-Patent-Class-556-402; US-Patent-Class-501-88; US-Patent-Class-501-91; US-Patent-Class-501-92) Avail: US Patent and Trademark Office CSCL 11B

The present invention relates to a polyorgano borosilane ceramic precursor polymer comprising a plurality of repeating units of the formula: (R(sup 1) single bond B)(sub p) being linked together at B by second units of the formula: single bond (R sup 2) single bond (Si single bond R sup 3) single bond (sub q), where R(sup 1) is a lower alkyl, cycloalkyl, phenyl, or (R(sup 2)R(sup 3) single bond Si single bond B single bond)(sub n) and R(sup 2) and R(sup 3) are each independently selected from hydrogen, lower

alkyl, vinyl, cycloalkyl, or aryl, n is an integer between 1 and 100; p is an integer between 1 and 100; and q is an integer between 1 and 100. These materials are prepared by combining an organo borohalide of the formula R(sup 4) single bond B single bond (X sup 1) (sub 2) where R(sup 4) is selected from halogen, lower alkyl, cycloalkyl, or aryl, and an organo halosilane of the formula: R(sup 2)(R sup 3)Si(X sup 2)(sub 2) where R(sup 2) and R (sup 3) are each independently selected from lower alkyl, cycloalkyl, or aryl, and X(sup 1) and X(sup 2) are each independently selected from halogen, in an anhydrous aprotic solvent having a boiling point at ambient pressure of not greater than 160 C with in excess of four equivalents of an alkali metal, heating the reaction mixture and recovering the polyorgano borosilane. These silicon boron polymers are useful to generate high-temperature ceramic materials, such as SiC, SiB4, and B4C, upon thermal degradation above 600 C.

Official Gazette of the U.S. Patent and Trademark Office

N90-21178# United Kingdom Atomic Energy Authority, Harwell (England). Metals Technology Centre.

EFFECTS OF TITANIUM ON SOME SURFACE PROPERTIES OF NITRIDE CERAMICS

C. M. E. vanThoor, J. A. Hemsworth, M. G. Nicholas, and R. M. Crispin Jun. 1989 21 p

(AERE-R-13566) Avail: NTIS HC A03/MF A01

The presence of titanium at nitride ceramic/braze interfaces can promote both wetting and bonding. Previously, titanium was added to brazes and the effects of segregation to the interfaces and reaction with the ceramics were examined. In this study, the ceramic surfaces were coated with titanium before they were contacted by brazes or solders. Ion assisted coatings were applied to sialon, Si3N4 and AlN, and sputter ion platings of titanium were applied to sialon. Coating adhesion measured by scratch testing was better for the sputter ion platings than the ion assisted coatings. The platings were also better wetted, by an Ag-Cu eutectic braze, and produced joints 50 percent stronger than those achievable with a commercially developed Ag-Cu-Ti active metal braze. Author

N90-21179# United Kingdom Atomic Energy Authority, Harwell (England). Materials Development Div.

ON THE STABILITY OF AMORPHOUS SILICA COATINGS FOR HIGH TEMPERATURE SERVICE

K. S. Coley, S. R. J. Saunders (National Physical Lab., Teddington, England), M. J. Bennett, C. F. Ayres, A. T. Tuson, and C. F. Knights Mar. 1989 21 p

(AERE-R-13425) Avail: NTIS HC A03/MF A01

Amorphous silica coatings significantly improve the resistance of Incoloy 800H to attack in aggressive atmospheres at temperatures up to 1000 C. Eventually, however, failure occurs due to crystallization of the silica and solid/solid interactions between the coating and substrate. The processes involved were studied using several surface analytical techniques. Crystalline silica nucleated beneath a layer of alloy, which was depleted in chromium on forming a pre-coating oxide layer. Due to the difference in chemical stability of amorphous and crystalline silica, Si and O diffused through the depleted alloy layer from the outer amorphous to the inner crystalline phase, resulting in migration of this alloy layer towards the coating surface. Diffusion calculations suggest migration rates that are reasonably consistent with those observed experimentally. Author

N90-21180*# Old Dominion Univ., Norfolk, VA. Dept. of Mechanical Engineering and Mechanics.

DETERMINATIONS OF MOLECULAR WEIGHT AND MOLECULAR WEIGHT DISTRIBUTION OF HIGH POLYMERS BY THE RHEOLOGICAL PROPERTIES Progress Report, period ending 30 Jun. 1989

J. Y. Huang, T. H. Hou, and S. N. Tiwari Aug. 1989 82 p (Grant NAG1-569)

(NASA-CR-186450; NAS 1.26:186450) Avail: NTIS HC A05/MF A01 CSCL 11C

Several methods are reviewed by which the molecular weight (MW) and the molecular weight distribution (MWD) of polymeric material were determined from the rheological properties. A poly(arylene ether) polymer with six different molecular weights was used in this investigation. Experimentally measured MW and MWD were conducted by GPC/LALLS (gel permeation chromatography/low angle laser light scattering), and the rheological properties of the melts were measured by a Rheometric System Four rheometer. It was found that qualitative information of the MW and MWD of these polymers could be derived from the viscoelastic properties, with the methods proposed by Zeichner and Patel, and by Dormier et al., by shifting the master curves of the dynamic storage modulus, G', and the loss modulus, G'', along the frequency axis. Efforts were also made to calculate quantitative profiles of MW and MWD for these polymers from their rheological properties. The technique recently proposed by Wu was evaluated. It was found that satisfactory results could only be obtained for polymers with single modal distribution in the molecular weight. Author

N90-21181*# National Aeronautics and Space Administration. Lewis Research Center, Cleveland, OH.

FEASIBILITY OF INTERCALATED GRAPHITE RAILGUN ARMATURES

James R. Gaier, Clarence E. Gooden, Doreen Yashan, and Steven Naud (Naval Coastal Systems Center, Panama City, FL.) Apr. 1990 7 p Presented at the 5th Symposium on Electromagnetic Launch Technology, Fort Walton Beach, FL, 2-5 Apr. 1990; sponsored by IEEE

(NASA-TM-102546; E-5332; NAS 1.15:102546) Avail: NTIS HC A02/MF A01 CSCL 11C

Graphite intercalation compounds may provide an excellent material for the fabrication of electro-magnetic railgun armatures. As a pulse of power is fed into the armature the intercalate could be excited into the plasma state around the edges of the armature, while the bulk of the current would be carried through the graphite block. Such an armature would have the desirable characteristics of both diffuse plasma armatures and bulk conduction armatures. In addition, the highly anisotropic nature of these materials could enable the electrical and thermal conductivity to be tailored to meet the specific requirements of electromagnetic railgun armatures. Preliminary investigations were performed in an attempt to determine the feasibility of using graphite intercalation compounds as railgun armatures. Issues of fabrication, resistivity, stability, and electrical current spreading are addressed for the case of highly oriented pyrolytic graphite. Author

N90-21182*# National Aeronautics and Space Administration. Lewis Research Center, Cleveland, OH.

STUDIES OF MECHANO-CHEMICAL INTERACTIONS IN THE TRIBOLOGICAL BEHAVIOR OF MATERIALS

Kazuhisa Miyoshi 1990 22 p Presented at the 8th International Conference on Thin Films, San Diego, CA, 2-6 Apr. 1990; sponsored by the American Vacuum Society

(NASA-TM-102545; E-5301; NAS 1.15:102545) Avail: NTIS HC A03/MF A01 CSCL 11C

Mechano-chemical interaction studies can contribute to the understanding of wear and friction of materials. Specific examples of experimental results relative to the subject are discussed. There are two parts: one describes the synergistic effect of corrosion and wear of iron sliding on sapphire in sulfuric acid, and the other describes the effect of surface films on the wear and friction of plasma-deposited diamondlike carbon (amorphous hydrogenated carbon) films in sliding contact with silicon nitride. The concentration of acid (pH) is an important factor in controlling the iron loss caused by wear-corrosion processes in sulfuric acid. The mechanical action can cause chemical reactions to proceed much faster than they would otherwise. The diamondlike carbon (DLC) films are shown to behave tribologically much like bulk diamond. In a dry nitrogen environment, a mechano-chemical reaction produces a substance which greatly decreases the coefficient of friction. In a moist air environment, mechano-chemical interactions drastically reduce the wear life of DLC films and water vapor greatly increases friction. Author

N90-21183# Dynamet Technology, Inc., Burlington, MA.
DUCTILE ALLOY ENCAPSULATED CERAMIC ARMOR DEVELOPMENT Final Report, Jun. 1987 - Nov. 1989
Susan M. Abkowitz, Paul Weihrauch, Stanley Abkowitz, Stephen A. Mariano, and Dino J. Papetti (Army Materials Technology Lab., Watertown, MA.) Jan. 1990 68 p
(Contract DAAL04-87-C-0029; DA Proj. 1L6-65502-MM-40)
(AD-A217632; MTL-TR-90-2) Avail: NTIS HC A04/MF A01 CSCL 11/6

Development of a fabrication process for encapsulating or cladding ballistic resistant ceramic materials with ductile metal alloys is described. Cladding is accomplished by powder metallurgy (P/M) technology in which an envelope of elemental metal powders, blended with elemental metal powders, blended with elemental or master alloy powder additions, is cold isostatically pressed around the ceramic in an inexpensive, re-usable elastomeric mold. The P/M envelope is further densified by vacuum sintering optionally followed by hot isostatic pressing. The metal cladding can also be heat treated for further enhancement of its mechanical properties. Besides the potential for improving ballistic armor performance, this P/M method of cladding offers wider flexibility in the design of ceramic armor systems allowing for the manufacture of multi-tile and multi-ceramic designs with the ceramic elements arranged and oriented in many different arrays. The metal cladding also provides a means of attaching armor plates by welding, thus offering advantages in the repair and maintainability of armored vehicles. The report describes the details of the optimized P/M cladding process of ceramics with titanium and aluminum base materials. Also described are efforts to evaluate and enhance the quality and strength of the bonding between the ceramics and strength of the bonding between the ceramics and the metal cladding. GRA

N90-21184# Department of the Navy, Washington, DC.
HIGH GLOSS CORROSION-RESISTANT COATINGS Patent Application
Charles R. Hegedus, inventor (to Navy), Donald J. Hirst, inventor (to Navy), Anthony T. Eng, inventor (to Navy), and William J. Green, inventor (to Navy) 28 Nov. 1989 23 p
(AD-D014403; US-Patent-Appl-SN-442085) Avail: NTIS HC A03/MF A01 CSCL 11/3

The patent application discloses a high-gloss, corrosion-resistant coating which can be applied directly to a surface comprising about 30 to 82 percent by weight of a polymeric binder and 18 to 70 percent by weight of a pigment system consisting essentially of zinc molybdate, zinc salt of benzoic acids, and zinc phosphate in specific ratio's. The coating exhibits good adhesion, flexibility, chemical- and weather-resistance. GRA

N90-21185# Department of the Navy, Washington, DC.
A NEW CLASS OF LUBRICANTS DERIVED FROM ARCHAEBACTERIAL LIPIDS Patent Application
Eddi L. Chang, inventor (to Navy) 29 Nov. 1989 13 p
(AD-D014429; US-Patent-Appl-SN-442961) Avail: NTIS HC A03/MF A01 CSCL 11/8

A new class of lubricants based on the general features of archaebacterial lipids but not limited to lipids solely extracted from archaebacteria is described. These lubricant/additive molecules have the following features: bipolarity, ether bonds, and branched biphytanyl chains. The molecules can be double chained or single chained. This new class has the potential to be highly thermally and chemically stable due to the above mentioned features. GRA

N90-21186# Sandia National Labs., Albuquerque, NM.
AGING AND COMPATIBILITY OF TNF-DOPED MYLAR
C. Arnold, Jr. 1990 3 p Presented at the 16th DOE Compatibility, Aging and Service Life Conference, Livermore, CA, 24-26 Apr. 1990
(Contract DE-AC04-76DP-00789)
(DE90-008508; SAND-90-0653C; CONF-9004146-1) Avail: NTIS HC A01/MF A01

TNF-doped Mylar is a new radiation-hard dielectric that has recently been qualified as a viable substitute for Mylar in capacitors. The advantage of TNF-doped Mylar is that it satisfies both the nuclear safety and radiation hardness requirements of weapons. Mylar is not radiation-hard. Aging and compatibility studies were carried out to insure that: (1) TNF does not diffuse from the film during fabrication of the capacitor or during storage; and (2) there are no compatibility problems with aluminum foil (the conductor) or Fluorinert (the secondary dielectric). Losses of TNF were barely detectable during the vacuum bakes used in fabricating capacitors or during accelerated aging tests carried out below T(sub g) (70 C) over a two year period in air. In other accelerated tests, no compatibility problems were detected with aluminum or Fluorinert. TNF-doped Mylar is now being used in the MC-4109 capacitor that was called out for use in SRAM II. No age-related or compatibility-related problems with TNF-doped Mylar are anticipated. DOE

N90-21187*# National Aeronautics and Space Administration. Goddard Space Flight Center, Greenbelt, MD.
FRACTURE TOUGHNESS AND CRACK GROWTH OF ZERODUR
Michael J. Viens Washington Apr. 1990 26 p
(NASA-TM-4185; NAS 1.15:4185) Avail: NTIS HC A03/MF A01 CSCL 11C

The fracture toughness and crack growth parameters of Zerodur, a low expansion glass ceramic material, were determined. The fracture toughness was determined using indentation techniques and was found to be 0.9 MPa x m(sup 1/2). The crack growth parameters were determined using indented biaxial specimens subjected to static and dynamic loading in an aqueous environment. The crack growth parameters n and 1n(B) were found to be 30.7 and -6.837, respectively. The crack growth parameters were also determined using indented biaxial specimens subjected to dynamic loading in an ambient 50 percent relative humidity environment. The crack growth parameters n and 1n(B) at 50 percent relative humidity were found to be 59.3 and -17.51, respectively. Author

N90-21188# Technology Assessment and Transfer, Inc., Annapolis, MD.
IMPROVED THERMO-OXIDATIVE-DEPOSITION SCREENING TESTS FOR TURBINE LUBRICANTS Final Report, Sep. 1986 - Jun. 1989
Larry Fehrenbacher, Robert Schafrik, and Jacqueline Macia 12 Nov. 1989 79 p
(Contract F33615-86-C-2697)
(AD-A217795; WRDC-20) Avail: NTIS HC A05/MF A01 CSCL 11/8

This research applied combined Thermogravimetric Analysis (TGA) and Differential Scanning Calorimetry (DSC) techniques to establish a potential new laboratory screening method for simulating and differentiating the high temperature lubricant degradation phenomena of oils in operational turbine engines. GRA

N90-21189 Department of the Navy, Washington, DC.
COMBINATION PRIMER/TOPCOAT COATING Patent
Charles R. Hegedus, inventor (to Navy) and William J. Green, inventor (to Navy) 5 Dec. 1989 4 p Filed 28 Mar. 1989 Supersedes AD-D014166
(AD-D014445; US-Patent-Appl-SN-331200;
US-Patent-Class-524-204) Avail: US Patent and Trademark Office CSCL 11/3

A coating for metallic or polymeric composite substrates is disclosed which performs both as a primer and as a topcoat. It comprises a two component aliphatic polyurethane binder, with titanium dioxide, zinc molybdate, zinc phosphate, an organo-zinc salt, and titanium dioxide vesiculated bead pigments in controlled amounts. The coating exhibits good adhesion, corrosion inhibition, flexibility, chemical and weather resistance, and opacity. GRA

N90-21190# Department of the Navy, Arlington, VA.
ENERGY BEAM TREATMENT FOR IMPROVED ADHESION OF COATINGS TO SURFACES Patent Application

Irwin L. Singer, inventor (to Navy) 31 Oct. 1989 38 p
(AD-D014449; US-Patent-Appl-SN-429959) Avail: NTIS HC A03/MF A01 CSCL 11/3

The present invention relates to engineering materials in general and more specifically to the coating of bulk engineering material with corrosion, oxidation or wear resistant inorganic materials. Coatings are needed for protecting engineering components against mechanical, tribological and corrosive/oxidative degradation. In particular, engineering ceramics, by virtue of their light weight, high strength and thermal stability, have great potential for many high temperature applications. However, several of the best and toughest candidate ceramics, e.g., silicon carbide, silicon nitride, and tungsten carbide, require oxide coatings to resist corrosion and oxidation at high temperatures (900 C and up). The coating of a substrate with a coating different from and non-reactive with the substrate is improved by energetic surface alloying of the substrate prior to coating. The ion implantation alters the stoichiometry of the substrate, creating a substrate surface which is reactive with the coating. For example, the bonding of TiN to Si3N4 is enhanced by implanting the substrate surface with Ti. GRA

N90-21191*# National Aeronautics and Space Administration. Marshall Space Flight Center, Huntsville, AL.
THE CORROSION PROTECTION OF 6061-T6 ALUMINUM BY A POLYURETHANE-SEALED ANODIZED COAT
M. D. Danford Apr. 1990 33 p
(NASA-TM-100394; NAS 1.15:100394) Avail: NTIS HC A03/MF A01 CSCL 11C

The corrosion protection of 6061-T6 anodized aluminum afforded by a newly patented polyurethane seal was studied using the ac impedance technique. Values of the average corrosion rates over a 27-day exposure period in 3.5 percent NaCl solutions at pH 5.2 and pH 9.5 compared very favorably for Lockheed-prepared polyurethane-sealed and dichromate-sealed coats of the same thickness. Average corrosion rates for both specimens over the first 7 days of exposure compared well with those for a hard anodized, dichromate-sealed coat, but rose well above those for the hard anodized coat over the entire 27-day period. This is attributed both to the greater thickness of the hard anodized coat, and possibly to its inherently better corrosion protective capability. Author

N90-21192*# National Aeronautics and Space Administration. Lewis Research Center, Cleveland, OH.
RESISTIVITY OF PRISTINE AND INTERCALATED GRAPHITE FIBER EPOXY COMPOSITES
James R. Gaier, Paul D. Hambourger (Cleveland State Univ., OH.), and Melissa E. Slabe 1989 18 p Presented at the 19th Biennial Conference on Carbon, University Park, PA, 25-30 Jun. 1989; sponsored by American Carbon Society
(Contract NCC3-19)
(NASA-TM-102576; E-5406; NAS 1.15:102576) Avail: NTIS HC A03/MF A01 CSCL 11C

Laminar composites were fabricated from pristine and bromine intercalated Amoco P-55, P-75, and P-100 graphite fibers and Hysol-Grafil EAG101-1 film epoxy. The thickness and r.f. eddy current resistivity of several samples were measured at grid points and averaged point by point to obtain final values. Although the values obtained this way have high precision (less than 3 percent deviation), the resistivity values appear to be 20 to 90 percent higher than resistivities measured on high aspect ratio samples using multi-point techniques, and by those predicted by theory. The temperature dependence of the resistivity indicates that the fibers are neither damaged nor deintercalated by the composite fabrication process. The resistivity of the composites is a function of sample thickness (i.e., resin content). Composite resistivity is dominated by fiber resistivity, so lowering the resistivity of the fibers, either through increased graphitization or intercalation, results in a lower composite resistivity. A modification of the simple rule of mixtures model appears to predict the conductivity of high aspect ratio samples measured along a fiber direction, but a directional dependence appears which is not predicted by the theory. The resistivity of these materials is clearly more complex than that of homogeneous materials. Author

N90-21193# Melbourne Univ., Parkville (Australia). School of Physics.
ZELED ANALYSIS OF APERIODICITY AND BOND LENGTHS IN CERAMIC POWDERS
Katherine L. Smith (Australian Nuclear Science and Technology Organisation, Menai.) and Timothy J. White 1989 21 p
(DE90-612932; UM-P-89/13) Avail: NTIS (US Sales Only) HC A03/MF A01

It is demonstrated that zero energy loss electron diffraction (ZELED) may be used to determine local correlations of bond length in ultra fine-grained (le100 10(exp -10) m) aperiodic ceramic precursor powders. Furthermore, it is suggested that during calcination the onset of crystallization may be recognized by monitoring the number and intensity of discrete bond lengths. The potential of this technique is illustrated using an alkoxide derived powder produced during the fabrication of titanate high level nuclear waste ceramics. ZELED is compared with extended x ray absorption fine structure (EXAFS) spectroscopy, to which it is similar in many respects, and the strengths and weaknesses of both techniques are highlighted. DOE

N90-21194# International Centre for Theoretical Physics, Trieste (Italy).
GENERALIZED RANDOM PHASE APPROXIMATION FOR MULTICOMPONENT POLYMER SYSTEMS
Mustapha Benmouna Sep. 1989 11 p Submitted for publication
(DE90-613691; IC-89/256) Avail: NTIS (US Sales Only) HC A03/MF A01

The extension of dynamical Random Phase Approximation to Polymer solutions is discussed. A generalized expression of the excluded volume parameter is given as a function of space and time. It is written in terms of static response and memory functions of the intermediate scattering functions for total and bare systems. A dynamic response function of the solvent is also given and its effects on various dynamical properties of the system are investigated. DOE

N90-21195# Japan Atomic Energy Research Inst., Tokyo.
LOW ENERGY ION GENERATOR
Yoshiaki Nakase Oct. 1989 75 p In JAPANESE; ENGLISH summary
(DE90-759905; JAERI-M-89-151) Avail: NTIS (US Sales Only) HC A04/MF A01

In order to investigate the modification of a polymer surface by ion bombardment, a low energy ion generator has been constructed. System design construction, generator components such as power system and evacuation system, the results of performance tests are described. A maximum beam intensity of Kr(+) was 1.6 mA at 35 kV on a Ti-target. From the preliminary experimental results of Kr(+) irradiation, the coloration (carbonization) of the polymer surface, i.e. the increase of optical density, was observed. The relationship between the optical density change of irradiated polymer film and Kr(+) beam currents as measured by Faraday Cup will provide a convenient method to estimate absorbed ion energy in the film. DOE

N90-21196# Los Alamos National Lab., NM. Defense Laser Technology.
DIAMOND: A HIGH POWER OPTICAL MATERIAL
Sidney Singer 1990 19 p Presented at the International Conference on Optical Science and Engineering, Hague (Netherlands), 12-16 Mar. 1990
(Contract W-7405-eng-36)
(DE90-008941; LA-UR-90-839; CONF-900368-3) Avail: NTIS HC A03/MF A01

Single crystal chemically/isotopically pure synthetic diamond operated at low temperature offers an unusual opportunity for a small transparent optic that may transmit as much as tens to

hundreds of megawatts of light, even in the presence of high peak power in the light beam. This property stems from the probable very low absorption of light in such material and the nature of the phonon energy transport at low temperature. DOE

N90-21197# Oak Ridge National Lab., TN. Structural Ceramics Group.
RESEARCH ADVANCES IN FINE CERAMICS
P. F. Beecher 2 Apr. 1990 17 p Presented at the International Forum on Fine Ceramics, Nagoya (Japan), 12-13 Mar. 1990; and at the International Fine Ceramics Workshop, Nagoya (Japan), 15-16 Mar. 1990
(Contract DE-AC05-84OR-21400)
(DE90-008983; ORNL/FTR-3572) Avail: NTIS HC A03/MF A01

The author attended both the International Forum on Fine Ceramics and the International Fine Ceramics Workshop in Nagoya, Japan. The Forum speakers presented overviews on research advances in the development of and the economics of electronics, ceramics, hard materials, and structural ceramics. The Workshop was devoted to presentations on recent research findings primarily on the mechanical behavior and processing of structural ceramics. The author presented two invited talks: one on the toughening behavior of whisker-reinforced ceramics, and one on mechanical properties at elevated temperatures. He also held separate discussions with researchers from Nippon Kokan K.K. (NKK) and Toshiba on their research on the properties of silicon nitride ceramics. These researchers and those of other Japanese laboratories have made excellent progress in developing silicon nitride ceramics with high fracture toughness/resistance which also appear to have promising properties at elevated temperatures. DOE

N90-21198* National Aeronautics and Space Administration. Langley Research Center, Hampton, VA.
PROCESS FOR CROSSLINKING METHYLENE-CONTAINING AROMATIC POLYMERS WITH IONIZING RADIATION Patent
Vernon L. Bell, inventor (to NASA) and Stephen J. Havens, inventor (to NASA) (Kentron International, Inc., Hampton, VA.) 20 Mar. 1990 11 p Filed 11 Mar. 1986 Supersedes N86-24840 (24 - 15, p 2439)
(NASA-Case-LAR-13448-1; US-Patent-4,910,233; US-Patent-Appl-SN-838654; US-Patent-Class-522-162; US-Patent-Class-264-022; US-Patent-Class-522-165; US-Patent-Class-528-176; US-Patent-Class-528-308) Avail: US Patent and Trademark Office CSCL 11C

A process for crosslinking aromatic polymers containing radiation-sensitive methylene groups (-CH2-) by exposing the polymers to ionizing radiation thereby causing crosslinking of the polymers through the methylene groups is described. Crosslinked polymers are resistant to most organic solvents such as acetone, alcohols, hydrocarbons, methylene, chloride, chloroform, and other halogenated hydrocarbons, to common fuels and to hydraulic fluids in contrast to readily soluble uncrosslinked polymers. In addition, the degree of crosslinking of the polymers depends upon the percentage of the connecting groups which are methylene which ranges from 5 to 50 pct and preferably from 25 to 50 pct of the connecting groups, and is also controlled by the level of irradiation which ranges from 25 to 1000 Mrads and preferably from 25 to 250 Mrads. The temperature of the reaction conditions ranges from 25 to 200 C and preferably at or slightly above the glass transition temperature of the polymer. The crosslinked polymers are generally more resistant to degradation at elevated temperatures such as greater than 150 C, have a reduced tendency to creep under load, and show no significant embrittlement of parts fabricated from the polymers.
Official Gazette of the U.S. Patent and Trademark Office

N90-21199# Oak Ridge National Lab., TN.
REVIEW OF THE STATE OF THE TECHNOLOGY FOR JOINING CERAMICS FOR HIGH-TEMPERATURE STRUCTURAL APPLICATIONS
A. J. Moorhead and Hyoun-Ee Kim 1990 8 p Presented at the 5th International Symposium on Advanced Technology in Welding, Materials Processing and Evaluation, Tokyo, Japan, 17-19 Apr. 1990
(Contract DE-AC05-84OR-21400)
(DE90-009224; CONF-9004154-1) Avail: NTIS HC A02/MF A01

Three major processes are reviewed for joining ceramics for structural applications; i.e., those which impose significant stresses, at elevated temperatures, and in corrosive environments. Included are discussions on diffusion welding, brazing with filler metals, and brazing with nonmetallic filler materials (glasses). DOE

N90-21200# Michigan Univ., Ann Arbor. Dept. of Materials Science and Engineering.
THE STRUCTURAL BASIS FOR FATIGUE INITIATION IN GLASSY POLYMERS Progress Report No. 2
Albert F. Yee and David W. Gidley Mar. 1990 5 p
(Contract DE-FG02-88ER-45366)
(DE90-009342; DOE/ER-45366/2) Avail: NTIS HC A01/MF A01

Glassy polymers are often subjected to cyclic loading and consequent failure in energy-related applications. At high amplitudes of loading they fail by ductile deformation, while at intermediate amplitudes the failures are brittle. In the latter case a large fraction of the useful lifetime is spent in the incubation period. Research is aimed at understanding this initiation process. Since much of the behavior including embrittlement observed in preliminary experiments are similar to those found in physical aging of glassy polymers, some of the techniques used for studying physical aging are also employed here; viz., DSC, stress relaxation, and positron annihilation lifetime studies (PAT). Glassy polycarbonate is used throughout. DOE

28 PROPELLANTS AND FUELS

Includes rocket propellants, igniters, and oxidizers; their storage and handling procedures; and aircraft fuels.

For related information see also *07 Aircraft Propulsion and Power, 20 Spacecraft Propulsion and Power,* and *44 Energy Production and Conversion.*

N90-21201# Materials Research Labs., Maribyrnong (Australia).
METHODS FOR IMPROVING THE FLOWABILITY OF A PERCUSSION PRIMER COMPOSITION
Leo V. deYong, Mark Fitzgerald, and Brian Whiffen 1989 35 p
(MRL-TR-89-32; ARL-005-734) Avail: NTIS HC A03/MF A01

A vibrating hopper was used to evaluate and determine methods for improvement of the flowability of the percussion primer composition MRL(X) 408. The flowability was enhanced by granulation using both water and binder systems and using flow modifiers (silicon dioxide). Addition of binders reduced the sensitivity of the composition and, when filled into primers, increased the value of peak pressure and the rise time to peak pressure.
Author

N90-21202# Materials Research Labs., Maribyrnong (Australia).
AN EVALUATION OF METAL SALTS OF 3-NITRO-1,2,4-TRIAZOL-5-ONE (NTO) AS POTENTIAL PRIMARY EXPLOSIVES
Lance D. Redman and Robert J. Spear 1989 17 p
(MRL-TN-563; AR-006-283) Avail: NTIS HC A03/MF A01

Sodium, potassium, and ammonium salts of NTO were prepared, and used as intermediates to prepare a range of heavy metal salts; silver, lead, mercuric, barium, cadmium, strontium, cupric, nickel and stannous. Normal salts were prepared in all cases, and acid salts for sodium, potassium, lead and mercuric. The ammonium salt was shown to be identical to that reported previously. Response to mechanical and thermal stimuli is typical of sensitive secondary explosives. It is concluded that these materials do not have any potential for use as primary (initiating) explosives. Author

N90-21203# Materials Research Labs., Maribyrnong (Australia).
PREPARATION, CHARACTERISATION AND COOKOFF BEHAVIOUR OF BOOSTER COMPOSITIONS PREPARED FROM RDX AND ACRYLIC OR ETHYLENE-VINYL ACETATE DISPERSIONS
Ian J. Dagley, Luciana Montelli, Robert P. Parker, and Craig N. Louey 1989 36 p
(MRL-TR-89-44; AR-005-750) Avail: NTIS HC A03/MF A01

A range of potential booster explosives was prepared using RDX and commercially available acrylic and ethylene-vinyl acetate dispersions. The dispersions were coagulated in hot aqueous slurries of RDX by electrolyte addition and the use of thermal coagulation aids, a process compatible with existing Australian production plant and methods. Generally the polymer coatings on the RDX crystals were porous and the precipitated particles had not coalesced to form polymer films. In these cases the compositions were no less sensitive to impact than RDX. Several softer polymers gave effective coatings and desensitized the RDX. Film formation was enhanced using plasticizers, and flow properties were improved by applying an additional coating of zinc stearate. Vacuum thermal stability in most cases was excellent. The six compositions rated as most promising were prepared on a larger scale and their impact sensitiveness, shock sensitivity and cookoff behavior were assessed. Compositions with sensitiveness less than that of tetryl have been produced; however further desensitization, particularly to slow cookoff, must be achieved to produce an acceptable insensitive booster composition. The use of plasticizers to enhance coating efficiencies and the incorporation of other explosives to modify cookoff response should be examined. Author

N90-21204# Materials Research Labs., Maribyrnong (Australia).
DETERMINATION OF DETONATION PARAMETERS OF BOOSTER EXPLOSIVES AT SMALL CHARGE DIAMETERS
Robert J. Spear and Michael G. Wolfson 1989 30 p
(MRL-TR-89-45; AR-006-287) Avail: NTIS HC A03/MF A01

An experimental method for determining velocity of detonation (VOD) of unconfined explosives at small charge diameters was developed. The experimental technique uses readily available components and is relatively easy to set up. VOD is measured by ultra-high speed streak photography; variation in magnification on the streak record was detected. VOD was determined on conventional booster explosives based on RDX/polyethylene wax (PEW), DNBF, and two candidate insensitive booster explosives PBXW-7 and ADNBF. All were pressed to 80 to 95 percent TMD (theoretical maximum density), and diameters ranged from 12.75 mm to 1.52 mm. A surprisingly strong dependence between the critical diameter estimated from these firings and percent TMD was observed. It is suggested that further measurements should be made for explosives pressed to 80 to 95 percent TMD, which is typical of production filling and where only very limited data are available. Comment is made on the potential of PBXW-7 and ADNBF to replace conventional booster explosives in fuzes for insensitive munitions. Author

N90-21205# Sandia National Labs., Albuquerque, NM.
SHOCK INITIATION SENSITIVITY OF DAMAGED TP-H1207C COMPOSITE PROPELLANT
L. J. Weirick 1989 15 p Presented at the 1990 JANNAF Propulsion Systems Hazards Meeting, Laurel, MD, 3-5 Apr. 1990
(Contract DE-AC04-76DP-00789)
(DE90-008509; SAND-89-2580C; CONF-9004147-2) Avail: NTIS HC A03/MF A01

A series of impact experiments on a composite and an energetic propellant and their simulants was recently completed using a light-gas gun. Previous experiments were done to obtain Hugoniot data, to investigate the pressure threshold at which a reaction occurs, to measure spall damage at various impact pressures, and to measure the shock attenuation of these materials. Recently, digitizing oscilloscopes with very high speed (1 GHz/1 ns per point), improved vertical resolution (8 bit), and large storage capacity (62 K points) were added to the laser interferometer system. These additions made possible the accurate measurement of the magnitude of impacts with very short loading histories (approx. 50 ns) which may be followed by long delay times (approx. 15 microsec) before a reaction is initiated or a subsequent impact occurs. Experiments have been performed where a flyer plate on the front of a projectile induced an initial shock of 1.94 GPa through a composite propellant, TP-H1207C, target producing a damaged propellant. After an induced delay of (approx. 4.5 microsec), a second impact shock is imposed into the damaged propellant possibly causing it to react. By using secondary impactors of various impedances, the second impact pressure can be lowered until the damaged propellant no longer reacts. This pressure is the initiation threshold pressure for the damaged propellant. For the case of TP-H1207C initially subjected to a 1.94 GPa pressure pulse, the sensitized material initiation threshold was found to be 1.46 GPa. This value contrasts with the previously measured initiation threshold of approx. 4.1 GPa for undamaged TP-H1207C. DOE

N90-21206# Los Alamos National Lab., NM.
DISCRETE MODELING OF BEDS OF PROPELLANT EXPOSED TO STRONG STIMULUS
D. Scott Stewart (Illinois Univ., Urbana.) and Blaine W. Asay 1989 23 p Presented at the Workshop on Dynamical Issues in Combustion Theory, Minneapolis, MN, 13-17 Nov. 1989 Submitted for publication
(Contracts W-7405-eng-36; LANL-9-XG-83931P-1)
(DE90-008932; LA-UR-90-898; CONF-891179-1) Avail: NTIS HC A03/MF A01

This paper is a description of experimental and theoretical modeling concepts that are being developed to describe the behavior of confined propellant beds made of discrete particles, when subjected to a strong stimulus such as the impact of a penetrating jet. A principal goal is to discover basic mechanisms within the bed that control a reactive wave that either fails and extinguishes, or propagates as a rapid burning or detonating wave. This paper is an extended version of a lecture given by D.S. Stewart at the Institute for Mathematics and its Application in November of 1989. DOE

29 MATERIALS PROCESSING

Includes space-based development of products and processes for commercial applications.
For biological materials see *55 Space Biology.*

N90-21207*# National Aeronautics and Space Administration, Washington, DC.
MICROGRAVITY SCIENCE AND APPLICATIONS BIBLIOGRAPHY, 1989 REVISION
May 1990 64 p
(NASA-TM-4192; NAS 1.15:4192) Avail: NTIS HC A04/MF A01 CSCL 22A

This edition of the Microgravity Science and Applications (MSA) Bibliography is a compilation of government reports, contractor reports, conference proceedings, and journal articles dealing with flight experiments utilizing a low gravity environment to elucidate and control various processes, or with ground based activities that provide supported research. It encompasses literature published but not cited in the 1988 Revision and that literature which has been published in the past year. Subdivisions of the Bibliography include: electronic materials, metals, alloys, and composites; fluids, interfaces, and transport; glasses and ceramics; biotechnology; combustion science; experimental technology, facilities, and instrumentation. Also included are publications from the European, Soviet, and Japanese programs. Author

N90-21208*# Alabama Univ., Huntsville. Dept. of Chemistry.
CRITICAL POINT WETTING DROP TOWER EXPERIMENT Final Report
William F. Kaukler 18 Apr. 1990 26 p
(Grant NAG8-511)

(NASA-CR-186513; NAS 1.26:186513) Avail: NTIS HC A03/MF A01 CSCL 22A

The 100 m Drop Tower at NASA-Marshall was used to provide the step change in acceleration from 1.0 to 0.0005 g. An inter-fluid meniscus oscillates vertically within a cylindrical container when suddenly released from earth's gravity and taken into a microgravity environment. Oscillations damp out from energy dissipative mechanisms such as viscosity and interfacial friction. Damping of the oscillations by the later mechanism is affected by the nature of the interfacial junction between the fluid-fluid interface and the container wall. In earlier stages of the project, the meniscus shape which developed during microgravity conditions was applied to evaluations of wetting phenomena near the critical temperature. Variations in equilibrium contact angle against the container wall were expected to occur under critical wetting conditions. However, it became apparent that the meaningful phenomenon was the damping of interfacial oscillations. This latter concept makes up the bulk of this report. Perfluoromethyl cyclohexane and isopropanol in glass were the materials used for the experiment. The wetting condition of the fluids against the wall changes at the critical wetting transition temperature. This change in wetting causes a change in the damping characteristics of the interfacial excursions during oscillation and no measurable change in contact angle. The effect of contact line friction measured above and below the wetting transition temperature was to increase the period of vertical oscillation for the vapor-liquid interface when below the wetting transition temperature. Author

N90-21209* National Aeronautics and Space Administration. Marshall Space Flight Center, Huntsville, AL.

APPARATUS FOR MIXING SOLUTIONS IN LOW GRAVITY ENVIRONMENTS Patent

Daniel C. Carter, inventor (to NASA) and Mary B. Broom, inventor (to NASA) (Universities Space Research Association, Huntsville, AL.) 20 Mar. 1990 8 p Filed 15 Sep. 1988

(NASA-Case-MFS-26047-1; US-Patent-4,909,933; US-Patent-Appl-SN-244369; US-Patent-Class-210-95; US-Patent-Class-210-94; US-Patent-Class-210-205; US-Patent-Class-210-247; US-Patent-Class-210-257.1; US-Patent-Class-210-321.6; US-Patent-Class-210-340) Avail: US Patent and Trademark Office CSCL 12A

An apparatus is disclosed for allowing mixing of solutions in low gravity environments so as to carry out crystallization of proteins and other small molecules or other chemical syntheses, under conditions that maximize crystal growth and minimize disruptive turbulent effects. The apparatus is comprised of a housing, a plurality of chambers, and a cylindrical rotatable valve disposed between at least two of the chambers, said valve having an internal passageway so as to allow fluid movement between the chambers by rotation of the valve. In an alternate embodiment of the invention, a valve is provided having an additional internal passage way so that fluid from a third chamber can be mixed with the fluids of the first two chambers. This alternate embodiment of the invention is particularly desirable when it is necessary to provide a termination step to the crystal growth, or if a second synthetic step is required.

Official Gazette of the U.S. Patent and Trademark Office

31 ENGINEERING (GENERAL)

Includes vacuum technology; control engineering; display engineering; cryogenics; and fire prevention.

N90-21210*# National Aeronautics and Space Administration. Lewis Research Center, Cleveland, OH.

INFLUENCE OF THE DEPOSITION CONDITIONS ON RADIOFREQUENCY MAGNETRON SPUTTERED MoS2 FILMS

Pierre A. Steinmann and Talivaldis Spalvins Apr. 1990 11 p

(NASA-TP-2994; E-5181; NAS 1.60:2994) Avail: NTIS HC A03/MF A01 CSCL 13B

By varying the radiofrequency (RF) power, the Ar pressure, and the potential on the substrates, MoS(x) films of various stoichiometry, density, adhesion, and morphology were produced. An increase of RF power increased the deposition rate and density of the MoS2 films as well as improved adhesion. However, the stoichiometry remained constant. An increase of Ar pressure increased the deposition rate but decreased the density, wheras both stoichiometry and adhesion were maximized at around 20 mtorr Ar pressure. Furthermore, a transition from compact film growth to columnar film growth was observed when the pressure was varied from 5 to 15 mtorr. Substoichiometric films were grown when a negative (bias) voltage was applied to the substrates.

Author

N90-21211# Department of the Army, Washington, DC.

METHOD OF MAKING A LONG LIFE HIGH CURRENT DENSITY CATHODE FROM TUNGSTEN AND IRIDIUM POWDERS USING A QUARTERNARY COMPOUND AS THE IMPREGNANT Patent Application

Louis E. Branovich, inventor (to Army), Bernard Smith, inventor (to Army), Gerard L. Freeman, inventor (to Army), and Donald W. Eckart, inventor (to Army) 2 Jan. 1990 8 p

(AD-D014425; US-Patent-Appl-SN-459629) Avail: NTIS HC A02/MF A01 CSCL 09/1

A long life high current density cathode is made from a mixture of tungsten and iridium powders by processing the mixture of powders with an activator into a porous billet, and then impregnating the billet with a quaternary compound including barium, oxygen, a metal selected from the group consisting of osmium, iridium, rhodium, and rhenium, and a metal selected from the group consisting of strontium, calcium, scandium and titanium, by firing the billet in a dry hydrogen furnace at a temperature at which the impregnant melts. GRA

N90-21212# Applied Research Associates, Inc., Panama City, FL.

SELECTIVE AUTOMATIC FIRE EXTINGUISHER FOR COMPUTERS (SAFECOMP): DEVELOPMENTAL TEST AND EVALUATION/INITIAL OPERATIONAL TEST AND EVALUATION Final Report

Jan. 1990 92 p

(Contract F08635-88-C-0067)

(AD-A217790) Avail: NTIS HC A05/MF A01 CSCL 13/12

The purpose of this test was to verify the operational effectiveness and suitability of the SAFECOMP (Selective Automatic Fire Extinguisher for Computers) fire detection, suppression, and notification system in a realistic operational environment. It is concluded that the SAFECOMP system provides fire detection and suppression inside the computer cabinet without release of a large quantity of fire extinguishing agent. The small amount of Halon 1211 (one pound) in SAFECOMP is safe, leaves no residue and has a very low ozone depletion potential (ODP) of 2.4 per pound as compared to total flood system with hundreds of pounds of Halon 1301 and an ODP of 12. SAFECOMP will replace Halon 1301 total flood systems at an installation and life-cycle cost savings of 90 + percent. The SAFECOMP system has been validated and the performance specifications met. The system has the potential to meet and exceed all of the objectives required for an automatic computer-electronic fire extinguishing system for worldwide Air Force use. GRA

N90-21213# Department of Defense Explosives Safety Board, Alexandria, VA.

MINUTES OF THE 23RD EXPLOSIVES SAFETY SEMINAR, VOLUME 1

Aug. 1988 1275 p Seminar held in Atlanta, GA, 9-11 Aug. 1988

(AD-A218264) Avail: NTIS HC A99/MF E12

Some topics of the conference include: Fragment hazards; Airblast interactions; Explosives risk assessment; Structural damage from blast; Demilitarization, disposal, decontamination; Quantity distance application; Fire protection - deluge systems; Debris hazards testing and analysis; Far field airblast effects and mitigation designs consideration; Electrostatic discharge (ESD); Underground explosion effects - large scale tests; Wall and window response

to blast loads; Explosives facility design considerations, Accident/explosion effects; and Shock sensitivity of explosives.
Author

N90-21214# Department of Defense Explosives Safety Board, Alexandria, VA.
MINUTES OF THE 23RD EPLOSIVES SAFETY SEMINAR, VOLUME 2
Aug. 1988 1195 p Seminar held in Atlanta, GA, 9-11 Aug. 1988
(AD-A218265) Avail: NTIS HC A99/MF E12 CSCL 13/2

Some areas of discussion at this seminar were: Hazards and risks of the disposal of chemical munitions using a cryogenic process; Special equipment for demilitarization of lethal chemical agent filled munitions; explosive containment room (ECR) repair Johnston Atoll chemical agent disposal system; Sympathetic detonation testing; Blast loads, external and internal; Structural reponse testing of walls, doors, and valves; Underground explosion effects, external airblast; Explosives shipping, transportation safety and port licensing; Explosive safety management; Underground explosion effects, model test and soil rock effects; Chemical risk and protection of workers; and Full scale explosives storage test.
Author

N90-21215* National Aeronautics and Space Administration. Pasadena Office, CA.
ACOUSTIC CONVECTIVE SYSTEM Patent
Eugene H. Trinh, inventor (to NASA) and Judith L. Robey, inventor (to NASA) (California Inst. of Tech., Pasadena.) 22 Aug. 1989 6 p Filed 23 Mar. 1988
(Contract NAS7-918)
(NASA-Case-NPO-17278-1-CU; US-Patent-4,858,717; US-Patent-Appl-SN-172100; US-Patent-Class-181-0.5; US-Patent-Class-361-383; US-Patent-Class-361-384; US-Patent-Class-361-385; US-Patent-Class-62-467) Avail: US Patent and Trademark Office CSCL 13B

A small and simple system is provided for cooling or heating a small component by flowing air or other fluid over it, which does not require any macroscopic moving parts. The system includes a transducer and reflector that are spaced apart with the component between them, and with the transducer being operated at a frequency resonant to the spacing between it and the reflector. The resulting standing wave pattern produces acoustic streaming which results in the circulating of air or other fluid in the environment across the component. The system is especially useful in the reduced gravity environment of outer space because of the absence of any buoyancy-induced convection there.
Official Gazette of the U.S. Patent and Trademark Office

N90-21216* National Aeronautics and Space Administration. Langley Research Center, Hampton, VA.
PRESSURE RIG FOR REPETITIVE CASTING Patent
Peter Vasquez, inventor (to NASA), William R. Hutto, inventor (to NASA), and Albert R. Philips, inventor (to NASA) 12 Sep. 1989 6 p Filed 29 Aug. 1988 Continuation-in-part of US-Patent-Appl-SN-067846, filed 30 Jun. 1987, abandoned
(NASA-Case-LAR-14050-1; US-Patent-4,865,114; US-Patent-Appl-SN-237657; US-Patent-Class-164-284; US-Patent-Class-164-113; US-Patent-Class-249-127; US-Patent-Appl-SN-067846) Avail: US Patent and Trademark Office CSCL 13H

The invention is a pressure rig for repetitive casting of metal. The pressure rig performs like a piston for feeding molten metal into a mold. Pressure is applied to an expandable rubber diaphragm which expands like a balloon to force the metal into the mold. A ceramic cavity which holds molten metal is lined with blanket-type insulating material, necessitating only a relining for subsequent use and eliminating the lengthy cavity preparation inherent in previous rigs. In addition, the expandable rubber diaphragm is protected by the insulating material thereby decreasing its vulnerability to heat damage. As a result of the improved design the life expectancy of the pressure rig contemplated by the present invention is more than doubled. Moreover, the improved heat protection has allowed the casting of brass and other alloys with higher melting temperatures than possible in the conventional pressure rigs.
Official Gazette of the U.S. Patent and Trademark Office

N90-21217# Fermi National Accelerator Lab., Batavia, IL.
MATERIALS FOR ULTRA-HIGH VACUUM
G. Lee 15 Aug. 1989 3 p
(Contract DE-AC02-76CH-03000)
(DE90-007908; FNAL-TM-1615) Avail: NTIS HC A01/MF A01

This report discusses materials for use in ultrahigh vacuum systems of 1 times 10(exp -9) Torr or lower. The author briefly discusses alloys, solders, insulators and joining methods for vacuum systems.
DOE

N90-21218# Brookhaven National Lab., Upton, NY.
ICE-MAKING HEAT EXCHANGER EVALUATION AND TEST PLAN
J. W. Andrews, R. W. Leigh, and M. W. Piraino Jan. 1990 17 p
(Contract DE-AC02-76CH-00016)
(DE90-008824; BNL-43844) Avail: NTIS HC A03/MF A01

Several approaches to making ice for district cooling are identified and their current status discussed. Recommendations for future work are given, with a detailed plan for one phase of the work.
DOE

N90-21219*# National Aeronautics and Space Administration. Marshall Space Flight Center, Huntsville, AL.
A GENERAL-PURPOSE BALLOON-BORNE POINTING SYSTEM FOR SOLAR SCIENTIFIC INSTRUMENTS
M. E. Polites Washington May 1990 22 p
(NASA-TP-3013; NAS 1.60:3013) Avail: NTIS HC A03/MF A01 CSCL 13I

A general purpose balloonborne pointing system for accommodating a wide variety of solar scientific instruments is described. It is designed for precise pointing, low cost, and quick launch. It offers the option of three-axis control, pitch-yaw-roll, or two-axis control, pitch-yaw, depending on the needs of the solar instrument. Simulation results are presented that indicate good pointing capability at Sun elevation angles ranging from 10 to 80 deg.
Author

N90-21220# Sandia National Labs., Albuquerque, NM. Packaging Technology Div.
THE DEVELOPMENT OF ULTRAVIOLET-OZONE CLEANING AS A PRODUCTION PROCESS IN THE PACKAGING OF INTEGRATED CIRCUITS
S. E. Garrett Mar. 1990 22 p
(Contract DE-AC04-76DP-00789)
(DE90-007960; SAND-88-3188) Avail: NTIS HC A03/MF A01

Ultraviolet-ozone (UV-ozone) cleaning was implemented as a production process to improve the cleanliness of metallized ceramic parts before a hermetic solder-sealing operation. The UV-ozone cleaning was developed as an in situ process that maintained a low moisture content in the sealed package. Sealing yields were improved by as much as 30 pct with this procedure. Seal quality and therefore, reliability, were also increased. Possible detrimental effects caused by UV-ozone cleaning were investigated. In particular, the possibility for silver from the silver-filled epoxy to electromigrate was studied. UV-ozone cleaning was not found to be a factor in this phenomena. Qualification lots were given Electrical, Group B, Group D, and Life Tests to determine if the UV-ozone cleaning had any detrimental effects on the parts' reliability. No detrimental effects were found on standard complementary metal oxide semiconductor technology integrated circuits. Some evidence has shown, however, that the memory retention of both large-scale integrated and discrete silicon nitride oxide semiconductor structures degrade(s) after UV-ozone cleaning.
DOE

32 COMMUNICATIONS AND RADAR

Includes radar; land and global communications; communications theory; and optical communications.

For related information see also *04 Aircraft Communications and Navigation* and *17 Space Communications, Spacecraft Communications, Command and Tracking.* For search and rescue see *03 Air Transportation and Safety,* and *16 Space Transportation.*

N90-21221 British Broadcasting Corp., London (England). Dept. of Research.

DIRECT RADIO BROADCASTING BY SATELLITE (DRBS): A REVIEW OF THE TECHNICAL FACTORS AND SYSTEM APPROACHES SUITABLE FOR MOBILE AND FIXED RECEPTION

D. Kail (Kingston Polytechnic, Kingston-Upon-Thames, England) 1989 26 p

(BBC-RD-1989/4) Avail: Issuing Activity

Direct Radio Broadcasting by Satellite (DRBS) offers many advantages while presenting new and challenging problems. The feasibility of a satellite system to broadcast high-quality stereo audio signals to fixed, portable, and mobile receivers using digital coding is examined. Technical options, including satellite orbits, operating frequencies, and digital coding methods are discussed, together with link-margin calculations. Seemingly intractable problems of transmitting high bit rate digital signals through highly dispersive mobile channels are then examined, together with methods of channel characterization and measurement. Finally, countermeasures to multipath propagation are discussed in detail; these include diversity systems, spread-spectrum, adaptive channel equalization and forward error control coding. Whereas the geostationary orbit is satisfactory for low latitude countries, it is concluded that a Molniya type elliptically orbiting satellite system may offer the best prospect for a technically successful, bandwidth efficient, DRBS system for the UK and other higher latitude countries. However, much additional study is necessary to develop the tentative conclusions drawn here. Author

N90-21222# Materials Research Labs., Ascot Vale (Australia).

THE MEASUREMENT OF SURFACE REFLECTIVITY AT MILLIMETRE WAVELENGTHS

P. W. Dixon and K. J. Gaylor 1989 30 p

(MRL-TN-559; ARL-005-729) Avail: NTIS HC A03/MF A01

An experimental facility was constructed to measure the surface reflectivity of materials at millimeter wavelengths. The facility can be used to measure the bistatic, monostatic or specular reflection from flat samples at horizontal, vertical or cross polarizations. The reflectivity of some representative materials of defense interest was measured at 35 GHz. Author

N90-21223# Advisory Group for Aerospace Research and Development, Neuilly-Sur-Seine (France). Avionics Panel.

HIGH RESOLUTION AIR- AND SPACEBORNE RADAR

Oct. 1989 224 p In ENGLISH and FRENCH Symposium held in The Hague, Netherlands, 8-12 May 1989

(AGARD-CP-459; ISBN-92-835-0530-1) Copyright Avail: NTIS HC A10/MF A02; Non-NATO Nationals requests available only from AGARD/Scientific Publications Executive

Imaging techniques are important sources of information in military operations. They may serve for purposes such as target detection and location, reconnaissance, classification and identification of fixed or moving objects as well as for orientation over unknown terrain. Despite considerable advances in electro-optical imaging systems the radar sensor has become an attractive alternative for several reasons: large range performance, penetration of weather, smoke, dust and foilage, day and night operation. On the other hand high resolution radar techniques such as synthetic aperture radar (SAR) and inverse synthetic aperture radar (ISAR) promise geometrical resolution of about 1 m and less. For individual titles, see N90-21224 through N90-21246.

N90-21224# Messerschmitt-Boelkow-Blohm G.m.b.H., Ottobrunn (Germany, F.R.).

CONCEPTS FOR HIGH RESOLUTION SPACE BASED SAR/ISAR SYSTEMS: PRELIMINARY DESIGN CONSIDERATIONS

C. Boesswetter, A. P. Wolframm, T. K. Pike, and J. M. Hermer (Thomson-CSF, Montrouge, France) *In* AGARD, High Resolution Air- and Spaceborne Radar Oct. 1989 9 p (For primary document see N90-21223 14-32)

Copyright Avail: NTIS HC A10/MF A02; Non-NATO Nationals requests available only from AGARD/Scientific Publications Executive

Some results are presented of preliminary feasibility considerations for a next generation space based multimode Synthetic Aperature Radar (SAR) and/or Inverse SAR system. A key element of next generation SAR systems, as currently designed for future remote sensing applications, is the active phased array antenna. Based on this antenna technology, some new operational modes are discussed, which currently are not available. Different beam pointing techniques (mono beam or multibeam in azimuth elevation) for strip mapping SAR modes as well as for Moving Target Indicator (MTI) ISAR modes are addressed. Basic requirements for selection of orbits are also discussed. The MTI/ISAR mode intended to detect and possibly classify from space, clusters of fast moving small targets against the clutter background of the earth surface, probably constitutes the highest risk in terms of requirements for onboard real time processing capabilities, pointing accuracies and coverage. Author

N90-21225# Marconi Space Systems Ltd., Portsmouth (England).

TRADE-OFFS IN A SPACE BASED SURVEILLANCE RADAR

Ian McMillan *In* AGARD, High Resolution Air- and Spaceborne Radar Oct. 1989 9 p Sponsored in part by ESA and Ministry of Defence Procurement Executive, England (For primary document see N90-21223 14-32)

Copyright Avail: NTIS HC A10/MF A02; Non-NATO Nationals requests available only from AGARD/Scientific Publications Executive

The design of a dual polarization high resolution synthetic aperature space based radar is discussed along with features which allow an adaptable operation mode to be utilized for ocean or land observation. The requirements for wide coverage for ocean observation at lower spatial resolution and smaller area coverage at high resolution of specific target areas in one instrument presents the designer with a significant challenge. The instrument incorporates dual polarization receiver features with selectable polarization transmit. Wide coverage transmit beams are utilized with a narrow steerable receive beam which follows the time dependent return signals in angle. The transmission of raw measurements to ground based facilities is impractical for high resolution and the instrument must perform on board much of the necessary data analysis. The technology tradeoffs applicable to such an instrument design for deployment and use in space are examined and the choices made in recent work are presented. A concept design incorporating a phased array with distributed transmit/receive modules with local intelligence and an all radio frequency and control optical distribution system and control system is examined. Author

N90-21226# Allgemeine Elektrizitaets-Gesellschaft, Ulm (Germany, F.R.).

A FREQUENCY AGILE 94 GHz PULSE-DOPPLER RADAR WITH DUAL POLARISATION CAPABILITY

Helmut Barth, Wolfgang Manzel, Alfred Plattner, and Joerg Schroth *In* AGARD, High Resolution Air- and Spaceborne Radar Oct. 1989 6 p (For primary document see N90-21223 14-32)

Copyright Avail: NTIS HC A10/MF A02; Non-NATO Nationals requests available only from AGARD/Scientific Publications Executive

The design of a coherent, frequency agile 94 GHz radar frontend is reported. This radar includes features like pulse frequency agility in steps of 10 MHz within a bandwidth of 400 MHz and fixed or

staggered pulse repetition frequency in a wide range between 1 and 50 kHz. The output power of 16 Watts and the antenna gain of 45 dB result in an effective radiated power of 89 dBm. The polarization of the transmitted wave is switchable from pulse to pulse either from RHC to LHC or from horizontal to vertical. This depends on the primary feed horn used for the 300 mm cassegrain antenna. Co- and cross-polarized echo signals are received and processed by two separate but identical receiver channels. Line scanning with a rate of 20 scans per sec is done by a flat rotating mirror. Author

N90-21227# Forschungsinstitut fuer Funk und Mathematik, Werthoven (Germany, F.R.). Dept. of Electronics.
APPLICATION OF SUPERRESOLUTION METHODS FOR AIRBORNE RADAR
U. Nickel *In* AGARD, High Resolution Air- and Spaceborne Radar Oct. 1989 6 p (For primary document see N90-21223 14-32)
Copyright Avail: NTIS HC A10/MF A02; Non-NATO Nationals requests available only from AGARD/Scientific Publications Executive

The usefulness of superresolution methods for airborne radar is examined. Angular resolution of closely flying targets is an interesting application. For SAR images, superresolution methods do not seem to be very helpful. A survey is given of the possible methods and problems and constraints are pointed out. Author

N90-21228# Physics and Electronics Lab. TNO, The Hague (Netherlands).
THE PHARUS PROJECT: DESIGN OF A POLARIMETRIC C-BAND SAR IN THE NETHERLANDS
P. Hoogeboom and P. J. Koomen *In* AGARD, High Resolution Air- and Spaceborne Radar Oct. 1989 7 p Sponsored in part by Ministry of Defense and National Remote Sensing Board Prepared in cooperation with National Aerospace Lab., Amsterdam, Netherlands and Technische Hogeschool, Delft, Netherlands (For primary document see N90-21223 14-32)
Copyright Avail: NTIS HC A10/MF A02; Non-NATO Nationals requests available only from AGARD/Scientific Publications Executive

In the Netherlands, a digital side looking aperture radar system (X band) was used for many years in radar remote sensing research. Examples of results and the system's key features are given. Calibration and high geometric and radiometric accuracy were the keywords to success in remote sensing for this system. Based on this experience, a polarimetric C band aircraft SAR is designed. In its final version, it will make use of a phased array antenna with solid state amplifiers. Before this system can be developed, a number of problems must be solved. In a preparatory study, a SAR testbed will be constructed to test parts of the technology that will be used in the final system and to gain experience with airborne SAR in general. This testbed is described. The data processing for the PHARUS (PHased ARray Universal SAR) requires the development of software tools, that take geometric and radiometric corrections into account, as well as the calibration. This in turn requires accurate measurements of the aircraft position and attitude. Author

N90-21229# Messerschmitt-Boelkow-Blohm G.m.b.H., Ottobrunn (Germany, F.R.).
ROSAR (HELICOPTER-ROTOR BASED SYNTHETIC APERTURE RADAR)
Helmut Klausing, Horst Kaltschmidt, and Wolfgang Keydel (Deutsche Forschungs- und Versuchsanstalt fuer Luft- und Raumfahrt, Wesseling, Germany, F.R.) *In* AGARD, High Resolution Air- and Spaceborne Radar Oct. 1989 12 p (For primary document see N90-21223 14-32)
Copyright Avail: NTIS HC A10/MF A02; Non-NATO Nationals requests available only from AGARD/Scientific Publications Executive

ROSAR is a synthetic aperture radar concept based on rotating antennas of a helicopter for pilot sight target detection and target localization with high resolution. The ROSAR concept has potential benefits for civil and military helicopterborne imaging applications, if the antennas are mounted at the tips of the rotor blades. The concept has two main potential benefits, the imaging field of view is 360 deg and there is no need for a forward velocity of the carrier platform. As opposed to SAR systems based on linear movement of the antenna, ROSAR imaging is based on synthetic aperture of a circular shape. Thus, the image formation process requires a polar format processing architecture. The ROSAR principle is also applicable for other radar mapping systems with rotating antennas, not only for helicopters. Author

N90-21230# Marconi Space Systems Ltd., Portsmouth (England).
CAPABILITIES OF BISTATIC SYNTHETIC APERTURE RADAR FOR COVERT BATTLEFIELD SURVEILLANCE
C. D. Hall *In* AGARD, High Resolution Air- and Spaceborne Radar Oct. 1989 8 p (For primary document see N90-21223 14-32)
Copyright Avail: NTIS HC A10/MF A02; Non-NATO Nationals requests available only from AGARD/Scientific Publications Executive

The capabilities of bistatic synthetic aperture radar to provide rapid update rate, real time covert radar surveillance to the military user are considered. The spatial resolution and sensitivity achievable from a tactical system using a small remotely piloted vehicle-borne transmitter and a static ground based receiver are discussed and the relative advantages of two distinct types of emission modulation are examined. Finally, a number of areas requiring further study are identified. Author

N90-21231# Selenia S.p.A., Rome (Italy). Dept. of Radar.
MMW SAR ON RPV FOR BATTLEFIELD SURVEILLANCE
A. Farina, U. Carletti, E. DAddio, C. Morabito, and R. Pangrazi *In* AGARD, High Resolution Air- and Spaceborne Radar Oct. 1989 11 p (For primary document see N90-21223 14-32)
Copyright Avail: NTIS HC A10/MF A02; Non-NATO Nationals requests available only from AGARD/Scientific Publications Executive

The capabilities and features of airborne synthetic aperture radar (SAR), operating in the millimeter wave (mmw) region, are discussed with reference to a battlefield surveillance application. The SAR system provides high resolution real time imaging of the battlefield and moving target detection, under adverse environmental conditions (e.g., weather, dust, smoke, obscurants). The most relevant and original aspects of the system described are the band of operation (i.e., mmw in lieu of the more traditional microwave region) and the use of an unmanned platform. The former implies reduced weight and size requirements, thus allowing use of small unmanned platforms. The latter enhances the system operational effectiveness by permitting accomplishment of recognition missions in depth beyond the forward edge battle area. An overall system architecture is described based on the onboard sensor, the platform, the communication equipment, and a mobile ground station. The relevant problem of detecting and imaging of moving target is also described. Author

N90-21232# Alcatel Espace, Toulouse (France).
PROGRAMMABLE GENERATION OF LINEAR FREQUENCY MODULATED PULSES [GENERATION PROGRAMMABLE DES IMPULSIONS MODULEES LINEAIREMENT EN FREQUENCE]
Jacques Richard and Jean-Marc Fallot *In* AGARD, High Resolution Air- and Spaceborne Radar Oct. 1989 12 p In FRENCH (For primary document see N90-21223 14-32)
Copyright Avail: NTIS HC A10/MF A02; Non-NATO Nationals requests available only from AGARD/Scientific Publications Executive

The ability to program pulse characteristics emitted from satellite-borne radar is necessary for future radars. In an altimeter radar, a very short pulse allows the accurate measurement of centimeters of distance above the ocean but is not useful above ice or land, because of a weaker signal and large contours encountered beneath the surface. The diminishing signal range on ice and land increases the transmission loss and widens the

signal acquisition in the case of an altimeter radar using the full-deramp technique. In a SAR or SLAR incapable of changing its pulse characteristics, the transverse resolution image is inversely proportional to the sine of the incidence angle. For example, certain images contain between 15 to 65 degs of incidence, with the resolution increased by a factor of 3 to 5. The use of a chirp with a programmable range solves the problem without a large transmission loss. The techniques for programming the chirp characteristics are discussed. Most of the techniques are numerical, with some interesting technical examples given. Transl. by E.R.

N90-21233# Deutsche Forschungs- und Versuchsanstalt fuer Luft- und Raumfahrt, Wesseling (Germany, F.R.). Inst. for Radio Frequency Technology.

REAL-TIME ADAPTIVE RADIOMETRIC CORRECTION FOR IMAGING RADARS SYSTEMS

Joao R. Moreira and Winfried Poetzsch *In* AGARD, High Resolution Air- and Spaceborne Radar Oct. 1989 6 p (For primary document see N90-21223 14-32)

Copyright Avail: NTIS HC A10/MF A02; Non-NATO Nationals requests available only from AGARD/Scientific Publications Executive

A new solution is given of a real time radiometric image correction that also minimizes the quantization and saturation noise introduced by the process of analog-to-digital conversion of raw data of coherent and noncoherent imaging radar systems. The implementation of this procedure was successfully performed with the experimental SAR System (E-SAR) of the DLR. Author

N90-21234# Siemens A.G., Munich (Germany, F.R.). Telecommunication/Semiconductors.

CONCEPT FOR A SPACEBORNE SYNTHETIC APERTURE RADAR (SAR) SENSOR BASED ON ACTIVE PHASED ARRAY TECHNOLOGY

A. Brunner, E. Langer, H. Oettl, and K. H. Zeller (Deutsche Forschungs- und Versuchsanstalt fuer Luft- und Raumfahrt, Oberpfaffenhofen, Germany, F.R.) *In* AGARD, High Resolution Air- and Spaceborne Radar Oct. 1989 10 p (For primary document see N90-21223 14-32)

Copyright Avail: NTIS HC A10/MF A02; Non-NATO Nationals requests available only from AGARD/Scientific Publications Executive

For surveillance with spaceborne remote sensing systems, quite often a spatial resolution of 1 m or less is requested. A SAR concept is presented for a low flying satellite. Assuming a peak power of 5 kW and using active phased array technology, a swath width of about 30 km at an off nadir angle of 35 deg is considered to be reasonable. A wide swath width combined with a high resolution can only be achieved if a fixed antenna beam is used for transmitting which illuminates the whole swath width, while a very narrow antenna beam scans the swath in the manner as the reflected pulse travels from the near range to the far range across the swath width. For the active antenna system, a high efficiency of the transmit/receive modulus, low losses in the feeding network and doubly polarized radiating elements with high polarization purity are considered of utmost importance. An antenna based on the slotted waveguide principle is described. The technology of the GaAs based modules with special respect to space requirement resulting in an economic solution of the power generation below 3 W per module is described. Author

N90-21235# Organisatie voor Toegepast Natuurwetenschappelijk Onderzoek, The Hague (Netherlands). Radar and Communications Div.

A MOTION COMPENSATION STUDY FOR THE PHARUS PROJECT

M. P. G. Otten *In* AGARD, High Resolution Air- and Spaceborne Radar Oct. 1989 12 p (For primary document see N90-21223 14-32)

Copyright Avail: NTIS HC A10/MF A02; Non-NATO Nationals requests available only from AGARD/Scientific Publications Executive

In the PHARUS project, a polarimetric C band SAR is being developed, which will be preceded by a nonpolarimetric test system called PHARS. A motion compensation study is also part of preparatory studies for the final PHARUS design. A SAR data simulator was developed as a tool for the study of the effects of aircraft motion on the SAR image. From the SAR mapping geometry, a terrain description, the radar parameters, and detailed trajectory and attitude data of a non-maneuvering aircraft, the simulator generates raw data with a given range resolution. This can be processed, by azimuth compression, into the SAR image. A secondary purpose of the simulation is to determine the impact of several design parameter choices, and to provide well defined test input for SAR processing software. The results of test runs with real flight data were verified theoretically, and have shown the need for motion compensation. It was also shown that a major advantage of simulation, in that it can take many factors into account at the same time, including for instance the SAR processing method, which is hard to do theoretically. Author

N90-21236# Deutsche Forschungs- und Versuchsanstalt fuer Luft- und Raumfahrt, Wesseling (Germany, F.R.). Inst. for Radio Frequency Technology.

A SOLUTION FOR REAL TIME MOTION COMPENSATION FOR SAR WITHOUT USING INERTIAL NAVIGATION SYSTEMS

Joao R. Moreira *In* AGARD, High Resolution Air- and Spaceborne Radar Oct. 1989 6 p (For primary document see N90-21223 14-32)

Copyright Avail: NTIS HC A10/MF A02; Non-NATO Nationals requests available only from AGARD/Scientific Publications Executive

A new solution is given for real time motion compensation. The main idea is to extract all the necessary motions of the aircraft from the radar backscatter signal using a new radar configuration and new methods for evaluating the azimuth spectra of the radar signal. Hence an inertial navigation system becomes unnecessary for many applications. The motion compensation parameters for real time motion error correction are the range delay, the range dependent phase shift and the pulse repetition frequency. The motions of the aircraft to be extracted are the displacement in line of sight direction, the aircraft's yaw and drift angle and forward velocity. Results show that a three look image with an azimuth resolution of 3m in the L-band using a small aircraft is achievable and the implementation of this method in real time using an array processor is feasible. Author

N90-21237# Thomson-CSF, Malakoff (France).

SAR AND ISAR IMAGERY OF MARINE TARGETS [L'IMAGERIE DES CIBLES MARINES A LA FRONTIERE ENTRE LE SAR ET L'ISAR]

Marie Fenou *In* AGARD, High Resolution Air- and Spaceborne Radar Oct. 1989 10 p In FRENCH (For primary document see N90-21223 14-32)

Copyright Avail: NTIS HC A10/MF A02; Non-NATO Nationals requests available only from AGARD/Scientific Publications Executive

For a working arrangement of marine targets of an airport radar used for ocean surveillance, Thomson-CSF developed a high resolution imaging system. A waveform was used to get natural resolution from the antenna. The usual method for synthetic imagery of synthetic aperture radar or inverse SAR is not directly applicable because the target and radar are not stable. The adaptation of a treatment considers the specificity of the problem and its location between SAR and ISAR treatment. On the other hand, the resulting image is a hybrid of the two, and its interpretation is not possible until the two phenomena are stable. Improvements in the signature are seen from effective returns by manual identification or automatic target detection. Transl. by E.R.

N90-21238# Forschungsinstitut fuer Hochfrequenzphysik, Werthhoven (Germany, F.R.).

PROBLEMS IN ISAR PROCESSING WITH RANGE RESOLUTION BY STEPPED FREQUENCY BURSTS

Gerd Kraemer *In* AGARD, High Resolution Air- and Spaceborne Radar Oct. 1989 5 p (For primary document see N90-21223

14-32)
Copyright Avail: NTIS HC A10/MF A02; Non-NATO Nationals requests available only from AGARD/Scientific Publications Executive

If a target image is reconstructed from an ISAR (Inverse Synthetic Aperture Radar) measurement by immediate application of the Discrete Fourier Transform, the image becomes blurred with increasing distance from its center. It is shown that with an ISAR sensor applying stepped frequency bursts, samples of the 2-D Fourier Transform of a 2-D scatterer density are measured and how a target image can be reconstructed. Author

N90-21239# Deutsche Forschungs- und Versuchsanstalt fuer Luft- und Raumfahrt, Oberpfaffenhofen (Germany, F.R.). Inst. fuer Hochfrequenztechnik.
A FAST ISAR-IMAGING PROCESS AND ITS INHERENT DEGRADING EFFECTS ON IMAGE QUALITY
K.-H. Bethke and B. Roede *In* AGARD, High Resolution Air- and Spaceborne Radar Oct. 1989 12 p (For primary document see N90-21223 14-32)
Copyright Avail: NTIS HC A10/MF A02; Non-NATO Nationals requests available only from AGARD/Scientific Publications Executive

A method for a fast 2-D inverse synthetic aperture radar (ISAR) imaging process is presented. A coherent short pulse radar is used to sample amplitude and phase of the backscattered field from a continuously rotating object. This is being done while a narrow range gate is sweeping in range steps of 15 cm across the target plane at a typical speed of 150 m/s. Applying fast SAR principles, in an off-line process for each range cell, an acceptable good cross range resolution can be obtained when processing angle intervals of less than 30 deg. The influence of analytical approximations as well as the effect of moving scattering centers through several range resolution cells during the process interval can cause severe image degradations. Two methods for partial and complete compensation of these effects under the aspect of minimum loss in processing speed were developed and are presented. Author

N90-21240# Organisatie voor Toegepast Natuurwetenschappelijk Onderzoek, The Hague (Netherlands). Physics and Electronics Lab.
RADAR OBSERVATIONS OF A FORMATION OF TWO FIGHTERS: A CASE STUDY FOR ISAR IMAGING
Frits Willems *In* AGARD, High Resolution Air- and Spaceborne Radar Oct. 1989 12 p (For primary document see N90-21223 14-32)
Copyright Avail: NTIS HC A10/MF A02; Non-NATO Nationals requests available only from AGARD/Scientific Publications Executive

A study was made of Inverse Synthetic Aperture Radar imaging of a formation of two fighters. The observations are interpreted in terms of relative motions of the two aircraft by use of model study and computer simulation. Author

N90-21241# Forschungsinstitut fuer Funk und Mathematik, Werthoven (Germany, F.R.).
THE 1D-ISAR IMAGING OF MANOEUVERING AIRCRAFT
J. Ender *In* AGARD, High Resolution Air- and Spaceborne Radar Oct. 1989 9 p (For primary document see N90-21223 14-32)
Copyright Avail: NTIS HC A10/MF A02; Non-NATO Nationals requests available only from AGARD/Scientific Publications Executive

Most operating radar systems don't provide sufficient range resolution to resolve flying targets in range direction. Nevertheless, high cross range resolution can be obtained by 1-D imaging. This procedure will be successful only, if the target motion is compensated with a high accuracy. A motion compensation technique is introduced based on Kalman forward-backward smoothing on radar position estimates together with spectral information. An iterative error correction procedure (autofocus) yields a cross range image with sufficient resolution. Correct scaling and estimation of the imaging axis direction are derived from the flight path by a simple orientation model. Some experimental study of this kind of ISAR processing was done with the electronic radar phased array. Echo sequences of targets of opportunity were recorded and off-line processed. With the autofocus procedure, coherence times up to 6 sec could be achieved providing resolution cells in the magnitude of 1 m. Images during straight flight periods as well as along curved flight paths were generated. The reliability of the information given by the signatures was examined. Author

N90-21242# Selenia S.p.A., Rome (Italy). Dept. of Radar.
RADAR TARGET IMAGE BY ISAR CASE STUDY
S. Marini, S. Pardini, and F. Prodi *In* AGARD, High Resolution Air- and Spaceborne Radar Oct. 1989 14 p (For primary document see N90-21223 14-32)
Copyright Avail: NTIS HC A10/MF A02; Non-NATO Nationals requests available only from AGARD/Scientific Publications Executive

Target imaging based on Inverse Synthetic Aperture Radar techniques are described. Theoretical and experimental results are presented. Theoretical topics illustrate the set of processing functions needed to obtain the target image starting from the radar echoes. Key processing steps include motion compensation and reconstruction of the reflectivity function. An experimental setup based on a currently available tracking radar, a data recorder and off-line processing facilities are illustrated. A high cross range resolution image of a MB-339 aircraft was obtained by processing recorded radar echoes from a Selenia X band tracking radar. Author

N90-21243*# National Aeronautics and Space Administration. Langley Research Center, Hampton, VA.
AIRBORNE DOPPLER RADAR FLIGHT EXPERIMENTS FOR THE DETECTION OF MICROBURSTS
Hans-J. C. Blume, C. D. Lytle, W. R. Jones, E. M. Bracalente, and C. L. Britt (Research Triangle Inst., Research Triangle Park, NC.) *In* AGARD, High Resolution Air- and Spaceborne Radar Oct. 1989 14 p (For primary document see N90-21223 14-32)
Copyright Avail: NTIS HC A10/MF A02; Non-NATO Nationals requests available only from AGARD/Scientific Publications Executive CSCL 17I

In the interest of aviation safety, NASA and the FAA are jointly conducting research to determine the applicability of airborne, coherent Doppler radar techniques to detect early microburst in wind shear conditions during aircraft takeoff and landing. Researchers have developed a computer model of the radar which predicts its response when viewing a simulated microburst against the simulated clutter background of an airport, the so-called radar microburst ground clutter model. Studies employing this model revealed that Doppler radar can accurately detect microburst ahead of the aircraft in time for pilot evasive response, but flight experiments will be required for complete performance evaluation of the system. An experimental X band radar is being developed for future flight experiments to verify the simulation modeling results. A description of the experimental radar, recording equipment, and its installation on the NASA 515 aircraft is presented. The flight experiments to be conducted are also described. Author

N90-21244# Deutsche Forschungs- und Versuchsanstalt fuer Luft- und Raumfahrt, Oberpfaffenhofen (Germany, F.R.). Inst. for Radio Frequency Technology.
CONCEPT AND RESULTS OF THE DLR REALTIME SAR PROCESSOR
Alberto Moreira *In* AGARD, High Resolution Air- and Spaceborne Radar Oct. 1989 6 p (For primary document see N90-21223 14-32)
Copyright Avail: NTIS HC A10/MF A02; Non-NATO Nationals requests available only from AGARD/Scientific Publications Executive

A real time azimuth processor was developed for the airborne E-SAR system (Experimental Synthetic Aperture Radar). The processor works with an unfocused compression method. This

method greatly simplifies the data processing and is easily implemented by a moving average approach. A SAR image processed by a traditional unfocused processing method has a lower contrast, higher sidelobes, and worse resolution than in the focused case. A new algorithm was developed, so that a triangular amplitude weighting could be implemented into the unfocused processing method without additional complications. Images processed in real time are presented. They show good contrast and strong suppression of the sidelobes. The processor hardware can be implemented with reduced costs in small aircraft and is suitable for several applications such as the detection of oil pollution over the sea. Author

N90-21245# Aerospatiale, Les Mureaux (France). Dept. Mesures.
IMAGE SIMULATION OF GEOMETRIC TARGETS FOR SYNTHETIC APERTURE RADAR [SIMULATION D'IMAGES DE CIBLES GEOMETRIQUES POUR RADAR A OUVERTURE SYNTHETIQUE]
J. M. Nasr *In* AGARD, High Resolution Air- and Spaceborne Radar Oct. 1989 7 p In FRENCH (For primary document see N90-21223 14-32)
Copyright Avail: NTIS HC A10/MF A02; Non-NATO Nationals requests available only from AGARD/Scientific Publications Executive

A new technique for image simulation which comes from a synthetic aperture radar is presented. The method is based on the embedding of an artificially simulated target in a real radar image captured by an operational antenna window on a satellite (SEASAT or SIR-B). A L and C band was used for the capture. The target dimensions studied were large enough for use with long waves provided the calculation techniques used with high frequencies were for an equivalent area radar (SER). The calculation of SER allows the capture of a raw signal received from the antennas. So that the possibility of simulation is low, some restrictions are made. The results are sufficiently interesting enough to let the study of the behavior of a particular target become of use to civilians or the military, in the functional bounds of radar waves. Transl. by E.R.

N90-21246# Thomson-CSF, Paris (France).
SAR IMAGE CODING [CODAGE D'IMAGES SAR]
P. Tourtier *In* AGARD, High Resolution Air- and Spaceborne Radar Oct. 1989 6 p In FRENCH (For primary document see N90-21223 14-32)
Copyright Avail: NTIS HC A10/MF A02; Non-NATO Nationals requests available only from AGARD/Scientific Publications Executive

The Synthetic Aperture Radar imagery causes a very large flow rate, to the extent that the data flow is at a record level. The image coding technique reduces the flow rate so that the original quality is preserved. This permits the reduction of the transmission channel capacity and improves the flow rate. A different technique is presented for data flow compression. The technique performs best at low cosine transform and is described in detail. The results obtained by Thomson-CSF show that a compression rate of the magnitude of 4 or 5 is possible without visible image degradation. Transl. by E.R.

N90-21247# Scientech, Inc., Idaho Falls, ID.
BOEING 727-100 TEST PROJECT (HIGH ENERGY RADIATED FIELD TESTS) Final Report, Dec. 1985 - Jan. 1986
T. Crowther, L. J. Ybarrondo, N. Skousen, and M. Hintze Jul. 1989 148 p
(Contract DTFA03-88-A-00027)
(DOT/FAA/CT-88/33) Avail: NTIS HC A07/MF A01

Discussed here is a radio frequency (RF) coupling test on a BOEING 727-100 commercial aircraft. The objective of the test was to measure the coupling, or penetration, of RF signals in a BOEING 727-100 in the frequency range of 1.0 MHz to 6.0 GHz. The RF field levels generated inside the airplane during flight are probably not a health hazard with respect to passengers and crew because exposure time to high intensity RF fields is of short duration. However, this project has demonstrated that RF energy can couple into aircraft compartments and onto electrical wiring. The extent to which existing RF sources can impose unwanted electrical signals or voltages on critical aircraft components during flyby are shown. Author

N90-21248# Federal Aviation Administration, Atlantic City, NJ.
FEASIBILITY OF USING FREQUENCY OFFSET ON VERY HIGH FREQUENCY AIR/GROUND VOICE CHANNELS
Martin Badinelli, Arthur Cushman, and Philip Randazzo Mar. 1990 48 p
(DOT/FAA/CT-TN89/71) Avail: NTIS HC A03/MF A01

In some large Federal Aviation Administration (FAA) air traffic control sectors, the controller manually switches between multiple ground transmitters to communicate with aircraft at opposite ends of the sector. This puts an additional burden on the controller. Aeronautical Radio, Inc. (ARINC) uses a frequency offset system which produces five frequencies from one channel assignment. ARINC provides this service to commercial air carriers who use receivers designed to ARINC specifications. These receivers are capable of eliminating the audio heterodyne generated by the offsetting process. The commercial air carriers use this system for airline business. The testing performed at the FAA Technical Center to evaluate this system as a means of controlling the air traffic in large sectors is described. The tests indicate that a frequency offset system cannot be used with general aviation aircraft receivers because many cannot filter out the audio heterodyne. Use of frequency offset may be possible in high altitude sectors where commercial aviation receivers, which meet ARINC specifications, are used if some additional concerns are resolved. Author

N90-21249# Computer Resource Management, Inc., Vienna, VA.
NATIONAL AIRSPACE SYSTEM AIR-GROUND COMMUNICATIONS OPERATIONAL CONCEPT
William Trent, Rodney Kuhn, and Thomas Pickerell Feb. 1990 46 p
(Contract DTFA01-88-Y-01073)
(DOT/FAA/DS-90/2; NAS-SR-1361) Avail: NTIS HC A03/MF A01

A requirement for the National Airspace System (NAS) is to provide for air-ground communications, as identified in the NAS System Requirement Specification, NAS-SR-1000. A concept of operations for air-ground communications is presented. Air-ground communications capabilities are described and the relationships are shown between subsystems, facilities, information, and operators/users. A common perspective is provided for personnel involved in air-ground communication activities. Assistance is provided for determining whether air-ground communications meet formal requirements and also for coordinating the organizations involved. Author

N90-21250*# National Aeronautics and Space Administration. Lewis Research Center, Cleveland, OH.
NUMERICAL ARC SEGMENTATION ALGORITHM FOR A RADIO CONFERENCE (NASARC), VERSION 4.0: USER'S MANUAL
Wayne A. Whyte, Jr., Ann O. Heyward, Denise S. Ponchak, Rodney L. Spence, and John E. Zuzek 6 Oct. 1988 112 p
(NASA-TM-101454; E-4987; NAS 1.15:101454) Avail: NTIS HC A06/MF A01 CSCL 17B

The information in the NASARC (Version 4.0) Technical Manual (NASA-TM-101453) and NASARC (Version 4.0) User's Manual (NASA-TM-101454) relates to the state of Numerical Arc Segmentation Algorithm for a Radio Conference (NASARC) software development through November 1, 1988. The Technical Manual describes the NASARC concept and the algorithms used to implement the concept. The User's Manual provides information on computer system considerations, installation instructions, description of input files, and program operation instructions. Significant revisions were incorporated in the Version 4.0 software over prior versions. These revisions have further enhanced the

modeling capabilities of the NASARC procedure and provide improved arrangements of predetermined arcs within the geostationary orbit. Array dimensions within the software were structured to fit within the currently available 12-megabyte memory capacity of the International Frequency Registration Board (IFRB) computer facility. A piecewise approach to predetermined arc generation in NASARC (Version 4.) allows worldwide planning problem scenarios to be accommodated within computer run time and memory constraints with enhanced likelihood and ease of solution. Author

N90-21251# Department of the Army, Washington, DC.
A REAL-TIME REJECTION CIRCUIT TO AUTOMATICALLY REJECT MULTIPLE INTERFERING HOPPING SIGNALS WHILE PASSING A LOWER LEVEL DESIRED SIGNAL Patent Application
William J. Skudera, Jr., inventor (to Army) and Stuart D. Albert, inventor (to Army) 8 Jan. 1990 24 p
(AD-D014424; US-Patent-Appl-SN-461943) Avail: NTIS HC A03/MF A01 CSCL 09/1

A real-time rejection circuit for passing low level desired signals in the presence of one or more strong, interfering signals. A chirp-z transform system separates the various frequency components of a received signal into frequency segregated time domain signals. A power splitter separates the time domain signal into two paths. One path includes a modulator or switch that is normally biased ON for passing the time domain signal. The second path includes a diode detector that produces pulses of sufficient strength when a strong interfering component is present to override the bias and turn the modulator OFF for a sufficient period of time to attenuate the unwanted frequency components in the other path. The modulator output will primarily contain the low level desired frequency components that are passed through an inverse transform device for producing a frequency domain signal of the desired signal uncorrupted by unwanted signals. GRA

N90-21252# Department of Agriculture, Edinburg, TX. Animal and Plant Health Inspection Service.
AN INTRODUCTION TO HIGH FREQUENCY RADIOTELETYPE SYSTEMS
Roger R. Pinnau 1 Oct. 1989 39 p
(PB90-145533) Avail: NTIS HC A03/MF A01 CSCL 17B

A basic introductory guide is provided to modern High Frequency (HF) data communications systems. Described are modern commercial radioteletype systems, data communication protocols, and various secrets of the trade. Author

N90-21253# Helsinki Univ. of Technology, Espoo (Finland). Lab. of Engineering Geology and Geophysics.
COMPUTER PROCESSING OF MULTI-CHANNEL ELECTROMAGNETIC DATA FROM AN AIRBORNE GEOPHYSICAL SURVEY SYSTEM
Markku Peltoniemi and Matti Viikari (G-Syst Oy, Espoo, Finland) 1989 54 p
(PB90-138413; TKK-IGE-A12; ISBN-951-754-930-X; ISSN-0785-9732) Avail: NTIS HC A04/MF A01 CSCL 20N

A multichannel airborne electromagnetic survey system is described with special reference to data processing requirements. A set of computer programs was developed that permits the original electromagnetic data to be corrected and transformed into different types of output ready for graphic presentation as stacked profiles or contour maps. The corrections are performed in an interactive mode of operation with a graphic terminal or workstation, and they include all filtering, leveling, and editing subroutines necessary for producing final, true anomaly values. The transformation subroutines accomplish the transformation of the true anomaly data into values of apparent conductivity, conductance, and depth with one layer, two layer, or vertical half-plane models. Examples of the different outputs of the data processing software are presented. Author

N90-21254# British Broadcasting Corp., Kingswood (England). Engineering Div.
HDTV BANDWIDTH REDUCTION USING MOTION COMPENSATION AND DATV
G. A. Thomas 1989 32 p
(BBC-RD-1989/10) Avail: Issuing Activity

Recent work, described in BBC Research Department Report BBC RD 1986/5, has examined the use of a motion-adaptive bandwidth reduction system to reduce the bandwidth of a high-definition television (HDTV) signal by a factor of four. Such a reduction is required in order to enable HDTV signals to be transmitted in channels that are likely to be available in the near future. The system was capable of transmitting a highly detailed image in stationary parts of the television picture, although the resolution of moving picture areas was reduced. Such a system has been termed Digitally Assisted Television (DATV). The addition of motion compensation to such a bandwidth reduction system, with the aim of being able to transmit signals with high spatial resolution in all parts of the picture except those whose motion cannot be estimated accurately is considered. Full details of the algorithm, which was developed using computer simulation, are given. The motion-compensated bandwidth reduction system was evaluated in a series of subjective tests as a part of the Eureka 95 HDTV project. The tests examined both the quality of the decoded HDTV picture and the quality of the compatible picture produced when the bandwidth-reduced signal is viewed on a MAC receiver that is not equipped with an HDTV decoder. The tests showed that the addition of motion compensation significantly improved the quality of the decoded picture at the expense of that of the compatible picture. Author

N90-21255# British Broadcasting Corp., Kingswood (England). Engineering Div.
PREDICTION OF VHF/UHF MOBILE RECEPTION IN URBAN AREAS: COMPARISON WITH MEASUREMENTS IN LONDON
J. Middleton 1989 9 p
(BBC-RD-1989/11) Avail: NTIS HC A02/MF A01

The BBC's interest in mobile reception stems from its ancillary service requirements at VHF and UHF and also the increasing use of the VHF-FM band for broadcast reception in cars. This has stimulated interest in predicting field strengths for mobile reception at both VHF and UHF. The results of high density field strength measurements in the London area using a receiving antenna height of 1.4 m are described. Comparisons are made with predictions using a modified version of the long established BBC method originally developed for predicting interference levels at a 10 m receiving antenna height. To date, these comparisons show good agreement. Author

N90-21256# Federal Aviation Administration, Atlantic City, NJ.
DATA LINK PROCESSOR (DLP) PROJECT TRANSITION PLAN
Gary Morfitt and Noel A. Doucett Apr. 1990 22 p
(DOT/FAA/CT-TN89/68) Avail: NTIS HC A03/MF A01

The provision for two-way communication with aircraft, via a digital data link, has long been considered a means of providing significant enhancements for safe and efficient flight operations. The data link processor (DLP) currently being tested will initially perform the ground-based data link processing functions necessary to provide appropriately equipped aircraft with pilot requested aviation weather data from a National Weather Data Base via the Mode Select Beacon System (Mode S). The weather data base will contain six products: surface observations (SA), terminal forecasts (FT), pilot reports (UA), wind and temperature aloft forecasts (FD), radar summaries (SD), and hazardous weather advisories. The DLP project transition plan presents those activities and the organizations that are responsible to effect the transition of the DLP into the Federal Aviation Administration (FAA) Technical Center. This plan identifies the functional interfaces, equipment description, testing, training, and logistics support necessary for an orderly transition at the FAA Technical Center. Author

N90-21257# Naval Postgraduate School, Monterey, CA.
THE 4TH ANNUAL REVIEW OF PROGRESS IN APPLIED COMPUTATIONAL ELECTROMAGNETICS
24 Mar. 1988 615 p Review held in Monterey, CA, 22-24 Mar. 1988
(AD-A217912) Avail: NTIS HC A99/MF A04

Some topics discussed at this conference include: A finite element analysis of lightning induced Maxwell current densities; Transient electromagnetic coupling to a cavity with metallic walls; Finite element computer programs for microstrip, waveguides and cavities; A time domain differential solver for electromagnetic scattering problems; A high frequency reformulation of the FDTD algorithm in generalized coordinates; Using impedance matrix frequency derivatives for estimating broadband transfer functions; The MAFIA approach to solving Maxwell's equations in three dimensions; Numerical integration schemes in calculating the Fourier coefficiencies of the free space Green's Function; and A lattice representation for back face removal in electromagnetic scattering. Author

N90-21258# Naval Postgraduate School, Monterey, CA.
THE 5TH ANNUAL REVIEW OF PROGRESS IN APPLIED COMPUTATIONAL ELECTROMAGNETICS
1989 874 p Review held in Monterey, CA, 20-24 Mar. 1989 Sponsored in part by DOD; ECOM; Army Information Systems Engineering Command; NOSC; NPS; and Applied Computational Electromagnetics Society
(Contract W-7405-eng-48)
(AD-A217994) Avail: NTIS HC A99/MF E06 CSCL 20/3

Some topics discussed include: General Purpose Electromagnetic Codes; Comparison of Antenna and Scattering Patterns by the NEC and ESP Codes; Junction: A Computer Code for the Computation of Radiation and Scattering by Arbitrary Conducting Wire/Surface Configurations; Microwave Circuits; Three-Dimensional Full-Wave Analysis of Passive Microstrip Components Using the TLM Method; The Field Theoretic MMIC Computation Enhanced by the Variational Principle; The Dispersion Characteristics of the FD-TD Method in Cylindrical Waveguides; Electromagnetic Compatibility and Interference; Scattering from Cylindrical Dielectric Slabs: A Method of Moments Approach; Radar Cross Section Calculation of Partially Coated Conducting Bodies; Calculation of Admittance of Slots on a Body of Revolution using the Method of Moments; Electromagnetic Code Validation by the Infrared Measurement Method; Finite Differences and Finite Elements; Simple Method to Compute the Current Distribution, Input Impedance and Efficiency of Thick Unloaded and Loaded Dipole Antennas; Four-Element Monopole Array; Analysis of Microstrip Antennas using the TLM Method; A New Fast Fourier Integral Transform: Rediscovering the Significance of Lanczos Sigma Effect Multipliers as a Digital Finite Impulse Response Windows in the Frequency Domain; Implementation and Performance of MMP Programs on Transputers; and Input/Output and Interface Issues. GRA

N90-21259# Naval Ocean Systems Center, San Diego, CA.
PROCEEDINGS OF THE JOINT NOSC/NRL (NAVAL OCEAN SYSTEMS CENTER/NAVAL RESEARCH LABORATORY) InP MICROWAVE/MILLIMETER WAVE TECHNOLOGY WORKSHOP Final Report
Dec. 1989 451 p Workshop held in San Diego, CA, 25-26 Jan. 1989
(AD-A218216; NOSC/TD-1712) Avail: NTIS HC A20/MF A03 CSCL 20/14

Technical highlights include: drift problem with MIS devices under attack with epitaxial dielectrics, heat pulse processing, silicon substrates, silicon wedge dielectrics, gentle plasma etching, sulfidation (5 percent drift over 100,000 sec, 4V drain, 4V gate), hydrogenation (2 percent drift); ion implantation damages to 3 microns or more even for the shortest anneal cycle; limits to HJ device performance related to epitaxial layer design (at present HBT working at 30 percent beta max); atomic planar doping in use for MODFET on InP with matching-V sat about 1.6 to 1.8 x 10(exp 7) cm/sec; small drain current drift observed in SiO2 based HIGFET-drift less than 4 percent over 15 hours; InAlAs-InGaAs planar-doped HEMTs lattice matched to InP, 0-.25 micron T-gate, 900 mS/mm, 0.5 dB NF at 18 GHz, and hot electron InP/InGaAs HBT ft=140 GHz, fmax=70GHz. GRA

N90-21260 Department of the Navy, Washington, DC.
AUTOMATIC CLASSIFICATION OF IMAGES Patent
John A. Knecht, inventor (to Navy) and Darrell L. Chenoweth, inventor (to Navy) 14 Nov. 1989 8 p Filed 28 Oct. 1983
(AD-D014437; US-Patent-4,881,270; US-Patent-Appl-SN-546755; US-Patent-Class-382-17) Avail: US Patent and Trademark Office CSCL 17/11

A method and system for classifying a raster scanned target image by collapsing the image into a vector corresponding to a horizontal line of the image, mathematically transforming this vector into a feature vector which corresponds to the power spectrum of the collapsed image, and comparing the feature vector with stored decision rules corresponding to classes of possible target objects to determine if the image represents an object in one of the classes. GRA

N90-21261*# National Aeronautics and Space Administration. Lewis Research Center, Cleveland, OH.
BIT-ERROR-RATE TESTING OF FIBER OPTIC DATA LINKS FOR MMIC-BASED PHASED ARRAY ANTENNAS
K. A. Shalkhauser, R. R. Kunath, and A. S. Daryoush (Drexel Univ., Philadelphia, PA.) Jan. 1990 10 p Presented at the Optoelectronics and Laser Applications in Science and Engineering Conference, Los Angeles, CA, 14-19 Jan. 1990; sponsored in part by the Society of Photo-Optical Instrumentation Engineers
(NASA-TM-102523; E-5330; NAS 1.15:102523) Avail: NTIS HC A02/MF A01 CSCL 17B

The measured bit-error-rate (BER) performance of a fiber optic data link to be used in satellite communications systems is presented and discussed. In the testing, the link was measured for its ability to carry high burst rate, serial-minimum shift keyed (SMSK) digital data similar to those used in actual space communications systems. The fiber optic data link, as part of a dual-segment injection-locked RF fiber optic link system, offers a means to distribute these signals to the many radiating elements of a phased array antenna. Test procedures, experimental arrangements, and test results are presented. Author

N90-21262*# Virginia Polytechnic Inst. and State Univ., Blacksburg.
CALIBRATION OF HEWLETT-PACKARD NETWORK ANALYZERS: A PRECISION VIEWPOINT Final Report
W. A. Davis and D. M. Keller Mar. 1990 76 p
(Contract NAS1-18106)
(NASA-CR-181989; NAS 1.26:181989) Avail: NTIS HC A05/MF A01 CSCL 17B

Alternative calibration procedures are examined for Hewlett-Packard vector network analyzers which lead to an improved open-circuit capacitance model, and hence, higher measurement accuracy. Author

N90-21263*# National Aeronautics and Space Administration. Lewis Research Center, Cleveland, OH.
A NEW RECTANGULAR WAVEGUIDE TO COPLANAR WAVEGUIDE TRANSITION
George E. Ponchak and Rainee N. Simons 1990 4 p Presented at the 1990 IEEE MTT-S International Microwave Symposium, Dallas, TX, 8-10 May 1990
(Grant NAG3-816)
(NASA-TM-102477; E-5264; NAS 1.15:102477) Avail: NTIS HC A01/MF A01 CSCL 20N

A new rectangular waveguide to coplanar waveguide (CPW) transition is described. The transition uses a ridge in one of the broad walls of the waveguide and a nonradiating slot in the opposite wall to split and rotate the electromagnetic fields of the rectangular waveguide TE10 mode into the CPW fields. Author

N90-21264# International Centre for Theoretical Physics, Trieste (Italy).
ULTRARELATIVISTIC ENVELOPE SOLITONS IN ELECTRON-POSITRON PLASMA OF THE PULSAR MAGNETOSPHERE
U. A. Mofiz Aug. 1989 11 p Submitted for publication
(DE90-613289; IC-89/176) Avail: NTIS (US Sales Only) HC A03/MF A01

The non-linear propagation of intense electromagnetic radiation in pulsar magnetospheres is investigated. The radiation is considered to be a circularly polarized electromagnetic wave, in whose field electrons and positrons acquire ultrarelativistic velocities. The non-linear frequency shift due to the wave plasma interaction is found to cause the wave localization and it produces a new kind of envelope soliton, which in coupling with the ambient magnetic field generates an intense ambipolar field along the magnetic lines. DOE

N90-21265# International Centre for Theoretical Physics, Trieste (Italy).
ON THE CREATION OF GRAVITATIONAL WAVE BY PHOTON IN EXTERNAL ELECTROMAGNETIC FIELD
Ngoe Long Hoang and Khac Huong Le (Academy of Science of Vietnam, Hanoi.) Aug. 1989 12 p
(DE90-613366; IC-89/233) Avail: NTIS (US Sales Only) HC A03/MF A01

The creation of the gravitational wave by the photon in an electromagnetic field is considered. It is shown that when the momentum of the photon is perpendicular to the field, the probability of the gravitational wave creation is largest in the direction of the motion of the photon. A numerical evaluation shows that the probability of creation in the direction mentioned is much larger than that in the direction considered, namely in the direction perpendicular to the photon momentum and may have the observable value in the present technical conditions. DOE

N90-21266# Lawrence Livermore National Lab., CA.
A CORRELATION-SPECTRAL METHOD FOR LINE DETECTION ON NOISY DATA
Shin-yee Lu and Farid Dowla Feb. 1990 8 p
(Contract W-7405-eng-48)
(DE90-007925; UCID-21936) Avail: NTIS HC A02/MF A01

Fourier angular features extracted by using a correlation-spectral method are applied to the detection of line patterns in noisy wake data. A large scale image is first segmented into fixed size windows. Angular features are then extracted in each window. Directionality in a window is indicated by the peaks in its feature set. The spurious horizontal and vertical directions caused by the nonperiodity of the pattern in a window can be reduced by removing the mean from the window before feature extraction. The result for wake detection shows good agreement with human visual detection. DOE

N90-21267# Sandia National Labs., Albuquerque, NM.
IS GALERKIN'S METHOD REALLY BETTER
Andrew F. Peterson (Georgia Inst. of Tech., Atlanta.) and Roy E. Jorgenson 1990 12 p Presented at the 6th Annual Review of Progress in Applied Computational Electromagnetics, Monterey, CA, 20-22 Mar. 1990
(Contract DE-AC04-76DP-00789)
(DE90-008804; SAND-90-0242C; CONF-9003128-1) Avail: NTIS HC A03/MF A01

The selection of basis and testing functions within a method-of-moments discretization is an important issue in computational electromagnetics. There appears to be widespread belief that Galerkin's method (selecting the same functions for basis and testing) will generally produce better results than some other choice. To investigate this issue, a variety of discretizations have been studied for several canonical electromagnetics problems. Results suggest that the accuracy of the discretization depends primarily on the order or smoothness of the basis and testing functions, and that there is nothing particularly noteworthy about the accuracy obtained with Galerkin's method. DOE

N90-21268# Instituto de Pesquisas Espaciais, Sao Jose dos Campos (Brazil).
ON BOARD CROSS SUPPORT SCENARIOS
Eduardo Whitaker Bergamini Nov. 1989 49 p Presented at the Consultative Committee for Space Data Systems, Ottawa, Ontario, 24 Sep. - 4 Oct. 1989
(INPE-5005-PRE/1562) Avail: NTIS HC A03/MF A01

A concept for On Board Cross Support Scenarios is presented. In this case, the cross support is characterized as a Communication Service. To some extent, a basic specification, covering aspects of Protocol, Service and Management is proposed for structuring the cross support communication service. The already established CCSDS recommendations for Conventional and Advanced Orbiting Systems, are commented as part of specific On Board Cross Supporting Scenarios. The complementary nature of the proposed concepts is enhanced with respect to the already existing scenarios, which are based on the current CCSDS recommendations. Therefore, if judged appropriate, the concepts which are presented could be a start for development of new CCSDS recommendations directed to On Board Cross Support for Space Data Systems.
Author

N90-21269# Helsinki Univ. of Technology, Espoo (Finland). Electromagnetics Lab.
NEW FERRITE-FILLED WAVEGUIDING STRUCTURES ANALYSED BY THE AVERAGING METHOD
Sergei A. Tretyakov, Markku I. Oksanen, and Andrei S. Cherepanov Aug. 1989 24 p Sponsored in part by Ministry of Education and Academy of Finland
(PB90-165671; ISBN-951-754-982-2; ISSN-0784-848X; Rept-51)
Avail: NTIS HC A03/MF A01 CSCL 20N

Waves in some sophisticated waveguiding structures, filled with magnetized ferrite, are investigated. Anisotropic boundary conditions are supposed to be valid on some of the walls of the waveguides, whence the results allow, for instance, an analysis of ferrite-filled corrugated waveguides and microstrip lines with corrugated strips. For solving the related electromagnetic problems, a new approximate technique, averaging method, is used. The main idea is to average field inside a waveguide assuming that the tangential components are locally quasi-static. The present technique can be used when one of the transversal dimensions of a waveguide is much smaller than the wavelength in that direction.
Author

N90-21270# Helsinki Univ. of Technology, Espoo (Finland). Electromagnetic Lab.
GENERALIZED WKB APPROXIMATION FOR STRATIFIED ISOTROPIC CHIRAL STRUCTURES
Ismo V. Lindell and Ari H. Sihvola Sep. 1989 24 p
(PB90-165689; ISBN-951-22-0027-9; ISSN-0784-848X; Rept-52)
Avail: NTIS HC A03/MF A01 CSCL 20N

The WKB (Wentzel-Kramer-Brillouin) method and its generalization, well known to be applicable to a certain class of achiral isotropic inhomogeneous media, are extended to stratified chiral media for waves with normal incidence. The method is based on an expansion in wave fields, certain combinations of the electric and magnetic fields whose properties are also extensively studied. It is seen that for sufficiently slowly varying media, the reflection dyadic due to the stratification can be expressed in closed integral form and, for normal incidence, the result is independent on the chirality parameter kappa applied. The method can be further extended for chiral media to what is known as the Bremmer series method for achiral media.
Author

33 ELECTRONICS AND ELECTRICAL ENGINEERING

Includes test equipment and maintainability; components, e.g., tunnel diodes and transistors; microminiaturization; and integrated circuitry.

For related information see also *60 Computer Operations and Hardware* and *76 Solid-State Physics.*

N90-21271*# National Aeronautics and Space Administration. Lewis Research Center, Cleveland, OH.

ADVANCED LAUNCH SYSTEM (ALS): ELECTRICAL ACTUATION AND POWER SYSTEMS IMPROVE OPERABILITY AND COST PICTURE

Gale R. Sundberg 1990 8 p Proposed for presentation at the National Aerospace and Electronics Conference, Dayton, OH, 21-25 May 1990; sponsored by IEEE

(NASA-TM-102547; E-5358; NAS 1.15:102547) Avail: NTIS HC A02/MF A01 CSCL 09C

To obtain the Advanced Launch System (ALS) primary goals of reduced costs and improved operability, there must be significant reductions in the launch operations and servicing requirements relative to current vehicle designs and practices. One of the primary methods for achieving these goals is by using vehicle electrical power system and controls for all actuation and avionics requirements. A brief status review of the ALS and its associated Advanced Development Program is presented to demonstrate maturation of those technologies that will help meet the overall operability and cost goals. The electric power and actuation systems are highlighted as a specific technology ready not only to meet the stringent ALS goals (cryogenic field valves and thrust vector controls with peak power demands to 75 hp), but also those of other launch vehicles, military and civilian aircraft, lunar/Martian vehicles, and a multitude of commercial applications. Author

N90-21272*# National Aeronautics and Space Administration. Lewis Research Center, Cleveland, OH.

ELECTROMECHANICAL ACTUATION FOR THRUST VECTOR CONTROL APPLICATIONS

Mary Ellen Roth 1990 5 p Proposed for presentation at the National Aerospace and Electronics Conference (NAECON), Dayton, OH, 21-25 May 1990; sponsored by IEEE

(Contract NAS3-25799)

(NASA-TM-102548; E-5359; NAS 1.15:102548) Avail: NTIS HC A01/MF A01 CSCL 09A

At present, actuation systems for the Thrust Vector Control (TVC) for launch vehicles are hydraulic systems. The Advanced Launch System (ALS), a joint initiative between NASA and the Air Force, is a launch vehicle that is designed to be cost effective, highly reliable and operationally efficient with a goal of reducing the cost per pound to orbit. As part of this initiative, an electromechanical actuation system is being developed as an attractive alternative to the hydraulic systems used today. NASA-Lewis is developing and demonstrating an Induction Motor Controller Actuation System with a 40 hp peak rating. The controller will integrate 20 kHz resonant link Power Management and Distribution (PMAD) technology and Pulse Population Modulation (PPM) techniques to implement Field Oriented Vector Control (FOVC) of a new advanced induction motor. Through PPM, multiphase variable frequency, variable voltage waveforms can be synthesized from the 20 kHz source. FOVC shows that varying both the voltage and frequency and their ratio (V/F), permits independent control of both torque and speed while operating at maximum efficiency at any point on the torque-speed curve. The driver and the FOVC will be microprocessor controlled. For increased system reliability, a Built-in Test (BITE) capability will be included. This involves introducing testability into the design of a system such that testing is calibrated and exercised during the design, manufacturing, maintenance and prelaunch activities. An actuator will be integrated with the motor controller for performance testing of the EMA TVC system. The design and fabrication of the motor controller is being done by General Dynamics Space Systems Division. The University of Wisconsin-Madison will assist in the design of the advanced induction motor and in the implementation of the FOVC theory. A 75 hp electronically controlled dynamometer will be used to test the motor controller in all four quadrants of operation using flight type control algorithms. Integrated testing of the controller and actuator will be conducted at a facility yet to be named. The EMA system described above is discussed in detail. Author

N90-21273*# National Aeronautics and Space Administration. Lewis Research Center, Cleveland, OH.

COPLANAR WAVEGUIDE FED PHASED ARRAY ANTENNA

Rainee N. Simons, George E. Ponchak, R. Q. Lee, and N. S. Fernandez (Puerto Rico Univ., Rio Piedras.) 1990 6 p Proposed for presentation at the 1990 IEEE AP-S International Symposium and URSI Radio Science Meeting, Dallas, TX, 7-1 May 1990

(NASA-TM-102522; E-5327; NAS 1.15:102522) Avail: NTIS HC A02/MF A01 CSCL 09A

A K-band four element linear phased array was designed and tested. Coplanar waveguide (CPW) is used for the microwave distribution system. A CPW to twin strip transition is used to interface with the printed dipole antennas. MMIC phased shifters are used for phase control. Author

N90-21274*# National Aeronautics and Space Administration. Lewis Research Center, Cleveland, OH.

RECENT RESULTS FROM ADVANCED RESEARCH ON SPACE SOLAR CELLS AT NASA

Dennis J. Flood 1990 9 p Presented at the International Solar Energy Conference, Miami, FL, 1-4 Apr. 1990; sponsored by ASME

(NASA-TM-102485; E-5251; NAS 1.15:102485) Avail: NTIS HC A02/MF A01 CSCL 10A

The NASA program in space photovoltaic research and development encompasses a wide range of emerging options for future space power systems, and includes both cell and array technology development. The long range goals are to develop technology capable of achieving 300 W/kg for planar arrays, and 300 W/sq m for concentrator arrays. InP and GaAs planar and concentrator cell technologies are under investigation for their potential high efficiency and good radiation resistance. The Advanced Photovoltaic Solar Array (APSA) program is a near term effort aimed at demonstrating 130 W/kg beginning of life specific power using thin (62 pm) silicon cells. It is intended to be technology transparent to future high efficiency cells and provides the baseline for development of the 300 W/kg array. Author

N90-21275*# National Aeronautics and Space Administration. Lewis Research Center, Cleveland, OH.

OPTICAL CONTROL OF AN 8-ELEMENT Ka-BAND PHASED ARRAY USING A HIGH-SPEED OPTOELECTRONIC INTERCONNECT

M. A. Richard, P. C. Claspy, K. B. Bhasin, and M. Bendett (Honeywell, Inc., Bloomington, MN.) 1990 6 p Proposed for presentation at the 1990 AP-S International Symposium, Dallas, TX, 7-11 May 1990; sponsored by IEEE

(NASA-TM-102550; E-5365; NAS 1.15:102550) Avail: NTIS HC A02/MF A01 CSCL 09C

Optical distribution of control signals in electronically steered phased array antennas is being considered. A demonstration experiment is described in which a high speed hybrid GaAs optoelectronic integrated circuit (OEIC) was used to control an eight element phased array antenna. The OEIC, which accepts a serial optical control signal as input and converts it to 16 demultiplexed parallel outputs, was used to control the monolithic GaAs phase shifters of a Ka-band patch panel array antenna. Antenna pattern switching speeds of 2.25 microsec, limited by interface circuitry, were observed. Author

N90-21276# National Inst. of Standards and Technology, Boulder, CO. Electromagnetic Fields Div.

SYSTEMATIC ERRORS IN POWER MEASUREMENTS MADE WITH A DUAL SIX-PORT ANA

Cletus A. Hoer Jul. 1989 55 p
(PB90-145160; NIST/TN-1332) Avail: NTIS HC A04/MF A01 CSCL 09C

The systematic error in measuring power with a dual 6-port Automatic Network Analyzer was determined. Equations for estimating systematic errors due to imperfections in the test port connector, imperfections in the connector on the power standard, and imperfections in the impedance standards used to calibrate the 6-port for measuring reflection coefficient were developed. These are the largest sources of error associated with the 6-port. For 7 mm connectors, all systematic errors which are associated with the 6-port add up to a worst-case uncertainty of + or - 0.00084 in measuring the ratio of the effective efficiency of a bolometric power sensor relative to that of a standard power sensor. Author

N90-21277*# National Aeronautics and Space Administration. Lewis Research Center, Cleveland, OH.
INTENSITY TO FREQUENCY CONVERSION TECHNIQUE IN INTENSITY MODULATED FIBER OPTIC SENSING SYSTEMS
G. Adamovsky and T. W. Carr (Case Western Reserve Univ., Cleveland, OH.) Mar. 1990 7 p
(NASA-TM-102562; E-5376; NAS 1.15:102562) Avail: NTIS HC A02/MF A01 CSCL 09C

A novel sensing technique based on intensity-to-frequency conversion is explained and demonstrated. Experimental data are presented and a comparison with a theoretical model is made. Author

N90-21278*# National Aeronautics and Space Administration. Lewis Research Center, Cleveland, OH.
COPLANAR WAVEGUIDE DISCONTINUITIES FOR P-I-N DIODE SWITCHES AND FILTER APPLICATIONS
N. I. Dib, P. B. Katehi, George E. Ponchak, and Rainee N. Simons (Case Western Reserve Univ., Cleveland, OH.) 1990 10 p Presented at the 1990 IEEE MTT-S International Microwave Symposium, Dallas, TX, 8-10 May 1990
(Grant NSF ECS-86-57951)
(NASA-TM-102534; E-5343; NAS 1.15:102534) Avail: NTIS HC A02/MF A01 CSCL 09C

A full wave space domain integral equation (SDIE) analysis of coplanar waveguide (CPW) two port discontinuities is presented. An experimental setup to measure the S-parameters of such discontinuities is described. Experimental and theoretical results for CPW realizations of pass-band and stop-band filters are presented. The S-parameters of such structures are plotted in the frequency range 5 to 25 GHz. Author

N90-21279*# National Aeronautics and Space Administration. Langley Research Center, Hampton, VA.
AN ASSESSMENT OF THE POTENTIAL OF CONTINUOUS-WAVE RANGING FOR MEASURING THE DISTANCE TO A HIGHLY REFLECTIVE, INFINITE SHEET
C. P. Hearn, M. C. Bailey, M. J. Czerner, K. L. Dudley, and E. Vedeler Apr. 1990 50 p
(NASA-TM-101680; NAS 1.15:101680) Avail: NTIS HC A03/MF A01 CSCL 09C

The feasibility of a continuous-wave, distance-measuring technique for measuring the distance from a spacecraft antenna to a highly ionized plasma surface is examined. The reflection coefficient angle is computed for several aperture models. It is concluded that aperture size and the presence of a nonablating dielectric cover over the antenna are critical factors. Author

N90-21280# Honeywell, Inc., Bloomington, MN. Systems and Research Center.
HIGH EFFICIENCY OCTAVE BANDWIDTH MILLIMETER WAVE POWER AMPLIFIER Final Report, 1 Apr. 1987 - 31 Mar. 1989
Vladimir Sokolov, Stanley Swirhun, James B. Beyer, and S. N. Prasad (Wisconsin Univ., Madison.) Aug. 1989 85 p
(Contract N00014-87-C-0157)
(AD-A218245; AD-E501191) Avail: NTIS HC A05/MF A01 CSCL 09/1

Millimeter (MM) wave monolithic distributed amplifiers are designed to cover the 30 to 60 GHz frequency band. Both low-pass bandpass and negative resistance compensated designs are developed. The MMIC designs are based on pseudomorphic MODFET devices having 1/4 micron gates fabricated on 3-inch wafers using a hybrid e-beam/optical stepper lithography technique. In addition to standard pseudomorphic MODFET structures with uniformly doped AlGaAs, psuedo-pulsed-doped structures were also developed to address low drain breakdown voltage problems. 60 GHz monolithic gain cells with 10 mW output power were also developed. GRA

N90-21281# Army Missile Command, Redstone Arsenal, AL.
POWER TRANSMISSION DEVICE Patent Application
William F. Otto, inventor (to Army), Miles E. Holloman, inventor (to Army), and Debbee Jordan, inventor (to Army) 26 Dec. 1989 9 p
(AD-D014430; US-Patent-Appl-SN-456899) Avail: NTIS HC A02/MF A01 CSCL 09/1

A power transmission device for transmitting electric power optically to remote locations is described. The device includes a laser for generating a laser light beam and a optical glass monofilament having a glass core and a outer cladding layer designed to convey the light beams directed into one end of said monofilament to the other and thereof. Means are provided for directing the laser beam into the receiving end for the monofilament at a predetermined angle which causes the light beam to exit from the other end of the monofilament at the same predetermined angle in a conical annulus of light. A conical reflector is disposed within the conical annulus of light exiting from the exit end of the fiber optical monofilament and has surfaces that intercepts the light beams within the conical annulus and reflects them along a different path. Disposed around the conical reflector is a plurality of photovoltaic cells in a position to intercept the reflected light beams and to convert the light beams to electric current. The photovoltaic cells are connected in series to increase the amount of voltage produced by the transmission device. GRA

N90-21282*# Analex Corp., Cleveland, OH.
APERTURE TAPER DETERMINATION FOR THE HALF-SCALE ACCURATE ANTENNA REFLECTOR Final Report
Kevin M. Lambert Apr. 1990 22 p
(Contract NAS3-24564)
(NASA-CR-185215; E-5373; NAS 1.26:185215) Avail: NTIS HC A03/MF A01 CSCL 09C

A simulation is described of a proposed microwave reflectance measurement in which the half scale reflector is used in a compact range type of application. The simulation is used to determine an acceptable aperture taper for the reflector which will allow for accurate measurements. Information on the taper is used in the design of a feed for the reflector. Author

N90-21283*# National Aeronautics and Space Administration. Lewis Research Center, Cleveland, OH.
CIVIL AIR TRANSPORT: A FRESH LOOK AT POWER-BY-WIRE AND FLY-BY-LIGHT
Gale R. Sundberg May 1990 6 p Presented at the National Aerospace and Electronics Conference, Dayton, OH, 21-25 May 1990; sponsored by IEEE
(NASA-TM-102574; E-5402; NAS 1.15:102574) Avail: NTIS HC A02/MF A01 CSCL 09C

Power-by-wire (PBW) is a key element under subsonic transport flight systems technology with potential savings of over 10 percent in gross take-off-weight and in fuel consumption compared to today's transport aircraft. The PBW technology substitutes electrical actuation in place of centralized hydraulics, uses internal starter-motor/generators and eliminates the need for variable engine bleed air to supply cabin comfort. The application of advanced fiber optics to the electrical power system controls, to built-in-test (BITE) equipment, and to fly-by-light (FBL) flight controls provides additional benefits in lightning and high energy radio frequency (HERF) immunity over existing mechanical or even

fly-by-wire controls. The program plan is reviewed and a snapshot is given of the key technologies and their benefits to all future aircraft, both civil and military. Author

N90-21284# Joint Publications Research Service, Arlington, VA.
JPRS REPORT: SCIENCE AND TECHNOLOGY. USSR: ELECTRONICS AND ELECTRICAL ENGINEERING
28 Mar. 1990 64 p Transl. into ENGLISH of various Russian documents
(JPRS-UEE-90-002) Avail: NTIS HC A04/MF A01

Abstracts of research in electronics and electrical engineering are given. Research in broadcasting, consumer electronics, antennas, radio wave propagation, reliability, industrial electronics, electron devices, computers, microwave theory and techniques, electromagnetic compatibility, power engineering, electromagnetic fields, quantum electronics and solid state circuits is covered. R.J.F.

N90-21285# Fermi National Accelerator Lab., Batavia, IL.
THE DESIGN OF A LARGE APERTURE HIGH FIELD DIPOLE
Fady Harfoush, Mike Harrison, Jim Kerby, Karl Koepke, Paul Mantsch, Tom Nicol, Alan Riddiford, and Jay Theilacker Dec. 1989 149 p
(Contract DE-AC02-76CH-03000)
(DE90-007910; FNAL-TM-1641) Avail: NTIS HC A08/MF A01

The impetus for this design report originated in the Snowmass 88 meeting where the subject of higher energies within the constraints of the existing Tevatron tunnel enclosure was investigated. It was determined that beam transport to the fixed target experimental areas was possible up to an energy of approx. 1.5 Tev. Collider operation was feasible at somewhat higher energies (1.8 Tev), primarily limited by the ability to design a single turn beam abort system within the constraints of the straight section length. A new accelerator in the existing tunnel would, of necessity, have a similar though not identical lattice and straight section layout to the present Tevatron. Thus when issues arose in the magnet design requiring input from the accelerator standpoint, it was assumed a Tevatron like machine. The possibility of using these high field magnets as elements in the existing Tevatron to create new warm space, for another Interaction Region for example, also emphasizes compatibility with the present machine. DOE

N90-21286# Helsinki Univ. of Technology, Espoo (Finland). Lab. of Thermal Engineering.
THE DEVELOPMENT OF A SIMULATION PROGRAM OF THE ANODE SIDE FOR ALUMINUM/AIR BATTERIES
C. N. Rooker (Technische Hogeschool, Twente, Netherlands) 30 Aug. 1989 78 p
(PB90-165754) Avail: NTIS HC A05/MF A01 CSCL 10C

A simulation program of the anode side of aluminum/air batteries in Turbo Pascal version 5.0 was developed. On this side two reactions occur, namely the oxidation of the aluminum self and the evolution of hydrogen. This last one is not wanted, because it reduces the capacity of the battery. The program shows graphics of the oxidation, the total current density, the hydrogen-flux and the efficiency of the cell versus the potential vs Hg/HgO. All this is based on a mathematic model of the electron transfer. Experimental testing of a germanium-crystal coated with platinum in IR-spectroscopy is also described. The crystal used this way is not effective. Author

N90-21287*# National Aeronautics and Space Administration. Lewis Research Center, Cleveland, OH.
PEELED FILM GaAs SOLAR CELLS FOR SPACE POWER
D. M. Wilt, F. L. DeAngelo, R. D. Thomas, S. G. Bailey, G. A. Landis, D. J. Brinker, and N. S. Fatemi (Sverdrup Technology, Inc., Cleveland, OH.) May 1990 8 p
(NASA-TM-103125; E-5453; NAS 1.15:103125) Avail: NTIS HC A02/MF A01 CSCL 10A

Gallium arsenide (GaAs) peeled film solar cells were fabricated, by Organo-Metallic Vapor Phase Epitaxy (OMVPE), incorporating an aluminum arsenide (AlAs) parting layer between the device structure and the GaAs substrate. This layer was selectively removed by etching in dilute hydrofloric (HF) acid to release the epitaxial film. Test devices exhibit high series resistance due to insufficient back contact area. A new design is presented which uses a coverglass superstrate for structural support and incorporates a coplanar back contact design. Devices based on this design should have a specific power approaching 700 W/Kg. Author

34 FLUID MECHANICS AND HEAT TRANSFER

Includes boundary layers; hydrodynamics; fluidics; mass transfer; and ablation cooling.

For related information see also *02 Aerodynamics* and *77 Thermodynamics and Statistical Physics.*

N90-21288 California Univ., Davis.
NUMERICAL SIMULATION OF VORTEX BREAKDOWN Ph.D. Thesis
Jasim Uddin Ahmad 1989 155 p
Avail: Univ. Microfilms Order No. DA9002715

The Vortex Breakdown for confined and unconfined, viscous and inviscid, steady and unsteady, incompressible and compressible, laminar, axisymmetric flows are simulated using both stream function-vorticity and primitive variables. For inviscid calculations, a model equation is solved with different algorithms and results are obtained for both compressible and incompressible steady flows with swirl. For viscous flows, Navier-Stokes equations are transformed to a form which is valid for zero Mach number, hence, the incompressible flow is a special case. A stream function-vorticity formulation for incompressible flow is presented with various numerical algorithms including Newton's method for steady flows and time integration of the unsteady equations, using direct solver and successive line relaxation precedures. Also, a method based on inverse iterations, for inviscid flows is extended to viscous flows, where a norm of the solution is prescribed and the swirling parameter is calculated as a part of the solution. For primitive variable calculations, a fully implicit, fully coupled solution procedure, based on Newton's method, is employed. Central differences are used everywhere for incompressible flows, while an upwind difference scheme in a conservative form for the convective terms is implemented for compressible flows. The temperature effect for incompressible flows is simulated using the Boussinesq approximation. Solutions are presented for a wide range of parameters and are compared with the experimental data as well as with other published results. The effect of compressibility on the breakdown is also studied and results indicate that for subsonic flows, breakdown occurs at a higher swirling velocity. Dissert. Abstr.

N90-21289*# Institute for Computer Applications in Science and Engineering, Hampton, VA.
ON THE INSTABILITY OF GOERTLER VORTICES TO NONLINEAR TRAVELLING WAVES Final Report
Sharon O. Seddougui and Andrew P. Bassom (Exeter Univ., England) Jan. 1990 45 p Submitted for publication
(Contract NAS1-18605)
(NASA-CR-181994; ICASE-90-1; NAS 1.26:181994) Avail: NTIS HC A03/MF A01 CSCL 20D

Recent theoretical work by Hall and Seddougui (1989) has shown that strongly nonlinear, high wavenumber Goertler vortices developing within a boundary layer flow are susceptible to a secondary instability which takes the form of travelling waves confined to a thin region centered at the outer edge of the vortex. The case is considered in which the secondary mode could be satisfactorily described by a linear stability theory and herein the objective is to extend this investigation of Hall and Seddougui (1989) into the nonlinear regime. It was found that at this stage not only does the secondary mode become nonlinear but it also interacts with itself so as to modify the governing equations for the primary Goertler vortex. In this case then, the vortex and the

travelling wave drive each other and, indeed, the whole flow structure is described by an infinite set of coupled, nonlinear differential equations. A Stuart-Watson type of weakly nonlinear analysis of these equations is undertaken and concluded, in particular, that on this basis there exist stable flow configurations in which the travelling mode is of finite amplitude. Implications of the findings for practical situations are discussed and it is shown that the theoretical conclusions drawn here are in good qualitative agreement with available experimental observations. Author

N90-21290*# Institute for Computer Applications in Science and Engineering, Hampton, VA.
SURFACE-COOLING EFFECTS ON COMPRESSIBLE BOUNDARY-LAYER INSTABILITY Final Report
Sharon O. Seddougui, R. I. Bowles, and F. T. Smith (University Coll., London, England) Feb. 1990 51 p Submitted for publication
(Contract NAS1-18605)
(NASA-CR-182003; ICASE-90-19; NAS 1.26:182003) Avail: NTIS HC A04/MF A01 CSCL 20D

The influence of surface cooling on compressible boundary layer instability is discussed theoretically for both viscous and inviscid modes, at high Reynolds numbers. The cooling enhances the surface heat transfer and shear stress, creating a high heat transfer sublayer. This has the effect of distorting and accentuating the viscous Tollmien-Schlichting modes to such an extent that their spatial growth rates become comparable with, and can even exceed, the growth rates of inviscid modes, including those found previously. This is for moderate cooling, and it applies at any Mach number. In addition, the moderate cooling destabilizes otherwise stable viscous or inviscid modes, in particular triggering outward-traveling waves at the edge of the boundary layer in the supersonic regime. Severe cooling is also discussed as it brings compressible dynamics directly into play within the viscous sublayer. All the new cooled modes found involve the heat transfer sublayer quite actively, and they are often multi-structured in form and may be distinct from those observed in previous computational and experimental investigations. The corresponding nonlinear processes are also pointed out with regard to transition in the cooled compressible boundary layer. Finally, comparisons with Lysenko and Maslov's (1984) experiments on surface cooling are presented. Author

N90-21291*# National Aeronautics and Space Administration. Lewis Research Center, Cleveland, OH.
A COST-EFFECTIVE STRATEGY FOR NONOSCILLATORY CONVECTION WITHOUT CLIPPING
B. P. Leonard and H. S. Niknafs (Norton Co., Stow, OH.) Mar. 1990 24 p
(NASA Order C-99066-G)
(NASA-TM-102538; ICOMP-90-09; E-5336; NAS 1.15:102538) Avail: NTIS HC A03/MF A01 CSCL 20D

Clipping of narrow extrema and distortion of smooth profiles is a well known problem associated with so-called high resolution nonoscillatory convection schemes. A strategy is presented for accurately simulating highly convective flows containing discontinuities such as density fronts or shock waves, without distorting smooth profiles or clipping narrow local extrema. The convection algorithm is based on non-artificially diffusive third-order upwinding in smooth regions, with automatic adaptive stencil expansion to (in principle, arbitrarily) higher order upwinding locally, in regions of rapidly changing gradients. This is highly cost effective because the wider stencil is used only where needed-in isolated narrow regions. A recently developed universal limiter assures sharp monotonic resolution of discontinuities without introducing artificial diffusion or numerical compression. An adaptive discriminator is constructed to distinguish between spurious overshoots and physical peaks; this automatically relaxes the limiter near local turning points, thereby avoiding loss of resolution in narrow extrema. Examples are given for one-dimensional pure convection of scalar profiles at constant velocity. Author

N90-21292*# North Carolina Agricultural and Technical State Univ., Greensboro. Dept. of Mechanical Engineering.
COMPACT SCHEME FOR SYSTEMS OF EQUATIONS APPLIED TO FUNDAMENTAL PROBLEMS OF MECHANICS OF CONTINUA Final Report
Jerzy Z. Klimkowski 1990 58 p
(Grant NAG1-812)
(NASA-CR-186494; NAS 1.26:186494) Avail: NTIS HC A04/MF A01 CSCL 20D

Compact scheme formulation was used in the treatment of boundary conditions for a system of coupled diffusion and Poisson equations. Models and practical solutions of specific engineering problems arising in solid mechanics, chemical engineering, heat transfer and fuid mechanics are described and analyzed for efficiency and accuracy. Only 2-D cases are discussed and a new method of numerical treatment of boundary conditions common in the fundamental problems of mechanics of continua is presented. Author

N90-21293# Department of the Navy, Washington, DC.
ABLATIVE COOLING OF AERODYNAMICALLY HEATED RADOMES Patent Application
Leon H. Schindel, inventor (to Navy) and Richard T. Driftmyer, inventor (to Navy) 14 Dec. 1989 15 p
(AD-D014426; US-Patent-Appl-SN-450754) Avail: NTIS HC A03/MF A01 CSCL 17/9

This invention relates generally to the cooling of surfaces aerodynamically heated by flow of air relative thereto, and more particularly to the cooling of radiation transmissive nose cone surfaces of missiles having properties adversely affected by aerodynamic heating during air travel at high velocities. A radome type nose cone shell subjected to aerodynamic heating during projectile travel, is ablatively cooled by evaporation of metal coolant from a solidified coating thereof adhering to the external surface of a porous section of the cone shell through which the coolant seeps from internal storage at a rate regulated by formation of the solidified coating. The evaporating coolant from the coating mixes with the air in the flow stream to form a protective boundary layer extending downstream from the porous section of the nose cone shell. The coolant is melted by said aerodynamic heating during internal storage within the nose cone shell for seepage outflow from the porous section and has the requisite heats of evaporation and fusion to effect alternate freezing and thawing thereof in response to withdrawal of heat by the cooling process for establishment and maintenance of the flow regulating coating. GRA

N90-21294*# National Aeronautics and Space Administration. Ames Research Center, Moffett Field, CA.
THERMAL CONTROL SYSTEM CORROSION STUDY
Robert Yee, Rolfe A. Folsom, and Phillip E. Mucha Feb. 1990 55 p
(NASA-TM-102220; A-89226; NAS 1.15:102220) Avail: NTIS HC A04/MF A01 CSCL 20D

During the development of an expert system for autonomous control of the Space Station Thermal Control System (TCS), the thermal performance of the Brassboard TCS began to gradually degrade. This degradation was due to filter clogging by metallic residue. A study was initiated to determine the source of the residue and the basic cause of the corrosion. The investigation focused on the TCS design, materials compatibility, Ames operating and maintenance procedures, and chemical analysis of the residue and of the anhydrous ammonia used as the principal refrigerant. It was concluded that the corrosion mechanisms involved two processes: the reaction of water alone with large, untreated aluminum parts in a high pH environment and the presence of chlorides and chloride salts. These salts will attack the aluminum oxide layer and may enable galvanic corrosion between the aluminum and the more noble stainless steel and other metallic elements present. Recommendations are made for modifications to the system design, the materials used, and the operating and maintenance procedures, which should largely prevent the recurrence of these corrosion mechanisms. Author

N90-21295*# National Aeronautics and Space Administration. Lewis Research Center, Cleveland, OH.

LIQUID TRANSFER CRYOGENIC TEST FACILITY: INITIAL HYDROGEN AND NITROGEN NO-VENT FILL DATA

Matthew E. Moran, Ted W. Nyland, and S. Stephen Papell (Analex Corp., Cleveland, OH.) Mar. 1990 28 p

(NASA-TM-102572; E-5396; NAS 1.15:102572) Avail: NTIS HC A03/MF A01 CSCL 20D

The Liquid Transfer Cryogenic Test Facility is a versatile testbed for ground-based cryogenic fluid storage, handling, and transfer experimentation. The test rig contains two well instrumented tanks, and a third interchangeable tank, designed to accommodate liquid nitrogen or liquid hydrogen testing. The internal tank volumes are approx. 18, 5, and 1.2 cu. ft. Tank pressures can be varied from 2 to 30 psia. Preliminary no vent fill tests with nitrogen and hydrogen were successfully completed with the test rig. Initial results indicate that no vent fills of nitrogen above 90 percent full are achievable using this test configuration, in a 1-g environment, and with inlet liquid temperatures as high as 143 R, and an average tank wall temperature of nearly 300 R. This inlet temperature corresponds to a saturation pressure of 19 psia for nitrogen. Hydrogen proved considerably more difficult to transfer between tanks without venting. The highest temperature conditions resulting in a fill level greater than 90 percent were with an inlet liquid temperature of 34 R, and an estimated tank wall temperature of slightly more than 100 R. Saturation pressure for hydrogen at this inlet temperature is 10 psia. All preliminary no vent fill tests were performed with a top mounted full cone nozzle for liquid injection. The nozzle produces a 120 degree conical droplet spray at a differential pressure of 10 psi. Pressure in the receiving tank was held to less than 30 psia for all tests. Author

N90-21296*# National Aeronautics and Space Administration. Lewis Research Center, Cleveland, OH.

THERMAL RADIATION CHARACTERISTICS OF NONISOTHERMAL CYLINDRICAL ENCLOSURES USING A NUMERICAL RAY TRACING TECHNIQUE

Joseph F. Baumeister 1990 9 p Proposed for presentation at the 5th Thermophysics and Heat Transfer Conference, Seattle, WA, 18-20 Jun. 1990; cosponsored by AIAA and ASME

(NASA-TM-102527; E-5335; NAS 1.15:102527) Avail: NTIS HC A02/MF A01 CSCL 20D

Analysis of energy emitted from simple or complex cavity designs can lead to intricate solutions due to nonuniform radiosity and irradiation within a cavity. A numerical ray tracing technique was applied to simulate radiation propagating within and from various cavity designs. To obtain the energy balance relationships between isothermal and nonisothermal cavity surfaces and space, the computer code NEVADA was utilized for its statistical technique applied to numerical ray tracing. The analysis method was validated by comparing results with known theoretical and limiting solutions, and the electrical resistance network method. In general, for nonisothermal cavities the performance (apparent emissivity) is a function of cylinder length-to-diameter ratio, surface emissivity, and cylinder surface temperatures. The extent of nonisothermal conditions in a cylindrical cavity significantly affects the overall cavity performance. Results are presented over a wide range of parametric variables for use as a possible design reference. Author

N90-21297*# National Aeronautics and Space Administration. Langley Research Center, Hampton, VA.

COMPUTER CODES FOR THE EVALUATION OF THERMODYNAMIC PROPERTIES, TRANSPORT PROPERTIES, AND EQUILIBRIUM CONSTANTS OF AN 11-SPECIES AIR MODEL

Richard A. Thompson, Kam-Pui Lee, and Roop N. Gupta (Scientific Research and Technology, Inc., Hampton, VA.) Feb. 1990 48 p

(NASA-TM-102602; NAS 1.15:102602) Avail: NTIS HC A03/MF A01 CSCL 20D

The computer codes developed provide data to 30000 K for the thermodynamic and transport properties of individual species and reaction rates for the prominent reactions occurring in an 11-species nonequilibrium air model. These properties and the reaction-rate data are computed through the use of curve-fit relations which are functions of temperature (and number density for the equilibrium constant). The curve fits were made using the most accurate data believed available. A detailed review and discussion of the sources and accuracy of the curve-fitted data used herein are given in NASA RP 1232. Author

N90-21298 Virginia Univ., Charlottesville.

A QUASI-LAGRANGIAN MOVING GRID TECHNIQUE FOR INVESTIGATING COMPRESSIBLE FLOWS Ph.D. Thesis

Leon P. Anderson, Jr. 1989 171 p

Avail: Univ. Microfilms Order No. DA9002818

A quasi-Langrangian moving grid numerical technique for investigating compressible flows is discussed. A flexible and versatile method which contains the advantages of both Lagrangian and Eulerian approaches to solving compressible flows was developed. The method moves the grid so that it is required to be Lagrangian in only one coordinate direction. This flexibility permits the use of an adaptive grid scheme in other directions. In order to increase the versatility of the method further, the basic flow equations are solved by a finite volume technique. The method is tested by using an unsplit MacCormack discritization scheme. Test calculations are performed for supersonic flows over a 15 deg wedge and a 15 deg corner. Test results from the calculations agree well with exact solutions. The potential of the method for calculating two-dimensional jet flows is illustrated by results of calculations for underexpanded, inviscid jets, exhausting to the atmosphere. Calculations are performed for various exit pressure to atmospheric pressure ratios and Mach numbers. One of the jet test cases uses an adaptive grid scheme in one of the coordinate directions. All of the results show excellent agreement with solutions predicted by the Method of Characteristics. Dissert. Abstr.

N90-21299 Carnegie-Mellon Univ., Pittsburgh, PA.

ANALYSIS AND FINITE ELEMENT APPROXIMATION OF SOME OPTIMAL CONTROL PROBLEMS ASSOCIATED WITH THE NAVIER-STOKES EQUATIONS Ph.D. Thesis

Lisheng Hou 1989 161 p

Avail: Univ. Microfilms Order No. DA9006210

The finite element approximation of several optimal control problems associated with the stationary Navier-Stokes equations is studied. The controls may be the distributed type (external body force), Dirichlet type (velocity on the boundary), Neumann type (stress on the boundary), or a combination of these. The optimization goal is either to minimize the viscous drag or to obtain a best approximation in the L sup 4 (omega) sense to some desired flow field. For the various cases the existence of optimal solutions is proved, and using Lagrange multiplier techniques, an optimality system of equations is derived. The regularity of solutions of the optimality systems is studied. Finally, finite element algorithms are defined and optimal error estimates are obtained. Dissert. Abstr.

N90-21300*# National Aeronautics and Space Administration. Lewis Research Center, Cleveland, OH.

NAVIER-STOKES ANALYSIS OF TURBINE BLADE HEAT TRANSFER

R. J. Boyle 1990 21 p Prepared for presentation at the 35th International Gas Turbine and Aeroengine Congress and Exposition, Brussels, Belgium, 11-14 Jun. 1990; sponsored in part by ASME

(NASA-TM-102496; E-5219; NAS 1.15:102496) Avail: NTIS HC A03/MF A01 CSCL 20D

Comparisons with experimental heat transfer and surface pressures were made for seven turbine vane and blade geometries using a quasi-three-dimensional thin-layer Navier-Stokes analysis. Comparisons are made for cases with both separated and unseparated flow over a range of Reynolds numbers and freestream turbulence intensities. The analysis used a modified Baldwin-Lomax turbulent eddy viscosity mode. Modifications were made to account for the effects of: (1) freestream turbulence on both transition

and leading edge heat transfer; (2) strong favorable pressure gradients on relaminarization; and (3) variable turbulent Prandtl number heat transfer. In addition, the effect of heat transfer on the near wall model of Deissler is compared with the Van Driest model. Author

N90-21301*# Michigan State Univ., East Lansing. Dept. of Mechanical Engineering.
THE EFFECTS OF FORCING ON A SINGLE STREAM SHEAR LAYER AND ITS PARENT BOUNDARY LAYER
Richard C. Haw and John F. Foss 1990 194 p
(Grant NAG3-671)
(NASA-CR-186529; NAS 1.26:186529; MSU-Engr-90-006; TSF1-R-014) Avail: NTIS HC A09/MF A01 CSCL 20D

Forcing and its effect on fluid flows has become an accepted tool in the study and control of flow systems. It has been used both as a diagnostic tool, to explore the development and interaction of coherent structures, and as a method of controlling the behavior of the flow. A number of forcing methods have been used in order to provide a perturbation to the flow; among these are the use of an oscillating trailing edge, acoustically driven slots, external acoustic forcing, and mechanical piston methods. The effect of a planar mechanical piston forcing on a single stream shear layer is presented; it can be noted that this is one of the lesser studied free shear layers. The single stream shear layer can be characterized by its primary flow velocity scale and the thickness of the separating boundary layer. The velocity scale is constant over the length of the flow field; theta (x) can be used as a width scale to characterize the unforced shear layer. In the case of the forced shear layer the velocity field is a function of phase time and definition of a width measure becomes somewhat problematic. Author

N90-21302# George Washington Univ., Washington, DC. School of Engineering and Applied Science.
CEPSTRUM ANALYSIS AND APPLICATIONS TO COMPUTATIONAL FLUID DYNAMIC SOLUTIONS M.S. Thesis
Kristine R. Meadows 16 Apr. 1990 119 p
Avail: NTIS HC A06/MF A01

A novel approach to the problem of spurious reflections introduced by artificial boundary conditions in computational fluid dynamic (CFD) solutions is proposed. Instead of attempting to derive non-reflecting boundary conditions, the approach is to accept the fact that spurious reflections occur, but to remove these reflections with cepstrum analysis, a signal processing technique which has been successfully used to remove echoes from experimental data. First, the theory of the cepstrum method is presented. This includes presentation of two types of cepstra: The Power Cepstrum and the Complex Cepstrum. The definitions of the cepstrum methods are applied theoretically and numerically to the analytical solution of sinusoidal plane wave propagation in a duct. One-D and 3-D time dependent solutions to the Euler equations are computed, and hard-wall conditions are prescribed at the numerical boundaries. The cepstrum method is applied, and the reflections from the boundaries are removed from the solutions. One-D and 3-D solutions are computed with so called nonreflecting boundary conditions, and these solutions are compared to those obtained by prescribing hard wall conditions and processing with the cepstrum. Author

N90-21303*# National Aeronautics and Space Administration. Lewis Research Center, Cleveland, OH.
PROTEUS TWO-DIMENSIONAL NAVIER-STOKES COMPUTER CODE, VERSION 1.0. VOLUME 1: ANALYSIS DESCRIPTION
Charles E. Towne, John R. Schwab, Thomas J. Benson, and Ambady Suresh (Sverdrup Technology, Inc., Cleveland, OH.) Mar. 1990 71 p
(NASA-TM-102551; E-5366; NAS 1.15:102551) Avail: NTIS HC A04/MF A01 CSCL 20D

A new computer code was developed to solve the two-dimensional or axisymmetric, Reynolds averaged, unsteady compressible Navier-Stokes equations in strong conservation law form. The thin-layer or Euler equations may also be solved. Turbulence is modeled using an algebraic eddy viscosity model. The objective was to develop a code for aerospace applications that is easy to use and easy to modify. Code readability, modularity, and documentation were emphasized. The equations are written in nonorthogonal body-fitted coordinates, and solved by marching in time using a fully-coupled alternating direction-implicit procedure with generalized first- or second-order time differencing. All terms are linearized using second-order Taylor series. The boundary conditions are treated implicitly, and may be steady, unsteady, or spatially periodic. Simple Cartesian or polar grids may be generated internally by the program. More complex geometries require an externally generated computational coordinate system. The documentation is divided into three volumes. Volume 1 is the Analysis Description, and describes in detail the governing equations, the turbulence model, the linearization of the equations and boundary conditions, the time and space differencing formulas, the ADI solution procedure, and the artificial viscosity models. Author

N90-21304# Massachusetts Univ., Amherst. Dept. of Chemical Engineering.
MIXING OF VISCOUS FLUIDS: BEHAVIOR OF MICROSTRUCTURES AND CHAOS Progress Report, 1 Mar. 1990 - 28 Feb. 1991
Julio M. Ottino Nov. 1989 19 p
(Contract DE-FG02-85ER-13333)
(DE90-008871; DOE/ER-13333/6) Avail: NTIS HC A03/MF A01

The work corresponding to the third year follows largely the plans outlined in the previous progress report (second year) and the original proposal. The work involved computational and experimental studies in two main areas: (1) investigations of chaotic mixing of single fluids in two-dimensional time-periodic flows, and (2) dynamics of active microstructures in such flows (e.g., stretching, breakup, coagulation, etc.). In this report, we briefly discuss the two main areas of research, and list publications, journals, presentations, proceedings, and lectures for the third year of the grant. DOE

N90-21305# National Inst. of Standards and Technology, Gaithersburg, MD. Center for Building Technology.
AN EXPERIMENTAL EVALUATION OF TWO NONAZEOTROPIC REFRIGERANT MIXTURES IN A WATER-TO-WATER BREADBOARD HEAT PUMP
Michael Kauffeld, William Mulroy, Mark McLinden, and David Didion Feb. 1990 64 p
(Contract DE-AC05-84OR-21400)
(DE90-009016; ORNL/M-1117) Avail: NTIS HC A04/MF A01

As part of the Department of Energy/Oak Ridge National Laboratory Building Equipment Research program, the National Institute of Standards and Technology constructed an experimental, easily reconfigurable, water-to-water, breadboard heat pump apparatus in order to compare pure R22 to nonazeotropic refrigerant mixtures. Performance of the heat pump charged with a range of compositions of the binary mixtures R22/RI14 and R13/R12 were compared to R22. The advantage claimed for mixtures in this application is improved thermodynamic efficiency as a result of gliding refrigerant temperatures in the evaporator and condenser in low lift, high glide applications typical of air conditioning. DOE

N90-21306*# National Aeronautics and Space Administration. Lewis Research Center, Cleveland, OH.
PROTEUS TWO-DIMENSIONAL NAVIER-STOKES COMPUTER CODE, VERSION 1.0. VOLUME 2: USER'S GUIDE
Charles E. Towne, John R. Schwab, Thomas J. Benson, and Ambady Suresh (Sverdrup Technology, Inc., Cleveland, OH.) Mar. 1990 110 p
(NASA-TM-102552; E-5367; NAS 1.15:102552) Avail: NTIS HC A06/MF A01 CSCL 20D

A new computer code was developed to solve the two-dimensional or axisymmetric, Reynolds averaged, unsteady compressible Navier-Stokes equations in strong conservation law

form. The thin-layer or Euler equations may also be solved. Turbulence is modeled using an algebraic eddy viscosity model. The objective was to develop a code for aerospace applications that is easy to use and easy to modify. Code readability, modularity, and documentation were emphasized. The equations are written in nonorthogonal body-fitted coordinates, and solved by marching in time using a fully-coupled alternating direction-implicit procedure with generalized first- or second-order time differencing. All terms are linearized using second-order Taylor series. The boundary conditions are treated implicitly, and may be steady, unsteady, or spatially periodic. Simple Cartesian or polar grids may be generated internally by the program. More complex geometries require an externally generated computational coordinate system. The documentation is divided into three volumes. Volume 2 is the User's Guide, and describes the program's general features, the input and output, the procedure for setting up initial conditions, the computer resource requirements, the diagnostic messages that may be generated, the job control language used to run the program, and several test cases. Author

N90-21307*# National Aeronautics and Space Administration. Lewis Research Center, Cleveland, OH.

PROTEUS TWO-DIMENSIONAL NAVIER-STOKES COMPUTER CODE, VERSION 1.0. VOLUME 3: PROGRAMMER'S REFERENCE

Charles E. Towne, John R. Schwab, Thomas J. Benson, and Ambady Suresh (Sverdrup Technology, Inc., Cleveland, OH.) Mar. 1990 249 p

(NASA-TM-102553; E-5368; NAS 1.15:102553) Avail: NTIS HC A11/MF A02 CSCL 20D

A new computer code was developed to solve the 2-D or axisymmetric, Reynolds-averaged, unsteady compressible Navier-Stokes equations in strong conservation law form. The thin-layer or Euler equations may also be solved. Turbulence is modeled using an algebraic eddy viscosity model. The objective was to develop a code for aerospace applications that is easy to use and easy to modify. Code readability, modularity, and documentation were emphasized. The equations are written in nonorthogonal body-fitted coordinates, and solved by marching in time using a fully-coupled alternating-direction-implicit procedure with generalized first- or second-order time differencing. All terms are linearized using second-order Taylor series. The boundary conditions are treated implicitly, and may be steady, unsteady, or spatially periodic. Simple Cartesian or polar grids may be generated internally by the program. More complex geometries require an externally generated computational coordinate system. The documentation is divided into three volumes. Volume 3 is the Programmer's Reference, and describes the program structure, the FORTRAN variables stored in common blocks, and the details of each subprogram. Author

N90-21308# Queensland Univ., Brisbane (Australia). Dept. of Civil Engineering.

DEPTH-AVERAGED EQUATIONS FOR TURBULENT FREE-SURFACE FLOW

D. A. Paterson and C. J. Apelt Dec. 1988 49 p

(PB90-164781; RR-CE100; ISBN-0-86776-323-X) Avail: NTIS HC A03/MF A01 CSCL 20D

Depth-averaged equations were derived for the calculation of turbulent free-surface flows under the action of gravity. The turbulence model used is the large Reynolds number version of the kappa-epsilon model of turbulence. Nearly complete equations are first derived and it is concluded that approximations of some sort are required before they can be solved. Four approximations are introduced; none of these is as crude as approximations often used. It is not, for example, assumed that the bed slope or the slope of the water surface is negligible and so these equations will apply in steep channels and in flows with rapid changes in cross section. Author

N90-21309# Technische Hogeschool, Delft (Netherlands). Dept. of Aerospace Engineering.

NOTES ON THE UNSTEADY RECTILINEAR MOTION OF A PERFECT GAS. PART 8: GENERAL THEORY AND GENERAL WAVES IN A HOMENTROPIC GAS

J. A. Steketee Jan. 1989 43 p

(PB90-167149; LR-575-Pt-8) Avail: NTIS HC A03/MF A01 CSCL 20D

Some classical theory is collected and some results are presented on the unsteady rectilinear flow of a perfect gas. Some general theory is reviewed including the characteristic equations and homentropic flows are considered including the homentropic simple waves. The unusual feature of the presentation is that the Lagrangian variables is used throughout. The homentropic general waves are considered. A detailed discussion is presented of the general solutions of the Euler-Poisson-Darboux equations which occur. Author

N90-21310# Technische Hogeschool, Delft (Netherlands). Dept. of Aerospace Engineering.

THE MODELLING OF HEAT AND MASS TRANSFER NEAR SOLID BOUNDARIES AND COMPARISON WITH EXPERIMENTAL RESULTS

P. J. M. Elands Nov. 1988 104 p Prepared in cooperation with Prins Maurits Lab. TNO, Rijswijk (Netherlands)

(PB90-167040; SFCC/Pub-54; LR-567; PML-1988-C159) Avail: NTIS HC A06/MF A01 CSCL 20D

The modelling of heat and mass transfer processes occurring in solid fuel combustion chambers, and the incorporation of these processes in the COPPEF (Computer Program for Parabolic and Elliptic Flows) computer code is discussed. After a general description of the COPPEF computer code, the calculation of the flow in the vicinity of a solid wall is discussed. Special attention is given to the incorporation of solid wall boundary conditions in the equations describing turbulence. Numerical tests with COPPEF and a comparison of computational and experimental data are also discussed. Author

N90-21311# Case Western Reserve Univ., Cleveland, OH. Dept. of Mechanical and Aerospace Engineering.

LASER VELOCIMETER MEASUREMENTS OF MULTIPHASE FLOW OF SOLIDS Final Report, Sep. 1986 - Apr. 1989

J. R. Kadambi, R. C. Chen, and S. Bhunia 1989 114 p

(Contract DE-FG22-86PC-90961)

(DE90-007604; DOE/PC-90961/T9) Avail: NTIS HC A06/MF A01

A unique refractive index matched facility for studying solid-liquid multiphase flow has been developed. The refractive index matching of the solid and the liquid allows the use of non-intrusive Laser Doppler Velocimetry (LDV) to measure the solid and the liquid velocities. These measurements will be useful in developing a better understanding of solid-liquid flows, especially solid-liquid and solid-solid interactions. Silica gel and 50 percent sodium iodide solution in water (refractive index approx. 1.443) are used as the refractive index matched solid and liquid respectively. A two color back scatter mode LDV is used for making velocity measurements. Tests were conducted in solid-liquid slurries with volumetric solid concentration levels of 5 percent and 15 percent in the Reynolds number (Re) range of 400 to 9200. Silica gel particles of mean diameter 40 microns were used. Measurements included mapping of the solid and liquid velocities and obtaining the pressure drop data. Signal processing technique utilizing histogram of velocity measurements made at a point and signal amplitude discrimination was successfully used for differentiating between solid and liquid velocities. DOE

N90-21312# Texas Univ., Austin. Inst. for Fusion Studies.

THE EFFECT OF VISCOSITY ON THE RESISTIVE TEARING MODE WITH THE PRESENCE OF SHEAR FLOW

X. L. Chen and P. J. Morrison Jan. 1990 15 p

(Contract DE-FG05-80ET-53088)

(DE90-009340; DOE/ET-53088/414; IFSR-414) Avail: NTIS HC A03/MF A01

The effect of small isotropic viscosity on the constant psi tearing mode in the presence of shear flow, is analyzed by the boundary layer approach. It is found that the influence of viscosity depends upon the parameter (G'(0)/F'(0)), where G'(0) and F'(0) denote that shear and magnetic field shear at the magnetic null plane, respectively. When the absolute value of G'(0)/F'(0) is much less than 1, the tearing mode growth rate is suppressed by the viscosity, but not completely stabilized. When the absolute value of G'(0)/F'(0) is approximately in the order of O(1) and the viscosity is comparable with the resistivity, the growth rate vanishes as (1 - G'(0) squared/F'(0) squared) (sup 1/3), when G'(0) squared yields F'(0) squared from below. In the case where 1 - G'(0) squared/F'(0) squared is less than 0 matching cannot be achieved. DOE

N90-20999# Arnold Engineering Development Center, Arnold Air Force Station, TN.
OPTIMIZATION OF AERODYNAMIC DESIGNS USING COMPUTATIONAL FLUID DYNAMICS
D. H. Huddleston and C. W. Mastin (Mississippi State Univ., Mississippi State.) *In* AGARD, Computational Methods for Aerodynamic Design (Inverse) and Optimization Mar. 1990 10 p Prepared in cooperation with Sverdrup Technology, Inc., Arnold AFS, TN (For primary document see N90-20976 14-05)
Copyright Avail: NTIS HC A15/MF A02; Non-NATO Nationals requests available only from AGARD/Scientific Publications Executive

N90-21030# Rolls-Royce Ltd., Derby (England).
DETAILED HEAT TRANSFER MEASUREMENTS IN NOZZLE GUIDE VANE PASSAGES IN LINEAR AND ANNULAR CASCADES IN THE PRESENCE OF SECONDARY FLOWS
N. W. Harvey, Z. Wang, P. T. Ireland, and T. V. Jones (Oxford Univ., England) *In* AGARD, Secondary Flows in Turbomachines Feb. 1990 13 p Sponsored in part by the Ministry of Defence and Rolls-Royce Plc., England (For primary document see N90-21009 14-07)
Copyright Avail: NTIS HC A15/MF A02; Non-NATO Nationals requests available only from AGARD/Scientific Publications Executive

N90-21031# Virginia Polytechnic Inst. and State Univ., Blacksburg. Dept. of Mechanical Engineering.
EFFECTS OF SECONDARY FLOW ON HEAT TRANSFER IN ROTATING PASSAGES
Joan G. Moore and John Moore *In* AGARD, Secondary Flows in Turbomachines Feb. 1990 13 p Sponsored by Rolls-Royce Plc. (For primary document see N90-21009 14-07)
Copyright Avail: NTIS HC A15/MF A02; Non-NATO Nationals requests available only from AGARD/Scientific Publications Executive

N90-21032# Office National d'Etudes et de Recherches Aerospatiales, Paris (France).
THEORETICAL STUDY OF THE FLOW IN A ROTATING CHANNEL. EXPERIMENTAL STUDY THROUGH FLOW VISUALIZATION IN A CURVED CHANNEL
Joel Guidez, Pierre-Jacques Michard, and Denis Dutoya *In* AGARD, Secondary Flows in Turbomachines Feb. 1990 14 p Sponsored by Direction des Recherches et Etudes Techniques (For primary document see N90-21009 14-07)
Copyright Avail: NTIS HC A15/MF A02; Non-NATO Nationals requests available only from AGARD/Scientific Publications Executive

35 INSTRUMENTATION AND PHOTOGRAPHY

Includes remote sensors; measuring instruments and gages; detectors; cameras and photographic supplies; and holography.

For aerial photography see *43 Earth Resources and Remote Sensing.* For related information see also *06 Aircraft Instrumentation,* and *19 Spacecraft Instrumentation.*

N90-21313*# National Aeronautics and Space Administration. Ames Research Center, Moffett Field, CA.
PROCEEDINGS OF THE THIRD INFRARED DETECTOR TECHNOLOGY WORKSHOP
Craig R. McCreight, comp. Oct. 1989 459 p Workshop held at Moffett Field, CA, 7-9 Feb. 1989
(NASA-TM-102209; A-89200; NAS 1.15:102209) Avail: NTIS HC A20/MF A03 CSCL 14B

This volume consists of 37 papers which summarize results presented at the Third Infrared Detector Technology Workshop, held February 7-9, 1989, at Ames Research Center. The workshop focused on infrared (IR) detector, detector array, and cryogenic electronic technologies relevant to low-background space astronomy. Papers on discrete IR detectors, cryogenic readouts, extrinsic and intrinsic IR arrays, and recent results from ground-based observations with integrated arrays were given. Recent developments in the second-generation Hubble Space Telescope (HST) infrared spectrometer and in detectors and arrays for the European Space Agency's Infrared Space Observatory (ISO) are also included, as are status reports on the Space Infrared Telescope Facility (SIRTF) and the Stratospheric Observatory for Infrared Astronomy (SOFIA) projects. For individual titles, see N90-21314 through N90-21350.

N90-21314*# Arizona Univ., Tucson.
REQUIREMENTS OF IR SPACE ASTRONOMY **c89**
Frank J. Low *In* NASA, Ames Research Center, Proceedings of the Third Infrared Detector Technology Workshop Oct. 1989 p 1-4 (For primary document see N90-21313 14-35)
Avail: NTIS HC A20/MF A03 CSCL 03A

An introduction to a series of infrared detector technology workshops is given. The establishment of goals and new requirements is addressed in a general way. The Shuttle Infrared telescope Facility (SIRIF) goals are listed. Given that the wavelength coverage is established at 2 to 750 microns and the unvignetted field of view is 7 arcmin, the field should be fully utilized at each wavelength, diffraction should be critically sampled, and each detector should be background limited. Author

N90-21315*# California Univ., Berkeley. Lawrence Berkeley Lab.
STRESSED Ge:Ga PHOTOCONDUCTORS FOR SPACE-BASED ASTRONOMY. (IS THERE LIFE BEYOND 120 MICRON)
J. W. Beeman, E. E. Haller, W. L. Hansen, P. N. Luke, and P. L. Richards (California Univ., Berkeley.) *In* NASA, Ames Research Center, Proceedings of the Third Infrared Detector Technology Workshop Oct. 1989 p 5-2 (For primary document see N90-21313 14-35)
Avail: NTIS HC A20/MF A03 CSCL 14B

Information is given in viewgraph form. Information is given on the characteristics of stressed Ge:Ga, a spring type stress cavity, mounting hardware, materials parameters affecting dark current, and the behavior of low dark current stressed Ge:Ga. It is concluded that detectors exist today for background-limited detection at 200 microns, that researchers are narrowing in on the significant parameters that effect dark current in stressed photoconductors, that these findings may be applied to other photoconductor materials, and that some creative problem solving for an ionizing effect reset mechanism is needed. Author

N90-21316*# California Univ., Los Angeles. Dept. of Materials Science and Engineering.
NEAR CONTACT PHENOMENA AND TRANSIENT EFFECTS IN FAR INFRARED PHOTOCONDUCTORS
Nancy M. Haegel *In* NASA, Ames Research Center, Proceedings of the Third Infrared Detector Technology Workshop, Oct. 1989 p 25-34 Sponsored in part by the David and Lucile Packard Foundation (For primary document see N90-21313 14-35)
(Grant NSF DMR-88-09298)
Avail: NTIS HC A20/MF A03 CSCL 14B

A combination of experimental and modeling work is summarized in two areas: first, the calculation of excess free carrier and space charge distributions near contacts and their effects on device resistivity, and second, the characterization of a slow transient response (tau approx. 1 sec) in Ge:Be detectors which is due to trapping associated with Be(+) formation. In both cases, analytical models, based on continuity and rate equations, have been developed to enable the application of these findings to a wide variety of photoconductor materials. Author

N90-21317*# California Univ., Berkeley. Dept. of Physics.
A 100 MICRO KELVIN BOLOMETER SYSTEM FOR SIRTF
G. M. Bernstein, P. T. Timbie, and P. L. Richards *In* NASA, Ames Research Center, Proceedings of the Third Infrared Detector Technology Workshop Oct. 1989 p 35-44 (For primary document see N90-21313 14-35)
(Contract NAS2-12578)
Avail: NTIS HC A20/MF A03 CSCL 14B

Progress toward a prototype of 100 mK bolometric detection system for the Space Infrared Telescope Facility (SIRTF) is described. Two adiabatic demagnetization refrigerators (ADR's) were constructed and used to investigate the capabilities necessary for orbital operation. The first, a laboratory ADR, demonstrated a hold time at 0.1 K of over 12 hours, with temperature stability approx. 3 micro-K RMS achieved by controlling the magnetic field. A durable salt pill and an efficient support system have been demonstrated. A second ADR, the SIRTF flight prototype, has been built and will be flown on a balloon. Techniques for magnetic shielding, low heat leak current leads, and a mechanical heat switch are being developed in this ADR. Plans for construction of 100 mK bolometers are discussed. Three important cosmological investigations which will be carried out by these longest wavelength SIRTF detectors are described. Author

N90-21318*# National Aeronautics and Space Administration. Ames Research Center, Moffett Field, CA.
A PROGRESS REPORT ON USING BOLOMETERS COOLED BY ADIABATIC DEMAGNETIZATION REFRIGERATION
L. Lesyna, T. Roellig, M. Savage (Sterling Software, Moffett Field, CA.), and Michael W. Werner *In its* Proceedings of the Third Infrared Detector Technology Workshop Oct. 1989 p 45-57 (For primary document see N90-21313 14-35)
Avail: NTIS HC A20/MF A03 CSCL 14B

For sensitive detection of astronomical continuum radiation in the 200 micron to 3 mm wavelength range, bolometers are presently the detectors of choice. In order to approach the limits imposed by photon noise in a cryogenically cooled telescope in space, bolometers must be operated at temperatures near 0.1 K. Researchers report progress in building and using bolometers that operate at these temperatures. The most sensitive bolometer had an estimated noise equivalent power (NEP) of 7 x 10(exp 017) W Hz(exp -1/2). Researchers also briefly discuss the durability of paramagnetic salts used to cool the bolometers. Author

N90-21319*# Rockwell International Science Center, Anaheim, CA.
THE SOLID STATE PHOTOMULTIPLIER: STATUS OF PHOTON COUNTING BEYOND THE NEAR-INFRARED
K. M. Hays, R. A. LaViolette, M. G. Stapelbroek, and M. D. Petroff *In* NASA, Ames Research Center, Proceedings of the Third Infrared Detector Technology Workshop Oct. 1989 p 59-80 (For primary document see N90-21313 14-35)
Avail: NTIS HC A20/MF A03 CSCL 14B

Rockwell International's Solid State Photomultiplier (SSPM) is an impurity-band avalanche device which can count individual photons with wavelengths between 0.4 and 28 micrometers. Its response to a photon is a pulse of between 10(exp 4) and 10(exp 5) conduction electrons, making it an important device for use in phenomenology. The characteristics of the SSPM make it a potentially important device for use in astronomical applications. Contract NAS2-12400 was initiated in June 1986 to conduct modeling and characterization studies of the SSPM to provide a basis for assessing its use in astronomical systems. Some SSPM models and results of measurements which characterize the group of SSPMs recently fabricated on this contract are discussed.
Author

N90-21320*# Arizona Univ., Tucson. Steward Observatory.
THE POTENTIAL FOR HIGH PERFORMANCE HgCdTe ARRAYS AT 4 MICRONS
G. H. Rieke, M. A. Sarfaraz, Marcia J. Rieke, and Erick T. Young *In* NASA, Ames Research Center, Proceedings of the Third Infrared Detector Technology Workshop Oct. 1989 p 81-84 Sponsored by NASA (For primary document see N90-21313 14-35)
Avail: NTIS HC A20/MF A03 CSCL 14B

The potential of existing technology at Rockwell International in terms of the goals for astronomical detector arrays in the 3 to 5 micron interval is evaluated. Measurements have been obtained for a number of samples of HgCdTe diodes manufactured by Rockwell International. All the diodes reported on here had cutoff wavelengths at high temperatures of 4.6 to 4.7 microns. Although no confirming measurements were made, the cutoff wavelength is expected to move to 5 microns or beyond at the low temperatures of our tests. Diode sizes ranged from 20 to 150 microns. The test program yielded full diode curves and relative response at 3.4 microns for the sample diodes as a function of temperature. Dark currents are quoted below as the current passing through the diode with a back bias of 50 mV. The various diode types showed a wide range of behavior, both with regard to dark current and responsibility. The test results for one of the best diode types are illustrated. This detector has a size of 148 microns and a cutoff wavelength of 4.61 microns. Author

N90-21321*# California Univ., Berkeley.
GERMANIUM BLOCKED IMPURITY BAND (BIB) DETECTORS
E. E. Haller, H. Baumann, J. W. Beeman, W. L. Hansen, P. N. Luke (California Univ., Berkeley. Lawrence Berkeley Lab.), M. Lutz, C. S. Rossington, and I. C. Wu *In* NASA, Ames Research Center, Proceedings of the Third Infrared Detector Technology Workshop Oct. 1989 p 85-115 (For primary document see N90-21313 14-35)
Avail: NTIS HC A20/MF A03 CSCL 14B

Information is given in viewgraph form. The advantages of the Si blocked impurity band (BIB) detector invented by M. D. Petroff and M. G. Stabelbroek are noted: smaller detection volume leading to a reduction of cosmic ray interference, extended wavelength response because of dopant wavefunction overlap, and photoconductive gain of unity. It is argued that the stated advantages of Si BIB detectors should be realizable for Ge BIB detectors. Information is given on detector development, subtrate choice and preparation, wafer polising, epitaxy, characterization of epi layers, and preliminary Ge BIB detector test results. Author

N90-21322*# Jet Propulsion Lab., California Inst. of Tech., Pasadena.
EXTRINSIC GERMANIUM BLOCKED IMPURITY BANK (BIB) DETECTORS
Timothy N. Krabach, James E. Huffman, and Dan M. Watson (Rochester Univ., NY.) *In* NASA, Ames Research Center, Proceedings of the Third Infrared Detector Technology Workshop Oct. 1989 p 117-123 (For primary document see N90-21313 14-35)
Avail: NTIS HC A20/MF A03 CSCL 14B

Ge:Ga blocked-impurity-band (BIB) detectors with long wavelength thresholds greater than 190 microns and peak quantum efficiencies of 4 percent, at an operating temperature of 1.8 K,

have been fabricated. These proof of concept devices consist of a high purity germanium blocking layer epitaxially grown on a Ga-doped Ge substrate. This demonstration of BIB behavior in germanium enables the development of far infrared detector arrays similar to the current silicon-based devices. Present efforts are focussed on improving the chemical vapor deposition process used to create the blocking layer and on the lithographic processing required to produce monolithic detector arrays in germanium. Approaches to test the impurity levels in both the blocking and active layers are considered. Author

N90-21323*# Arizona Univ., Tucson. Steward Observatory.
Ga:Ge ARRAY DEVELOPMENT
Erick T. Young, G. H. Rieke, Frank J. Low, E. E. Haller, and J. W. Beeman (California Univ., Berkeley. Lawrence Berkeley Lab.) *In* NASA, Ames Research Center, Proceedings of the Third Infrared Detector Technology Workshop Oct. 1989 p 125-133 (For primary document see N90-21313 14-35)
(Contract NASw-3703; NAGw-1285)
Avail: NTIS HC A20/MF A03 CSCL 14B

Work at the University of Arizona and at Lawrence Berkeley Laboratory on the development of a far infrared array camera for the Multiband Imaging Photometer on the Space Infrared Telescope Facility (SIRTF) is discussed. The camera design uses stacked linear arrays of Ge:Ga photoconductors to make a full two-dimensional array. Initial results from a 1 x 16 array using a thermally isolated J-FET readout are presented. Dark currents below 300 electrons s(exp -1) and readout noises of 60 electrons were attained. Operation of these types of detectors in an ionizing radiation environment are discussed. Results of radiation testing using both low energy gamma rays and protons are given. Work on advanced C-MOS cascode readouts that promise lower temperature operation and higher levels of performance than the current J-FET based devices is described. Author

N90-21324*# Amber Engineering Co., Santa Barbara, CA.
COMMON SOURCE CASCODE AMPLIFIERS FOR INTEGRATING IR-FPA APPLICATIONS
James T. Woolaway and Erick T. Young (Arizona Univ., Tucson.) *In* NASA, Ames Research Center, Proceedings of the Third Infrared Detector Technology Workshop Oct. 1989 p 135-146 (For primary document see N90-21313 14-35)
(Contract NAS2-12578)
Avail: NTIS HC A20/MF A03 CSCL 14B

Space based astronomical infrared measurements present stringent performance requirements on the infrared detector arrays and their associated readout circuitry. To evaluate the usefulness of commercial CMOS technology for astronomical readout applications a theoretical and experimental evaluation was performed on source follower and common-source cascode integrating amplifiers. Theoretical analysis indicates that for conditions where the input amplifier integration capacitance is limited by the detectors capacitance the input referred rms noise electrons of each amplifier should be equivalent. For conditions of input gate limited capacitance the source follower should provide lower noise. Measurements of test circuits containing both source follower and common source cascode circuits showed substantially lower input referred noise for the common-source cascode input circuits. Noise measurements yielded 4.8 input referred rms noise electrons for an 8.5 minute integration. The signal and noise gain of the common-source cascode amplifier appears to offer substantial advantages in acheiving predicted noise levels. Author

N90-21325*# Santa Barbara Research Center, Goleta, CA.
STUDY OF ADVANCED InSb ARRAYS FOR SIRTF (SPACE INFRARED TELESCOPE FACILITY)
Alan Hoffman and Robert Feitt *In* NASA, Ames Research Center, Proceedings of the Third Infrared Detector Technology Workshop Oct. 1989 p 147-156 (For primary document see N90-21313 14-35)
Avail: NTIS HC A20/MF A03 CSCL 14B

The Santa Barbara Research Center has completed a study leading to the development of advanced Indium Antimonide detector arrays for the Space Infrared Telescope Facility (SIRTF) Focal Plane Array Detector (FPAD) Subsystem of the Infrared Array Camera (IRAC) Band 1. The overall goal of the study was to perform design tradeoff studies, analysis and research to develop a Direct Readout Integrated Circuit to be hybridized to an advanced, high performance InSb detector array that would satisfy the technical requirements for Band 1 as specified in the IRAC Instrument Requirements Document (IRD), IRAC-202. The overall goal of the study was divided into both a near-term goal and a far-term goal. The near-term goal identifies current technology available that approaches, and in some cases meets the program technological goals as specified in IRAC-202. The far-term goal identifies technology development required to completely achieve SIRTF program goals. Analyses of potential detector materials indicates that InSb presently meets all Band 1 requirements and is considered to be the baseline approach due to technical maturity. The major issue with regard to photovoltaic detectors such as InSb and HgCdTe is to achieve a reduction in detector capacitance. Author

N90-21326*# Rochester Univ., NY. Dept. of Physics and Astronomy.
InSb DRO ARRAY CHARACTERISTICS
W. J. Forrest, J. L. Pipher, Z. Ninkov, and J. D. Garnett *In* NASA, Ames Research Center, Proceedings of the Third Infrared Detector Technology Workshop Oct. 1989 p 157-182 (For primary document see N90-21313 14-35)
Avail: NTIS HC A20/MF A03 CSCL 14B

Researchers tested 58 x 62 low-doped InSb diode arrays bonded to MOSFET readouts for their performance potential in a low background space environment. Of primary concern were the quantum efficiency, dark current and read noise. The quantum efficiency (45 percent at 3.3 microns) and dark current (less than 2.4e(-)/s) were found to be adequate for the Space Infrared Telescope Facility (SIRTF) experiments, while the read noise (200 e(-) RMS) was found to be wanting. More subtle concerns, such as image quality, linearity/calibratibility and flat fielding were also investigated. In these respects the arrays appear to be well suited for the high sensitivity, photometric accuracy, and image clarity demanded by the SIRTF experiments. Author

N90-21327*# Joint Astronomy Centre, Hilo, HI.
EXPERIENCE WITH THE UKIRT InSb ARRAY CAMERA
Ian S. McLean, Mark M. Casali, Gillian S. Wright, and Colin Aspin *In* NASA, Ames Research Center, Proceedings of the Third Infrared Detector Technology Workshop Oct. 1989 p 183-200 Original contains color illustrations (For primary document see N90-21313 14-35)
Avail: NTIS HC A20/MF A03 CSCL 14B

The cryogenic infrared camera, IRCAM, has been operating routinely on the 3.8 m UK Infrared Telescope on Mauna Kea, Hawaii for over two years. The camera, which uses a 62x58 element Indium Antimonide array from Santa Barbara Research Center, was designed and built at the Royal Observatory, Edinburgh which operates UKIRT on behalf of the UK Science and Engineering Research Council. Over the past two years at least 60% of the available time on UKIRT has been allocated for IRCAM observations. Described here are some of the properties of this instrument and its detector which influence astronomical performance. Observational techniques and the power of IR arrays with some recent astronomical results are discussed. Author

N90-21328*# National Aeronautics and Space Administration. Goddard Space Flight Center, Greenbelt, MD.
REDUCTION AND ANALYSIS TECHNIQUES FOR INFRARED IMAGING DATA
Mark McCaughrean *In* NASA, Ames Research Center, Proceedings of the Third Infrared Detector Technology Workshop Oct. 1989 p 201-219 (For primary document see N90-21313 14-35)
Avail: NTIS HC A20/MF A03 CSCL 14B

Infrared detector arrays are becoming increasingly available to

the astronomy community, with a number of array cameras already in use at national observatories, and others under development at many institutions. As the detector technology and imaging instruments grow more sophisticated, more attention is focussed on the business of turning raw data into scientifically significant information. Turning pictures into papers, or equivalently, astronomy into astrophysics, both accurately and efficiently, is discussed. Also discussed are some of the factors that can be considered at each of three major stages; acquisition, reduction, and analysis, concentrating in particular on several of the questions most relevant to the techniques currently applied to near infrared imaging. Author

N90-21329*# Rochester Univ., NY.
DISCOVERY OF LOW MASS OBJECTS IN TAURUS **c89**
W. J. Forrest, Z. Ninkov, J. D. Garnett, M. F. Skrutskie, and M. Shure (Hawaii Univ., Honolulu.) *In* NASA, Ames Research Center, Proceedings of the Third Infrared Detector Technology Workshop Oct. 1989 p 221-230 (For primary document see N90-21313 14-35)
Avail: NTIS HC A20/MF A03 CSCL 03A

In infrared (2.2 micron, K-band) search of small regions (25 in square) near 26 members of the Taurus star-forming association has revealed 20 dim (K = 13-16 mag) stellar objects near 13 of them. Of these 20 objects, 9 are exceptionally red. It is argued that these 9 are probably also Taurus members. From the luminosities (0.4 to 4 times 10 the -3 power luminosity) and ages (estimated at 10(exp 6) years), masses can be determined by reference to theoretical low-mass cooling curves. The masses are in the range 0.005 to 0.015 solar mass, i.e., low-mass brown dwarfs. Proper motion studies of 7 of the objects visible on the POSS plates conducted by Burton Jones establish that 4 are highly probable Taurus members while 1 is a possible member. Author

N90-21330*# National Aeronautics and Space Administration. Ames Research Center, Moffett Field, CA.
HIGH RESOLUTION IMAGING OF THE VENUS NIGHT SIDE USING A ROCKWELL 128X128 HgCdTe ARRAY **c89**
K.-W. Hodapp, W. Sinton, B. Ragent, and D. Allen (Anglo-Australian Observatory, Epping.) *In its* Proceedings of the Third Infrared Detector Technology Workshop Oct. 1989 p 231-235 (For primary document see N90-21313 14-35)
Avail: NTIS HC A20/MF A03 CSCL 03A

The University of Hawaii operates an infrared camera with a 128x128 HgCdTe detector array on loan from JPL's High Resolution Imaging Spectrometer (HIRIS) project. The characteristics of this camera system are discussed. The infrared camera was used to obtain images of the night side of Venus prior to and after inferior conjunction in 1988. The images confirm Allen and Crawford's (1984) discovery of bright features on the dark hemisphere of Venus visible in the H and K bands. Our images of these features are the best obtained to date. Researchers derive a pseudo rotation period of 6.5 days for these features and 1.74 microns brightness temperatures between 425 K and 480 K. The features are produced by nonuniform absorption in the middle cloud layer (47 to 57 Km altitude) of thermal radiation from the lower Venus atmosphere (20 to 30 Km altitude). A more detailed analysis of the data is in progress. Author

N90-21331*# National Optical Astronomy Lab. Tucson, AZ.
INFRARED GROUND-BASED ASTRONOMY WITH THE HUGHES 256 X 256 PtSi ARRAY **c89**
A. Fowler, R. Joyce, I. Gatley, J. Gates, and J. Herring (Hughes Aircraft Co., Carlsbad, CA.) *In* NASA, Ames Research Center, Proceedings of the Third Infrared Detector Technology Workshop Oct. 1989 p 237-246 Sponsored in part by NSF (For primary document see N90-21313 14-35)
Avail: NTIS HC A20/MF A03 CSCL 03A

It is shown that large format PtSi Schottky diode infrared arrays, the Hughes 256 X 256 hybrid Schottky array in particular, are competitive alternatives to the smaller format photovoltaic arrays for ground-based astronomy. The modest quantum efficiency of the PtSi compared to the photovoltaic devices is more than compensated for by the larger format. The use of hybrid technology yields effective fill factors of nearly 100 percent, and the low dark current, noise, excellent imaging characteristics, cost, and solid nitrogen operating temperature add to the effectiveness of this array for ground-based imaging. In addition to discussing the characteristics of this array, researchers present laboratory test data and astronomical results achieved at Kitt Peak. Author

N90-21332*# California Univ., Berkeley.
STRESSED DETECTOR ARRAYS FOR AIRBORNE ASTRONOMY **c89**
G. J. Stacey, J. W. Beeman, E. E. Haller, N. Geis, A. Poglitsch, and M. Rumitz (Max-Planck-Inst. fuer Physik und Astrophysik, Garching, Germany, F.R.) *In* NASA, Ames Research Center, Proceedings of the Third Infrared Detector Technology Workshop Oct. 1989 p 247-258 (For primary document see N90-21313 14-35)
Avail: NTIS HC A20/MF A03 CSCL 03A

The development of stressed Ge:Ga detector arrays for far-infrared astronomy from the Kuiper Airborne Observatory (KAO) is discussed. Researchers successfully constructed and used a three channel detector array on five flights from the KAO, and have conducted laboratory tests of a two-dimensional, 25 elements (5x5) detector array. Each element of the three element array performs as well as the researchers' best single channel detector, as do the tested elements of the 25 channel system. Some of the exciting new science possible with far-infrared detector arrays is also discussed. Author

N90-21333*# Air Force Geophysics Lab., Hanscom AFB, MA.
AFGL TEN MICRON MOSAIC ARRAY SPECTROMETER: RECENT RESULTS
Paul D. LeVan *In* NASA, Ames Research Center, Proceedings of the Third Infrared Detector Technology Workshop Oct. 1989 p 259-265 (For primary document see N90-21313 14-35)
Avail: NTIS HC A20/MF A03 CSCL 14B

Recent measurements were made with a novel mosaic array prism spectrometer on long period variable stars of carbon and oxygen-rich atmospheres. These stars have generally large IR excesses and show strong SiC and silicate emission features, respectively. A comparison is provided by published spectra obtained with the IRAS Low Resolution Spectrometer. Emission feature equivalent widths are independent of the absolute photometric level of the spectra and provide information on the relative variation of the feature and continuum fluxes between the epochs of the space and groundbased observations. Author

N90-21334*# National Aeronautics and Space Administration. Goddard Space Flight Center, Greenbelt, MD.
INITIAL ASTRONOMICAL RESULTS WITH A NEW 5-14 MICRON Si:Ga 58X62 DRO ARRAY CAMERA
Dan Gezari, Walter Folz, and Larry Woods *In* NASA, Ames Research Center, Proceedings of the Third Infrared Detector Technology Workshop Oct. 1989 p 267-282 (For primary document see N90-21313 14-35)
Avail: NTIS HC A20/MF A03 CSCL 14B

A new array camera system was developed using a 58 x 62 pixel Si:Ga (gallium doped silicon) DRO (direct readout) photoconductor array detector manufactured by Hughes/Santa Barbara Research Center (SBRC). The camera system is a broad band photometer designed for 5 to 14 micron imaging with large ground-based optical telescopes. In a typical application a 10 micron photon flux of about 10(exp 9) photons sec(exp -1) m(exp -2) microns(exp -1) arcsec(exp -2) is incident in the telescope focal plane, while the detector well capacity of these arrays is 10(exp 5) to 10 (exp 6) electrons. However, when the real efficiencies and operating conditions are accounted for, the 2-channel 3596 pixel array operates with about 1/2 full wells at 10 micron and 10% bandwidth with high duty cycle and no real experimental compromises. Author

N90-21335*# Texas Univ., Austin.
PRELIMINARY RESULTS ON TWO-DIMENSIONAL INTERFEROMETRY OF HL Tau **c89**
Eric V. Tollestrup and Paul M. Harvey *In* NASA, Ames Research Center, Proceedings of the Third Infrared Detector Technology Workshop Oct. 1989 p 283-293 (For primary document see N90-21313 14-35)
Avail: NTIS HC A20/MF A03 CSCL 03A

Preliminary two-dimensional speckle interferometry results of HL Tau were found to be qualitatively similar to those found with one-dimensional slit scanning techniques; results consist of a resolved component (approximately 0.7 arcsec in size) and an unresolved component. Researchers are currently reducing the rest of the data (taken on three different telescopes and at three different wavelengths) and are also exploring other high resolution methods like the shift and add technique and selecting only the very best images for processing. The availability of even better two-dimensional arrays within the next couple of years promises to make speckle interferometry and other high resolution techniques very powerful and exiting tools for probing a variety of objects in the subarcsec regime. Author

N90-21336*# Honeywell Electro-Optics Center, Lexington, MA.
SHORT WAVELENGTH HgCdTe STARING FOCAL PLANE FOR LOW BACKGROUND ASTRONOMY APPLICATIONS **c89**
D. Hall (Hawaii Univ., Honolulu.), J. Stobie, N. Hartle, D. Lacroix, and K. Maschhoff *In* NASA, Ames Research Center, Proceedings of the Third Infrared Detector Technology Workshop Oct. 1989 p 295-310 (For primary document see N90-21313 14-35)
(Contract JPL-958095)
Avail: NTIS HC A20/MF A03 CSCL 03A

The design of a 128x128 staring short wave infrared (SWIR) HgCdTe focal plane incorporating charge integrating trans-impedance input preamplifiers is presented. The preamplifiers improve device linearity and uniformity, and provide signal gain ahead of the miltiplexer and readout circuitry. Detector's with cutoff wavelength of 2.5 microns and operated at 80 K have demonstrated impedances in excess of 10(exp 16) ohms with 60 percent quantum efficiency. Focal plane performance using a smaller format device is presented which demonstrates the potential of this approach. Although the design is capable of achieving less than 30 rms electrons with todays technology, initial small format devices demonstrated a read noise of 100 rms electrons and were limited by the atypical high noise performance of the silicon process run. Luminescence from the active silicon circuitry in the multiplexer limits the minimum detector current to a few hundred electrons per second. Approaches to eliminate this excessive source of current is presented which should allow the focal plane to achieve detector background limited performance. Author

N90-21337*# Rockwell International Science Center, Thousand Oaks, CA.
LOW NOISE HgCdTe 128 X 128 SWIR FPA FOR HUBBLE SPACE TELESCOPE **c89**
Michael Blessinger, Kadri Vural, William Kleinhans, Marcia J. Rieke, Rodger Thompson, and Robert Rasche (Arizona Univ., Tucson.) *In* NASA, Ames Research Center, Proceedings of the Third Infrared Detector Technology Workshop Oct. 1989 p 311-320 (For primary document see N90-21313 14-35)
Avail: NTIS HC A20/MF A03 CSCL 03A

Large area focal plane arrays of unprecedented performance were developed for use in Near Infrared Camera and Multi-Object Spectrometer (NICMOS), a proposed Hubble Space Telescope refurbishment instrument. These FPAs are 128x128-element, HgCdTe hybrid arrays with a cutoff wavelength of 2.5 microns. The multiplexer consists of a CMOS field effect transistor switch array with a typical mean readout noise of less than 30 electrons. The detectors typically have a mean dark current of less than 10 electrons/s at 77 K, with currents below 2 electrons measured at 60 K (both at 0.5 V reverse bias). The mean quantum efficiency is 40 to 60 percent at 77 K for 1.0 to 2.4 microns. Functional pixel yield is typically greater than 99 percent, and the power consumption is approximately 0.2 mW (during readout only). Author

N90-21338*# Arizona Univ., Tucson. Steward Observatory.
LABORATORY AND TELESCOPE USE OF THE NICMOS2 128 X 128 HgCdTe ARRAY **c89**
Marcia J. Rieke, E. F. Montgomery, G. H. Rieke, Kadri Vural, Michael Blessinger, and William Kleinhans (Valley Oak Semiconductor, Inc., Westlake Village, CA.) *In* NASA, Ames Research Center, Proceedings of the Third Infrared Detector Technology Workship Oct. 1989 p 321-330 (For primary document see N90-21313 14-35)
(Contract NAS5-30008)
Avail: NTIS HC A20/MF A03 CSCL 03A

The second generation of Hubble Space Telescope (HST) instruments will include a near-infrared instrument. This choice has driven the development of near-infrared arrays to larger sizes and lower read noises. Rockwell International has delivered an array for use in the Near Infrared Camera and Multi-Object Spectrometer (NICMOS) instrument; this array has been dubbed NICMOS2. NICMOS2 is a 128x128 array of HgCdTe diodes In-bonded to a switched MOSFET readout. The readout was specifically designed for astronomical use with the HST requirement of low read noise a prime goal. These arrays use detector material which is similar to that used by Rockwell in previous arrays (e.g., HgCdTe produced on a sapphire substrate), but the NICMOS2 devices differ substantially from other 128x128 arrays produced by Rockwell in having a read noise of only 30 electrons when read out using appropriate correlated sampling. NICMOS2 has now been characterized in the laboratory, and it has been used on groundbased telescopes. Author

N90-21339*# Arizona Univ., Tucson. Steward Observatory.
FUTURE DIRECTIONS FOR NICMOS ARRAYS
R. Thompson, Marcia J. Rieke, Erick T. Young, D. McCarthy, Robert Rasche, Michael Blessinger, Kadri Vural, and William Kleinhans (Valley Oak Semiconductor, Inc., Westlake Village, CA.) *In* NASA, Ames Research Center, Proceedings of the Third Infrared Detector Technology Workshop Oct. 1989 p 331-336 (For primary document see N90-21313 14-35)
Avail: NTIS HC A20/MF A03 CSCL 14B

The Near Infrared Camera and Multi-Object Spectrometer (NICMOS) for the Hubble Space Telescope (HST) requires focal plane arrays of 256x256 pixels for both its cameras and its spectrometers. The new arrays, developed by the Rockwell Corporation for NICMOS, have 40 microns pixels of HgCdTe bump bonded to a switched MOSFET readout. Expected read noise and dark current for the arrays at 60 K are 30 e and 1 e/sec. respectively. The basis for these numbers is previous experience with 128x128 arrays. Author

N90-21340*# European Space Agency. European Space Research and Technology Center, ESTEC, Noordwijk (Netherlands). Space Science Dept.
INTRODUCTION TO THE INFRARED SPACE OBSERVATORY (ISO) **c89**
M. F. Kessler and F. Sibille (Observatoire de Lyon, France) *In* NASA, Ames Research Center, Proceedings of the Third Infrared Detector Technology Workshop Oct. 1989 p 337-344 (For primary document see N90-21313 14-35)
Avail: NTIS HC A20/MF A03 CSCL 03A

The Infrared Space Observatory (ISO) is an astronomical satellite, which will operate at infrared wavelengths (2.5 to 200 microns) for a period of at least 18 months. Imaging, spectroscopic, photometric and polarimetric observations will be obtained by four scientific instruments in the focal plane of its 60-cm diameter, cryogenically-cooled telescope. Two-thirds of ISO's observing time will be available to the astronomical community. ISO is a fully approved and funded project of the European Space Agency (ESA) with a foreseen launch date of May 1993. Author

N90-21341*# Space Research Organization Netherlands, Groningen.
DESIGN AND STATUS OF THE DETECTOR BLOCK FOR THE ISO-SWS
W. Luinge, D. A. Beintema, L. Haser, R. Katterloher (Max-Planck-Inst. fuer Extraterrestrische Physik, Garching, Germany, F.R.), and G. Ploeger *In* NASA, Ames Research Center, Proceedings of the Third Infrared Detector Technology Workshop Oct. 1989 p 345-349 (For primary document see N90-21313 14-35)
Avail: NTIS HC A20/MF A03 CSCL 14B

The Short Wave Spectrometer (SWS) is one of the two spectrometers for the Infrared Space Observatory (ISO). It consists of a pair of grating spectrometers and a Fabry-Perot interferometer. Together, the grating spectrometers cover the wavelength range 2.4 to 45 microns, at a resolution between 1000 and 2000. The Fabry-Perot interferometer, in series with one of the grating spectrometers, provides a resolution of about 20,000 at the wavelengths between 15 and 35 microns. The SWS is being built by the Space Research Organization of the Netherlands and the Max Planck Institute for Extraterrestrial Physics in Garching, Germany. The spectrometer has 52 discrete detectors, most of which are bulk detectors. In the design of the spectrometer, the main emphasis is on the sensitivity of the individual channels, rather than on the number of detectors. This was one of the main reasons to select non-destructive read-out circuits, with a separate heated-JFET pre-amplifier for each individual detector. The signals are amplified and filtered in parallel. The engineering tests on the SWS detector block have not yet been completed. The design of the detector block is described and the present problem areas are indicated. Author

N90-21342*# Max-Planck-Inst. fuer Astronomie, Heidelberg (Germany, F.R.).
STATUS OF THE ISOPHOT DETECTOR DEVELOPMENT
J. Wolf, D. Lemke, M. Burgdorf, U. Groezinger, and Ch. Hajduk *In* NASA, Ames Research Center, Proceedings of the Third Infrared Detector Technology Workshop Oct. 1989 p 351-363 (For primary document see N90-21313 14-35)
Avail: NTIS HC A20/MF A03 CSCL 14B

ISOPHOT is one of the four focal plane experiments of the European Space Agency's Infrared Space Observatory (ISO). Scheduled for a 1993 launch, it will operate extrinsic silicon and germanium photoconductors at low temperature and low background during the longer than 18 month mission. These detectors cover the wavelength range from 2.5 to 200 microns and are used as single elements and in arrays. A cryogenic preamplifier was developed to read out a total number of 223 detector pixels. Author

N90-21343*# Centre d'Etude Spatiale des Rayonnements, Toulouse (France).
ISO/LWS: DETECTOR STATUS
C. LeNaour, C. Delettrez, M. Griffin, P. Ade, D. Robinson, and D. Vickers (London Univ., England) *In* NASA, Ames Research Center, Proceedings of the Third Infrared Detector Technology Workshop Oct. 1989 p 365-380 (For primary document see N90-21313 14-35)
Avail: NTIS HC A20/MF A03 CSCL 14B

The aim of the long wavelength spectrometer (LWS) of the Infrared Space Observatory is to perform spectrometry in the wavelength range 45 to 200 microns using two resolution modes. The resolution will be around 200 in the medium resolution mode while it will reach 10(exp 4) in the high resolution mode. The sensitivity of this instrument will be close to 10(exp -18) W/sq. root Hz. A schematic view of the focal plane unit is presented. The detectors divide the wavelength range into ten spectral channels. The spectral range and position of each detector is indicated. Each detector will cover approximately a spectral bandwidth sufficient to allow for a 50 percent redundancy in the case of detector failure. There are three types of detectors. SW1 is a Ge:Be photoconductor covering the 45 to 55 micron region. LW1, SW2, SW3, SW4, SW5 are unstressed Ge:Ga photoconductors which cover the 50 to 120 micron region. LW2, LW3, LW4, LW5 are uniaxially stressed Ge:GA photoconductors covering the range from 100 to 200 microns. The stress applied to each detector will be adjusted in order to get the peak response in the corresponding wavelength range, and to minimize the dark current of the shorter wavelength stressed detectors. Stressed and unstressed detectors are located alternatively in order to receive the first and second order of the diffracted beam. Author

N90-21344*# Observatoire de Lyon (France).
ISO CAMERA ARRAY DEVELOPMENT STATUS
F. Sibille, C. Cesarsky, P. Agnese, and D. Rouan (Observatoire de Paris-Meudon, France) *In* NASA, Ames Research Center, Proceedings of the Third Infrared Detector Technology Workshop Oct. 1989 p 381-385 (For primary document see N90-21313 14-35)
Avail: NTIS HC A20/MF A03 CSCL 14B

A short outline is given of the Infrared Space Observatory Camera (ISOCAM), one of the 4 instruments onboard the Infrared Space Observatory (ISO), with the current status of its two 32x32 arrays, an InSb charge injection device (CID) and a Si:Ga direct read-out (DRO), and the results of the in orbit radiation simulation with gamma ray sources. A tentative technique for the evaluation of the flat fielding accuracy is also proposed. Author

N90-21345*# National Aeronautics and Space Administration. Ames Research Center, Moffett Field, CA.
SIRTF IN HIGH EARTH ORBIT **c85**
Michael W. Werner, Walter F. Brooks, Larry A. Manning, and Peter Eisenhardt (California Univ., Berkeley.) *In its* Proceedings of the Third Infrared Detector Technology Workshop Oct. 1989 p 387-400 (For primary document see N90-21313 14-35)
Avail: NTIS HC A20/MF A03 CSCL 03A

The goals, requirements and operation of the Space Infrared Telescope Facility (SIRTF) are discussed. Emphasis is upon an analysis of the options of high and low earth orbits for the mission. The consensus was that the high earth orbit offers significant scientific and engineering advantages for SIRTF. Author

N90-21346*# National Aeronautics and Space Administration. Ames Research Center, Moffett Field, CA.
SOFIA: STRATOSPHERIC OBSERVATORY FOR INFRARED ASTRONOMY **c89**
E. F. Erickson *In its* Proceedings of the Third Infrared Detector Technology Workshop Oct. 1989 p 401-402 (For primary document see N90-21313 14-35)
Avail: NTIS HC A20/MF A03 CSCL 03A

SOFIA will be a three meter class telescope operating in a Boeing 747, offering astronomers routine access to infrared wavelengths unavailable from the ground, and with the means to observe transient astronomical events from anywhere in the world. The concept is based on 15 years of experience with NASA's Kuiper Airborne Observatory (KAO), which SOFIA will replace in the mid 1990's. SOFIA's wavelength range covers nearly four decades of the electromagnetic spectrum: from the visible, throughout the infrared and submillimeter, to the microwave region. Relative to the KAO, SOFIA will be roughly ten times more sensitive for compact sources, enabling observations of fainter objects and measurements at higher spectral resolution. Also, it will have three times the angular resolving power for wavelengths greater than 30 microns, permitting more detailed imaging at far infrared wavelengths. Author

N90-21347*# National Aeronautics and Space Administration. Ames Research Center, Moffett Field, CA.
LABORATORY CHARACTERIZATION OF DIRECT READOUT Si:Sb AND Si:Ga INFRARED DETECTOR ARRAYS
Mark E. McKelvey, Nicolas N. Moss, R. E. McMurray, Jr., John A. Estrada, John H. Goebel, Craig R. McCreight, Maureen L. Savage, Frank Junga, and Thomas Whittemore (Lockheed Missiles and Space Co., Palo Alto, CA.) *In its* Proceedings of the Third

Infrared Detector Technology Workshop Oct. 1989 p 403-412 (For primary document see N90-21313 14-35)
Avail: NTIS HC A20/MF A03 CSCL 14B

Highlights of recent results obtained at Ames Research Center in performance evaluations of infrared detector arrays are presented. Antimony- and gallium-doped silicon direct readout 58x62 element hybrid devices from Ames' ongoing detector technology development program are described. The observed characteristics meet most of the performance goals specified by the Space Infrared Telescope Facility (SIRTF) instrument teams and compare favorably with the best performance reported for discrete non-integrating extrinsic silicon detectors. Initial results of radiation environment testing are reported, and non-ideal behavior demonstrated by these test devices is discussed. Author

N90-21348*# Rockwell International Science Center, Thousand Oaks, CA.
HgCdTe 256X256 NWIR FPA
Kadri Vural, Michael Blessinger, Jenkon Chen, and William Kleinhans (Valley Oak Semiconductor, Inc., Westlake Village, CA.) *In* NASA, Ames Research Center, Proceedings of the Third Infrared Detector Technology Workshop Oct. 1989 p 413-419 (For primary document see N90-21313 14-35)
Avail: NTIS HC A20/MF A03 CSCL 14B

Researchers developed a HgCdTe 256x256 focal plane array (FPA) which operates in the 1 to 5 micron band. This is presently the largest demonstrated HgCdTe FPA. The detector material is HgCdTe on sapphire (PACE-1 technology) which has a low thermal expansion mismatch with silicon. The multiplexer is a CMOS FET-switch device processed through a commercial silicon foundry. The multiplexer input is direct injection and the charge capacity is about 2 times 10 to the 7th power electrons. The kTC limited read noise is 400 electrons. Researchers demonstrated high background imaging using the device. The broadband quantum efficiency is measured to be 59 percent. Dark currents less than 0.1 pA were measured at 77 K for detectors processed on PACE-1 material with 4.9 microns cutoff. The dark currents decrease as the temperature is lowered, and researchers are presently studying the T less than 77 K characteristics. The interconnect yield is greater than 95 percent. The devices are available for astronomical applications. Author

N90-21349*# Cornell Univ., Ithaca, NY. Dept. of Astronomy.
IMPROVED Si:As BIBIB (BACK-ILLUMINATED BLOCKED-IMPURITY-BAND) HYBRID ARRAYS
T. Herter, N. Rowlands, S. V. W. Beckwith, G. E. Gull, D. B. Reynolds, D. H. Seib, and M. G. Stapelbroek (Rockwell International Science Center, Thousand Oaks, CA.) *In* NASA, Ames Research Center, Proceedings of the Third Infrared Detector Technology Workshop Oct. 1989 p 427-438 (For primary document see N90-21313 14-35)
(Contract NAS2-12524)
Avail: NTIS HC A20/MF A03 CSCL 14B

Results of a program to increase the short wavelength (less than 10 microns) detective quantum efficiency, eta/beta, of Si:As Impurity Band Conduction arrays are presented. The arrays are epitaxially grown Back-Illuminated Blocked (BIB) Impurity-Band (BIBIB) 10x50 detectors bonded to switched-FET multiplexers. It is shown that the 4.7 microns detective quantum efficiency increases proportionately with the thickness of the infrared active layer. A BIB array with a thick active layer, designed for low dark current, exhibits eta/beta = 7 to 9 percent at 4.7 microns for applied bias voltages between 3 and 5 V. The product of quantum efficiency and photoelectric gain, etaG, increases from 0.3 to 2.5 as the voltage increases from 3 to 5 V. Over this voltage range, the dark current increases from 8 to 120 e(-)s(-1) at a device temperature of 4.2 K and is under 70 e(-)s(-1) for all voltages at 2 K. Because of device gain, the effective dark current (equivalent photon rate) is less than 3 e(-)s(-1) under all operating conditions. The effective read noise (equivalent photon noise) is found to be less than 12 electrons under all operating conditions and for integration times between 0.05 and 100 seconds. Author

N90-21350*# Max-Planck-Inst. fuer Astronomie, Heidelberg (Germany, F.R.).
TESTS OF THE ROCKWELL Si:As BACK-ILLUMINATED BLOCKED-IMPURITY BAND (BIBIB) DETECTORS
J. Wolf, U. Groezinger, M. Burgdorf, and A. Salama (European Space Agency. European Space Research and Technology Center, ESTEC, Noordwijk, Netherlands) *In* NASA, Ames Research Center, Proceedings of the Third Infrared Detector Technology Workshop Oct. 1989 p 439-449 (For primary document see N90-21313 14-35)
Avail: NTIS HC A20/MF A03 CSCL 14B

Two arrays of Rockwell's Si:As back-illuminated blocked-impurity-band detectors were tested at the Max-Planck-Institute for Astronomy (MPIA) at low background and low temperature for possible use in the astronomical space experiment IOSPHOT. For these measurements special test equipment was put together. A cryostat was mechanically modified to accommodate the arrays and speical peripheral electronics was added to a microprocessor system to drive the cold multiplexer and to acquire the output data. The first device, a 16x50 element array on a fan-out board was used to test individual pixels with a trans-impedance-amplifier at a photon background of 10(exp 8) Ph s(-1)cm(-2) and at temperatures of 2.7 to 4.4 K. The noise-equivalent-power NEP is in the range 5 - 7 x 10(exp -18) WHz(exp -1/2), the responsivity is less than or equal to 100 AW(exp -1)(f = 10 Hz). The second device was a 10x50 array including a cold readout electronics of switched FETs (SWIFET). Measurements of this array were done in a background range of 5 x 10(exp 5) to 5 x 10(exp 11) Ph s(exp-1)cm(exp-2) and at operating temperatures between 3.0 and 4.8 K. The NEP ranges from less than 10(exp -18) at the lowest background to 2 x 10(exp -16) WHz(exp -1/2) at the highest flux. Author

N90-21351*# National Aeronautics and Space Administration. Lewis Research Center, Cleveland, OH.
FOUNDATIONS OF MEASUREMENT AND INSTRUMENTATION
Isidore Warshawsky Apr. 1990 232 p
(NASA-RP-1222; E-3786; NAS 1.61:1222) Avail: NTIS HC A11/MF A02 CSCL 14B

The user of instrumentation has provided an understanding of the factors that influence instrument performance, selection, and application, and of the methods of interpreting and presenting the results of measurements. Such understanding is prerequisite to the successful attainment of the best compromise among reliability, accuracy, speed, cost, and importance of the measurement operation in achieving the ultimate goal of a project. Some subjects covered are dimensions; units; sources of measurement error; methods of describing and estimating accuracy; deduction and presentation of results through empirical equations, including the method of least squares; experimental and analytical methods of determining the static and dynamic behavior of instrumentation systems, including the use of analogs. Author

N90-21352# Polytechnic Univ., Farmingdale, NY.
LOW FREQUENCY GYROTRON AMPLIFIER INVESTIGATION, PHASE 2 Final Report, 1 Jul. 1988 - 15 Sep. 1989
Bernard R. Cheo 15 Nov. 1989 40 p
(Contract DAAL03-88-K-0119)
(AD-A217096; POLY-WRI-1567-89; ARO-25893.3-PH) Avail: NTIS HC A03/MF A01 CSCL 09/1

The dispersion relation of a periodically disc loaded cylindrical waveguide is delivered for the H11 mode, in connection with a wide band gyro-TWA analysis. The results are shown to match accurately with the experimental results. The characteristic impedance of this cold circuit is also derived and shown to match experimental results accurately through measurements of the return loss of the circuit. The possibility of absolute instabilities is discussed. GRA

N90-21353 Department of the Navy, Washington, DC.
METHOD FOR HOLOGRAPHIC CORRECTION OF BEAMS OF COHERENT LIGHT Patent
C. Gilbreath-Frandsen, inventor (to Navy) and James W. Wagner,

inventor (to Navy) 7 Nov. 1989 8 p Filed 5 Dec. 1986
(AD-D014406; US-Patent-4,878,718; US-Patent-Appl-SN-938314;
US-Patent-Class-350-3.69) Avail: US Patent and Trademark
Office CSCL 20/14

A method for producing desired changes in a beam of coherent light radiating at lambda 1, comprising the steps of: (1) splitting a beam of coherent light radiating at lambda 1, correcting one of the beams to achieve a desired wavefront and recombining this beam with the first, where a record medium (1) is placed such that the beams are separated by an angle determined by Bragg's law and the line spacing of the interference pattern formed by the two beams; (2) developing the first medium such that a diffraction grating of spacing d1 is recorded in a material, specifically sensitive to lambda 1, which will become the master; (3) illuminating the master with a second wavelength lambda 2, selected by choice of a second medium which possesses very high diffraction efficiency. The second beam is split into two parts. The first is directed to the master. This diffracted order is recombined with the second beam. These beams are separated by an angle determined by Bragg's law and the line spacing of the interference pattern formed by the two beams. The record of the second medium (2) is placed at this jucture. A second grating with grating spacing d2 is recorded in this medium containing a record of the first hologram diffracted from the master, which forms the working hologram; and (4) illuminating the working hologram with the original beam at lambda 1, at an incidence angle specific to the grating spacing d2 and lambda 1, wherein the desired wavefront at lambda 1, is diffracted. GRA

N90-21354 Department of the Navy, Washington, DC.
APPARATUS AND METHOD FOR LOCATING THE AXIS OF SYMMETRY (CENTER OF CIRCULAR CROSS SECTION) OF THREE DIMENSIONAL OBJECTS Patent
Joseph M. Londino, Jr., inventor (to Navy) 7 Nov. 1989 8 p Filed 22 Apr. 1988 Supersedes AD-D013841
(AD-D014407; US-Patent-4,878,296; US-Patent-Appl-SN-184217)
Avail: US Patent and Trademark Office CSCL 13/9

An apparatus and method for locating the vertical axis of symmetry of a surface of horizontal circular cross-section. The apparatus has a plumb structure that establishes a vertical line of sight, and a horizontal translating structure that preselectedly locates the plumb in the two horizontal dimensions. The plumb has at least three arms whose ends are constrained to lie on a circular perimeter which, because the arms are fixed to the plumb, is horizontally disposed. The translating structure and the arms are manipulated so that the end of the arms touch the surface, constraining the line of sight to be colinear with the axis of symmetry. A laser can make the axis visible. The apparatus and method are useable to locate the focal axis and focus of a parabolic antenna. GRA

N90-21355# Department of the Navy, Washington, DC.
HIGH POWER, HIGH SENSITIVITY MICROWAVE CALORIMETER Patent Application
Fredrick M. Mako, inventor (to Navy) and John A. Pasour, inventor (to Navy) 22 May 1989 18 p
(AD-D014427; US-Patent-Appl-SN-354559) Avail: NTIS HC A03/MF A01 CSCL 14/2

A microwave calorimeter is disclosed for substantially measuring the total microwave energy in an applied microwave pulse. The microwave calorimeter includes: a housing having a highly reflective interior surface, a microwave device disposed in the housing for substantially absorbing microwave energy transmitted into the housing and for producing a thermal response proportional to the amount of microwave energy being absorbed, and a measurement device responsive to the thermal response for determining the amount of microwave energy being absorbed by the microwave absorbing device. GRA

N90-21356# Joint Inst. for Nuclear Research, Dubna (USSR). Lab. of Nuclear Problems.
MICROCHANNEL PHOTOMULTIPLIERS IN TIME SPECTROMETER
J. Wawryszczuk et al 1988 5 p In RUSSIAN; ENGLISH summary
(DE90-616417; JINR-13-88-855) Avail: NTIS (US Sales Only)
HC A01/MF A01

Performance of the time spectrometer of gamma-gamma coincidences is described. The spectrometer is developed on the basis of the standard POLON and ORTEG blocks with new microchannel photomultipliers FEhU 165. The time resolution of 152 ps was obtained in detection of gamma-quanta of (60)Co and 235 ps in detection of annihilation gamma-quanta of (22)Na. The FEhU 165 photomultiplier is shown to be useful for investigation of time processes in the subnanosecond range. DOE

N90-21357# Los Alamos National Lab., NM.
THE RAP UNIT: A REMOTE AUTORANGING PICOAMMETER
E. Ray Martin, Karen M. Bennion, and David F. Jones (Jomar Systems, Inc., Los Alamos, NM.) Mar. 1990 95 p
(Contract W-7405-eng-36)
(DE90-007711; LA-11778-MS) Avail: NTIS HC A05/MF A01

A digital instrument for remote acquisition of low-level current measurements is described. Primarily designed for operation with ionization chambers, this instrument provides the capability of local or remote operation over the current range from 10(exp -11) to 10(exp -4) A. It is capable of autoranging operation, or it can be placed in a hold mode where the range is specified. The digital communication link is an optically-isolated 60-mA current loop for noise-free operation, and the unit can be daisy-chained for multiple-unit communication. DOE

N90-21358* National Aeronautics and Space Administration. Pasadena Office, CA.
ALTERNATING GRADIENT PHOTODETECTOR Patent
Albert W. Overhauser, inventor (to NASA) and Joseph Maserjian, inventor (to NASA) (California Inst. of Tech., Pasadena.) 22 Aug. 1989 9 p Filed 5 Nov. 1987
(NASA-Case-NPO-17235-1-CO; US-Patent-4,860,074;
US-Patent-Appl-SN-116811; US-Patent-Class-357-30;
US-Patent-Class-357-58; US-Patent-Class-357-90;
US-Patent-Class-357-4; US-Patent-Class-357-29) Avail: US Patent and Trademark Office CSCL 14B

A far infrared (FIR) range responsive photodetector is disclosed. There is a substrate of degenerate germanium. A plurality of alternating impurity-band and high resistivity layers of germanium are disposed on the substrate. The impurity-band layers have a doping concentration therein sufficiently high to include donor bands which can release electrons upon impingement by FIR photons of energy hv greater than an energy gap epsilon. The high resistivity layers have a doping concentration therein sufficiently low as to not include conducting donor bands and are depleted of electrons. Metal contacts are provided for applying an electrical field across the substrate and the plurality of layers. In the preferred embodiment as shown, the substrate is degenerate n-type (N++) germanium; the impurity-band layers are n+ layers of germanium doped to approximately the low 10(exp 16)/cu cm range; and, the high resistivity layers are n-layers of germanium doped to a maximum of approximately 10(exp)/cu cm. Additionally, the impurity-band layers have a thickness less than a conduction-electron diffusion length in germanium and likely to be in the range of 0.1 to 1.0 micron, the plurality of impurity-bands is of a number such that the flux of FIR photons passing therethrough will be substantially totally absorbed therein, the thickness of the high resistivity layers is such compared to the voltage applied that the voltage drop in each the high resistivity layers controls the occurence of impact ionization in the impurity-band layers to a desired level.

Official Gazette of the U.S. Patent and Trademark Office

N90-21359# Advisory Group for Aerospace Research and Development, Neuilly-Sur-Seine (France). Guidance and Control Panel.
THE ANATOMY OF THE GYROSCOPE, PART 3
Frank W. Cousins and John L. Hollington, ed. (Smiths Industries Aerospace and Defence Systems Ltd., Cheltenham, England)

1990 298 p
(AGARD-AG-313) Copyright Avail: NTIS HC A13/MF A02; Non-NATO Nationals requests available only from AGARD/Scientific Publications Executive

The gyroscope and its applications are collated with the technical information to be found in the patent literature, augmented by that found in textbooks and technical journels. A detailed consideration is given to early mechanical gyroscopes. Included is a discussion of gyroscopic gears, vibratory gyroscopes, interferometric gyroscopes, and the use of the gyroscope in optical and related devices and deals finally with the difficult problem of gyroscopic inertial drives. Author

N90-21360*# National Aeronautics and Space Administration. Lewis Research Center, Cleveland, OH.
A FIBER OPTIC SENSOR FOR NONCONTACT MEASUREMENT OF SHAFT SPEED, TORQUE, AND POWER
George C. Madzsar 1990 11 p Presented at the 36th International Instrumentation Symposium, Denver, CO, 6-10 May 1990; sponsored by Instrument Society of America
(NASA-TM-102481; E-5271; NAS 1.15:102481) Avail: NTIS HC A03/MF A01 CSCL 14B

A fiber optic sensor which enables noncontact measurement of the speed, torque and power of a rotating shaft was fabricated and tested. The sensor provides a direct measurement of shaft rotational speed and shaft angular twist, from which torque and power can be determined. Angles of twist between 0.005 and 10 degrees were measured. Sensor resolution is limited by the sampling rate of the analog to digital converter, while accuracy is dependent on the spot size of the focused beam on the shaft. Increasing the sampling rate improves measurement resolution, and decreasing the focused spot size increases accuracy. Digital processing allows for enhancement of an electronically or optically degraded signal. Author

N90-21361*# National Aeronautics and Space Administration. Lewis Research Center, Cleveland, OH.
ATTACHMENT OF LEAD WIRES TO THIN FILM THERMOCOUPLES MOUNTED ON HIGH TEMPERATURE MATERIALS USING THE PARALLEL GAP WELDING PROCESS
Raymond Holanda, Walter S. Kim, Eric Pencil, Mary Groth (Cincinnati Univ., OH.), and Gerald A. Danzey 1990 19 p Presented at the 177th Meeting of the Electrochemical Society, Montreal, Quebec, 6-11 May 1990
(NASA-TM-102442; E-5218; NAS 1.15:102442) Avail: NTIS HC A03/MF A01 CSCL 14B

Parallel gap resistance welding was used to attach lead wires to sputtered thin film sensors. Ranges of optimum welding parameters to produce an acceptable weld were determined. The thin film sensors were Pt13Rh/Pt thermocouples; they were mounted on substrates of MCrAlY-coated superalloys, aluminum oxide, silicon carbide and silicon nitride. The entire sensor system is designed to be used on aircraft engine parts. These sensor systems, including the thin-film-to-lead-wire connectors, were tested to 1000 C. Author

N90-21362# International Centre for Theoretical Physics, Trieste (Italy).
PRODUCTION OF DIFFRACTION GRATINGS USING HOLOGRAPHIC INTERFEROMETRY
F. N. Ecevit, H. Guven, and R. Aydin (Middle East Technical Univ., Ankara, Turkey) Sep. 1989 10 p
(DE90-612841; IC-89/278) Avail: NTIS (US Sales Only) HC A02/MF A01

Holographic transmission gratings are produced using low power He-Ne laser and the 488-nm Ar-ion laser line. From the observed data of the Hg spectrum and the 488.0-nm, 514.5-nm and 632.8-nm laser lines the fringe spacings of the gratings are calculated. Using the gratings produced with the He-Ne laser the Rydberg constant is determined by measuring the diffraction angles of the Balmer series in the H-atomic spectrum. DOE

N90-21363# Sandia National Labs., Albuquerque, NM. Sensor Components Div.
SOFTWARE TO CHARACTERIZE TUNING FORK RESONATORS USED IN THE QUARTZ DIGITAL ACCELEROMETER
Clarence Collins Mar. 1990 46 p
(Contract DE-AC04-76DP-00789)
(DE90-007913; SAND-89-0855) Avail: NTIS HC A03/MC A01

This report documents the software developed to characterize tuning fork resonators used in the Quartz Digital Accelerometer. The results, after characterizing numerous resonators, indicate a resonant frequency sensitivity to input drive level. Also, the resonant frequency increased for some of the tuning fork resonators but decreased for others. The characterization process used to obtain these results is summarized. DOE

N90-21364# Sandia National Labs., Albuquerque, NM.
IN-SITU PERMEABLE FLOW SENSOR
1990 2 p Presented at the Conference on Support for the US Environmental and Waste Management Industry by DOE, Los Alamos, NM, 14 Mar. 1990
(Contract DE-AC04-76DP-00789)
(DE90-008806; SAND-90-0737C; CONF-9003129-1) Avail: NTIS HC A01/MF A01

The In-situ Permeable Flow Sensor is a new type of implantable instrument under development at Sandia National Laboratories that uses thermal boundary layer pertubation techniques to rapidly determine the three-dimensional velocity vector of groundwater flow in soils or permeable geologic media. This sensor is based on the refinement of previous technology, the Convective Heat Flow Probe, developed for the scientific study of the flow of geothermal fluids in thermally active regions of the earth's crust. The Convective Heat Flow Probe was designed as a logging tool for use in open or uncased boreholes. The newer In-situ Permeable Flow Sensor is based on the same theoretical principles but is designed to be permanently buried at waste or cleanup sites where long term monitoring of groundwater flow is of interest. This instrument is sensitive to permeable flows as low as a few meters per year. DOE

N90-21365# Lawrence Livermore National Lab., CA.
ERROR CORRECTION OF THE DEA (DIGITAL ELECTRONIC AUTOMATION) COORDINATE MEASURING MACHINES AT LLNL
Donald L. Carter 14 Nov. 1989 16 p Presented at the IMOG Measurement and Technology Subgroup on Seminar on Coordinate Measurement Machine User, Livermore, CA, 14-15 Nov. 1989
(Contract W-7405-eng-48)
(DE90-008913; UCRL-102937; CONF-8911177-1) Avail: NTIS HC A03/MF A01

The Lawrence Livermore National Laboratory (LLNL) uses Coordinate Measuring Machines (CMM) manufactured by Digital Electronic Automation, Inc. (DEA) to provide in-process and final measurements of various components as they are assembled and aligned for later experimentation. The machines achieve their accuracy by using real-time passive error compensation to correct for all 21 parametric error components. LLNL does its own parametric testing and downloading of error correction data into the CMM's computer. This paper describes the theory, the parametric tests, the data or map, and the final checkout of the machines. DOE

N90-21366# Westinghouse Savannah River Co., Aiken, SC.
FIBER OPTIC VOID FRACTION SENSOR
S. E. Reed and J. W. Berthold 1989 23 p Presented at the LEOS 1989 Annual Conference, Orlando, FL, 15-16 Oct. 1989
(Contract DE-AC09-89SR-18035)
(DE90-009124; DP-MS-89-1; CONF-8910213-2) Avail: NTIS HC A03/MF A01

Reliable and accurate sensors and instrumentation for void fraction measurements are not commercially available. We have developed a fiber optic method to make these measurements as a part of a three-phase program: proof of principle, design and

fabrication, installation and use during a series of flow channel tests. This paper covers the design, testing, and results for this fiber optic void fraction probe, designed to measure the concentration of liquid water in the flow channel. DOE

N90-21367# Fermi National Accelerator Lab., Batavia, IL. Particle Detector Group.
DEVELOPMENT OF INTRINSIC IPT SCINTILLATOR
Alan D. Bross 31 Jul. 1989 11 p Presented at the Workshop on Scintillating Fiber Detector Development for the SSC, Batavia, IL, 14-16 Nov. 1988
(Contract DE-AC02-76CH-03000)
(DE90-007906; FNAL-TM-1587; CONF-8811199-4) Avail: NTIS HC A03/MF A01

We report on the development of a new polystyrene based plastic scintillator. Optical absorption, fluorescence and light output measurements are presented. Preliminary results of radiation damage effects are also given and compared to the effects on a commercial plastic scintillator, NE 110. DOE

N90-21368# Quaid-i-Azam Univ., Islamabad (Pakistan). Dept. of Physics.
PHASE-ONLY HOLOGRAPHIC FILTERS AND THEIR APPLICATIONS M.S. Thesis
Shahid Qamar 1989 149 p
(PB90-166802) Avail: NTIS HC A07/MF A01 CSCL 14E

Software was developed to perform the computer simulation of optical pattern recognition using phase-only and conventional matched filters. The filters are fabricated using the technique of Computer Generated Hologram based on Lohmann's method. When phase-only filter is used in a optical correlator, correlation-like response that has a considerably higher peak intensity than the conventional matched filter is obtained. Author

N90-21369# Technische Hogeschool, Delft (Netherlands). Dept. of Aerospace Engineering.
UNIVIMP: A UNIVERSAL INSTRUMENT FOR THE SURVEY OF INITIAL IMPERFECTIONS OF THIN-WALLED SHELLS
A. W. H. Klompe Dec. 1988 18 p
(PB90-167065; LR-570) Avail: NTIS HC A03/MF A01 CSCL 14B

In all research into the influence of initial imperfections on the elastic stability of thin-walled structures, experimentation plays an important part; in the first place because the imperfections have to be measured, the results being the basis for the subsequent theoretical analysis; secondly, in order to verify the validity of the theoretical approach or to check the results of calculations, the compressive collapse load of the structure in question has to be determined experimentally, in particular the former purpose calls for specialized equipment, which is not commercially available in most cases. The Universal instrument for the survey of initial imperfections of thin-walled shells is designed to test cylinders with a diameter of 240, 360 and 480 mm and a height of respectively 240, 360 and 480 mm. The report gives a description of the apparatus. Author

N90-21370# Sandia National Labs., Albuquerque, NM. Intelligent Machine Principles Div.
MODELING ELASTOMER DISPLACEMENTS FOR TACTILE SENSING APPLICATIONS
J. L. Novak Feb. 1990 34 p
(Contract DE-AC04-76DP-00789)
(DE90-007959; SAND-89-1089) Avail: NTIS HC A03/MF A01

Many capacitance-based tactile sensors measure the displacements of an elastic substrate at multiple sites. A large number of sensing applications, however, require knowledge of the surface forces. This report considers the problem of reconstructing these surface forces from the measured displacements. Two models for reconstruction are considered. Contacts in which the area is much smaller than the dimensions of the compliant surface are modelled using a linear elastic half-space. Analyses of the deformations using this model confirm a strong coupling between normal and tangential displacements for normal, tangential or arbitrary loads. Using a spatial frequency formulation, the minimum spatial sampling densities for reconstructing displacements (as a prerequisite to reconstructing forces) are shown to be significantly smaller than those required for reconstructing strains. The second model, the bonded spring, is introduced for surface contacts which extend over the entire sensor surface. A nonlinear stress-strain relationship is included since tactile sensors undergo relatively large deformations. An empirical relationship between elastic pad geometry and the effective modulus of elasticity is also presented. DOE

N90-21371# Lawrence Livermore National Lab., CA.
ABSOLUTE MULTILAYER CHARACTERIZATION AT HIGH SPATIAL RESOLUTION VIA REAL-TIME SOFT X RAY IMAGING
Larry Madison Mar. 1990 17 p Presented at the National Society of Black Physicists Annual Meeting, Baton Rouge, LA, 21-24 Mar. 1990 Submitted for publication
(Contract W-7405-eng-48)
(DE90-009181; UCRL-100498-Rev-1; CONF-9003115-1) Avail: NTIS HC A03/MF A01

An imaging-based technique has been modeled for its suitability and performance in measuring the spatial distribution of the absolute soft x ray characterization of flat multilayer mirrors. Such a technique, if implemented experimentally, is anticipated to have substantially higher throughput (wafers/day) than is possible from prevailing non-imaging means. DOE

36 LASERS AND MASERS

Includes parametric amplifiers.
For related information see also *76 Solid-State Physics.*

N90-21372 Rochester Univ., NY.
DEVELOPMENT OF AN ULTRA-BRIGHT LASER AND AN APPLICATION TO MULTI-PHOTON IONIZATION Ph.D. Thesis
Donna Theo Strickland 1989 162 p
Avail: Univ. Microfilms Order No. DA8913596

Conventional amplifiers have not been able to amplify short pulses to high energies either because the stored energy of the gain medium was too low or the high peak powers in the amplifier would cause nonlinear effects and eventually damage to occur. Chirped radar was developed over forty years ago to solve a similar problem in the radar field. The optical analog to chirped radar, Chirped Pulse Amplification (CPA) has been studied here and a prototype laser system has been developed. The CPA technique uses fiber and grating pulse compression techniques. Short pulses are stretched several times their initial duration by group velocity dispersion, either in an optical fiber or a pair of gratings. The long pulses are then amplified in a high energy gain medium, without reaching the peak power limitation. The high energy pulse can be recompressed to its original pulse duration by a second dispersive delay line, with the opposite dispersion. The prototype system focuses 50 ps pulses from a cw mode-locked Nd:YLF oscillator into an optical fiber. The bandwidth is stretched to approximately 4 nm and the pulse width is stretched to 150 ps. The duration is further stretched by a grating pair to 500 ps. The long pulses are amplified in three stages to an energy of 0.5 J. The amplified pulses are compressed to a 1 ps duration by a second pair of gratings. Dissert. Abstr.

N90-21373 Maryland Univ., College Park.
GENERATION OF ULTRASHORT LASER PULSES FROM NEODYMIUM GLASS OSCILLATOR AND REGENERATIVE AMPLIFIER Ph.D. Thesis
Li Yan 1989 242 p
Avail: Univ. Microfilms Order No. DA8924260

Physical processes affecting generation, amplification, and compression of high repetition rate, ultrashort laser pulses from a Nd:phosphate glass oscillator-regenerative amplifier system are studied. Characteristics of the three-element optical resonators were studied, and an optimal configuration was found. Thermal

stress induced fracture, thermal birefringence and thermal lensing of the Nd:phosphate glass under longitudinal pumping were investigated. The spectral properties of continuous wave (CW) lasing showed that the Nd:phosphate glass laser is a weakly inhomogeneously broadened laser. The nonlinear atomic frequency pulling was the limiting factor in generating coherent short laser pulses by active modelocking. The oscillator generated bandwidth limited, CW actively modelocked pulses with less than 10 picosecond duration. A high repetition rate Nd:phosphate glass regenerative amplifier was developed, which increased the pulse energy up to approximately 40 microJ at 370 Hz. The strong intracavity self-phase modulation during regenerative amplification of short picosecond pulse was used to broaden the pulse bandwidth to approximately 35 A. Using a pair of external cavity gratings, the amplified and spectrally broadened and chirped pulses were directly compressed to 0.55 ps with greater than 10 microJ pulse energy after compression. An optical fiber further broadened the pulse bandwidth to more than 500 A. A second pair of gratings shortened the pulses to 30 femtosecond, the shortest pulses ever generated at 1.054 microns. Dissert. Abstr.

N90-21374# United Kingdom Atomic Energy Authority, Harwell (England). National NDT Centre.
SOME RECENT APPLICATIONS OF LASER ULTRASOUND TO THE CHARACTERISATION OF MATERIALS
C. B. Scruby, F. K. Brocklehurst, B. C. Moss, and D. J. Buttle Jul. 1989 32 p
(AERE-R-13438) Avail: NTIS HC A03/MF A01

Laser techniques for ultrasonic generation and reception have potential for a wide range of non-contact measurements, chiefly because they can be used for defect detection and materials characterization at elevated temperatures. However, these techniques have other advantages. Unlike contact transducers, they do not disturb elastic wave propagation by loading the surface of the specimen. They are also capable of much higher temporal and spatial resolution than can be obtained by most conventional techniques. Some recent applications of this technology to a range of materials are presented. The first two exploit the non-contact characteristics of laser ultrasound for surface characterization following, respectively, plasma-sprayed coating and laser hardening. The remaining applications exploit the high temporal and spatial resolution for the acoustic characterization of various composite materials, i.e., glass-fiber and carbon-fiber reinforced plastics, and a metal matrix composite. Author

N90-21375# Department of the Navy, Arlington, VA.
X RAY LASER WITH ENHANCED X RAY GAIN THROUGH PHOTODEPOPULATION Patent Application
Raymond C. Elton, inventor (to Navy) 29 Sep. 1989 15 p
(AD-D014448; US-Patent-Appl-SN-414499) Avail: NTIS HC A03/MF A01 CSCL 09/3

The present invention relates to x ray lasers employing hydrogenic lasing ions of nuclear charge Z, for n=2 to 4 or 6 excitation, and radiating ions of nuclear charge Z/2 for decreasing the n=2 population density of the hydrogenic lasing ions of nuclear charge Z. It is an object of the invention to increase the population inversion and gain to saturation, to improve the overall efficiency, and to increase the plasma size by decreasing the population density N2. GRA

N90-21376# Israel Academy of Sciences and Humanities, Jerusalem.
TENTH INTERNATIONAL FREE ELECTRON LASER CONFERENCE
1988 140 p Conference held in Jerusalem (Israel), 29 Aug. - 2 Sep. 1988; sponsored in part by Ministry of Science and Development; Weizmann Inst. of Science; Tel Aviv Univ.; Navy and AF
(DE90-614773; INIS-mf-11580; CONF-8808146) Avail: NTIS (US Sales Only) HC A07/MF A01

The volume contains over a hundred abstracts of lectures covering a wide variety of subjects in the field of free electron lasers. Many features of lasing were observed over a range of problems, and experiments which resulted in finding ideal or near-ideal techniques for gaining better and more efficient optical power have been carried out. DOE

N90-21377# Los Alamos National Lab., NM.
CLOUD HOLE-BORING WITH LONG PULSE CO2 LASERS
Gerard P. Quigley, Robert B. Webster, and George W. York 1990 12 p Presented at the SPIE Optics, Electro-Optics and Laser Applications in Science and Engineering Conference and Exhibition, Los Angeles, CA, 15-19 Jan. 1990
(Contract W-7405-eng-36)
(DE90-008946; LA-UR-90-768; CONF-900140-18) Avail: NTIS HC A03/MF A01

Chemically generated CO2 laser pulses at 10.6 microns were used to clear a 5 cm diameter hole through a stratus-like cloud in a laboratory cloud chamber. The results show that 100 percent clearing can be achieved. The mechanism is shown to be droplet shattering followed by evaporation. Under the conditions of the experiment, the channel closure is dominated by turbulent mixing and not droplet recondensation. DOE

N90-21378# Rochester Univ., NY. Lab. for Laser Energetics.
LLE REVIEW Quarterly Report, Oct. - Dec. 1989
D. K. Bradley, ed. 1989 67 p Sponsored by Empire State Electric Energy Research Corp., New York, NY; New York State Energy Research and Development Authority; and Ontario Hydro
(Contract DE-FC03-85DP-40200)
(DE90-008958; DOE/DP-40200/112) Avail: NTIS HC A04/MF A01

This volume of the LLE Review, covering the period October to December 1989, contains an article discussing saturation effects and power-balance considerations in the design of high-power lasers and an article describing numerical modeling of the effects of power imbalances on target behavior. The advanced technology section reports on the development of a liquid crystal laser-beam apodizer and an experiment to study the high-intensity ionization of noble gases. Finally, the activities of the National Laser Users Facility and the GDL and OMEGA laser facilities are summarized. The highlights of this issue are: The problem of achieving power balance in high-efficiency, multibeam lasers has been studied in terms of gain-saturation effects and the nonlinear nature of harmonic frequency conversion. It is shown that power imbalance can be minimized by balancing the gains and losses in equivalent amplification stages in each beamline. The effects of target implosion behavior of various power-imbalance sources in the OMEGA laser system have been studied using the two-dimensional hydrodynamics code ORCHID. The simulations show good agreement with an experiment in which a deliberate power imbalance was applied to the target drive. Laser-beam apodizers with large clear apertures have been fabricated using cholesteric liquid crystals. DOE

N90-21379# California Univ., Berkeley. Lawrence Berkeley Lab. Accelerator and Fusion Research Div.
ON STORAGE RINGS FOR SHORT WAVELENGTH FELS
Swapan Chattopadhyay Jan. 1990 23 p Presented at the SPIE Optics, Electro-Optics and Laser Applications in Science and Engineering Conference and Exhibition, Los Angeles, CA, 15-19 Jan. 1990
(Contract DE-AC03-76SF-00098)
(DE90-009059; LBL-28483; CONF-900140-16) Avail: NTIS HC A03/MF A01

Significant advances have been made recently in the understanding of free electron laser (FEL) physics and the technology of associated systems. We have witnessed experimental successes in the operation of FELs from the far infrared to the visible and near UV. All of the basic physics of FELs, as advanced up to date, in the small and high gain regimes (including exponential growth from noise, optical guiding, etc.) have been proved experimentally in the near or far infrared. These successes motivate us to explore the design of FEL systems at even shorter wavelengths, in the UV, XUV and soft x-ray regions,

assuming that the same physics remain valid at these wavelengths. This paper is concerned with issues in the physics and design of storage rings as drivers of short wavelength FELs. DOE

N90-21380# National Inst. of Standards and Technology, Gaithersburg, MD. Center for Atomic, Molecular and Optical Physics.
LASER STUDIES OF CHEMICAL DYNAMICS AT THE GAS-SOLID INTERFACE Progress Report, Jan. 1987 - Jun. 1989
Richard R. Cavanagh and David S. King 1990 14 p
(Contract DE-AI05-84ER-13150)
(DE90-008698; DOE/ER-13150/T3) Avail: NTIS HC A03/MF A01

The DOE funded research program Laser Studies of Chemical Dynamics at the Gas-Solid Interface has taken a detailed, microscopic view of molecules desorbed from surfaces in order to gain an understanding of energy flow and interaction potentials and how these control chemical reactivity at interfaces. Successful completion of these experiments required technical expertise both in surface science and laser-based molecular dynamics, a collaborative situation that exists in the NIST center for Atomic, Molecular and Optical Physics. During the three year period covered by this progress report, our goal was to use state-resolved techniques to examine a single chemisorption system in detail, and to observe how changes in the interaction potential or method of surface excitation are manifest in the desorption dynamics. The system chosen was NO/Pt(111). Studies were undertaken in which the effects on the NO-Pt interaction potential of coadsorbates--both weakly (CO) and strongly (NH(sub 3)) interacting-- could be examined. In addition, attempts were to be made to study non-equilibrium dynamics by using pulsed laser heating. DOE

37 MECHANICAL ENGINEERING

Includes auxiliary systems (nonpower); machine elements and processes; and mechanical equipment.

N90-21381# Royal Aerospace Establishment, Farnborough (England).
PERFORATION OF A REINFORCED CONCRETE WALL BY A RIGID MISSILE
C. Berriaud (Commissariat a l'Energie Atomique, Saclay, France) 22 Sep. 1988 21 p Transl. into ENGLISH of Perforation d'une Paroi en Beton Arme par un Projectile Rigide, 1980 Presented at conference held in Paris, France, 17 Jan. 1980
(AD-A210025; RAE-Trans-2165; BR110032; CEA-CONF-5079)
Avail: NTIS HC A03/MF A01 CSCL 13/9

The results of a large experimental program in which cylindrical steel projectiles were fired at slabs of reinforced concrete are given. A scale of one third with respect to the wall of a nuclear reactor was largely used, and the effects of the variation of the following parameters were studied: projectile speed, mass, ratio of diameter of projectile to thickness of the slab, and the characteristics of the steel reinforcement. A homogeneous perforation formula is proposed for the computation of the thickness of reinforced concrete which will be perforated by a given missile, and its range of validity is specified. A comparison with other formulae found in the literature is made. Author

N90-21382# International Society for Terrain-Vehicle Systems, Hanover, NH.
PROCEEDINGS OF THE 4TH EUROPEAN CONFERENCE, VOLUME 2
Mar. 1989 111 p Conference held in Wageningen, Netherlands, 21-23 Mar. 1989 Sponsored in part by Army
(AD-A216521) Avail: NTIS HC A06/MF A01 CSCL 08/10

Topics addressed include: Terrain-Vehicle Systems and Sustained Soil Quality; Soil-Vehicle Interaction and Sustained Soil Quality; Advances in Mobility Devices and Soil-Vehicle Modelling; Soil compaction at wood hauling and wood skidding with heavy-duty tractors; Field Traffic and Sustained Soil Quality for Plant Growth - Agriculture and Forestry Aspects; Terrain-Vehicle Systems and Soil Quality - Military Aspects; Advances in Mobility Devices and Soil-Vehicle Modeling. GRA

N90-21383# Stanford Univ., CA. Aerospace Robotics Lab.
END POINT CONTROL OF FLEXIBLE MANIPULATORS Final Report, Oct. 1985 - Oct. 1988
Robert H. Cannon, Jr. Oct. 1988 105 p
(Contract MDA903-86-K-0037)
(AD-A217319) Avail: NTIS HC A06/MF A01 CSCL 13/9

Research toward a technology for very quick, precise two-arm cooperative manipulation with the use of end-point control is covered. The research addresses precision force control and dynamic cooperation of two manipulators. Unavoidable flexibility in the drive trains of robots and the robots' mounts make precise end-point control of flexible robots important. This research is part of a series of experiments requiring increasingly more advanced control capability and working with exaggerated flexibility to force solution of fundamental problems. The report covers: (1) cooperating two-link arms with flexible drive trains; (2) control of a flexible robot arm with a two degree-of-freedom mini-manipulator; and (3) force control of a two-link arm with a flexible drive train. GRA

N90-21384 Department of the Navy, Washington, DC.
EXPANDING RING JOINT Patent
Kent G. Whitham, inventor (to Navy) 7 Nov. 1989 7 p Filed 5 Dec. 1988
(AD-D014398; US-Patent-4,878,695; US-Patent-Appl-SN-280056)
Avail: US Patent and Trademark Office CSCL 13/5

This investigation relates to an apparatus and method for producing a rigid joint between two interlocked tubular members and in particular between two tubular members have cylindrical mating ends. This patent involves a joint having no external protrusions consisting of the mating cylindrical ends of two tubular members joined by interlocking cogs on the male and female ends of the tubular members, and a pair of facing ramp surfaced rings disposed in the joint with one ring integral with or affixed immovably to the male end of one tubular member, the other ring rotatably disposed upon that same member within the joint so that when the movable ring is rotated by means of a spanner wrench or equivalent tool relative to the stationary ring, the juxtaposed ramp surfaces ride upon each other causing the movable ring to move axially relative to but in continuing contact with the stationary ring until contact with the female end of the other tubular member in the joint is established and the joint is thereby made rigid. The spaces thus created between the ramps of the rings are filled with material that becomes solid or set screws radially disposed in the movable ring to engage an annular slot about the male end of the one tubular member and underlying the movable ring can be used to thereafter immobilize that ring. GRA

N90-21385# Department of the Navy, Arlington, VA.
HEAT ENGINE BASED ON SHAPE MEMORY ALLOYS Patent Application
David Goldstein, inventor (to Navy) 1 Dec. 1989 12 p
(AD-D014400; US-Patent-Appl-SN-444350) Avail: NTIS HC A03/MF A01 CSCL 10/1

This patent application discloses a tubular gear made of shape memory alloy in sheet form, having longitudinal corrugations and being floating supported for rotation about an axis fixedly spaced from the rotational axis of a roller gear in meshing engagement with the corrugations. The tubular gear is sequentially deformed by exposure to radiated heat causing the shape memory alloy to expand circumferentially and by said meshing engagement with roller gear. Such deformation of the tubular gear within differential temperature regions established by restricted exposure to the radiated heat, induces and sustains rotation of the tubular gear to convert the heat energy into mechanical energy. GRA

N90-21386# Department of the Navy, Washington, DC.
DOUBLE VALVE MECHANISM FOR AN ACOUSTIC MODULATOR Patent Application
Robert B. Anderson, inventor (to Navy) 23 Aug. 1989 17 p
(AD-D014401; US-Patent-Appl-SN-397549) Avail: NTIS HC A03/MF A01 CSCL 20/1

A double valve mechanism which is the functioning part of an acoustic modulator which regulates airflow by creating air pressure variations. A pair of cylindrical shaped members, each of which has a plurality of elongated ports therein move relative to each other through electro-magnetic excitation. The motion of the two cylindrical shaped members is reciprocating causing the ports to first open and then close, thereby modulating the air flowing through the acoustic modulator. Linear motion of the cylindrical shaped members to displace the same port area is only one half of the linear motion required in a previous design, resulting in an acoustic energy output waveform having a frequency which is double the frequency of an electrical sinusoidal input signal supplied to the acoustic modulator. GRA

N90-21387*# Ohio State Univ., Columbus. Dept. of Mechanical Engineering.
A REVIEW OF GEAR HOUSING DYNAMICS AND ACOUSTICS LITERATURE Interim Report
Teik Chin Lim and Rajendra Singh Oct. 1989 85 p
(Grant NAG3-773; DA Proj. 1L1-62209-A47-A)
(NASA-CR-185148; NAS 1.26:185148; AVSCOM-TM-89-C-009)
Avail: NTIS HC A05/MF A01 CSCL 13I

A review of the available literature on gear housing vibration and noise radiation is presented. Analytical and experimental methodologies used for bearing dynamics, housing vibration and noise, mounts and suspensions, and the overall gear and housing system are discussed. Typical design guidelines, as outlined by various investigators, are also included. Results of this review indicate that although many attempts were made to characterize the dynamics of gearbox system components, no comprehensive set of design criteria currently exist. Moreover, the literature contains conflicting reports concerning relevant design guidelines. Author

N90-21388# Uniroyal Plastics Co., Inc., Mishawaka, IN. Engineered Systems Div.
COLLAPSIBLE FABRIC TANK TESTING Final Technical Report, Oct. 1987 - Sep. 1989
Don V. Perkins 29 Sep. 1989 201 p
(Contract DAAK70-87-C-0078)
(AD-A217861; FC-2094) Avail: NTIS HC A10/MF A02 CSCL 21/4

A test program was conducted on military fuel and water static storage tanks which involved the following: (1) Weatherometer aging of government supplied tanks to 2000 hours, (2) Fuel testing of tank materials for 14, 28 and 42 days in Fuel B and MIL-F-46162B + EGME at 160 F, (3) Three different types of abrasion testing, (4) Development of non-destructive test methods to predict tank serviceability and remaining service life, (5) Analysis of packaging and handling of tanks with recommendations for increasing storage and service life. GRA

N90-21389# Mega Research, Inc., Rancho Palos Verdes, CA.
IMPROVED ANALYTICAL CAPABILITIES FOR FOIL AIR BEARINGS, PHASE 1 Final Report, 15 Sep. 1988 - 15 Sep. 1989
Erh-Rong Wu and Phyllis M. K. Wu Jan. 1990 38 p
(Contract F33615-88-C-2851; AF Proj. 3005)
(AD-A218071; SBIR-88-LUB-1; WRDC-TR-89-2149) Avail: NTIS HC A03/MF A01 CSCL 13/9

Completion of this Phase 1 study has presented an advanced analytic tool for predicting the performance of foil bearings and solid-walled bearings as well, operating at speeds wherein the Reynolds number is no longer small and the effects of the fluid inertia, the heat transfer and the turbulent flow become significant. The tool uses the 3-D Navier-Stokes approach for the fluid film thermohydrodynamics and the thermoelasticity treatment for the foil deformation. The Navier-Stokes approach is more complicated than the Reynolds equation approach, conventional or modified for the inclusion of inertia or turbulence. Nevertheless, the N-S approach has the capability of investigating the local behaviors of the lubricant and the foil. Especially, the prediction of temperature variation may eventually help explain the hot spots or burned spots which are often observed in a failed bearing. Two computer programs, 3DNSBRGJ (journal) and 3DNSBRGT (thrust) are developed through this Phase 1 study. The programs are capable of calculating bearing performance characteristics, and the velocity components, the temperature distribution, the foil deflection, the turbulence energy distribution and its dissipation rate. GRA

N90-21390* National Aeronautics and Space Administration. Lyndon B. Johnson Space Center, Houston, TX.
DOUBLE SWIVEL TOGGLE RELEASE Patent
Guy L. King and William C. Schneider 12 Sep. 1989 8 p
Filed 23 Feb. 1989
(NASA-Case-MSC-21436-1; US-Patent-4,864,910;
US-Patent-Appl-SN-313839; US-Patent-Class-89-1.14;
US-Patent-Class-89-1.57; US-Patent-Class-102-378;
US-Patent-Class-194-82.26; US-Patent-Class-194-82.29) Avail: US Patent and Trademark Office CSCL 13I

A pyrotechnic actuated structural release device is disclosed which is mechanically two fault tolerant for release. The device comprises a fastener plate and fastener body each attachable to one of a pair of structures to be joined. The fastener plate and the fastener body are fastened by a dual swivel toggle member. The toggle member is supported at one end on the fastener plate and mounted for universal pivotal movement thereon. Its other end is received in a central opening in the fastener body, and has a universally mounted retainer ring member. The toggle member is restrained by three retractable latching pins symmetrically disposed in equiangular spacing about the axis of the toggle member and positionable in latching engagement with the retainer ring member on the toggle member. Each pin is retractable by a pyrotechnic charge, the expanding gases of which are applied to a pressure receiving face on the latch pins to effect retraction from the ring member. While retraction of all three pins releases the ring member, the fastener is mechanically two fault tolerant since the failure of any single one or pair of the latch pins to retract results in an asymmetrical loading on the ring member and its dual pivotal movement ensures a release.
Official Gazette of the U.S. Patent and Trademark Office

N90-21391 Texas Univ., Austin.
DEVELOPMENT OF A DYNAMIC MODELING TECHNIQUE AND ITS APPLICATION TO THE ANALYSIS AND CONTROL OF A HIGH-PRECISION ROBOTIC MANIPULATOR Ph.D. Thesis
Whang Cho 1989 211 p
Avail: Univ. Microfilms Order No. DA9005555

A systematic dynamic formulation technique yielding closed form equations of motion is developed for the modeling of a broad class of multibody dynamic systems ranging from simple open chain linkages to highly complex hybrid linkage structures consisting of multiple open and closed chains. The necessary formulations are based on the concept of kinematic influence coefficients (KIC). This work involves the extension of the concept in a more structured format enabling a more generic treatment of large class of systems. A particular application of this technique is made to investigate the kinematic and dynamic characteristics of a redundant planar shoulder with special macro/micro geometry. In this structure the small scale system is embedded in the large scale system, as opposed to the more elementary serial structures. The benefit of the proposed structure is the increased static and dynamic resolutions in rotational and translational motions of output. A robust controller using feedback linearization is designed to demonstrate the tracking capability of the proposed parallel type robotic manipulator under modeling uncertainties. The architecture of the proposed controller may be used to control a general class of macro/micro robotic manipulator system without excessive computational requirements. Dissert. Abstr.

N90-21392 Wisconsin Univ., Madison.
COMPUTER-AIDED DESIGN OF FLYWHEEL TRANSMISSION SYSTEMS Ph.D. Thesis
Tung-Ming Hsieh 1989 158 p
Avail: Univ. Microfilms Order No. DA8917654

A comprehensive flywheel vehicle performance simulation program was developed to study the fuel economy and performance of proposed flywheel vehicles. The program is a generic model of various components that can be assembled to simulate flywheel hybrid vehicles with different configurations and control strategies. Results from the program can be formatted to accomplish parametric studies of flywheel vehicles. Numerical optimization methods are compared and the Complex Search Method is implemented to search for an optimal design of the flywheel vehicle resulting in specific design, control strategy and a given set of components. An efficient random number generator is implemented to generate random numbers for constructing feasible design points which satisfy explicit constraints during the optimal search of design parameters. Parametric studies of major design factors on fuel economy are made. Two different configurations of flywheel transmission are used to serve as a basis of optimal design study for flywheel vehicles.

Dissert. Abstr.

N90-21393 Wisconsin Univ., Madison.
APPLICATION OF OPTIMIZATION IN DESIGN AND MOTION CONTROL OF ROBOT MANIPULATORS Ph.D. Thesis
Ahmad Reza Kashani 1989 148 p
Avail: Univ. Microfilms Order No. DA8916427

Optimal design methodologies are developed for actuator sizing and motion control of robot manipulators with applications in manufacturing. Using the dynamic load carrying capacity as the objective function, an algorithm is developed for sizing the joint actuators of robot manipulators. This allows designing robotic systems for high performance material handling applications. In addition, an optimal design strategy is combined with a motion control algorithm and a computational architecture for robotic applications in plunge surface grinding. The optimal design methodology is used to select joint stiffness via appropriate feed-back and feed-forward gains in the control system. The objective function is the deviation of the characteristic equation of the linearized model of the robot manipulator from the desired target dynamics. A new computational architecture is also developed to speed up the necessary computations. Author

N90-21394*# National Aeronautics and Space Administration. Lewis Research Center, Cleveland, OH.
TRANSMISSION RESEARCH ACTIVITIES AT NASA LEWIS RESEARCH CENTER
D. G. Lewicki 1990 31 p Presented at the Helicopter Transmission Design and Maintenance Workshop, Quebec City, Quebec, 21-25 May 1990; sponsored by Canadian Department of National Defense Prepared in cooperation with Army Aviation Systems Command, Cleveland, OH
(DA Proj. 1L1-2211-A-47-A)
(NASA-TM-103132; E-5469; NAS 1.15:103132; AVSCOM-TM-90-C-006) Avail: NTIS HC A03/MF A01 CSCL 13I

A joint research program, to advance the technology of rotorcraft transmissions, consists of analytical and experimental efforts to achieve the overall goals of reducing transmission weight and noise, while increasing life and reliability. Recent activities in the areas of transmission and related component research are highlighted. Current areas include specific technologies in support of military rotary wing aviation, gearing technology, transmission noise reduction studies, a recent interest in gearbox diagnostics, and advanced transmission system studies. Results of recent activities are presented along with near term research plans.

Author

N90-21395*# Mechanical Technology, Inc., Latham, NY.
INTERNAL ROTOR FRICTION INSTABILITY Final Report, Nov. 1983 - Oct. 1987
J. Walton, A. Artiles, J. Lund, J. Dill, and E. Zorzi Feb. 1990 169 p
(Contract NAS8-35601)
(NASA-CR-183942; NAS 1.26:183942; MTI-88TR39) Avail: NTIS HC A08/MF A01 CSCL 13I

The analytical developments and experimental investigations performed in assessing the effect of internal friction on rotor systems dynamic performance are documented. Analytical component models for axial splines, Curvic splines, and interference fit joints commonly found in modern high speed turbomachinery were developed. Rotor systems operating above a bending critical speed were shown to exhibit unstable subsynchronous vibrations at the first natural frequency. The effect of speed, bearing stiffness, joint stiffness, external damping, torque, and coefficient of friction, was evaluated. Testing included material coefficient of friction evaluations, component joint quantity and form of damping determinations, and rotordynamic stability assessments. Under conditions similar to those in the SSME turbopumps, material interfaces experienced a coefficient of friction of approx. 0.2 for lubricated and 0.8 for unlubricated conditions. The damping observed in the component joints displayed nearly linear behavior with increasing amplitude. Thus, the measured damping, as a function of amplitude, is not represented by either linear or Coulomb friction damper models. Rotordynamic testing of an axial spline joint under 5000 in.-lb of static torque, demonstrated the presence of an extremely severe instability when the rotor was operated above its first flexible natural frequency. The presence of this instability was predicted by nonlinear rotordynamic time-transient analysis using the nonlinear component model developed under this program. Corresponding rotordynamic testing of a shaft with an interference fit joint demonstrated the presence of subsynchronous vibrations at the first natural frequency. While subsynchronous vibrations were observed, they were bounded and significantly lower in amplitude than the synchronous vibrations.

Author

N90-21396# Rockwell International Corp., Golden, CO. Aerospace Operations.
THE EFFECTS OF A NEARBY SUBSEQUENT FUSION WELD ON THE PROPERTIES OF AN INERTIA FRICTION WELD
S. Tsang, D. Yashan, P. A. Kneale, and B. B. Lawton 31 Dec. 1989 24 p
(Contract DE-AC04-76DP-03533)
(DE90-007972; RFP-4256) Avail: NTIS HC A03/MF A01

Effects of performing a subsequent fusion weld were evaluated. This case involved a defocused electron beam weld near the interface of an inertia friction weld between 1100 F aluminum and Type 316 stainless steel. The primary methods of evaluation were metallography and measuring the tensile strength change of the inertia friction weld before and after performing the fusion weld in the proximity of this friction weld. When tensile tested, the friction welds fractured in the 1100 F aluminum base metal. Strength degradation, referred to as the electron beam weld damage, was mainly due to softening of the aluminum base metal in and around the heat-affected zone of the friction weld. This softening effect was due to grain growth, which resulted from the heat cycle of the electron beam weld as determined by the weld parameters. Other possible effects on the extent of the damage are steel mating surface geometry and temper of the 1100 F aluminum, both of which appear to influence the grain growth process.

DOE

N90-21397# Oak Ridge National Lab., TN. Engineering Physics and Mathematics Div.
A NEW APPROACH TO SOLVE THE KINEMATICS RESOLUTION OF A REDUNDANT ROBOT
Philippe Belmans and Jean-Christophe Culioli Mar. 1990 19 p
(Contract DE-AC05-84OR-21400)
(DE90-010213; ORNL/TM-11435; CESAR-89/53) Avail: NTIS HC A03/MF A01

A classical redundancy resolution scheme for an m-degree of freedom robot involves the numerical or symbolic computation of the Moore-Penrose pseudo-inverse of the Jacobian matrix, which

in turn leads to a least norm solution for the joint velocities. Since the Jacobian matrix may be ill-conditioned, the computation of the inverse may often turn out to be lengthy and/or inaccurate. An alternative method is proposed to find this least norm solution. Namely the original underdetermined problem is modified by transforming it into a set of determined new problems. The solutions of these problems are computed in parallel and their least norm simplex combination was found. It is proven that if the dimension of the task-space is n, only (m (minus) n + 1) such solutions are needed. It is also shown that the approach can take into account obstacle avoidance and maximum of manipulability or any other type of analytical criterion. The method is applied to a planar redundant arm. DOE

38 QUALITY ASSURANCE AND RELIABILITY

Includes product sampling procedures and techniques; and quality control.

N90-21398# United Kingdom Atomic Energy Authority, Harwell (England). Materials Physics and Metallurgy Div.

ON-LINE ASSESSMENT OF WELD QUALITY USING ULTRASONICS

C. Duffill, B. C. G. Haywood, C. B. Scruby, and I. J. Stares Jul. 1989 25 p

(AERE-R-13401) Avail: NTIS HC A03/MF A01

There is a recognized industrial need for active methods to control weld parameters in order to give improved fusion weld quality. In particular, it is important to control weld penetration, weld pool size and position, and defect formation. Ultrasonic waves are able to penetrate within the material and provide information about the nature and position of the solid-liquid interface together with any other discontinuities or defects during the welding process. The application of pulse-echo ultrasonics is presented, using both compression and shear waves, to the characterization of the solid-liquid interface surrounding the weld-pool in stainless steel. A theoretical model is used to plot the ray paths in the severe temperature gradients surrounding the weld-pool and thereby calculate the correction needed to take into account thermal effects. There was good overall agreement between theory and experimental data. It is concluded that, provided the ultrasonic data processing instrumentation is capable of rapid signal averaging and on-line analysis, this technique has considerable potential for weld quality control. Because compression waves can be transmitted through the molten metal in the pool, the technique can also be used to detect some weld defects on-line, such as inclusions, porosity, and lack of fusion. Author

N90-21399*# National Aeronautics and Space Administration. Lewis Research Center, Cleveland, OH.

AEROPROPULSION FACILITIES CONFIGURATION CONTROL: PROCEDURES MANUAL

James J. Lavelle Mar. 1990 24 p

(NASA-TM-102541; E-5351; NAS 1.15:102541) Avail: NTIS HC A03/MF A01 CSCL 14D

Lewis Research Center senior management directed that the aeropropulsion facilities be put under configuration control. A Configuration Management (CM) program was established by the Facilities Management Branch of the Aeropropulsion Facilities and Experiments Division. Under the CM program, a support service contractor was engaged to staff and implement the program. The Aeronautics Directorate has over 30 facilities at Lewis of various sizes and complexities. Under the program, a Facility Baseline List (FBL) was established for each facility, listing which systems and their documents were to be placed under configuration control. A Change Control System (CCS) was established requiring that any proposed changes to FBL systems or their documents were to be processed as per the CCS. Limited access control of the FBL master drawings was implemented and an audit system established to ensure all facility changes are properly processed. This procedures manual sets forth the policy and responsibilities to ensure all key documents constituting a facilities configuration are kept current, modified as needed, and verified to reflect any proposed change. This is the essence of the CM program. Author

N90-21400# Defense Contract Administration Services Region, Saint Louis, MO.

QUALITY AT A GLANCE

Donald S. Parsons, Jr., comp. Jan. 1990 33 p

(AD-A217297) Avail: NTIS HC A03/MF A01 CSCL 05/1

This document contains summaries of fifteen of the well known books which underlie the Total Quality Management philosophy. Members of the DCASR St. Louis staff offer comments and opinions on how the authors have presented the quality concept in today's business environment. GRA

N90-21401*# National Aeronautics and Space Administration. Lewis Research Center, Cleveland, OH.

ULTRASONIC AND RADIOGRAPHIC EVALUATION OF ADVANCED AEROSPACE MATERIALS: CERAMIC COMPOSITES

Edward R. Generazio 1990 12 p Presented at Physics Dept. Seminars, University Heights, OH, 11 Apr. 1990; sponsored by John Carroll Univ.

(NASA-TM-102540; E-5403; NAS 1.15:102540) Avail: NTIS HC A03/MF A01 CSCL 14D

Two conventional nondestructive evaluation techniques were used to evaluate advanced ceramic composite materials. It was shown that neither ultrasonic C-scan nor radiographic imaging can individually provide sufficient data for an accurate nondestructive evaluation. Both ultrasonic C-scan and conventional radiographic imaging are required for preliminary evaluation of these complex systems. The material variations that were identified by these two techniques are porosity, delaminations, bond quality between laminae, fiber alignment, fiber registration, fiber parallelism, and processing density flaws. The degree of bonding between fiber and matrix cannot be determined by either of these methods. An alternative ultrasonic technique, angular power spectrum scanning (APSS) is recommended for quantification of this interfacial bond. Author

N90-21402*# National Aeronautics and Space Administration. Lewis Research Center, Cleveland, OH.

REVIEW AND STATISTICAL ANALYSIS OF THE ULTRASONIC VELOCITY METHOD FOR ESTIMATING THE POROSITY FRACTION IN POLYCRYSTALLINE MATERIALS

D. J. Roth, S. M. Swickard, D. B. Stang, and M. R. DeGuire (Case Western Reserve Univ., Cleveland, OH.) Mar. 1990 45 p

(NASA-TM-102501; E-5298; NAS 1.15:102501) Avail: NTIS HC A03/MF A01 CSCL 14D

A review and statistical analysis of the ultrasonic velocity method for estimating the porosity fraction in polycrystalline materials is presented. Initially, a semi-empirical model is developed showing the origin of the linear relationship between ultrasonic velocity and porosity fraction. Then, from a compilation of data produced by many researchers, scatter plots of velocity versus percent porosity data are shown for Al2O3, MgO, porcelain-based ceramics, PZT, SiC, Si3N4, steel, tungsten, UO2,(U0.30Pu0.70)C, and YBa2Cu3O(7-x). Linear regression analysis produced predicted slope, intercept, correlation coefficient, level of significance, and confidence interval statistics for the data. Velocity values predicted from regression analysis for fully-dense materials are in good agreement with those calculated from elastic properties. Author

N90-21403# California Univ., Berkeley. Lawrence Berkeley Lab. Earth Sciences Div.

A CASTING AND IMAGING TECHNIQUE FOR DETERMINING VOID GEOMETRY AND RELATIVE PERMEABILITY BEHAVIOR OF A SINGLE FRACTURE SPECIMEN

B. L. Cox, K. Pruess, and P. Persoff Jan. 1990 6 p Presented at the 15th Workshop on Geothermal Reservoir Engineering, Stanford, CA, 23-25 Jan. 1990

(Contract DE-AC03-76SF-00098)
(DE90-009192; LBL-28485; CONF-900115-2) Avail: NTIS HC A02/MF A01

A casting technique has been developed for making translucent replicas of the void space of natural rock fractures. Attenuation of light shined through the cast combined with digital image analysis provides a pointwise definition of fracture apertures. The technique has been applied to a fracture specimen from Dixie Valley, Nevada, and the measured void space geometry has been used to develop theoretical predictions of two-phase relative permeability. A strong anisotropy in relative permeabilities has been found, which is caused by highly anisotropic spatial correlations among fracture apertures. DOE

N90-21404# Lawrence Livermore National Lab., CA.
HIGH EXPLOSIVES (PBX9502) CHARACTERIZATION USING COMPUTERIZED TOMOGRAPHY
H. E. Martz, G. P. Roberson, M. F. Skeate, D. J. Schneberk, S. G. Azevedo, and S. K. Lynch (Mason and Hanger-Silas Mason Co., Inc., Amarillo, TX.) 14 Feb. 1990 104 p
(Contract W-7405-eng-48)
(DE90-008170; UCRL-ID-103318) Avail: NTIS HC A06/MF A01

X ray computed axial tomography (CAT or CT) is an advanced imaging technique which provides three-dimensional nondestructive inspection and characterization of materials, components and assemblies. The Lawrence Livermore National Laboratory (LLNL) and the Mason and Hanger-Silas Mason Co., Pantex Plant are cooperating to examine the use of CT Technology to inspect high-explosive (HE) pressings. The goals of this joint project are to study the HE pressing process using computed tomography scanners, to provide a foundation for the further development of industrial CT scanners, and to work with the private sector on the design and implementation of an automated CT inspection scanner to be used in the manufacturing process of high explosives at the Pantex Plant. The early detection of defective HE pressings will reduce the cost and improve the safety of the high-explosives production cycle. At present, all pressings are bulk density tested. In addition, samples are randomly selected from each pressing lot for destructive core sampling to obtain an estimate of internal density gradients. CT is a viable technology for a high-explosives inspection system. CT measures density variations, detects foreign inclusions and voids with a probability of detection as good as or better than present inspection techniques. In addition, CT can be fully automated to allow for a 100 percent sample inspection. DOE

39 STRUCTURAL MECHANICS

Includes structural element design and weight analysis; fatigue; and thermal stress.

For applications see *05 Aircraft Design, Testing and Performance* and *18 Spacecraft Design, Testing and Performance.*

N90-21405*# Old Dominion Univ., Hampton, VA.
THE EFFECT OF ELASTIC BOUNDARY CONDITIONS ON THE DYNAMIC RESPONSE OF RECTANGULAR PLATES M.S. Thesis
Terry K. Brewer May 1988 116 p
(Contract NAS1-17993)
(NASA-CR-186059; NAS 1.26:186059) Avail: NTIS HC A06/MF A01 CSCL 20K

Natural frequencies and forced steady-state harmonic response for the vibration of uniform rectangular plates with edges elastically restrained against rotation and transverse translation are addressed. A single mode Rayleigh-Ritz solution is derived using functions that describe the normal modes of vibration of a beam whose ends are elastically restrained. The finite element solution is obtained for comparison. MACSYMA symbolic manipulation system is implemented as an aid to the mathematical rigor of the Ritz approach, and NASTRAN finite element code is used to model the mechanical system. Comparisons are made to published results and the solutions of this study are found to give lower frequencies for some values of boundary restraint. Steady-state harmonic amplitudes of displacement and acceleration are found to agree favorably for the two solutions. Low predictions of steady-state strain from NASTRAN result in some cases when compared to the Ritz values. Finally, a subjective assessment is made about the merit of using MACSYMA and NASTRAN. Author

N90-21406 Stanford Univ., CA.
FOURIER SERIES METHODS FOR PLATES AND SHELLS WITH CRACKS AND INCLUSIONS Ph.D. Thesis
Seung-Hyun Yoo 1989 119 p
Avail: Univ. Microfilms Order No. DA8925983

Fourier series methods are applied to the analysis of plates and shells with cracks and inclusions. Although these methods typically were used for stress analysis, their application to the case of discontinuities is relatively recent. The equations are expressed in terms of the Fourier series at the discontinuity line using the conditions on the discontinuity and the continuity conditions on the remaining parts. This approach is computationally more efficient than finite element method or other classical methods because it avoids the solution of integral equation or fine meshing around the discontinuity. Important quantities such as stress intensity factors and natural frequency factors of the plates can be easily calculated. These methods are extended to solve rectangular plates with rectangular inclusions. The effects of size, location and orthotropy of such inclusions are investigated. As a direct extension of this approach, cylindrical panels with cracks are considered. Static behavior is studied using Novozhilov's equations and, Donnell-Mushtari-Vlasov equations are used for free vibration analysis. Dissert. Abstr.

N90-21407 Brown Univ., Providence, RI.
PROBLEMS ASSOCIATED WITH RESIDUAL AND MISMATCH STRESSES IN THIN FILM STRUCTURES Ph.D. Thesis
Jean-Claude Ramirez 1989 64 p
Avail: Univ. Microfilms Order No. DA9002281

Two problems dealing with thin film structures are addressed. The results of a combined experimental and analytical investigation of the effects of mechanical stress on threshold voltage in MESFETs are reported. The theoretical aspect involves a 2-D finite element simulation of the same device structure on which measurements were made. In contrast with an approximate analytical calculation reported in the literature in which the stress concentrations which occur at the gate edges were represented by concentrated line forces acting in the plane of the substrate surface, the substrate stresses and resultant piezoelectric charge distributions calculated, take into account the 2-D nature of the geometry of the gate. Accounting for the 2-D nature of the overlayer yields piezoelectric charge distributions that differ from those predicted using the more approximate concentrated force model. The experimental portion involves measurement of DC parameters of devices using the application of external mechanical loads. These loads are intended to simulate mechanical stresses which arise during device processing. By introducing this stress without any additional thermal processing, the impact of residual stresses via the piezoelectric effect on parameters such as threshold voltage can be examined separately from other effects, such as stress enhanced diffusion. A model is constructed of a thin film of a rigid-plastic material bonded to a linear elastic substrate subject to a state of mismatch strain between the two materials. The purpose is to investigate the existence of deformation localization in the film that is periodic along the direction of the bi-material interface. Bifurcation phenomena could be a possible precursor to debonding phenomena. The conditions necessary for these undulations to appear are given by a bifurcation equation which relates the internal film stress to the relative stiffness of the substrate and the thickness of the film. Dissert. Abstr.

N90-21408 Harvard Univ., Cambridge, MA.
MECHANICS OF INTERFACE FRACTURE Ph.D. Thesis

Zhigang Suo 1989 113 p
Avail: Univ. Microfilms Order No. DA8926182

Knowledge on the mechanics of interface fracture is summarized. Emphasis is placed on the analytical and numerical results obtained in the recent years. The materials considered are limited to linearly elastic ones, but nonlinear behaviors are allowed in a small zone around crack tips. Various fundamental issues involved in the definition of interfacial toughness are discussed. An engineering fracture mechanics scheme is stated, including data conversion in the experimental determination of toughness and assessment of a given interface by using the measured toughness. A collection of basic solutions is presented. These solutions are intended to calibrate fracture specimens, evaluate structures, and model fracture behaviors at microscopic levels. The parallel results for anisotropic bimaterials are also presented. A brief survey of the elements of anisotropic elasticity is included with application to crack analysis as the goal. Efforts were made to demonstrate the similarity of the solution structures between isotropic and anisotropic bimaterials. Throughout the work key problems waiting for further development are identified and discussed. Dissert. Abstr.

N90-21409*# National Aeronautics and Space Administration. Langley Research Center, Hampton, VA.
FATIGUE DAMAGE GROWTH MECHANISMS IN CONTINUOUS FIBER REINFORCED TITANIUM MATRIX COMPOSITES
W. S. Johnson, R. A. Naik, and W. D. Pollock (Analytical Services and Materials, Inc., Hampton, VA.) Jan. 1990 12 p Presented at the Fatigue 90 Conference, Honolulu, HI, 15-20 Jul. 1990
(NASA-TM-102594; NAS 1.15:102594) Avail: NTIS HC A03/MF A01 CSCL 20K

The role of fiber/matrix interface strength, residual thermal stresses, and fiber and matrix properties on fatigue damage accumulation in continuous fiber metal matrix composites (MMC) is discussed. Results from titanium matrix silicon carbide fiber composites is the primary topic of discussion. Results were obtained from both notched and unnotched specimens at room and elevated temperatures. The stress in the 0 deg fibers was identified as the controlling factor in fatigue life. Fatigue of the notched specimens indicated that cracks can grow in the matrix materials without breaking fibers. Author

N90-21410*# Lockheed Missiles and Space Co., Palo Alto, CA.
THE COMPUTATIONAL STRUCTURAL MECHANICS TESTBED GENERIC STRUCTURAL-ELEMENT PROCESSOR MANUAL
Gary M. Stanley and Shahram Nour-Omid Mar. 1990 306 p
(Contract NAS1-18444)
(NASA-CR-181728; NAS 1.26:181728; LMSC-D878511) Avail: NTIS HC A14/MF A02 CSCL 20K

The usage and development of structural finite element processors based on the CSM Testbed's Generic Element Processor (GEP) template is documented. By convention, such processors have names of the form ESi, where i is an integer. This manual is therefore intended for both Testbed users who wish to invoke ES processors during the course of a structural analysis, and Testbed developers who wish to construct new element processors (or modify existing ones). Author

N90-21411*# Analytical Services and Materials, Inc., Hampton, VA.
DIRECT FORMULATION OF A 4-NODE HYBRID SHELL ELEMENT WITH ROTATIONAL DEGREES OF FREEDOM
Mohammad A. Aminpour Washington, DC NASA Apr. 1990 27 p
(Contract NAS1-18599)
(NASA-CR-4282; NAS 1.26:4282) Avail: NTIS HC A03/MF A01 CSCL 20K

A simple 4-node assumed-stress hybrid quadrilateral shell element with rotational or drilling degrees of freedom is formulated. The element formulation is based directly on a 4-node element. This direct formulation requires fewer computations than a similar element that is derived from an internal 8-node isoparametric element in which the midside degrees of freedom are eliminated in favor of rotational degree of freedom at the corner nodes. The formulation is based on the principle of minimum complementary energy. The membrane part of the element has 12 degrees of freedom including rotational degrees of freedom. The bending part of the element also has 12 degrees of freedom. The bending part of the quadratic variations for both in-plane and out-of-plane displacement fields and linear variations for both in-plane and out-of-plane rotation fields are assumed along the edges of the element. The element Cartesian-coordinate system is chosen such as to make the stress field invariant with respect to node numbering. The membrane part of the stress field is based on a 9-parameter equilibrating stress field, while the bending part is based on a 13-parameter equilibrating stress field. The element passes the patch test, is nearly insensitive to mesh distortion, does not lock, possesses the desirable invariance properties, has no spurious modes, and produces accurate and reliable results. Author

N90-21412*# National Aeronautics and Space Administration. Langley Research Center, Hampton, VA.
INTEGRATED MODELING AND ANALYSIS OF A SPACE-TRUSS ARTICLE
Alan E. Stockwell (Lockheed Engineering and Sciences Co., Hampton, VA.), Sharon E. Perez, and Richard S. Pappa Mar. 1990 28 p Presented at the MSC World Users' Conference, Los Angeles, CA, 26-30 Mar. 1990
(NASA-TM-102615; NAS 1.15:102615) Avail: NTIS HC A03/MF A01 CSCL 20K

MSC/NASTRAN is being used in the Controls-Structures Interaction (CSI) program at NASA Langley Research Center as a key analytical tool for structural analysis as well as the basis for control law development, closed-loop performance evaluation, and system safety checks. Guest investigators from academia and industry are performing dynamics and control experiments on a flight-like deployable space truss called Mini-Mast to determine the effectiveness of various active-vibration control laws. MSC/NASTRAN was used to calculate natural frequencies and mode shapes below 100 Hz to describe the dynamics of the 20-meter-long lightweight Mini-Mast structure. Gravitational effects contribute significantly to structural stiffness and are accounted for through a two-phase solution in which the differential stiffness matrix is calculated and then used in the eigensolution. Reduced modal models are extracted for control law design and evaluation of closed-loop system performance. Predicted actuator forces from controls simulations are then applied to the extended model to predict member loads and stresses. These pre-test analyses reduce risks associated with the structural integrity of the test article, which is a major concern in closed-loop control experiments due to potential instabilities. Author

N90-21413*# Old Dominion Univ., Norfolk, VA.
USER MANUAL FOR VICONOPT: AN EXACT ANALYSIS AND OPTIMUM DESIGN PROGRAM COVERING THE BUCKLING AND VIBRATION OF PRISMATIC ASSEMBLIES OF FLAT IN-PLANE LOADED, ANISOTROPIC PLATES, WITH APPROXIMATIONS FOR DISCRETE SUPPORTS, AND TRANSVERSE STIFFENERS
F. W. Williams, M. S. Anderson, D. Kennedy, R. Butler, and G. Aston Apr. 1990 183 p Prepared in cooperation with Wales Univ. Inst. of Science and Technology, Cardiff
(Contracts NAS1-18584; NCCw-000002)
(NASA-CR-181966; NAS 1.26:181966) Avail: NTIS HC A09/MF A01 CSCL 20K

A computer program which is designed for efficient, accurate buckling and vibration analysis and optimum design of composite panels is described. The capabilities of the program are given along with detailed user instructions. It is written in FORTRAN 77 and is operational on VAX, IBM, and CDC computers and should be readily adapted to others. Several illustrations of the various aspects of the input are given along the example problems illustrating the use and application of the program. Author

N90-21414*# National Aeronautics and Space Administration. Marshall Space Flight Center, Huntsville, AL.
COMPENDIUM OF FRACTURE MECHANICS PROBLEMS
R. Stallworth, C. Wilson, and C. Meyers Apr. 1990 173 p
(NASA-TM-100393; NAS 1.15:100393) Avail: NTIS HC A08/MF A01 CSCL 20K

Fracture mechanics analysis results are presented from the following structures/components analyzed at Marshall Space Flight Center (MSFC) between 1982 and 1989: space shuttle main engine (SSME), Hubble Space Telescope (HST), external tank attach ring, B-1 stand LOX inner tank, and solid rocket booster (SRB). Results from the SSME high pressure fuel turbopump (HPFTP) second stage blade parametric analysis determine a critical flaw size for a wide variety of stress intensity values. The engine 0212 failure analysis was a time dependent fracture life assessment. Results indicated that the disk ruptured due to an overspeed condition. Results also indicated that very small flaws in the curvic coupling area could propagate and lead to failure under normal operating conditions. It was strongly recommended that a nondestructive evaluation inspection schedule be impiemented. The main ring of the HST, scheduled to launch in 1990, was analyzed by safe-life and fail-safe analyses. First safe-life inspection criteria curves for the ring inner and outer skins and the fore and aft channels were derived. Afterwards the skins and channels were determined to be fail-safe by analysis. A conservative safe-life analysis was done on the 270 redesign external tank attach ring. Results from the analysis were used to determine the nondestructive evaluation technique required. Author

N90-21415 Georgia Inst. of Tech., Atlanta.
ELASTIC-PLASTIC INSTABILITY OF PLANE FRAMES Ph.D. Thesis
Salah-Eldin Abdel-Mo Mohamed 1989 145 p
Avail: Univ. Microfilms Order No. DA9005490

A numerical procedure for the nonlinear elastic instability analysis of nonorthogonal frames and elastic-plastic instability analysis of orthogonal and nonorthogonal frames is presented. The procedure is based on nonlinear kinematic relations and linearly elastic material behavior except at the plastic regions (concentrated plasticity). The frames can have either rigid or flexible connections and the supports can be with or without elastic rotational restraint. The nonlinear flexible connections are presented by a polynomial model. The mathematical formulation is presented in detail and the solution methodology is outlined and demonstrated through several examples. Through the chosen examples, the following types of responses were observed: Elastic bifurcation instability, elastic limit point instability, elasto-plastic limit point instability, and plastic collapse. The effect of several parameters is assessed in order to enhance understanding of frame behavior. These include the effect of nonuniform geometry, of rotational restraints at the supports, of rise to span ratio, of beam to column stiffness ratio, of load eccentricity, and of joint flexible connections. It is also demonstrated that the elastic dynamic critical loads for gabled frames with fixed supports and rigid joints are less than the elastic static critical loads by 15 to 30 percent. It is also found that the assumption of linear (instead of nonlinear, polynomial) connections behavior is not acceptable. It is further concluded that true behavior of frames structures can be obtained only by incorporating both stability and strength in the analysis. Dissert. Abstr.

N90-21416 Stevens Inst. of Tech., Hoboken, NJ.
DEVELOPMENT OF A FRACTURE ANALYSIS TECHNIQUE FOR USE WITH A GENERAL-PURPOSE FINITE ELEMENT PROGRAM Ph.D. Thesis
Jennifer Cordes 1989 140 p
Avail: Univ. Microfilms Order No. DA9001129

A fracture-critical analytical model was developed and tested for prediction of failure in structural components. The analytic model creates a fictitious crack region adjacent to an actual crack or notch and uses finite element analysis to predict actual crack initiation, crack growth, and ultimate failure of the component. Unlike other approaches, this model: (1) predicts directly the loading condition causing failure in a structural component; (2) predicts failure in either a brittle or a ductile material; and (3) predicts the mode of failure (yielding or fracture) in a ductile material. The method was developed for use with a general-purpose finite element program. The fictitious crack model is based upon the Dugdale and Barenblatt damage zone models. In the fictitious crack model, the damage zone is represented by cohesive forces which act along surfaces at the crack front. As the applied load is increased, the size of the damage zone increases and the overall stiffness of the structure decreases. When the maximum load on the structure is reached, unstable crack growth occurs and the cohesive forces go to zero. In the finite element model, the cohesive forces are represented by nonlinear springs. The springs provide the material nonlinearities associated with a growing damage zone. Geometric nonlinearities associated with the large strain at the crack tip can also be included in the analysis. The analytical model was tested by comparing predicted results to experimental results described in the literature. In general, predicted results were within 12 percent of experimental failure loads for an aluminum late with a central precrack, an aluminum plate with a center hole and radial cracks, a graphite/epoxy plate with a center hole, a graphite/epoxy beam with a center crack, and a glass/epoxy with a matrix crack. Author

N90-21417 Illinois Univ., Chicago.
DETERMINATION OF STRESSES AROUND CUTOUTS IN MULTILAYERED COMPOSITE PLATE AND SHELL STRUCTURES Ph.D. Thesis
Missoum Moumene 1989 151 p
Avail: Univ. Microfilms Order No. DA9003736

A finite element formulation for evaluating stresses around cutouts in thin to moderately thick laminated composite plate- and shell-type structures is presented. First, the eight-noded isoparametric quadrilateral element with independent rotational and displacement degrees of freedom is extended to laminated composite elements. The element includes an arbitrary number of bonded layers, each of which may have a different thickness, orientation of principal material directions, and elastic properties. The transverse shear deformation, which is a predominant factor in the analysis of laminated composite structures, is taken into account in developing the stiffness matrix. Second, the formulated element is considered for accurate determination of stresses around cutouts in composite as well as isotropic plate- and shell-type structures. The powerfulness of the element is established to such stress concentration problems. Several isotropic and advanced composite structures with circular hole, subjected to different types of loading are analyzed. Numerical results show that the present element is as efficient and accurate as the customary used triangular element. It is the first multilayered quadrilateral element that is employed efficiently and successfully for the finite element studies of shells and plates with cutouts. Dissert. Abstr.

N90-21418# Case Western Reserve Univ., Cleveland, OH.
STRESS ANALYSIS AND MINIMUM WEIGHT DESIGN OF HONEYCOMB SANDWICH PLATES Ph.D. Thesis
Yong-Seok Shin 1989 116 p
Avail: Univ. Microfilms Order No. DA9004512

A computer aided analytical solution is presented for the analysis and design of minimum weight hex-cell and square cell honeycomb core sandwich plates subjected to a uniformly distributed load. The design variables are the configuration parameters. The constraints considered are the maximum stress and deflection, the core cell buckling, and the face local deflection on the perforated region of the core as well as the bounds of the design variables. In order to evaluate the mechanical behavior, a higher order sandwich plate theory is developed. This theory predicts the deflections and stresses accurately when compared to the 3-D elasticity solutions. The intercell buckling analysis is accomplished under the combined stress condition consisting of nonuniform bending, shear, and transverse normal stress. The optimal design problem is cast into a model of a nonlinear mathematical programming problem which is solved with the Generalized Reduced Gradient direction generation method. The

optimum face thickness, core depth, cell wall thickness, and cell size are determined for the stainless steel honeycomb sandwich panels by way of example. Dissert. Abstr.

N90-21419 Southampton Univ. (England).
WAVE RECEPTANCE ANALYSIS OF VIBRATING BEAMS AND STIFFENED PLATES Ph.D. Thesis
Yavuz Yaman 1989 402 p
Avail: Univ. Microfilms Order No. BRDX87379

Analytical methods for the analysis of harmonically forced vibrations of multi-supported beams and stiffened plates are developed. The methods are based on the response of infinite, uninterrupted structures to a single external excitation from which families of waves propagate outwards in all directions. The structures considered are uniform in thickness. The beams have a single-point force. The plates are finite in width with the two opposite parallel edges being simply supported along the length. A line forcing varies sinusoidally between those edges. The first part analyses the dynamics of infinite, uninterrupted structures. Special attention is subsequently paid to three-layered sandwich structures and their dispersion characteristics are also investigated. The second part considers finite structures. An analytical approach is presented for single-bay and multi-bay structures with arbitrary support spacing. Influences of support elastic/inertial characteristics are investigated in detail. Effects of end reflections are fully dealt with. The third part deals with the free and forced vibrations of infinite, periodic structures. Particular attention is focused on the effects of stiffness characteristics and cross-sectional distortion of the stiffeners. Part four outlines experimental work undertaken to validate the above theories. The experimental and theoretical results are compared.
Dissert. Abstr.

N90-21420*# Sverdrup Technology, Inc., Cleveland, OH.
THERMOMECHANICAL DEFORMATION TESTING AND MODELING IN THE PRESENCE OF METALLURGICAL INSTABILITIES M.S. Thesis - Akron Univ. Final Report
Michael G. Castelli Jan. 1990 172 p
(Contract NAS3-25266)
(NASA-CR-185188; E-5243; NAS 1.26:185188) Avail: NTIS HC A08/MF A01 CSCL 20K

A number of viscoplastic constitutive models were developed to describe deformation behavior under complex combinations of thermal and mechanical loading. Questions remain, however, regarding the validity of procedures used to characterize these models for specific structural alloys. One area of concern is that the majority of experimental data available for this purpose are determined under isothermal conditions. This experimental study is aimed at determining whether viscoplastic constitutive theories characterized using an isothermal data base can adequately model material response under the complex thermomechanical loading conditions typical of power generation service. The approach adopted was to conduct a series of carefully controlled thermomechanical experiments on a nickel-based superalloy, Hastelloy Alloy X. Previous investigations had shown that this material experiences metallurgical instabilities leading to complex hardening behavior, termed dynamic strain aging. Investigating this phenomenon under full thermomechanical conditions leads to a number of challenging experimental difficulties which up to the present work were unresolved. To correct this situation, a number of advances were made in thermomechanical testing techniques. Advanced methods for dynamic temperature gradient control, phasing control and thermal strain compensation were developed and incorporated into real time test control software. These advances allowed the thermomechanical data to be analyzed with minimal experimental uncertainty. The thermomechanical results were evaluated on both a phenomenological and microstructural basis. Phenomenological results revealed that the thermomechanical hardening trends were not bounded by those displayed under isothermal conditions. For the case of Hastelloy Alloy X (and similar dynamic strain aging materials), this strongly suggests that some form of thermomechanical testing is necessary when characterizing a thermoviscoplastic deformation model. Transmission electron microscopy was used to study the microstructural physics, and analyze the unique phenomenological behavior. Author

N90-21421*# Analytical Services and Materials, Inc., Hampton, VA.
DELAMINATION FAILURE IN A UNIDIRECTIONAL CURVED COMPOSITE LAMINATE
Roderick H. Martin Apr. 1990 44 p
(Contract NAS1-18599)
(NASA-CR-182018; NAS 1.26:182018) Avail: NTIS HC A03/MF A01 CSCL 20K

Delamination failure in a unidirectional curved composite laminate was investigated. The curved laminate failed unstably by delaminations developing around the curved region of the laminate at different depths through the thickness until virtually all bending stiffness was lost. Delamination was assumed to initiate at the location of the highest radial stress in the curved region. A closed form curved beam elasticity solution and a 2-D finite element analysis (FEA) were conducted to determine this location. The variation in the strain energy release rate, G, with delamination growth was then determined using the FEA. A strength-based failure criteria adequately predicted the interlaminar tension failure which caused initial delamination onset. Using the G analysis the delamination was predicted to extend into the arm and leg of the laminate, predominantly in mode I. As the initial delamination grew arould the curved region, the maximum radial stress in the newly formed inner sublaminate increased to a level sufficient to cause a new delamination to initiate in the sublaminate with no increase in applied load. This failure progression was observed experimentally. Author

N90-21422*# National Aeronautics and Space Administration. Langley Research Center, Hampton, VA.
NASA AIRFRAME STRUCTURAL INTEGRITY PROGRAM
Charles E. Harris Apr. 1990 20 p
(NASA-TM-102637; NAS 1.15:102637) Avail: NTIS HC A03/MF A01 CSCL 20K

NASA initiated a research program with the long-term objective of supporting the aerospace industry in addressing issues related to the aging of the commercial transport fleet. The program combines advanced fatigue crack growth prediction methodology with innovative nondestructive examination technology with the focus on multi-stage damage (MSD) at rivited connections. A fracture mechanics evaluation of the concept of pressure proof testing the fuselage to screen for MSD was completed. A successful laboratory demonstration of the ability of the thermal flux method to detect disbonds at rivited lap splice joints was conducted. All long-term program elements were initiated, and the plans for the methodology verification program are being coordinated with the airframe manufacturers. Author

N90-21423# Laboratorio de Computacao Cientifica, Rio de Janeiro (Brazil).
A NUMERICAL MODEL FOR THE DETERMINATION OF PERIODIC SOLUTIONS OF PIPES SUBJECTED TO NON-CONSERVATIVE LOADS
P. A. Velloso and A. C. Galeio May 1989 13 p
(DE90-614756; LNCC-006/89) Avail: NTIS (US Sales Only) HC A03/MF A01

This paper deals with nonlinear vibrations of pipes subjected to non-conservative loads. Periodic solutions of these problems are determined using a variational approach based on Hamilton's Principle combined with a Fourier series expansion to describe the displacement field time dependence. A finite element model which utilizes Hemite's cubic interpolation for both axial and transversal displacement amplitudes is used. This model is applied to the problem of a pipe subjected to a tangential and a normal follower force. The numerical results obtained with this model are compared with the corespondent solutions determined using a total Lagrangian description for the Principle of Virtual Work, coupled with Newmark's step-by-step integration procedure. It is shown that for small to moderate displacement amplitudes the

one-term Fourier series approximation compares fairly well with the predicted solution. For large displacements as least a two-term approximation should be utilized. DOE

N90-21424*# National Aeronautics and Space Administration. Langley Research Center, Hampton, VA.
AN EVALUATION OF THE PRESSURE PROOF TEST CONCEPT FOR THIN SHEET 2024-T3
D. S. Dawicke (Analytical Services and Materials, Inc., Hampton, VA.), C. C. Poe, Jr., James C. Newman, Jr., and Charles E. Harris Apr. 1990 32 p
(NASA-TM-101675; NAS 1.15:101675) Avail: NTIS HC A03/MF A01 CSCL 20K

The concept of pressure proof testing of fuselage structures with fatigue cracks to insure structural integrity was evaluated from a fracture mechanics viewpoint. A generic analytical and experimental investigation was conducted on uniaxially loaded flat panels with crack configurations and stress levels typical of longitudinal lap splice joints in commercial transport aircraft fuselages. The results revealed that the remaining fatigue life after a proof test was longer than that without the proof test because of crack growth retardation due to increased crack closure. However, based on a crack length that is slightly less than the critical value at the maximum proof test stress, the minimum assured life or proof test interval must be no more than 550 pressure cycles for a 1.33 proof factor and 1530 pressure cycles for a 1.5 proof factor to prevent in-flight failures. Author

N90-21425# Technische Hogeschool, Delft (Netherlands). Dept. of Aerospace Engineering.
FLUTTER OF SLENDER BODIES UNDER AXIAL STRESS
R. Coene Nov. 1988 22 p
(PB90-167024; LR-563) Avail: NTIS HC A03/MF A01 CSCL 20K

Solutions of the equations of motion of flexible slender bodies with constant body sections are derived. For a certain axial stress the divergence speed and the flutter speed are obtained. The new results are compared with a classical waving flag result in 2-D flow. The theoretical predictions compare favorably with experimental results for some paper strips. Author

N90-21426# Queensland Univ., Brisbane (Australia). Dept. of Civil Engineering.
ELASTO-PLASTIC LARGE DEFORMATION ANALYSIS OF THIN-WALLED STRUCTURES
F. G. A. Al-Bermani and S. Kitipornchai Apr. 1989 43 p
Sponsored by Australian Research Council
(PB90-164757; RR-CE101; ISBN-0-86776-336-1; ISSN-0784-3143) Avail: NTIS HC A03/MF A01 CSCL 20K

An elasto-plastic, large deformation analysis of thin walled structures is presented. A solution procedure for treating both the geometric and material nonlinearities, based on an updated Lagrangian formulation is proposed. The procedure is suitable for analyzing large scale space frames since the structures may be modelled using only a single beam-column element per member. It is achieved by incorporating a displacement stiffness matrix which provides the necessary coupling between the axial stretching and the flexural and torsional deformations. The geometric and the displacement stiffness matrices for a general thin walled beam-column element are used. Plastic hinge formation, the interaction of element forces at the hinges, and elastic unloading are taken into account in the analysis. Several numerical examples are presented to demonstrate the accuracy and efficiency of the method. Author

N90-21427# Technische Hogeschool, Delft (Netherlands). Dept. of Aerospace Engineering.
FRACTOGRAPHIC ANALYSIS OF THE CRACK GROWTH RATE AND THE SHEAR LIP DEVELOPMENT OF 2024-T3 SPECIMENS UNDER SIMPLE VARIABLE-AMPLITUDE LOADING
M. R. Ling and J. Schijve Nov. 1988 61 p
(PB90-167032; LR-566) Avail: NTIS HC A04/MF A01 CSCL 20K

Sequence effects on fatigue crack growth under variable amplitude (VA) load histories were studied. The crack surfaces of 2024 sheet materials obtained in fatigue tests under two simple VA load sequences were studied under the electron microscopes (TEM and SEM). Phenomena, like the giant striation induced by the first overload cycle, the delayed retardation after applying overload(s), etc., were observed and evaluated. The crack growth rates during and after the overload(s) and underload(s) were measured and compared with the predictions. Possible effects of the shear lip width on the crack growth were estimated by new crack growth data. Comparisons between the test results and the CA data obtained with the corresponding shear lip width are provided. Author

N90-21428# Helsinki Univ. of Technology, Espoo (Finland). Dept. of Mechanical Engineering.
A MODIFICATION OF A LOW-ORDER REISSNER-MINDLIN PLATE BENDING ELEMENT
Leopoldo P. Franca (Laboratorio de Computacao Cientifica, Rio de Janeiro, Brazil) and Rolf Stenberg Aug. 1989 17 p
Sponsored by Ministere Francais des Affaires Etrangeres
(PB90-165630; ISBN-951-754-997-0; ISSN-0783-9375; Rept-9) Avail: NTIS HC A03/MF A01 CSCL 20K

A modification of a recent plate bending element by Arnold and Falk is proposed. The optimal convergence rate of the original method is preserved, but the modification is considerably easier to implement. Author

N90-21429# Technische Hogeschool, Delft (Netherlands). Dept. of Aerospace Engineering.
REVIEW OF FORMULAE FOR THE BUCKLING OF SIMPLY-SUPPORTED, ORTHOTROPIC PLATES UNDER SHEAR LOAD, INCLUDING TRANSVERSE SHEAR EFFECTS
P. G. vanBladel Nov. 1988 60 p
(PB90-167073; LR-571) Avail: NTIS HC A04/MF A01 CSCL 20K

Some approaches to the calculation of the buckling load of simply-supported, rectangular orthotropic plates loaded in shear, with and without transverse shear deformation are reviewed. The purpose is to find simple, yet reliable formulae. At the same time, infinitely long panels are addressed. The effectiveness of the parabolic interaction formula for compression and shear is also evaluated. Author

N90-21430# Sandia National Labs., Albuquerque, NM.
AN INTERNAL/EXTERNAL PRESSURE, TENSION/COMPRESSION MULTIAXIAL FATIGUE SYSTEM
Ray J. Bourcier, Wendell B. Jones, and David T. Schmale 1990 4 p Presented at the ASTM Symposium on Rapid Load Fracture Testing, San Francisco, CA, 23 Apr. 1990
(Contract DE-AC04-76DP-00789)
(DE90-009510; SAND-90-1080C; CONF-900474-1) Avail: NTIS HC A01/MF A01

As computers become increasingly powerful, the constitutive models used in structural analysis codes become increasingly sophisticated. With the current generation of supercomputers, it now seems reasonable to consider incorporating relatively detailed representations of the multiaxial deformation response of engineering alloys. To aid in the development of such models and to allow measurement of their constituent parameters, a complex multiaxial deformation test system was designed. The system to be described was developed to perform non-proportional cycling of thin-walled metal tubes using internal/external fluid pressure and tensile/compressive axial loading. It was added to an existing MTS 490 kN load frame with a PDP 11/34-based computer control system. Features of interest include: specimen grips, the high pressure chamber, the hydraulic intensifier and controller, and associated valving and switching. Initial software for this system was written on the PDP 11/34 in the MTS MultiUser-BASIC language to perform simple proportional multiaxial

cyclic deformation to a prescribed effective plastic strain limit.
DOE

42 GEOSCIENCES (GENERAL)

N90-21431# Joint Publications Research Service, Washington, DC.
JPRS REPORT. SCIENCE AND TECHNOLOGY. USSR: EARTH SCIENCES
6 Dec. 1988 21 p Transl. into ENGLISH of various Russian documents
(JPRS-UES-88-004) Avail: NTIS HC A03/MF A01
Abstracts of articles dealing with research in the Earth sciences are given. Subject areas include geology, oceanography, and atmospheric physics. R.J.F.

N90-21432# Joint Publications Research Service, Washington, DC.
JPRS REPORT. SCIENCE AND TECHNOLOGY. USSR: EARTH SCIENCES
5 May 1989 26 p Transl. into ENGLISH of various Russian documents
(JPRS-UES-89-002) Avail: NTIS HC A03/MF A01
Abstracts of research in the Earth Sciences are given. The topics covered include arctic and Antarctic research, geology, meteorology, oceanography, and atmospheric physics. R.J.F.

N90-21433# Joint Publications Research Service, Arlington, VA.
JPRS REPORT: SCIENCE AND TECHNOLOGY. USSR: EARTH SCIENCES
19 Apr. 1990 27 p Transl. into ENGLISH of various Russian documents
(JPRS-UES-90-005) Avail: NTIS HC A03/MF A01
Science and technology abstracts are given. Topics in geology, oceanography, atmospheric physics and ecology are covered.
R.J.F.

N90-21434# Joint Publications Research Service, Arlington, VA.
JPRS REPORT: SCIENCE AND TECHNOLOGY. USSR: LIFE SCIENCES
29 Mar. 1990 39 p Transl. into ENGLISH of various Russian documents
(JPRS-ULS-90-002) Avail: NTIS HC A03/MF A01
Abstracts of research in life sciences are given. Research in agricultural science, biochemistry, biophysics, biotechnology, epidemiology, genetics, immunology, industrial medicine, laser bioeffects, microbiology, military medicine, molecular biology, nonionizing radiation effects, pharmacology, and toxology is covered. R.J.F.

43 EARTH RESOURCES AND REMOTE SENSING

Includes remote sensing of earth resources by aircraft and spacecraft; photogrammetry; and aerial photography.

For instrumentation see *35 Instrumentation and Photography.*

N90-21435# Instituto de Pesquisas Espaciais, Sao Jose dos Campos (Brazil).
PROGRAMME OF THE INTERNATIONAL TRAINING COURSE ON REMOTE SENSING FOR AFRICAN SPECIALISTS
Tania Maria Sausen Apr. 1989 40 p Presented at a Training Course, Sao Jose dos Campos, Brazil, Aug. 1987 - Apr. 1988
(INPE-4878-NTE/290) Avail: NTIS HC A03/MF A01
The Institute for Space Research of Brazil (Instituto de Pesquisas Espaciais - INPE) is a Brazilian research and development organization working for more than 15 years with Remote Sensing. One of INPE's main concerns is the transference of technology to different users in its country and abroad. This is done through remote sensing courses, training orientation, master degree programs and specialization programs such as the 2nd International Course on Remote Sensing. This course was offered by the Brazilian Government in cooperation with INPE and the Space Application Division of the United Nations Organization and was intended for specialists from African countries. The objective of this course is to qualify specialists from developing countries in remote sensing research and techniques for survey and monitoring of natural resources. Author

N90-21436*# National Aeronautics and Space Administration. Goddard Space Flight Center, Greenbelt, MD.
SHADE IMAGES OF FORESTED AREAS OBTAINED FROM LANDSAT MSS DATA
Yosio Edemir Shimabukuro (Instituto de Pesquisas Espaciais, Sao Jose dos Campos, Brazil) and James A. Smith Feb. 1989 10 p Presented at the 22nd International Symposium on Remote Sensing of Environment, Abidjan, Ivory Coast, 20-26 Oct. 1988
(NASA-TM-102939; NAS 1.15:102939; INPE-4797-PRE/1451)
Avail: NTIS HC A02/MF A01 CSCL 05B
The pixel size in the present day Remote Sensing systems is large enough to include different types of land cover. Depending upon the target area, several components may be present within the pixel. In forested areas, generally, three main components are present: tree canopy, soil (understory), and shadow. The objective is to generate a shade (shadow) image of forested areas from multispectral measurements of LANDSAT MSS (Multispectral Scanner) data by implementing a linear mixing model, where shadow is considered as one of the primary components in a pixel. The shade images are related to the observed variation in forest structure, i.e., the proportion of inferred shadow in a pixel is related to different forest ages, forest types, and tree crown cover. The Constrained Least Squares (CLS) method is used to generate shade images for forest of eucalyptus and vegetation of cerrado using LANDSAT MSS imagery over Itapeva study area in Brazil. The resulted shade images may explain the difference on ages for forest of eucalyptus and the difference on three crown cover for vegetation of cerrado. Author

N90-21437# Instituto de Pesquisas Espaciais, Sao Jose dos Campos (Brazil).
RESULTS OF THE GONDWANA PROJECT: AN EXAMPLE OF INTERCONTINENTAL GEOLOGIC CORRELATION UTILIZING LANDSAT IMAGERY [RESULTADOS DO PROJETO GONDWANA: UM EXEMPLO DE CORRELACAO GEOLOGICA INTERCONTINENTAL UTILIZANDO IMAGENS LANDSAT]
Roberto PereiradaCunha, Paulo Roberto Martini, and Edison Crepani Aug. 1989 13 p In PORTUGUESE; ENGLISH summary Presented at the 3rd Brazilian Symposium on Remote Sensing, Rio de Janeiro, Brazil, 28-30 Nov. 1984
(INPE-4870-PRE/1481) Avail: NTIS HC A03/MF A01
The main results in INPE's GONDWANA Project are presented. The project focus was on a geological comparison between Northeast Brazil and West Africa using LANDSAT and RADAR imageries. It is shown that Northeast Brazil and West Africa in the Late Proterozoic were under a same regional stress configuration characterized by similar styles of deformation. When the maps of both areas are placed in a pre-drift configuration (Bullard type) Northeast Brazil and West Africa display a regional strike-slip pattern similar to Hercynian or Tibetan terrains. Author

N90-21438# Instituto de Pesquisas Espaciais, Sao Jose dos Campos (Brazil).
REMOTE SENSING APPLIED TO SEA WATER QUALITY RESEARCHES IN COASTAL REGIONS: A REVIEW
Claudia ZuccariFernandesBraga and Myrian deMouraAbdon Sep. 1989 20 p In PORTUGUESE; ENGLISH summary Presented at the 3rd Congresso Brasileiro de Defesa do Meio Ambiente, Rio de Janeiro, Brazil, 24-28 Jul. 1989
(INPE-4935-PRE/1425) Avail: NTIS HC A03/MF A01
Research on water quality in coastal areas with remote sensing data utilization is examined. Water quality parameters which give

better correlations with spectral data obtained by satellites are presented. Methods for treatments and analyses of data used for monitoring different types of pollution in coastal areas are discussed. Author

N90-21439# Instituto de Pesquisas Espaciais, Sao Jose dos Campos (Brazil).
WHEAT YIELD ESTIMATION AT THE FARM LEVEL USING LANDSAT TM AND AGROMETEOROLOGICAL DATA
Bernardo Friedrich T Rudorff and Getulio T. Batista Dec. 1989 24 p Sponsored in part by the Fundacao Banco do Brasil Submitted for publication
(INPE-5017-RPE/611) Avail: NTIS HC A03/MF A01

Wheat plays an important role in the Brazilian commodity production. Therefore, objective and reliable methods for yield estimation are needed especially at the farm level where several management actions have to be taken. TM LANDSAT and agrometeorological data were integrated in a model for wheat yield estimation at the farm level for a test site in the south of Sao Paulo State. LANDSAT data for the crop years of 1986 (three acquisitions) and 1987 (two acquisitions), agronomic and meteorological data were related to yield estimates at the field level (200 fields approximately). Results have shown that a vegetation index derived from TM LANDSAT explained 60 and 40 percent of wheat yield variability for the two crop years analyzed. The joint use of both vegetation index and agrometeorological data in a single model improved significantly the results as compared to either vegetation index or agrometeorological data separately. The proposed model is to be validated for future crop seasons; nevertheless, it provided objective and reasonably accurate results for wheat estimation on the two crop seasons analyzed. Author

N90-21440# Instituto de Pesquisas Espaciais, Sao Jose dos Campos (Brazil).
GEOBOTANICAL REMOTE SENSING: A REVIEW
Waldir Renato Paradella and William David Bruce (Canada Centre for Remote Sensing, Ottawa, Ontario) Aug. 1989 56 p In PORTUGUESE; ENGLISH summary Submitted for publication
(INPE-5026-PRE/1565) Avail: NTIS HC A04/MF A01

Recent advances in Remote Sensing technology have encouraged research toward the developments of new approaches to the application of the concept of Geobotany to geological mapping and resource exploration (mineral and hydrocarbon). The relationship between Geobotany and Remote Sensing is examined from a conceptual perspective. As a consequence of this, a basic distinction between Background Geobotany and Target Geobotany is established. The theoretical basis for this distinction, their practical interdependence and their operational potential as geological mapping and exploration tools are also analyzed. A current update to recent bibliographic works is also provided of Geobotany and Remote Sensing. Author

N90-21441# Instituto de Pesquisas Espaciais, Sao Jose dos Campos (Brazil).
AGRICULTURAL YIELD ESTIMATION OF SUGARCANE BASED ON AGROMETEOROLOGICAL-SPECTRAL MODEL
Bernardo Friedrich T Rudorff and Getulio T. Batista Nov. 1989 46 p Submitted for publication Sponsored in part by Banco do Brasil Foundation
(INPE-5016-RPE/610) Avail: NTIS HC A03/MF A01

This work has the objective to assess the performance of a yield estimation model for sugarcane (Succharum officinarum). The model uses orbital gathered spectral data along with yield estimated from an agrometeorological model. The test site includes the sugarcane plantations of the Barra Grande Plant located in Lencois Paulista municipality in Sao Paulo State. Production data of four crop years were analyzed. Yield data observed in the first crop year (1983/84) were regressed against spectral and agrometeorological data of that same year. This provided the model to predict the yield for the following crop year i.e., 1984/85. The model to predict the yield of subsequent years (up to 1987/88) were developed similarly, incorporating all previous years data. The yield estimations obtained from these models explained 69, 54, and 50 percent of the yield variation in the 1984/85, 1985/86, and 1986/87 crop years, respectively. The accuracy of yield estimations based on spectral data only (vegetation index model) and on agrometeorological data only (agrometeorological model) were also investigated. Author

N90-21442# Instituto de Pesquisas Espaciais, Sao Jose dos Campos (Brazil).
MONITORING OF AGROCATTLE-RAISING PROJECTS THROUGH VISUAL/DIGITAL ANALYSIS OF LANDSAT-TM IMAGERY SOUTH OF PARA STATE [MONITORAMENTO DE PROJETOS AGROPECUARIOS ATRAVES DA ANALISE VISUAL/DIGITAL DE IMAGENS LANDSAT-TM NO SUL DO ESTADO DO PARA]
Jose SimeaodeMedeiros, Roberto W. OliveiraDias, Francisco LunaToledo, and Edson EijiSano (Superintendancy of the Development of the Amazon Region, Recife, Brazil) Sep. 1989 14 p In PORTUGUESE; ENGLISH summary Presented at the 5th Brazilian Symposium on Remote Sensing, Natal, Brazil, Oct. 1988
(INPE-4982-PRE/1542) Avail: NTIS HC A03/MF A01

A study was carried out in order to develop a methodology for the agrocattle-raising projects mapping in order to create ancillary data for guiding and helping the SUDAM fiscalization and evaluation system. A study area in the Amazonic region, south of Para state, located approximately in 8 deg 30 min to 9 deg 15 min latitude and 5 deg 00 min to 51 deg 00 min longitude, with ten agrocattle-raising properties was selected. An interactive procedure using both visual image interpretation and digital processing of TM LANDSAT data was developed. The following classes were mapped as follows: natural, vegetation, clean pasture, dirty pasture, very dirty pasture, raising pasture, bare soil, infrastructure natural vegetation regeneration, burned area, roads and reservoirs. The pastureland qualities, from the deforest total area to pastureland formation (85.775 ha) were observed. It was noted that 57 percent are occupied by the class dirty pasture (49.148 ha), and 24 percent are occupied by the class very dirty pasture (20.753 ha). Author

N90-21443# Instituto de Pesquisas Espaciais, Sao Jose dos Campos (Brazil).
SURVEY OF LAND USE THROUGH REMOTE SENSING [COBERTURA E USO DA TERRA ATRAVES DE SENSORIAMENTO REMOTO]
Madalena NieroPereira, Maria deLourdesNdeOKurkdjian, and Celina Foresti Nov. 1989 120 p In PORTUGUESE; ENGLISH summary
(INPE-5032-MD/042) Avail: NTIS HC A06/MF A01

Different products are shown for remote sensing used for land use survey; land use classification systems; definition and example of land use identification criterias through the utilization of remote sensing techniques and methologies for digital processing/monitoring of land use. As an addition to this information a practical example of land use survey is shown in all phases, developed at INPE using LANDSAT-TM data. Author

N90-21444# Instituto de Pesquisas Espaciais, Sao Jose dos Campos (Brazil).
A KNOWLEDGE-BASED INFORMATION BASED FOR CROP AREA ESTIMATION
Flavio Roberto Dias Velasco, Leila Maria Garcia Fonseca, Guaraci Jose Erthal, Leonardo SantAnnaBins, and Antonio Miguel Vieir Monteiro Oct. 1989 9 p Presented at the 4th Simposio Latinoamericano sobre Sensores Remotos, Bariloche, Argentina, 20-24 Nov. 1989 Sponsored in part by SID Informatica, Projeto Estra
(INPE-4990-PRE/1555) Avail: NTIS HC A02/MF A01

For reasons of accuracy and timeliness, it is interesting that a system for crop production estimation be as automatic as possible, making use of digital processing of satellite images. Some mandatory as well as desirable requirements are discussed for such a system and the architecture of a computer information system designed to estimate crop area based on satellite images

is presented. To meet the requirements, it is proposed a knowledge-bases system to estimate crop area through the integration of satellite image information with maps (thematic and conventional) and tabular census data. The information needed is extracted by independent knowledge sources (KS) (experts) and communicated and integrated through a global structured memory area (blackboard model). Author

N90-21445# Instituto de Pesquisas Espaciais, Sao Jose dos Campos (Brazil). Departamento de Processamento de Imagens.
ANALYSIS AND MODELLING OF SPATIAL DATA PROPOSAL OF A SYSTEM FOR CBERS
Diogenes Salas Alves, Gilberto Camara Neto, Ricardo Cartaxo ModestodeSouza, Juan Carlos PintodeGarrido, and Fernando Augusto Mit li Oct. 1989 8 p Presented at the 4th Simposio Latinoamericano sobre Sensores Remotos, Bariloche, Argentina, 20-24 Nov. 1989
(INPE-4911-PRE/1512) Avail: NTIS HC A02/MF A01

Requirements are introduced for an analysis/modeling system of spatial information, aimed at combining remotely sensed data with information from other sources. The work was conceived as an aid for INPE's CBERS Ground Applications Segment, that encompasses development of an integrated system to perform the tasks of reception, production and spatial analysis. Current requirements concern aspects of visualization, input, storage, retrieval and manipulation of spatial data. A special topic formulates some guidelines for software development. Author

N90-21446# Instituto de Pesquisas Espaciais, Sao Jose dos Campos (Brazil).
PROJECT CANASATE: REMOTE SENSING APPLIED TO SUGAR CANE CROP SURVEY [PROJETO CANASATE: SENSORIAMENTO REMOTO APLICADO AO LEVANTAMENTO DA CULTURA CANAVIEIRA]
Francisco Jose Mendonca, Getulio TeixeiraBatista, and Antonio TebaldiTardin Jul. 1989 18 p In PORTUGUESE; ENGLISH summary Presented at the 3rd Brazilian Symposium on Remote Sensing, Rio de Janeiro, Brazil, 28-30 Mar. 1984
(INPE-4902-PRE/1503) Avail: NTIS HC A03/MF A01

The objective of the CANASATE project is the development of a system for area estimation and mapping of sugar cane plantations at the national level, using remote sensing techniques. In this project, the sugar cane region was divided into: Area 1, corresponding to Sao Paulo, Rio de Janeiro and Parana States, where satellite data are used; Area 2, corresponding to Pernambuco and Alagoas States, where aerial photographs are used, for these states present constant cloud cover problems during LANDSAT overpasses; and Area 3, corresponding to other states where there exists at least one operating sugar or alcohol production plant. The methological approach is based on the visual interpretation of LANDSAT images at the scale of 1:250,000, through the exploration of spatial, temporal and multispectral characteristics of these data, as well as on aircraft data with support of field work. A statistical sampling procedure will be used for mapping accuracy assessment. The interpreted sugar cane theme will be transferred to available cartographic bases for final presentation. A digitizer and a plotter attached to a microcomputer will be used for sugar cane area estimation at a municipal level. Author

N90-21447# Instituto de Pesquisas Espaciais, Sao Jose dos Campos (Brazil).
GENERATION OF TRIANGULAR FORM MODELS IN A MICROCOMPUTER ENVIRONMENT [GERACAO DE MODELOS DE GRADE TRIANGULAR EM AMBIENTE DE MICROCOMPUTADOR]
Carlos Alberto Felgueiras, Claudia Akiko Urashima, and Marcia LopesCancioPSoares Oct. 1989 9 p In PORTUGUESE; ENGLISH summary Presented at the 4th Latin American Symposium on Remote Sensing, Bariloche, Argentina, 20-24 Nov. 1989
(INPE-4974-PRE/1539) Avail: NTIS HC A02/MF A01

A methology is presented to generate digital terrain models in a triangular irregular form. The methodology is implemented in a microcomputer IBM-PC like environment. To compensate the limitations of processing speed and main memory of this environment, data structures, and the memory need to be optimized to allow the program to work with large amount of samples. An analysis of the time cost versus the amount of samples is performed. Author

N90-21448# Instituto de Pesquisas Espaciais, Sao Jose dos Campos (Brazil).
DIGITAL PROCESSING OF TM/LANDSAT DATA IN MONITORING INTERIOR WATER [PROCESSAMENTO DIGITAL DE DADOS TM/LANDSAT NO MONITORAMENTO DE AGUAS INTERIORES]
Moacir GodoyJunior and Evlyn Marcia Leao MoraesNovo Nov. 1989 24 p In PORTUGUESE; ENGLISH summary
(INPE-4956-PRE/1533) Avail: NTIS HC A03/MF A01

Results are presented from an experiment performed to assess the performance of the median recursive filter for stripping removal from TM/LANDSAT data. The experiment consisted of comparing the resulting images in terms of their potential for water and land use classification. This comparison was performed taking into account two types of remote sensor data user: the user interested in manual interpretation and the user interested in digital interpretation. As far as the potential for manual interpretation is concerned, the different images were compared in terms of the digital filtering effects on the elements of importance for the information extraction: color, texture, shape, and contrast. The image performance in terms of digital classification was assessed by comparing the classification matrix resulting from the application of a maximum likelihood algorithm to each data set: reflectance image; reflectance filtered image; and composite image. The performance of each data set was assessed through the percent of correct classification produced by the samples used to train the system. The results indicate that the filtered image allowed greater separability between optically distinct water classes, however presenting a poor performance for non-aquatic targets as far as digital analysis was concerned. For manual analysis, however, the composite image was the best. Author

N90-21449# Instituto de Pesquisas Espaciais, Sao Jose dos Campos (Brazil).
CHARACTERIZATION OF LINEAR STRUCTURES FROM REMOTE SENSING DATA; ESPINHACO MERIDIONAL (MG) SIERRA [CARACTERIZACAO DE ESTRUTURAS LINEARES A PARTIR DE DADOS DE SENSORIAMENTO REMOTE; SERRA DO ESPINHACO MERIDIONAL (MG)]
Marx PrestesBarbosa and Hans Daniel Schorscher Nov. 1989 12 p In PORTUGUESE; ENGLISH summary Presented at the 3rd Brazilian Symposium on Remote Sensing, Rio de Janeiro, Brazil, 28-30 Nov. 1984
(INPE-4905-PRE/1506) Avail: NTIS HC A03/MF A01

Studies in the scale of 1:250,000 based on data interpretation of photographic LANDSAT and radar imagery of RADAMBRASIL project in geologic terrains limited by parallels 19 deg 00 min and 20 deg 00 min of south latitude and by meridians 42 deg 00 min and 45 deg 00 min of west longitude show the following lithostructural frame work. The area is represented by rocks of the Complexo Migmatitico-Granulitico of Minas Gerais state in the east, south, and southeast; by rocks of Espinhaco Meridional in the center north; by rocks of the Quadrilatero Ferrifero in the south; and by rocks of the Supergrupo Sao Francisco in the centerwest. Through the analysis of textural elements of drainage and relief six principal directions were discriminated: NS, N2O deg-40 deg E, N40 deg-70 deg E, EW, N40 deg-70 deg W, and N2O deg-40 deg E. In the areas where occur the rocks of the Supergrupo Sao Francisco on the directions N2O deg-40 deg W, N2O deg-40 deg W, N2O deg-40 deg E and N40 deg-70 deg E have regional expression, whereas the other directions have only isolated reflexes. In evolutionary terms it can be inferred that the rocks of the Supergrupo Sao Francisco were poorly affected only by the last event of tectonoorogenetic reativation that formed the folds and thrust faults in the Espinhaco evidenced by the directions of strike slip faults N2O deg-40 deg E, N2O deg-40 deg W, N40

deg-70 deg E, and N40 deg-70 deg W. After this reativation the east part of the study regions was affected by tectonic processes of distensible character evidenced by injection of magmatic material of different ages. Author

N90-21450# Instituto de Pesquisas Espaciais, Sao Jose dos Campos (Brazil).

GEOLOGY OF ESPINHACO MERIDIONAL, INCLUDING THE QUADRILATERO FERRIFERO: INTEGRATION THROUGH REMOTE SENSING DATA [GEOLOGIA DO ESPINHACO MERIDIONAL, INCLUINDO O QUADRILATERO FERRIFERO: INTEGRACAO ATRAVES DE DADOS DE SENSORIAMENTO REMOTO]

Marx Prestes Barbosa, Athos RibeirodosSantos, Paulo Veneziani, Hans Daniel Schorscher, and Pedro Angelo AlmeidaAbreu (Centro de Geologia Eschwege, Diamantina, Brazil) Nov. 1989 18 p In PORTUGUESE; ENGLISH summary Presented at the 3rd Brazilian Symposium on Remote Sensing, Rio de Janeiro, Brazil, 28-30 Nov. 1984

(INPE-4904-PRE/1505) Avail: NTIS HC A03/MF A01

Results of the interpretation of remote sensing photographic products (MSS, RBV, TM and SLAR images RADAMBRASIL Project), applied to the region of Southern Espinhaco, Quadrilatero Ferrifero, and adjacent parts of the Migmatitic-Granulitic Complex in Minas Gerais State, are presented. The area is composed principally of precambrian metamorphic rocks, arquean to upper proterozoic in age, and phanerozoic rocks represented by basaltic magmatism and restricted sedimentary basins, developed in the Tertiary and Quaternay periods. The region presents complex polycyclic evolution by superimposed precambrian orogenesis and tectonomagmatic reactivations in phanerozoic times. The main results are: integrated regional geological map (1:250,000) and photolineaments map (1:250,000). The integrated geological map contributes to the regional geology, emphasizing lithostratigraphic and structural aspects of the area including information unpublished in previous studies. The photolineaments map shows the importance of the four principal fracturing systems (N-S, E-W, NW-SE and NE-SW) conditioning the tectonic evolution of this region. Author

N90-21451# Instituto de Pesquisas Espaciais, Sao Jose dos Campos (Brazil).

MONITORING VEGETATION OF BRAZIL: POTENTIALITIES OF MULTI-SENSORS APPROACH

Yosio Edemir Shimabukuro, Pedro Hernandez Filho, Marcos daCostaPereira, and Joao Roberto dosSantos Oct. 1989 12 p Presented at the Conference on Global Natural Resource Monitoring and Assessment: Preparing for the 21st Century, Venezia, Italy, 24-30 Sep. 1989 Submitted for publication

(INPE-4993-PRE/1555) Avail: NTIS HC A03/MF A01

The large territorial extension of Brazil (8.5 million square kilometers) makes remote sensing technology an important tool for monitoring the Brazilian natural resources. A research history has shown the application of satellite data for studying vegetation cover, primarily on a regional level, using MSS and TM/LANDSAT and more recently HRV/SPOT data. It is well known that the detailed knowledge of the geographic and seasonal patterns of terrestrial vegetation is a necessary factor to understand global climate, biospheric productivity and human impact on the environment. Currently, there are several data collection platforms with sensors of different spatial, spectral, and temporal characteristics which are very useful to study vegetation cover. The AVHRR/NOAA, for instance, having much less spatial detail than LANDSAT sensors but providing daily worldwide data collection show the great potential for monitoring global vegetation and its dynamic. On the other hand, data provided by LANDSAT and SPOT sensors have been used for regional studies. The potentialities are presented of multi-sensors (AVHRR/NOAA, MSS and TM/LANDSAT and HRV/SPOT) for monitoring vegetation of Brazil. The results of the analyzed procedures show the potential of multi-sensors for mapping, estimation of biomass, and phenology conditions of the vegetation and the human impact on the environment (deforestation, biomass burning, etc.). Author

N90-21452# Instituto de Pesquisas Espaciais, Sao Jose dos Campos (Brazil).

EVOLUTION OF REMOTE SENSING APPLIED TO VEGETATION AND FOREST AT INPE [EVOLUCAO DO SENSORIAMENTO REMOTO APLICADO EM VEGETACAO E FLORESTA NO INPE]

Vitor CelsodeCarvalho, Yosio Edemir Shimabukuro, and Pedro HernandezFilho Dec. 1989 16 p In PORTUGUESE; ENGLISH summary Presented at the 6th State Forest Conference, Nova Prata, Brazil, 19-24 Sep. 1988

(INPE-4970-PRE/1538) Avail: NTIS HC A03/MF A01

Brazil, with a territorial extension of 8.5 millions square kilometers, scarce economic resources, and an unequal and concentrated populational distribution presents operational difficulties to the knowledge and evaluation of its natural resources. Analyzing this problem, the Federal government decided to start, in the decade of the sixties, the development of research related to the spatial area, having as one of its objectives the utilization of orbital data to the execution of the natural resources survey. The Institute for Space Research (INPE) is the main civilian organization responsible for the development of this research through its Research and Applications Department (DPA) in the remote sensing area. The studies realized by the vegetation and forest group of the DPA are presented, which has as its main purpose the study of the vegetal cover using remote sensing techniques, including characterization and/or mapping, evaluation and/or inventory, and management and/or monitoring, in natural environments in forest plantation areas, or in ecological conservation areas. Author

N90-21453# Instituto de Pesquisas Espaciais, Sao Jose dos Campos (Brazil).

ANALYSIS OF WATER QUALITY PARAMETERS OF THE PIAUI RIVER (SE), BRAZIL, THROUGH FIELD AND TM/LANDSAT SENSOR DATA [ANALISE DE PARAMETROS DE QUALIDADE DE AGUA DO RIO PIAUI (SE), BRASIL, ATRAVES DE DADOS DE CAMPO E DO SENSOR TM/LANDSAT]

Myrian deMouraAbdon and Valdineide B. Santana (Universidade Federal de Sergipe, Aracaju, Brazil) Sep. 1989 7 p In PORTUGUESE; ENGLISH summary Presented at the 14th Brazilian Conference on Cartography, Gramado, Brazil, 21-26 May 1989

(INPE-4918-PRE/1417) Avail: NTIS HC A02/MF A01

Water transparency, depth, tides, temperature, and salt content data for the surface waters of Piaui River, Sergipe State, Brazil, were collected simultaneously with the recording of digital TM/LANDSAT satellite images in the visible, near, mid, and thermal infrared spectral bands. Correlation analysis of field and satellite data in their original or processed form were performed. The results are presented and discussed based on the correlation coefficients with the objective of advancing the methods for studies of water quality through remote sensing. Author

N90-21454# Instituto de Pesquisas Espaciais, Sao Jose dos Campos (Brazil).

EVALUATION OF THE MANGROVE AREAS OF THE RIO PIAUI (SE) THROUGH REMOTE SENSING [AVALIACAO DAS AREAS DE MANGUEZAL DO RIO PIAUI(SE) ATRAVES DE SENSORIAMENTO REMOTO]

Myrian deMouraAbdon, Carmem Regina SEspindola, Dalton deMorissonValeriano, Ernesto Getulio MVieira, Alberto W. Setzer, Maria AuxiliadoraSantos, and Yara Schaeffer-Novelli (Sao Paulo Univ., Brazil) Aug. 1989 8 p In PORTUGUESE; ENGLISH summary Presented at the Latin American Symposium on Remote Sensing, Gramado, Brazil, 10-15 Aug. 1986; sponsored in part by INPE/SELPER/SBC

(INPE-4909-PRE/1510) Avail: NTIS HC A02/MF A01

The purpose of this work is to estimate the areas of mangroves at the estuary of the River Piaui (SE) with remote sensing techniques, and also to evaluate any degradation of these areas associated to the growing industrialization in the region. Aereal panchromatic photos in the 1:25.000 scale from 20/12/84 were used to produce a ground truth map where mangrove areas were

identified from other ground cover features. Digital multispectral and multitemporal analysis of MSS/LANDSAT (26/03/79) and TM/LANDSAT (19/07/84) imagery produced thematic maps of the region, which showed that no significant clearing occurred in mangrove areas for the 1979 to 1984 period. Author

N90-21455# Instituto de Pesquisas Espaciais, Sao Jose dos Campos (Brazil).

AERIAL PHOTOGRAPHY AS AN AID FOR AGRICULTURAL CREDIT CONTROL

Bernardo Friedrich T Rudorff, Getulio T. Batista, and Antonio T. Tardin Dec. 1989 34 p Sponsored in part by Bank of Brazil Submitted for publication

(INPE-5019-RPE/613) Avail: NTIS HC A03/MF A01

This work had the objective to develop a methodology for the control process of governmental loans for agriculture with the support of aerial photographs. The study area, the Irece region, is located in Bahia State and comprises the municipal areas of Irece, Lapao, Gabriel, and Joao Dourado. For monitoring the proper use of agricultural loans provided by Banco do Brasil S.A. (Bank of Brazil), aerial photographs were used in a first phase after the plowing or at crop emergence stage and in a second phase just before harvesting. Vertical aerial photographs were obtained in color prints at the scales of 1:30,000 and 1:15,000, respectively for the first and second phases. The farms with granted loans were outlined over the aerial photographs using cadastral maps at the scale of 1:5,000 and 1:25,000. The aerial photographs obtained in the first phase were used to assess the area of soil prepared for planting and it was possible to assess 92 percent of the farms when compared to the area agreed to be olanted in the loan contract. For the second phase the aerial photographs were utilized, both to identify the crop and to evaluate the planted area in accordance with the loan contract. In this phase, 50 percent of the loan contracts were analyzed of which 27.7 percent were in irregular situation in relation to planted crop or area reduction. From the aircraft mission to the delivery of results to the local branch of the Bank 15 and 20 days were spent, respectively, for the first and second phases. This experience has shown that both technically and economically the loan control can be done operationally using aerial photography in the region of Irece.

Author

N90-21456# Instituto de Pesquisas Espaciais, Sao Jose dos Campos (Brazil).

INTRODUCTION OF DIGITAL IMAGE PROCESSING BY REMOTE SENSORS APPLIED TO GEOLOGY [INTRODUCAO AO PROCESSAMENTO DIGITAL DE IMAGENS DE SENSORES REMOTOS APLICADO A GEOLOGIA]

Waldir Renato Paradella Feb. 1990 42 p In PORTUGUESE; ENGLISH summary

(INPE-5023-RPE/616) Avail: NTIS HC A03/MF A01

Orbital remote sensing data are available for geologic applications in a paper or digital format through computer compatible tapes (CCT's). The current trend based on the use of computer to analyze digital data consolidates a set of techniques adapted to geologic problems: the digital enhancements. Familiarization with the techniques is fundamental for the geologists with interest in extracting the maximum information from orbital remote sensing products. The main enhancement techniques such as, contrast stretch, band-ratios; principal component transformation, decorrelation stretch; IHS and digital filtering are discussed through an introductory approach. A basic bibliographic on these subjects is also provided. Author

N90-21457# Instituto de Pesquisas Espaciais, Sao Jose dos Campos (Brazil).

MULTITEMPORAL ANALYSIS OF LANDSAT/TM DIGITAL IMAGERY IN THE DETECTION OF AREAS AFFECTED BY CATERPILLAR (SIBINE FUSCA) ATTACK IN THE DENDE (ELAIS GUINEENSIS) PALM PLANTATION [ANALISE MULTITEMPORAL DE IMAGENS DIGITAIS DO LANDSAT TM NA DETECCAO DE AREAS AFETADAS POR ATAQUE DE LAGARTAS (SIBINE FUSCA) NA CULTURA DE DENDE (ELAIS GUINEENSIS]

Jose Simeao deMedeiros and Edson EijiSano (Organization of American States.) Sep. 1989 8 p In PORTUGUESE; ENGLISH summary Presented at the 5th Brazilian Symposium on Remote Sensing, Natal, Brazil, Oct. 1988

(INPE-4979-PRE/1544) Avail: NTIS HC A02/MF A01

The purpose was to detect the areas affected by caterpillars (Sibine fusca) attack in a dende palm plantation (Elais quineensis), through LANDSAT data multitemporal analysis. The test site was selected within Denpasa's farm (Dende do Para S.A.), located 45 km away from Belem (PA). The TM bands 3, 4, and 5 acquired in two different dates (July 24, 1984 and July 17, 1986), were used. After attenuation of path radiance and images registration, a supervised temporal/spectral classification was performed, which made it possible to define with precision, the areas attacked by caterpillars. Author

N90-21458# Instituto de Pesquisas Espaciais, Sao Jose dos Campos (Brazil).

EVALUATION OF CLASSIFICATION PERFORMANCE AND PROPORTION ESTIMATE OF THE SUGAR CANE CROP THROUGH PROCEDURE-INPE UTILIZING LANDSAT DATA [AVALIACAO DO DESEMPENHO DA CLASSIFICACAO E ESTIMATIVA DA PROPORCAO DA CULTURA DA CANA-DE-ACUCAR PELO PROCEDIMENTO-INPE, UTILIZANDO DADOS DO LANDSAT]

Bernardo Friedrich T Rudorff and Getulio TeixeiraBatista Aug. 1989 17 p In PORTUGUESE; ENGLISH summary Presented at the 3rd Brazilian Symposium on Remote Sensing, Rio de Janeiro, Brazil, 28-30 Nov. 1984

(INPE-4899-PRE/1500) Avail: NTIS HC A03/MF A01

The objective was to determine the effect of crop density, satellite data acquisition period and the number of spectral bands on the classification performance and proportion estimate of sugar cane in sampling segments (9 x 11 km approximately). Multitemporal and multispectral LANDSAT/MSS data were analyzed in IMAGE-100 (INPE's Image Analysis System) using the PROCEDURE-INPE. Four LANDSAT/MSS registered passes for each one of the four studied segments located in regions of high density (two segments) and low density (two segments) of sugar cane were analyzed. All possible combinations of four acquisition dates were classified using the maximum likelihood decision rule. This procedure requires the labeling of 100 pixels randomly distributed in the segment. Both labeling and classification performance assessment were done using thematic maps obtained either from CIR aerial photographs or from topographic charts. Results showed similar classification performance for all combinations of date acquisitions. The effect of crop concentration on classification performance seems to be significant. The algorithm for bias correction improved the sugarcane proportion estimation.

Author

N90-21459# Instituto de Pesquisas Espaciais, Sao Jose dos Campos (Brazil).

CONTRIBUTION FOR THE STUDY OF THE EVOLUTION OF PART OF THE ESPINHACO SUPERGROUP AND ITS FOUNDATION THROUGH FRACTURE ANALYSIS [CONTRIBUICAO PARA O ESTUDO DA EVOLUCAO DE PARTE DO SUPERGRUPO ESPINHACO E DE SEU EMBASAMENTO ATRAVES DA ANALISE DE FRATURAMENTO]

Paulo Veneziani and Hans Daniel Schorscher (Sao Paulo Univ., Brazil) Nov. 1989 17 p In PORTUGUESE; ENGLISH

summary Presented at the 3rd Brazilian Sy.nposium on Remote Sensing, Rio de Janeiro, Brazil, 28-30 Nov. 1984
(INPE-4907-PRE/1508) Avail: NTIS HC A03/MF A01

The interpretation of remote sensing products (MSS, RBV, TM and SLAR images) was applied to the region of Espinhaco Meridional, Minas Gerais, Brazil. This region is located between 18 deg 00 min and 19 deg 00 min of South latitude and 44 deg 30 min and 42 deg 00 min of West longitude. The study was based on the analysis of joint trends, geological data from literature and field works. Preliminary results were obtained at the scale of 1:250,000 integrated geological map; joint trends maps; photolineaments map. The analysis of patterns of fracturing showed the importance of N-S, E-W, NE-SW, and NW-SE events of ruptile and ruptile ductile tectonics. The trends are related to polycyclic polygenetic activities (archean to mesozoic) developed by synsedimentary generative strain of distension and orogenetic compression. The structures and deformation of the Espinhaco ridge are compatible with moderate ensialic plate techtonic evolution. Author

N90-21460# Instituto de Pesquisas Espaciais, Sao Jose dos Campos (Brazil).
WHEAT PRODUCTIVITY ESTIMATE THROUGH FIELD RADIOMETRY [ESTIMATIVA DA PRODUTIVIDADEDO TRIGO ATRAVES DE RADIOMETRIA DE CAMPO]
Bernardo Friedrich T Rudorff and Getulio T. Batista Nov. 1989 21 p In PORTUGUESE; ENGLISH summary Presented at the 4th SELPER Symposium, Sao Carlos de Bariloche, Argentina, 20-24 Nov. 1989
(INPE-4994-PRE/1556) Avail: NTIS HC A03/MF A01

The spectral behavior of three varieties of wheat (Anahuac, IAC-24, and BH-1146) was analyzed using field radiometry throughout the 1988 growing season, in the region of Assis, SP. The field radiometric data were obtained in the visible and near infrared portion of the electromagnetic spectrum of 30 sampled fields distributed in commercially planted fields. The radiometric data were transformed into vegetation indices and related to agronomic variables (grain yield, green phytomass, and dry phytomass) obtained in the ten measurement campaigns carried out weekly beginning at initial stages of growing (30 days after planting approximately) until harvesting. The main objective was to verify the potential of spectral data to estimate grain yield of wheat growing in tropical region. It was observed that the vegetation index obtained at sprouting to flowering states was quite well related to the final grain yield and correlation coefficients of 0.82 to 0.93 were obtained. The radiometric data were analyzed multitemporally also, where the vegetation indices were integrated throughout the growing cycle and related to the final yield. Results obtained clearly indicated that the reflected energy at certain stages of the crop development and at certain wavelength bands are well related to the final grain yield. Author

N90-21461# Instituto de Pesquisas Espaciais, Cachoeira Paulista (Brazil).
SUBSYSTEM TM PRECISION: PROGRESS AND PERSPECTIVE [SUBSISTEMA TM PRECISION: AVANCOS E PERSPECTIVAS]
Paulo Cesar RegoBezerra and Julio Cesar LimaDAlge Oct. 1989 6 p In PORTUGUESE; ENGLISH summary Presented at the 5th Brazilian Symposium on Remote Sensing, Natal, Brazil, 11-15 Oct. 1989
(INPE-5006-PRE/1563) Avail: NTIS HC A02/MF A01

System corrected (bulk) TM-LANDSAT images produced by INPE show an internal geometric quality of about 1.5 pixel but a geodetic accuracy of only around 50 pixels, mainly due to inaccurate telemetry data broadcasted by the satellite. Because of this, efforts are being carried for the implementation of a precision subsystem capable to generate TM images with a geodetic accuracy of at least 1.5 pixel. This work presents the results of the first correction model tested, which is based on the refinement of the broadcast ephemeris. Author

N90-21462# Instituto de Pesquisas Espaciais, Sao Jose dos Campos (Brazil).
POSSIBLE USE OF SATELLITE DATA FOR FLOOD PLAIN MAPPING [POTENCIALIDADE DO USO DE DADOS DE SATELITE NO MAPEAMENTO DE PLANICIES DE INUNDACAO]
Rui Carlos VieiradaSilva (Universidade Federal do Rio de Janeiro, Brazil), Sergio dosAnjosFerreiraPinto, and Madalena NieroPereira Nov. 1989 15 p In PORTUGUESE; ENGLISH summary Presented at the 8th Brazilian Symposium on Water Resources, Foz do Iguacu, Brazil, 26-30 Nov. 1989
(INPE-4968-PRE/1537) Avail: NTIS HC A03/MF A01

The objective is to evaluate the possibility of using satellite imagery (LANDSAT) to obtain basic parameters which permit the calibration of a flood plain mathematical model. Multitemporal satellite imagery of 1979, 1983, and 1985 of the Sao Francisco basin between the city of Carinhanha and the Sobradinho reservatory (Bahia State) were used to analyze the spatial and temporal distribution of flood plain which are important to formulate the mathematical model. Author

N90-21463# Instituto de Pesquisas Espaciais, Sao Jose dos Campos (Brazil).
PERFORMANCE EVALUATION OF MSS/LANDSAT DATA IN THE ESTIMATION OF FLUVIAL CHANNEL WIDTH [AVALIACAO DO DESEMPENHO DOS DADOS MSS/LANDSAT NA ESTIMATIVA DE LARGURA DE CANAIS FLUVIAIS]
Evlyn Marcia LeaodeMoraesNovo, Sergio dosAnjosFerreiraPinto, Madalena NieroPereira, and Roberto Rosa (Universidade Federal de Uberlandia, Brazil) Nov. 1989 19 p In PORTUGUESE; ENGLISH summary Presented at the 3rd Brazilian Symposium on Remote Sensing, Rio de Janeiro, Brazil, 28-30 Nov. 1984
(INPE-4906-PRE/1507) Avail: NTIS HC A03/MF A01

The problem in change evaluation of water surfaces using MSS/LANDSAT image is in the determination of measuring error during data acquisition. The error is determined by the pixel size (80m x 80m). The pixels situated in the border line of the fluvial channels can be classified as water or vegetation. The following situation can occur in the determination of the water surface to estimate the fluvial channel width: the pixel is composed by 50 percent of water and 50 percent of vegetation and is classified as water; the pixel is composed by 50 percent of water and 50 percent of vegetation and is classified as vegetation; the pixel has more portion of water and is classified as water, and vice-versa. On this way it was possible to obtain an error equivalent to one pixel to each border of the fluvial channel. The objective was to verify the error obtained in the water surface measuring using MSS/LANDSAT images. An image corresponding to the low water stage (August 27, 1977) of path 220/row 27, and scale 1:250,000 was chosen. The study area corresponds to a section of the Parana River, bordering the states of Sao Paulo and Mato Grosso, some cross sections in the analyzed image were selected supposing that the water surface referring to the low water situation can be considered a good estimator of the fluvial channel width. The similar cross-sections were selected in the topographic charts (scale 1:50,000). A statistical analysis was carried out (regression analysis) to find the best regression line between the data obtained from the image (X) and topographic charts (Y). The preliminary results show that the image overestimates the narrow fluvial channels and underestimates the larger fluvial channels. Author

N90-21464# Instituto de Pesquisas Espaciais, Sao Jose dos Campos (Brazil).
PERFORMANCE EVALUATION OF MORPHOLOGICAL EDGE DETECTORS [AVALIACAO DO DESEMPENHO DE DETETORES MORFOLOGICOS DE BORDA]
Nelson DelfinodAvilaMascarenhas and Erivaldo AntoniodaSilva Oct. 1989 10 p In PORTUGESE Presented at the 4th Latin American Symposium on Remote Sensing, Bariloche, Argentina, 20-24 Nov. 1989
(INPE-4975-PRE/1540) Avail: NTIS HC A02/MF A01

Recently, a mathematical morphology theory served as the basis for proposed new edge detectors in imagery. The

performance of six morphological edge detectors is compared from the point of view of sensitivity to its response and orientation of the edge. Also prepared is an application example for the detector in an edge description for LANDSAT-TM imagery of urban areas. Transl. by B.G.

N90-21465# Instituto de Pesquisas Espaciais, Sao Jose dos Campos (Brazil).
REGIONAL REMOTE SENSING LABORATORY [LABORATORIO REGIONAL DE SENSORIAMENTO REMOTO]
Rene Antonio Novaes Mar. 1989 10 p In PORTUGESE; In PORTUGUESE; ENGLISH summary Presented at the 3rd Brazilian Symposium on Remote Sensing, Rio de Janeiro, Brazil, 28-30 Nov. 1984
(INPE-4922-PRE/1519) Avail: NTIS HC A02/MF A01

The policies establishing INPE's remote sensing laboratory are the same goals which directed the formation of remote sensing at INPE, in 1967, which was to establish, develop, and expand the benefits following the use of remote sensing techniques for all national territory. This work seeks to show knowledge and/or advantages of the formation of the laboratories and the organization, structure, and operations of the first Regional Remote Sensing Laboratory at Campina Grande-Paraiba. Transl. by B.G.

N90-21466# Los Alamos National Lab., NM.
PRINCIPLES OF THE RADIOSITY METHOD FOR CANOPY REFLECTANCE MODELING
S. A. W. Gerstl and C. C. Borel Mar. 1990 4 p Presented at the 1990 International Geoscience and Remote Sensing Symposium, College Park, MD, 20-24 May 1990 Submitted for publication
(Contract W-7405-eng-36)
(DE90-008943; LA-UR-90-782; CONF-900567-3) Avail: NTIS HC A02/MF A01

The radiosity method is introduced to plant canopy reflectance modeling. We review the physics principles of the radiosity method which originates in thermal radiative transfer analyses when hot and cold surfaces are considered within a given enclosure. The radiosity equation, which is an energy balance equation for discrete surfaces, is described and contrasted with the radiative transfer equation, which is a volumetric energy balance equation. Comparing the strengths and weaknesses of the radiosity method and the radiative transfer method, we conclude that both methods are complementary to each other. Results of sample calculations are given for canopy models with up to 20,000 discrete leaves. DOE

44 ENERGY PRODUCTION AND CONVERSION

Includes specific energy conversion systems, e.g., fuel cells; global sources of energy; geophysical conversion; and windpower.

For related information see also *07 Aircraft Propulsion and Power, 20 Spacecraft Propulsion and Power,* and *28 Propellants and Fuels.*

N90-21467# Ceramatec, Inc., Salt Lake City, UT.
DEVELOPMENT OF PLANAR GEOMETRY SOLID OXIDE FUEL CELL TECHNOLOGY, PHASE 2 Annual Report, Oct. 1987 - Oct. 1988
Ashok C. Khandkar, S. Elangovan, and Dave W. Prouse Nov. 1989 100 p
(Contract GRI-5086-294-1292)
(PB90-131293; PROG-8860710; GRI-89/0161) Avail: NTIS HC A05/MF A01 CSCL 10A

The progress made towards the development of planar geometry solid oxide fuel cell (SOFC) technology is documented. The thrust was to develop stack technology via the development of planar-ribbed interconnects, and to demonstrate improved cell performance. The problem related to anode adhesion and delamination during cell operation was addressed using alternate materials as well as by developing optimized processes. In addition, the cell performance was optimized iteratively. Successful single cell tests conducted demonstrated an improved cell performance of 300 mA/sq cm at 0.5V using different anode gas compositions. In addition, the edge seal material was qualified in both out-of-cell and in-cell tests to be adequate for a cumulative cell test time of over 1000 hrs. Cell diagnostic techniques were developed for out-of-cell component qualification. Diagnostic tests conducted on single cells indicate that the major polarization loss occurs at the anode. Interconnect materials were synthesized, characterized and pressureless sintered in air. Problems encountered with densification were solved using transient liquid phase densification aids and controlled atmosphere and pressure while sintering. Author

N90-21468# Pacific Northwest Lab., Richland, WA.
ALTERNATIVE MATERIALS FOR SOLID OXIDE FUEL CELLS
J. L. Bates, L. A. Chick, P. C. Rieke, and W. J. Weber May 1989 10 p Presented at the 1st Annual Fuel Cells Contractors Review Meeting, Morgantown, WV, 2-4 May 1989
(Contract DE-AC06-76RL-01830)
(DE90-008615; PNL-SA-16902; CONF-890572-2) Avail: NTIS HC A03/MF A01

This project is an effort to modify state-of-the-art Solid Oxide Fuel Cells (SOFC) materials or develop analogous SOFC materials as electrodes and interconnections that will provide improved electrical, thermal expansion and electrochemical properties. Work includes four tasks: material synthesis and processing technology in order to modify alternative interconnection materials (powders) that can be sintered in air below 1823 K with and without the use of metal additives as sintering aids; evaluation of additive effects on structure, synthesis and electrical and thermal properties of alternative interconnection materials based on La(M')(Cr, M'')O3 and Y(M')(Cr, M'')CrO3; evaluation of electrical and thermal properties of alternative interconnection of materials as functions of composition, structure and synthesis/fabrication methods; and electrochemical behavior of material interfaces is being studied to evaluate simple SOFC geometries. DOE

N90-21469*# National Aeronautics and Space Administration. Lewis Research Center, Cleveland, OH.
O2 REDUCTION AT THE IFC ORBITER FUEL CELL O2 ELECTRODE
William L. Fielder and Joseph Singer Apr. 1990 15 p
(NASA-TM-102580; E-5411; NAS 1.15:102580) Avail: NTIS HC A03/MF A01 CSCL 10B

O2 reduction Tafel data were obtained for the IFC Orbiter fuel cell O2 electrode (Au-10 percent Pt catalyst) at temperatures between 24 and 81 C. BET measurements gave an electrode surface area of about 2040 sq cm per sq cm of geometric area. The Tafel data could be fitted to three straight line regions. For current densities less than 0.001 A/sq cm, the slope was essentially independent of temperature with a value of about 0.032 V/decade. Above 0.001 A/sq cm, the two regions, designated in the present study as the 0.04 and 0.12 V/decate regions, were temperature dependent. The apparent energies of activation for these two regions were about 9.3 and 6.5 kcal/mol, respectively. Tafel data (1 atmosphere O2) were extrapolated to 120 C for predicting changes in overpotential with increasing temperature. A mechanism is presented for O2 reduction. Author

N90-21470# Solar Kinetics, Inc., Dallas, TX.
DESIGN AND DEMONSTRATION OF AN IMPROVED STRETCHED-MEMBRANE HELIOSTAT
Dec. 1989 101 p
(Contracts DE-AC04-76DP-00789; SNL-33-1227)
(DE90-007904; SAND-89-7028) Avail: NTIS HC A06/MF A01

Improvements to a stretched-membrane heliostat have been designed and implemented under contract with Sandia National Laboratories. Specific improvements were made to the mirror module to improve performance and reduce costs. The performance of the heliostat in windy conditions was improved by adding a restraint to the rear membrane. An open-section ring was used to increase structural efficiency. The rear structure was

redesigned to take advantage of common manufacturing techniques and lower cost materials. The control system was improved, and a means of achieving passive defocus was achieved. Finally, membrane preload was applied with nonconsumable tooling. An 8 percent reduction in mirror-module cost was realized. The improved design was successfully demonstrated with a 50 sq m prototype. This prototype had improved optical stability in fluctuating winds. Its slope error in calm winds was measured to be 1.3 mrad. DOE

N90-21471# Department of Energy, Washington, DC. Office of the Deputy Assistant Secretary for Oil, Gas, Shale, and Special Technologies.
FUEL CELL SYSTEMS PROGRAM PLAN, FY 1990
Oct. 1989 40 p
(DE90-008178; DOE/FE-0106P) Avail: NTIS HC A03/MF A01

A principal goal of the Office of Fossil Energy is to increase the utilization of domestic fuels in an environmentally benign manner, through the development and transfer to the private sector of advanced energy conversion technology. Successful efforts to achieve this goal contribute to the stability and reliability of reasonably priced energy supplies, enhance the competitiveness of domestic fuels and energy technologies in domestic and international markets, and contribute to the development of cost effective strategies for control of acid rain and global warming. Several advanced energy conversion technologies are now under development by DOE which can help to achieve these objectives. Fuel cells are among those technologies. This report briefly describes fuel cell technology and the program plan of U.S. DOE fuel cell program. DOE

N90-21472# Minnesota Mining and Mfg. Co., Saint Paul. Applied Technologies Lab.
IMPROVEMENT OF SMALL-AREA, AMORPHOUS-SILICON THIN-FILM PHOTOVOLTAICS ON POLYMER SUBSTRATE Final Report, 1 Mar. 1988 - 30 Jun. 1989
Michael F. Weber Feb. 1990 30 p
(Contracts DE-AC02-83CH-10093; SERI-ZB-8-0-7271-1)
(DE90-000314; SERI/TP-211-3656) Avail: NTIS HC A03/MF A01

This report describes a contract to produce, using roll-to-roll deposition on polyamide substrate, a small-area amorphous-silicon p-i-n photovoltaic (PV) cell with an energy conversion efficiency of 10 percent under air mass 1.5 insolation. Three improvements were attempted to achieve this goal: (1) zinc oxide, a transparent conducting oxide, was used as a top contact; the zinc oxide conductivity was improved to 8 to 9 ohms/square sheet resistance with less than 8 percent average optical absorption, (2) the red light response was improved with dielectric enhanced metal reflecting electrodes, which increased the short-circuit current density by more than 1 mA/sq cm; a three-layer dielectric mirror coating was also designed that can increase the current density by another 1 mA/sq cm, and (3) improving the fill factor of the n-i-p (reverse structured) devices was also achieved in a multichamber deposition system. The overall energy conversion efficiency of the PV cell was 8.36 percent. Major obstacles to higher efficiencies are: (1) controlling the thin-film defects that cause electrical shunts in devices fabricated on enhanced reflection electrodes, and (2) controlling impurities and introducing dopant profiles near the p/i interface in a continuous web deposition system. DOE

N90-21473# Chronar Corp., Princeton, NJ.
RESEARCH ON AMORPHOUS SILICON-BASED THIN FILM PHOTOVOLTAIC DEVICES. TASK B: RESEARCH ON STABLE HIGH EFFICIENCY LARGE AREA, AMORPHOUS SILICON-BASED SUBMODULES Semiannual Report, 16 Mar. - 30 Nov. 1989
A. E. Delahoy, F. B. Ellis, C. Kothandaraman, H. Schade, T. Tonon, and H. Weakliem Mar. 1990 38 p
(Contracts DE-AC02-83CH-10093; SERI-ZB-7-06003-1)
(DE90-000320; SERI/TP-211-3667) Avail: NTIS HC A03/MF A01

The primary objective of this subcontract is to develop amorphous silicon p-i-n/p-i-n tandem junction photovoltaic submodules (greater than 900 sq cm) having an aperture area efficiency of at least 9 percent. A further objective is to demonstrate 8 percent tandem submodules that degrade by no more than 5 percent under standard light soaking conditions. The main lines of investigation during this period concerned with exploration of novel types of p-layers, the properties and applications of doped zinc oxide films to a -Si:H cells, the effects of various surface treatments of SnO2 and ZnO transparent conducting oxides (TCO's) on cell performance, the dependence of cell stability on substrate and junction type, and the development of techniques to enable the full potential performance of the a -Si:H to be realized in a module configuration. DOE

N90-21474# Pacific Northwest Lab., Richland, WA.
SPACE POWER GENERATION AND DISTRIBUTION
E. P. Coomes, R. D. Widrig, and B. M. Johnson Jan. 1990 5 p Presented at the 7th Symposium on Space Nuclear Power Systems, Albuquerque, NM, 7-11 Jan. 1990
(Contract DE-AC06-76RL-01830)
(DE90-008676; PNL-SA-17792; CONF-900109-24) Avail: NTIS HC A02/MF A01

The availability of power in space is currently constrained by the Ever-Ready Energizer approach: individual power sources tailored to each satellite for each mission. This document describes an alternative approach known as power beaming, which integrates power generation and distribution, opening space to many new applications. Power beaming is the basis for a completely new space power architecture and a fully integrated transportable space power infrastructure. The power-beaming architecture supporting near-Earth missions can be replicated as mankind explores farther into the solar system. A power-beaming architecture would support manned lunar activities including the establishment of a permanent base on the moon. As mankind ventures farther to Mars and even the asteroids, a power-beaming space power architecture would support these activities as well. DOE

N90-21475# Sandia National Labs., Albuquerque, NM.
RECENT PROGRESS IN PHOTOVOLTAIC CONCENTRATOR MODULE TECHNOLOGY
Elizabeth H. Richards, Jay L. Chamberlain, and Eldon C. Boes 1990 11 p Presented at the Solar 1990: 19th American Solar Energy Society Annual Conference, Austin, TX, 18-20 Mar. 1990
(Contract DE-AC04-76DP-00789)
(DE90-009007; SAND-89-2987C; CONF-900315-2) Avail: NTIS HC A03/MF A01

Significant progress is continuing in the development of photovoltaic (PV) concentrator technology. New record cell and module efficiencies have been achieved, and improvements in cells, cell assemblies, and modules are increasing reliability and decreasing cost. The number of firms actively pursuing PV concentrator module technology has increased substantially in the last three years. Two new concentrator systems were installed last year, and we are likely to see more in the near future. This paper describes the most significant developments of the last two years, including descriptions of PV concentrator module development and reliability activities, advances in concentrator cell technology, the new PV concentrator array installations, a new Concentrator Initiative Program, and results of the latest costing study. DOE

N90-21476# California Univ., Berkeley. Lawrence Berkeley Lab. Windows and Daylighting Group.
FAILURE AND DEGRADATION MODES IN SELECTED SOLAR MATERIALS: A REVIEW
Carl M. Lampert, ed. May 1989 143 p
(Contract DE-AC03-76SF-00098)
(DE90-009075; LBL-27814) Avail: NTIS HC A07/MF A01

Research and development programs involved in solar heating and solar cooling technology are presented. Each report is cataloged individually. DOE

45 ENVIRONMENT POLLUTION

Includes atmospheric, noise, thermal, and water pollution.

N90-21477# National Oceanic and Atmospheric Administration, Washington, DC. Marine Applications Branch.
MECCA PROGRAM DOCUMENTATION
Kurt W. Hess Sep. 1989 260 p
(NOAA-TR-NESDIS-46) Avail: NTIS HC A12/MF A02

The National Environmental Satellite, Data, and Information Service (NESDIS) has developed and tested a three-dimensional time-dependent numerical model of coastal circulation called MECCA (Model for Estuarine and Coastal Circulation Assessment). MECCA was created to study environmental impacts on sensitive marine areas and to assess the use of satellite data for estuarine research. The model was designed to simulate tidal, wind-driven, and density-driven currents in bays and on the shallow continental shelf. MECCA has been applied to study the salinity and temperature distribution in Chesapeake Bay and the Chesapeake Bay/Shelf area. The equations and boundary conditions for coastal circulation are listed. The numerical methods used to solve the equations are explained. How the grid was designed and how to select input data are explained. The computer program which implements the model, MECCA, is discussed as a series of steps with flow diagrams. The input and output files are discussed and examples are given of each. Instructions for running the program interactively are also given. Author

N90-21478# Finnish Meteorological Inst., Helsinki. Air Quality Dept.
TRANSFORMATION AND DEPOSITION OF AIRBORNE GASEOUS AND PARTICULATE POLLUTANTS DURING TRANSPORT OVER THE BALTIC SEA
Virpi T. Lindfors and Sylvain M. Joffre 1989 39 p In FINNISH; ENGLISH summary
(Publ-Air-Quality-5; ISBN-951-697-300-0; ISSN-0782-6095) Avail: NTIS HC A03/MF A01

Researchers used the concentration data and meteorological information collected during a cruise over the Baltic Sea in April-June, 1985, to study transformation and deposition processes of atmospheric pollutants in marine conditions. A simple Lagrangian-type long-range transport model was found to give reasonable predictions of sulphur dioxide and sulphate concentration levels also in sea areas, provided that accurate emission data is available, and that the model parameters are chosen appropriately. Local episodes could also be fairly well simulated. The dry deposition rate of sulphur dioxide, and transformation rate to sulphate were determined by studying selected transport cases between the ship and coastal stations. The dry deposition rate varied from 0.607 10(exp-5) s(exp-1) to 3.38 10(exp-1) s(exp-1), with an average of 1.65 10(exp-5) s(exp-1). The transformation rate was 0.3 10(exp-5) s(exp-1), but the results were controversial, and very sensitive to model parameterization, and to the simplifying assumptions. The experimentally determined dry deposition velocities of sulphur dioxide agreed with the predictions of a theoretical model for boundary layer heights 250 to 500 m. Researchers also estimated the dry deposition of gaseous and particulate sulphur and nitrogen compounds in different regions of the Baltic proper, using the measured concentrations and theoretical dry deposition velocities, calculated from the meteorological data. Author

N90-21479*# Jet Propulsion Lab., California Inst. of Tech., Pasadena.
ENVIRONMENTAL PROJECTS, VOLUME 11.
ENVIRONMENTAL ASSESSMENT: ADDITION TO OPERATIONS BUILDING, MARS SITE
15 Feb. 1990 69 p
(Contract NAS7-918)
(NASA-CR-186449; JPL-Publ-87-4; NAS 1.26:186449) Avail: NTIS HC A04/MF A01 CSCL 13B

An Environmental Assessment was performed of the proposed addition to building G-86 at the Mars Site, which will provide space for new electronic equipment to consolidate the Deep Space Network (DSN) support facilities from other Goldstone Deep Space Communication Complex (GDSCC) sites at the Mars Site, and will include a fifth telemetry and command group with its associated link monitor, control processor, and operator consoles. The addition of these facilities will increase the capability of the DSN to support future sophisticated NASA spacecraft missions such as the International Solar and Terrestrial Physics (ISTP) Program. The planned construction of this building addition requires an Environmental Assessment (EA) document that records the existing environmental conditions at the Mars Site, that analyzes the environmental effects that possibly could be expected from the construction and use of the new building addition, and that recommends measures to be taken to mitigate any possible deleterious environmental effects. Author

N90-21480*# Jet Propulsion Lab., California Inst. of Tech., Pasadena.
ENVIRONMENTAL PROJECTS, VOLUME 10.
ENVIRONMENTAL ASSESSMENT: NEW 34-METER ANTENNA AT APOLLO SITE
15 Jan. 1990 82 p
(Contract NAS7-918)
(NASA-CR-186448; JPL-Publ-87-4; NAS 1.26:186448) Avail: NTIS HC A05/MF A01 CSCL 13B

The Goldstone Deep Space Communications Complex (GDSCC) is part of NASA's Deep Space Network (DSN), one of the world's largest and most sensitive scientific telecommunications and radio navigation networks. A detailed description of the GDSCC is presented. At present the Venus Station has an unused 9-meter antenna and a 26-meter (85 ft) antenna known as DSS-13. Construction of a new 34-meter (111.5 ft) antenna at the Venus site is under way to replace the present DSS-13 26-meter antenna. The proposed construction at the Apollo Site of a new, high efficiency, 34-meter, multifrequency beam waveguide-type antenna to replace the aging, 20-year old, DSS-12 34-meter antenna located at the Echo Site is analyzed. This new 34-meter antenna, to be constructed at the Apollo Site and to be known as DSS-18, will be of a design similar to the new DSS-13 34-meter antenna now being constructed at the Venus Site. When the new 34-meter antenna is completed and operational at the Apollo Site (planned for 1993), the old DSS-12 34-meter antenna at the Echo Site will be decommissioned, dismantled, and removed. Author

N90-21481# NSI Technology Services Corp., Corvallis, OR.
EFFECTS OF AIR POLLUTION ON WESTERN FORESTS
Richard K. Olson, ed. and Allen S. Lefohn, ed. (ASL and Associates, Helena, MT.) Jun. 1989 557 p Symposium held in Anaheim, CA, 29-30 Jun. 1989 Sponsored in part by Air and Waste Management Association, Pittsburgh, PA; Forest Service, Washington, DC; National Park Service, Washington, DC and California Air Resources Board, Sacramento
(PB90-131111; EPA/600/D-89/195) Avail: NTIS HC A24/MF A03 CSCL 13B

Topics addressed include air quality and deposition, forest condition and growth trends, physiological mechanism of effects, and effects of air pollution on forest soils. Among the conclusions reached were: (1) large areas of forests in California have been damaged by ozone; (2) highly acidic clouds impact forests in Washington, California and Colorado; (3) most western forest soils are not currently at risk from acid deposition; and (4) forests in southern Arizona are experiencing unexplained growth declines. Author

N90-21482# EA Engineering Science and Technology, Inc., Sparks, MD.
GAITHERSBURG NIKE CONTROL AND LAUNCH AREA PRELIMINARY ASSESSMENT/SITE INSPECTION, GAITHERSBURG, MARYLAND Final Report, Jan. 1989 - Jan. 1990
Steven A. Brown and Kenneth W. Kilmer Jan. 1990 340 p
(Contract DAAA15-88-D-0005)

(AD-A217791; EA-10559.04; CETHA-BC-CR-90028) Avail: NTIS HC A15/MF A02 CSCL 13/2

This report summarizes the findings of the Preliminary Assessment/Site Inspection study completed at the former Gaithersburg Nike Launch and Control Site. This study was conducted to assess the environmental conditions at this facility relative to past Army operations. The control area has been identified for closure in the Base Realignments and Closures report completed by the Defense Secretary's Commission in December 1988. The Launch and Control Sites are located 1.5 miles apart and a separate, though similar, sampling plan was developed for each site. Ground-water, surface water, surface sediment and soil samples were collected and analyzed for priority pollutant parameters at these sites. The assessment of the data collected indicates that no compounds exceeded current maximum contaminant levels (MCL). GRA

N90-21483# Department of Energy, Washington, DC. Office of Planning and Environment.

A FOSSIL ENERGY PERSPECTIVE ON GLOBAL CLIMATE CHANGE

D. W. South, N. Bhatti, M. E. Fernau, J. L. Gillette, R. C. Hemphill, H. A. Hootman, and D. S. Rothman Jan. 1990 99 p

(DE90-007894; DOE/FE-0164) Avail: NTIS HC A06/MF A01

This report discusses global climate change from a fossil energy power generation perspective. As such, it highlights the substantial uncertainties that underlie the forecasts of greenhouse gas (GHG) emissions, GHG concentrations, and climate change--forecasts that some believe provide the basis for current initiatives to reduce or eliminate fossil fuel use. In addition, this report demonstrates that if it is determined that GHG emissions should be reduced, fossil-fuel-based technologies must play a role in this process. DOE

N90-21484# Brookhaven National Lab., Upton, NY. Atmospheric Sciences Div.

SOURCE ATTRIBUTION FOR TROPOSPHERIC OZONE IN THE US

Carmen M. Benkovitz and Lawrence I. Kleinman Jan. 1990 150 p

(Contract DE-AC02-76CH-00016)

(DE90-007994; BNL-52227) Avail: NTIS HC A07/MF A01

A methodology has been developed that allows fast evaluation of the relative contributions of different emission sectors to the production of tropospheric O3; it can be used to evaluate numerous emissions control strategies. Regional scale hydrocarbon and ozone concentrations are calculated using a trajectory model with a linear description of hydrocarbon oxidation. Emitted hydrocarbons are assumed to react under the influence of an externally specified chemical environment. Emitted compounds are oxidized forming peroxy radicals which can oxidize NO, combine to form peroxides, or form adducts such as PAN. Secondary compounds can react further until complete oxidation occurs. Formation of O3 is associated with NO to NO2 conversions. The linearity of the governing equations allows calculated hydrocarbon and O3 concentrations to be attributed to specific source regions, precursor compounds, or industrial categories. Anthropogenic and biogenic emission inventories for the contiguous U.S. are used to calculate O3 and hydrocarbon concentrations for a summer month, both at the national and the regional levels. DOE

N90-21485# Oak Ridge National Lab., TN.

MODELING LARGE-SCALE VEGETATION DYNAMICS

I. Colin Prentice, Robert A. Monserud, Thomas M. Smith (Virginia Univ., Charlottesville.), and William R. Emanuel 16 Jun. 1989 17 p Presented at the Global Vegetation Change: Considerations for Developing A Long-term Research Plan, Laxenburg (Austria), 16-21 Apr. 1988

(Contract DE-AC05-84OR-21400; NSF BSR-84-17923)

(DE90-008883; CONF-8804214-2) Avail: NTIS HC A03/MF A01

Environmental changes affect vegetation. The dependence of plant cell processes on light, temperature, moisture, and nutrients is the basis for this, but with time the consequences of environmental changes extend to variations in community characteristics including species composition, biomass, leaf-area profiles, and the continental distributions of natural vegetation zones or biomass. In this chapter, we discuss models that are useful in analyzing responses of vegetation to large-scale environmental changes. We emphasize climate, but most concepts and approaches are pertinent to other global changes as well. First, we summarize the natural processes that dictate vegetation dynamics under changing environmental conditions. Models that relate natural vegetation distribution to climate are then described. These can be purely correlative --- based on observed relationships between vegetation and climate, without regard to the mechanisms involved. But to simulate transient responses, we need dynamic models that represent community processes including competition. We summarize a class of such models that are suited to small landscape or patch analysis. We conclude by outlining a scheme for applying these models in large-scale studies, by a Monte Carlo method that samples spatial variability in the environment. DOE

N90-21486# Instituto de Pesquisas Espaciais, Sao Jose dos Campos (Brazil).

RADON CONCENTRATION OVER THE BRAZILIAN AMAZON BASIN DURING THE WET SEASON (BELEM-MANAUS GTE-ABLE-2B FLIGHT OF APRIL 24, 1987)

D. J. R. Nordemann and E. B. Pereira Aug. 1989 12 p Presented at the AGU Spring Meeting, Baltimore, MD, May 1988

(INPE-4892-PRE/1493) Avail: NTIS HC A03/MF A01

Rn-222 was measured by an airborne radon-meter using Po-218 electrostatic precipitation and alpha-ray spectrometry. All radon concentrations were found to be very low (less than 17 pCi/cu m) in regard to the current values found in the literature for other continental regions of the world. This is probably related to the lower diffusivity of radon in damp soils leading to a low radon emanation during the rainy season. Over the Atlantic Ocean, at the mouth of the Amazon River, a value of (5.5 + or - 3.0) pCi/cu m (at 3000 m) may be considered as an indicator of mass of air that was charged with radon over continental areas during the past few days. Between Belem and Santarem, the radon concentrations were higher at low altitude (4.9 + or - 2.9) and (16.4 + or - 5.8) pCi/cu m at 300 m than they were at high altitude (0.0 + or - 1.0) and (0.0 + or - 1.0) pCi/cu m at 3000 m, these last values being associated with subsidence phenomenon over this area that is corroborated by the meteorological analysis. Between Santarem and Manaus, the radon concentrations were slightly lower at low altitude suggesting a possible overturning of the atmospheric structure associated with strong convective activity. Author

N90-21487# Pacific Northwest Lab., Richland, WA.

AN EVALUATION OF THE RELATIONSHIP BETWEEN THE PRODUCTION AND USE OF ENERGY AND ATMOSPHERIC METHANE EMISSIONS

David W. Barns and J. A. Edmonds Apr. 1990 241 p

(Contract DE-AC06-76OR-01830)

(DE90-007982; DOE/NBB-0088P) Avail: NTIS HC A11/MF A02

The purpose of this document is to examine the role energy plays in the emission of CH4 to the atmosphere. We begin with an overview of the CH4 cycle, briefly discussing the current understanding of sources and sinks for CH4. We then proceed to a detailed discussion of the energy-related sources of CH4 to the atmosphere. These include coal mining, natural gas production and distribution, combustion of traditional biomass, and landfill methane. This examination will then be used to develop estimates of the total global energy-related emissions of CH4. DOE

46 GEOPHYSICS

Includes aeronomy; upper and lower atmosphere studies; ionospheric and magnetospheric physics; and geomagnetism.

For space radiation see *93 Space Radiation.*

N90-21488# Massachusetts Inst. of Tech., Cambridge. Center for Space Research.
CENTER OF EXCELLENCE IN THEORETICAL GEOPLASMA RESEARCH Final Report, 1 Oct. 1986 - 30 Sep. 1989
Tom T. S. Chang 10 Nov. 1989 79 p
(Contract F49620-86-C-0128; AF Proj. 3484)
(AD-A215035; AFOSR-89-1512TR) Avail: NTIS HC A05/MF A01 CSCL 04/1

Topics addressed include: Transverse Acceleration and Heating of Ionospheric Ions and the Formation of Ion Conics; Transverse Heating of Ionospheric Ions Along Auroral Field Lines; Acceleration of Ionospheric Ions by Lower Hybrid Waves in the Discrete Auroral Region; Two Dimensional Particle-in-Cell Plasma Simulation of High-Latitude Lower Hybrid Turbulence and Charged Particle Acceleration; Studies of Inhomogeneous Plasma Turbulence in the Auroral Region; A Kinetic Treatment of the Nonclassical Polar Wind; Double Layer Formation and Ion Hole Theory along Auroral Field Lines; Flux Transfer Events and Ionosphere-Magnetosphere Coupling; Auroral Kilometric Radiation and Relativistic Magnetized Anisotropic Plasmas; Plasma Radiations in the Low-Altitude Ionosphere due to Moving Conducting Objects; Gyroresonance Generated Ion Conic Populations; Low-Altitude Transverse Ion Acceleration; and Counterstreaming Electrons. GRA

N90-21489# Northwest Research Associates, Inc., Bellevue, WA.
INVESTIGATIONS INTO THE PROPERTIES, CONDITIONS, AND EFFECTS OF THE IONOSPHERE Report No. 9, 16 Dec. 1987 - 31 Dec. 1988
G. D. Biello, E. J. Fremouw, B. W. Reinisch, and E. P. Szuszczewicz (Science Applications International Corp., Bellevue, WA.) 15 Jan. 1989 37 p
(Contract F19628-87-C-0003)
(AD-A217807; NWRA-CR-89-R039; AFGL-TR-89-0028) Avail: NTIS HC A03/MF A01

The investigations address ionospheric composition, structure, specification, scintillation and chemistry as well as remote sensing of the ionosphere through ultraviolet sensors. Specific work is carried out under individual task requirement notices (TRNs) written for conduct and/or support of investigations in the following six categories; laboratory measurements; field measurements; aircraft measurements; rocket, balloon, shuttle, and satellite measurements; analytical and theoretical investigations; and scientific and engineering analysis. A summary of the work performed during the period 16 December 1987 through 31 December 1988 is provided. GRA

N90-21490# Weidlinger Associates, Los Altos, CA.
A NUMERICAL AND THEORETICAL STUDY OF SEISMIC WAVE DIFFRACTION IN COMPLEX GEOLOGIC STRUCTURE Final Report, Apr. 1984 - Jul. 1988
Gregory L. Wojcik 14 Apr. 1989 103 p
(Contract F19628-84-C-0102; AF Proj. 2309)
(AD-A218209; R8928; GL-TR-88-0291) Avail: NTIS HC A06/MF A01 CSCL 08/11

This report presents results of a theoretical study on wave propagation and diffraction effects in irregular geologic media. The first objective of the study is to demonstrate and validate some large-scale finite element methods for analyzing linear and nonlinear seismic effects in the surficial geologies relevant to several Air Force missions. The second objective is to solve the hitherto intractable problem of vector edge diffraction, which strongly influences seismic wave interactions at the geologic discontinuities ubiquitous in near-surface structure. The first paper describes a variety of linear and nonlinear, finite element seismic simulations at small- and large-scale, and their performance on minicomputers and supercomputers, particularly the Cray-2. The second paper develops a rigorous theory of vector wave diffraction for the canonical planar wedge problem. The third paper presents a numerical evaluation and verification of the two-dimensional diffraction theory for various types of incident plane-wave polarization. The diffraction solutions described here are used to verify discrete numerical solutions in the neighborhood of sharp edges. Validation is required because basis functions for the discrete solvers do not support the field singularities that actually occur at an edge. In fact, the exact solution evaluated here indicates that edge-diffracted seismic wave fields calculated by discrete numerical methods probably exhibits significant errors. GRA

N90-21491 Georgia Inst. of Tech., Atlanta.
THE EXTENSION OF RAPID DISTORTION THEORY TO STRATIFIED SHEAR FLOWS Ph.D. Thesis
Bryan Alan Baum 1989 108 p
Avail: Univ. Microfilms Order No. DA9005469

The combined effect of stratification and shear on the development of initially isotropic turbulence is investigated. The motivation is due to the common occurrence of shear driven turbulence in the atmosphere and the ocean where the presence of stratification may have important implications in the energy budgets. The focus is not only in the overall turbulence kinetic energy (TKE) and turbulence potential energy (TPE) budgets, but the mechanics of the intercomponent energy transfer. The flow idealization consists of an initially isotropic turbulent air parcel which, at $t = O$, is subjected to both a mean shear and stratification. The equations of motion and of turbulent transport describing this system are derived and simplified using rapid, distortion theory (RDT). The novelty is that with this formulation, any arbitrary height dependent background wind and potential temperature profile may be imposed. The numerical results reported are compared successfully to results previously reported in the literature. When both stratification and uniform shear are imposed on the turbulent air parcel, it is found that stratification acts to limit the generation of TKE. A significant portion of TKE may be converted to TPE. The pressure-strain terms, which act to redistribute energy between components, show a strong sensitivity to stratification. Stratification acts to reduce the magnitude of the velocity correlation but has the greatest effect on the vertical component (w'w'). One result is that counter-gradient heat fluxes develop in response to the imposition of a stabilizing potential temperature gradient.
Dissert. Abstr.

N90-21492 Utah Univ., Salt Lake City.
THE INFLUENCE OF LATERAL BOUNDARY CONDITIONS, FIXED SURFACE FORCINGS, AND SYNOPTIC SITUATIONS UPON PREDICTABILITY ESTIMATES USING LIMITED AREA NUMERICAL MODELS Ph.D. Thesis
Tomislava Vukicevic 1989 140 p
Avail: Univ. Microfilms Order No. DA9004151

The predictability of synoptic scale and mesoscale atmosphere motions is investigated using limited area numerical forecast models. The influence of one-way interacting lateral boundary conditions upon predictability is studied using a 2-D barotropic numerical model and a complete mesoscale limited area model. It is shown that the initial perturbations grow only in domains larger than a critical size and damp in smaller domains. It is found that a main mechanism by which one-way interacting lateral boundary conditions constrain the evolution of initial perturbations is by setting the upper wavelength limit upon horizontal scales that are free to evolve in accordance to model dynamics. A major contributor to the differences between predictability properties of global numerical models and limited area models is the one-way interacting lateral boundary constraint in the latter case. On the other hand, it is shown that large scale growing boundary perturbations contaminate the internal solution rather quickly. This indicates that operational, medium range forecasts with nested limited area numerical models may not show significant improvement relative to the same integrations performed with global models. Dissert. Abstr.

N90-21493*# California Inst. of Tech., Pasadena.
AGE CONSTRAINTS FOR THE PRESENT FAULT CONFIGURATION IN THE IMPERIAL VALLEY, CALIFORNIA: EVIDENCE FOR NORTHWESTWARD PROPAGATION OF THE GULF OF CALIFORNIA RIFT SYSTEM
Shawn Larsen and Robert Reilinger (Massachusetts Inst. of Tech., Cambridge.) 1990 29 p
(Grant NAG5-814)
(NASA-CR-186541; NAS 1.26:186541) Avail: NTIS HC A03/MF A01 CSCL 08G

Releveling and other geophysical data for the Imperial Valley of southern California suggest the northern section of the Imperial-Brawley fault system, which includes the Mesquite Basin and Brawley Seismic Zone, is much younger than the 4 to 5 million year age of the valley itself. A minimum age of 3000 years is calculated for the northern segment of the Imperial fault from correlations between surface topography and geodetically observed seismic/interseismic vertical movements. Calculations of a maximum age of 80,000 years is based upon displacements in the crystalline basement along the Imperial fault, inferred from seismic refraction surveys. This young age supports recent interpretations of heat flow measurements, which also suggest that the current patterns of seismicity and faults in the Imperial Valley are not long lived. The current fault geometry and basement morphology suggest northwestward growth of the Imperial fault and migration of the Brawley Seismic Zone. It is suggested that this migration is a manifestation of the propagation of the Gulf of California rift system into the North American continent. Author

N90-21494# Instituto de Pesquisas Espaciais, Sao Jose dos Campos (Brazil).
LOW LATITUDE F-REGION DYNAMICAL PROCESSES FROM ATOMIC OXYGEN NIGHTGLOW EMISSIONS
J. A. Bittencourt and Y. Sahai Jun. 1989 30 p Presented at the 1st Latin-American Conference on Space Geophysics, San Paulo, Brazil, 21-23 Nov. 1988
(INPE-4999-PRE/1561) Avail: NTIS HC A03/MF A01

Simultaneous observations of permitted and forbidden atomic oxygen airglow emissions have been used in the past by several investigators to study nighttime dynamical processes in the low latitude F region ionospheric plasma. Simultaneous measurements of the emissions OI 135.6 nm (or OI 777.4 nm) and OI 630.0 nm, either from satellite or from ground-based instrumentation, can be used to infer the F region peak electron density, n (e), and height, h. Results are presented showing the use of this remote sensing technique to study low latitude ionospheric dynamical processes, including mapping of F region plasma irregularities and transequatorial plasma bubbles, ionospheric effects due to thermospheric neutral winds and ionospheric response during magnetically disturbed conditions. Author

N90-21495# Commonwealth Scientific and Industrial Research Organization, Mordialoc (Australia). Div. of Atmospheric Research.
ZONES OF FEASIBILITY FOR RETRIEVAL OF SURFACE PRESSURE FROM OBSERVATIONS OF ABSORPTION IN THE A BAND OF OXYGEN
D. M. OBrien and R. M. Mitchell 1989 15 p
(DAR-TP-19; ISBN-0-643-05086-8) Copyright Avail: NTIS HC A03/MF A01

The study by the authors in 1987 demonstrated the feasibility of remote sensing of surface pressure based on analysis of the oxygen A-band as observed in sunlight reflected from the sea. The results of the earlier work are used to map the regions on the sea where the technique should allow retrieval of pressure with an accuracy of 2 hPa. The regions are shown to be extensive and to be rather insensitive to the surface wind speed. Author

N90-21496# Commonwealth Scientific and Industrial Research Organization, Mordialoc (Australia). Div. of Atmospheric Research.
SENSITIVITY STUDIES IN A TWO-DIMENSIONAL ATMOSPHERIC TRANSPORT MODEL
J. V. Mansbridge and I. G. Enting 1989 36 p
(DAR-TP-18; ISBN-0-643-05070-1) Copyright Avail: NTIS HC A03/MF A01

A series of sensitivity studies carried out on a 2-D atmospheric transport model is described. The model was used to deduce sources of total carbon given surface observations of CO2. It was found that the deduced sources are very sensitive to the vertical resolution in the model if the procedure used to specify the lower boundary condition and deduce the tracer source is only accurate to first order in the vertical grid spacing. A number of improved formulations of this lower boundary condition are suggested and tested. Author

N90-21497# National Center for Atmospheric Research, Boulder, CO. Climate and Global Dynamics Div.
THEORY AND APPLICATION OF NONLINEAR NORMAL MODE INITIALIZATION
Ronald M. Errico Nov. 1989 148 p
(Grant NSF ATM-87-09659)
(PB90-166000; NCAR/TN-344-1A) Avail: NTIS HC A07/MF A01 CSCL 04A

A comprehensive summary of the theory and application of nonlinear normal model initialization (NNMI) is presented. NNMI was developed in the late 1970s for initialization of models used for numerical weather prediction (NWP). The purpose of initialization is discussed, followed by a brief history of solutions to the problem of initialization. Attention is focused on NNMI rather than on earlier schemes. A simple model is used to introduce and describe normal modes and the phenomenon of linear geostrophic adjustment; nonlinear aspects are reintroduced and NNMI described; the applications of NNMI to global and regional models are presented; and the relationship of NNMI to quasi-geostrophic theory is discussed. A summary stressing the use of NNMI is presented. Although not as detailed as a textbook, this technical note is intended as an aid for a graduate in dynamic meteorology.
Author

47 METEOROLOGY AND CLIMATOLOGY

Includes weather forecasting and modification.

N90-21498# National Oceanic and Atmospheric Administration, Washington, DC. Office of Research and Applications.
PRELIMINARY REPORT ON THE DEMONSTRATION OF THE VAS CO2 CLOUD PARAMETERS (COVER, HEIGHT, AND AMOUNT) IN SUPPORT OF ASOS
W. P. Menzel and K. I. Strabala (Wisconsin Univ., Madison.) Nov. 1989 25 p
(NOAA-TM-NESDIS-29) Avail: NTIS HC A03/MF A01

A demonstration of the utility of the Visible Spin Scan radiometer Atmospheric Sounder (VAS) CO2 cloud parameters (cover, height, amount) for augmenting conventional ground observations was undertaken. The geostationary multispectral observations are readily synchronized with the ground reports and are available over North America. Three weeks of comparisons in summer 1989 of the satellite derived cloud information with surface observations show that the satellite can supplement surface measurements of cloud cover above 10,000 feet. Preliminary conclusions are that: above 400 mb (25,000 feet) the satellite information is more reliable; between 400 and 700 mb (10,000 feet) the satellite and ground observations are complementary; and below 700 mb the surfce observation is preferable. The VAS cloud product derivation is explained, a few illustrative examples are presented, the statistics of the three weeks of intercomparisons are summarized, and guidelines for interpreting the satellite results are suggested.
Author

N90-21499# Finnish Meteorological Inst., Helsinki. Dept. of Geophysics.
OBSERVATIONS OF ATMOSPHERIC ELECTRICITY, 1988
Tapio J. Tuomi 1989 60 p

(Geophysical-Publ-10; ISBN-951-697-304-3; ISSN-0782-6087)
Avail: NTIS HC A04/MF A01

Ground level atmospheric electricity is continuously measured at two stations, Helsinki (Helsinki-Vantaa Airport) and Kevo (Kevo Subarctic Research Station), and this publication summarizes the results of the so-called fair-weather or undisturbed hours. At Helsinki continuous recording of the potential gradient, the air-earth current density and the two polar conductivities of air was practiced. At Kevo the atmospheric electric station recorded the potential gradient and current density, but not the conductivity. Author

N90-21500# Federal Aviation Administration, Atlantic City, NJ. Technical Center.
METEOROLOGIST WEATHER PROCESSOR (MWP) INTEGRATION TEST PLAN
Wilfred Huber and Bruce E. Ware (Data Transformation Corp., Houston, TX.) Mar. 1990 27 p
(DOT/FAA/CT-TN89/62) Avail: NTIS HC A03/MF A01

The Meteorologist Weather Processor (MWP) System is an element of the National Airspace System (NAS) modernization. The initial MWP is a leased interim system which will be replaced after 5 years by an end-state system which will meet all of the requirements of NAS-SS-1000 for the Meteorologist Weather Processor/Central Flow Meteorologist Weather Processor (MWP/CFMWP). The contractor, Harris Corporation, is responsible for all aspects of system support including communications and maintenance. The MWP will be capable of processing weather data from a variety of sources including alphanumeric and graphic products, radar weather data, and satellite imagery. These weather products will be used by the Center Weather Service Unit (CWSU) meteorologists, Traffic Management Unit (TMU) personnel in briefing pilots, and air traffic control (ATC) personnel concerning weather products. Author

N90-21501*# Wisconsin Univ., Madison. Space Science and Engineering Center.
USE OF MICROWAVE SATELLITE DATA TO STUDY VARIATIONS IN RAINFALL OVER THE INDIAN OCEAN Final Report, 1 Aug. 1986 - 28 Feb. 1990
Barry B. Hinton, David W. Martin, Brian Auvine, and William S. Olson Mar. 1990 61 p
(Grant NAGw-920)
(NASA-CR-186408; NAS 1.26:186408) Avail: NTIS HC A04/MF A01 CSCL 04B

The University of Wisconsin Space Science and Engineering Center mapped rainfall over the Indian Ocean using a newly developed Scanning Multichannel Microwave Radiometer (SMMR) rain-retrieval algorithm. The short-range objective was to characterize the distribution and variability of Indian Ocean rainfall on seasonal and annual scales. In the long-range, the objective is to clarify differences between land and marine regimes of monsoon rain. Researchers developed a semi-empirical algorithm for retrieving Indian Ocean rainfall. Tools for this development have come from radiative transfer and cloud liquid water models. Where possible, ground truth information from available radars was used in development and testing. SMMR rainfalls were also compared with Indian Ocean gauge rainfalls. Final Indian Ocean maps were produced for months, seasons, and years and interpreted in terms of historical analysis over the sub-continent. Author

N90-21502*# Pennsylvania State Univ., University Park. Dept. of Meteorology.
PREDICTABILITY OF WEATHER AND CLIMATE IN A COUPLED OCEAN-ATMOSPHERE MODEL: A DYNAMICAL SYSTEMS APPROACH Ph.D. Thesis
Jon M. Nese Aug. 1989 4 p
(Grant NAGw-1434)
(NASA-CR-186499; NAS 1.26:186499) Avail: NTIS HC A01/MF A01 CSCL 04B

A dynamical systems approach is used to quantify the instantaneous and time-averaged predictability of a low-order moist general circulation model. Specifically, the effects on predictability of incorporating an active ocean circulation, implementing annual solar forcing, and asynchronously coupling the ocean and atmosphere are evaluated. The predictability and structure of the model attractors is compared using the Lyapunov exponents, the local divergence rates, and the correlation, fractal, and Lyapunov dimensions. The Lyapunov exponents measure the average rate of growth of small perturbations on an attractor, while the local divergence rates quantify phase-spatial variations of predictability. These local rates are exploited to efficiently identify and distinguish subtle differences in predictability among attractors. In addition, the predictability of monthly averaged and yearly averaged states is investigated by using attractor reconstruction techniques.
Author

N90-21503# National Oceanic and Atmospheric Administration, Boulder, CO. Wave Propagation Lab.
EDITING WIND PROFILER MEASUREMENTS
David B. Wuertz and Bob L. Weber Aug. 1989 84 p
(PB90-130147; NOAA-TR-ERL-438-WPL-62) Avail: NTIS HC A05/MF A01 CSCL 04B

An algorithm is described for editing profiler measurements of wind components over height and/or over time. The algorithm identifies and edits those measurements that do not fall within a continuously connected pattern. The algorithm is based on the premise that a fundamental component of any editor is a model that defines continuity. A simple continuity model is used to provide many examples to demonstrate that wind profiler measurements can be edited automatically and objectively with confidence.
Author

N90-21504# Oregon State Univ., Corvallis. Dept. of Atmospheric Sciences.
METEOROLOGICAL INFLUENCES ON MOUNTAIN CLOUDWATER CHEMISTRY IN THE EASTERN UNITED STATES
Richard J. Vong, Bruce H. Bailey, Michael J. Markus, and Volker A. Mohnen (State Univ. of New York, Albany.) 1986 6 p Presented at the International Conference on Forest Decline Research: State of Knowledge and Perspectives, Friedrichshafen, Fed. Republic of Germany, 2-6 Oct. 1989 Sponsored by Environmental Research Lab., Corvallis, OR
(PB90-132432; EPA/600/D-89/263) Avail: NTIS HC A02/MF A01 CSCL 04B

To relate cloudwater composition with large scale circulation features, cloud events sampled during the 1986 to 1988 field seasons by the U.S. EPA Mountain Cloudwater Chemistry Program (MCCP) were classified according to the principal synoptic features responsible for cloud production. The scheme classifies cloud events according to a mountain's location relative to surface weather map features for hours when cloud was observed at the sites. Goals were to: (1) understand the extreme variability in cloud water chemistry; (2) analyze the effect of the part-time, nonrandom sampling protocol (every cloud hour was sampled during several multiple week sampling intensives but no events were sampled for other multiple week periods); and (3) establish meteorological scenarios for cloud water interception models. Author

N90-21505# Air Force Inst. of Tech., Wright-Patterson AFB, OH.
TROPICAL CYCLONE TRACK PREDICTABILITY AND THE ADJOINT METHOD OF DATA ASSIMILATION M.S. Thesis - Colorado State Univ.
Bruce W. Thompson 1989 87 p
(AD-A218324; AFIT/CI/CIA-89-065) Avail: NTIS HC A05/MF A01 CSCL 04/2

This thesis explores a new method to improve hurricane track forecasts. This is done by modifying the model's initial conditions using the adjoint method developed by Talagrand and Courtier (1987). The idea is to run the model forward using the governing equation, and then run the model backwards using the adjoint equation. The result of the forward integration is the distance function, and the result of the backward integration is the gradient of the distance function, where the distance function is a scalar measure of the distance between the observed and model

hurricane track. The gradient of the distance function is used in a minimization scheme that modifies the initial conditions. These new initial conditions produce a model track closer to the observed track. Like Talagrand and Courtier, we derive the adjoint method using the spectral nondivergent vorticity equation. However, to eliminate computational error, here we use the Adams-Bashforth time integration scheme instead of the leapfrog method. Experiments were run using the nondivergent barotropic model to indicate how the adjoint method can improve hurricane track forecasts. GRA

N90-21506 Nevada Univ., Reno.
NUMERICAL SIMULATIONS OF THE CLOUD-CAPPED MARINE BOUNDARY LAYER Ph.D. Thesis
Darko Rudolf Koracin 1989 151 p
Avail: Univ. Microfilms Order No. DA9008162

A one-dimensional, second-moment, turbulent closure model (including both shortwave and longwave radiative transfer) is applied to the subtropical, cloud-capped marine boundary layer (MABL) in the vicinity of ocean temperature fronts. Simulations have shown that in convective conditions the cloud and subcloud layers have decoupled turbulence structure by the influence of solar radiative heating within the cloud. During nighttime, the cloud and subcloud layers are usually recoupled by the effect of redistribution of longwave cooling at cloud top within the whole MABL. As warm air flows over cooler water, negative buoyancy occurs close to the sea surface and a stable internal boundary layer (IBL) develops in which shear production of turbulent kinetic energy balances the negative buoyancy and small-scale dissipation of energy. The IBL decouples subcloud and cloud layers from the surface and confines the moisture in it for the time scale of the order of several hours to one day. The present study has shown that nighttime recoupling between the cloud and subcloud layers would not occur on the colder water side of the ocean front due to the reduced surface forcing and consequently insufficient redistribution of longwave cooling at the cloud top. On the time scale of one to two days, these simulations have shown that the IBL can overcome stable interface between the cloud and subcloud layers and promote rapid cloud development by transferring accumulated moisture aloft. Dissert. Abstr.

N90-21507 Nevada Univ., Reno.
PRECIPITATION MECHANISMS IN TROPICAL AND MIDLATITUDE CONVECTIVE CLOUDS Ph.D. Thesis
Kyung-Eak Kim 1989 287 p
Avail: Univ. Microfilms Order No. DA9004375

Microphysical data from aircraft penetrations in convective clouds over Montana and the ocean off Florida are analyzed to investigate the precipitation mechanisms operating in tropical and midlatitude regions where summertime convective clouds always include the freezing level. Special emphasis is placed on the analysis of broadening of droplet size spectrum, ice multiplication, and entrainment and mixing process in the development of precipitation. The analysis of mixing process is attempted using a new method developed on a theoretical basis. Using the analysis results, the precipitation mechanisms in three convective cloud systems, which have different environmental characters, are compared, and conceptual models of precipitation development of these systems are organized. Dissert. Abstr.

N90-21508# Federal Aviation Administration, Atlantic City, NJ. Technical Center.
ANALYSIS OF DISTRIBUTIONS OF VISUAL METEOROLOGICAL CONDITIONS (VMC) HELIPORT DATA Technical Report, Nov. 1988
Christopher J. Wolf Mar. 1990 1055 p
(DOT/FAA/CT-TN89/67) Avail: NTIS HC A99/MF E09

The FAA Technical Center's Visual Meteorological Conditions (VMC) project was designed to provide data for the validation of the Heliport Design Advisory Circular (AC 150/5390-2) visual approach/departure surface criteria. Procedures for the analysis of data collected during this project were specified by the Design and Operations Criteria Division, AAS-100. These procedures are based on an assumption of the Gaussian, or Normal, distribution. The results of the VMC Project, based on the assumption of Normal data, are documented in DOT/FAA/CT-TN87/40, Heliport Visual Approach and Departure Airspace Tests. During the data reduction and analysis phase of the VMC project, questions were raised as to validity of the assumption of the Normal distribution for the characterization of VMC data. An effort undertaken to look at the VMC data for the purpose of drawing conclusions about the proper distributional assumption is documented. Several different procedures were used to test the original assumption. Information is provided on the tests used in this effort and on several alternate distributions, i.e., the Beta and Gamma distributions. Author

N90-21509# Federal Aviation Administration, Washington, DC. Flightcrew Systems Research Branch.
WINDSHEAR CASE STUDY: DENVER, COLORADO, JULY 11, 1988 Final Report
Herbert W. Schlickenmaier Nov. 1989 470 p
(DOT/FAA/DS-89/19) Avail: NTIS HC A20/MF A03

On Monday 11 July 1988 between 2207 and 2213 UTC (16:07 to 16:13 MDT), four successive United flights had inadvertent encounters with microburst windshear conditions while on final approach to Denver Stapleton Airport (DEN), each resulting in a missed approach, subsequent delay, and uneventful arrival. A fifth flight executed a missed approach without encountering the phenomena. All of the flight crews were trained utilizing the resources of the Windshear Training Aid. There was no damage to aircraft and no passenger injuries. At the time the aircraft encountered the microburst, the Terminal Doppler Weather Radar (TDWR) Operations Test and Experiment (OT&E) was in progress and detected divergent flow that intersected the operating zones for the approach runways. The radar used to test the TDWR algorithm was the Massachusetts Institute of Technology Lincoln Laboratory 10 cm Doppler radar. This Windshear Case Study outlines the technical details of the encounter, as well as describes insights gained from this confrontation that should be applied to future investigations of aircraft encountering windshear. Information was summarized from several sources including flight crew comments, air traffic control (ATC) operations and surveillance radar data, flight data recorders, data from the TDWR and the Low-Level Wind Shear Alert System (LLWAS), technical details of the event meteorology, and data from the Terminal Area Simulation System (TASS). Author

48 OCEANOGRAPHY

Includes biological, dynamic, and physical oceanography; and marine resources.

For related information see also *43 Earth Resources and Remote Sensing.*

N90-21510# Materials Research Labs., Maribyrnong (Australia).
AN OUTLINE FOR THE ANALYSIS OF WAVE INDUCED BOTTOM PRESSURE FLUCTUATIONS
G. Saiva 1989 36 p
(MRL-TN-558; AR-005-725) Avail: NTIS HC A03/MF A01

A computer program is outlined which replaces the manual Draper-Tucker analysis of bottom pressure fluctuations induced by surface waves. The analysis described in this note is basically concerned with the analysis of individual bottom pressure records, i.e., with the short term statistics. Short term statistics collected over a number of years enable the deduction of the medium term wave climate statistics, which are essential for the planning of mine warfare operations. They are used for the estimation of the effects that the waves might have on the effectiveness of pressure mines during a particular month, season or year. The long term statistics are of limited interest to mine warfare studies. Author

N90-21511# Oak Ridge National Lab., TN. Environmental Sciences Div.
MODELING THE UPPER OCEAN AND ITS INTERACTION WITH THE ATMOSPHERE

Tsing-Hung Peng 28 Mar. 1990 12 p Presented at the International Meeting on Modeling the Physics, Biology and Chemistry of the Upper Ocean and its Interaction with the Atmosphere, London (England), 12-13 Mar. 1990
(Contract DE-AC05-84OR-21400)
(DE90-008980; ORNL/FTR-3555) Avail: NTIS HC A03/MF A01

The author attended the International Meeting on Modeling the Physics, Biology and Chemistry of the Upper Ocean and its Interaction with the Atmosphere in London, England, and presented a lecture entitled Modeling the Seasonality of CO2 in the North Atlantic. Most lectures focused on the modeling of the upper ocean, with a particular emphasis in the area of marine biology and marine ecosystems. Models ranged from simple box ocean models to general circulation models. At the end of the conference, it became clear that a better understanding of global change in climate atmospheric CO2 variations requires a closer link between the studies of marine biology and ocean physics and chemistry.
DOE

51 LIFE SCIENCES (GENERAL)

N90-21512# Lawrence Livermore National Lab., CA. Biomedical Sciences Div.
DOES DNA CYTOMETRY HAVE A PLACE IN THE CLINICAL LABORATORY
Brian Mayall, Frederic Waldman, Karen Chew, Konstantin Christov, William Goodson, Britt-Marie Ljung, and Helene S. Smith (Brush, Geraldine Cancer Research Inst., San Francisco, CA) 24 Jan. 1990 4 p Presented at the European Society for Analytical Cellular Pathology on Advances in Analytical Cellular Pathology, Schloss Elmau, Fed. Republic of Germany, 12-17 Nov. 1989 Sponsored in part by Lab. for Cell Analysis, Univ. of California, San Francisco; Univ. of California Program for Analytical Cytology; and Brush (Geraldine) Cancer Research Inst., San Francsico, CA
(Contract W-7405-eng-48; CA-44768)
(DE90-007652; UCRL-102862; CONF-8911174-1) Avail: NTIS HC A01/MF A01

We are investigating the potential utility of cellular markers, including cellular proliferation and DNA cytometry, as independent diagnostic and prognostic markers in human breast cancer. However, as the clinical laboratory is responsible for providing physicians with data relevant to the patient, it is essential first to establish the validity of such markers before their use is recommended. Prospective validation is time-consuming and costly for tests of human malignancies, such as breast cancer, which may follow a lengthy and indolent course requiring patients to be followed for a decade or more before their clinical outcome is known. Therefore, retrospective studies on archival material are used whenever possible. Cell proliferation is recognized as an important diagnostic and prognostic marker for human breast cancer and a tritiated thymidine DNA labeling index greater than 5 percent is associated with a markedly less favorable outcome. Incorporation of bromodeoxyuridine (BrdUrd) into the DNA of S phase cells gives a similar labeling index. Unfortunately, paraffin-embedded archival material is rarely pre-labeled, and so DNA cytometry of either whole nuclei disaggregated from thick sections or partial nuclei in thin sections must be used as an indirect approach to estimate cellular proliferative activity. We are particularly interested in validating the DNA cytometry of thin sections and in relating the DNA histogram to in vivo BrdUrd labeling index, which is our standard for cellular proliferation.
DOE

N90-21513*# Lockheed Engineering and Sciences Co., Washington, DC.
USSR SPACE LIFE SCIENCES DIGEST, ISSUE 26
Lydia Razran Stone, ed., Mary Ann Frey, ed., Ronald Teeter, ed., Victoria Garshnek, ed., and Joseph Rowe, ed. (Library of Congress, Washington, DC.) Washington, DC NASA May 1990 104 p
(Contract NASw-4292)
(NASA-CR-392231; NAS 1.26:392231) Avail: NTIS HC A06/MF A01 CSCL 06C

This is the twenty-sixth issue of NASA's USSR Space Life Sciences Digest. It contains abstracts of 35 journal papers or book chapters published in Russian and of 8 Soviet books. In addition, the proceedings of an Intercosmos conference on space biology and medicine are summarized.
Author

N90-21514# Pacific Northwest Lab., Richland, WA.
BIOLOGICAL EFFECTS OF ELF (EXTREMELY-LOW-FREQUENCY) ELECTRIC AND MAGNETIC FIELDS
L. E. Anderson Oct. 1989 7 p Presented at the US/USSR Cooperative Agreement on Physical Factors in the Environment, Prague, Czechoslovakia, 24 Sep. - 10 Oct. 1989
(Contract DE-AC06-76RL-01830)
(DE90-008634; PNL-SA-17321; CONF-8909315-1) Avail: NTIS HC A02/MF A01

Studies were conducted at the Pacific Northwest Laboratory to examine extremely-low-frequency (ELF) electromagnetic fields for possible biological effects in animals. Two areas of investigation are reported here: studies on the nervous system, including behavior and neuroendocrine function, and experiments on cancer development in animals. In behavioral experiments, preliminary data suggest that short term memory may be affected in albino rats exposed to combined ELF and static magnetic fields. Neuroendocrine studies were conducted to demonstrate an apparent stress-related response in rats exposed to 60-Hz electric fields. Finally, using a chemically-induced mammary tumor model, experiments were conducted in which rats, chronically exposed to 60-Hz electric fields, showed an enhancement in the number of tumors per tumor bearing animal.
DOE

N90-21515# Los Alamos National Lab., NM.
ARTIFICIAL LIFE: THE COMING EVOLUTION
J. Doyne Farmer and Alleta dA. Belin (Shute, Mihaly and Weinberger, Santa Fe, NM.) 1990 26 p Presented at the Indirect Liquefaction Contractors Review Meeting, Pittsburgh, PA, 13-15 Nov. 1989 Prepared in cooperation with Santa Fe Coll., NM
(Contract W-7405-eng-36)
(DE90-008860; LA-UR-90-378; CONF-891131) Avail: NTIS HC A03/MF A01

Within fifty to a hundred years a new class of organisms is likely to emerge. These organisms will be artificial in the sense that they will originally be designed by humans. However, they will reproduce, and will evolve into something other than their initial form; they will be alive under any reasonable definition of the word. These organisms will evolve in a fundamentally different manner than contemporary biological organisms, since their reproduction will be under at least partial conscious control, giving it a Lamarckian component. The pace of evolutionary change consequently will be extremely rapid. The advent of artificial life will be the most significant historical event since the emergence of human beings. The impact on humanity and the biosphere could be enormous, larger than the industrial revolution, nuclear weapons, or environmental pollution. We must take steps now to shape the emergence of artificial organisms; they have potential to be either the ugliest terrestrial disaster, or the most beautiful creation of humanity.
DOE

N90-21516# Cornell Univ., Ithaca, NY.
ANAEROBIC METABOLISM OF AROMATIC COMPOUNDS BY PHOTOTROPHIC BACTERIA: BIOCHEMICAL ASPECTS Annual Progress Report, 1 Apr. - 15 Nov. 1989
Jane Gibson 1989 4 p Presented at the Annual Meeting of the American Society for Microbiology, Anaheim, CA, May 1990
(Contract DE-FG02-86ER-13495)
(DE90-009503; DOE/ER-13495/T3) Avail: NTIS HC A01/MF A01

Two aspects of the work proposed have received major emphasis during the period since the grant was activated: isolation

and characterization of transposon insertion mutants of Rhodopseudomonas palusrtis defective in phototrophic growth on aromatic compounds, and attempts to purify and characterize the Coenzyme A ligase enzyme involved in activating 4-hydroxybenzoate. The HPLC apparatus was installed in August, and calibration of columns both for metabolite and for protein separations was initiated. A start has also been made on synthesis of Coenzyme A thioesters of compounds that are potential intermediates in the anaerobic degradation pathways. DOE

52 AEROSPACE MEDICINE

Includes physiological factors; biological effects of radiation; and effects of weightlessness on man and animals.

N90-21517 Pennsylvania State Univ., University Park.
KINEMATIC AND KINETIC ANALYSES OF DROP LANDINGS Ph.D. Thesis
Jill Lynn McNitt-Gray 1989 163 p
Avail: Univ. Microfilms Order No. DA8922084

During a landing impact, large forces which create the potential for injury are applied to the human body. In particular, the risk to the lower extremities during gymnastics landings has been proven to be high. The forces experienced may be modified by the human by selectively controlling the joint motion. To determine the effect of impact velocity (2.5 to 5.0 m/s) and landing experience on the strategy selected, the preferred landing strategies used by six male collegiate gymnasts and six male recreational athletes from three drop heights (.32 to 1.28 m) were characterized using mechanical descriptors. Kinematic and kinetic 2D data were acquired simultaneously using high speed film (202.4 fps) and a force plate (1000 Hz). Reaction forces, net joint moments, lower extremity joint motion, joint work, and the generated momentum of each segment were used to characterize the strategies. Results indicated that statistically significant (ANOVA, p less than .05) increases in joint flexion (with the exception of ankle joint flexion), angular velocity, net moments, work, and impact force resulted as impact velocity increased. Gymnasts and recreational athletes demonstrated similar adjustment patterns to increases in landing impact velocities; however, significant differences in degree of joint flexion and total landing phase time over impact velocity conditions were found. Dissert. Abstr.

N90-21518# Institute for Perception RVO-TNO, Soesterberg (Netherlands).
SPACE ADAPTATION SYNDROME INDUCED BY A LONG DURATION +3Gx CENTRIFUGE RUN Final Report
W. Bles, J. E. Bos, R. Furrer, B. deGraaf, R. J. A. W. Hosman, H. W. Kortschot, J. R. Krol, A. Kuipers, J. T. Marcus, and E. Messerschmid (Stuttgart Univ., Germany, F.R.) et al 31 Jul. 1989 45 p
(AD-A218248; IZF-1989-25; TDCK-89-1055) Avail: NTIS HC A03/MF A01 CSCL 06/10

The three European scientists astronauts of the D1 Spacelab Mission were exposed to a 1 1/2 hours +3G centrifuge run in supine position resulting in a linear acceleration along the x-axis (3Gx). Afterwards they experienced motion sickness symptoms which were for each of the astronauts similar to the symptoms of the Space Adaption Syndrome as experienced during their space flight in 1985. These motion sickness symptoms lasted up to 6 hours. In otolith function tests following the centrifuge run, changes in visual vestibular interaction were observed which replicated findings obtained immediately after their space flight. GRA

N90-21519* National Aeronautics and Space Administration. Langley Research Center, Hampton, VA.
RAPIDLY QUANTIFYING THE RELATIVE DISTENTION OF A HUMAN BLADDER Patent
John A. Companion, inventor (to NASA), Joseph S. Heyman, inventor (to NASA), Beth A. Mineo, inventor (to NASA), Albert R. Cavalier, inventor (to NASA), and Travis N. Blalock, inventor (to NASA) (Department of Education, Washington, DC.) 1 Aug. 1989 13 p Filed 10 Nov. 1987 Continuation-in-part of US-Patent-Appl-SN-929869, filed 13 Nov. 1986, abandoned (NASA-Case-LAR-13901-1-NP; US-Patent-4,852,578; US-Patent-Appl-SN-118993; US-Patent-Appl-SN-929869; US-Patent-Class-128-661.03) Avail: US Patent and Trademark Office CSCL 06B

A device and method of rapidly quantifying the relative distention of the bladder in a human subject are disclosed. The ultrasonic transducer which is positioned on the subject in proximity to the bladder is excited by a pulser under the command of a microprocessor to launch an acoustic wave into the patient. This wave interacts with the bladder walls and is reflected back to the ultrasonic transducer, when it is received, amplified and processed by the receiver. The resulting signal is digitized by an analog-to-digital converter under the command of the microprocessor and is stored in the data memory. The software in the microprocessor determines the relative distention of the bladder as a function of the propagated ultrasonic energy; and based on programmed scientific measurements and individual, anatomical, and behavioral characterists of the specific subject as contained in the program memory, sends out a signal to turn on any or all of the audible alarm, the visible alarm, the tactile alarm, and the remote wireless alarm.

Official Gazette of the U.S. Patent and Trademark Office

N90-21520# Australian Radiation Lab., Melbourne.
PROCEEDINGS OF A WORKSHOP ON CARCINOGENIC POTENTIAL OF EXTREMELY LOW FREQUENCY MAGNETIC FIELDS
Vincent Delpizzo, ed. and Donald W. Keam, ed. Feb. 1989 177 p Workshop held in Melbourne (Australia), 17 May 1988
(DE90-614340; ARL/TR-082; CONF-8805357) Avail: NTIS (US Sales Only) HC A09/MF A01

The debate over the suspected link between Extremely Low Frequency (ELF) magnetic fields and cancer is entering its second decade, but the end is not in sight. The epidemiological evidence is now somewhat stronger, mainly due to the Savitz study of residential exposure and childhood cancer, but far from overwhelming. The results of in-vitro studies are fragmentary, sometimes contradictory and, overall, confusing. Well designed animal studies are virtually non-existent. A plausible biological model has not yet been established. Although scant, the present body of knowledge is very complex encompassing several disciplines and this workshop brought together researchers of vastly different backgrounds. The nine papers presented deal with an overview of ELF and cancer; the biochemistry of processes implicated in ELF carcinogenesis; possible mechanisms of cancer promotion; the status of in-vitro ELF cellular interactions; epidemiological studies, both occupational and residential, and the use of wire coding configurations as indicators of magnetic field exposures in such studies. Discussion follows each paper. DOE

53 BEHAVIORAL SCIENCES

Includes psychological factors; individual and group behavior; crew training and evaluation; and psychiatric research.

N90-21521*# Essex Corp., Orlando, FL.
DEVELOPMENT OF MICROCOMPUTER-BASED MENTAL ACUITY TESTS FOR REPEATED-MEASURES STUDIES Final Report
R. S. Kennedy, R. L. Wilkes, D. R. Baltzley, and J. E. Fowlkes 25 Jan. 1990 73 p
(Contract NAS9-17326)
(NASA-CR-185607; NAS 1.26:185607) Avail: NTIS HC A04/MF A01 CSCL 05I

The purpose of this report is to detail the development of the Automated Performance Test System (APTS), a computer battery of mental acuity tests that can be used to assess human performance in the presence of toxic elements and environmental stressors. There were four objectives in the development of APTS.

First, the technical requirements for developing APTS followed the tenets of the classical theory of mental tests which requires that tests meet set criteria like stability and reliability (the lack of which constitutes insensitivity). To be employed in the study of the exotic conditions of protracted space flight, a battery with multiple parallel forms is required. The second criteria was for the battery to have factorial multidimensionality and the third was for the battery to be sensitive to factors known to compromise performance. A fourth objective was for the tests to converge on the abilities entailed in mission specialist tasks. A series of studies is reported in which candidate APTS tests were subjected to an examination of their psychometric properties for repeated-measures testing. From this work, tests were selected that possessed the requisite metric properties of stability, reliability, and factor richness. In addition, studies are reported which demonstrate the predictive validity of the tests to holistic measures of intelligence. Author

54 MAN/SYSTEM TECHNOLOGY AND LIFE SUPPORT

Includes human engineering; biotechnology; and space suits and protective clothing.

For related information see also *16 Space Transportation.*

N90-21522# National Aeronautical Lab., Bangalore (India). Computational and Theoretical Fluid Dynamics Div.
HUMAN FACTORS IN FIGHTER SOFTWARE DEVELOPMENT
Rajendra K. Bera Jan. 1990 11 p
(PD-CF-9003) Avail: NTIS HC A03/MF A01

In the development of any large scale software, human factors play a crucial role. This is even more true for fighter software which are embedded, real time, distributed, and fault tolerant. Those human factors which play an important role in the development of fighter software are examined. Author

N90-21523# Naval Air Development Center, Warminster, PA. Air Vehicle and Crew Systems Technology Dept.
THE EFFECT OF WINDSCREEN BOWS AND HUD PITCH LADDER FORMAT ON PILOT PERFORMANCE DURING SIMULATED FLIGHT Final Report, Oct. 1987 - Sep. 1988
John E. Deaton, Michael J. Barnes, Nancy J. Lindsey, Janettarose L. Greene, and Jonathan Kern (Veda, Inc., Warminster, PA.) 21 May 1989 19 p
(AD-A218139; NADC-89084-60) Avail: NTIS HC A03/MF A01 CSCL 01/3

During the upgrade of the F-14 to the F-14D, pilots have expressed their concerns regarding the obscuration of the forward field-of-view due to the new Head-Up Display (HUD) supports in conjunction with preexisting windscreen bows. An additional issue involves the proposed use of the HUD as the primary flight reference instrument. The HUD pitch ladder has been criticized for not providing enough information to enhance recovery from unusual attitudes. The purpose of the present study was, therefore, twofold: (1) to measure the levels of target detection with and without windscreen bows, and (2) to measure unusual attitude recovery performance using two different HUD pitch ladder formats - Standard versus Enhanced. During simulated flight, twelve subjects were required to make visual detections of enemy aircraft with and without the windscreen bow. Additionally, subjects were required to recover from various pitch/roll combinations. GRA

55 SPACE BIOLOGY

Includes exobiology; planetary biology; and extraterrestrial life.

No abstracts in this category.

59 MATHEMATICAL AND COMPUTER SCIENCES (GENERAL)

N90-21524*# National Aeronautics and Space Administration. Langley Research Center, Hampton, VA.
A TIME-ACCURATE ADAPTIVE GRID METHOD AND THE NUMERICAL SIMULATION OF A SHOCK-VORTEX INTERACTION
Michael J. Bockelie and Peter R. Eiseman (Columbia Univ., New York, NY.) Washington Jun. 1990 20 p
(Grants NAG1-427; AF-AFOSR-0307-86)
(NASA-TP-2998; L-16727; NAS 1.60:2998) Avail: NTIS HC A03/MF A01 CSCL 12A

A time accurate, general purpose, adaptive grid method is developed that is suitable for multidimensional steady and unsteady numerical simulations. The grid point movement is performed in a manner that generates smooth grids which resolve the severe solution gradients and the sharp transitions in the solution gradients. The temporal coupling of the adaptive grid and the PDE solver is performed with a grid prediction correction method that is simple to implement and ensures the time accuracy of the grid. Time accurate solutions of the 2-D Euler equations for an unsteady shock vortex interaction demonstrate the ability of the adaptive method to accurately adapt the grid to multiple solution features. Author

60 COMPUTER OPERATIONS AND HARDWARE

Includes hardware for computer graphics, firmware, and data processing.

For components see *33 Electronics and Electrical Engineering.*

N90-21525* National Aeronautics and Space Administration. Pasadena Office, CA.
VLSI BINARY UPDOWN COUNTER Patent
Trieu-Kie Truong, inventor (to NASA), In-Shek Hsu, inventor (to NASA), and Irving S. Reed, inventor (to NASA) (California Inst. of Tech., Pasadena.) 4 Jul. 1989 7 p Filed 13 Jan. 1988
(NASA-Case-NPO-17205-1-CU; US-Patent-4,845,728;
US-Patent-Appl-SN-143434; US-Patent-Class-377-123;
US-Patent-Class-377-111; US-Patent-Class-377-114;
US-Patent-Class-377-116; US-Patent-Class-377-126;
US-Patent-Class-377-69; US-Patent-Class-377-79) Avail: US Patent and Trademark Office CSCL 09B

A pipeline binary updown counter is comprised of simple stages that may be readily replicated. Each stage is defined by the Boolean logic equation: A(sub n)(t) = A(sub n)(t - 1) exclusive OR (U AND P(sub n)) inclusive OR (D AND Q(sub n)), where A(sub n)(t) denotes the value of the nth bit at time t. The input to the counter has three values represented by two binary signals U and D such that if both are zero, the input is zero, if U = 0 and D = 1, the input is -1 and if U = 1 and D = 0, the input is +1. P(sub n) represents a product of A(sub k)'s for 1 is less than or equal to k is less than or equal to -1, while Q(sub n) represents the product of bar A's for 1 is less than or equal to K is less than or equal to n - 1, where bar A(sub k) is the complement of A(sub k) and P(sub n) and Q(sub n) are expressed as the following two equations: P(sub n) = A(sub n - 1) A(sub n - 2)...A(sub 1) and Q(sub n) = bar A(sub n - 1) bar A(sub n - 2)...bar A(sub 1), which can be written in recursive form as P(sub n) = P(sub n - 1) AND bar A(sub n - 1) and Q(sub n) = Q(sub n - 1) AND bar A(sub n - 1) with the initial values P(sub 1) = 1 and Q(sub 1) = 1.
Official Gazette of the U.S. Patent and Trademark Office

N90-21526# Office of Technology Assessment, Washington, DC.
HIGH PERFORMANCE COMPUTING AND NETWORKING FOR SCIENCE

Sep. 1989 52 p
(PB90-131228; OTA-BP-CIT-59; LC-89-600758) Avail: NTIS HC A04/MF A01; also available SOD HC $2.25 as 052-003-01164-6 CSCL 09B

Key issues concerning the Federal role in supporting national high performance computing facilities and in developing a national research and education network are explored. Author

N90-21527* National Aeronautics and Space Administration. Pasadena Office, CA.
FAULT TOLERANT HYPERCUBE COMPUTER SYSTEM ARCHITECTURE Patent
Herb S. Madan, inventor (to NASA) and Edward Chow, inventor (to NASA) (California Inst. of Tech., Pasadena.) 19 Sep. 1989 18 p Filed 29 Oct. 1987
(NASA-Case-NPO-16859-1-CU; US-Patent-4,868,818; US-Patent-Appl-SN-113956; US-Patent-Class-371-11.3; US-Patent-Class-364-229.4; US-Patent-Class-364-267.9; US-Patent-Class-364-975.5; US-Patent-Class-364-940.67; US-Patent-Class-364-942.51; US-Patent-Class-364-944) Avail: US Patent and Trademark Office CSCL 09B

A fault-tolerant multiprocessor computer system of the hypercube type comprising a hierarchy of computers of like kind which can be functionally substituted for one another as necessary is disclosed. Communication between the working nodes is via one communications network while communications between the working nodes and watch dog nodes and load balancing nodes higher in the structure is via another communications network separate from the first. A typical branch of the hierarchy reporting to a master node or host computer comprises, a plurality of first computing nodes; a first network of message conducting paths for interconnecting the first computing nodes as a hypercube. The first network provides a path for message transfer between the first computing nodes; a first watch dog node; and a second network of message connecting paths for connecting the first computing nodes to the first watch dog node independent from the first network, the second network provides an independent path for test message and reconfiguration affecting transfers between the first computing nodes and the first switch watch dog node. There is additionally, a plurality of second computing nodes; a third network of message conducting paths for interconnecting the second computing nodes as a hypercube. The third network provides a path for message transfer between the second computing nodes; a fourth network of message conducting paths for connecting the second computing nodes to the first watch dog node independent from the third network. The fourth network provides an independent path for test message and reconfiguration affecting transfers between the second computing nodes and the first watch dog node; and a first multiplexer disposed between the first watch dog node and the second and fourth networks for allowing the first watch dog node to selectively communicate with individual ones of the computing nodes through the second and fourth networks; as well as, a second watch dog node operably connected to the first multiplexer whereby the second watch dog node can selectively communicate with individual ones of the computing nodes through the second and fourth networks. The branch is completed by a first load balancing node; and a second multiplexer connected between the first load balancing node and the first and second watch dog nodes, allowing the first load balancing node to selectively communicate with the first and second watch dog nodes.
Official Gazette of the U.S. Patent and Trademark Office

N90-21528# Tokyo Univ., Tanashi (Japan). Inst. for Nuclear Study.
CAMAC MEMORY MODULE: MEMO-32
Masaru Ikeda Sep. 1989 16 p In JAPANESE; ENGLISH summary
(DE90-759846; INS-T-490) Avail: NTIS (US Sales Only) HC A03/MF A01

For high-speed data transfer from the CAMAC front-end electronics to an on-line computer, two types of CAMAC memory modules (MEMO-32 and MEMO-32Q) have been developed. These modules snoop the data on the CAMAC dataway and write them on a memory by one CAMAC command; F(0). This feature reduces the number of CAMAC actions for data acquisition. With these modules, even an inexpensive system consisting of a personal computer and an auxiliary Crate Controller can handle a large amount of data in high speed. The modules have been used for experiments with the large acceptance spectrometer, TAGX, at the 1.3-GeV ES. DOE

61 COMPUTER PROGRAMMING AND SOFTWARE

Includes computer programs, routines, alogorithms, and specific applications, e.g., CAD/CAM.

N90-21529*# Alabama Univ., Huntsville.
COOPERATING INTELLIGENT SYSTEMS Final Report
Daniel Rochowiak Aug. 1989 43 p
(Contract NCC8-13)
(NASA-CR-184982; NAS 1.26:184982; UAH-RR-804) Avail: NTIS HC A03/MF A01 CSCL 09B

Some of the issues connected to the development of a bureaucratic system are discussed. Emphasis is on a layer multiagent approach to distributed artificial intelligence (DAI). The division of labor in a bureaucracy is considered. The bureaucratic model seems to be a fertile model for further examination since it allows for the growth and change of system components and system protocols and rules. The first part of implementing the system would be the construction of a frame based reasoner and the appropriate B-agents and E-agents. The agents themselves should act as objects and the E-objects in particular should have the capability of taking on a different role. No effort was made to address the problems of automated failure recovery, problem decomposition, or implementation. Instead what has been achieved is a framework that can be developed in several distinct ways, and which provides a core set of metaphors and issues for further research. Author

N90-21530# National Inst. of Standards and Technology, Gaithersburg, MD. National Computer Systems Lab.
SOFTWARE VERIFICATION AND VALIDATION: ITS ROLE IN COMPUTER ASSURANCE AND ITS RELATIONSHIP WITH SOFTWARE PROJECT MANAGEMENT STANDARDS Report, Jul. 1988 - May 1989
Dolores R. Wallace and Roger U. Fujii (Logicon, Inc., San Pedro, CA.) Sep. 1989 40 p
(PB90-111691; NIST/SP-500/165; LC-89-600754) Avail: NTIS HC A03/MF A01; SOD HC $2.25 as 003-003-02959-9 CSCL 09B

How the software verification and validation (V and V) methodology and V and V standards provide a strong framework for developing quality software is described. First, software V and V is described along with objectives, recommended tasks, and guidance for selecting techniques to perform V and V. The difference is explained between V and V and quality assurance, development system engineering, and user organization functions. It is explained that V and V produces maximum benefits when it is performed independent of development functions and a brief discussion is provided of how V and V benefits change when embedded in quality assurance, development systems engineering, and user organizations. An analysis of two studies of V and V's cost effectiveness concludes that cost benefits of V and V's early error detection outweigh the cost of performing V and V. Author

N90-21531*# Maryland Univ., College Park. Inst. for Advanced Computer Studies.
MAINTENANCE = REUSE-ORIENTED SOFTWARE DEVELOPMENT
Victor R. Basili May 1989 14 p Presented at the Conference on Software Maintenance, Phoenix, AZ, Oct. 1988

(Contract NsG-5123; N00014-87-K-0307)
(NASA-CR-186455; NAS 1.26:186455; UMIACS-TR-89-48; CS-TR-2244) Avail: NTIS HC A03/MF A01 CSCL 09B

Maintenance is viewed as a reuse process. In this context, a set of models that can be used to support the maintenance process is discussed. A high level reuse framework is presented that characterizes the object of reuse, the process for adapting that object for its target application, and the reused object within its target application. Based upon this framework, a qualitative comparison is offered of the three maintenance process models with regard to their strengths and weaknesses and the circumstances in which they are appropriate. To provide a more systematic, quantitative approach for evaluating the appropriateness of the particular maintenance model, a measurement scheme is provided, based upon the reuse framework, in the form of an organized set of questions that need to be answered. To support the reuse perspective, a set of reuse enablers are discussed. Author

N90-21532*# Maryland Univ., College Park. Inst. for Advanced Computer Studies.

INTEGRATING AUTOMATED SUPPORT FOR A SOFTWARE MANAGEMENT CYCLE INTO THE TAME SYSTEM

Toshihiko Sunazuka (Nippon Electric Co. Ltd., Tokyo, Japan) and Victor R. Basili Jul. 1989 21 p Sponsored in part by Nippon Electric Co., Ltd.
(Grant NsG-5123)
(NASA-CR-186457; NAS 1.26:186457; UMIACS-TR-89-75; CS-TR-2289) Avail: NTIS HC A03/MF A01 CSCL 09B

Software managers are interested in the quantitative management of software quality, cost and progress. An integrated software management methodology, which can be applied throughout the software life cycle for any number purposes, is required. The TAME (Tailoring A Measurement Environment) methodology is based on the improvement paradigm and the goal/question/metric (GQM) paradigm. This methodology helps generate a software engineering process and measurement environment based on the project characteristics. The SQMAR (software quality measurement and assurance technology) is a software quality metric system and methodology applied to the development processes. It is based on the feed forward control principle. Quality target setting is carried out before the plan-do-check-action activities are performed. These methodologies are integrated to realize goal oriented measurement, process control and visual management. A metric setting procedure based on the GQM paradigm, a management system called the software management cycle (SMC), and its application to a case study based on NASA/SEL data are discussed. The expected effects of SMC are quality improvement, managerial cost reduction, accumulation and reuse of experience, and a highly visual management reporting system. Author

N90-21533*# Cornell Univ., Ithaca, NY. Dept. of Computer Science.

FAST CAUSAL MULTICAST

Kenneth P. Birman, Andre Schiper (Ecole Polytechnique Federale de Lausanne, Switzerland), and Pat Stephenson 10 Apr. 1990 33 p
(Contract NAG2-593; N00140-87-C-8904; ARPA Order 6037)
(NASA-CR-186495; NAS 1.26:186495) Avail: NTIS HC A03/MF A01 CSCL 09B

A new protocol is presented that efficiently implements a reliable, causally ordered multicast primitive and is easily extended into a totally ordered one. Intended for use in the ISIS toolkit, it offers a way to bypass the most costly aspects of ISIS while benefiting from virtual synchrony. The facility scales with bounded overhead. Measured speedups of more than an order of magnitude were obtained when the protocol was implemented within ISIS. One conclusion is that systems such as ISIS can achieve performance competitive with the best existing multicast facilities - a finding contradicting the widespread concern that fault-tolerance may be unacceptably costly. Author

N90-21534# Laguna Research Lab., Fallbrook, CA.

QUADRATIC HADAMARD MEMORIES 1

Hendricus G. Loos Dec. 1989 29 p
(Contract DAAH01-88-C-0887; ARPA Order 6429)
(AD-A217224; TR-1) Avail: NTIS HC A03/MF A01 CSCL 12/6

A novel associative memory is discussed which overcomes the early saturation problem of Hopfield memories, without resorting to dilute state vectors or nonlocal learning rules. The memory uses a Bidirectional Linear Transformer (BLT) which transforms the bipolar input vector x into a vector u, which is a linear combination of Hadamard vectors. The matrix of the BLT is of Hebbian form, equal to the sum of outer products of stored vectors q to infinity and Hadamard vectors h to infinity. The Hadamard vectors are considered to serve as labels for the stored vectors. The BLT is followed by a Dominant Label Selector (DLS), which finds the dominant Hadamard component in the linear combination u, and returns the associated Hadamard vector to the BLT, to be processed in the BLT backstroke. This report deals with the DLS, which may be seen as an associative memory which stores N orthogonal bipolar vectors, the Hadamard vectors. A DLS architecture has been found which gives perfect associative recall of these stored vectors. The method involves a quadratic activation which, on account of a group property of Hadamard vectors, requires no more physical connections than a fully connected Hopfield memory of the same dimension. GRA

N90-21535*# Old Dominion Univ., Norfolk, VA. Dept. of Electrical and Computer Engineering.

STRATEGIES FOR CONCURRENT PROCESSING OF COMPLEX ALGORITHMS IN DATA DRIVEN ARCHITECTURES Final Report, period ending 15 Aug. 1989

John W. Stoughton, Roland R. Mielke, and Sukhamony Som Apr. 1990 179 p
(Grant NAG1-683)
(NASA-CR-186515; NAS 1.26:186515) Avail: NTIS HC A09/MF A01 CSCL 09B

The performance modeling and enhancement for periodic execution of large-grain, decision-free algorithms in data flow architectures is examined. Applications include real-time implementation of control and signal processing algorithms where performance is required to be highly predictable. The mapping of algorithms onto the specified class of data flow architectures is realized by a marked graph model called ATAMM (Algorithm To Architecture Mapping Model). Performance measures and bounds are established. Algorithm transformation techniques are identified for performance enhancement and reduction of resource (computing element) requirements. A systematic design procedure is described for generating operating conditions for predictable performance both with and without resource constraints. An ATAMM simulator is used to test and validate the performance prediction by the design procedure. Experiments on a three resource testbed provide verification of the ATAMM model and the design procedure. Author

N90-21536*# National Aeronautics and Space Administration. Goddard Space Flight Center, Greenbelt, MD.

ANNOTATED BIBLIOGRAPHY OF SOFTWARE ENGINEERING LABORATORY LITERATURE

Melanie Buhler and Jon Valett Nov. 1989 236 p
(NASA-TM-103313; NAS 1.15:103313; SEL-82-806) Avail: NTIS HC A11/MF A02 CSCL 09B

An annotated bibliography is presented of technical papers, documents, and memorandums produced by or related to the Software Engineering Laboratory. The bibliography was updated and reorganized substantially since the original version (SEL-82-006, November 1982). All materials were grouped into eight general subject areas for easy reference: (1) The Software Engineering Laboratory; (2) The Software Engineering Laboratory: Software Development Documents; (3) Software Tools; (4) Software Models; (5) Software Measurement; (6) Technology Evaluations; (7) Ada Technology; and (8) Data Collection. Subject and author

indexes further classify these documents by specific topic and individual author. Author

N90-21537*# National Aeronautics and Space Administration. Goddard Space Flight Center, Greenbelt, MD.
COLLECTED SOFTWARE ENGINEERING PAPERS, VOLUME 7
Nov. 1989 162 p
(NASA-TM-103312; NAS 1.15:103312; SEL-89-006) Avail: NTIS HC A08/MF A01 CSCL 09B

A collection is presented of selected technical papers produced by participants in the Software Engineering Laboratory (SEL) during the period Dec. 1988 to Oct. 1989. The purpose of the document is to make available, in one reference, some results of SEL research that originally appeared in a number of different forums. For the convenience of this presentation, the seven papers contained here are grouped into three major categories: (1) Software Measurement and Technology Studies; (2) Measurement Environment Studies; and (3) Ada Technology Studies. The first category presents experimental research and evaluation of software measurement and technology; the second presents studies on software environments pertaining to measurement. The last category represents Ada technology and includes research, development, and measurement studies. Author

N90-21538*# National Aeronautics and Space Administration. Goddard Space Flight Center, Greenbelt, MD.
LESSONS LEARNED IN THE TRANSITION TO Ada FROM FORTRAN AT NASA/GODDARD
Carolyn Elizabeth Brophy Nov. 1989 161 p
(NASA-TM-103311; NAS 1.15:103311; SEL-89-005) Avail: NTIS HC A08/MF A01 CSCL 09B

Two dynamics satellite simulators are developed from the same requirements, one in Ada and the other in FORTRAN. The purpose of the research was to find out how well the prescriptive Ada development model worked to develop the Ada simulator. The FORTRAN simulator development, as well as past FORTRAN developments, provided a baseline for comparison. Since this was the first simulator developed, the prescriptive Ada development model had many similarities to the usual FORTRAN development model. However, it was modified to include longer design and shorter testing phases, which is generally expected with Ada developments. One result was that the percentage of time the Ada project spent in the various development activities was very similar to the percentage of time spent in these activities when doing a FORTRAN project. Another finding was the difficulty the Ada team had with unit testing as well as with integration. It was realized that adding additional steps to the design phase, such as an abstract data type analysis, and certain guidelines to the implementation phase, such as to use primarily library units and nest sparingly, would have made development easier. These are among the recommendations made to be incorporated in a new Ada development model next time. Author

N90-21539*# National Aeronautics and Space Administration. Goddard Space Flight Center, Greenbelt, MD.
EVOLUTION OF Ada TECHNOLOGY IN THE FLIGHT DYNAMICS AREA: IMPLEMENTATION/TESTING PHASE ANALYSIS
Kelvin L. Quimby, Linda Esker, John Miller, Laurie Smith (Computer Sciences Corp., Greenbelt, MD.), Mike Stark, and Frank McGarry Nov. 1989 100 p
(NASA-TM-103310; NAS 1.15:103310; SEL-89-004) Avail: NTIS HC A05/MF A01 CSCL 09B

An analysis is presented of the software engineering issues related to the use of Ada for the implementation and system testing phases of four Ada projects developed in the flight dynamics area. These projects reflect an evolving understanding of more effective use of Ada features. In addition, the testing methodology used on these projects has changed substantially from that used on previous FORTRAN projects. Author

N90-21540*# National Aeronautics and Space Administration. Goddard Space Flight Center, Greenbelt, MD.
COLLECTED SOFTWARE ENGINEERING PAPERS, VOLUME 6
Nov. 1988 157 p
(NASA-TM-103309; NAS 1.15:103309; SEL-88-002) Avail: NTIS HC A08/MF A01 CSCL 09B

A collection is presented of technical papers produced by participants in the Software Engineering Laboratory (SEL) during the period 1 Jun. 1987 to 1 Jan. 1989. The purpose of the document is to make available, in one reference, some results of SEL research that originally appeared in a number of different forums. For the convenience of this presentation, the twelve papers contained here are grouped into three major categories: (1) Software Measurement and Technology Studies; (2) Measurement Environment Studies; and (3) Ada Technology Studies. The first category presents experimental research and evaluation of software measurement and technology; the second presents studies on software environments pertaining to measurement. The last category represents Ada technology and includes research, development, and measurement studies. Author

N90-21541*# National Aeronautics and Space Administration. Goddard Space Flight Center, Greenbelt, MD.
SYSTEM TESTING OF A PRODUCTION Ada (TRADEMARK) PROJECT: THE GRODY STUDY
Jeffrey Seigle, Linda Esker, and Ying-Liang Shi (Computer Sciences Corp., Greenbelt, MD.) [1990] 40 p
(NASA-TM-103308; NAS 1.15:103308; SEL-88-001) Avail: NTIS HC A03/MF A01 CSCL 09B

The use of the Ada language and design methodologies that utilize its features has a strong impact on all phases of the software development project lifecycle. At the National Aeronautics and Space Administration/Goddard Space Flight Center (NASA/GSFC), the Software Engineering Laboratory (SEL) conducted an experiment in parallel development of two flight dynamics systems in FORTRAN and Ada. The teams found some qualitative differences between the system test phases of the two projects. Although planning for system testing and conducting of tests were not generally affected by the use of Ada, the solving of problems found in system testing was generally facilitated by Ada constructs and design methodology. Most problems found in system testing were not due to difficulty with the language or methodology but to lack of experience with the application. Author

N90-21542*# National Aeronautics and Space Administration. Goddard Space Flight Center, Greenbelt, MD.
EVOLUTION OF Ada TECHNOLOGY IN THE FLIGHT DYNAMICS AREA: DESIGN PHASE ANALYSIS
Kelvin L. Quimby and Linda Esker (Computer Sciences Corp., Greenbelt, MD.) Dec. 1988 66 p
(NASA-TM-103307; NAS 1.15:103307; SEL-88-003) Avail: NTIS HC A04/MF A01 CSCL 09B

The software engineering issues related to the use of the Ada programming language during the design phase of an Ada project are analyzed. Discussion shows how an evolving understanding of these issues is reflected in the design processes of three generations of Ada projects. Author

N90-21543*# National Aeronautics and Space Administration. Goddard Space Flight Center, Greenbelt, MD.
SOFTWARE MANAGEMENT ENVIRONMENT (SME) CONCEPTS AND ARCHITECTURE
William Decker and Jon Valett Aug. 1989 67 p
(NASA-TM-103306; NAS 1.15:103306; SEL-89-003) Avail: NTIS HC A04/MF A01 CSCL 09B

The concepts and architecture of the Software Management Environment (SME) currently under development for the Systems Development Branch of the Flight Dynamics Division of the Goddard Space Flight Center (GSFC) are presented. The SME will provide an integrated set of management tools that can assist software development managers in the management and planning of flight dynamics software development projects. Author

N90-21544*# National Aeronautics and Space Administration. Goddard Space Flight Center, Greenbelt, MD.
IMPLEMENTATION OF A PRODUCTION Ada PROJECT: THE GRODY STUDY
Sara Godfrey and Carolyn Elizabeth Brophy (Maryland Univ., College Park.) Sep. 1989 149 p
(NASA-TM-103305; SEL-89-002; NAS 1.15:103305) Avail: NTIS HC A07/MF A01 CSCL 09B

The use of the Ada language and design methodologies that encourage full use of its capabilities have a strong impact on all phases of the software development project life cycle. At the National Aeronautics and Space Administration/Goddard Space Flight Center (NASA/GSFC), the Software Engineering Laboratory (SEL) conducted an experiment in parallel development of two flight dynamics systems in FORTRAN and Ada. The differences observed during the implementation, unit testing, and integration phases of the two projects are described and the lessons learned during the implementation phase of the Ada development are outlined. Included are recommendations for future Ada development projects. Author

N90-21545*# National Aeronautics and Space Administration. Goddard Space Flight Center, Greenbelt, MD.
SOFTWARE ENGINEERING LABORATORY (SEL) DATABASE ORGANIZATION AND USER'S GUIDE
Maria So, Gerard Heller, Sandra Steinberg (Computer Sciences Corp., Greenbelt, MD.), and Douglas Spiegel May 1989 176 p
(NASA-TM-103304; SEL-89-001; NAS 1.15:103304) Avail: NTIS HC A09/MF A01 CSCL 09B

The organization of the Software Engineering Laboratory (SEL) database is presented. Included are definitions and detailed descriptions of the database tables and views, the SEL data, and system support data. The mapping from the SEL and system support data to the base tables is described. In addition, techniques for accessing the database, through the Database Access Manager for the SEL (DAMSEL) system and via the ORACLE structured query language (SQL), are discussed. Author

N90-21546# Joint Inst. for Nuclear Research, Dubna (USSR). Lab. of Nuclear Problems.
CAD WORK STATION FOR ELECTRONICS DESIGNER
A. G. Asmolov 1988 8 p In RUSSIAN; ENGLISH summary
(DE90-616473; JINR-R-10-88-870) Avail: NTIS (US Sales Only) HC A02/MF A01

Computer aided design work station on base of a personnel computer intended for designing and debugging of digital and analog CAMAC units is described. A set of hardware and software which essentially diminishes time of designing and checkout of electronics is presented. DOE

N90-21547# Joint Inst. for Nuclear Research, Dubna (USSR). Lab. of Computing Techniques and Automation.
THE PARALLEL ALGORITHM FOR SOLVING THE THREE-DIMENSIONAL INTEGRAL MAGNETOSTATIC EQUATIONS
P. G. Akishin, E. P. Zhidkov, and V. D. Kravtson 1988 6 p In JAPANESE; ENGLISH summary
(DE90-616529; JINR-R-11-88-918) Avail: NTIS (US Sales Only) HC A02/MF A01

The paper deals with solving integral equations of a three-dimensional magnetostatic field. The interative process reduced to matrix multiplication by a vector is used for solving the nonlinear discretized system of equations. The parallel algorithms are proposed for all basic moments of solving the problem: computations of the coefficients of the discretized equations and the magnetic field of coils, the iterative process of solution of the nonlinear system and recalculation of the field for the interesting points. Some numerical results confirming the efficiency of the algorithm proposed are given. DOE

N90-21548# Sandia National Labs., Albuquerque, NM.
TOWARD A NEW CIM (COMPUTER INTEGRATED MANUFACTURING) ARCHITECTURE FOR SANDIA LABORATORIES
James R. Yoder 1990 8 p Presented at CIMCOM '90: International Conference on CIM Architecture, Gaithersburg, MD, 22-24 May 1990
(Contract DE-AC04-76DP-00789)
(DE90-008677; SAND-89-2685C; CONF-9005152-1) Avail: NTIS HC A02/MF A01

Sandia National Laboratories has experienced several generations of design and engineering automation. Each successive iteration brought improvement to a specific function. The changes in technology were point optimized, i.e., the improvements were made to narrow functional areas and not necessarily to the entire organization. Further, implementation plans rarely included the transfer of information from one function to another. Consequently, the Laboratories began a significant effort to design an overall architecture under which integration of disparate activities could take place and which would serve to provide an information path between all functions. The current version of the architecture is described and a description of the process that led to the architecture is provided. DOE

N90-21549# Sandia National Labs., Albuquerque, NM.
THE CAD/CAM PRODUCT DATA STANDARDS: IGES/PDES (INITIAL GRAPHICS EXCHANGE SPECIFICATION/PRODUCT DATA EXCHANGE STANDARDS, THE PRESENT AND THE FUTURE
Larry OConnell 1990 5 p Presented at the 1990 Update for Standards in Industrial Automation: Status and Future, St. Louis, MO, 14-16 May 1990
(Contract DE-AC04-76DP-00789)
(DE90-008803; SAND-90-0482C; CONF-9005151-1) Avail: NTIS HC A01/MF A01

The Initial Graphics Exchange Specification (IGES) has more capability than most people infer from the name. It can already provide some product data for manufacturing and test of products and, in particular, products having electrical and electronic aspects. The Product Data Exchange Specification (PDES) promises to do even better. Both of these efforts address the demonstrated need to move product descriptions from one computer-aided system to another in a way that maximizes the utility of the data received. Receiving systems can use these product descriptions (usually after some augmentation) to perform simulations, numerically controlled fabrication operations, process planning and variety of inspections and tests. PDES is expected to support Computer Integrated Manufacturing with the emphasis on Integrated. DOE

N90-21550# Oak Ridge National Lab., TN.
SIGNIF: A C FUNCTION TO COMPUTE SIGNIFICANT DIGITS
B. M. Horwedel and J. E. Horwedel 1990 18 p Presented at the SAS User Group International Conference (SUGI-15), Nashville, TN, 1-4 Apr. 1990
(Contract DE-AC05-84OR-21400)
(DE90-009242; CONF-9004161-1) Avail: NTIS HC A03/MF A01

This poster presents a C function, SIGNIF, that can be called from a SAS program to return a value rounded to a specified number of significant digits. The rules for rounding a number to n significant digits as implemented by SIGNIF are: truncate the number to n digits, and treat the excess digits as a decimal fraction; if the fraction is greater than 1/2, increment the least significant digit; if the fraction is less than 1/2, do not increment; if the fraction equals 1/2, increment the least significant digit only if it is odd. DOE

N90-21551# Oak Ridge National Lab., TN. Mathematical Science Section.
PARALLEL TRIDIAGONALIZATION OF A GENERAL MATRIX USING DISTRIBUTED-MEMORY MULTIPROCESSORS
G. A. Geist 1989 8 p Presented at the 4th SIAM Conference on Parallel Processing for Scientific Computing, Chicago, IL, 11-13

Dec. 1989
(Contract DE-AC05-84OR-21400)
(DE90-008902; CONF-891273-3) Avail: NTIS HC A02/MF A01

Recently there has been a renewed interest in finding reliable methods for reducing general matrices to tridiagonal form. We have developed a serial reduction algorithm that appears to be very reliable in practice by incorporating an optimal pivot search and two recovery schemes. In this paper we describe a parallel version of our algorithm. The algorithm was developed as one step in the process of finding eigenvalues of nonsymmetric matrices. Our original parallel eigenvalue routines reduced the matrix to Hessenberg form and then applied QR iteration, but the performance of the QR iteration was disappointing. Our new parallel algorithm reduces the matrix to tridiagonal form and then applies LR iteration. Using an iPSC/2, we compare the performance of the new parallel algorithm with our previous parallel algorithm and show that the new algorithm is nearly an order of magnitude faster, allowing us to solve much larger problems than previously attempted. DOE

N90-21552*# Sverdrup Technology, Inc., Cleveland, OH.
HYPERCLUSTER PARALLEL PROCESSING LIBRARY USER'S MANUAL Final Report
Angela Quealy Apr. 1990 75 p
(Contract NAS3-25266)
(NASA-CR-185231; NAS 1.26:185231) Avail: NTIS HC A04/MF A01 CSCL 09B

This User's Manual describes the Hypercluster Parallel Processing Library, composed of FORTRAN-callable subroutines which enable a FORTRAN programmer to manipulate and transfer information throughout the Hypercluster at NASA Lewis Research Center. Each subroutine and its parameters are described in detail. A simple heat flow application using Laplace's equation is included to demonstrate the use of some of the library's subroutines. The manual can be used initially as an introduction to the parallel features provided by the library. Thereafter it can be used as a reference when programming an application. Author

N90-21553*# Illinois Univ., Urbana-Champaign. Civil Engineering Systems Lab.
ARCHITECTURE INDEPENDENT ENVIRONMENT FOR DEVELOPING ENGINEERING SOFTWARE ON MIMD COMPUTERS
Karim A. Valimohamed and L. A. Lopez Jan. 1990 152 p
Sponsored in part by Apollo Computer, Inc., Chelmsford, MA
(Grant NAG1-525622)
(NASA-CR-186562; NAS 1.26:186562; UILU-ENG-90-2001; ISSN-0735-2867) Avail: NTIS HC A08/MF A01 CSCL 09B

Engineers are constantly faced with solving problems of increasing complexity and detail. Multiple Instruction stream Multiple Data stream (MIMD) computers have been developed to overcome the performance limitations of serial computers. The hardware architectures of MIMD computers vary considerably and are much more sophisticated than serial computers. Developing large scale software for a variety of MIMD computers is difficult and expensive. There is a need to provide tools that facilitate programming these machines. First, the issues that must be considered to develop those tools are examined. The two main areas of concern were architecture independence and data management. Architecture independent software facilitates software portability and improves the longevity and utility of the software product. It provides some form of insurance for the investment of time and effort that goes into developing the software. The management of data is a crucial aspect of solving large engineering problems. It must be considered in light of the new hardware organizations that are available. Second, the functional design and implementation of a software environment that facilitates developing architecture independent software for large engineering applications are described. The topics of discussion include: a description of the model that supports the development of architecture independent software; identifying and exploiting concurrency within the application program; data coherence; engineering data base and memory management. Author

N90-21554*# Georgia Inst. of Tech., Atlanta. School of Aerospace Engineering.
CURVATURE CONTINUITY OF CUBIC BEZIER CURVES IN THE SOLID MODELING AEROSPACE RESEARCH TOOLS DESIGN SOFTWARE Interim Report
Robert L. Roach and John R. Forrest [1990] 19 p
(Grant NAG1-1039)
(NASA-CR-186583; NAS 1.26:186583) Avail: NTIS HC A03/MF A01 CSCL 09B

Preliminary results are presented of an investigation into the development of a procedure to provide curvature continuity between biparametric cubic Bezier surface patches in the computer-aided design package known as SMART (Solid Modeling Aerospace Research Tools). This initial effort was aimed at providing the designer with the ability to locally impose curvature continuity at the intersection of two Bezier curves without disrupting either the curvature or slope continuity that may exist at the ends of these curves. Such a method was found if the original Bezier control points are all coplanar. If they are not, then it is possible to find a minimum deviation from exact curvature continuity. In cases where this is not sufficient, then an entire piecewise curve must be made curvature continuous simultaneously. A method was developed based on cubic splines which is very fast. The procedure returns new Bezier control points which have both slope and curvature continuity. Author

N90-20998# Princeton Univ., NJ.
AERODYNAMIC DESIGN VIA CONTROL THEORY
Antony Jameson *In* AGARD, Computational Methods for Aerodynamic Design (Inverse) and Optimization Mar. 1990 32 p (For primary document see N90-20976 14-05)
Copyright Avail: NTIS HC A15/MF A02; Non-NATO Nationals requests available only from AGARD/Scientific Publications Executive

62 COMPUTER SYSTEMS

Includes computer networks and special application computer systems.

N90-21555*# Cornell Univ., Ithaca, NY. Dept. of Computer Science.
EXPLOITING VIRTUAL SYNCHRONY IN DISTRIBUTED SYSTEMS
Kenneth P. Birman and Thomas A. Joseph 1987 16 p
(Contracts NAG2-593; MDA903-85-C-0124; N00140-87-C-8904; NSF DCR-84-12582; ARPA Order 5378)
(NASA-CR-182855; NAS 1.26:182855) Copyright Avail: NTIS HC A03/MF A01 CSCL 09B

Applications of a virtually synchronous environment are described for distributed programming, which underlies a collection of distributed programming tools in the ISIS2 system. A virtually synchronous environment allows processes to be structured into process groups, and makes events like broadcasts to the group as an entity, group membership changes, and even migration of an activity from one place to another appear to occur instantaneously, in other words, synchronously. A major advantage to this approach is that many aspects of a distributed application can be treated independently without compromising correctness. Moreover, user code that is designed as if the system were synchronous can often be executed concurrently. It is argued that this approach to building distributed and fault tolerant software is more straightforward, more flexible, and more likely to yield correct solutions than alternative approaches. Author

N90-21556*# Institute for Computer Applications in Science and Engineering, Hampton, VA.
PERFORMANCE BOUNDS ON PARALLEL SELF-INITIATING DISCRETE-EVENT Final Report
David M. Nicol (College of William and Mary, Hampton, VA.) Mar. 1990 30 p Submitted for publication Sponsored in part by Virginia Center for Innovative Technology

(Contract NAS1-18605; NAG1-060; NSF ASC-88-19393)
(NASA-CR-182010; NAS 1.26:182010; ICASE-90-21) Avail: NTIS HC A03/MF A01 CSCL 09B

The use is considered of massively parallel architectures to execute discrete-event simulations of what is termed self-initiating models. A logical process in a self-initiating model schedules its own state re-evaluation times, independently of any other logical process, and sends its new state to other logical processes following the re-evaluation. The interest is in the effects of that communication on synchronization. The performance is considered of various synchronization protocols by deriving upper and lower bounds on optimal performance, upper bounds on Time Warp's performance, and lower bounds on the performance of a new conservative protocol. The analysis of Time Warp includes the overhead costs of state-saving and rollback. The analysis points out sufficient conditions for the conservative protocol to outperform Time Warp. The analysis also quantifies the sensitivity of performance to message fan-out, lookahead ability, and the probability distributions underlying the simulation. Author

N90-21557*# Illinois Univ., Urbana-Champaign. Coordinated Science Lab.
NETRA: A PARALLEL ARCHITECTURE FOR INTEGRATED VISION SYSTEMS 2: ALGORITHMS AND PERFORMANCE EVALUATION
Alok N. Choudhary, Janak H. Patel, and Narendra Ahuja Dec. 1989 46 p
(Grant NAG1-613)
(NASA-CR-186510; NAS 1.26:186510; UILU-ENG-89-2242; CSG-118) Avail: NTIS HC A03/MF A01 CSCL 09B

In part 1 architecture of NETRA is presented. A performance evaluation of NETRA using several common vision algorithms is also presented. Performance of algorithms when they are mapped on one cluster is described. It is shown that SIMD, MIMD, and systolic algorithms can be easily mapped onto processor clusters, and almost linear speedups are possible. For some algorithms, analytical performance results are compared with implementation performance results. It is observed that the analysis is very accurate. Performance analysis of parallel algorithms when mapped across clusters is presented. Mappings across clusters illustrate the importance and use of shared as well as distributed memory in achieving high performance. The parameters for evaluation are derived from the characteristics of the parallel algorithms, and these parameters are used to evaluate the alternative communication strategies in NETRA. Furthermore, the effect of communication interference from other processors in the system on the execution of an algorithm is studied. Using the analysis, performance of many algorithms with different characteristics is presented. It is observed that if communication speeds are matched with the computation speeds, good speedups are possible when algorithms are mapped across clusters. Author

N90-21558# Los Alamos National Lab., NM. Theoretical Div.
APPLICATION OF NEURAL NETS TO SYSTEM IDENTIFICATION AND BIFURCATION ANALYSIS OF REAL WORLD EXPERIMENTAL DATA
R. A. Admoaitis, R. M. Farber, J. L. Hudson, I. G. Kevrekidis, M. Kube (Virginia Univ., Charlottesville.), and A. S. Lapedes Feb. 1990 13 p Presented at the 1990 International Conference on Neural Networks, Lyons, France, Mar. 1990
(Contract W-7405-eng-36)
(DE90-007539; LA-UR-90-515; CONF-900398-1) Avail: NTIS HC A03/MF A01

Results on the use of neural nets, and the closely related radial basis nets, to analyze experimental time series from electro-chemical systems are reported. It is shown how the nets may be used to derive a map that describes the nonlinear system, and how reserving an extra input line of the network allows one to learn the system behavior dependent on a control variable. Pruning of the network after training appears to result in elimination of spurious connection weights and enhanced predictive accuracy. Subsequent analysis of the learned map using techniques of bifurcation theory allows both nonlinear system identification and accurate and efficient predictions of long-term system behavior. The electrochemical system that was used involved the electrodissolution of copper in phosphoric acid. This system exhibits interesting low dimensional dynamics such transitions from steady state to oscillatory behavior and from period-one to period-two oscillations. This analysis provides an example of methodology that can be fruitful in understanding systems for which no adequate phenomenological model exists, or for which predictions of system behavior given a large scale, complicated model is inherently impractical. DOE

N90-21559# Argonne National Lab., IL. Mathematics and Computer Science Div.
ACTIVITIES AND OPERATIONS OF THE ADVANCED COMPUTING RESEARCH FACILITY Report, Jan. 1989 - Jan. 1990
Gail W. Pieper Feb. 1990 24 p
(Contract W-31-109-eng-38)
(DE90-007957; ANL-90/12) Avail: NTIS HC A03/MF A01

This report reviews the activities and operations of the Advanced Computing Research Facility (ACRF) for the period January 1, 1989, through January 31, 1990. The ACRF is operated by the Mathematics and Computer Science Division at Argonne National Laboratory. The facility's principal objective is to foster research in parallel computing. Toward this objective, the ACRF continues to operate experimental advanced computers and to sponsor new technology transfer efforts and new research projects. DOE

N90-21560# Sandia National Labs., Albuquerque, NM.
MULTIGRID ON MASSIVELY PARALLEL COMPUTERS
David E. Womble and Brenton C. Young (Stanford Univ., CA.) 1990 6 p Presented at the 5th Distributed Memory Computing Conference, Charleston, SC, 9-12 Apr. 1990
(Contract DE-AC04-76DP-00789)
(DE90-008999; SAND-89-2872C; CONF-9004159-1) Avail: NTIS HC A02/MF A01

Multigrid is a fast iterative method used to solve linear partial differential equations. However, because the solution of very small problems is inherent in the multigrid iteration, it is difficult to implement efficiently on a massively parallel computer. In this paper, we present an implementation of the multigrid v-cycle that has achieved 84 percent efficiency on the 1,024 processor NCUBE/ten. We also present a model for the efficiency of multigrid on a parallel computer that depends only on the efficiency of the smoother at each level. This model can be used to verify that it is indeed difficult to obtain extremely high efficiencies (95 to 100 percent), but that it is relatively easy to obtain moderately high efficiencies (70 to 85 percent). DOE

63 CYBERNETICS

Includes feedback and control theory, artificial intelligence, robotics and expert systems.

For related information see also *54 Man/System Technology and Life Support.*

N90-21561# Japan Atomic Energy Research Inst., Ibaraki.
THE DEVELOPMENT OF COMPUTATIONAL ALGORITHMS FOR MANIPULATOR INVERSE KINEMATICS
Shinobu Sasaki Oct. 1989 107 p In JAPANESE; ENGLISH summary
(DE90-759877; JAERI-M-89-137) Avail: NTIS (US Sales Only) HC A06/MF A01

A solution technique of the inverse kinematics for multi-joint robot manipulators has been considered to be one of the most cumbersome treatments due to non-linearity properties inclusive of trigonometric functions. The most traditional approach is to use the Jacobian matrix on linearization assumptions. This iterative technique, however, is attended with numerical problems having significant influences on the solution characteristics such as initial guess dependence and singularities. Taking these facts into consideration, new approaches have been proposed from different

standpoints, which are based on polynomial transformation of kinematic models, the minimization technique in mathematical programming, vector-geometrical concept, and the separation of joint variables associated with the optimization problem. In terms of computer simulations, each approach was identified to be a useful algorithm which leads to theoretically accurate solutions to complicated inverse problems. In this way, the short-term goal of our studies on manipulator inverse problem in the R and D project of remote handling technology was accomplished with success, and consequently the present report sums up the results of basic studies on this matter. DOE

N90-21562# Japan Atomic Energy Research Inst., Ibaraki. Dept. of Reactor Engineering.
ADAPTIVE LEARNING FUZZY CONTROL OF A MOBILE ROBOT
Nov. 1989 29 p In JAPANESE; ENGLISH summary
(DE90-759898; JAERI-M-89-191) Avail: NTIS (US Sales Only) HC A03/MF A01

In this report a problem is studied to construct a fuzzy controller for a mobile robot to move autonomously along a given reference direction curve, for which control rules are generated and acquired through an adaptive learning process. An adaptive learning fuzzy controller has been developed for a mobile robot. Good properties of the controller are shown through the travelling experiments of the mobile robot. DOE

N90-21563# Argonne National Lab., IL. Mathematics and Computer Science Div.
OTTER (ORGANIZED TECHNIQUES FOR THEOREM-PROVING AND EFFECTIVE RESEARCH) 2.0 USERS GUIDE
William W. McCune Mar. 1990 31 p
(Contract W-31-109-eng-38)
(DE90-007978; ANL-90/9) Avail: NTIS HC A03/MF A01

Organized Techniques for Theorem-proving and Effective Research (OTTER) is a resolution-style theorem-proving program for first-order logic with equality. OTTER includes the inference rules binary resolution, hyperresolution, UR-resolution, and binary paramodulation. Some of its other abilities are conversion from first-order formulas to clauses, forward and back subsumption, factoring, weighting, answer literals, term ordering, forward and back demodulation, evaluable functions and predicates, and Knuth-Bendix completion. OTTER is coded in C, it is free, and it is portable to many different kinds of computers. DOE

N90-21564*# National Aeronautics and Space Administration. Lewis Research Center, Cleveland, OH.
A REAL TIME NEURAL NET ESTIMATOR OF FATIGUE LIFE
T. Troudet (Sverdrup Technology, Inc., Cleveland, OH.) and W. Merrill 1990 11 p Presented at the International Joint Conference on Neural Networks, San Diego, CA, 17-21 Jun. 1990; cosponsored by IEEE and INNS
(NASA-TM-103117; E-5217; NAS 1.15:103117) Avail: NTIS HC A03/MF A01 CSCL 09B

A neural net architecture is proposed to estimate, in real-time, the fatigue life of mechanical components, as part of the Intelligent Control System for Reusable Rocket Engines. Arbitrary component loading values were used as input to train a two hidden-layer feedforward neural net to estimate component fatigue damage. The ability of the net to learn, based on a local strain approach, the mapping between load sequence and fatigue damage has been demonstrated for a uniaxial specimen. Because of its demonstrated performance, the neural computation may be extended to complex cases where the loads are biaxial or triaxial, and the geometry of the component is complex (e.g., turbopump blades). The generality of the approach is such that load/damage mappings can be directly extracted from experimental data without requiring any knowledge of the stress/strain profile of the component. In addition, the parallel network architecture allows real-time life calculations even for high frequency vibrations. Owing to its distributed nature, the neural implementation will be robust and reliable, enabling its use in hostile environments such as rocket engines. This neural net estimator of fatigue life is seen as the enabling technology to achieve component life prognosis, and therefore would be an important part of life extending control for reusable rocket engines. Author

64 NUMERICAL ANALYSIS

Includes iteration, difference equations, and numerical approximation.

N90-21565# Stanford Univ., CA. Dept. of Statistics.
A NOTE ON OVERDISPERSED EXPONENTIAL FAMILIES
A. E. Gelfand and S. R. Dalal 5 Dec. 1989 23 p
(Contract N00014-89-J-1627)
(AD-A216277; TR-425) Avail: NTIS HC A03/MF A01 CSCL 12/3

The issue of creating overdispersion in a given one parameter one dimensional exponential family by extending it to a two parameter exponential family with the same support is considered. An easily verifiable sufficient condition for this is derived. It is shown that a large class of families satisfy this condition and that this class includes Efron's (1986) and Lindsay's (1986) family as special cases. This class is also closely related to Jorgensen's (1988) Exponential Dispersion Models. UMP unbiased tests for testing overdispersion are exhibited and it is shown that in this context Cox's overdispersion test is a special case. A graphical display is developed to select a family of the general class which should be used with a given set of data to overdisperse a given target one parameter family. Two real data illustrations are given. GRA

N90-21566*# Institute for Computer Applications in Science and Engineering, Hampton, VA.
ON THE CONTINUOUS DEPENDENCE WITH RESPECT TO SAMPLING OF THE LINEAR QUADRATIC REGULATOR PROBLEM FOR DISTRIBUTED PARAMETER SYSTEMS Final Report
I. G. Rosen and C. Wang (University of Southern California, Los Angeles.) Mar. 1990 43 p Submitted for publication
Sponsored in part by Univ. of Southern California
(Contract NAS1-18605; AF-AFOSR-0356-87)
(NASA-CR-182012; NAS 1.26:182012; ICASE-90-23) Avail: NTIS HC A03/MF A01 CSCL 12A

The convergence of solutions to the discrete or sampled time linear quadratic regulator problem and associated Riccati equation for infinite dimensional systems to the solutions to the corresponding continuous time problem and equation, as the length of the sampling interval (the sampling rate) tends toward zero (infinity) is established. Both the finite and infinite time horizon problems are studied. In the finite time horizon case, strong continuity of the operators which define the control system and performance index together with a stability and consistency condition on the sampling scheme are required. For the infinite time horizon problem, in addition, the sampled systems must be stabilizable and detectable, uniformly with respect to the sampling rate. Classes of systems for which this condition can be verified are discussed. Results of numerical studies involving the control of a heat/diffusion equation, a hereditary of delay system, and a flexible beam are presented and discussed. Author

N90-21567*# National Aeronautics and Space Administration. Lewis Research Center, Cleveland, OH.
HIGH ACCURACY SOLUTIONS OF INCOMPRESSIBLE NAVIER-STOKES EQUATIONS
Murli M. Gupta Mar. 1990 27 p
(NASA Order C-99066-G)
(NASA-TM-102539; ICOMP-90-10; E-5350; NAS 1.15:102539)
Avail: NTIS HC A03/MF A01 CSCL 12A

In recent years, high accuracy finite difference approximations were developed for partial differential equations of elliptic type, with particular emphasis on the convection-diffusion equation. These approximations are of compact type, have a local truncation error of fourth order, and allow the use of standard iterative

schemes to solve the resulting systems of algebraic equations. These high accuracy approximations are extended to the solution of Navier-Stokes equations. Solutions are obtained for the model problem of driven cavity and are compared with solutions obtained using other approximations and those obtained by other authors. It is discovered that the high order approximations do indeed produce high accuracy solutions and have a potential for use in solving important problems of viscous fluid flows. Author

N90-21568*# North Carolina Agricultural and Technical State Univ., Greensboro. Dept. of Mechanical Engineering.
COMPACT FINITE VOLUME METHODS FOR THE DIFFUSION EQUATION
Milton E. Rose 16 Sep. 1989 41 p
(Grant NAG1-812)
(NASA-CR-186477; NAS 1.26:186477; JCP-4406) Avail: NTIS HC A03/MF A01 CSCL 12A

An approach to treating initial-boundary value problems by finite volume methods is described, in which the parallel between differential and difference arguments is closely maintained. By using intrinsic geometrical properties of the volume elements, it is possible to describe discrete versions of the div, curl, and grad operators which lead, using summation-by-parts techniques, to familiar energy equations as well as the div curl = 0 and curl grad = 0 identities. For the diffusion equation, these operators describe compact schemes whose convergence is assured by the energy equations and which yield both the potential and the flux vector with second order accuracy. A simplified potential form is especially useful for obtaining numerical results by multigrid and alternating direction implicit (ADI) methods. The treatment of general curvilinear coordinates is shown to result from a specialization of these general results. Author

N90-21569# Texas A&M Univ., College Station. Dept. of Mathematics.
[DETERMINATION OF UNKNOWN COEFFICIENTS IN PARTICAL DIFFERENTIAL EQUATIONS] Report, 1 Jan. - 31 Dec. 1989
William Rundell and Michael Pilant 31 Dec. 1989 121 p
(Contract N00014-89-J-1108)
(AD-A217169) Avail: NTIS HC A06/MF A01 CSCL 12/1

This research concerns undetermined coefficient problems in partial differential equations, in particular those problems where the unknown coefficients depend only on the dependent variables. The problems modeled by these equations are related to the determination of unknown physical laws or relationships. The nonlinear terms which were sought to recover in the model problems correspond to material properties that have physical significance; temperature dependent specific heats, conductivities, reaction terms, to name a few. Examples of such problems are: the determination of an unknown reaction term f(dot) in u sub t - u sub xx = f(u), or the conductivity k(dot) in the equation Del dot k(u) Del u = 0. These functions are determined by giving only overposed boundary data. This type of problem is distinct from those that involve media with unknown inhomogeneities; that is, the differential equations contain an unknown coefficient that depends on the independent spatial variable. In a given physical problem both situations may occur, that is, the unknowns have both spatial as well temperature dependence. This is a considerably more difficult problem and has received little attention in its full generality, instead both the limiting cases of dependence on a single one of these variables have and has received the vast majority of the research efforts. For those cases where the media is isotropic, the assumption that the unknowns depend only on the independent variable may be a reasonable one. GRA

N90-21570*# National Aeronautics and Space Administration. Lewis Research Center, Cleveland, OH.
ULTRA-SHARP NONOSCILLATORY CONVECTION SCHEMES FOR HIGH-SPEED STEADY MULTIDIMENSIONAL FLOW
B. P. Leonard and Simin Mokhtari (Akron Univ., OH.) Apr. 1990 50 p
(NASA Order C-99066-G)
(NASA-TM-102568; ICOMP-90-12; E-5320; NAS 1.15:102568)
Avail: NTIS HC A03/MF A01 CSCL 12A

For convection-dominated flows, classical second-order methods are notoriously oscillatory and often unstable. For this reason, many computational fluid dynamicists have adopted various forms of (inherently stable) first-order upwinding over the past few decades. Although it is now well known that first-order convection schemes suffer from serious inaccuracies attributable to artificial viscosity or numerical diffusion under high convection conditions, these methods continue to enjoy widespread popularity for numerical heat transfer calculations, apparently due to a perceived lack of viable high accuracy alternatives. But alternatives are available. For example, nonoscillatory methods used in gasdynamics, including currently popular TVD schemes, can be easily adapted to multidimensional incompressible flow and convective transport. This, in itself, would be a major advance for numerical convective heat transfer, for example. But, as is shown, second-order TVD schemes form only a small, overly restrictive, subclass of a much more universal, and extremely simple, nonoscillatory flux-limiting strategy which can be applied to convection schemes of arbitrarily high order accuracy, while requiring only a simple tridiagonal ADI line-solver, as used in the majority of general purpose iterative codes for incompressible flow and numerical heat transfer. The new universal limiter and associated solution procedures form the so-called ULTRA-SHARP alternative for high resolution nonoscillatory multidimensional steady state high speed convective modelling. Author

N90-21571*# Mississippi State Univ., Mississippi State. Dept. of Aerospace Engineering.
ADAPTIVE GRID EMBEDDING FOR THE TWO-DIMENSIONAL FLUX-SPLIT EULER EQUATIONS M.S. Thesis
Gary Patrick Warren May 1990 77 p
(NASA-CR-186533; NAS 1.26:186533) Avail: NTIS HC A05/MF A01 CSCL 12A

A numerical algorithm is presented for solving the 2-D flux-split Euler equations using a multigrid method with adaptive grid embedding. The method uses an unstructured data set along with a system of pointers for communication on the irregularly shaped grid topologies. An explicit two-stage time advancement scheme is implemented. A multigrid algorithm is used to provide grid level communication and to accelerate the convergence of the solution to steady state. Results are presented for a subcritical airfoil and a transonic airfoil with 3 levels of adaptation. Comparisons are made with a structured upwind Euler code which uses the same flux integration techniques of the present algorithm. Good agreement is obtained with converged surface pressure coefficients. The lift coefficients of the adaptive code are within 2 1/2 percent of the structured code for the sub-critical case and within 4 1/2 percent of the structured code for the transonic case using approximately one-third the number of grid points. Author

N90-21572# International Centre for Theoretical Physics, Trieste (Italy).
ON INDUCED HERMITIAN METRICS FOR HOLOMORPHIC VECTOR BUNDLES
Hoang Le Minh (Ho Chi Minh City Univ., Vietnam) Sep. 1989 16 p Submitted for publication
(DE90-612737; IC-89/272) Avail: NTIS (US Sales Only) HC A03/MF A01

An explicit computation of induced Hermitian metrics on holomorphic vector bundles is given. As an example the Fubini-Study metrics for complex projective spaces and Grassmannians are considered. DOE

N90-21573# International Centre for Theoretical Physics, Trieste (Italy).
THE MONAD CONSTRUCTION AND HERMETIAN-EINSTEIN METRICS
Hoang Le Minh (Ho Chi Minh City Univ., Vietnam) Sep. 1989 12 p Submitted for publication

(DE90-612738; IC-89/273) Avail: NTIS (US Sales Only) HC A03/MF A01

Methods of linear algebra are used to determine Hermitian-Einstein metrics on some holomorphic vector bundles associated with the monad construction over complex projective spaces and Grassmannians. DOE

N90-21574# International Centre for Theoretical Physics, Trieste (Italy).

ON A NON CLASSICAL OBLIQUE DERIVATIVE PROBLEM FOR PARABOLIC SINGULAR INTEGRO-DIFFERENTIAL OPERATORS

Nguyen Minh Chuong and Le Quang Trung (Moscow State Univ., USSR) Oct. 1989 10 p Submitted for publication
(DE90-612739; IC-89/304) Avail: NTIS (US Sales Only) HC A02/MF A01

In this paper an oblique derivative problem for parabolic singular integro-differential operators was studied. In this problem the direction of the derivative may be tangent to the boundary of the domain. By the large parameter method theorems of existence and uniqueness of solutions of the problem were obtained. DOE

N90-21575# International Centre for Theoretical Physics, Trieste (Italy).

ON THE EQUATION: DELTA u+c=Ke(SUP u)

Duong Minh Duc Oct. 1989 26 p Submitted for publication
(DE90-612741; IC-89/326) Avail: NTIS (US Sales Only) HC A03/MF A01

The Sobolev inequality was established for limiting case. Using this result, the method of McOwen, the Ekeland variational principle and the generalized critical values results, the existence was studied of solutions of the equation: delta u+c=Ke(sup u) for the case in which K and c may not tend to zero as x tends to infinity. DOE

N90-21576# International Centre for Theoretical Physics, Trieste (Italy).

WEIERSTRASS PREPARATION AND DIVISION THEOREMS FOR THE RING OF GERMS OF SUPERANALYTIC FUNCTIONS

Christian L. Yankov (Sofia Univ., Bulgaria) Nov. 1989 12 p Submitted for publication
(DE90-612742; IC-89/368) Avail: NTIS (US Sales Only) HC A03/MF A01

The aim of this paper is to show that Weierstrass preparation and division theorems hold for the ring of germs of superanalytic functions at a given point. This ring is the tensor product of the ring of germs of analytic functions at that point and a finite-dimensional complex Grassmann algebra. DOE

N90-21577# Joint Inst. for Nuclear Research, Dubna (USSR). Lab. of Nuclear Problems.

EXTENSION OF THE CONSTRAINTS ALGEBRA FOR THE CLOSED STRING WITH THE FIXED TOPOLOGY WORLD SHEET

1988 18 p In RUSSIAN
(DE90-612745; JINR-R-2-88-862) Avail: NTIS (US Sales Only) HC A03/MF A01

The recently proposed way of choosing the gauging, when the constraints and additional conditions make up a closed algebra, is extended to the case of generalized graded Krichever-Novikov algebras. The central element of the extended algebra is shown to be represented by a nonexact form on the closed contour of the string world sheet. Realization of the given algebra is obtained in terms of string variables. For this purpose, classical dynamics of the closed boson string with the world sheet of fixed genus is discussed. Dynamic variables are introduced covariantly, and the Hamilton equations are obtained in terms of these variables. These equations are equivalent to the Lagrange ones only in the case of the harmonic time function. DOE

N90-21578# Joint Inst. for Nuclear Research, Dubna (USSR). Lab. of Nuclear Problems.

EXTENSION OF THE KRICHEVER-NOVIKOV ALGEBRA IN THE CLOSED STRING THEORY

R. M. Kashaev and A. A. Osipov 1988 8 p In RUSSIAN; ENGLISH summary
(DE90-612746; JINR-R-2-88-863) Avail: NTIS (US Sales Only) HC A02/MF A01

Possible special extensions of the Krichever-Novikov algebra are discussed. Among them there is an extension which can be interpreted as the closed algebra of constraints and additional conditions in the theory of the boson string with the fixed topology world sheet. Realization of the given algebra is obtained in terms of string variables. The conclusion is drawn that the symmetry of the quantum system studied is wider than the usual BRST-invariance. This is the group of the global symmetry OSP (1.1/2). DOE

N90-21579# International Centre for Theoretical Physics, Trieste (Italy).

A LAGRANGIAN FORMALISM FOR NONEQUILIBRIUM ENSEMBLES

Y. Sobouti (Atomic Energy Organization of Iran, Teheran.) Aug. 1989 13 p Submitted for publication Sponsored in part by Shiraz Univ., Iran and Atomic Energy Organization of Iran
(DE90-612748; IC-89/231) Avail: NTIS (US Sales Only) HC A03/MF A01

It is suggested to formulate a nonequilibrium ensemble theory by maximizing a time-integrated entropy constrained by Liouville's equation. This leads to distribution functions of the form f = Z(sup -1)exp(-g/kT), where g(p,q,t) is a solution of Liouville's equation. A further requirement that the entropy should be an additive functional of the integrals of Liouville's equation, limits the choice of g to linear superpositions of the nonlinearly independent integrals of motion. Time-dependent and time-independent integrals may participate in this superposition. DOE

N90-21580# International Centre for Theoretical Physics, Trieste (Italy).

PERIODIC SOLUTIONS FOR HAMILTONIAN SYSTEMS IN A NONCONVEX POTENTIAL WELL

Li Shujie (Scuola Internazionale Superiore di Studi Avanzati, Trieste, Italy) Oct. 1989 11 p Submitted for publication
(DE90-612752; IC-89/296) Avail: NTIS (US Sales Only) HC A03/MF A01

Recently there has been a considerable amount of work on the existence of T-periodic solutions for Hamiltonian systems with singular potentials. In this paper the existence of T-periodic solutions for non-conservative second-order dynamical systems in a nonconvex potential well is studied. DOE

N90-21581# International Centre for Theoretical Physics, Trieste (Italy).

THE N = 2 SUPERCONFORMAL ALGEBRAS ON HYPERELLIPTIC SURFACES AND THEIR COULOMB GAS REALIZATION

De-Hai Zhang and Chao-Shang Huang (Academy of Sciences, Peking, China) Aug. 1989 12 p Submitted for publication
(DE90-612790; IC-89/235) Avail: NTIS (US Sales Only) HC A03/MF A01

The N = 2 superconformal algebras on Z sub 2 hyperelliptic surfaces are given. Existence of more discrete symmetries lead to the existing four different sectors as the primary fields. These algebras can be realized by a supersymmetric Coulomb gas system. DOE

N90-21582# International Centre for Theoretical Physics, Trieste (Italy).

LINKING NUMBERS AND VARIATIONAL METHOD

Ichiro Oda (Chiba Univ., Japan) and Shigeaki Yahikozawa Sep. 1989 19 p Submitted for publication
(DE90-612793; IC-89/287) Avail: NTIS (US Sales Only) HC A03/MF A01

The ordinary and generalized linking numbers for two surfaces of dimension p and n-p-1 in an n-dimensional manifold are derived. We use a variational method based on the properties of topological quantum field theory in order to derive them. DOE

N90-21583# International Centre for Theoretical Physics, Trieste (Italy).
FUSION ALGEBRA AND FUSING MATRICES
Yi-Hong Gao, Miao Li (International School for Advanced Studies, Trieste, Italy), and Ming Yu Sep. 1989 23 p Submitted for publication
(DE90-612798; IC-89/316) Avail: NTIS (US Sales Only) HC A03/MF A01

It is shown that the Wilson line operators in topological field theories form a fusion algebra. In general, the fusion algebra is a relation among the fusing (F) matrices. In the case of the SU(2) WZW model, some special F matrix elements are found in this way, and the remaining F matrix elements are then determined up to a sign. In addition, the S(j) modular transformation of the one point blocks on the torus is worked out. The results are found to agree with those obtained from the quantum group method. DOE

N90-21584# Lawrence Livermore National Lab., CA.
A PARALLEL MULTIGRID METHOD FOR SOLVING ELLIPTIC PARTIAL DIFFERENTIAL EQUATIONS M.S. Thesis
Theodore E. Ferretta Feb. 1989 76 p
(Contract W-7405-eng-48)
(DE90-007929; UCRL-53918) Avail: NTIS HC A05/MF A01

This paper introduces a parallel multigrid method for solving elliptic partial differential equations. This method combines two other methods, both of which are popular methods. One of the methods is a multigrid method, essentially a sequential method. The other is a parallel domain decomposition method, a variation on the Schwarz alternating procedure. Each method is explained individually, before the combined method is explained. The combined method is then compared to each of the individual methods, demonstrating the superiority of the combined method over each of its parent methods. As a model problem Poisson's equation is used. The computer on which the various methods were tested is an Alliant FX/8, a shared memory multiprocessor machine having 8 processors which can be run simultaneously in executing parallel code. DOE

N90-21585# Lawrence Livermore National Lab., CA.
DIFFERENTIAL-ALGEBRAIC EQUATIONS AS STIFF ORDINARY DIFFERENTIAL EQUATIONS
Michael Knorrenschild May 1989 23 p
(Contract W-7405-eng-48)
(DE90-007922; UCID-21964; ISCR-1989-01) Avail: NTIS HC A03/MF A01

In this paper we show that differential-algebraic systems of index-1 can always be viewed as reduced problems from singular perturbed ordinary differential equations (ODEs). Applying implicit Runge-Kutta methods to the singular perturbed system, we gain new insight into the relationship of order-reduction phenomena observed for stiff ODEs to that for differential-algebraic equations. We show that the order of convergence achieved for index-1-differential/algebraic equations is at least the order of B-convergence. DOE

N90-21586# Los Alamos National Lab., NM.
STABILITY OF A SOLITARY WAVE SOLUTION TO A SET OF COUPLED BOUSSINESQ-LIKE EQUATIONS
Peter L. Christiansen, Salvatore Rionaro (Naples Univ., Italy), Peter S. Lomdahl, and Virginia Muto 1989 12 p Presented at the 5th International Conference on Waves and Stability in Continuous Media, Sorrento (Italy), 9-14 Oct. 1989 Prepared in cooperation with Technical Univ. of Denmark, Lyngby
(Contract W-7405-eng-36)
(DE90-008927; LA-UR-90-955; CONF-8910207-2) Avail: NTIS HC A03/MF A01

A set of coupled partial differential equations of Boussinesq type are derived in the continuum limit of a Toda lattice with a transverse degree of freedom. The stability of a new hybrid wave solution with longitudinal and transversal components is investigated by approximate calculation of the Hamiltonian for infinitesimal displacement of the longitudinal and transversal strains relatively and by numerical solution. DOE

N90-21587# Los Alamos National Lab., NM.
COMPARISON OF THE ALGEBRAIC RECONSTRUCTION TECHNIQUE WITH THE MAXIMUM ENTROPY RECONSTRUCTION TECHNIQUE FOR A VARIETY OF DETECTION TASKS
K. M. Hanson (Food and Drug Administration, Rockville, MD.) and K. J. Myers 1990 13 p Presented at the SPIE Technical Conference and Exhibition on Medical Imaging, Newport Beach, CA, 4-9 Feb. 1990
(Contract W-7405-eng-36)
(DE90-008933; LA-UR-90-897; CONF-900238-2) Avail: NTIS HC A03/MF A01

A method for comparing reconstruction algorithms is presented based on the ability to perform certain detection tasks on the resulting images. The reconstruction algorithms compared are the algebraic reconstruction technique and the maximum entropy reconstruction method. Task performance is assessed through a Monte Carlo simulation of the complete imaging process, including the generation of a set of object scenes, followed by data-taking, reconstruction, and performance of the specified task by a machine observer. For these detection tasks the figure of merit used for comparison is the detectability index. When each algorithm is run with approximately optimized parameters, these studies find comparable values for the detectability index. DOE

N90-21588# Helsinki Univ. of Technology, Espoo (Finland). Inst. of Mathematics.
ON THE STABILITY OF A CERTAIN DIFFERENCE SCHEME
Jukka Tuomela Aug. 1989 15 p
(PB90-165614; RR-A268; ISBN-951-754-995-4; ISSN-0784-3143)
Avail: NTIS HC A03/MF A01 CSCL 12A

The stability questions of time integration of the wave equation and the geometrical properties of the finite element mesh to the stability condition of the step size are considered. Some numerical examples are given. GRA

N90-21589# Helsinki Univ. of Technology, Espoo (Finland). Inst. of Mathematics.
A REMARK ON THE KELVIN TRANSFORM AND A NON-LINEAR PARTIAL DIFFERENTIAL EQUATION
Peter Lindqvist Jun. 1989 9 p
(PB90-165622; RR-A267; ISBN-851-754-933-4; ISSN-0784-3143)
Avail: NTIS HC A02/MF A01 CSCL 12A

The p-harmonic functions are preserved under reflections in spheres only if the exponent p, 1 less than p less than infinity, is equal to the dimension of the underlying Euclidean space. In the linear case p = 2 the Kelvin transform corrects this lack of invariance. The author shows that the Kelvin transform has no reasonable counterpart for general values of the exponent p. Author

65 STATISTICS AND PROBABILITY

Includes data sampling and smoothing; Monte Carlo method; and stochastic processes.

No abstracts in this category.

66 SYSTEMS ANALYSIS

Includes mathematical modeling; network analysis; and operations research.

No abstracts in this category.

67 THEORETICAL MATHEMATICS

Includes topology and number theory.

N90-21590# Stanford Univ., CA. Systems Optimization Lab.
A MONOTONE COMPLEMENTARITY PROBLEM IN HILBERT SPACE
Jen-Chih Yao Apr. 1990 5 p
(Contracts DE-FG03-87ER-25028; N00014-89-J-1659; NSF DMS-89-13089)
(DE90-009755; SU-SOL-90-7) Avail: NTIS HC A01/MF A01

An existence theorem for a complementarity problem involving a weakly coercive monotone mapping over an arbitrary closed convex cone in a real Hilbert space is established. DOE

70 PHYSICS (GENERAL)

For precision time and time interval (PTTI) see *35 Instrumentation and Photography;* for geophysics, astrophysics or solar physics see *46 Geophysics, 90 Astrophysics,* or *92 Solar Physics.*

N90-21591# National Inst. of Standards and Technology, Gaithersburg, MD. National Measurement Lab.
CENTER FOR ATOMIC, MOLECULAR, AND OPTICAL PHYSICS: TECHNICAL ACTIVITIES Report, FY 1989
Katharine B. Gebbie Dec. 1989 364 p
(PB90-133158; NISTIR-89/4184) Avail: NTIS HC A16/MF A02 CSCL 20C

The research and technical activities of the Center for Atomic, Molecular and Optical Physics (CAMOP) are summarized. The activities include work in the areas of fundamental constants, radiation physics, surface science, molecular spectroscopy, electron and optical physics, atomic and plasma spectroscopy, time and frequency, quantum metrology, and quantum physics. Author

N90-21592# Joint Inst. for Nuclear Research, Dubna (USSR). Lab. of High Energy.
ONCE MORE ABOUT THE SIZES OF FAST-MOVING OBJECTS
V. N. Streltsov 1988 5 p In RUSSIAN; ENGLISH summary
(DE90-615204; JINR-R-2-88-843) Avail: NTIS (US Sales Only) HC A01/MF A01

It is noted that visual (longitudinal) sizes of fast moving objects are essentially connected with the results of measuring procedure being the basis of the concept of relativistic length (CRL). CRL is based on the radar method for distance measuring and its consequence if the elongation formula is used. It is stressed that according to up to date notion the elementary particle interactions are in fact the radar character. Therefore, the relativistic length plays an important role in the microworld physics. In particular, within the CRL the known difficulty due to the existence of fundamental length is solved. Besides on the basis of CRL the solution of the Rindler-Denur paradox with electrostatic energy of the capacitor is given. DOE

N90-21593# Joint Publications Research Service, Arlington, VA.
JPRS REPORT: SCIENCE AND TECHNOLOGY. USSR: PHYSICS AND MATHEMATICS
27 Mar. 1990 25 p Transl. into ENGLISH of various Russian documents
(JPRS-UPM-90-002) Avail: NTIS HC A03/MF A01

Abstracts of research in science and technology are given. Research in lasers, nuclear physics, optics, spectroscopy, plasma physics, and superconductivity is covered. R.J.F.

N90-21594# International Centre for Theoretical Physics, Trieste (Italy).
A MODIFIED MOEBIUS INVERSE FORMULA AND ITS APPLICATIONS IN PHYSICS
Nan-Xian Chen (Beijing Univ., China) Oct. 1989 9 p Submitted for publication Sponsored in part by National Foundation of Natural Science, China
(DE90-612740; IC-89/314) Avail: NTIS (US Sales Only) HC A02/MF A01

A new theorem of inverse formula is introduced for a kind of infinite series. Thus some new results for important inverse problems in physics are presented in this paper. These are the inverse problems for obtaining the phonon density of states, the inverse blackbody radiation problem for remote sensing, and the solution for inverse Ewald summation. Of more importance, it shows the possibility of the application of number theory to physical problems. DOE

N90-21595# Instituto de Pesquisas Espaciais, Sao Jose dos Campos (Brazil).
FINITE ELEMENT ALGORITHMS FOR HYPERBOLIC CONSERVATION LAWS WITH FORCING TERMS
Philippe Remy Bernar Devloo and Sonia Maria GomesdeGonzalezVillalobos Dec. 1989 63 p
(Contract FINEP-53-89-0363-00; CNPq-302714/88-0/MA/FV)
(INPE-5024-RPE/617) Avail: NTIS HC A04/MF A01

Several finite element algorithms are presented and analyzed for the simulation of first order convection problems with forcing terms. The analysis presented was motivated by the necessity of having a better understanding of numerical schemes used to model the flow in a hydrazine micro-thruster. First, the finite element algorithm as applied to pure convection problems is introduced. Its implementation is described for a sequence of equations from a scalar linear equation up to multicomponent gas dynamics equations in one dimension. Then three different finite element implementations for the approximation of hyperbolic systems for conversation laws with forcing term are studied. The last part is dedicated to the analysis and implementation of numerical boundary conditions. Two aspects are considered implementing insufficient boundary condition in a stable fashion and implementing nonlinear boundary conditions for nonlinear systems of conservation laws. Author

71 ACOUSTICS

Includes sound generation, transmission and attenuation. For noise pollution see *45 Environmental Pollution.*

N90-21596# Vibration Inst., Clarendon Hills, IL.
THE SHOCK AND VIBRATION DIGEST, VOLUME 22, NO. 2 Monthly Report
Vicki M. Pate, ed. Feb. 1990 68 p
Avail: NTIS HC A04/MF A01

In addition to a feature article on the state of the art of the acoustics of active and passive mufflers, abstracts of numerous articles dealing with shock and vibration are given. Topics covered include machine tools, compressors, structural analysis, vehicles, testing systems, shock absorbers, structural components, experimental techniques and tests, seismic environments, computational and mathematical modeling techniques, and standards and specifications. For individual titles, see N90-21597 through N90-21597.

N90-21597# Indian Inst. of Science, Bangalore. Dept. of Mechanical Engineering.
STATE OF THE ART OF ACOUSTICS OF ACTIVE AND PASSIVE MUFFLERS
M. L. Munjal *In* Vibration Inst., The Shock and Vibration Digest, Volume 22, No. 2 Feb. 1990 p 3-12 (For primary document see N90-21596 14-71)
Avail: NTIS HC A04/MF A01

Significant advances made in the analysis and design of mufflers over the last four years are reviewed. Active, passive, reflective, and dissipative mufflers are discussed. While emphasis is on the frequency domain analysis, the time domain analysis is included. Applicability of the various contributions is highlighted. Author

N90-21598*# Texas A&M Univ., College Station. Turbomachinery Lab.
RECTANGULAR SUBSONIC JET FLOW FIELD MEASUREMENTS Final Report
Gerald L. Morrison and David H. Swan Mar. 1990 162 p (Grant NAG1-630)
(NASA-CR-181925; NAS 1.26:181925; TL-89-JETS-GLM-1)
Avail: NTIS HC A08/MF A01 CSCL 20A

Flow field measurements of three subsonic rectangular cold air jets are presented. The three cases had aspect ratios of 1x2, 1x4 at a Mach number of 0.09 and an aspect ratio of 1x2 at a Mach number of 0.9. All measurements were made using a 3-D laser Doppler anemometer system. The data includes the mean velocity vector, all Reynolds stress tensor components, turbulent kinetic energy and velocity correlation coefficients. The data are presented in tabular and graphical form. No analysis of the measured data or comparison to other published data is made. Author

N90-21599# Swedish Inst. for Materials Testing, Boras. Acoustics Lab.
AIRBORNE SOUND INSULATION OF SLITS, JOINTS, AND SEALING STRIPES
Kaj Bodlund and Carl-Axel Carlsson 1989 88 p In SWEDISH; ENGLISH summary
(PB90-128976; SP-RAPP-1989:28; ISBN-91-7848-179-1; ISSN-0284-5172) Avail: NTIS HC A05/MF A01 CSCL 20A

A test method is described by which it is possible to determine the airborne sound insulation of slits, joints, and sealing stripes. The method is based on sound intensity measurements close to the test object on the receiver side. The method was used for studies of slit-shaped apertures with or without sealing strips and absorbents. The results were compared with available theories for hard-walled slits and the method proved to give reproducible and realistic results. Constructions with sealing strips must be hermetic. If the joint is not airtight, the sound insulation may decrease by 10 dB or more. Joints and slits shall always be as small as possible. Every expansion of a slit is negative to the sound insulation and there is a resonance phenomenon when the depth of the slit equals half the wavelength. Author

N90-21600*# Sverdrup Technology, Inc., Cleveland, OH.
MICROGRAVITY ACOUSTIC MIXING FOR PARTICLE CLOUD COMBUSTORS Final Report
Frederic Pla and Robert I. Rubinstein Mar. 1990 153 p (Contract NAS3-25266)
(NASA-CR-185159; E-5347; NAS 1.26:185159) Avail: NTIS HC A08/MF A01 CSCL 20A

Experimental and theoretical investigations of acoustic mixing procedures designed to uniformly distribute fuel particles in a combustion tube for application in the proposed Particle Cloud Combustion Experiment (PCCE) are described. Two acoustic mixing methods are investigated: mixing in a cylindrical tube using high frequency spinning modes generated by suitably phased, or quadrature speakers, and acoustic premixing in a sphere. Quadrature mixing leads to rapid circumferential circulation of the powder around the tube. Good mixing is observed in the circulating regions. However, because axial inhomogeneities are necessarily present in the acoustic field, this circulation does not extend throughout the tube. Simultaneous operation of the quadrature-speaker set and the axial-speaker was observed to produce considerably enhanced mixing compared to operation of the quadrature-speaker set alone. Mixing experiments using both types of speakers were free of the longitudinal powder drift observed using axial-speakers alone. Vigorous powder mixing was obtained in the sphere for many normal modes: however, in no case was the powder observed to fill the sphere entirely. Theoretical analysis indicated that mixing under steady conditions cannot fill more than a hemisphere except under very unusual conditions. Premixing in a hemisphere may be satisfactory; otherwise, complete mixing in microgravity might be possible by operating the speaker in short bursts. A general conclusion is that acoustic transients are more likely to produce good mixing than steady state conditions. The reason is that in steady conditions, flow structures like nodal planes are possible and often even unavoidable. These tend to separate the mixing region into cells across which powder cannot be transferred. In contrast, transients not only are free of such structures, they also have the characteristics, desirable for mixing, of randomness and disorder. This conclusion is corroborated by mixing experiments using axial waves. Author

N90-21601 Edinburgh Univ. (Scotland).
THE OPTICAL MEASUREMENT OF ACOUSTIC VELOCITY FIELDS Ph.D. Thesis
John P. Sharpe 1988 177 p
Avail: Univ. Microfilms Order No. BRD-87614

The application of two different optical techniques to the measurement of acoustic velocity fields is described. Firstly, the application of laser Doppler anemometry to the measurement of the vibrational velocities associated with acoustic fields is described. Secondly, the technique of particle image velocimetry is introduced to measure the nonlinear, non-zero mean motions which arise when higher intensity sound fields are present. For the first case consideration is given to the special requirements involved in measuring acoustic vibrational velocities: theory is then developed relating the photon correlation function to the sound field velocity distribution for the cases of periodic and noisy sound fields. A technique which can be used to measure the phase of the velocity with respect to the pressure is also described. Experiments are then described which test the technique and successful measurements are made of complex acoustic impedance. These latter measurements lead to the consideration of acoustic streaming and to the realization that it could be measured using particle image velocimetry. This technique is then applied to Rayleigh streaming and the measurements are shown to agree well with theory. Dissert. Abstr.

N90-21602*# General Electric Co., Schenectady, NY.
THE RADIATION OF SOUND FROM A PROPELLER AT ANGLE OF ATTACK Final Report
Ramani Mani Washington, DC NASA Jan. 1990 53 p (Contract NAS3-23721)
(NASA-CR-4264; E-5139; NAS 1.26:4264) Avail: NTIS HC A04/MF A01 CSCL 20A

The mechanism by which the noise generated at the blade passing frequency by a propeller is altered when the propeller axis is at an angle of attack to the freestream is examined. The measured noise field is distinctly non axially symmetric under such conditions with far field sound pressure levels both diminished and increased relative to the axially symmetric values produced with the propeller at zero angle of attack. Attempts have been made to explain this non axially symmetric sound field based on the unsteady (once per rev) loading experienced by the propeller blades when the propeller axis is at non zero angle of attack. A calculation based on this notion appears to greatly underestimate the measured azimuthal asymmetry of noise for high tip speed, highly loaded propellers. A new mechanism is proposed; namely, that at angle of attack, there is a non axially symmetric modulation of the radiative efficiency of the steady loading and thickness noise which is the primary cause of the non axially symmetric sound field at angle of attack for high tip speed, heavily loaded propellers with a large number of blades. A calculation of this

effect to first order in the crossflow Mach number (component of freestream Mach number normal to the propeller axis) is carried out and shows much better agreement with measured noise data on the angle of attack effect. Author

N90-21603*# National Aeronautics and Space Administration. Langley Research Center, Hampton, VA.
ACTIVE CONTROL OF MULTI-DIMENSIONAL RANDOM SOUND IN DUCTS
R. J. Silcox and S. J. Elliott May 1990 12 p Presented at Acoustics 90, Southampton, England, 28-30 Mar. 1990
(NASA-TM-102653; NAS 1.15:102653) Avail: NTIS HC A03/MF A01 CSCL 20A

Previous work has demonstrated how active control may be applied to the control of random noise in ducts. These implementations, however, have been restricted to frequencies where only plane waves are propagating in the duct. In spite of this, the need for this technology at low frequencies has progressed to the point where commercial products that apply these concepts are currently available. Extending the frequency range of this technology requires the extension of current single channel controllers to multi-variate control systems as well as addressing the problems inherent in controlling higher order modes. The application of active control in the multi-dimensional propagation of random noise in waveguides is examined. An adaptive system is implemented using measured system frequency response functions. Experimental results are presented illustrating attained suppressions of 15 to 30 dB for random noise propagating in multiple modes. Author

N90-21604*# Pennsylvania State Univ., State College. Noise Control Lab.
FREE-FIELD PROPAGATION OF HIGH INTENSITY NOISE Final Report, 1 Dec. 1979 - 28 Feb. 1983
Joseph P. Welz and Oliver H. McDaniel 1990 78 p
(Grant NAG1-4)
(NASA-CR-186577; NAS 1.26:186577) Avail: NTIS HC A05/MF A01 CSCL 20A

Observed spectral data from supersonic jet aircraft are known to contain much more high frequency energy than can be explained by linear acoustic propagation theory. It is believed that the high frequency energy is an effect of nonlinear distortion due to the extremely high acoustic levels generated by the jet engines. The objective, to measure acoustic waveform distortion for spherically diverging high intensity noise, was reached by using an electropneumatic acoustic source capable of generating sound pressure levels in the range of 140 to 160 decibels (re 20 micro Pa). The noise spectrum was shaped to represent the spectra generated by jet engines. Two microphones were used to capture the acoustic pressure waveform at different points along the propagation path in order to provide a direct measure of the waveform distortion as well as spectral distortion. A secondary objective was to determine that the observed distortion is an acoustic effect. To do this an existing computer prediction code that deals with nonlinear acoustic propagation was used on data representative of the measured data. The results clearly demonstrate that high intensity jet noise does shift the energy in the spectrum to the higher frequencies along the propagation path. In addition, the data from the computer model are in good agreement with the measurements, thus demonstrating that the waveform distortion can be accounted for with nonlinear acoustic theory. Author

N90-21605*# Lockheed Engineering and Sciences Co., Hampton, VA.
SONIC BOOM SIGNATURE DATA FROM CRUCIFORM MICROPHONE ARRAY EXPERIMENTS DURING THE 1966-1967 EAFB NATIONAL SONIC BOOM EVALUATION PROGRAM
H. H. Hubbard and D. J. Maglieri (Eagle Engineering, Inc., Hampton, VA.) May 1990 54 p
(Contracts NAS1-19000; NAS9-17900)
(NASA-CR-182027; NAS 1.26:182027) Avail: NTIS HC A04/MF A01 CSCL 20A

Tables are provided of measured sonic boom signature data derived from supersonic flyover tests of the XB-70, B-58 and F-104 aircraft for ranges of altitude and Mach number. These tables represent a convenient hard copy version of available electronic files and complement preliminary information included in a reference National Sonic Boom Evaluation Office document. Author

72 ATOMIC AND MOLECULAR PHYSICS

Includes atomic structure, electron properties, and molecular spectra.

N90-21606*# Alaska Univ., Fairbanks. Geophysical Inst.
SR90, STRONTIUM SHAPED-CHARGE CRITICAL IONIZATION VELOCITY EXPERIMENT
Eugene M. Wescott, Hans Stenbaek-Nielsen, Daniel W. Swift, Arnoldo Valenzuela, and David Rees (University Coll., London, England) [1990] 25 p
(Grants NAGw-269; NAG6-1)
(NASA-CR-186501; NAS 1.26:186501) Avail: NTIS HC A03/MF A01 CSCL 20H

In May 1986 an experiment was performed to test Alfven's critical ionization velocity (CIV) effect in free space, using the first high explosive shaped charge with a conical liner of strontium metal. The release, made at 540 km altitude at dawn twilight, was aimed at 48 deg to B. The background electron density was 1.5 x 10(exp 4) cu cm. A faint field-aligned Sr(+) ion streak with tip velocity of 2.6 km/s was observed from two optical sites. Using two calibration methods, it was calculated that between 4.5 x 10(exp 20) and 2 x 10(exp 21) ions were visible. An ionization time constant of 1920 s was calculated for Sr from the solar UV spectrum and ionization cross section which combined with a computer simulation of the injection predicts 1.7 x 10(exp 21) solar UV ions in the low-velocity part of the ion streak. Thus all the observed ions are from solar UV ionization of the slow (less than critical) velocity portion of the neutral jet. The observed neutral Sr velocity distribution and computer simulations indicate that 2 x 10(exp 21) solar UV ions would have been created from the fast (greater than critical) part of the jet. They would have been more diffuse, and were not observed. Using this fact it was estimated that any CIV ions created were less than 10(exp 21). It was concluded that future Sr CIV free space experiments should be conducted below the UV shadow height and in much larger background plasma density. Author

N90-21607# California Univ., Berkeley. Lawrence Berkeley Lab.
CURRENT EXPERIMENTS IN ELEMENTARY PARTICLE PHYSICS
C. G. Wohl, F. E. Armstrong, T. G. Trippe, G. P. Yost, Y. Oyanagi, D. C. Dodder, Yu. G. Ryabov, S. R. Slabospitsky, R. Frosch, and A. Olin (Tri-Univ. Meson Facility, Vancouver, British Columbia) Sep. 1989 179 p
(Contract DE-AC03-76SF-00098)
(DE90-008062; LBL-91-Rev-9/89) Avail: NTIS HC A09/MF A01

This report contains summaries of 736 current and recent experiments in elementary particle physics (experiments that finished taking data before 1982 are excluded). Included are experiments at Brookhaven, CERN, CESR, DESY, Fermilab, Tokyo Institute of Nuclear Studies, Moscow Institute of Theoretical and Experimental Physics, Joint Institute for Nuclear Research (Dubna), KEK, LAMPF, Novosibirsk, PSI/SIN, Saclay, Serpukhov, SLAC, and TRIUMF, and also several underground experiments. Also given are instructions for searching online the computer database (maintained under the SLAC/SPIRES system) that contains the summaries. Properties of the fixed-target beams at most of the laboratories are summarized. DOE

N90-21608# International Centre for Theoretical Physics, Trieste (Italy).
POLARIZATION: EFFECTS ON SECOND HARMONIC POWER IN LIGHT SCATTERING BY FREE ELECTRONS
V. P. Verma (Allahabad Univ., India) Oct. 1989 12 p Submitted for publication
(DE90-612842; IC-89/331) Avail: NTIS (US Sales Only) HC A03/MF A01

The effect of polarization over 2 omega radiated power in the plane e.m. wave scattering by free electrons is studied. It is found that the second harmonic time averaged power radiated due to scattering of circularly polarized wave is larger than the power generated in the scattering of plane-polarized incident radiation. Radiated power is directly proportional to the square of the wavelength and also the energy flux of incident intense polarized radiation. It is observed that the instantaneous power corresponding to circularly polarized incident light is maximum at theta=pi/2. In the case of linearly polarized beam the maximum is again observed at scattering angle, theta=pi/2 provided the initial polarization angle phi(sub 0)=pi/4. DOE

N90-21609# Melbourne Univ., Parkville (Australia). School of Physics.
LARGE BASIS SPACE EFFECTS IN ELECTRON SCATTERING FORM FACTORS OF LIGHT NUCLEI
K. Amos and C. Steward 1989 20 p
(DE90-613501; UM-P-89/38) Avail: NTIS (US Sales Only) HC A03/MF A01

Large basis space projected Hartree-Fock wave functions have been used to calculate the longitudinal and transverse (electric) form factors from the excitations of 2 sub 1(+) and 4 sub 1(+) states in C-12, Ne-20 and Mg-24. The results obtained by use of such large basis space models of structure are compared with limited basis space (Shell model) predictions to show how diverse momentum transfer dependent corrections can be. DOE

N90-21610# Los Alamos National Lab., NM.
GAMMA-RAY PRODUCTION CROSS SECTION MEASUREMENTS USING A WHITE NEUTRON SOURCE FROM 1 TO 400 MeV
S. A. Wender, R. O. Nelson, and C. M. Laymon 1990 15 p Presented at the Specialists' Meeting on Measurement, Calculation and Evaluation of Photon Production Cross Sections, Smolenice, Czechoslovakia, 5-7 Feb. 1990
(Contract W-7405-eng-36)
(DE90-008906; LA-UR-90-1035; CONF-9002109-1) Avail: NTIS HC A03/MF A01

The continuous energy (white) neutron source at the Los Alamos Meson Physics Facility (LAMPF) is used to measure photon-production cross sections over a wide range of neutron energies. Detector systems were or are being developed to measure gamma rays in the energy range from hundreds of keV up to several hundreds of MeV. In particular a high resolution Ge detector system is used to detect gamma rays from several hundred keV to over 6 MeV. A 5 crystal BGO detector system is used for measuring gamma-rays from 1 MeV to approximately 20 MeV. A large volume BGO detector with an active shield is used to measure gamma rays in the range from 5 to 40 MeV. A multi-element gamma-ray telescope is presently being developed to measure gamma rays with energies from 50 MeV up to several hundred MeV. DOE

N90-21611# Oak Ridge National Lab., TN.
US-JAPAN WORKSHOP ON ATOMIC COLLISIONS IN SOLIDS: ABSTRACTS OF LECTURES
Mar. 1990 17 p Workshop held in Honolulu, HI, 2-9 Feb. 1990
(Contract DE-AC05-84OR-21400)
(DE90-008979; CONF-900276) Avail: NTIS HC A03/MF A01

Abstracts are contained for the following topics: techniques of scanning probe microscopy; new types of radiation; a search for wake-riding electrons using slow antiproton beams; antiproton wake: theory; bending of swift ion beams by graphite foils; angular momentum distribution of autoionizing rydberg states: produced by 64 MeV S ions in collisions with C foils; multiphonon energy exchange in atom-surface collisions; plans for positron experiments; resonant coherent excitation: experiment; line shapes in resonant coherent excitation: theory; MUSE experiments and Monte Carlo simulation; inelastic interactions of electrons and positrons with solids; density fluctuation detection; cluster-impact fusion; a model for cluster-impact fusion; thoughts on cold fusion; and plasmon decay. DOE

N90-21612# Los Alamos National Lab., NM. Physics Div.
A MEASUREMENT OF THE GRAVITATIONAL ACCELERATION OF THE ANTIPROTON
Michael H. Holzscheiter 1990 6 p Presented at the Recontres De Moriond 1990: New and Exotic Phenomena, Les Arcs, France, 20-27 Jan. 1990
(Contract W-7405-eng-36)
(DE90-008903; LA-UR-90-1014; CONF-900183-3) Avail: NTIS HC A02/MF A01

A fundamental experiment in gravity proposed by the authors, is the measurement of the gravitational force on antimatter. This measurement would constitute the first direct test of the Weak Equivalence Principle (WEP) for antimatter. The availability of low energy antiprotons at CERN has made such an experiment feasible, and a proposal to carry out such a measurement was accepted by the CERN Program Committee. The use of a time-of-flight technique similar to that pioneered by Fairbank and Witteborn in their measurement of the gravitational force on an electron is planned. Very slow particles are launched into a vertical drift tube and the time-of-flight spectrum of these particles is recorded. This spectrum will exhibit a cut-off point directly related to the gravitational acceleration of the particles. Obtaining very slow antiprotons involves several stages of deceleration. Antiprotons from LEAR will be initially decelerated from 2 MeV to tens of kilovolts by passing them through a thin foil. After capture and cooling in a series of ion traps, the antiprotons will be in a thermal distribution with a temperature of a few degrees Kelvin. These ultra-cold antiprotons will then be released a few at a time into the drift tube. A detector will measure the arrival time of the particles at the exit of the drift tube. H(-) ion, which have almost identical electromagnetic properties to the antiprotons, will be used for comparison and as a calibration standard. DOE

N90-21613# Institute for Advanced Study, Princeton, NJ.
RINGS
R. L. Davis 1989 10 p Presented at the Cambridge Cosmic Strings Workshop, Cambridge, MA, Jul. 1989
(Contract DE-AC02-76ER-02220)
(DE90-009035; CONF-8907186-1; IASSNS-HEP-89/48) Avail: NTIS HC A02/MF A01

The essence of vortex physics is that at certain low energy scales elementary excitations of a point particle theory can behave like strings rather than particles. Vortices are the resulting string-like solutions; their thickness sets the distance scale beyond which physics is string-like rather than particle-like. String degrees of freedom are massless in the sense that excitations on a string can have an arbitrarily low frequency. Non-string degrees of freedom correspond to massive particles and are absent from the low energy spectrum. This article considers only field theories with vortices at low energies. The possible existence of a class of solitons in these vortex theories will be discussed. They are vortex rings: they are localized and finite in energy, and able to carry the quantum numbers of point particles. Rings are thus particle-like solutions of a vortex theory, which is itself a limit of a point particle field theory. DOE

N90-21614# Wisconsin Univ., Milwaukee.
INELASTIC ELECTRON SCATTERING FROM SURFACES
Annual Technical Progress Report
S. Y. Tong 1989 7 p
(Contract DE-FG02-84ER-45076)
(DE90-009365; DOE/ER-45076/T1) Avail: NTIS HC A02/MF A01

Research is discussed which is being done on inelastic electron scattering by surface phonons and proposed experiments in this area. DOE

73 NUCLEAR AND HIGH-ENERGY PHYSICS

Includes elementary and nuclear particles; and reactor theory.

For space radiation see *93 Space Radiation.*

N90-21615# Joint Inst. for Nuclear Research, Dubna (USSR). Lab. of Nuclear Problems.

MESOOPTICAL FOURIER TRANSFORM MICROSCOPE: A NEW DEVICE FOR HIGH ENERGY PHYSICS

A. Ya. Astakhov et al 1988 22 p In RUSSIAN; ENGLISH summary

(DE90-616423; JINR-E-13-88-892) Avail: NTIS (US Sales Only) HC A03/MF A01

A new device for high energy physics, Mesooptical Fourier Transform Microscope (MFTM), designed for observation of straight line particle tracks in nuclear emulsion is described. The MFTM works without any mechanical or electronical depth scanning and can be considered as a selectively viewing eye. The computer controlled system containing MFTM as the main unit is given. This system can be used for fast search particle tracks and events produced by high energy neutrinos from accelerators. The results of the first experimental test of the computer controlled MFTM are presented. The performances of this system are described and discussed. It is shown that the angular resolution of the MFTM is 1 angular minute and the measurement time is equal to 30 ms. As all operations in the MFTM go without any depth scanning this new system works at least two orders of magnitude faster than any known system with a traditional optical microscope. DOE

N90-21616# Brookhaven National Lab., Upton, NY.

STRANGENESS ENHANCEMENT IN 14.6 A GeV/c Si+Au INTERACTIONS?

Ole Hansen 1990 8 p Presented at the 18th International Workshop on Gross Properties of Nuclei and Nuclear Excitations, Hirschegg, Austria, 15-20 Jan. 1990

(Contract DE-AC02-76CH-00016)

(DE90-008826; BNL-44347; CONF-900181-2) Avail: NTIS HC A02/MF A01

The questions of strangeness enhancement and of J/(psi) suppression have become central in the discussion of high energy heavy ion physics. Both phenomena have been predicted as signs of the formation of a deconfined quark-gluon phase of matter, both have been observed and both may be explainable also in terms of ordinary hadronic matter. In this note the question of K(+) and K(-) enhancement will be discussed from a much less elevated point of view, namely as a question of enhanced (or suppressed) over what. What is the relevant comparison for A(sub p) + A(sub t) data. DOE

N90-21617# Lawrence Livermore National Lab., CA.

PROPOSAL FOR FY86 LAWRENCE LIVERMORE NATIONAL LABORATORY PARTICLE BEAM RESEARCH

A. C. Smith 15 Mar. 1990 91 p

(Contracts W-7405-eng-48; N60921-84-WR-W0095; ARPA Order 4395)

(DE90-007936; UCRL-ID-103333) Avail: NTIS HC A05/MF A01

This document represents a combination FY 85 annual report plus the FY 96 proposal for Charged Particle Beam (CPB) research by the Lawrence Livermore National Laboratory's (LLNL's) Beam Research Program. Our report on FY 85 activities focuses on a set of experiments in which the ATA electron beam was propagated through a 1-foot-diameter, 8.5-m-long tank at pressures ranging from the ion-focused regime up to 500 Torr of dry, synthetic air. Based on the optimistic results from this first set of experiments, we propose in FY 86 to extend the tank length to 20 m. We will operate ATA at higher beam current to improve our understanding of intra-accelerator transport physics and to resolve, to our satisfaction, lead pulse stability issues centering around the beam's robustness against the hose instability as a function of beam conditioning. We expect these experiments to yield a wealth of detailed experimental propagation data which will help us prepare for propagating the ATA beam into the open air, an event planned for the end of FY 86. The principal elements are ATA operating time, constructing a flexible lead pulse/conductivity channel tracking facility, and preparing the atmospheric air line for the open air propagation tests. We believe our plans reflect and intelligent and practical symbiotic relationship with SDIO-sponsored Free Electron Laser experiments, also planned on ATA for FY 86, but with very different electron beam current and emittance requirements. DOE

N90-21618# Lawrence Livermore National Lab., CA.

CHARGED-PARTICLE BEAM RESEARCH PROGRAM Quarterly Report, Jul. - Sep. 1989

Nov. 1989 21 p

(Contract W-7405-eng-48; ARPA Order 4395)

(DE90-007937; UCID-21791-3) Avail: NTIS HC A03/MF A01

The following topics on charged-particle beam research program are discussed: management and application; beam propagation theory and computations; accelerator theory; ATA operations supporting the CPB experimental program; multiple pulse propagation experiment; diagnostics development and handling; and compact accelerator technology development beam research program publications. DOE

74 OPTICS

Includes light phenomena; and optical devices.

For lasers see *36 Lasers and Masers.*

N90-21619# Research Support Instruments, Inc., Cockeysville, MD.

UV SPECTROMETER SYSTEM AFGL 801 A HUP Final Report, 12 Jan. 1979 - 31 Oct. 1988

J. C. E. Berends, R. C. Eppig, and J. T. Riley May 1989 385 p

(Contract F19628-79-C-0044)

(AD-A217805; GL-TR-89-0137) Avail: NTIS HC A17/MF A02 CSCL 14/2

Seven spectrometers, covering the ultraviolet and visible spectral regions were designed, built, and tested under this contract. One UV Spectrometer was packaged with a telescope, scan platform and electronics, and flown on Shuttle Mission STS-4. Several other spectrometers were similarly packaged for a subsequent Shuttle experiment. Ground support equipment was provided for the units. GRA

N90-21620 Department of the Navy, Washington, DC.

PASSIVE STABILIZATION OF A FIBER OPTIC NONLINEAR INTERFEROMETRIC SENSOR Patent

Kee P. Koo, inventor (to Navy), Frank Bucholtz, inventor (to Navy), and Anthony Dandridge, inventor (to Navy) 21 Nov. 1989 9 p Filed 20 May 1988 Supersedes AD-D013914

(AD-D014438; US-Patent-4,881,813; US-Patent-Appl-SN-196705; US-Patent-Class-356-345) Avail: US Patent and Trademark Office CSCL 20/6

Three sampling circuits, a subtraction circuit, and a divider circuit cooperate to sample an output signal from a nonlinear interferometric sensor at proper times, to subtract output signal samples to obtain a difference signal, and to divide an output signal sample into the difference signal to remove noise-induced modulation from the output signal. GRA

N90-21621# Brigham Young Univ., Provo, UT. Dept. of Physics.

THE INVESTIGATION OF MULTILAYER X RAY REFLECTORS AS X RAY OPTICAL ELEMENTS Final Report

Larry V. Knight 15 Dec. 1989 52 p
(Contract DE-AS03-88DP-10741)
(DE90-009044; DOE/DP-10741/1) Avail: NTIS HC A04/MF A01

At Brigham Young University (BYU), we have been involved in x ray optics for several years. In the last several years the intensity of this effort has significantly increased. A review of this work is included in the previous report. The work done in the last phase of this work on multilayer x ray mirrors focused on a code to predict the curvature of etched silicon wafers and a study of the development of an x ray interferometer for plasma diagnostics. The work was also partially supported by the State of Utah under the Centers of Excellence program and the interferometer work was done in collaboration with MOXTEK, Inc., an x ray optics company which received support for some of the work through The Department of Defense. DOE

N90-21082*# Lockheed Missiles and Space Co., Palo Alto, CA.
ASCIE: AN INTEGRATED EXPERIMENT TO STUDY CSI IN LARGE SEGMENTED OPTICAL SYSTEMS
Jean-Noel Aubrun and Kenneth R. Lorell *In* NASA, Langley Research Center, NASA/DOD Controls-Structures Interaction Technology 1989 Aug. 1989 p 349-36 (For primary document see N90-21062 14-18)
Avail: NTIS HC A23/MF A03 CSCL 20F

N90-21090*# National Aeronautics and Space Administration. Langley Research Center, Hampton, VA.
STRAIN AND DYNAMIC MEASUREMENTS USING FIBER OPTIC SENSORS EMBEDDED INTO GRAPHITE/EPOXY TUBES
D. W. DeHart, T. Doederlein, J. Koury (Air Force Astronautics Lab., Edwards AFB, CA.), R. S. Rogowski, J. S. Heyman, and M. S. Holben, Jr. *In its* NASA/DOD Controls-Structures Interaction Technology 1989 Aug. 1989 p 497-506 (For primary document see N90-21062 14-18)
Avail: NTIS HC A23/MF A03 CSCL 20F

75 PLASMA PHYSICS

Includes magnetohydrodynamics and plasma fusion.
For ionospheric plasmas see *46 Geophysics.* For space plasmas see *90 Astrophysics.*

N90-21622# Maryland Univ., College Park. Lab. for Plasma Research.
EXPERIMENTAL STUDY OF POPULATION INVERSION AND SPECTRAL LINE BROADENING IN A PLASMA CONTAINING A MIXTURE OF HIGH Z AND LOW Z IONS Final Technical Report, 8 Apr. 1987 - 18 Oct. 1988
H. R. Griem Oct. 1988 42 p
(Contract DE-AS08-87DP-10684)
(DE90-007552; DOE/DP-10684/1) Avail: NTIS HC A03/MF A01

Laser produced plasmas were studied using spherical targets continuing layers of high Z and low Z materials. The emphasis was on quantitative spectroscopy of ions in a very dense, recombining plasma. The targets used consisted of carbon-copper, carbon-gold, and aluminum-gold mixtures, instead of the originally proposed Fe or Mo mixtures with carbon. The thickness of the Cu and the Au layers were varied in order to study the effect of higher Z ion cooling the plasma. Indeed, a pronounced cooling effect was observed by increasing the thickness of the Au layer in targets with Al-Au layers. Electron temperatures were studied by measuring the 1s-2p/1s(sup 2)-1s2p line ratio of Al XIII to Al XII. The experimental measurements, together with a collisional radiative model and a 1-D hydrodynamic code, indicate that the electron temperature falls from 1500 eV with no gold to 950 eV with a 500 A layer of gold. DOE

N90-21623# Academy of Sciences (USSR), Novosibirsk. Inst. Yadernoj Fiziki.
STUDY ON ROTATING PLASMA WITH SUBMILLIMETER LASER INTERFEROMETER
1988 27 p In RUSSIAN
(DE90-615387; IYaF-88-144) Avail: NTIS (US Sales Only) HC A03/MF A01

Increase of plasma rotation rate and plasma density in crossed fields was the purpose of experiments, conducted at PSP-2 device. Results of measuring radial profile of plasma density and its dynamics in PSP-2 device by submillimeter laser interferometer are presented. Plasma probing was conducted along six chord and one diameter. Directions channel sensitivity, equal to (0.4 divided by 0.8) x 10(exp -3) of nl sub min = (2.7 divided by 5.3) x 10(exp 11)/sq cm was achieved. Effect of neutral gas, delivered from the wall of internal liner, on distribution and absolute value of plasma density was shown. Coefficient of radial plasma diffusion for oscillations, occurring at high rates of plasma rotation, was evaluated according to results of interferometric and spectral measurements. DOE

N90-21624# Academy of Sciences (USSR), Novosibirsk. Inst. Yadernoj Fiziki.
LANGMUIR WAVE INTERACTION WITH ION ACOUSTIC WAVE
N. S. Buchelnikova and E. P. Matochkin 1988 69 p In RUSSIAN; ENGLISH summary
(DE90-615407; IYaF-88-163) Avail: NTIS (US Sales Only) HC A04/MF A01

The conversion of the Langmuir wave on the ion-acoustic wave leads to the excitation of Langmuir wave modes. The damping of the electric field is determined by the trapping of the electrons by the main conversion modes and by the stochastic instability of the electron motion (the stochastic layers formation). The evolution of the stochastic layers of the conversion modes leads to the acceleration of a part of the electrons and to the formation of the short tails of the velocity distribution function. The evolution of the large scale stochasticity leads to the heating of the main part of the electrons. DOE

N90-21625 Wisconsin Univ., Madison.
HELIUM TRANSPORT IN PLASMA EDGE REGIONS Ph.D. Thesis
Hanaa Hassan Abou-Gabal 1989 175 p
Avail: Univ. Microfilms Order No. DA8923307

The transport of neutral helium atoms near diverter or limiter target plates in fusion devices was studied. Two simulation codes, based on Monte Carlo techniques, were developed. The first treats the problem in one-dimensional geometry and the second considers two-dimensional effects. The atomic processes of ionization of helium atoms by electron impact and elastic scattering with plasma ions are included. The total and differential elastic scattering cross-sections were calculated classically using an ab initio calculation of the interatomic potential. The thermal motion and the streaming of the ions along the magnetic field, which can be at an angle to the target plate, are included. Results obtained with the one-dimensional code show significant effects of elastic collisions below about 10 eV, causing a substantial fraction of the helium atoms to be reflected back to the target plate. This effect can be beneficial for the pumping of helium from the discharge chamber. The two-dimensional Monte Carlo code was used to study helium recycling near a flat, vented target plate. A parametric study is performed to examine the dependence of the pumping efficiency on plasma parameters and geometric aspects. Results show that the pumping of neutral helium can be increased by shortening and widening the ports as well as by increasing the angle between the magnetic field and the target plate. Also, keeping the ion temperature below about 10 eV and the plasma density around a few 10(exp 14) cu cm near the targe plate can be beneficial for the pumping of helium gas. Author

N90-21626# Instituto de Pesquisas Energeticas e Nucleares, Sao Paulo (Brazil).
A SIMPLIFIED THEORETICAL MODEL FOR THE LASER-INDUCED OPTOGALVANIC EFFECT
Armando Mirace 1990 14 p
(DE90-613121; INIS-BR-1796) Avail: NTIS (US Sales Only) HC A03/MF A01

A simplified theoretical model for an estimate of the optogalvanic effect induced in an electric discharge by resonant laser radiation is presented. This theory is based on the solution of a two-level system rate equation, where the upper level of the stimulated transition is connected to the ground state (lower level) through radiative and collisional processes. The developed relations show that the magnitude and temporal evolution (in the case of pulsed excitation) of the optogalvanic signal depend on the electronic plasma density, electron temperature and on the density of light absorbing centers. DOE

N90-21627# International Centre for Theoretical Physics, Trieste (Italy).
RELATIVISTIC STIMULATED BRILLOUIN AND RAMAN SCATTERING IN A LASER-PRODUCED PLASMA
M. Salimullah and M. H. A. Hassan Nov. 1989 13 p
(DE90-613123; IC-89/360) Avail: NTIS (US Sales Only) HC A03/MF A01

An investigation is made on the relativistic effect on the nonlinear stimulated scattering of a large-amplitude laser radiation in the presence of the self-generated magnetic field in a laser-produced plasma. The relativistic Vlasov equation expressed in terms of the guiding-center coordinates has been solved to obtain the response of the magnetized plasma electrons. It is noted that the extreme relativistic effect increases the growth rates of the stimulated scattering by a factor of c and v(sub e), where c and v(sub e) are the free-space speed of light and thermal velocity of the plasma electrons. DOE

N90-21628# Instituto de Pesquisas Espaciais, Sao Jose dos Campos (Brazil).
CHARACTERIZATION OF THE PLASMA IN MAGNETIC MULTIDIPOLE DISCHARGES M.S. Thesis
Julio Guimaraes Ferreira Sep. 1988 228 p In PORTUGUESE; ENGLISH summary
(DE90-613219; INPE-4704-TDL/343; TDL-343) Avail: (US Sales Only) NTIS HC A11/MF A02

A characterization of the discharge of the quiescent plasma machine of INPE, and an identification of the most relevant processes in the definition of its plasma properties, were achieved. Measurements of plasma properties, the floating potential, the temperature of the electrons, and the density of the plasma, for pressures ranging from 10(exp -3) to 10(exp -1)Pa and for discharge potentials for 45V to 120V were accomplished. These measurements were made with a Langmuir spherical probe with 1mm in diameter. In the whole range of operation, the presence of two populations of electrons with distinct temperatures in the energy range from 1 to 10eV was observed, although for pressures approaching 10(exp -1)Pa the plasma tended to a single population of electrons with temperature of 1eV. The difference between plasma and floating potentials was observed to become smaller as the pressure raised, and the potential difference between plasma and anode reached a value around 2V when pressure rose above 10(exp -2)Pa. The plasma density increases approximately linearly with pressure, for values below 10(exp -2)Paa, but above 10(exp -1)Pa its increase with pressure is quite reduced. A study on the collision processes in the plasma volume and on loss processes to surfaces allowed to interpret qualitatively the observed plasma behavior and to estimate, by means of simple expressions, some of the plasma parameters. The loss area for ions and primary electrons were estimated from experimental results. A simple quantitative model which allows the calculation of plasma density in the whole range of operation, reproduced the correct order of magnitude of experimental values. However, an additional work, both theoretical and experimental, is required to obtain better agreement between experimental and theoretical values. DOE

N90-21629# International Centre for Theoretical Physics, Trieste (Italy).
ON THE RELATIVISTIC VLASOV EQUATION IN GUIDING-CENTER COORDINATES
M. Salimullah, M. B. Chaudhry, and M. H. A. Hassan Nov. 1989 8 p Submitted for publication
(DE90-613241; IC-89/358) Avail: NTIS (US Sales Only) HC A02/MF A01

The relativistic Vlasov equation has been expressed in terms of the guiding-center coordinates in a hot magnetized plasma. It is noted that the relativistic effect reduces the cyclotron resonance frequency for electrostatic and electromagnetic waves propagating transverse to the direction of the static magnetic field in the plasma. DOE

N90-21630# Japan Atomic Energy Research Inst., Ibaraki. Dept. of Thermonuclear Fusion.
NUMERICAL CODE AEOLUS-E1 FOR ANALYSING FREE-BOUNDARY RESISTIVE MHD MODE
Gen-ichi Kurita, Masafumi Azumi, Tomonori Takizuka, Toshihide Tsunematsu, and Tatsuoki Takeda Oct. 1989 58 p In JAPANESE; ENGLISH summary
(DE90-759903; JAERI-M-89-157) Avail: NTIS (US Sales Only) HC A04/MF A01

Numerical code AEOLUS-E1 for analyzing a free-boundary resistive MHD mode in a tokamak is developed. A reduced set of the resistive MHD equation is solved as a single-helicity free-boundary problem based on pseudo-vacuum model in a cylindrical geometry. The code can solve problems including effects of coupling to external circuit and interaction between plasma and limiter. DOE

N90-21631# Wisconsin Univ., Madison. Dept. of Physics Research.
A SELF-CONSISTENT THEORY OF RADIAL TRANSPORT OF FIELD-ALIGNED CURRENT BY MICROTURBULENCE
P. W. Terry and P. H. Diamond (California Univ., San Diego, La Jolla.) Feb. 1990 30 p Sponsored by Sloan (Alfred P.) Foundation and NSF
(Contracts DE-FG02-89ER-53291; DE-FG03-88ER-53275)
(DE90-007920; DOE/ER-53291/150) Avail: NTIS HC A03/MF A01

The radial transport of field aligned current due to collisionless microturbulence is examined self-consistently. The self-consistent treatment of mode coupling shown to constrain the transport in such a way that the relaxation of current gradients is regulated solely by electrostatic fluctuations which couple to ion dissipation, even in the presence of temperature gradients and temperature anisotropy. As a consequence, the radial flux of parallel current induced by collisionless microinstabilities is insufficient to account for the dynamo in reversed field pinch plasmas. DOE

N90-21632# Connecticut Univ., Storrs.
ATOMIC PROCESSES IN HIGH TEMPERATURE PLASMAS Annual Report
Yukap Hahn Mar. 1990 8 p
(Contract DE-FG02-85ER-53205)
(DE90-008873; DOE/ER-53205/4) Avail: NTIS HC A02/MF A01

Much theoretical and experimental effort has been expended in recent years to study those atomic processes which are specially relevant to understanding high temperature laboratory plasmas. For magnetically confined fusion plasmas, the temperature range of interest spans from the hundreds of eV at plasma edges to 10 keV at the center of the plasma, where most of the impurity ions are nearly fully ionized. These highly stripped ions interact strongly with electrons in the plasma, leading to further excitation and ionization of the ions, as well as electron capture. Radiations are emitted during these processes, which easily escape to plasma container walls, thus cooling the plasma. One of the dominant modes of radiation emission has been identified with dielectronic recombination. This paper reviews this work. DOE

N90-21633# Los Alamos National Lab., NM. Theoretical Div.
DYNAMICS OF CAVITONS IN STRONG LANGMUIR TURBULENCE
D. F. DuBois, Harvey A. Rose, and David Russell 1990 56 p Presented at the Topical Conference on Research Trends in Nonlinear and Relativistic Effects in Plasmas, LaJolla, CA, 5-8 Feb. 1990
(Contract W-7405-eng-36)
(DE90-008918; LA-UR-90-1000; CONF-900264-4) Avail: NTIS HC A04/MF A01

Recent studies of Langmuir turbulence as described by Zakharov's model will be reviewed. For parameters of interest in laser-plasma experiments and for ionospheric hf heating experiments a significant fraction of the turbulent energy is in nonlinear caviton excitations which are localized in space and time. A local caviton model will be presented which accounts for the nucleation-collapse-burnout cycles of individual cavitons as well as their space-time correlations. This model is in detailed agreement with many features of the electron density fluctuation spectra in the ionosphere modified by powerful hf waves as measured by incoherent scatter radar. Recently such observations have verified a prediction of the theory that free Langmuir waves are emitted in the caviton collapse process. Observations and theoretical considerations also imply that when the pump frequency is slightly lower than the ambient electron plasma frequency cavitons may evolve to states in which they are ordered in space and time. The sensitivity of the high frequency Langmuir field dynamics to the low frequency ion density fluctuations and the related caviton nucleation process will be discussed. DOE

N90-21634# Foreign Applied Sciences Assessment Center, La Jolla, CA.
WEST EUROPEAN MAGNETIC CONFINEMENT FUSION RESEARCH Technical Assessment Report
R. D. Hazeltine, K. W. Gentle, J. T. Hogan, M. Porkolab, D. J. Sigmar, D. Steiner, and K. I. Thomassen Jan. 1990 273 p Prepared in cooperation with Science Applications International Corp., McLean, VA
Avail: NTIS HC A12/MF A02

A technical assessment and review of the West European program in magnetic confinement fusion by a panel of U.S. scientists and engineers active in fusion research is presented. Findings are based on the scientific and technical literature, on laboratory reports and preprints, and on the personal experiences and collaborations of the panel members. Concerned primarily with developments during the past 10 years, the report assesses West European fusion research in seven technical areas: tokamak experiments; magnetic confinement technology and engineering; fusion nuclear technology; alternate concepts; theory; fusion computations; and program organization. The main conclusion emerging from the analysis is that West European fusion research has attained a position of leadership in the international fusion program. This distinction reflects in large measure the remarkable achievements of the Joint European Torus (JET). However, West European fusion prominence extends beyond tokamak experimental physics: the program has demonstrated a breadth of skill in fusion science and technology that is not excelled in the international effort. Author

N90-21635# General Atomic Co., San Diego, CA.
APPLIED PLASMA PHYSICS Annual Report, 1 Oct. 1988 - 30 Sep. 1989
Feb. 1990 61 p
(Contract DE-AC03-89ER-53277)
(DE90-007932; GA-A-19923) Avail: NTIS HC A04/MF A01

The following topics on controlled magnetic fusion are discussed: applied plasma physics overview; fusion plasma theory; fusion user service center; diagnostics; and ergodic and resonant magnetic divertor experiments on text. DOE

N90-21636# General Atomic Co., San Diego, CA.
FUSION TECHNOLOGY DEVELOPMENT Annual Report, 1 Oct. 1988 - 30 Sep. 1989
Feb. 1990 27 p
(Contract DE-AC03-89ER-52153)
(DE90-007933; GA-A-19924) Avail: NTIS HC A03/MF A01

This report discusses the following topics on magnetic fusion: RF technologies; plasma facing components; reactor design studies; fusion nuclear technologies; and fusion materials development. DOE

N90-21637# Lawrence Livermore National Lab., CA.
AN EXTENDED DIFFUSIVE MODEL FOR CALCULATING THERMAL DIFFUSIVITY FROM SINGLE MONOPOLE TOKAMAK HEAT PULSE PROPAGATION
Marty Marinak (California Univ., Berkeley.) Feb. 1990 31 p
(Contract W-7405-eng-48)
(DE90-007958; UCRL-ID-103119) Avail: NTIS HC A03/MF A01

The problem of deducing chi (sub e) from measurements of the propagation of a monopole heatpulse is considered. An extended diffusive model, which takes into account perturbed sources and sinks is extended to the case of a monopole heat input. Chi (sub e) is expressed as a function of two observables, the heat pulse velocity and the radial damping rate. Two simple expressions valid for two different ranges of the radius of the poloidal waist of the beam power profile are given. The expressions are valid in the heat pulse measurement region, extending radially 0.05a beyond the beam power waist to near 0.6a. The inferred chi (sub e) is a local value, not an average value of the radial chi (sub e) profile. DOE

N90-21638# Los Alamos National Lab., NM.
FUSION BURN DYNAMICS IN DENSE Z-PINCH (DZP)
R. A. Krakowski Apr. 1990 78 p
(Contract W-7405-eng-36)
(DE90-007976; LA-11757-MS) Avail: NTIS HC A05/MF A01

The fusion burn dynamics and energy yield of the dense Z-pinch (DZP) are examined using a profile-averaged, zero-dimensional, time dependent model. A range of conditions (fuel, line density, voltage, fusion-product heating, enthalpy endloss, density and temperature profiles, current rise rate, electrode impurities) are examined. Magnetohydrodynamic stability is assumed, and initial conditions are based on those ideally existing after the melting and ionization of a solid fiber of fusion fuel. Plasma conditions required of neutron sources for materials testing and for possible commercial power production are described. If f(sub B) approx. greater than 0.8 fractional fuel burnup is possible in a nominal 800-ns DT discharge (200-ns current-rise phase at 20 MV/m followed by a 500-ns constant-current crowbarred phase), reactor-relevant values of Q(sub p) may be possible. For the simpler (and shorter) constant-voltage discharge (e.g., no voltage crowbar) the value of Q(sub p) is in the range 5 to 10 for discharges below 200-ns duration. Smaller levels of fuel burnup, shorter discharges, or generally lower levels of Q(sub p) will require a reversible energy transfer system to meet reactor energy-balance requirements. Imposition of a plasma current rise-time constraint that may be needed for stable plasma operation (e.g., I greater than 10(exp 12) A/s) will burnup, Q(sub p) and discharge time to an extent where reversible energy/transfer system will be required to meet reactor energy balance requirements. DOE

N90-21639# Texas Univ., Austin. Inst. for Fusion Studies.
MHD MODES DRIVEN BY ANOMALOUS ELECTRON VISCOSITY AND THEIR ROLE IN FAST SAWTOOTH CRASHES
A. Y. Aydemir 13 Feb. 1990 27 p
(Contract DE-FG05-80ET-53088)
(DE90-009311; DOE/ET-53088/408; IFSR-408) Avail: NTIS HC A03/MF A01

The dispersion relations are derived for both small and large delta' modes (m is greater than or = to 2, and m = 1 modes, respectively) driven by anomalous electron viscosity. Under the assumption that the anomalous kinematic electron viscosity is comparable to the anomalous electron thermal diffusivity, we find that the viscous mode typically has a higher growth rate than the

corresponding resistive mode. Computational results in cylindrical and toroidal geometries are compared with theory and some nonlinear results are presented for viscous m = 1 modes in both circular and D-shaped boundaries and their possible rile in fast sawtooth crashes are discussed. DOE

N90-21640# Texas Univ., Austin. Inst. for Fusion Studies.
NONLINEAR INTERACTION OF PHOTONS AND PHONONS IN ELECTRON-POSITRON PLASMAS
T. Tajima and T. Taniuti Mar. 1990 45 p
(Contract DE-FG05-80ET-53088; NSF ATM-88-11128)
(DE90-009341; DOE/ET-53088/425; IFSR-425) Avail: NTIS HC A03/MF A01

Nonlinear interaction of electromagnetic waves and acoustic modes in an electron-positron plasma is investigated. The plasma of electrons and positrons is quite plastic so that the imposition of electromagnetic (EM) waves causes depression of the plasma and other structural imprints on it through either the nonresonant or resonant interaction. The theory shows that the nonresonant interaction can lead to the coalescence of photons and collapse of plasma cavity in higher (greater than or = to 2) dimensions. The resonant interaction, in which the group velocity of EM waves is equal to the phase velocity of acoustic waves, is analyzed and a set of basic equations of the system is derived via the reductive perturbation theory. New solutions of solitary types were found: bright solitons, kink solitons, and dark solitons as the solutions to these equations. The computation hints their stability. An impact of the present theory on astrophysical plasma settings is expected, including the cosmological relativistically hot electron-positron plasma. DOE

N90-21641# Texas Univ., Austin. Inst. for Fusion Studies.
TRANSITION FROM RESISTIVE-g TO ETA-i DRIVEN TURBULENCE IN STELLARATOR SYSTEMS
B.-G. Hong, W. Horton, S. Hamaguchi, M. Wakatani, M. Yagi, and H. Sugama (Kyoto Univ., Uji, Japan) Feb. 1990 19 p
(Contract DE-FG05-80ET-53088)
(DE90-009382; DOE/ET-53088/417; IFSR-417) Avail: NTIS HC A03/MF A01

By an electromagnetic incompressible two fluid model describing both ion temperature gradient drift modes (eta(sub i) modes) and resistive interchange modes (g modes), a new type of eta(sub i) mode is studied in cylindrical geometry including magnetic shear and an averaged curvature of Heliotron/Torsatron. This eta(sub i) mode is destabilized by the coupling to the unstable g mode. Finite plasma pressure beta increases the growth rate of this mode and the radial mode width also increases with plasma pressure beta indicating large anomalous transport in the Hiliotron/Torsatron configuration. The transport from eta(sub i) mode exceeds that from resistive g when the mean-free-path exceeds the machine circumference. For plasma beta above two to three times the Suydam limit the m = 1/n = 1 growth rate increases from the eta(sub i) mode value to the MHD value. DOE

N90-21642# Oak Ridge National Lab., TN.
FULL WAVE COMPUTATION OF ELECTROMAGNETIC WAVE EXCITATION, PROPAGATION, AND ABSORPTION AT THE ION CYCLOTRON FREQUENCY IN FUSION EXPERIMENTS
D. B. Batchelor and E. F. Jaeger 1990 10 p Presented at the 6th Annual Review of Progress in Applied Computational Electromagnetics, Monterey, CA, 20-22 Mar. 1990
(Contract DE-AC05-84OR-21400)
(DE90-009399; CONF-9003128-2) Avail: NTIS HC A02/MF A01

High-power electromagnetic waves at frequencies ranging from a few megahertz to a few hundred gigahertz serve many important functions in modern fusion experiments. Probably the most important application is plasma heating. Ignition of a fusion reactor will require a plasma to be heated until the average particle energy is approximately 10 keV (temperature is greater than 10(exp 8) K). This is routinely accomplished in existing large devices. Waves at the ion cyclotron frequency (typically f = 30 to 100 MHz) are very important for fusion devices because of low cost/unit power compared to other frequency regimes and because of their ability to directly heat fusile ions. These waves are also useful for modifying the velocity distribution for improved stability and to drive currents which affect plasma equilibrium. Study of this frequency range is, however, greatly complicated by long wavelengths compared to device size, nonsymmetric device geometry, and the tendency of the waves to linearly transform to shorter wavelength modes. Geometrical optics is generally inapplicable. Thus, codes were developed to solve the vector wave equation in toroidal geometry for hot plasmas having anisotropic, spatially nonuniform, dispersive constitutive relations. The code ORION developed at Oak Ridge National Laboratory is described and illustrative applications are presented for a range of fusion experiments. Specific applications of the code include detailed modeling of the antennas used to launch the waves, calculation of wave propagation throughout the plasma, and modeling of the absorption of the waves by the plasma. DOE

N90-21643# Texas Univ., Austin. Inst. for Fusion Studies.
INSTABILITIES AND VORTEX DYNAMICS IN SHEAR FLOW OF MAGNETIZED PLASMAS
T. Tajima, W. Horton, P. J. Morrison, J. Schutkeker, T. Kamimura, K. Mima, and Y. Abe Mar. 1990 64 p
(Contract DE-FG05-80ET-53088)
(DE90-009448; DOE/ET-53088/418; IFSR-418) Avail: NTIS HC A04/MF A01

Gradient-driven instabilities and the subsequent nonlinear evolution of generated vortices in sheared E x B flows are investigated for magnetized plasmas with and without gravity (magnetic curvature) and magnetic shear by using theory and implicit particle simulations. In the linear eigenmode analysis, the instabilities considered are the Kelvin-Helmholtz (K-H) instability and the resistive interchange instability. The presence of the shear flow can stabilize these instabilities. The dynamics of the K-H instability and the vortex dynamics can be uniformly described by the initial flow pattern with a vorticity localization parameter (epsilon). The observed growth of the K-H modes is exponential in time for linearly unstable modes, secular for marginal mode, and absent until driven nonlinearly for linearly stable modes. The distance between two vortex centers experiences rapid merging while the angle (theta) between the axis of vortices and the external shear flow increases. These vortices proceed toward their overall coalescence, while shedding small-scale vortices and waves. The main features of vortex dynamics of the nonlinear coalescence and the tilt or the rotational instabilities of vortices are shown to be given by using a low dimension Hamiltonian representation for interacting vortex cores in the shear flow. DOE

76 SOLID-STATE PHYSICS

Includes superconductivity.

For related information, see also *33 Electronics and Electrical Engineering* and *36 Lasers and Masers*.

N90-21644# Argonne National Lab., IL.
DEFORMATION PROCESSING OF YBa2Cu3O(SUB x)
K. C. Goretta, M. J. McGuire, A. Brandstaedter (Institute for Reactor Research, Juelich, Germany, F.R.), J. P. Singh, R. B. Poeppel, A. J. Schultz, and J. L. Routbort Jan. 1990 13 p Presented at the 1990 Spring Meeting of the Metallurgical Society, Anaheim, CA, 20-21 Feb. 1990 Sponsored in part by American Nuclear Society
(Contract W-31-109-eng-38)
(DE90-007795; CONF-900206-3) Avail: NTIS HC A03/MF A01

Generalized plasticity of polycrystalline YBa2 Cu3 O sub x at high temperatures was achieved by diffusional flow; from 850 to 980 C, strain rates of approximately 10 (exp -4) s(exp -1) were obtained without fracture. The strain rate for a given stress and temperature increased with decreasing oxygen partial pressure. Although dislocations are mobile at elevated temperature, they

are limited almost exclusively to the basal planes and hence deformation from their motion does not contribute significantly to total strain. DOE

N90-21645# Argonne National Lab., IL.
TOUGHENED YBa2Cu3O(SUB x)/ZrO2 COMPOSITES
K. C. Goretta, M. Kullberg, D. Baer (Institute for Reactor Research, Juelich, Germany, F.R.), S. E. Dorris, U. Balachandran, R. B. Poeppel, and J. L. Routbort Jan. 1990 12 p Presented at the 119th TMS (The Minerals, Metals and Metallurgical Society) Annual Meeting and Exhibit, Anaheim, CA, 18-22 Feb. 1990 Sponsored in part by American Nuclear Society
(Contract W-31-109-eng-38)
(DE90-007796; CONF-900206-2) Avail: NTIS HC A03/MF A01

Tetragonal ZrO2 particles have been added to YBa2 Cu3 O sub x to improve the fracture toughness of the superconductor. For some processing procedures, toughness was increased from 1 to 3 MPa(m)(sup 0.5), but in some cases ZrO2 reacted with YBa2 Cu3 O sub x and destroyed its superconductivity. Coating the ZrO2 with Y2 BaCuO5 is being explored to minimize the reaction between ZrO2 and YBa2 Cu3 O sub x. DOE

N90-21646# Litton Systems, Inc., Charlotte, NC. Airtron Div.
CONTRACT CRYSTAL GROWTH AND FABRICATION SERVICES Quarterly Technical Report No. 3, Nov. 1989 - Jan. 1990
M. H. Randles, R. Metzl, D. M. Murrell, and J. E. Creamer 9 Feb. 1990 4 p
(Contract N00014-89-C-2222)
(AD-A218327) Avail: NTIS HC A01/MF A01 CSCL 20/2

This program is intended to give the scientists at the Naval Research Laboratory the ability to evaluate new solid state laser crystals. The five crystals grown were gadolinium scandium gallium garnet (GSGG) doped with erbium and/or thulium. The presumed congruent composition for undoped GSGG is GD2.96Sc1.9Ga-3.14O12. If it is assumed that the distribution coefficients are unity then the crystal compositions will be the same. GRA

N90-21647# International Centre for Theoretical Physics, Trieste (Italy).
COUPLED MAGNETOPLASMON-PHONON MODES AT THE SURFACE OF A SEMI-INFINITE SEMICONDUCTOR SUPERLATTICE
J. C. Granada Nov. 1989 20 p Submitted for publication
(DE90-612904; IC-89/370) Avail: NTIS (US Sales Only) HC A03/MF A01

Surface excitations, which can occur at the interface of an ionic crystal and a semiconductor superlattice in a transversal magnetic field, are investigated. It is shown that, under certain conditions, the propagation of a surface wave with frequencies lower than the electron cyclotron resonance frequency is possible. This mode has a negative group velocity. It is demonstrated that the resonance between surface polaritons and cyclotron oscillations of the electron system causes a small splitting of the surface polariton frequency. The behavior of the starting points of the surface coupling modes is also discussed. DOE

N90-21648# Melbourne Univ., Parkville (Australia). School of Physics.
RETABULATION OF SPACE GROUP EXTINCTIONS FOR ELECTRON DIFFRACTION
P. Goodman and M. Tanaka (Tohoku Univ., Sendai, Japan) 1989 16 p
(DE90-612933; UM-P-89/29) Avail: NTIS (US Sales Only) HC A03/MF A01

The space group tables previously published by one of the authors and others are here presented in a revised and compacted form designed to make for compatability with existing tables for x ray diffraction. 136 of the 230 space groups are subject to dynamic extinctions due to glide planes and screw axes, and the observables from these space groups in specific settings are tabulated. DOE

N90-21649# Melbourne Univ., Parkville (Australia). School of Physics.
AN ATTEMPT TO MEASURE COLD-FUSION EFFECTS
M. N. Thompson, G. N. Taylor, R. P. Rassool, A. D. Bates, S. C. McDonald, and S. Guggenheimer 1989 4 p
(DE90-613248; UM-P-89/41) Avail: NTIS (US Sales Only) HC A01/MF A01

Recent press releases by Fleischmann and Pons at Utah State University and Jones et al., at Brigham Young University reported nuclear fusion of deuterium. These announcements suggested a significant new effect, following electrolysis of heavy water at room temperature, using palladium or titanium cathodes. The size of the reported reaction rate had powerful implications for future commercial use of the technique in power production. Attempts have been made to repeat the experiments in order to test the results. Two different types of experiments, one set involving electrolysis of heavy water, and another involving deuterium gas impregnation of titanium metal, were undertaken. None of the experiments gave any indication of fusion. DOE

N90-21650# International Centre for Theoretical Physics, Trieste (Italy).
CHERN-SIMONS SUPERCONDUCTIVITY AT FINITE TEMPERATURE
S. Randjbar-Daemi, Abdus Salam, and J. Strathdee Sep. 1989 43 p Submitted for publication
(DE90-613393; IC-89/283) Avail: NTIS (US Sales Only) HC A03/MF A01

A simple gauge theory discussed recently in the literature as a model of high temperature superconductors is examined. The model contains a Maxwell field and a Chern-Simons field coupled to fermions in 2+1-dimensional spacetime. This model has been shown to exhibit a kind of Meissner effect at zero temperature which originates in the 1-loop mixing between the two gauge fields. We use a Euclidean effective action formulation to show that the effect persists at all finite temperatures. Although a long range magnetic type interaction arises at non-zero temperatures, in competition with the finite range forces which dominate the zero temperature interaction, the effect varies smoothly with temperature. In our perturbation treatment, we find no indication of a critical transition at which the Meissner effect is extinguished. DOE

N90-21651# International Centre for Theoretical Physics, Trieste (Italy).
SPECIFIC HEAT AND CRITICAL FLUCTUATIONS IN ANISOTROPIC HIGH-T(SUB C) OXIDE SUPERCONDUCTORS
L. N. Shehata Oct. 1989 15 p Submitted for publication
(DE90-613394; IC-89/315) Avail: NTIS (US Sales Only) HC A03/MF A01

The specific heat due to the fluctuation of the order parameter is evaluated from the Modified Ginzburg-Landau free energy functional for high T sub c superconductors. The Ginzburg criterion was estimated from the Gaussian fluctuation contribution to the specific heat. The obtained criterion implies that the breakdown of the Modified Ginzburg-Landau mean-field theory takes place in a rather wide temperature range for the new superconductors. Comparison with the available experimental data is presented. DOE

N90-21652# International Centre for Theoretical Physics, Trieste (Italy).
ON THE SUBSTITUTION OF Sr IONS AT Y SITES IN YB(SUBa2)Cu3O(SUB7-d)
S. A. Siddiqi, K. Sreedhar, D. Drobac, C. Infante, F. C. Matacotta, and P. Ganguly (Indian Inst. of Science, Bangalore.) Oct. 1989 6 p Submitted for publication
(DE90-613395; IC-89/333) Avail: NTIS (US Sales Only) HC A02/MF A01

The effect of Sr substitution at the Ba sites in YBa2 Cu3 O sub 7-d has been studied; attempts to substitute Sr exclusively at Y sites have not been successful. We have been able to substitute Sr at Y sites only when the Ba ions are simultaneously substituted

by Sr to give solid solutions of the type Y sub 1-x Sr sub x Ba sub 2-2x Sr sub 2x Cu3 O(sub 7-)x(sub /2-d). These examples show superconducting transitions higher than 78 K without significant deterioration in the magnitude of the ac susceptibility. The substitutions are best understood in terms of site constraints on the ions occupying the Y and Ba sites. DOE

N90-21653# Weizmann Inst. of Science, Rehovoth (Israel). Dept. of Nuclear Physics.
AN ULTRA-SMALL CAPACITANCE JOSEPHSON JUNCTION
Efrat Shimshoni, Yuval Gefen, and Shimon Levit Jan. 1989 34 p
(DE90-613396; WIS-PH-89/01) Avail: NTIS HC A03/MF A01

We consider a voltage biased ultra-small capacitance Josephson junction, with the coupling to the external source containing both resistive and inductive elements. In addition we include a phenomenological coupling to an external heat bath. Our goal is to extend and generalize previous studies of current biased ultra-small junctions. Charging effects, due to the presence of discrete charge carriers in the junction, play a crucial role. In particular, we find an infinite resistance branch in the I-V characteristic for a d.c. bias, and resistive steps in the I-V curve when the external bias contains an additional a.c. component. These effects are reminiscent of the Coulomb blockade and the inverse Shapiro steps, respectively, predicted earlier in the context of current biased circuits. As a response to an a.c. voltage bias we also predict spikes of the voltage across the junction and a noisy background, when this voltage is plotted as a function of either the external d.c. biasing voltage or the external frequency. Our analysis shows that various circuitry components may qualitatively affect the response of the junction to an external bias. DOE

N90-21654# Melbourne Univ., Parkville (Australia). School of Physics.
DEFORMATION AND MICROSTRUCTURE OF RUTILE
M. G. Blanchin, L. A. Bursill, and C. Lafage (Lyon-1 Univ., France) 1989 74 p Submitted for publication
(DE90-614113; UM-P-89/36) Avail: NTIS (US Sales Only) HC A04/MF A01

Studies of the mechanical properties of rutiles are described, in particular the behavior of the elastic limit under compression with respect to variations in temperature (pure rutile), intrinsic non-stoichiometry (pure rutile reduced under low oxygen pressure) and extrinsic non-stoichiometry (rutile doped with chromia and alumina). A wide range of values is obtained, which may be understood in terms of the interaction of dislocations belonging to the slip systems (101) (101) and (110) (001) with impurities, non-stoichiometric small and extended defects and precipitates. Transmission electron microscopy at medium resolution as well as high resolution electron microscopy were used to relate mechanical behavior with microstructure. DOE

N90-21655# California Univ., Berkeley. Lawrence Berkeley Lab. Materials and Chemical Sciences Div.
ANISOTROPY OF GRAIN GROWTH IN ALUMINA
Juergen Roedel and Andreas M. Glaeser Sep. 1989 40 p Presented at the 91st Annual Meeting of the American Ceramic Society, Indianapolis, IN, 23-27 Apr. 1989 Prepared in cooperation with California Univ., Berkeley
(Contract DE-AC03-76SF-00098)
(DE90-009045; LBL-27360; CONF-890421-12) Avail: NTIS HC A03/MF A01

Grain growth in theoretically dense undoped and MgO-doped polycrystalline alumina was studied, and average grain boundary migration rates were compared to those of a-plane and c-plane sapphire during migration into the same undoped and MgO-doped materials. The results are discussed in terms of a grain size dependent grain boundary mobility, grain boundary energy product, M(sub b)(gamma)(sub b). The grain size dependencies of the M(sub b)(gamma)(sub b) products for seed and matrix grains differ. Seed orientation appears to affect the nature of solute-boundary interactions. The importance of grain boundary structure on migration characteristics is also indicated by a demonstration of twin formation enhanced grain growth. DOE

N90-21656# California Univ., Berkeley. Lawrence Berkeley Lab. Materials and Chemical Sciences Div.
HIGH VOLTAGE/HIGH RESOLUTION STUDIES OF METAL AND SEMICONDUCTOR INTERFACES
K. H. Westmacott and U. Dahmen Nov. 1989 10 p Presented at the Symposium on Electron Microscopy in Plasticity, Holzhau, German Democratic Republic, 8-13 Oct. 1989
(Contract DE-AC03-76SF-00098)
(DE90-009065; LBL-26274; CONF-8910380-1) Avail: NTIS HC A02/MF A01

The application of high resolution transmission electron microscopy to the study of homo- or hetero-phase interface structures requires specimens that meet stringent criteria. In some systems the necessary geometric imaging conditions are established naturally, thus greatly simplifying the analysis. This is illustrated for a diamond-hexagonal/diamond-cubic interface in deformed silicon, a Sigma 99 tilt boundary in a pure aluminum bicrystal, and a germanium precipitate in an aluminum matrix. DOE

N90-21657# California Univ., Berkeley. Lawrence Berkeley Lab. National Center for Electron Microscopy.
SIMULATED IMAGE MAPS FOR USE IN EXPERIMENTAL HIGH-RESOLUTION ELECTRON MICROSCOPY
M. A. OKeefe, U. Dahmen, and C. J. D. Hetherington Dec. 1989 6 p Presented at the Materials Research Society Fall Meeting, Boston, MA, 27 Nov. - 2 Dec. 1989
(Contract DE-AC03-76SF-00098)
(DE90-009176; LBL-27503; CONF-891119-114) Avail: NTIS HC A02/MF A01

A map of all possible high-resolution images may be simulated for a crystalline specimen in a chosen orientation for any particular transmission electron microscope. These maps are useful during experimental high-resolution electron microscopy and make it possible to locate optimum imaging conditions even for foil thicknesses beyond the weak-phase object limit. Although defects such as grain boundaries are not generally periodic, image maps of perfect crystals can be used to optimize defect contrast during operation of the microscope by reference to the image of the perfect crystal neighboring the defect. DOE

N90-21658# Lawrence Livermore National Lab., CA.
THERMOGRAVIMETRIC ANALYSIS OF Nd(2-x)Ce(x)CuO(4-DELTA)
J. L. Peng, R. L. Greene, P. Klavins, R. N. Shelton (California Univ., Davis.), and H. B. Radousky Feb. 1990 5 p Presented at the Materials Research Society Fall Meeting, Boston, MA, 27 Nov. - 2 Dec. 1989
(Contract W-7405-eng-48)
(DE90-009184; UCRL-JC-103340; CONF-891119-116) Avail: NTIS HC A01/MF A01

Samples of Nd(sub 2-x) Ca(sub x)CuO(sub 4-(delta)) were prepared by the usual solid state reaction technique and characterized by x ray diffraction, resistivity, and magnetization measurements. The thermogravimetric analysis (TGA) was used to observe the sample weight change as a function of temperature in a variety of gas atmospheres. The oxygen content was determined by a TGA technique incorporating the results of x ray diffraction. We confirmed that for x = 0.15, a small value of (delta) (of order 0.05) is vital to superconductivity. DOE

N90-21659# Lawrence Livermore National Lab., CA.
SHOCK COMPRESSION OF SOLIDS: A TUTORIAL
W. J. Nellis 1990 72 p Presented at the American Physical Society Meeting, Anaheim, CA, 11-16 Mar. 1990
(Contract W-7405-eng-48)
(DE90-009185; UCRL-JC-103276; CONF-900384-1) Avail: NTIS HC A04/MF A01

The focus of this tutorial will be on fundamentals of shock-

compression physics, the states achieved, and laboratory experiments with research-size specimens. Shock pressures can be applied to assemblies of virtually arbitrary size using explosive systems. Hence, results of laboratory shock-compression research can be scaled to industrial quantities as well. DOE

N90-21660# Midwest Research Inst., Golden, CO.
CHARACTERIZATION AND COMPARISON OF OPTICALLY TRANSPARENT CONDUCTING FILMS
R. G. Gordon (Harvard Univ., Cambridge, MA.) Mar. 1990 54 p
(Contracts DE-AC02-83CH-10093; SERI-XX-8-18148-1; NSF DMR-88-02306)
(DE90-000319; SERI/TP-211-3666) Avail: NTIS HC A04/MF A01

Textured tin oxide films with high light-trapping efficiency, high electrical conductivity and high transparency were successfully grown at high rates by chemical vapor deposition (CVD). This process has achieved large-scale commercial production of substrates for amorphous silicon solar cells. Highly transparent and highly conductive films of fluorine-doped zinc oxide were formed by a new CVD process. Increases in the texture (light-trapping) and growth rate are needed to make this a practical process for making substrates for solar cells. Decreases in deposition temperature are needed to make successful back contacts. A hybrid transparent conducting oxide (TCO) consisting of textured tin oxide covered with a thin, smooth fluorine-doped zinc oxide layer combines the best features of these two materials. It shows efficient light-trapping because of the textured tin oxide, combined with the good resistance of zinc oxide to the hydrogen plasma used to deposit the amorphous silicon. Highly conductive and reflective titanium nitride was deposited under conditions mild enough to form back contacts on amorphous silicon solar cells. Actual cells will be coated and tested in the next contract period. Further optimization of the deposition conditions for these materials should be carried out in collaboration with solar cell manufacturers. DOE

N90-21661# Lawrence Livermore National Lab., CA. Thermal-Fluids Group.
PROGRAM CICC: FLOW AND HEAT TRANSFER IN CABLE IN CONDUIT CONDUCTORS, USER'S MANUAL
Robert L. Wong 14 Feb. 1990 64 p
(Contract W-7405-eng-48)
(DE90-007924; UCID-21941) Avail: NTIS HC A04/MF A01

This report is the user's manual for program CICC and it's graphics postprocessor, CICCP. CICC was written for use in the thermofluids design of the cryogenic superconducting magnets which utilize helium-cooled, cable-in-conduit conductors (CICC). The program models the transient thermodynamic and fluid-dynamic system response to the occurrence of normal-zone heating in the superconductor. References 1 and 2 have previously been written describing the equations used in the program, the solution method, and the experimental verification. DOE

N90-21662# Lawrence Livermore National Lab., CA. Chemistry and Materials Science.
MICROSTRUCTURE OF Au/Nb MULTILAYERS
Alan F. Jankowski and P. L. Perry Feb. 1990 16 p Presented at the 8th International Triennial Conference on Thin Films and the 17th International Conference on Metallurgical Coatings, San Diego, CA, 1-6 Apr. 1990
(Contract W-7405-eng-48)
(DE90-008722; UCRL-102016; CONF-900419-3) Avail: NTIS HC A03/MF A01

Au/Nb multilayers are prepared using magnetron sputter deposition. The close-packed orientation of the films are revealed using x ray diffraction. Although in bulk form (111) Au and (110) Nb have a near zero lattice misfit, the average lattice spacing of the multilayer is found to vary as a function of the direction of the composition modulation. Similar lattice distortions of the multilayer structure are known for fcc/fcc metallic superlattices, as Au/Ni. Lattice imaging of the Au/Nb multilayers, in cross-section, provides a direct means to complete an initial characterization of the atomic rearrangements in the modulation direction. DOE

N90-21663# Lawrence Livermore National Lab., CA.
NEW SURFACE ATOMIC STRUCTURES FOR COLUMN 5 OVERLAYERS ON THE (110) SURFACES OF 3-5 COMPOUND SEMICONDUCTORS
John P. LaFemina, C. B. Duke (Xerox Webster Research Center, NY.), and Christian Mailihot Feb. 1990 34 p Presented at the Physics and Chemistry of Semiconductor Interfaces, Clearwater Beach, FL, 31 Jan. - 2 Feb. 1990
(Contracts W-7405-eng-48; DE-AC06-76RL-01830)
(DE90-009003; UCRL-JC-103212; CONF-900123-1) Avail: NTIS HC A03/MF A01

Two new minimum-energy surface structures were identified for p(1 x 1) overlayers of Sb on the (110) surface of III-V compound semiconductors using a tight-binding total-energy formalism previously developed for these systems. The first is the commensurate chain structure in which Sb zig-zag chains are commensurate with, and on top of, the Ga-As unreconstructed surface zig-zag chains. This structure differs from the previously found epitaxial-chain structure by virtue of the registry of the Sb chains on top of rather than in between the substrate Ga-As chains. Like the epitaxial chain structure, it is compatible with both scanning tunneling microscopy (STM) and photoemission data. The second is an overlapping chain structure in which the Sb chains are 180 deg out-of-phase with, and on top of, the Ga-As substrate chains. This structure is, however, incompatible with both low energy electron diffraction and STM data for GaAs(110)-p(1 x 1)-Sb although it may be a possible structure for other systems. Computations for GaP(110)-p(1 x 1)-Sb and InSb(110)- p(1 x 1)-Sb reveal that the energy difference between the commensurate chain and traditional epitaxial structure is approximately constant over this range of overlayer/substrate lattice mismatch. DOE

N90-21664# Argonne National Lab., IL. Materials and Components Technology Div.
DETERMINATION OF INTERNAL STRAINS IN HIGH-TEMPERATURE SUPERCONDUCTOR COMPOSITES BY INTENSE PULSED NEUTRON SOURCE
J. P. Singh, D. S. Kupperman, S. Majumdar, and R. L. Hitterman Feb. 1990 10 p Presented at the International Conference on Micromechanics of Failure of Quasi-Brittle Materials, Albuquerque, NM, 7-8 Jun. 1990
(Contract W-31-109-eng-38)
(DE90-007799; CONF-9006122-4) Avail: NTIS HC A02/MF A01

Results are presented for the effect of silver (Ag) addition on microstructure, mechanical properties, and internal strains in YBa2Cu3O(7-delta)-Ag superconducting composites. A 2.2 fold increase in strength was obtained as a result of approx. 20 vol percent Ag addition to YBa2Cu3O(7-delta) without any adverse effects on superconducting properties. The increase in strength is believed to be due to an increase in density as well as due to the development of internal compressive strains in the YBa2Cu3O(7-delta) matrix as a result of Ag addition. The internal strains developed due to thermal expansion mismatch between YBa2Cu3O(7-delta) and Ag were measured by neutron diffraction using Intense Pulsed Neutron Source at Argonne National Laboratory. Creep may play an important role in relaxing the residual strains in composite constituents. DOE

N90-21665# Oak Ridge National Lab., TN. Mathematical Sciences Section.
MODELING HIGH-TEMPERATURE SUPERCONDUCTORS AND METALLIC ALLOYS ON THE INTEL IPSC/860
G. A. Geist, B. W. Peyton, W. A. Shelton, and G. M. Stocks 1990 10 p Presented at the 5th Distributed Memory Computing Conference, Charleston, SC, 9-12 Apr. 1990
(Contract DE-AC05-84OR-21400)
(DE90-009402; CONF-9004159-2) Avail: NTIS HC A02/MF A01

Oak Ridge National Laboratory has embarked on several computational Grand Challenges, which require the close cooperation of physicists, mathematicians, and computer scientists. One of these projects is the determination of the material properties of alloys from first principles and, in particular, the electronic structure of high-temperature superconductors. While the present focus of the project is on superconductivity, the approach is general enough to permit study of other properties of metallic alloys such as strength and magnetic properties. This paper describes the progress to date on this project. We include a description of a self-consistent KKR-CPA method, parallelization of the model, and the incorporation of a dynamic load balancing scheme into the algorithm. We also describe the development and performance of a consolidated KKR-CPA code capable of running on CRAYs, workstations, and several parallel computers without source code modification. Performance of this code on the Intel iPSC/860 is also compared to a CRAY 2, CRAY YMP, and several workstations. Finally, some density of state calculations of two perovskite superconductors are given. DOE

N90-21666# Lawrence Livermore National Lab., CA.
PROGRESS IN THE MATERIAL DEVELOPMENT OF LiCaAlF(6):Cr(3+) LASER CRYSTALS
M. D. Shinn, L. L. Chase, J. A. Caird, S. A. Payne, L. J. Atherton, and W. L. Kway Mar. 1990 11 p Presented at the OSA Topical Meeting on Advanced Solid-State Lasers, Salt Lake City, UT, 5-7 Mar. 1990
(Contract W-7405-eng-48)
(DE90-009542; UCRL-102248; CONF-900373-1) Avail: NTIS HC A03/MF A01

High Cr(3+) doping levels, up to 8 mole percent, and low losses were obtained with the tunable solid-state laser material LiCaAlF(6):Cr(3+) (Cr:LiCAF). Measurements and calculations show that high pumping and extraction efficiencies are possible with the improved material. DOE

77 THERMODYNAMICS AND STATISTICAL PHYSICS

Includes quantum mechanics; theoretical physics; and Bose and Fermi statistics.

For related information see also *25 Inorganic and Physical Chemistry* and *34 Fluid Mechanics and Heat Transfer.*

N90-21667# Los Alamos National Lab., NM.
NONOPTIMAL ENTROPY GENERATION BY HEAT TRANSFER IN CRYOGENIC DOMAIN
Dusan P. Sekulic (Novi Sad Univ., Yugoslavia) and Frederick J. Edeskuty 1990 9 p Presented at the Florence World Energy Research Symposium, Florence, Italy, 28 May - 1 Jun. 1990
(Contract W-7405-eng-36; JF-DOE-818)
(DE90-007544; LA-UR-90-590; CONF-900508-1) Avail: NTIS HC A02/MF A01

The entropy generation caused by heat conduction has been analyzed for physical situations related to cryostats. The situations under consideration are characterized by heat conduction with presence or absence of heat generation and/or heat convection. The existing information regarding the thermodynamic optimal design is compared with more realistic nonoptimal situations. The difference between the optimal and nonoptimal entropy generation has been analyzed from the quantitative point of view. It has been shown that the nonoptimal temperature distribution through a cryostat component might be a realistic option from the thermal design point of view. DOE

N90-21668# Joint Inst. for Nuclear Research, Dubna (USSR). Lab. of High Energy.
CHARACTERISTICS CONSEQUENCES OF SPACE-TIME COORDINATE RELATIVIZATION
V. N. Streltsov 1988 11 p In RUSSIAN; ENGLISH summary
(DE90-615201; JINR-R-2-88-748) Avail: NTIS (US Sales Only) HC A03/MF A01

The possibility is discussed of using right and left Feynman clocks (made on the base of parity nonconservation) for practical realization of anisotropic time space. Characteristic properties of anisotropic (noncommutative) planimetry are considered. The difference between rotation in the Euclidean plane and rotation in the Minkowski plane is emphasized. It is noted that from the Minkowski space symmetry relatively inversions and reinterpretation principle the existence of antiparticles (as objects with negative energy moving back in time) follows. Attention is paid to the interconnection between space and time inversions. A possible nonconservation of leptonic charge in K(sub l(sub 3))(sup 0) decays is indicated as a consequence of the T-invariance violation. DOE

N90-21669# Joint Inst. for Nuclear Research, Dubna (USSR). Lab. of Theoretical Physics.
THE GENERALLY COVARIANT REPRESENTATION OF ENERGY-MOMENTUM PSEUDOTENSOR OF GRAVITATIONAL FIELD
M. N. Tentyukov 1988 6 p In RUSSIAN; ENGLISH summary
(DE90-615203; JINR-R-2-88-838) Avail: NTIS (US Sales Only) HC A02/MF A01

The number of known energy momentum pseudotensors of the gravitational field are considered. On the manifold with the background affine connection these pseudotensors are the tensor functionals of the background connection. Some properties of these functionals are analyzed. DOE

N90-21670# International Centre for Theoretical Physics, Trieste (Italy).
LOCAL SUPERSYMMETRY IN NON-RELATIVISTIC SYSTEMS
L. F. Urrutia and J. Zanelli (Chile Univ., Santiago.) Oct. 1989 16 p Submitted for publication Sponsored in part by Centro de Estudios Cientificos, de Santiago, Chile; FONDECYT, Chile; and CONACYT, Mexico
(DE90-612751; IC-89/295) Avail: NTIS (US Sales Only) HC A03/MF A01

Classical and quantum non-relativistic interacting systems invariant under local supersymmetry are constructed by the method of taking square roots of the bosonic constraints which generate timelike reparameterization, leaving the action unchanged. In particular, the square root of the Schroedinger constraint is shown to be the non-relativistic limit of the Dirac constraint. Contact is made with the standard models of Supersymmetric Quantum Mechanics through the reformulation of the locally invariant systems in terms of their true degrees of freedom. Contrary to the field theory case, it is shown that the locally invariant systems are completely equivalent to the corresponding globally invariant ones, the latter being the Heisenberg picture description of the former, with respect to some fermionic time. DOE

N90-21671# International Centre for Theoretical Physics, Trieste (Italy).
QUANTIZATION OF THE N = 2m SIMPLE SUPERGRAVITY IN d = 2 + 1
Omer F. Dayi Sep. 1989 12 p Submitted for publication
(DE90-612765; IC-89/286) Avail: NTIS (US Sales Only) HC A03/MF A01

In d=2+1 simple supergravity is a trivial theory and it has a Chern-Simons interpretation. Thus the overall sign of each one of the fermionic terms in the action for N greater than 1 is arbitrary. By making use of these facts it is shown that for the N=2m simple supergravity in d=2+1 there exists a real polarization and an explicit construction of the physical Hilbert space is possible. DOE

N90-21672# International Centre for Theoretical Physics, Trieste (Italy).
CONSERVED CONFORMAL CURRENTS IN CURVED SPACE-TIME
A. L. Marrakchi (Mohammed V Univ., Rabat, Morocco) Oct. 1989 14 p Submitted for publication

(DE90-612766; IC-89/328) Avail: NTIS (US Sales Only) HC A03/MF A01

Conformal transformations in curved space-time are considered. Their conserved currents are calculated. It is shown that they reduce at flat limit to the well known conserved conformal currents in flat space-time. The conformal equivalence principle is then elaborated. DOE

N90-21673# Pontificia Univ. Catolica, Rio de Janeiro (Brazil). Dept. de Fisica.

THE GRAVITATIONAL LENS EFFECT AND ITS OPTICAL EQUIVALENTS M.S. Thesis

Luciane RangeldeFreitas 1987 68 p In PORTUGUESE; ENGLISH summary

(DE90-612767; INIS-BR-1780) Avail: NTIS (US Sales Only) HC A04/MF A01

The evolution of the use of the so called gravitational lens effect from a simple observational test of the General Relativity theory to an instrument to measure cosmological parameters is presented. A detailed analysis of how a gravitational lens deflects light without forming images is shown for the case of the deflector with spherical symmetry. In addition, the exact optical equivalent of a cylindrical gravitational lens, which forms true images, is proposed. Finally, the problem of the formation of multiple images and the related astronomical observations is discussed. DOE

N90-21674# International Centre for Theoretical Physics, Trieste (Italy).

STRING DYNAMICS IN CURVED SPACE-TIME REVISITED

A. L. Marrakchi and L. P. Singh (Utkal Univ., Bhubaneswar, India) Sep. 1989 8 p Submitted for publication

(DE90-612796; IC-89/298) Avail: NTIS (US Sales Only) HC A02/MF A01

The equations of motion of the general background of curved space-time, Einstein's equations, are derived simply by demanding the renormalized energy-momentum tensor of a bosonic string propagating in this background to be traceless. The energy-momentum tensor of such a string is then separable into a holomorphic and an antiholomorphic parts as a consequence of the conformal invariance of the theory regained at the quantum level. DOE

N90-21675# International Centre for Theoretical Physics, Trieste (Italy).

THERMAL DECAY OF AN INITIALLY HOT ISOTHERMAL WATER BODY WITH APPLICATION TO THERMAL ENERGY STORAGE

S. K. Adjepong and A. R. Bestman Nov. 1989 18 p Submitted for publication

(DE90-614742; IC-89/348) Avail: NTIS (US Sales Only) HC A03/MF A01

The thermal decay of an initially hot isothermal water body contained in a tank has been studied. Analytical solutions (including a group-theoretic solution) have been obtained for the one-dimensional heat conduction equation with heat loss from the sides of the tank. The convective heat transfer coefficient is assumed to vary with space and time rather than constantly over the surface of the tank. A very good agreement is obtained between the group-theoretic solution and a numerical solution using the Crank-Nicholson finite difference scheme. The analytical results have been discussed in terms of underlying physical mechanisms. DOE

N90-21676# Sandia National Labs., Albuquerque, NM. Computational Mechanics Div.

THE CHEMKIN THERMODYNAMIC DATA BASE

Robert J. Kee, Fran M. Rupley, and James A. Miller Mar. 1990 155 p

(Contract DE-AC04-76DR-00789)

(DE90-007953; SAND-87-8215B) Avail: NTIS HC A08/MF A01

The Chemkin general-purpose chemical kinetics package uses a data base that contains polynomial fits to specific heats, standard state enthalpies, and standard state entropies. The fourteen coefficient fits are in the same form as used in the NASA Complex Chemical Equilibrium Program (Gordon and McBride, 1971). This report represents a compilation of the data that is currently in use at Sandia National Laboratories. DOE

N90-21677# Washington Univ., Saint Louis, MO. Dept. of Physics.

STUDIES IN QUANTUM FIELD THEORY Progress Report, 1 Apr. 1989 - 31 Mar. 1990

1990 15 p

(Contract DE-AC02-78ER-04915)

(DE90-008731; DOE/ER-04915/4) Avail: NTIS HC A03/MF A01

During the period 1 April to 31 March 1990 the theoretical physics group supported by Department of Energy Contract No. AC02-78ER04915.A015 and consisting of Professors Bender and Shrauner, Associate Professor Papanicolaou, Assistant Professor Ogilvie, and Senior Research Associate Visser has made progress in many areas of theoretical and mathematical physics. Professors Bender and Shrauner, Associate Professor Papanicolaou, Assistant Professor Ogilvie, and Research Associate Visser are currently conducting research in many areas of high energy theoretical and mathematical physics. These areas include: strong-coupling approximation; classical solutions of non-Abelian gauge theories; mean-field approximation in quantum field theory; path integral and coherent state representations in quantum field theory; lattice gauge calculations; the nature of perturbation theory in large order; quark condensation in QCD; chiral symmetry breaking; the 1/N expansion in quantum field theory; effective potential and action in quantum field theories, including QCD; studies of the early universe and inflation, and quantum gravity. DOE

N90-21678# Institute for Advanced Study, Princeton, NJ. School of Natural Sciences.

SOME GLOBAL PROBLEMS IN GAUGE THEORIES (VARIATIONS ON A THEME OF AHARONOV AND BOHM)

Frank Wilczek Dec. 1989 23 p Presented at the Conference on Thirty Years of the Aharonov-Bohm Effect, Columbia, SC, 1989

(Contract DE-FG02-90ER-40542)

(DE90-009034; CONF-890001-1; IASSNS-HEP-90/19) Avail: NTIS HC A03/MF A01

Several situations are discussed, in which the sort of global considerations made famous by Aharonov and Bohm in their discussion of the interaction of charged particles with magnetic flux tubes have important physical implications. It is argued that discrete gauge symmetries in the continuum make sense, and manifest themselves most clearly in Aharonov-Bohm type scattering of charged particles off string singularities. The existence of such discrete symmetries has important implications for the quantum mechanics of topologically non-trivial space-times in general and black holes in particular. It is argued that in the non-abelian case essentially new features arise, most notably that the symmetry group of the homogeneous ground state generally ceases to be globally defined in the presence of a string. When continuous rather than discrete symmetries are involved, a variety of fascinating and as yet poorly understood dynamical effects occur. Perhaps the most striking is a new form of string superconductivity, that exists for purely topological reasons, and is not well modeled by regarding the string as a superconducting wire. DOE

N90-21679# Institute for Advanced Study, Princeton, NJ.

THE 2 + 1 DIMENSIONAL QUANTUM GRAVITY AND THE BRAID GROUP

Steven Carlip Oct. 1989 11 p Presented at the Workshop on Physics, Braids and Links, Banff, Alberta, Aug. 1989

(Contract DE-AC02-76ER-02220)

(DE90-009036; CONF-8908219-1; IASSNS-HEP-89/51) Avail: NTIS HC A03/MF A01

The following topics on quantum gravity are discussed: 2 + 1 gravity as a Chern-Simons theory; quantization; dynamics; the Braid group; and the emergence of space and time. DOE

80 SOCIAL SCIENCES (GENERAL)

Includes educational matters.

No abstracts in this category.

81 ADMINISTRATION AND MANAGEMENT

Includes management planning and research.

N90-21680*# National Aeronautics and Space Administration, Washington, DC.
SMALL BUSINESS INNOVATION RESEARCH. ABSTRACTS OF 1988 PHASE 1 AWARDS
Mar. 1990 90 p
(NASA-TM-102991; NAS 1.15:102991; SBIR-88-2) Avail: NTIS HC A05/MF A01 CSCL 05A

Non-proprietary proposal abstracts of Phase 1 Small Business Innovation Research (SBIR) projects supported by NASA are presented. Projects in the fields of aeronautical propulsion, aerodynamics, acoustics, aircraft systems, materials and structures, teleoperators and robots, computer sciences, information systems, data processing, spacecraft propulsion, bioastronautics, satellite communication, and space processing are covered. R.J.F.

N90-21681*# National Aeronautics and Space Administration, Washington, DC.
SMALL BUSINESS INNOVATION RESEARCH. ABSTRACTS OF COMPLETED 1987 PHASE 1 PROJECTS
Dec. 1989 95 p
(NASA-TM-101797; NAS 1.15:101797; SBIR-87-2) Avail: NTIS HC A05/MF A01 CSCL 05A

Non-proprietary summaries of Phase 1 Small Business Innovation Research (SBIR) projects supported by NASA in the 1987 program year are given. Work in the areas of aeronautical propulsion, aerodynamics, acoustics, aircraft systems, materials and structures, teleoperators and robotics, computer sciences, information systems, spacecraft systems, spacecraft power supplies, spacecraft propulsion, bioastronautics, satellite communication, and space processing are covered. R.J.F.

N90-20930*# Massachusetts Inst. of Tech., Cambridge. Flight Transportation Lab.
TIME AND TRUTH IN PLANS
Lyman R. Hazelton, Jr. *In* NASA, Langley Research Center, Joint University Program for Air Transportation Research, 1988-1989 Mar. 1990 p 77-91 (For primary document see N90-20921 14-01)
(Grant NGL-22-009-640)
Avail: NTIS HC A10/MF A02 CSCL 01C

82 DOCUMENTATION AND INFORMATION SCIENCE

Includes information management; information storage and retrieval technology; technical writing; graphic arts; and micrography.

For computer documentation see *61 Computer Programming and Software.*

N90-21682# Vrije Univ., Amsterdam (Netherlands). Faculteit Wiskunde en Informatica.
A FORMAL APPROACH TO USER MODELS IN DATA RETRIEVAL
Andre J. Kok Apr. 1989 18 p
(Grant NWO-612-319-008)
(PB90-124728; IR-186) Avail: NTIS HC A03/MF A01 CSCL 05B

A formal foundation for modelling the interests of users interacting with a data base is given. This is done in three steps: First a logic is defined for describing interests of a user in the availability of certain data. Then a special modal operator, analogous to the possibility operator of the standard Kripke possible-world semantics, is defined for expressing the predictive qualities of a user model. It will be shown that modelling predictions of possible interests of a user can best be formalized by means of a KT system. Finally, a notational convention for describing the results of user modelling methods is introduced. Author

N90-21683# National Library of Medicine, Bethesda, MD.
MEDICAL SUBJECT HEADINGS: ANNOTATED ALPHABETIC LIST, 1990
Jul. 1989 1085 p
(PB90-100009; NLM/MED-90/01; ISSN-0147-5711) Avail: NTIS HC A99/MF E09 CSCL 05B

An alphabetic list of all subject descriptors used by indexers and catalogers at the National Library of Medicine is presented. It includes: subject headings, cross references, geographic headings, non-MeSH terms, check tags, three numbers, notes for indexers, catalogers, and online searchers. Author

N90-21684# National Library of Medicine, Bethesda, MD.
PERMUTED MEDICAL SUBJECT HEADINGS, 1990
Jul. 1989 473 p
(PB90-100025; NLM/MED-90/03; ISSN-1045-2338) Avail: NTIS HC A20/MF A03 CSCL 05B

Permuted Medical Subject Headings, 1990 is a computer-generated display of all terms, i.e., descriptors and cross references, in the alphabetic list of the National Library of Medicine's Medical Subject Headings (MeSH) for 1990, as well as all citation type, check tag, and geographic descriptors in the Annotated Alphabetic Mesh, 1990. The Permuted MeSH takes each significant word that appears in each MeSH term and then lists all the MeSH terms in which that word appears. Author

N90-21685# Oak Ridge Gaseous Diffusion Plant, TN.
ARMY WAR COLLEGE FINAL PROTOTYPE OPTICAL DISK SYSTEM TESTING AND EVALUATION REPORT
Al J. Klein and Stephen J. Gillespie Mar. 1990 59 p
(Contract DE-AC05-84OR-21400)
(DE90-008852; K/DSRD-276) Avail: NTIS HC A04/MF A01

This report documents the continuation of the PC-based optical disk retrieval-storage system testing and evaluation activities that Data Systems Research and Development (DSRD) staff have performed over the last year for the Army War College (AWC), Carlisle, Pennsylvania. A previous report (see Army War College Optical Disk System Test and Evaluation Report, K/DSRD-74, April 1989) detailed the performance testing results of the initial two prototype optical disk systems evaluated by DSRD. Based on the results of this prototype system testing and evaluation, the AWC selected the SAIC/LaserData system for further development and testing. This report describes the development activities that were performed to enhance the SAIC/LaserData system and details the tests and evaluations that were performed under an environment similar to that which would be encountered at the sponsor's site. The prototype optical disk system that was tested and evaluated consists of two stations: a master scanning station for scanning, indexing, and storing of documents onto master and distribution disks and retrieval station for retrieving and displaying information contained on the distribution disks. DOE

N90-21686# California Univ., Berkeley. Lawrence Berkeley Lab.
STORM: A STATISTICAL OBJECT REPRESENTATION MODEL
Maurizio Rafanelli (Consiglio Nazionale delle Ricerche, Rome, Italy) and Arie Shoshani Nov. 1989 18 p
(Contract DE-AC03-76SF-00098)
(DE90-009048; LBL-28103) Avail: NTIS HC A03/MF A01

The structure and semantic properties of the entities stored in

statistical databases are explored. Such entities are called statistical objects (SOs) and a new statistical object representation model, based on a graph representation is proposed. A number of SO representational problems were identified in current models and a methodology was proposed for their solution. DOE

N90-21687# Sandia National Labs., Albuquerque, NM. Product Data Systems Management and Development Div.
THE ULTIMATE CASE TOOL
John K. Sharp 1990 3 p Presented at the Conference on Lasers and Electro-Optics, Anaheim, CA, 21-25 May 1990
(Contract DE-AC04-76DP-00078)
(DE90-009351; SAND-90-0871C; CONF-900530-3) Avail: NTIS HC A01/MF A01

The theory and practice of information engineering is being actively developed at Sandia National Laboratories. The main output of Sandia is information. Information is created, analyzed, and distributed. It is the life blood of the design laboratory. The proper management of information will have a large, positive impact on staff productivity. In order to achieve the potential benefits of shared information a commonly understood approach is needed, and the approach must be implemented in a CASE (Computer-Aided Software Engineering) tool that spans the entire life cycle of information. The commonly understood approach used at Sandia is natural language. More specifically, it is a structured subset of English. Users and system developers communicate requirements and commitments that they both understand. The approach is based upon NIAM (Nijssen's Information Analysis Methodology). In the last three years four NIAM training classes have been given at Sandia. The classes were all at the introductory level, with the latest class last October having an additional seminar highlighting successful projects. The continued growth in applications using NIAM requires an advanced class. The class will develop an information model for the Ultimate CASE Tool. The requirements that were established for the Ultimate CASE Tool and the initial models are presented. DOE

83 ECONOMICS AND COST ANALYSIS

Includes cost effectiveness studies.

No abstracts in this category.

84 LAW, POLITICAL SCIENCE AND SPACE POLICY

Includes NASA appropriation hearings; aviation law; space law and policy; international law; international cooperation; and patent policy.

No abstracts in this category.

85 URBAN TECHNOLOGY AND TRANSPORTATION

Includes applications of space technology to urban problems; technology transfer; technology assessment; and surface and mass transportation.

For related information see also *03 Air Transportation and Safety, 16 Space Transportation,* and *44 Energy Production and Conversion.*

N90-21688# Oak Ridge Y-12 Plant, TN. Dept. of Fabrication Systems.
ADVANCED MANUFACTURING TECHNOLOGY: A DEPARTMENT OF ENERGY TECHNOLOGY TRANSFER INITIATIVE
R. S. Steele, Jr. and W. E. Barkman 1 Feb. 1990 8 p Presented at the 2nd International Conference on Computer Integrated Manufacturing, Troy, NY, 21-23 May 1990
(Contract DE-AC05-84OR-21400)
(DE90-008601; Y/DX-916; CONF-9005134-1) Avail: NTIS HC A02/MF A01

This paper describes a new initiative called the Advanced Manufacturing Technology (AMT) Program that is managed for the U.S. Department of Energy (DOE) by Martin Marietta Energy Systems in Oak Ridge, Tennessee. The AMT Program seeks to assist the U.S. manufacturing community regain some of the market share that it has lost to competiting companies in both Europe and the Far East. One key element to this program is the establishment of teaching and development facilities called manufacturing technology centers (MTCs) which will showcase unclassified DOE manufacturing technologies. This paper describes some of the precision flexible manufacturing system (PFMS) technology that is available through the Oak Ridge Y-12 Plant. This technology will be highlighted in the first of the MTCs that is being established. DOE

N90-21345*# National Aeronautics and Space Administration. Ames Research Center, Moffett Field, CA.
SIRTF IN HIGH EARTH ORBIT
Michael W. Werner, Walter F. Brooks, Larry A. Manning, and Peter Eisenhardt (California Univ., Berkeley.) *In its* Proceedings of the Third Infrared Detector Technology Workshop Oct. 1989 p 387-400 (For primary document see N90-21313 14-35)
Avail: NTIS HC A20/MF A03 CSCL 03A

88 SPACE SCIENCES (GENERAL)

No abstracts in this category.

89 ASTRONOMY

Includes radio, gamma-ray, and infrared astronomy, and astrometry.

N90-21689# Instituto de Pesquisas Espaciais, Sao Jose dos Campos (Brazil).
NEW WATER VAPOR MASERS IN THE SOUTHERN HEMISPHERE
E. ScaliseJunior and J. L. MonteirodoVale Dec. 1988 13 p Presented at the 6th Japan-Brazil Symposium on Science and Technology, Sao Jose dos Campos, Brazil, 10-12 Aug. 1988
(Contract FINEP-537-CT)
(INPE-4844-PRE/1473) Avail: NTIS HC A03/MF A01

A search for water vapor masers was conducted in the direction of selected strong point sources detected by the Infrared Astronomical Satellite - IRAS. Three hundred twenty-five points were observed and 18 water maser sources were detected. The

detection rate was 5.6 percent. The new sources are discussed and compared with the previously known galactic masers.
Author

N90-21690 Leicester Univ. (England).
DESIGN AND OPTIMISATION OF THIN FOIL X RAY TELESCOPES Ph.D. Thesis
Lalit Jalota 1988 201 p
Avail: Univ. Microfilms Order No. BRD-87322

The use of thin foil conical profile x ray mirrors for high energy, large aperture, and lightweight telescopes is investigated. The telescope performance is studied using analytical solutions and ray tracing simulations. Expressions for the number of mirrors in a module, the collecting area, the efficiency of aperture utilization, and the resolution are calculated for on-axis sources. For off-axis sources, ray tracing is used and expressions to describe the performance are derived empirically. The sensitivity and effect of singly reflected rays on the image are also investigated, and the comparison is made with Wolter(I) profile optics. A technique for the production of super-smooth surfaces using a layer of acrylic lacquer is described. Several materials have been coated using this method to assess their suitability as potential mirror substrates. To quantitatively assess the quality of both substrate and lacquer finishes, a program of x ray scattering measurements has been carried out. Several different types of surfaces have been examined both before and after lacquer to remove surface features of different spatial wavelengths. An epoxy replicated test flat is also examined which provides an interesting comparison with the lacquer coating technique for the production of thin x ray mirrors. As a consequence of the wide range of materials examined it has been possible to compare most of the different techniques for producing thin x ray mirrors. There is no one solution for all applications and thin foil mirrors are indeed a competitive technology. Dissert. Abstr.

N90-21691# Los Alamos National Lab., NM. Theoretical Div.
RECENT ADVANCES IN THE STUDIES OF THE NOVA OUTBURST
Sumner Starrfield 1989 5 p Presented at the 11th North American Workshop on CV's and LMXRE's, Santa Fe, NM, 9-13 Oct. 1989
(Contract W-7405-eng-36)
(DE90-008936; LA-UR-90-874; CONF-8910381-1) Avail: NTIS HC A01/MF A01

This conference marks 13 years since the first North American Cataclysmic Variable workshop (NACVW) was held in 1976 at the University of Illinois. It, therefore, seems appropriate to briefly review the progress that was made in understanding the nova outburst. Recent detailed reviews of both the nova binary systems and their outbursts can be found in the proceedings of the Madrid IAU Symposium No. 122 on the Physics of Classical Novae (Cassatella and Viotti 1990), Gehrz (1988), Shara (1989), Starrfield (1988, 1989), and Bode and Evans (1989). Because of the existence of these reviews, only a few of the developments that have had a major impact on studies of the outburst are described. DOE

N90-21692# Los Alamos National Lab., NM. IGPP and Theoretical Div.
MULTI-WAVELENGTH OBSERVATIONS OF NOVAE IN OUTBURST
Sumner Starrfield 1989 12 p Presented at the IAU Coll. No. 122, on Physics of Classical Novae, Madrid (Spain), 27-30 Jun. 1989
(Contract W-7405-eng-36)
(DE90-008934; LA-UR-90-876; CONF-8906225-5) Avail: NTIS HC A03/MF A01

This review serves as the introduction to the observational studies of novae and a number of results that will be emphasized by other reviewers is mentioned. Therefore, the physical framework is provided for multi-wavelength observations as applied to studies of novae. The outburst were divided into phases based on the physical effects that are occurring at that time. The first phase is the rise to bolometric maximum and occurs on a convective time scale. The second phase is the rise to visual maximum and occurs on the time scale for the envelope to expand to approx. 10(exp 12) cm. The third phase is the time when the nova is emitting at constant bolometric luminosity, but declining optical magnitude, and it lasts until most of the accreted material has been either exhausted or eroded from the surface of the white dwarf. The fourth and final phase is the return to quiescence (turn-off phase) and it occurs at the time that nuclear burning is ending. Each of these phases are discussed in turn. DOE

N90-21693# Los Alamos National Lab., NM.
THE 1989 OUTBURST OF V404 CYGNI: A VERY UNUSUAL X RAY NOVA
R. M. Wagner, Sumner Starrfield, A. Cassatella, R. Gonzalez-Riestra, T. J. Kreidl, S. B. Howell, R. M. Hjellming, X-H. Han, C. Shader, and G. Sonneborn (National Aeronautics and Space Administration. Goddard Space Flight Center, Greenbelt, MD.) et al 1989 6 p Presented at the IAU Coll. No. 122 on Physics of Classical Novae, Madrid (Spain), 27-30 Jun. 1989
(Contract W-7405-eng-36)
(DE90-008935; LA-UR-90-875; CONF-8906225-4) Avail: NTIS HC A02/MF A01

On May 22, 1989, the Japanese Ginga Team discovered a new x ray source that was cataloged as GS 2023+338. This source was subsequently identified as coincident in position with a previously known nova cataloged as V404 Cygni. Its last recorded outburst was in 1938 when it rose to about 12th mag. Spectroscopic data were obtained and confirmed the nature of the outburst. Additional ground based data were obtained by us at CTIO and the VLA. The x ray behavior of this object was reported to be very unusual and it reached a peak of about 17 crab about one week after discovery. Since then it has varied widely in magnitude at all wavelengths at which it has been studied. A brief summary of the observations that were obtained up to the time of the meeting and shortly thereafter is presented. DOE

N90-21694*# Los Alamos National Lab., NM.
MODEL ATMOSPHERES FOR NOVAE DURING THE EARLY STAGES
Rainer Wehrse, P. H. Hauschildt, G. Shaviv (Technion - Israel Inst. of Tech., Haifa.), and Sumner Starrfield 1989 14 p Presented at the Physics of Classical Novae: IAU Colloquium No. 122, Madrid, Spain, 27-30 Jun. 1989
(Contracts NAS5-28731; NAG5-481; W-7405-eng-36; NSF AST-85-16173; NSF AST-88-18215)
(NASA-CR-180498; NAS 1.26:180498; DE90-008938; LA-UR-90-870; CONF-8906225-3) Avail: NTIS HC A03/MF A01 CSCL 03A

Continuum and line blanketing models for the photospheres of novae in the early stages of their outbursts are presented. The expanding envelopes are characterized by a very slow increase of density with decreasing radius which leads to very large geometrical extensions and large temperature differences between the inner and outer parts. The spectra show a large IR excess and a small Balmer jump which may be either in absorption or in emission. For the parameters considered (T sub eff = 10(exp 4), 1.5 x 10(exp 4), 2 x 10(exp 4) K, R = 10(exp 11) cm, solar composition), most lines are in absorption. The effects of both modifications in the temperature structure (e.g., by heating from shock fronts) and changes in the abundances of the heavy elements on the emergent spectra are briefly discussed. DOE

N90-21314*# Arizona Univ., Tucson.
REQUIREMENTS OF IR SPACE ASTRONOMY
Frank J. Low *In* NASA, Ames Research Center, Proceedings of the Third Infrared Detector Technology Workshop Oct. 1989 p 1-4 (For primary document see N90-21313 14-35)
Avail: NTIS HC A20/MF A03 CSCL 03A

N90-21329*# Rochester Univ., NY.
DISCOVERY OF LOW MASS OBJECTS IN TAURUS
W. J. Forrest, Z. Ninkov, J. D. Garnett, M. F. Skrutskie, and M. Shure (Hawaii Univ., Honolulu.) *In* NASA, Ames Research Center,

Proceedings of the Third Infrared Detector Technology Workshop Oct. 1989 p 221-230 (For primary document see N90-21313 14-35)
Avail: NTIS HC A20/MF A03 CSCL 03A

N90-21330*# National Aeronautics and Space Administration. Ames Research Center, Moffett Field, CA.
HIGH RESOLUTION IMAGING OF THE VENUS NIGHT SIDE USING A ROCKWELL 128X128 HgCdTe ARRAY
K.-W. Hodapp, W. Sinton, B. Ragent, and D. Allen (Anglo-Australian Observatory, Epping.) *In its* Proceedings of the Third Infrared Detector Technology Workshop Oct. 1989 p 231-235 (For primary document see N90-21313 14-35)
Avail: NTIS HC A20/MF A03 CSCL 03A

N90-21331*# National Optical Astronomy Lab. Tucson, AZ.
INFRARED GROUND-BASED ASTRONOMY WITH THE HUGHES 256 X 256 PtSi ARRAY
A. Fowler, R. Joyce, I. Gatley, J. Gates, and J. Herring (Hughes Aircraft Co., Carlsbad, CA.) *In* NASA, Ames Research Center, Proceedings of the Third Infrared Detector Technology Workshop Oct. 1989 p 237-246 Sponsored in part by NSF (For primary document see N90-21313 14-35)
Avail: NTIS HC A20/MF A03 CSCL 03A

N90-21332*# California Univ., Berkeley.
STRESSED DETECTOR ARRAYS FOR AIRBORNE ASTRONOMY
G. J. Stacey, J. W. Beeman, E. E. Haller, N. Geis, A. Poglitsch, and M. Rumitz (Max-Planck-Inst. fuer Physik und Astrophysik, Garching, Germany, F.R.) *In* NASA, Ames Research Center, Proceedings of the Third Infrared Detector Technology Workshop Oct. 1989 p 247-258 (For primary document see N90-21313 14-35)
Avail: NTIS HC A20/MF A03 CSCL 03A

N90-21335*# Texas Univ., Austin.
PRELIMINARY RESULTS ON TWO-DIMENSIONAL INTERFEROMETRY OF HL Tau
Eric V. Tollestrup and Paul M. Harvey *In* NASA, Ames Research Center, Proceedings of the Third Infrared Detector Technology Workshop Oct. 1989 p 283-293 (For primary document see N90-21313 14-35)
Avail: NTIS HC A20/MF A03 CSCL 03A

N90-21336*# Honeywell Electro-Optics Center, Lexington, MA.
SHORT WAVELENGTH HgCdTe STARING FOCAL PLANE FOR LOW BACKGROUND ASTRONOMY APPLICATIONS
D. Hall (Hawaii Univ., Honolulu.), J. Stobie, N. Hartle, D. Lacroix, and K. Maschhoff *In* NASA, Ames Research Center, Proceedings of the Third Infrared Detector Technology Workshop Oct. 1989 p 295-310 (For primary document see N90-21313 14-35)
(Contract JPL-958095)
Avail: NTIS HC A20/MF A03 CSCL 03A

N90-21337*# Rockwell International Science Center, Thousand Oaks, CA.
LOW NOISE HgCdTe 128 X 128 SWIR FPA FOR HUBBLE SPACE TELESCOPE
Michael Blessinger, Kadri Vural, William Kleinhans, Marcia J. Rieke, Rodger Thompson, and Robert Rasche (Arizona Univ., Tucson.) *In* NASA, Ames Research Center, Proceedings of the Third Infrared Detector Technology Workshop Oct. 1989 p 311-320 (For primary document see N90-21313 14-35)
Avail: NTIS HC A20/MF A03 CSCL 03A

N90-21338*# Arizona Univ., Tucson. Steward Observatory.
LABORATORY AND TELESCOPE USE OF THE NICMOS2 128 X 128 HgCdTe ARRAY
Marcia J. Rieke, E. F. Montgomery, G. H. Rieke, Kadri Vural, Michael Blessinger, and William Kleinhans (Valley Oak Semiconductor, Inc., Westlake Village, CA.) *In* NASA, Ames Research Center, Proceedings of the Third Infrared Detector Technology Workship Oct. 1989 p 321-330 (For primary document see N90-21313 14-35)
(Contract NAS5-30008)
Avail: NTIS HC A20/MF A03 CSCL 03A

N90-21340*# European Space Agency. European Space Research and Technology Center, ESTEC, Noordwijk (Netherlands). Space Science Dept.
INTRODUCTION TO THE INFRARED SPACE OBSERVATORY (ISO)
M. F. Kessler and F. Sibille (Observatoire de Lyon, France) *In* NASA, Ames Research Center, Proceedings of the Third Infrared Detector Technology Workshop Oct. 1989 p 337-344 (For primary document see N90-21313 14-35)
Avail: NTIS HC A20/MF A03 CSCL 03A

N90-21346*# National Aeronautics and Space Administration. Ames Research Center, Moffett Field, CA.
SOFIA: STRATOSPHERIC OBSERVATORY FOR INFRARED ASTRONOMY
E. F. Erickson *In its* Proceedings of the Third Infrared Detector Technology Workshop Oct. 1989 p 401-402 (For primary document see N90-21313 14-35)
Avail: NTIS HC A20/MF A03 CSCL 03A

90 ASTROPHYSICS

Includes cosmology; celestial mechanics; space plasmas; and interstellar and interplanetary gases and dust.
For related information see also *75 Plasma Physics.*

N90-21695# Chalmers Univ. of Technology, Goeteborg (Sweden). Space Observatory.
THE MOLECULAR CLOUD CONTENT OF EARLY TYPE GALAXIES. 2: A MOLECULAR RING IN NGC 404
Tommy Wiklind and Christian Henkel (Max-Planck-Inst. fuer Radioastronomie, Bonn, Germany, F.R.) 1989 54 p
(PB90-124348; Rept-89/25) Avail: NTIS HC A04/MF A01 CSCL 03B

The authors are presently engaged in a CO survey of early type galaxies detected by the IRAS satellite, in the Northern and Southern Hemispheres. Here, the molecular cloud content of early type galaxies is discussed. Researchers present observations of the molecular gas in NGC 404 which shows surprisingly strong CO emission in the two lowest rotational transitions. The observational data is also used to obtain a better estimate of the distance and of the morphological classification (E versus SO) of the galaxy. Author

N90-21696 State Univ. of New York, Stony Brook.
THE DYNAMICS OF SCALAR FIELDS IN THE EARLY UNIVERSE Ph.D. Thesis
Hume A. Feldman 1989 149 p
Avail: Univ. Microfilms Order No. DA8926323

The dynamical evolution of weakly coupled scalar fields in the early universe is discussed. Such fields would be out of thermal equilibrium, and their initial distribution highly inhomogeneous. The classical evolution was studied in the pre-inflationary, radiation dominated universe, and under which conditions the fields dynamically relax to configurations which give inflation was discussed. The effects of thermal fluctuations in a model of new inflation with a double-well potential are studied. The stochastic approach to inflation is extended to cover a situation in which spatial gradient terms and acceleration terms in the equation of motion of the scalar field dominate. These effects are explored numerically to complement the analytical investigation. A critical value of the strength of the coupling to the thermal bath is found, above which thermal fluctuations do not allow the inflationary period to begin. The evolution of the scalar field is followed until the onset of the inflationary period. Gravitational perturbations about the Friedmann-Robertson-Walker metric are taken into account. Making use of gauge invariant variables, it is shown, both analytical and numerically, that provided the initial gravitational perturbations

are not too large, they do not prevent the dynamical relaxation of the scalar field configuration to an almost homogeneous configuration which leads inflation. A detailed derivation of the Einstein equations and the equation of motion for the scalar fields and their perturbations including the effects of back reaction in the analysis, is given. Different gauge choices are explored and discussed. Numerical simulation of the dynamical evolution of both the scalar field and the metric perturbation variable is done.
Dissert. Abstr.

N90-21697 Edinburgh Univ. (Scotland).
THE EVOLUTION AND GEOMETRY OF THE OUTER PARTS OF THE SMALL MAGELLANIC CLOUD Ph.D. Thesis
D. Hatzidimitriou 1989 276 p
Avail: Univ. Microfilms Order No. BRD-86402

The purpose is to achieve an improved and more complete understanding of the structure and evolutionary history of the Small Magellanic Cloud (SMC), the second nearest galaxy to the Milky Way. The focus was on the northeastern and west/southwestern parts of the SMC, including populations at projected distances larger than 2.2 kpc from the center of the SMC. These regions were scarcely studied in detail in the past. The observational material consisted of good quality B and R photographic plates taken with the U.K. Schmidt Telescope in Australia, digitized by the COSMOS automatic microdensitometer and calibrated by a series of CCD photometric sequences obtained at the European Southern Observatory (with the 1.5 m Danish Telescope) and at the Anglo-Australian Observatory (with the 4 m telescope). Color-magnitude diagrams were constructed over the whole of the area measured. The analysis of the properties of these diagrams resulted in establishing the population synthesis in the outer parts of the SMC as a function of position with respect to the center, and probing the geometrical structure (in three dimensions) of these outlying regions of the SMC, which led to the discovery of a significant line-of-sight depth in the NE outer parts. A study of the carbon star population in the SMC outer regions was also conducted, using UKST prism plates. The carbon stars were used as probes of the intermediate-age populations in the outer parts of the SMC.
Dissert. Abstr.

N90-21698 Harvard Univ., Cambridge, MA.
RELATIVISTIC PROCESSES IN ACTIVE GALACTIC NUCLEI Ph.D. Thesis
Timothy Ralph White 1989 158 p
Avail: Univ. Microfilms Order No. DA8926193

Processes in relativistic plasmas in the context of active galactic nuclei (AGN) are examined. Two problems are addressed relating to the central, energy producing regions of these objects in an attempt to develop diagnostics for the conditions present there. The spectra of AGNs can be characterized by a smooth continuum, between infrared and x ray energies, and an excess of emission in the ultraviolet, referred to as the UV-bump which is interpreted as emission from cool, optically thick matter. From estimates of the temperature of this matter and the total luminosities in the bump and the continuum, it is established that for many of these objects, this interpretation requires thermal matter to occupy roughly the same spatial region near the central object as the continuum emitting plasma. This cool matter will then reprocess part of the continuum emission, leading to a broad hump in the x ray spectra between approximately 10 and 300 keV. The implications when a UV-bump is present but the x ray hump is not are discussed. The origin of the continuum spectrum, which extends to MeV energies, is investigated. The thermal, optically thin accretion disks of the 1970s are synthesized with the microphysics of thermal electron-positron pair plasmas of the 1980's. In disks cooled by externally produced photons, pairs have little qualitative effect. However, in disks cooled by internally produced photons, there exists a critical accretion rate above which pair equilibrium can not be maintained and steady-state disks do not exist. Below the critical rate, two self-consistent disk solutions exist at each radius, one with a low density of pairs, and one with a high density of pairs. The time-dependent behavior of these disks was studied and it was found that the disk, when in the unstable, high pair density state or at accretion rates exceeding the critical value, collapses toward an optically thick state. The observational consequences of these conclusions are discussed.
Dissert. Abstr.

N90-21699 Wisconsin Univ., Madison.
THOMSON SCATTERING IN A MAGNETIC FIELD Ph.D. Thesis
Barbara Anne Whitney 1989 286 p
Avail: Univ. Microfilms Order No. DA8923355

Solutions to the equation of transfer for electron scattering in a magnetic field are presented. The cross sections for electron scattering are derived, and the radiative transfer is done using Monte Carlo methods. Emergent Intensity and polarization are presented for various orientations of constant magnetic field and for various atmosphere thicknesses. Several atmosphere results are combined to give the flux from a dipole star. Several interesting features of magnetic white dwarfs are reproduced, such as the rotation of the position angle of the polarization by 90 deg. These results, along with the discussion of the differential and integrated cross sections, provide insight into the subject of radiative transfer in a magnetic field.
Dissert. Abstr.

N90-21700 Wisconsin Univ., Madison.
A THEORETICAL STUDY OF CIRCUMSTELLAR DUST AROUND Ae/Be STARS Ph.D. Thesis
Wilfred Henry Sorrell 1989 133 p
Avail: Univ. Microfilms Order No. DA8923348

Numerical radiative transfer models are used to discuss the properties of circumstellar dust grains around Ae/Be stars showing strong infrared excess emission. It is assumed that the dust grains consist of a silicate-graphite mixture distributed in a spherical shell around the stars. It is further assumed that a black body spectrum is a useful approximation to the continuous energy distribution of the redden star. The stars selected for study are six Herbig Ae/Be stars, five peculiar shell stars, and the central object in the Red Rectangle Nebula. Observed flux data over the wavelength bands 1200A to 100 microns are assembled from the various sources in the literature. Such data make possible to carry out a multi-wavelength study from the far-UV to the far-IR. In addition to modeling the continuum energy distribution, special attention is given to fitting observed dust spectroscopic features with corresponding features expected from model silicate and graphite grains. By comparing model absorption curves and energy distributions to observations, it is then possible to strengthen constraints on dust-grain composition, abundance, and grain size distributions.
Dissert. Abstr.

N90-21701 Edinburgh Univ. (Scotland).
THE LARGE SCALE STRUCTURE OF THE UNIVERSE IN PANCAKE MODELS OF GALAXY FORMATION Ph.D. Thesis
James G. More 1988 158 p
Avail: Univ. Microfilms Order No. BRD-87606

The evolution of characteristic structures in neutrino or adiabatic baryon-dominated models of galaxy formation is investigated. The collapse of protocluster or protosupercluster clouds is discussed in terms of the behavior of non-rotating, homogeneous triaxial ellipsoids, predicting that galaxies should populate filamentary or quasi-spherical structures rather than the generic flat structures (pancakes). Secondly, a numerical code was designed which allows fast cosmological hydrodynamics. The effect of explosions on the standard pancake picture for galaxy formation was investigated. Blast waves created by the early evolution of galaxies can not produce the anti-biasing effect required to reconcile the rapid evolution of clustering in n-body simulations of neutrino models with observations of galaxies at redshifts greater than one.
Author

N90-21702 North Carolina Univ., Chapel Hill.
TOWARD QUANTUM CORRECTIONS IN BLACK HOLE THERMODYNAMICS Ph.D. Thesis
Jeffrey Melmed 1989 90 p
Avail: Univ. Microfilms Order No. DA9007299

Motivated by the incertitude of the stability of black holes in

thermal equilibrium with their own radiation, yet lacking a closed renormalized effective action for gravity, the issue of stability is addressed from the point of view of quantum field theory in curved space. A conformally coupled scalar field is employed to model the one loop partition function which is then used to describe a finite black hole radiation system in the canonical ensemble. A boundary correct effective action is proposed based on an extension of the recently introduced Brown and Ottewill conformal approach. During the process of that extension, the required boundary correct C sub 2 coefficient, which appears as the fourth order gravitational counterterm in the renormalization of the conformal scalar field action, and which is intimately connected to the anomalous trace of the quantum stress tensor, is found in geometrical terms. The resulting effective theory is applied to radiation systems in flat space and in Schwarzschild spacetimes where thermal quantities are computed by the method of York. In flat space, explicit modifications were found to the Planckian thermal radiation quantities coming from the geometry of the cavity wall. In Schwarzschild it was found that the radiation does not effect the known zero-loop thermal stability, at least to the same level of approximation which is implicit in the quantum stress tensor of Page. Dissert. Abstr.

N90-21703 Texas Univ., Austin.
THE THERMO-MECHANICAL BEHAVIOR OF COMETARY NUCLEI Ph.D. Thesis
Jacklyn Rena Green 1989 163 p
Avail: Univ. Microfilms Order No. DA9005584

The thermo-mechanical behavior of cometary nuclei is investigated in terms of the properties of the porous ice composing them. The time-dependent thermal gradients and the material properties dictate the thermal stress response and possible fracture. Thermal conductivity, specific heat, coefficient of thermal expansion, Young's modulus, and Poisson's ratio are studied analytically as functions of porosity and composition. More extensive numerical calculations, employing the method of finite elements, yield the thermal conductivity as a function of porosity, pore shape, pore size, ice composition, pore vapor composition, pore orientation with respect to heat flow, pore size distribution, pore packing geometry, grain-grain interface size, and heat transport mechanism. Numerical techniques are employed to simulate the large-scale thermal and stress response of two-dimensional, planar comet surface layers. The thermal and stress profiles are calculated as functions of porosity, pore shape, and presence of pore space vapor. The numerical results are compared with analytical results for the development of thermal stress in a sphere under the same conditions. Fracture mechanics calculations of Griffith crack propagation are employed to investigate the occurrence of catastrophic fracture. Author

N90-21704 Case Western Reserve Univ., Cleveland, OH.
EVOLUTIONARY EFFECTS IN B STARS Ph.D. Thesis
Stephen James Hulbert 1989 94 p
Avail: Univ. Microfilms Order No. DA9004509

Evolutionary changes in the chemical composition of B stars are investigated through the study of B-type blue stragglers. In OB associations many of the suspected blue stragglers are OBN stars; OB stars that exhibit unusually strong nitrogen lines. One of the promising theories that accounts for the nitrogen abundance peculiarity involves the rotationally induced mixing of the star. This mixing can deposit CN processed material from the interior of the star on the surface, thus affecting the observed abundance of carbon and nitrogen. Similar abundance peculiarities were sought in B-type stragglers in three open clusters to clarify their evolutionary status. In one case such an abundance signature was found. Relative to the solar values, the star, CPD-53 7353 in NGC 6067, has an enhanced nitrogen abundance and depleted carbon abundance which is consistent with the theoretical predictions for the OB blue stragglers. Dissert. Abstr.

N90-21705 Kentucky Univ., Lexington.
PROBLEMS IN RADIATIVE TRANSFER IN ASTROPHYSICS: AN ESCAPE PROBABILITY TREATMENT OF LINE OVERLAP AND A MODEL OF THE MASERS AROUND VX Sgr Ph.D. Thesis
Philip Brian Lockett 1989 111 p
Avail: Univ. Microfilms Order No. DA9005799

The escape probability formalism is used to treat two problems in astrophysical radiative transfer. The first problem concerns line overlap, which occurs when two or more spectral lines lie close enough together that there is a significant probability that a photon emitted in one of the lines can be absorbed in another. The second problem involved creating a detailed model of the masers around the supergiant star, VX Sgr. An escape probability procedure was developed that accounts for the effects of line overlap by integrating the amount of absorption in each of the overlapping lines. This method was used to test the accuracy of a simpler escape probability formalism developed by Elitzur and Netzer that utilized rectangular line profiles. Good agreement between the two methods was found for a wide range of physical conditions. The more accurate method was also used to examine the effects of line overlap of the far infrared lines of the OH molecule. This overlap did have important effects on the level populations and could cause maser emission. A detailed model of the OH 1612 and water masers around VX Sgr were also developed. The masers can be adequately explained using reasonable estimates for the physical parameters. It is possible to provide a tighter constraint on the highly uncertain mass loss rate from the star. Modeling the SiO masers was less successful. Their explanation will require a more exact method of treating the many levels involved and also a more accurate knowledge of the relevant physical input parameters. Dissert. Abstr.

N90-21706 Texas Univ., Austin.
SMALL SCALE STRUCTURES AND DENSITY OF STAR-FORMING REGIONS Ph.D. Thesis
Shudong Zhou 1989 167 p
Avail: Univ. Microfilms Order No. DA9005701

Star formation in our own galaxy is described. Based on recent developments in the field, several crucial observations were designed and carried out to check both the basis and predictions of theoretical models of low-mass star formation, and to provide the observational basis for models of high-mass star formation. In the area of low-mass star formation, CS molecular line survey has revealed the presence of supersonic turbulence in nearby dense cores, sites of the low-mass star formation, contrary to previous NH3 observations which showed only subsonic turbulence. The result presents a potential problem for the current theory of low-mass star formation which considers only subsonic turbulence. A detailed study of the low-mass dense core, B335, has been that the density profile around its embedded star is proportional to r(sup -alpha) where alpha is between 1.5 and 2.0, in good agreement with theoretical predictions. In the area of high-mass star formation, a detailed study of NGC 2071, a nearby region with an approx. 5 solar-mass young stellar object was made. The CS observations have yielded a density law of n varies as r(exp -1) in the region, which implies the dominance of gas self-gravity and turbulence, based on numerical models of dense core evolution. In regions of both low-mass and high-mass star formation, the distributions of the two molecules, CS and NH3, are clearly different; this difference may be caused by variations in local chemical processes. Thus, caution is advised in choosing molecules as tracers of the much more abundant, but generally unobservable, H2. At least in NGC 2071, CS is shown to be a better gas tracer than NH3. Author

N90-21707# International Centre for Theoretical Physics, Trieste (Italy).
A MECHANISM FOR THE FORMATION OF KNOTS, KINKS AND DISCONTINUOUS EVENTS IN THE PLASMA TAIL OF COMETS
Shui Wang Aug. 1989 28 p Submitted for publication

(DE90-613285; IC-89/218) Avail: NTIS (US Sales Only) HC A03/MF A01

In this paper, we investigate the growth rates and eigenmodes of the streaming sausage, kink and tearing instabilities in the plasma tail of comets. The results show that both the sausage and kink modes can be excited by the sheared plasma flow, which is low at the centre of the plasma sheet and high on the two sides of the plasma sheet. The streaming sausage mode grows faster than the streaming kink mode when beta sub L less than 1.5. When beta sub L greater than 1.5, the streaming kink instability has a higher growth rate. The instability condition for both the streaming sausage and kink modes is found to be V sub L greater than or approx. 1.2 V sub AL. Here beta sub L is the ratio between the plasma and magnetic pressures, V sub AL, the Alfven velocity and V sub L, the plasma flow velocity in the lobes of the cometary tail. In the presence of a finite resistivity, the streaming sausage mode evolves into the streaming tearing mode, which leads to the formation of magnetic islands. We suggest that some of the knots, kinks and disconnection events observed in the plasma tail of comets may be associated with the streaming sausage, kink and tearing instabilities, respectively. DOE

N90-21708# International Centre for Theoretical Physics, Trieste (Italy).
HORIZON PROBLEM IN COSMOLOGICAL MODELS WITH NON ZERO
Mariusz P. Dabrowski, Jerzy Stelmach, and Ryszard Byrka (Warsaw Univ., Poland) Aug. 1989 24 p
(DE90-613367; IC-89/234) Avail: NTIS (US Sales Only) HC A03/MF A01

The influence of the small cosmological constant on the angle under which we observe today the particle horizon corresponding to the last scattering epoch is investigated. Numerical calculations are performed as well for the recombination epoch (z sub R = 1300) as for the model in which the last scattering of photons took place more recently (5 less than z sub S less than 15) due to reheating. It is shown that even the small admissible Lambda-term may change this angle remarkably (up to 50 percent) depending on the density of the matter. Moreover, the positive cosmological constant lowers the angle while the negative one enlarges it. In models with reheating, the values of redshifts for which the horizon problem may be solved are found. The surface of the last scattering in these models is also calculated. Numerical values of all integrals appearing in the paper are found using elliptic functions. DOE

91 LUNAR AND PLANETARY EXPLORATION

Includes planetology; and manned and unmanned flights.
For spacecraft design or space stations see *18 Spacecraft Design, Testing and Performance.*

N90-21709# Lawrence Livermore National Lab., CA. Special Studies Program.
MARS IN THIS CENTURY: THE OLYMPIA PROJECT
Roderick A. Hyde, Muriel Y. Ishikawa, and Lowell L. Wood 1988 17 p Presented at the 4th National Space Symposium, Colorado Springs, CO, 12-15 Apr. 1988
(Contract W-7405-eng-48)
(DE90-008356; UCRL-98567; CONF-8804105-2) Avail: NTIS HC A03/MF A01

Manned exploration of the inner solar system, typified by a manned expedition of Mars, this side of the indefinite future involves fitting a technical peg into the political hole. If Apollo-level resources are assumed unavailable for such exploratory programs, then non-Apollo means and methods must be employed, involving greater technical and human risks, or else such exploration must be deferred indefinitely. Sketched here is an example of such a relatively high risk alternative, one which could land men on Mars in the next decade, and return them to earth. Two of its key features are a teleoperated rocket fuel generating facility on the lunar surface and an interplanetary mission staging space station at L(sub 4), which would serve to enable a continuing solar system exploratory program, with annual mission commencements to points as distant as the Jovian moons. The estimated cost to execute this infrastructure building manned Mars mission is $3 billion, with follow on missions estimated to cost no more than $1 billion each. DOE

92 SOLAR PHYSICS

Includes solar activity, solar flares, solar radiation and sunspots.
For related information see *93 Space Radiation.*

N90-21710# Institute of Plasma Physics, Prague (Czechoslovakia).
SOLAR FLARES AND DYNAMICS OF LANGMUIR WAVES IN CURRENT-CARRYING PLASMAS
K. Jungwirth and M. Karlicky May 1989 41 p
(IPPCZ-291) Avail: NTIS HC A03/MF A01

The dynamics of intense Langmuir waves in current-carrying plasmas is studied both analytically and numerically. Starting with the widely used Zakharov equations, adapted to these systems, specific features of this problem are pointed out. Further, the role of resonant particles is analyzed. By using 1-D macroparticle numerical code, nonlinear regimes of the modified-decay and modulational instabilities are then modelled. Efficient cooperation of essentially ponderomotive and electron-ion drift effects is demonstrated. It appears that the heating of a current-carrying plasma can be activated through releasing of the inductively stored energy, due to the enhanced conversion of energy associated with the electron drift motion. The underlying physics is discussed and its relationship to the solar flare theory is suggested. Author

N90-21711*# Tufts Univ., Medford, MA.
VLA OBSERVATIONS OF THE CORONAL PLASMA
Kenneth R. Lang 1989 11 p Presented at the 142nd IAU Symposium on Basic Plasma Processes on the Sun, Bangalore, India, 1-5 Dec. 1989 Sponsored in part by NSF
(Grants NAG5-501; AF-AFOSR-0147-89)
(NASA-CR-186540; NAS 1.26:186540) Avail: NTIS HC A03/MF A01 CSCL 03B

VLA observations at 20 cm wavelength specify the brightness temperature and magnetic structure of plasma constrained within coronal loops in solar active regions. Comparisons with simultaneous SMM observations at soft x ray wavelengths lead to measurements of physical parameters like electron density, electron temperature and magnetic field strength. Such comparisons also indicate coronal loops can be detected at either radio or x ray wavelengths while remaining invisible in the other spectral domain, and that the dominant radiation mechanisms can be thermal bremsstrahlung or thermal gyroresonance radiation. VLA observations at the longer 90 cm wavelength reveal the thermal emission of a hot transition sheath enveloping a cooler, underlying H alpha filament seen in absorption. The 20 cm VLA observations indicate that the precursor, impulsive and post-flare components of solar flares originate in spatially separated and resolved sources. The 90 cm VLA data indicate that time-correlated radio bursts can occur in active regions on opposite sides of the solar equator. These regions are apparently linked by large scale, trans-equatorial magnetic loops at least 2.6 x 10(exp 5) km (or 6 feet) long; these loops act as magnetic conduits for relativistic electrons moving at one-third the velocity of light. Author

N90-21712# Mission Research Corp., Los Alamos, NM.
SUBSTORMS: THEIR EXPANSION AND RECOVERY PHASES
Edward W. Hones 1990 16 p Presented at the Workshop on Magnetospheric Substorms and Solar Flares, Honolulu, HI, 26-30 Mar. 1990 Prepared in cooperation with Los Alamos National Lab., NM
(Contract W-7405-eng-36)

(DE90-008970; LA-UR-90-1037; CONF-9003131-1) Avail: NTIS HC A03/MF A01

Solar flares and magnetospheric substorms are each presumably processes by which energy is released from storage in magnetic fields and converted into kinetic energy of plasma and energetic particles. There are a number of analogies between flares and substorms. Substorms, their expansion and recovery phases, and a model by which they are presently explained are briefly discussed. Two features of substorms, the retreating neutral line and the separatrix layer are offered as features which might have identifiable (observable) analogies in flares. DOE

N90-21713# Instituto de Pesquisas Espaciais, Sao Jose dos Campos (Brazil).

HIGH ENERGY PHENOMENA DURING SOLAR FLARES Ph.D. Thesis [FENOMENOS DE ALTA ENERGIA EM EXPLOSOES SOLARES]

Emilia Correia Nov. 1989 104 p In PORTUGUESE; ENGLISH summary

(INPE-4961-TDL/390) Avail: NTIS HC A06/MF A01

The main purpose is to analyze the characteristics of peculiar solar events that could be produced by ultrarelativistic electrons and try to define the new boundary conditions for the primary energy release during impulsive phase. It seems that submillimeter emission in solar flares is not a rare phenomenon, there is not much evidence, due to the lack of observations in this range of the spectrum. During May 1984 the Sun was observed at 90 GHz with high time resolution and high sensitivity, and evidence was obtained. The May 21, 1984 event, at 1326 UT is the best example of the high energy manifestation during the spectrum and gave us new boundary conditions for the physical phenomena in the Sun. The May 21 event required a detailed analysis of the current interpretation models and suggested the presence of relativistic electrons during the impulsive phase. In this case Syncrotron/inverse compton mechanism was suggested to explain sub-millimeter/x ray emission and short pulse duration. The new boundary conditions for primary energy release favored Tajima and Sakai's model, based in magnetic island coalescence theory. Author

N90-21714# Instituto de Pesquisas Espaciais, Sao Jose dos Campos (Brazil).

COMPARISON OF QUIET TIME GEOMAGNETIC DAILY VARIATION (Sq) IN H COMPONENT AT EUSEBIO AND CACHOEIRA PAULISTA

R. P. Kane, N. B. Trivedi, A. L. Padilha, and J. M. daCosta Jun. 1989 10 p Presented at the 40th Annual Meeting of the Sociedade Brasileira para o Progresso da Ciencia, Sao Paulo, Brazil, 1988

(INPE-4985-PRE/1547) Avail: NTIS HC A02/MF A01

Quiet time daily variations at Eusebio for the high solar activity period of 1978 to 79 were previously studied. Results are presented for quiet time daily variations (Sq) in the H-field at Eusebio and are compared with the similar variations observed at Cachoeira Paulista for the period of low solar activity in the year 1986. Eusebio is situated in the region of Equatorial Electrojet and Cachoeira Paulista is a low latitude station situated in the region of South Atlantic Magnetic Anomaly. Author

93 SPACE RADIATION

Includes cosmic radiation; and inner and outer earth's radiation belts.

For biological effects of radiation see *52 Aerospace Medicine*. For theory see *73 Nuclear and High-Energy Physics*.

N90-21715*# National Aeronautics and Space Administration. Langley Research Center, Hampton, VA.

SIMPLIFIED MODEL FOR SOLAR COSMIC RAY EXPOSURE IN MANNED EARTH ORBITAL FLIGHTS

John W. Wilson, Govind S. Khandelwal, Judy L. Shinn, John E. Nealy, Lawrence W. Townsend, and Francis A. Cucinotta (Rockwell International Corp., Houston, TX.) Washington May 1990 15 p

(NASA-TM-4182; L-16738; NAS 1.15:4182) Avail: NTIS HC A03/MF A01 CSCL 03B

A simple calculational model is derived for use in estimating solar cosmic ray exposure to critical body organs in low-Earth orbit at the center of a large spherical shield of fixed thickness. The effects of the Earth's geomagnetic field, including storm conditions and the astronauts' self-shielding, are evaluated explicitly. The magnetic storm model is keyed to the planetary index K(sub p). Author

N90-21716 Minnesota Univ., Minneapolis.

FRAGMENTATION OF RELATIVISTIC HEAVY NUCLEI WITH APPLICATION TO COSMIC RAY PROPAGATION Ph.D. Thesis

James Richard Cummings 1989 270 p

Avail: Univ. Microfilms Order No. DA9001006

Cross sections were measured for charge changing interactions of several nuclei with 26 less than or equal to Z less than or equal to 79, at energies from 0.5 to 1.6 GeV/nucleon, on targets of C, CH2 (and H by derivation), Al, and Cu. These measurements are summarized, which are the result of a series of experiments at the Lawrence Berkeley Laboratories Bevalac particle accelerator designed to calibrate and aid in the interpretation of the results from the High Energy Astronomical Observatory 3 Heavy Nuclei Experiment satellite instrument. The latest run is examined in detail. A global expression was found with few free parameters for cross sections of nuclei near these energies and charges which has good chi squared values when fit to all measured cross sections. The expression is a greatly improved fit to these data compared to the standard, but much more complex, semi-empirical relations. The experiments also indicate that unexpectedly large mass losses occur in these interactions. This result has important implications for the calculated isotopic yield from nuclear interactions near these energies and charges. Application is discussed of the global fit and mass change information to the propagation of ultra-heavy cosmic rays from the source to the point of detection. Author

N90-21717 California Inst. of Tech., Pasadena.

A BALLOON MEASUREMENT OF THE ISOTOPIC COMPOSITION OF GALACTIC COSMIC RAY IRON Ph.D. Thesis

Jon Eric Grove 1989 249 p

Avail: Univ. Microfilms Order No. DA9000564

The isotopic composition of galactic cosmic ray iron in the energy interval of approximately 1550 to 2200 MeV/nucleon was measured using a balloon-borne mass spectrometer. The instrument was flown from Palestine, Texas, in May 1984 for greater than 35 hours at an atmospheric depth of approximately 6 g/sq cm. Masses were derived by the Cerenkov-Energy technique. The Cerenkov counter employed a silica aerogel radiator with an index of refraction n = 1.1. Particle energies were measured in a stack of NaI(Tl) scintillators, which also provided particle trajectories. A detailed discussion of the sources of mass uncertainty is presented, including an analytic model of the contribution from fluctuations in the Cerenkov yield from knock-on electrons. The achieved mass resolution is approximately 0.65 amu, which is consistent with the theoretical estimate. An Fe-54/Fe-56 abundance ratio of 0.14(sup +0.18)(sub -0.11) and an 84 percent confidence upper limit of Fe-58/Fe-56 is less than or = to 0.07 at the top of the atmosphere is reported. Combining the data with those of precious measurements of the composition of iron at lower energies, and using a model of the galactic propagation, cosmic-ray source abundance ratios of Fe-54/Fe-56 = 0.064(sup +0.032)(sub -0.027) and Fe-58/F3-56 is less than or = to 0.062 were derived. These values are consistent with the composition of solar system iron and place restrictions on the conditions under which cosmic-ray iron is synthesized. Dissert. Abstr.

N90-21718 Wisconsin Univ., Madison.

A SEARCH FOR VERY HIGH ENERGY GAMMA RAYS FROM

THE CRAB PULSAR-NEBULA Ph.D. Thesis
Almus Thomas Kenter 1989 283 p
Avail: Univ. Microfilms Order No. DA8923382

The Haleakala Gamma Ray Observatory (HGO) uses the Cerenkov Technique to look for point sources of greater than or = 0.3 TeV gamma rays. The Crab pulsar (PSR0531 + 21) is a well studied, isolated, radio pulsar in a supernova remnant. This pulsar is unique in that it has been observed at virtually all wavelengths. Recent reports indicate that the pulsar and nebula are emitting TeV gamma rays both continuously and sporadically. During the period of October 1986 through February 1988 the HGO observed the Crab pulsar-nebula for 174 hours. The data set was examined for several types of emission; continuous pulsed, continuous nonpulsed, episodic pulsed and episodic nonpulsed. No conclusive evidence for emission was found in the data set.
Dissert. Abstr.

N90-21719*# Tufts Univ., Medford, MA.
FLARE STARS AT RADIO WAVELENGTHS
Kenneth R. Lang 1989 14 p Presented at the 137th IAU Symposium on Flare Stars, Byurakan, Armenia, USSR, 23-27 Oct. 1989 Sponsored in part by NSF
(Grants NAG5-501; AF-AFOSR-0147-89)
(NASA-CR-186539; NAS 1.26:186539) Avail: NTIS HC A03/MF A01 CSCL 03B

The radio emission from dMe flare stars is discussed using Very Large Array and Arecibo observations as examples. Active flare stars emit weak, unpolarized, quiescent radio radiation that may be always present. Although thermal bremsstrahlung and/or thermal gyroresonance radiation account for the slowly-varying, quiescent radio radiation of solar active regions, these processes cannot account for the long-wavelength quiescent radiation observed from nearby dMe flare stars. It has been attributed to nonthermal gyrosynchrotron radiation, but some as yet unexplained mechanism must be continually producing the energetic electrons. Long duration, narrow-band radiation is also emitted from some nearby dMe stars at 20 cm wavelength. Such radiation may be attributed to coherent plasma radiation or to coherent electron-cyclotron masers. Impulsive stellar flares exhibit rapid variations that require radio sources that are smaller than the star in size, and high brightness temperatures greater than 10(exp 15) K that are also explained by coherent radiation processes. Quasi-periodic temporal fluctuations suggest pulsations during some radio flares. Evidence for frequency structure and positive or negative frequency drifts during radio flares from dMe stars is also presented. Author

99 GENERAL

N90-21720# European Office of Aerospace Research and Development, London (England).
[RESEARCH PROGRAMS IN AERONAUTICAL ENGINEERING, SOLID STATE PHYSICS, AND MATERIALS SCIENCE AT TECHNION-ISRAEL INSTITUTE OF TECHNOLOGY, HAIFA, ISRAEL]
Vincent L. Donlan Jun. 1989 11 p
(EOARD-LR-89-068) Avail: NTIS HC A03/MF A01

Research programs in aeronautical engineering, solid state physics, and materials science currently under way at Technion are described. Topics covered are: advanced rocket propellants; hypervelocity impacts at glancing angles; thin shell composite structures; thrust-vectored jet engines; vibration mode analysis of aeroelastic structures; ion implantation and annealing of HgCdTe; reduction of 1/f noise in elevated temperature HgCdTe detectors; intersubband infrared absorption in undoped 3-5 quantum well structures; strained layer InGaAs lasers; thin film sputtering of ternary alloys; and ceramics and cermets. Author

N90-21721*# National Aeronautics and Space Administration. Lyndon B. Johnson Space Center, Houston, TX.
RESEARCH AND TECHNOLOGY Annual Report, 1989
Mar. 1990 171 p
(NASA-TM-102161; F-603; NAS 1.15:102161) Avail: NTIS HC A08/MF A01 CSCL 05B

Johnson Space Center (JSC) accomplishments in new and advanced concepts during 1989 are highlighted. This year, reports are grouped in sections, Medical Science, Solar System Sciences, Space Transportation Technology, and Space Systems Technology. Summary sections describing the role of JSC in each program are followed by descriptions of significant tasks. Descriptions are suitable for external consumption, free of technical jargon, and illustrated to increase ease of comprehension. Author

Typical Subject Index Listing

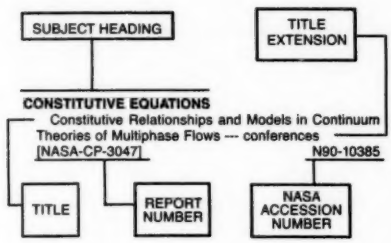

The subject heading is a key to the subject content of the document. Titles, report numbers, and accession numbers of pertinent documents are provided under each subject heading. When the title is insufficiently descriptive of the document content, a title extension has been added, separated from the title by three hyphens. The report number helps to indicate the type of document cited (e.g., NASA report, NASA translation, NASA contractor report). The NASA accession number is the number by which the document abstracts are arranged in this journal and by which the document is sold or requested. The titles, with title extensions if present, are arranged under each subject heading in ascending accession number order. The subject headings have been selected from the latest revision of the *NASA Thesaurus* (NASA SP-7064).

A

A STARS
A theoretical study of circumstellar dust around Ae/Be stars N90-21700
ABLATIVE NOSE CONES
Ablative cooling of aerodynamically heated radomes [AD-D014426] N90-21293
ABSORPTION SPECTRA
Zones of feasibility for retrieval of surface pressure from observations of absorption in the A band of oxygen [DAR-TP-19] N90-21495
ABSORPTION SPECTROSCOPY
Study of new technique of solid combustible materials to determination of volatile elements by flame atomic absorption spectrophotometry [DE90-612907] N90-21147
ABSORPTIVITY
Full wave computation of electromagnetic wave excitation, propagation, and absorption at the ion cyclotron frequency in fusion experiments [DE90-009399] N90-21642
ABUNDANCE
Evolutionary effects in B stars N90-21704
A balloon measurement of the isotopic composition of galactic cosmic ray iron N90-21717
ACCELERATION STRESSES (PHYSIOLOGY)
Space adaptation syndrome induced by a long duration +3Gx centrifuge run [AD-A218248] N90-21518
ACCELEROMETERS
Software to characterize tuning fork resonators used in the Quartz Digital Accelerometer [DE90-007913] N90-21363
ACCIDENTS
Final safety analysis report for the Ulysses Mission. Volume 2: Accident model document-appendices [DE90-008695] N90-21104
Final safety analysis report for the Ulysses Mission [DE90-008690] N90-21106
Final safety analysis report for the Ulysses mission. Volume 1: Reference design document [DE90-008693] N90-21107
ACCRETION DISKS
Relativistic processes in active galactic nuclei N90-21698
ACCURACY
Foundations of measurement and instrumentation [NASA-RP-1222] N90-21351
Error correction of the DEA (Digital Electronic Automation) coordinate measuring machines at LLNL [DE90-008913] N90-21365
ACETATES
Preparation, characterisation and cookoff behaviour of booster compositions prepared from RDX and acrylic or ethylene-vinyl acetate dispersions [MRL-TR-89-44] N90-21203
ACIDITY
Effects of Air Pollution on Western Forests [PB90-131111] N90-21481
ACOUSTIC EMISSION
Acoustic characterisation of an aluminium silicon carbide metal matrix composite [AERE-R-13273] N90-21121
ACOUSTIC EXCITATION
Double valve mechanism for an acoustic modulator [AD-D014401] N90-21386
ACOUSTIC FREQUENCIES
The radiation of sound from a propeller at angle of attack [NASA-CR-4264] N90-21602
ACOUSTIC IMPEDANCE
The optical measurement of acoustic velocity fields N90-21601
ACOUSTIC MEASUREMENT
High-resolution Brillouin gain spectroscopy in solids [DE90-009475] N90-21155
The optical measurement of acoustic velocity fields N90-21601
ACOUSTIC PROPERTIES
Relating flow between counter-rotating propellers to aerodynamic interaction noise N90-20944
Acoustic characterisation of an aluminium silicon carbide metal matrix composite [AERE-R-13273] N90-21121
ACOUSTIC STREAMING
Microgravity acoustic mixing for particle cloud combustors [NASA-CR-185159] N90-21600
The optical measurement of acoustic velocity fields N90-21601
ACOUSTIC VELOCITY
The optical measurement of acoustic velocity fields N90-21601
ACOUSTICS
Acoustic convective system [NASA-CASE-NPO-17278-1-CU] N90-21215
Double valve mechanism for an acoustic modulator [AD-D014401] N90-21386
The Shock and Vibration Digest, volume 22, no. 2 N90-21596
State of the art of acoustics of active and passive mufflers N90-21597
The optical measurement of acoustic velocity fields N90-21601
ACRYLIC RESINS
Preparation, characterisation and cookoff behaviour of booster compositions prepared from RDX and acrylic or ethylene-vinyl acetate dispersions [MRL-TR-89-44] N90-21203
ACTIVE CONTROL
PACOSS program status and results N90-21065
A distributed finite-element modeling and control approach for large flexible structures N90-21071
Controller reduction for effective interdisciplinary design of active structures N90-21077
A survey of experiments and experimental facilities for active control of flexible structures N90-21079
Experimental evaluation of active-member control of precision structures N90-21084
In-house experiments in large space structures at the Air Force Wright Aeronautical Laboratories Flight Dynamics Laboratory N90-21092
Attitude control modes for the MECB remote sensing satellites [INPE-4755-PRE/1427] N90-21094
Active control of multi-dimensional random sound in ducts [NASA-TM-102653] N90-21603
ACTIVE GALACTIC NUCLEI
Relativistic processes in active galactic nuclei N90-21698
ACTS
NASA's Advanced Communications Technology Satellite (ACTS): Will it benefit commercial/military satellites [AD-A217710] N90-21100
ACTUATORS
Advanced Launch System (ALS): Electrical actuation and power systems improve operability and cost picture [NASA-TM-102547] N90-21271
Electromechanical actuation for thrust vector control applications [NASA-TM-102548] N90-21272
Civil air transport: A fresh look at power-by-wire and fly-by-light [NASA-TM-102574] N90-21283
Application of optimization in design and motion control of robot manipulators N90-21393
ACUITY
Development of microcomputer-based mental acuity tests for repeated-measures studies [NASA-CR-185607] N90-21521
ADA (PROGRAMMING LANGUAGE)
Lessons learned in the transition to Ada from FORTRAN at NASA/Goddard [NASA-TM-103311] N90-21538
Evolution of Ada technology in the flight dynamics area: Implementation/testing phase analysis [NASA-TM-103310] N90-21539
System testing of a production Ada (trademark) project: The GRODY study [NASA-TM-103308] N90-21541
Evolution of Ada technology in the flight dynamics area: Design phase analysis [NASA-TM-103307] N90-21542
Implementation of a production Ada project: The GRODY study [NASA-TM-103305] N90-21544
ADAPTIVE CONTROL
Rule-based mechanisms of learning for intelligent adaptive flight control N90-20939
Design of a helicopter automatic flight control system using adaptive control N90-21040
CSI technology validation on an LSS ground experiment facility N90-21089
Adaptive learning fuzzy control of a mobile robot [DE90-759898] N90-21562
ADHESION
High gloss corrosion-resistant coatings [AD-D014403] N90-21184
Combination primer/topcoat coating [AD-D014445] N90-21189
Energy beam treatment for improved adhesion of coatings to surfaces [AD-D014449] N90-21190
Development of planar geometry solid oxide fuel cell technology, phase 2 [PB90-131293] N90-21467
ADHESIVE BONDING
Crack stoppers and ARALL laminates [PB90-166588] N90-21142
ADIABATIC CONDITIONS
A 100 micro Kelvin bolometer system for SIRTF N90-21317
ADIABATIC DEMAGNETIZATION COOLING
A progress report on using bolometers cooled by adiabatic demagnetization refrigeration N90-21318
ADVANCED LAUNCH SYSTEM (STS)
Advanced Launch System (ALS): Electrical actuation and power systems improve operability and cost picture [NASA-TM-102547] N90-21271

Electromechanical actuation for thrust vector control applications
[NASA-TM-102548] N90-21272

AERIAL EXPLOSIONS
Minutes of the 23rd Explosives Safety Seminar, volume 2
[AD-A218265] N90-21214

AERIAL PHOTOGRAPHY
Project CANASATE: Remote sensing applied to sugar cane crop survey
[INPE-4902-PRE/1503] N90-21446
Aerial photography as an aid for agricultural credit control
[INPE-5019-RPE/613] N90-21455
Evaluation of classification performance and proportion estimate of the sugar cane crop through PROCEDURE-INPE utilizing LANDSAT data
[INPE-4899-PRE/1500] N90-21458

AERIAL RECONNAISSANCE
Cockpit display of hazardous wind shear information N90-20924

AEROASSIST
Optimal trajectories for the aeroassisted flight experiment. Part 3: Formulation, results, and analysis
[NASA-CR-186165] N90-21051

AEROBRAKING
Mechanistic model for catalytic recombination during aerobraking maneuvers
[NASA-CR-185611] N90-21059
Heavily loaded joints for assembling aerobrake support trusses
[NASA-CR-181992] N90-21099

AERODYNAMIC CHARACTERISTICS
Measurement and prediction of propeller blade surface pressure distributions N90-20961
Computational Methods for Aerodynamic Design (Inverse) and Optimization
[AGARD-CP-463] N90-20976
Aerodynamic design techniques at DLR Institute for Design Aerodynamics N90-20979
Aerodynamic design by optimization N90-20986
Aerodynamic design via control theory N90-20998
Optimization of aerodynamic designs using computational fluid dynamics N90-20999

AERODYNAMIC COEFFICIENTS
An aerodynamic tradeoff study of the scissor wing configuration
[NASA-CR-186576] N90-20965

AERODYNAMIC CONFIGURATIONS
An aerodynamic tradeoff study of the scissor wing configuration
[NASA-CR-186576] N90-20965
An intensive procedure for the design of pressure-specified three-dimensional configurations at subsonic and supersonic speeds by means of a higher-order panel method N90-20982
Numerical optimization of wings in transonic flow N90-20997

AERODYNAMIC DRAG
Flight test investigation of certification issues pertaining to general-aviation-type aircraft with natural laminar flow
[NASA-CR-181967] N90-20952
Constrained spanload optimization for minimum drag of multi-lifting-surface configurations N90-20992
Exhaust nozzles for propulsion systems with emphasis on supersonic cruise aircraft
[NASA-RP-1235] N90-21037

AERODYNAMIC HEATING
Ablative cooling of aerodynamically heated radomes
[AD-D014426] N90-21293

AERODYNAMIC INTERFERENCE
The MANTA: An RPV design to investigate forces and moments on a lifting surface
[NASA-CR-186227] N90-20971

AERODYNAMIC LOADS
Parametric resonance in horizontal axis wind turbines N90-20962
The MANTA: An RPV design to investigate forces and moments on a lifting surface
[NASA-CR-186227] N90-20971
A computational design method for shock free transonic cascades and airfoils N90-20986
The radiation of sound from a propeller at angle of attack
[NASA-CR-4264] N90-21602

AERODYNAMIC NOISE
Relating flow between counter-rotating propellers to aerodynamic interaction noise N90-20944

AERODYNAMICS
Progress in inverse design and optimization in aerodynamics N90-20977
LACE flight dynamics experiment N90-21086
Small business innovation research. Abstracts of 1988 phase 1 awards
[NASA-TM-102991] N90-21680
Small business innovation research. Abstracts of completed 1987 phase 1 projects
[NASA-TM-101797] N90-21681

AEROELASTICITY
Performance data from a wind-tunnel test of two main-rotor blade designs for a utility-class helicopter
[NASA-TM-4183] N90-20974
Experimental aeroelasticity history, status and future in brief
[NASA-TM-102651] N90-21047

AEROMANEUVERING
Optimal trajectories for the aeroassisted flight experiment. Part 3: Formulation, results, and analysis
[NASA-CR-186165] N90-21051

AERONAUTICAL ENGINEERING
In-house experiments in large space structures at the Air Force Wright Aeronautical Laboratories Flight Dynamics Laboratory N90-21092
Small business innovation research. Abstracts of 1988 phase 1 awards
[NASA-TM-102991] N90-21680
Research programs in aeronautical engineering, solid state physics, and materials science at Technion-Israel Institute of Technology, Haifa, Israel
[EOARD-LR-89-068] N90-21720

AEROSPACE ENGINEERING
USSR Space Life Sciences Digest, Issue 26
[NASA-CR-392231] N90-21513

AEROSPACE ENVIRONMENTS
Proceedings of the 13th International Congress on Instrumentation in Aerospace Simulation Facilities
[EOARD-LR-89-069] N90-21046
United States Air Force Academy get-away-special flexible beam experiment N90-21088

AEROSPACE INDUSTRY
NASA airframe structural integrity program
[NASA-TM-102637] N90-21422

AEROSPACE MEDICINE
Human centrifuge controller
[NAL-TM-SE-8901] N90-21043
USSR Space Life Sciences Digest, Issue 26
[NASA-CR-392231] N90-21513

AEROSPACE PLANES
HOTOL structures and materials at British Aerospace, Warton, UK
[EOARD-LR-90-001] N90-21001
Performance of an aero-space plane propulsion nozzle N90-21034

AEROSPACE SYSTEMS
PACOSS program status and results N90-21065
Initial operational capability of the ASTREX large space structures test bed N90-21091
Curvature continuity of cubic Bezier curves in the solid modeling aerospace research tools design software
[NASA-CR-186583] N90-21554
Research and Technology
[NASA-TM-102161] N90-21721

AEROTHERMODYNAMICS
Probabilistic modeling for simulation of aerodynamic uncertainties in propulsion systems
[NASA-TM-102472] N90-21036
Navier-Stokes analysis of turbine blade heat transfer
[NASA-TM-102496] N90-21300

AGING (MATERIALS)
Aging and compatibility of TNF-doped Mylar
[DE90-008508] N90-21186

AGRICULTURE
Agricultural yield estimation of sugarcane based on agrometeorological-spectral model
[INPE-5016-RPE/610] N90-21441
Aerial photography as an aid for agricultural credit control
[INPE-5019-RPE/613] N90-21455

AGROMETEOROLOGY
Wheat yield estimation at the farm level using LANDSAT TM and agrometeorological data
[INPE-5017-RPE/611] N90-21439
Agricultural yield estimation of sugarcane based on agrometeorological-spectral model
[INPE-5016-RPE/610] N90-21441

AIR COOLING
Acoustic convective system
[NASA-CASE-NPO-17278-1-CU] N90-21215

AIR FLOW
The MANTA: An RPV design to investigate forces and moments on a lifting surface
[NASA-CR-186227] N90-20971
Acoustic convective system
[NASA-CASE-NPO-17278-1-CU] N90-21215

AIR JETS
Rectangular subsonic jet flow field measurements
[NASA-CR-181925] N90-21598

AIR LAND INTERACTIONS
Observations of atmospheric electricity, 1988
[GEOPHYSICAL-PUBL-10] N90-21499

AIR NAVIGATION
Joint University Program for Air Transportation Research, 1988-1989
[NASA-CP-3063] N90-20921
Ridge regression processing N90-20931

AIR POLLUTION
Transformation and deposition of airborne gaseous and particulate pollutants during transport over the Baltic Sea
[PUBL-AIR-QUALITY-5] N90-21478
Effects of Air Pollution on Western Forests
[PB90-131111] N90-21481
An evaluation of the relationship between the production and use of energy and atmospheric methane emissions
[DE90-007982] N90-21487

AIR QUALITY
Final Safety Analysis Report for the Ulysses Mission. Volume 3 (Book 1): Nuclear risk analysis document
[DE90-008691] N90-21101
Effects of Air Pollution on Western Forests
[PB90-131111] N90-21481

AIR TRAFFIC CONTROL
Joint University Program for Air Transportation Research, 1988-1989
[NASA-CP-3063] N90-20921
Investigation of air transportation technology at the Massachusetts Institute of Technology, 1988-1989 N90-20922
Automatic speech recognition in air traffic control N90-20923
Cockpit display of hazardous wind shear information N90-20924
Investigation of air transportation technology at Princeton University, 1988-1989 N90-20935
Plan for the FAA air traffic operational evaluation of the Automated Surface Observing System (ASOS)
[DOT/FAA/CT-TN89/56] N90-20968
Feasibility of using frequency offset on very high frequency air/ground voice channels
[DOT/FAA/CT-TN89/71] N90-21248
National airspace system air-ground communications operational concept
[DOT/FAA/DS-90/2] N90-21249
Meteorologist Weather Processor (MWP) integration test plan
[DOT/FAA/CT-TN89/62] N90-21500
Windshear case study: Denver, Colorado, July 11, 1988
[DOT/FAA/DS-89/19] N90-21509

AIR TRAFFIC CONTROLLERS (PERSONNEL)
Meteorologist Weather Processor (MWP) integration test plan
[DOT/FAA/CT-TN89/62] N90-21500

AIR TRANSPORTATION
Joint University Program for Air Transportation Research, 1988-1989
[NASA-CP-3063] N90-20921
Investigation of air transportation technology at the Massachusetts Institute of Technology, 1988-1989 N90-20922
Automatic speech recognition in air traffic control N90-20923
Investigation of air transportation technology at Princeton University, 1988-1989 N90-20935

AIR WATER INTERACTIONS
MECCA program documentation
[NOAA-TR-NESDIS-46] N90-21477
The extension of rapid distortion theory to stratified shear flows N90-21491
Predictability of weather and climate in a coupled ocean-atmosphere model: A dynamical systems approach
[NASA-CR-186499] N90-21502
Numerical simulations of the cloud-capped marine boundary layer N90-21506
Modeling the upper ocean and its interaction with the atmosphere
[DE90-008980] N90-21511

AIRBORNE SURVEILLANCE RADAR
Application of superresolution methods for airborne radar N90-21227
Airborne Doppler radar flight experiments for the detection of microbursts N90-21243

AIRBORNE/SPACEBORNE COMPUTERS
Computer processing of multi-channel electromagnetic data from an airborne geophysical survey system
[PB90-138413] N90-21253

AIRCRAFT ACCIDENTS
Annual review of aircraft accident data: US general aviation calendar year 1987
[PB90-138066] N90-20966

AIRCRAFT BRAKES
Brake performance of the McDonnell Douglas DC-10-30/40 during high speed, high energy rejected takeoffs
[PB90-917004] N90-21000

AIRCRAFT CARRIERS
Census of US civil aircraft
[PB90-120296] N90-20920
AIRCRAFT COMPARTMENTS
Boeing 727-100 test project (high energy radiated field tests)
[DOT/FAA/CT-88/33] N90-21247
AIRCRAFT CONFIGURATIONS
Subsonic flutter analysis using MSC/NASTRAN
[PB90-166786] N90-21041
AIRCRAFT CONSTRUCTION MATERIALS
Ultrasonic and radiographic evaluation of advanced aerospace materials: Ceramic composites
[NASA-TM-102540] N90-21401
AIRCRAFT CONTROL
Joint University Program for Air Transportation Research, 1988-1989
[NASA-CP-3063] N90-20921
Neural networks for aircraft control N90-20937
Perspectives on the use of rule-based control N90-20940
AIRCRAFT DESIGN
Aerofoil design techniques N90-20978
A system for transonic wing design with geometric constraints based on an inverse method N90-20983
Numerical optimization of wings in transonic flow N90-20997
Aerodynamic design via control theory N90-20998
AIRCRAFT ENGINES
Structural tailoring of select fiber composite structures
[NASA-TM-102484] N90-21137
Attachment of lead wires to thin film thermocouples mounted on high temperature materials using the parallel gap welding process
[NASA-TM-102442] N90-21361
Aeropropulsion facilities configuration control: Procedures manual
[NASA-TM-102541] N90-21399
Small business innovation research. Abstracts of completed 1987 phase 1 projects
[NASA-TM-101797] N90-21681
AIRCRAFT HAZARDS
Investigation of air transportation technology at the Massachusetts Institute of Technology, 1988-1989 N90-20922
Cockpit display of hazardous wind shear information N90-20924
Modeling of surface roughness effects on glaze ice accretion N90-20925
Ultrasonic techniques for aircraft ice accretion measurement N90-20926
Investigation of surface water behavior during glaze ice accretion N90-20927
The influence of ice accretion physics on the forecasting of aircraft icing conditions N90-20928
Cockpit display of hazardous weather information N90-20929
Advanced instrumentation for aircraft icing research
[NASA-CR-185225] N90-21006
AIRCRAFT INSTRUMENTS
Simulator comparison of thumball, thumb switch, and touch screen input concepts for interaction with a large screen cockpit display format
[NASA-TM-102587] N90-21005
AIRCRAFT MODELS
Aerofoil design techniques N90-20978
AIRCRAFT PERFORMANCE
Flight test investigation of certification issues pertaining to general-aviation-type aircraft with natural laminar flow
[NASA-CR-181967] N90-20952
Flight path reconstruction using extended Kalman filtering techniques
[PD-FC-9001] N90-20970
Supersonic through-flow fan engine and aircraft mission performance
[NASA-TM-102304] N90-21038
The 1D-ISAR imaging of manoeuvering aircraft N90-21241
AIRCRAFT PILOTS
The effect of windscreen bows and HUD pitch ladder format on pilot performance during simulated flight
[AD-A218139] N90-21523
AIRCRAFT POWER SUPPLIES
Civil air transport: A fresh look at power-by-wire and fly-by-light
[NASA-TM-102574] N90-21283
AIRCRAFT RELIABILITY
The role of structural analysis in airworthiness certification
[BR112064] N90-20972
AIRCRAFT SAFETY
Weather data dissemination to aircraft N90-20934
Statistics on aircraft gas turbine engine rotor failures that occurred in US commercial aviation during 1986
[DOT/FAA/CT-89/30] N90-21008
AIRCRAFT STABILITY
An aerodynamic tradeoff study of the scissor wing configuration
[NASA-CR-186576] N90-20985
AIRCRAFT STRUCTURES
Computer-aided structural optimisation of aircraft structures
[BR112837] N90-20973
AIRFOIL PROFILES
Optimum hypersonic airfoils with attached shocks N90-20960
The MANTA: An RPV design to investigate forces and moments on a lifting surface
[NASA-CR-186227] N90-20971
Inverse design of airfoil contours: Constraints, numerical method, and applications N90-20980
An efficient airfoil design method using the Navier-Stokes equations N90-20981
Numerical optimization of target pressure distributions for subsonic and transonic airfoil design N90-20993
Adaptive grid embedding for the two-dimensional flux-split Euler equations
[NASA-CR-186533] N90-21571
AIRFOILS
Ultrasonic techniques for aircraft ice accretion measurement N90-20926
Comparison of C- and O-grid generation methods using a NACA 0012 airfoil
[AD-A216375] N90-20948
Progress in inverse design and optimization in aerodynamics N90-20977
An efficient airfoil design method using the Navier-Stokes equations N90-20981
A fast collocation method for transonic airfoil design N90-20984
A computational design method for shock free transonic cascades and airfoils N90-20986
A tool for automatic design of airfoils in different operating conditions N90-20994
The use of numerical optimization for helicopter airfoil and blade design N90-20995
Aerodynamic design by optimization N90-20996
Optimization of aerodynamic designs using computational fluid dynamics N90-20999
The effects of compressor endwall flow on airfoil incidence and deviation N90-21011
Research on cascade secondary and tip-leakage flows: Periodicity and surface flow visualization N90-21026
AIRFRAMES
NASA airframe structural integrity program
[NASA-TM-102637] N90-21422
AIRGLOW
Low latitude F-region dynamical processes from atomic oxygen nightglow emissions
[INPE-4999-PRE/1561] N90-21494
AIRLINE OPERATIONS
Indianapolis Downtown Heliport: Operations analysis and marketing history
[REPT-90RR-13] N90-21049
AIRPORTS
Criteria for polymer concrete on airport pavements
[DOT/FAA/DS-89/18] N90-21045
AIRSPACE
An early overview of tiltrotor aircraft characteristics and pilot procedures in civil transport applications
[DOT/FAA/DS-89/37] N90-21003
ALGEBRA
High accuracy solutions of incompressible Navier-Stokes equations
[NASA-TM-102539] N90-21567
Weierstrass preparation and division theorems for the ring of germs of superanalytic functions
[DE90-612742] N90-21576
Extension of the constraints algebra for the closed string with the fixed topology world sheet
[DE90-612745] N90-21577
Extension of the Krichever-Novikov algebra in the closed string theory
[DE90-612746] N90-21578
The N = 2 superconformal algebras on hyperelliptic surfaces and their Coulomb gas realization
[DE90-612790] N90-21581
Fusion algebra and fusing matrices
[DE90-612798] N90-21583
Differential-algebraic equations as stiff ordinary differential equations
[DE90-007922] N90-21585
Comparison of the algebraic reconstruction technique with the maximum entropy reconstruction technique for a variety of detection tasks
[DE90-008933] N90-21587
ALGORITHMS
Comparison of C- and O-grid generation methods using a NACA 0012 airfoil
[AD-A216375] N90-20948
An overlapped grid method for multigrid, finite volume/difference flow solvers: MaGGiE
[NASA-CR-182006] N90-20953
A two-dimensional unsteady analysis for transonic and supersonic cascade flows N90-20955
Flight path reconstruction using extended Kalman filtering techniques
[PD-FC-9001] N90-20970
A homotopy approach to the solutions of minimum-fuel space-flight rendezvous problems N90-21053
Numerical simulation model for hydrazine attitude control thrusters. Part 1: Model description
[INPE-4952-RPE/601] N90-21115
Modeling the temperature dependence of the thermal conductivity of aluminum nitride
[DE90-009428] N90-21154
Capabilities of bistatic synthetic aperture radar for covert battlefield surveillance N90-21230
Concept and results of the DLR realtime SAR processor N90-21244
Numerical Arc Segmentation Algorithm for a Radio Conference (NASARC), version 4.0: User's manual
[NASA-TM-101454] N90-21250
The 4th Annual Review of Progress in Applied Computational Electromagnetics
[AD-A217912] N90-21257
A correlation-spectral method for line detection on noisy data
[DE90-007925] N90-21266
Electromechanical actuation for thrust vector control applications
[NASA-TM-102548] N90-21272
Numerical simulation of vortex breakdown N90-21288
A cost-effective strategy for nonoscillatory convection without clipping
[NASA-TM-102538] N90-21291
Analysis and finite element approximation of some optimal control problems associated with the Navier-Stokes equations N90-21299
Digital processing of TM/LANDSAT data in monitoring interior water
[INPE-4956-PRE/1533] N90-21448
Editing wind profiler measurements
[PB90-130147] N90-21503
Windshear case study: Denver, Colorado, July 11, 1988
[DOT/FAA/DS-89/19] N90-21509
Strategies for concurrent processing of complex algorithms in data driven architectures
[NASA-CR-186515] N90-21535
The parallel algorithm for solving the three-dimensional integral magnetostatic equations
[DE90-616529] N90-21547
Parallel tridiagonalization of a general matrix using distributed-memory multiprocessors
[DE90-008902] N90-21551
Performance bounds on parallel self-initiating discrete-event
[NASA-CR-182010] N90-21556
NETRA: A parallel architecture for integrated vision systems 2: Algorithms and performance evaluation
[NASA-CR-186510] N90-21557
Adaptive grid embedding for the two-dimensional flux-split Euler equations
[NASA-CR-186533] N90-21571
Comparison of the algebraic reconstruction technique with the maximum entropy reconstruction technique for a variety of detection tasks
[DE90-008933] N90-21587
Finite element algorithms for hyperbolic conservation laws with forcing terms
[INPE-5024-RPE/617] N90-21595
Modeling high-temperature superconductors and metallic alloys on the Intel IPSC/860
[DE90-009402] N90-21665
ALIGNMENT
Error correction of the DEA (Digital Electronic Automation) coordinate measuring machines at LLNL
[DE90-008913] N90-21365
ALKYL COMPOUNDS
Boron-containing organosilane polymers and ceramic materials thereof
[NASA-CASE-ARC-11649-2-SB] N90-21177
ALTERNATING CURRENT
A comparative study of electric power distribution systems for spacecraft
[NASA-CR-186531] N90-21113
ALTIMETERS
Programmable generation of linear frequency modulated pulses N90-21232
ALUMINIDES
Titanium aluminides: Processing, properties and potential
[AERE-R-13198] N90-21158

Surface characterization of hydrogen charged and uncharged alpha-2 and gamma titanium aluminide alloys using AES and REELS
[NASA-CR-186561] N90-21171

ALUMINUM
Formation of subsurface aluminum layers in beryllium by ion implantation and post-implant annealing
[DE90-007975] N90-21172
The corrosion protection of 6061-T6 aluminum by a polyurethane-sealed anodized coat
[NASA-TM-100394] N90-21191

ALUMINUM ALLOYS
Crack stoppers and ARALL laminates
[PB90-166588] N90-21142
Grain boundary precipitation in Ni3Al based alloys
[AERE-R-13362] N90-21161
Lecture on ordered intermetallic alloys
[DE90-009011] N90-21169
Fatigue crack growth from narrow-band Gaussian spectrum loading in 6063 aluminum alloy
[DE90-008957] N90-21173
Determination of Li-Al alloy extent in tubular aluminum elements by small source neutron radiology
[DE90-009142] N90-21174
Ductile alloy encapsulated ceramic armor development
[AD-A217632] N90-21183
Fractographic analysis of the crack growth rate and the shear lip development of 2024-T3 specimens under simple variable-amplitude loading
[PB90-167032] N90-21427

ALUMINUM ARSENIDES
Peeled film GaAs solar cells for space power
[NASA-TM-103125] N90-21287

ALUMINUM CARBIDES
Acoustic characterisation of an aluminium silicon carbide metal matrix composite
[AERE-R-13273] N90-21121

ALUMINUM CHLORIDES
Ionic equilibrium between octahedral and tetrahedral complexes in liquid aluminium-sodium fluoride mixtures
[DE90-613690] N90-21150

ALUMINUM FLUORIDES
Ionic equilibrium between octahedral and tetrahedral complexes in liquid aluminium-sodium fluoride mixtures
[DE90-613690] N90-21150

ALUMINUM NITRIDES
Modeling the temperature dependence of the thermal conductivity of aluminum nitride
[DE90-009428] N90-21154

ALUMINUM OXIDES
Anisotropy of grain growth in alumina
[DE90-009045] N90-21655

AMAZON REGION (SOUTH AMERICA)
Monitoring of agrocattle-raising projects through visual/digital analysis of LANDSAT-TM imagery south of Para state
[INPE-4982-PRE/1542] N90-21442
Multitemporal analysis of LANDSAT/TM digital imagery in the detection of areas affected by caterpillar (sibine fusca) attack in the dende (elais guineensis) palm plantation
[INPE-4979-PRE/1544] N90-21457
Radon concentration over the Brazilian Amazon Basin during the wet season (Belem-Manaus GTE-ABLE-2B flight of April 24, 1987)
[INPE-4892-PRE/1493] N90-21486

AMBIGUITY
Ambiguity bootstrapping to determine GPS orbits and baselines
[AD-A218206] N90-21052

AMMONIUM COMPOUNDS
An evaluation of metal salts of 3-nitro-1,2,4-triazol-5-one (NTO) as potential primary explosives
[MRL-TN-563] N90-21202

AMMUNITION
Minutes of the 23rd Explosives Safety Seminar, volume 1
[AD-A218264] N90-21213

AMORPHOUS MATERIALS
Research on amorphous silicon-based thin film photovoltaic devices. Task B: Research on stable high efficiency large area, amorphous silicon-based submodules
[DE90-000320] N90-21473

AMPLIFICATION
Development of an ultra-bright laser and an application to multi-photon ionization N90-21372
LLE review
[DE90-008958] N90-21378

AMPLIFIERS
Common source cascode amplifiers for integrating IR-FPA applications N90-21324
Generation of ultrashort laser pulses from neodymium glass oscillator and regenerative amplifier N90-21373

ANAEROBES
Anaerobic metabolism of aromatic compounds by phototrophic bacteria: Biochemical aspects
[DE90-009503] N90-21516

ANALOG COMPUTERS
CAD work station for electronics designer
[DE90-616473] N90-21546

ANALYTIC FUNCTIONS
Weierstrass preparation and division theorems for the ring of germs of superanalytic functions
[DE90-612742] N90-21576

ANGULAR MOMENTUM
US-Japan Workshop on Atomic Collisions in Solids: Abstracts of lectures
[DE90-008979] N90-21611

ANGULAR VELOCITY
Kinematic and kinetic analyses of drop landings N90-21517

ANISOTROPY
Specific heat and critical fluctuations in anisotropic high-T(sub c) oxide superconductors
[DE90-613394] N90-21651

ANNEALING
Formation of subsurface aluminum layers in beryllium by ion implantation and post-implant annealing
[DE90-007975] N90-21172
Proceedings of the Joint NOSC/NRL (Naval Ocean Systems Center/Naval Research Laboratory) InP Microwave/Millimeter Wave Technology Workshop
[AD-A218216] N90-21259

ANNOTATIONS
Medical subject headings: Annotated alphabetic list, 1990
[PB90-100009] N90-21683

ANNUAL VARIATIONS
Use of microwave satellite data to study variations in rainfall over the Indian Ocean
[NASA-CR-186408] N90-21501

ANODES
The development of a simulation program of the anode side for aluminum/air batteries
[PB90-165754] N90-21286
Development of planar geometry solid oxide fuel cell technology, phase 2
[PB90-131293] N90-21467

ANODIZING
The corrosion protection of 6061-T6 aluminum by a polyurethane-sealed anodized coat
[NASA-TM-100394] N90-21191

ANOMALIES
A homotopy approach to the solutions of minimum-fuel space-flight rendezvous problems N90-21053
MHD modes driven by anomalous electron viscosity and their role in fast sawtooth crashes
[DE90-009311] N90-21639

ANTENNA ARRAYS
Concepts for high resolution space based SAR/ISAR systems: Preliminary design considerations N90-21224
Coplanar waveguide fed phased array antenna
[NASA-TM-102522] N90-21273
Optical control of an 8-element Ka-band phased array using a high-speed optoelectronic interconnect
[NASA-TM-102550] N90-21275

ANTENNA DESIGN
A spaceborne optical interferometer: The JPL CSI mission focus N90-21063
Aperture taper determination for the half-scale accurate antenna reflector
[NASA-CR-185215] N90-21282

ANTENNAS
Full wave computation of electromagnetic wave excitation, propagation, and absorption at the ion cyclotron frequency in fusion experiments
[DE90-009399] N90-21642

ANTIPARTICLES
US-Japan Workshop on Atomic Collisions in Solids: Abstracts of lectures
[DE90-008979] N90-21611

ANTIPROTONS
A measurement of the gravitational acceleration of the antiproton
[DE90-008903] N90-21612

APERTURES
Millimeter wave near-field study
[NASA-CR-182014] N90-21058
An assessment of the potential of continuous-wave ranging for measuring the distance to a highly reflective, infinite sheet
[NASA-TM-101680] N90-21279
Aperture taper determination for the half-scale accurate antenna reflector
[NASA-CR-185215] N90-21282

APPROXIMATION
An approximate viscous shock layer method for calculating the hypersonic flow over blunt-nosed bodies N90-20947
On the dynamics of polymer mixtures in solution using the RPA
[DE90-613689] N90-21149
Ordering mechanism in substitutional Ni-Cr alloys: Theory and experiment
[DE90-006268] N90-21156
Modified tight-binding approximation and electron-phonon spectral function for transition metals
[DE90-614022] N90-21166
Generalized random phase approximation for multicomponent polymer systems
[DE90-613691] N90-21194
New ferrite-filled waveguiding structures analysed by the averaging method
[PB90-165671] N90-21269

ARCHAEBACTERIA
A new class of lubricants derived from archaebacterial lipids
[AD-D014429] N90-21185

ARCHITECTURE (COMPUTERS)
Controlled multibody dynamics simulation for large space structures N90-21068
Computational architecture for integrated controls and structures design N90-21076
Application of optimization in design and motion control of robot manipulators N90-21393
A knowledge-based information based for crop area estimation
[INPE-4990-PRE/1555] N90-21444
Fault tolerant hypercube computer system architecture
[NASA-CASE-NPO-16859-1-CU] N90-21527
Software Management Environment (SME) concepts and architecture
[NASA-TM-103306] N90-21543
Software Engineering Laboratory (SEL) database organization and user's guide
[NASA-TM-103304] N90-21545
Toward a new CIM (Computer Integrated Manufacturing) architecture for Sandia Laboratories
[DE90-008677] N90-21548
Architecture independent environment for developing engineering software on MIMD computers
[NASA-CR-186562] N90-21553
Performance bounds on parallel self-initiating discrete-event
[NASA-CR-182010] N90-21556
NETRA: A parallel architecture for integrated vision systems 2: Algorithms and performance evaluation
[NASA-CR-186510] N90-21557
Activities and operations of the Advanced Computing Research Facility
[DE90-007957] N90-21559
STORM: A statistical object representation model
[DE90-009048] N90-21686

ARITHMETIC
VLSI binary updown counter
[NASA-CASE-NPO-17205-1-CU] N90-21525

ARMATURES
Laser controlled semiconductor armature for electromagnetic launchers
[AD-D014435] N90-21055
Feasibility of intercalated graphite railgun armatures
[NASA-TM-102546] N90-21181

ARMOR
Ductile alloy encapsulated ceramic armor development
[AD-A217632] N90-21183

ARSENIC
Improved Si:As BIBIB (Back-Illuminated Blocked-Impurity-Band) hybrid arrays N90-21349

ARTIFICIAL INTELLIGENCE
Time and truth in plans N90-20930
Perspectives on the use of rule-based control N90-20940

ARTIFICIAL SATELLITES
Design of a digital model following controller of reaction wheel torques
[INPE-4753-PRE/1425] N90-21093
Space environment simulation of the SCD-01 satellite through heating plates
[INPE-4988-PRE/1550] N90-21105
Lessons learned in the transition to Ada from FORTRAN at NASA/Goddard
[NASA-TM-103311] N90-21538

ASSOCIATIVE PROCESSING (COMPUTERS)
Quadratic Hadamard Memories 1
[AD-A217224] N90-21534

ASTRONAUTS
Space adaptation syndrome induced by a long duration +3Gx centrifuge run
[AD-A218248] N90-21518

ASTRONOMICAL MODELS
The large scale structure of the universe in pancake models of galaxy formation N90-21701

Horizon problem in cosmological models with non zero
[DE90-613367] N90-21706

ASTRONOMICAL SPECTROSCOPY
Stressed detector arrays for airborne astronomy N90-21332

ASTRONOMY
Common source cascode amplifiers for integrating IR-FPA applications N90-21324
Experience with the UKIRT InSb array camera N90-21327
Initial astronomical results with a new 5-14 micron Si:Ga 58x62 DRO array camera N90-21334
Laboratory and telescope use of the NICMOS2 128 x 128 HgCdTe array N90-21338
HgCdTe 256x256 NWIR FPA N90-21348
Tests of the Rockwell Si:As Back-Illuminated Blocked-Impurity Band (BIBIB) detectors N90-21350

ASTROPHYSICS
Problems in radiative transfer in astrophysics: An escape probability treatment of line overlap and a model of the masers around VX Sgr N90-21705

ATMOSPHERIC BOUNDARY LAYER
The influence of lateral boundary conditions, fixed surface forcings, and synoptic situations upon predictability estimates using limited area numerical models N90-21492
Sensitivity studies in a two-dimensional atmospheric transport model
[DAR-TP-18] N90-21496
Numerical simulations of the cloud-capped marine boundary layer N90-21506

ATMOSPHERIC CHEMISTRY
Meteorological influences on mountain cloudwater chemistry in the eastern United States
[PB90-132432] N90-21504

ATMOSPHERIC CIRCULATION
The influence of lateral boundary conditions, fixed surface forcings, and synoptic situations upon predictability estimates using limited area numerical models N90-21492
Sensitivity studies in a two-dimensional atmospheric transport model
[DAR-TP-18] N90-21496
Meteorological influences on mountain cloudwater chemistry in the eastern United States
[PB90-132432] N90-21504

ATMOSPHERIC COMPOSITION
Preliminary report on the demonstration of the VAS CO2 cloud parameters (cover, height, and amount) in support of ASOS
[NOAA-TM-NESDIS-29] N90-21498

ATMOSPHERIC EFFECTS
Investigations into the properties, conditions, and effects of the ionosphere
[AD-A217807] N90-21489

ATMOSPHERIC ELECTRICITY
Observations of atmospheric electricity, 1988
[GEOPHYSICAL-PUBL-10] N90-21499

ATMOSPHERIC ENTRY
Optimal trajectories for the aeroassisted flight experiment. Part 3: Formulation, results, and analysis
[NASA-CR-166165] N90-21051

ATMOSPHERIC ENTRY SIMULATION
Optimal trajectories for the aeroassisted flight experiment. Part 3: Formulation, results, and analysis
[NASA-CR-166165] N90-21051

ATMOSPHERIC MODELS
Sensitivity studies in a two-dimensional atmospheric transport model
[DAR-TP-18] N90-21496
Predictability of weather and climate in a coupled ocean-atmosphere model: A dynamical systems approach
[NASA-CR-186499] N90-21502
Windshear case study: Denver, Colorado, July 11, 1988
[DOT/FAA/DS-89/19] N90-21509
Modeling the upper ocean and its interaction with the atmosphere
[DE90-008980] N90-21511
Model atmospheres for novae during the early stages
[NASA-CR-180498] N90-21694

ATMOSPHERIC PHYSICS
JPRS report. Science and technology. USSR: Earth sciences
[JPRS-UES-88-004] N90-21431
JPRS report. Science and technology. USSR: Earth sciences
[JPRS-UES-89-002] N90-21432
JPRS report: Science and technology. USSR: Earth sciences
[JPRS-UES-90-005] N90-21433

ATMOSPHERIC PRESSURE
Zones of feasibility for retrieval of surface pressure from observations of absorption in the A band of oxygen
[DAR-TP-19] N90-21495

ATMOSPHERIC RADIATION
A radiological assessment of nuclear power and propulsion operations near Space Station Freedom
[NASA-CR-185185] N90-21108

ATMOSPHERIC SOUNDING
Preliminary report on the demonstration of the VAS CO2 cloud parameters (cover, height, and amount) in support of ASOS
[NOAA-TM-NESDIS-29] N90-21498

ATOM CONCENTRATION
Mechanistic model for catalytic recombination during aerobraking maneuvers
[NASA-CR-185611] N90-21059

ATOMIC COLLISIONS
US-Japan Workshop on Atomic Collisions in Solids: Abstracts of lectures
[DE90-008979] N90-21611

ATOMIC PHYSICS
Center for Atomic, Molecular, and Optical Physics: Technical activities
[PB90-133158] N90-21591
Helium transport in plasma edge regions N90-21625
Atomic processes in high temperature plasmas
[DE90-008873] N90-21632

ATOMIC SPECTRA
Study of new technique of solid combustible materials to determination of volatile elements by flame atomic absorption spectrophotometry
[DE90-612907] N90-21147

ATOMIC STRUCTURE
Ordering mechanism in substitutional Ni-Cr alloys: Theory and experiment
[DE90-006268] N90-21156
New surface atomic structures for column 5 overlayers on the (110) surfaces of 3-5 compound semiconductors
[DE90-009003] N90-21663

ATTITUDE (INCLINATION)
Optimization of the effective GPS data rate N90-20932

ATTITUDE CONTROL
LACE flight dynamics experiment N90-21086
Design of a digital model following controller of reaction wheel torques
[INPE-4753-PRE/1425] N90-21093
Attitude control modes for the MECB remote sensing satellites
[INPE-4755-PRE/1427] N90-21094
Numerical simulation model for hydrazine attitude control thrusters. Part 1: Model description
[INPE-4952-RPE/601] N90-21115

AUDIO SIGNALS
Direct Radio Broadcasting by Satellite (DRBS): A review of the technical factors and system approaches suitable for mobile and fixed reception
[BBC-RD-1989/4] N90-21221

AUGER EFFECT
Surface characterization of hydrogen charged and uncharged alpha-2 and gamma titanium aluminide alloys using AES and REELS
[NASA-CR-186561] N90-21171

AUGER SPECTROSCOPY
Magnetron sputtered boron films and Ti/B multilayer structures
[DE90-009190] N90-21153

AUSTRALIA
A requirement for Australian research: Access to big science facilities, a report by the Australian National Committee for Crystallography
[DE90-614784] N90-21048

AUTOMATED PILOT ADVISORY SYSTEM
The influence of ice accretion physics on the forecasting of aircraft icing conditions N90-20928

AUTOMATIC CONTROL
Thermal control system corrosion study
[NASA-TM-102220] N90-21294

AUTOMATIC FLIGHT CONTROL
Design of a helicopter automatic flight control system using adaptive control N90-21040

AUTONOMOUS NAVIGATION
Autonomous integrated GPS/INS navigation experiment for OMV. Phase 1: Feasibility study
[NASA-CR-4267] N90-20969

AUTORADIOGRAPHY
Neutron autoradiography of hydrogen
[DE90-612930] N90-21148

AVIONICS
Joint University Program for Air Transportation Research, 1988-1989
[NASA-CP-3063] N90-20921
Optimization of the effective GPS data rate N90-20932
Advanced Launch System (ALS): Electrical actuation and power systems improve operability and cost picture
[NASA-TM-102547] N90-21271

AXIAL FLOW
Relating flow between counter-rotating propellers to aerodynamic interaction noise N90-20944

AXIAL FLOW TURBINES
Calculation of the secondary flow in an axial turbine N90-21022
Research on cascade secondary and tip-leakage flows: Periodicity and surface flow visualization N90-21026
Computational prediction and measurement of the flow in axial turbine cascades and stages N90-21028

AXIAL STRESS
Flutter of slender bodies under axial stress
[PB90-167024] N90-21425

AXISYMMETRIC FLOW
The radiation of sound from a propeller at angle of attack
[NASA-CR-4264] N90-21602

B

B STARS
A theoretical study of circumstellar dust around Ae/Be stars N90-21700
Evolutionary effects in B stars N90-21704

B-58 AIRCRAFT
Sonic boom signature data from cruciform microphone array experiments during the 1966-1967 EAFB national sonic boom evaluation program
[NASA-CR-182027] N90-21605

B-70 AIRCRAFT
Sonic boom signature data from cruciform microphone array experiments during the 1966-1967 EAFB national sonic boom evaluation program
[NASA-CR-182027] N90-21605

BACKGROUND NOISE
An ultra-small capacitance Josephson junction
[DE90-613396] N90-21653

BACTERIA
Anaerobic metabolism of aromatic compounds by phototrophic bacteria: Biochemical aspects
[DE90-009503] N90-21516

BALLISTICS
Ductile alloy encapsulated ceramic armor development
[AD-A217632] N90-21183

BALLOON SOUNDING
Investigations into the properties, conditions, and effects of the ionosphere
[AD-A217807] N90-21489

BALLOON-BORNE INSTRUMENTS
A general-purpose balloon-borne pointing system for solar scientific instruments
[NASA-TP-3013] N90-21219

BALTIC SEA
Transformation and deposition of airborne gaseous and particulate pollutants during transport over the Baltic Sea
[PUBL-AIR-QUALITY-5] N90-21478

BANACH SPACE
Periodic solutions for Hamiltonian systems in a nonconvex potential well
[DE90-612752] N90-21580

BANDPASS FILTERS
Coplanar waveguide discontinuities for P-I-N diode switches and filter applications
[NASA-TM-102534] N90-21278

BANDSTOP FILTERS
Coplanar waveguide discontinuities for P-I-N diode switches and filter applications
[NASA-TM-102534] N90-21278

BANDWIDTH
HDTV bandwidth reduction using motion compensation and DATV
[BBC-RD-1989/10] N90-21254

BARIUM OXIDES
Deformation processing of YBa2Cu3O(sub x)
[DE90-007795] N90-21644

BASALT
Geology of Espinhaco Meridional, including the Quadrilatero Ferrifero: Integration through remote sensing data
[INPE-4904-PRE/1505] N90-21450

BEACONS
Data Link Processor (DLP) project transition plan
[DOT/FAA/CT-TN89/68] N90-21256

BEAM CURRENTS
Proposal for FY86 Lawrence Livermore National Laboratory particle beam research
[DE90-007936] N90-21617

BEAMS (RADIATION)
Energy beam treatment for improved adhesion of coatings to surfaces
[AD-D014449] N90-21190
BEHAVIOR
Biological effects of ELF (Extremely-Low-Frequency) electric and magnetic fields
[DE90-008634] N90-21514
BENDING
A modification of a low-order Reissner-Mindlin plate bending element
[PB90-165630] N90-21428
BERYLLIUM
Formation of subsurface aluminum layers in beryllium by ion implantation and post-implant annealing
[DE90-007975] N90-21172
BIBLIOGRAPHIES
A compendium of sources of fracture toughness and fatigue crack growth data for metallic alloys, part 4
[NASA-TM-102646] N90-21164
Microgravity science and applications bibliography, 1989 revision
[NASA-TM-4192] N90-21207
JPRS report: Science and technology. USSR: Electronics and electrical engineering
[JPRS-UEE-90-002] N90-21284
Tenth International Free Electron Laser Conference
[DE90-614773] N90-21376
JPRS report. Science and technology. USSR: Earth sciences
[JPRS-UES-88-004] N90-21431
JPRS report. Science and technology. USSR: Earth sciences
[JPRS-UES-89-002] N90-21432
JPRS report: Science and technology. USSR: Earth sciences
[JPRS-UES-90-005] N90-21433
JPRS report: Science and technology. USSR: Life sciences
[JPRS-ULS-90-002] N90-21434
Geobotanical remote sensing: A review
[INPE-5026-PRE/1565] N90-21440
Annotated bibliography of software engineering laboratory literature
[NASA-TM-103313] N90-21536
Collected software engineering papers, volume 7
[NASA-TM-103312] N90-21537
Collected software engineering papers, volume 6
[NASA-TM-103309] N90-21540
JPRS report: Science and technology. USSR: Physics and mathematics
[JPRS-UPM-90-002] N90-21593
The Shock and Vibration Digest, volume 22, no. 2 N90-21596
Current experiments in elementary particle physics
[DE90-008062] N90-21607
Small business innovation research. Abstracts of 1988 phase 1 awards
[NASA-TM-102991] N90-21680
Small business innovation research. Abstracts of completed 1987 phase 1 projects
[NASA-TM-101797] N90-21681
BICRYSTALS
High voltage/high resolution studies of metal and semiconductor interfaces
[DE90-009065] N90-21656
BILLETS
Method of making a long life high current density cathode from tungsten and iridium powders using a quarternary compound as the impregnant
[AD-D014425] N90-21211
BINARY DATA
VLSI binary updown counter
[NASA-CASE-NPO-17205-1-CU] N90-21525
BINDERS (MATERIALS)
High gloss corrosion-resistant coatings
[AD-D014403] N90-21184
Methods for improving the flowability of a percussion primer composition
[MRL-TR-89-32] N90-21201
BIOASTRONAUTICS
Small business innovation research. Abstracts of 1988 phase 1 awards
[NASA-TM-102991] N90-21680
Small business innovation research. Abstracts of completed 1987 phase 1 projects
[NASA-TM-101797] N90-21681
BIOCHEMISTRY
Final safety analysis report for the Ulysses Mission. Volume 3 (Book 2): Nuclear risk analysis document-appendices
[DE90-008692] N90-21102
JPRS report: Science and technology. USSR: Life sciences
[JPRS-ULS-90-002] N90-21434
Biological effects of ELF (Extremely-Low-Frequency) electric and magnetic fields
[DE90-008634] N90-21514
Anaerobic metabolism of aromatic compounds by phototrophic bacteria: Biochemical aspects
[DE90-009503] N90-21516
BIOLOGICAL EFFECTS
Biological effects of ELF (Extremely-Low-Frequency) electric and magnetic fields
[DE90-008634] N90-21514
BIOPHYSICS
Modelling of molecular structures and properties in physical chemistry and biophysics
[AD-A214561] N90-21145
JPRS report: Science and technology. USSR: Life sciences
[JPRS-ULS-90-002] N90-21434
BIOTECHNOLOGY
Artificial life: The coming evolution
[DE90-008860] N90-21515
BISMUTH ALLOYS
Phase equilibria and solution thermodynamics of bismuth-lead alloys
[PB90-138421] N90-21163
BISTATIC REFLECTIVITY
The measurement of surface reflectivity at millimetre wavelengths
[MRL-TN-559] N90-21222
BIT ERROR RATE
Bit-error-rate testing of fiber optic data links for MMIC-based phased array antennas
[NASA-TM-102523] N90-21261
BLACK BODY RADIATION
A modified Moebius inverse formula and its applications in physics
[DE90-612740] N90-21594
Model atmospheres for novae during the early stages
[NASA-CR-180498] N90-21694
BLACK HOLES (ASTRONOMY)
Toward quantum corrections in black hole thermodynamics N90-21702
BLADDER
Rapidly quantifying the relative distention of a human bladder
[NASA-CASE-LAR-13901-1-NP] N90-21519
BLADE TIPS
Losses in the tip-leakage flow of a planar cascade of turbine blades N90-21027
Analysis of the rotor tip leakage flow with tip cooling air ejection N90-21029
BLAST LOADS
Minutes of the 23rd Explosives Safety Seminar, volume 1
[AD-A218264] N90-21213
Minutes of the 23rd Eplosives Safety Seminar, volume 2
[AD-A218265] N90-21214
BLUE STARS
Evolutionary effects in B stars N90-21704
BLUNT BODIES
An approximate viscous shock layer method for calculating the hypersonic flow over blunt-nosed bodies N90-20947
BLUNT LEADING EDGES
Effects of nose bluntness and shock-shock interactions on blunt bodies in viscous hypersonic flows
[NASA-CR-186451] N90-20950
BOEING AIRCRAFT
Boeing 727-100 test project (high energy radiated field tests)
[DOT/FAA/CT-88/33] N90-21247
BOEING 747 AIRCRAFT
SOFIA: Stratospheric Observatory for Infrared Astronomy N90-21346
BOILING
Boron-containing organosilane polymers and ceramic materials thereof
[NASA-CASE-ARC-11649-2-SB] N90-21177
BOLOMETERS
Systematic errors in power measurements made with a dual six-port ANA
[PB90-145160] N90-21276
A 100 micro Kelvin bolometer system for SIRTF N90-21317
A progress report on using bolometers cooled by adiabatic demagnetization refrigeration N90-21318
BOLTZMANN-VLASOV EQUATION
Relativistic stimulated Brillouin and Raman scattering in a laser-produced plasma
[DE90-613123] N90-21627
On the relativistic Vlasov equation in guiding-center coordinates
[DE90-613241] N90-21629
BOOLEAN ALGEBRA
VLSI binary updown counter
[NASA-CASE-NPO-17205-1-CU] N90-21525
BOOSTER ROCKET ENGINES
Hydrocarbon-fuel/combustion-chamber-liner materials compatibility
[NASA-CR-185203] N90-21165
BOOSTERS (EXPLOSIVES)
Preparation, characterisation and cookoff behaviour of booster compositions prepared from RDX and acrylic or ethylene-vinyl acetate dispersions
[MRL-TR-89-44] N90-21203
Determination of detonation parameters of booster explosives at small charge diameters
[MRL-TR-89-45] N90-21204
BOREHOLES
In-situ permeable flow sensor
[DE90-008806] N90-21364
BORON
Magnetron sputtered boron films and Ti/B multilayer structures
[DE90-009190] N90-21153
Grain boundary precipitation in Ni3Al based alloys
[AERE-R-13362] N90-21161
Lecture on ordered intermetallic alloys
[DE90-009011] N90-21189
Boron-containing organosilane polymers and ceramic materials thereof
[NASA-CASE-ARC-11649-2-SB] N90-21177
BOSONS
Extension of the constraints algebra for the closed string with the fixed topology world sheet
[DE90-612745] N90-21577
Extension of the Krichever-Novikov algebra in the closed string theory
[DE90-612746] N90-21578
String dynamics in curved space-time revisited
[DE90-612796] N90-21674
BOUNDARY LAYER FLOW
Relating flow between counter-rotating propellers to aerodynamic interaction noise N90-20944
Comparison of C- and O-grid generation methods using a NACA 0012 airfoil
[AD-A216375] N90-20948
On the instability of Goertler vortices to nonlinear travelling waves
[NASA-CR-181994] N90-21289
The effects of forcing on a single stream shear layer and its parent boundary layer
[NASA-CR-186529] N90-21301
BOUNDARY LAYER STABILITY
On the instability of Goertler vortices to nonlinear travelling waves
[NASA-CR-181904] N90-21289
BOUNDARY LAYER TRANSITION
Flight test investigation of certification issues pertaining to general-aviation-type aircraft with natural laminar flow
[NASA-CR-181967] N90-20952
BOUNDARY VALUE PROBLEMS
A system for transonic wing design with geometric constraints based on an inverse method N90-20983
Subsonic and transonic blade design by means of analysis codes N90-20985
A computational design method for shock free transonic cascades and airfoils N90-20986
Compact scheme for systems of equations applied to fundamental problems of mechanics of continua
[NASA-CR-186494] N90-21292
Theory and application of nonlinear normal mode initialization
[PB90-166000] N90-21497
Compact finite volume methods for the diffusion equation
[NASA-CR-186477] N90-21568
Finite element algorithms for hyperbolic conservation laws with forcing terms
[INPE-5024-RPE/617] N90-21595
High energy phenomena during solar flares
[INPE-4961-TDL/390] N90-21713
BOUSSINESQ APPROXIMATION
Numerical simulation of vortex breakdown N90-21288
Stability of a solitary wave solution to a set of coupled Boussinesq-like equations
[DE90-008927] N90-21586
BRAZIL
Evolution of remote sensing applied to vegetation and forest at INPE
[INPE-4970-PRE/1538] N90-21452
Analysis of water quality parameters of the Piaui River (SE), Brazil, through field and TM/LANDSAT sensor data
[INPE-4918-PRE/1417] N90-21453
Aerial photography as an aid for agricultural credit control
[INPE-5019-RPE/613] N90-21455

Contribution for the study of the evolution of part of the Espinhaco supergroup and its foundation through fracture analysis
[INPE-4907-PRE/1508] N90-21459
Wheat productivity estimate through field radiometry
[INPE-4994-PRE/1556] N90-21460
Regional remote sensing laboratory
[INPE-4922-PRE/1519] N90-21465
Radon concentration over the Brazilian Amazon Basin during the wet season (Belem-Manaus GTE-ABLE-2B flight of April 24, 1987)
[INPE-4892-PRE/1493] N90-21486

BRAZILIAN SPACE PROGRAM
Space environment simulation of the SCD-01 satellite through heating plates
[INPE-4988-PRE/1550] N90-21105

BRAZING
Effects of titanium on some surface properties of nitride ceramics
[AERE-R-13566] N90-21178
Review of the state of the technology for joining ceramics for high-temperature structural applications
[DE90-009224] N90-21199

BREADBOARD MODELS
An experimental evaluation of two nonazeotropic refrigerant mixtures in a water-to-water breadboard heat pump
[DE90-009016] N90-21305

BREMSSTRAHLUNG
VLA observations of the coronal plasma
[NASA-CR-186540] N90-21711
Flare stars at radio wavelengths
[NASA-CR-186539] N90-21719

BRIGHTNESS TEMPERATURE
VLA observations of the coronal plasma
[NASA-CR-186540] N90-21711
Flare stars at radio wavelengths
[NASA-CR-186539] N90-21719

BRILLOUIN EFFECT
Relativistic stimulated Brillouin and Raman scattering in a laser-produced plasma
[DE90-613123] N90-21627

BRILLOUIN ZONES
High-resolution Brillouin gain spectroscopy in solids
[DE90-009475] N90-21155

BROADCASTING
Direct Radio Broadcasting by Satellite (DRBS): A review of the technical factors and system approaches suitable for mobile and fixed reception
[BBC-RD-1989/4] N90-21221
Prediction of VHF/UHF mobile reception in urban areas: Comparison with measurements in London
[BBC-RD-1989/11] N90-21255
JPRS report: Science and technology. USSR: Electronics and electrical engineering
[JPRS-UEE-90-002] N90-21284

BROWN DWARF STARS
Discovery of low mass objects in Taurus N90-21329

BUCKLING
Compressive behavior of laminated composite structures N90-21134
User manual for VICONOPT: An exact analysis and optimum design program covering the buckling and vibration of prismatic assemblies of flat in-plane loaded, anisotropic plates, with approximations for discrete supports, and transverse stiffeners
[NASA-CR-181966] N90-21413
Review of formulae for the buckling of simply-supported, orthotropic plates under shear load, including transverse shear effects
[PB90-167073] N90-21429

C

C BAND
The PHARUS project: Design of a polarimetric C-band SAR in the Netherlands N90-21228
A motion compensation study for the PHARUS project N90-21235

C-141 AIRCRAFT
Stressed detector arrays for airborne astronomy N90-21332

CADASTRAL MAPPING
Aerial photography as an aid for agricultural credit control
[INPE-5019-RPE/613] N90-21455

CALCULUS OF VARIATIONS
A Lagrangian formalism for nonequilibrium ensembles
[DE90-612748] N90-21579
Linking numbers and variational method
[DE90-612793] N90-21582

CALIBRATING
Calibration of Hewlett-Packard network analyzers: A precision viewpoint
[NASA-CR-181989] N90-21262
Systematic errors in power measurements made with a dual six-port ANA
[PB90-145160] N90-21276
Software to characterize tuning fork resonators used in the Quartz Digital Accelerometer
[DE90-007913] N90-21363
Error correction of the DEA (Digital Electronic Automation) coordinate measuring machines at LLNL
[DE90-008913] N90-21365
Absolute multilayer characterization at high spatial resolution via real-time soft x ray imaging
[DE90-009181] N90-21371
Mechanics of interface fracture N90-21408
Possible use of satellite data for flood plain mapping
[INPE-4968-PRE/1537] N90-21462
SR90, strontium shaped-charge critical ionization velocity experiment
[NASA-CR-186501] N90-21606

CALORIMETERS
Improved Thermo-Oxidative-Deposition screening tests for turbine lubricants
[AD-A217795] N90-21188
High power, high sensitivity microwave calorimeter
[AD-D014427] N90-21355

CAMERAS
Ga:Ge array development N90-21323
Study of advanced InSb arrays for SIRTF (Space Infrared Telescope Facility) N90-21325
Experience with the UKIRT InSb array camera N90-21327
Reduction and analysis techniques for infrared imaging data N90-21328
High resolution imaging of the Venus night side using a Rockwell 128x128 HgCdTe array N90-21330
Initial astronomical results with a new 5-14 micron Si:Ga 58x62 DRO array camera N90-21334
Low noise HgCdTe 128 x 128 SWIR FPA for Hubble space telescope N90-21337
Future directions for NICMOS arrays N90-21339
Status of the isophot detector development N90-21342
ISO camera array development status N90-21344

CANARD CONFIGURATIONS
Constrained spanload optimization for minimum drag of multi-lifting-surface configurations N90-20992

CANCER
Proceedings of a workshop on Carcinogenic Potential of Extremely Low Frequency Magnetic Fields
[DE90-614340] N90-21520

CANOPIES (VEGETATION)
Principles of the radiosity method for canopy reflectance modeling
[DE90-008943] N90-21466

CANTILEVER BEAMS
United States Air Force Academy get-away-special flexible beam experiment N90-21088

CAPACITANCE
Simulator comparison of thumball, thumb switch, and touch screen input concepts for interaction with a large screen cockpit display format
[NASA-TM-102587] N90-21005
Calibration of Hewlett-Packard network analyzers: A precision viewpoint
[NASA-CR-181989] N90-21262
An ultra-small capacitance Josephson junction
[DE90-613396] N90-21653

CAPS (EXPLOSIVES)
Minutes of the 23rd Explosives Safety Seminar, volume 1
[AD-A218264] N90-21213

CARBON
Direct sublimation of NaCl salt from carbon matrixes
[DE90-007927] N90-21139

CARBON CYCLE
Modeling the upper ocean and its interaction with the atmosphere
[DE90-008980] N90-21511

CARBON DIOXIDE
Source attribution for tropospheric ozone in the US
[DE90-007994] N90-21484
Preliminary report on the demonstration of the VAS CO2 cloud parameters (cover, height, and amount) in support of ASOS
[NOAA-TM-NESDIS-29] N90-21498

CARBON DIOXIDE CONCENTRATION
Sensitivity studies in a two-dimensional atmospheric transport model
[DAR-TP-18] N90-21496

CARBON DIOXIDE LASERS
Cloud hole-boring with long pulse CO2 lasers
[DE90-008946] N90-21377

CARBON STARS
The evolution and geometry of the outer parts of the small Magellanic cloud N90-21697

CARBONIZATION
Low energy ion generator
[DE90-759905] N90-21195

CARCINOGENS
Proceedings of a workshop on Carcinogenic Potential of Extremely Low Frequency Magnetic Fields
[DE90-614340] N90-21520

CARTESIAN COORDINATES
Direct formulation of a 4-node hybrid shell element with rotational degrees of freedom
[NASA-CR-4282] N90-21411

CASCADE FLOW
A two-dimensional unsteady analysis for transonic and supersonic cascade flows N90-20955
A computational design method for shock free transonic cascades and airfoils N90-20986
An inverse method for the design of turbomachine blades N90-20988
Secondary flows and Reynolds stress distributions downstream of a turbine cascade at different expansion ratios N90-21015
An investigation of secondary flows in nozzle guide vanes N90-21016
Secondary flow in a turbine guide vane with low aspect ratio N90-21018
Measurement of the flow field in the blade passage and side-wall region of a plane turbine cascade N90-21019
Centrifugal impeller geometry and its influence on secondary flows N90-21020
Calculation of the three dimensional turbulent flow in a linear turbine blade N90-21021
Research on cascade secondary and tip-leakage flows: Periodicity and surface flow visualization N90-21026
Losses in the tip-leakage flow of a planar cascade of turbine blades N90-21027
Computational prediction and measurement of the flow in axial turbine cascades and stages N90-21028
Detailed heat transfer measurements in nozzle guide vane passages in linear and annular cascades in the presence of secondary flows N90-21030
The effect of secondary flow on the redistribution of the total temperature field downstream of a stationary turbine cascade N90-21033

CASTING
Strengthening mechanisms of tungsten powder reinforced uranium
[DE90-009331] N90-21144
Pressure rig for repetitive casting
[NASA-CASE-LAR-14050-1] N90-21216
A casting and imaging technique for determining void geometry and relative permeability behavior of a single fracture specimen
[DE90-009192] N90-21403

CASTINGS
A casting and imaging technique for determining void geometry and relative permeability behavior of a single fracture specimen
[DE90-009192] N90-21403

CATALYTIC ACTIVITY
Mechanistic model for catalytic recombination during aerobraking maneuvers
[NASA-CR-185611] N90-21059

CATHODES
Method of making a long life high current density cathode from tungsten and iridium powders using a quarternary compound as the impregnant
[AD-D014425] N90-21211
An attempt to measure cold-fusion effects
[DE90-613248] N90-21649

CAVITIES
Pressure rig for repetitive casting
[NASA-CASE-LAR-14050-1] N90-21216
Thermal radiation characteristics of nonisothermal cylindrical enclosures using a numerical ray tracing technique
[NASA-TM-102527] N90-21296

CAVITONS
Dynamics of cavitons in strong Langmuir turbulence
[DE90-008918] N90-21633

CELLS (BIOLOGY)
Does DNA cytometry have a place in the clinical laboratory
[DE90-007652] N90-21512

CEMENTS
Criteria for polymer concrete on airport pavements
[DOT/FAA/DS-89/18] N90-21045

CENSUS
Census of US civil aircraft
[PB90-120296] N90-20920

CENTRIFUGAL COMPRESSORS
Flow in a forward swept centrifugal fan, volumes 1 and 2 N90-20959

CENTRIFUGES
Space adaptation syndrome induced by a long duration +3Gx centrifuge run
[AD-A218248] N90-21518

CEPSTRAL ANALYSIS
Cepstrum analysis and applications to computational fluid dynamic solutions N90-21302
CERAMIC BONDING
Ductile alloy encapsulated ceramic armor development
[AD-A217632] N90-21183
CERAMIC MATRIX COMPOSITES
Nicalon/siliconoxycarbide ceramic composites
[NASA-TM-102563] N90-21133
Small business innovation research. Abstracts of completed 1987 phase 1 projects
[NASA-TM-101797] N90-21681
CERAMICS
Nicalon/siliconoxycarbide ceramic composites
[NASA-TM-102563] N90-21133
Boron-containing organosilane polymers and ceramic materials thereof
[NASA-CASE-ARC-11649-2-SB] N90-21177
Effects of titanium on some surface properties of nitride ceramics
[AERE-R-13568] N90-21178
Ductile alloy encapsulated ceramic armor development
[AD-A217632] N90-21183
Fracture toughness and crack growth of Zerodur
[NASA-TM-4185] N90-21187
Energy beam treatment for improved adhesion of coatings to surfaces
[AD-D014449] N90-21190
ZELED analysis of aperiodicity and bond lengths in ceramic powders
[DE90-612932] N90-21193
Research advances in fine ceramics
[DE90-008963] N90-21197
Review of the state of the technology for joining ceramics for high-temperature structural applications
[DE90-009224] N90-21199
Pressure rig for repetitive casting
[NASA-CASE-LAR-14050-1] N90-21216
Ultrasonic and radiographic evaluation of advanced aerospace materials: Ceramic composites
[NASA-TM-102540] N90-21401
Research programs in aeronautical engineering, solid state physics, and materials science at Technion-Israel Institute of Technology, Haifa, Israel
[EOARD-LR-89-068] N90-21720
CERENKOV RADIATION
A balloon measurement of the isotopic composition of galactic cosmic ray iron N90-21717
A search for very high energy gamma rays from the Crab pulsar-nebula N90-21718
CERMETS
Research programs in aeronautical engineering, solid state physics, and materials science at Technion-Israel Institute of Technology, Haifa, Israel
[EOARD-LR-89-068] N90-21720
CERTIFICATION
Sole means navigation and integrity through hybrid Loran-C and NAVSTAR GPS N90-20933
Brake performance of the McDonnell Douglas DC-10-30/40 during high speed, high energy rejected takeoffs
[PB90-917004] N90-21000
CHANNEL CAPACITY
SAR image coding N90-21246
Feasibility of using frequency offset on very high frequency air/ground voice channels
[DOT/FAA/CT-TN89/71] N90-21248
CHARACTERIZATION
Surface characterization of hydrogen charged and uncharged alpha-2 and gamma titanium aluminide alloys using AES and REELS
[NASA-CR-186561] N90-21171
Evolution of remote sensing applied to vegetation and forest at INPE
[INPE-4970-PRE/1538] N90-21452
Characterization of the plasma in magnetic multidipole discharges
[DE90-613219] N90-21628
CHARGE DISTRIBUTION
Near contact phenomena and transient effects in far infrared photoconductors N90-21316
CHARGE INJECTION DEVICES
ISO camera array development status N90-21344
CHARGE TRANSFER
Modelling of molecular structures and properties in physical chemistry and biophysics
[AD-A214561] N90-21145
CHARGED PARTICLES
Charged-particle beam research program
[DE90-007937] N90-21618
Some global problems in gauge theories (variations on a theme of Aharonov and Bohm)
[DE90-009034] N90-21678
CHEMICAL ANALYSIS
A solution level indicator system
[DE90-007939] N90-21151
Analytical sciences
[DE90-007965] N90-21152
An evaluation of metal salts of 3-nitro-1,2,4-triazol-5-one (NTO) as potential primary explosives
[MRL-TN-563] N90-21202
Thermal control system corrosion study
[NASA-TM-102220] N90-21294
CHEMICAL ATTACK
Combination primer/topcoat coating
[AD-D014445] N90-21189
CHEMICAL BONDS
Modelling of molecular structures and properties in physical chemistry and biophysics
[AD-A214561] N90-21145
Boron-containing organosilane polymers and ceramic materials thereof
[NASA-CASE-ARC-11649-2-SB] N90-21177
A new class of lubricants derived from archaebacterial lipids
[AD-D014429] N90-21185
New surface atomic structures for column 5 overlayers on the (110) surfaces of 3-5 compound semiconductors
[DE90-009003] N90-21683
CHEMICAL COMPOSITION
Grain boundary precipitation in Ni3Al based alloys
[AERE-R-13362] N90-21161
Methods for improving the flowability of a percussion primer composition
[MRL-TR-89-32] N90-21201
Evolutionary effects in B stars N90-21704
A balloon measurement of the isotopic composition of galactic cosmic ray iron N90-21717
CHEMICAL EFFECTS
Anaerobic metabolism of aromatic compounds by phototrophic bacteria: Biochemical aspects
[DE90-009503] N90-21516
CHEMICAL ENGINEERING
Compact scheme for systems of equations applied to fundamental problems of mechanics of continua
[NASA-CR-186494] N90-21292
CHEMICAL EQUILIBRIUM
Ionic equilibrium between octahedral and tetrahedral complexes in liquid aluminium-sodium fluoride mixtures
[DE90-613890] N90-21150
Controlled production and characterization of metastable intermetallics
[DE90-009384] N90-21176
CHEMICAL REACTIONS
Computation of nonequilibrium chemically reacting flows in hypersonic flow field N90-20954
Modelling of molecular structures and properties in physical chemistry and biophysics
[AD-A214561] N90-21145
Compatibility of Au base thick films with solder alloys: Solid state growth of intermetallics
[DE90-009285] N90-21175
Shock initiation sensitivity of damaged TP-H1207C composite propellant
[DE90-008509] N90-21205
Transformation and deposition of airborne gaseous and particulate pollutants during transport over the Baltic Sea
[PUBL-AIR-QUALITY-5] N90-21478
Thermogravimetric analysis of Nd(2-x)Ce(x)CuO(4-delta)
[DE90-009184] N90-21658
CHEMISORPTION
Laser studies of chemical dynamics at the gas-solid interface
[DE90-008698] N90-21380
CHESAPEAKE BAY (US)
MECCA program documentation
[NOAA-TR-NESDIS-46] N90-21477
CHIPS (MEMORY DEVICES)
VLSI single-chip (255,223) Reed-Solomon encoder with interleaver
[NASA-CASE-NPO-17280-1-CU] N90-21061
CHIRAL DYNAMICS
Generalized WKB approximation for stratified isotropic chiral structures
[PB90-165689] N90-21270
Studies in quantum field theory
[DE90-006731] N90-21677
CHROMATOGRAPHY
Analytical sciences
[DE90-007965] N90-21152
CHROMIUM ALLOYS
Ordering mechanism in substitutional Ni-Cr alloys: Theory and experiment
[DE90-006268] N90-21156
High-temperature oxidation and sulfidation of Fe-20Cr-16Ni-4Al-1Y2O3 oxide-dispersion-strengthened alloy
[DE90-007897] N90-21168
On the stability of amorphous silica coatings for high temperature service
[AERE-R-13425] N90-21179
CIRCUITS
A real-time rejection circuit to automatically reject multiple interfering hopping signals while passing a lower level desired signal
[AD-D014424] N90-21251
JPRS report: Science and technology. USSR: Electronics and electrical engineering
[JPRS-UEE-90-002] N90-21284
Common source cascode amplifiers for integrating IR-FPA applications N90-21324
Short wavelength HgCdTe staring focal plane for low background astronomy applications N90-21336
An ultra-small capacitance Josephson junction
[DE90-613396] N90-21653
CITIES
Possible use of satellite data for flood plain mapping
[INPE-4968-PRE/1537] N90-21462
Performance evaluation of morphological edge detectors
[INPE-4975-PRE/1540] N90-21464
CIVIL AVIATION
Census of US civil aircraft
[PB90-120296] N90-20920
Civil air transport: A fresh look at power-by-wire and fly-by-light
[NASA-TM-102574] N90-21283
CLADDING
Ductile alloy encapsulated ceramic armor development
[AD-A217632] N90-21183
CLASSIFICATIONS
Modeling and control of flexible space platforms with articulated payloads N90-21073
Automatic classification of images
[AD-D014437] N90-21260
Survey of land use through remote sensing
[INPE-5032-MD/042] N90-21443
Digital processing of TM/LANDSAT data in monitoring interior water
[INPE-4958-PRE/1533] N90-21448
Multitemporal analysis of LANDSAT/TM digital imagery in the detection of areas affected by caterpillar (sibine fusca) attack in the dende (elais guineensis) palm plantation
[INPE-4979-PRE/1544] N90-21457
Evaluation of classification performance and proportion estimate of the sugar cane crop through PROCEDURE-INPE utilizing LANDSAT data
[INPE-4899-PRE/1500] N90-21458
CLEANING
The development of ultraviolet-ozone cleaning as a production process in the packaging of integrated circuits
[DE90-007960] N90-21220
CLEARING
Cloud hole-boring with long pulse CO2 lasers
[DE90-008946] N90-21377
CLIMATE
Modeling large-scale vegetation dynamics
[DE90-008883] N90-21485
Predictability of weather and climate in a coupled ocean-atmosphere model: A dynamical systems approach
[NASA-CR-186499] N90-21502
CLIMATE CHANGE
A fossil energy perspective on global climate change
[DE90-007894] N90-21483
Modeling the upper ocean and its interaction with the atmosphere
[DE90-008980] N90-21511
CLIMATOLOGY
A fossil energy perspective on global climate change
[DE90-007894] N90-21483
CLINICAL MEDICINE
JPRS report: Science and technology. USSR: Life sciences
[JPRS-ULS-90-002] N90-21434
CLOUD COVER
Preliminary report on the demonstration of the VAS CO2 cloud parameters (cover, height, and amount) in support of ASOS
[NOAA-TM-NESDIS-29] N90-21498
CLOUDS
Cloud hole-boring with long pulse CO2 lasers
[DE90-008946] N90-21377

CLOUDS (METEOROLOGY)
Preliminary report on the demonstration of the VAS CO2 cloud parameters (cover, height, and amount) in support of ASOS
[NOAA-TM-NESDIS-29] N90-21498
Meteorological influences on mountain cloudwater chemistry in the eastern United States
[PB90-132432] N90-21504
Numerical simulations of the cloud-capped marine boundary layer N90-21506
CLUTTER
Problems in ISAR processing with range resolution by stepped frequency bursts N90-21238
CMOS
Common source cascode amplifiers for integrating IR-FPA applications N90-21324
Low noise HgCdTe 128 x 128 SWIR FPA for Hubble space telescope N90-21337
HgCdTe 256x256 NWIR FPA N90-21348
COALESCING
Investigation of surface water behavior during glaze ice accretion N90-20927
High energy phenomena during solar flares
[INPE-4961-TDL/390] N90-21713
COASTAL WATER
Remote sensing applied to sea water quality researches in coastal regions: A review
[INPE-4935-PRE/1425] N90-21438
COASTS
MECCA program documentation
[NOAA-TR-NESDIS-46] N90-21477
COATINGS
Design and optimisation of thin foil x ray telescopes N90-21690
COCKPITS
Cockpit display of hazardous wind shear information N90-20924
Simulator comparison of thumball, thumb switch, and touch screen input concepts for interaction with a large screen cockpit display format
[NASA-TM-102587] N90-21005
The effect of windscreen bows and HUD pitch ladder format on pilot performance during simulated flight
[AD-A218139] N90-21523
CODERS
VLSI single-chip (255,223) Reed-Solomon encoder with interleaver
[NASA-CASE-NPO-17280-1-CU] N90-21061
CODING
Direct Radio Broadcasting by Satellite (DRBS): A review of the technical factors and system approaches suitable for mobile and fixed reception
[BBC-RD-1989/4] N90-21221
Lessons learned in the transition to Ada from FORTRAN at NASA/Goddard
[NASA-TM-103311] N90-21538
COEFFICIENT OF FRICTION
Studies of mechano-chemical interactions in the tribological behavior of materials
[NASA-TM-102545] N90-21182
Internal rotor friction instability
[NASA-CR-183942] N90-21395
COGNITION
Time and truth in plans N90-20930
COHERENT LIGHT
Method for holographic correction of beams of coherent light
[AD-D014406] N90-21353
COLD WORKING
Ductile alloy encapsulated ceramic armor development
[AD-A217632] N90-21183
COLLISIONLESS PLASMAS
Relativistic stimulated Brillouin and Raman scattering in a laser-produced plasma
[DE90-613123] N90-21627
On the relativistic Vlasov equation in guiding-center coordinates
[DE90-613241] N90-21629
A self-consistent theory of radial transport of field-aligned current by microturbulence
[DE90-007920] N90-21631
COLLOCATION
A fast collocation method for transonic airfoil design N90-20984
COLOR PHOTOGRAPHY
Aerial photography as an aid for agricultural credit control
[INPE-5019-RPE/613] N90-21455
COLOR-MAGNITUDE DIAGRAM
The evolution and geometry of the outer parts of the small Magellanic cloud N90-21697
COMBUSTION
Full-scale air transport category fuselage burnthrough tests
[DOT/FAA/CT-TN89/65] N90-20967
Study of new technique of solid combustible materials to determination of volatile elements by flame atomic absorption spectrophotometry
[DE90-612907] N90-21147
COMBUSTION CHAMBERS
Hydrocarbon-fuel/combustion-chamber-liner materials compatibility
[NASA-CR-185203] N90-21165
The modelling of heat and mass transfer near solid boundaries and comparison with experimental results
[PB90-167040] N90-21310
Microgravity acoustic mixing for particle cloud combustors
[NASA-CR-185159] N90-21600
COMBUSTION PRODUCTS
A fossil energy perspective on global climate change
[DE90-007894] N90-21483
COMET NUCLEI
The thermo-mechanical behavior of cometary nuclei N90-21703
COMET TAILS
A mechanism for the formation of knots, kinks and discontinuous events in the plasma tail of comets
[DE90-613285] N90-21707
COMETS
A mechanism for the formation of knots, kinks and discontinuous events in the plasma tail of comets
[DE90-613285] N90-21707
COMMERCE
Quality at a glance
[AD-A217297] N90-21400
Small business innovation research. Abstracts of 1988 phase 1 awards
[NASA-TM-102991] N90-21680
Small business innovation research. Abstracts of completed 1987 phase 1 projects
[NASA-TM-101797] N90-21681
COMMUNICATION NETWORKS
Fault tolerant hypercube computer system architecture
[NASA-CASE-NPO-16859-1-CU] N90-21527
COMPLEX SYSTEMS
Perspectives on the use of rule-based control N90-20940
COMPOSITE MATERIALS
Fracture of sandwiched composites N90-21136
Resistance mechanics for laminated composite materials
[INPE-4919-RPE/594] N90-21141
Combination primer/topcoat coating
[AD-D014445] N90-21189
Toughened YBa2Cu3O(sub x)/ZrO2 composites
[DE90-007796] N90-21645
COMPOSITE PROPELLANTS
Shock initiation sensitivity of damaged TP-H1207C composite propellant
[DE90-008509] N90-21205
COMPOSITE STRUCTURES
Filament winding of composite cylinders N90-21119
Fracture and longevity of composite structures
[AD-A217827] N90-21127
Multi-objective shape and material optimization of composite structures including damping
[NASA-TM-102579] N90-21132
Compressive behavior of laminated composite structures N90-21134
Structural tailoring of select fiber composite structures
[NASA-TM-102484] N90-21137
User manual for VICONOPT: An exact analysis and optimum design program covering the buckling and vibration of prismatic assemblies of flat in-plane loaded, anisotropic plates, with approximations for discrete supports, and transverse stiffeners
[NASA-CR-181966] N90-21413
Research programs in aeronautical engineering, solid state physics, and materials science at Technion-Israel Institute of Technology, Haifa, Israel
[EOARD-LR-89-068] N90-21720
COMPRESSIBILITY
Numerical simulation of vortex breakdown N90-21288
An internal/external pressure, tension/compression multiaxial fatigue system
[DE90-009510] N90-21430
COMPRESSIBLE BOUNDARY LAYER
Surface-cooling effects on compressible boundary-layer instability
[NASA-CR-182003] N90-21290
COMPRESSIBLE FLOW
Comparison of C- and O-grid generation methods using a NACA 0012 airfoil
[AD-A216375] N90-20948
Numerical method for designing 3D turbomachinery blade rows N90-20990
PROTEUS two-dimensional Navier-Stokes computer code, version 1.0. Volume 1: Analysis description
[NASA-TM-102551] N90-21303
PROTEUS two-dimensional Navier-Stokes computer code, version 1.0. Volume 2: User's guide
[NASA-TM-102552] N90-21306
COMPRESSING
Shock compression of solids: A tutorial
[DE90-009185] N90-21659
COMPRESSION LOADS
Fracture and longevity of composite structures
[AD-A217827] N90-21127
UNIVIMP: A universal instrument for the survey of initial imperfections of thin-walled shells
[PB90-167065] N90-21369
COMPRESSIVE STRENGTH
Compressive behavior of laminated composite structures N90-21134
COMPRESSOR BLADES
Inverse computation of transonic internal flows with application for multi-point-design of supercritical compressor blades N90-20987
COMPRESSOR ROTORS
Flow in a forward swept centrifugal fan, volumes 1 and 2 N90-20959
COMPRESSORS
Secondary flows and radial mixing predictions in axial compressors N90-21010
COMPUTATIONAL FLUID DYNAMICS
On total variation diminishing schemes for transonic turbulent flow computation N90-20945
Comparison of C- and O-grid generation methods using a NACA 0012 airfoil
[AD-A216375] N90-20948
Convergence acceleration of hypersonic flow calculations: A nonlinear relaxation factor N90-20957
Computational Methods for Aerodynamic Design (Inverse) and Optimization
[AGARD-CP-463] N90-20976
An efficient airfoil design method using the Navier-Stokes equations N90-20981
A computational design method for shock free transonic cascades and airfoils N90-20986
Inverse computation of transonic internal flows with application for multi-point-design of supercritical compressor blades N90-20987
An inverse method for the design of turbomachine blades N90-20988
Optimization of aerodynamic designs using computational fluid dynamics N90-20999
Secondary Flows in Turbomachines
[AGARD-CP-469] N90-21009
Secondary flows and radial mixing predictions in axial compressors N90-21010
A study on secondary flow and spanwise mixing in axial flow compressors N90-21012
Parabolized calculations of turbulent three dimensional flows in a turbine duct N90-21013
Experimental and numerical study on basic phenomena of secondary flows in turbines N90-21014
An investigation of secondary flows in nozzle guide vanes N90-21016
Secondary flow predictions for a transonic nozzle guide vane N90-21017
Secondary flow in a turbine guide vane with low aspect ratio N90-21018
Centrifugal impeller geometry and its influence on secondary flows N90-21020
Calculation of the three dimensional turbulent flow in a linear turbine blade N90-21021
Calculation of the secondary flow in an axial turbine N90-21022
Secondary flow calculations for axial and radial compressors N90-21024
Computational prediction and measurement of the flow in axial turbine cascades and stages N90-21028
Analysis of the rotor tip leakage flow with tip cooling air ejection N90-21029
Theoretical study of the flow in a rotating channel. Experimental study through flow visualization in a curved channel N90-21032
A cost-effective strategy for nonoscillatory convection without clipping
[NASA-TM-102538] N90-21291
Cepstrum analysis and applications to computational fluid dynamic solutions N90-21302
PROTEUS two-dimensional Navier-Stokes computer code, version 1.0. Volume 1: Analysis description
[NASA-TM-102551] N90-21303
PROTEUS two-dimensional Navier-Stokes computer code, version 1.0. Volume 2: User's guide
[NASA-TM-102552] N90-21306
PROTEUS two-dimensional Navier-Stokes computer code, version 1.0. Volume 3: Programmer's reference
[NASA-TM-102553] N90-21307
COMPUTATIONAL GRIDS
Comparison of C- and O-grid generation methods using a NACA 0012 airfoil
[AD-A216375] N90-20948

An overlapped grid method for multigrid, finite volume/difference flow solvers: MaGGIE
[NASA-CR-182008] N90-20953
Convergence acceleration of hypersonic flow calculations: A nonlinear relaxation factor N90-20957
A fast collocation method for transonic airfoil design N90-20984
A computational design method for shock free transonic cascades and airfoils N90-20986
Secondary flow predictions for a transonic nozzle guide vane N90-21017
Resistivity of pristine and intercalated graphite fiber epoxy composites
[NASA-TM-102576] N90-21192
A quasi-Lagrangian moving grid technique for investigating compressible flows N90-21298
A time-accurate adaptive grid method and the numerical simulation of a shock-vortex interaction
[NASA-TP-2998] N90-21524
Compact finite volume methods for the diffusion equation
[NASA-CR-186477] N90-21568
Adaptive grid embedding for the two-dimensional flux-split Euler equations
[NASA-CR-186533] N90-21571

COMPUTER AIDED DESIGN

The role of structural analysis in airworthiness certification
[BR112064] N90-20972
Computer-aided structural optimisation of aircraft structures
[BR112837] N90-20973
Computer-aided design of flywheel transmission systems N90-21392
CAD work station for electronics designer
[DE90-616473] N90-21546
The CAD/CAM product data standards: IGES/PDES (Initial Graphics Exchange Specification/Product Data Exchange Standards, the present and the future
[DE90-008803] N90-21549
Curvature continuity of cubic Bezier curves in the solid modeling aerospace research tools design software
[NASA-CR-186583] N90-21554

COMPUTER AIDED MANUFACTURING

Toward a new CIM (Computer Integrated Manufacturing) architecture for Sandia Laboratories
[DE90-008677] N90-21548
The CAD/CAM product data standards: IGES/PDES (Initial Graphics Exchange Specification/Product Data Exchange Standards, the present and the future
[DE90-008803] N90-21549

COMPUTER AIDED TOMOGRAPHY

High explosives (PBX9502) characterization using computerized tomography
[DE90-008170] N90-21404

COMPUTER COMPATIBLE TAPES

Introduction of digital image processing by remote sensors applied to geology
[INPE-5023-RPE/616] N90-21456

COMPUTER GRAPHICS

Modeling the temperature dependence of the thermal conductivity of aluminum nitride
[DE90-009428] N90-21154
High explosives (PBX9502) characterization using computerized tomography
[DE90-008170] N90-21404
The CAD/CAM product data standards: IGES/PDES (Initial Graphics Exchange Specification/Product Data Exchange Standards, the present and the future
[DE90-008803] N90-21549
Simulated image maps for use in experimental high-resolution electron microscopy
[DE90-009176] N90-21657

COMPUTER INFORMATION SECURITY

Software verification and validation: Its role in computer assurance and its relationship with software project management standards
[PB90-111691] N90-21530

COMPUTER NETWORKS

High performance computing and networking for science
[PB90-131228] N90-21526
Toward a new CIM (Computer Integrated Manufacturing) architecture for Sandia Laboratories
[DE90-008677] N90-21548

COMPUTER PROGRAMMING

Human centrifuge controller
[NAL-TM-SE-8901] N90-21043
Numerical Arc Segmentation Algorithm for a Radio Conference (NASARC), version 4.0: User's manual
[NASA-TM-101454] N90-21250
Software to characterize tuning fork resonators used in the Quartz Digital Accelerometer
[DE90-007913] N90-21363
Maintenance = reuse-oriented software development
[NASA-CR-186455] N90-21531
Integrating automated support for a software management cycle into the TAME system
[NASA-CR-186457] N90-21532
Annotated bibliography of software engineering laboratory literature
[NASA-TM-103313] N90-21536
Collected software engineering papers, volume 7
[NASA-TM-103312] N90-21537
Evolution of Ada technology in the flight dynamics area: Implementation/testing phase analysis
[NASA-TM-103310] N90-21539
Collected software engineering papers, volume 6
[NASA-TM-103309] N90-21540
System testing of a production Ada (trademark) project: The GRODY study
[NASA-TM-103308] N90-21541
Evolution of Ada technology in the flight dynamics area: Design phase analysis
[NASA-TM-103307] N90-21542
Software Management Environment (SME) concepts and architecture
[NASA-TM-103306] N90-21543
Implementation of a production Ada project: The GRODY study
[NASA-TM-103305] N90-21544
Software Engineering Laboratory (SEL) database organization and user's guide
[NASA-TM-103304] N90-21545
Exploiting virtual synchrony in distributed systems
[NASA-CR-182855] N90-21555
Numerical code AEOLUS-E1 for analysing free-boundary resistive MHD mode
[DE90-759903] N90-21630
Program CICC: Flow and heat transfer in Cable In Conduit Conductors, user's manual
[DE90-007924] N90-21661

COMPUTER PROGRAMS

An overlapped grid method for multigrid, finite volume/difference flow solvers: MaGGIE
[NASA-CR-182008] N90-20953
Convergence acceleration of hypersonic flow calculations: A nonlinear relaxation factor N90-20957
Aerofoil design techniques N90-20978
Constrained spanload optimization for minimum drag of multi-lifting-surface configurations N90-20992
Aerodynamic design by optimization N90-20996
Numerical optimization of wings in transonic flow N90-20997
Experimental and numerical study on basic phenomena of secondary flows in turbines N90-21014
Secondary flow in a turbine guide vane with low aspect ratio N90-21018
Generation and decay of secondary flows and their impact on aerodynamic performance of modern turbomachinery components N90-21023
Computational prediction and measurement of the flow in axial turbine cascades and stages N90-21028
Supersonic nozzle design of arbitrary cross-section N90-21035
Controlled multibody dynamics simulation for large space structures N90-21068
Detection of potential space station control/structure interaction with CO-ST-IN N90-21074
Filament winding of composite cylinders N90-21119
A computational model of the perforation of multi-layer metallic laminates
[MRL-RR-9-89] N90-21128
Structural tailoring of select fiber composite structures
[NASA-TM-102484] N90-21137
Computer processing of multi-channel electromagnetic data from an airborne geophysical survey system
[PB90-138413] N90-21253
The 4th Annual Review of Progress in Applied Computational Electromagnetics
[AD-A217912] N90-21257
The 5th Annual Review of Progress in Applied Computational Electromagnetics
[AD-A217994] N90-21258
Thermal radiation characteristics of nonisothermal cylindrical enclosures using a numerical ray tracing technique
[NASA-TM-102527] N90-21296
Computer codes for the evaluation of thermodynamic properties, transport properties, and equilibrium constants of an 11-species air model
[NASA-TM-102602] N90-21297
PROTEUS two-dimensional Navier-Stokes computer code, version 1.0. Volume 1: Analysis description
[NASA-TM-102551] N90-21303
PROTEUS two-dimensional Navier-Stokes computer code, version 1.0. Volume 2: User's guide
[NASA-TM-102552] N90-21306
PROTEUS two-dimensional Navier-Stokes computer code, version 1.0. Volume 3: Programmer's reference
[NASA-TM-102553] N90-21307
The modelling of heat and mass transfer near solid boundaries and comparison with experimental results
[PB90-167040] N90-21310
Phase-only holographic filters and their applications
[PB90-166802] N90-21368
Improved analytical capabilities for foil air bearings, phase 1
[AD-A218071] N90-21389
Aeropropulsion facilities configuration control: Procedures manual
[NASA-TM-102541] N90-21399
The computational structural mechanics testbed generic structural-element processor manual
[NASA-CR-181728] N90-21410
Stress analysis and minimum weight design of honeycomb sandwich plates N90-21418
An internal/external pressure, tension/compression multiaxial fatigue system
[DE90-009510] N90-21430
MECCA program documentation
[NOAA-TR-NESDIS-46] N90-21477
An outline for the analysis of wave induced bottom pressure fluctuations
[MRL-TN-558] N90-21510
Software verification and validation: Its role in computer assurance and its relationship with software project management standards
[PB90-111691] N90-21530
Integrating automated support for a software management cycle into the TAME system
[NASA-CR-186457] N90-21532
Collected software engineering papers, volume 7
[NASA-TM-103312] N90-21537
Lessons learned in the transition to Ada from FORTRAN at NASA/Goddard
[NASA-TM-103311] N90-21538
Evolution of Ada technology in the flight dynamics area: Implementation/testing phase analysis
[NASA-TM-103310] N90-21539
Collected software engineering papers, volume 6
[NASA-TM-103309] N90-21540
Software Management Environment (SME) concepts and architecture
[NASA-TM-103306] N90-21543
Implementation of a production Ada project: The GRODY study
[NASA-TM-103305] N90-21544
CAD work station for electronics designer
[DE90-616473] N90-21546
The CAD/CAM product data standards: IGES/PDES (Initial Graphics Exchange Specification/Product Data Exchange Standards, the present and the future
[DE90-008803] N90-21549
SIGNIF: A C function to compute significant digits
[DE90-009242] N90-21550
Hypercluster parallel processing library user's manual
[NASA-CR-185231] N90-21552
Curvature continuity of cubic Bezier curves in the solid modeling aerospace research tools design software
[NASA-CR-186583] N90-21554
OTTER (Organized Techniques for Theorem-proving and Effective Research) 2.0 users guide
[DE90-007978] N90-21563
Modeling high-temperature superconductors and metallic alloys on the Intel IPSC/860
[DE90-009402] N90-21665
STORM: A statistical object representation model
[DE90-009048] N90-21686

COMPUTER STORAGE DEVICES

CAMAC memory module: MEMO-32
[DE90-759846] N90-21528
Quadratic Hadamard Memories 1
[AD-A217224] N90-21534

COMPUTER SYSTEMS DESIGN

System testing of a production Ada (trademark) project: The GRODY study
[NASA-TM-103308] N90-21541
Evolution of Ada technology in the flight dynamics area: Design phase analysis
[NASA-TM-103307] N90-21542

COMPUTER SYSTEMS PERFORMANCE

Selective automatic fire extinguisher for computers (SAFECOMP): Developmental test and evaluation/initial operational test and evaluation
[AD-A217790] N90-21212
Strategies for concurrent processing of complex algorithms in data driven architectures
[NASA-CR-186515] N90-21535
System testing of a production Ada (trademark) project: The GRODY study
[NASA-TM-103308] N90-21541

COMPUTER SYSTEMS PROGRAMS

Architecture independent environment for developing engineering software on MIMD computers
[NASA-CR-186562] N90-21553

COMPUTER TECHNIQUES
Development of microcomputer-based mental acuity tests for repeated-measures studies
[NASA-CR-185607] N90-21521
Multigrid on massively parallel computers
[DE90-008999] N90-21560
The ultimate CASE tool
[DE90-009351] N90-21687
COMPUTER VISION
NETRA: A parallel architecture for integrated vision systems 2: Algorithms and performance evaluation
[NASA-CR-186510] N90-21557
COMPUTERIZED SIMULATION
Autonomous integrated GPS/INS navigation experiment for OMV. Phase 1: Feasibility study
[NASA-CR-4267] N90-20969
Calculation of the three dimensional turbulent flow in a linear turbine blade N90-21021
The numerical simulation of multistage turbomachinery flows N90-21025
Controlled multibody dynamics simulation for large space structures N90-21068
Detection of potential space station control/structure interaction with CO-ST-IN N90-21074
Computational architecture for integrated controls and structures design N90-21076
LACE flight dynamics experiment N90-21086
Filament winding of composite cylinders N90-21119
Fiber pushout test: A three-dimensional finite element computational simulation
[NASA-TM-102565] N90-21131
Minutes of the 23rd Eplosives Safety Seminar, volume 2
[AD-A218265] N90-21214
Radar observations of a formation of two fighters: A case study for ISAR imaging N90-21240
Airborne Doppler radar flight experiments for the detection of microbursts N90-21243
The development of a simulation program of the anode side for aluminum/air batteries
[PB90-165754] N90-21286
Phase-only holographic filters and their applications
[PB90-166802] N90-21368
Computer-aided design of flywheel transmission systems N90-21392
Problems associated with residual and mismatch stresses in thin film structures N90-21407
An internal/external pressure, tension/compression multiaxial fatigue system
[DE90-009510] N90-21430
A time-accurate adaptive grid method and the numerical simulation of a shock-vortex interaction
[NASA-TP-2998] N90-21524
SR90, strontium shaped-charge critical ionization velocity experiment
[NASA-CR-186501] N90-21606
Helium transport in plasma edge regions N90-21625
Design and optimisation of thin foil x ray telescopes N90-21690
COMPUTERS
Selective automatic fire extinguisher for computers (SAFECOMP): Developmental test and evaluation/initial operational test and evaluation
[AD-A217790] N90-21212
CONCENTRATORS
Recent progress in photovoltaic concentrator module technology
[DE90-009007] N90-21475
CONCRETES
Criteria for polymer concrete on airport pavements
[DOT/FAA/DS-89/18] N90-21045
Perforation of a reinforced concrete wall by a rigid missile
[AD-A210025] N90-21381
CONCURRENT PROCESSING
Strategies for concurrent processing of complex algorithms in data driven architectures
[NASA-CR-186515] N90-21535
CONDUCTION ELECTRONS
Alternating gradient photodetector
[NASA-CASE-NPO-17235-1-CO] N90-21358
CONDUCTORS
Program CICC: Flow and heat transfer in Cable In Conduit Conductors, user's manual
[DE90-007924] N90-21661
CONFERENCES
Joint University Program for Air Transportation Research, 1988-1989
[NASA-CP-3063] N90-20921
Computational Methods for Aerodynamic Design (inverse) and Optimization
[AGARD-CP-463] N90-20976
Secondary Flows in Turbomachines
[AGARD-CP-469] N90-21009
Proceedings of the 13th International Congress on Instrumentation in Aerospace Simulation Facilities
[EOARD-LR-89-069] N90-21046
NASA/DOD Controls-Structures Interaction Technology 1989
[NASA-CP-3041] N90-21062
Modelling of molecular structures and properties in physical chemistry and biophysics
[AD-A214561] N90-21145
Minutes of the 23rd Explosives Safety Seminar, volume 1
[AD-A218264] N90-21213
Minutes of the 23rd Eplosives Safety Seminar, volume 2
[AD-A218265] N90-21214
The 4th Annual Review of Progress in Applied Computational Electromagnetics
[AD-A217912] N90-21257
The 5th Annual Review of Progress in Applied Computational Electromagnetics
[AD-A217994] N90-21258
Proceedings of the Joint NOSC/NRL (Naval Ocean Systems Center/Naval Research Laboratory) InP Microwave/Millimeter Wave Technology Workshop
[AD-A218216] N90-21259
Proceedings of the Third Infrared Detector Technology Workshop
[NASA-TM-102209] N90-21313
Tenth International Free Electron Laser Conference
[DE90-614773] N90-21376
Proceedings of the 4th European Conference, volume 2
[AD-A216521] N90-21382
US-Japan Workshop on Atomic Collisions in Solids: Abstracts of lectures
[DE90-008979] N90-21611
Recent advances in the studies of the nova outburst
[DE90-008936] N90-21691
CONFIGURATION MANAGEMENT
Aeropropulsion facilities configuration control: Procedures manual
[NASA-TM-102541] N90-21399
CONFORMAL MAPPING
The N = 2 superconformal algebras on hyperelliptic surfaces and their Coulomb gas realization
[DE90-612790] N90-21581
Fusion algebra and fusing matrices
[DE90-612798] N90-21583
Conserved conformal currents in curved space-time
[DE90-612766] N90-21672
CONICAL BODIES
Discrete-vortex model for the symmetric-vortex flow on cones
[NASA-TP-2989] N90-20948
CONICAL SHELLS
Ablative cooling of aerodynamically heated radomes
[AD-D014426] N90-21293
CONNECTORS
Systematic errors in power measurements made with a dual six-port ANA
[PB90-145160] N90-21276
CONSERVATION LAWS
Finite element algorithms for hyperbolic conservation laws with forcing terms
[INPE-5024-RPE/617] N90-21595
CONSTRUCTION
Nonlinear and distributed parameter models of the mini-mast truss N90-21070
CONTAMINANTS
Transformation and deposition of airborne gaseous and particulate pollutants during transport over the Baltic Sea
[PUBL-AIR-QUALITY-5] N90-21478
Gaithersburg Nike control and launch area preliminary assessment/site inspection, Gaithersburg, Maryland
[AD-A217791] N90-21482
CONTINUITY EQUATION
Curvature continuity of cubic Bezier curves in the solid modeling aerospace research tools design software
[NASA-CR-186583] N90-21554
CONTINUOUS RADIATION
An assessment of the potential of continuous-wave ranging for measuring the distance to a highly reflective, infinite sheet
[NASA-TM-101680] N90-21279
CONTINUUM MECHANICS
Compact scheme for systems of equations applied to fundamental problems of mechanics of continua
[NASA-CR-186494] N90-21292
CONTOURS
Inverse design of airfoil contours: Constraints, numerical method, and applications N90-20980
CONTRAROTATING PROPELLERS
Relating flow between counter-rotating propellers to aerodynamic interaction noise N90-20944
CONTROL STICKS
Simulator comparison of thumball, thumb switch, and touch screen input concepts for interaction with a large screen cockpit display format
[NASA-TM-102587] N90-21005
CONTROL SYSTEMS DESIGN
Joint University Program for Air Transportation Research, 1988-1989
[NASA-CP-3063] N90-20921
Rule-based mechanisms of learning for intelligent adaptive flight control N90-20939
Perspectives on the use of rule-based control N90-20940
Stochastic robustness of linear control systems N90-20941
Design of a helicopter automatic flight control system using adaptive control N90-21040
Human centrifuge controller
[NAL-TM-SE-8901] N90-21043
NASA/DOD Controls-Structures Interaction Technology 1989
[NASA-CP-3041] N90-21062
A spaceborne optical interferometer: The JPL CSI mission focus N90-21063
Zenith Star: A structural control challenge N90-21064
PACOSS program status and results N90-21065
Controlled multibody dynamics simulation for large space structures N90-21068
A distributed finite-element modeling and control approach for large flexible structures N90-21071
Effective techniques for the identification and accommodation of disturbances N90-21072
Modeling and control of flexible space platforms with articulated payloads N90-21073
Detection of potential space station control/structure interaction with CO-ST-IN N90-21074
Optimization of the structural and control system for LSS with reduced-order model N90-21075
Computational architecture for integrated controls and structures design N90-21076
Controller reduction for effective interdisciplinary design of active structures N90-21077
Recent experience in simultaneous control-structure optimization N90-21078
A survey of experiments and experimental facilities for active control of flexible structures N90-21079
NASA CSI suspension methods overview N90-21080
ASCIE: An integrated experiment to study CSI in large segmented optical systems N90-21082
CSI sensing and control: Analytical and experimental results N90-21083
Experimental evaluation of active-member control of precision structures N90-21084
Controls, Astrophysics, and Structures Experiment in Space (CASES) N90-21085
CSI technology validation on an LSS ground experiment facility N90-21089
Initial operational capability of the ASTREX large space structures test bed N90-21091
In-house experiments in large space structures at the Air Force Wright Aeronautical Laboratories Flight Dynamics Laboratory N90-21092
Attitude control modes for the MECB remote sensing satellites
[INPE-4755-PRE/1427] N90-21094
A general-purpose balloon-borne pointing system for solar scientific instruments
[NASA-TP-3013] N90-21219
CONTROL THEORY
Joint University Program for Air Transportation Research, 1988-1989
[NASA-CP-3063] N90-20921
An expert system for wind shear avoidance N90-20938
Experimental and theoretical investigation of optimal control methods with model reduction N90-21039
Suboptimal and hybrid numerical solution schemes for orbit transfer manoeuvres
[INPE-4991-PRE/1556] N90-21054
Modeling and control of flexible space platforms with articulated payloads N90-21073
CSI sensing and control: Analytical and experimental results N90-21083
Integrated modeling and analysis of a space-truss article
[NASA-TM-102615] N90-21412
CONTROLLABILITY
End point control of flexible manipulators
[AD-A217319] N90-21383
CONTROLLERS
Perspectives on the use of rule-based control N90-20940
Experimental and theoretical investigation of optimal control methods with model reduction N90-21039

Human centrifuge controller
[NAL-TM-SE-8901] N90-21043
Effective techniques for the identification and accommodation of disturbances N90-21072
Computational architecture for integrated controls and structures design N90-21076
Controller reduction for effective interdisciplinary design of active structures N90-21077
Design of a digital model following controller of reaction wheel torques
[INPE-4753-PRE/1425] N90-21093
Electromechanical actuation for thrust vector control applications
[NASA-TM-102548] N90-21272
Development of a dynamic modeling technique and its application to the analysis and control of a high-precision robotic manipulator N90-21391
Active control of multi-dimensional random sound in ducts
[NASA-TM-102653] N90-21603

CONVECTION
A cost-effective strategy for nonoscillatory convection without clipping
[NASA-TM-102538] N90-21291
Finite element algorithms for hyperbolic conservation laws with forcing terms
[INPE-5024-RPE/617] N90-21595
Thermal decay of an initially hot isothermal water body with application to thermal energy storage
[DE90-614742] N90-21675

CONVECTION CLOUDS
Precipitation mechanisms in tropical and midlatitude convective clouds N90-21507

CONVECTIVE FLOW
Acoustic convective system
[NASA-CASE-NPO-17278-1-CU] N90-21215
A cost-effective strategy for nonoscillatory convection without clipping
[NASA-TM-102538] N90-21291

CONVECTIVE HEAT TRANSFER
Acoustic convective system
[NASA-CASE-NPO-17278-1-CU] N90-21215
ULTRA-SHARP nonoscillatory convection schemes for high-speed steady multidimensional flow
[NASA-TM-102568] N90-21570

CONVERGENCE
Convergence acceleration of hypersonic flow calculations: A nonlinear relaxation factor N90-20957
A modification of a low-order Reissner-Mindlin plate bending element
[PB90-165630] N90-21428
Differential-algebraic equations as stiff ordinary differential equations
[DE90-007922] N90-21585

CONVEXITY
A monotone complementarity problem in Hilbert space
[DE90-009755] N90-21590

COOLANTS
An experimental evaluation of two nonazeotropic refrigerant mixtures in a water-to-water breadboard heat pump
[DE90-009016] N90-21305

COOLING
Analysis of the rotor tip leakage flow with tip cooling air ejection N90-21029
Detailed heat transfer measurements in nozzle guide vane passages in linear and annular cascades in the presence of secondary flows N90-21030
Thermal decay of an initially hot isothermal water body with application to thermal energy storage
[DE90-614742] N90-21675

COORDINATES
Error correction of the DEA (Digital Electronic Automation) coordinate measuring machines at LLNL
[DE90-008913] N90-21365

COPOLYMERS
Nicalon/siliconoxycarbide ceramic composites
[NASA-TM-102563] N90-21133
On the dynamics of polymer mixtures in solution using the RPA
[DE90-613889] N90-21149
Generalized random phase approximation for multicomponent polymer systems
[DE90-613691] N90-21194

COPPER
Hydrocarbon-fuel/combustion-chamber-liner materials compatibility
[NASA-CR-185203] N90-21165

COPPER ALLOYS
High temperature fatigue behavior of tungsten copper composites
[NASA-TM-102404] N90-21138

COPPER OXIDES
Deformation processing of YBa2Cu3O(sub x)
[DE90-007795] N90-21644

CORONAL LOOPS
VLA observations of the coronal plasma
[NASA-CR-186540] N90-21711

CORRELATION COEFFICIENTS
Review and statistical analysis of the ultrasonic velocity method for estimating the porosity fraction in polycrystalline materials
[NASA-TM-102501] N90-21402

CORROSION
A corrosion fatigue/stress corrosion testing facility at Materials Research Laboratory
[MRL-TN-568] N90-21044
Current fluctuations associated with localised corrosion: Mechanistic studies of the early stages of pitting and stress corrosion cracking of stainless steel
[AERE-R-13531] N90-21159
Corrosion behavior of mild steel in high pH aqueous media
[PB90-131152] N90-21162
High-temperature oxidation and sulfidation of Fe-20Cr-16Ni-4Al-1Y2O3 oxide-dispersion-strengthened alloy
[DE90-007897] N90-21168
The corrosion protection of 6061-T6 aluminum by a polyurethane-sealed anodized coat
[NASA-TM-100394] N90-21191

CORROSION PREVENTION
High gloss corrosion-resistant coatings
[AD-D014403] N90-21184
Combination primer/topcoat coating
[AD-D014445] N90-21189
The corrosion protection of 6061-T6 aluminum by a polyurethane-sealed anodized coat
[NASA-TM-100394] N90-21191

CORROSION RESISTANCE
High-temperature oxidation and sulfidation of Fe-20Cr-16Ni-4Al-1Y2O3 oxide-dispersion-strengthened alloy
[DE90-007897] N90-21168
High gloss corrosion-resistant coatings
[AD-D014403] N90-21184

CORROSION TESTS
A corrosion fatigue/stress corrosion testing facility at Materials Research Laboratory
[MRL-TN-568] N90-21044

COSMIC DUST
Cosmic Dust Collection Facility: Scientific objectives and programmatic relations
[NASA-TM-102160] N90-21098

COSMIC RAYS
Fragmentation of relativistic heavy nuclei with application to cosmic ray propagation N90-21716

COSMIC X RAYS
Recent advances in the studies of the nova outburst
[DE90-008936] N90-21691

COSMOLOGY
Studies in quantum field theory
[DE90-008731] N90-21677
The large scale structure of the universe in pancake models of galaxy formation N90-21701
Horizon problem in cosmological models with non zero
[DE90-613367] N90-21708

COST ANALYSIS
Criteria for polymer concrete on airport pavements
[DOT/FAA/DS-89/18] N90-21045
Mars in this century: The Olympia Project
[DE90-008356] N90-21709

COST EFFECTIVENESS
A cost-effective strategy for nonoscillatory convection without clipping
[NASA-TM-102538] N90-21291

COUNTERS
VLSI binary updown counter
[NASA-CASE-NPO-17205-1-CU] N90-21525

COUNTING
The solid state photomultiplier: Status of photon counting beyond the near-infrared N90-21319

COUPLED MODES
Coupled magnetoplasmon-phonon modes at the surface of a semi-infinite semiconductor superlattice
[DE90-612904] N90-21647

COUPLINGS
Modeling and control of flexible space platforms with articulated payloads N90-21073

CRACK ARREST
Crack stoppers and ARALL laminates
[PB90-166588] N90-21142

CRACK INITIATION
Combined effect of matrix cracking and stress-free edge on delamination
[NASA-TM-102591] N90-21126
Micromechanics analysis of space simulated thermal deformations and stresses in continuous fiber reinforced composites
[NASA-TM-102633] N90-21140

CRACK OPENING DISPLACEMENT
Fracture of sandwiched composites N90-21136

CRACK PROPAGATION
A corrosion fatigue/stress corrosion testing facility at Materials Research Laboratory
[MRL-TN-568] N90-21044
Three-dimensional elastic-plastic analysis of shallow cracks in single-edge-crack-tension specimens
[NASA-TM-102636] N90-21130
Crack stoppers and ARALL laminates
[PB90-166588] N90-21142
A compendium of sources of fracture toughness and fatigue crack growth data for metallic alloys, part 4
[NASA-TM-102648] N90-21164
Fatigue crack growth from narrow-band Gaussian spectrum loading in 6063 aluminum alloy
[DE90-008957] N90-21173
Fracture toughness and crack growth of Zerodur
[NASA-TM-4185] N90-21187
Development of a fracture analysis technique for use with a general-purpose finite element program N90-21416
NASA airframe structural integrity program
[NASA-TM-102637] N90-21422
An evaluation of the pressure proof test concept for thin sheet 2024-T3
[NASA-TM-101675] N90-21424
Fractographic analysis of the crack growth rate and the shear lip development of 2024-T3 specimens under simple variable-amplitude loading
[PB90-167032] N90-21427

CRACK TIPS
Mechanics of interface fracture N90-21408

CRACKS
Three-dimensional elastic-plastic analysis of shallow cracks in single-edge-crack-tension specimens
[NASA-TM-102636] N90-21130
Fourier series methods for plates and shells with cracks and inclusions N90-21406
An evaluation of the pressure proof test concept for thin sheet 2024-T3
[NASA-TM-101675] N90-21424
Fractographic analysis of the crack growth rate and the shear lip development of 2024-T3 specimens under simple variable-amplitude loading
[PB90-167032] N90-21427

CRAY COMPUTERS
Modeling high-temperature superconductors and metallic alloys on the Intel IPSC/860
[DE90-009402] N90-21665

CREATIVITY
On the creation of gravitational wave by photon in external electromagnetic field
[DE90-613366] N90-21265

CREEP PROPERTIES
Titanium aluminides: Processing, properties and potential
[AERE-R-13198] N90-21158

CRITICAL LOADING
Elastic-plastic instability of plane frames N90-21415

CRITICAL POINT
Critical point wetting drop tower experiment
[NASA-CR-186513] N90-21208

CRITICAL VELOCITY
SR90, strontium shaped-charge critical ionization velocity experiment
[NASA-CR-186501] N90-21606

CROP GROWTH
Agricultural yield estimation of sugarcane based on agrometeorological-spectral model
[INPE-5016-RPE/610] N90-21441
A knowledge-based information based for crop area estimation
[INPE-4990-PRE/1555] N90-21444
Wheat productivity estimate through field radiometry
[INPE-4994-PRE/1556] N90-21460

CROSSLINKING
Process for crosslinking methylene-containing aromatic polymers with ionizing radiation
[NASA-CASE-LAR-13448-1] N90-21198

CRYOGENIC FLUID STORAGE
Liquid Transfer Cryogenic Test Facility: Initial hydrogen and nitrogen no-vent fill data
[NASA-TM-102572] N90-21295

CRYOGENICS
Advanced Launch System (ALS): Electrical actuation and power systems improve operability and cost picture
[NASA-TM-102547] N90-21271
Liquid Transfer Cryogenic Test Facility: Initial hydrogen and nitrogen no-vent fill data
[NASA-TM-102572] N90-21295
Experience with the UKIRT InSb array camera N90-21327
Status of the isophot detector development N90-21342

Program CICC: Flow and heat transfer in Cable In Conduit Conductors, user's manual
[DE90-007924] N90-21661
Nonoptimal entropy generation by heat transfer in cryogenic domain
[DE90-007544] N90-21667

CRYOPUMPING
BASG thermomechanical pump helium 2 transfer tests
[NASA-CR-177541] N90-21097

CRYOSTATS
Nonoptimal entropy generation by heat transfer in cryogenic domain
[DE90-007544] N90-21667

CRYSTAL DEFECTS
Progress in the material development of LiCaAlF(6):Cr(3+) laser crystals
[DE90-009542] N90-21666

CRYSTAL DISLOCATIONS
Deformation and microstructure of rutile
[DE90-614113] N90-21654

CRYSTAL GROWTH
Apparatus for mixing solutions in low gravity environments
[NASA-CASE-MFS-26047-1] N90-21209
Contract crystal growth and fabrication services
[AD-A218327] N90-21646
Anisotropy of grain growth in alumina
[DE90-009045] N90-21655

CRYSTAL LATTICES
On the substitution of Sr ions at Y sites in YB(suba2)Cu3O(sub7-d)
[DE90-613395] N90-21652

CRYSTAL STRUCTURE
ZELED analysis of aperiodicity and bond lengths in ceramic powders
[DE90-612932] N90-21193
Heat engine based on shape memory alloys
[AD-D014400] N90-21385
Contract crystal growth and fabrication services
[AD-A218327] N90-21646
Shock compression of solids: A tutorial
[DE90-009185] N90-21659

CRYSTALLINITY
LaRC TPI 1500 series polymers
[NASA-CR-181899] N90-21129

CRYSTALLIZATION
LaRC TPI 1500 series polymers
[NASA-CR-181899] N90-21129
ZELED analysis of aperiodicity and bond lengths in ceramic powders
[DE90-612932] N90-21193
Apparatus for mixing solutions in low gravity environments
[NASA-CASE-MFS-26047-1] N90-21209

CRYSTALLOGRAPHY
A requirement for Australian research: Access to big science facilities, a report by the Australian National Committee for Crystallography
[DE90-614784] N90-21048
Retabulation of space group extinctions for electron diffraction
[DE90-612933] N90-21648

CRYSTALS
Modeling the temperature dependence of the thermal conductivity of aluminum nitride
[DE90-009428] N90-21154
Contract crystal growth and fabrication services
[AD-A218327] N90-21646
Simulated image maps for use in experimental high-resolution electron microscopy
[DE90-009176] N90-21657

CUES
Stereopsis cueing effects on hover-in-turbulence performance in a simulated rotorcraft
[NASA-TP-2980] N90-21004

CURRENT DENSITY
Method of making a long life high current density cathode from tungsten and iridium powders using a quarternary compound as the impregnant
[AD-D014425] N90-21211
Observations of atmospheric electricity, 1988
[GEOPHYSICAL-PUBL-10] N90-21499

CURVATURE
Curvature continuity of cubic Bezier curves in the solid modeling aerospace research tools design software
[NASA-CR-186583] N90-21554
On the equation: Delta u+c=Ke(sup u)
[DE90-612741] N90-21575

CYCLIC LOADS
Characterization of failure processes in tungsten copper composites under fatigue loading conditions
[NASA-TM-102371] N90-21123

CYCLOTRON FREQUENCY
Full wave computation of electromagnetic wave excitation, propagation, and absorption at the ion cyclotron frequency in fusion experiments
[DE90-009399] N90-21642

CYCLOTRON RESONANCE DEVICES
Low frequency gyrotron amplifier investigation, phase 2
[AD-A217096] N90-21352

CYGNUS CONSTELLATION
The 1989 outburst of V404 Cygni: A very unusual x ray nova
[DE90-008935] N90-21693

CYLINDRICAL BODIES
Filament winding of composite cylinders N90-21119

CYTOLOGY
Does DNA cytometry have a place in the clinical laboratory
[DE90-007652] N90-21512

CYTOMETRY
Does DNA cytometry have a place in the clinical laboratory
[DE90-007652] N90-21512

D

DAMAGE
Use of unbalanced laminates as a screening method for microcracking
[NASA-TM-102517] N90-21124
Two-dimensional damage models of fiber-reinforced composites N90-21135

DAMAGE ASSESSMENT
Relevance of impacter shape to nonvisible damage and residual tensile strength of a thick graphite/epoxy laminate
[NASA-TM-102599] N90-21122
Cross-sectional examination of the damage zone in impacted specimens of carbon/epoxy and carbon/PEEK composites
[NASA-TM-100391] N90-21125

DAMPING
United States Air Force Academy get-away-special flexible beam experiment N90-21088

DATA ACQUISITION
The MANTA: An RPV design to investigate forces and moments on a lifting surface
[NASA-CR-186227] N90-20971
Performance evaluation of MSS/LANDSAT data in the estimation of fluvial channel width
[INPE-4906-PRE/1507] N90-21463
CAMAC memory module: MEMO-32
[DE90-759846] N90-21528

DATA BASE MANAGEMENT SYSTEMS
The Chemkin Thermodynamic Data Base
[DE90-007953] N90-21676
The ultimate CASE tool
[DE90-009351] N90-21687

DATA BASES
The influence of ice accretion physics on the forecasting of aircraft icing conditions N90-20928
Software Engineering Laboratory (SEL) database organization and user's guide
[NASA-TM-103304] N90-21545
The Chemkin Thermodynamic Data Base
[DE90-007953] N90-21676
A formal approach to user models in data retrieval
[PB90-124728] N90-21682

DATA COLLECTION PLATFORMS
The MANTA: An RPV design to investigate forces and moments on a lifting surface
[NASA-CR-186227] N90-20971
Monitoring vegetation of Brazil: Potentialities of multi-sensors approach
[INPE-4993-PRE/1555] N90-21451

DATA COMPRESSION
Weather data dissemination to aircraft N90-20934
Concept and results of the DLR realtime SAR processor N90-21244

DATA FLOW ANALYSIS
Architecture independent environment for developing engineering software on MIMD computers
[NASA-CR-186562] N90-21553

DATA LINKS
Weather data dissemination to aircraft N90-20934
Data Link Processor (DLP) project transition plan
[DOT/FAA/CT-TN89/68] N90-21256
Bit-error-rate testing of fiber optic data links for MMIC-based phased array antennas
[NASA-TM-102523] N90-21261

DATA MANAGEMENT
Architecture independent environment for developing engineering software on MIMD computers
[NASA-CR-186562] N90-21553

DATA PROCESSING
Principles of the radiosity method for canopy reflectance modeling
[DE90-008943] N90-21486
Meteorologist Weather Processor (MWP) integration test plan
[DOT/FAA/CT-TN89/62] N90-21500
The CAD/CAM product data standards: IGES/PDES (Initial Graphics Exchange Specification/Product Data Exchange Standards, the present and the future
[DE90-008803] N90-21549
Small business innovation research. Abstracts of 1988 phase 1 awards
[NASA-TM-102991] N90-21680

DATA RETRIEVAL
A formal approach to user models in data retrieval
[PB90-124728] N90-21682

DATA STORAGE
Rapidly quantifying the relative distention of a human bladder
[NASA-CASE-LAR-13901-1-NP] N90-21519

DATA SYSTEMS
Cockpit display of hazardous wind shear information N90-20924
Weather data dissemination to aircraft N90-20934
On board cross support scenarios
[INPE-5005-PRE/1562] N90-21268
Analysis and modelling of spatial data proposal of a system for CBERS
[INPE-4911-PRE/1512] N90-21445

DATA TRANSMISSION
Optimization of the effective GPS data rate N90-20932
VLSI single-chip (255,223) Reed-Solomon encoder with interleaver
[NASA-CASE-NPO-17280-1-CU] N90-21061
SAR image coding N90-21246
An introduction to high frequency radioteletype systems
[PB90-145533] N90-21252
A correlation-spectral method for line detection on noisy data
[DE90-007925] N90-21266
Subsystem TM Precision: Progress and perspective
[INPE-5006-PRE/1563] N90-21461
CAMAC memory module: MEMO-32
[DE90-759846] N90-21528

DC 10 AIRCRAFT
Brake performance of the McDonnell Douglas DC-10-30/40 during high speed, high energy rejected takeoffs
[PB90-917004] N90-21000

DECISION THEORY
Automatic classification of images
[AD-D014437] N90-21260

DEEP SPACE NETWORK
Environmental projects, volume 11. Environmental assessment: Addition to operations building, Mars site
[NASA-CR-186449] N90-21479
Environmental projects, volume 10. Environmental assessment: New 34-meter antenna at Apollo site
[NASA-CR-186448] N90-21480

DEFECTS
UNIVIMP: A universal instrument for the survey of initial imperfections of thin-walled shells
[PB90-167065] N90-21369
Compendium of fracture mechanics problems
[NASA-TM-100393] N90-21414

DEFORMATION
A computational model of the perforation of multi-layer metallic laminates
[MRL-RR-9-89] N90-21128
Micromechanics analysis of space simulated thermal deformations and stresses in continuous fiber reinforced composites
[NASA-TM-102633] N90-21140
Modeling elastomer displacements for tactile sensing applications
[DE90-007959] N90-21370
Heat engine based on shape memory alloys
[AD-D014400] N90-21385
Improved analytical capabilities for foil air bearings, phase 1
[AD-A218071] N90-21389
Thermomechanical deformation testing and modeling in the presence of metallurgical instabilities
[NASA-CR-185188] N90-21420
Review of formulae for the buckling of simply-supported, orthotropic plates under shear load, including transverse shear effects
[PB90-167073] N90-21429
Results of the Gondwana Project: An example of intercontinental geologic correlation utilizing LANDSAT imagery
[INPE-4870-PRE/1481] N90-21437

Contribution for the study of the evolution of part of the Espinhaco supergroup and its foundation through fracture analysis
[INPE-4907-PRE/1508] N90-21459
Deformation processing of YBa2Cu3O(sub x)
[DE90-007795] N90-21644

DEGRADATION
Evaluation of the mangrove areas of the Rio Piaui (SE) through remote sensing
[INPE-4909-PRE/1510] N90-21454
Failure and degradation modes in selected solar materials: A review
[DE90-009075] N90-21476

DEGREES OF FREEDOM
Direct formulation of a 4-node hybrid shell element with rotational degrees of freedom
[NASA-CR-4282] N90-21411

DEICING
Modeling of surface roughness effects on glaze ice accretion N90-20925

DELAMINATING
Cross-sectional examination of the damage zone in impacted specimens of carbon/epoxy and carbon/PEEK composites
[NASA-TM-100391] N90-21125
Combined effect of matrix cracking and stress-free edge on delamination
[NASA-TM-102591] N90-21126
Fracture and longevity of composite structures
[AD-A217827] N90-21127
Compressive behavior of laminated composite structures N90-21134
Delamination failure in a unidirectional curved composite laminate
[NASA-CR-182018] N90-21421
Development of planar geometry solid oxide fuel cell technology, phase 2
[PB90-131293] N90-21467

DELTA WINGS
Experimental and numerical investigation of the vortex flow over a sharp edged delta wing: with and without sideslip
[PB90-167131] N90-20964

DEOXYRIBONUCLEIC ACID
Does DNA cytometry have a place in the clinical laboratory
[DE90-007652] N90-21512

DEPOSITION
Influence of the deposition conditions on radiofrequency magnetron sputtered MoS2 films
[NASA-TP-2994] N90-21210
Improvement of small-area, amorphous-silicon thin-film photovoltaics on polymer substrate
[DE90-000314] N90-21472
Transformation and deposition of airborne gaseous and particulate pollutants during transport over the Baltic Sea
[PUBL-AIR-QUALITY-5] N90-21478
Effects of Air Pollution on Western Forests
[PB90-131111] N90-21481

DEPTH
A solution level indicator system
[DE90-007939] N90-21151

DERIVATION
On a non classical oblique derivative problem for parabolic singular integro-differential operators
[DE90-612739] N90-21574

DESIGN ANALYSIS
Design of a natural laminar flow airfoil for an unmanned aircraft
[PD-CF-9004] N90-20975
Aerodynamic design techniques at DLR Institute for Design Aerodynamics N90-20979
Inverse design of airfoil contours: Constraints, numerical method, and applications N90-20980
An efficient airfoil design method using the Navier-Stokes equations N90-20981
A system for transonic wing design with geometric constraints based on an inverse method N90-20983
A fast collocation method for transonic airfoil design N90-20984
Subsonic and transonic blade design by means of analysis codes N90-20985
A computational design method for shock free transonic cascades and airfoils N90-20986
Inverse computation of transonic internal flows with application for multi-point-design of supercritical compressor blades N90-20987
An inverse method for the design of turbomachine blades N90-20988
Application of an inverse method to the design of a radial inflow turbine N90-20989
Aerodynamic optimization by simultaneously updating flow variables and design parameters N90-20991
Numerical optimization of target pressure distributions for subsonic and transonic airfoil design N90-20993
A tool for automatic design of airfoils in different operating conditions N90-20994
The use of numerical optimization for helicopter airfoil and blade design N90-20995
Aerodynamic design by optimization N90-20996
Numerical optimization of wings in transonic flow N90-20997
Aerodynamic design via control theory N90-20998
Optimization of aerodynamic designs using computational fluid dynamics N90-20999
Recent experience in simultaneous control-structure optimization N90-21078
Global nonlinear optimization of spacecraft protective structures design
[NASA-TM-100367] N90-21095
Design and status of the detector block for the ISO-SWS N90-21341

DETECTION
Determination of Li-Al alloy extent in tubular aluminum elements by small source neutron radiology
[DE90-009142] N90-21174
A correlation-spectral method for line detection on noisy data
[DE90-007925] N90-21266
Modeling elastomer displacements for tactile sensing applications
[DE90-007959] N90-21370
The effect of windscreen bows and HUD pitch ladder format on pilot performance during simulated flight
[AD-A218139] N90-21523

DETONATION
Determination of detonation parameters of booster explosives at small charge diameters
[MRL-TR-89-45] N90-21204
Discrete modeling of beds of propellant exposed to strong stimulus
[DE90-006932] N90-21206

DEVIATION
The effects of compressor endwall flow on airfoil incidence and deviation N90-21011

DIAMETERS
Determination of detonation parameters of booster explosives at small charge diameters
[MRL-TR-89-45] N90-21204

DIAMONDS
Studies of mechano-chemical interactions in the tribological behavior of materials
[NASA-TM-102545] N90-21182
Diamond: A high power optical material
[DE90-008941] N90-21196

DIELECTRICS
Proceedings of the Joint NOSC/NRL (Naval Ocean Systems Center/Naval Research Laboratory) InP Microwave/Millimeter Wave Technology Workshop
[AD-A218216] N90-21259
An assessment of the potential of continuous-wave ranging for measuring the distance to a highly reflective, infinite sheet
[NASA-TM-101680] N90-21279

DIELS-ALDER REACTIONS
Bis(4-(3,4-dimethylenepyrrolidyl)-phenyl) methane
[NASA-CASE-LAR-13965-1-CU] N90-21118

DIFFERENCE EQUATIONS
On the stability of a certain difference scheme
[PB90-165614] N90-21588

DIFFERENTIAL EQUATIONS
Numerical simulation model for hydrazine attitude control thrusters. Part 1: Model description
[INPE-4952-RPE/601] N90-21115
PROTEUS two-dimensional Navier-Stokes computer code, version 1.0. Volume 3: Programmer's reference
[NASA-TM-102553] N90-21307
Compact finite volume methods for the diffusion equation
[NASA-CR-186477] N90-21568
Adaptive grid embedding for the two-dimensional flux-split Euler equations
[NASA-CR-186533] N90-21571
On a non classical oblique derivative problem for parabolic singular integro-differential operators
[DE90-612739] N90-21574
Differential-algebraic equations as stiff ordinary differential equations
[DE90-007922] N90-21585

DIFFERENTIAL PRESSURE
Liquid Transfer Cryogenic Test Facility: Initial hydrogen and nitrogen no-vent fill data
[NASA-TM-102572] N90-21295

DIFFRACTION PATTERNS
Method for holographic correction of beams of coherent light
[AD-D014406] N90-21353

DIFFUSION
Generalized random phase approximation for multicomponent polymer systems
[DE90-613691] N90-21194
Mixing of viscous fluids: Behavior of microstructures and chaos
[DE90-008871] N90-21304
Compact finite volume methods for the diffusion equation
[NASA-CR-186477] N90-21568

DIFFUSION LENGTH
Alternating gradient photodetector
[NASA-CASE-NPO-17235-1-CO] N90-21358

DIGITAL COMPUTERS
Data Link Processor (DLP) project transition plan
[DOT/FAA/CT-TN89/68] N90-21256
Activities and operations of the Advanced Computing Research Facility
[DE90-007957] N90-21559

DIGITAL DATA
Data Link Processor (DLP) project transition plan
[DOT/FAA/CT-TN89/68] N90-21256
Bit-error-rate testing of fiber optic data links for MMIC-based phased array antennas
[NASA-TM-102523] N90-21261
Digital processing of TM/LANDSAT data in monitoring interior water
[INPE-4956-PRE/1533] N90-21448
Introduction of digital image processing by remote sensors applied to geology
[INPE-5023-RPE/616] N90-21456
Multitemporal analysis of LANDSAT/TM digital imagery in the detection of areas affected by caterpillar (sibine fusca) attack in the dende (elais guineensis) palm plantation
[INPE-4979-PRE/1544] N90-21457

DIGITAL SIMULATION
Comparison of C- and O-grid generation methods using a NACA 0012 airfoil
[AD-A216375] N90-20948
Generation of triangular form models in a microcomputer environment
[INPE-4974-PRE/1539] N90-21447

DIGITAL SYSTEMS
Error correction of the DEA (Digital Electronic Automation) coordinate measuring machines at LLNL
[DE90-008913] N90-21365

DIGITS
SIGNIF: A C function to compute significant digits
[DE90-009242] N90-21550

DIMENSIONAL ANALYSIS
Fiber pushout test: A three-dimensional finite element computational simulation
[NASA-TM-102565] N90-21131

DIODES
Coplanar waveguide discontinuities for P-I-N diode switches and filter applications
[NASA-TM-102534] N90-21278
The potential for high performance HgCdTe arrays at 4 microns N90-21320
InSb DRO array characteristics N90-21326
Laboratory and telescope use of the NICMOS2 128 x 128 HgCdTe array N90-21338

DIRAC EQUATION
Local supersymmetry in non-relativistic systems
[DE90-612751] N90-21670

DIRECT CURRENT
A comparative study of electric power distribution systems for spacecraft
[NASA-CR-186531] N90-21113

DIRICHLET PROBLEM
Inverse design of airfoil contours: Constraints, numerical method, and applications N90-20980
Analysis and finite element approximation of some optimal control problems associated with the Navier-Stokes equations N90-21299

DISPLACEMENT
Modeling elastomer displacements for tactile sensing applications
[DE90-007959] N90-21370
Age constraints for the present fault configuration in the Imperial Valley, California: Evidence for northwestward propagation of the Gulf of California rift system
[NASA-CR-186541] N90-21493

DISPLAY DEVICES
Investigation of air transportation technology at the Massachusetts Institute of Technology, 1988-1989 N90-20922
Cockpit display of hazardous wind shear information N90-20924
Cockpit display of hazardous weather information N90-20929
Stereopsis cueing effects on hover-in-turbulence performance in a simulated rotorcraft
[NASA-TP-2980] N90-21004
Simulator comparison of thumball, thumb switch, and touch screen input concepts for interaction with a large screen cockpit display format
[NASA-TM-102587] N90-21005

A note on overdispersed exponential families
[AD-A216277] N90-21565

DISTANCE
An assessment of the potential of continuous-wave ranging for measuring the distance to a highly reflective, infinite sheet
[NASA-TM-101680] N90-21279

DISTORTION
Element-specific modal formulations for large-displacement multibody dynamics N90-21069
Wave receptance analysis of vibrating beams and stiffened plates N90-21419
The extension of rapid distortion theory to stratified shear flows N90-21491
Free-field propagation of high intensity noise
[NASA-CR-186577] N90-21604

DISTRIBUTED AMPLIFIERS
High efficiency octave bandwidth millimeter wave power amplifier
[AD-A216245] N90-21280

DISTRIBUTED PARAMETER SYSTEMS
A distributed finite-element modeling and control approach for large flexible structures N90-21071
On the continuous dependence with respect to sampling of the linear quadratic regulator problem for distributed parameter systems
[NASA-CR-182012] N90-21566

DISTRIBUTED PROCESSING
Cooperating intelligent systems
[NASA-CR-184962] N90-21529
Fast causal multicast
[NASA-CR-186495] N90-21533
Parallel tridiagonalization of a general matrix using distributed-memory multiprocessors
[DE90-008902] N90-21551
Exploiting virtual synchrony in distributed systems
[NASA-CR-182855] N90-21555

DISTRIBUTION FUNCTIONS
Analysis of distributions of Visual Meteorological Conditions (VMC) heliport data
[DOT/FAA/CT-TN89/67] N90-21508

DISTURBANCES
Effective techniques for the identification and accommodation of disturbances N90-21072

DIURNAL VARIATIONS
Comparison of quiet time geomagnetic daily variation (Sq) in H component at Eusebio and Cachoeira Paulista
[INPE-4985-PRE/1547] N90-21714

DOPPLER RADAR
Advanced instrumentation for aircraft icing research
[NASA-CR-185225] N90-21006
Airborne Doppler radar flight experiments for the detection of microbursts N90-21243

DOWNLINKING
VLSI single-chip (255,223) Reed-Solomon encoder with interleaver
[NASA-CASE-NPO-17280-1-CU] N90-21061

DRAG REDUCTION
A fast collocation method for transonic airfoil design N90-20984
Constrained spanload optimization for minimum drag of multi-lifting-surface configurations N90-20992

DRAINAGE
Characterization of linear structures from remote sensing data; Espinhaco Meridional (MG) sierra
[INPE-4905-PRE/1506] N90-21449

DROP SIZE
Precipitation mechanisms in tropical and midlatitude convective clouds N90-21507

DROP TOWERS
Critical point wetting drop tower experiment
[NASA-CR-186513] N90-21208

DRYING
Wheat productivity estimate through field radiometry
[INPE-4994-PRE/1556] N90-21460

DUCTS
Numerical method for designing 3D turbomachinery blade rows N90-20990
Inflatable fuel tank buffer
[AD-D014446] N90-21002
Parabolized calculations of turbulent three dimensional flows in a turbine duct N90-21013
Effects of secondary flow on heat transfer in rotating passages N90-21031
Active control of multi-dimensional random sound in ducts
[NASA-TM-102653] N90-21603

DURABILITY
The effect of leveling coatings on the atomic oxygen durability of solar concentrator surfaces
[NASA-TM-102557] N90-21110

DUST
A theoretical study of circumstellar dust around Ae/Be stars N90-21700

DYNAMIC CHARACTERISTICS
Development of a dynamic modeling technique and its application to the analysis and control of a high-precision robotic manipulator N90-21391
Modeling large-scale vegetation dynamics
[DE90-008883] N90-21485

DYNAMIC CONTROL
Controlled multibody dynamics simulation for large space structures N90-21068
End point control of flexible manipulators
[AD-A217319] N90-21383
Integrated modeling and analysis of a space-truss article
[NASA-TM-102615] N90-21412

DYNAMIC LOADS
Fatigue crack growth from narrow-band Gaussian spectrum loading in 6063 aluminum alloy
[DE90-008957] N90-21173
Fracture toughness and crack growth of Zerodur
[NASA-TM-4185] N90-21187
A numerical model for the determination of periodic solutions of pipes subjected to non-conservative loads
[DE90-614756] N90-21423

DYNAMIC MODELS
Modelling of molecular structures and properties in physical chemistry and biophysics
[AD-A214561 j] N90-21145
Development of a dynamic modeling technique and its application to the analysis and control of a high-precision robotic manipulator N90-21391

DYNAMIC RESPONSE
Experimental aeroelasticity history, status and future in brief
[NASA-TM-102651] N90-21047
Nonlinear and distributed parameter models of the mini-mast truss N90-21070
Controller reduction for effective interdisciplinary design of active structures N90-21077
The effect of elastic boundary conditions on the dynamic response of rectangular plates
[NASA-CR-186059] N90-21405

DYNAMIC STRUCTURAL ANALYSIS
Performance data from a wind-tunnel test of two main-rotor blade designs for a utility-class helicopter
[NASA-TM-4183] N90-20974
Nonlinear and distributed parameter models of the mini-mast truss N90-21070
Controller reduction for effective interdisciplinary design of active structures N90-21077
Controls, Astrophysics, and Structures Experiment in Space (CASES) N90-21085
Space truss zero gravity dynamics N90-21087
Fourier series methods for plates and shells with cracks and inclusions N90-21406
User manual for VICONOPT: An exact analysis and optimum design program covering the buckling and vibration of prismatic assemblies of flat in-plane loaded, anisotropic plates, with approximations for discrete supports, and transverse stiffeners
[NASA-CR-181966] N90-21413
Wave receptance analysis of vibrating beams and stiffened plates N90-21419
Elasto-plastic large deformation analysis of thin-walled structures
[PB90-164757] N90-21426

DYNAMICAL SYSTEMS
Periodic solutions for Hamiltonian systems in a nonconvex potential well
[DE90-612752] N90-21580

E

EARTH (PLANET)
JPRS report. Science and technology. USSR: Earth sciences
[JPRS-UES-88-004] N90-21431

EARTH GRAVITATION
Critical point wetting drop tower experiment
[NASA-CR-186513] N90-21208

EARTH MAGNETOSPHERE
Center of excellence in theoretical geoplasma research
[AD-A215035] N90-21488
Substorms: Their expansion and recovery phases
[DE90-008970] N90-21712

EARTH OBSERVATIONS (FROM SPACE)
Trade-offs in a space based surveillance radar N90-21225

EARTH ORBITAL ENVIRONMENTS
Simplified model for solar cosmic ray exposure in manned Earth orbital flights
[NASA-TM-4182] N90-21715

EARTH ORBITS
Optimal trajectories for the aeroassisted flight experiment. Part 3: Formulation, results, and analysis
[NASA-CR-186165] N90-21051
SIRTF in high earth orbit N90-21345

EARTH RESOURCES
Monitoring vegetation of Brazil: Potentialities of multi-sensors approach
[INPE-4993-PRE/1555] N90-21451

ECONOMICS
Evolution of remote sensing applied to vegetation and forest at INPE
[INPE-4970-PRE/1538] N90-21452
Advanced manufacturing technology: A Department of Energy technology transfer initiative
[DE90-008601] N90-21688

EDDY VISCOSITY
PROTEUS two-dimensional Navier-Stokes computer code, version 1.0. Volume 2: User's guide
[NASA-TM-102552] N90-21306
PROTEUS two-dimensional Navier-Stokes computer code, version 1.0. Volume 3: Programmer's reference
[NASA-TM-102553] N90-21307

EDGE DETECTION
Performance evaluation of morphological edge detectors
[INPE-4975-PRE/1540] N90-21464

EDGE LOADING
Combined effect of matrix cracking and stress-free edge on delamination
[NASA-TM-102591] N90-21126

EDITING
Editing wind profiler measurements
[PB90-130147] N90-21503

EDITING ROUTINES (COMPUTERS)
Editing wind profiler measurements
[PB90-130147] N90-21503

EDUCATION
Programme of the International Training Course on Remote Sensing for African Specialists
[INPE-4878-NTE/290] N90-21435
The ultimate CASE tool
[DE90-009351] N90-21687

EIGENVALUES
Parallel tridiagonalization of a general matrix using distributed-memory multiprocessors
[DE90-008902] N90-21551

EINSTEIN EQUATIONS
The monad construction and Hermetian-Einstein metrics
[DE90-612738] N90-21573
String dynamics in curved space-time revisited
[DE90-612796] N90-21674
The dynamics of scalar fields in the early universe N90-21696

ELASTIC DEFORMATION
A review of gear housing dynamics and acoustics literature
[NASA-CR-185148] N90-21387
Elasto-plastic large deformation analysis of thin-walled structures
[PB90-164757] N90-21426
Deformation and microstructure of rutile
[DE90-614113] N90-21654

ELASTIC PROPERTIES
Three-dimensional elastic-plastic analysis of shallow cracks in single-edge-crack-tension specimens
[NASA-TM-102636] N90-21130
Review and statistical analysis of the ultrasonic velocity method for estimating the porosity fraction in polycrystalline materials
[NASA-TM-102501] N90-21402
Mechanics of interface fracture N90-21408
Delamination failure in a unidirectional curved composite laminate
[NASA-CR-182018] N90-21421

ELASTIC SCATTERING
Helium transport in plasma edge regions N90-21625

ELASTODYNAMICS
Element-specific modal formulations for large-displacement multibody dynamics N90-21069

ELASTOMERS
Modeling elastomer displacements for tactile sensing applications
[DE90-007959] N90-21370

ELASTOPLASTICITY
Elastic-plastic instability of plane frames N90-21415
Elasto-plastic large deformation analysis of thin-walled structures
[PB90-164757] N90-21426

ELASTOSTATICS
Two-dimensional damage models of fiber-reinforced composites N90-21135

ELECTRIC CURRENT
Power transmission device
[AD-D014430] N90-21281

The RAP unit: A remote autoranging picoammeter
[DE90-007711] N90-21357
Solar flares and dynamics of Langmuir waves in current-carrying plasmas
[IPPCZ-291] N90-21710

ELECTRIC DISCHARGES
A simplified theoretical model for the laser-induced optogalvanic effect
[DE90-613121] N90-21626

ELECTRIC EQUIPMENT TESTS
The RAP unit: A remote autoranging picoammeter
[DE90-007711] N90-21357

ELECTRIC FIELDS
Generalized WKB approximation for stratified isotropic chiral structures
[PB90-165689] N90-21270
Proceedings of a workshop on Carcinogenic Potential of Extremely Low Frequency Magnetic Fields
[DE90-614340] N90-21520
Langmuir wave interaction with ion acoustic wave
[DE90-615407] N90-21624

ELECTRIC POTENTIAL
Alternating gradient photodetector
[NASA-CASE-NPO-17235-1-CO] N90-21358
An ultra-small capacitance Josephson junction
[DE90-613396] N90-21653

ELECTRIC POWER SUPPLIES
Advanced Launch System (ALS): Electrical actuation and power systems improve operability and cost picture
[NASA-TM-102547] N90-21271

ELECTRIC POWER TRANSMISSION
A comparative study of electric power distribution systems for spacecraft
[NASA-CR-186531] N90-21113

ELECTRIC WIRE
The RAP unit: A remote autoranging picoammeter
[DE90-007711] N90-21357

ELECTRICAL ENGINEERING
JPRS report: Science and technology. USSR: Electronics and electrical engineering
[JPRS-UEE-90-002] N90-21284

ELECTRICAL IMPEDANCE
The 5th Annual Review of Progress in Applied Computational Electromagnetics
[AD-A217994] N90-21258

ELECTRICAL MEASUREMENT
The RAP unit: A remote autoranging picoammeter
[DE90-007711] N90-21357

ELECTRICAL PROPERTIES
Alternative materials for solid oxide fuel cells
[DE90-008615] N90-21468

ELECTRICAL RESISTIVITY
Resistivity of pristine and intercalated graphite fiber epoxy composites
[NASA-TM-102576] N90-21192
Near contact phenomena and transient effects in far infrared photoconductors N90-21316
Alternating gradient photodetector
[NASA-CASE-NPO-17235-1-CO] N90-21358

ELECTROCHEMICAL CORROSION
Thermal control system corrosion study
[NASA-TM-102220] N90-21294

ELECTROCHEMISTRY
Analytical sciences
[DE90-007965] N90-21152
Application of neural nets to system identification and bifurcation analysis of real world experimental data
[DE90-007539] N90-21558
An attempt to measure cold-fusion effects
[DE90-613248] N90-21649

ELECTRODES
O2 reduction at the IFC orbiter fuel cell O2 electrode
[NASA-TM-102580] N90-21469

ELECTROLYSIS
An attempt to measure cold-fusion effects
[DE90-613248] N90-21649

ELECTROLYTES
Effect of KOH concentration on LEO cycle life of IPV nickel-hydrogen flight battery cells
[NASA-TM-103127] N90-21116

ELECTROMAGNETIC ACCELERATION
Railgun performance with a two-stage light-gas gun injector
[DE90-009183] N90-21057

ELECTROMAGNETIC COMPATIBILITY
The 5th Annual Review of Progress in Applied Computational Electromagnetics
[AD-A217994] N90-21258

ELECTROMAGNETIC COUPLING
Boeing 727-100 test project (high energy radiated field tests)
[DOT/FAA/CT-88/33] N90-21247

ELECTROMAGNETIC FIELDS
Boeing 727-100 test project (high energy radiated field tests)
[DOT/FAA/CT-88/33] N90-21247
The 5th Annual Review of Progress in Applied Computational Electromagnetics
[AD-A217994] N90-21258
A new rectangular waveguide to coplanar waveguide transition
[NASA-TM-102477] N90-21263
On the creation of gravitational wave by photon in external electromagnetic field
[DE90-613366] N90-21265
Proceedings of a workshop on Carcinogenic Potential of Extremely Low Frequency Magnetic Fields
[DE90-614340] N90-21520
Polarization: Effects on second harmonic power in light scattering by free electrons
[DE90-612842] N90-21606

ELECTROMAGNETIC INTERACTIONS
The 4th Annual Review of Progress in Applied Computational Electromagnetics
[AD-A217912] N90-21257
Once more about the sizes of fast-moving objects
[DE90-615204] N90-21592

ELECTROMAGNETIC PROPERTIES
The measurement of surface reflectivity at millimetre wavelengths
[MRL-TN-559] N90-21222

ELECTROMAGNETIC PROPULSION
Laser controlled semiconductor armature for electromagnetic launchers
[AD-D014435] N90-21055

ELECTROMAGNETIC RADIATION
Is Galerkin's method really better
[DE90-008804] N90-21267
Center of excellence in theoretical geoplasma research
[AD-A215035] N90-21488
Proceedings of a workshop on Carcinogenic Potential of Extremely Low Frequency Magnetic Fields
[DE90-614340] N90-21520

ELECTROMAGNETIC SCATTERING
The 4th Annual Review of Progress in Applied Computational Electromagnetics
[AD-A217912] N90-21257

ELECTROMAGNETIC WAVE TRANSMISSION
Ultrarelativistic envelope solitons in electron-positron plasma of the pulsar magnetosphere
[DE90-613289] N90-21264
Full wave computation of electromagnetic wave excitation, propagation, and absorption at the ion cyclotron frequency in fusion experiments
[DE90-009399] N90-21642

ELECTROMAGNETISM
Computer processing of multi-channel electromagnetic data from an airborne geophysical survey system
[PB90-138413] N90-21253
Biological effects of ELF (Extremely-Low-Frequency) electric and magnetic fields
[DE90-008634] N90-21514

ELECTRON BEAMS
On storage rings for short wavelength FELs
[DE90-009059] N90-21379
Proposal for FY86 Lawrence Livermore National Laboratory particle beam research
[DE90-007936] N90-21617

ELECTRON CAPTURE
Atomic processes in high temperature plasmas
[DE90-008873] N90-21632

ELECTRON CYCLOTRON HEATING
Applied plasma physics
[DE90-007932] N90-21635

ELECTRON DENSITY (CONCENTRATION)
SR90, strontium shaped-charge critical ionization velocity experiment
[NASA-CR-186501] N90-21606
An extended diffusive model for calculating thermal diffusivity from single monopole tokamak heat pulse propagation
[DE90-007958] N90-21637
Instabilities and vortex dynamics in shear flow of magnetized plasmas
[DE90-009448] N90-21643

ELECTRON DIFFRACTION
ZELED analysis of aperiodicity and bond lengths in ceramic powders
[DE90-612932] N90-21193
Retabulation of space group extinctions for electron diffraction
[DE90-612933] N90-21648

ELECTRON ENERGY
Experimental study of population inversion and spectral line broadening in a plasma containing a mixture of high Z and low Z ions
[DE90-007552] N90-21622
A simplified theoretical model for the laser-induced optogalvanic effect
[DE90-613121] N90-21626

ELECTRON IMPACT
Helium transport in plasma edge regions N90-21625

ELECTRON MICROSCOPY
Grain boundary precipitation in Ni3Al based alloys
[AERE-R-13362] N90-21161
High voltage/high resolution studies of metal and semiconductor interfaces
[DE90-009065] N90-21656
Simulated image maps for use in experimental high-resolution electron microscopy
[DE90-009176] N90-21657

ELECTRON PHONON INTERACTIONS
Modified tight-binding approximation and electron-phonon spectral function for transition metals
[DE90-614022] N90-21166

ELECTRON SCATTERING
Large basis space effects in electron scattering form factors of light nuclei
[DE90-613501] N90-21609
Inelastic electron scattering from surfaces
[DE90-009365] N90-21614
Thomson scattering in a magnetic field N90-21699

ELECTRON SPECTROSCOPY
Magnetron sputtered boron films and Ti/B multilayer structures
[DE90-009190] N90-21153

ELECTRON TRANSFER
The development of a simulation program of the anode side for aluminum/air batteries
[PB90-165754] N90-21286

ELECTRON-POSITRON PAIRS
Relativistic processes in active galactic nuclei N90-21698

ELECTRON-POSITRON PLASMAS
Ultrarelativistic envelope solitons in electron-positron plasma of the pulsar magnetosphere
[DE90-613289] N90-21264
Nonlinear interaction of photons and phonons in electron-positron plasmas
[DE90-009341] N90-21640

ELECTRONIC CONTROL
Human centrifuge controller
[NAL-TM-SE-8901] N90-21043

ELECTRONIC EQUIPMENT
Environmental projects, volume 11. Environmental assessment: Addition to operations building, Mars site
[NASA-CR-186449] N90-21479
The CAD/CAM product data standards: IGES/PDES (Initial Graphics Exchange Specification/Product Data Exchange Standards, the present and the future
[DE90-008803] N90-21549

ELECTRONIC PACKAGING
The development of ultraviolet-ozone cleaning as a production process in the packaging of integrated circuits
[DE90-007960] N90-21220

ELECTRONS
Modified tight-binding approximation and electron-phonon spectral function for transition metals
[DE90-614022] N90-21166
Polarization: Effects on second harmonic power in light scattering by free electrons
[DE90-612842] N90-21606
Large basis space effects in electron scattering form factors of light nuclei
[DE90-613501] N90-21609
Langmuir wave interaction with ion acoustic wave
[DE90-615407] N90-21624
MHD modes driven by anomalous electron viscosity and their role in fast sawtooth crashes
[DE90-009311] N90-21639
High energy phenomena during solar flares
[INPE-4961-TDL/390] N90-21713
A balloon measurement of the isotopic composition of galactic cosmic ray iron N90-21717

ELECTROSTATIC WAVES
Langmuir wave interaction with ion acoustic wave
[DE90-615407] N90-21624

ELECTROSTATICS
Radon concentration over the Brazilian Amazon Basin during the wet season (Belem-Manaus GTE-ABLE-2B flight of April 24, 1987)
[INPE-4892-PRE/1493] N90-21486
Once more about the sizes of fast-moving objects
[DE90-615204] N90-21592

ELEMENTARY PARTICLES
Current experiments in elementary particle physics
[DE90-008062] N90-21607

ELLIPTIC DIFFERENTIAL EQUATIONS
A parallel multigrid method for solving elliptic partial differential equations
[DE90-007929] N90-21584

ELLIPTIC FUNCTIONS
On the equation: Delta u+c=Ke(sup u)
[DE90-612741] N90-21575

EMBEDDING
Strain and dynamic measurements using fiber optic sensors embedded into graphite/epoxy tubes N90-21090
Structural tailoring of select fiber composite structures [NASA-TM-102484] N90-21137
Image simulation of geometric targets for synthetic aperture radar N90-21245
EMBRITTLEMENT
Magneto acoustic emission apparatus for testing materials for embrittlement [NASA-CASE-LAR-13817-1] N90-21170
EMERGENCIES
Perspectives on the use of rule-based control N90-20940
EMISSION
A fossil energy perspective on global climate change [DE90-007894] N90-21483
Source attribution for tropospheric ozone in the US [DE90-007994] N90-21484
Radon concentration over the Brazilian Amazon Basin during the wet season (Belem-Manaus GTE-ABLE-2B flight of April 24, 1987) [INPE-4892-PRE/1493] N90-21486
An evaluation of the relationship between the production and use of energy and atmospheric methane emissions [DE90-007982] N90-21487
EMISSION SPECTRA
Remote sensing applied to sea water quality researches in coastal regions: A review [INPE-4935-PRE/1425] N90-21438
Free-field propagation of high intensity noise [NASA-CR-186577] N90-21604
EMITTANCE
Thermal radiation characteristics of nonisothermal cylindrical enclosures using a numerical ray tracing technique [NASA-TM-102527] N90-21296
Problems in radiative transfer in astrophysics: An escape probability treatment of line overlap and a model of the masers around VX Sgr N90-21705
ENCAPSULATING
Ductile alloy encapsulated ceramic armor development [AD-A217632] N90-21183
END PLATES
Double swivel toggle release [NASA-CASE-MSC-21436-1] N90-21390
ENERGY ABSORPTION
Low energy ion generator [DE90-759905] N90-21195
High power, high sensitivity microwave calorimeter [AD-D014427] N90-21355
ENERGY BUDGETS
The extension of rapid distortion theory to stratified shear flows N90-21491
ENERGY CONVERSION
Substorms: Their expansion and recovery phases [DE90-008970] N90-21712
ENERGY DISSIPATION
An investigation of secondary flows in nozzle guide vanes N90-21016
Losses in the tip-leakage flow of a planar cascade of turbine blades N90-21027
Surface characterization of hydrogen charged and uncharged alpha-2 and gamma titanium aluminide alloys using AES and REELS [NASA-CR-186561] N90-21171
ENERGY METHODS
An approximate viscous shock layer method for calculating the hypersonic flow over blunt-nosed bodies N90-20947
ENERGY SPECTRA
Gamma-ray production cross section measurements using a white neutron source from 1 to 400 MeV [DE90-008906] N90-21610
ENERGY TECHNOLOGY
An evaluation of the relationship between the production and use of energy and atmospheric methane emissions [DE90-007982] N90-21487
ENERGY TRANSFER
The numerical simulation of multistage turbomachinery flows N90-21025
The extension of rapid distortion theory to stratified shear flows N90-21491
The generally covariant representation of energy-momentum pseudotensor of gravitational field [DE90-615203] N90-21689
ENGINE DESIGN
Supersonic through-flow fan engine and aircraft mission performance [NASA-TM-102304] N90-21038
Recent Stirling engine loss-understanding results [NASA-TM-103122] N90-21114
ENGINE FAILURE
Statistics on aircraft gas turbine engine rotor failures that occurred in US commercial aviation during 1986 [DOT/FAA/CT-89/30] N90-21008
Compendium of fracture mechanics problems [NASA-TM-100393] N90-21414
ENGINE PARTS
Attachment of lead wires to thin film thermocouples mounted on high temperature materials using the parallel gap welding process [NASA-TM-102442] N90-21361
ENTHALPY
The structural basis for fatigue initiation in glassy polymers [DE90-009342] N90-21200
The Chemkin Thermodynamic Data Base [DE90-007953] N90-21676
ENTROPY
A Lagrangian formalism for nonequilibrium ensembles [DE90-612748] N90-21579
Nonoptimal entropy generation by heat transfer in cryogenic domain [DE90-007544] N90-21667
ENVIRONMENT EFFECTS
Final safety analysis report for the Ulysses Mission [DE90-008690] N90-21106
MECCA program documentation [NOAA-TR-NESDIS-46] N90-21477
Environmental projects, volume 11. Environmental assessment: Addition to operations building, Mars site [NASA-CR-186449] N90-21479
ENVIRONMENT SIMULATION
Proceedings of the 13th International Congress on Instrumentation in Aerospace Simulation Facilities [EOARD-LR-89-069] N90-21046
ENVIRONMENTAL SURVEYS
Gaithersburg Nike control and launch area preliminary assessment/site inspection, Gaithersburg, Maryland [AD-A217791] N90-21482
ENVIRONMENTS
Modeling large-scale vegetation dynamics [DE90-008883] N90-21485
EPIDEMIOLOGY
Proceedings of a workshop on Carcinogenic Potential of Extremely Low Frequency Magnetic Fields [DE90-614340] N90-21520
EPITAXY
Improved Si:As BIBIB (Back-Illuminated Blocked-Impurity-Band) hybrid arrays N90-21349
EPOXY MATRIX COMPOSITES
Cross-sectional examination of the damage zone in impacted specimens of carbon/epoxy and carbon/PEEK composites [NASA-TM-100391] N90-21125
Resistivity of pristine and intercalated graphite fiber epoxy composites [NASA-TM-102576] N90-21192
EPOXY RESINS
Criteria for polymer concrete on airport pavements [DOT/FAA/DS-89/18] N90-21045
EQUATIONS OF MOTION
Parametric resonance in horizontal axis wind turbines N90-20962
Design of a helicopter automatic flight control system using adaptive control N90-21040
Modeling and control of flexible space platforms with articulated payloads N90-21073
United States Air Force Academy get-away-special flexible beam experiment N90-21088
Notes on the unsteady rectilinear motion of a perfect gas. Part 8: General theory and general waves in a homentropic gas [PB90-167149] N90-21309
Development of a dynamic modeling technique and its application to the analysis and control of a high-precision robotic manipulator N90-21391
A new approach to solve the kinematics resolution of a redundant robot [DE90-010213] N90-21397
Flutter of slender bodies under axial stress [PB90-167024] N90-21425
The extension of rapid distortion theory to stratified shear flows N90-21491
Extension of the constraints algebra for the closed string with the fixed topology world sheet [DE90-612745] N90-21577
Instabilities and vortex dynamics in shear flow of magnetized plasmas [DE90-009448] N90-21643
The dynamics of scalar fields in the early universe N90-21696
EQUIPMENT SPECIFICATIONS
Goes I-M and beyond: Science requirements and technology challenges N90-21067
EQUIVALENCE
The gravitational lens effect and its optical equivalents [DE90-612767] N90-21673
ERROR ANALYSIS
LDV measurements and the flow analysis in the vortex region of a radial inflow turbine N90-21007
Foundations of measurement and instrumentation [NASA-RP-1222] N90-21351
ERRORS
Systematic errors in power measurements made with a dual six-port ANA [PB90-145160] N90-21276
Performance evaluation of MSS/LANDSAT data in the estimation of fluvial channel width [INPE-4906-PRE/1507] N90-21483
SIGNIF: A C function to compute significant digits [DE90-009242] N90-21550
ESTIMATES
A knowledge-based information based for crop area estimation [INPE-4990-PRE/1555] N90-21444
ESTIMATING
Systematic errors in power measurements made with a dual six-port ANA [PB90-145160] N90-21276
Agricultural yield estimation of sugarcane based on agrometeorological-spectral model [INPE-5016-RPE/610] N90-21441
Performance evaluation of MSS/LANDSAT data in the estimation of fluvial channel width [INPE-4906-PRE/1507] N90-21483
ESTUARIES
Evaluation of the mangrove areas of the Rio Piaui (SE) through remote sensing [INPE-4909-PRE/1510] N90-21454
MECCA program documentation [NOAA-TR-NESDIS-46] N90-21477
ETCHING
The investigation of multilayer x ray reflectors as x ray optical elements [DE90-009044] N90-21621
EUCLIDEAN GEOMETRY
A remark on the Kelvin transform and a non-linear partial differential equation [PB90-165822] N90-21589
Characteristics consequences of space-time coordinate relativization [DE90-615201] N90-21668
EULER EQUATIONS OF MOTION
Some aspects of Essentially Nonoscillatory (ENO) formulations for the Euler equations, part 3 [NASA-CR-4285] N90-20949
Computation of nonequilibrium chemically reacting flows in hypersonic flow field N90-20954
An evaluation of the two-dimensional Euler and Navier-Stokes calculations based on a flux-vector splitting [PB90-166778] N90-20963
Optimization of aerodynamic designs using computational fluid dynamics N90-20999
Cepstrum analysis and applications to computational fluid dynamic solutions N90-21302
PROTEUS two-dimensional Navier-Stokes computer code, version 1.0. Volume 1: Analysis description [NASA-TM-102551] N90-21303
PROTEUS two-dimensional Navier-Stokes computer code, version 1.0. Volume 2: User's guide [NASA-TM-102552] N90-21306
Adaptive grid embedding for the two-dimensional flux-split Euler equations [NASA-CR-186533] N90-21571
EULER-LAGRANGE EQUATION
A quasi-Lagrangian moving grid technique for investigating compressible flows N90-21298
EUROPE
Microgravity science and applications bibliography, 1989 revision [NASA-TM-4192] N90-21207
EXCITATION
Large basis space effects in electron scattering form factors of light nuclei [DE90-613501] N90-21609
EXHAUST GASES
An evaluation of the relationship between the production and use of energy and atmospheric methane emissions [DE90-007982] N90-21487
EXHAUST NOZZLES
Exhaust nozzles for propulsion systems with emphasis on supersonic cruise aircraft [NASA-RP-1235] N90-21037
EXHAUST VELOCITY
The effects of magnetic nozzle configurations on plasma thrusters [NASA-CR-186465] N90-21109

EXOBIOLOGY
USSR Space Life Sciences Digest, Issue 26
[NASA-CR-392231] N90-21513
EXPANDABLE STRUCTURES
Collapsible fabric tank testing
[AD-A217861] N90-21388
EXPANSION
Expanding ring joint
[AD-D014396] N90-21384
EXPERT SYSTEMS
Investigation of air transportation technology at Princeton University, 1988-1989 N90-20935
An expert system for wind shear avoidance N90-20938
Rule-based mechanisms of learning for intelligent adaptive flight control N90-20939
Progress in inverse design and optimization in aerodynamics N90-20977
Thermal control system corrosion study
[NASA-TM-102220] N90-21294
A knowledge-based information based for crop area estimation
[INPE-4990-PRE/1555] N90-21444
Cooperating intelligent systems
[NASA-CR-184982] N90-21529
EXPLOSIVES
An evaluation of metal salts of 3-nitro-1,2,4-triazol-5-one (NTO) as potential primary explosives
[MRL-TN-563] N90-21202
Determination of detonation parameters of booster explosives at small charge diameters
[MRL-TR-89-45] N90-21204
Minutes of the 23rd Explosives Safety Seminar, volume 1
[AD-A218264] N90-21213
Minutes of the 23rd Eplosives Safety Seminar, volume 2
[AD-A218265] N90-21214
High explosives (PBX9502) characterization using computerized tomography
[DE90-006170] N90-21404
EXPONENTIAL FUNCTIONS
A note on overdispersed exponential families
[AD-A216277] N90-21565
EXPOSURE
Simplified model for solar cosmic ray exposure in manned Earth orbital flights
[NASA-TM-4182] N90-21715
EXTERNAL STORE SEPARATION
An overlapped grid method for multigrid, finite volume/difference flow solvers: MaGGiE
[NASA-CR-182008] N90-20953
EXTERNAL TANKS
Compendium of fracture mechanics problems
[NASA-TM-100393] N90-21414
EXTINCTION
Retabulation of space group extinctions for electron diffraction
[DE90-612933] N90-21648
EXTRACTION
Digital processing of TM/LANDSAT data in monitoring interior water
[INPE-4956-PRE/1533] N90-21448

F

F REGION
Low latitude F-region dynamical processes from atomic oxygen nightglow emissions
[INPE-4999-PRE/1561] N90-21494
F-104 AIRCRAFT
Sonic boom signature data from cruciform microphone array experiments during the 1966-1967 EAFB national sonic boom evaluation program
[NASA-CR-182027] N90-21605
FABRICATION
Reinforcement-matrix interface effects in metal matrix composites
[MRL-TN-562] N90-21120
The investigation of multilayer x ray reflectors as x ray optical elements
[DE90-009044] N90-21621
Toughened YBa2Cu3O(sub x)/ZrO2 composites
[DE90-007796] N90-21645
Contract crystal growth and fabrication services
[AD-A218327] N90-21646
Shock compression of solids: A tutorial
[DE90-009185] N90-21659
Advanced manufacturing technology: A Department of Energy technology transfer initiative
[DE90-006601] N90-21688
FABRICS
Collapsible fabric tank testing
[AD-A217861] N90-21388
FABRY-PEROT INTERFEROMETERS
Design and status of the detector block for the ISO-SWS N90-21341
FAILURE
On the stability of amorphous silica coatings for high temperature service
[AERE-R-13425] N90-21179
Double swivel toggle release
[NASA-CASE-MSC-21436-1] N90-21390
FAILURE ANALYSIS
Effect of KOH concentration on LEO cycle life of IPV nickel-hydrogen flight battery cells
[NASA-TM-103127] N90-21116
Characterization of failure processes in tungsten copper composites under fatigue loading conditions
[NASA-TM-102371] N90-21123
Fracture and longevity of composite structures
[AD-A217827] N90-21127
Compressive behavior of laminated composite structures N90-21134
Two-dimensional damage models of fiber-reinforced composites N90-21135
The structural basis for fatigue initiation in glassy polymers
[DE90-009342] N90-21200
Compendium of fracture mechanics problems
[NASA-TM-100393] N90-21414
Development of a fracture analysis technique for use with a general-purpose finite element program N90-21416
FAILURE MODES
Compressive behavior of laminated composite structures N90-21134
Resistance mechanics for laminated composite materials
[INPE-4919-RPE/594] N90-21141
Development of a fracture analysis technique for use with a general-purpose finite element program N90-21416
Delamination failure in a unidirectional curved composite laminate
[NASA-CR-182018] N90-21421
Failure and degradation modes in selected solar materials: A review
[DE90-009075] N90-21476
FAR INFRARED RADIATION
Extrinsic germanium Blocked Impurity Bank (BIB) detectors N90-21322
Ga:Ge array development N90-21323
Stressed detector arrays for airborne astronomy N90-21332
Alternating gradient photodetector
[NASA-CASE-NPO-17235-1-CO] N90-21358
FARM CROPS
Agricultural yield estimation of sugarcane based on agrometeorological-spectral model
[INPE-5016-RPE/610] N90-21441
A knowledge-based information based for crop area estimation
[INPE-4990-PRE/1555] N90-21444
Project CANASATE: Remote sensing applied to sugar cane crop survey
[INPE-4902-PRE/1503] N90-21446
Aerial photography as an aid for agricultural credit control
[INPE-5019-RPE/613] N90-21455
Evaluation of classification performance and proportion estimate of the sugar cane crop through PROCEDURE-INPE utilizing LANDSAT data
[INPE-4899-PRE/1500] N90-21458
Wheat productivity estimate through field radiometry
[INPE-4994-PRE/1556] N90-21460
FASTENERS
Double swivel toggle release
[NASA-CASE-MSC-21436-1] N90-21390
FATIGUE (MATERIALS)
Characterization of failure processes in tungsten copper composites under fatigue loading conditions
[NASA-TM-102371] N90-21123
Crack stoppers and ARALL laminates
[PB90-166588] N90-21142
Titanium aluminides: Processing, properties and potential
[AERE-R-13198] N90-21158
Fatigue crack growth from narrow-band Gaussian spectrum loading in 6063 aluminum alloy
[DE90-008957] N90-21173
The structural basis for fatigue initiation in glassy polymers
[DE90-009342] N90-21200
Fatigue damage growth mechanisms in continuous fiber reinforced titanium matrix composites
[NASA-TM-102594] N90-21409
NASA airframe structural integrity program
[NASA-TM-102637] N90-21422
An internal/external pressure, tension/compression multiaxial fatigue system
[DE90-009510] N90-21430
A real time neural net estimator of fatigue life
[NASA-TM-103117] N90-21564
FATIGUE LIFE
Fatigue damage growth mechanisms in continuous fiber reinforced titanium matrix composites
[NASA-TM-102594] N90-21409
An evaluation of the pressure proof test concept for thin sheet 2024-T3
[NASA-TM-101675] N90-21424
A real time neural net estimator of fatigue life
[NASA-TM-103117] N90-21564
FATIGUE TESTS
A corrosion fatigue/stress corrosion testing facility at Materials Research Laboratory
[MRL-TN-568] N90-21044
Fractographic analysis of the crack growth rate and the shear lip development of 2024-T3 specimens under simple variable-amplitude loading
[PB90-167032] N90-21427
FAULT TOLERANCE
Neural networks for aircraft control N90-20937
Double swivel toggle release
[NASA-CASE-MSC-21436-1] N90-21390
Fault tolerant hypercube computer system architecture
[NASA-CASE-NPO-16859-1-CU] N90-21527
Exploiting virtual synchrony in distributed systems
[NASA-CR-182855] N90-21555
FEEDBACK CONTROL
Stochastic robustness of linear control systems N90-20941
Optimization of the structural and control system for LSS with reduced-order model N90-21075
Controller reduction for effective interdisciplinary design of active structures N90-21077
On the continuous dependence with respect to sampling of the linear quadratic regulator problem for distributed parameter systems
[NASA-CR-182012] N90-21566
FERRITES
New ferrite-filled waveguiding structures analysed by the averaging method
[PB90-165671] N90-21269
FERRY SPACECRAFT
The partnership: Space shuttle, space science, and space station
[NASA-TM-102900] N90-21050
FEYNMAN DIAGRAMS
Characteristics consequences of space-time coordinate relativization
[DE90-615201] N90-21668
FIBER COMPOSITES
Characterization of failure processes in tungsten copper composites under fatigue loading conditions
[NASA-TM-102371] N90-21123
Use of unbalanced laminates as a screening method for microcracking
[NASA-TM-102517] N90-21124
Fracture and longevity of composite structures
[AD-A217827] N90-21127
Multi-objective shape and material optimization of composite structures including damping
[NASA-TM-102579] N90-21132
Two-dimensional damage models of fiber-reinforced composites N90-21135
Structural tailoring of select fiber composite structures
[NASA-TM-102484] N90-21137
High temperature fatigue behavior of tungsten copper composites
[NASA-TM-102404] N90-21138
Micromechanics analysis of space simulated thermal deformations and stresses in continuous fiber reinforced composites
[NASA-TM-102633] N90-21140
Fatigue damage growth mechanisms in continuous fiber reinforced titanium matrix composites
[NASA-TM-102594] N90-21409
Small business innovation research. Abstracts of 1988 phase 1 awards
[NASA-TM-102991] N90-21680
FIBER OPTICS
Advanced instrumentation for aircraft icing research
[NASA-CR-185225] N90-21006
Strain and dynamic measurements using fiber optic sensors embedded into graphite/epoxy tubes N90-21090
Bit-error-rate testing of fiber optic data links for MMIC-based phased array antennas
[NASA-TM-102523] N90-21261
Intensity to frequency conversion technique in intensity modulated fiber optic sensing systems
[NASA-TM-102562] N90-21277

Civil air transport: A fresh look at power-by-wire and fly-by-light
[NASA-TM-102574] N90-21283
A fiber optic sensor for noncontact measurement of shaft speed, torque, and power
[NASA-TM-102481] N90-21360
Fiber optic void fraction sensor
[DE90-009124] N90-21366
Passive stabilization of a fiber optic nonlinear interferometric sensor
[AD-D014438] N90-21620

FIBER ORIENTATION
Resistivity of pristine and intercalated graphite fiber epoxy composites
[NASA-TM-102576] N90-21192

FIBERS
Fiber pushout test: A three-dimensional finite element computational simulation
[NASA-TM-102565] N90-21131

FIELD ALIGNED CURRENTS
A self-consistent theory of radial transport of field-aligned current by microturbulence
[DE90-007920] N90-21631

FIELD EFFECT TRANSISTORS
InSb DRO array characteristics N90-21326
Low noise HgCdTe 128 x 128 SWIR FPA for Hubble space telescope N90-21337
Laboratory and telescope use of the NICMOS2 128 x 128 HgCdTe array N90-21338
HgCdTe 256x256 NWIR FPA N90-21348
Improved Si:As BIBIB (Back-Illuminated Blocked-Impurity-Band) hybrid arrays N90-21349
Problems associated with residual and mismatch stresses in thin film structures N90-21407

FIELD STRENGTH
Prediction of VHF/UHF mobile reception in urban areas: Comparison with measurements in London
[BBC-RD-1989/11] N90-21255

FIELD THEORY (PHYSICS)
Linking numbers and variational method
[DE90-612793] N90-21582
Fusion algebra and fusing matrices
[DE90-612798] N90-21583
Rings
[DE90-009035] N90-21613
Studies in quantum field theory
[DE90-008731] N90-21677

FIGHTER AIRCRAFT
Radar observations of a formation of two fighters: A case study for ISAR imaging N90-21240
Human factors in fighter software development
[PD-CF-9003] N90-21522

FILAMENT WINDING
Filament winding of composite cylinders N90-21119

FILLING
Rapidly quantifying the relative distention of a human bladder
[NASA-CASE-LAR-13901-1-NP] N90-21519

FINANCIAL MANAGEMENT
Aerial photography as an aid for agricultural credit control
[INPE-5019-RPE/613] N90-21455

FINITE DIFFERENCE THEORY
A fast collocation method for transonic airfoil design N90-20984
Application of an inverse method to the design of a radial inflow turbine N90-20989
Numerical method for designing 3D turbomachinery blade rows N90-20990
Optimization of aerodynamic designs using computational fluid dynamics N90-20999
PROTEUS two-dimensional Navier-Stokes computer code, version 1.0. Volume 3: Programmer's reference
[NASA-TM-102553] N90-21307
High accuracy solutions of incompressible Navier-Stokes equations
[NASA-TM-102539] N90-21567

FINITE ELEMENT METHOD
Comparison of C- and O-grid generation methods using a NACA 0012 airfoil
[AD-A216375] N90-20948
The role of structural analysis in airworthiness certification
[BR112064] N90-20972
An inverse method for the design of turbomachine blades N90-20988
A study on secondary flow and spanwise mixing in axial flow compressors N90-21012
Analysis of the rotor tip leakage flow with tip cooling air ejection N90-21029
Element-specific modal formulations for large-displacement multibody dynamics N90-21069
A distributed finite-element modeling and control approach for large flexible structures N90-21071
Stress analysis of rocket motors with viscoelastic propellant by a mixed finite element model N90-21112
Numerical simulation model for hydrazine attitude control thrusters. Part 1: Model description
[INPE-4952-RPE/601] N90-21115
Combined effect of matrix cracking and stress-free edge on delamination
[NASA-TM-102591] N90-21126
Three-dimensional elastic-plastic analysis of shallow cracks in single-edge-crack-tension specimens
[NASA-TM-102636] N90-21130
Fiber pushout test: A three-dimensional finite element computational simulation
[NASA-TM-102565] N90-21131
Micromechanics analysis of space simulated thermal deformations and stresses in continuous fiber reinforced composites
[NASA-TM-102633] N90-21140
The 4th Annual Review of Progress in Applied Computational Electromagnetics
[AD-A217912] N90-21257
Analysis and finite element approximation of some optimal control problems associated with the Navier-Stokes equations N90-21299
Fourier series methods for plates and shells with cracks and inclusions N90-21406
Problems associated with residual and mismatch stresses in thin film structures N90-21407
The computational structural mechanics testbed generic structural-element processor manual
[NASA-CR-181728] N90-21410
Direct formulation of a 4-node hybrid shell element with rotational degrees of freedom
[NASA-CR-4282] N90-21411
Development of a fracture analysis technique for use with a general-purpose finite element program N90-21416
Determination of stresses around cutouts in multilayered composite plate and shell structures N90-21417
Delamination failure in a unidirectional curved composite laminate
[NASA-CR-182018] N90-21421
A numerical and theoretical study of seismic wave diffraction in complex geologic structure
[AD-A218209] N90-21490
On the stability of a certain difference scheme
[PB90-165614] N90-21588
Finite element algorithms for hyperbolic conservation laws with forcing terms
[INPE-5024-RPE/617] N90-21595
The thermo-mechanical behavior of cometary nuclei N90-21703

FINITE VOLUME METHOD
An overlapped grid method for multigrid, finite volume/difference flow solvers: MaGGiE
[NASA-CR-182008] N90-20953
A computational design method for shock free transonic cascades and airfoils N90-20986
Compact finite volume methods for the diffusion equation
[NASA-CR-186477] N90-21568

FIRE EXTINGUISHERS
Selective automatic fire extinguisher for computers (SAFECOMP): Developmental test and evaluation/initial operational test and evaluation
[AD-A217790] N90-21212

FIRES
Full-scale air transport category fuselage burnthrough tests
[DOT/FAA/CT-TN89/65] N90-20967

FIRING (IGNITING)
Preparation, characterisation and cookoff behaviour of booster compositions prepared from RDX and acrylic or ethylene-vinyl acetate dispersions
[MRL-TR-89-44] N90-21203

FLAME SPECTROSCOPY
Study of new technique of solid combustible materials to determination of volatile elements by flame atomic absorption spectrophotometry
[DE90-612907] N90-21147

FLAMMABILITY
Full-scale air transport category fuselage burnthrough tests
[DOT/FAA/CT-TN89/65] N90-20967

FLAPPING
Parametric resonance in horizontal axis wind turbines N90-20962

FLARE STARS
Flare stars at radio wavelengths
[NASA-CR-186539] N90-21719

FLAT PLATES
User manual for VICONOPT: An exact analysis and optimum design program covering the buckling and vibration of prismatic assemblies of flat in-plane loaded, anisotropic plates, with approximations for discrete supports, and transverse stiffeners
[NASA-CR-181966] N90-21413

FLEXIBILITY
High gloss corrosion-resistant coatings
[AD-D014403] N90-21184
End point control of flexible manipulators
[AD-A217319] N90-21383

FLEXIBLE BODIES
NASA/DOD Controls-Structures Interaction Technology 1989
[NASA-CP-3041] N90-21062
A survey of experiments and experimental facilities for active control of flexible structures N90-21079

FLEXIBLE SPACECRAFT
NASA CSI suspension methods overview N90-21080

FLIGHT CHARACTERISTICS
Flight path reconstruction using extended Kalman filtering techniques
[PD-FC-9001] N90-20970

FLIGHT CONDITIONS
Measurement and prediction of propeller blade surface pressure distributions N90-20961
The use of numerical optimization for helicopter airfoil and blade design N90-20995
Data Link Processor (DLP) project transition plan
[DOT/FAA/CT-TN89/68] N90-21256

FLIGHT CONTROL
Optimization of the effective GPS data rate N90-20932
Investigation of air transportation technology at Princeton University, 1988-1989 N90-20935
Application of stochastic robustness to aircraft control systems N90-20936
An expert system for wind shear avoidance N90-20938
Rule-based mechanisms of learning for intelligent adaptive flight control N90-20939
Civil air transport: A fresh look at power-by-wire and fly-by-light
[NASA-TM-102574] N90-21283

FLIGHT CREWS
Windshear case study: Denver, Colorado, July 11, 1988
[DOT/FAA/DS-89/19] N90-21509

FLIGHT INSTRUMENTS
The effect of windscreen bows and HUD pitch ladder format on pilot performance during simulated flight
[AD-A218139] N90-21523

FLIGHT OPERATIONS
Data Link Processor (DLP) project transition plan
[DOT/FAA/CT-TN89/68] N90-21256

FLIGHT PATHS
Flight path reconstruction using extended Kalman filtering techniques
[PD-FC-9001] N90-20970

FLIGHT RECORDERS
Windshear case study: Denver, Colorado, July 11, 1988
[DOT/FAA/DS-89/19] N90-21509

FLIGHT SIMULATION
An early overview of tiltrotor aircraft characteristics and pilot procedures in civil transport applications
[DOT/FAA/DS-89/37] N90-21003
Stereopsis cueing effects on hover-in-turbulence performance in a simulated rotorcraft
[NASA-TP-2980] N90-21004
USSR Space Life Sciences Digest, Issue 26
[NASA-CR-392231] N90-21513
The effect of windscreen bows and HUD pitch ladder format on pilot performance during simulated flight
[AD-A218139] N90-21523

FLIGHT STABILITY TESTS
The MANTA: An RPV design to investigate forces and moments on a lifting surface
[NASA-CR-186227] N90-20971

FLIGHT TESTS
Flight test investigation of certification issues pertaining to general-aviation-type aircraft with natural laminar flow
[NASA-CR-181967] N90-20952

FLIGHT VEHICLES
Experimental aeroelasticity history, status and future in brief
[NASA-TM-102651] N90-21047

FLOOD PLAINS
Possible use of satellite data for flood plain mapping
[INPE-4968-PRE/1537] N90-21462

FLOODS
Performance evaluation of MSS/LANDSAT data in the estimation of fluvial channel width
[INPE-4906-PRE/1507] N90-21463

FLOW CHARACTERISTICS
Aerodynamic optimization by simultaneously updating flow variables and design parameters N90-20991
LaRC TPI 1500 series polymers
[NASA-CR-181899] N90-21129

FLOW DISTRIBUTION
Laser-velocimeter-measured flow field around an advanced, swept, eight-blade propeller at Mach 0.8
[NASA-TP-2462] N90-20942
Users manual for the NASA Lewis Ice Accretion Prediction Code (LEWICE)
[NASA-CR-185129] N90-20943
On total variation diminishing schemes for transonic turbulent flow computation N90-20945
Discrete-vortex model for the symmetric-vortex flow on cones
[NASA-TP-2969] N90-20946
An approximate viscous shock layer method for calculating the hypersonic flow over blunt-nosed bodies N90-20947
Comparison of C- and O-grid generation methods using a NACA 0012 airfoil
[AD-A216375] N90-20948
Some aspects of Essentially Nonoscillatory (ENO) formulations for the Euler equations, part 3
[NASA-CR-4285] N90-20949
Effects of nose bluntness and shock-shock interactions on blunt bodies in viscous hypersonic flows
[NASA-CR-186451] N90-20950
Computation of nonequilibrium chemically reacting flows in hypersonic flow field N90-20954
Measurement of lift development on rapidly-accelerated wings N90-20956
Convergence acceleration of hypersonic flow calculations: A nonlinear relaxation factor N90-20957
Computation of viscous flow around a propeller-shaft configuration with infinite-pitch rectangular blades N90-20958
Flow in a forward swept centrifugal fan, volumes 1 and 2 N90-20959
Optimum hypersonic airfoils with attached shocks N90-20960
An evaluation of the two-dimensional Euler and Navier-Stokes calculations based on a flux-vector splitting
[PB90-166778] N90-20963
Experimental and numerical investigation of the vortex flow over a sharp edged delta wing; with and without sideslip
[PB90-167131] N90-20964
Aerodynamic design techniques at DLR Institute for Design Aerodynamics N90-20979
Aerodynamic design via control theory N90-20998
Secondary Flows in Turbomachines
[AGARD-CP-469] N90-21009
Measurement of the flow field in the blade passage and side-wall region of a plane turbine cascade N90-21019
Centrifugal impeller geometry and its influence on secondary flows N90-21020
The effect of secondary flow on the redistribution of the total temperature field downstream of a stationary turbine cascade N90-21033
Supersonic nozzle design of arbitrary cross-section N90-21035
Subsonic flutter analysis using MSC/NASTRAN
[PB90-166786] N90-21041
Computer codes for the evaluation of thermodynamic properties, transport properties, and equilibrium constants of an 11-species air model
[NASA-TM-102602] N90-21297
Analysis and finite element approximation of some optimal control problems associated with the Navier-Stokes equations N90-21299
The effects of forcing on a single stream shear layer and its parent boundary layer
[NASA-CR-186529] N90-21301
Flutter of slender bodies under axial stress
[PB90-167024] N90-21425
Adaptive grid embedding for the two-dimensional flux-split Euler equations
[NASA-CR-186533] N90-21571
Rectangular subsonic jet flow field measurements
[NASA-CR-181925] N90-21598

FLOW EQUATIONS
Some aspects of Essentially Nonoscillatory (ENO) formulations for the Euler equations, part 3
[NASA-CR-4285] N90-20949
Multigrid accelerated relaxation solution of transonic full potential flow equation
[PD-CF-8942] N90-20951
Computation of nonequilibrium chemically reacting flows in hypersonic flow field N90-20954
Aerodynamic design via control theory N90-20998
A quasi-Lagrangian moving grid technique for investigating compressible flows N90-21298
Depth-averaged equations for turbulent free-surface flow
[PB90-164781] N90-21308
Finite element algorithms for hyperbolic conservation laws with forcing terms
[INPE-5024-RPE/617] N90-21595

FLOW MEASUREMENT
Laser velocimeter measurements of multiphase flow of solids
[DE90-007604] N90-21311

FLOW VELOCITY
Relating flow between counter-rotating propellers to aerodynamic interaction noise N90-20944
LDV measurements and the flow analysis in the vortex region of a radial inflow turbine N90-21007
SAR image coding N90-21246
The effects of forcing on a single stream shear layer and its parent boundary layer
[NASA-CR-186529] N90-21301
Laser velocimeter measurements of multiphase flow of solids
[DE90-007604] N90-21311

FLOW VISUALIZATION
Research on cascade secondary and tip-leakage flows: Periodicity and surface flow visualization N90-21026
Theoretical study of the flow in a rotating channel. Experimental study through flow visualization in a curved channel N90-21032

FLOWMETERS
In-situ permeable flow sensor
[DE90-008806] N90-21364

FLUID DYNAMICS
The modelling of heat and mass transfer near solid boundaries and comparison with experimental results
[PB90-167040] N90-21310
High accuracy solutions of incompressible Navier-Stokes equations
[NASA-TM-102539] N90-21567

FLUID FILMS
Improved analytical capabilities for foil air bearings, phase 1
[AD-A218071] N90-21389

FLUID FLOW
Direct sublimation of NaCl salt from carbon matrixes
[DE90-007927] N90-21139
Apparatus for mixing solutions in low gravity environments
[NASA-CASE-MFS-26047-1] N90-21209
Mixing of viscous fluids: Behavior of microstructures and chaos
[DE90-008871] N90-21304
The effect of viscosity on the resistive tearing mode with the presence of shear flow
[DE90-009340] N90-21312
In-situ permeable flow sensor
[DE90-008806] N90-21364
Fiber optic void fraction sensor
[DE90-009124] N90-21366
Instabilities and vortex dynamics in shear flow of magnetized plasmas
[DE90-009448] N90-21643

FLUORINE COMPOUNDS
Progress in the material development of LiCaAlF(6):Cr(3+) laser crystals
[DE90-009542] N90-21666

FLUTTER ANALYSIS
Subsonic flutter analysis using MSC/NASTRAN
[PB90-166786] N90-21041
Flutter of slender bodies under axial stress
[PB90-167024] N90-21425

FLUX VECTOR SPLITTING
An evaluation of the two-dimensional Euler and Navier-Stokes calculations based on a flux-vector splitting
[PB90-166778] N90-20963

FLYWHEELS
Computer-aided design of flywheel transmission systems N90-21392

FOCAL PLANE DEVICES
Study of advanced InSb arrays for SIRTF (Space Infrared Telescope Facility) N90-21325
Short wavelength HgCdTe staring focal plane for low background astronomy applications N90-21336
Low noise HgCdTe 128 x 128 SWIR FPA for Hubble space telescope N90-21337
Future directions for NICMOS arrays N90-21339
Status of the isophot detector development N90-21342
HgCdTe 256x256 NWIR FPA N90-21348

FOCUSING
Simulated image maps for use in experimental high-resolution electron microscopy
[DE90-009176] N90-21657

FOIL BEARINGS
Improved analytical capabilities for foil air bearings, phase 1
[AD-A218071] N90-21389

FOILS (MATERIALS)
Design and optimisation of thin foil x ray telescopes N90-21690

FOKKER-PLANCK EQUATION
Nonlinear interaction of photons and phonons in electron-positron plasmas
[DE90-009341] N90-21640

FORCE DISTRIBUTION
The MANTA: An RPV design to investigate forces and moments on a lifting surface
[NASA-CR-186227] N90-20971

FORCED VIBRATION
Wave receptance analysis of vibrating beams and stiffened plates N90-21419

FOREBODIES
Effects of nose bluntness and shock-shock interactions on blunt bodies in viscous hypersonic flows
[NASA-CR-186451] N90-20950

FOREST MANAGEMENT
Proceedings of the 4th European Conference, volume 2
[AD-A216521] N90-21382
Modeling large-scale vegetation dynamics
[DE90-008883] N90-21485

FORESTS
Shade images of forested areas obtained from LANDSAT MSS data
[NASA-TM-102939] N90-21436
Evolution of remote sensing applied to vegetation and forest at INPE
[INPE-4970-PRE/1538] N90-21452
Effects of Air Pollution on Western Forests
[PB90-131111] N90-21481

FORKS
Software to characterize tuning fork resonators used in the Quartz Digital Accelerometer
[DE90-007913] N90-21363

FORM FACTORS
Large basis space effects in electron scattering form factors of light nuclei
[DE90-613501] N90-21609

FORMALISM
A Lagrangian formalism for nonequilibrium ensembles
[DE90-612748] N90-21579
Problems in radiative transfer in astrophysics: An escape probability treatment of line overlap and a model of the masers around VX Sgr N90-21705

FORMULAS (MATHEMATICS)
A modified Moebius inverse formula and its applications in physics
[DE90-612740] N90-21594

FORTRAN
Lessons learned in the transition to Ada from FORTRAN at NASA/Goddard
[NASA-TM-103311] N90-21538

FOSSIL FUELS
A fossil energy perspective on global climate change
[DE90-007894] N90-21483

FOURIER ANALYSIS
Millimeter wave near-field study
[NASA-CR-182014] N90-21058
A correlation-spectral method for line detection on noisy data
[DE90-007925] N90-21266

FOURIER SERIES
Fourier series methods for plates and shells with cracks and inclusions N90-21406

FOURIER TRANSFORMATION
Fracture of sandwiched composites N90-21136
Problems in ISAR processing with range resolution by stepped frequency bursts N90-21238
Mesooptical Fourier transform microscope: A new device for high energy physics
[DE90-616423] N90-21615

FRACTOGRAPHY
Fractographic analysis of the crack growth rate and the shear lip development of 2024-T3 specimens under simple variable-amplitude loading
[PB90-167032] N90-21427

FRACTURE MECHANICS
A corrosion fatigue/stress corrosion testing facility at Materials Research Laboratory
[MRL-TN-568] N90-21044
Use of unbalanced laminates as a screening method for microcracking
[NASA-TM-102517] N90-21124
Fracture and longevity of composite structures
[AD-A217827] N90-21127
Three-dimensional elastic-plastic analysis of shallow cracks in single-edge-crack-tension specimens
[NASA-TM-102636] N90-21130
Two-dimensional damage models of fiber-reinforced composites N90-21135
Shock initiation sensitivity of damaged TP-H1207C composite propellant
[DE90-008509] N90-21205
Mechanics of interface fracture N90-21408
Compendium of fracture mechanics problems
[NASA-TM-100393] N90-21414

Development of a fracture analysis technique for use with a general-purpose finite element program N90-21416
NASA airframe structural integrity program [NASA-TM-102637] N90-21422
An evaluation of the pressure proof test concept for thin sheet 2024-T3 [NASA-TM-101675] N90-21424
Determination of internal strains in high-temperature superconductor composites by intense pulsed neutron source [DE90-007799] N90-21664
The thermo-mechanical behavior of cometary nuclei N90-21703

FRACTURE STRENGTH
A compendium of sources of fracture toughness and fatigue crack growth data for metallic alloys, part 4 [NASA-TM-102646] N90-21164
Fracture toughness and crack growth of Zerodur [NASA-TM-4185] N90-21187
Research advances in fine ceramics [DE90-008983] N90-21197

FRACTURES (MATERIALS)
Fracture of sandwiched composites N90-21136

FRACTURING
Acoustic characterisation of an aluminium silicon carbide metal matrix composite [AERE-R-13273] N90-21121
A casting and imaging technique for determining void geometry and relative permeability behavior of a single fracture specimen [DE90-009192] N90-21403
Contribution for the study of the evolution of part of the Espinhaco supergroup and its foundation through fracture analysis [INPE-4907-PRE/1508] N90-21459
The thermo-mechanical behavior of cometary nuclei N90-21703

FRAGMENTATION
Statistics on aircraft gas turbine engine rotor failures that occurred in US commercial aviation during 1986 [DOT/FAA/CT-89/30] N90-21008
Final safety analysis report for the Ulysses Mission. Volume 2: Accident model document-appendices [DE90-008695] N90-21104
Fragmentation of relativistic heavy nuclei with application to cosmic ray propagation N90-21716

FRAMES
Elastic-plastic instability of plane frames N90-21415

FREDHOLM EQUATIONS
Fracture of sandwiched composites N90-21136

FREE ELECTRON LASERS
Tenth International Free Electron Laser Conference [DE90-614773] N90-21376
On storage rings for short wavelength FELs [DE90-009059] N90-21379
Proposal for FY86 Lawrence Livermore National Laboratory particle beam research [DE90-007936] N90-21617

FREE ELECTRONS
Polarization: Effects on second harmonic power in light scattering by free electrons [DE90-612842] N90-21608

FREE VIBRATION
On total variation diminishing schemes for transonic turbulent flow computation N90-20945
Stress analysis of rocket motors with viscoelastic propellant by a mixed finite element model N90-21112
Wave receptance analysis of vibrating beams and stiffened plates N90-21419

FREQUENCY CONVERTERS
Intensity to frequency conversion technique in intensity modulated fiber optic sensing systems [NASA-TM-102562] N90-21277

FREQUENCY HOPPING
A real-time rejection circuit to automatically reject multiple interfering hopping signals while passing a lower level desired signal [AD-D014424] N90-21251

FREQUENCY MODULATION
Programmable generation of linear frequency modulated pulses N90-21232

FREQUENCY RANGES
A frequency agile 94 GHz pulse-Doppler radar with dual polarisation capability N90-21226

FREQUENCY SCANNING
A frequency agile 94 GHz pulse-Doppler radar with dual polarisation capability N90-21226

FRICTION FACTOR
Fiber pushout test: A three-dimensional finite element computational simulation [NASA-TM-102565] N90-21131

FRICTION WELDING
The effects of a nearby subsequent fusion weld on the properties of an inertia friction weld [DE90-007972] N90-21396

FUEL CELLS
Development of planar geometry solid oxide fuel cell technology, phase 2 [PB90-131293] N90-21467
Alternative materials for solid oxide fuel cells [DE90-008615] N90-21468
O2 reduction at the IFC orbiter fuel cell O2 electrode [NASA-TM-102580] N90-21469

FUEL COMBUSTION
The modelling of heat and mass transfer near solid boundaries and comparison with experimental results [PB90-167040] N90-21310

FUEL CONSUMPTION
Civil air transport: A fresh look at power-by-wire and fly-by-light [NASA-TM-102574] N90-21283
Computer-aided design of flywheel transmission systems N90-21392

FUEL SPRAYS
Microgravity acoustic mixing for particle cloud combustors [NASA-CR-185159] N90-21600

FUEL TANKS
Inflatable fuel tank buffer [AD-D014446] N90-21002

FULL SCALE TESTS
Full-scale air transport category fuselage burnthrough tests [DOT/FAA/CT-TN89/65] N90-20967

FUSELAGES
Full-scale air transport category fuselage burnthrough tests [DOT/FAA/CT-TN89/65] N90-20967
NASA airframe structural integrity program [NASA-TM-102637] N90-21422
An evaluation of the pressure proof test concept for thin sheet 2024-T3 [NASA-TM-101675] N90-21424

FUSION REACTORS
Fusion technology development [DE90-007933] N90-21636

FUSION WELDING
The effects of a nearby subsequent fusion weld on the properties of an inertia friction weld [DE90-007972] N90-21396
On-line assessment of weld quality using ultrasonics [AERE-R-13401] N90-21398

FUZZY SYSTEMS
Adaptive learning fuzzy control of a mobile robot [DE90-759898] N90-21562

G

GALACTIC COSMIC RAYS
A balloon measurement of the isotopic composition of galactic cosmic ray iron N90-21717

GALACTIC EVOLUTION
The large scale structure of the universe in pancake models of galaxy formation N90-21701

GALACTIC STRUCTURE
The evolution and geometry of the outer parts of the small Magellanic cloud N90-21697

GALERKIN METHOD
Is Galerkin's method really better [DE90-008804] N90-21267

GALLIUM
Stressed Ge:Ga photoconductors for space-based astronomy. (Is there life beyond 120 micron) N90-21315
Extrinsic germanium Blocked Impurity Bank (BIB) detectors N90-21322
Ga:Ge array development N90-21323
Initial astronomical results with a new 5-14 micron Si:Ga 58x62 DRO array camera N90-21334

GALLIUM ARSENIDES
Peeled film GaAs solar cells for space power [NASA-TM-103125] N90-21287
New surface atomic structures for column 5 overlayers on the (110) surfaces of 3-5 compound semiconductors [DE90-009003] N90-21663

GAMMA RAY BURSTS
The 1989 outburst of V404 Cygni: A very unusual x ray nova [DE90-008935] N90-21693

GAMMA RAY SPECTROMETERS
Microchannel photomultipliers in time spectrometer [DE90-616417] N90-21356

GAMMA RAYS
Gamma-ray production cross section measurements using a white neutron source from 1 to 400 MeV [DE90-008906] N90-21610
A search for very high energy gamma rays from the Crab pulsar-nebula N90-21718

GAS BEARINGS
Improved analytical capabilities for foil air bearings, phase 1 [AD-A218071] N90-21389

GAS DYNAMICS
Computation of nonequilibrium chemically reacting flows in hypersonic flow field N90-20954
Finite element algorithms for hyperbolic conservation laws with forcing terms [INPE-5024-RPE/617] N90-21595

GAS FLOW
Notes on the unsteady rectilinear motion of a perfect gas. Part 8: General theory and general waves in a homentropic gas [PB90-167149] N90-21309

GAS INJECTION
Analysis of the rotor tip leakage flow with tip cooling air ejection N90-21029

GAS IONIZATION
Helium transport in plasma edge regions N90-21625

GAS TURBINE ENGINES
Statistics on aircraft gas turbine engine rotor failures that occurred in US commercial aviation during 1986 [DOT/FAA/CT-89/30] N90-21008

GAS-SOLID INTERFACES
Laser studies of chemical dynamics at the gas-solid interface [DE90-008698] N90-21380

GAUGE INVARIANCE
Quantization of the N = 2m simple supergravity in d = 2 + 1 [DE90-612765] N90-21671
Some global problems in gauge theories (variations on a theme of Aharonov and Bohm) [DE90-009034] N90-21678

GAUGE THEORY
Chern-Simons superconductivity at finite temperature [DE90-613393] N90-21650
Studies in quantum field theory [DE90-008731] N90-21677
Some global problems in gauge theories (variations on a theme of Aharonov and Bohm) [DE90-009034] N90-21678

GEAR TEETH
A review of gear housing dynamics and acoustics literature [NASA-CR-185148] N90-21387

GEARS
Heat engine based on shape memory alloys [AD-D014400] N90-21385
A review of gear housing dynamics and acoustics literature [NASA-CR-185148] N90-21387
Transmission research activities at NASA Lewis Research Center [NASA-TM-103132] N90-21394

GENERAL AVIATION AIRCRAFT
Census of US civil aircraft [PB90-120296] N90-20920
Annual review of aircraft accident data: US general aviation calendar year 1987 [PB90-138066] N90-20966

GENETIC ENGINEERING
Artificial life: The coming evolution [DE90-008860] N90-21515

GENETICS
Artificial life: The coming evolution [DE90-008860] N90-21515

GEOBOTANY
Geobotanical remote sensing: A review [INPE-5026-PRE/1565] N90-21440

GEOCHRONOLOGY
Age constraints for the present fault configuration in the Imperial Valley, California: Evidence for northwestward propagation of the Gulf of California rift system [NASA-CR-186541] N90-21493

GEODETIC ACCURACY
Ambiguity bootstrapping to determine GPS orbits and baselines [AD-A218206] N90-21052
Subsystem TM Precision: Progress and perspective [INPE-5006-PRE/1563] N90-21481

GEODYNAMICS
Age constraints for the present fault configuration in the Imperial Valley, California: Evidence for northwestward propagation of the Gulf of California rift system [NASA-CR-186541] N90-21493

GEOGRAPHIC INFORMATION SYSTEMS
Analysis and modelling of spatial data proposal of a system for CBERS [INPE-4911-PRE/1512] N90-21445
Generation of triangular form models in a microcomputer environment [INPE-4974-PRE/1539] N90-21447

GEOLOGICAL FAULTS
Characterization of linear structures from remote sensing data; Espinhaco Meridional (MG) sierra
[INPE-4905-PRE/1506] N90-21449
Geology of Espinhaco Meridional, including the Quadrilatero Ferrifero: Integration through remote sensing data
[INPE-4904-PRE/1505] N90-21450
Age constraints for the present fault configuration in the Imperial Valley, California: Evidence for northwestward propagation of the Gulf of California rift system
[NASA-CR-186541] N90-21493

GEOLOGY
JPRS report. Science and technology. USSR: Earth sciences
[JPRS-UES-88-004] N90-21431
JPRS report. Science and technology. USSR: Earth sciences
[JPRS-UES-89-002] N90-21432
Results of the Gondwana Project: An example of intercontinental geologic correlation utilizing LANDSAT imagery
[INPE-4870-PRE/1481] N90-21437
Geobotanical remote sensing: A review
[INPE-5026-PRE/1565] N90-21440
Geology of Espinhaco Meridional, including the Quadrilatero Ferrifero: Integration through remote sensing data
[INPE-4904-PRE/1505] N90-21450
Introduction of digital image processing by remote sensors applied to geology
[INPE-5023-RPE/616] N90-21456
Contribution for the study of the evolution of part of the Espinhaco supergroup and its foundation through fracture analysis
[INPE-4907-PRE/1508] N90-21459

GEOMAGNETISM
Comparison of quiet time geomagnetic daily variation (Sq) in H component at Eusebio and Cachoeira Paulista
[INPE-4985-PRE/1547] N90-21714

GEOMETRIC DILUTION OF PRECISION
Ridge regression processing N90-20931

GEOMETRY
A system for transonic wing design with geometric constraints based on an inverse method N90-20983
Subsonic and transonic blade design by means of analysis codes N90-20985

GEOPHYSICS
Computer processing of multi-channel electromagnetic data from an airborne geophysical survey system
[PB90-138413] N90-21253
Age constraints for the present fault configuration in the Imperial Valley, California: Evidence for northwestward propagation of the Gulf of California rift system
[NASA-CR-186541] N90-21493

GEOSYNCHRONOUS ORBITS
Numerical Arc Segmentation Algorithm for a Radio Conference (NASARC), version 4.0: User's manual
[NASA-TM-101454] N90-21250

GERMANIUM
Stressed Ge:Ga photoconductors for space-based astronomy. (Is there life beyond 120 micron) N90-21315
Germanium Blocked Impurity Band (BIB) detectors N90-21321
Extrinsic germanium Blocked Impurity Bank (BIB) detectors N90-21322
Ga:Ge array development N90-21323

GET AWAY SPECIALS (STS)
United States Air Force Academy get-away-special flexible beam experiment N90-21088

GLASS
The structural basis for fatigue initiation in glassy polymers
[DE90-009342] N90-21200

GLASS LASERS
Generation of ultrashort laser pulses from neodymium glass oscillator and regenerative amplifier N90-21373

GLOBAL POSITIONING SYSTEM
Ridge regression processing N90-20931
Optimization of the effective GPS data rate N90-20932
Sole means navigation and integrity through hybrid Loran-C and NAVSTAR GPS N90-20933
Autonomous integrated GPS/INS navigation experiment for OMV. Phase 1: Feasibility study
[NASA-CR-4267] N90-20969
Ambiguity bootstrapping to determine GPS orbits and baselines
[AD-A218206] N90-21052

GOALS
Requirements of IR space astronomy N90-21314

GOERTLER INSTABILITY
On the instability of Goertler vortices to nonlinear travelling waves
[NASA-CR-181994] N90-21289

GOLD
Compatibility of Au base thick films with solder alloys: Solid state growth of intermetallics
[DE90-009265] N90-21175
Microstructure of Au/Nb multilayers
[DE90-008722] N90-21662

GOLD ISOTOPES
Strangeness enhancement in 14.6 A GeV/c Si+Au interactions?
[DE90-008826] N90-21616

GRADIENTS
Alternating gradient photodetector
[NASA-CASE-NPO-17235-1-CO] N90-21358

GRAIN BOUNDARIES
Characterization of failure processes in tungsten copper composites under fatigue loading conditions
[NASA-TM-102371] N90-21123
A STEM study of changing grain boundary chemistry during the sensitisation of AISI 304 stainless steel
[AERE-R-13418] N90-21157
Current fluctuations associated with localised corrosion: Mechanistic studies of the early stages of pitting and stress corrosion cracking of stainless steel
[AERE-R-13531] N90-21159
Mathematical modelling of intergranular attack in stainless steels: A preliminary study
[AERE-M-3698] N90-21160
Grain boundary precipitation in Ni3Al based alloys
[AERE-R-13362] N90-21161
Grain boundary chemistry effects on irradiation-assisted stress corrosion cracking
[DE90-008623] N90-21167
Anisotropy of grain growth in alumina
[DE90-009045] N90-21655
High voltage/high resolution studies of metal and semiconductor interfaces
[DE90-009065] N90-21656
Simulated image maps for use in experimental high-resolution electron microscopy
[DE90-009176] N90-21657

GRAIN SIZE
Methods for improving the flowability of a percussion primer composition
[MRL-TR-89-32] N90-21201

GRAPHITE
Resistivity of pristine and intercalated graphite fiber epoxy composites
[NASA-TM-102576] N90-21192

GRAPHITE-EPOXY COMPOUNDS
Strain and dynamic measurements using fiber optic sensors embedded into graphite/epoxy tubes N90-21090
Filament winding of composite cylinders N90-21119
Relevance of impacter shape to nonvisible damage and residual tensile strength of a thick graphite/epoxy laminate
[NASA-TM-102599] N90-21122

GRATINGS (SPECTRA)
Production of diffraction gratings using holographic interferometry
[DE90-612841] N90-21362

GRAVITATION
The 2 + 1 dimensional quantum gravity and the Braid group
[DE90-009036] N90-21679

GRAVITATION THEORY
Studies in quantum field theory
[DE90-008731] N90-21677

GRAVITATIONAL EFFECTS
Toward quantum corrections in black hole thermodynamics N90-21702

GRAVITATIONAL FIELDS
A measurement of the gravitational acceleration of the antiproton
[DE90-008903] N90-21612
The generally covariant representation of energy-momentum pseudotensor of gravitational field
[DE90-615203] N90-21669

GRAVITATIONAL LENSES
The gravitational lens effect and its optical equivalents
[DE90-612767] N90-21673

GRAVITATIONAL WAVES
On the creation of gravitational wave by photon in external electromagnetic field
[DE90-613366] N90-21265

GREENHOUSE EFFECT
A fossil energy perspective on global climate change
[DE90-007894] N90-21483

GRID GENERATION (MATHEMATICS)
A time-accurate adaptive grid method and the numerical simulation of a shock-vortex interaction
[NASA-TP-2998] N90-21524

GROUND STATIONS
Environmental projects, volume 10. Environmental assessment: New 34-meter antenna at Apollo site
[NASA-CR-186448] N90-21480

GROUND SUPPORT SYSTEMS
Environmental projects, volume 11. Environmental assessment: Addition to operations building, Mars site
[NASA-CR-186449] N90-21479
Environmental projects, volume 10. Environmental assessment: New 34-meter antenna at Apollo site
[NASA-CR-186448] N90-21480

GROUND TESTS
NASA/DOD Controls-Structures Interaction Technology 1989
[NASA-CP-3041] N90-21062
An air-bearing weight offload system for ground test of heavy LSS structures N90-21081
CSI technology validation on an LSS ground experiment facility N90-21089

GROUND TRUTH
Evaluation of the mangrove areas of the Rio Piaui (SE) through remote sensing
[INPE-4909-PRE/1510] N90-21454

GROUND WATER
Final safety analysis report for the Ulysses Mission. Volume 3 (Book 2): Nuclear risk analysis document-appendices
[DE90-008692] N90-21102
Corrosion behavior of mild steel ih high pH aqueous media
[PB90-131152] N90-21162
In-situ permeable flow sensor
[DE90-006806] N90-21364

GROUND-AIR-GROUND COMMUNICATION
National airspace system air-ground communications operational concept
[DOT/FAA/DS-90/2] N90-21249

GROUP THEORY
The 2 + 1 dimensional quantum gravity and the Braid group
[DE90-009036] N90-21679

GROUP VELOCITY
Development of an ultra-bright laser and an application to multi-photon ionization N90-21372

GROWTH
Evaluation of the mangrove areas of the Rio Piaui (SE) through remote sensing
[INPE-4909-PRE/1510] N90-21454

GUIDE VANES
LDV measurements and the flow analysis in the vortex region of a radial inflow turbine N90-21007
An investigation of secondary flows in nozzle guide vanes N90-21016
Secondary flow predictions for a transonic nozzle guide vane N90-21017
Secondary flow in a turbine guide vane with low aspect ratio N90-21018
Detailed heat transfer measurements in nozzle guide vane passages in linear and annular cascades in the presence of secondary flows N90-21030

GYROSCOPIC STABILITY
The anatomy of the gyroscope, part 3
[AGARD-AG-313] N90-21359

H

HAMILTONIAN FUNCTIONS
Periodic solutions for Hamiltonian systems in a nonconvex potential well
[DE90-612752] N90-21580

HARDNESS
Strengthening mechanisms of tungsten powder reinforced uranium
[DE90-009331] N90-21144

HARMONIC ANALYSIS
Parametric resonance in horizontal axis wind turbines N90-20962

HARMONIC FUNCTIONS
A remark on the Kelvin transform and a non-linear partial differential equation
[PB90-165622] N90-21589

HARTREE APPROXIMATION
Large basis space effects in electron scattering form factors of light nuclei
[DE90-613501] N90-21609

HAULING
Transportation monitoring unit qualification
[NASA-CR-183930] N90-21060

HEAD-UP DISPLAYS
The effect of windscreen bows and HUD pitch ladder format on pilot performance during simulated flight
[AD-A218139] N90-21523

HEALTH
Boeing 727-100 test project (high energy radiated field tests)
[DOT/FAA/CT-88/33] N90-21247

HEAT EXCHANGERS
Ice-making heat exchanger evaluation and test plan
[DE90-008824] N90-21218

An experimental evaluation of two nonazeotropic refrigerant mixtures in a water-to-water breadboard heat pump
[DE90-009016] N90-21305

HEAT FLUX
Principles of the radiosity method for canopy reflectance modeling
[DE90-008943] N90-21466

HEAT PUMPS
An experimental evaluation of two nonazeotropic refrigerant mixtures in a water-to-water breadboard heat pump
[DE90-009016] N90-21305

HEAT RESISTANT ALLOYS
Attachment of lead wires to thin film thermocouples mounted on high temperature materials using the parallel gap welding process
[NASA-TM-102442] N90-21361

HEAT SHIELDING
Mechanistic model for catalytic recombination during aerobraking maneuvers
[NASA-CR-185611] N90-21059

HEAT STORAGE
Thermal decay of an initially hot isothermal water body with application to thermal energy storage
[DE90-614742] N90-21675

HEAT TRANSFER
Ultrasonic techniques for aircraft ice accretion measurement N90-20926
Users manual for the NASA Lewis Ice Accretion Prediction Code (LEWICE)
[NASA-CR-185129] N90-20943
Secondary Flows in Turbomachines
[AGARD-CP-469] N90-21009
Detailed heat transfer measurements in nozzle guide vane passages in linear and annular cascades in the presence of secondary flows N90-21030
Effects of secondary flow on heat transfer in rotating passages N90-21031
Theoretical study of the flow in a rotating channel. Experimental study through flow visualization in a curved channel N90-21032
Surface-cooling effects on compressible boundary-layer instability
[NASA-CR-182003] N90-21290
Compact scheme for systems of equations applied to fundamental problems of mechanics of continua
[NASA-CR-186494] N90-21292
Navier-Stokes analysis of turbine blade heat transfer
[NASA-TM-102496] N90-21300
An experimental evaluation of two nonazeotropic refrigerant mixtures in a water-to-water breadboard heat pump
[DE90-009016] N90-21305
The modelling of heat and mass transfer near solid boundaries and comparison with experimental results
[PB90-167040] N90-21310
ULTRA-SHARP nonoscillatory convection schemes for high-speed steady multidimensional flow
[NASA-TM-102568] N90-21570
Program CICC: Flow and heat transfer in Cable In Conduit Conductors, user's manual
[DE90-007924] N90-21661
Nonoptimal entropy generation by heat transfer in cryogenic domain
[DE90-007544] N90-21667

HEAT TRANSFER COEFFICIENTS
Ultrasonic techniques for aircraft ice accretion measurement N90-20926

HEAT TREATMENT
Energy beam treatment for improved adhesion of coatings to surfaces
[AD-D014449] N90-21190

HEATERS
Space environment simulation of the SCD-01 satellite through heating plates
[INPE-4988-PRE/1550] N90-21105

HEATING
Boron-containing organosilane polymers and ceramic materials thereof
[NASA-CASE-ARC-11649-2-SB] N90-21177
Acoustic convective system
[NASA-CASE-NPO-17278-1-CU] N90-21215

HEAVY NUCLEI
Fragmentation of relativistic heavy nuclei with application to cosmic ray propagation N90-21716

HEAVY WATER
An attempt to measure cold-fusion effects
[DE90-613248] N90-21649

HELICOPTER CONTROL
Design of a helicopter automatic flight control system using adaptive control N90-21040
ROSAR (Helicopter-Rotor based Synthetic Aperture Radar) N90-21229

HELICOPTER DESIGN
Design of a helicopter automatic flight control system using adaptive control N90-21040

HELICOPTER PERFORMANCE
Performance data from a wind-tunnel test of two main-rotor blade designs for a utility-class helicopter
[NASA-TM-4183] N90-20974
An early overview of tiltrotor aircraft characteristics and pilot procedures in civil transport applications
[DOT/FAA/DS-89/37] N90-21003
Indianapolis Downtown Heliport: Operations analysis and marketing history
[REPT-90RR-13] N90-21049

HELICOPTERS
The use of numerical optimization for helicopter airfoil and blade design N90-20995

HELIOSTATS
Design and demonstration of an improved stretched-membrane heliostat
[DE90-007904] N90-21470

HELIPORTS
Indianapolis Downtown Heliport: Operations analysis and marketing history
[REPT-90RR-13] N90-21049
Analysis of distributions of Visual Meteorological Conditions (VMC) heliport data
[DOT/FAA/CT-TN89/67] N90-21508

HELIUM ISOTOPES
BASG thermomechanical pump helium 2 transfer tests
[NASA-CR-177541] N90-21097

HELIUM PLASMA
Helium transport in plasma edge regions N90-21625

HERMITIAN POLYNOMIAL
On induced Hermitian metrics for holomorphic vector bundles
[DE90-612737] N90-21572

HETERODYNING
Feasibility of using frequency offset on very high frequency air/ground voice channels
[DOT/FAA/CT-TN89/71] N90-21248

HIERARCHIES
Fault tolerant hypercube computer system architecture
[NASA-CASE-NPO-16859-1-CU] N90-21527

HIGH CURRENT
Method of making a long life high current density cathode from tungsten and iridium powders using a quarternary compound as the impregnant
[AD-D014425] N90-21211

HIGH ELECTRON MOBILITY TRANSISTORS
Proceedings of the Joint NOSC/NRL (Naval Ocean Systems Center/Naval Research Laboratory) InP Microwave/Millimeter Wave Technology Workshop
[AD-A218216] N90-21259

HIGH ENERGY ELECTRONS
High energy phenomena during solar flares
[INPE-4961-TDL/390] N90-21713

HIGH ENERGY INTERACTIONS
The design of a large aperture high field dipole
[DE90-007910] N90-21285
Mesooptical Fourier transform microscope: A new device for high energy physics
[DE90-616423] N90-21615
A search for very high energy gamma rays from the Crab pulsar-nebula N90-21718

HIGH FREQUENCIES
Feasibility of using frequency offset on very high frequency air/ground voice channels
[DOT/FAA/CT-TN89/71] N90-21248
An introduction to high frequency radioteletype systems
[PB90-145533] N90-21252

HIGH POLYMERS
Determinations of molecular weight and molecular weight distribution of high polymers by the rheological properties
[NASA-CR-186450] N90-21180

HIGH POWER LASERS
Laser controlled semiconductor armature for electromagnetic launchers
[AD-D014435] N90-21055

HIGH RESOLUTION
High-resolution Brillouin gain spectroscopy in solids
[DE90-009475] N90-21155
Application of superresolution methods for airborne radar N90-21227
HDTV bandwidth reduction using motion compensation and DATV
[BBC-RD-1989/10] N90-21254
High resolution imaging of the Venus night side using a Rockwell 128x128 HgCdTe array N90-21330
Simulated image maps for use in experimental high-resolution electron microscopy
[DE90-009176] N90-21657

HIGH SPEED
Aerofoil design techniques N90-20978

HIGH STRENGTH
Energy beam treatment for improved adhesion of coatings to surfaces
[AD-D014449] N90-21190

HIGH TEMPERATURE
Bis(4-(3,4-dimethylenepyrrolidyl)-phenyl) methane
[NASA-CASE-LAR-13965-1-CU] N90-21118
High temperature fatigue behavior of tungsten copper composites
[NASA-TM-102404] N90-21138
Pressure rig for repetitive casting
[NASA-CASE-LAR-14050-1] N90-21216

HIGH TEMPERATURE ENVIRONMENTS
Review of the state of the technology for joining ceramics for high-temperature structural applications
[DE90-009224] N90-21199

HIGH TEMPERATURE PLASMAS
Atomic processes in high temperature plasmas
[DE90-008873] N90-21632

HIGH TEMPERATURE SUPERCONDUCTORS
Determination of internal strains in high-temperature superconductor composites by intense pulsed neutron source
[DE90-007799] N90-21664
Modeling high-temperature superconductors and metallic alloys on the Intel IPSC/860
[DE90-009402] N90-21665

HILBERT SPACE
A monotone complementarity problem in Hilbert space
[DE90-009755] N90-21590
Quantization of the N = 2m simple supergravity in d = 2 + 1
[DE90-612765] N90-21671

HISTORIES
The anatomy of the gyroscope, part 3
[AGARD-AG-313] N90-21359

HOLOGRAPHIC INTERFEROMETRY
Production of diffraction gratings using holographic interferometry
[DE90-612841] N90-21362

HOLOGRAPHY
Method for holographic correction of beams of coherent light
[AD-D014406] N90-21353
Phase-only holographic filters and their applications
[PB90-166802] N90-21368

HOMOTOPY THEORY
A homotopy approach to the solutions of minimum-fuel space-flight rendezvous problems N90-21053

HONEYCOMB CORES
Stress analysis and minimum weight design of honeycomb sandwich plates N90-21418

HONEYCOMB STRUCTURES
Stress analysis and minimum weight design of honeycomb sandwich plates N90-21418

HOT-FILM ANEMOMETERS
Relating flow between counter-rotating propellers to aerodynamic interaction noise N90-20944

HOUSINGS
A review of gear housing dynamics and acoustics literature
[NASA-CR-185148] N90-21387

HOVERING
Stereopsis cueing effects on hover-in-turbulence performance in a simulated rotorcraft
[NASA-TP-2980] N90-21004

HUBBLE SPACE TELESCOPE
Proceedings of the Third Infrared Detector Technology Workshop
[NASA-TM-102209] N90-21313
Low noise HgCdTe 128 x 128 SWIR FPA for Hubble space telescope N90-21337
Laboratory and telescope use of the NICMOS2 128 x 128 HgCdTe array N90-21338
Future directions for NICMOS arrays N90-21339
Compendium of fracture mechanics problems
[NASA-TM-100393] N90-21414

HUMAN BODY
Kinematic and kinetic analyses of drop landings N90-21517

HUMAN CENTRIFUGES
Human centrifuge controller
[NAL-TM-SE-8901] N90-21043

HUMAN FACTORS ENGINEERING
Investigation of air transportation technology at the Massachusetts Institute of Technology, 1988-1989 N90-20922
Human factors in fighter software development
[PD-CF-9003] N90-21522
The effect of windscreen bows and HUD pitch ladder format on pilot performance during simulated flight
[AD-A218139] N90-21523

HUMAN PERFORMANCE
Development of microcomputer-based mental acuity tests for repeated-measures studies
[NASA-CR-185607] N90-21521

HURRICANES
Tropical cyclone track predictability and the adjoint method of data assimilation
[AD-A216324] N90-21505
HYBRID NAVIGATION SYSTEMS
Sole means navigation and integrity through hybrid Loran-C and NAVSTAR GPS N90-20933
HYDRAZINES
Numerical simulation model for hydrazine attitude control thrusters. Part 1: Model description
[INPE-4952-RPE/601] N90-21115
HYDROCARBON FUELS
Hydrocarbon-fuel/combustion-chamber-liner materials compatibility
[NASA-CR-185203] N90-21165
HYDRODYNAMIC RAM EFFECT
Inflatable fuel tank buffer
[AD-D014446] N90-21002
HYDRODYNAMICS
LLE review
[DE90-008958] N90-21378
The large scale structure of the universe in pancake models of galaxy formation N90-21701
HYDROGEN
Neutron autoradiography of hydrogen
[DE90-612930] N90-21148
Surface characterization of hydrogen charged and uncharged alpha-2 and gamma titanium aluminide alloys using AES and REELS
[NASA-CR-186561] N90-21171
HYPERBOLIC FUNCTIONS
Some aspects of Essentially Nonoscillatory (ENO) formulations for the Euler equations, part 3
[NASA-CR-4265] N90-20649
HYPERCUBE MULTIPROCESSORS
Fault tolerant hypercube computer system architecture
[NASA-CASE-NPO-16859-1-CU] N90-21527
HYPERSONIC FLOW
An approximate viscous shock layer method for calculating the hypersonic flow over blunt-nosed bodies N90-20947
Effects of nose bluntness and shock-shock interactions on blunt bodies in viscous hypersonic flows
[NASA-CR-186451] N90-20950
Computation of nonequilibrium chemically reacting flows in hypersonic flow field N90-20954
Convergence acceleration of hypersonic flow calculations: A nonlinear relaxation factor N90-20957
Optimum hypersonic airfoils with attached shocks N90-20960
HYPERSONIC SHOCK
Optimum hypersonic airfoils with attached shocks N90-20960
HYPERVELOCITY GUNS
Laser controlled semiconductor armature for electromagnetic launchers
[AD-D014435] N90-21055
HYPERVELOCITY IMPACT
Global nonlinear optimization of spacecraft protective structures design
[NASA-TM-100387] N90-21095

I

ICE
Modeling of surface roughness effects on glaze ice accretion N90-20925
Ultrasonic techniques for aircraft ice accretion measurement N90-20926
Investigation of surface water behavior during glaze ice accretion N90-20927
The influence of ice accretion physics on the forecasting of aircraft icing conditions N90-20928
Ice-making heat exchanger evaluation and test plan
[DE90-008824] N90-21218
ICE FORMATION
Investigation of air transportation technology at the Massachusetts Institute of Technology, 1988-1989 N90-20922
Modeling of surface roughness effects on glaze ice accretion N90-20925
Ultrasonic techniques for aircraft ice accretion measurement N90-20926
Investigation of surface water behavior during glaze ice accretion N90-20927
The influence of ice accretion physics on the forecasting of aircraft icing conditions N90-20928
Users manual for the NASA Lewis Ice Accretion Prediction Code (LEWICE)
[NASA-CR-185129] N90-20943
Advanced instrumentation for aircraft icing research
[NASA-CR-185225] N90-21006
ICE PREVENTION
Modeling of surface roughness effects on glaze ice accretion N90-20925
IDEAL GAS
Notes on the unsteady rectilinear motion of a perfect gas. Part 8: General theory and general waves in a homentropic gas
[PB90-167149] N90-21309
IDENTIFYING
Effective techniques for the identification and accommodation of disturbances N90-21072
IGNEOUS ROCKS
Geology of Espinhaco Meridional, including the Quadrilatero Ferrifero: Integration through remote sensing data
[INPE-4904-PRE/1505] N90-21450
ILLUMINATING
Modified touchdown zone lighting
[DOT/FAA/CT-TN89/70] N90-21042
IMAGE ANALYSIS
Results of the Gondwana Project: An example of intercontinental geologic correlation utilizing LANDSAT imagery
[INPE-4870-PRE/1481] N90-21437
Evaluation of classification performance and proportion estimate of the sugar cane crop through PROCEDURE-INPE utilizing LANDSAT data
[INPE-4899-PRE/1500] N90-21458
Performance evaluation of MSS/LANDSAT data in the estimation of fluvial channel width
[INPE-4906-PRE/1507] N90-21463
Performance evaluation of morphological edge detectors
[INPE-4975-PRE/1540] N90-21464
IMAGE CONTRAST
Shade images of forested areas obtained from LANDSAT MSS data
[NASA-TM-102939] N90-21436
IMAGE CORRELATORS
Digital processing of TM/LANDSAT data in monitoring interior water
[INPE-4956-PRE/1533] N90-21448
IMAGE MOTION COMPENSATION
A motion compensation study for the PHARUS project N90-21235
A solution for real time motion compensation for SAR without using inertial navigation systems N90-21236
The 1D-ISAR imaging of manoeuvering aircraft N90-21241
IMAGE PROCESSING
A fast ISAR-imaging process and its inherent degrading effects on image quality N90-21239
Automatic classification of images
[AD-D014437] N90-21260
A correlation-spectral method for line detection on noisy data
[DE90-007925] N90-21266
Absolute multilayer characterization at high spatial resolution via real-time soft x ray imaging
[DE90-009181] N90-21371
A casting and imaging technique for determining void geometry and relative permeability behavior of a single fracture specimen
[DE90-009192] N90-21403
High explosives (PBX9502) characterization using computerized tomography
[DE90-008170] N90-21404
Monitoring of agrocattle-raising projects through visual/digital analysis of LANDSAT-TM imagery south of Para state
[INPE-4982-PRE/1542] N90-21442
A knowledge-based information based for crop area estimation
[INPE-4990-PRE/1555] N90-21444
Digital processing of TM/LANDSAT data in monitoring interior water
[INPE-4956-PRE/1533] N90-21448
Introduction of digital image processing by remote sensors applied to geology
[INPE-5023-RPE/616] N90-21456
Principles of the radiosity method for canopy reflectance modeling
[DE90-008943] N90-21466
NETRA: A parallel architecture for integrated vision systems 2: Algorithms and performance evaluation
[NASA-CR-186510] N90-21557
Mesooptical Fourier transform microscope: A new device for high energy physics
[DE90-616423] N90-21615
Simulated image maps for use in experimental high-resolution electron microscopy
[DE90-009176] N90-21657
IMAGE RECONSTRUCTION
Problems in ISAR processing with range resolution by stepped frequency bursts N90-21238
Comparison of the algebraic reconstruction technique with the maximum entropy reconstruction technique for a variety of detection tasks
[DE90-008933] N90-21587
IMAGE RESOLUTION
Application of superresolution methods for airborne radar N90-21227
A fast ISAR-imaging process and its inherent degrading effects on image quality N90-21239
The 1D-ISAR imaging of manoeuvering aircraft N90-21241
InSb DRO array characteristics N90-21326
IMAGES
HDTV bandwidth reduction using motion compensation and DATV
[BBC-RD-1989/10] N90-21254
Automatic classification of images
[AD-D014437] N90-21260
IMAGING RADAR
Real-time adaptive radiometric correction for imaging radars systems N90-21233
IMAGING TECHNIQUES
SAR and ISAR imagery of marine targets N90-21237
Image simulation of geometric targets for synthetic aperture radar N90-21245
Ga:Ge array development N90-21323
Reduction and analysis techniques for infrared imaging data N90-21328
High resolution imaging of the Venus night side using a Rockwell 128x128 HgCdTe array N90-21330
Infrared ground-based astronomy with the Hughes 256 X 256 PtSi array N90-21331
Initial astronomical results with a new 5-14 micron Si:Ga 58x62 DRO array camera N90-21334
SOFIA: Stratospheric Observatory for Infrared Astronomy N90-21346
HgCdTe 256x256 NWIR FPA N90-21348
Ultrasonic and radiographic evaluation of advanced aerospace materials: Ceramic composites
[NASA-TM-102540] N90-21401
IMPACT DAMAGE
Relevance of impacter shape to nonvisible damage and residual tensile strength of a thick graphite/epoxy laminate
[NASA-TM-102599] N90-21122
A computational model of the perforation of multi-layer metallic laminates
[MRL-RR-9-89] N90-21128
IMPACT LOADS
Final safety analysis report for the Ulysses Mission. Volume 2: Accident model document-appendices
[DE90-008695] N90-21104
Shock initiation sensitivity of damaged TP-H1207C composite propellant
[DE90-008509] N90-21205
IMPACT TESTS
Simple light gas guns for hypervelocity studies
[DE90-008907] N90-21056
Cross-sectional examination of the damage zone in impacted specimens of carbon/epoxy and carbon/PEEK composites
[NASA-TM-100391] N90-21125
IMPEDANCE
Systematic errors in power measurements made with a dual six-port ANA
[PB90-145160] N90-21276
Low frequency gyrotron amplifier investigation, phase 2
[AD-A217096] N90-21352
A simplified theoretical model for the laser-induced optogalvanic effect
[DE90-613121] N90-21626
IMPELLERS
Flow in a forward swept centrifugal fan, volumes 1 and 2 N90-20959
Application of an inverse method to the design of a radial inflow turbine N90-20989
Centrifugal impeller geometry and its influence on secondary flows N90-21020
IMPREGNATING
Method of making a long life high current density cathode from tungsten and iridium powders using a quarternary compound as the impregnant
[AD-D014425] N90-21211
IMPURITIES
Improved Si:As BIBIB (Back-Illuminated Blocked-Impurity-Band) hybrid arrays N90-21349
IN-FLIGHT MONITORING
Optimization of the effective GPS data rate N90-20932
INCIDENCE
The effects of compressor endwall flow on airfoil incidence and deviation N90-21011
INCLUSIONS
Fourier series methods for plates and shells with cracks and inclusions N90-21406
INCOMPRESSIBLE FLOW
High accuracy solutions of incompressible Navier-Stokes equations
[NASA-TM-102539] N90-21567

ULTRA-SHARP nonoscillatory convection schemes for high-speed steady multidimensional flow
[NASA-TM-102568] N90-21570
Transition from resistive-g to eta-i driven turbulence in stellarator systems
[DE90-009382] N90-21641
INDIAN OCEAN
Use of microwave satellite data to study variations in rainfall over the Indian Ocean
[NASA-CR-186408] N90-21501
INDIUM ANTIMONIDES
Study of advanced InSb arrays for SIRTF (Space Infrared Telescope Facility) N90-21325
INDUCTION MOTORS
Electromechanical actuation for thrust vector control applications
[NASA-TM-102548] N90-21272
INELASTIC SCATTERING
US-Japan Workshop on Atomic Collisions in Solids: Abstracts of lectures
[DE90-008979] N90-21611
Inelastic electron scattering from surfaces
[DE90-009365] N90-21614
INERTIAL NAVIGATION
Optimization of the effective GPS data rate N90-20932
Autonomous integrated GPS/INS navigation experiment for OMV. Phase 1: Feasibility study
[NASA-CR-4267] N90-20969
INFERENCE
Time and truth in plans N90-20930
INFLATABLE STRUCTURES
Inflatable fuel tank buffer
[AD-D014446] N90-21002
INFORMATION DISSEMINATION
High performance computing and networking for science
[PB90-131228] N90-21526
INFORMATION FLOW
Strategies for concurrent processing of complex algorithms in data driven architectures
[NASA-CR-186515] N90-21535
INFORMATION RETRIEVAL
A formal approach to user models in data retrieval
[PB90-124728] N90-21682
INFORMATION SYSTEMS
Investigation of air transportation technology at the Massachusetts Institute of Technology, 1988-1989 N90-20922
A knowledge-based information based for crop area estimation
[INPE-4990-PRE/1555] N90-21444
A formal approach to user models in data retrieval
[PB90-124728] N90-21682
Army War College final prototype optical disk system testing and evaluation report
[DE90-008852] N90-21685
The ultimate CASE tool
[DE90-009351] N90-21687
INFORMATION THEORY
The ultimate CASE tool
[DE90-009351] N90-21687
INFORMATION TRANSFER
Weather data dissemination to aircraft N90-20934
INFRARED ASTRONOMY
Proceedings of the Third Infrared Detector Technology Workshop
[NASA-TM-102209] N90-21313
Discovery of low mass objects in Taurus N90-21329
Infrared ground-based astronomy with the Hughes 256 X 256 PtSi array N90-21331
Stressed detector arrays for airborne astronomy N90-21332
Preliminary results on two-dimensional interferometry of HL Tau N90-21335
Short wavelength HgCdTe staring focal plane for low background astronomy applications N90-21336
Introduction to the Infrared Space Observatory (ISO) N90-21340
SIRTF in high earth orbit N90-21345
SOFIA: Stratospheric Observatory for Infrared Astronomy N90-21346
INFRARED ASTRONOMY SATELLITE
AFGL ten micron mosaic array spectrometer: Recent results N90-21333
The molecular cloud content of early type galaxies. 2: A molecular ring in NGC 404
[PB90-124348] N90-21695
INFRARED DETECTORS
Proceedings of the Third Infrared Detector Technology Workshop
[NASA-TM-102209] N90-21313
The potential for high performance HgCdTe arrays at 4 microns N90-21320
Extrinsic germanium Blocked Impurity Bank (BIB) detectors N90-21322
Common source cascode amplifiers for integrating IR-FPA applications N90-21324
Reduction and analysis techniques for infrared imaging data N90-21328
Stressed detector arrays for airborne astronomy N90-21332
Design and status of the detector block for the ISO-SWS N90-21341
SOFIA: Stratospheric Observatory for Infrared Astronomy N90-21346
Laboratory characterization of direct readout Si:Sb and Si:Ga infrared detector arrays N90-21347
Improved Si:As BIBIB (Back-Illuminated Blocked-Impurity-Band) hybrid arrays N90-21349
INFRARED IMAGERY
Proceedings of the 13th International Congress on Instrumentation in Aerospace Simulation Facilities
[EOARD-LR-89-069] N90-21046
Reduction and analysis techniques for infrared imaging data N90-21328
INFRARED PHOTOGRAPHY
Investigation of air transportation technology at the Massachusetts Institute of Technology, 1988-1989 N90-20922
INFRARED RADIATION
Study of new technique of solid combustible materials to determination of volatile elements by flame atomic absorption spectrophotometry
[DE90-612907] N90-21147
Common source cascode amplifiers for integrating IR-FPA applications N90-21324
Experience with the UKIRT InSb array camera N90-21327
High resolution imaging of the Venus night side using a Rockwell 128x128 HgCdTe array N90-21330
Infrared ground-based astronomy with the Hughes 256 X 256 PtSi array N90-21331
Short wavelength HgCdTe staring focal plane for low background astronomy applications N90-21336
New water vapor masers in the Southern Hemisphere
[INPE-4844-PRE/1473] N90-21689
INFRARED RADIOMETERS
HgCdTe 256x256 NWIR FPA N90-21348
INFRARED SPACE OBSERVATORY (ISO)
Proceedings of the Third Infrared Detector Technology Workshop
[NASA-TM-102209] N90-21313
Introduction to the Infrared Space Observatory (ISO) N90-21340
Design and status of the detector block for the ISO-SWS N90-21341
Status of the isophot detector development N90-21342
ISO/LWS: Detector status N90-21343
ISO camera array development status N90-21344
INFRARED SPECTRA
On the substitution of Sr ions at Y sites in YB(suba2)Cu3O(sub7-d)
[DE90-613395] N90-21652
INFRARED SPECTROMETERS
Proceedings of the Third Infrared Detector Technology Workshop
[NASA-TM-102209] N90-21313
High resolution imaging of the Venus night side using a Rockwell 128x128 HgCdTe array N90-21330
Low noise HgCdTe 128 x 128 SWIR FPA for Hubble space telescope N90-21337
Laboratory and telescope use of the NICMOS2 128 x 128 HgCdTe array N90-21338
Future directions for NICMOS arrays N90-21339
INFRARED TELESCOPES
Requirements of IR space astronomy N90-21314
A 100 micro Kelvin bolometer system for SIRTF N90-21317
Study of advanced InSb arrays for SIRTF (Space Infrared Telescope Facility) N90-21325
Experience with the UKIRT InSb array camera N90-21327
Laboratory characterization of direct readout Si:Sb and Si:Ga infrared detector arrays N90-21347
INITIATION
An evaluation of metal salts of 3-nitro-1,2,4-triazol-5-one (NTO) as potential primary explosives
[MRL-TN-563] N90-21202
INJECTORS
Railgun performance with a two-stage light-gas gun injector
[DE90-009183] N90-21057
INJURIES
Kinematic and kinetic analyses of drop landings N90-21517
INLET FLOW
Application of an inverse method to the design of a radial inflow turbine N90-20989
LDV measurements and the flow analysis in the vortex region of a radial inflow turbine N90-21007
INSECTS
Multitemporal analysis of LANDSAT/TM digital imagery in the detection of areas affected by caterpillar (sibine fusca) attack in the dende (elais guineensis) palm plantation
[INPE-4979-PRE/1544] N90-21457
INSPECTION
High explosives (PBX9502) characterization using computerized tomography
[DE90-008170] N90-21404
Compendium of fracture mechanics problems
[NASA-TM-100393] N90-21414
INSULATION
Pressure rig for repetitive casting
[NASA-CASE-LAR-14050-1] N90-21216
Airborne sound insulation of slits, joints, and sealing stripes
[PB90-128976] N90-21599
INTAKE SYSTEMS
Inflatable fuel tank buffer
[AD-D014446] N90-21002
INTEGERS
Boron-containing organosilane polymers and ceramic materials thereof
[NASA-CASE-ARC-11649-2-SB] N90-21177
INTEGRAL EQUATIONS
On a non classical oblique derivative problem for parabolic singular integro-differential operators
[DE90-612739] N90-21574
INTEGRATED CIRCUITS
The development of ultraviolet-ozone cleaning as a production process in the packaging of integrated circuits
[DE90-007960] N90-21220
Coplanar waveguide fed phased array antenna
[NASA-TM-102522] N90-21273
Optical control of an 8-element Ka-band phased array using a high-speed optoelectronic interconnect
[NASA-TM-102550] N90-21275
INTELLIGENCE
Development of microcomputer-based mental acuity tests for repeated-measures studies
[NASA-CR-185607] N90-21521
INTERACTIONS
Detection of potential space station control/structure interaction with CO-ST-IN N90-21074
Optimization of the structural and control system for LSS with reduced-order model N90-21075
Computational architecture for integrated controls and structures design N90-21076
Controller reduction for effective interdisciplinary design of active structures N90-21077
Recent experience in simultaneous control-structure optimization N90-21078
A survey of experiments and experimental facilities for active control of flexible structures N90-21079
NASA CSI suspension methods overview N90-21080
ASCIE: An integrated experiment to study CSI in large segmented optical systems N90-21082
CSI sensing and control: Analytical and experimental results N90-21083
Experimental evaluation of active-member control of precision structures N90-21084
Controls, Astrophysics, and Structures Experiment in Space (CASES) N90-21085
CSI technology validation on an LSS ground experiment facility N90-21089
Initial operational capability of the ASTREX large space structures test bed N90-21091
INTERATOMIC FORCES
Helium transport in plasma edge regions N90-21625
INTERCALATION
Feasibility of intercalated graphite railgun armatures
[NASA-TM-102546] N90-21181
Resistivity of pristine and intercalated graphite fiber epoxy composites
[NASA-TM-102576] N90-21192
INTERCEPTION
Power transmission device
[AD-D014430] N90-21281
INTERFACES
High voltage/high resolution studies of metal and semiconductor interfaces
[DE90-009065] N90-21656
INTERFERENCE FIT
Internal rotor friction instability
[NASA-CR-183942] N90-21395
INTERFEROMETERS
A spaceborne optical interferometer: The JPL CSI mission focus N90-21063
Preliminary results on two-dimensional interferometry of HL Tau N90-21335
Passive stabilization of a fiber optic nonlinear interferometric sensor
[AD-D014438] N90-21620

The investigation of multilayer x ray reflectors as x ray optical elements
[DE90-009044] N90-21621

INTERFEROMETRY
The anatomy of the gyroscope, part 3
[AGARD-AG-313] N90-21359
Passive stabilization of a fiber optic nonlinear interferometric sensor
[AD-D014438] N90-21620

INTERGRANULAR CORROSION
A STEM study of changing grain boundary chemistry during the sensitisation of AISI 304 stainless steel
[AERE-R-13418] N90-21157

INTERMETALLICS
Lecture on ordered intermetallic alloys
[DE90-009011] N90-21169
Compatibility of Au base thick films with solder alloys: Solid state growth of intermetallics
[DE90-009265] N90-21175
Controlled production and characterization of metastable intermetallics
[DE90-009364] N90-21176

INTERNAL FRICTION
Internal rotor friction instability
[NASA-CR-183942] N90-21395

INTERPLANETARY FLIGHT
Mars in this century: The Olympia Project
[DE90-008356] N90-21709

INTERPOLATION
An overlapped grid method for multigrid, finite volume/difference flow solvers: MaGGiE
[NASA-CR-182008] N90-20953

INVARIANCE
Local supersymmetry in non-relativistic systems
[DE90-612751] N90-21670
Conserved conformal currents in curved space-time
[DE90-612766] N90-21672

INVISCID FLOW
Numerical method for designing 3D turbomachinery blade rows N90-20990
Surface-cooling effects on compressible boundary-layer instability
[NASA-CR-182003] N90-21290

ION ACOUSTIC WAVES
Langmuir wave interaction with ion acoustic wave
[DE90-615407] N90-21624

ION BEAMS
Low energy ion generator
[DE90-759905] N90-21195

ION IMPLANTATION
Formation of subsurface aluminum layers in beryllium by ion implantation and post-implant annealing
[DE90-007975] N90-21172
Energy beam treatment for improved adhesion of coatings to surfaces
[AD-D014449] N90-21190
Proceedings of the Joint NOSC/NRL (Naval Ocean Systems Center/Naval Research Laboratory) InP Microwave/Millimeter Wave Technology Workshop
[AD-A218216] N90-21259

ION TEMPERATURE
Helium transport in plasma edge regions N90-21625

IONIC COLLISIONS
Atomic processes in high temperature plasmas
[DE90-008873] N90-21632

IONIC CRYSTALS
Coupled magnetoplasmon-phonon modes at the surface of a semi-infinite semiconductor superlattice
[DE90-612904] N90-21647

IONIZATION
Alternating gradient photodetector
[NASA-CASE-NPO-17235-1-CO] N90-21358
Development of an ultra-bright laser and an application to multi-photon ionization N90-21372
LLE review
[DE90-008958] N90-21378
SR90, strontium shaped-charge critical ionization velocity experiment
[NASA-CR-186501] N90-21606
Atomic processes in high temperature plasmas
[DE90-008873] N90-21632

IONIZATION CHAMBERS
The RAP unit: A remote autoranging picoammeter
[DE90-007711] N90-21357

IONIZING RADIATION
Process for crosslinking methylene-containing aromatic polymers with ionizing radiation
[NASA-CASE-LAR-13448-1] N90-21198
Ga:Ge array development N90-21323

IONOSPHERIC COMPOSITION
Investigations into the properties, conditions, and effects of the ionosphere
[AD-A217807] N90-21489

IONOSPHERIC DISTURBANCES
Center of excellence in theoretical geoplasma research
[AD-A215035] N90-21488

IONOSPHERIC HEATING
Center of excellence in theoretical geoplasma research
[AD-A215035] N90-21488

IONOSPHERIC ION DENSITY
Dynamics of cavitons in strong Langmuir turbulence
[DE90-008918] N90-21633

IONS
Ionic equilibrium between octahedral and tetrahedral complexes in liquid aluminium-sodium fluoride mixtures
[DE90-613690] N90-21150
X ray laser with enhanced x ray gain through photodepopulation
[AD-D014448] N90-21375

IRIDIUM
Method of making a long life high current density cathode from tungsten and iridium powders using a quarternary compound as the impregnant
[AD-D014425] N90-21211

IRON
Studies of mechano-chemical interactions in the tribological behavior of materials
[NASA-TM-102545] N90-21182
A balloon measurement of the isotopic composition of galactic cosmic ray iron N90-21717

IRON ALLOYS
On the stability of amorphous silica coatings for high temperature service
[AERE-R-13425] N90-21179

IRRADIATION
Grain boundary chemistry effects on irradiation-assisted stress corrosion cracking
[DE90-008623] N90-21167
Low energy ion generator
[DE90-759905] N90-21195
Ga:Ge array development N90-21323
A simplified theoretical model for the laser-induced optogalvanic effect
[DE90-613121] N90-21626

IRREGULARITIES
Low latitude F-region dynamical processes from atomic oxygen nightglow emissions
[INPE-4999-PRE/1561] N90-21494

ISOLATION
Vibration isolation versus vibration compensation on multiple payload platforms N90-21066

ISOTOPES
Fragmentation of relativistic heavy nuclei with application to cosmic ray propagation N90-21716
A balloon measurement of the isotopic composition of galactic cosmic ray iron N90-21717

ISOTROPIC MEDIA
Generalized WKB approximation for stratified isotropic chiral structures
[PB90-165689] N90-21270

ISOTROPIC TURBULENCE
The extension of rapid distortion theory to stratified shear flows N90-21491

ITERATION
A two-dimensional unsteady analysis for transonic and supersonic cascade flows N90-20955
Convergence acceleration of hypersonic flow calculations: A nonlinear relaxation factor N90-20957
Application of an inverse method to the design of a radial inflow turbine N90-20989
Computational prediction and measurement of the flow in axial turbine cascades and stages N90-21028
Multigrid on massively parallel computers
[DE90-008999] N90-21560
High accuracy solutions of incompressible Navier-Stokes equations
[NASA-TM-102539] N90-21567
A parallel multigrid method for solving elliptic partial differential equations
[DE90-007929] N90-21584

ITERATIVE SOLUTION
The parallel algorithm for solving the three-dimensional integral magnetostatic equations
[DE90-616529] N90-21547

J

JAPAN
Microgravity science and applications bibliography, 1989 revision
[NASA-TM-4192] N90-21207

JET ENGINE FUELS
Concentric layer ramjet fuel
[AD-D014443] N90-21111

JET ENGINES
Research programs in aeronautical engineering, solid state physics, and materials science at Technion-Israel Institute of Technology, Haifa, Israel
[EOARD-LR-89-068] N90-21720

JET FLOW
Rectangular subsonic jet flow field measurements
[NASA-CR-181925] N90-21598

JFET
The potential for high performance HgCdTe arrays at 4 microns N90-21320

JOINTS (JUNCTIONS)
Heavily loaded joints for assembling aerobrake support trusses
[NASA-CR-181992] N90-21099
Fiber pushout test: A three-dimensional finite element computational simulation
[NASA-TM-102565] N90-21131
Expanding ring joint
[AD-D014398] N90-21384
The development of computational algorithms for manipulator inverse kinematics
[DE90-759877] N90-21561

JOSEPHSON JUNCTIONS
An ultra-small capacitance Josephson junction
[DE90-613396] N90-21653

K

K-EPSILON TURBULENCE MODEL
Depth-averaged equations for turbulent free-surface flow
[PB90-164781] N90-21308

KALMAN FILTERS
Autonomous integrated GPS/INS navigation experiment for OMV. Phase 1: Feasibility study
[NASA-CR-4267] N90-20969
Flight path reconstruction using extended Kalman filtering techniques
[PD-FC-9001] N90-20970

KINEMATIC EQUATIONS
Flight path reconstruction using extended Kalman filtering techniques
[PD-FC-9001] N90-20970

KINEMATICS
Development of a dynamic modeling technique and its application to the analysis and control of a high-precision robotic manipulator N90-21391
A new approach to solve the kinematics resolution of a redundant robot
[DE90-010213] N90-21397
Elastic-plastic instability of plane frames N90-21415
Kinematic and kinetic analyses of drop landings N90-21517
The development of computational algorithms for manipulator inverse kinematics
[DE90-759877] N90-21561

KINETIC ENERGY
Secondary flow calculations for axial and radial compressors N90-21024

KINETICS
Center of excellence in theoretical geoplasma research
[AD-A215035] N90-21488
The development of computational algorithms for manipulator inverse kinematics
[DE90-759877] N90-21561
Anisotropy of grain growth in alumina
[DE90-009045] N90-21655

KNOWLEDGE BASES (ARTIFICIAL INTELLIGENCE)
Cooperating intelligent systems
[NASA-CR-184982] N90-21529

L

LABORATORIES
Analytical sciences
[DE90-007965] N90-21152
Regional remote sensing laboratory
[INPE-4922-PRE/1519] N90-21465

LAGRANGE MULTIPLIERS
Suboptimal and hybrid numerical solution schemes for orbit transfer manoeuvres
[INPE-4991-PRE/1556] N90-21054

LAMINAR FLOW
Flight test investigation of certification issues pertaining to general-aviation-type aircraft with natural laminar flow
[NASA-CR-181967] N90-20952

LAMINAR FLOW AIRFOILS
Design of a natural laminar flow airfoil for an unmanned aircraft
[PD-CF-9004] N90-20975
Aerofoil design techniques N90-20978

LAMINAR MIXING
Mixing of viscous fluids: Behavior of microstructures and chaos
[DE90-008871] N90-21304
LAMINATES
Relevance of impacter shape to nonvisible damage and residual tensile strength of a thick graphite/epoxy laminate
[NASA-TM-102599] N90-21122
Use of unbalanced laminates as a screening method for microcracking
[NASA-TM-102517] N90-21124
Combined effect of matrix cracking and stress-free edge on delamination
[NASA-TM-102591] N90-21126
A computational model of the perforation of multi-layer metallic laminates
[MRL-RR-9-89] N90-21128
Compressive behavior of laminated composite structures N90-21134
Resistance mechanics for laminated composite materials
[INPE-4919-RPE/594] N90-21141
Crack stoppers and ARALL laminates
[PB90-166588] N90-21142
Determination of stresses around cutouts in multilayered composite plate and shell structures N90-21417
Delamination failure in a unidirectional curved composite laminate
[NASA-CR-182018] N90-21421
LAND USE
Survey of land use through remote sensing
[INPE-5032-MD/042] N90-21443
Digital processing of TM/LANDSAT data in monitoring interior water
[INPE-4956-PRE/1533] N90-21448
Aerial photography as an aid for agricultural credit control
[INPE-5019-RPE/613] N90-21455
LANDING
Kinematic and kinetic analyses of drop landings N90-21517
LANDING AIDS
Modified touchdown zone lighting
[DOT/FAA/CT-TN89/70] N90-21042
LANDSAT SATELLITES
Wheat yield estimation at the farm level using LANDSAT TM and agrometeorological data
[INPE-5017-RPE/611] N90-21439
Monitoring vegetation of Brazil: Potentialities of multi-sensors approach
[INPE-4993-PRE/1555] N90-21451
LARGE SPACE STRUCTURES
NASA/DOD Controls-Structures Interaction Technology 1989
[NASA-CP-3041] N90-21062
PACOSS program status and results N90-21065
Controlled multibody dynamics simulation for large space structures N90-21068
Nonlinear and distributed parameter models of the mini-mast truss N90-21070
Optimization of the structural and control system for LSS with reduced-order model N90-21075
An air-bearing weight offload system for ground test of heavy LSS structures N90-21081
Controls, Astrophysics, and Structures Experiment in Space (CASES) N90-21085
LACE flight dynamics experiment N90-21086
Space truss zero gravity dynamics N90-21087
CSI technology validation on an LSS ground experiment facility N90-21089
Strain and dynamic measurements using fiber optic sensors embedded into graphite/epoxy tubes N90-21090
Initial operational capability of the ASTREX large space structures test bed N90-21091
In-house experiments in large space structures at the Air Force Wright Aeronautical Laboratories Flight Dynamics Laboratory N90-21092
Preliminary design approach for large high precision segmented reflectors
[NASA-TM-102605] N90-21096
LASER APPLICATIONS
Production of diffraction gratings using holographic interferometry
[DE90-612841] N90-21362
Some recent applications of laser ultrasound to the characterisation of materials
[AERE-R-13438] N90-21374
LASER BEAMS
Power transmission device
[AD-D014430] N90-21281
LASER DOPPLER VELOCIMETERS
Laser-velocimeter-measured flow field around an advanced, swept, eight-blade propeller at Mach 0.8
[NASA-TP-2462] N90-20942
LDV measurements and the flow analysis in the vortex region of a radial inflow turbine N90-21007
Laser velocimeter measurements of multiphase flow of solids
[DE90-007604] N90-21311
The optical measurement of acoustic velocity fields N90-21601
LASER GYROSCOPES
The anatomy of the gyroscope, part 3
[AGARD-AG-313] N90-21359
LASER INTERFEROMETRY
Study on rotating plasma with submillimeter laser interferometer
[DE90-615387] N90-21623
LASER OUTPUTS
X ray laser with enhanced x ray gain through photodepopulation
[AD-D014448] N90-21375
Cloud hole-boring with long pulse CO2 lasers
[DE90-008946] N90-21377
LASER PLASMAS
X ray laser with enhanced x ray gain through photodepopulation
[AD-D014448] N90-21375
Experimental study of population inversion and spectral line broadening in a plasma containing a mixture of high Z and low Z ions
[DE90-007552] N90-21622
LASER PUMPING
Progress in the material development of LiCaAlF(6):Cr(3+) laser crystals
[DE90-009542] N90-21666
LASER TARGETS
LLE review
[DE90-008958] N90-21378
Experimental study of population inversion and spectral line broadening in a plasma containing a mixture of high Z and low Z ions
[DE90-007552] N90-21622
LASERS
Apparatus and method for locating the axis of symmetry (center of circular cross section) of three dimensional objects
[AD-D014407] N90-21354
LLE review
[DE90-008958] N90-21378
Laser studies of chemical dynamics at the gas-solid interface
[DE90-008698] N90-21380
Space power generation and distribution
[DE90-008676] N90-21474
JPRS report: Science and technology. USSR: Physics and mathematics
[JPRS-UPM-90-002] N90-21593
A simplified theoretical model for the laser-induced optogalvanic effect
[DE90-613121] N90-21626
Relativistic stimulated Brillouin and Raman scattering in a laser-produced plasma
[DE90-613123] N90-21627
Army War College final prototype optical disk system testing and evaluation report
[DE90-008852] N90-21685
Research programs in aeronautical engineering, solid state physics, and materials science at Technion-Israel Institute of Technology, Haifa, Israel
[EOARD-LR-89-068] N90-21720
LASING
Generation of ultrashort laser pulses from neodymium glass oscillator and regenerative amplifier N90-21373
Tenth International Free Electron Laser Conference
[DE90-614773] N90-21376
LATTICE VIBRATIONS
Modified tight-binding approximation and electron-phonon spectral function for transition metals
[DE90-614022] N90-21166
LAUNCH VEHICLES
Advanced Launch System (ALS): Electrical actuation and power systems improve operability and cost picture
[NASA-TM-102547] N90-21271
LAUNCHERS
Laser controlled semiconductor armature for electromagnetic launchers
[AD-D014435] N90-21055
LAUNCHING
NASA's Advanced Communications Technology Satellite (ACTS): Will it benefit commercial/military satellites
[AD-A217710] N90-21100
LAUNCHING SITES
Gaithersburg Nike control and launch area preliminary assessment/site inspection, Gaithersburg, Maryland
[AD-A217791] N90-21482
LEAD ALLOYS
Phase equilibria and solution thermodynamics of bismuth-lead alloys
[PB90-138421] N90-21183
LEAKAGE
Research on cascade secondary and tip-leakage flows: Periodicity and surface flow visualization N90-21026
Losses in the tip-leakage flow of a planar cascade of turbine blades N90-21027
Analysis of the rotor tip leakage flow with tip cooling air ejection N90-21029
LEAST SQUARES METHOD
A note on overdispersed exponential families
[AD-A216277] N90-21565
LEVELING
The effect of leveling coatings on the atomic oxygen durability of solar concentrator surfaces
[NASA-TM-102557] N90-21110
LIBRARIES
Hypercluster parallel processing library user's manual
[NASA-CR-185231] N90-21552
Medical subject headings: Annotated alphabetic list, 1990
[PB90-100009] N90-21683
LIFE (DURABILITY)
Effect of KOH concentration on LEO cycle life of IPV nickel-hydrogen flight battery cells
[NASA-TM-103127] N90-21116
Method of making a long life high current density cathode from tungsten and iridium powders using a quarternary compound as the impregnant
[AD-D014425] N90-21211
LIFE SCIENCES
USSR Space Life Sciences Digest, Issue 26
[NASA-CR-392231] N90-21513
LIFT
Measurement of lift development on rapidly-accelerated wings N90-20956
LIFT DRAG RATIO
An aerodynamic tradeoff study of the scissor wing configuration
[NASA-CR-186576] N90-20965
LIGHT BEAMS
Diamond: A high power optical material
[DE90-008941] N90-21196
Method for holographic correction of beams of coherent light
[AD-D014406] N90-21353
LIGHT GAS GUNS
Simple light gas guns for hypervelocity studies
[DE90-008907] N90-21056
Railgun performance with a two-stage light-gas gun injector
[DE90-009183] N90-21057
LIGHT SCATTERING
Determinations of molecular weight and molecular weight distribution of high polymers by the rheological properties
[NASA-CR-186450] N90-21180
Polarization: Effects on second harmonic power in light scattering by free electrons
[DE90-612842] N90-21608
Large basis space effects in electron scattering form factors of light nuclei
[DE90-613501] N90-21609
LIGHT SOURCES
Railgun performance with a two-stage light-gas gun injector
[DE90-009183] N90-21057
LIGHT TRANSMISSION
Diamond: A high power optical material
[DE90-008941] N90-21196
LINE SPECTRA
Zones of feasibility for retrieval of surface pressure from observations of absorption in the A band of oxygen
[DAR-TP-19] N90-21495
Experimental study of population inversion and spectral line broadening in a plasma containing a mixture of high Z and low Z ions
[DE90-007552] N90-21622
Problems in radiative transfer in astrophysics: An escape probability treatment of line overlap and a model of the masers around VX Sgr N90-21705
LINEAR ACCELERATORS
Gamma-ray production cross section measurements using a white neutron source from 1 to 400 MeV
[DE90-008906] N90-21610
LINEAR QUADRATIC REGULATOR
On the continuous dependence with respect to sampling of the linear quadratic regulator problem for distributed parameter systems
[NASA-CR-182012] N90-21566
LINEAR SYSTEMS
Stochastic robustness of linear control systems N90-20941

LININGS
Hydrocarbon-fuel/combustion-chamber-liner materials compatibility
[NASA-CR-185203] N90-21165
LIOUVILLE EQUATIONS
A Lagrangian formalism for nonequilibrium ensembles
[DE90-612748] N90-21579
LIPIDS
A new class of lubricants derived from archaebacterial lipids
[AD-D014429] N90-21185
LIQUID CHROMATOGRAPHY
Determinations of molecular weight and molecular weight distribution of high polymers by the rheological properties
[NASA-CR-186450] N90-21180
LIQUID CRYSTALS
LLE review
[DE90-006958] N90-21378
LIQUID HELIUM 2
BASG thermomechanical pump helium 2 transfer tests
[NASA-CR-177541] N90-21097
LIQUID INJECTION
Liquid Transfer Cryogenic Test Facility: Initial hydrogen and nitrogen no-vent fill data
[NASA-TM-102572] N90-21295
LIQUID PROPELLANT ROCKET ENGINES
Numerical simulation model for hydrazine attitude control thrusters. Part 1: Model description
[INPE-4952-RPE/601] N90-21115
LIQUID SURFACES
Inflatable fuel tank buffer
[AD-D014446] N90-21002
LIQUIDS
A solution level indicator system
[DE90-007939] N90-21151
Laser velocimeter measurements of multiphase flow of solids
[DE90-007604] N90-21311
LISTS
Medical subject headings: Annotated alphabetic list, 1990
[PB90-100009] N90-21683
LITHIUM ALLOYS
Determination of Li-Al alloy extent in tubular aluminum elements by small source neutron radiology
[DE90-009142] N90-21174
LITHOGRAPHY
Extrinsic germanium Blocked Impurity Band (BIB) detectors N90-21322
LOAD DISTRIBUTION (FORCES)
Stress analysis and minimum weight design of honeycomb sandwich plates N90-21418
LOADS (FORCES)
Heavily loaded joints for assembling aerobrake support trusses
[NASA-CR-181992] N90-21099
LOCKS (FASTENERS)
Expanding ring joint
[AD-D014398] N90-21384
LOGIC PROGRAMMING
VLSI binary updown counter
[NASA-CASE-NPO-17205-1-CU] N90-21525
LORAN C
Sole means navigation and integrity through hybrid Loran-C and NAVSTAR GPS N90-20933
LOW ASPECT RATIO
Secondary flow in a turbine guide vane with low aspect ratio N90-21018
LOW FREQUENCIES
Proceedings of a workshop on Carcinogenic Potential of Extremely Low Frequency Magnetic Fields
[DE90-614340] N90-21520
LOW VISIBILITY
Modified touchdown zone lighting
[DOT/FAA/CT-TN89/70] N90-21042
LUBRICANTS
A new class of lubricants derived from archaebacterial lipids
[AD-D014429] N90-21185
Improved Thermo-Oxidative-Deposition screening tests for turbine lubricants
[AD-A217795] N90-21188
Influence of the deposition conditions on radiofrequency magnetron sputtered MoS2 films
[NASA-TP-2994] N90-21210
Improved analytical capabilities for foil air bearings, phase 1
[AD-A218071] N90-21389
LUMINOSITY
Discovery of low mass objects in Taurus N90-21329
Recent advances in the studies of the nova outburst
[DE90-008936] N90-21691
Multi-wavelength observations of novae in outburst
[DE90-008934] N90-21692
LUNAR BASES
Space power generation and distribution
[DE90-008676] N90-21474
Mars in this century: The Olympia Project
[DE90-008356] N90-21709

M

MACHINE LEARNING
Rule-based mechanisms of learning for intelligent adaptive flight control N90-20939
Adaptive learning fuzzy control of a mobile robot
[DE90-759898] N90-21582
MACHINING
Advanced manufacturing technology: A Department of Energy technology transfer initiative
[DE90-006601] N90-21688
MAGAZINES (SUPPLY CHAMBERS)
Minutes of the 23rd Explosives Safety Seminar, volume 1
[AD-A218264] N90-21213
MAGELLANIC CLOUDS
The evolution and geometry of the outer parts of the small Magellanic cloud N90-21697
MAGMA
Geology of Espinhaco Meridional, including the Quadrilatero Ferrifero: Integration through remote sensing data
[INPE-4904-PRE/1505] N90-21450
MAGNETIC COOLING
A 100 micro Kelvin bolometer system for SIRTF N90-21317
MAGNETIC DIPOLES
The design of a large aperture high field dipole
[DE90-007910] N90-21285
Characterization of the plasma in magnetic multidipole discharges
[DE90-613219] N90-21628
MAGNETIC EFFECTS
The effects of magnetic nozzle configurations on plasma thrusters
[NASA-CR-186465] N90-21109
MAGNETIC FIELDS
The effects of magnetic nozzle configurations on plasma thrusters
[NASA-CR-186465] N90-21109
Generalized WKB approximation for stratified isotropic chiral structures
[PB90-165689] N90-21270
A 100 micro Kelvin bolometer system for SIRTF N90-21317
The parallel algorithm for solving the three-dimensional integral magnetostatic equations
[DE90-616529] N90-21547
Relativistic stimulated Brillouin and Raman scattering in a laser-produced plasma
[DE90-613123] N90-21627
On the relativistic Vlasov equation in guiding-center coordinates
[DE90-613241] N90-21629
MHD modes driven by anomalous electron viscosity and their role in fast sawtooth crashes
[DE90-009311] N90-21639
Coupled magnetoplasmon-phonon modes at the surface of a semi-infinite semiconductor superlattice
[DE90-612904] N90-21647
Recent advances in the studies of the nova outburst
[DE90-008936] N90-21691
Thomson scattering in a magnetic field N90-21699
MAGNETIC STORMS
Substorms: Their expansion and recovery phases
[DE90-008970] N90-21712
MAGNETIC VARIATIONS
Comparison of quiet time geomagnetic daily variation (Sq) in H component at Eusebio and Cachoeira Paulista
[INPE-4985-PRE/1547] N90-21714
MAGNETIZATION
Center of excellence in theoretical geoplasma research
[AD-A215035] N90-21488
MAGNETOACOUSTIC WAVES
Magneto acoustic emission apparatus for testing materials for embrittlement
[NASA-CASE-LAR-13817-1] N90-21170
MAGNETOHYDRODYNAMIC FLOW
The effects of magnetic nozzle configurations on plasma thrusters
[NASA-CR-186465] N90-21109
MAGNETOHYDRODYNAMIC STABILITY
The effect of viscosity on the resistive tearing mode with the presence of shear flow
[DE90-009340] N90-21312
Fusion burn dynamics in Dense Z-Pinch (DZP)
[DE90-007976] N90-21638
MHD modes driven by anomalous electron viscosity and their role in fast sawtooth crashes
[DE90-009311] N90-21639
Transition from resistive-g to eta-i driven turbulence in stellarator systems
[DE90-009382] N90-21641
Instabilities and vortex dynamics in shear flow of magnetized plasmas
[DE90-009448] N90-21643
Solar flares and dynamics of Langmuir waves in current-carrying plasmas
[IPPCZ-291] N90-21710
MAGNETOHYDRODYNAMICS
Numerical code AEOLUS-E1 for analysing free-boundary resistive MHD mode
[DE90-759903] N90-21630
MAGNETOSTATICS
The parallel algorithm for solving the three-dimensional integral magnetostatic equations
[DE90-616529] N90-21547
MAGNETRON SPUTTERING
Magnetron sputtered boron films and Ti/B multilayer structures
[DE90-009190] N90-21153
Influence of the deposition conditions on radiofrequency magnetron sputtered MoS2 films
[NASA-TP-2994] N90-21210
MAINTENANCE
Brake performance of the McDonnell Douglas DC-10-30/40 during high speed, high energy rejected takeoffs
[PB90-917004] N90-21000
Vibration isolation versus vibration compensation on multiple payload platforms N90-21066
Thermal control system corrosion study
[NASA-TM-102220] N90-21294
Maintenance = reuse-oriented software development
[NASA-CR-186455] N90-21531
MAN MACHINE SYSTEMS
Simulator comparison of thumball, thumb switch, and touch screen input concepts for interaction with a large screen cockpit display format
[NASA-TM-102587] N90-21005
MANAGEMENT PLANNING
Quality at a glance
[AD-A217297] N90-21400
Software Management Environment (SME) concepts and architecture
[NASA-TM-103306] N90-21543
MANAGEMENT SYSTEMS
Detection of potential space station control/structure interaction with CO-ST-IN N90-21074
Integrating automated support for a software management cycle into the TAME system
[NASA-CR-186457] N90-21532
MANIFOLDS (MATHEMATICS)
The monad construction and Hermetian-Einstein metrics
[DE90-612738] N90-21573
On a non classical oblique derivative problem for parabolic singular integro-differential operators
[DE90-612739] N90-21574
Linking numbers and variational method
[DE90-612793] N90-21582
MANIPULATORS
Modeling elastomer displacements for tactile sensing applications
[DE90-007959] N90-21370
End point control of flexible manipulators
[AD-A217319] N90-21383
Development of a dynamic modeling technique and its application to the analysis and control of a high-precision robotic manipulator N90-21391
Application of optimization in design and motion control of robot manipulators N90-21393
The development of computational algorithms for manipulator inverse kinematics
[DE90-759877] N90-21561
MANNED MARS MISSIONS
Mars in this century: The Olympia Project
[DE90-008356] N90-21709
MANUALS
Software Engineering Laboratory (SEL) database organization and user's guide
[NASA-TM-103304] N90-21545
MANUFACTURING
Filament winding of composite cylinders N90-21119
JPRS report: Science and technology. USSR: Electronics and electrical engineering
[JPRS-UEE-90-002] N90-21284
High explosives (PBX9502) characterization using computerized tomography
[DE90-008170] N90-21404
Design and demonstration of an improved stretched-membrane heliostat
[DE90-007904] N90-21470

Advanced manufacturing technology: A Department of Energy technology transfer initiative
[DE90-008601] N90-21688

MANY BODY PROBLEM
Controlled multibody dynamics simulation for large space structures N90-21068
Element-specific modal formulations for large-displacement multibody dynamics N90-21069
The large scale structure of the universe in pancake models of galaxy formation N90-21701

MAPPING
Monitoring of agrocattle-raising projects through visual/digital analysis of LANDSAT-TM imagery south of Para state
[INPE-4982-PRE/1542] N90-21442
Project CANASATE: Remote sensing applied to sugar cane crop survey
[INPE-4902-PRE/1503] N90-21446
Possible use of satellite data for flood plain mapping
[INPE-4968-PRE/1537] N90-21462
A monotone complementarity problem in Hilbert space
[DE90-009755] N90-21590
Simulated image maps for use in experimental high-resolution electron microscopy
[DE90-009176] N90-21657
STORM: A statistical object representation model
[DE90-009048] N90-21686

MARINE BIOLOGY
Modeling the upper ocean and its interaction with the atmosphere
[DE90-008980] N90-21511

MARINE ENVIRONMENTS
SAR and ISAR imagery of marine targets N90-21237

MARINE METEOROLOGY
Numerical simulations of the cloud-capped marine boundary layer N90-21506

MARINE PROPULSION
Computation of viscous flow around a propeller-shaft configuration with infinite-pitch rectangular blades N90-20958

MARKET RESEARCH
Indianapolis Downtown Heliport: Operations analysis and marketing history
[REPT-90RR-13] N90-21049

MARKETING
Indianapolis Downtown Heliport: Operations analysis and marketing history
[REPT-90RR-13] N90-21049

MARKING
Does DNA cytometry have a place in the clinical laboratory
[DE90-007652] N90-21512

MASS TRANSFER
Numerical simulation model for hydrazine attitude control thrusters. Part 1: Model description
[INPE-4952-RPE/601] N90-21115
The modelling of heat and mass transfer near solid boundaries and comparison with experimental results
[PB90-167040] N90-21310

MASSIVELY PARALLEL PROCESSORS
Performance bounds on parallel self-initiating discrete-event
[NASA-CR-182010] N90-21556
Multigrid on massively parallel computers
[DE90-008999] N90-21560

MATCHED FILTERS
Phase-only holographic filters and their applications
[PB90-166802] N90-21368

MATERIALS HANDLING
Application of optimization in design and motion control of robot manipulators N90-21393

MATHEMATICAL LOGIC
OTTER (Organized Techniques for Theorem-proving and Effective Research) 2.0 users guide
[DE90-007978] N90-21563

MATHEMATICAL MODELS
Discrete-vortex model for the symmetric-vortex flow on cones
[NASA-TP-2989] N90-20946
A two-dimensional unsteady analysis for transonic and supersonic cascade flows N90-20955
Parametric resonance in horizontal axis wind turbines N90-20962
An efficient airfoil design method using the Navier-Stokes equations N90-20981
An intensive procedure for the design of pressure-specified three-dimensional configurations at subsonic and supersonic speeds by means of a higher-order panel method N90-20982
Subsonic and transonic blade design by means of analysis codes N90-20985
Inverse computation of transonic internal flows with application for multi-point-design of supercritical compressor blades N90-20987
Numerical method for designing 3D turbomachinery blade rows N90-20990
Constrained spanload optimization for minimum drag of multi-lifting-surface configurations N90-20992
Secondary flows and radial mixing predictions in axial compressors N90-21010
A study on secondary flow and spanwise mixing in axial flow compressors N90-21012
Parabolized calculations of turbulent three dimensional flows in a turbine duct N90-21013
Experimental and numerical study on basic phenomena of secondary flows in turbines N90-21014
Secondary flow calculations for axial and radial compressors N90-21024
The numerical simulation of multistage turbomachinery flows N90-21025
Research on cascade secondary and tip-leakage flows: Periodicity and surface flow visualization N90-21026
Analysis of the rotor tip leakage flow with tip cooling air ejection N90-21029
Experimental and theoretical investigation of optimal control methods with model reduction N90-21039
Design of a helicopter automatic flight control system using adaptive control N90-21040
Subsonic flutter analysis using MSC/NASTRAN
[PB90-166786] N90-21041
NASA/DOD Controls-Structures Interaction Technology 1989
[NASA-CP-3041] N90-21062
Element-specific modal formulations for large-displacement multibody dynamics N90-21069
Nonlinear and distributed parameter models of the mini-mast truss N90-21070
A distributed finite-element modeling and control approach for large flexible structures N90-21071
Modeling and control of flexible space platforms with articulated payloads N90-21073
Optimization of the structural and control system for LSS with reduced-order model N90-21075
Recent experience in simultaneous control-structure optimization N90-21078
CSI sensing and control: Analytical and experimental results N90-21083
Experimental evaluation of active-member control of precision structures N90-21084
LACE flight dynamics experiment N90-21086
Stress analysis of rocket motors with viscoelastic propellant by a mixed finite element model N90-21112
A computational model of the perforation of multi-layer metallic laminates
[MRL-RR-9-89] N90-21128
Resistance mechanics for laminated composite materials
[INPE-4919-RPE/594] N90-21141
Mathematical modelling of intergranular attack in stainless steels: A preliminary study
[AERE-M-3698] N90-21160
Intensity to frequency conversion technique in intensity modulated fiber optic sensing systems
[NASA-TM-102562] N90-21277
Numerical simulation of vortex breakdown N90-21288
Computer codes for the evaluation of thermodynamic properties, transport properties, and equilibrium constants of an 11-species air model
[NASA-TM-102602] N90-21297
PROTEUS two-dimensional Navier-Stokes computer code, version 1.0. Volume 1: Analysis description
[NASA-TM-102551] N90-21303
PROTEUS two-dimensional Navier-Stokes computer code, version 1.0. Volume 2: User's guide
[NASA-TM-102552] N90-21306
PROTEUS two-dimensional Navier-Stokes computer code, version 1.0. Volume 3: Programmer's reference
[NASA-TM-102553] N90-21307
Near contact phenomena and transient effects in far infrared photoconductors N90-21316
Modeling elastomer displacements for tactile sensing applications
[DE90-007959] N90-21370
On-line assessment of weld quality using ultrasonics
[AERE-R-13401] N90-21398
Elastic-plastic instability of plane frames N90-21415
Development of a fracture analysis technique for use with a general-purpose finite element program N90-21416
Thermomechanical deformation testing and modeling in the presence of metallurgical instabilities
[NASA-CR-185188] N90-21420
A numerical model for the determination of periodic solutions of pipes subjected to non-conservative loads
[DE90-614756] N90-21423
A modification of a low-order Reissner-Mindlin plate bending element
[PB90-165830] N90-21428
Possible use of satellite data for flood plain mapping
[INPE-4968-PRE/1537] N90-21462
Modeling large-scale vegetation dynamics
[DE90-008883] N90-21485
The influence of lateral boundary conditions, fixed surface forcings, and synoptic situations upon predictability estimates using limited area numerical models N90-21492
Theory and application of nonlinear normal mode initialization
[PB90-166000] N90-21497
Numerical simulations of the cloud-capped marine boundary layer N90-21506
Extension of the constraints algebra for the closed string with the fixed topology world sheet
[DE90-612745] N90-21577
Stability of a solitary wave solution to a set of coupled Boussinesq-like equations
[DE90-008927] N90-21586
US-Japan Workshop on Atomic Collisions in Solids: Abstracts of lectures
[DE90-008979] N90-21611
A simplified theoretical model for the laser-induced optogalvanic effect
[DE90-613121] N90-21626
An extended diffusive model for calculating thermal diffusivity from single monopole tokamak heat pulse propagation
[DE90-007958] N90-21637
Transition from resistive-g to eta-i driven turbulence in stellarator systems
[DE90-009362] N90-21641
Model atmospheres for novae during the early stages
[NASA-CR-180498] N90-21694
The dynamics of scalar fields in the early universe N90-21696
A theoretical study of circumstellar dust around Ae/Be stars N90-21700
Small scale structures and density of star-forming regions N90-21706
Substorms: Their expansion and recovery phases
[DE90-008970] N90-21712
Simplified model for solar cosmic ray exposure in manned Earth orbital flights
[NASA-TM-4182] N90-21715
A balloon measurement of the isotopic composition of galactic cosmic ray iron N90-21717

MATRICES (MATHEMATICS)
The parallel algorithm for solving the three-dimensional integral magnetostatic equations
[DE90-616529] N90-21547
Parallel tridiagonalization of a general matrix using distributed-memory multiprocessors
[DE90-008902] N90-21551
Fusion algebra and fusing matrices
[DE90-612798] N90-21583

MATRIX MATERIALS
Reinforcement-matrix interface effects in metal matrix composites
[MRL-TN-562] N90-21120

MAXIMUM ENTROPY METHOD
Comparison of the algebraic reconstruction technique with the maximum entropy reconstruction technique for a variety of detection tasks
[DE90-008933] N90-21587

MAXIMUM LIKELIHOOD ESTIMATES
Flight path reconstruction using extended Kalman filtering techniques
[PD-FC-9001] N90-20970
Evaluation of classification performance and proportion estimate of the sugar cane crop through PROCEDURE-INPE utilizing LANDSAT data
[INPE-4899-PRE/1500] N90-21458

MEASUREMENT
Foundations of measurement and instrumentation
[NASA-RP-1222] N90-21351

MEASURING INSTRUMENTS
Foundations of measurement and instrumentation
[NASA-RP-1222] N90-21351
The RAP unit: A remote autoranging picoammeter
[DE90-007711] N90-21357
Error correction of the DEA (Digital Electronic Automation) coordinate measuring machines at LLNL
[DE90-008913] N90-21365
Rapidly quantifying the relative distention of a human bladder
[NASA-CASE-LAR-13901-1-NP] N90-21519

MECHANICAL DRIVES
End point control of flexible manipulators
[AD-A217319] N90-21383

MECHANICAL PROPERTIES
Reinforcement-matrix interface effects in metal matrix composites
[MRL-TN-562] N90-21120
Resistance mechanics for laminated composite materials
[INPE-4919-RPE/594] N90-21141

Compatibility of Au base thick films with solder alloys: Solid state growth of intermetallics
[DE90-009285] N90-21175
Review of the state of the technology for joining ceramics for high-temperature structural applications
[DE90-009224] N90-21199

MECHANICAL SHOCK
The Shock and Vibration Digest, volume 22, no. 2
N90-21596

MEDICAL SCIENCE
Medical subject headings: Annotated alphabetic list, 1990
[PB90-100009] N90-21683
Permuted medical subject headings, 1990
[PB90-100025] N90-21684
Research and Technology
[NASA-TM-102161] N90-21721

MELTING
Pressure rig for repetitive casting
[NASA-CASE-LAR-14050-1] N90-21216

MELTS (CRYSTAL GROWTH)
LaRC TPI 1500 series polymers
[NASA-CR-181899] N90-21129

MEMBRANES
Design and demonstration of an improved stretched-membrane heliostat
[DE90-007904] N90-21470

MEMORY (COMPUTERS)
Numerical Arc Segmentation Algorithm for a Radio Conference (NASARC), version 4.0: User's manual
[NASA-TM-101454] N90-21250
CAMAC memory module: MEMO-32
[DE90-759846] N90-21526
Quadratic Hadamard Memories 1
[AD-A217224] N90-21534

MENISCI
Critical point wetting drop tower experiment
[NASA-CR-186513] N90-21208

MENTAL PERFORMANCE
Development of microcomputer-based mental acuity tests for repeated-measures studies
[NASA-CR-185607] N90-21521

MERCURY CADMIUM TELLURIDES
The potential for high performance HgCdTe arrays at 4 microns N90-21320
High resolution imaging of the Venus night side using a Rockwell 128x128 HgCdTe array N90-21330
Short wavelength HgCdTe staring focal plane for low background astronomy applications N90-21336
Low noise HgCdTe 128 x 128 SWIR FPA for Hubble space telescope N90-21337
Laboratory and telescope use of the NICMOS2 128 x 128 HgCdTe array N90-21338
HgCdTe 256x256 NWIR FPA N90-21348

MERIDIONAL FLOW
Secondary flow calculations for axial and radial compressors N90-21024

MESOSCALE PHENOMENA
The influence of lateral boundary conditions, fixed surface forcings, and synoptic situations upon predictability estimates using limited area numerical models
N90-21492

MESOSPHERE
Investigations into the properties, conditions, and effects of the ionosphere
[AD-A217607] N90-21489

MESSAGE PROCESSING
Fast causal multicast
[NASA-CR-186495] N90-21533

METABOLISM
Anaerobic metabolism of aromatic compounds by phototrophic bacteria: Biochemical aspects
[DE90-009503] N90-21516

METAL AIR BATTERIES
The development of a simulation program of the anode side for aluminum/air batteries
[PB90-165754] N90-21286

METAL COATINGS
High gloss corrosion-resistant coatings
[AD-D014403] N90-21184

METAL FATIGUE
A compendium of sources of fracture toughness and fatigue crack growth data for metallic alloys, part 4
[NASA-TM-102646] N90-21164

METAL FIBERS
Characterization of failure processes in tungsten copper composites under fatigue loading conditions
[NASA-TM-102371] N90-21123
High temperature fatigue behavior of tungsten copper composites
[NASA-TM-102404] N90-21138

METAL MATRIX COMPOSITES
Reinforcement-matrix interface effects in metal matrix composites
[MRL-TN-562] N90-21120
Acoustic characterisation of an aluminium silicon carbide metal matrix composite
[AERE-R-13273] N90-21121
High temperature fatigue behavior of tungsten copper composites
[NASA-TM-102404] N90-21138
Optimal fabrication processes for unidirectional metal-matrix composites: A computational simulation
[NASA-TM-102559] N90-21143
Fatigue damage growth mechanisms in continuous fiber reinforced titanium matrix composites
[NASA-TM-102594] N90-21409

METAL OXIDE SEMICONDUCTORS
Study of advanced InSb arrays for SIRTF (Space Infrared Telescope Facility) N90-21325

METAL POWDER
Method of making a long life high current density cathode from tungsten and iridium powders using a quarternary compound as the impregnant
[AD-D014425] N90-21211

METAL SURFACES
Surface characterization of hydrogen charged and uncharged alpha-2 and gamma titanium aluminide alloys using AES and REELS
[NASA-CR-186561] N90-21171
Inelastic electron scattering from surfaces
[DE90-009365] N90-21614

METALLOGRAPHY
Analytical sciences
[DE90-007965] N90-21152

METAMORPHISM (GEOLOGY)
Geology of Espinhaco Meridional, including the Quadrilatero Ferrifero: Integration through remote sensing data
[INPE-4904-PRE/1505] N90-21450

METASTABLE STATE
Controlled production and characterization of metastable intermetallics
[DE90-009384] N90-21176

METEORITE COLLISIONS
Global nonlinear optimization of spacecraft protective structures design
[NASA-TM-100387] N90-21095

METEOROLOGICAL PARAMETERS
Weather data dissemination to aircraft N90-20934
Data Link Processor (DLP) project transition plan
[DOT/FAA/CT-TN89/68] N90-21256
Transformation and deposition of airborne gaseous and particulate pollutants during transport over the Baltic Sea
[PUBL-AIR-QUALITY-5] N90-21478

METEOROLOGICAL RADAR
Cockpit display of hazardous wind shear information
N90-20924
Meteorologist Weather Processor (MWP) integration test plan
[DOT/FAA/CT-TN89/62] N90-21500

METEOROLOGICAL SERVICES
Plan for the FAA air traffic operational evaluation of the Automated Surface Observing System (ASOS)
[DOT/FAA/CT-TN89/56] N90-20968
Meteorologist Weather Processor (MWP) integration test plan
[DOT/FAA/CT-TN89/62] N90-21500

METEOROLOGY
JPRS report. Science and technology. USSR: Earth sciences
[JPRS-UES-89-002] N90-21432
Transformation and deposition of airborne gaseous and particulate pollutants during transport over the Baltic Sea
[PUBL-AIR-QUALITY-5] N90-21478
Meteorologist Weather Processor (MWP) integration test plan
[DOT/FAA/CT-TN89/62] N90-21500
Windshear case study: Denver, Colorado, July 11, 1988
[DOT/FAA/DS-89/19] N90-21509

METHANATION
An evaluation of the relationship between the production and use of energy and atmospheric methane emissions
[DE90-007982] N90-21487

METHANE
Bis(4-(3,4-dimethylenepyrrolidyl)-phenyl) methane
[NASA-CASE-LAR-13965-1-CU] N90-21118
An evaluation of the relationship between the production and use of energy and atmospheric methane emissions
[DE90-007982] N90-21487

METHOD OF CHARACTERISTICS
A quasi-Lagrangian moving grid technique for investigating compressible flows N90-21298

METHOD OF MOMENTS
Is Galerkin's method really better
[DE90-008804] N90-21267

METHYLENE
Process for crosslinking methylene-containing aromatic polymers with ionizing radiation
[NASA-CASE-LAR-13448-1] N90-21198

METRIC SPACE
On induced Hermitian metrics for holomorphic vector bundles
[DE90-612737] N90-21572
The monad construction and Hermetian-Einstein metrics
[DE90-612738] N90-21573

METROLOGY
Center for Atomic, Molecular, and Optical Physics: Technical activities
[PB90-133158] N90-21591

MICROANALYSIS
Cosmic Dust Collection Facility: Scientific objectives and programmatic relations
[NASA-TM-102160] N90-21098

MICROBIOLOGY
JPRS report: Science and technology. USSR: Life sciences
[JPRS-ULS-90-002] N90-21434

MICROBURSTS (METEOROLOGY)
Cockpit display of hazardous weather information
N90-20929
Airborne Doppler radar flight experiments for the detection of microbursts N90-21243
Windshear case study: Denver, Colorado, July 11, 1988
[DOT/FAA/DS-89/19] N90-21509

MICROCHANNEL PLATES
Microchannel photomultipliers in time spectrometer
[DE90-616417] N90-21356

MICROCOMPUTERS
Generation of triangular form models in a microcomputer environment
[INPE-4974-PRE/1539] N90-21447
Development of microcomputer-based mental acuity tests for repeated-measures studies
[NASA-CR-185607] N90-21521
CAD work station for electronics designer
[DE90-616473] N90-21546

MICROCRACKS
Use of unbalanced laminates as a screening method for microcracking
[NASA-TM-102517] N90-21124

MICRODENSITOMETERS
The evolution and geometry of the outer parts of the small Magellanic cloud N90-21697

MICROGRAVITY APPLICATIONS
Microgravity science and applications bibliography, 1989 revision
[NASA-TM-4192] N90-21207

MICROMECHANICS
Multi-objective shape and material optimization of composite structures including damping
[NASA-TM-102579] N90-21132
Two-dimensional damage models of fiber-reinforced composites N90-21135
Micromechanics analysis of space simulated thermal deformations and stresses in continuous fiber reinforced composites
[NASA-TM-102633] N90-21140
Optimal fabrication processes for unidirectional metal-matrix composites: A computational simulation
[NASA-TM-102559] N90-21143

MICROMETEOROLOGY
Precipitation mechanisms in tropical and midlatitude convective clouds N90-21507

MICROSTRIP TRANSMISSION LINES
New ferrite-filled waveguiding structures analysed by the averaging method
[PB90-165671] N90-21269

MICROSTRUCTURE
Characterization of failure processes in tungsten copper composites under fatigue loading conditions
[NASA-TM-102371] N90-21123
Strengthening mechanisms of tungsten powder reinforced uranium
[DE90-009331] N90-21144
Controlled production and characterization of metastable intermetallics
[DE90-009384] N90-21176
Absolute multilayer characterization at high spatial resolution via real-time soft x ray imaging
[DE90-009181] N90-21371
Thermomechanical deformation testing and modeling in the presence of metallurgical instabilities
[NASA-CR-185188] N90-21420
Deformation processing of YBa2Cu3O(sub x)
[DE90-007795] N90-21644
Deformation and microstructure of rutile
[DE90-614113] N90-21654
Anisotropy of grain growth in alumina
[DE90-009045] N90-21655

Microstructure of Au/Nb multilayers
[DE90-008722] N90-21662
Determination of internal strains in high-temperature superconductor composites by intense pulsed neutron source
[DE90-007799] N90-21664

MICROWAVE AMPLIFIERS
High efficiency octave bandwidth millimeter wave power amplifier
[AD-A218245] N90-21280

MICROWAVE ANTENNAS
Millimeter wave near-field study
[NASA-CR-182014] N90-21058
Optical control of an 8-element Ka-band phased array using a high-speed optoelectronic interconnect
[NASA-TM-102550] N90-21275

MICROWAVE CIRCUITS
The 5th Annual Review of Progress in Applied Computational Electromagnetics
[AD-A217994] N90-21258
Coplanar waveguide fed phased array antenna
[NASA-TM-102522] N90-21273

MICROWAVE EQUIPMENT
High power, high sensitivity microwave calorimeter
[AD-D014427] N90-21355

MICROWAVE RADIOMETERS
HgCdTe 256x256 NWIR FPA N90-21348
Use of microwave satellite data to study variations in rainfall over the Indian Ocean
[NASA-CR-186408] N90-21501

MICROWAVES
JPRS report: Science and technology. USSR: Electronics and electrical engineering
[JPRS-UEE-90-002] N90-21284

MILITARY SPACECRAFT
NASA's Advanced Communications Technology Satellite (ACTS): Will it benefit commercial/military satellites
[AD-A217710] N90-21100

MILLIMETER WAVES
Millimeter wave near-field study
[NASA-CR-182014] N90-21058
MMW SAR on RPV for battlefield surveillance N90-21231
High efficiency octave bandwidth millimeter wave power amplifier
[AD-A218245] N90-21280

MIMD (COMPUTERS)
Architecture independent environment for developing engineering software on MIMD computers
[NASA-CR-186562] N90-21553

MINERAL EXPLORATION
Geobotanical remote sensing: A review
[INPE-5026-PRE/1565] N90-21440

MINIMUM DRAG
Constrained spanload optimization for minimum drag of multi-lifting-surface configurations N90-20992

MINKOWSKI SPACE
Characteristics consequences of space-time coordinate relativization
[DE90-615201] N90-21668

MIRA VARIABLES
AFGL ten micron mosaic array spectrometer: Recent results N90-21333

MIRRORS
Absolute multilayer characterization at high spatial resolution via real-time soft x ray imaging
[DE90-009181] N90-21371
Design and demonstration of an improved stretched-membrane heliostat
[DE90-007904] N90-21470
The investigation of multilayer x ray reflectors as x ray optical elements
[DE90-009044] N90-21621

MISSILE DEFENSE
Zenith Star: A structural control challenge N90-21064

MISSILES
Perforation of a reinforced concrete wall by a rigid missile
[AD-A210025] N90-21381
Gaithersburg Nike control and launch area preliminary assessment/site inspection, Gaithersburg, Maryland
[AD-A217791] N90-21482

MISSION PLANNING
A spaceborne optical interferometer: The JPL CSI mission focus N90-21063

MIXING
Secondary flows and radial mixing predictions in axial compressors N90-21010
A study on secondary flow and spanwise mixing in axial flow compressors N90-21012
Phase equilibrium of mixtures consisting of molecules with large size and shape differences (thermodynamic modeling of Supercritical Fluid Extraction and Retrograde Condensation, SFE/RC)
[PB90-131285] N90-21146
Apparatus for mixing solutions in low gravity environments
[NASA-CASE-MFS-26047-1] N90-21209
Microgravity acoustic mixing for particle cloud combustors
[NASA-CR-185159] N90-21600

MOBILITY
Proceedings of the 4th European Conference, volume 2
[AD-A216521] N90-21382

MODEL REFERENCE ADAPTIVE CONTROL
Rule-based mechanisms of learning for intelligent adaptive flight control N90-20939

MODELS
Design of a digital model following controller of reaction wheel torques
[INPE-4753-PRE/1425] N90-21093
Proceedings of the 4th European Conference, volume 2
[AD-A216521] N90-21382
Generation of triangular form models in a microcomputer environment
[INPE-4974-PRE/1539] N90-21447

MODFETS
Proceedings of the Joint NOSC/NRL (Naval Ocean Systems Center/Naval Research Laboratory) InP Microwave/Millimeter Wave Technology Workshop
[AD-A218216] N90-21259

MODULATORS
Double valve mechanism for an acoustic modulator
[AD-D014401] N90-21386

MODULES
Recent progress in photovoltaic concentrator module technology
[DE90-009007] N90-21475

MOISTURE CONTENT
Meteorological influences on mountain cloudwater chemistry in the eastern United States
[PB90-132432] N90-21504

MOLECULAR BIOLOGY
JPRS report: Science and technology. USSR: Life sciences
[JPRS-ULS-90-002] N90-21434
Artificial life: The coming evolution
[DE90-008860] N90-21515

MOLECULAR CHAINS
A new class of lubricants derived from archaebacterial lipids
[AD-D014429] N90-21185

MOLECULAR CLOUDS
The molecular cloud content of early type galaxies. 2: A molecular ring in NGC 404
[PB90-124348] N90-21695

MOLECULAR GASES
The molecular cloud content of early type galaxies. 2: A molecular ring in NGC 404
[PB90-124348] N90-21695

MOLECULAR SPECTROSCOPY
Center for Atomic, Molecular, and Optical Physics: Technical activities
[PB90-133158] N90-21591

MOLECULAR STRUCTURE
Nicalon/siliconoxycarbide ceramic composites
[NASA-TM-102563] N90-21133
Modelling of molecular structures and properties in physical chemistry and biophysics
[AD-A214561] N90-21145

MOLECULAR WEIGHT
Determinations of molecular weight and molecular weight distribution of high polymers by the rheological properties
[NASA-CR-186450] N90-21180

MOLECULES
Phase equilibrium of mixtures consisting of molecules with large size and shape differences (thermodynamic modeling of Supercritical Fluid Extraction and Retrograde Condensation, SFE/RC)
[PB90-131285] N90-21146

MOLNIYA SATELLITES
Direct Radio Broadcasting by Satellite (DRBS): A review of the technical factors and system approaches suitable for mobile and fixed reception
[BBC-RD-1989/4] N90-21221

MOLTEN SALTS
Ionic equilibrium between octahedral and tetrahedral complexes in liquid aluminium-sodium fluoride mixtures
[DE90-613690] N90-21150

MOMENTUM
Kinematic and kinetic analyses of drop landings N90-21517

MOMENTUM TRANSFER
The numerical simulation of multistage turbomachinery flows N90-21025
The generally covariant representation of energy-momentum pseudotensor of gravitational field
[DE90-615203] N90-21669

MONOPOLES
An extended diffusive model for calculating thermal diffusivity from single monopole tokamak heat pulse propagation
[DE90-007958] N90-21637

MONSOONS
Use of microwave satellite data to study variations in rainfall over the Indian Ocean
[NASA-CR-186408] N90-21501

MONTE CARLO METHOD
Ordering mechanism in substitutional Ni-Cr alloys: Theory and experiment
[DE90-006268] N90-21156

MORPHOLOGY
Influence of the deposition conditions on radiofrequency magnetron sputtered MoS2 films
[NASA-TP-2994] N90-21210
Performance evaluation of morphological edge detectors
[INPE-4975-PRE/1540] N90-21464

MOSAICS
AFGL ten micron mosaic array spectrometer: Recent results N90-21333

MOTION SICKNESS
Space adaptation syndrome induced by a long duration +3Gx centrifuge run
[AD-A218248] N90-21518

MOUNTAINS
Meteorological influences on mountain cloudwater chemistry in the eastern United States
[PB90-132432] N90-21504

MOVING TARGET INDICATORS
Concepts for high resolution space based SAR/ISAR systems: Preliminary design considerations N90-21224

MUFFLERS
The Shock and Vibration Digest, volume 22, no. 2 N90-21596
State of the art of acoustics of active and passive mufflers N90-21597

MULTICHANNEL COMMUNICATION
Computer processing of multi-channel electromagnetic data from an airborne geophysical survey system
[PB90-138413] N90-21253

MULTIPATH TRANSMISSION
Direct Radio Broadcasting by Satellite (DRBS): A review of the technical factors and system approaches suitable for mobile and fixed reception
[BBC-RD-1989/4] N90-21221

MULTIPHASE FLOW
Laser velocimeter measurements of multiphase flow of solids
[DE90-007604] N90-21311

MULTIPLEXING
Short wavelength HgCdTe staring focal plane for low background astronomy applications N90-21336
HgCdTe 256x256 NWIR FPA N90-21348
Improved Si:As BIBIB (Back-Illuminated Blocked-Impurity-Band) hybrid arrays N90-21349
Fault tolerant hypercube computer system architecture
[NASA-CASE-NPO-16859-1-CU] N90-21527

MULTIPROCESSING (COMPUTERS)
Fault tolerant hypercube computer system architecture
[NASA-CASE-NPO-16859-1-CU] N90-21527
Parallel tridiagonalization of a general matrix using distributed-memory multiprocessors
[DE90-008902] N90-21551
NETRA: A parallel architecture for integrated vision systems 2: Algorithms and performance evaluation
[NASA-CR-186510] N90-21557
A parallel multigrid method for solving elliptic partial differential equations
[DE90-007929] N90-21584

MULTISPECTRAL RADAR
A frequency agile 94 GHz pulse-Doppler radar with dual polarisation capability N90-21226

MULTISTATIC RADAR
Capabilities of bistatic synthetic aperture radar for covert battlefield surveillance N90-21230

MYLAR (TRADEMARK)
Aging and compatibility of TNF-doped Mylar
[DE90-008508] N90-21186

N

NACELLES
Measurement and prediction of propeller blade surface pressure distributions N90-20961
Aerodynamic design techniques at DLR Institute for Design Aerodynamics N90-20979

NASA PROGRAMS
A survey of experiments and experimental facilities for active control of flexible structures N90-21079
Small business innovation research. Abstracts of 1988 phase 1 awards [NASA-TM-102991] N90-21680
Small business innovation research. Abstracts of completed 1987 phase 1 projects [NASA-TM-101797] N90-21681
NASA SPACE PROGRAMS
The partnership: Space shuttle, space science, and space station [NASA-TM-102900] N90-21050
NASTRAN
Subsonic flutter analysis using MSC/NASTRAN [PB90-166786] N90-21041
Experimental evaluation of active-member control of precision structures N90-21084
LACE flight dynamics experiment N90-21086
NATIONAL AEROSPACE PLANE PROGRAM
Effects of nose bluntness and shock-shock interactions on blunt bodies in viscous hypersonic flows [NASA-CR-186451] N90-20950
NATIONAL AIRSPACE SYSTEM
Weather data dissemination to aircraft N90-20934
National airspace system air-ground communications operational concept [DOT/FAA/DS-90/2] N90-21249
Meteorologist Weather Processor (MWP) integration test plan [DOT/FAA/CT-TN89/62] N90-21500
NAVIER-STOKES EQUATION
On total variation diminishing schemes for transonic turbulent flow computation N90-20945
Comparison of C- and O-grid generation methods using a NACA 0012 airfoil [AD-A216375] N90-20948
An evaluation of the two-dimensional Euler and Navier-Stokes calculations based on a flux-vector splitting [PB90-166778] N90-20963
An efficient airfoil design method using the Navier-Stokes equations N90-20981
Optimization of aerodynamic designs using computational fluid dynamics N90-20999
Parabolized calculations of turbulent three dimensional flows in a turbine duct N90-21013
Centrifugal impeller geometry and its influence on secondary flows N90-21020
Calculation of the secondary flow in an axial turbine N90-21022
Generation and decay of secondary flows and their impact on aerodynamic performance of modern turbomachinery components N90-21023
Analysis of the rotor tip leakage flow with tip cooling air ejection N90-21029
Effects of secondary flow on heat transfer in rotating passages N90-21031
Theoretical study of the flow in a rotating channel. Experimental study through flow visualization in a curved channel N90-21032
Numerical simulation of vortex breakdown N90-21288
Analysis and finite element approximation of some optimal control problems associated with the Navier-Stokes equations N90-21299
Navier-Stokes analysis of turbine blade heat transfer [NASA-TM-102496] N90-21300
PROTEUS two-dimensional Navier-Stokes computer code, version 1.0. Volume 1: Analysis description [NASA-TM-102551] N90-21303
PROTEUS two-dimensional Navier-Stokes computer code, version 1.0. Volume 2: User's guide [NASA-TM-102552] N90-21306
PROTEUS two-dimensional Navier-Stokes computer code, version 1.0. Volume 3: Programmer's reference [NASA-TM-102553] N90-21307
High accuracy solutions of incompressible Navier-Stokes equations [NASA-TM-102539] N90-21567
NAVIGATION
Sole means navigation and integrity through hybrid Loran-C and NAVSTAR GPS N90-20933
NAVIGATION AIDS
Sole means navigation and integrity through hybrid Loran-C and NAVSTAR GPS N90-20933
NAVIGATION SATELLITES
Sole means navigation and integrity through hybrid Loran-C and NAVSTAR GPS N90-20933
NAVSTAR SATELLITES
Optimization of the effective GPS data rate N90-20932
Sole means navigation and integrity through hybrid Loran-C and NAVSTAR GPS N90-20933
NEAR FIELDS
Millimeter wave near-field study [NASA-CR-182014] N90-21058
NEAR INFRARED RADIATION
Attitude control modes for the MECB remote sensing satellites [INPE-4755-PRE/1427] N90-21094
Low noise HgCdTe 128 x 128 SWIR FPA for Hubble space telescope N90-21337
Laboratory and telescope use of the NICMOS2 128 x 128 HgCdTe array N90-21338
Future directions for NICMOS arrays N90-21339
NEBULAE
A search for very high energy gamma rays from the Crab pulsar-nebula N90-21718
NEGATIVE RESISTANCE CIRCUITS
High efficiency octave bandwidth millimeter wave power amplifier [AD-A216245] N90-21280
NEODYMIUM LASERS
Development of an ultra-bright laser and an application to multi-photon ionization N90-21372
Generation of ultrashort laser pulses from neodymium glass oscillator and regenerative amplifier N90-21373
NETWORK ANALYSIS
Calibration of Hewlett-Packard network analyzers: A precision viewpoint [NASA-CR-181989] N90-21262
NEURAL NETS
Neural networks for aircraft control N90-20937
Application of neural nets to system identification and bifurcation analysis of real world experimental data [DE90-007539] N90-21558
A real time neural net estimator of fatigue life [NASA-TM-103117] N90-21564
NEUTRAL ATMOSPHERES
Low latitude F-region dynamical processes from atomic oxygen nightglow emissions [INPE-4999-PRE/1561] N90-21494
NEUTRAL GASES
Helium transport in plasma edge regions N90-21625
NEUTRON BEAMS
A requirement for Australian research: Access to big science facilities, a report by the Australian National Committee for Crystallography [DE90-614784] N90-21048
NEUTRON DIFFRACTION
A requirement for Australian research: Access to big science facilities, a report by the Australian National Committee for Crystallography [DE90-614784] N90-21048
NEUTRON RADIOGRAPHY
Neutron autoradiography of hydrogen [DE90-612930] N90-21148
Determination of Li-Al alloy extent in tubular aluminum elements by small source neutron radiology [DE90-009142] N90-21174
NEUTRON SOURCES
Gamma-ray production cross section measurements using a white neutron source from 1 to 400 MeV [DE90-008906] N90-21610
Determination of internal strains in high-temperature superconductor composites by intense pulsed neutron source [DE90-007799] N90-21664
NEWTON METHODS
Computer-aided structural optimisation of aircraft structures [BR112837] N90-20973
NICKEL ALLOYS
Ordering mechanism in substitutional Ni-Cr alloys: Theory and experiment [DE90-006268] N90-21156
Grain boundary precipitation in Ni3Al based alloys [AERE-R-13362] N90-21161
High-temperature oxidation and sulfidation of Fe-20Cr-16Ni-4Al-1Y2O3 oxide-dispersion-strengthened alloy [DE90-007897] N90-21168
Lecture on ordered intermetallic alloys [DE90-009011] N90-21169
On the stability of amorphous silica coatings for high temperature service [AERE-R-13425] N90-21179
NICKEL HYDROGEN BATTERIES
Effect of KOH concentration on LEO cycle life of IPV nickel-hydrogen flight battery cells [NASA-TM-103127] N90-21116
NIGHT
High resolution imaging of the Venus night side using a Rockwell 128x128 HgCdTe array N90-21330
NIGHTGLOW
Low latitude F-region dynamical processes from atomic oxygen nightglow emissions [INPE-4999-PRE/1561] N90-21494
NIOBIUM
Microstructure of Au/Nb multilayers [DE90-008722] N90-21662
NITRIDES
Effects of titanium on some surface properties of nitride ceramics [AERE-R-13566] N90-21178
NITROGEN
Evolutionary effects in B stars N90-21704
NITROGEN OXIDES
Source attribution for tropospheric ozone in the US [DE90-007994] N90-21484
NOISE INTENSITY
Airborne sound insulation of slits, joints, and sealing stripes [PB90-128976] N90-21599
Free-field propagation of high intensity noise [NASA-CR-186577] N90-21604
NOISE MEASUREMENT
The Shock and Vibration Digest, volume 22, no. 2 N90-21596
State of the art of acoustics of active and passive mufflers N90-21597
Airborne sound insulation of slits, joints, and sealing stripes [PB90-128976] N90-21599
NOISE PROPAGATION
Active control of multi-dimensional random sound in ducts [NASA-TM-102653] N90-21603
Free-field propagation of high intensity noise [NASA-CR-186577] N90-21604
NOISE REDUCTION
A review of gear housing dynamics and acoustics literature [NASA-CR-185148] N90-21387
Transmission research activities at NASA Lewis Research Center [NASA-TM-103132] N90-21394
The Shock and Vibration Digest, volume 22, no. 2 N90-21596
State of the art of acoustics of active and passive mufflers N90-21597
Airborne sound insulation of slits, joints, and sealing stripes [PB90-128976] N90-21599
Passive stabilization of a fiber optic nonlinear interferometric sensor [AD-D014438] N90-21620
NOISE SPECTRA
Free-field propagation of high intensity noise [NASA-CR-186577] N90-21604
NONDESTRUCTIVE TESTS
Neutron autoradiography of hydrogen [DE90-612930] N90-21148
Magneto acoustic emission apparatus for testing materials for embrittlement [NASA-CASE-LAR-13817-1] N90-21170
Some recent applications of laser ultrasound to the characterisation of materials [AERE-R-13438] N90-21374
Collapsible fabric tank testing [AD-A217861] N90-21388
Ultrasonic and radiographic evaluation of advanced aerospace materials: Ceramic composites [NASA-TM-102540] N90-21401
NONLINEAR PROGRAMMING
Suboptimal and hybrid numerical solution schemes for orbit transfer manoeuvres [INPE-4991-PRE/1556] N90-21054
NONLINEAR SYSTEMS
Nonlinear and distributed parameter models of the mini-mast truss N90-21070
Elastic-plastic instability of plane frames N90-21415
Determination of unknown coefficients in partical differential equations [AD-A217169] N90-21569
NONLINEARITY
Mechanics of interface fracture N90-21408
Theory and application of nonlinear normal mode initialization [PB90-166000] N90-21497
A remark on the Kelvin transform and a non-linear partial differential equation [PB90-165622] N90-21589
Passive stabilization of a fiber optic nonlinear interferometric sensor [AD-D014438] N90-21620
Nonlinear interaction of photons and phonons in electron-positron plasmas [DE90-009341] N90-21640
NONOSCILLATORY ACTION
Some aspects of Essentially Nonoscillatory (ENO) formulations for the Euler equations, part 3 [NASA-CR-4285] N90-20949

NORMAL DENSITY FUNCTIONS
Analysis of distributions of Visual Meteorological Conditions (VMC) heliport data
[DOT/FAA/CT-TN89/67] N90-21508
NOSES (FOREBODIES)
Effects of nose bluntness and shock-shock interactions on blunt bodies in viscous hypersonic flows
[NASA-CR-186451] N90-20950
NOTCH STRENGTH
Fatigue damage growth mechanisms in continuous fiber reinforced titanium matrix composites
[NASA-TM-102594] N90-21409
NOVAE
Recent advances in the studies of the nova outburst
[DE90-008936] N90-21691
Multi-wavelength observations of novae in outburst
[DE90-008934] N90-21692
The 1989 outburst of V404 Cygni: A very unusual x ray nova
[DE90-008935] N90-21693
Model atmospheres for novae during the early stages
[NASA-CR-180498] N90-21694
NOZZLE DESIGN
An investigation of secondary flows in nozzle guide vanes N90-21016
Secondary flow predictions for a transonic nozzle guide vane N90-21017
Detailed heat transfer measurements in nozzle guide vane passages in linear and annular cascades in the presence of secondary flows N90-21030
Supersonic nozzle design of arbitrary cross-section N90-21035
Technical Evaluation Motor no. 5 (TEM-5)
[NASA-CR-183932] N90-21117
NOZZLE FLOW
Secondary flow predictions for a transonic nozzle guide vane N90-21017
Secondary flow in a turbine guide vane with low aspect ratio N90-21018
The effect of secondary flow on the redistribution of the total temperature field downstream of a stationary turbine cascade N90-21033
NOZZLE GEOMETRY
Performance of an aero-space plane propulsion nozzle N90-21034
NUCLEAR ELECTRIC PROPULSION
A radiological assessment of nuclear power and propulsion operations near Space Station Freedom
[NASA-CR-185185] N90-21108
NUCLEAR EMULSIONS
Mesooptical Fourier transform microscope: A new device for high energy physics
[DE90-616423] N90-21615
NUCLEAR EXPLOSIONS
Final safety analysis report for the Ulysses mission. Volume 2 (Book 1): Accident model document
[DE90-008694] N90-21103
NUCLEAR FUSION
West European magnetic confinement fusion research N90-21634
Fusion burn dynamics in Dense Z-Pinch (DZP)
[DE90-007976] N90-21638
An attempt to measure cold-fusion effects
[DE90-613248] N90-21649
NUCLEAR GYROSCOPES
The anatomy of the gyroscope, part 3
[AGARD-AG-313] N90-21359
NUCLEAR INTERACTIONS
Strangeness enhancement in 14.6 A GeV/c Si+Au interactions?
[DE90-008826] N90-21616
Fragmentation of relativistic heavy nuclei with application to cosmic ray propagation N90-21716
NUCLEAR MEDICINE
JPRS report: Science and technology. USSR: Life sciences
[JPRS-ULS-90-002] N90-21434
NUCLEAR PHYSICS
JPRS report: Science and technology. USSR: Physics and mathematics
[JPRS-UPM-90-002] N90-21593
Current experiments in elementary particle physics
[DE90-008062] N90-21607
NUCLEAR RADIATION
Final Safety Analysis Report for the Ulysses Mission. Volume 3 (Book 1): Nuclear risk analysis document
[DE90-008691] N90-21101
Final safety analysis report for the Ulysses Mission. Volume 3 (Book 2): Nuclear risk analysis document-appendices
[DE90-008692] N90-21102
Final safety analysis report for the Ulysses mission. Volume 2 (Book 1): Accident model document
[DE90-008694] N90-21103
NUCLEAR REACTIONS
Gamma-ray production cross section measurements using a white neutron source from 1 to 400 MeV
[DE90-008906] N90-21610
NUCLEAR REACTORS
Simple light gas guns for hypervelocity studies
[DE90-008907] N90-21056
West European magnetic confinement fusion research N90-21634
Full wave computation of electromagnetic wave excitation, propagation, and absorption at the ion cyclotron frequency in fusion experiments
[DE90-009399] N90-21642
NUMBER THEORY
A modified Moebius inverse formula and its applications in physics
[DE90-612740] N90-21594
NUMERICAL ANALYSIS
MECCA program documentation
[NOAA-TR-NESDIS-46] N90-21477
NUMERICAL INTEGRATION
Supersonic nozzle design of arbitrary cross-section N90-21035
NUMERICAL STABILITY
Stability of a solitary wave solution to a set of coupled Boussinesq-like equations
[DE90-008927] N90-21586
NUMERICAL WEATHER FORECASTING
The influence of lateral boundary conditions, fixed surface forcings, and synoptic situations upon predictability estimates using limited area numerical models N90-21492
Theory and application of nonlinear normal mode initialization
[PB90-166000] N90-21497

O

OBJECT PROGRAMS
STORM: A statistical object representation model
[DE90-009048] N90-21686
OBSERVATORIES
Experience with the UKIRT InSb array camera N90-21327
SOFIA: Stratospheric Observatory for Infrared Astronomy N90-21346
The evolution and geometry of the outer parts of the small Magellanic cloud N90-21697
OCCULTATION
The effect of windscreen bows and HUD pitch ladder format on pilot performance during simulated flight
[AD-A218139] N90-21523
OCEAN BOTTOM
An outline for the analysis of wave induced bottom pressure fluctuations
[MRL-TN-558] N90-21510
OCEAN MODELS
Predictability of weather and climate in a coupled ocean-atmosphere model: A dynamical systems approach
[NASA-CR-186499] N90-21502
Modeling the upper ocean and its interaction with the atmosphere
[DE90-008980] N90-21511
OCEAN SURFACE
Zones of feasibility for retrieval of surface pressure from observations of absorption in the A band of oxygen
[DAR-TP-19] N90-21495
Modeling the upper ocean and its interaction with the atmosphere
[DE90-008980] N90-21511
OCEANOGRAPHY
JPRS report. Science and technology. USSR: Earth sciences
[JPRS-UES-88-004] N90-21431
JPRS report. Science and technology. USSR: Earth sciences
[JPRS-UES-89-002] N90-21432
JPRS report: Science and technology. USSR: Earth sciences
[JPRS-UES-90-005] N90-21433
OCEANS
Numerical simulations of the cloud-capped marine boundary layer N90-21506
OCTAHEDRONS
Ionic equilibrium between octahedral and tetrahedral complexes in liquid aluminium-sodium fluoride mixtures
[DE90-613690] N90-21150
ON-LINE SYSTEMS
Effective techniques for the identification and accommodation of disturbances N90-21072
On-line assessment of weld quality using ultrasonics
[AERE-R-13401] N90-21398
OPENINGS
Cloud hole-boring with long pulse CO2 lasers
[DE90-008948] N90-21377
Determination of stresses around cutouts in multilayered composite plate and shell structures N90-21417
OPERATORS (MATHEMATICS)
On a non classical oblique derivative problem for parabolic singular integro-differential operators
[DE90-612739] N90-21574
OPTICAL COMMUNICATION
Optical control of an 8-element Ka-band phased array using a high-speed optoelectronic interconnect
[NASA-TM-102550] N90-21275
OPTICAL DISKS
Army War College final prototype optical disk system testing and evaluation report
[DE90-008852] N90-21685
OPTICAL EQUIPMENT
ASCIE: An integrated experiment to study CSI in large segmented optical systems N90-21082
The anatomy of the gyroscope, part 3
[AGARD-AG-313] N90-21359
OPTICAL FIBERS
Development of an ultra-bright laser and an application to multi-photon ionization N90-21372
OPTICAL MEASUREMENT
The optical measurement of acoustic velocity fields N90-21601
OPTICAL MICROSCOPES
Mesooptical Fourier transform microscope: A new device for high energy physics
[DE90-616423] N90-21615
OPTICAL PROPERTIES
Laser controlled semiconductor armature for electromagnetic launchers
[AD-D014435] N90-21055
Power transmission device
[AD-D014430] N90-21281
Characterization and comparison of optically transparent conducting films
[DE90-000319] N90-21660
OPTICAL RADAR
Development of an ultra-bright laser and an application to multi-photon ionization N90-21372
OPTIMAL CONTROL
Experimental and theoretical investigation of optimal control methods with model reduction N90-21039
Suboptimal and hybrid numerical solution schemes for orbit transfer manoeuvres
[INPE-4991-PRE/1556] N90-21054
Analysis and finite element approximation of some optimal control problems associated with the Navier-Stokes equations N90-21299
OPTIMIZATION
Optimization of the effective GPS data rate N90-20932
Computer-aided structural optimisation of aircraft structures
[BR112837] N90-20973
Computational Methods for Aerodynamic Design (inverse) and Optimization
[AGARD-CP-463] N90-20976
Progress in inverse design and optimization in aerodynamics N90-20977
Aerodynamic optimization by simultaneously updating flow variables and design parameters N90-20991
Constrained spanload optimization for minimum drag of multi-lifting-surface configurations N90-20992
Numerical optimization of target pressure distributions for subsonic and transonic airfoil design N90-20993
A tool for automatic design of airfoils in different operating conditions N90-20994
The use of numerical optimization for helicopter airfoil and blade design N90-20995
Aerodynamic design by optimization N90-20996
Numerical optimization of wings in transonic flow N90-20997
Aerodynamic design via control theory N90-20998
Optimization of aerodynamic designs using computational fluid dynamics N90-20999
A homotopy approach to the solutions of minimum-fuel space-flight rendezvous problems N90-21053
Optimization of the structural and control system for LSS with reduced-order model N90-21075
Computational architecture for integrated controls and structures design N90-21076
Recent experience in simultaneous control-structure optimization N90-21078
Global nonlinear optimization of spacecraft protective structures design
[NASA-TM-100387] N90-21095
Multi-objective shape and material optimization of composite structures including damping
[NASA-TM-102579] N90-21132

Optimal fabrication processes for unidirectional metal-matrix composites: A computational simulation [NASA-TM-102559] N90-21143
Modeling the temperature dependence of the thermal conductivity of aluminum nitride [DE90-009428] N90-21154
Application of optimization in design and motion control of robot manipulators N90-21393
Design and demonstration of an improved stretched-membrane heliostat [DE90-007904] N90-21470
Nonoptimal entropy generation by heat transfer in cryogenic domain [DE90-007544] N90-21667
Design and optimisation of thin foil x ray telescopes N90-21690

ORBIT CALCULATION
Ambiguity bootstrapping to determine GPS orbits and baselines [AD-A218206] N90-21052

ORBITAL MANEUVERING VEHICLES
Autonomous integrated GPS/INS navigation experiment for OMV. Phase 1: Feasibility study [NASA-CR-4267] N90-20869
Optimal trajectories for the aeroassisted flight experiment. Part 3: Formulation, results, and analysis [NASA-CR-166165] N90-21051

ORBITAL SERVICING
The partnership: Space shuttle, space science, and space station [NASA-TM-102900] N90-21050

ORDER-DISORDER TRANSFORMATIONS
Ordering mechanism in substitutional Ni-Cr alloys: Theory and experiment [DE90-006268] N90-21156

ORGANIC MATERIALS
Process for crosslinking methylene-containing aromatic polymers with ionizing radiation [NASA-CASE-LAR-13448-1] N90-21198

ORGANISMS
Artificial life: The coming evolution [DE90-008860] N90-21515

ORGANIZATIONS
Cooperating intelligent systems [NASA-CR-184982] N90-21529

ORGANOMETALLIC POLYMERS
Combination primer/topcoat coating [AD-D014445] N90-21189

ORGANS
Simplified model for solar cosmic ray exposure in manned Earth orbital flights [NASA-TM-4182] N90-21715

ORTHOTROPIC PLATES
Review of formulae for the buckling of simply-supported, orthotropic plates under shear load, including transverse shear effects [PB90-167073] N90-21429

OSCILLATING FLOW
ULTRA-SHARP nonoscillatory convection schemes for high-speed steady multidimensional flow [NASA-TM-102568] N90-21570

OSCILLATORS
Development of an ultra-bright laser and an application to multi-photon ionization N90-21372
Generation of ultrashort laser pulses from neodymium glass oscillator and regenerative amplifier N90-21373

OXIDATION
High-temperature oxidation and sulfidation of Fe-20Cr-16Ni-4Al-1Y2O3 oxide-dispersion-strengthened alloy [DE90-007897] N90-21168
Improved Thermo-Oxidative-Deposition screening tests for turbine lubricants [AD-A217795] N90-21188

OXIDATION RESISTANCE
Titanium aluminides: Processing, properties and potential [AERE-R-13198] N90-21158

OXIDES
Development of planar geometry solid oxide fuel cell technology, phase 2 [PB90-131293] N90-21467
Specific heat and critical fluctuations in anisotropic high-T(sub c) oxide superconductors [DE90-613394] N90-21651

OXYGEN
O2 reduction at the IFC orbiter fuel cell O2 electrode [NASA-TM-102580] N90-21469
Zones of feasibility for retrieval of surface pressure from observations of absorption in the A band of oxygen [DAR-TP-19] N90-21495

OXYGEN ATOMS
The effect of leveling coatings on the atomic oxygen durability of solar concentrator surfaces [NASA-TM-102557] N90-21110
Low latitude F-region dynamical processes from atomic oxygen nightglow emissions [INPE-4999-PRE/1561] N90-21494

OZONE
The development of ultraviolet-ozone cleaning as a production process in the packaging of integrated circuits [DE90-007960] N90-21220
Effects of Air Pollution on Western Forests [PB90-131111] N90-21481
Source attribution for tropospheric ozone in the US [DE90-007994] N90-21484

P

P-I-N JUNCTIONS
Coplanar waveguide discontinuities for P-I-N diode switches and filter applications [NASA-TM-102534] N90-21278
Research on amorphous silicon-based thin film photovoltaic devices. Task B: Research on stable high efficiency large area, amorphous silicon-based submodules [DE90-000320] N90-21473

PAIR PRODUCTION
Nonlinear interaction of photons and phonons in electron-positron plasmas [DE90-009341] N90-21640

PANEL METHOD (FLUID DYNAMICS)
Users manual for the NASA Lewis Ice Accretion Prediction Code (LEWICE) [NASA-CR-185129] N90-20943
An intensive procedure for the design of pressure-specified three-dimensional configurations at subsonic and supersonic speeds by means of a higher-order panel method N90-20982
A system for transonic wing design with geometric constraints based on an inverse method N90-20983
A fast collocation method for transonic airfoil design N90-20984
Probabilistic modeling for simulation of aerodynamic uncertainties in propulsion systems [NASA-TM-102472] N90-21036

PANELS
Preliminary design approach for large high precision segmented reflectors [NASA-TM-102605] N90-21096

PARABOLIC ANTENNAS
Apparatus and method for locating the axis of symmetry (center of circular cross section) of three dimensional objects [AD-D014407] N90-21354

PARALLEL PROCESSING (COMPUTERS)
Cooperating intelligent systems [NASA-CR-184982] N90-21529
Parallel tridiagonalization of a general matrix using distributed-memory multiprocessors [DE90-008902] N90-21551
Hypercluster parallel processing library user's manual [NASA-CR-185231] N90-21552
Performance bounds on parallel self-initiating discrete-event [NASA-CR-182010] N90-21556
NETRA: A parallel architecture for integrated vision systems 2: Algorithms and performance evaluation [NASA-CR-186510] N90-21557
Application of neural nets to system identification and bifurcation analysis of real world experimental data [DE90-007539] N90-21558
Activities and operations of the Advanced Computing Research Facility [DE90-007957] N90-21559
A parallel multigrid method for solving elliptic partial differential equations [DE90-007929] N90-21584
Modeling high-temperature superconductors and metallic alloys on the Intel IPSC/860 [DE90-009402] N90-21665

PARALLEL PROGRAMMING
Hypercluster parallel processing library user's manual [NASA-CR-185231] N90-21552

PARAMETER IDENTIFICATION
CSI technology validation on an LSS ground experiment facility N90-21089

PARAMETERIZATION
Modeling the temperature dependence of the thermal conductivity of aluminum nitride [DE90-009428] N90-21154

PARTIAL DIFFERENTIAL EQUATIONS
Application of an inverse method to the design of a radial inflow turbine N90-20989
Multigrid on massively parallel computers [DE90-008999] N90-21560
High accuracy solutions of incompressible Navier-Stokes equations [NASA-TM-102539] N90-21567
Determination of unknown coefficients in partical differential equations [AD-A217169] N90-21569
On the equation: Delta u+c=Ke(sup u) [DE90-612741] N90-21575
A parallel multigrid method for solving elliptic partial differential equations [DE90-007929] N90-21584
Stability of a solitary wave solution to a set of coupled Boussinesq-like equations [DE90-008927] N90-21586
A remark on the Kelvin transform and a non-linear partial differential equation [PB90-165622] N90-21589

PARTICLE ACCELERATION
Langmuir wave interaction with ion acoustic wave [DE90-615407] N90-21624

PARTICLE ACCELERATOR TARGETS
The design of a large aperture high field dipole [DE90-007910] N90-21285

PARTICLE ACCELERATORS
Current experiments in elementary particle physics [DE90-008062] N90-21607
A measurement of the gravitational acceleration of the antiproton [DE90-008903] N90-21612

PARTICLE BEAMS
Charged-particle beam research program [DE90-007937] N90-21618

PARTICLE COLLISIONS
Inelastic electron scattering from surfaces [DE90-009365] N90-21614
Characterization of the plasma in magnetic multidipole discharges [DE90-613219] N90-21628

PARTICLE ENERGY
A balloon measurement of the isotopic composition of galactic cosmic ray iron N90-21717

PARTICLE INTERACTIONS
Once more about the sizes of fast-moving objects [DE90-615204] N90-21592
Some global problems in gauge theories (variations on a theme of Aharonov and Bohm) [DE90-009034] N90-21678

PARTICLE MOTION
Once more about the sizes of fast-moving objects [DE90-615204] N90-21592

PARTICLE THEORY
Rings [DE90-009035] N90-21613

PARTICLE TRACKS
Mesooptical Fourier transform microscope: A new device for high energy physics [DE90-616423] N90-21615

PASCAL (PROGRAMMING LANGUAGE)
The development of a simulation program of the anode side for aluminum/air batteries [PB90-165754] N90-21286

PASSAGEWAYS
Apparatus for mixing solutions in low gravity environments [NASA-CASE-MFS-26047-1] N90-21209

PATENTS
Bis(4-(3,4-dimethylenepyrrolidyl)-phenyl) methane [NASA-CASE-LAR-13965-1-CU] N90-21118

PATIENTS
Rapidly quantifying the relative distention of a human bladder [NASA-CASE-LAR-13901-1-NP] N90-21519

PATTERN RECOGNITION
Phase-only holographic filters and their applications [PB90-166802] N90-21368

PAVEMENTS
Criteria for polymer concrete on airport pavements [DOT/FAA/DS-89/18] N90-21045

PAYLOADS
Modeling and control of flexible space platforms with articulated payloads N90-21073
An air-bearing weight offload system for ground test of heavy LSS structures N90-21081
Controls, Astrophysics, and Structures Experiment in Space (CASES) N90-21085

PEEK
Cross-sectional examination of the damage zone in impacted specimens of carbon/epoxy and carbon/PEEK composites [NASA-TM-100391] N90-21125

PENETRATION
Boeing 727-100 test project (high energy radiated field tests) [DOT/FAA/CT-88/33] N90-21247

PERCOLATION
Mathematical modelling of intergranular attack in stainless steels: A preliminary study
[AERE-M-3698] N90-21160
PERCUSSION
Methods for improving the flowability of a percussion primer composition
[MRL-TR-89-32] N90-21201
PERFORATING
Perforation of a reinforced concrete wall by a rigid missile
[AD-A210025] N90-21381
PERFORMANCE PREDICTION
Secondary flow predictions for a transonic nozzle guide vane N90-21017
Generation and decay of secondary flows and their impact on aerodynamic performance of modern turbomachinery components N90-21023
Computational prediction and measurement of the flow in axial turbine cascades and stages N90-21028
Development of a fracture analysis technique for use with a general-purpose finite element program N90-21416
PERFORMANCE TESTS
Performance data from a wind-tunnel test of two main-rotor blade designs for a utility-class helicopter
[NASA-TM-4183] N90-20974
Secondary flow predictions for a transonic nozzle guide vane N90-21017
Space environment simulation of the SCD-01 satellite through heating plates
[INPE-4988-PRE/1550] N90-21105
Effect of KOH concentration on LEO cycle life of IPV nickel-hydrogen flight battery cells
[NASA-TM-103127] N90-21116
Selective automatic fire extinguisher for computers (SAFECOMP): Developmental test and evaluation/initial operational test and evaluation
[AD-A217790] N90-21212
The development of a simulation program of the anode side for aluminum/air batteries
[PB90-165754] N90-21286
Germanium Blocked Impurity Band (BIB) detectors N90-21321
Ga:Ge array development N90-21323
NETRA: A parallel architecture for integrated vision systems 2: Algorithms and performance evaluation
[NASA-CR-186510] N90-21557
PERIODIC VARIATIONS
Research on cascade secondary and tip-leakage flows: Periodicity and surface flow visualization N90-21026
PERMEABILITY
Criteria for polymer concrete on airport pavements
[DOT/FAA/DS-89/18] N90-21045
A casting and imaging technique for determining void geometry and relative permeability behavior of a single fracture specimen
[DE90-009192] N90-21403
PERTURBATION
The dynamics of scalar fields in the early universe N90-21696
PERTURBATION THEORY
Discrete modeling of beds of propellant exposed to strong stimulus
[DE90-008932] N90-21206
The effects of forcing on a single stream shear layer and its parent boundary layer
[NASA-CR-186529] N90-21301
Chern-Simons superconductivity at finite temperature
[DE90-613393] N90-21650
PHARMACOLOGY
JPRS report: Science and technology. USSR: Life sciences
[JPRS-ULS-90-002] N90-21434
PHASE CHANGE MATERIALS
Failure and degradation modes in selected solar materials: A review
[DE90-009075] N90-21476
PHASE DETECTORS
Advanced instrumentation for aircraft icing research
[NASA-CR-185225] N90-21006
PHASE DIAGRAMS
Phase equilibria and solution thermodynamics of bismuth-lead alloys
[PB90-138421] N90-21163
Controlled production and characterization of metastable intermetallics
[DE90-009384] N90-21176
PHASE LOCKED SYSTEMS
Strain and dynamic measurements using fiber optic sensors embedded into graphite/epoxy tubes N90-21090
PHASE MODULATION
Weather data dissemination to aircraft N90-20934
PHASED ARRAYS
The PHARUS project: Design of a polarimetric C-band SAR in the Netherlands N90-21228
Concept for a spaceborne Synthetic Aperture Radar (SAR) sensor based on active phased array technology N90-21234
A motion compensation study for the PHARUS project N90-21235
Bit-error-rate testing of fiber optic data links for MMIC-based phased array antennas
[NASA-TM-102523] N90-21261
Coplanar waveguide fed phased array antenna
[NASA-TM-102522] N90-21273
Optical control of an 8-element Ka-band phased array using a high-speed optoelectronic interconnect
[NASA-TM-102550] N90-21275
PHENYLS
Bis(4-(3,4-dimethylenepyrrolidyl)-phenyl) methane
[NASA-CASE-LAR-13965-1-CU] N90-21118
Boron-containing organosilane polymers and ceramic materials thereof
[NASA-CASE-ARC-11649-2-SB] N90-21177
PHONONS
A modified Moebius inverse formula and its applications in physics
[DE90-612740] N90-21594
Nonlinear interaction of photons and phonons in electron-positron plasmas
[DE90-009341] N90-21640
Coupled magnetoplasmon-phonon modes at the surface of a semi-infinite semiconductor superlattice
[DE90-612904] N90-21647
PHOSPHORIC ACID FUEL CELLS
Fuel cell systems program plan, FY 1990
[DE90-008178] N90-21471
PHOTOCONDUCTORS
Stressed Ge:Ga photoconductors for space-based astronomy. (Is there life beyond 120 micron) N90-21315
Near contact phenomena and transient effects in far infrared photoconductors N90-21316
Germanium Blocked Impurity Band (BIB) detectors N90-21321
Ga:Ge array development N90-21323
Stressed detector arrays for airborne astronomy N90-21332
Initial astronomical results with a new 5-14 micron Si:Ga 58x62 DRO array camera N90-21334
Status of the isophot detector development N90-21342
ISO/LWS: Detector status N90-21343
PHOTOGRAPHS
Characterization of linear structures from remote sensing data; Espinhaco Meridional (MG) sierra
[INPE-4905-PRE/1506] N90-21449
Geology of Espinhaco Meridional, including the Quadrilatero Ferrifero: Integration through remote sensing data
[INPE-4904-PRE/1505] N90-21450
PHOTOINTERPRETATION
Monitoring of agrocattle-raising projects through visual/digital analysis of LANDSAT-TM imagery south of Para state
[INPE-4982-PRE/1542] N90-21442
Survey of land use through remote sensing
[INPE-5032-MD/042] N90-21443
PHOTOMAPPING
Digital processing of TM/LANDSAT data in monitoring interior water
[INPE-4956-PRE/1533] N90-21448
PHOTOMETERS
Ga:Ge array development N90-21323
Initial astronomical results with a new 5-14 micron Si:Ga 58x62 DRO array camera N90-21334
Alternating gradient photodetector
[NASA-CASE-NPO-17235-1-CO] N90-21358
PHOTOMETRY
InSb DRO array characteristics N90-21326
AFGL ten micron mosaic array spectrometer: Recent results N90-21333
Introduction to the Infrared Space Observatory (ISO) N90-21340
PHOTOMULTIPLIER TUBES
The solid state photomultiplier: Status of photon counting beyond the near-infrared N90-21319
Microchannel photomultipliers in time spectrometer
[DE90-616417] N90-21356
PHOTONS
On the creation of gravitational wave by photon in external electromagnetic field
[DE90-613366] N90-21265
The solid state photomultiplier: Status of photon counting beyond the near-infrared N90-21319
Gamma-ray production cross section measurements using a white neutron source from 1 to 400 MeV
[DE90-008906] N90-21610
Nonlinear interaction of photons and phonons in electron-positron plasmas
[DE90-009341] N90-21640
Problems in radiative transfer in astrophysics: An escape probability treatment of line overlap and a model of the masers around VX Sgr N90-21705
Horizon problem in cosmological models with non zero
[DE90-613367] N90-21708
PHOTOOXIDATION
Source attribution for tropospheric ozone in the US
[DE90-007994] N90-21484
PHOTOTROPISM
Anaerobic metabolism of aromatic compounds by phototrophic bacteria: Biochemical aspects
[DE90-009503] N90-21516
PHOTOVOLTAIC CELLS
Infrared ground-based astronomy with the Hughes 256 X 256 PtSi array N90-21331
Research on amorphous silicon-based thin film photovoltaic devices. Task B: Research on stable high efficiency large area, amorphous silicon-based submodules
[DE90-000320] N90-21473
Recent progress in photovoltaic concentrator module technology
[DE90-009007] N90-21475
PHOTOVOLTAIC CONVERSION
Recent results from advanced research on space solar cells at NASA
[NASA-TM-102485] N90-21274
Improvement of small-area, amorphous-silicon thin-film photovoltaics on polymer substrate
[DE90-000314] N90-21472
PHOTOVOLTAIC EFFECT
Power transmission device
[AD-D014430] N90-21281
Short wavelength HgCdTe staring focal plane for low background astronomy applications N90-21336
PHYSICAL CHEMISTRY
Modelling of molecular structures and properties in physical chemistry and biophysics
[AD-A214561] N90-21145
PHYSICAL EXERCISE
Kinematic and kinetic analyses of drop landings N90-21517
PICOSECOND PULSES
Generation of ultrashort laser pulses from neodymium glass oscillator and regenerative amplifier N90-21373
PIEZOELECTRICITY
Experimental evaluation of active-member control of precision structures N90-21084
PILOT PERFORMANCE
An early overview of tiltrotor aircraft characteristics and pilot procedures in civil transport applications
[DOT/FAA/DS-89/37] N90-21003
Stereopsis cueing effects on hover-in-turbulence performance in a simulated rotorcraft
[NASA-TP-2980] N90-21004
PILOTLESS AIRCRAFT
Design of a natural laminar flow airfoil for an unmanned aircraft
[PD-CF-9004] N90-20975
PIPES (TUBES)
Determination of Li-Al alloy extent in tubular aluminum elements by small source neutron radiology
[DE90-009142] N90-21174
A numerical model for the determination of periodic solutions of pipes subjected to non-conservative loads
[DE90-614756] N90-21423
Program CICC: Flow and heat transfer in Cable In Conduit Conductors, user's manual
[DE90-007924] N90-21661
PITTING
Current fluctuations associated with localised corrosion: Mechanistic studies of the early stages of pitting and stress corrosion cracking of stainless steel
[AERE-R-13531] N90-21159
Corrosion behavior of mild steel ih high pH aqueous media
[PB90-131152] N90-21162
PIXELS
Shade images of forested areas obtained from LANDSAT MSS data
[NASA-TM-102939] N90-21436
Subsystem TM Precision: Progress and perspective
[INPE-5006-PRE/1563] N90-21481
PLANAR STRUCTURES
A homotopy approach to the solutions of minimum-fuel space-flight rendezvous problems N90-21053
A new rectangular waveguide to coplanar waveguide transition
[NASA-TM-102477] N90-21263
Coplanar waveguide fed phased array antenna
[NASA-TM-102522] N90-21273

Coplanar waveguide discontinuities for P-I-N diode switches and filter applications
[NASA-TM-102534] N90-21278
Elastic-plastic instability of plane frames N90-21415

PLANE WAVES
A numerical and theoretical study of seismic wave diffraction in complex geologic structure
[AD-A218209] N90-21490
Active control of multi-dimensional random sound in ducts
[NASA-TM-102653] N90-21603

PLANETARY RADIATION
High resolution imaging of the Venus night side using a Rockwell 128x128 HgCdTe array N90-21330

PLANTING
Wheat productivity estimate through field radiometry
[INPE-4994-PRE/1556] N90-21460

PLASMA BUBBLES
Low latitude F-region dynamical processes from atomic oxygen nightglow emissions
[INPE-4999-PRE/1561] N90-21494

PLASMA CONTROL
West European magnetic confinement fusion research N90-21634
Applied plasma physics
[DE90-007932] N90-21635

PLASMA COOLING
Experimental study of population inversion and spectral line broadening in a plasma containing a mixture of high Z and low Z ions
[DE90-007552] N90-21622

PLASMA DENSITY
Study on rotating plasma with submillimeter laser interferometer
[DE90-615387] N90-21623
Helium transport in plasma edge regions N90-21625
A simplified theoretical model for the laser-induced optogalvanic effect
[DE90-613121] N90-21626
Characterization of the plasma in magnetic multidipole discharges
[DE90-613219] N90-21628

PLASMA DIAGNOSTICS
The investigation of multilayer x ray reflectors as x ray optical elements
[DE90-009044] N90-21621
Study on rotating plasma with submillimeter laser interferometer
[DE90-615387] N90-21623
Characterization of the plasma in magnetic multidipole discharges
[DE90-613219] N90-21628
Applied plasma physics
[DE90-007932] N90-21635

PLASMA DIFFUSION
Study on rotating plasma with submillimeter laser interferometer
[DE90-615387] N90-21623

PLASMA DRIFT
Solar flares and dynamics of Langmuir waves in current-carrying plasmas
[IPPCZ-291] N90-21710

PLASMA ENGINES
The effects of magnetic nozzle configurations on plasma thrusters
[NASA-CR-186485] N90-21109

PLASMA ETCHING
Proceedings of the Joint NOSC/NRL (Naval Ocean Systems Center/Naval Research Laboratory) InP Microwave/Millimeter Wave Technology Workshop
[AD-A218216] N90-21259

PLASMA HEATING
Fusion burn dynamics in Dense Z-Pinch (DZP)
[DE90-007976] N90-21638
Full wave computation of electromagnetic wave excitation, propagation, and absorption at the ion cyclotron frequency in fusion experiments
[DE90-009399] N90-21642
Solar flares and dynamics of Langmuir waves in current-carrying plasmas
[IPPCZ-291] N90-21710

PLASMA LOSS
Characterization of the plasma in magnetic multidipole discharges
[DE90-613219] N90-21628

PLASMA PHYSICS
JPRS report: Science and technology. USSR: Physics and mathematics
[JPRS-UPM-90-002] N90-21593
Numerical code AEOLUS-E1 for analysing free-boundary resistive MHD mode
[DE90-759903] N90-21630

PLASMA TURBULENCE
Center of excellence in theoretical geoplasma research
[AD-A215035] N90-21488

PLASMA WAVES
On the relativistic Vlasov equation in guiding-center coordinates
[DE90-613241] N90-21629
Dynamics of cavitons in strong Langmuir turbulence
[DE90-008918] N90-21633

PLASMAS (PHYSICS)
Instabilities and vortex dynamics in shear flow of magnetized plasmas
[DE90-009448] N90-21643
Solar flares and dynamics of Langmuir waves in current-carrying plasmas
[IPPCZ-291] N90-21710

PLASMONS
US-Japan Workshop on Atomic Collisions in Solids: Abstracts of lectures
[DE90-008979] N90-21611
Coupled magnetoplasmon-phonon modes at the surface of a semi-infinite semiconductor superlattice
[DE90-612904] N90-21647

PLASTIC DEFORMATION
Elasto-plastic large deformation analysis of thin-walled structures
[PB90-164757] N90-21426

PLASTIC PROPERTIES
Three-dimensional elastic-plastic analysis of shallow cracks in single-edge-crack-tension specimens
[NASA-TM-102636] N90-21130
Deformation processing of YBa2Cu3O(sub x)
[DE90-007795] N90-21644

PLASTICIZERS
Preparation, characterisation and cookoff behaviour of booster compositions prepared from RDX and acrylic or ethylene-vinyl acetate dispersions
[MRL-TR-89-44] N90-21203

PLATE THEORY
Direct formulation of a 4-node hybrid shell element with rotational degrees of freedom
[NASA-CR-4282] N90-21411

PLATES
Wave receptance analysis of vibrating beams and stiffened plates N90-21419
A modification of a low-order Reissner-Mindlin plate bending element
[PB90-165630] N90-21428

PLATES (STRUCTURAL MEMBERS)
Micromechanics analysis of space simulated thermal deformations and stresses in continuous fiber reinforced composites
[NASA-TM-102633] N90-21140
Determination of stresses around cutouts in multilayered composite plate and shell structures N90-21417

POINT SOURCES
New water vapor masers in the Southern Hemisphere
[INPE-4844-PRE/1473] N90-21689
A search for very high energy gamma rays from the Crab pulsar-nebula N90-21718

POINTING CONTROL SYSTEMS
A general-purpose balloon-borne pointing system for solar scientific instruments
[NASA-TP-3013] N90-21219

POISSON EQUATION
Compact scheme for systems of equations applied to fundamental problems of mechanics of continua
[NASA-CR-186494] N90-21292

POLAR ORBITS
Attitude control modes for the MECB remote sensing satellites
[INPE-4755-PRE/1427] N90-21094

POLAR REGIONS
Center of excellence in theoretical geoplasma research
[AD-A215035] N90-21488

POLARIMETERS
The PHARUS project: Design of a polarimetric C-band SAR in the Netherlands N90-21228

POLARIMETRY
A motion compensation study for the PHARUS project N90-21235
Introduction to the Infrared Space Observatory (ISO) N90-21340
Status of the isophot detector development N90-21342

POLARIZATION (WAVES)
A frequency agile 94 GHz pulse-Doppler radar with dual polarisation capability N90-21226
A numerical and theoretical study of seismic wave diffraction in complex geologic structure
[AD-A218209] N90-21490

POLARIZED LIGHT
Polarization: Effects on second harmonic power in light scattering by free electrons
[DE90-612842] N90-21608

POLICIES
Regional remote sensing laboratory
[INPE-4922-PRE/1519] N90-21485

POLLUTION TRANSPORT
Sensitivity studies in a two-dimensional atmospheric transport model
[DAR-TP-18] N90-21496

POLONIUM ISOTOPES
Radon concentration over the Brazilian Amazon Basin during the wet season (Belem-Manaus GTE-ABLE-2B flight of April 24, 1987)
[INPE-4892-PRE/1493] N90-21486

POLYCARBONATES
The structural basis for fatigue initiation in glassy polymers
[DE90-009342] N90-21200

POLYCRYSTALS
Formation of subsurface aluminum layers in beryllium by ion implantation and post-implant annealing
[DE90-007975] N90-21172
Review and statistical analysis of the ultrasonic velocity method for estimating the porosity fraction in polycrystalline materials
[NASA-TM-102501] N90-21402

POLYESTERS
Criteria for polymer concrete on airport pavements
[DOT/FAA/DS-89/18] N90-21045
Low energy ion generator
[DE90-759905] N90-21195

POLYIMIDES
Bis(4-(3,4-dimethylenepyrrolidyl)-phenyl) methane
[NASA-CASE-LAR-13965-1-CU] N90-21118

POLYMER BLENDS
On the dynamics of polymer mixtures in solution using the RPA
[DE90-613689] N90-21149

POLYMER CHEMISTRY
Determinations of molecular weight and molecular weight distribution of high polymers by the rheological properties
[NASA-CR-186450] N90-21180

POLYMER MATRIX COMPOSITES
Use of unbalanced laminates as a screening method for microcracking
[NASA-TM-102517] N90-21124

POLYMER PHYSICS
Determinations of molecular weight and molecular weight distribution of high polymers by the rheological properties
[NASA-CR-186450] N90-21180

POLYMERIC FILMS
Low energy ion generator
[DE90-759905] N90-21195
Improvement of small-area, amorphous-silicon thin-film photovoltaics on polymer substrate
[DE90-000314] N90-21472

POLYMERIZATION
Process for crosslinking methylene-containing aromatic polymers with ionizing radiation
[NASA-CASE-LAR-13448-1] N90-21198
The structural basis for fatigue initiation in glassy polymers
[DE90-009342] N90-21200

POLYNOMIALS
Elastic-plastic instability of plane frames N90-21415

POLYSTYRENE
Development of intrinsic IPT scintillator
[DE90-007906] N90-21367

POLYURETHANE RESINS
The corrosion protection of 6061-T6 aluminum by a polyurethane-sealed anodized coat
[NASA-TM-100394] N90-21191

POPULATION INVERSION
X ray laser with enhanced x ray gain through photodepopulation
[AD-D014448] N90-21375
Experimental study of population inversion and spectral line broadening in a plasma containing a mixture of high Z and low Z ions
[DE90-007552] N90-21622

POROSITY
Review and statistical analysis of the ultrasonic velocity method for estimating the porosity fraction in polycrystalline materials
[NASA-TM-102501] N90-21402

POROUS MATERIALS
Method of making a long life high current density cathode from tungsten and iridium powders using a quarternary compound as the impregnant
[AD-D014425] N90-21211
Ablative cooling of aerodynamically heated radomes
[AD-D014426] N90-21293

POSITION (LOCATION)
Apparatus and method for locating the axis of symmetry (center of circular cross section) of three dimensional objects
[AD-D014407] N90-21354

POTASSIUM
An evaluation of metal salts of 3-nitro-1,2,4-triazol-5-one (NTO) as potential primary explosives
[MRL-TN-563] N90-21202
POTASSIUM HYDROXIDES
Effect of KOH concentration on LEO cycle life of IPV nickel-hydrogen flight battery cells
[NASA-TM-103127] N90-21116
POTENTIAL FLOW
Users manual for the NASA Lewis Ice Accretion Prediction Code (LEWICE)
[NASA-CR-185129] N90-20943
Discrete-vortex model for the symmetric-vortex flow on cones
[NASA-TP-2989] N90-20946
Multigrid accelerated relaxation solution of transonic full potential flow equation
[PD-CF-8942] N90-20951
POTENTIAL GRADIENTS
Observations of atmospheric electricity, 1988
[GEOPHYSICAL-PUBL-10] N90-21499
POWDER (PARTICLES)
ZELED analysis of aperiodicity and bond lengths in ceramic powders
[DE90-612932] N90-21193
Method of making a long life high current density cathode from tungsten and iridium powders using a quarternary compound as the impregnant
[AD-D014425] N90-21211
Alternative materials for solid oxide fuel cells
[DE90-008615] N90-21468
Shock compression of solids: A tutorial
[DE90-009185] N90-21659
POWDER METALLURGY
Ductile alloy encapsulated ceramic armor development
[AD-A217632] N90-21183
POWDERED ALUMINUM
Ductile alloy encapsulated ceramic armor development
[AD-A217632] N90-21183
POWER AMPLIFIERS
High efficiency octave bandwidth millimeter wave power amplifier
[AD-A218245] N90-21280
POWER BEAMING
Space power generation and distribution
[DE90-008676] N90-21474
POWER TRANSMISSION
Power transmission device
[AD-D014430] N90-21281
PREAMPLIFIERS
Short wavelength HgCdTe staring focal plane for low background astronomy applications N90-21336
Status of the isophot detector development N90-21342
PRECAMBRIAN PERIOD
Geology of Espinhaco Meridional, including the Quadrilatero Ferrifero: Integration through remote sensing data
[INPE-4904-PRE/1505] N90-21450
Contribution for the study of the evolution of part of the Espinhaco supergroup and its foundation through fracture analysis
[INPE-4907-PRE/1508] N90-21459
PRECIPITATION (METEOROLOGY)
Precipitation mechanisms in tropical and midlatitude convective clouds N90-21507
PRECIPITATION HARDENING
Thermomechanical deformation testing and modeling in the presence of metallurgical instabilities
[NASA-CR-185188] N90-21420
PRECISION
Foundations of measurement and instrumentation
[NASA-RP-1222] N90-21351
PREDICTION ANALYSIS TECHNIQUES
Measurement and prediction of propeller blade surface pressure distributions N90-20961
Aerodynamic design via control theory N90-20998
Secondary Flows in Turbomachines
[AGARD-CP-469] N90-21009
Secondary flows and radial mixing predictions in axial compressors N90-21010
The effects of compressor endwall flow on airfoil incidence and deviation N90-21011
Secondary flow in a turbine guide vane with low aspect ratio N90-21018
Calculation of the secondary flow in an axial turbine N90-21022
Losses in the tip-leakage flow of a planar cascade of turbine blades N90-21027
Computer codes for the evaluation of thermodynamic properties, transport properties, and equilibrium constants of an 11-species air model
[NASA-TM-102602] N90-21297
Improved analytical capabilities for foil air bearings, phase 1
[AD-A218071] N90-21389
NASA airframe structural integrity program
[NASA-TM-102637] N90-21422
PREDICTIONS
The influence of lateral boundary conditions, fixed surface forcings, and synoptic situations upon predictability estimates using limited area numerical models N90-21492
Predictability of weather and climate in a coupled ocean-atmosphere model: A dynamical systems approach
[NASA-CR-186499] N90-21502
Tropical cyclone track predictability and the adjoint method of data assimilation
[AD-A216324] N90-21505
PRESSURE DISTRIBUTION
Measurement and prediction of propeller blade surface pressure distributions N90-20961
An intensive procedure for the design of pressure-specified three-dimensional configurations at subsonic and supersonic speeds by means of a higher-order panel method N90-20982
A system for transonic wing design with geometric constraints based on an inverse method N90-20983
Numerical optimization of target pressure distributions for subsonic and transonic airfoil design N90-20993
Numerical optimization of wings in transonic flow N90-20997
Secondary Flows in Turbomachines
[AGARD-CP-469] N90-21009
Double valve mechanism for an acoustic modulator
[AD-D014401] N90-21386
PRESSURE EFFECTS
Shock initiation sensitivity of damaged TP-H1207C composite propellant
[DE90-008509] N90-21205
An internal/external pressure, tension/compression multiaxial fatigue system
[DE90-009510] N90-21430
PRESSURE OSCILLATIONS
An outline for the analysis of wave induced bottom pressure fluctuations
[MRL-TN-558] N90-21510
PRESSURE REDUCTION
Secondary flow predictions for a transonic nozzle guide vane N90-21017
PRESSURE VESSELS
An internal/external pressure, tension/compression multiaxial fatigue system
[DE90-009510] N90-21430
PRIMERS
Methods for improving the flowability of a percussion primer composition
[MRL-TR-89-32] N90-21201
PRIMERS (COATINGS)
Combination primer/topcoat coating
[AD-D014445] N90-21189
PRISMS
AFGL ten micron mosaic array spectrometer: Recent results N90-21333
PROBABILITY THEORY
Stochastic robustness of linear control systems N90-20941
Probabilistic modeling for simulation of aerodynamic uncertainties in propulsion systems
[NASA-TM-102472] N90-21036
Final safety analysis report for the Ulysses Mission. Volume 2: Accident model document-appendices
[DE90-008695] N90-21104
Problems in radiative transfer in astrophysics: An escape probability treatment of line overlap and a model of the masers around VX Sgr N90-21705
PROBLEM SOLVING
Subsonic and transonic blade design by means of analysis codes N90-20985
Mechanics of interface fracture N90-21408
Cooperating intelligent systems
[NASA-CR-184982] N90-21529
Multigrid on massively parallel computers
[DE90-008999] N90-21560
High accuracy solutions of incompressible Navier-Stokes equations
[NASA-TM-102539] N90-21567
Numerical code AEOLUS-E1 for analysing free-boundary resistive MHD mode
[DE90-759903] N90-21630
STORM: A statistical object representation model
[DE90-009048] N90-21686
PROCESS CONTROL (INDUSTRY)
Deformation processing of YBa2Cu3O(sub x)
[DE90-007795] N90-21644
Toughened YBa2Cu3O(sub x)/ZrO2 composites
[DE90-007796] N90-21645
PRODUCTIVITY
Wheat productivity estimate through field radiometry
[INPE-4994-PRE/1556] N90-21460
Advanced manufacturing technology: A Department of Energy technology transfer initiative
[DE90-008601] N90-21688
PROGRAM VERIFICATION (COMPUTERS)
Software verification and validation: Its role in computer assurance and its relationship with software project management standards
[PB90-111691] N90-21530
PROJECT MANAGEMENT
Fuel cell systems program plan, FY 1990
[DE90-008178] N90-21471
Software verification and validation: Its role in computer assurance and its relationship with software project management standards
[PB90-111691] N90-21530
PROJECT PLANNING
Fuel cell systems program plan, FY 1990
[DE90-008178] N90-21471
PROJECTILES
Simple light gas guns for hypervelocity studies
[DE90-008907] N90-21056
Railgun performance with a two-stage light-gas gun injector
[DE90-009183] N90-21057
Ablative cooling of aerodynamically heated radomes
[AD-D014426] N90-21293
Perforation of a reinforced concrete wall by a rigid missile
[AD-A210025] N90-21381
PROP-FAN TECHNOLOGY
Structural tailoring of select fiber composite structures
[NASA-TM-102484] N90-21137
PROPELLANT EXPLOSIONS
Discrete modeling of beds of propellant exposed to strong stimulus
[DE90-008932] N90-21206
PROPELLANT GRAINS
Concentric layer ramjet fuel
[AD-D014443] N90-21111
PROPELLANT SENSITIVITY
Shock initiation sensitivity of damaged TP-H1207C composite propellant
[DE90-008509] N90-21205
PROPELLANTS
Stress analysis of rocket motors with viscoelastic propellant by a mixed finite element model N90-21112
Discrete modeling of beds of propellant exposed to strong stimulus
[DE90-008932] N90-21206
PROPELLER BLADES
Relating flow between counter-rotating propellers to aerodynamic interaction noise N90-20944
Measurement and prediction of propeller blade surface pressure distributions N90-20961
Aerofoil design techniques N90-20978
PROPELLER DRIVE
Computation of viscous flow around a propeller-shaft configuration with infinite-pitch rectangular blades N90-20958
PROPELLER EFFICIENCY
Computation of viscous flow around a propeller-shaft configuration with infinite-pitch rectangular blades N90-20958
PROPELLER NOISE
The radiation of sound from a propeller at angle of attack
[NASA-CR-4264] N90-21602
PROPELLERS
Laser-velocimeter-measured flow field around an advanced, swept, eight-blade propeller at Mach 0.8
[NASA-TP-2462] N90-20942
Relating flow between counter-rotating propellers to aerodynamic interaction noise N90-20944
Aerodynamic optimization by simultaneously updating flow variables and design parameters N90-20991
PROPULSION SYSTEM CONFIGURATIONS
Performance of an aero-space plane propulsion nozzle N90-21034
Probabilistic modeling for simulation of aerodynamic uncertainties in propulsion systems
[NASA-TM-102472] N90-21036
Exhaust nozzles for propulsion systems with emphasis on supersonic cruise aircraft
[NASA-RP-1235] N90-21037
PROPULSION SYSTEM PERFORMANCE
Performance of an aero-space plane propulsion nozzle N90-21034
Probabilistic modeling for simulation of aerodynamic uncertainties in propulsion systems
[NASA-TM-102472] N90-21036
Exhaust nozzles for propulsion systems with emphasis on supersonic cruise aircraft
[NASA-RP-1235] N90-21037

Technical Evaluation Motor no. 5 (TEM-5) [NASA-CR-183932] N90-21117
PROTECTION
Pressure rig for repetitive casting [NASA-CASE-LAR-14050-1] N90-21216
PROTECTIVE CLOTHING
Minutes of the 23rd Explosives Safety Seminar, volume 2 [AD-A218265] N90-21214
PROTECTIVE COATINGS
The effect of leveling coatings on the atomic oxygen durability of solar concentrator surfaces [NASA-TM-102557] N90-21110
High gloss corrosion-resistant coatings [AD-D014403] N90-21184
Combination primer/topcoat coating [AD-D014445] N90-21189
Energy beam treatment for improved adhesion of coatings to surfaces [AD-D014449] N90-21190
PROTOCOL (COMPUTERS)
On board cross support scenarios [INPE-5005-PRE/1562] N90-21268
Cooperating intelligent systems [NASA-CR-184962] N90-21529
Fast causal multicast [NASA-CR-186495] N90-21533
PSYCHOLOGICAL TESTS
Development of microcomputer-based mental acuity tests for repeated-measures studies [NASA-CR-185607] N90-21521
PSYCHOLOGY
Joint University Program for Air Transportation Research, 1988-1989 [NASA-CP-3063] N90-20921
PUBLIC HEALTH
Final Safety Analysis Report for the Ulysses Mission. Volume 3 (Book 1): Nuclear risk analysis document [DE90-008691] N90-21101
PULSAR MAGNETOSPHERES
Ultrarelativistic envelope solitons in electron-positron plasma of the pulsar magnetosphere [DE90-613289] N90-21264
PULSARS
Ultrarelativistic envelope solitons in electron-positron plasma of the pulsar magnetosphere [DE90-613289] N90-21264
A search for very high energy gamma rays from the Crab pulsar-nebula N90-21718
PULSE COMPRESSION
Development of an ultra-bright laser and an application to multi-photon ionization N90-21372
PULSE DOPPLER RADAR
A frequency agile 94 GHz pulse-Doppler radar with dual polarisation capability N90-21226
PULSE DURATION
Intensity to frequency conversion technique in intensity modulated fiber optic sensing systems [NASA-TM-102562] N90-21277
PULSE GENERATORS
Programmable generation of linear frequency modulated pulses N90-21232
PULSED LASERS
Generation of ultrashort laser pulses from neodymium glass oscillator and regenerative amplifier N90-21373
PUMPS
BASG thermomechanical pump helium 2 transfer tests [NASA-CR-177541] N90-21097
PYROLYTIC GRAPHITE
Feasibility of intercalated graphite railgun armatures [NASA-TM-102546] N90-21181
PYROTECHNICS
Double swivel toggle release [NASA-CASE-MSC-21436-1] N90-21390

Q

QUALIFICATIONS
Sole means navigation and integrity through hybrid Loran-C and NAVSTAR GPS N90-20933
QUALITY
Proceedings of the 4th European Conference, volume 2 [AD-A216521] N90-21382
QUALITY CONTROL
Quality at a glance [AD-A217297] N90-21400
Software verification and validation: Its role in computer assurance and its relationship with software project management standards [PB90-111691] N90-21530
Advanced manufacturing technology: A Department of Energy technology transfer initiative [DE90-008601] N90-21688
QUANTUM EFFICIENCY
InSb DRO array characteristics N90-21326
Infrared ground-based astronomy with the Hughes 256 X 256 PtSi array N90-21331
Short wavelength HgCdTe staring focal plane for low background astronomy applications N90-21336
Improved Si:As BIBIB (Back-Illuminated Blocked-Impurity-Band) hybrid arrays N90-21349
QUANTUM ELECTRONICS
JPRS report: Science and technology. USSR: Electronics and electrical engineering [JPRS-UEE-90-002] N90-21284
QUANTUM MECHANICS
Center for Atomic, Molecular, and Optical Physics: Technical activities [PB90-133158] N90-21591
Local supersymmetry in non-relativistic systems [DE90-612751] N90-21670
QUANTUM THEORY
Linking numbers and variational method [DE90-612793] N90-21582
Fusion algebra and fusing matrices [DE90-612798] N90-21583
Studies in quantum field theory [DE90-008731] N90-21677
The 2 + 1 dimensional quantum gravity and the Braid group [DE90-009036] N90-21679
Toward quantum corrections in black hole thermodynamics N90-21702

R

RADAR ANTENNAS
ROSAR (Helicopter-Rotor based Synthetic Aperture Radar) N90-21229
Concept for a spaceborne Synthetic Aperture Radar (SAR) sensor based on active phased array technology N90-21234
RADAR BEAMS
Concepts for high resolution space based SAR/ISAR systems: Preliminary design considerations N90-21224
Trade-offs in a space based surveillance radar N90-21225
RADAR CROSS SECTIONS
The 5th Annual Review of Progress in Applied Computational Electromagnetics [AD-A217994] N90-21258
RADAR DATA
Windshear case study: Denver, Colorado, July 11, 1988 [DOT/FAA/DS-88/19] N90-21509
RADAR DETECTION
Concept for a spaceborne Synthetic Aperture Radar (SAR) sensor based on active phased array technology N90-21234
Airborne Doppler radar flight experiments for the detection of microbursts N90-21243
Concept and results of the DLR realtime SAR processor N90-21244
RADAR ECHOES
A fast ISAR-imaging process and its inherent degrading effects on image quality N90-21239
Radar target image by ISAR case study N90-21242
RADAR IMAGERY
SAR and ISAR imagery of marine targets N90-21237
Radar observations of a formation of two fighters: A case study for ISAR imaging N90-21240
The 1D-ISAR imaging of manoeuvering aircraft N90-21241
Radar target image by ISAR case study N90-21242
Image simulation of geometric targets for synthetic aperture radar N90-21245
SAR image coding N90-21246
Automatic classification of images [AD-D014437] N90-21260
Results of the Gondwana Project: An example of intercontinental geologic correlation utilizing LANDSAT imagery [INPE-4870-PRE/1481] N90-21437
Characterization of linear structures from remote sensing data; Espinhaco Meridional (MG) sierra [INPE-4905-PRE/1506] N90-21449
RADAR MEASUREMENT
Problems in ISAR processing with range resolution by stepped frequency bursts N90-21238
Investigations into the properties, conditions, and effects of the ionosphere [AD-A217807] N90-21489
RADAR RESOLUTION
High Resolution Air- and Spaceborne Radar [AGARD-CP-459] N90-21223
RADAR SCANNING
MMW SAR on RPV for battlefield surveillance N90-21231
RADAR SCATTERING
The PHARUS project: Design of a polarimetric C-band SAR in the Netherlands N90-21228
A solution for real time motion compensation for SAR without using inertial navigation systems N90-21236
RADAR TARGETS
Radar target image by ISAR case study N90-21242
RADAR TRACKING
Trade-offs in a space based surveillance radar N90-21225
Capabilities of bistatic synthetic aperture radar for covert battlefield surveillance N90-21230
Radar observations of a formation of two fighters: A case study for ISAR imaging N90-21240
Radar target image by ISAR case study N90-21242
RADIATION DAMAGE
Stressed Ge:Ga photoconductors for space-based astronomy. (Is there life beyond 120 micron) N90-21315
Development of intrinsic IPT scintillator [DE90-007906] N90-21367
RADIATION DETECTORS
Stressed Ge:Ga photoconductors for space-based astronomy. (Is there life beyond 120 micron) N90-21315
Germanium Blocked Impurity Band (BIB) detectors N90-21321
Short wavelength HgCdTe staring focal plane for low background astronomy applications N90-21336
Status of the isophot detector development N90-21342
ISO/LWS: Detector status N90-21343
Tests of the Rockwell Si:As Back-Illuminated Blocked-Impurity Band (BIBIB) detectors N90-21350
RADIATION DOSAGE
A radiological assessment of nuclear power and propulsion operations near Space Station Freedom [NASA-CR-185185] N90-21108
Simplified model for solar cosmic ray exposure in manned Earth orbital flights [NASA-TM-4182] N90-21715
RADIATION EFFECTS
Final Safety Analysis Report for the Ulysses Mission. Volume 3 (Book 1): Nuclear risk analysis document [DE90-008691] N90-21101
Final safety analysis report for the Ulysses Mission. Volume 3 (Book 2): Nuclear risk analysis document-appendices [DE90-008692] N90-21102
Final safety analysis report for the Ulysses mission. Volume 2 (Book 1): Accident model document [DE90-008694] N90-21103
Grain boundary chemistry effects on irradiation-assisted stress corrosion cracking [DE90-008823] N90-21167
Aging and compatibility of TNF-doped Mylar [DE90-008508] N90-21186
Study of advanced InSb arrays for SIRTF (Space Infrared Telescope Facility) N90-21325
ISO camera array development status N90-21344
Laboratory characterization of direct readout Si:Sb and Si:Ga infrared detector arrays N90-21347
JPRS report: Science and technology. USSR: Life sciences [JPRS-ULS-90-002] N90-21434
Biological effects of ELF (Extremely-Low-Frequency) electric and magnetic fields [DE90-008634] N90-21514
RADIATION HAZARDS
Final Safety Analysis Report for the Ulysses Mission. Volume 3 (Book 1): Nuclear risk analysis document [DE90-008691] N90-21101
Final safety analysis report for the Ulysses Mission. Volume 3 (Book 2): Nuclear risk analysis document-appendices [DE90-008692] N90-21102
Final safety analysis report for the Ulysses mission. Volume 2 (Book 1): Accident model document [DE90-008694] N90-21103
Final safety analysis report for the Ulysses mission. Volume 1: Reference design document [DE90-008693] N90-21107
Boeing 727-100 test project (high energy radiated field tests) [DOT/FAA/CT-88/33] N90-21247
RADIATION PROTECTION
Final safety analysis report for the Ulysses Mission. Volume 3 (Book 2): Nuclear risk analysis document-appendices [DE90-008692] N90-21102
Final safety analysis report for the Ulysses Mission. Volume 2: Accident model document-appendices [DE90-008695] N90-21104

RADIATION SHIELDING
Simplified model for solar cosmic ray exposure in manned Earth orbital flights
[NASA-TM-4182] N90-21715
RADIATIVE TRANSFER
Numerical simulations of the cloud-capped marine boundary layer N90-21506
Thomson scattering in a magnetic field N90-21699
A theoretical study of circumstellar dust around Ae/Be stars N90-21700
Problems in radiative transfer in astrophysics: An escape probability treatment of line overlap and a model of the masers around VX Sgr N90-21705
RADIO ANTENNAS
Environmental projects, volume 10. Environmental assessment: New 34-meter antenna at Apollo site
[NASA-CR-186448] N90-21480
RADIO COMMUNICATION
An introduction to high frequency radioteletype systems
[PB90-145533] N90-21252
Prediction of VHF/UHF mobile reception in urban areas: Comparison with measurements in London
[BBC-RD-1989/11] N90-21255
RADIO EMISSION
New water vapor masers in the Southern Hemisphere
[INPE-4844-PRE/1473] N90-21689
Flare stars at radio wavelengths
[NASA-CR-186539] N90-21719
RADIO FREQUENCIES
Influence of the deposition conditions on radiofrequency magnetron sputtered MoS2 films
[NASA-TP-2994] N90-21210
Boeing 727-100 test project (high energy radiated field tests)
[DOT/FAA/CT-88/33] N90-21247
RADIO TRANSMISSION
JPRS report: Science and technology. USSR: Electronics and electrical engineering
[JPRS-UEE-90-002] N90-21284
RADIO WAVES
Flare stars at radio wavelengths
[NASA-CR-186539] N90-21719
RADIOACTIVE DECAY
Characteristics consequences of space-time coordinate relativization
[DE90-615201] N90-21668
RADIOISOTOPE BATTERIES
Final Safety Analysis Report for the Ulysses Mission. Volume 3 (Book 1): Nuclear risk analysis document
[DE90-008691] N90-21101
Final safety analysis report for the Ulysses mission. Volume 2 (Book 1): Accident model document
[DE90-008694] N90-21103
RADIOLOGY
Final safety analysis report for the Ulysses Mission. Volume 3 (Book 2): Nuclear risk analysis document-appendices
[DE90-008692] N90-21102
A radiological assessment of nuclear power and propulsion operations near Space Station Freedom
[NASA-CR-185185] N90-21108
RADIOMETERS
Wheat productivity estimate through field radiometry
[INPE-4994-PRE/1556] N90-21460
RADIOMETRIC CORRECTION
Real-time adaptive radiometric correction for imaging radars systems N90-21233
RADIOMETRIC RESOLUTION
Real-time adaptive radiometric correction for imaging radars systems N90-21233
RADOMES
Ablative cooling of aerodynamically heated radomes
[AD-D014426] N90-21293
RADON ISOTOPES
Radon concentration over the Brazilian Amazon Basin during the wet season (Belem-Manaus GTE-ABLE-2B flight of April 24, 1987)
[INPE-4892-PRE/1493] N90-21486
RAILGUN ACCELERATORS
Laser controlled semiconductor armature for electromagnetic launchers
[AD-D014435] N90-21055
Railgun performance with a two-stage light-gas gun injector
[DE90-009183] N90-21057
Feasibility of intercalated graphite railgun armatures
[NASA-TM-102546] N90-21181
RAIN
Use of microwave satellite data to study variations in rainfall over the Indian Ocean
[NASA-CR-186408] N90-21501
RAMAN SPECTRA
Relativistic stimulated Brillouin and Raman scattering in a laser-produced plasma
[DE90-613123] N90-21627
RAMJET ENGINES
Concentric layer ramjet fuel
[AD-D014443] N90-21111
RANDOM NOISE
Effective techniques for the identification and accommodation of disturbances N90-21072
Active control of multi-dimensional random sound in ducts
[NASA-TM-102653] N90-21603
RANGEFINDING
An assessment of the potential of continuous-wave ranging for measuring the distance to a highly reflective, infinite sheet
[NASA-TM-101680] N90-21279
Development of a dynamic modeling technique and its application to the analysis and control of a high-precision robotic manipulator N90-21391
RARE GASES
LLE review
[DE90-008958] N90-21378
RATS
Biological effects of ELF (Extremely-Low-Frequency) electric and magnetic fields
[DE90-008634] N90-21514
RAY TRACING
Thermal radiation characteristics of nonisothermal cylindrical enclosures using a numerical ray tracing technique
[NASA-TM-102527] N90-21296
Design and optimisation of thin foil x ray telescopes N90-21690
RDX
Preparation, characterisation and cookoff behaviour of booster compositions prepared from RDX and acrylic or ethylene-vinyl acetate dispersions
[MRL-TR-89-44] N90-21203
REACTION KINETICS
Computer codes for the evaluation of thermodynamic properties, transport properties, and equilibrium constants of an 11-species air model
[NASA-TM-102602] N90-21297
Laser studies of chemical dynamics at the gas-solid interface
[DE90-008698] N90-21380
The Chemkin Thermodynamic Data Base
[DE90-007953] N90-21676
REACTION WHEELS
Design of a digital model following controller of reaction wheel torques
[INPE-4753-PRE/1425] N90-21093
REACTIVITY
Hydrocarbon-fuel/combustion-chamber-liner materials compatibility
[NASA-CR-185203] N90-21165
REACTOR DESIGN
Fusion technology development
[DE90-007933] N90-21636
REACTOR MATERIALS
Fusion technology development
[DE90-007933] N90-21636
REACTOR TECHNOLOGY
West European magnetic confinement fusion research N90-21634
Fusion technology development
[DE90-007933] N90-21636
READOUT
Laboratory characterization of direct readout Si:Sb and Si:Ga infrared detector arrays N90-21347
REAL TIME OPERATION
Rule-based mechanisms of learning for intelligent adaptive flight control N90-20939
Perspectives on the use of rule-based control N90-20940
Effective techniques for the identification and accommodation of disturbances N90-21072
Effect of KOH concentration on LEO cycle life of IPV nickel-hydrogen flight battery cells
[NASA-TM-103127] N90-21116
Real-time adaptive radiometric correction for imaging radars systems N90-21233
A solution for real time motion compensation for SAR without using inertial navigation systems N90-21236
Concept and results of the DLR realtime SAR processor N90-21244
A real-time rejection circuit to automatically reject multiple interfering hopping signals while passing a lower level desired signal
[AD-D014424] N90-21251
Strategies for concurrent processing of complex algorithms in data driven architectures
[NASA-CR-186515] N90-21535
A real time neural net estimator of fatigue life
[NASA-TM-103117] N90-21564
RECEIVERS
Ridge regression processing N90-20931
Direct Radio Broadcasting by Satellite (DRBS): A review of the technical factors and system approaches suitable for mobile and fixed reception
[BBC-RD-1989/4] N90-21221
Feasibility of using frequency offset on very high frequency air/ground voice channels
[DOT/FAA/CT-TN89/71] N90-21248
RECOMBINATION COEFFICIENT
Mechanistic model for catalytic recombination during aerobraking maneuvers
[NASA-CR-185611] N90-21059
RECOMBINATION REACTIONS
Mechanistic model for catalytic recombination during aerobraking maneuvers
[NASA-CR-185611] N90-21059
Atomic processes in high temperature plasmas
[DE90-008873] N90-21632
RECONNAISSANCE
Design of a natural laminar flow airfoil for an unmanned aircraft
[PD-CF-9004] N90-20975
RECTANGULAR PLATES
The effect of elastic boundary conditions on the dynamic response of rectangular plates
[NASA-CR-186059] N90-21405
Fourier series methods for plates and shells with cracks and inclusions N90-21406
Review of formulae for the buckling of simply-supported, orthotropic plates under shear load, including transverse shear effects
[PB90-167073] N90-21429
RECTANGULAR WAVEGUIDES
A new rectangular waveguide to coplanar waveguide transition
[NASA-TM-102477] N90-21263
RED SHIFT
The large scale structure of the universe in pancake models of galaxy formation N90-21701
Horizon problem in cosmological models with non zero
[DE90-613367] N90-21708
REDUCED GRAVITY
Space truss zero gravity dynamics N90-21087
Microgravity science and applications bibliography, 1989 revision
[NASA-TM-4192] N90-21207
Critical point wetting drop tower experiment
[NASA-CR-186513] N90-21208
Apparatus for mixing solutions in low gravity environments
[NASA-CASE-MFS-28047-1] N90-21209
Acoustic convective system
[NASA-CASE-NPO-17278-1-CU] N90-21215
Microgravity acoustic mixing for particle cloud combustors
[NASA-CR-185159] N90-21600
REDUCTION (CHEMISTRY)
O2 reduction at the IFC orbiter fuel cell O2 electrode
[NASA-TM-102580] N90-21469
REDUNDANCY
A new approach to solve the kinematics resolution of a redundant robot
[DE90-010213] N90-21397
REFLECTANCE
The measurement of surface reflectivity at millimetre wavelengths
[MRL-TN-559] N90-21222
An assessment of the potential of continuous-wave ranging for measuring the distance to a highly reflective, infinite sheet
[NASA-TM-101680] N90-21279
Fiber optic void fraction sensor
[DE90-009124] N90-21366
Absolute multilayer characterization at high spatial resolution via real-time soft x ray imaging
[DE90-009181] N90-21371
Digital processing of TM/LANDSAT data in monitoring interior water
[INPE-4956-PRE/1533] N90-21448
REFLECTOR ANTENNAS
Aperture taper determination for the half-scale accurate antenna reflector
[NASA-CR-185215] N90-21282
REFLECTORS
ASCIE: An integrated experiment to study CSI in large segmented optical systems N90-21082
Preliminary design approach for large high precision segmented reflectors
[NASA-TM-102605] N90-21096
Power transmission device
[AD-D014430] N90-21281
REFRACTORY MATERIALS
Titanium aluminides: Processing, properties and potential
[AERE-R-13198] N90-21158

Boron-containing organosilane polymers and ceramic materials thereof
[NASA-CASE-ARC-11649-2-SB] N90-21177
Attachment of lead wires to thin film thermocouples mounted on high temperature materials using the parallel gap welding process
[NASA-TM-102442] N90-21361

REFRIGERANTS
Thermal control system corrosion study
[NASA-TM-102220] N90-21294
An experimental evaluation of two nonazeotropic refrigerant mixtures in a water-to-water breadboard heat pump
[DE90-009016] N90-21305

REFRIGERATING
A progress report on using bolometers cooled by adiabatic demagnetization refrigeration N90-21316

REFRIGERATORS
A 100 micro Kelvin bolometer system for SIRTF N90-21317

REGENERATORS
Generation of ultrashort laser pulses from neodymium glass oscillator and regenerative amplifier N90-21373

REGRESSION ANALYSIS
Review and statistical analysis of the ultrasonic velocity method for estimating the porosity fraction in polycrystalline materials
[NASA-TM-102501] N90-21402
Performance evaluation of MSS/LANDSAT data in the estimation of fluvial channel width
[INPE-4906-PRE/1507] N90-21463

REINFORCING FIBERS
Reinforcement-matrix interface effects in metal matrix composites
[MRL-TN-562] N90-21120

REJECTION
A real-time rejection circuit to automatically reject multiple interfering hopping signals while passing a lower level desired signal
[AD-D014424] N90-21251

RELATIVISTIC EFFECTS
String dynamics in curved space-time revisited
[DE90-612796] N90-21674

RELATIVISTIC PARTICLES
High energy phenomena during solar flares
[INPE-4961-TDL/390] N90-21713
Fragmentation of relativistic heavy nuclei with application to cosmic ray propagation N90-21716

RELATIVISTIC PLASMAS
Ultrarelativistic envelope solitons in electron-positron plasma of the pulsar magnetosphere
[DE90-613289] N90-21264
Relativistic stimulated Brillouin and Raman scattering in a laser-produced plasma
[DE90-613123] N90-21627
Relativistic processes in active galactic nuclei N90-21698

RELATIVITY
Once more about the sizes of fast-moving objects
[DE90-615204] N90-21592
The gravitational lens effect and its optical equivalents
[DE90-612767] N90-21673

RELAXATION METHOD (MATHEMATICS)
Multigrid accelerated relaxation solution of transonic full potential flow equation
[PD-CF-8942] N90-20951

RELEASING
Double swivel toggle release
[NASA-CASE-MSC-21436-1] N90-21390

RELIABILITY
Development of microcomputer-based mental acuity tests for repeated-measures studies
[NASA-CR-185607] N90-21521

REMOTE SENSING
Programme of the International Training Course on Remote Sensing for African Specialists
[INPE-4878-NTE/290] N90-21435
Shade images of forested areas obtained from LANDSAT MSS data
[NASA-TM-102939] N90-21436
Remote sensing applied to sea water quality researches in coastal regions: A review
[INPE-4935-PRE/1425] N90-21438
Geobotanical remote sensing: A review
[INPE-5026-PRE/1565] N90-21440
Survey of land use through remote sensing
[INPE-5032-MD/042] N90-21443
Analysis and modelling of spatial data proposal of a system for CBERS
[INPE-4911-PRE/1512] N90-21445
Project CANASATE: Remote sensing applied to sugar cane crop survey
[INPE-4902-PRE/1503] N90-21446
Monitoring vegetation of Brazil: Potentialities of multi-sensors approach
[INPE-4993-PRE/1555] N90-21451
Evolution of remote sensing applied to vegetation and forest at INPE
[INPE-4970-PRE/1538] N90-21452
Introduction of digital image processing by remote sensors applied to geology
[INPE-5023-RPE/616] N90-21456
Regional remote sensing laboratory
[INPE-4922-PRE/1519] N90-21465
Use of microwave satellite data to study variations in rainfall over the Indian Ocean
[NASA-CR-186406] N90-21501

REMOTELY PILOTED VEHICLES
The MANTA: An RPV design to investigate forces and moments on a lifting surface
[NASA-CR-186227] N90-20971
MMW SAR on RPV for battlefield surveillance N90-21231

REPORTS
A compendium of sources of fracture toughness and fatigue crack growth data for metallic alloys, part 4
[NASA-TM-102646] N90-21164

REQUIREMENTS
Requirements of IR space astronomy N90-21314

RESEARCH AND DEVELOPMENT
A requirement for Australian research: Access to big science facilities, a report by the Australian National Committee for Crystallography
[DE90-614784] N90-21048
Goes I-M and beyond: Science requirements and technology challenges N90-21067
Research and Technology
[NASA-TM-102161] N90-21721

RESEARCH FACILITIES
Proceedings of the 13th International Congress on Instrumentation in Aerospace Simulation Facilities
[EOARD-LR-89-069] N90-21046
A survey of experiments and experimental facilities for active control of flexible structures N90-21079
Cosmic Dust Collection Facility: Scientific objectives and programmatic relations
[NASA-TM-102160] N90-21096
Microgravity science and applications bibliography, 1989 revision
[NASA-TM-4192] N90-21207
Aeropropulsion facilities configuration control: Procedures manual
[NASA-TM-102541] N90-21399
Activities and operations of the Advanced Computing Research Facility
[DE90-007957] N90-21559
Research and Technology
[NASA-TM-102161] N90-21721

RESERVOIRS
Monitoring of agrocattle-raising projects through visual/digital analysis of LANDSAT-TM imagery south of Para state
[INPE-4982-PRE/1542] N90-21442
Thermal decay of an initially hot isothermal water body with application to thermal energy storage
[DE90-614742] N90-21675

RESIDUAL STRENGTH
Relevance of impacter shape to nonvisible damage and residual tensile strength of a thick graphite/epoxy laminate
[NASA-TM-102599] N90-21122

RESIDUAL STRESS
Use of unbalanced laminates as a screening method for microcracking
[NASA-TM-102517] N90-21124
Fiber pushout test: A three-dimensional finite element computational simulation
[NASA-TM-102565] N90-21131
Optimal fabrication processes for unidirectional metal-matrix composites: A computational simulation
[NASA-TM-102559] N90-21143
Problems associated with residual and mismatch stresses in thin film structures N90-21407
Determination of internal strains in high-temperature superconductor composites by intense pulsed neutron source
[DE90-007799] N90-21664

RESIDUES
Thermal control system corrosion study
[NASA-TM-102220] N90-21294

RESONANCE
Parametric resonance in horizontal axis wind turbines N90-20962

RESONANT FREQUENCIES
Software to characterize tuning fork resonators used in the Quartz Digital Accelerometer
[DE90-007913] N90-21363
The effect of elastic boundary conditions on the dynamic response of rectangular plates
[NASA-CR-186059] N90-21405
Integrated modeling and analysis of a space-truss article
[NASA-TM-102615] N90-21412

RESONATORS
Software to characterize tuning fork resonators used in the Quartz Digital Accelerometer
[DE90-007913] N90-21363

REUSABLE ROCKET ENGINES
Probabilistic modeling for simulation of aerodynamic uncertainties in propulsion systems
[NASA-TM-102472] N90-21036
A real time neural net estimator of fatigue life
[NASA-TM-103117] N90-21564

REVISIONS
Maintenance = reuse-oriented software development
[NASA-CR-186455] N90-21531

REYNOLDS NUMBER
Navier-Stokes analysis of turbine blade heat transfer
[NASA-TM-102496] N90-21300

REYNOLDS STRESS
Secondary flows and Reynolds stress distributions downstream of a turbine cascade at different expansion ratios N90-21015

RHEOLOGY
Nicalon/siliconoxycarbide ceramic composites
[NASA-TM-102563] N90-21133
Determinations of molecular weight and molecular weight distribution of high polymers by the rheological properties
[NASA-CR-186450] N90-21180

RICCATI EQUATION
On the continuous dependence with respect to sampling of the linear quadratic regulator problem for distributed parameter systems
[NASA-CR-182012] N90-21566

RIEMANN MANIFOLD
Extension of the Krichever-Novikov algebra in the closed string theory
[DE90-612746] N90-21578

RIGID STRUCTURES
Detection of potential space station control/structure interaction with CO-ST-IN N90-21074

RING STRUCTURES
Expanding ring joint
[AD-D014398] N90-21384

RISK
Final safety analysis report for the Ulysses Mission
[DE90-008690] N90-21106
Kinematic and kinetic analyses of drop landings N90-21517

RIVERS
Analysis of water quality parameters of the Piaui River (SE), Brazil, through field and TM/LANDSAT sensor data
[INPE-4918-PRE/1417] N90-21453
Evaluation of the mangrove areas of the Rio Piaui (SE) through remote sensing
[INPE-4909-PRE/1510] N90-21454
Performance evaluation of MSS/LANDSAT data in the estimation of fluvial channel width
[INPE-4906-PRE/1507] N90-21463

ROADS
Monitoring of agrocattle-raising projects through visual/digital analysis of LANDSAT-TM imagery south of Para state
[INPE-4982-PRE/1542] N90-21442

ROBOT ARMS
End point control of flexible manipulators
[AD-A217319] N90-21383
Development of a dynamic modeling technique and its application to the analysis and control of a high-precision robotic manipulator N90-21391
Application of optimization in design and motion control of robot manipulators N90-21393

ROBOT DYNAMICS
Application of optimization in design and motion control of robot manipulators N90-21393

ROBOTICS
Controlled multibody dynamics simulation for large space structures N90-21068
Application of optimization in design and motion control of robot manipulators N90-21393
Adaptive learning fuzzy control of a mobile robot
[DE90-759898] N90-21562
Small business innovation research. Abstracts of 1988 phase 1 awards
[NASA-TM-102991] N90-21680

ROBOTS
A solution level indicator system
[DE90-007939] N90-21151
Modeling elastomer displacements for tactile sensing applications
[DE90-007959] N90-21370
End point control of flexible manipulators
[AD-A217319] N90-21383

A new approach to solve the kinematics resolution of a redundant robot
[DE90-010213] N90-21397
The development of computational algorithms for manipulator inverse kinematics
[DE90-759877] N90-21561
Adaptive learning fuzzy control of a mobile robot
[DE90-759898] N90-21562
ROBUSTNESS (MATHEMATICS)
Application of stochastic robustness to aircraft control systems N90-20936
Stochastic robustness of linear control systems N90-20941
ROCK MECHANICS
A casting and imaging technique for determining void geometry and relative permeability behavior of a single fracture specimen
[DE90-009192] N90-21403
ROCKET ENGINES
Stress analysis of rocket motors with viscoelastic propellant by a mixed finite element model N90-21112
ROCKET PROPELLANTS
Research programs in aeronautical engineering, solid state physics, and materials science at Technion-Israel Institute of Technology, Haifa, Israel
[EOARD-LR-89-068] N90-21720
ROCKS
Characterization of linear structures from remote sensing data; Espinhaco Meridional (MG) sierra
[INPE-4905-PRE/1506] N90-21449
ROLLERS
Heat engine based on shape memory alloys
[AD-D014400] N90-21385
ROTARY WING AIRCRAFT
Stereopsis cueing effects on hover-in-turbulence performance in a simulated rotorcraft
[NASA-TP-2980] N90-21004
Transmission research activities at NASA Lewis Research Center
[NASA-TM-103132] N90-21394
ROTARY WINGS
Performance data from a wind-tunnel test of two main-rotor blade designs for a utility-class helicopter
[NASA-TM-4183] N90-20974
ROSAR (Helicopter-Rotor based Synthetic Aperture Radar) N90-21229
ROTATING FLUIDS
Theoretical study of the flow in a rotating channel. Experimental study through flow visualization in a curved channel N90-21032
ROTATING PLASMAS
Study on rotating plasma with submillimeter laser interferometer
[DE90-615387] N90-21623
ROTATING SHAFTS
A fiber optic sensor for noncontact measurement of shaft speed, torque, and power
[NASA-TM-102481] N90-21360
ROTATION
Apparatus for mixing solutions in low gravity environments
[NASA-CASE-MFS-26047-1] N90-21209
Heat engine based on shape memory alloys
[AD-D014400] N90-21385
Direct formulation of a 4-node hybrid shell element with rotational degrees of freedom
[NASA-CR-4282] N90-21411
ROTOR AERODYNAMICS
Measurement and prediction of propeller blade surface pressure distributions N90-20961
ROTOR BLADES
Analysis of the rotor tip leakage flow with tip cooling air ejection N90-21029
ROTOR BLADES (TURBOMACHINERY)
An inverse method for the design of turbomachine blades N90-20988
Experimental and numerical study on basic phenomena of secondary flows in turbines N90-21014
Measurement of the flow field in the blade passage and side-wall region of a plane turbine cascade N90-21019
Effects of secondary flow on heat transfer in rotating passages N90-21031
ROTOR DYNAMICS
Design of a helicopter automatic flight control system using adaptive control N90-21040
Internal rotor friction instability
[NASA-CR-183942] N90-21395
ROTORS
Statistics on aircraft gas turbine engine rotor failures that occurred in US commercial aviation during 1986
[DOT/FAA/CT-89/30] N90-21008
Internal rotor friction instability
[NASA-CR-183942] N90-21395
RUNWAY LIGHTS
Modified touchdown zone lighting
[DOT/FAA/CT-TN89/70] N90-21042
RUNWAYS
Modified touchdown zone lighting
[DOT/FAA/CT-TN89/70] N90-21042
RUTILE
Deformation and microstructure of rutile
[DE90-614113] N90-21654

S

SAFETY
Final safety analysis report for the Ulysses Mission. Volume 2: Accident model document-appendices
[DE90-008695] N90-21104
Final safety analysis report for the Ulysses Mission
[DE90-008690] N90-21106
Final safety analysis report for the Ulysses mission. Volume 1: Reference design document
[DE90-008693] N90-21107
SAFETY MANAGEMENT
Brake performance of the McDonnell Douglas DC-10-30/40 during high speed, high energy rejected takeoffs
[PB90-917004] N90-21000
Minutes of the 23rd Explosives Safety Seminar, volume 2
[AD-A218265] N90-21214
SALINITY
Analysis of water quality parameters of the Piaui River (SE), Brazil, through field and TM/LANDSAT sensor data
[INPE-4918-PRE/1417] N90-21453
MECCA program documentation
[NOAA-TR-NESDIS-46] N90-21477
SAMPLING
On the continuous dependence with respect to sampling of the linear quadratic regulator problem for distributed parameter systems
[NASA-CR-182012] N90-21566
SANDWICH STRUCTURES
Stress analysis and minimum weight design of honeycomb sandwich plates N90-21418
Wave receptance analysis of vibrating beams and stiffened plates N90-21419
SATELLITE COMMUNICATION
NASA's Advanced Communications Technology Satellite (ACTS): Will it benefit commercial/military satellites
[AD-A217710] N90-21100
Small business innovation research. Abstracts of 1988 phase 1 awards
[NASA-TM-102991] N90-21680
Small business innovation research. Abstracts of completed 1987 phase 1 projects
[NASA-TM-101797] N90-21681
SATELLITE IMAGERY
Shade images of forested areas obtained from LANDSAT MSS data
[NASA-TM-102939] N90-21436
Results of the Gondwana Project: An example of intercontinental geologic correlation utilizing LANDSAT imagery
[INPE-4870-PRE/1481] N90-21437
Wheat yield estimation at the farm level using LANDSAT TM and agrometeorological data
[INPE-5017-RPE/611] N90-21439
Monitoring of agrocattle-raising projects through visual/digital analysis of LANDSAT-TM imagery south of Para state
[INPE-4982-PRE/1542] N90-21442
A knowledge-based information based for crop area estimation
[INPE-4990-PRE/1555] N90-21444
Analysis of water quality parameters of the Piaui River (SE), Brazil, through field and TM/LANDSAT sensor data
[INPE-4918-PRE/1417] N90-21453
Evaluation of the mangrove areas of the Rio Piaui (SE) through remote sensing
[INPE-4909-PRE/1510] N90-21454
Introduction of digital image processing by remote sensors applied to geology
[INPE-5023-RPE/616] N90-21456
Multitemporal analysis of LANDSAT/TM digital imagery in the detection of areas affected by caterpillar (sibine fusca) attack in the dende (elais guineensis) palm plantation
[INPE-4979-PRE/1544] N90-21457
Evaluation of classification performance and proportion estimate of the sugar cane crop through PROCEDURE-INPE utilizing LANDSAT data
[INPE-4899-PRE/1500] N90-21458
Subsystem TM Precision: Progress and perspective
[INPE-5006-PRE/1563] N90-21461
Possible use of satellite data for flood plain mapping
[INPE-4968-PRE/1537] N90-21462
Performance evaluation of morphological edge detectors
[INPE-4975-PRE/1540] N90-21464
SATELLITE OBSERVATION
Goes I-M and beyond: Science requirements and technology challenges N90-21067
Investigations into the properties, conditions, and effects of the ionosphere
[AD-A217807] N90-21489
SATELLITE-BORNE RADAR
Programmable generation of linear frequency modulated pulses N90-21232
SCALARS
The dynamics of scalar fields in the early universe N90-21696
SCATTERING
Fiber optic void fraction sensor
[DE90-009124] N90-21366
Relativistic stimulated Brillouin and Raman scattering in a laser-produced plasma
[DE90-613123] N90-21627
SCATTERING CROSS SECTIONS
Thomson scattering in a magnetic field N90-21699
SCATTERING FUNCTIONS
Generalized random phase approximation for multicomponent polymer systems
[DE90-613691] N90-21194
SCHEDULING
Investigation of air transportation technology at the Massachusetts Institute of Technology, 1988-1989 N90-20922
Time and truth in plans N90-20930
SCHOTTKY DIODES
Infrared ground-based astronomy with the Hughes 256 X 256 PtSi array N90-21331
SCHROEDINGER EQUATION
Local supersymmetry in non-relativistic systems
[DE90-612751] N90-21670
SCINTILLATION COUNTERS
Development of intrinsic IPT scintillator
[DE90-007906] N90-21367
SEA WATER
Remote sensing applied to sea water quality researches in coastal regions: A review
[INPE-4935-PRE/1425] N90-21438
SEALERS
The corrosion protection of 6061-T6 aluminum by a polyurethane-sealed anodized coat
[NASA-TM-100394] N90-21191
SEALS (STOPPERS)
The development of ultraviolet-ozone cleaning as a production process in the packaging of integrated circuits
[DE90-007960] N90-21220
SECONDARY FLOW
Secondary Flows in Turbomachines
[AGARD-CP-469] N90-21009
Secondary flows and radial mixing predictions in axial compressors N90-21010
The effects of compressor endwall flow on airfoil incidence and deviation N90-21011
A study on secondary flow and spanwise mixing in axial flow compressors N90-21012
Experimental and numerical study on basic phenomena of secondary flows in turbines N90-21014
Secondary flows and Reynolds stress distributions downstream of a turbine cascade at different expansion ratios N90-21015
An investigation of secondary flows in nozzle guide vanes N90-21016
Secondary flow predictions for a transonic nozzle guide vane N90-21017
Secondary flow in a turbine guide vane with low aspect ratio N90-21018
Measurement of the flow field in the blade passage and side-wall region of a plane turbine cascade N90-21019
Calculation of the three dimensional turbulent flow in a linear turbine blade N90-21021
Calculation of the secondary flow in an axial turbine N90-21022
Generation and decay of secondary flows and their impact on aerodynamic performance of modern turbomachinery components N90-21023
Secondary flow calculations for axial and radial compressors N90-21024
Research on cascade secondary and tip-leakage flows: Periodicity and surface flow visualization N90-21026
Losses in the tip-leakage flow of a planar cascade of turbine blades N90-21027
Computational prediction and measurement of the flow in axial turbine cascades and stages N90-21028
Detailed heat transfer measurements in nozzle guide vane passages in linear and annular cascades in the presence of secondary flows N90-21030
Effects of secondary flow on heat transfer in rotating passages N90-21031

Theoretical study of the flow in a rotating channel. Experimental study through flow visualization in a curved channel N90-21032
The effect of secondary flow on the redistribution of the total temperature field downstream of a stationary turbine cascade N90-21033

SEDIMENTS
Gaithersburg Nike control and launch area preliminary assessment/site inspection, Gaithersburg, Maryland [AD-A217791] N90-21482

SEGMENTS
ASCIE: An integrated experiment to study CSI in large segmented optical systems N90-21082

SEISMIC WAVES
A numerical and theoretical study of seismic wave diffraction in complex geologic structure [AD-A218209] N90-21490

SEISMOLOGY
A numerical and theoretical study of seismic wave diffraction in complex geologic structure [AD-A218209] N90-21490

SELF CONSISTENT FIELDS
A self-consistent theory of radial transport of field-aligned current by microturbulence [DE90-007920] N90-21631

SEMICONDUCTOR DEVICES
Germanium Blocked Impurity Band (BIB) detectors N90-21321
New surface atomic structures for column 5 overlayers on the (110) surfaces of 3-5 compound semiconductors [DE90-009003] N90-21663

SEMICONDUCTORS (MATERIALS)
Coupled magnetoplasmon-phonon modes at the surface of a semi-infinite semiconductor superlattice [DE90-612904] N90-21647
High voltage/high resolution studies of metal and semiconductor interfaces [DE90-009065] N90-21656
New surface atomic structures for column 5 overlayers on the (110) surfaces of 3-5 compound semiconductors [DE90-009003] N90-21663

SENSITIVITY
Preparation, characterisation and cookoff behaviour of booster compositions prepared from RDX and acrylic or ethylene-vinyl acetate dispersions [MRL-TR-89-44] N90-21203

SEPARATED FLOW
Measurement of the flow field in the blade passage and side-wall region of a plane turbine cascade N90-21019
Navier-Stokes analysis of turbine blade heat transfer [NASA-TM-102496] N90-21300

SERIES EXPANSION
A modified Moebius inverse formula and its applications in physics [DE90-612740] N90-21594

SERVICE LIFE
Flow in a forward swept centrifugal fan, volumes 1 and 2 N90-20959
Fracture and longevity of composite structures [AD-A217827] N90-21127
Aging and compatibility of TNF-doped Mylar [DE90-008508] N90-21186
Collapsible fabric tank testing [AD-A217861] N90-21388

SHAFTS (MACHINE ELEMENTS)
Parametric resonance in horizontal axis wind turbines N90-20962

SHAPE MEMORY ALLOYS
Heat engine based on shape memory alloys [AD-D014400] N90-21385

SHAPED CHARGES
Minutes of the 23rd Explosives Safety Seminar, volume 1 [AD-A218264] N90-21213
SR90, strontium shaped-charge critical ionization velocity experiment [NASA-CR-186501] N90-21606

SHAPES
A tool for automatic design of airfoils in different operating conditions N90-20994
Optimization of aerodynamic designs using computational fluid dynamics N90-20999
Supersonic nozzle design of arbitrary cross-section N90-21035

SHARP LEADING EDGES
Experimental and numerical investigation of the vortex flow over a sharp edged delta wing; with and without sideslip [PB90-167131] N90-20964

SHEAR FLOW
The effect of viscosity on the resistive tearing mode with the presence of shear flow [DE90-009340] N90-21312
The extension of rapid distortion theory to stratified shear flows N90-21491
Instabilities and vortex dynamics in shear flow of magnetized plasmas [DE90-009448] N90-21643

SHEAR LAYERS
The effects of forcing on a single stream shear layer and its parent boundary layer [NASA-CR-186529] N90-21301

SHEAR STRENGTH
Fiber pushout test: A three-dimensional finite element computational simulation [NASA-TM-102565] N90-21131

SHELLS (STRUCTURAL FORMS)
Fourier series methods for plates and shells with cracks and inclusions N90-21406
Direct formulation of a 4-node hybrid shell element with rotational degrees of freedom [NASA-CR-4282] N90-21411
Determination of stresses around cutouts in multilayered composite plate and shell structures N90-21417
Elasto-plastic large deformation analysis of thin-walled structures [PB90-164757] N90-21426

SHOCK ABSORBERS
The Shock and Vibration Digest, volume 22, no. 2 N90-21596

SHOCK LAYERS
An approximate viscous shock layer method for calculating the hypersonic flow over blunt-nosed bodies N90-20947

SHOCK LOADS
Shock compression of solids: A tutorial [DE90-009185] N90-21659

SHOCK RESISTANCE
Shock initiation sensitivity of damaged TP-H1207C composite propellant [DE90-008509] N90-21205

SHOCK WAVE INTERACTION
A time-accurate adaptive grid method and the numerical simulation of a shock-vortex interaction [NASA-TP-2998] N90-21524

SHOCK WAVE PROPAGATION
Nonlinear interaction of photons and phonons in electron-positron plasmas [DE90-009341] N90-21640

SHOCK WAVES
Shock compression of solids: A tutorial [DE90-009185] N90-21659

SIDE-LOOKING RADAR
The PHARUS project: Design of a polarimetric C-band SAR in the Netherlands N90-21228

SIDESLIP
Experimental and numerical investigation of the vortex flow over a sharp edged delta wing; with and without sideslip [PB90-167131] N90-20964

SIGNAL ANALYZERS
Ridge regression processing N90-20931

SIGNAL DETECTION
Fiber optic void fraction sensor [DE90-009124] N90-21366

SIGNAL DETECTORS
A real-time rejection circuit to automatically reject multiple interfering hopping signals while passing a lower level desired signal [AD-D014424] N90-21251
Passive stabilization of a fiber optic nonlinear interferometric sensor [AD-D014438] N90-21620

SIGNAL PROCESSING
Ridge regression processing N90-20931
Magneto acoustic emission apparatus for testing materials for embrittlement [NASA-CASE-LAR-13817-1] N90-21170
Intensity to frequency conversion technique in intensity modulated fiber optic sensing systems [NASA-TM-102562] N90-21277
Cepstrum analysis and applications to computational fluid dynamic solutions N90-21302
Strategies for concurrent processing of complex algorithms in data driven architectures [NASA-CR-186515] N90-21535

SIGNAL REFLECTION
Cepstrum analysis and applications to computational fluid dynamic solutions N90-21302

SIGNAL STABILIZATION
Passive stabilization of a fiber optic nonlinear interferometric sensor [AD-D014438] N90-21620

SIGNAL TRANSMISSION
HDTV bandwidth reduction using motion compensation and DATV [BBC-RD-1989/10] N90-21254

SIGNATURE ANALYSIS
Sonic boom signature data from cruciform microphone array experiments during the 1966-1967 EAFB national sonic boom evaluation program [NASA-CR-182027] N90-21605

SILICON
Proceedings of the Joint NOSC/NRL (Naval Ocean Systems Center/Naval Research Laboratory) InP Microwave/Millimeter Wave Technology Workshop [AD-A218216] N90-21259
Initial astronomical results with a new 5-14 micron Si:Ga 58x62 DRO array camera N90-21334
Improved Si:As BIBIB (Back-Illuminated Blocked-Impurity-Band) hybrid arrays N90-21349
Improvement of small-area, amorphous-silicon thin-film photovoltaics on polymer substrate [DE90-000314] N90-21472
Research on amorphous silicon-based thin film photovoltaic devices. Task B: Research on stable high efficiency large area, amorphous silicon-based submodules [DE90-000320] N90-21473

SILICON CARBIDES
Acoustic characterisation of an aluminium silicon carbide metal matrix composite [AERE-R-13273] N90-21121
Ductile alloy encapsulated ceramic armor development [AD-A217632] N90-21183

SILICON DIOXIDE
On the stability of amorphous silica coatings for high temperature service [AERE-R-13425] N90-21179
Methods for improving the flowability of a percussion primer composition [MRL-TR-89-32] N90-21201

SILICON ISOTOPES
Strangeness enhancement in 14.6 A GeV/c Si+Au interactions? [DE90-008826] N90-21616

SILICON NITRIDES
Research advances in fine ceramics [DE90-008983] N90-21197

SILICON POLYMERS
Boron-containing organosilane polymers and ceramic materials thereof [NASA-CASE-ARC-11649-2-SB] N90-21177

SILVER
Determination of internal strains in high-temperature superconductor composites by intense pulsed neutron source [DE90-007799] N90-21664

SIMULATION
Aperture taper determination for the half-scale accurate antenna reflector [NASA-CR-185215] N90-21282
Numerical simulations of the cloud-capped marine boundary layer N90-21506
Finite element algorithms for hyperbolic conservation laws with forcing terms [INPE-5024-RPE/617] N90-21595

SIMULATORS
Simulator comparison of thumball, thumb switch, and touch screen input concepts for interaction with a large screen cockpit display format [NASA-TM-102587] N90-21005
CSI technology validation on an LSS ground experiment facility N90-21089
Lessons learned in the transition to Ada from FORTRAN at NASA/Goddard [NASA-TM-103311] N90-21538

SINGLE CRYSTALS
Diamond: A high power optical material [DE90-008941] N90-21196

SINGLE STAGE TO ORBIT VEHICLES
HOTOL structures and materials at British Aerospace, Warton, UK [EOARD-LR-90-001] N90-21001

SINTERING
Development of planar geometry solid oxide fuel cell technology, phase 2 [PB90-131293] N90-21467
Alternative materials for solid oxide fuel cells [DE90-008615] N90-21468

SLENDER BODIES
Flutter of slender bodies under axial stress [PB90-167024] N90-21425

SLEWING
NASA CSI suspension methods overview N90-21080

SLITS
Airborne sound insulation of slits, joints, and sealing stripes [PB90-128976] N90-21599

SOBOLEV SPACE
On the equation: Delta u+c=Ke(sup u) [DE90-612741] N90-21575

SODIUM
An evaluation of metal salts of 3-nitro-1,2,4-triazol-5-one (NTO) as potential primary explosives
[MRL-TN-563] N90-21202
SODIUM CHLORIDES
Direct sublimation of NaCl salt from carbon matrixes
[DE90-007927] N90-21139
Ionic equilibrium between octahedral and tetrahedral complexes in liquid aluminium-sodium fluoride mixtures
[DE90-613690] N90-21150
SODIUM FLUORIDES
Ionic equilibrium between octahedral and tetrahedral complexes in liquid aluminium-sodium fluoride mixtures
[DE90-613690] N90-21150
SOFTWARE ENGINEERING
Human centrifuge controller
[NAL-TM-SE-8901] N90-21043
Numerical Arc Segmentation Algorithm for a Radio Conference (NASARC), version 4.0: User's manual
[NASA-TM-101454] N90-21250
Human factors in fighter software development
[PD-CF-9003] N90-21522
Maintenance = reuse-oriented software development
[NASA-CR-186455] N90-21531
Integrating automated support for a software management cycle into the TAME system
[NASA-CR-186457] N90-21532
Lessons learned in the transition to Ada from FORTRAN at NASA/Goddard
[NASA-TM-103311] N90-21538
Toward a new CIM (Computer Integrated Manufacturing) architecture for Sandia Laboratories
[DE90-008677] N90-21548
SOFTWARE TOOLS
Fast causal multicast
[NASA-CR-186495] N90-21533
Annotated bibliography of software engineering laboratory literature
[NASA-TM-103313] N90-21536
Exploiting virtual synchrony in distributed systems
[NASA-CR-182855] N90-21555
The ultimate CASE tool
[DE90-009351] N90-21687
SOIL MECHANICS
Proceedings of the 4th European Conference, volume 2
[AD-A216521] N90-21382
SOIL SCIENCE
Wheat productivity estimate through field radiometry
[INPE-4994-PRE/1556] N90-21460
SOILS
Monitoring of agrocattle-raising projects through visual/digital analysis of LANDSAT-TM imagery south of Para state
[INPE-4982-PRE/1542] N90-21442
Effects of Air Pollution on Western Forests
[PB90-131111] N90-21481
Gaithersburg Nike control and launch area preliminary assessment/site inspection, Gaithersburg, Maryland
[AD-A217791] N90-21482
Radon concentration over the Brazilian Amazon Basin during the wet season (Belem-Manaus GTE-ABLE-2B flight of April 24, 1987)
[INPE-4892-PRE/1493] N90-21486
SOLAR ARRAYS
Controls, Astrophysics, and Structures Experiment in Space (CASES) N90-21085
Recent results from advanced research on space solar cells at NASA
[NASA-TM-102485] N90-21274
Infrared ground-based astronomy with the Hughes 256 X 256 PtSi array N90-21331
SOLAR CELLS
Recent results from advanced research on space solar cells at NASA
[NASA-TM-102485] N90-21274
Peeled film GaAs solar cells for space power
[NASA-TM-103125] N90-21287
Characterization and comparison of optically transparent conducting films
[DE90-000319] N90-21660
SOLAR COLLECTORS
The effect of leveling coatings on the atomic oxygen durability of solar concentrator surfaces
[NASA-TM-102557] N90-21110
Recent results from advanced research on space solar cells at NASA
[NASA-TM-102485] N90-21274
SOLAR COOLING
Failure and degradation modes in selected solar materials: A review
[DE90-009075] N90-21476
SOLAR COSMIC RAYS
Simplified model for solar cosmic ray exposure in manned Earth orbital flights
[NASA-TM-4182] N90-21715
SOLAR ENERGY
Design and demonstration of an improved stretched-membrane heliostat
[DE90-007904] N90-21470
SOLAR ENERGY CONVERSION
Failure and degradation modes in selected solar materials: A review
[DE90-009075] N90-21476
SOLAR FLARES
Solar flares and dynamics of Langmuir waves in current-carrying plasmas
[IPPCZ-291] N90-21710
Substorms: Their expansion and recovery phases
[DE90-008970] N90-21712
High energy phenomena during solar flares
[INPE-4961-TDL/390] N90-21713
SOLAR HEATING
Failure and degradation modes in selected solar materials: A review
[DE90-009075] N90-21476
SOLAR INSTRUMENTS
A general-purpose balloon-borne pointing system for solar scientific instruments
[NASA-TP-3013] N90-21219
SOLAR SYSTEM
Cosmic Dust Collection Facility: Scientific objectives and programmatic relations
[NASA-TM-102160] N90-21098
Research and Technology
[NASA-TM-102161] N90-21721
SOLDERED JOINTS
Compatibility of Au base thick films with solder alloys: Solid state growth of intermetallics
[DE90-009285] N90-21175
SOLDERS
Compatibility of Au base thick films with solder alloys: Solid state growth of intermetallics
[DE90-009285] N90-21175
SOLID ELECTROLYTES
Alternative materials for solid oxide fuel cells
[DE90-008615] N90-21468
SOLID MECHANICS
Compact scheme for systems of equations applied to fundamental problems of mechanics of continua
[NASA-CR-186494] N90-21292
SOLID PROPELLANT ROCKET ENGINES
Transportation monitoring unit qualification
[NASA-CR-183930] N90-21060
Technical Evaluation Motor no. 5 (TEM-5)
[NASA-CR-183932] N90-21117
SOLID PROPELLANTS
The modelling of heat and mass transfer near solid boundaries and comparison with experimental results
[PB90-167040] N90-21310
SOLID STATE
The solid state photomultiplier: Status of photon counting beyond the near-infrared N90-21319
SOLID STATE LASERS
Contract crystal growth and fabrication services
[AD-A218327] N90-21648
Progress in the material development of LiCaAlF(6):Cr(3+) laser crystals
[DE90-009542] N90-21666
SOLIDIFICATION
Shock compression of solids: A tutorial
[DE90-009185] N90-21659
SOLIDS
High-resolution Brillouin gain spectroscopy in solids
[DE90-009475] N90-21155
Laser velocimeter measurements of multiphase flow of solids
[DE90-007604] N90-21311
Shock compression of solids: A tutorial
[DE90-009185] N90-21659
SOLITARY WAVES
Ultrarelativistic envelope solitons in electron-positron plasma of the pulsar magnetosphere
[DE90-613289] N90-21264
Nonlinear interaction of photons and phonons in electron-positron plasmas
[DE90-009341] N90-21640
SOLUBILITY
Phase equilibrium of mixtures consisting of molecules with large size and shape differences (thermodynamic modeling of Supercritical Fluid Extraction and Retrograde Condensation, SFE/RC)
[PB90-131285] N90-21146
SOLUTIONS
Generalized random phase approximation for multicomponent polymer systems
[DE90-613691] N90-21194
SOLVENTS
Phase equilibrium of mixtures consisting of molecules with large size and shape differences (thermodynamic modeling of Supercritical Fluid Extraction and Retrograde Condensation, SFE/RC)
[PB90-131285] N90-21146
Generalized random phase approximation for multicomponent polymer systems
[DE90-613691] N90-21194
SONIC BOOMS
Sonic boom signature data from cruciform microphone array experiments during the 1966-1967 EAFB national sonic boom evaluation program
[NASA-CR-182027] N90-21605
SOUND FIELDS
Microgravity acoustic mixing for particle cloud combustors
[NASA-CR-185159] N90-21600
The optical measurement of acoustic velocity fields N90-21601
The radiation of sound from a propeller at angle of attack
[NASA-CR-4264] N90-21602
SOUND PRESSURE
The radiation of sound from a propeller at angle of attack
[NASA-CR-4264] N90-21602
Free-field propagation of high intensity noise
[NASA-CR-186577] N90-21604
SOUND WAVES
Rapidly quantifying the relative distention of a human bladder
[NASA-CASE-LAR-13901-1-NP] N90-21519
Free-field propagation of high intensity noise
[NASA-CR-186577] N90-21604
SOUTHERN HEMISPHERE
New water vapor masers in the Southern Hemisphere
[INPE-4844-PRE/1473] N90-21689
SPACE ADAPTATION SYNDROME
Space adaptation syndrome induced by a long duration +3Gx centrifuge run
[AD-A218248] N90-21518
SPACE BASED RADAR
High Resolution Air- and Spaceborne Radar
[AGARD-CP-459] N90-21223
Concepts for high resolution space based SAR/ISAR systems: Preliminary design considerations N90-21224
Trade-offs in a space based surveillance radar N90-21225
Concept for a spaceborne Synthetic Aperture Radar (SAR) sensor based on active phased array technology N90-21234
SPACE CHARGE
Near contact phenomena and transient effects in far infrared photoconductors N90-21316
SPACE COLONIES
The partnership: Space shuttle, space science, and space station
[NASA-TM-102900] N90-21050
SPACE COMMUNICATION
On board cross support scenarios
[INPE-5005-PRE/1562] N90-21268
Environmental projects, volume 11. Environmental assessment: Addition to operations building, Mars site
[NASA-CR-186449] N90-21479
Environmental projects, volume 10. Environmental assessment: New 34-meter antenna at Apollo site
[NASA-CR-186448] N90-21480
SPACE ENVIRONMENT SIMULATION
Space environment simulation of the SCD-01 satellite through heating plates
[INPE-4988-PRE/1550] N90-21105
SPACE ERECTABLE STRUCTURES
Preliminary design approach for large high precision segmented reflectors
[NASA-TM-102605] N90-21096
Heavily loaded joints for assembling aerobrake support trusses
[NASA-CR-181992] N90-21099
SPACE INFRARED TELESCOPE FACILITY
BASG thermomechanical pump helium 2 transfer tests
[NASA-CR-177541] N90-21097
Proceedings of the Third Infrared Detector Technology Workshop
[NASA-TM-102209] N90-21313
A 100 micro Kelvin bolometer system for SIRTF N90-21317
Ga:Ge array development N90-21323
Study of advanced InSb arrays for SIRTF (Space Infrared Telescope Facility) N90-21325
InSb DRO array characteristics N90-21326
SIRTF in high earth orbit N90-21345
Laboratory characterization of direct readout Si:Sb and Si:Ga infrared detector arrays N90-21347

SPACE LOGISTICS
The partnership: Space shuttle, space science, and space station
[NASA-TM-102900] N90-21050
SPACE OBSERVATIONS (FROM EARTH)
VLA observations of the coronal plasma
[NASA-CR-186540] N90-21711
SPACE PLASMAS
VLA observations of the coronal plasma
[NASA-CR-186540] N90-21711
SPACE PLATFORMS
Modeling and control of flexible space platforms with articulated payloads N90-21073
SPACE PROCESSING
Small business innovation research. Abstracts of 1988 phase 1 awards
[NASA-TM-102991] N90-21680
Small business innovation research. Abstracts of completed 1987 phase 1 projects
[NASA-TM-101797] N90-21681
SPACE RENDEZVOUS
A homotopy approach to the solutions of minimum-fuel space-flight rendezvous problems N90-21053
SPACE SHUTTLE BOOSTERS
Compendium of fracture mechanics problems
[NASA-TM-100393] N90-21414
SPACE SHUTTLE MAIN ENGINE
Compendium of fracture mechanics problems
[NASA-TM-100393] N90-21414
SPACE SHUTTLE PAYLOADS
The partnership: Space shuttle, space science, and space station
[NASA-TM-102900] N90-21050
United States Air Force Academy get-away-special flexible beam experiment N90-21088
UV spectrometer system AFGL 801 A HUP
[AD-A217805] N90-21619
SPACE SHUTTLES
The partnership: Space shuttle, space science, and space station
[NASA-TM-102900] N90-21050
Optimal trajectories for the aeroassisted flight experiment. Part 3: Formulation, results, and analysis
[NASA-CR-186165] N90-21051
SPACE STATION PAYLOADS
Vibration isolation versus vibration compensation on multiple payload platforms N90-21066
SPACE STATIONS
The partnership: Space shuttle, space science, and space station
[NASA-TM-102900] N90-21050
Detection of potential space station control/structure interaction with CO-ST-IN N90-21074
Cosmic Dust Collection Facility: Scientific objectives and programmatic relations
[NASA-TM-102160] N90-21096
Thermal control system corrosion study
[NASA-TM-102220] N90-21294
SPACE TRANSPORTATION
Research and Technology
[NASA-TM-102161] N90-21721
SPACE WEAPONS
Zenith Star: A structural control challenge N90-21064
SPACE-TIME FUNCTIONS
Characteristics consequences of space-time coordinate relativization
[DE90-615201] N90-21668
Conserved conformal currents in curved space-time
[DE90-612766] N90-21672
String dynamics in curved space-time revisited
[DE90-612796] N90-21674
SPACEBORNE ASTRONOMY
Proceedings of the Third Infrared Detector Technology Workshop
[NASA-TM-102209] N90-21313
Stressed Ge:Ga photoconductors for space-based astronomy. (Is there life beyond 120 micron) N90-21315
SPACEBORNE EXPERIMENTS
A spaceborne optical interferometer: The JPL CSI mission focus N90-21063
Tests of the Rockwell Si:As Back-Illuminated Blocked-Impurity Band (BIBIB) detectors N90-21350
SPACEBORNE LASERS
Zenith Star: A structural control challenge N90-21064
SPACEBORNE TELESCOPES
Requirements of IR space astronomy N90-21314
SPACECRAFT CONFIGURATIONS
Global nonlinear optimization of spacecraft protective structures design
[NASA-TM-100387] N90-21095
SPACECRAFT CONSTRUCTION MATERIALS
HOTOL structures and materials at British Aerospace, Warton, UK
[EOARD-LR-90-001] N90-21001
Ultrasonic and radiographic evaluation of advanced aerospace materials: Ceramic composites
[NASA-TM-102540] N90-21401
SPACECRAFT DESIGN
The partnership: Space shuttle, space science, and space station
[NASA-TM-102900] N90-21050
Zenith Star: A structural control challenge N90-21064
SPACECRAFT ENVIRONMENTS
Stressed Ge:Ga photoconductors for space-based astronomy. (Is there life beyond 120 micron) N90-21315
SPACECRAFT EQUIPMENT
Acoustic convective system
[NASA-CASE-NPO-17278-1-CU] N90-21215
SPACECRAFT LAUNCHING
LACE flight dynamics experiment N90-21086
Advanced Launch System (ALS): Electrical actuation and power systems improve operability and cost picture
[NASA-TM-102547] N90-21271
SPACECRAFT MANEUVERS
Suboptimal and hybrid numerical solution schemes for orbit transfer manoeuvres
[INPE-4991-PRE/1556] N90-21054
Attitude control modes for the MECB remote sensing satellites
[INPE-4755-PRE/1427] N90-21094
SPACECRAFT POWER SUPPLIES
A comparative study of electric power distribution systems for spacecraft
[NASA-CR-186531] N90-21113
Recent Stirling engine loss-understanding results
[NASA-TM-103122] N90-21114
Recent results from advanced research on space solar cells at NASA
[NASA-TM-102485] N90-21274
Peeled film GaAs solar cells for space power
[NASA-TM-103125] N90-21287
Space power generation and distribution
[DE90-008676] N90-21474
Small business innovation research. Abstracts of completed 1987 phase 1 projects
[NASA-TM-101797] N90-21681
SPACECRAFT PROPULSION
A radiological assessment of nuclear power and propulsion operations near Space Station Freedom
[NASA-CR-185185] N90-21108
Small business innovation research. Abstracts of 1988 phase 1 awards
[NASA-TM-102991] N90-21680
Small business innovation research. Abstracts of completed 1987 phase 1 projects
[NASA-TM-101797] N90-21681
SPACECRAFT STRUCTURES
PACOSS program status and results N90-21065
Global nonlinear optimization of spacecraft protective structures design
[NASA-TM-100387] N90-21095
SPACECREWS
A radiological assessment of nuclear power and propulsion operations near Space Station Freedom
[NASA-CR-185185] N90-21108
SPACING
Production of diffraction gratings using holographic interferometry
[DE90-612641] N90-21362
SPATIAL RESOLUTION
Capabilities of bistatic synthetic aperture radar for covert battlefield surveillance N90-21230
Concept for a spaceborne Synthetic Aperture Radar (SAR) sensor based on active phased array technology N90-21234
A solution for real time motion compensation for SAR without using inertial navigation systems N90-21236
A fast ISAR-imaging process and its inherent degrading effects on image quality N90-21239
Radar target image by ISAR case study N90-21242
Absolute multilayer characterization at high spatial resolution via real-time soft x ray imaging
[DE90-009181] N90-21371
Some recent applications of laser ultrasound to the characterisation of materials
[AERE-R-13438] N90-21374
SPECIFIC HEAT
Specific heat and critical fluctuations in anisotropic high-T(sub c) oxide superconductors
[DE90-613394] N90-21651
The Chemkin Thermodynamic Data Base
[DE90-007953] N90-21676
The thermo-mechanical behavior of cometary nuclei N90-21703
SPECKLE INTERFEROMETRY
Preliminary results on two-dimensional interferometry of HL Tau N90-21335
SPECTRA
Modified tight-binding approximation and electron-phonon spectral function for transition metals
[DE90-614022] N90-21166
SPECTRAL RESOLUTION
A solution for real time motion compensation for SAR without using inertial navigation systems N90-21236
SPECTROGRAPHS
SIRTF in high earth orbit N90-21345
SPECTROMETERS
AFGL ten micron mosaic array spectrometer: Recent results N90-21333
Design and status of the detector block for the ISO-SWS N90-21341
Status of the isophot detector development N90-21342
ISO/LWS: Detector status N90-21343
SPECTROPHOTOMETRY
Study of new technique of solid combustible materials to determination of volatile elements by flame atomic absorption spectrophotometry
[DE90-612907] N90-21147
SPECTROSCOPY
High-resolution Brillouin gain spectroscopy in solids
[DE90-009475] N90-21155
Introduction to the Infrared Space Observatory (ISO) N90-21340
SPECTRUM ANALYSIS
Wheat productivity estimate through field radiometry
[INPE-4994-PRE/1556] N90-21460
SPECULAR REFLECTION
The effect of leveling coatings on the atomic oxygen durability of solar concentrator surfaces
[NASA-TM-102557] N90-21110
The measurement of surface reflectivity at millimetre wavelengths
[MRL-TN-559] N90-21222
SPEECH RECOGNITION
Investigation of air transportation technology at the Massachusetts Institute of Technology, 1988-1989 N90-20922
Automatic speech recognition in air traffic control N90-20923
SPHERES
A remark on the Kelvin transform and a non-linear partial differential equation
[PB90-165622] N90-21589
SPIRAL GALAXIES
The molecular cloud content of early type galaxies. 2: A molecular ring in NGC 404
[PB90-124348] N90-21695
SPLINES
Internal rotor friction instability
[NASA-CR-183942] N90-21395
STABILITY
Elastic-plastic instability of plane frames N90-21415
On the stability of a certain difference scheme
[PB90-165614] N90-21588
STABILITY TESTS
Computation of nonequilibrium chemically reacting flows in hypersonic flow field N90-20954
STABILIZATION
CSI sensing and control: Analytical and experimental results N90-21083
The extension of rapid distortion theory to stratified shear flows N90-21491
STABILIZERS (FLUID DYNAMICS)
The MANTA: An RPV design to investigate forces and moments on a lifting surface
[NASA-CR-186227] N90-20971
STAINLESS STEELS
A STEM study of changing grain boundary chemistry during the sensitisation of AISI 304 stainless steel
[AERE-R-13418] N90-21157
Current fluctuations associated with localised corrosion: Mechanistic studies of the early stages of pitting and stress corrosion cracking of stainless steel
[AERE-R-13531] N90-21159
Mathematical modelling of intergranular attack in stainless steels: A preliminary study
[AERE-M-3698] N90-21160
Materials for ultra-high vacuum
[DE90-007908] N90-21217
On-line assessment of weld quality using ultrasonics
[AERE-R-13401] N90-21396
STAR FORMATION
Small scale structures and density of star-forming regions N90-21706
STARS
Preliminary results on two-dimensional interferometry of HL Tau N90-21335

STATE ESTIMATION
Flight path reconstruction using extended Kalman filtering techniques
[PD-FC-9001] N90-20970
Experimental and theoretical investigation of optimal control methods with model reduction N90-21039
STATIC LOADS
Fracture toughness and crack growth of Zerodur
[NASA-TM-4185] N90-21187
STATIC TESTS
Technical Evaluation Motor no. 5 (TEM-5)
[NASA-CR-183932] N90-21117
STATISTICAL ANALYSIS
Ridge regression processing N90-20931
Annual review of aircraft accident data: US general aviation calendar year 1987
[PB90-138066] N90-20966
Statistics on aircraft gas turbine engine rotor failures that occurred in US commercial aviation during 1986
[DOT/FAA/CT-89/30] N90-21008
Quality at a glance
[AD-A217297] N90-21400
Review and statistical analysis of the ultrasonic velocity method for estimating the porosity fraction in polycrystalline materials
[NASA-TM-102501] N90-21402
Project CANASATE: Remote sensing applied to sugar cane crop survey
[INPE-4902-PRE/1503] N90-21446
Performance evaluation of MSS/LANDSAT data in the estimation of fluvial channel width
[INPE-4906-PRE/1507] N90-21463
An outline for the analysis of wave induced bottom pressure fluctuations
[MRL-TN-558] N90-21510
SIGNIF: A C function to compute significant digits
[DE90-009242] N90-21550
STORM: A statistical object representation model
[DE90-009048] N90-21686
STATORS
The numerical simulation of multistage turbomachinery flows N90-21025
The effect of secondary flow on the redistribution of the total temperature field downstream of a stationary turbine cascade N90-21033
STEADY FLOW
Convergence acceleration of hypersonic flow calculations: A nonlinear relaxation factor N90-20957
ULTRA-SHARP nonoscillatory convection schemes for high-speed steady multidimensional flow
[NASA-TM-102568] N90-21570
STEELS
Corrosion behavior of mild steel in high pH aqueous media
[PB90-131152] N90-21162
Magneto acoustic emission apparatus for testing materials for embrittlement
[NASA-CASE-LAR-13817-1] N90-21170
STELLAR ATMOSPHERES
Model atmospheres for novae during the early stages
[NASA-CR-180498] N90-21694
STELLAR COLOR
The evolution and geometry of the outer parts of the small Magellanic cloud N90-21697
STELLAR ENVELOPES
A theoretical study of circumstellar dust around Ae/Be stars N90-21700
STELLAR EVOLUTION
Multi-wavelength observations of novae in outburst
[DE90-008934] N90-21692
Evolutionary effects in B stars N90-21704
STELLAR FLARES
Flare stars at radio wavelengths
[NASA-CR-186539] N90-21719
STELLAR MAGNITUDE
Recent advances in the studies of the nova outburst
[DE90-008936] N90-21691
The evolution and geometry of the outer parts of the small Magellanic cloud N90-21697
STELLAR MASS
Discovery of low mass objects in Taurus N90-21329
Small scale structures and density of star-forming regions N90-21706
STELLAR MODELS
Multi-wavelength observations of novae in outburst
[DE90-008934] N90-21692
Small scale structures and density of star-forming regions N90-21706
STELLAR ROTATION
Thomson scattering in a magnetic field N90-21699
STELLAR SPECTRA
AFGL ten micron mosaic array spectrometer: Recent results N90-21333
Preliminary results on two-dimensional interferometry of HL Tau N90-21335
STELLARATORS
Transition from resistive-g to eta-i driven turbulence in stellarator systems
[DE90-009382] N90-21641
STIFFNESS
Wave receptance analysis of vibrating beams and stiffened plates N90-21419
STIRLING CYCLE
Recent Stirling engine loss-understanding results
[NASA-TM-103122] N90-21114
STIRLING ENGINES
Recent Stirling engine loss-understanding results
[NASA-TM-103122] N90-21114
STOCHASTIC PROCESSES
Application of stochastic robustness to aircraft control systems N90-20936
Stochastic robustness of linear control systems N90-20941
Effective techniques for the identification and accommodation of disturbances N90-21072
Quadratic Hadamard Memories 1
[AD-A217224] N90-21534
STOICHIOMETRY
Energy beam treatment for improved adhesion of coatings to surfaces
[AD-D014449] N90-21190
Influence of the deposition conditions on radiofrequency magnetron sputtered MoS2 films
[NASA-TP-2994] N90-21210
STOPPING
Brake performance of the McDonnell Douglas DC-10-30/40 during high speed, high energy rejected takeoffs
[PB90-917004] N90-21000
STORAGE RINGS (PARTICLE ACCELERATORS)
On storage rings for short wavelength FELs
[DE90-009059] N90-21379
STORAGE TANKS
Collapsible fabric tank testing
[AD-A217861] N90-21388
STRAIN DISTRIBUTION
Direct formulation of a 4-node hybrid shell element with rotational degrees of freedom
[NASA-CR-4282] N90-21411
STRAIN ENERGY RELEASE RATE
Combined effect of matrix cracking and stress-free edge on delamination
[NASA-TM-102591] N90-21126
Delamination failure in a unidirectional curved composite laminate
[NASA-CR-182018] N90-21421
STRAIN HARDENING
Strengthening mechanisms of tungsten powder reinforced uranium
[DE90-009331] N90-21144
STRAIN MEASUREMENT
Strain and dynamic measurements using fiber optic sensors embedded into graphite/epoxy tubes N90-21090
STRANGENESS
Strangeness enhancement in 14.6 A GeV/c Si+Au interactions?
[DE90-008826] N90-21616
STRATA
Concentric layer ramjet fuel
[AD-D014443] N90-21111
STRATEGY
Controller reduction for effective interdisciplinary design of active structures N90-21077
STRATIFICATION
The extension of rapid distortion theory to stratified shear flows N90-21491
STRESS (PHYSIOLOGY)
Biological effects of ELF (Extremely-Low-Frequency) electric and magnetic fields
[DE90-008634] N90-21514
STRESS ANALYSIS
Stress analysis of rocket motors with viscoelastic propellant by a mixed finite element model N90-21112
Micromechanics analysis of space simulated thermal deformations and stresses in continuous fiber reinforced composites
[NASA-TM-102633] N90-21140
Fourier series methods for plates and shells with cracks and inclusions N90-21406
Determination of stresses around cutouts in multilayered composite plate and shell structures N90-21417
Stress analysis and minimum weight design of honeycomb sandwich plates N90-21418
Elasto-plastic large deformation analysis of thin-walled structures
[PB90-164757] N90-21426
Design and demonstration of an improved stretched-membrane heliostat
[DE90-007904] N90-21470
STRESS CONCENTRATION
Determination of stresses around cutouts in multilayered composite plate and shell structures N90-21417
STRESS CORROSION
Grain boundary chemistry effects on irradiation-assisted stress corrosion cracking
[DE90-008623] N90-21167
STRESS CORROSION CRACKING
A corrosion fatigue/stress corrosion testing facility at Materials Research Laboratory
[MRL-TN-568] N90-21044
A STEM study of changing grain boundary chemistry during the sensitisation of AISI 304 stainless steel
[AERE-R-13418] N90-21157
Current fluctuations associated with localised corrosion: Mechanistic studies of the early stages of pitting and stress corrosion cracking of stainless steel
[AERE-R-13531] N90-21159
Grain boundary chemistry effects on irradiation-assisted stress corrosion cracking
[DE90-008623] N90-21167
STRESS DISTRIBUTION
Secondary flows and Reynolds stress distributions downstream of a turbine cascade at different expansion ratios N90-21015
Direct formulation of a 4-node hybrid shell element with rotational degrees of freedom
[NASA-CR-4282] N90-21411
STRESS INTENSITY FACTORS
Fracture of sandwiched composites N90-21136
Fatigue crack growth from narrow-band Gaussian spectrum loading in 6063 aluminum alloy
[DE90-008957] N90-21173
STRESS TENSORS
Rectangular subsonic jet flow field measurements
[NASA-CR-181925] N90-21598
STRESS-STRAIN RELATIONSHIPS
Element-specific modal formulations for large-displacement multibody dynamics N90-21069
Nicalon/siliconoxycarbide ceramic composites
[NASA-TM-102563] N90-21133
Modeling elastomer displacements for tactile sensing applications
[DE90-007959] N90-21370
STRESSES
Stressed Ge:Ga photoconductors for space-based astronomy. (Is there life beyond 120 micron) N90-21315
STRING THEORY
Extension of the constraints algebra for the closed string with the fixed topology world sheet
[DE90-612745] N90-21577
Extension of the Krichever-Novikov algebra in the closed string theory
[DE90-612746] N90-21578
Rings
[DE90-009035] N90-21613
String dynamics in curved space-time revisited
[DE90-612796] N90-21674
STRIP TRANSMISSION LINES
The 4th Annual Review of Progress in Applied Computational Electromagnetics
[AD-A217912] N90-21257
STRONGLY COUPLED PLASMAS
Center of excellence in theoretical geoplasma research
[AD-A215035] N90-21488
STRONTIUM
SR90, strontium shaped-charge critical ionization velocity experiment
[NASA-CR-186501] N90-21606
STRUCTURAL ANALYSIS
The role of structural analysis in airworthiness certification
[BR112064] N90-20972
Computer-aided structural optimisation of aircraft structures
[BR112837] N90-20973
Zenith Star: A structural control challenge N90-21064
A distributed finite-element modeling and control approach for large flexible structures N90-21071
Mechanics of interface fracture N90-21408
The computational structural mechanics testbed generic structural-element processor manual
[NASA-CR-181728] N90-21410
Direct formulation of a 4-node hybrid shell element with rotational degrees of freedom
[NASA-CR-4282] N90-21411
Integrated modeling and analysis of a space-truss article
[NASA-TM-102615] N90-21412
The Shock and Vibration Digest, volume 22, no. 2 N90-21596

Research programs in aeronautical engineering, solid state physics, and materials science at Technion-Israel Institute of Technology, Haifa, Israel
[EOARD-LR-89-066] N90-21720

STRUCTURAL BASINS
Radon concentration over the Brazilian Amazon Basin during the wet season (Belem-Manaus GTE-ABLE-2B flight of April 24, 1987)
[INPE-4892-PRE/1493] N90-21486

STRUCTURAL DESIGN
Computational Methods for Aerodynamic Design (Inverse) and Optimization
[AGARD-CP-463] N90-20976
Progress in inverse design and optimization in aerodynamics N90-20977
Inverse design of airfoil contours: Constraints, numerical method, and applications N90-20980
An intensive procedure for the design of pressure-specified three-dimensional configurations at subsonic and supersonic speeds by means of a higher-order panel method N90-20982
An inverse method for the design of turbomachine blades N90-20988
Application of an inverse method to the design of a radial inflow turbine N90-20989
Aerodynamic optimization by simultaneously updating flow variables and design parameters N90-20991
Calculation of the secondary flow in an axial turbine N90-21022
Generation and decay of secondary flows and their impact on aerodynamic performance of modern turbomachinery components N90-21023
Effects of secondary flow on heat transfer in rotating passages N90-21031
NASA/DOD Controls-Structures Interaction Technology 1989
[NASA-CP-3041] N90-21062
Vibration isolation versus vibration compensation on multiple payload platforms N90-21066
Element-specific modal formulations for large-displacement multibody dynamics N90-21069
Modeling and control of flexible space platforms with articulated payloads N90-21073
Detection of potential space station control/structure interaction with CO-ST-IN N90-21074
Optimization of the structural and control system for LSS with reduced-order model N90-21075
Computational architecture for integrated controls and structures design N90-21076
Controller reduction for effective interdisciplinary design of active structures N90-21077
Recent experience in simultaneous control-structure optimization N90-21078
A survey of experiments and experimental facilities for active control of flexible structures N90-21079
NASA CSI suspension methods overview N90-21080
ASCIE: An integrated experiment to study CSI in large segmented optical systems N90-21082
CSI sensing and control: Analytical and experimental results N90-21083
Experimental evaluation of active-member control of precision structures N90-21084
Controls, Astrophysics, and Structures Experiment in Space (CASES) N90-21085
LACE flight dynamics experiment N90-21086
CSI technology validation on an LSS ground experiment facility N90-21089
Initial operational capability of the ASTREX large space structures test bed N90-21091
In-house experiments in large space structures at the Air Force Wright Aeronautical Laboratories Flight Dynamics Laboratory N90-21092
Preliminary design approach for large high precision segmented reflectors
[NASA-TM-102605] N90-21096
Multi-objective shape and material optimization of composite structures including damping
[NASA-TM-102579] N90-21132
Structural tailoring of select fiber composite structures
[NASA-TM-102484] N90-21137
Review of the state of the technology for joining ceramics for high-temperature structural applications
[DE90-009224] N90-21199
Development of a fracture analysis technique for use with a general-purpose finite element program N90-21416

STRUCTURAL ENGINEERING
Initial operational capability of the ASTREX large space structures test bed N90-21091

STRUCTURAL FAILURE
NASA airframe structural integrity program
[NASA-TM-102637] N90-21422
An evaluation of the pressure proof test concept for thin sheet 2024-T3
[NASA-TM-101675] N90-21424

STRUCTURAL MEMBERS
Heat engine based on shape memory alloys
[AD-D014400] N90-21385

STRUCTURAL PROPERTIES (GEOLOGY)
Characterization of linear structures from remote sensing data; Espinhaco Meridional (MG) sierra
[INPE-4905-PRE/1506] N90-21449
Geology of Espinhaco Meridional, including the Quadrilatero Ferrifero: Integration through remote sensing data
[INPE-4904-PRE/1505] N90-21450
A numerical and theoretical study of seismic wave diffraction in complex geologic structure
[AD-A218209] N90-21490

STRUCTURAL STABILITY
Initial operational capability of the ASTREX large space structures test bed N90-21091

STRUCTURAL VIBRATION
PACOSS program status and results N90-21065
Nonlinear and distributed parameter models of the mini-mast truss N90-21070
The effect of elastic boundary conditions on the dynamic response of rectangular plates
[NASA-CR-186059] N90-21405

STRUTS
Heavily loaded joints for assembling aerobrake support trusses
[NASA-CR-181992] N90-21099

SUBJECTS
Medical subject headings: Annotated alphabetic list, 1990
[PB90-100009] N90-21683
Permuted medical subject headings, 1990
[PB90-100025] N90-21684

SUBLIMATION
Direct sublimation of NaCl salt from carbon matrixes
[DE90-007927] N90-21139

SUBMILLIMETER WAVES
Study on rotating plasma with submillimeter laser interferometer
[DE90-615387] N90-21623

SUBROUTINES
Hypercluster parallel processing library user's manual
[NASA-CR-185231] N90-21552

SUBSONIC FLOW
Subsonic and transonic blade design by means of analysis codes N90-20985
Numerical optimization of target pressure distributions for subsonic and transonic airfoil design N90-20993
Subsonic flutter analysis using MSC/NASTRAN
[PB90-166786] N90-21041
Rectangular subsonic jet flow field measurements
[NASA-CR-181925] N90-21598

SUBSONIC FLUTTER
Subsonic flutter analysis using MSC/NASTRAN
[PB90-166786] N90-21041

SUBSONIC SPEED
An intensive procedure for the design of pressure-specified three-dimensional configurations at subsonic and supersonic speeds by means of a higher-order panel method N90-20982

SUBSTRATES
Proceedings of the Joint NOSC/NRL (Naval Ocean Systems Center/Naval Research Laboratory) InP Microwave/Millimeter Wave Technology Workshop
[AD-A218216] N90-21259
Alternating gradient photodetector
[NASA-CASE-NPO-17235-1-CO] N90-21358
Improvement of small-area, amorphous-silicon thin-film photovoltaics on polymer substrate
[DE90-000314] N90-21472

SUGAR CANE
Agricultural yield estimation of sugarcane based on agrometeorological-spectral model
[INPE-5016-RPE/610] N90-21441
Project CANASATE: Remote sensing applied to sugar cane crop survey
[INPE-4902-PRE/1503] N90-21446
Evaluation of classification performance and proportion estimate of the sugar cane crop through PROCEDURE-INPE utilizing LANDSAT data
[INPE-4899-PRE/1500] N90-21458

SULFIDATION
High-temperature oxidation and sulfidation of Fe-20Cr-16Ni-4Al-1Y2O3 oxide-dispersion-strengthened alloy
[DE90-007897] N90-21168

SULFUR DIOXIDES
Transformation and deposition of airborne gaseous and particulate pollutants during transport over the Baltic Sea
[PUBL-AIR-QUALITY-5] N90-21478

SUPERCOMPUTERS
High performance computing and networking for science
[PB90-131228] N90-21526

SUPERCONDUCTING MAGNETS
The design of a large aperture high field dipole
[DE90-007910] N90-21285

SUPERCONDUCTING SUPER COLLIDER
The design of a large aperture high field dipole
[DE90-007910] N90-21285

SUPERCONDUCTIVITY
Modified tight-binding approximation and electron-phonon spectral function for transition metals
[DE90-614022] N90-21166
JPRS report: Science and technology. USSR: Physics and mathematics
[JPRS-UPM-90-002] N90-21593
Chern-Simons superconductivity at finite temperature
[DE90-613393] N90-21650
On the substitution of Sr ions at Y sites in YB(suba2)Cu3O(sub7-d)
[DE90-613395] N90-21652
Thermogravimetric analysis of Nd(2-x)Ce(x)CuO(4-delta)
[DE90-009184] N90-21656
Some global problems in gauge theories (variations on a theme of Aharonov and Bohm)
[DE90-009034] N90-21678

SUPERCONDUCTORS
Deformation processing of YBa2Cu3O(sub x)
[DE90-007795] N90-21644
Toughened YBa2Cu3O(sub x)/ZrO2 composites
[DE90-007796] N90-21645
Specific heat and critical fluctuations in anisotropic high-T(sub c) oxide superconductors
[DE90-613394] N90-21651
Shock compression of solids: A tutorial
[DE90-009185] N90-21659

SUPERCRITICAL AIRFOILS
Aerodynamic design techniques at DLR Institute for Design Aerodynamics N90-20979

SUPERCRITICAL FLOW
Aerofoil design techniques N90-20978
Inverse design of airfoil contours: Constraints, numerical method, and applications N90-20980
Inverse computation of transonic internal flows with application for multi-point-design of supercritical compressor blades N90-20987

SUPERCRITICAL FLUIDS
Phase equilibrium of mixtures consisting of molecules with large size and shape differences (thermodynamic modeling of Supercritical Fluid Extraction and Retrograde Condensation, SFE/RC)
[PB90-131285] N90-21146

SUPERGRAVITY
Quantization of the N = 2m simple supergravity in d = 2 + 1
[DE90-612765] N90-21671

SUPERLATTICES
Coupled magnetoplasmon-phonon modes at the surface of a semi-infinite semiconductor superlattice
[DE90-612904] N90-21647
Microstructure of Au/Nb multilayers
[DE90-006722] N90-21662

SUPERSONIC COMBUSTION RAMJET ENGINES
Performance of an aero-space plane propulsion nozzle N90-21034

SUPERSONIC FLIGHT
An aerodynamic tradeoff study of the scissor wing configuration
[NASA-CR-186576] N90-20965

SUPERSONIC FLOW
A two-dimensional unsteady analysis for transonic and supersonic cascade flows N90-20955
Exhaust nozzles for propulsion systems with emphasis on supersonic cruise aircraft
[NASA-RP-1235] N90-21037
A quasi-Lagrangian moving grid technique for investigating compressible flows N90-21298

SUPERSONIC NOZZLES
Supersonic nozzle design of arbitrary cross-section N90-21035
Exhaust nozzles for propulsion systems with emphasis on supersonic cruise aircraft
[NASA-RP-1235] N90-21037

SUPERSONIC SPEED
An intensive procedure for the design of pressure-specified three-dimensional configurations at subsonic and supersonic speeds by means of a higher-order panel method N90-20982

SUPERSONIC TRANSPORTS
Supersonic through-flow fan engine and aircraft mission performance
[NASA-TM-102304] N90-21038

SUPERSONIC TURBINES
Supersonic through-flow fan engine and aircraft mission performance
[NASA-TM-102304] N90-21038

SUPERSYMMETRY
The N = 2 superconformal algebras on hyperelliptic surfaces and their Coulomb gas realization
[DE90-612790] N90-21581
Local supersymmetry in non-relativistic systems
[DE90-612751] N90-21670
SUPPORTS
Vibration isolation versus vibration compensation on multiple payload platforms N90-21066
SURFACE COOLING
Surface-cooling effects on compressible boundary-layer instability
[NASA-CR-182003] N90-21290
Ablative cooling of aerodynamically heated radomes
[AD-D014426] N90-21293
SURFACE PROPERTIES
Low energy ion generator
[DE90-759905] N90-21195
The measurement of surface reflectivity at millimetre wavelengths
[MRL-TN-559] N90-21222
Depth-averaged equations for turbulent free-surface flow
[PB90-164781] N90-21308
Modeling elastomer displacements for tactile sensing applications
[DE90-007959] N90-21370
Absolute multilayer characterization at high spatial resolution via real-time soft x ray imaging
[DE90-009181] N90-21371
SURFACE ROUGHNESS
Investigation of surface water behavior during glaze ice accretion N90-20927
SURFACE ROUGHNESS EFFECTS
Modeling of surface roughness effects on glaze ice accretion N90-20925
SURFACE TEMPERATURE
Thermal radiation characteristics of nonisothermal cylindrical enclosures using a numerical ray tracing technique
[NASA-TM-102527] N90-21296
SURFACE VEHICLES
Proceedings of the 4th European Conference, volume 2
[AD-A216521] N90-21382
SURFACE WATER
Investigation of surface water behavior during glaze ice accretion N90-20927
Analysis of water quality parameters of the Piaui River (SE), Brazil, through field and TM/LANDSAT sensor data
[INPE-4918-PRE/1417] N90-21453
SURFACE WAVES
An outline for the analysis of wave induced bottom pressure fluctuations
[MRL-TN-558] N90-21510
SURVEILLANCE
MMW SAR on RPV for battlefield surveillance N90-21231
SURVEILLANCE RADAR
High Resolution Air- and Spaceborne Radar
[AGARD-CP-459] N90-21223
Trade-offs in a space based surveillance radar N90-21225
SURVEYS
A survey of experiments and experimental facilities for active control of flexible structures N90-21079
Survey of land use through remote sensing
[INPE-5032-MD/042] N90-21443
Project CANASATE: Remote sensing applied to sugar cane crop survey
[INPE-4902-PRE/1503] N90-21446
Evolution of remote sensing applied to vegetation and forest at INPE
[INPE-4970-PRE/1538] N90-21452
The molecular cloud content of early type galaxies. 2: A molecular ring in NGC 404
[PB90-124348] N90-21695
SUSPENDING (HANGING)
An air-bearing weight offload system for ground test of heavy LSS structures N90-21081
SUSPENSION SYSTEMS (VEHICLES)
NASA CSI suspension methods overview N90-21080
SWIRLING
Numerical simulation of vortex breakdown N90-21288
SWITCHES
Simulator comparison of thumball, thumb switch, and touch screen input concepts for interaction with a large screen cockpit display format
[NASA-TM-102587] N90-21005
SWITCHING CIRCUITS
Laser controlled semiconductor armature for electromagnetic launchers
[AD-D014435] N90-21055
NASA's Advanced Communications Technology Satellite (ACTS): Will it benefit commercial/military satellites
[AD-A217710] N90-21100
SWIVELS
Double swivel toggle release
[NASA-CASE-MSC-21436-1] N90-21390
SYMMETRY
Apparatus and method for locating the axis of symmetry (center of circular cross section) of three dimensional objects
[AD-D014407] N90-21354
SYNCHROTRON RADIATION
A requirement for Australian research: Access to big science facilities, a report by the Australian National Committee for Crystallography
[DE90-614784] N90-21048
SYNTHESIS (CHEMISTRY)
Bis(4-(3,4-dimethylenepyrrolidyl)-phenyl) methane
[NASA-CASE-LAR-13965-1-CU] N90-21118
Apparatus for mixing solutions in low gravity environments
[NASA-CASE-MFS-26047-1] N90-21209
Method of making a long life high current density cathode from tungsten and iridium powders using a quarternary compound as the impregnant
[AD-D014425] N90-21211
Alternative materials for solid oxide fuel cells
[DE90-008615] N90-21468
SYNTHETIC APERTURE RADAR
High Resolution Air- and Spaceborne Radar
[AGARD-CP-459] N90-21223
Concepts for high resolution space based SAR/ISAR systems: Preliminary design considerations N90-21224
Trade-offs in a space based surveillance radar N90-21225
Application of superresolution methods for airborne radar N90-21227
ROSAR (Helicopter-Rotor based Synthetic Aperture Radar) N90-21229
Capabilities of bistatic synthetic aperture radar for covert battlefield surveillance N90-21230
Real-time adaptive radiometric correction for imaging radars systems N90-21233
Concept for a spaceborne Synthetic Aperture Radar (SAR) sensor based on active phased array technology N90-21234
A motion compensation study for the PHARUS project N90-21235
A solution for real time motion compensation for SAR without using inertial navigation systems N90-21236
SAR and ISAR imagery of marine targets N90-21237
Problems in ISAR processing with range resolution by stepped frequency bursts N90-21238
A fast ISAR-imaging process and its inherent degrading effects on image quality N90-21239
Radar observations of a formation of two fighters: A case study for ISAR imaging N90-21240
The 1D-ISAR imaging of manoeuvering aircraft N90-21241
Radar target image by ISAR case study N90-21242
Concept and results of the DLR realtime SAR processor N90-21244
Image simulation of geometric targets for synthetic aperture radar N90-21245
SAR image coding N90-21246
SYSTEM IDENTIFICATION
CSI sensing and control: Analytical and experimental results N90-21083
In-house experiments in large space structures at the Air Force Wright Aeronautical Laboratories Flight Dynamics Laboratory N90-21092
Application of neural nets to system identification and bifurcation analysis of real world experimental data
[DE90-007539] N90-21558
SYSTEMS ANALYSIS
Detection of potential space station control/structure interaction with CO-ST-IN N90-21074
SYSTEMS ENGINEERING
NASA/DOD Controls-Structures Interaction Technology 1989
[NASA-CP-3041] N90-21062
Software verification and validation: Its role in computer assurance and its relationship with software project management standards
[PB90-111691] N90-21530
Evolution of Ada technology in the flight dynamics area: Implementation/testing phase analysis
[NASA-TM-103310] N90-21539
SYSTEMS INTEGRATION
ASCIE: An integrated experiment to study CSI in large segmented optical systems N90-21082
SYSTEMS SIMULATION
Probabilistic modeling for simulation of aerodynamic uncertainties in propulsion systems
[NASA-TM-102472] N90-21036

T

TAKEOFF
Brake performance of the McDonnell Douglas DC-10-30/40 during high speed, high energy rejected takeoffs
[PB90-917004] N90-21000
HOTOL structures and materials at British Aerospace, Warton, UK
[EOARD-LR-90-001] N90-21001
TAPERING
Aperture taper determination for the half-scale accurate antenna reflector
[NASA-CR-185215] N90-21282
TARGET ACQUISITION
ROSAR (Helicopter-Rotor based Synthetic Aperture Radar) N90-21229
MMW SAR on RPV for battlefield surveillance N90-21231
SAR and ISAR imagery of marine targets N90-21237
Radar target image by ISAR case study N90-21242
TARGET RECOGNITION
High Resolution Air- and Spaceborne Radar
[AGARD-CP-459] N90-21223
Automatic classification of images
[AD-D014437] N90-21260
The effect of windscreen bows and HUD pitch ladder format on pilot performance during simulated flight
[AD-A218139] N90-21523
TARGETS
Determination of Li-Al alloy extent in tubular aluminum elements by small source neutron radiology
[DE90-009142] N90-21174
Image simulation of geometric targets for synthetic aperture radar N90-21245
TAYLOR SERIES
PROTEUS two-dimensional Navier-Stokes computer code, version 1.0. Volume 3: Programmer's reference
[NASA-TM-102553] N90-21307
TEARING MODES (PLASMAS)
The effect of viscosity on the resistive tearing mode with the presence of shear flow
[DE90-009340] N90-21312
MHD modes driven by anomalous electron viscosity and their role in fast sawtooth crashes
[DE90-009311] N90-21639
TECHNICAL WRITING
A compendium of sources of fracture toughness and fatigue crack growth data for metallic alloys, part 4
[NASA-TM-102646] N90-21164
TECHNOLOGICAL FORECASTING
Experimental aeroelasticity history, status and future in brief
[NASA-TM-102651] N90-21047
NASA's Advanced Communications Technology Satellite (ACTS): Will it benefit commercial/military satellites
[AD-A217710] N90-21100
TECHNOLOGIES
Goes I-M and beyond: Science requirements and technology challenges N90-21067
TECHNOLOGY ASSESSMENT
Review of the state of the technology for joining ceramics for high-temperature structural applications
[DE90-009224] N90-21199
High performance computing and networking for science
[PB90-131228] N90-21526
TECHNOLOGY TRANSFER
Programme of the International Training Course on Remote Sensing for African Specialists
[INPE-4878-NTE/290] N90-21435
Regional remote sensing laboratory
[INPE-4922-PRE/1519] N90-21465
Toward a new CIM (Computer Integrated Manufacturing) architecture for Sandia Laboratories
[DE90-008677] N90-21548
Advanced manufacturing technology: A Department of Energy technology transfer initiative
[DE90-008601] N90-21688
TECTONICS
Characterization of linear structures from remote sensing data; Espinhaco Meridional (MG) sierra
[INPE-4905-PRE/1506] N90-21449
Geology of Espinhaco Meridional, including the Quadrilatero Ferrifero: Integration through remote sensing data
[INPE-4904-PRE/1505] N90-21450
Contribution for the study of the evolution of part of the Espinhaco supergroup and its foundation through fracture analysis
[INPE-4907-PRE/1508] N90-21459

TELEMETRY
VLSI single-chip (255,223) Reed-Solomon encoder with interleaver
[NASA-CASE-NPO-17280-1-CU] N90-21061
Subsystem TM Precision: Progress and perspective
[INPE-5006-PRE/1563] N90-21461
Environmental projects, volume 11. Environmental assessment: Addition to operations building, Mars site
[NASA-CR-186449] N90-21479
TELEOPERATORS
Mars in this century: The Olympia Project
[DE90-008356] N90-21709
TELESCOPES
Experimental evaluation of active-member control of precision structures N90-21084
Initial astronomical results with a new 5-14 micron Si:Ga 58x62 DRO array camera N90-21334
Introduction to the Infrared Space Observatory (ISO) N90-21340
SOFIA: Stratospheric Observatory for Infrared Astronomy N90-21348
TELETYPEWRITERS
An introduction to high frequency radioteletype systems
[PB90-145533] N90-21252
TELEVISION SYSTEMS
HDTV bandwidth reduction using motion compensation and DATV
[BBC-RD-1989/10] N90-21254
Prediction of VHF/UHF mobile reception in urban areas: Comparison with measurements in London
[BBC-RD-1989/11] N90-21255
TEMPERATE REGIONS
Precipitation mechanisms in tropical and midlatitude convective clouds N90-21507
TEMPERATURE CONTROL
Space environment simulation of the SCD-01 satellite through heating plates
[INPE-4988-PRE/1550] N90-21105
Thermal control system corrosion study
[NASA-TM-102220] N90-21294
TEMPERATURE DEPENDENCE
Modeling the temperature dependence of the thermal conductivity of aluminum nitride
[DE90-009428] N90-21154
O2 reduction at the IFC orbiter fuel cell O2 electrode
[NASA-TM-102580] N90-21469
Chern-Simons superconductivity at finite temperature
[DE90-613393] N90-21650
TEMPERATURE DISTRIBUTION
The effect of secondary flow on the redistribution of the total temperature field downstream of a stationary turbine cascade N90-21033
MECCA program documentation
[NOAA-TR-NESDIS-46] N90-21477
TEMPERATURE EFFECTS
Transportation monitoring unit qualification
[NASA-CR-183930] N90-21060
LaRC TPI 1500 series polymers
[NASA-CR-181899] N90-21129
Micromechanics analysis of space simulated thermal deformations and stresses in continuous fiber reinforced composites
[NASA-TM-102633] N90-21140
Optimal fabrication processes for unidirectional metal-matrix composites: A computational simulation
[NASA-TM-102559] N90-21143
A STEM study of changing grain boundary chemistry during the sensitisation of AISI 304 stainless steel
[AERE-R-13418] N90-21157
Titanium aluminides: Processing, properties and potential
[AERE-R-13198] N90-21158
On the stability of amorphous silica coatings for high temperature service
[AERE-R-13425] N90-21179
Research advances in fine ceramics
[DE90-008983] N90-21197
Pressure rig for repetitive casting
[NASA-CASE-LAR-14050-1] N90-21216
Deformation and microstructure of rutile
[DE90-614113] N90-21654
Thermogravimetric analysis of Nd(2-x)Ce(x)CuO(4-delta)
[DE90-009184] N90-21658
TEMPERATURE GRADIENTS
Thermomechanical deformation testing and modeling in the presence of metallurgical instabilities
[NASA-CR-185188] N90-21420
TEMPERATURE MEASUREMENT
Analysis of water quality parameters of the Piaui River (SE), Brazil, through field and TM/LANDSAT sensor data
[INPE-4918-PRE/1417] N90-21453
TEMPORAL RESOLUTION
Some recent applications of laser ultrasound to the characterisation of materials
[AERE-R-13438] N90-21374
Evaluation of the mangrove areas of the Rio Piaui (SE) through remote sensing
[INPE-4909-PRE/1510] N90-21454
Multitemporal analysis of LANDSAT/TM digital imagery in the detection of areas affected by caterpillar (sibine fusca) attack in the dende (elais guineensis) palm plantation
[INPE-4979-PRE/1544] N90-21457
TENSILE PROPERTIES
The effects of a nearby subsequent fusion weld on the properties of an inertia friction weld
[DE90-007972] N90-21396
TENSILE STRENGTH
Relevance of impacter shape to nonvisible damage and residual tensile strength of a thick graphite/epoxy laminate
[NASA-TM-102599] N90-21122
TENSORS
The generally covariant representation of energy-momentum pseudotensor of gravitational field
[DE90-615203] N90-21669
TERMS
Medical subject headings: Annotated alphabetic list, 1990
[PB90-100009] N90-21683
Permuted medical subject headings, 1990
[PB90-100025] N90-21684
TERRAIN
Proceedings of the 4th European Conference, volume 2
[AD-A216521] N90-21382
TERRAIN ANALYSIS
Generation of triangular form models in a microcomputer environment
[INPE-4974-PRE/1539] N90-21447
TEST FACILITIES
A corrosion fatigue/stress corrosion testing facility at Materials Research Laboratory
[MRL-TN-568] N90-21044
Liquid Transfer Cryogenic Test Facility: Initial hydrogen and nitrogen no-vent fill data
[NASA-TM-102572] N90-21295
TEST FIRING
Technical Evaluation Motor no. 5 (TEM-5)
[NASA-CR-183932] N90-21117
TETRAHEDRONS
Ionic equilibrium between octahedral and tetrahedral complexes in liquid aluminium-sodium fluoride mixtures
[DE90-613690] N90-21150
TEXTURES
Characterization of linear structures from remote sensing data; Espinhaco Meridional (MG) sierra
[INPE-4905-PRE/1506] N90-21449
THEMATIC MAPPING
Geobotanical remote sensing: A review
[INPE-5026-PRE/1565] N90-21440
Survey of land use through remote sensing
[INPE-5032-MD/042] N90-21443
Digital processing of TM/LANDSAT data in monitoring interior water
[INPE-4956-PRE/1533] N90-21448
Analysis of water quality parameters of the Piaui River (SE), Brazil, through field and TM/LANDSAT sensor data
[INPE-4918-PRE/1417] N90-21453
Evaluation of the mangrove areas of the Rio Piaui (SE) through remote sensing
[INPE-4909-PRE/1510] N90-21454
Evaluation of classification performance and proportion estimate of the sugar cane crop through PROCEDURE-INPE utilizing LANDSAT data
[INPE-4899-PRE/1500] N90-21458
Performance evaluation of morphological edge detectors
[INPE-4975-PRE/1540] N90-21464
THEOREM PROVING
OTTER (Organized Techniques for Theorem-proving and Effective Research) 2.0 users guide
[DE90-007978] N90-21563
THEORETICAL PHYSICS
Periodic solutions for Hamiltonian systems in a nonconvex potential well
[DE90-612752] N90-21580
THERMAL CONDUCTIVITY
Modeling the temperature dependence of the thermal conductivity of aluminum nitride
[DE90-009428] N90-21154
An experimental evaluation of two nonazeotropic refrigerant mixtures in a water-to-water breadboard heat pump
[DE90-009016] N90-21305
Nonoptimal entropy generation by heat transfer in cryogenic domain
[DE90-007544] N90-21667
The thermo-mechanical behavior of cometary nuclei N90-21703
THERMAL CYCLING TESTS
Use of unbalanced laminates as a screening method for microcracking
[NASA-TM-102517] N90-21124
THERMAL DEGRADATION
Boron-containing organosilane polymers and ceramic materials thereof
[NASA-CASE-ARC-11649-2-SB] N90-21177
THERMAL DIFFUSIVITY
An extended diffusive model for calculating thermal diffusivity from single monopole tokamak heat pulse propagation
[DE90-007958] N90-21637
THERMAL EXPANSION
Use of unbalanced laminates as a screening method for microcracking
[NASA-TM-102517] N90-21124
Modeling the temperature dependence of the thermal conductivity of aluminum nitride
[DE90-009428] N90-21154
The thermo-mechanical behavior of cometary nuclei N90-21703
THERMAL FATIGUE
High temperature fatigue behavior of tungsten copper composites
[NASA-TM-102404] N90-21138
THERMAL PLASMAS
Relativistic processes in active galactic nuclei N90-21698
THERMAL RADIATION
Thermal radiation characteristics of nonisothermal cylindrical enclosures using a numerical ray tracing technique
[NASA-TM-102527] N90-21296
Heat engine based on shape memory alloys
[AD-D014400] N90-21385
Principles of the radiosity method for canopy reflectance modeling
[DE90-008943] N90-21466
THERMAL STABILITY
Energy beam treatment for improved adhesion of coatings to surfaces
[AD-D014449] N90-21190
THERMAL STRESSES
Fiber pushout test: A three-dimensional finite element computational simulation
[NASA-TM-102565] N90-21131
Micromechanics analysis of space simulated thermal deformations and stresses in continuous fiber reinforced composites
[NASA-TM-102633] N90-21140
Optimal fabrication processes for unidirectional metal-matrix composites: A computational simulation
[NASA-TM-102559] N90-21143
The thermo-mechanical behavior of cometary nuclei N90-21703
THERMIONIC CONVERTERS
Final safety analysis report for the Ulysses mission. Volume 1: Reference design document
[DE90-008693] N90-21107
THERMOCOUPLES
Attachment of lead wires to thin film thermocouples mounted on high temperature materials using the parallel gap welding process
[NASA-TM-102442] N90-21361
THERMODYNAMIC EQUILIBRIUM
Phase equilibria and solution thermodynamics of bismuth-lead alloys
[PB90-138421] N90-21163
The dynamics of scalar fields in the early universe N90-21696
Toward quantum corrections in black hole thermodynamics N90-21702
THERMODYNAMIC PROPERTIES
Investigation of surface water behavior during glaze ice accretion N90-20927
Phase equilibrium of mixtures consisting of molecules with large size and shape differences (thermodynamic modeling of Supercritical Fluid Extraction and Retrograde Condensation, SFE/RC)
[PB90-131285] N90-21146
Computer codes for the evaluation of thermodynamic properties, transport properties, and equilibrium constants of an 11-species air model
[NASA-TM-102602] N90-21297
High power, high sensitivity microwave calorimeter
[AD-D014427] N90-21355
THERMODYNAMICS
BASG thermomechanical pump helium 2 transfer tests
[NASA-CR-177541] N90-21097

High temperature fatigue behavior of tungsten copper composites
[NASA-TM-102404] N90-21138
Phase equilibrium of mixtures consisting of molecules with large size and shape differences (thermodynamic modeling of Supercritical Fluid Extraction and Retrograde Condensation, SFE/RC)
[PB90-131285] N90-21146
Ice-making heat exchanger evaluation and test plan
[DE90-008824] N90-21218
An experimental evaluation of two nonazeotropic refrigerant mixtures in a water-to-water breadboard heat pump
[DE90-009016] N90-21305
Thermal decay of an initially hot isothermal water body with application to thermal energy storage
[DE90-614742] N90-21675
The Chemkin Thermodynamic Data Base
[DE90-007953] N90-21676
The thermo-mechanical behavior of cometary nuclei N90-21703

THERMOELECTRIC GENERATORS
Final Safety Analysis Report for the Ulysses Mission. Volume 3 (Book 1): Nuclear risk analysis document
[DE90-008691] N90-21101
Final safety analysis report for the Ulysses mission. Volume 2 (Book 1): Accident model document
[DE90-008694] N90-21103
Final safety analysis report for the Ulysses Mission
[DE90-008690] N90-21106

THERMOGRAVIMETRY
Improved Thermo-Oxidative-Deposition screening tests for turbine lubricants
[AD-A217795] N90-21188
Thermogravimetric analysis of Nd(2-x)Ce(x)CuO(4-delta)
[DE90-009184] N90-21658

THERMONUCLEAR REACTIONS
US-Japan Workshop on Atomic Collisions in Solids: Abstracts of lectures
[DE90-008979] N90-21611
Fusion burn dynamics in Dense Z-Pinch (DZP)
[DE90-007976] N90-21638

THERMOPLASTIC RESINS
Determinations of molecular weight and molecular weight distribution of high polymers by the rheological properties
[NASA-CR-186450] N90-21180

THERMOSPHERE
Low latitude F-region dynamical processes from atomic oxygen nightglow emissions
[INPE-4999-PRE/1561] N90-21494

THICK FILMS
Compatibility of Au base thick films with solder alloys: Solid state growth of intermetallics
[DE90-009285] N90-21175

THICKNESS
Ultrasonic techniques for aircraft ice accretion measurement N90-20926

THIN FILMS
The effect of leveling coatings on the atomic oxygen durability of solar concentrator surfaces
[NASA-TM-102557] N90-21110
Magnetron sputtered boron films and Ti/B multilayer structures
[DE90-009190] N90-21153
Influence of the deposition conditions on radiofrequency magnetron sputtered MoS2 films
[NASA-TP-2994] N90-21210
Peeled film GaAs solar cells for space power
[NASA-TM-103125] N90-21287
Attachment of lead wires to thin film thermocouples mounted on high temperature materials using the parallel gap welding process
[NASA-TM-102442] N90-21361
Problems associated with residual and mismatch stresses in thin film structures N90-21407
Improvement of small-area, amorphous-silicon thin-film photovoltaics on polymer substrate
[DE90-000314] N90-21472
Research on amorphous silicon-based thin film photovoltaic devices. Task B: Research on stable high efficiency large area, amorphous silicon-based submodules
[DE90-000320] N90-21473
Inelastic electron scattering from surfaces
[DE90-009365] N90-21614
Shock compression of solids: A tutorial
[DE90-009185] N90-21659
Characterization and comparison of optically transparent conducting films
[DE90-000319] N90-21660
Microstructure of Au/Nb multilayers
[DE90-008722] N90-21662

THIN WALLED SHELLS
Compressive behavior of laminated composite structures N90-21134
UNIVIMP: A universal instrument for the survey of initial imperfections of thin-walled shells
[PB90-167065] N90-21369

THOMSON SCATTERING
Thomson scattering in a magnetic field N90-21699

THREE AXIS STABILIZATION
Attitude control modes for the MECB remote sensing satellites
[INPE-4755-PRE/1427] N90-21094
A general-purpose balloon-borne pointing system for solar scientific instruments
[NASA-TP-3013] N90-21219

THREE DIMENSIONAL BODIES
Apparatus and method for locating the axis of symmetry (center of circular cross section) of three dimensional objects
[AD-D014407] N90-21354

THREE DIMENSIONAL FLOW
On total variation diminishing schemes for transonic turbulent flow computation N90-20945
Secondary Flows in Turbomachines
[AGARD-CP-469] N90-21009
Parabolized calculations of turbulent three dimensional flows in a turbine duct N90-21013
Experimental and numerical study on basic phenomena of secondary flows in turbines N90-21014
An investigation of secondary flows in nozzle guide vanes N90-21016
Measurement of the flow field in the blade passage and side-wall region of a plane turbine cascade N90-21019
Centrifugal impeller geometry and its influence on secondary flows N90-21020
Calculation of the three dimensional turbulent flow in a linear turbine blade N90-21021
Generation and decay of secondary flows and their impact on aerodynamic performance of modern turbomachinery components N90-21023

THREE DIMENSIONAL MODELS
A fast collocation method for transonic airfoil design N90-20984
Numerical method for designing 3D turbomachinery blade rows N90-20990
Supersonic nozzle design of arbitrary cross-section N90-21035

THROATS
Supersonic nozzle design of arbitrary cross-section N90-21035

THRUST VECTOR CONTROL
Electromechanical actuation for thrust vector control applications
[NASA-TM-102548] N90-21272

TIDES
Analysis of water quality parameters of the Piaui River (SE), Brazil, through field and TM/LANDSAT sensor data
[INPE-4918-PRE/1417] N90-21453
MECCA program documentation
[NOAA-TR-NESDIS-46] N90-21477

TILT ROTOR AIRCRAFT
An early overview of tiltrotor aircraft characteristics and pilot procedures in civil transport applications
[DOT/FAA/DS-89/37] N90-21003

TIME
Time and truth in plans N90-20930
String dynamics in curved space-time revisited
[DE90-612796] N90-21674

TIME SERIES ANALYSIS
Application of neural nets to system identification and bifurcation analysis of real world experimental data
[DE90-007539] N90-21558

TIME SIGNALS
A real-time rejection circuit to automatically reject multiple interfering hopping signals while passing a lower level desired signal
[AD-D014424] N90-21251

TIMING DEVICES
The RAP unit: A remote autoranging picoammeter
[DE90-007711] N90-21357

TIN OXIDES
Characterization and comparison of optically transparent conducting films
[DE90-000319] N90-21660

TITANIUM
Titanium aluminides: Processing, properties and potential
[AERE-R-13198] N90-21158
Effects of titanium on some surface properties of nitride ceramics
[AERE-R-13566] N90-21178

TITANIUM ALLOYS
Surface characterization of hydrogen charged and uncharged alpha-2 and gamma titanium aluminide alloys using AES and REELS
[NASA-CR-186561] N90-21171

TITANIUM NITRIDES
Effects of titanium on some surface properties of nitride ceramics
[AERE-R-13566] N90-21178

TOKAMAK DEVICES
Numerical code AEOLUS-E1 for analysing free-boundary resistive MHD mode
[DE90-759903] N90-21630
West European magnetic confinement fusion research N90-21634
Applied plasma physics
[DE90-007932] N90-21635
An extended diffusive model for calculating thermal diffusivity from single monopole tokamak heat pulse propagation
[DE90-007958] N90-21637

TOLLMIEN-SCHLICHTING WAVES
Surface-cooling effects on compressible boundary-layer instability
[NASA-CR-182003] N90-21290

TOPOGRAPHY
Evaluation of classification performance and proportion estimate of the sugar cane crop through PROCEDURE-INPE utilizing LANDSAT data
[INPE-4899-PRE/1500] N90-21458
Performance evaluation of MSS/LANDSAT data in the estimation of fluvial channel width
[INPE-4906-PRE/1507] N90-21463

TOPOLOGY
Extension of the constraints algebra for the closed string with the fixed topology world sheet
[DE90-612745] N90-21577
Fusion algebra and fusing matrices
[DE90-612798] N90-21583

TORQUE
Design of a digital model following controller of reaction wheel torques
[INPE-4753-PRE/1425] N90-21093
A fiber optic sensor for noncontact measurement of shaft speed, torque, and power
[NASA-TM-102481] N90-21360

TORQUEMETERS
A fiber optic sensor for noncontact measurement of shaft speed, torque, and power
[NASA-TM-102481] N90-21360

TORSION
Parametric resonance in horizontal axis wind turbines N90-20962

TOUCH
Modeling elastomer displacements for tactile sensing applications
[DE90-007959] N90-21370

TOUCHDOWN
Modified touchdown zone lighting
[DOT/FAA/CT-TN89/70] N90-21042

TOUGHNESS
Mechanics of interface fracture N90-21408

TOXICOLOGY
JPRS report: Science and technology. USSR: Life sciences
[JPRS-ULS-90-002] N90-21434

TRACE ELEMENTS
Study of new technique of solid combustible materials to determination of volatile elements by flame atomic absorption spectrophotometry
[DE90-612907] N90-21147
Small scale structures and density of star-forming regions N90-21706

TRACKING (POSITION)
Tropical cyclone track predictability and the adjoint method of data assimilation
[AD-A218324] N90-21505

TRAJECTORIES
Optimal trajectories for the aeroassisted flight experiment. Part 3: Formulation, results, and analysis
[NASA-CR-186165] N90-21051

TRAJECTORY OPTIMIZATION
Optimal trajectories for the aeroassisted flight experiment. Part 3: Formulation, results, and analysis
[NASA-CR-186165] N90-21051

TRANSFER ORBITS
Optimal trajectories for the aeroassisted flight experiment. Part 3: Formulation, results, and analysis
[NASA-CR-186165] N90-21051
Suboptimal and hybrid numerical solution schemes for orbit transfer manoeuvres
[INPE-4991-PRE/1556] N90-21054

TRANSFORMATIONS (MATHEMATICS)
A remark on the Kelvin transform and a non-linear partial differential equation
[PB90-165622] N90-21589

TRANSITION TEMPERATURE
On the substitution of Sr ions at Y sites in YB(suba2)Cu3O(sub7-d)
[DE90-613395] N90-21652
TRANSMISSION LOSS
Programmable generation of linear frequency modulated pulses N90-21232
Subsystem TM Precision: Progress and perspective
[INPE-5006-PRE/1563] N90-21461
TRANSMISSIONS (MACHINE ELEMENTS)
Computer-aided design of flywheel transmission systems N90-21392
Transmission research activities at NASA Lewis Research Center
[NASA-TM-103132] N90-21394
TRANSMITTANCE
Power transmission device
[AD-D014430] N90-21281
TRANSMITTERS
Feasibility of using frequency offset on very high frequency air/ground voice channels
[DOT/FAA/CT-TN89/71] N90-21248
TRANSONIC FLIGHT
A tool for automatic design of airfoils in different operating conditions N90-20994
TRANSONIC FLOW
On total variation diminishing schemes for transonic turbulent flow computation N90-20945
Multigrid accelerated relaxation solution of transonic full potential flow equation
[PD-CF-8942] N90-20951
A two-dimensional unsteady analysis for transonic and supersonic cascade flows N90-20955
Subsonic and transonic blade design by means of analysis codes N90-20985
Inverse computation of transonic internal flows with application for multi-point-design of supercritical compressor blades N90-20987
Numerical optimization of target pressure distributions for subsonic and transonic airfoil design N90-20993
Numerical optimization of wings in transonic flow N90-20997
Secondary flow in a turbine guide vane with low aspect ratio N90-21018
TRANSPARENCE
Characterization and comparison of optically transparent conducting films
[DE90-000319] N90-21660
TRANSPORT AIRCRAFT
Full-scale air transport category fuselage burnthrough tests
[DOT/FAA/CT-TN89/65] N90-20967
Simulator comparison of thumball, thumb switch, and touch screen input concepts for interaction with a large screen cockpit display format
[NASA-TM-102587] N90-21005
Civil air transport: A fresh look at power-by-wire and fly-by-light
[NASA-TM-102574] N90-21283
An evaluation of the pressure proof test concept for thin sheet 2024-T3
[NASA-TM-101675] N90-21424
TRANSPORT PROPERTIES
Computer codes for the evaluation of thermodynamic properties, transport properties, and equilibrium constants of an 11-species air model
[NASA-TM-102602] N90-21297
TRANSPORT THEORY
The numerical simulation of multistage turbomachinery flows N90-21025
A self-consistent theory of radial transport of field-aligned current by microturbulence
[DE90-007920] N90-21631
Transition from resistive-g to eta-i driven turbulence in stellarator systems
[DE90-009382] N90-21641
TRANSPORTATION
Transportation monitoring unit qualification
[NASA-CR-183930] N90-21060
TRANSVERSE ACCELERATION
Center of excellence in theoretical geoplasma research
[AD-A215035] N90-21488
TRAPPED PARTICLES
Langmuir wave interaction with ion acoustic wave
[DE90-615407] N90-21624
TRAVELING WAVES
On the instability of Goertler vortices to nonlinear travelling waves
[NASA-CR-181994] N90-21289
TREES (PLANTS)
Shade images of forested areas obtained from LANDSAT MSS data
[NASA-TM-102939] N90-21436
TRENDS
Contribution for the study of the evolution of part of the Espinhaco supergroup and its foundation through fracture analysis
[INPE-4907-PRE/1508] N90-21459
TRIANGULATION
Generation of triangular form models in a microcomputer environment
[INPE-4974-PRE/1539] N90-21447
TRIBOLOGY
Studies of mechano-chemical interactions in the tribological behavior of materials
[NASA-TM-102545] N90-21182
TROPICAL REGIONS
Wheat productivity estimate through field radiometry
[INPE-4994-PRE/1556] N90-21460
Low latitude F-region dynamical processes from atomic oxygen nightglow emissions
[INPE-4999-PRE/1561] N90-21494
Precipitation mechanisms in tropical and midlatitude convective clouds N90-21507
TROPOSPHERE
Source attribution for tropospheric ozone in the US
[DE90-007994] N90-21484
TRUSSES
Nonlinear and distributed parameter models of the mini-mast truss N90-21070
A distributed finite-element modeling and control approach for large flexible structures N90-21071
An air-bearing weight offload system for ground test of heavy LSS structures N90-21081
Experimental evaluation of active-member control of precision structures N90-21084
Space truss zero gravity dynamics N90-21087
In-house experiments in large space structures at the Air Force Wright Aeronautical Laboratories Flight Dynamics Laboratory N90-21092
Heavily loaded joints for assembling aerobrake support trusses
[NASA-CR-181992] N90-21099
Integrated modeling and analysis of a space-truss article
[NASA-TM-102615] N90-21412
TUNGSTEN
Method of making a long life high current density cathode from tungsten and iridium powders using a quarternary compound as the impregnant
[AD-D014425] N90-21211
TUNGSTEN ALLOYS
High temperature fatigue behavior of tungsten copper composites
[NASA-TM-102404] N90-21138
Strengthening mechanisms of tungsten powder reinforced uranium
[DE90-009331] N90-21144
TUNING
Software to characterize tuning fork resonators used in the Quartz Digital Accelerometer
[DE90-007913] N90-21363
TURBINE BLADES
Subsonic and transonic blade design by means of analysis codes N90-20985
Calculation of the three dimensional turbulent flow in a linear turbine blade N90-21021
Calculation of the secondary flow in an axial turbine N90-21022
Losses in the tip-leakage flow of a planar cascade of turbine blades N90-21027
Navier-Stokes analysis of turbine blade heat transfer
[NASA-TM-102496] N90-21300
TURBINE ENGINES
Improved Thermo-Oxidative-Deposition screening tests for turbine lubricants
[AD-A217795] N90-21188
TURBINE PUMPS
Probabilistic modeling for simulation of aerodynamic uncertainties in propulsion systems
[NASA-TM-102472] N90-21036
TURBOCOMPRESSORS
The effects of compressor endwall flow on airfoil incidence and deviation N90-21011
A study on secondary flow and spanwise mixing in axial flow compressors N90-21012
Secondary flow calculations for axial and radial compressors N90-21024
TURBOFAN ENGINES
Supersonic through-flow fan engine and aircraft mission performance
[NASA-TM-102304] N90-21038
TURBOMACHINERY
Computational Methods for Aerodynamic Design (Inverse) and Optimization
[AGARD-CP-463] N90-20976
Numerical method for designing 3D turbomachinery blade rows N90-20990
Secondary Flows in Turbomachines
[AGARD-CP-469] N90-21009
Generation and decay of secondary flows and their impact on aerodynamic performance of modern turbomachinery components N90-21023
The numerical simulation of multistage turbomachinery flows N90-21025
TURBULENCE
Stereopsis cueing effects on hover-in-turbulence performance in a simulated rotorcraft
[NASA-TP-2980] N90-21004
LDV measurements and the flow analysis in the vortex region of a radial inflow turbine N90-21007
Secondary flows and Reynolds stress distributions downstream of a turbine cascade at different expansion ratios N90-21015
Numerical simulations of the cloud-capped marine boundary layer N90-21506
A self-consistent theory of radial transport of field-aligned current by microturbulence
[DE90-007920] N90-21631
Dynamics of cavitons in strong Langmuir turbulence
[DE90-006918] N90-21633
Transition from resistive-g to eta-i driven turbulence in stellarator systems
[DE90-009382] N90-21641
TURBULENCE MODELS
An approximate viscous shock layer method for calculating the hypersonic flow over blunt-nosed bodies N90-20947
An efficient airfoil design method using the Navier-Stokes equations N90-20981
Centrifugal impeller geometry and its influence on secondary flows N90-21020
PROTEUS two-dimensional Navier-Stokes computer code, version 1.0. Volume 1: Analysis description
[NASA-TM-102551] N90-21303
TURBULENT DIFFUSION
Parabolized calculations of turbulent three dimensional flows in a turbine duct N90-21013
The numerical simulation of multistage turbomachinery flows N90-21025
TURBULENT FLOW
On total variation diminishing schemes for transonic turbulent flow computation N90-20945
Parabolized calculations of turbulent three dimensional flows in a turbine duct N90-21013
Calculation of the three dimensional turbulent flow in a linear turbine blade N90-21021
Effects of secondary flow on heat transfer in rotating passages N90-21031
Depth-averaged equations for turbulent free-surface flow
[PB90-164781] N90-21308
TURBULENT HEAT TRANSFER
Improved analytical capabilities for foil air bearings, phase 1
[AD-A216071] N90-21389
TURBULENT MIXING
Cloud hole-boring with long pulse CO2 lasers
[DE90-008946] N90-21377
TVD SCHEMES
On total variation diminishing schemes for transonic turbulent flow computation N90-20945
Some aspects of Essentially Nonoscillatory (ENO) formulations for the Euler equations, part 3
[NASA-CR-4285] N90-20949
ULTRA-SHARP nonoscillatory convection schemes for high-speed steady multidimensional flow
[NASA-TM-102568] N90-21570
TWO DIMENSIONAL FLOW
An evaluation of the two-dimensional Euler and Navier-Stokes calculations based on a flux-vector splitting
[PB90-166778] N90-20963
PROTEUS two-dimensional Navier-Stokes computer code, version 1.0. Volume 1: Analysis description
[NASA-TM-102551] N90-21303
TWO DIMENSIONAL MODELS
Two-dimensional damage models of fiber-reinforced composites N90-21135
Sensitivity studies in a two-dimensional atmospheric transport model
[DAR-TP-18] N90-21496

U

U.S.S.R.
Microgravity science and applications bibliography, 1989 revision
[NASA-TM-4192] N90-21207
JPRS report: Science and technology. USSR: Electronics and electrical engineering
[JPRS-UEE-90-002] N90-21284

JPRS report. Science and technology. USSR: Earth sciences
[JPRS-UES-88-004] N90-21431
JPRS report. Science and technology. USSR: Earth sciences
[JPRS-UES-89-002] N90-21432
JPRS report: Science and technology. USSR: Life sciences
[JPRS-ULS-90-002] N90-21434
JPRS report: Science and technology. USSR: Physics and mathematics
[JPRS-UPM-90-002] N90-21593

ULTRAHIGH FREQUENCIES
Prediction of VHF/UHF mobile reception in urban areas: Comparison with measurements in London
[BBC-RD-1989/11] N90-21255

ULTRAHIGH VACUUM
Materials for ultra-high vacuum
[DE90-007908] N90-21217

ULTRASONIC WAVE TRANSDUCERS
Ultrasonic techniques for aircraft ice accretion measurement N90-20926

ULTRASONICS
Some recent applications of laser ultrasound to the characterisation of materials
[AERE-R-13438] N90-21374
On-line assessment of weld quality using ultrasonics
[AERE-R-13401] N90-21398

ULTRAVIOLET RADIATION
UV spectrometer system AFGL 801 A HUP
[AD-A217805] N90-21619

ULTRAVIOLET SPECTRA
The development of ultraviolet-ozone cleaning as a production process in the packaging of integrated circuits
[DE90-007960] N90-21220

ULTRAVIOLET SPECTROMETERS
UV spectrometer system AFGL 801 A HUP
[AD-A217805] N90-21619

ULYSSES MISSION
Final safety analysis report for the Ulysses Mission. Volume 2: Accident model document-appendices
[DE90-008695] N90-21104
Final safety analysis report for the Ulysses Mission
[DE90-008690] N90-21106
Final safety analysis report for the Ulysses mission. Volume 1: Reference design document
[DE90-008693] N90-21107

UNDERGROUND EXPLOSIONS
Minutes of the 23rd Eplosives Safety Seminar, volume 2
[AD-A218265] N90-21214

UNIVERSE
The dynamics of scalar fields in the early universe N90-21696
The large scale structure of the universe in pancake models of galaxy formation N90-21701
Horizon problem in cosmological models with non zero
[DE90-613367] N90-21708

UNIVERSITIES
Joint University Program for Air Transportation Research, 1988-1989
[NASA-CP-3063] N90-20921

UNIVERSITY PROGRAM
Investigation of air transportation technology at Princeton University, 1988-1989 N90-20935

UNSTEADY FLOW
A two-dimensional unsteady analysis for transonic and supersonic cascade flows N90-20955
Measurement of lift development on rapidly-accelerated wings N90-20956
PROTEUS two-dimensional Navier-Stokes computer code, version 1.0. Volume 1: Analysis description
[NASA-TM-102551] N90-21303
Notes on the unsteady rectilinear motion of a perfect gas. Part 8: General theory and general waves in a homentropic gas
[PB90-167149] N90-21309

UPLINKING
Weather data dissemination to aircraft N90-20934

URANIUM
Strengthening mechanisms of tungsten powder reinforced uranium
[DE90-009331] N90-21144

USER MANUALS (COMPUTER PROGRAMS)
Users manual for the NASA Lewis Ice Accretion Prediction Code (LEWICE)
[NASA-CR-185129] N90-20943
Numerical Arc Segmentation Algorithm for a Radio Conference (NASARC), version 4.0: User's manual
[NASA-TM-101454] N90-21250
PROTEUS two-dimensional Navier-Stokes computer code, version 1.0. Volume 2: User's guide
[NASA-TM-102552] N90-21306
The computational structural mechanics testbed generic structural-element processor manual
[NASA-CR-181728] N90-21410
User manual for VICONOPT: An exact analysis and optimum design program covering the buckling and vibration of prismatic assemblies of flat in-plane loaded, anisotropic plates, with approximations for discrete supports, and transverse stiffeners
[NASA-CR-181966] N90-21413
Hypercluster parallel processing library user's manual
[NASA-CR-185231] N90-21552
OTTER (Organized Techniques for Theorem-proving and Effective Research) 2.0 users guide
[DE90-007978] N90-21563
Program CICC: Flow and heat transfer in Cable In Conduit Conductors, user's manual
[DE90-007924] N90-21661

USER REQUIREMENTS
Goes I-M and beyond: Science requirements and technology challenges N90-21067

V

VALVES
Apparatus for mixing solutions in low gravity environments
[NASA-CASE-MFS-26047-1] N90-21209
Double valve mechanism for an acoustic modulator
[AD-D014401] N90-21386

VANES
Navier-Stokes analysis of turbine blade heat transfer
[NASA-TM-102496] N90-21300

VAPOR DEPOSITION
Extrinsic germanium Blocked Impurity Bank (BIB) detectors N90-21322
Characterization and comparison of optically transparent conducting films
[DE90-000319] N90-21660

VAPOR PHASE EPITAXY
Peeled film GaAs solar cells for space power
[NASA-TM-103125] N90-21287
Germanium Blocked Impurity Band (BIB) detectors N90-21321

VARIABLE STARS
AFGL ten micron mosaic array spectrometer: Recent results N90-21333

VARIABLE SWEEP WINGS
An aerodynamic tradeoff study of the scissor wing configuration
[NASA-CR-186576] N90-20965

VARIATIONAL PRINCIPLES
Direct formulation of a 4-node hybrid shell element with rotational degrees of freedom
[NASA-CR-4262] N90-21411

VARIATIONS
Specific heat and critical fluctuations in anisotropic high-T(sub c) oxide superconductors
[DE90-613394] N90-21651
A mechanism for the formation of knots, kinks and discontinuous events in the plasma tail of comets
[DE90-613285] N90-21707

VECTOR ANALYSIS
A numerical and theoretical study of seismic wave diffraction in complex geologic structure
[AD-A218209] N90-21490

VECTOR SPACES
On induced Hermitian metrics for holomorphic vector bundles
[DE90-612737] N90-21572

VEGETATION
Wheat yield estimation at the farm level using LANDSAT TM and agrometeorological data
[INPE-5017-RPE/611] N90-21439
Monitoring of agrocattle-raising projects through visual/digital analysis of LANDSAT-TM imagery south of Para state
[INPE-4982-PRE/1542] N90-21442
Monitoring vegetation of Brazil: Potentialities of multi-sensors approach
[INPE-4993-PRE/1555] N90-21451
Evolution of remote sensing applied to vegetation and forest at INPE
[INPE-4970-PRE/1538] N90-21452
Multitemporal analysis of LANDSAT/TM digital imagery in the detection of areas affected by caterpillar (sibine fusca) attack in the dende (elais guineensis) palm plantation
[INPE-4979-PRE/1544] N90-21457
Performance evaluation of MSS/LANDSAT data in the estimation of fluvial channel width
[INPE-4906-PRE/1507] N90-21463
Modeling large-scale vegetation dynamics
[DE90-008883] N90-21485

VELOCITY
Laser velocimeter measurements of multiphase flow of solids
[DE90-007804] N90-21311

VELOCITY DISTRIBUTION
The optical measurement of acoustic velocity fields N90-21601

VELOCITY MEASUREMENT
A fiber optic sensor for noncontact measurement of shaft speed, torque, and power
[NASA-TM-102481] N90-21360
The optical measurement of acoustic velocity fields N90-21601

VENTING
Liquid Transfer Cryogenic Test Facility: Initial hydrogen and nitrogen no-vent fill data
[NASA-TM-102572] N90-21295

VENUS (PLANET)
High resolution imaging of the Venus night side using a Rockwell 128x128 HgCdTe array N90-21330

VENUS ATMOSPHERE
High resolution imaging of the Venus night side using a Rockwell 128x128 HgCdTe array N90-21330

VERY HIGH FREQUENCIES
Prediction of VHF/UHF mobile reception in urban areas: Comparison with measurements in London
[BBC-RD-1989/11] N90-21255

VERY LARGE SCALE INTEGRATION
VLSI single-chip (255,223) Reed-Solomon encoder with interleaver
[NASA-CASE-NPO-17280-1-CU] N90-21061
VLSI binary updown counter
[NASA-CASE-NPO-17205-1-CU] N90-21525

VIBRATION
User manual for VICONOPT: An exact analysis and optimum design program covering the buckling and vibration of prismatic assemblies of flat in-plane loaded, anisotropic plates, with approximations for discrete supports, and transverse stiffeners
[NASA-CR-181966] N90-21413
The Shock and Vibration Digest, volume 22, no. 2 N90-21596
The optical measurement of acoustic velocity fields N90-21601

VIBRATION DAMPING
PACOSS program status and results N90-21065
Vibration isolation versus vibration compensation on multiple payload platforms N90-21066
Nonlinear and distributed parameter models of the mini-mast truss N90-21070
LACE flight dynamics experiment N90-21086
Initial operational capability of the ASTREX large space structures test bed N90-21091
Multi-objective shape and material optimization of composite structures including damping
[NASA-TM-102579] N90-21132
A review of gear housing dynamics and acoustics literature
[NASA-CR-185148] N90-21387
Internal rotor friction instability
[NASA-CR-183942] N90-21395

VIBRATION EFFECTS
Transportation monitoring unit qualification
[NASA-CR-183930] N90-21060

VIBRATION MODE
Experimental and theoretical investigation of optimal control methods with model reduction N90-21039
Integrated modeling and analysis of a space-truss article
[NASA-TM-102615] N90-21412

VIBRATION TESTS
The Shock and Vibration Digest, volume 22, no. 2 N90-21596

VISCOELASTICITY
Stress analysis of rocket motors with viscoelastic propellant by a mixed finite element model N90-21112
LaRC TPI 1500 series polymers
[NASA-CR-181899] N90-21129
Determinations of molecular weight and molecular weight distribution of high polymers by the rheological properties
[NASA-CR-186450] N90-21180

VISCOPLASTICITY
Thermomechanical deformation testing and modeling in the presence of metallurgical instabilities
[NASA-CR-185188] N90-21420

VISCOSITY
Measurement of lift development on rapidly-accelerated wings N90-20956
The effect of viscosity on the resistive tearing mode with the presence of shear flow
[DE90-009340] N90-21312

VISCOUS FLOW
Relating flow between counter-rotating propellers to aerodynamic interaction noise N90-20944

Comparison of C- and O-grid generation methods using a NACA 0012 airfoil
[AD-A216375] N90-20948
Effects of nose bluntness and shock-shock interactions on blunt bodies in viscous hypersonic flows
[NASA-CR-186451] N90-20950
Computation of viscous flow around a propeller-shaft configuration with infinite-pitch rectangular blades N90-20958
Centrifugal impeller geometry and its influence on secondary flows N90-21020
Generation and decay of secondary flows and their impact on aerodynamic performance of modern turbomachinery components N90-21023
PROTEUS two-dimensional Navier-Stokes computer code, version 1.0. Volume 2: User's guide
[NASA-TM-102552] N90-21306

VISCOUS FLUIDS
Mixing of viscous fluids: Behavior of microstructures and chaos
[DE90-006871] N90-21304

VISIBILITY
Modified touchdown zone lighting
[DOT/FAA/CT-TN89/70] N90-21042
Apparatus and method for locating the axis of symmetry (center of circular cross section) of three dimensional objects
[AD-D014407] N90-21354
Analysis of distributions of Visual Meteorological Conditions (VMC) heliport data
[DOT/FAA/CT-TN89/67] N90-21508

VISIBLE INFRARED SPIN SCAN RADIOMETER
Preliminary report on the demonstration of the VAS CO2 cloud parameters (cover, height, and amount) in support of ASOS
[NOAA-TM-NESDIS-29] N90-21498

VOIDS
Fiber optic void fraction sensor
[DE90-009124] N90-21366
A casting and imaging technique for determining void geometry and relative permeability behavior of a single fracture specimen
[DE90-009192] N90-21403

VOLATILITY
Improved Thermo-Oxidative-Deposition screening tests for turbine lubricants
[AD-A217795] N90-21188

VORTEX BREAKDOWN
Numerical simulation of vortex breakdown N90-21288

VORTEX RINGS
Rings
[DE90-009035] N90-21613

VORTEX SHEDDING
Secondary flows and Reynolds stress distributions downstream of a turbine cascade at different expansion ratios N90-21015

VORTICES
Discrete-vortex model for the symmetric-vortex flow on cones
[NASA-TP-2989] N90-20946
Measurement of lift development on rapidly-accelerated wings N90-20956
Experimental and numerical investigation of the vortex flow over a sharp edged delta wing; with and without sideslip
[PB90-167131] N90-20964
LDV measurements and the flow analysis in the vortex region of a radial inflow turbine N90-21007
Experimental and numerical study on basic phenomena of secondary flows in turbines N90-21014
Secondary flows and Reynolds stress distributions downstream of a turbine cascade at different expansion ratios N90-21015
On the instability of Goertler vortices to nonlinear travelling waves
[NASA-CR-181994] N90-21289
A time-accurate adaptive grid method and the numerical simulation of a shock-vortex interaction
[NASA-TP-2998] N90-21524
Instabilities and vortex dynamics in shear flow of magnetized plasmas
[DE90-009448] N90-21643

VORTICITY
Secondary flow calculations for axial and radial compressors N90-21024

VORTICITY EQUATIONS
Tropical cyclone track predictability and the adjoint method of data assimilation
[AD-A218324] N90-21505

VULNERABILITY
Pressure rig for repetitive casting
[NASA-CASE-LAR-14050-1] N90-21216

W

WAFERS
Germanium Blocked Impurity Band (BIB) detectors N90-21321
The investigation of multilayer x ray reflectors as x ray optical elements
[DE90-009044] N90-21621

WAKES
Comparison of C- and O-grid generation methods using a NACA 0012 airfoil
[AD-A216375] N90-20948
A correlation-spectral method for line detection on noisy data
[DE90-007925] N90-21266

WALL FLOW
Aerodynamic optimization by simultaneously updating flow variables and design parameters N90-20991
The effects of compressor endwall flow on airfoil incidence and deviation N90-21011

WALLS
Perforation of a reinforced concrete wall by a rigid missile
[AD-A210025] N90-21381

WARNING SYSTEMS
Joint University Program for Air Transportation Research, 1988-1989
[NASA-CP-3063] N90-20921
Cockpit display of hazardous weather information N90-20929
Selective automatic fire extinguisher for computers (SAFECOMP): Developmental test and evaluation/initial operational test and evaluation
[AD-A217790] N90-21212
Rapidly quantifying the relative distention of a human bladder
[NASA-CASE-LAR-13901-1-NP] N90-21519

WATER
Depth-averaged equations for turbulent free-surface flow
[PB90-164781] N90-21308
Digital processing of TM/LANDSAT data in monitoring interior water
[INPE-4956-PRE/1533] N90-21448
Thermal decay of an initially hot isothermal water body with application to thermal energy storage
[DE90-614742] N90-21675

WATER CIRCULATION
MECCA program documentation
[NOAA-TR-NESDIS-46] N90-21477

WATER DEPTH
Analysis of water quality parameters of the Piaui River (SE), Brazil, through field and TM/LANDSAT sensor data
[INPE-4918-PRE/1417] N90-21453

WATER MASERS
New water vapor masers in the Southern Hemisphere
[INPE-4844-PRE/1473] N90-21689

WATER QUALITY
Remote sensing applied to sea water quality researches in coastal regions: A review
[INPE-4935-PRE/1425] N90-21438
Analysis of water quality parameters of the Piaui River (SE), Brazil, through field and TM/LANDSAT sensor data
[INPE-4918-PRE/1417] N90-21453

WATER VAPOR
New water vapor masers in the Southern Hemisphere
[INPE-4844-PRE/1473] N90-21689

WAVE DIFFRACTION
A numerical and theoretical study of seismic wave diffraction in complex geologic structure
[AD-A218209] N90-21490

WAVE DISPERSION
MHD modes driven by anomalous electron viscosity and their role in fast sawtooth crashes
[DE90-009311] N90-21639
Coupled magnetoplasmon-phonon modes at the surface of a semi-infinite semiconductor superlattice
[DE90-612904] N90-21647

WAVE EQUATIONS
Stability of a solitary wave solution to a set of coupled Boussinesq-like equations
[DE90-008927] N90-21586
On the stability of a certain difference scheme
[PB90-165614] N90-21588

WAVE EXCITATION
Full wave computation of electromagnetic wave excitation, propagation, and absorption at the ion cyclotron frequency in fusion experiments
[DE90-009399] N90-21642

WAVE FRONTS
Method for holographic correction of beams of coherent light
[AD-D014406] N90-21353

WAVE FUNCTIONS
Modified tight-binding approximation and electron-phonon spectral function for transition metals
[DE90-814022] N90-21166
Large basis space effects in electron scattering form factors of light nuclei
[DE90-613501] N90-21609

WAVE INTERACTION
A numerical and theoretical study of seismic wave diffraction in complex geologic structure
[AD-A218209] N90-21490
Langmuir wave interaction with ion acoustic wave
[DE90-615407] N90-21624

WAVE PROPAGATION
Discrete modeling of beds of propellant exposed to strong stimulus
[DE90-008932] N90-21206
A numerical and theoretical study of seismic wave diffraction in complex geologic structure
[AD-A218209] N90-21490
On the relativistic Vlasov equation in guiding-center coordinates
[DE90-613241] N90-21629
Full wave computation of electromagnetic wave excitation, propagation, and absorption at the ion cyclotron frequency in fusion experiments
[DE90-009399] N90-21642

WAVEFORMS
SAR and ISAR imagery of marine targets N90-21237

WAVEGUIDE ANTENNAS
The 5th Annual Review of Progress in Applied Computational Electromagnetics
[AD-A217994] N90-21258
Coplanar waveguide fed phased array antenna
[NASA-TM-102522] N90-21273

WAVEGUIDES
New ferrite-filled waveguiding structures analysed by the averaging method
[PB90-165671] N90-21269
Coplanar waveguide discontinuities for P-I-N diode switches and filter applications
[NASA-TM-102534] N90-21278
Low frequency gyrotron amplifier investigation, phase 2
[AD-A217096] N90-21352
Active control of multi-dimensional random sound in ducts
[NASA-TM-102653] N90-21603

WEAR
Studies of mechano-chemical interactions in the tribological behavior of materials
[NASA-TM-102545] N90-21182

WEAR RESISTANCE
Energy beam treatment for improved adhesion of coatings to surfaces
[AD-D014449] N90-21190

WEATHER
Investigation of air transportation technology at the Massachusetts Institute of Technology, 1988-1989 N90-20922
Cockpit display of hazardous wind shear information N90-20924
Cockpit display of hazardous weather information N90-20929
Weather data dissemination to aircraft N90-20934
Plan for the FAA air traffic operational evaluation of the Automated Surface Observing System (ASOS)
[DOT/FAA/CT-TN89/56] N90-20968
Final safety analysis report for the Ulysses Mission. Volume 3 (Book 2): Nuclear risk analysis document-appendices
[DE90-008692] N90-21102
Meteorologist Weather Processor (MWP) integration test plan
[DOT/FAA/CT-TN89/62] N90-21500
Analysis of distributions of Visual Meteorological Conditions (VMC) heliport data
[DOT/FAA/CT-TN89/67] N90-21508

WEATHER FORECASTING
The influence of ice accretion physics on the forecasting of aircraft icing conditions N90-20928
Predictability of weather and climate in a coupled ocean-atmosphere model: A dynamical systems approach
[NASA-CR-186499] N90-21502
Tropical cyclone track predictability and the adjoint method of data assimilation
[AD-A218324] N90-21505

WEATHERING
Collapsible fabric tank testing
[AD-A217861] N90-21388

WEIERSTRASS FUNCTIONS
Weierstrass preparation and division theorems for the ring of germs of superanalytic functions
[DE90-612742] N90-21576

WEIGHT REDUCTION
Multi-objective shape and material optimization of composite structures including damping
[NASA-TM-102579] N90-21132
Transmission research activities at NASA Lewis Research Center
[NASA-TM-103132] N90-21394
WEIGHTING FUNCTIONS
A note on overdispersed exponential families
[AD-A216277] N90-21565
WEIGHTLESSNESS
Space truss zero gravity dynamics N90-21087
In-house experiments in large space structures at the Air Force Wright Aeronautical Laboratories Flight Dynamics Laboratory N90-21092
BASG thermomechanical pump helium 2 transfer tests
[NASA-CR-177541] N90-21097
WELD STRENGTH
On-line assessment of weld quality using ultrasonics
[AERE-R-13401] N90-21398
WELDED JOINTS
The effects of a nearby subsequent fusion weld on the properties of an inertia friction weld
[DE90-007972] N90-21396
WELDING
Materials for ultra-high vacuum
[DE90-007908] N90-21217
Attachment of lead wires to thin film thermocouples mounted on high temperature materials using the parallel gap welding process
[NASA-TM-102442] N90-21361
WENTZEL-KRAMER-BRILLOUIN METHOD
Generalized WKB approximation for stratified isotropic chiral structures
[PB90-165689] N90-21270
WETTING
Critical point wetting drop tower experiment
[NASA-CR-186513] N90-21208
WHEAT
Wheat yield estimation at the farm level using LANDSAT TM and agrometeorological data
[INPE-5017-RPE/611] N90-21439
Wheat productivity estimate through field radiometry
[INPE-4994-PRE/1556] N90-21460
WHEELS
Design of a digital model following controller of reaction wheel torques
[INPE-4753-PRE/1425] N90-21093
WHISKER COMPOSITES
Research advances in fine ceramics
[DE90-008983] N90-21197
WIND MEASUREMENT
Editing wind profiler measurements
[PB90-130147] N90-21503
WIND PROFILES
Editing wind profiler measurements
[PB90-130147] N90-21503
WIND SHEAR
Joint University Program for Air Transportation Research, 1988-1989
[NASA-CP-3063] N90-20921
Investigation of air transportation technology at the Massachusetts Institute of Technology, 1988-1989 N90-20922
Cockpit display of hazardous wind shear information N90-20924
Cockpit display of hazardous weather information N90-20929
Investigation of air transportation technology at Princeton University, 1988-1989 N90-20935
An expert system for wind shear avoidance N90-20938
Airborne Doppler radar flight experiments for the detection of microbursts N90-21243
Windshear case study: Denver, Colorado, July 11, 1988
[DOT/FAA/DS-89/19] N90-21509
WIND TUNNEL TESTS
Investigation of air transportation technology at the Massachusetts Institute of Technology, 1988-1989 N90-20922
Laser-velocimeter-measured flow field around an advanced, swept, eight-blade propeller at Mach 0.8
[NASA-TP-2462] N90-20942
An approximate viscous shock layer method for calculating the hypersonic flow over blunt-nosed bodies N90-20947
Performance data from a wind-tunnel test of two main-rotor blade designs for a utility-class helicopter
[NASA-TM-4183] N90-20974
Advanced instrumentation for aircraft icing research
[NASA-CR-185225] N90-21006
Measurement of the flow field in the blade passage and side-wall region of a plane turbine cascade N90-21019
Detailed heat transfer measurements in nozzle guide vane passages in linear and annular cascades in the presence of secondary flows N90-21030
Experimental aeroelasticity history, status and future in brief
[NASA-TM-102651] N90-21047
WIND TUNNELS
Modeling of surface roughness effects on glaze ice accretion N90-20925
WIND TURBINES
Parametric resonance in horizontal axis wind turbines N90-20962
WINDS ALOFT
Low latitude F-region dynamical processes from atomic oxygen nightglow emissions
[INPE-4999-PRE/1561] N90-21494
WINDSHIELDS
The effect of windscreen bows and HUD pitch ladder format on pilot performance during simulated flight
[AD-A218139] N90-21523
WING PROFILES
Measurement of lift development on rapidly-accelerated wings N90-20956
WINGS
Progress in inverse design and optimization in aerodynamics N90-20977
Aerofoil design techniques N90-20978
A system for transonic wing design with geometric constraints based on an inverse method N90-20983
Constrained spanload optimization for minimum drag of multi-lifting-surface configurations N90-20992
Numerical optimization of wings in transonic flow N90-20997
WIRE
Attachment of lead wires to thin film thermocouples mounted on high temperature materials using the parallel gap welding process
[NASA-TM-102442] N90-21361
WIRING
Boeing 727-100 test project (high energy radiated field tests)
[DOT/FAA/CT-88/33] N90-21247
WORDS (LANGUAGE)
Permuted medical subject headings, 1990
[PB90-100025] N90-21684

X

X RAY DIFFRACTION
Retabulation of space group extinctions for electron diffraction
[DE90-612933] N90-21648
Thermogravimetric analysis of Nd(2-x)Ce(x)CuO(4-delta)
[DE90-009184] N90-21658
X RAY IMAGERY
Absolute multilayer characterization at high spatial resolution via real-time soft x ray imaging
[DE90-009181] N90-21371
X RAY LASERS
X ray laser with enhanced x ray gain through photodepopulation
[AD-D014448] N90-21375
X RAY SCATTERING
Design and optimisation of thin foil x ray telescopes N90-21690
X RAY TELESCOPES
Design and optimisation of thin foil x ray telescopes N90-21690
X RAYS
The investigation of multilayer x ray reflectors as x ray optical elements
[DE90-009044] N90-21621
Design and optimisation of thin foil x ray telescopes N90-21690
Relativistic processes in active galactic nuclei N90-21698
High energy phenomena during solar flares
[INPE-4961-TDL/390] N90-21713

Y

YIELD STRENGTH
A computational model of the perforation of multi-layer metallic laminates
[MRL-RR-9-89] N90-21128
YTTRIUM OXIDES
Deformation processing of YBa2Cu3O(sub x)
[DE90-007795] N90-21644
On the substitution of Sr ions at Y sites in YB(suba2)Cu3O(sub7-d)
[DE90-613395] N90-21652

Z

ZERO ANGLE OF ATTACK
The radiation of sound from a propeller at angle of attack
[NASA-CR-4264] N90-21602
ZETA PINCH
Fusion burn dynamics in Dense Z-Pinch (DZP)
[DE90-007976] N90-21638
ZINC OXIDES
Characterization and comparison of optically transparent conducting films
[DE90-000319] N90-21660

PERSONAL AUTHOR INDEX

Typical Personal Author Index Listing

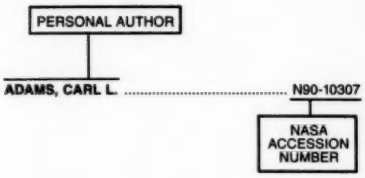

Listings in this index are arranged alphabetically by personal author. The NASA accession number denotes the number by which the citation is identified.

A

ABE, Y. N90-21643
ABKOWITZ, STANLEY N90-21183
ABKOWITZ, SUSAN M. N90-21183
ABOU-GABAL, HANAA HASSAN N90-21625
ADAMCZYK, J. J. N90-21025
ADAMOVSKY, G. N90-21277
ADE, P. N90-21343
ADJEPONG, S. K. N90-21675
ADMOAITIS, R. A. N90-21558
AGNESE, P. N90-21344
AHMAD, JASIM UDDIN N90-21288
AHUJA, NARENDRA N90-21557
AKDENIZ, Z. N90-21150
AKISHIN, P. G. N90-21547
AKMANDOR, I. S. N90-20986
AL-BERMANI, F. G. A. N90-21426
ALBERT, STUART D. N90-21251
ALLEN, D. N90-21330
ALLISON, SIDNEY G. N90-21170
ALLONGUE, M. N90-20995
ALMEIDAABREU, PEDRO ANGELO N90-21450
ALVES, DIOGENES SALAS N90-21445
AMINPOUR, MOHAMMAD A. N90-21411
AMOS, K. N90-21609
ANDERSON, L. E. N90-21514
ANDERSON, LEON P., JR. N90-21298
ANDERSON, M. S. N90-21413
ANDERSON, ROBERT B. N90-21386
ANDREWS, HAROLD N90-21003
ANDREWS, J. W. N90-21218
ANTAL, J. J. N90-21174
ANTONIODASILVA, ERIVALDO N90-21464
APELT, C. J. N90-21308
ARMSTRONG, F. E. N90-21607
ARNOLD, C., JR. N90-21186
ARTILES, A. N90-21395
ASAY, BIAINE W. N90-21206
ASAY, J. R. N90-21057
ASMOLOV, A. G. N90-21546
ASPIN, COLIN N90-21327
ASTAKHOV, A. YA. N90-21615
ASTON, G. N90-21413
ASWATH, C. N90-21043
ATHERTON, L. J. N90-21666
AUBRUN, JEAN-NOEL N90-21082
AUVINE, BRIAN N90-21501
AUXILIADORASANTOS, MARIA N90-21454
AVANS, S. L. N90-21095
AYDEMIR, A. Y. N90-21639
AYDIN, R. N90-21362
AYRES, C. F. N90-21179
AZEVEDO, S. G. N90-21404
AZUMI, MASAFUMI N90-21630

B

BACHALO, W. N90-21006
BADINELLI, MARTIN N90-21248
BAE, YOON-YEONG N90-21034
BAER, D. N90-21645
BAI, JIA-MO N90-21129
BAILEY, BRUCE H. N90-21504
BAILEY, M. C. N90-21279
BAILEY, S. G. N90-21287
BALACHANDRAN, U. N90-21645
BALAS, MARK J. N90-21077
BALKWILL, P. N90-21159
BALTZLEY, D. R. N90-21521
BANDEL, HANNSKARL N90-21099
BARBEN, C. L. N90-21151
BARBOSA, MARX PRESTES N90-21450
BARKMAN, W. E. N90-21688
BARNES, MICHAEL J. N90-21523
BARNS, DAVID W. N90-21487
BARON, A. N90-20994
BARTH, HELMUT N90-21226
BARTHOLOMEW, P. N90-20972
N90-20973
BASILI, VICTOR R. N90-21531
N90-21532
BASSOM, ANDREW P. N90-21289
BATCHELOR, D. B. N90-21642
BATES, A. D. N90-21649
BATES, J. L. N90-21468
BATES, JACK R. N90-21002
BATISTA, GETULIO T. N90-21439
N90-21441
N90-21455
N90-21460
BAUM, BRYAN ALAN N90-21491
BAUMANN, H. N90-21321
BAUMEISTER, JOSEPH F. N90-21296
BAXTER, B. J. N90-21044
BAYSAL, OKTAY N90-20953
BEACH, T. A. N90-21025
BECKWITH, S. V. W. N90-21349
BEECHER, P. F. N90-21197
BEEMAN, J. W. N90-21315
N90-21321
N90-21323
N90-21332
BEINTEMA, D. A. N90-21341
BELIN, ALLETA DA. N90-21515
BELL, VERNON L. N90-21198
BELMANS, PHILIPPE N90-21397
BELVIN, W. KEITH N90-21076
BENDETT, M. N90-21275
BENKOVITZ, CARMEN M. N90-21484
BENMOUNA, MUSTAPHA N90-21149
N90-21194
BENNETT, M. J. N90-21179
BENNION, KAREN M. N90-21357
BENSON, THOMAS J. N90-21303
N90-21306
N90-21307
BERA, RAJENDRA K. N90-21522
BERENDS, J. C. E. N90-21619
BERGAMINI, EDUARDO WHITAKER N90-21268
BERKOWITZ, BRIAN M. N90-20925
N90-20943
BERNARD, J. N90-21022
BERNSTEIN, G. M. N90-21317
BERRIAUD, C. N90-21381
BERTACHINIDEALMEIDAPRADO, ANTONIO FERNANDO N90-21054
BERTHOLD, J. W. N90-21366
BESTMAN, A. R. N90-21675
BETHKE, K.-H. N90-21239
BEYER, JAMES B. N90-21280
BHASIN, K. B. N90-21275
BHATTI, N. N90-21483
BHUNIA, S. N90-21311
BIELLO, G. D. N90-21489
BIRMAN, KENNETH P. N90-21533
N90-21555
BISCHEL, WILLIAM K. N90-21155
BITTENCOURT, J. A. N90-21494
BLACKWOOD, GARY N90-21084
BLALOCK, TRAVIS N. N90-21519
BLANCHIN, M. G. N90-21654
BLELLOCH, PAUL ANDREW N90-21074
BLES, W. N90-21518
BLESSINGER, MICHAEL N90-21337
N90-21338
N90-21339
N90-21348
BLUME, HANS-J. C. N90-21243
BOCCI, A. J. N90-20978
BOCK, K.-W. N90-20996
BOCKELIE, MICHAEL J. N90-21524
BODLUND, KAJ N90-21599
BOES, ELDON C. N90-21475
BOESSWETTER, C. N90-21224
BOFFADOSSI, MAURIZIO N90-20984
BOLCH, WESLEY E. N90-21108
BOREL, C. C. N90-21486
BORGES, JOAO EDUARDO N90-20989
BOS, J. E. N90-21518
BOURCIER, RAY J. N90-21430
BOVINO, LAWRENCE J. N90-21055
BOWLES, DAVID E. N90-21140
BOWLES, KENNETH J. N90-21124
BOWLES, R. I. N90-21290
BOYLE, R. J. N90-21300
BRACALENTE, E. M. N90-21243
BRADLEY, D. K. N90-21378
BRANDSMA, F. J. N90-20983
BRANDSTAEDTER, A. N90-21644
BRANOVICH, LOUIS E. N90-21211
BREWER, TERRY K. N90-21405
BRINKER, D. J. N90-21287
BRITT, C. L. N90-21243
BROCKLEHURST, F. K. N90-21374
BROOKS, WALTER F. N90-21345
BROOM, MARY B. N90-21209
BROPHY, CAROLYN ELIZABETH N90-21538
N90-21544
BROSS, ALAN D. N90-21367
BROWN, DAVID WARD N90-21172
BROWN, STEVEN A. N90-21482
BROWNLEE, D. E. N90-21098
BRUCE, WILLIAM DAVID N90-21440
BRUEMMER, S. M. N90-21167
BRUNNER, A. N90-21234
BRYAN, KEVIN N90-20971
BUBB, KEITH W. N90-21088
BUCHELNIKOVA, N. S. N90-21624
BUCHOLTZ, FRANK N90-21620
BUHLER, MELANIE N90-21536
BUNCH, T. E. N90-21098
BURCH, I. A. N90-21044
BURDETTE, GEORGE W. N90-21111
BURGDORF, M. N90-21342
N90-21350
BURSILL, L. A. N90-21654
BUSCHE, DONNA M. N90-21108
BUTLER, R. N90-21413
BUTTLE, D. J. N90-21121
N90-21374
BYRKA, RYSZARD N90-21708

C

CAIRD, J. A. N90-21666
CALIUS, EMILIO P. N90-21119
CAMBIER, L. N90-21021
CANNON, ROBERT H., JR. N90-21383
CANTRELL, JOHN H. N90-21170
CARLETTI, U. N90-21231
CARLIP, STEVEN N90-21679
CARLSSON, CARL-AXEL N90-21599
CARNEY, KELLY N90-21074
CARR, T. W. N90-21277
CARSCALLEN, W. E. N90-21033
CARTER, DANIEL C. N90-21209
CARTER, DONALD L. N90-21365
CASALI, MARK M. N90-21327
CASSATELLA, A. N90-21693
CASTEJONGARCIA, EZIO N90-21105
CASTELLI, MICHAEL G. N90-21420
CAVALIER, ALBERT R. N90-21519
CAVANAGH, RICHARD R. N90-21380
CELESTINA, M. L. N90-21025
CELSODECARVALHO, VITOR N90-21452

CESARSKY, C. N90-21344
CETINKAYA, T. A. N90-20986
CHAKRAVARTHY, SUKUMAR R. N90-20949
CHAMBERLAIN, JAY L. N90-21475
CHAMIS, CHRISTOS C. N90-21131
N90-21132
N90-21137
CHANG, C. W. N90-21066
CHANG, EDDI L. N90-21185
CHANG, TOM T. S. N90-21488
CHAPPELL, P. J. C. N90-21120
CHARLOT, L. A. N90-21167
CHASE, L. L. N90-21668
CHATTOPADHYAY, SWAPAN N90-21379
CHAUDHRY, M. B. N90-21629
CHEN, JENKON N90-21348
CHEN, MING-HSIUNG N90-20945
CHEN, NAN-XIAN N90-21594
CHEN, R. C. N90-21311
CHEN, TIMOTHY S. N90-21177
CHEN, X. L. N90-21312
CHENOWETH, DARRELL L. N90-21260
CHEO, BERNARD R. N90-21352
CHEREPANOV, ANDREI S. N90-21269
CHEUNG, SAMSON HOK-CHI N90-20957
CHEW, KAREN N90-21512
CHIANG, TING-LUNG N90-20954
CHICK, L. A. N90-21468
CHO, WHANG N90-21391
CHOUDHARY, ALOK N. N90-21557
CHOW, EDWARD N90-21527
CHRISTIANSEN, PETER L. N90-21586
CHRISTOV, KONSTANTIN N90-21512
CHU, CHENG-CHIH N90-21084
CHUONG, NGUYEN MINH N90-21574
CLASPY, P. C. N90-21275
COENE, R. N90-21425
COLEY, K. S. N90-21179
COLLINS, CLARENCE N90-21363
COLLINS, JOHN N90-20967
COLLINS, TIMOTHY J. N90-21096
COMBS, DAN N90-20971
COMBS, S. K. N90-21056
COMPANION, JOHN A. N90-21519
CONDRON, DAVID N90-20971
CONROY, PAULA J. N90-21133
COOK, M. N90-21060
N90-21117
COOLEY, VICTOR M. N90-21080
COOMES, E. P. N90-21474
CORDES, JENNIFER N90-21416
CORREIA, EMILIA N90-21713
COSGROVE, COLIN B., JR. N90-21100
COUNSELMAN, CHARLES C., III N90-21052
COUSINS, FRANK W. N90-21359
COX, B. L. N90-21403
CREAMER, J. E. N90-21646
CREPANI, EDISON N90-21437
CRISPIN, R. M. N90-21178
CROUCH, IAN G. N90-21128
CROWTHER, T. N90-21247
CUCINOTTA, FRANCIS A. N90-21715
CULBERTSON, PHILIP E. N90-21050
CULIOLI, JEAN-CHRISTOPHE N90-21397
CUMMINGS, JAMES RICHARD N90-21716
CUSHMAN, ARTHUR N90-21248
CZERNER, M. J. N90-21279

D

DABROWSKI, MARIUSZ P. N90-21708
DACOSTA, J. M. N90-21714
DACOSTAPEREIRA, MARCOS N90-21451
DACUNHATRIVELATO, GILBERTO N90-21093
DADDIO, E. N90-21231
DAGLEY, IAN J. N90-21203
DAHMEN, U. N90-21656
N90-21657
DALAL, S. R. N90-21565
DANDRIDGE, ANTHONY N90-21620
DANFORD, M. D. N90-21191
DANZEY, GERALD A. N90-21361
DARYOUSH, A. S. N90-21261
DAVIS, R. L. N90-21613
DAVIS, W. A. N90-21262
DAWICKE, D. S. N90-21424
DAYI, OMER F. N90-21671
DEANGELO, F. L. N90-21287
DEATON, JOHN E. N90-21523
DECKER, WILLIAM N90-21543
DEGRAAF, B. N90-21518
DEGROH, KIM K. N90-21110
DEGUIRE, M. R. N90-21402
DEHART, D. W. N90-21090
DELAHOY, A. E. N90-21473
DELETTREZ, C. N90-21343
DELFINODAVILAMASCARENHAS, NELSON N90-21464
DELOURDESNDEOKURKDJIAN, MARIA N90-21443
DELPIZZO, VINCENT N90-21520
DELUCIA, R. A. N90-21008
DEMEDEIROS, JOSE SIMEAO N90-21457
DEMORISSONVALERIANO, DALTON N90-21454
DEMOURAABDON, MYRIAN N90-21438
N90-21453
N90-21454
DEPONTE, SERGIO N90-20984
DERUYCK, J. N90-21010
DESTARAC, D. N90-20997
DETEMPLE-LAAKE, E. N90-21019
DEUTSCH, LESLIE J. N90-21061
DEVER, THERESE M. N90-21110
DEVLOO, PHILIPPE REMY BERNARD N90-21115
N90-21595
DEYONG, LEO V. N90-21201
DIAMOND, P. H. N90-21631
DIB, N. I. N90-21278
DIDION, DAVID N90-21305
DILL, J. N90-21395
DINWIDDIE, RALPH B. N90-21154
DIXON, P. W. N90-21222
DO, DUNG N90-20967
DODDER, D. C. N90-21607
DOEDERLEIN, T. N90-21090
DOMINY, R. G. N90-21016
DONASCIMENTOFEITOSA, EVERALDO ALENCAR
N90-20962
DONLAN, VINCENT L. N90-21720
DORRIS, S. E. N90-21645
DOSANJOSFERREIRAPINTO, SERGIO N90-21462
N90-21463
DOSSANTOS, JOAO ROBERTO N90-21451
DOTY, WAYNE A. N90-20952
DOUCETT, NOEL A. N90-21256
DOUVIKAS, D. N90-21024
DOWLA, FARID N90-21266
DRIFTMYER, RICHARD T. N90-21293
DRING, ROBERT P. N90-21011
DROBAC, D. N90-21652
DUBOIS, D. F. N90-21633
DUC, DUONG MINH N90-21575
DUDENHOEFER, JAMES E. N90-21114
DUDLEY, K. L. N90-21279
DUFFILL, C. N90-21398
DUKE, C. B. N90-21663
DUTOYA, DENIS N90-21032
DYER, MARK J. N90-21155

E

ECEVIT, F. N. N90-21362
ECKART, DONALD W. N90-21211
EDESKUTY, FREDERICK J. N90-21667
EDMONDS, J. A. N90-21487
EIJISANO, EDSON N90-21442
N90-21457
EISEMAN, PETER R. N90-21524
EISENHARDT, PETER N90-21345
ELANDS, P. J. M. N90-21310
ELANGOVAN, S. N90-21467
ELDRED, D. B. N90-21089
ELLIOTT, S. J. N90-21603
ELLIS, F. B. N90-21473
ELTON, RAYMOND C. N90-21375
EMANUEL, WILLIAM R. N90-21485
ENDER, J. N90-21241
ENG, ANTHONY T. N90-21184
ENTING, I. G. N90-21496
EPPIG, R. C. N90-21619
ERICKSON, E. F. N90-21348
ERKILET, MURAT N90-21012
ERRICO, RONALD M. N90-21497
ERTHAL, GUARACI JOSE N90-21444
ESCANDE, B. N90-21021
ESKER, LINDA N90-21539
N90-21541
N90-21542
ESTRADA, JOHN A. N90-21347

F

FALCHETTI, F. N90-21022
FALLOT, JEAN-MARC N90-21232
FANSON, JAMES N90-21084
FARBER, R. M. N90-21558
FARINA, A. N90-21231
FARIS, GREGORY W. N90-21155
FARMER, J. DOYNE N90-21515
FATEMI, N. S. N90-21287
FEHRENBACHER, LARRY N90-21188
FEITT, ROBERT N90-21325
FELDMAN, HUME A. N90-21696
FELGUEIRAS, CARLOS ALBERTO N90-21447
FENOU, MARIE N90-21237
FENTON, B. C. N90-21008
FERNANDEZ, N. S. N90-21273
FERNAU, M. E. N90-21483
FERRAINOLO, JOHN J. N90-21164
FERRAND, P. N90-21013
FERREIRA, JULIO GUIMARAES N90-21628
FERRETTA, THEODORE E. N90-21584
FIELDER, WILLIAM L. N90-21469
FILHO, PEDRO HERNANDEZ N90-21451
FISHER, SHALOM N90-21086
FITZGERALD, MARK N90-21201
FITZSIMONS, PHILIP MATTHEW N90-21040
FLOOD, DENNIS J. N90-21274
FLUSS, M. J. N90-21156
FOLSOM, ROLFE A. N90-21294
FOLZ, WALTER N90-21334
FONSECA, LEILA MARIA GARCIA N90-21444
FOREMAN, R. J. N90-21153
FORESTI, CELINA N90-21443
FORNASIER, L. N90-20982
FORREST, JOHN R. N90-21554
FORREST, W. J. N90-21326
N90-21329
FOSS, JOHN F. N90-21301
FOWLER, A. N90-21331
FOWLKES, J. E. N90-21521
FRAKER, ANNA C. N90-21162
FRANCA, LEOPOLDO P. N90-21428
FRANCIS, JOHN P. N90-21111
FRANCISCUS, LEO C. N90-21038
FRAY, J. M. J. N90-20983
FREEMAN, GERARD L. N90-21211
FREITAG, ROBERT F. N90-21050
FREMOUW, E. J. N90-21489
FREY, MARY ANN N90-21513
FROSCH, R. N90-21607
FUJII, ROGER U. N90-21530
FURRER, R. N90-21518

G

GABB, TIMOTHY P. N90-21123
N90-21138
GAGE, MARK L. N90-21165
GAIER, JAMES R. N90-21181
N90-21192
GAINER, THOMAS G. N90-20946
GALEIO, A. C. N90-21423
GALLUS, H. E. N90-21026
GANGULY, P. N90-21652
GAO, YI-HONG N90-21583
GARINO, ED N90-20971
GARNETT, J. D. N90-21326
N90-21329
GARRETT, S. E. N90-21220
GARSHNEK, VICTORIA N90-21513
GATES, J. N90-21331
GATLEY, I. N90-21331
GAYLOR, K. J. N90-21222
GEBBIE, KATHARINE B. N90-21591
GEFEN, YUVAL N90-21653
GEIS, N. N90-21332
GEIST, G. A. N90-21551
N90-21665
GELFAND, A. E. N90-21565
GENERAZIO, EDWARD R. N90-21401
GENTLE, K. W. N90-21634
GERSTL, S. A. W. N90-21466
GEYER, GEORGE N90-20967
GEZARI, DAN N90-21334
GHIELMI, L. N90-20994
GIBSON, JANE N90-21516
GIDLEY, DAVID W. N90-21200
GILBREATH-FRANDSEN, C. N90-21353
GILLESPIE, STEPHEN J. N90-21685
GILLETTE, J. L. N90-21483
GILLIAM, FRED T. N90-21046
GISQUET, D. N90-20997
GLAESER, ANDREAS M. N90-21655
GODFREY, SARA N90-21544
GODOYJUNIOR, MOACIR N90-21448
GOEBEL, JOHN H. N90-21347
GOLDSTEIN, DAVID N90-21385
GOMESDEGONZALEZVILLALOBOS, SONIA MARIA
N90-21115
N90-21595
GONZALEZ-RIESTRA, R. N90-21693
GOODEN, CLARENCE E. N90-21181
GOODMAN, P. N90-21648
GOODSON, WILLIAM N90-21512
GORDON, R. G. N90-21660

GORDON, ROBERT W. N90-21092
GORETTA, K. C. N90-21644
N90-21645
GRAHAM, RON N90-21074
GRANADA, J. C. N90-21647
GRANTZ, ARTHUR CHRISTIAN N90-20947
GRAVES, PHILIP C. N90-21073
GREEN, DAVID L. N90-21003
GREEN, JACKLYN RENA N90-21703
GREEN, WILLIAM J. N90-21184
N90-21189
GREENE, JANETTAROSE L. N90-21523
GREENE, R. L. N90-21658
GRIEM, H. R. N90-21622
GRIFFIN, M. N90-21343
GROEZINGER, U. N90-21342
N90-21350
GROTH, MARY N90-21361
GROUNDS, D. N90-21098
GROVE, JON ERIC N90-21717
GRUN, E. N90-21098
GUGGENHEIMER, S. N90-21649
GUIDEZ, JOEL N90-21032
GULL, G. E. N90-21349
GUPTA, MURLI M. N90-21567
GUPTA, ROOP N. N90-21297
GUVEN, H. N90-21362
GYEKENYESI, JOHN Z. N90-21133

H

HADDAD, A. N90-21035
HAEGEL, NANCY M. N90-21316
HAH, C. N90-21023
HAHN, YUKAP N90-21632
HAJDUK, CH. N90-21342
HALL, C. A. N90-21057
HALL, C. D. N90-21230
HALL, D. N90-21336
HALL, STEPHEN W. N90-21116
HALLER, E. E. N90-21315
N90-21321
N90-21323
N90-21332
HAMAGUCHI, S. N90-21641
HAMBOURGER, PAUL D. N90-21192
HAMED, AWATEF N90-21036
HAMPTON, LAWRENCE N90-20967
HAN, X-H. N90-21693
HANDELMAN, DAVID A. N90-20939
N90-20940
HANSEN, JAMES G. R. N90-21001
HANSEN, OLE N90-21616
HANSEN, W. L. N90-21315
N90-21321
HANSMAN, R. JOHN, JR. N90-20924
N90-20925
N90-20926
N90-20927
N90-20928
N90-20929
HANSON, K. M. N90-21587
HARDING, S. C. N90-21016
HARFOUSH, FADY N90-21285
HARRIS, CHARLES E. N90-21422
N90-21424
HARRIS, JONICE S. N90-21162
HARRISON, MIKE N90-21285
HARTLE, N. N90-21336
HARVEY, N. W. N90-21030
HARVEY, PAUL M. N90-21335
HASELTON, H. H. N90-21056
HASER, L. N90-21341
HASSAN, M. H. A. N90-21627
N90-21629
HATZIDIMITRIOU, D. N90-21697
HAUSCHILDT, P. H. N90-21694
HAVENS, STEPHEN J. N90-21198
HAW, RICHARD C. N90-21301
HAWKE, R. S. N90-21057
HAYS, K. M. N90-21319
HAYWOOD, B. C. G. N90-21398
HAZELTINE, R. D. N90-21634
HAZELTON, LYMAN R., JR. N90-20930
HEARN, C. P. N90-21279
HEATH, W. A. N90-21057
HEDGEPETH, JOHN M. N90-21096
HEGEDUS, CHARLES R. N90-21184
N90-21189
HELLER, GERARD N90-21545
HEMPHILL, R. C. N90-21483
HEMSWORTH, J. A. N90-21178
HENKEL, CHRISTIAN N90-21695
HERBERT, A. W. N90-21160
HERMER, J. M. N90-21224
HERNANDEZFILHO, PEDRO N90-21452
HERRING, J. N90-21331
HERTER, T. N90-21349
HESS, KURT W. N90-21477
HETHERINGTON, C. J. D. N90-21657
HEYMAN, J. S. N90-21090
HEYMAN, JOSEPH S. N90-21519
HEYWARD, ANN O. N90-21250
HICKMAN, ALBERT PEET N90-21155
HICKMAN, R. J. N90-21057
HICKMAN, T. N90-21152
HINTON, BARRY B. N90-21501
HINTZE, M. N90-21247
HIPPSLEY, C. A. N90-21161
HIRSCH, CH. N90-21010
HIRST, DONALD J. N90-21184
HITTERMAN, R. L. N90-21664
HJELLMING, R. M. N90-21693
HOANG, NGOE LONG N90-21265
HODAPP, K.-W. N90-21330
HOER, CLETUS A. N90-21276
HOERZ, FRED N90-21098
HOFFMAN, ALAN N90-21325
HOFFMANN, W. N90-21018
N90-21020
HOFFREN, JAAKKO N90-20963
HOGAN, J. T. N90-21634
HOLANDA, RAYMOND N90-21361
HOLBEN, M. S., JR. N90-21090
HOLLINGTON, JOHN L. N90-21359
HOLLOMAN, MILES E. N90-21281
HOLZSCHEITER, MICHAEL H. N90-21612
HONES, EDWARD W. N90-21712
HONG, B.-G. N90-21641
HOOGEBOOM, P. N90-21228
HOOTMAN, H. A. N90-21483
HORNER, GARNETT C. N90-21079
HORSTMANN, K.-H. N90-20979
HORTON, G. C. N90-21017
HORTON, W. N90-21641
N90-21643
HORWEDEL, B. M. N90-21550
HORWEDEL, J. E. N90-21550
HOSMAN, R. J. A. W. N90-21518
HOU, LISHENG N90-21299
HOU, T. H. N90-21180
HOU, TAN-HUNG N90-21129
HOUSH, CLINTON S. N90-20965
HOUSNER, J. M. N90-21068
HOWARD, BRIAN T. N90-20942
HOWELL, R. H. N90-21156
HOWELL, S. B. N90-21693
HSIEH, TUNG-MING N90-21392
HSU, IN-SHEK N90-21061
N90-21525
HSU, MING-TA S. N90-21177
HUANG, CHAO-SHANG N90-21581
HUANG, J. Y. N90-21180
HUBBARD, H. H. N90-21605
HUBER, WILFRED N90-21500
HUDDLESTON, D. H. N90-20999
HUDSON, C. MICHAEL N90-21164
HUDSON, J. L. N90-21558
HUFFMAN, JAMES E. N90-21322
HULBERT, STEPHEN JAMES N90-21704
HURWITZ, FRANCES I. N90-21133
HUTTO, WILLIAM R. N90-21216
HYDE, RODERICK A. N90-21709

I

II, FERNANDO AUGUSTO MITSUO N90-21445
IKEDA, MASARU N90-21528
INFANTE, C. N90-21652
IRELAND, P. T. N90-21030
ISHIKAWA, MURIEL Y. N90-21709

J

JACQUOTTE, OLIVIER-PIERRE N90-20988
JAEGER, E. F. N90-21642
JALOTA, LALIT N90-21690
JAMES, R. N90-21161
JAMESON, ANTONY N90-20998
JANKOWSKI, A. F. N90-21153
JANKOWSKI, ALAN F. N90-21682
JASPER, LOUIS J., JR. N90-21055
JOFFRE, SYLVAIN M. N90-21478
JOHNSON, B. M. N90-21474
JOHNSON, C. D. N90-21072
JOHNSON, D. D. N90-21156
JOHNSON, W. S. N90-21409
JONES, DAVID F. N90-21357
JONES, DENISE R. N90-21005
JONES, PAUL H. N90-21042
JONES, T. V. N90-21030
JONES, W. R. N90-21243
JONES, WENDELL B. N90-21430
JORDAN, DEBBEE N90-21281
JORGENSON, ROY E. N90-21287
JOSEPH, THOMAS A. N90-21555
JOSHI, SURESH M. N90-21073
JOSLYN, H. DAVID N90-21011
JOYCE, R. N90-21331
JUANG, JER-NAN N90-21079
JUNGA, FRANK N90-21347
JUNGWIRTH, K. N90-21710
JUNKINS, J. L. N90-21083
JUSINSKI, LEONARD E. N90-21155

K

KADAMBI, J. R. N90-21311
KAIL, D. N90-21221
KALDELLIS, J. N90-21024
KALTSCHMIDT, HORST N90-21229
KAMIMURA, T. N90-21643
KANE, R. P. N90-21714
KAO, YUNG-FU N90-20955
KARLICKY, M. N90-21710
KARLSSON, JOAKIM N90-20923
KASHAEV, R. M. N90-21578
KASHANI, AHMAD REZA N90-21393
KATEHI, P. B. N90-21278
KATTERLOHER, R. N90-21341
KAUFFELD, MICHAEL N90-21305
KAUFMAN, M. J. N90-21176
KAUKLER, WILLIAM F. N90-21208
KEAM, DONALD W. N90-21520
KEE, ROBERT J. N90-21676
KEFAUVER, NEILL N90-21058
KELLER, D. M. N90-21262
KENNEDY, D. N90-21413
KENNEDY, R. S. N90-21521
KENTER, ALMUS THOMAS N90-21718
KERBY, JIM N90-21285
KERN, JONATHAN N90-21523
KESSLER, M. F. N90-21340
KEVREKIDIS, I. G. N90-21558
KEYDEL, WOLFGANG N90-21229
KHAN, M. Z. SHAH N90-21044
KHANDELWAL, GOVIND S. N90-21715
KHANDKAR, ASHOK C. N90-21467
KHOT, N. S. N90-21075
KILMER, KENNETH W. N90-21482
KIM, HYOUN-EE N90-21199
KIM, HYOUNG-TAE N90-20958
KIM, KYUNG-EAK N90-21507
KIM, WALTER S. N90-21361
KIM, YONG-SUK N90-21123
N90-21138
KING, DAVID S. N90-21380
KING, GUY L. N90-21390
KING, ROGER J. N90-21113
KIRBY, MARK S. N90-20926
KITIPORNCHAI, S. N90-21426
KLAUSING, HELMUT N90-21229
KLAVINS, P. N90-21658
KLEIN, AL J. N90-21685
KLEINHANS, WILLIAM N90-21337
N90-21338
N90-21339
N90-21348
KLEINMAN, LAWRENCE I. N90-21484
KLIMETZEK, F. N90-20987
KLIMKOWSKI, JERZY Z. N90-21292
KLOMPE, A. W. H. N90-21369
KLOSE, GERHARD N90-21079
KNEALE, P. A. N90-21396
KNECHT, JOHN A. N90-21260
KNIGHT, LARRY V. N90-21621
KNIGHTS, C. F. N90-21179
KNORRENSCHILD, MICHAEL N90-21585
KO, SIU-PING N90-21134
KOEPKE, KARL N90-21285
KOESTER, H. N90-20979
KOK, ANDRE J. N90-21682
KONRAD, C. H. N90-21057
KOO, KEE P. N90-21620
KOOMEN, P. J. N90-21228
KORACIN, DARKO RUDOLF N90-21506
KORTSCHOT, H. W. N90-21518
KOSCHEL, W. N90-21029
KOTHANDARAMAN, C. N90-21473
KOURY, J. N90-21090
KRABACH, TIMOTHY N. N90-21322
KRAEMER, GERD N90-21238
KRAIN, H. N90-21020
KRAKOWSKI, R. A. N90-21638

KRAVTSON, V. D. N90-21547
KRAWIZCKI, MELISSA ANN N90-21144
KREIDL, T. J. N90-21693
KROL, J. R. N90-21518
KUBE, M. N90-21558
KUHL, MARK R. N90-20931
KUHN, RODNEY N90-21249
KUIPERS, A. N90-21518
KULLBERG, M. N90-21645
KUNATH, R. R. N90-21261
KUPPERMAN, D. S. N90-21664
KURITA, GEN-ICHI N90-21630
KUZENSKY, A. L. N90-21166
KWAY, W. L. N90-21666
KYR, DOUG N90-21074

L

LACROIX, D. N90-21336
LAFAGE, C. N90-21654
LAFEMINA, JOHN P. N90-21663
LAGACE, PAUL A. N90-21127
LAKSHMINARASIMHA, A. N. N90-21007
LAMBERSON, STEVEN E. N90-21068
LAMBERT, KEVIN M. N90-21282
LAMPERT, CARL M. N90-21476
LANDIS, G. A. N90-21287
LANG, KENNETH R. N90-21711
N90-21719
LANGER, E. N90-21234
LANGSTON, L. S. N90-21026
LAPEDES, A. S. N90-21558
LAROCCA, F. N90-20990
LARSEN, SHAWN N90-21493
LASH, THOMAS A. N90-21088
LASKIN, R. A. N90-21063
LAVELLE, JAMES J. N90-21399
LAVIOLETTE, R. A. N90-21319
LAWTON, B. B. N90-21396
LAYMON, C. M. N90-21610
LE, KHAC HUONG N90-21265
LEAODEMORAESNOVO, EVLYN MARCIA N90-21463
LEBOEUF, F. N90-21013
LEE, G. N90-21217
LEE, KAM-PUI N90-21297
LEE, R. Q. N90-21273
LEE, W. Y. N90-21051
LEFOHN, ALLEN S. N90-21481
LEIGH, R. W. N90-21218
LEMKE, D. N90-21342
LENAOUR, C. N90-21343
LEONARD, B. P. N90-21291
N90-21570
LEONARD, O. N90-20985
LESSARD, VICTOR R. N90-20953
LESYNA, L. N90-21318
LEVAN, PAUL D. N90-21333
LEVINTOV, BORIS N90-21099
LEVIT, SHIMON N90-21653
LEWICKI, D. G. N90-21394
LI, MIAO N90-21583
LICHTENFELTS, FRED N90-20926
LIM, TEIK CHIN N90-21387
LIMADALGE, JULIO CESAR N90-21461
LIN, WEH-HUEI N90-21136
LIN, YUNG TUN N90-21112
LINDELL, ISMO V. N90-21270
LINDFORS, VIRPI T. N90-21478
LINDQVIST, PETER N90-21589
LINDSEY, NANCY J. N90-21523
LING, M. R. N90-21427
LINSE, DENNIS N90-20937
LIU, C. T. N90-21189
LJUNG, BRITT-MARIE N90-21512
LOCKETT, PHILIP BRIAN N90-21705
LOMDAHL, PETER S. N90-21586
LONDINO, JOSEPH M., JR. N90-21354
LOOS, HENDRICUS G. N90-21534
LOPESCANCIOPSOARES, MARCIA N90-21447
LOPESDEOLIVEIRAESOUZA, MARCELO N90-21093
LOPEZ, L. A. N90-21553
LORELL, KENNETH R. N90-21082
LOUEY, CRAIG N. N90-21203
LOVETT, J. N., JR. N90-21095
LOW, FRANK J. N90-21314
N90-21323
LU, SHIN-YEE N90-21266
LUECKING, P. N90-21014
LUINGE, W. N90-21341
LUKE, P. N. N90-21315
N90-21321
LUNATOLEDO, FRANCISCO N90-21442
LUND, J. N90-21395
LUTTON, MARK J. N90-20948
LUTZ, M. N90-21321
LYNCH, S. K. N90-21404
LYTLE, C. D. N90-21243

M

MACIA, JACQUELINE N90-21188
MADAN, HERB S. N90-21527
MADISON, LARRY N90-21371
MADZSAR, GEORGE C. N90-21360
MAGLIERI, D. J. N90-21605
MAGOLD, N. J. N90-21125
MAILHOT, CHRISTIAN N90-21663
MAJUMDAR, S. N90-21664
MAKO, FREDRICK M. N90-21355
MAKOWIECKI, D. M. N90-21153
MALDONADO, JAIME J. N90-21038
MALIK, A. U. N90-21188
MALONE, J. B. N90-20981
MANI, RAMANI N90-21602
MANNING, LARRY A. N90-21345
MANSBRIDGE, J. V. N90-21496
MANSOORI, G. ALI N90-21146
MANTEGAZZA, CLAUDIO N90-20984
MANTSCH, PAUL N90-21285
MANZEL, WOLFGANG N90-21226
MARAZZI, R. N90-20994
MARCUS, J. T. N90-21518
MARIANO, STEPHEN A. N90-21183
MARINAK, MARTY N90-21637
MARINI, S. N90-21242
MARKUS, MICHAEL J. N90-21504
MAROTTA, A. S. N90-21174
MARRAKCHI, A. L. N90-21672
N90-21674
MARSHALL, DAVID T. N90-21106
MARSILIO, R. N90-20990
MARTIN, DAVID W. N90-21501
MARTIN, E. RAY N90-21357
MARTIN, RODERICK H. N90-21421
MARTINEZ, J. R. N90-21057
MARTINI, PAULO ROBERTO N90-21437
MARTZ, H. E. N90-21404
MASCHHOFF, K. N90-21336
MASERJIAN, JOSEPH N90-21358
MASTIN, C. W. N90-20999
MATACOTTA, F. C. N90-21652
MATOCHKIN, E. P. N90-21624
MAYALL, BRIAN N90-21512
MCCARTHY, D. N90-21339
MCCAUGHREAN, MARK N90-21328
MCCREIGHT, CRAIG R. N90-21313
N90-21347
MCCUNE, WILLIAM W. N90-21563
MCDANIEL, OLIVER H. N90-21604
MCDONALD, S. C. N90-21649
MCFARLAND, RICHARD H. N90-20934
MCGARRY, FRANK N90-21539
MCGUIRE, M. J. N90-21644
MCINTYRE, DAVID S. N90-20932
MCKELVEY, MARK E. N90-21347
MCKERNAN, M. A. N90-21153
MCLEAN, IAN S. N90-21327
MCLINDEN, MARK N90-21305
MCMILLAN, IAN N90-21225
MCMURRAY, R. E., JR. N90-21347
MCNITT-GRAY, JILL LYNN N90-21517
MEADOWS, KRISTINE R. N90-21302
MEALING, B. E. N90-20959
MEDIATE, BRUNO N90-20971
MELMED, JEFFREY N90-21702
MENDONCA, FRANCISCO JOSE N90-21446
MENZEL, W. P. N90-21498
MERRILL, W. N90-21564
MESSERSCHMID, E. N90-21518
METZL, R. N90-21646
MEYERS, C. N90-21414
MICHARD, PIERRE-JACQUES N90-21032
MIDDLETON, J. N90-21255
MIELE, A. N90-21051
MIELKE, ROLAND R. N90-21535
MIKULAS, MARTIN M., JR. N90-21096
MILLER, JAMES A. N90-21676
MILLER, JOHN N90-21539
MILLS, G. L. N90-21097
MILMAN, M. N90-21078
MILORA, S. L. N90-21056
MIMA, K. N90-21643
MIN, NAMKUNG N90-21170
MINEO, BETH A. N90-21519
MINH, HOANG LE N90-21572
N90-21573
MIRACE, ARMANDO N90-21626
MITAL, SUBODH K. N90-21131
MITCHELL, R. M. N90-21495
MIYOSHI, KAZUHISA N90-21182
MODESTODESOUZA, RICARDO CARTAXO N90-21445
MOFIZ, U. A. N90-21264
MOG, R. A. N90-21095
MOHAMED, SALAH-ELDIN ABDEL-MONEM N90-21415
MOHNEN, VOLKER A. N90-21504
MOKHTARI, SIMIN N90-21570
MONSERUD, ROBERT A. N90-21485
MONTEIRO, ANTONIO MIGUEL VIEIRA N90-21444
MONTEIRODOVALE, J. L. N90-21689
MONTELLI, LUCIANA N90-21203
MONTGOMERY, E. F. N90-21338
MOORE, JOAN G. N90-21031
MOORE, JOHN N90-21031
MOORHEAD, A. J. N90-21199
MORABITO, C. N90-21231
MORAESNOVO, EVLYN MARCIA LEAO N90-21448
MORAN, MATTHEW E. N90-21295
MORE, JAMES G. N90-21701
MOREIRA, ALBERTO N90-21244
MOREIRA, JOAO R. N90-21233
N90-21236
MOREL, M. N90-21143
MORFITT, GARY N90-21256
MORINE, L. A. N90-21064
MORRELL, FREDERICK R. N90-20921
MORRISON, GERALD L. N90-21598
MORRISON, P. J. N90-21312
N90-21643
MOSS, B. C. N90-21374
MOSS, NICOLAS N. N90-21347
MOUMENE, MISSOUM N90-21417
MUCHA, PHILLIP E. N90-21294
MULAC, R. A. N90-21025
MULROY, WILLIAM N90-21305
MUNJAL, M. L. N90-21597
MURRELL, D. M. N90-21646
MURTHY, P. L. N. N90-21143
MUTO, VIRGINIA N90-21586
MVIEIRA, ERNESTO GETULIO N90-21454
MYERS, K. J. N90-21587

N

NAARDING, S. H. J. N90-20964
NAIK, R. A. N90-21409
NAKASE, YOSHIAKI N90-21195
NARRAMORE, J. C. N90-20981
NASR, J. M. N90-21245
NATESAN, K. N90-21168
NAUD, STEVEN N90-21181
NEALY, JOHN E. N90-21715
NEKMOUCHE, L. N90-20985
NELLIS, W. J. N90-21659
NELSON, PAUL N90-21108
NELSON, R. O. N90-21610
NESE, JON M. N90-21502
NETO, GILBERTO CAMARA N90-21445
NETTLES, A. T. N90-21125
NEUMAN, HARVEY E. N90-20942
NEWELL, D. A. N90-21097
NEWMAN, JAMES C., JR. N90-21130
N90-21424
NEWMAN, ROBERT B. N90-21049
NEWSOM, JERRY R. N90-21062
NICHOLAS, M. G. N90-21178
NICHOLSON, D. M. N90-21156
NICKEL, U. N90-21227
NICOL, DAVID M. N90-21556
NICOL, TOM N90-21285
NIEHUIS, R. N90-21014
NIEROPEREIRA, MADALENA N90-21443
N90-21462
N90-21463
NIKNAFS, H. S. N90-21291
NINKOV, Z. N90-21326
N90-21329
NORDEMANN, D. J. R. N90-21486
NORRIS, G. A. N90-21091
NOUR-OMID, SHAHRAM N90-21410
NOVAES, RENE ANTONIO N90-21465
NOVAK, J. L. N90-21370
NUNES, DANTON N90-21094
NYLAND, TED W. N90-21295

O

OBRIEN, D. M. N90-21495
OBRIEN, T. K. N90-21126
OCONNELL, LARRY N90-21549
ODA, ICHIRO N90-21582
OETTL, H. N90-21234
OKEEFE, M. A. N90-21657
OKSANEN, MARKKU I. N90-21269
OLIN, A. N90-21607

OLIVEIRADIAS, ROBERTO W. N90-21442
OLSON, RICHARD K. N90-21481
OLSON, WILLIAM S. N90-21501
OLSSON, NILS N90-21099
ONN, DAVID G. N90-21154
OOSTHUIZEN, P. H. N90-21033
ORTNER, S. R. N90-21157
OSIPOV, A. A. N90-21578
OTTEN, M. P. G. N90-21235
OTTENBRITE, RAPHAEL M. N90-21118
OTTINO, JULIO M. N90-21304
OTTO, WILLIAM F. N90-21281
OVERHAUSER, ALBERT W. N90-21358
OWEN, DAVID TUDOR N90-20961
OYANAGI, Y. N90-21607
OZGUNER, UMIT N90-21092

P

PADILHA, A. L. N90-21714
PANDALAI, KRISH N90-21045
PANGRAZI, R. N90-21231
PAPADOPOULOS, DEMETRIOS S. N90-21124
PAPAILIOU, K. D. N90-21024
PAPELL, S. STEPHEN N90-21295
PAPETTI, DINO J. N90-21183
PAPPA, RICHARD S. N90-21412
PARADELLA, WALDIR RENATO N90-21440
N90-21456
PARAMESWARAN, V. N90-20970
PARDINI, S. N90-21242
PARK, K. C. N90-21076
PARKER, CRAIG B. N90-20934
PARKER, ROBERT P. N90-21203
PARKINSON, E. N90-21013
PARRISH, RUSSELL V. N90-21004
N90-21005
PARSONS, DONALD S., JR. N90-21400
PASOUR, JOHN A. N90-21355
PATE, VICKI M. N90-21596
PATEL, JANAK H. N90-21557
PATERSON, D. A. N90-21308
PATRICK, HOWARD VAN LIEW N90-20944
PAYNE, S. A. N90-21666
PEDDICORD, K. LEE N90-21108
PEISEN, DEBORAH J. N90-21049
PELTONIEMI, MARKKU N90-21253
PENCIL, ERIC N90-21361
PENG, J. L. N90-21658
PENG, TSING-HUNG N90-21511
PERDICHIZZI, ANTONIO N90-21015
PEREIRA, E. B. N90-21486
PEREIRADACUNHA, ROBERTO N90-21437
PEREZ, SHARON E. N90-21412
PERKINS, DON V. N90-21388
PERRY, P. L. N90-21662
PERSOFF, P. N90-21403
PETERSON, ANDREW F. N90-21267
PETROFF, M. D. N90-21319
PEYTON, B. W. N90-21665
PHILIPS, ALBERT R. N90-21216
PICKERELL, THOMAS N90-21249
PIEPER, GAIL W. N90-21559
PIKE, T. K. N90-21224
PILANT, MICHAEL N90-21569
PINNAU, ROGER R. N90-21252
PINSKI, F. J. N90-21156
PINTODEGARRIDO, JUAN CARLOS N90-21445
PIPHER, J. L. N90-21326
PIRAINO, M. W. N90-21218
PLA, FREDERIC N90-21600
PLAETSCHKE, E. N90-20970
PLATTNER, ALFRED N90-21226
PLOEGER, G. N90-21341
POE, C. C., JR. N90-21122
N90-21424
POEPPEL, R. B. N90-21644
N90-21645
POETZSCH, WINFRIED N90-21233
POGLITSCH, A. N90-21332
POLITES, M. E. N90-21219
POLLOCK, T. C. N90-21083
POLLOCK, W. D. N90-21409
POMMEL, F. N90-21013
PONCHAK, DENISE S. N90-21250
PONCHAK, GEORGE E. N90-21263
N90-21273
N90-21278
PONTESCARDOSO, HUMBERTO N90-21105
PORKOLAB, M. N90-21634
POTAPCZUK, MARK N90-20925
PRASAD, S. N. N90-21280
PRENTICE, I. COLIN N90-21485
PRESTESBARBOSA, MARX N90-21449
PRIOVOLOS, GEORGE J. N90-20969
PRODI, F. N90-21242
PROUSE, DAVE W. N90-21467
PRUESS, K. N90-21403

Q

QAMAR, SHAHID N90-21368
QUAIDE, W. L. N90-21098
QUAN, RALPH N90-21077
QUAST, THOMAS N90-20971
QUEALY, ANGELA N90-21552
QUEST, J. N90-21018
QUIGLEY, GERARD P. N90-21377
QUIMBY, KELVIN L. N90-21539
N90-21542
QUINN, WILLIAM F. N90-21110

R

RADESPIEL, R. N90-20979
RADOUSKY, H. B. N90-21658
RAFANELLI, MAURIZIO N90-21686
RAGENT, B. N90-21330
RAHMAN, Z. H. N90-21083
RAMAKER, R. N90-21078
RAMAMOORTHY, P. N90-20975
RAMIREZ, JEAN-CLAUDE N90-21407
RANDAZZO, PHILIP N90-21248
RANDJBAR-DAEMI, S. N90-21650
RANDLES, M. H. N90-21646
RANGELDEFREITAS, LUCIANE N90-21673
RAO, T. V. S. N90-21043
RASCHE, ROBERT N90-21337
N90-21339
RASSOOL, R. P. N90-21649
REDMAN, LANCE D. N90-21202
REED, IRVING S. N90-21061
N90-21525
REED, S. E. N90-21366
REES, DAVID N90-21606
REGOBEZERRA, PAULO CESAR N90-21461
REILINGER, ROBERT N90-21493
REINISCH, B. W. N90-21489
RENEAUX, J. N90-20995
N90-20997
RENKO, KARI N90-21041
REYNOLDS, D. B. N90-21349
RHODEHAMEL, HARLEY N90-20969
RIBEIRODOSSANTOS, ATHOS N90-21450
RICCITIELLO, SALVATORE R. N90-21177
RICE, R. B. N90-21081
RICHARD, JACQUES N90-21232
RICHARD, M. A. N90-21275
RICHARDS, ELIZABETH H. N90-21475
RICHARDS, K. E., JR. N90-21065
RICHARDS, P. L. N90-21315
N90-21317
RICKETTS, RODNEY H. N90-21047
RIDDIFORD, ALAN N90-21285
RIEKE, G. H. N90-21320
N90-21323
N90-21338
RIEKE, MARCIA J. N90-21320
N90-21337
N90-21338
N90-21339
RIEKE, P. C. N90-21468
RILEY, J. T. N90-21619
RIONARO, SALVATORE N90-21586
RIOSNETO, ATAIR N90-21054
RIVERA, ANN L. N90-21133
RIZK, M. H. N90-20991
ROACH, ROBERT L. N90-21554
ROBERSON, G. P. N90-21404
ROBEY, JUDITH L. N90-21215
ROBINSON, D. N90-21343
ROCHOWIAK, DANIEL N90-21529
ROEDE, B. N90-21239
ROEDEL, JUERGEN N90-21655
ROELLIG, T. N90-21318
ROGOWSKI, R. S. N90-21090
ROHARDT, C.-H. N90-20979
ROKHSAZ, KAMRAN N90-20965
ROMIG, A. D., JR. N90-21175
ROOKER, C. N. N90-21286
ROSA, ROBERTO N90-21463
ROSE, HARVEY A. N90-21633
ROSE, MILTON E. N90-21568
ROSEN, I. G. N90-21566
ROSSINGTON, C. S. N90-21321
ROTH, D. J. N90-21402
ROTH, MARY ELLEN N90-21272
ROTHMAN, D. S. N90-21483
ROUAN, D. N90-21344
ROUTBORT, J. L. N90-21644
N90-21645
ROWE, JOSEPH N90-21513
ROWLANDS, N. N90-21349
RUBINSTEIN, ROBERT I. N90-21137
N90-21600
RUDOFF, R. N90-21006
RUDORFF, BERNARDO FRIEDRICH THEODOR
N90-21439
N90-21441
N90-21455
N90-21458
N90-21460
RUFF, GARY A. N90-20943
RUMITZ, M. N90-21332
RUMMEL, Y. N90-21096
RUNDELL, WILLIAM N90-21569
RUPLEY, FRAN M. N90-21676
RUSSELL, DAVID N90-21633
RYABOV, YU. G. N90-21607
RYAN, LAURA E. N90-20936
N90-20941
RYAN, R. R. N90-21069

S

SAHAI, Y. N90-21494
SAIVA, G. N90-21510
SALAM, ABDUS N90-21650
SALAMA, A. N90-21350
SALAMA, M. N90-21078
SALAYMEH, S. R. N90-21174
SALIMULLAH, M. N90-21627
N90-21629
SALPEKAR, S. A. N90-21126
SALVINO, J. T. N90-21008
SANKAR, L. N. N90-20981
SANTANA, VALDINEIDE B. N90-21453
SANTANNABINS, LEONARDO N90-21444
SARANIERO, MICHAEL N90-21003
SARAVANOS, D. A. N90-21132
N90-21143
SARFARAZ, M. A. N90-21320
SASAKI, SHINOBU N90-21561
SAUNDERS, S. R. J. N90-21179
SAUSEN, TANIA MARIA N90-21435
SAUVE, J. L. N90-21057
SAVAGE, M. N90-21318
SAVAGE, MAUREEN L. N90-21347
SAWYER, RICHARD STEVEN N90-20956
SCALISEJUNIOR, E. N90-21689
SCHADE, H. N90-21473
SCHAEFFER-NOVELLI, YARA N90-21454
SCHAFRIK, ROBERT N90-21188
SCHAMEL, GEORGE CUSHEN, II N90-21039
SCHIJVE, J. N90-21142
N90-21427
SCHINDEL, LEON H. N90-21293
SCHIPER, ANDRE N90-21533
SCHLICKENMAIER, HERBERT W. N90-21509
SCHMALE, DAVID T. N90-21430
SCHMIDT, E. N90-20987
SCHMIDT, H. N90-21029
SCHNEBERK, D. J. N90-21404
SCHNEIDER, WILLIAM C. N90-21390
SCHORSCHER, HANS DANIEL N90-21449
N90-21450
N90-21459
SCHROTH, JOERG N90-21226
SCHUBERT, MARTIN N90-20971
SCHULTZ, A. J. N90-21644
SCHUTKEKER, J. N90-21643
SCHWAB, JOHN R. N90-21303
N90-21306
N90-21307
SCHWEIKA, W. N90-21156
SCRUBY, C. B. N90-21121
N90-21374
N90-21398
SEDDOUGUI, SHARON O. N90-21289
N90-21290
SEGAERT, P. N90-21010
SEIB, D. H. N90-21349
SEIGLE, JEFFREY N90-21541
SEKULIC, DUSAN P. N90-21667
SELBERG, BRUCE P. N90-20965
SERAFINI, JOHN A. N90-20942
SESPINDOLA, CARMEM REGINA N90-21454
SETZER, ALBERTO W. N90-21454
SHADER, C. N90-21693
SHALKHAUSER, K. A. N90-21261
SHANABARGER, M. R. N90-21171
SHANKAR, VIJAYALAXMI N90-21043
SHARKEY, JOHN P. N90-21085
SHARP, JOHN K. N90-21687

SHARPE, JOHN P. N90-21601
SHAVIV, G. N90-21694
SHAW, THOMAS LEOMIL N90-21141
SHEHATA, L. N. N90-21651
SHELTON, R. N. N90-21658
SHELTON, W. A. N90-21665
SHENK, WILLIAM E. N90-21067
SHI, YING-LIANG N90-21541
SHIMABUKURO, YOSIO EDEMIR N90-21436
N90-21451
N90-21452
SHIMSHONI, EFRAT N90-21653
SHIN, YONG-SEOK N90-21418
SHINN, JUDY L. N90-21715
SHINN, M. D. N90-21666
SHIVAKUMAR, KUNIGAL N. N90-21130
SHOSHANI, ARIE N90-21666
SHUJIE, LI N90-21560
SHURE, M. N90-21329
SIBILLE, F. N90-21340
N90-21344
SIDDIQI, S. A. N90-21652
SIGMAR, D. J. N90-21634
SIHVOLA, ARI H. N90-21270
SIIKONEN, TIMO N90-20963
SILCOX, R. J. N90-21603
SIMEAODEMEDEIROS, JOSE N90-21442
SIMONEN, E. P. N90-21167
SIMONS, RAINEE N. N90-21263
N90-21273
N90-21278
SIMPSON, ROBERT W. N90-20922
SINGER, IRWIN L. N90-21190
SINGER, JOSEPH N90-21469
SINGER, SIDNEY N90-21196
SINGH, D. J. N90-20950
SINGH, J. P. N90-20951
N90-21644
N90-21664
SINGH, L. P. N90-21674
SINGH, RAJENDRA N90-21387
SINGLETON, JEFFREY D. N90-20974
SINTON, W. N90-21330
SIRLIN, S. W. N90-21066
SJOLANDER, S. A. N90-21027
SKEATE, M. F. N90-21404
SKOUSEN, N. N90-21247
SKRUTSKIE, M. F. N90-21329
SKUDERA, WILLIAM J., JR. N90-21251
SLABE, MELISSA E. N90-21192
SLABOSPITSKY, S. R. N90-21607
SMITH, A. C. N90-21617
SMITH, BERNARD N90-21211
SMITH, F. T. N90-21290
SMITH, HELENE S. N90-21512
SMITH, J. N90-21006
SMITH, JAMES A. N90-21436
SMITH, KATHERINE L. N90-21193
SMITH, LAURIE N90-21539
SMITH, THOMAS M. N90-21485
SMITHRICK, JOHN J. N90-21116
SO, MARIA N90-21545
SOBIECZKY, HELMUT N90-20977
SOBOUTI, Y. N90-21579
SOKOLOV, VLADIMIR N90-21280
SOM, SUKHAMONY N90-21535
SONNEBORN, G. N90-21693
SORRELL, WILFRED HENRY N90-21700
SOUTAR, JOHN N90-20971
SOUTH, D. W. N90-21483
SPALVINS, TALIVALDIS N90-21210
SPARKS, DEAN W., JR. N90-21079
SPEAR, ROBERT J. N90-21202
N90-21204
SPENCE, RODNEY L. N90-21250
SPIEGEL, DOUGLAS N90-21545
SREEDHAR, K. N90-21652
SRILATHA, K. R. N90-20975
STACEY, G. J. N90-21332
STALLWORTH, R. N90-21414
STANG, D. B. N90-21402
STANLEY, GARY M. N90-21410
STAPELBROEK, M. G. N90-21319
N90-21349
STARES, I. J. N90-21398
STARK, MIKE N90-21539
STARRFIELD, SUMNER N90-21691
N90-21692
N90-21693
N90-21694
STEELE, R. S., JR. N90-21688
STEINBERG, SANDRA N90-21545
STEINER, D. N90-21634
STEINMANN, PIERRE A. N90-21210
STEKETEE, J. A. N90-21309
STELMACH, JERZY N90-21708
STENBAEK-NIELSEN, HANS N90-21606
STENBERG, ROLF N90-21428
STENGEL, ROBERT F. N90-20935
N90-20938
N90-20939
N90-20940
N90-20941
STEPHENS, J. J. N90-21175
STEPHENSON, PAT N90-21533
STEWARD, C. N90-21609
STEWART, D. SCOTT N90-21206
STEWART, J. N90-21159
STITT, LEONARD E. N90-21037
STOBIE, J. N90-21336
STOCKS, G. M. N90-21156
N90-21665
STOCKWELL, ALAN E. N90-21412
STONE, LYDIA RAZRAN N90-21513
STOUGHTON, JOHN W. N90-21535
STRABALA, K. I. N90-21498
STRANGWOOD, M. N90-21158
N90-21161
STRATHDEE, J. N90-21650
STRATTON, D. ALEXANDER N90-20938
STRELTSOV, V. N. N90-21592
N90-21668
STRICKLAND, DONNA THEO N90-21372
STUART, THOMAS A. N90-21113
STUBERT, B. N90-21014
SUGAMA, H. N90-21641
SUNAZUKA, TOSHIHIKO N90-21532
SUNDBERG, GALE R. N90-21271
N90-21283
SUO, ZHIGANG N90-21408
SURESH, AMBADY N90-21303
N90-21306
N90-21307
SUSOEFF, A. R. N90-21057
SWAN, DAVID H. N90-21598
SWANSON, ANDY N90-21087
SWICKARD, S. M. N90-21402
SWIFT, DANIEL W. N90-21606
SWIRHUN, STANLEY N90-21280
SZUSZCZEWICZ, E. P. N90-21489

T

TAJIMA, T. N90-21640
N90-21643
TAKEDA, TATSUOKI N90-21630
TAKIZUKA, TOMONORI N90-21630
TANAKA, M. N90-21648
TANIUTI, T. N90-21640
TARDIN, ANTONIO T. N90-21455
TASKINEN, PEKKA N90-21163
TAYLOR, G. N. N90-21649
TAYLOR, LAWRENCE W., JR. N90-21070
TAYLOR, SCOTT N90-20971
TEBALDITARDIN, ANTONIO N90-21448
TEETER, RONALD N90-21513
TEIXEIRABATISTA, GETULIO N90-21446
N90-21458
TENTYUKOV, M. N. N90-21669
TERRY, P. W. N90-21631
TETEREV, YU. G. N90-21148
TEW, ROY C. N90-21114
THEILACKER, JAY N90-21285
THIEME, LANNY G. N90-21114
THOMAS, G. A. N90-21254
THOMAS, J. KELLY N90-21108
THOMAS, R. D. N90-21287
THOMASSEN, K. I. N90-21634
THOMPSON, BRUCE W. N90-21505
THOMPSON, M. N. N90-21649
THOMPSON, R. N90-21339
THOMPSON, RICHARD A. N90-21297
THOMPSON, RODGER N90-21337
TIMBIE, P. T. N90-21317
TIWARI, S. N. N90-20950
N90-21180
TO, W. M. N90-21025
TOLLESTRUP, ERIC V. N90-21335
TONG, S. Y. N90-21614
TONON, T. N90-21473
TOSI, M. P. N90-21150
TOURTIER, P. N90-21246
TOWNE, CHARLES E. N90-21303
N90-21306
N90-21307
TOWNSEND, LAWRENCE W. N90-21715
TRENT, WILLIAM N90-21249
TRETYAKOV, SERGEI A. N90-21269
TRINH, EUGENE H. N90-21215
TRIPPE, T. G. N90-21607
TRIVEDI, N. B. N90-21714
TROUDET, T. N90-21564
TRUNG, LE QUANG N90-21574
TRUONG, TRIEU-KIE N90-21061
N90-21525
TSANG, S. N90-21396
TSUNEMATSU, TOSHIHIDE N90-21630
TUOMELA, JUKKA N90-21588
TUOMI, TAPIO J. N90-21499
TURCHI, P. E. A. N90-21156
TURCICH, ELIZABETH N90-20968
TURNOCK, STEPHEN R. N90-20927
TUSON, A. T. N90-21179

U

UBALDI, MARINA N90-21015
UCER, AHMET S. N90-20986
N90-21012
UPADHYAY, TRIVENI N. N90-20969
URASHIMA, CLAUDIA AKIKO N90-21447
URBACH, A. R. N90-21097
URRUTIA, L. F. N90-21670

V

VALENZUELA, ARNOLDO N90-21606
VALETT, JON N90-21536
N90-21543
VALIMOHAMED, KARIM A. N90-21553
VANBLADEL, P. G. N90-21429
VANDEBRAEMBUSSCHE, R. A. N90-20985
VANDEDAM, R. F. N90-20992
VANDENAVYLE, JAMES A. N90-21173
VANEGMOND, J. A. N90-20993
VANGRAAS, FRANK N90-20933
VANTHOOR, C. M. E. N90-21178
VARALLO, T. P. N90-21174
VARDANYAN, VAGARSHAK N90-21135
VASQUEZ, PETER N90-21216
VASSEL, A. N90-21158
VASUDEVAN, GOPAL N90-21053
VEDELER, E. N90-21279
VEERS, PAUL S. N90-21173
VELASCO, FLAVIO ROBERTO DIAS N90-21444
VELLOSO, P. A. N90-21423
VENEZIANI, PAULO N90-21450
N90-21459
VERHAAGEN, N. G. N90-20964
VERMA, V. P. N90-21608
VERRILLI, MICHAEL J. N90-21123
N90-21138
VICKERS, D. N90-21343
VIEIRADASILVA, RUI CARLOS N90-21462
VIENS, MICHAEL J. N90-21187
VIIKARI, MATTI N90-21253
VOLPE, G. N90-20980
VONG, RICHARD J. N90-21504
VORNBERGER, A. N90-21029
VUKICEVIC, TOMISLAVA N90-21492
VURAL, KADRI N90-21337
N90-21338
N90-21339
N90-21348

W

WACHS, A. L. N90-21156
WAGNER, BARBARA AGNES N90-20960
WAGNER, JAMES W. N90-21353
WAGNER, R. M. N90-21693
WAITES, HENRY B. N90-21085
WAKATANI, M. N90-21641
WALDMAN, FREDERIC N90-21512
WALKER, R. M. N90-21098
WALLACE, DOLORES R. N90-21530
WALTON, J. N90-21395
WANG, C. N90-21566
WANG, S. J. N90-21089
WANG, SHUI N90-21707
WANG, T. N90-21051
WANG, Z. N90-21030
WANKE, CRAIG N90-20924
N90-20929
WARE, BRUCE E. N90-20968
N90-21500
WARREN, GARY PATRICK N90-21571
WARSHAWSKY, ISIDORE N90-21351
WATSON, DAN M. N90-21322
WAWRYSZCZUK, J. N90-21356
WEAKLIEM, H. N90-21473
WEBER, BOB L. N90-21503
WEBER, MICHAEL F. N90-21472
WEBER, W. J. N90-21468
WEBSTER, HARRY N90-20967

WEBSTER, ROBERT B. N90-21377
WEGENER, D. N90-21018
WEHRSE, RAINER N90-21694
WEIHRAUCH, PAUL N90-21183
WEINER, MAURICE N90-21055
WEIRICK, L. J. N90-21205
WELLEN, H. N90-20973
WELLMAN, G. W. N90-21057
WELLS, D. B. N90-21159
WELZ, JOSEPH P. N90-21604
WENDER, S. A. N90-21610
WERNER, MICHAEL W. N90-21318
N90-21345
WESCOTT, EUGENE M. N90-21606
WESKAMP, K. N90-21028
WESTCOTT, C. N90-21159
WESTMACOTT, K. H. N90-21656
WHIFFEN, BRIAN N90-21201
WHIPPLE, DANIEL Y. N90-20942
WHITE, TIMOTHY J. N90-21193
WHITE, TIMOTHY RALPH N90-21698
WHITHAM, KENT G. N90-21384
WHITNEY, BARBARA ANNE N90-21699
WHITTEMORE, THOMAS N90-21347
WHYTE, WAYNE A., JR. N90-21250
WIDRIG, R. D. N90-21474
WIKLIND, TOMMY N90-21695
WILBUR, MATTHEW L. N90-20974
WILCZEK, FRANK N90-21678
WILKES, R. L. N90-21521
WILLEMS, FRITS N90-21240
WILLEY, RONALD J. N90-21059
WILLIAMS, D. E. N90-21159
WILLIAMS, F. W. N90-21413
WILLIAMS, STEVEN P. N90-21004
WILSON, C. N90-21414
WILSON, JOHN W. N90-21715
WILT, D. M. N90-21287
WITTY, PETER N90-20971
WOHL, C. G. N90-21607
WOJCIK, GREGORY L. N90-21490
WOLF, CHRISTOPHER J. N90-21508
WOLF, J. N90-21342
N90-21350
WOLFRAMM, A. P. N90-21224
WOLFSON, MICHAEL G. N90-21204
WOMBLE, DAVID E. N90-21580
WONG, ROBERT L. N90-21661
WOOD, LOWELL L. N90-21709
WOODARD, STANLEY E. N90-21080
WOODS, LARRY N90-21334
WOODWARD, RAY L. N90-21128
WOOLAWAY, JAMES T. N90-21324
WRIGHT, GILLIAN S. N90-21327
WRIGHT, JOSEPH N90-20967
WU, ERH-RONG N90-21389
WU, I. C. N90-21321
WU, PHYLLIS M. K. N90-21389
WU, S. C. N90-21068
WUERTZ, DAVID B. N90-21503

Y

YAGI, M. N90-21641
YAHIKOZAWA, SHIGEAKI N90-21582
YAMAGUCHI, KEIKO N90-20925
YAMAN, YAVUZ N90-21419
YAN, LI N90-21373
YANKOV, CHRISTIAN L. N90-21576
YAO, JEN-CHIH N90-21590
YARAS, M. I. N90-21027
YASHAN, D. N90-21396
YASHAN, DOREEN N90-21181
YBARRONDO, L. J. N90-21247
YEAGER, WILLIAM T., JR. N90-20974
YEE, ALBERT F. N90-21200
YEE, ROBERT N90-21294
YODER, JAMES R. N90-21548
YOO, H. H. N90-21089
YOO, SEUNG-HYUN N90-21406
YORK, GEORGE W. N90-21377
YORK, THOMAS M. N90-21109
YOST, G. P. N90-21607
YOST, WILLIAM T. N90-21170
YOUNG, BRENTON C. N90-21560
YOUNG, ERICK T. N90-21320
N90-21323
N90-21324
N90-21339
YOUNG, K. D. N90-21071
YU, MING N90-21583
YURKOVICH, STEVEN N90-21092

Z

ZANELLI, J. N90-21670
ZANNETTI, L. N90-20990
ZELLER, K. H. N90-21234
ZESCHKY, J. N90-21028
ZHANG, DE-HAI N90-21561
ZHAO, Z. G. N90-21051
ZHERNOV, A. P. N90-21166
ZHIDKOV, E. P. N90-21547
ZHOU, SHUDONG N90-21706
ZORZI, E. N90-21395
ZUCCARIFERNANDESBRAGA, CLAUDIA N90-21438
ZUNDELEVICH, YURY N90-21139
ZUNINO, PIETRO N90-21015
ZUZEK, JOHN E. N90-21250

Typical Corporate Source Index Listing

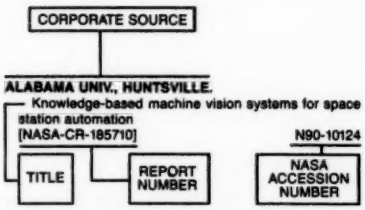

Listings in this index are arranged alphabetically by corporate source. The title of the document provides the user with a brief description of the subject matter. The report number helps to indicate the type of document cited (e.g., NASA report, translation, NASA contractor report). The NASA accession number denotes the number by which the citation is identified. The titles are arranged under each corporate source in ascending accession number order.

A

ACADEMY OF SCIENCES (USSR), NOVOSIBIRSK.
Study on rotating plasma with submillimeter laser interferometer
[DE90-615387] N90-21623
Langmuir wave interaction with ion acoustic wave
[DE90-615407] N90-21624

ADVISORY GROUP FOR AEROSPACE RESEARCH AND DEVELOPMENT, NEUILLY-SUR-SEINE (FRANCE).
Computational Methods for Aerodynamic Design (Inverse) and Optimization
[AGARD-CP-463] N90-20976
Secondary Flows in Turbomachines
[AGARD-CP-469] N90-21009
High Resolution Air- and Spaceborne Radar
[AGARD-CP-459] N90-21223
The anatomy of the gyroscope, part 3
[AGARD-AG-313] N90-21359

AEROJET TECHNICAL SYSTEMS CO., SACRAMENTO, CA.
Hydrocarbon-fuel/combustion-chamber-liner materials compatibility
[NASA-CR-185203] N90-21165

AEROMETRICS, INC., SUNNYVALE, CA.
Advanced instrumentation for aircraft icing research
[NASA-CR-185225] N90-21006

AERONAUTICA MACCHI S.P.A., VARESE (ITALY).
A tool for automatic design of airfoils in different operating conditions N90-20994

AEROSPATIALE, LES MUREAUX (FRANCE).
Image simulation of geometric targets for synthetic aperture radar N90-21245

AIR AND WASTE MANAGEMENT ASSOCIATION, PITTSBURGH, PA.
Effects of Air Pollution on Western Forests
[PB90-131111] N90-21481

AIR FORCE ACADEMY, CO.
United States Air Force Academy get-away-special flexible beam experiment N90-21088

AIR FORCE ASTRONAUTICS LAB., EDWARDS AFB, CA.
Initial operational capability of the ASTREX large space structures test bed N90-21091

AIR FORCE GEOPHYSICS LAB., HANSCOM AFB, MA.
AFGL ten micron mosaic array spectrometer: Recent results N90-21333

AIR FORCE INST. OF TECH., WRIGHT-PATTERSON AFB, OH.
Comparison of C- and O-grid generation methods using a NACA 0012 airfoil
[AD-A216375] N90-20948
NASA's Advanced Communications Technology Satellite (ACTS): Will it benefit commercial/military satellites
[AD-A217710] N90-21100
Tropical cyclone track predictability and the adjoint method of data assimilation
[AD-A216324] N90-21505

AIR FORCE WRIGHT AERONAUTICAL LABS., WRIGHT-PATTERSON AFB, OH.
Optimization of the structural and control system for LSS with reduced-order model N90-21075
Space truss zero gravity dynamics N90-21087
In-house experiments in large space structures at the Air Force Wright Aeronautical Laboratories Flight Dynamics Laboratory N90-21092

AIRCRAFT RESEARCH ASSOCIATION LTD., BEDFORD (ENGLAND).
Aerofoil design techniques N90-20978

ALABAMA UNIV., HUNTSVILLE.
Effective techniques for the identification and accommodation of disturbances N90-21072
Critical point wetting drop tower experiment
[NASA-CR-186513] N90-21208
Cooperating intelligent systems
[NASA-CR-184982] N90-21529

ALASKA UNIV., FAIRBANKS.
SR90, strontium shaped-charge critical ionization velocity experiment
[NASA-CR-186501] N90-21606

ALCATEL ESPACE, TOULOUSE (FRANCE).
Programmable generation of linear frequency modulated pulses N90-21232

ALLGEMEINE ELEKTRIZITAETS-GESELLSCHAFT, ULM (GERMANY, F.R.).
A frequency agile 94 GHz pulse-Doppler radar with dual polarisation capability N90-21226

ALLIED-SIGNAL AEROSPACE CO., KANSAS CITY, MO.
A solution level indicator system
[DE90-007939] N90-21151
Analytical sciences
[DE90-007965] N90-21152

AMBER ENGINEERING CO., SANTA BARBARA, CA.
Common source cascode amplifiers for integrating IR-FPA applications N90-21324

ANALEX CORP., CLEVELAND, OH.
Aperture taper determination for the half-scale accurate antenna reflector
[NASA-CR-185215] N90-21282

ANALYTICAL SERVICES AND MATERIALS, INC., HAMPTON, VA.
Direct formulation of a 4-node hybrid shell element with rotational degrees of freedom
[NASA-CR-4282] N90-21411
Delamination failure in a unidirectional curved composite laminate
[NASA-CR-182018] N90-21421

APPLIED RESEARCH ASSOCIATES, INC., PANAMA CITY, FL.
Selective automatic fire extinguisher for computers (SAFECOMP): Developmental test and evaluation/Initial operational test and evaluation
[AD-A217790] N90-21212

ARGONNE NATIONAL LAB., IL.
High-temperature oxidation and sulfidation of Fe-20Cr-16Ni-4Al-1Y2O3 oxide-dispersion-strengthened alloy
[DE90-007897] N90-21168
Activities and operations of the Advanced Computing Research Facility
[DE90-007957] N90-21559
OTTER (Organized Techniques for Theorem-proving and Effective Research) 2.0 users guide
[DE90-007978] N90-21563
Deformation processing of YBa2Cu3O(sub x)
[DE90-007795] N90-21644
Toughened YBa2Cu3O(sub x)/ZrO2 composites
[DE90-007796] N90-21645
Determination of internal strains in high-temperature superconductor composites by intense pulsed neutron source
[DE90-007799] N90-21664

ARIZONA UNIV., TUCSON.
Requirements of IR space astronomy N90-21314
The potential for high performance HgCdTe arrays at 4 microns N90-21320
Ga:Ge array development N90-21323
Laboratory and telescope use of the NICMOS2 128 x 128 HgCdTe array N90-21338
Future directions for NICMOS arrays N90-21339

ARMY AVIATION SYSTEMS COMMAND, CLEVELAND, OH.
Transmission research activities at NASA Lewis Research Center
[NASA-TM-103132] N90-21394

ARMY AVIATION SYSTEMS COMMAND, HAMPTON, VA.
Performance data from a wind-tunnel test of two main-rotor blade designs for a utility-class helicopter
[NASA-TM-4183] N90-20974

ARMY COMMUNICATIONS-ELECTRONICS COMMAND, FORT MONMOUTH, NJ.
Laser controlled semiconductor armature for electromagnetic launchers
[AD-D014435] N90-21055

ARMY MISSILE COMMAND, REDSTONE ARSENAL, AL.
Power transmission device
[AD-D014430] N90-21281

ARNOLD ENGINEERING DEVELOPMENT CENTER, ARNOLD AIR FORCE STATION, TN.
Optimization of aerodynamic designs using computational fluid dynamics N90-20999

AUSTRALIAN NATIONAL COMMITTEE FOR CRYSTALLOGRAPHY, CANBERRA.
A requirement for Australian research: Access to big science facilities, a report by the Australian National Committee for Crystallography
[DE90-614784] N90-21048

AUSTRALIAN RADIATION LAB., MELBOURNE.
Proceedings of a workshop on Carcinogenic Potential of Extremely Low Frequency Magnetic Fields
[DE90-614340] N90-21520

B

BALL AEROSPACE SYSTEMS DIV., BOULDER, CO.
BASG thermomechanical pump helium 2 transfer tests
[NASA-CR-177541] N90-21097

BOEING CO., SEATTLE, WA.
Heavily loaded joints for assembling aerobrake support trusses
[NASA-CR-181992] N90-21099

BRESCIA UNIV. (ITALY).
Secondary flows and Reynolds stress distributions downstream of a turbine cascade at different expansion ratios N90-21015

BRIGHAM YOUNG UNIV., PROVO, UT.
The investigation of multilayer x ray reflectors as x ray optical elements
[DE90-009044] N90-21621

BRITISH BROADCASTING CORP., KINGSWOOD (ENGLAND).
HDTV bandwidth reduction using motion compensation and DATV
[BBC-RD-1989/10] N90-21254
Prediction of VHF/UHF mobile reception in urban areas: Comparison with measurements in London
[BBC-RD-1989/11] N90-21255

BRITISH BROADCASTING CORP., LONDON (ENGLAND).
Direct Radio Broadcasting by Satellite (DRBS): A review of the technical factors and system approaches suitable for mobile and fixed reception
[BBC-RD-1989/4] N90-21221

BROOKHAVEN NATIONAL LAB., UPTON, NY.
Ice-making heat exchanger evaluation and test plan
[DE90-008824] N90-21218
Source attribution for tropospheric ozone in the US
[DE90-007994] N90-21484
Strangeness enhancement in 14.6 A GeV/c Si+Au interactions?
[DE90-008826] N90-21616

BROWN UNIV., PROVIDENCE, RI.
Problems associated with residual and mismatch stresses in thin film structures N90-21407

C

CALIFORNIA AIR RESOURCES BOARD, SACRAMENTO.
Effects of Air Pollution on Western Forests [PB90-131111] N90-21481
CALIFORNIA INST. OF TECH., PASADENA.
Age constraints for the present fault configuration in the Imperial Valley, California: Evidence for northwestward propagation of the Gulf of California rift system [NASA-CR-186541] N90-21493
A balloon measurement of the isotopic composition of galactic cosmic ray iron N90-21717
CALIFORNIA UNIV., BERKELEY.
A 100 micro Kelvin bolometer system for SIRTF N90-21317
Germanium Blocked Impurity Band (BIB) detectors N90-21321
Stressed detector arrays for airborne astronomy N90-21332
Anisotropy of grain growth in alumina [DE90-009045] N90-21655
CALIFORNIA UNIV., BERKELEY. LAWRENCE BERKELEY LAB.
Stressed Ge:Ga photoconductors for space-based astronomy. (Is there life beyond 120 micron) N90-21315
On storage rings for short wavelength FELs [DE90-009059] N90-21379
A casting and imaging technique for determining void geometry and relative permeability behavior of a single fracture specimen [DE90-009192] N90-21403
Failure and degradation modes in selected solar materials: A review [DE90-009075] N90-21476
Current experiments in elementary particle physics [DE90-008062] N90-21607
Anisotropy of grain growth in alumina [DE90-009045] N90-21655
High voltage/high resolution studies of metal and semiconductor interfaces [DE90-008065] N90-21656
Simulated image maps for use in experimental high-resolution electron microscopy [DE90-009178] N90-21657
STORM: A statistical object representation model [DE90-009048] N90-21686
CALIFORNIA UNIV., DAVIS.
Convergence acceleration of hypersonic flow calculations: A nonlinear relaxation factor N90-20957
Numerical simulation of vortex breakdown N90-21288
CALIFORNIA UNIV., LOS ANGELES.
Two-dimensional damage models of fiber-reinforced composites N90-21135
Near contact phenomena and transient effects in far infrared photoconductors N90-21316
CALIFORNIA UNIV., SANTA BARBARA.
Surface characterization of hydrogen charged and uncharged alpha-2 and gamma titanium aluminide alloys using AES and REELS [NASA-CR-186561] N90-21171
CARLETON UNIV., OTTAWA (ONTARIO).
Losses in the tip-leakage flow of a planar cascade of turbine blades N90-21027
CARNEGIE-MELLON UNIV., PITTSBURGH, PA.
Analysis and finite element approximation of some optimal control problems associated with the Navier-Stokes equations N90-21299
CASE WESTERN RESERVE UNIV., CLEVELAND, OH.
Laser velocimeter measurements of multiphase flow of solids [DE90-007804] N90-21311
Stress analysis and minimum weight design of honeycomb sandwich plates N90-21418
Evolutionary effects in B stars N90-21704
CENTRE D'ETUDE SPATIALE DES RAYONNEMENTS, TOULOUSE (FRANCE).
ISO/LWS: Detector status N90-21343
CENTRE NATIONAL DE LA RECHERCHE SCIENTIFIQUE, ECULLY (FRANCE).
Paraboloized calculations of turbulent three dimensional flows in a turbine duct N90-21013
CERAMATEC, INC., SALT LAKE CITY, UT.
Development of planar geometry solid oxide fuel cell technology, phase 2 [PB90-131293] N90-21467
CESSNA AIRCRAFT CO., WICHITA, KS.
Flight test investigation of certification issues pertaining to general-aviation-type aircraft with natural laminar flow [NASA-CR-181967] N90-20952
CHALMERS UNIV. OF TECHNOLOGY, GOETEBORG (SWEDEN).
The molecular cloud content of early type galaxies. 2: A molecular ring in NGC 404 [PB90-124348] N90-21695
CHRONAR CORP., PRINCETON, NJ.
Research on amorphous silicon-based thin film photovoltaic devices. Task B: Research on stable high efficiency large area, amorphous silicon-based submodules [DE90-000320] N90-21473
CINCINNATI UNIV., OH.
LDV measurements and the flow analysis in the vortex region of a radial inflow turbine N90-21007
COLORADO UNIV., BOULDER.
Controller reduction for effective interdisciplinary design of active structures N90-21077
COMMONWEALTH SCIENTIFIC AND INDUSTRIAL RESEARCH ORGANIZATION, MORDIALOC (AUSTRALIA).
Zones of feasibility for retrieval of surface pressure from observations of absorption in the A band of oxygen [DAR-TP-19] N90-21495
Sensitivity studies in a two-dimensional atmospheric transport model [DAR-TP-18] N90-21496
COMPUTER RESOURCE MANAGEMENT, INC., VIENNA, VA.
National airspace system air-ground communications operational concept [DOT/FAA/DS-90/2] N90-21249
CONNECTICUT UNIV., STORRS.
Research on cascade secondary and tip-leakage flows: Periodicity and surface flow visualization N90-21026
Atomic processes in high temperature plasmas [DE90-006873] N90-21632
CORNELL UNIV., ITHACA, NY.
Improved Si:As BIBIB (Back-Illuminated Blocked-Impurity-Band) hybrid arrays N90-21349
Anaerobic metabolism of aromatic compounds by phototrophic bacteria: Biochemical aspects [DE90-009503] N90-21516
Fast causal multicast [NASA-CR-186495] N90-21533
Exploiting virtual synchrony in distributed systems [NASA-CR-182855] N90-21555
COUNCIL FOR NATIONAL ACADEMIC AWARDS (ENGLAND).
Flow in a forward swept centrifugal fan, volumes 1 and 2 N90-20959
Supersonic nozzle design of arbitrary cross-section N90-21035

D

DEFENSE CONTRACT ADMINISTRATION SERVICES REGION, SAINT LOUIS, MO.
Quality at a glance [AD-A217297] N90-21400
DEPARTMENT OF AGRICULTURE, EDINBURG, TX.
An introduction to high frequency radioteletype systems [PB90-145533] N90-21252
DEPARTMENT OF DEFENSE EXPLOSIVES SAFETY BOARD, ALEXANDRIA, VA.
Minutes of the 23rd Explosives Safety Seminar, volume 1 [AD-A218264] N90-21213
Minutes of the 23rd Explosives Safety Seminar, volume 2 [AD-A218265] N90-21214
DEPARTMENT OF ENERGY, WASHINGTON, DC.
Fuel cell systems program plan, FY 1990 [DE90-006178] N90-21471
A fossil energy perspective on global climate change [DE90-007894] N90-21483
DEPARTMENT OF THE ARMY, WASHINGTON, DC.
Method of making a long life high current density cathode from tungsten and iridium powders using a quarternary compound as the impregnant [AD-D014425] N90-21211
A real-time rejection circuit to automatically reject multiple interfering hopping signals while passing a lower level desired signal [AD-D014424] N90-21251
DEPARTMENT OF THE NAVY, ARLINGTON, VA.
Energy beam treatment for improved adhesion of coatings to surfaces [AD-D014449] N90-21190
X ray laser with enhanced x ray gain through photodepopulation [AD-D014446] N90-21375
Heat engine based on shape memory alloys [AD-D014400] N90-21385
DEPARTMENT OF THE NAVY, WASHINGTON, DC.
Inflatable fuel tank buffer [AD-D014446] N90-21002
Concentric layer ramjet fuel [AD-D014443] N90-21111
High gloss corrosion-resistant coatings [AD-D014403] N90-21184
A new class of lubricants derived from archaebacterial lipids [AD-D014429] N90-21185
Combination primer/topcoat coating [AD-D014445] N90-21189
Automatic classification of images [AD-D014437] N90-21260
Ablative cooling of aerodynamically heated radomes [AD-D014426] N90-21293
Method for holographic correction of beams of coherent light [AD-D014406] N90-21353
Apparatus and method for locating the axis of symmetry (center of circular cross section) of three dimensional objects [AD-D014407] N90-21354
High power, high sensitivity microwave calorimeter [AD-D014427] N90-21355
Expanding ring joint [AD-D014398] N90-21384
Double valve mechanism for an acoustic modulator [AD-D014401] N90-21386
Passive stabilization of a fiber optic nonlinear interferometric sensor [AD-D014438] N90-21620
DEUTSCHE FORSCHUNGS- UND VERSUCHSANSTALT FUER LUFT- UND RAUMFAHRT, BRUNSWICK (GERMANY, F.R.).
Aerodynamic design techniques at DLR Institute for Design Aerodynamics N90-20979
DEUTSCHE FORSCHUNGS- UND VERSUCHSANSTALT FUER LUFT- UND RAUMFAHRT, GOETTINGEN (GERMANY, F.R.).
Progress in inverse design and optimization in aerodynamics N90-20977
DEUTSCHE FORSCHUNGS- UND VERSUCHSANSTALT FUER LUFT- UND RAUMFAHRT, OBERPFAFFENHOFEN (GERMANY, F.R.).
A fast ISAR-imaging process and its inherent degrading effects on image quality N90-21239
Concept and results of the DLR realtime SAR processor N90-21244
DEUTSCHE FORSCHUNGS- UND VERSUCHSANSTALT FUER LUFT- UND RAUMFAHRT, WESSELING (GERMANY, F.R.).
Real-time adaptive radiometric correction for imaging radars systems N90-21233
A solution for real time motion compensation for SAR without using inertial navigation systems N90-21236
DEUTSCHE FORSCHUNGSANSTALT FUER LUFT- UND RAUMFAHRT, COLOGNE (GERMANY, F.R.).
Secondary flow in a turbine guide vane with low aspect ratio N90-21018
Centrifugal impeller geometry and its influence on secondary flows N90-21020
DEUTSCHE FORSCHUNGSANSTALT FUER LUFT- UND RAUMFAHRT, GOETTINGEN (GERMANY, F.R.).
Measurement of the flow field in the blade passage and side-wall region of a plane turbine cascade N90-21019
DORNIER-WERKE G.M.B.H., FRIEDRICHSHAFEN (GERMANY, F.R.).
Aerodynamic design by optimization N90-20996
DRC CONSULTANTS, INC., FLUSHING, NY.
Heavily loaded joints for assembling aerobrake support trusses [NASA-CR-181992] N90-21099
DURHAM UNIV. (ENGLAND).
An investigation of secondary flows in nozzle guide vanes N90-21016
DYNAMET TECHNOLOGY, INC., BURLINGTON, MA.
Ductile alloy encapsulated ceramic armor development [AD-A217632] N90-21183

E

EA ENGINEERING SCIENCE AND TECHNOLOGY, INC., SPARKS, MD.
Gaithersburg Nike control and launch area preliminary assessment/site inspection, Gaithersburg, Maryland [AD-A217791] N90-21482

EDINBURGH UNIV. (SCOTLAND).
The optical measurement of acoustic velocity fields N90-21601
The evolution and geometry of the outer parts of the small Magellanic cloud N90-21697
The large scale structure of the universe in pancake models of galaxy formation N90-21701
ESSEX CORP., ORLANDO, FL.
Development of microcomputer-based mental acuity tests for repeated-measures studies [NASA-CR-185607] N90-21521
EUROPEAN OFFICE OF AEROSPACE RESEARCH AND DEVELOPMENT, LONDON (ENGLAND).
HOTOL structures and materials at British Aerospace, Warton, UK [EOARD-LR-90-001] N90-21001
Proceedings of the 13th International Congress on Instrumentation in Aerospace Simulation Facilities [EOARD-LR-89-069] N90-21046
Research programs in aeronautical engineering, solid state physics, and materials science at Technion-Israel Institute of Technology, Haifa, Israel [EOARD-LR-89-068] N90-21720
EUROPEAN SPACE AGENCY. EUROPEAN SPACE RESEARCH AND TECHNOLOGY CENTER, ESTEC, NOORDWIJK (NETHERLANDS).
Introduction to the Infrared Space Observatory (ISO) N90-21340

F

FEDERAL AVIATION ADMINISTRATION, ATLANTIC CITY, NJ.
Full-scale air transport category fuselage burnthrough tests [DOT/FAA/CT-TN89/65] N90-20967
Plan for the FAA air traffic operational evaluation of the Automated Surface Observing System (ASOS) [DOT/FAA/CT-TN89/56] N90-20968
Statistics on aircraft gas turbine engine rotor failures that occurred in US commercial aviation during 1986 [DOT/FAA/CT-89/30] N90-21008
Modified touchdown zone lighting [DOT/FAA/CT-TN89/70] N90-21042
Feasibility of using frequency offset on very high frequency air/ground voice channels [DOT/FAA/CT-TN89/71] N90-21248
Data Link Processor (DLP) project transition plan [DOT/FAA/CT-TN89/68] N90-21256
Meteorologist Weather Processor (MWP) integration test plan [DOT/FAA/CT-TN89/62] N90-21500
Analysis of distributions of Visual Meteorological Conditions (VMC) heliport data [DOT/FAA/CT-TN89/67] N90-21508
FEDERAL AVIATION ADMINISTRATION, WASHINGTON, DC.
Census of US civil aircraft [PB90-120296] N90-20920
An early overview of tiltrotor aircraft characteristics and pilot procedures in civil transport applications [DOT/FAA/DS-89/37] N90-21003
Criteria for polymer concrete on airport pavements [DOT/FAA/DS-89/18] N90-21045
Windshear case study: Denver, Colorado, July 11, 1988 [DOT/FAA/DS-89/19] N90-21509
FERMI NATIONAL ACCELERATOR LAB., BATAVIA, IL.
Materials for ultra-high vacuum [DE90-007908] N90-21217
The design of a large aperture high field dipole [DE90-007910] N90-21285
Development of intrinsic IPT scintillator [DE90-007906] N90-21367
FINNISH METEOROLOGICAL INST., HELSINKI.
Transformation and deposition of airborne gaseous and particulate pollutants during transport over the Baltic Sea [PUBL-AIR-QUALITY-5] N90-21478
Observations of atmospheric electricity, 1988 [GEOPHYSICAL-PUBL-10] N90-21499
FLORIDA UNIV., GAINESVILLE.
On total variation diminishing schemes for transonic turbulent flow computation N90-20945
FOREIGN APPLIED SCIENCES ASSESSMENT CENTER, LA JOLLA, CA.
West European magnetic confinement fusion research N90-21634
FOREST SERVICE, WASHINGTON, DC.
Effects of Air Pollution on Western Forests [PB90-131111] N90-21481
FORSCHUNGSINSTITUT FUER FUNK UND MATHEMATIK, WERTHOVEN (GERMANY, F.R.).
Application of superresolution methods for airborne radar N90-21227
The 1D-ISAR imaging of manoeuvering aircraft N90-21241
FORSCHUNGSINSTITUT FUER HOCHFREQUENZPHYSIK, WERTHHOVEN (GERMANY, F.R.).
Problems in ISAR processing with range resolution by stepped frequency bursts N90-21238

G

GENERAL ATOMIC CO., SAN DIEGO, CA.
Applied plasma physics [DE90-007932] N90-21635
Fusion technology development [DE90-007933] N90-21636
GENERAL ELECTRIC CO., PHILADELPHIA, PA.
Final safety analysis report for the Ulysses mission. Volume 2 (Book 1): Accident model document [DE90-008694] N90-21103
Final safety analysis report for the Ulysses Mission. Volume 2: Accident model document-appendices [DE90-008695] N90-21104
Final safety analysis report for the Ulysses mission. Volume 1: Reference design document [DE90-008693] N90-21107
GENERAL ELECTRIC CO., SCHENECTADY, NY.
Generation and decay of secondary flows and their impact on aerodynamic performance of modern turbomachinery components N90-21023
The radiation of sound from a propeller at angle of attack [NASA-CR-4264] N90-21602
GEORGE WASHINGTON UNIV., WASHINGTON, DC.
Cepstrum analysis and applications to computational fluid dynamic solutions N90-21302
GEORGIA INST. OF TECH., ATLANTA.
Design of a helicopter automatic flight control system using adaptive control N90-21040
Elastic-plastic instability of plane frames N90-21415
The extension of rapid distortion theory to stratified shear flows N90-21491
Curvature continuity of cubic Bezier curves in the solid modeling aerospace research tools design software [NASA-CR-186583] N90-21554
GRUMMAN AEROSPACE CORP., BETHPAGE, NY.
Inverse design of airfoil contours: Constraints, numerical method, and applications N90-20980

H

HARVARD UNIV., CAMBRIDGE, MA.
Mechanics of interface fracture N90-21408
Relativistic processes in active galactic nuclei N90-21698
HELSINKI UNIV. OF TECHNOLOGY, ESPOO (FINLAND).
An evaluation of the two-dimensional Euler and Navier-Stokes calculations based on a flux-vector splitting [PB90-166778] N90-20963
Subsonic flutter analysis using MSC/NASTRAN [PB90-166786] N90-21041
Phase equilibria and solution thermodynamics of bismuth-lead alloys [PB90-138421] N90-21163
Computer processing of multi-channel electromagnetic data from an airborne geophysical survey system [PB90-138413] N90-21253
New ferrite-filled waveguiding structures analysed by the averaging method [PB90-165671] N90-21269
Generalized WKB approximation for stratified isotropic chiral structures [PB90-165689] N90-21270
The development of a simulation program of the anode side for aluminum/air batteries [PB90-165754] N90-21286
A modification of a low-order Reissner-Mindlin plate bending element [PB90-165630] N90-21428
On the stability of a certain difference scheme [PB90-165814] N90-21588
A remark on the Kelvin transform and a non-linear partial differential equation [PB90-165622] N90-21589
HONEYWELL, INC., BLOOMINGTON, MN.
High efficiency octave bandwidth millimeter wave power amplifier [AD-A218245] N90-21280
HONEYWELL ELECTRO-OPTICS CENTER, LEXINGTON, MA.
Short wavelength HgCdTe staring focal plane for low background astronomy applications N90-21336

I

ILLINOIS UNIV., CHICAGO.
Phase equilibrium of mixtures consisting of molecules with large size and shape differences (thermodynamic modeling of Supercritical Fluid Extraction and Retrograde Condensation, SFE/RC) [PB90-131285] N90-21146
Determination of stresses around cutouts in multilayered composite plate and shell structures N90-21417
ILLINOIS UNIV., URBANA-CHAMPAIGN.
Architecture independent environment for developing engineering software on MIMD computers [NASA-CR-186562] N90-21553
NETRA: A parallel architecture for integrated vision systems 2: Algorithms and performance evaluation [NASA-CR-186510] N90-21557
INDIAN INST. OF SCIENCE, BANGALORE.
State of the art of acoustics of active and passive mufflers N90-21597
INSTITUTE FOR ADVANCED STUDY, PRINCETON, NJ.
Rings [DE90-009035] N90-21613
Some global problems in gauge theories (variations on a theme of Aharonov and Bohm) [DE90-009034] N90-21678
The 2 + 1 dimensional quantum gravity and the Braid group [DE90-009036] N90-21679
INSTITUTE FOR COMPUTER APPLICATIONS IN SCIENCE AND ENGINEERING, HAMPTON, VA.
On the instability of Goertler vortices to nonlinear travelling waves [NASA-CR-181994] N90-21289
Surface-cooling effects on compressible boundary-layer instability [NASA-CR-182003] N90-21290
Performance bounds on parallel self-initiating discrete-event [NASA-CR-182010] N90-21556
On the continuous dependence with respect to sampling of the linear quadratic regulator problem for distributed parameter systems [NASA-CR-182012] N90-21566
INSTITUTE FOR PERCEPTION RVO-TNO, SOESTERBERG (NETHERLANDS).
Space adaptation syndrome induced by a long duration +3Gx centrifuge run [AD-A218248] N90-21518
INSTITUTE OF PLASMA PHYSICS, PRAGUE (CZECHOSLOVAKIA).
Solar flares and dynamics of Langmuir waves in current-carrying plasmas [IPPCZ-291] N90-21710
INSTITUTO DE PESQUISAS ENERGETICAS E NUCLEARES, SAO PAULO (BRAZIL).
A simplified theoretical model for the laser-induced optogalvanic effect [DE90-613121] N90-21626
INSTITUTO DE PESQUISAS ESPACIAIS, CACHOEIRA PAULISTA (BRAZIL).
Subsystem TM Precision: Progress and perspective [INPE-5006-PRE/1563] N90-21461
INSTITUTO DE PESQUISAS ESPACIAIS, SAO JOSE DOS CAMPOS (BRAZIL).
Suboptimal and hybrid numerical solution schemes for orbit transfer manoeuvres [INPE-4991-PRE/1556] N90-21054
Design of a digital model following controller of reaction wheel torques [INPE-4753-PRE/1425] N90-21093
Attitude control modes for the MECB remote sensing satellites [INPE-4755-PRE/1427] N90-21094
Space environment simulation of the SCD-01 satellite through heating plates [INPE-4988-PRE/1550] N90-21105
Numerical simulation model for hydrazine attitude control thrusters. Part 1: Model description [INPE-4952-RPE/601] N90-21115
Resistance mechanics for laminated composite materials [INPE-4919-RPE/594] N90-21141
On board cross support scenarios [INPE-5005-PRE/1562] N90-21268
Programme of the International Training Course on Remote Sensing for African Specialists [INPE-4878-NTE/290] N90-21435
Results of the Gondwana Project: An example of intercontinental geologic correlation utilizing LANDSAT imagery [INPE-4870-PRE/1481] N90-21437
Remote sensing applied to sea water quality researches in coastal regions: A review [INPE-4935-PRE/1425] N90-21438

Wheat yield estimation at the farm level using LANDSAT TM and agrometeorological data
[INPE-5017-RPE/611] N90-21439
Geobotanical remote sensing: A review
[INPE-5026-PRE/1565] N90-21440
Agricultural yield estimation of sugarcane based on agrometeorological-spectral model
[INPE-5016-RPE/610] N90-21441
Monitoring of agrocattle-raising projects through visual/digital analysis of LANDSAT-TM imagery south of Para state
[INPE-4982-PRE/1542] N90-21442
Survey of land use through remote sensing
[INPE-5032-MD/042] N90-21443
A knowledge-based information based for crop area estimation
[INPE-4990-PRE/1555] N90-21444
Analysis and modelling of spatial data proposal of a system for CBERS
[INPE-4911-PRE/1512] N90-21445
Project CANASATE: Remote sensing applied to sugar cane crop survey
[INPE-4902-PRE/1503] N90-21446
Generation of triangular form models in a microcomputer environment
[INPE-4974-PRE/1539] N90-21447
Digital processing of TM/LANDSAT data in monitoring interior water
[INPE-4956-PRE/1533] N90-21448
Characterization of linear structures from remote sensing data; Espinhaco Meridional (MG) sierra
[INPE-4905-PRE/1506] N90-21449
Geology of Espinhaco Meridional, including the Quadrilatero Ferrifero: Integration through remote sensing data
[INPE-4904-PRE/1505] N90-21450
Monitoring vegetation of Brazil: Potentialities of multi-sensors approach
[INPE-4993-PRE/1555] N90-21451
Evolution of remote sensing applied to vegetation and forest at INPE
[INPE-4970-PRE/1538] N90-21452
Analysis of water quality parameters of the Piaui River (SE), Brazil, through field and TM/LANDSAT sensor data
[INPE-4918-PRE/1417] N90-21453
Evaluation of the mangrove areas of the Rio Piaui (SE) through remote sensing
[INPE-4909-PRE/1510] N90-21454
Aerial photography as an aid for agricultural credit control
[INPE-5019-RPE/613] N90-21455
Introduction of digital image processing by remote sensors applied to geology
[INPE-5023-RPE/616] N90-21456
Multitemporal analysis of LANDSAT/TM digital imagery in the detection of areas affected by caterpillar (sibine fusca) attack in the dende (elais guineensis) palm plantation
[INPE-4979-PRE/1544] N90-21457
Evaluation of classification performance and proportion estimate of the sugar cane crop through PROCEDURE-INPE utilizing LANDSAT data
[INPE-4899-PRE/1500] N90-21458
Contribution for the study of the evolution of part of the Espinhaco supergroup and its foundation through fracture analysis
[INPE-4907-PRE/1508] N90-21459
Wheat productivity estimate through field radiometry
[INPE-4994-PRE/1556] N90-21460
Possible use of satellite data for flood plain mapping
[INPE-4968-PRE/1537] N90-21462
Performance evaluation of MSS/LANDSAT data in the estimation of fluvial channel width
[INPE-4906-PRE/1507] N90-21463
Performance evaluation of morphological edge detectors
[INPE-4975-PRE/1540] N90-21464
Regional remote sensing laboratory
[INPE-4922-PRE/1519] N90-21465
Radon concentration over the Brazilian Amazon Basin during the wet season (Belem-Manaus GTE-ABLE-2B flight of April 24, 1987)
[INPE-4892-PRE/1493] N90-21486
Low latitude F-region dynamical processes from atomic oxygen nightglow emissions
[INPE-4999-PRE/1561] N90-21494
Finite element algorithms for hyperbolic conservation laws with forcing terms
[INPE-5024-RPE/617] N90-21595
Characterization of the plasma in magnetic multidipole discharges
[DE90-613219] N90-21628
New water vapor masers in the Southern Hemisphere
[INPE-4844-PRE/1473] N90-21689
High energy phenomena during solar flares
[INPE-4961-TDL/390] N90-21713
Comparison of quiet time geomagnetic daily variation (Sq) in H component at Eusebio and Cachoeira Paulista
[INPE-4985-PRE/1547] N90-21714

INSTITUTO SUPERIOR TECNICO, LISBON (PORTUGAL).

Application of an inverse method to the design of a radial inflow turbine N90-20989

INTERNATIONAL CENTRE FOR THEORETICAL PHYSICS, TRIESTE (ITALY).

On the dynamics of polymer mixtures in solution using the RPA
[DE90-613689] N90-21149
Ionic equilibrium between octahedral and tetrahedral complexes in liquid aluminium-sodium fluoride mixtures
[DE90-613690] N90-21150
Modified tight-binding approximation and electron-phonon spectral function for transition metals
[DE90-614022] N90-21166
Generalized random phase approximation for multicomponent polymer systems
[DE90-613691] N90-21194
Ultrarelativistic envelope solitons in electron-positron plasma of the pulsar magnetosphere
[DE90-613289] N90-21264
On the creation of gravitational wave by photon in external electromagnetic field
[DE90-613366] N90-21265
Production of diffraction gratings using holographic interferometry
[DE90-612841] N90-21362
On induced Hermitian metrics for holomorphic vector bundles
[DE90-612737] N90-21572
The monad construction and Hermetian-Einstein metrics
[DE90-612738] N90-21573
On a non classical oblique derivative problem for parabolic singular integro-differential operators
[DE90-612739] N90-21574
On the equation: Delta u+c=Ke(sup u)
[DE90-612741] N90-21575
Weierstrass preparation and division theorems for the ring of germs of superanalytic functions
[DE90-612742] N90-21576
A Lagrangian formalism for nonequilibrium ensembles
[DE90-612748] N90-21579
Periodic solutions for Hamiltonian systems in a nonconvex potential well
[DE90-612752] N90-21580
The N = 2 superconformal algebras on hyperelliptic surfaces and their Coulomb gas realization
[DE90-612790] N90-21581
Linking numbers and variational method
[DE90-612793] N90-21582
Fusion algebra and fusing matrices
[DE90-612796] N90-21583
A modified Moebius inverse formula and its applications in physics
[DE90-612740] N90-21594
Polarization: Effects on second harmonic power in light scattering by free electrons
[DE90-612842] N90-21608
Relativistic stimulated Brillouin and Raman scattering in a laser-produced plasma
[DE90-613123] N90-21627
On the relativistic Vlasov equation in guiding-center coordinates
[DE90-613241] N90-21629
Coupled magnetoplasmon-phonon modes at the surface of a semi-infinite semiconductor superlattice
[DE90-612904] N90-21647
Chern-Simons superconductivity at finite temperature
[DE90-613393] N90-21650
Specific heat and critical fluctuations in anisotropic high-T(sub c) oxide superconductors
[DE90-613394] N90-21651
On the substitution of Sr ions at Y sites in YB(suba2)Cu3O(sub7-d)
[DE90-613395] N90-21652
Local supersymmetry in non-relativistic systems
[DE90-612751] N90-21670
Quantization of the N = 2m simple supergravity in d = 2 + 1
[DE90-612765] N90-21671
Conserved conformal currents in curved space-time
[DE90-612766] N90-21672
String dynamics in curved space-time revisited
[DE90-612796] N90-21674
Thermal decay of an initially hot isothermal water body with application to thermal energy storage
[DE90-614742] N90-21675
A mechanism for the formation of knots, kinks and discontinuous events in the plasma tail of comets
[DE90-613285] N90-21707
Horizon problem in cosmological models with non zero
[DE90-613367] N90-21708

INTERNATIONAL SOCIETY FOR TERRAIN-VEHICLE SYSTEMS, HANOVER, NH.

Proceedings of the 4th European Conference, volume 2
[AD-A216521] N90-21382

IOWA STATE UNIV. OF SCIENCE AND TECHNOLOGY, AMES.

Fracture of sandwiched composites N90-21136

IOWA UNIV., IOWA CITY.

Computation of viscous flow around a propeller-shaft configuration with infinite-pitch rectangular blades N90-20958

ISRAEL ACADEMY OF SCIENCES AND HUMANITIES, JERUSALEM.

Tenth International Free Electron Laser Conference
[DE90-614773] N90-21376

J

JAPAN ATOMIC ENERGY RESEARCH INST., IBARAKI.

The development of computational algorithms for manipulator inverse kinematics
[DE90-759877] N90-21561
Adaptive learning fuzzy control of a mobile robot
[DE90-759898] N90-21562
Numerical code AEOLUS-E1 for analysing free-boundary resistive MHD mode
[DE90-759903] N90-21630

JAPAN ATOMIC ENERGY RESEARCH INST., TOKYO.

Low energy ion generator
[DE90-759905] N90-21195

JET PROPULSION LAB., CALIFORNIA INST. OF TECH., PASADENA.

VLSI single-chip (255,223) Reed-Solomon encoder with interleaver
[NASA-CASE-NPO-17280-1-CU] N90-21061
A spaceborne optical interferometer: The JPL CSI mission focus N90-21063
Vibration isolation versus vibration compensation on multiple payload platforms N90-21066
Recent experience in simultaneous control-structure optimization N90-21078
Experimental evaluation of active-member control of precision structures N90-21084
CSI technology validation on an LSS ground experiment facility N90-21089
Extrinsic germanium Blocked Impurity Bank (BIB) detectors N90-21322
Environmental projects, volume 11. Environmental assessment: Addition to operations building, Mars site
[NASA-CR-186449] N90-21479
Environmental projects, volume 10. Environmental assessment: New 34-meter antenna at Apollo site
[NASA-CR-186448] N90-21480

JOINT ASTRONOMY CENTRE, HILO, HI.

Experience with the UKIRT InSb array camera N90-21327

JOINT INST. FOR NUCLEAR RESEARCH, DUBNA (USSR).

Neutron autoradiography of hydrogen
[DE90-612930] N90-21148
Microchannel photomultipliers in time spectrometer
[DE90-616417] N90-21356
CAD work station for electronics designer
[DE90-616473] N90-21546
The parallel algorithm for solving the three-dimensional integral magnetostatic equations
[DE90-616529] N90-21547
Extension of the constraints algebra for the closed string with the fixed topology world sheet
[DE90-612745] N90-21577
Extension of the Krichever-Novikov algebra in the closed string theory
[DE90-612746] N90-21578
Once more about the sizes of fast-moving objects
[DE90-615204] N90-21592
Mesooptical Fourier transform microscope: A new device for high energy physics
[DE90-616423] N90-21615
Characteristics consequences of space-time coordinate relativization
[DE90-615201] N90-21668
The generally covariant representation of energy-momentum pseudotensor of gravitational field
[DE90-615203] N90-21669

JOINT PUBLICATIONS RESEARCH SERVICE, ARLINGTON, VA.

JPRS report: Science and technology. USSR: Electronics and electrical engineering
[JPRS-UEE-90-002] N90-21284

JPRS report: Science and technology. USSR: Earth sciences
[JPRS-UES-90-005] N90-21433
JPRS report: Science and technology. USSR: Life sciences
[JPRS-ULS-90-002] N90-21434
JPRS report: Science and technology. USSR: Physics and mathematics
[JPRS-UPM-90-002] N90-21583

JOINT PUBLICATIONS RESEARCH SERVICE, WASHINGTON, DC.
JPRS report. Science and technology. USSR: Earth sciences
[JPRS-UES-88-004] N90-21431
JPRS report. Science and technology. USSR: Earth sciences
[JPRS-UES-89-002] N90-21432

K

KENTUCKY UNIV., LEXINGTON.
Problems in radiative transfer in astrophysics: An escape probability treatment of line overlap and a model of the masers around VX Sgr N90-21705

L

LABORATORIO DE COMPUTACAO CIENTIFICA, RIO DE JANEIRO (BRAZIL).
A numerical model for the determination of periodic solutions of pipes subjected to non-conservative loads
[DE90-614756] N90-21423

LAGUNA RESEARCH LAB., FALLBROOK, CA.
Quadratic Hadamard Memories 1
[AD-A217224] N90-21534

LAWRENCE LIVERMORE NATIONAL LAB., CA.
Railgun performance with a two-stage light-gas gun injector
[DE90-009183] N90-21057
A distributed finite-element modeling and control approach for large flexible structures N90-21071
Direct sublimation of NaCl salt from carbon matrixes
[DE90-007927] N90-21139
Magnetron sputtered boron films and Ti/B multilayer structures
[DE90-009190] N90-21153
High-resolution Brillouin gain spectroscopy in solids
[DE90-009475] N90-21155
Ordering mechanism in substitutional Ni-Cr alloys: Theory and experiment
[DE90-006268] N90-21156
Formation of subsurface aluminum layers in beryllium by ion implantation and post-implant annealing
[DE90-007975] N90-21172
A correlation-spectral method for line detection on noisy data
[DE90-007925] N90-21266
Error correction of the DEA (Digital Electronic Automation) coordinate measuring machines at LLNL
[DE90-008913] N90-21365
Absolute multilayer characterization at high spatial resolution via real-time soft x ray imaging
[DE90-009181] N90-21371
High explosives (PBX9502) characterization using computerized tomography
[DE90-008170] N90-21404
Does DNA cytometry have a place in the clinical laboratory
[DE90-007652] N90-21512
A parallel multigrid method for solving elliptic partial differential equations
[DE90-007929] N90-21584
Differential-algebraic equations as stiff ordinary differential equations
[DE90-007922] N90-21585
Proposal for FY86 Lawrence Livermore National Laboratory particle beam research
[DE90-007936] N90-21617
Charged-particle beam research program
[DE90-007937] N90-21618
An extended diffusive model for calculating thermal diffusivity from single monopole tokamak heat pulse propagation
[DE90-007958] N90-21637
Thermogravimetric analysis of Nd(2-x)Ce(x)CuO(4-delta)
[DE90-009184] N90-21658
Shock compression of solids: A tutorial
[DE90-009185] N90-21659
Program CICC: Flow and heat transfer in Cable In Conduit Conductors, user's manual
[DE90-007924] N90-21661
Microstructure of Au/Nb multilayers
[DE90-008722] N90-21662
New surface atomic structures for column 5 overlayers on the (110) surfaces of 3-5 compound semiconductors
[DE90-009003] N90-21663
Progress in the material development of LiCaAlF(6):Cr(3+) laser crystals
[DE90-009542] N90-21666
Mars in this century: The Olympia Project
[DE90-008356] N90-21709

LEICESTER UNIV. (ENGLAND).
Design and optimisation of thin foil x ray telescopes N90-21690

LITTON SYSTEMS, INC., CHARLOTTE, NC.
Contract crystal growth and fabrication services
[AD-A218327] N90-21646

LOCKHEED ENGINEERING AND SCIENCES CO., HAMPTON, VA.
LaRC TPI 1500 series polymers
[NASA-CR-181899] N90-21129
Sonic boom signature data from cruciform microphone array experiments during the 1966-1967 EAFB national sonic boom evaluation program
[NASA-CR-182027] N90-21605

LOCKHEED ENGINEERING AND SCIENCES CO., WASHINGTON, DC.
USSR Space Life Sciences Digest, Issue 26
[NASA-CR-392231] N90-21513

LOCKHEED MISSILES AND SPACE CO., PALO ALTO, CA.
ASCIE: An integrated experiment to study CSI in large segmented optical systems N90-21082
The computational structural mechanics testbed generic structural-element processor manual
[NASA-CR-181728] N90-21410

LOS ALAMOS NATIONAL LAB., NM.
Strengthening mechanisms of tungsten powder reinforced uranium
[DE90-009331] N90-21144
Diamond: A high power optical material
[DE90-008941] N90-21196
Discrete modeling of beds of propellant exposed to strong stimulus
[DE90-008932] N90-21206
The RAP unit: A remote autoranging picoammeter
[DE90-007711] N90-21357
Cloud hole-boring with long pulse CO2 lasers
[DE90-008946] N90-21377
Principles of the radioeity method for canopy reflectance modeling
[DE90-008943] N90-21466
Artificial life: The coming evolution
[DE90-008860] N90-21515
Application of neural nets to system identification and bifurcation analysis of real world experimental data
[DE90-007539] N90-21558
Stability of a solitary wave solution to a set of coupled Boussinesq-like equations
[DE90-008927] N90-21586
Comparison of the algebraic reconstruction technique with the maximum entropy reconstruction technique for a variety of detection tasks
[DE90-008933] N90-21587
Gamma-ray production cross section measurements using a white neutron source from 1 to 400 MeV
[DE90-008906] N90-21610
A measurement of the gravitational acceleration of the antiproton
[DE90-008903] N90-21612
Dynamics of cavitons in strong Langmuir turbulence
[DE90-008918] N90-21633
Fusion burn dynamics in Dense Z-Pinch (DZP)
[DE90-007976] N90-21638
Nonoptimal entropy generation by heat transfer in cryogenic domain
[DE90-007544] N90-21667
Recent advances in the studies of the nova outburst
[DE90-008936] N90-21691
Multi-wavelength observations of novae in outburst
[DE90-008934] N90-21692
The 1989 outburst of V404 Cygni: A very unusual x ray nova
[DE90-008935] N90-21693
Model atmospheres for novae during the early stages
[NASA-CR-180498] N90-21694
Substorms: Their expansion and recovery phases
[DE90-008970] N90-21712

M

MARCONI SPACE SYSTEMS LTD., PORTSMOUTH (ENGLAND).
Trade-offs in a space based surveillance radar N90-21225
Capabilities of bistatic synthetic aperture radar for covert battlefield surveillance N90-21230

MARTIN MARIETTA AEROSPACE, DENVER, CO.
Zenith Star: A structural control challenge N90-21064
PACOSS program status and results N90-21065
An air-bearing weight offload system for ground test of heavy LSS structures N90-21081

MARTIN MARIETTA CORP., DENVER, CO.
Millimeter wave near-field study
[NASA-CR-182014] N90-21058

MARYLAND UNIV., COLLEGE PARK.
Generation of ultrashort laser pulses from neodymium glass oscillator and regenerative amplifier N90-21373
Maintenance = reuse-oriented software development
[NASA-CR-186455] N90-21531
Integrating automated support for a software management cycle into the TAME system
[NASA-CR-186457] N90-21532
Experimental study of population inversion and spectral line broadening in a plasma containing a mixture of high Z and low Z ions
[DE90-007552] N90-21622

MASSACHUSETTS INST. OF TECH., CAMBRIDGE.
Investigation of air transportation technology at the Massachusetts Institute of Technology, 1988-1989 N90-20922
Automatic speech recognition in air traffic control N90-20923
Cockpit display of hazardous wind shear information N90-20924
Ultrasonic techniques for aircraft ice accretion measurement N90-20926
Investigation of surface water behavior during glaze ice accretion N90-20927
The influence of ice accretion physics on the forecasting of aircraft icing conditions N90-20928
Cockpit display of hazardous weather information N90-20929
Time and truth in plans N90-20930
Ambiguity bootstrapping to determine GPS orbits and baselines
[AD-A218206] N90-21052
Fracture and longevity of composite structures
[AD-A217827] N90-21127
Center of excellence in theoretical geoplasma research
[AD-A215035] N90-21488

MASSACHUSETTS UNIV., AMHERST.
Mixing of viscous fluids: Behavior of microstructures and chaos
[DE90-008871] N90-21304

MATERIALS RESEARCH LABS., ASCOT VALE (AUSTRALIA).
The measurement of surface reflectivity at millimetre wavelengths
[MRL-TN-559] N90-21222

MATERIALS RESEARCH LABS., MARIBYRNONG (AUSTRALIA).
A corrosion fatigue/stress corrosion testing facility at Materials Research Laboratory
[MRL-TN-568] N90-21044
Reinforcement-matrix interface effects in metal matrix composites
[MRL-TN-562] N90-21120
A computational model of the perforation of multi-layer metallic laminates
[MRL-RR-9-89] N90-21128
Methods for improving the flowability of a percussion primer composition
[MRL-TR-89-32] N90-21201
An evaluation of metal salts of 3-nitro-1,2,4-triazol-5-one (NTO) as potential primary explosives
[MRL-TN-563] N90-21202
Preparation, characterisation and cookoff behaviour of booster compositions prepared from RDX and acrylic or ethylene-vinyl acetate dispersions
[MRL-TR-89-44] N90-21203
Determination of detonation parameters of booster explosives at small charge diameters
[MRL-TR-89-45] N90-21204
An outline for the analysis of wave induced bottom pressure fluctuations
[MRL-TN-558] N90-21510

MAX-PLANCK-INST. FUER ASTRONOMIE, HEIDELBERG (GERMANY, F.R.).
Status of the isophot detector development N90-21342
Tests of the Rockwell Si:As Back-Illuminated Blocked-Impurity Band (BIBIB) detectors N90-21350

MAYFLOWER COMMUNICATIONS CO., INC., READING, MA.
Autonomous integrated GPS/INS navigation experiment for OMV. Phase 1: Feasibility study
[NASA-CR-4267] N90-20989

MECHANICAL DYNAMICS, INC., ANN ARBOR, MI.
Element-specific modal formulations for large-displacement multibody dynamics N90-21069

MECHANICAL TECHNOLOGY, INC., LATHAM, NY.
Internal rotor friction instability
[NASA-CR-183942] N90-21395
MEGA RESEARCH, INC., RANCHO PALOS VERDES, CA.
Improved analytical capabilities for foil air bearings, phase 1
[AD-A218071] N90-21389
MELBOURNE UNIV., PARKVILLE (AUSTRALIA).
ZELED analysis of aperiodicity and bond lengths in ceramic powders
[DE90-612932] N90-21193
Large basis space effects in electron scattering form factors of light nuclei
[DE90-613501] N90-21609
Retabulation of space group extinctions for electron diffraction
[DE90-612933] N90-21648
An attempt to measure cold-fusion effects
[DE90-613248] N90-21649
Deformation and microstructure of rutile
[DE90-614113] N90-21654
MESSERSCHMITT-BOELKOW-BLOHM G.M.B.H., MUNICH (GERMANY, F.R.).
An intensive procedure for the design of pressure-specified three-dimensional configurations at subsonic and supersonic speeds by means of a higher-order panel method N90-20982
MESSERSCHMITT-BOELKOW-BLOHM G.M.B.H., OTTOBRUNN (GERMANY, F.R.).
Concepts for high resolution space based SAR/ISAR systems: Preliminary design considerations N90-21224
ROSAR (Helicopter-Rotor based Synthetic Aperture Radar) N90-21229
MICHIGAN STATE UNIV., EAST LANSING.
The effects of forcing on a single stream shear layer and its parent boundary layer
[NASA-CR-186529] N90-21301
MICHIGAN UNIV., ANN ARBOR.
The structural basis for fatigue initiation in glassy polymers
[DE90-009342] N90-21200
MIDDLE EAST TECHNICAL UNIV., ANKARA (TURKEY).
A computational design method for shock free transonic cascades and airfoils N90-20986
A study on secondary flow and spanwise mixing in axial flow compressors N90-21012
MIDWEST RESEARCH INST., GOLDEN, CO.
Characterization and comparison of optically transparent conducting films
[DE90-000319] N90-21660
MINNESOTA MINING AND MFG. CO., SAINT PAUL.
Improvement of small-area, amorphous-silicon thin-film photovoltaics on polymer substrate
[DE90-000314] N90-21472
MINNESOTA UNIV., MINNEAPOLIS.
Fragmentation of relativistic heavy nuclei with application to cosmic ray propagation N90-21716
MISSION RESEARCH CORP., LOS ALAMOS, NM.
Substorms: Their expansion and recovery phases
[DE90-008970] N90-21712
MISSISSIPPI STATE UNIV., MISSISSIPPI STATE.
Adaptive grid embedding for the two-dimensional flux-split Euler equations
[NASA-CR-186533] N90-21571
MISSOURI UNIV., ROLLA.
An aerodynamic tradeoff study of the scissor wing configuration
[NASA-CR-186576] N90-20965
MOTOREN- UND TURBINEN-UNION MUENCHEN G.M.B.H. (GERMANY, F.R.).
Experimental and numerical study on basic phenomena of secondary flows in turbines N90-21014

N

NATIONAL AERONAUTICAL LAB., BANGALORE (INDIA).
Multigrid accelerated relaxation solution of transonic full potential flow equation
[PD-CF-8942] N90-20951
Flight path reconstruction using extended Kalman filtering techniques
[PD-FC-9001] N90-20970
Design of a natural laminar flow airfoil for an unmanned aircraft
[PD-CF-9004] N90-20975
Human centrifuge controller
[NAL-TM-SE-8901] N90-21043
Human factors in fighter software development
[PD-CF-9003] N90-21522
NATIONAL AERONAUTICS AND SPACE ADMINISTRATION, WASHINGTON, DC.
The partnership: Space shuttle, space science, and space station
[NASA-TM-102900] N90-21050
Microgravity science and applications bibliography, 1989 revision
[NASA-TM-4192] N90-21207
Small business innovation research. Abstracts of 1988 phase 1 awards
[NASA-TM-102991] N90-21680
Small business innovation research. Abstracts of completed 1987 phase 1 projects
[NASA-TM-101797] N90-21681
NATIONAL AERONAUTICS AND SPACE ADMINISTRATION. AMES RESEARCH CENTER, MOFFETT FIELD, CA.
Boron-containing organosilane polymers and ceramic materials thereof
[NASA-CASE-ARC-11649-2-SB] N90-21177
Thermal control system corrosion study
[NASA-TM-102220] N90-21294
Proceedings of the Third Infrared Detector Technology Workshop
[NASA-TM-102209] N90-21313
A progress report on using bolometers cooled by adiabatic demagnetization refrigeration N90-21318
High resolution imaging of the Venus night side using a Rockwell 128x128 HgCdTe array N90-21330
SIRTF in high earth orbit N90-21345
SOFIA: Stratospheric Observatory for Infrared Astronomy N90-21346
Laboratory characterization of direct readout Si:Sb and Si:Ga infrared detector arrays N90-21347
NATIONAL AERONAUTICS AND SPACE ADMINISTRATION. GODDARD SPACE FLIGHT CENTER, GREENBELT, MD.
Goes I-M and beyond: Science requirements and technology challenges N90-21067
Fracture toughness and crack growth of Zerodur
[NASA-TM-4185] N90-21187
Reduction and analysis techniques for infrared imaging data N90-21328
Initial astronomical results with a new 5-14 micron Si:Ga 58x62 DRO array camera N90-21334
Shade images of forested areas obtained from LANDSAT MSS data
[NASA-TM-102939] N90-21436
Annotated bibliography of software engineering laboratory literature
[NASA-TM-103313] N90-21536
Collected software engineering papers, volume 7
[NASA-TM-103312] N90-21537
Lessons learned in the transition to Ada from FORTRAN at NASA/Goddard
[NASA-TM-103311] N90-21538
Evolution of Ada technology in the flight dynamics area: Implementation/testing phase analysis
[NASA-TM-103310] N90-21539
Collected software engineering papers, volume 6
[NASA-TM-103309] N90-21540
System testing of a production Ada (trademark) project: The GRODY study
[NASA-TM-103308] N90-21541
Evolution of Ada technology in the flight dynamics area: Design phase analysis
[NASA-TM-103307] N90-21542
Software Management Environment (SME) concepts and architecture
[NASA-TM-103306] N90-21543
Implementation of a production Ada project: The GRODY study
[NASA-TM-103305] N90-21544
Software Engineering Laboratory (SEL) database organization and user's guide
[NASA-TM-103304] N90-21545
NATIONAL AERONAUTICS AND SPACE ADMINISTRATION. LYNDON B. JOHNSON SPACE CENTER, HOUSTON, TX.
Cosmic Dust Collection Facility: Scientific objectives and programmatic relations
[NASA-TM-102160] N90-21098
Double swivel toggle release
[NASA-CASE-MSC-21436-1] N90-21390
Research and Technology
[NASA-TM-102161] N90-21721
NATIONAL AERONAUTICS AND SPACE ADMINISTRATION. LANGLEY RESEARCH CENTER, HAMPTON, VA.
Joint University Program for Air Transportation Research, 1988-1989
[NASA-CP-3063] N90-20921
Discrete-vortex model for the symmetric-vortex flow on cones
[NASA-TP-2989] N90-20948
Performance data from a wind-tunnel test of two main-rotor blade designs for a utility-class helicopter
[NASA-TM-4183] N90-20974
Stereopsis cueing effects on hover-in-turbulence performance in a simulated rotorcraft
[NASA-TP-2980] N90-21004
Simulator comparison of thumball, thumb switch, and touch screen input concepts for interaction with a large screen cockpit display format
[NASA-TM-102587] N90-21005
Experimental aeroelasticity history, status and future in brief
[NASA-TM-102651] N90-21047
NASA/DOD Controls-Structures Interaction Technology 1989
[NASA-CP-3041] N90-21062
Controlled multibody dynamics simulation for large space structures N90-21068
Nonlinear and distributed parameter models of the mini-mast truss N90-21070
Modeling and control of flexible space platforms with articulated payloads N90-21073
Computational architecture for integrated controls and structures design N90-21076
A survey of experiments and experimental facilities for active control of flexible structures N90-21079
NASA CSI suspension methods overview N90-21080
Strain and dynamic measurements using fiber optic sensors embedded into graphite/epoxy tubes N90-21090
Preliminary design approach for large high precision segmented reflectors
[NASA-TM-102605] N90-21096
Bis(4-(3,4-dimethylenepyrrolidyl)-phenyl) methane
[NASA-CASE-LAR-13965-1-CU] N90-21118
Relevance of impacter shape to nonvisible damage and residual tensile strength of a thick graphite/epoxy laminate
[NASA-TM-102599] N90-21122
Combined effect of matrix cracking and stress-free edge on delamination
[NASA-TM-102591] N90-21126
Three-dimensional elastic-plastic analysis of shallow cracks in single-edge-crack-tension specimens
[NASA-TM-102636] N90-21130
Micromechanics analysis of space simulated thermal deformations and stresses in continuous fiber reinforced composites
[NASA-TM-102633] N90-21140
A compendium of sources of fracture toughness and fatigue crack growth data for metallic alloys, part 4
[NASA-TM-102646] N90-21164
Magneto acoustic emission apparatus for testing materials for embrittlement
[NASA-CASE-LAR-13817-1] N90-21170
Process for crosslinking methylene-containing aromatic polymers with ionizing radiation
[NASA-CASE-LAR-13448-1] N90-21196
Pressure rig for repetitive casting
[NASA-CASE-LAR-14050-1] N90-21216
Airborne Doppler radar flight experiments for the detection of microbursts N90-21243
An assessment of the potential of continuous-wave ranging for measuring the distance to a highly reflective, infinite sheet
[NASA-TM-101680] N90-21279
Computer codes for the evaluation of thermodynamic properties, transport properties, and equilibrium constants of an 11-species air model
[NASA-TM-102602] N90-21297
Fatigue damage growth mechanisms in continuous fiber reinforced titanium matrix composites
[NASA-TM-102594] N90-21409
Integrated modeling and analysis of a space-truss article
[NASA-TM-102615] N90-21412
NASA airframe structural integrity program
[NASA-TM-102637] N90-21422
An evaluation of the pressure proof test concept for thin sheet 2024-T3
[NASA-TM-101675] N90-21424
Rapidly quantifying the relative distention of a human bladder
[NASA-CASE-LAR-13901-1-NP] N90-21519
A time-accurate adaptive grid method and the numerical simulation of a shock-vortex interaction
[NASA-TP-2998] N90-21524
Active control of multi-dimensional random sound in ducts
[NASA-TM-102653] N90-21603
Simplified model for solar cosmic ray exposure in manned Earth orbital flights
[NASA-TM-4182] N90-21715

NATIONAL AERONAUTICS AND SPACE ADMINISTRATION. LEWIS RESEARCH CENTER, CLEVELAND, OH.
Modeling of surface roughness effects on glaze ice accretion N90-20925
Laser-velocimeter-measured flow field around an advanced, swept, eight-blade propeller at Mach 0.8 [NASA-TP-2462] N90-20942
The numerical simulation of multistage turbomachinery flows N90-21025
Probabilistic modeling for simulation of aerodynamic uncertainties in propulsion systems [NASA-TM-102472] N90-21036
Supersonic through-flow fan engine and aircraft mission performance [NASA-TM-102304] N90-21038
Detection of potential space station control/structure interaction with CO-ST-IN N90-21074
The effect of leveling coatings on the atomic oxygen durability of solar concentrator surfaces [NASA-TM-102557] N90-21110
Recent Stirling engine loss-understanding results [NASA-TM-103122] N90-21114
Effect of KOH concentration on LEO cycle life of IPV nickel-hydrogen flight battery cells [NASA-TM-103127] N90-21116
Characterization of failure processes in tungsten copper composites under fatigue loading conditions [NASA-TM-102371] N90-21123
Use of unbalanced laminates as a screening method for microcracking [NASA-TM-102517] N90-21124
Fiber pushout test: A three-dimensional finite element computational simulation [NASA-TM-102565] N90-21131
Multi-objective shape and material optimization of composite structures including damping [NASA-TM-102579] N90-21132
Nicalon/siliconoxycarbide ceramic composites [NASA-TM-102563] N90-21133
Structural tailoring of select fiber composite structures [NASA-TM-102484] N90-21137
High temperature fatigue behavior of tungsten copper composites [NASA-TM-102404] N90-21138
Optimal fabrication processes for unidirectional metal-matrix composites: A computational simulation [NASA-TM-102559] N90-21143
Feasibility of intercalated graphite railgun armatures [NASA-TM-102546] N90-21181
Studies of mechano-chemical interactions in the tribological behavior of materials [NASA-TM-102545] N90-21182
Resistivity of pristine and intercalated graphite fiber epoxy composites [NASA-TM-102576] N90-21192
Influence of the deposition conditions on radiofrequency magnetron sputtered MoS2 films [NASA-TP-2994] N90-21210
Numerical Arc Segmentation Algorithm for a Radio Conference (NASARC), version 4.0: User's manual [NASA-TM-101454] N90-21250
Bit-error-rate testing of fiber optic data links for MMIC-based phased array antennas [NASA-TM-102523] N90-21261
A new rectangular waveguide to coplanar waveguide transition [NASA-TM-102477] N90-21263
Advanced Launch System (ALS): Electrical actuation and power systems improve operability and cost picture [NASA-TM-102547] N90-21271
Electromechanical actuation for thrust vector control applications [NASA-TM-102548] N90-21272
Coplanar waveguide fed phased array antenna [NASA-TM-102522] N90-21273
Recent results from advanced research on space solar cells at NASA [NASA-TM-102485] N90-21274
Optical control of an 8-element Ka-band phased array using a high-speed optoelectronic interconnect [NASA-TM-102550] N90-21275
Intensity to frequency conversion technique in intensity modulated fiber optic sensing systems [NASA-TM-102562] N90-21277
Coplanar waveguide discontinuities for P-I-N diode switches and filter applications [NASA-TM-102534] N90-21278
Civil air transport: A fresh look at power-by-wire and fly-by-light [NASA-TM-102574] N90-21283
Peeled film GaAs solar cells for space power [NASA-TM-103125] N90-21287
A cost-effective strategy for nonoscillatory convection without clipping [NASA-TM-102538] N90-21291
Liquid Transfer Cryogenic Test Facility: Initial hydrogen and nitrogen no-vent fill data [NASA-TM-102572] N90-21295
Thermal radiation characteristics of nonisothermal cylindrical enclosures using a numerical ray tracing technique [NASA-TM-102527] N90-21296
Navier-Stokes analysis of turbine blade heat transfer [NASA-TM-102496] N90-21300
PROTEUS two-dimensional Navier-Stokes computer code, version 1.0. Volume 1: Analysis description [NASA-TM-102551] N90-21303
PROTEUS two-dimensional Navier-Stokes computer code, version 1.0. Volume 2: User's guide [NASA-TM-102552] N90-21306
PROTEUS two-dimensional Navier-Stokes computer code, version 1.0. Volume 3: Programmer's reference [NASA-TM-102553] N90-21307
Foundations of measurement and instrumentation [NASA-RP-1222] N90-21351
A fiber optic sensor for noncontact measurement of shaft speed, torque, and power [NASA-TM-102481] N90-21360
Attachment of lead wires to thin film thermocouples mounted on high temperature materials using the parallel gap welding process [NASA-TM-102442] N90-21361
Transmission research activities at NASA Lewis Research Center [NASA-TM-103132] N90-21394
Aeropropulsion facilities configuration control: Procedures manual [NASA-TM-102541] N90-21399
Ultrasonic and radiographic evaluation of advanced aerospace materials: Ceramic composites [NASA-TM-102540] N90-21401
Review and statistical analysis of the ultrasonic velocity method for estimating the porosity fraction in polycrystalline materials [NASA-TM-102501] N90-21402
O2 reduction at the IFC orbiter fuel cell O2 electrode [NASA-TM-102580] N90-21469
A real time neural net estimator of fatigue life [NASA-TM-103117] N90-21564
High accuracy solutions of incompressible Navier-Stokes equations [NASA-TM-102539] N90-21567
ULTRA-SHARP nonoscillatory convection schemes for high-speed steady multidimensional flow [NASA-TM-102568] N90-21570

NATIONAL AERONAUTICS AND SPACE ADMINISTRATION. MARSHALL SPACE FLIGHT CENTER, HUNTSVILLE, AL.
Controls, Astrophysics, and Structures Experiment in Space (CASES) N90-21085
Global nonlinear optimization of spacecraft protective structures design [NASA-TM-100387] N90-21095
Cross-sectional examination of the damage zone in impacted specimens of carbon/epoxy and carbon/PEEK composites [NASA-TM-100391] N90-21125
The corrosion protection of 6061-T6 aluminum by a polyurethane-sealed anodized coat [NASA-TM-100394] N90-21191
Apparatus for mixing solutions in low gravity environments [NASA-CASE-MFS-26047-1] N90-21209
A general-purpose balloon-borne pointing system for solar scientific instruments [NASA-TP-3013] N90-21219
Compendium of fracture mechanics problems [NASA-TM-100393] N90-21414

NATIONAL AERONAUTICS AND SPACE ADMINISTRATION. PASADENA OFFICE, CA.
VLSI single-chip (255,223) Reed-Solomon encoder with interleaver [NASA-CASE-NPO-17280-1-CU] N90-21061
Acoustic convective system [NASA-CASE-NPO-17278-1-CU] N90-21215
Alternating gradient photodetector [NASA-CASE-NPO-17235-1-CO] N90-21358
VLSI binary updown counter [NASA-CASE-NPO-17205-1-CU] N90-21525
Fault tolerant hypercube computer system architecture [NASA-CASE-NPO-16859-1-CU] N90-21527

NATIONAL AEROSPACE LAB., AMSTERDAM (NETHERLANDS).
A system for transonic wing design with geometric constraints based on an inverse method N90-20983
Constrained spanload optimization for minimum drag of multi-lifting-surface configurations N90-20992
Numerical optimization of target pressure distributions for subsonic and transonic airfoil design N90-20993
The PHARUS project: Design of a polarimetric C-band SAR in the Netherlands N90-21228

NATIONAL CENTER FOR ATMOSPHERIC RESEARCH, BOULDER, CO.
Theory and application of nonlinear normal mode initialization [PB90-166000] N90-21497

NATIONAL INST. OF STANDARDS AND TECHNOLOGY, BOULDER, CO.
Systematic errors in power measurements made with a dual six-port ANA [PB90-145160] N90-21278

NATIONAL INST. OF STANDARDS AND TECHNOLOGY, GAITHERSBURG, MD.
Corrosion behavior of mild steel in high pH aqueous media [PB90-131152] N90-21162
An experimental evaluation of two nonazeotropic refrigerant mixtures in a water-to-water breadboard heat pump [DE90-009016] N90-21305
Laser studies of chemical dynamics at the gas-solid interface [DE90-008698] N90-21380
Software verification and validation: Its role in computer assurance and its relationship with software project management standards [PB90-111691] N90-21530
Center for Atomic, Molecular, and Optical Physics: Technical activities [PB90-133158] N90-21591

NATIONAL LIBRARY OF MEDICINE, BETHESDA, MD.
Medical subject headings: Annotated alphabetic list, 1990 [PB90-100009] N90-21683
Permuted medical subject headings, 1990 [PB90-100025] N90-21684

NATIONAL OCEANIC AND ATMOSPHERIC ADMINISTRATION, BOULDER, CO.
Editing wind profiler measurements [PB90-130147] N90-21503

NATIONAL OCEANIC AND ATMOSPHERIC ADMINISTRATION, WASHINGTON, DC.
MECCA program documentation [NOAA-TR-NESDIS-46] N90-21477
Preliminary report on the demonstration of the VAS CO2 cloud parameters (cover, height, and amount) in support of ASOS [NOAA-TM-NESDIS-29] N90-21498

NATIONAL OPTICAL ASTRONOMY LAB. TUCSON, AZ.
Infrared ground-based astronomy with the Hughes 256 X 256 PtSi array N90-21331

NATIONAL PARK SERVICE, WASHINGTON, DC.
Effects of Air Pollution on Western Forests [PB90-131111] N90-21481

NATIONAL RESEARCH COUNCIL OF CANADA, OTTAWA (ONTARIO).
The effect of secondary flow on the redistribution of the total temperature field downstream of a stationary turbine cascade N90-21033

NATIONAL TECHNICAL UNIV., ATHENS (GREECE).
Secondary flow calculations for axial and radial compressors N90-21024

NATIONAL TRANSPORTATION SAFETY BOARD, WASHINGTON, DC.
Annual review of aircraft accident data: US general aviation calendar year 1987 [PB90-138066] N90-20966
Brake performance of the McDonnell Douglas DC-10-30/40 during high speed, high energy rejected takeoffs [PB90-917004] N90-21000

NAVAL AIR DEVELOPMENT CENTER, WARMINSTER, PA.
The effect of windscreen bows and HUD pitch ladder format on pilot performance during simulated flight [AD-A218139] N90-21523

NAVAL OCEAN SYSTEMS CENTER, SAN DIEGO, CA.
Proceedings of the Joint NOSC/NRL (Naval Ocean Systems Center/Naval Research Laboratory) InP Microwave/Millimeter Wave Technology Workshop [AD-A218216] N90-21259

NAVAL POSTGRADUATE SCHOOL, MONTEREY, CA.
The 4th Annual Review of Progress in Applied Computational Electromagnetics [AD-A217912] N90-21257
The 5th Annual Review of Progress in Applied Computational Electromagnetics [AD-A217994] N90-21258

NAVAL RESEARCH LAB., WASHINGTON, DC.
LACE flight dynamics experiment N90-21086

NEBRASKA UNIV., LINCOLN.
Compressive behavior of laminated composite structures N90-21134

NEVADA UNIV., RENO.
Numerical simulations of the cloud-capped marine boundary layer N90-21506

Precipitation mechanisms in tropical and midlatitude convective clouds N90-21507

NORTH CAROLINA AGRICULTURAL AND TECHNICAL STATE UNIV., GREENSBORO.
Compact scheme for systems of equations applied to fundamental problems of mechanics of continua [NASA-CR-186494] N90-21292
Compact finite volume methods for the diffusion equation [NASA-CR-186477] N90-21568

NORTH CAROLINA STATE UNIV., RALEIGH.
Relating flow between counter-rotating propellers to aerodynamic interaction noise N90-20944
An approximate viscous shock layer method for calculating the hypersonic flow over blunt-nosed bodies N90-20947

NORTH CAROLINA UNIV., CHAPEL HILL.
Toward quantum corrections in black hole thermodynamics N90-21702

NORTHEASTERN UNIV., BOSTON, MA.
Mechanistic model for catalytic recombination during aerobraking maneuvers [NASA-CR-185611] N90-21059

NORTHWEST RESEARCH ASSOCIATES, INC., BELLEVUE, WA.
Investigations into the properties, conditions, and effects of the ionosphere [AD-A217807] N90-21489

NOTRE DAME UNIV., IN.
The MANTA: An RPV design to investigate forces and moments on a lifting surface [NASA-CR-186227] N90-20971

NSI TECHNOLOGY SERVICES CORP., CORVALLIS, OR.
Effects of Air Pollution on Western Forests [PB90-131111] N90-21481

NUCLEAR UTILITY SERVICES, INC., GAITHERSBURG, MD.
Final Safety Analysis Report for the Ulysses Mission. Volume 3 (Book 1): Nuclear risk analysis document [DE90-006691] N90-21101
Final safety analysis report for the Ulysses Mission. Volume 3 (Book 2): Nuclear risk analysis document-appendices [DE90-006692] N90-21102
Final safety analysis report for the Ulysses Mission [DE90-006690] N90-21106

O

OAK RIDGE GASEOUS DIFFUSION PLANT, TN.
Army War College final prototype optical disk system testing and evaluation report [DE90-006852] N90-21685

OAK RIDGE NATIONAL LAB., TN.
Simple light gas guns for hypervelocity studies [DE90-006907] N90-21056
Modeling the temperature dependence of the thermal conductivity of aluminum nitride [DE90-009428] N90-21154
Lecture on ordered intermetallic alloys [DE90-009011] N90-21169
Research advances in fine ceramics [DE90-006983] N90-21197
Review of the state of the technology for joining ceramics for high-temperature structural applications [DE90-009224] N90-21199
A new approach to solve the kinematics resolution of a redundant robot [DE90-010213] N90-21397
Modeling large-scale vegetation dynamics [DE90-006883] N90-21485
Modeling the upper ocean and its interaction with the atmosphere [DE90-006980] N90-21511
SIGNIF: A C function to compute significant digits [DE90-009242] N90-21550
Parallel tridiagonalization of a general matrix using distributed-memory multiprocessors [DE90-006902] N90-21551
US-Japan Workshop on Atomic Collisions in Solids: Abstracts of lectures [DE90-006979] N90-21611
Full wave computation of electromagnetic wave excitation, propagation, and absorption at the ion cyclotron frequency in fusion experiments [DE90-009399] N90-21642
Modeling high-temperature superconductors and metallic alloys on the Intel IPSC/860 [DE90-009402] N90-21665

OAK RIDGE Y-12 PLANT, TN.
Advanced manufacturing technology: A Department of Energy technology transfer initiative [DE90-006801] N90-21688

OBSERVATOIRE DE LYON (FRANCE).
ISO camera array development status N90-21344

OFFICE NATIONAL D'ETUDES ET DE RECHERCHES AEROSPATIALES, PARIS (FRANCE).
An inverse method for the design of turbomachine blades N90-20988
The use of numerical optimization for helicopter airfoil and blade design N90-20995
Numerical optimization of wings in transonic flow N90-20997
Calculation of the three dimensional turbulent flow in a linear turbine blade N90-21021
Theoretical study of the flow in a rotating channel. Experimental study through flow visualization in a curved channel N90-21032

OFFICE OF TECHNOLOGY ASSESSMENT, WASHINGTON, DC.
High performance computing and networking for science [PB90-131226] N90-21526

OHIO STATE UNIV., COLUMBUS.
The effects of magnetic nozzle configurations on plasma thrusters [NASA-CR-186465] N90-21109
A review of gear housing dynamics and acoustics literature [NASA-CR-185148] N90-21387

OHIO UNIV., ATHENS.
Ridge regression processing N90-20931
Optimization of the effective GPS data rate N90-20932
Sole means navigation and integrity through hybrid Loran-C and NAVSTAR GPS N90-20933
Weather data dissemination to aircraft N90-20934

OKLAHOMA UNIV., NORMAN.
Performance of an aero-space plane propulsion nozzle N90-21034

OLD DOMINION UNIV., HAMPTON, VA.
The effect of elastic boundary conditions on the dynamic response of rectangular plates [NASA-CR-186059] N90-21405

OLD DOMINION UNIV., NORFOLK, VA.
Effects of nose bluntness and shock-shock interactions on blunt bodies in viscous hypersonic flows [NASA-CR-186451] N90-20950
An overlapped grid method for multigrid, finite volume/difference flow solvers: MaGGiE [NASA-CR-182008] N90-20953
Determinations of molecular weight and molecular weight distribution of high polymers by the rheological properties [NASA-CR-186450] N90-21180
User manual for VICONOPT: An exact analysis and optimum design program covering the buckling and vibration of prismatic assemblies of flat in-plane loaded, anisotropic plates, with approximations for discrete supports, and transverse stiffeners [NASA-CR-181966] N90-21413
Strategies for concurrent processing of complex algorithms in data driven architectures [NASA-CR-186515] N90-21535

OREGON STATE UNIV., CORVALLIS.
Meteorological influences on mountain cloudwater chemistry in the eastern United States [PB90-132432] N90-21504

ORGANISATIE VOOR TOEGEPAST NATUURWETENSCHAPPELIJK ONDERZOEK, THE HAGUE (NETHERLANDS).
A motion compensation study for the PHARUS project N90-21235
Radar observations of a formation of two fighters: A case study for ISAR imaging N90-21240

P

PACIFIC NORTHWEST LAB., RICHLAND, WA.
Grain boundary chemistry effects on irradiation-assisted stress corrosion cracking [DE90-008623] N90-21167
Alternative materials for solid oxide fuel cells [DE90-008615] N90-21468
Space power generation and distribution [DE90-008676] N90-21474
An evaluation of the relationship between the production and use of energy and atmospheric methane emissions [DE90-007962] N90-21487
Biological effects of ELF (Extremely-Low-Frequency) electric and magnetic fields [DE90-008634] N90-21514

PENNSYLVANIA STATE UNIV., STATE COLLEGE.
Free-field propagation of high intensity noise [NASA-CR-186577] N90-21604

PENNSYLVANIA STATE UNIV., UNIVERSITY PARK.
Predictability of weather and climate in a coupled ocean-atmosphere model: A dynamical systems approach [NASA-CR-186499] N90-21502
Kinematic and kinetic analyses of drop landings N90-21517

PHYSICS AND ELECTRONICS LAB. TNO, THE HAGUE (NETHERLANDS).
The PHARUS project: Design of a polarimetric C-band SAR in the Netherlands N90-21228

POLITECNICO DI MILANO (ITALY).
A fast collocation method for transonic airfoil design N90-20984

POLITECNICO DI TORINO (ITALY).
Numerical method for designing 3D turbomachinery blade rows N90-20990

POLYTECHNIC UNIV., FARMINGDALE, NY.
Low frequency gyrotron amplifier investigation, phase 2 [AD-A217096] N90-21352

PONTIFICIA UNIV. CATOLICA, RIO DE JANEIRO (BRAZIL).
Study of new technique of solid combustible materials to determination of volatile elements by flame atomic absorption spectrophotometry [DE90-612907] N90-21147
The gravitational lens effect and its optical equivalents [DE90-612767] N90-21673

PRINCETON UNIV., NJ.
Investigation of air transportation technology at Princeton University, 1988-1989 N90-20935
Application of stochastic robustness to aircraft control systems N90-20936
Neural networks for aircraft control N90-20937
An expert system for wind shear avoidance N90-20938
Rule-based mechanisms of learning for intelligent adaptive flight control N90-20939
Perspectives on the use of rule-based control N90-20940
Stochastic robustness of linear control systems N90-20941
Aerodynamic design via control theory N90-20998

PRINS MAURITS LAB. TNO, RIJSWIJK (NETHERLANDS).
The modelling of heat and mass transfer near solid boundaries and comparison with experimental results [PB90-167040] N90-21310

PURDUE UNIV., WEST LAFAYETTE, IN.
A two-dimensional unsteady analysis for transonic and supersonic cascade flows N90-20955
Measurement of lift development on rapidly-accelerated wings N90-20956

Q

QUAID-I-AZAM UNIV., ISLAMABAD (PAKISTAN).
Phase-only holographic filters and their applications [PB90-166802] N90-21368

QUEENSLAND UNIV., BRISBANE (AUSTRALIA).
Depth-averaged equations for turbulent free-surface flow [PB90-164781] N90-21308
Elasto-plastic large deformation analysis of thin-walled structures [PB90-164757] N90-21426

R

RENSSELAER POLYTECHNIC INST., TROY, NY.
Optimum hypersonic airfoils with attached shocks N90-20960

RESEARCH SUPPORT INSTRUMENTS, INC., COCKEYSVILLE, MD.
UV spectrometer system AFGL 801 A HUP [AD-A217805] N90-21619

RICE UNIV., HOUSTON, TX.
Optimal trajectories for the aeroassisted flight experiment. Part 3: Formulation, results, and analysis [NASA-CR-186165] N90-21051

ROCHESTER UNIV., NY.
InSb DRO array characteristics N90-21326
Discovery of low mass objects in Taurus N90-21329
Development of an ultra-bright laser and an application to multi-photon ionization N90-21372
LLE review [DE90-008958] N90-21378

ROCKWELL INTERNATIONAL CORP., GOLDEN, CO.
The effects of a nearby subsequent fusion weld on the properties of an inertia friction weld [DE90-007972] N90-21396

ROCKWELL INTERNATIONAL SCIENCE CENTER, ANAHEIM, CA.
The solid state photomultiplier: Status of photon counting beyond the near-infrared N90-21319

ROCKWELL INTERNATIONAL SCIENCE CENTER, THOUSAND OAKS, CA.
Some aspects of Essentially Nonoscillatory (ENO) formulations for the Euler equations, part 3
[NASA-CR-4285] N90-20949
Low noise HgCdTe 128 x 128 SWIR FPA for Hubble space telescope N90-21337
HgCdTe 256x256 NWIR FPA N90-21348

ROLLS-ROYCE LTD., DERBY (ENGLAND).
Detailed heat transfer measurements in nozzle guide vane passages in linear and annular cascades in the presence of secondary flows N90-21030

ROYAL AEROSPACE ESTABLISHMENT, FARNBOROUGH (ENGLAND).
Secondary flow predictions for a transonic nozzle guide vane N90-21017
Perforation of a reinforced concrete wall by a rigid missile
[AD-A210025] N90-21381

ROYAL AIRCRAFT ESTABLISHMENT, FARNBOROUGH (ENGLAND).
The role of structural analysis in airworthiness certification
[BR112064] N90-20972
Computer-aided structural optimisation of aircraft structures
[BR112837] N90-20973

S

SANDIA NATIONAL LABS., ALBUQUERQUE, NM.
Fatigue crack growth from narrow-band Gaussian spectrum loading in 6063 aluminum alloy
[DE90-008957] N90-21173
Compatibility of Au base thick films with solder alloys: Solid state growth of intermetallics
[DE90-009285] N90-21175
Aging and compatibility of TNF-doped Mylar
[DE90-008508] N90-21186
Shock initiation sensitivity of damaged TP-H1207C composite propellant
[DE90-008509] N90-21205
The development of ultraviolet-ozone cleaning as a production process in the packaging of integrated circuits
[DE90-007960] N90-21220
Is Galerkin's method really better
[DE90-008804] N90-21267
Software to characterize tuning fork resonators used in the Quartz Digital Accelerometer
[DE90-007913] N90-21363
In-situ permeable flow sensor
[DE90-008806] N90-21364
Modeling elastomer displacements for tactile sensing applications
[DE90-007959] N90-21370
An internal/external pressure, tension/compression multiaxial fatigue system
[DE90-009510] N90-21430
Recent progress in photovoltaic concentrator module technology
[DE90-009007] N90-21475
Toward a new CIM (Computer Integrated Manufacturing) architecture for Sandia Laboratories
[DE90-008677] N90-21548
The CAD/CAM product data standards: IGES/PDES (Initial Graphics Exchange Specification/Product Data Exchange Standards, the present and the future
[DE90-008803] N90-21549
Multigrid on massively parallel computers
[DE90-008999] N90-21560
The Chemkin Thermodynamic Data Base
[DE90-007953] N90-21676
The ultimate CASE tool
[DE90-009351] N90-21687

SANTA BARBARA RESEARCH CENTER, GOLETA, CA.
Study of advanced InSb arrays for SIRTF (Space Infrared Telescope Facility) N90-21325

SANTA FE COLL., NM.
Artificial life: The coming evolution
[DE90-008860] N90-21515

SCIENCE APPLICATIONS INTERNATIONAL CORP., MCLEAN, VA.
West European magnetic confinement fusion research N90-21634

SCIENTECH, INC., IDAHO FALLS, ID.
Boeing 727-100 test project (high energy radiated field tests)
[DOT/FAA/CT-88/33] N90-21247

SELENIA S.P.A., ROME (ITALY).
MMW SAR on RPV for battlefield surveillance N90-21231
Radar target image by ISAR case study N90-21242

SIEMENS A.G., MUNICH (GERMANY, F.R.).
Concept for a spaceborne Synthetic Aperture Radar (SAR) sensor based on active phased array technology N90-21234

SOCIETE FRANCAISE DE CHIMIE-PHYSIQUE, PARIS.
Modelling of molecular structures and properties in physical chemistry and biophysics
[AD-A214561] N90-21145

SOCIETE NATIONALE D'ETUDE ET DE CONSTRUCTION DE MOTEURS D'AVIATION, MOISSY-CRAMAYEL (FRANCE).
Calculation of the secondary flow in an axial turbine N90-21022

SOLAR KINETICS, INC., DALLAS, TX.
Design and demonstration of an improved stretched-membrane heliostat
[DE90-007904] N90-21470

SOUTHAMPTON UNIV. (ENGLAND).
Measurement and prediction of propeller blade surface pressure distributions N90-20961
Parametric resonance in horizontal axis wind turbines N90-20962
Wave receptance analysis of vibrating beams and stiffened plates N90-21419

SPACE RESEARCH ORGANIZATION NETHERLANDS, GRONINGEN.
Design and status of the detector block for the ISO-SWS N90-21341

SRI INTERNATIONAL CORP., MENLO PARK, CA.
High-resolution Brillouin gain spectroscopy in solids
[DE90-009475] N90-21155

STANFORD UNIV., CA.
Filament winding of composite cylinders N90-21119
End point control of flexible manipulators
[AD-A217319] N90-21383
Fourier series methods for plates and shells with cracks and inclusions N90-21406
A note on overdispersed exponential families
[AD-A216277] N90-21565
A monotone complementarity problem in Hilbert space
[DE90-009755] N90-21590

STARMARK CORP., ARLINGTON, VA.
An early overview of tiltrotor aircraft characteristics and pilot procedures in civil transport applications
[DOT/FAA/DS-89/37] N90-21003

STATE UNIV. OF NEW YORK, STONY BROOK.
The dynamics of scalar fields in the early universe N90-21696

STEVENS INST. OF TECH., HOBOKEN, NJ.
Development of a fracture analysis technique for use with a general-purpose finite element program N90-21416

STUTTGART UNIV. (GERMANY, F.R.).
Inverse computation of transonic internal flows with application for multi-point-design of supercritical compressor blades N90-20987

SVERDRUP TECHNOLOGY, INC., ARNOLD AFS, TN.
Optimization of aerodynamic designs using computational fluid dynamics N90-20999

SVERDRUP TECHNOLOGY, INC., EGLIN AFB, FL.
Aerodynamic optimization by simultaneously updating flow variables and design parameters N90-20991

SVERDRUP TECHNOLOGY, INC., CLEVELAND, OH.
Users manual for the NASA Lewis Ice Accretion Prediction Code (LEWICE)
[NASA-CR-185129] N90-20943
Exhaust nozzles for propulsion systems with emphasis on supersonic cruise aircraft
[NASA-RP-1235] N90-21037
Thermomechanical deformation testing and modeling in the presence of metallurgical instabilities
[NASA-CR-185188] N90-21420
Hypercluster parallel processing library user's manual
[NASA-CR-185231] N90-21552
Microgravity acoustic mixing for particle cloud combustors
[NASA-CR-185159] N90-21600

SWEDISH INST. FOR MATERIALS TESTING, BORAS.
Airborne sound insulation of slits, joints, and sealing stripes
[PB90-128976] N90-21599

SYSTEMS CONTROL TECHNOLOGY, INC., ARLINGTON, VA.
Indianapolis Downtown Heliport: Operations analysis and marketing history
[REPT-90RR-13] N90-21049

T

TECHNICAL UNIV. OF DENMARK, LYNGBY.
Stability of a solitary wave solution to a set of coupled Boussinesq-like equations
[DE90-008927] N90-21586

TECHNISCHE HOCHSCHULE, AACHEN (GERMANY, F.R.).
Computational prediction and measurement of the flow in axial turbine cascades and stages N90-21028
Analysis of the rotor tip leakage flow with tip cooling air ejection N90-21029

TECHNISCHE HOGESCHOOL, DELFT (NETHERLANDS).
Experimental and numerical investigation of the vortex flow over a sharp edged delta wing; with and without sideslip
[PB90-167131] N90-20964
Crack stoppers and ARALL laminates
[PB90-166588] N90-21142
The PHARUS project: Design of a polarimetric C-band SAR in the Netherlands N90-21228
Notes on the unsteady rectilinear motion of a perfect gas. Part 8: General theory and general waves in a homentropic gas
[PB90-167149] N90-21309
The modelling of heat and mass transfer near solid boundaries and comparison with experimental results
[PB90-167040] N90-21310
UNIVIMP: A universal instrument for the survey of initial imperfections of thin-walled shells
[PB90-167065] N90-21369
Flutter of slender bodies under axial stress
[PB90-167024] N90-21425
Fractographic analysis of the crack growth rate and the shear lip development of 2024-T3 specimens under simple variable-amplitude loading
[PB90-167032] N90-21427
Review of formulae for the buckling of simply-supported, orthotropic plates under shear load, including transverse shear effects
[PB90-167073] N90-21429

TECHNOLOGY ASSESSMENT AND TRANSFER, INC., ANNAPOLIS, MD.
Improved Thermo-Oxidative-Deposition screening tests for turbine lubricants
[AD-A217795] N90-21188

TEXAS A&M UNIV., COLLEGE STATION.
CSI sensing and control: Analytical and experimental results N90-21083
A radiological assessment of nuclear power and propulsion operations near Space Station Freedom
[NASA-CR-185185] N90-21108
Determination of unknown coefficients in partical differential equations
[AD-A217169] N90-21569
Rectangular subsonic jet flow field measurements
[NASA-CR-181925] N90-21598

TEXAS UNIV., AUSTIN.
Computation of nonequilibrium chemically reacting flows in hypersonic flow field N90-20954
The effect of viscosity on the resistive tearing mode with the presence of shear flow
[DE90-009340] N90-21312
Preliminary results on two-dimensional interferometry of HL Tau N90-21395
Development of a dynamic modeling technique and its application to the analysis and control of a high-precision robotic manipulator N90-21391
MHD modes driven by anomalous electron viscosity and their role in fast sawtooth crashes
[DE90-009311] N90-21639
Nonlinear interaction of photons and phonons in electron-positron plasmas
[DE90-009341] N90-21640
Transition from resistive-g to eta-i driven turbulence in stellarator systems
[DE90-009382] N90-21641
Instabilities and vortex dynamics in shear flow of magnetized plasmas
[DE90-009448] N90-21643
The thermo-mechanical behavior of cometary nuclei N90-21703
Small scale structures and density of star-forming regions N90-21706

TEXTRON BELL HELICOPTER, FORT WORTH, TX.
An efficient airfoil design method using the Navier-Stokes equations N90-20981

THIOKOL CORP., BRIGHAM CITY, UT.
Transportation monitoring unit qualification
[NASA-CR-183930] N90-21060
Technical Evaluation Motor no. 5 (TEM-5)
[NASA-CR-183932] N90-21117

THOMSON-CSF, MALAKOFF (FRANCE).
SAR and ISAR imagery of marine targets N90-21237

THOMSON-CSF, PARIS (FRANCE).
SAR image coding N90-21246

TOKYO UNIV., TANASHI (JAPAN).
CAMAC memory module: MEMO-32
[DE90-759846] N90-21528

TOLEDO UNIV., OH.
A comparative study of electric power distribution systems for spacecraft
[NASA-CR-186531] N90-21113

TUFTS UNIV., MEDFORD, MA.
VLA observations of the coronal plasma
[NASA-CR-186540] N90-21711

Flare stars at radio wavelengths
[NASA-CR-186539] N90-21719

U

UNIROYAL PLASTICS CO., INC., MISHAWAKA, IN.
Collapsible fabric tank testing
[AD-A217861] N90-21388

UNITED KINGDOM ATOMIC ENERGY AUTHORITY, HARWELL (ENGLAND).
Acoustic characterisation of an aluminium silicon carbide metal matrix composite
[AERE-R-13273] N90-21121

A STEM study of changing grain boundary chemistry during the sensitisation of AISI 304 stainless steel
[AERE-R-13418] N90-21157

Titanium aluminides: Processing, properties and potential
[AERE-R-13198] N90-21158

Current fluctuations associated with localised corrosion: Mechanistic studies of the early stages of pitting and stress corrosion cracking of stainless steel
[AERE-R-13531] N90-21159

Mathematical modelling of intergranular attack in stainless steels: A preliminary study
[AERE-M-3698] N90-21160

Grain boundary precipitation in Ni3Al based alloys
[AERE-R-13362] N90-21161

Effects of titanium on some surface properties of nitride ceramics
[AERE-R-13566] N90-21178

On the stability of amorphous silica coatings for high temperature service
[AERE-R-13425] N90-21179

Some recent applications of laser ultrasound to the characterisation of materials
[AERE-R-13438] N90-21374

On-line assessment of weld quality using ultrasonics
[AERE-R-13401] N90-21398

UNITED TECHNOLOGIES RESEARCH CENTER, EAST HARTFORD, CT.
The effects of compressor endwall flow on airfoil incidence and deviation N90-21011

UTAH UNIV., SALT LAKE CITY.
The influence of lateral boundary conditions, fixed surface forcings, and synoptic situations upon predictability estimates using limited area numerical models N90-21492

V

VIBRATION INST., CLARENDON HILLS, IL.
The Shock and Vibration Digest, volume 22, no. 2 N90-21596

VIRGINIA POLYTECHNIC INST. AND STATE UNIV., BLACKSBURG.
Effects of secondary flow on heat transfer in rotating passages N90-21031

Experimental and theoretical investigation of optimal control methods with model reduction N90-21039

A homotopy approach to the solutions of minimum-fuel space-flight rendezvous problems N90-21053

Stress analysis of rocket motors with viscoelastic propellant by a mixed finite element model N90-21112

Calibration of Hewlett-Packard network analyzers: A precision viewpoint
[NASA-CR-181969] N90-21252

VIRGINIA UNIV., CHARLOTTESVILLE.
A quasi-Lagrangian moving grid technique for investigating compressible flows N90-21298

VON KARMAN INST. FOR FLUID DYNAMICS, RHODE-SAINT-GENESE (BELGIUM).
Subsonic and transonic blade design by means of analysis codes N90-20985

VRIJE UNIV., AMSTERDAM (NETHERLANDS).
Secondary flows and radial mixing predictions in axial compressors N90-21010

A formal approach to user models in data retrieval
[PB90-124726] N90-21682

W

WALES UNIV. INST. OF SCIENCE AND TECHNOLOGY, CARDIFF.
User manual for VICONOPT: An exact analysis and optimum design program covering the buckling and vibration of prismatic assemblies of flat in-plane loaded, anisotropic plates, with approximations for discrete supports, and transverse stiffeners
[NASA-CR-181966] N90-21413

WASHINGTON UNIV., SAINT LOUIS, MO.
Studies in quantum field theory
[DE90-008731] N90-21677

WASHINGTON UNIV., SEATTLE.
Controlled production and characterization of metastable intermetallics
[DE90-009384] N90-21176

WEIDLINGER ASSOCIATES, LOS ALTOS, CA.
A numerical and theoretical study of seismic wave diffraction in complex geologic structure
[AD-A218209] N90-21490

WEIZMANN INST. OF SCIENCE, REHOVOTH (ISRAEL).
An ultra-small capacitance Josephson junction
[DE90-613396] N90-21653

WESTINGHOUSE SAVANNAH RIVER CO., AIKEN, SC.
Determination of Li-Al alloy extent in tubular aluminum elements by small source neutron radiology
[DE90-009142] N90-21174

Fiber optic void fraction sensor
[DE90-009124] N90-21386

WISCONSIN UNIV., MADISON.
Computer-aided design of flywheel transmission systems N90-21392

Application of optimization in design and motion control of robot manipulators N90-21393

Use of microwave satellite data to study variations in rainfall over the Indian Ocean
[NASA-CR-186408] N90-21501

Helium transport in plasma edge regions N90-21625

A self-consistent theory of radial transport of field-aligned current by microturbulence
[DE90-007920] N90-21631

Thomson scattering in a magnetic field N90-21699

A theoretical study of circumstellar dust around Ae/Be stars N90-21700

A search for very high energy gamma rays from the Crab pulsar-nebula N90-21718

WISCONSIN UNIV., MILWAUKEE.
Inelastic electron scattering from surfaces
[DE90-009365] N90-21614

Typical Contract Number Index Listing

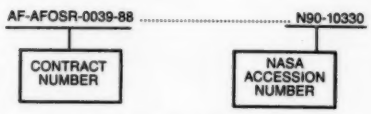

Listings in this index are arranged alphanumerically by contract number. Under each contract number the NASA accession numbers denoting documents that have been produced as a result of research done under that contract are arranged in ascending order. The NASA accession number denotes the number by which the citation is identified.

AF PROJ. 2302 ..... N90-21127
AF PROJ. 2309 ..... N90-21490
AF PROJ. 3005 ..... N90-21389
AF PROJ. 3484 ..... N90-21488
AF-AFOSR-0147-88 ..... N90-21711
N90-21719
AF-AFOSR-0206-85 ..... N90-21127
AF-AFOSR-0307-86 ..... N90-21524
AF-AFOSR-0356-87 ..... N90-21566
ARPA ORDER 4395 ..... N90-21617
N90-21618
ARPA ORDER 5378 ..... N90-21555
ARPA ORDER 6037 ..... N90-21533
ARPA ORDER 6429 ..... N90-21534
BARR-10-119 ..... N90-20929
CA-44768 ..... N90-21512
CNPQ-302714/88-0/MA/FV N90-21595
DA PROJ. 1L1-2211-A-47-A N90-21394
DA PROJ. 1L1-61102-AH-45 ..... N90-21004
DA PROJ. 1L1-62209-A47-A N90-21387
DA PROJ. 1L6-65502-MM-40 ..... N90-21183
DAAA15-88-D-0005 ..... N90-21482
DAAG29-84-K-0048 ..... N90-20939
N90-20940
DAAH01-88-C-0887 ..... N90-21534
DAAK70-87-C-0078 ..... N90-21388
DAAL03-88-K-0119 ..... N90-21352
DAAL04-87-C-0029 ..... N90-21183
DAJA89-M-0063 ..... N90-21145
DE-AC01-79ET-32043 ..... N90-21103
N90-21104
N90-21107
DE-AC01-87NE-32134 ..... N90-21101
N90-21102
N90-21106
DE-AC02-76CH-00016 ..... N90-21218
N90-21484
N90-21616
DE-AC02-76CH-03000 ..... N90-21217
N90-21285
N90-21367
DE-AC02-76ER-02220 ..... N90-21613
N90-21679
DE-AC02-78ER-04915 ..... N90-21677
DE-AC02-83CH-10093 ..... N90-21472
N90-21473
N90-21660
DE-AC03-76SF-00098 ..... N90-21379
N90-21403
N90-21476
N90-21607
N90-21655
N90-21656
N90-21657
N90-21686
DE-AC03-89ER-52153 ..... N90-21636
DE-AC03-89ER-53277 ..... N90-21635
DE-AC04-76DP-00078 ..... N90-21175
N90-21687
DE-AC04-76DP-00613 ..... N90-21151
N90-21152
DE-AC04-76DP-00789 ..... N90-21158
N90-21173
N90-21186
N90-21205
N90-21220
N90-21267
N90-21363
N90-21364
N90-21370
N90-21430
N90-21470
N90-21475
N90-21548
N90-21549
N90-21560
DE-AC04-76DP-03533 ..... N90-21396
DE-AC04-76DR-00789 ..... N90-21676
DE-AC05-84OR-21400 ..... N90-21056
N90-21154
N90-21156
N90-21169
N90-21197
N90-21199
N90-21305
N90-21397
N90-21485
N90-21511
N90-21550
N90-21551
N90-21611
N90-21642
N90-21665
N90-21685
N90-21688
DE-AC06-76OR-01830 ..... N90-21487
DE-AC06-76RL-01830 ..... N90-21167
N90-21468
N90-21474
N90-21514
N90-21663
DE-AC09-89SR-18035 ..... N90-21174
N90-21366
DE-AI05-84ER-13150 ..... N90-21380
DE-AS03-88DP-10741 ..... N90-21621
DE-AS06-87DP-10684 ..... N90-21622
DE-FC03-85DP-40200 ..... N90-21378
DE-FG02-84ER-45076 ..... N90-21614
DE-FG02-85ER-13333 ..... N90-21304
DE-FG02-85ER-53205 ..... N90-21632
DE-FG02-86ER-13495 ..... N90-21516
DE-FG02-88ER-45366 ..... N90-21200
DE-FG02-89ER-53291 ..... N90-21631
DE-FG02-90ER-40542 ..... N90-21678
DE-FG03-87ER-25026 ..... N90-21590
DE-FG03-88ER-53275 ..... N90-21631
DE-FG05-90ET-53088 ..... N90-21312
N90-21639
N90-21640
N90-21641
N90-21643
DE-FG06-87ER-45327 ..... N90-21176
DE-FG22-86PC-90961 ..... N90-21311
DTFA-01-86-Y-01015 ..... N90-21045
DTFA01-87-C-00014 ..... N90-21049
DTFA01-88-Y-01073 ..... N90-21249
DTFA01-89-P-01074 ..... N90-21003
DTFA03-88-A-00027 ..... N90-21247
FINEP-53-89-0363-00 ..... N90-21595
FINEP-537-CT N90-21689
F08635-88-C-0067 ..... N90-21212
F19628-79-C-0044 ..... N90-21619
F19628-84-C-0102 ..... N90-21490
F19628-86-K-0009 ..... N90-21052
F19628-87-C-0003 ..... N90-21489
F33615-86-C-2697 ..... N90-21188
F33615-88-C-2851 ..... N90-21389
F49620-86-C-0128 ..... N90-21488
GRI-5088-260-1244 ..... N90-21146
GRI-5088-294-1292 ..... N90-21467
JF-DOE-818 ..... N90-21667
JPL-956415 ..... N90-21051
JPL-958095 ..... N90-21336
LANL-9-XG-83931P-1 ..... N90-21206
MDA903-85-C-0124 ..... N90-21555
MDA903-86-K-0037 ..... N90-21383
NAGW-269 ..... N90-21606
NAGW-920 ..... N90-21501
NAGW-1285 ..... N90-21323
NAGW-1434 ..... N90-21502
NAG1-4 ..... N90-21604
NAG1-060 ..... N90-21556
NAG1-423 ..... N90-20950
NAG1-427 ..... N90-21524
NAG1-569 ..... N90-21180
NAG1-613 ..... N90-21557
NAG1-630 ..... N90-21598
NAG1-664 ..... N90-20953
NAG1-672 ..... N90-21118
NAG1-683 ..... N90-21535
NAG1-690 ..... N90-20929
NAG1-812 ..... N90-21292
N90-21568
NAG1-834 ..... N90-20938
NAG1-975 ..... N90-20965
NAG1-1039 ..... N90-21554
NAG1-525622 ..... N90-21553
NAG2-593 ..... N90-21533
N90-21555
NAG3-666 ..... N90-20925
N90-20926
N90-20927
N90-20928
NAG3-671 ..... N90-21301
NAG3-708 ..... N90-21113
NAG3-773 ..... N90-21387
NAG3-816 ..... N90-21263
NAG3-843 ..... N90-21109
NAG3-944 ..... N90-21108
NAG5-481 ..... N90-21694
NAG5-501 ..... N90-21711
N90-21719
NAG5-814 ..... N90-21493
NAG6-1 ..... N90-21606
NAG8-511 ..... N90-21208
NAG8-755 ..... N90-21051
NAG9-314 ..... N90-21059
NASA ORDER C-99066-G N90-21036
N90-21131
N90-21291
N90-21567
N90-21570
NASW-3703 ..... N90-21323
NASW-4292 ..... N90-21513
NASW-4435 ..... N90-20971
NAS1-17492 ..... N90-20949
NAS1-17993 ..... N90-21405
NAS1-18106 ..... N90-21262
NAS1-18224 ..... N90-21099
NAS1-18444 ..... N90-21410
NAS1-18455 ..... N90-21058
NAS1-18561 ..... N90-20952
NAS1-18584 ..... N90-21413
NAS1-18599 ..... N90-21411
N90-21421
NAS1-18605 ..... N90-21269
N90-21290
N90-21556
N90-21566
NAS1-19000 ..... N90-21129
N90-21605
NAS2-11979 ..... N90-21097
NAS2-12157 ..... N90-20991
NAS2-12524 ..... N90-21349
NAS2-12578 ..... N90-21317
N90-21324
NAS3-23721 ..... N90-21602
NAS3-24564 ..... N90-21282
NAS3-24855 ..... N90-20991
NAS3-25070 ..... N90-21165
NAS3-25266 ..... N90-20943
N90-21037
N90-21420
N90-21552
N90-21600
NAS3-25317 ..... N90-21006
NAS3-25799 ..... N90-21272

NAS5-28731 ..... N90-21694
NAS5-30006 ..... N90-21338
NAS7-918 ..... N90-21061
N90-21215
N90-21479
N90-21480
NAS8-30490 ..... N90-21060
N90-21117
NAS8-35601 ..... N90-21395
NAS8-38031 ..... N90-20969
NAS9-17326 ..... N90-21521
NAS9-17900 ..... N90-21605
NCCW-000002 ..... N90-21413
NCC2-63 ..... N90-21171
NCC3-19 ..... N90-21192
NCC8-13 ..... N90-21529
NGL-22-009-640 ..... N90-20925
N90-20926
N90-20927
N90-20928
N90-20929
N90-20930
NGL-31-001-252 ..... N90-20941
NGR-009-017 ..... N90-20933
NSERC-A1671 ..... N90-21027
NSF ASC-88-19393 ..... N90-21556
NSF AST-85-16173 ..... N90-21694
NSF AST-88-18215 ..... N90-21694
NSF ATM-87-09659 ..... N90-21497
NSF ATM-88-11128 ..... N90-21640
NSF BSR-84-17923 ..... N90-21485
NSF DCR-84-12582 ..... N90-21555
NSF DMR-88-02306 ..... N90-21660
NSF DMR-88-09298 ..... N90-21316
NSF DMS-89-13089 ..... N90-21590
NSF ECS-88-57951 ..... N90-21278
NSF 85-52702 ..... N90-20925
N90-20927
NSG-5123 ..... N90-21531
N90-21532
NWO-612-319-006 ..... N90-21662
N00014-87-C-0157 ..... N90-21280
N00014-87-K-0307 ..... N90-21531
N00014-89-C-2222 ..... N90-21646
N00014-89-J-1108 ..... N90-21569
N00014-89-J-1627 ..... N90-21565
N00014-89-J-1659 ..... N90-21590
N00140-87-C-8904 ..... N90-21533
N90-21555
N60921-84-WR-W0095 ..... N90-21617
SERI-XX-8-18148-1 ..... N90-21660
SERI-ZB-7-06003-1 ..... N90-21473
SERI-ZB-8-0-7271-1 ..... N90-21472
SNL-33-1227 ..... N90-21470
T/RF-41/E0010/E14 ..... N90-20982
W-31-109-ENG-38 ..... N90-21168
N90-21559
N90-21563
N90-21644
N90-21645
N90-21664
W-7405-ENG-36 ..... N90-21144
N90-21196
N90-21206
N90-21357
N90-21377
N90-21466
N90-21515
N90-21558
N90-21586
N90-21587
N90-21610
N90-21612
N90-21633
N90-21638
N90-21667
N90-21691
N90-21692
N90-21693
N90-21694
N90-21712
W-7405-ENG-48 ..... N90-21057
N90-21139
N90-21153
N90-21155
N90-21156
N90-21172
N90-21258
N90-21266
N90-21365
N90-21371
N90-21404
N90-21512
N90-21584
N90-21585
N90-21617
N90-21618
N90-21637
N90-21658
N90-21659
N90-21661
N90-21662
N90-21663
N90-21666
N90-21709
188-41-55 ..... N90-21334
188-78-44 ..... N90-21097
199-22-76-01 ..... N90-21715
314-40-32-10-23 ..... N90-21479
N90-21480
450-52-01-71 ..... N90-21098
505-45-33-64 ..... N90-20952
505-45-58 ..... N90-20942
505-60-01-02 ..... N90-20949
505-60-21-06 ..... N90-20946
505-61-11-01 ..... N30-21598
505-62-0K N90-21387
505-62-00 ..... N90-21296
505-62-01 ..... N90-21277
N90-21351
505-62-21 ..... N90-21036
N90-21291
N90-21300
N90-21303
N90-21306
N90-21307
N90-21552
N90-21567
N90-21570
505-63-1B N90-21132
N90-21420
505-63-5A N30-21387
505-63-01-01 ..... N90-21129
505-63-01-05 ..... N90-21122
N90-21126
N90-21130
N90-21164
N90-21421
N90-21422
N90-21424
505-63-01-09 ..... N90-21413
505-63-01-10 ..... N90-21410
N90-21411
505-63-11 ..... N90-21137
505-63-21 ..... N90-21047
505-63-51 ..... N90-21394
505-63-51-03 ..... N90-20974
505-63-51-09 ..... N90-21603
505-66-01-02 ..... N90-20921
505-66-11-02 ..... N90-21004
N90-21005
505-66-11 ..... N90-20943
N90-21006
505-66-91-01 ..... N90-20953
505-69-61 ..... N90-21037
N90-21038
505-90-21-01 ..... N90-21289
N90-21290
N90-21556
N90-21566
505-90-21-02 ..... N90-21524
506-40-31-02 ..... N90-21297
506-41-11 ..... N90-21274
N90-21287
506-41-21 ..... N90-21116
N90-21469
506-41-31 ..... N90-21110
506-41-41 ..... N90-21181
N90-21192
N90-21283
506-43-11 ..... N90-21182
N90-21210
N90-21402
506-43-21-04 ..... N90-21140
506-43-71-03 ..... N90-21409
506-44-2C N90-21263
N90-21273
N90-21278
506-44-20 ..... N90-21275
506-44-21-03 ..... N90-21058
N90-21262
N90-21279
506-45-31 ..... N90-21313
510-01-0A N90-21124
N90-21131
N90-21133
N90-21138
N90-21143
N90-21361
510-01-1A N90-21401
535-03-01 ..... N90-21602
537-03-21-03 ..... N90-21605
549-03-1A N90-21271
N90-21272
549-03-11 ..... N90-21294
553-13-00 ..... N90-21123
582-01-11 ..... N90-21564
590-13-11 ..... N90-21114
590-14-61-01 ..... N90-21412
590-21-11-300 ..... N90-21414
590-21-41 ..... N90-21360
590-33-31-01 ..... N90-21096
591-22-31-01 ..... N90-21099
591-23-00 ..... N90-21295
643-10-01 ..... N90-21250
650-60-20 ..... N90-21261
N90-21282
694-24-00 ..... N90-21600
992-15-00-00-72 ..... N90-21721

Typical Report Number Index Listing

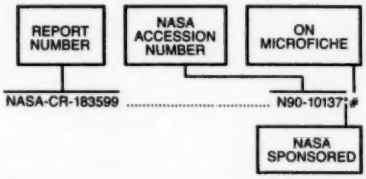

Listings in this index are arranged alphanumerically by report number. The NASA accession number denotes the number by which the citation is identified. An asterisk (*) indicates that the item is a NASA report. A pound sign (#) indicates that the item is available on microfiche.

A-89200 ..... N90-21313* #
A-89226 ..... N90-21294* #
A-90127 ..... N90-21097* #

AARL-P-90-1 ..... N90-21109* #

AD-A210025 ..... N90-21381 #
AD-A214561 ..... N90-21145 #
AD-A215035 ..... N90-21488 #
AD-A216277 ..... N90-21565 #
AD-A216375 ..... N90-20948 #
AD-A216521 ..... N90-21382 #
AD-A217096 ..... N90-21352 #
AD-A217169 ..... N90-21569 #
AD-A217224 ..... N90-21534 #
AD-A217297 ..... N90-21400 #
AD-A217319 ..... N90-21383 #
AD-A217632 ..... N90-21183 #
AD-A217710 ..... N90-21100 #
AD-A217790 ..... N90-21212 #
AD-A217791 ..... N90-21482 #
AD-A217795 ..... N90-21188 #
AD-A217805 ..... N90-21619 #
AD-A217807 ..... N90-21489 #
AD-A217827 ..... N90-21127 #
AD-A217861 ..... N90-21388 #
AD-A217912 ..... N90-21257 #
AD-A217994 ..... N90-21258 #
AD-A218071 ..... N90-21389 #
AD-A218139 ..... N90-21523 #
AD-A218206 ..... N90-21052 #
AD-A218209 ..... N90-21490 #
AD-A218216 ..... N90-21259 #
AD-A218245 ..... N90-21280 #
AD-A218248 ..... N90-21518 #
AD-A218264 ..... N90-21213 #
AD-A218265 ..... N90-21214 #
AD-A218324 ..... N90-21505 #
AD-A218327 ..... N90-21646 #

AD-D014398 ..... N90-21384
AD-D014400 ..... N90-21385 #
AD-D014401 ..... N90-21386 #
AD-D014403 ..... N90-21184 #
AD-D014406 ..... N90-21353
AD-D014407 ..... N90-21354
AD-D014424 ..... N90-21251 #
AD-D014425 ..... N90-21211 #
AD-D014426 ..... N90-21293 #
AD-D014427 ..... N90-21355 #
AD-D014429 ..... N90-21185 #
AD-D014430 ..... N90-21281 #
AD-D014435 ..... N90-21055 #
AD-D014437 ..... N90-21260
AD-D014438 ..... N90-21620
AD-D014443 ..... N90-21111
AD-D014445 ..... N90-21189
AD-D014446 ..... N90-21002
AD-D014448 ..... N90-21375 #
AD-D014449 ..... N90-21190 #

AD-E501191 ..... N90-21280 #

AERE-M-3698 ..... N90-21160 #

AERE-R-13198 ..... N90-21158 #
AERE-R-13273 ..... N90-21121 #
AERE-R-13362 ..... N90-21161 #
AERE-R-13401 ..... N90-21398 #
AERE-R-13418 ..... N90-21157 #
AERE-R-13425 ..... N90-21179 #
AERE-R-13438 ..... N90-21374 #
AERE-R-13531 ..... N90-21159 #
AERE-R-13566 ..... N90-21178 #

AERO-ASTRONAUTICS-242-PT-3 ..... N90-21051* #

AFGL-TR-89-0028 ..... N90-21489 #

AFIT/CI/CIA-88-242 ..... N90-21100 #
AFIT/CI/CIA-89-065 ..... N90-21505 #

AFIT/GAE/ENY/89D-21 ..... N90-20948 #

AFOSR-89-1512TR ..... N90-21488 #
AFOSR-90-0082TR ..... N90-21127 #

AGARD-AG-313 ..... N90-21359 #

AGARD-CP-459 ..... N90-21223 #
AGARD-CP-463 ..... N90-20976 #
AGARD-CP-469 ..... N90-21009 #

AIAA-89-2139 ..... N90-21038* #
AIAA-90-0978 ..... N90-21047* #

AMS-420 ..... N90-20920 #

ANL-90/9 ..... N90-21563 #
ANL-90/12 ..... N90-21559 #

ANL/FE-89-7 ..... N90-21168 #

AR-005-725 ..... N90-21510 #
AR-005-750 ..... N90-21203 #
AR-006-282 ..... N90-21120 #
AR-006-283 ..... N90-21202 #
AR-006-287 ..... N90-21204 #
AR-006-288 ..... N90-21044 #

ARL-005-729 ..... N90-21222 #
ARL-005-734 ..... N90-21201 #

ARL/TR-082 ..... N90-21520 #

ARO-25893.3-PH ..... N90-21352 #

AVSCOM-TM-89-C-009 ..... N90-21387* #
AVSCOM-TM-90-B-002 ..... N90-21126* #
AVSCOM-TM-90-B-004 ..... N90-20974* #
AVSCOM-TM-90-C-006 ..... N90-21394* #

AVSCOM-TR-90-B-002 ..... N90-21004* #

BBC-RD-1989/4 ..... N90-21221
BBC-RD-1989/10 ..... N90-21254 #
BBC-RD-1989/11 ..... N90-21255 #

BNL-43844 ..... N90-21218 #
BNL-44347 ..... N90-21615 #
BNL-52227 ..... N90-21484 #

BR110032 ..... N90-21381 #
BR112064 ..... N90-20972 #
BR112837 ..... N90-20973 #

CEA-CONF-5079 ..... N90-21381 #

CESAR-89/53 ..... N90-21397 #

CETHA-BC-CR-90028 ..... N90-21482 #

CONF-890001-1 ..... N90-21678 #
CONF-890421-12 ..... N90-21655 #

CONF-890554-4 ..... N90-21174 #
CONF-890572-2 ..... N90-21468 #
CONF-891119-82 ..... N90-21156 #
CONF-891119-114 ..... N90-21657 #
CONF-891119-116 ..... N90-21658 #
CONF-891131 ..... N90-21515 #
CONF-891179-1 ..... N90-21206 #
CONF-891273-3 ..... N90-21551 #
CONF-900109-24 ..... N90-21474 #
CONF-900115-2 ..... N90-21403 #
CONF-900123-1 ..... N90-21663 #
CONF-900140-16 ..... N90-21379 #
CONF-900140-18 ..... N90-21377 #
CONF-900181-2 ..... N90-21616 #
CONF-900183-3 ..... N90-21612 #
CONF-900206-2 ..... N90-21645 #
CONF-900206-3 ..... N90-21644 #
CONF-900238-2 ..... N90-21587 #
CONF-900264-4 ..... N90-21633 #
CONF-900276 ..... N90-21611 #
CONF-900315-2 ..... N90-21475 #
CONF-900368-3 ..... N90-21196 #
CONF-900373-1 ..... N90-21668 #
CONF-900384-1 ..... N90-21659 #
CONF-900398-1 ..... N90-21558 #
CONF-900403-9 ..... N90-21167 #
CONF-900419-3 ..... N90-21662 #
CONF-900474-1 ..... N90-21430 #
CONF-900508-1 ..... N90-21667 #
CONF-900530-3 ..... N90-21687 #
CONF-900567-3 ..... N90-21466 #
CONF-8804105-2 ..... N90-21709 #
CONF-8804214-2 ..... N90-21485 #
CONF-8805357 ..... N90-21520 #
CONF-8808146 ..... N90-21376 #
CONF-8811199-4 ..... N90-21367 #
CONF-8906225-3 ..... N90-21694* #
CONF-8906225-4 ..... N90-21693 #
CONF-8906225-5 ..... N90-21692 #
CONF-8907186-1 ..... N90-21613 #
CONF-8908219-1 ..... N90-21679 #
CONF-8909315-1 ..... N90-21514 #
CONF-8910207-2 ..... N90-21586 #
CONF-8910213-2 ..... N90-21386 #
CONF-8910319-3 ..... N90-21154 #
CONF-8910380-1 ..... N90-21656 #
CONF-8910381-1 ..... N90-21691 #
CONF-8911174-1 ..... N90-21512 #
CONF-8911177-1 ..... N90-21365 #
CONF-9002109-1 ..... N90-21610 #
CONF-9003115-1 ..... N90-21371 #
CONF-9003122-1 ..... N90-21056 #
CONF-9003128-1 ..... N90-21267 #
CONF-9003128-2 ..... N90-21642 #
CONF-9003129-1 ..... N90-21364 #
CONF-9003131-1 ..... N90-21712 #
CONF-9004136-8 ..... N90-21057 #
CONF-9004146-1 ..... N90-21186 #
CONF-9004146-4 ..... N90-21175 #
CONF-9004147-2 ..... N90-21205 #
CONF-9004154-1 ..... N90-21199 #
CONF-9004159-1 ..... N90-21560 #
CONF-9004159-2 ..... N90-21665 #
CONF-9004161-1 ..... N90-21550 #
CONF-9004164-1 ..... N90-21173 #
CONF-9005134-1 ..... N90-21688 #
CONF-9005148-1 ..... N90-21153 #
CONF-9005151-1 ..... N90-21549 #
CONF-9005152-1 ..... N90-21548 #
CONF-9006122-4 ..... N90-21664 #

CS-TR-2244 ..... N90-21531* #
CS-TR-2289 ..... N90-21532* #

CSG-118 ..... N90-21557* #

DAR-TP-18 ..... N90-21496 #
DAR-TP-19 ..... N90-21495 #

DE90-000314 ..... N90-21472 #
DE90-000319 ..... N90-21660 #
DE90-000320 ..... N90-21473 #
DE90-006268 ..... N90-21156 #

DE90-007539 ..... N90-21558 #
DE90-007544 ..... N90-21667 #
DE90-007552 ..... N90-21622 #
DE90-007604 ..... N90-21311 #
DE90-007652 ..... N90-21512 #
DE90-007711 ..... N90-21357 #
DE90-007795 ..... N90-21644 #
DE90-007796 ..... N90-21645 #
DE90-007799 ..... N90-21664 #
DE90-007894 ..... N90-21483 #
DE90-007897 ..... N90-21168 #
DE90-007904 ..... N90-21470 #
DE90-007906 ..... N90-21367 #
DE90-007908 ..... N90-21217 #
DE90-007910 ..... N90-21285 #
DE90-007913 ..... N90-21363 #
DE90-007920 ..... N90-21631 #
DE90-007922 ..... N90-21585 #
DE90-007924 ..... N90-21661 #
DE90-007925 ..... N90-21266 #
DE90-007927 ..... N90-21139 #
DE90-007929 ..... N90-21584 #
DE90-007932 ..... N90-21635 #
DE90-007933 ..... N90-21636 #
DE90-007936 ..... N90-21617 #
DE90-007937 ..... N90-21618 #
DE90-007939 ..... N90-21151 #
DE90-007953 ..... N90-21676 #
DE90-007957 ..... N90-21559 #
DE90-007958 ..... N90-21637 #
DE90-007959 ..... N90-21370 #
DE90-007960 ..... N90-21220 #
DE90-007965 ..... N90-21152 #
DE90-007972 ..... N90-21396 #
DE90-007975 ..... N90-21172 #
DE90-007976 ..... N90-21638 #
DE90-007978 ..... N90-21563 #
DE90-007982 ..... N90-21487 #
DE90-007994 ..... N90-21484 #
DE90-008062 ..... N90-21607 #
DE90-008170 ..... N90-21404 #
DE90-008178 ..... N90-21471 #
DE90-008356 ..... N90-21709 #
DE90-008508 ..... N90-21186 #
DE90-008509 ..... N90-21205 #
DE90-008601 ..... N90-21688 #
DE90-008615 ..... N90-21468 #
DE90-008623 ..... N90-21167 #
DE90-008634 ..... N90-21514 #
DE90-008676 ..... N90-21474 #
DE90-008677 ..... N90-21548 #
DE90-008690 ..... N90-21106 #
DE90-008691 ..... N90-21101 #
DE90-008692 ..... N90-21102 #
DE90-008693 ..... N90-21107 #
DE90-008694 ..... N90-21103 #
DE90-008695 ..... N90-21104 #
DE90-008698 ..... N90-21380 #
DE90-008722 ..... N90-21662 #
DE90-008731 ..... N90-21677 #
DE90-008803 ..... N90-21549 #
DE90-008804 ..... N90-21267 #
DE90-008806 ..... N90-21364 #
DE90-008824 ..... N90-21218 #
DE90-008826 ..... N90-21616 #
DE90-008852 ..... N90-21685 #
DE90-008860 ..... N90-21515 #
DE90-008871 ..... N90-21304 #
DE90-008873 ..... N90-21632 #
DE90-008883 ..... N90-21485 #
DE90-008902 ..... N90-21551 #
DE90-008903 ..... N90-21612 #
DE90-008906 ..... N90-21610 #
DE90-008907 ..... N90-21056 #
DE90-008913 ..... N90-21365 #
DE90-008918 ..... N90-21633 #
DE90-008927 ..... N90-21586 #
DE90-008932 ..... N90-21206 #
DE90-008933 ..... N90-21587 #
DE90-008934 ..... N90-21692 #
DE90-008935 ..... N90-21693 #
DE90-008936 ..... N90-21691 #
DE90-008938 ..... N90-21694* #
DE90-008941 ..... N90-21196 #
DE90-008943 ..... N90-21466 #
DE90-008946 ..... N90-21377 #
DE90-008957 ..... N90-21173 #
DE90-008958 ..... N90-21378 #
DE90-008970 ..... N90-21712 #
DE90-008979 ..... N90-21611 #
DE90-008980 ..... N90-21511 #
DE90-008983 ..... N90-21197 #
DE90-008999 ..... N90-21560 #
DE90-009003 ..... N90-21663 #
DE90-009007 ..... N90-21475 #
DE90-009011 ..... N90-21169 #
DE90-009016 ..... N90-21305 #
DE90-009034 ..... N90-21678 #
DE90-009035 ..... N90-21613 #
DE90-009036 ..... N90-21679 #
DE90-009044 ..... N90-21621 #
DE90-009045 ..... N90-21655 #
DE90-009048 ..... N90-21686 #
DE90-009059 ..... N90-21379 #
DE90-009065 ..... N90-21656 #
DE90-009075 ..... N90-21476 #
DE90-009124 ..... N90-21366 #
DE90-009142 ..... N90-21174 #
DE90-009176 ..... N90-21657 #
DE90-009181 ..... N90-21371 #
DE90-009183 ..... N90-21057 #
DE90-009184 ..... N90-21658 #
DE90-009185 ..... N90-21659 #
DE90-009190 ..... N90-21153 #
DE90-009192 ..... N90-21403 #
DE90-009224 ..... N90-21199 #
DE90-009242 ..... N90-21550 #
DE90-009285 ..... N90-21175 #
DE90-009311 ..... N90-21639 #
DE90-009331 ..... N90-21144 #
DE90-009340 ..... N90-21312 #
DE90-009341 ..... N90-21640 #
DE90-009342 ..... N90-21200 #
DE90-009351 ..... N90-21687 #
DE90-009365 ..... N90-21614 #
DE90-009382 ..... N90-21641 #
DE90-009384 ..... N90-21176 #
DE90-009399 ..... N90-21642 #
DE90-009402 ..... N90-21685 #
DE90-009428 ..... N90-21154 #
DE90-009448 ..... N90-21643 #
DE90-009475 ..... N90-21155 #
DE90-009503 ..... N90-21516 #
DE90-009510 ..... N90-21430 #
DE90-009542 ..... N90-21666 #
DE90-009755 ..... N90-21590 #
DE90-C10213 ..... N90-21397 #
DE90-612737 ..... N90-21572 #
DE90-612738 ..... N90-21573 #
DE90-612739 ..... N90-21574 #
DE90-612740 ..... N90-21594 #
DE90-612741 ..... N90-21575 #
DE90-612742 ..... N90-21576 #
DE90-612745 ..... N90-21577 #
DE90-612746 ..... N90-21578 #
DE90-612748 ..... N90-21579 #
DE90-612751 ..... N90-21670 #
DE90-612752 ..... N90-21580 #
DE90-612765 ..... N90-21671 #
DE90-612766 ..... N90-21672 #
DE90-612767 ..... N90-21673 #
DE90-612790 ..... N90-21581 #
DE90-612793 ..... N90-21582 #
DE90-612796 ..... N90-21674 #
DE90-612798 ..... N90-21583 #
DE90-612841 ..... N90-21362 #
DE90-612842 ..... N90-21608 #
DE90-612904 ..... N90-21647 #
DE90-612907 ..... N90-21147 #
DE90-612930 ..... N90-21148 #
DE90-612932 ..... N90-21193 #
DE90-612933 ..... N90-21648 #
DE90-613121 ..... N90-21626 #
DE90-613123 ..... N90-21627 #
DE90-613219 ..... N90-21628 #
DE90-613241 ..... N90-21629 #
DE90-613248 ..... N90-21649 #
DE90-613285 ..... N90-21707 #
DE90-613289 ..... N90-21264 #
DE90-613366 ..... N90-21265 #
DE90-613367 ..... N90-21708 #
DE90-613393 ..... N90-21650 #
DE90-613394 ..... N90-21651 #
DE90-613395 ..... N90-21652 #
DE90-613396 ..... N90-21653 #
DE90-613501 ..... N90-21609 #
DE90-613689 ..... N90-21149 #
DE90-613690 ..... N90-21150 #
DE90-613691 ..... N90-21194 #
DE90-614022 ..... N90-21166 #
DE90-614113 ..... N90-21654 #
DE90-614340 ..... N90-21520 #
DE90-614742 ..... N90-21675 #
DE90-614756 ..... N90-21423 #
DE90-614773 ..... N90-21376 #
DE90-614784 ..... N90-21048 #
DE90-615201 ..... N90-21668 #
DE90-615203 ..... N90-21669 #
DE90-615204 ..... N90-21592 #
DE90-615387 ..... N90-21623 #
DE90-615407 ..... N90-21624 #
DE90-616417 ..... N90-21356 #
DE90-616423 ..... N90-21615 #
DE90-616473 ..... N90-21546 #
DE90-616529 ..... N90-21547 #
DE90-759846 ..... N90-21528 #
DE90-759877 ..... N90-21561 #
DE90-759898 ..... N90-21562 #
DE90-759903 ..... N90-21630 #
DE90-759905 ..... N90-21195 #

DOE/DP-10684/1 ..... N90-21622 #
DOE/DP-10741/1 ..... N90-21621 #
DOE/DP-40200/112 ..... N90-21378 #

DOE/ER-04915/4 ..... N90-21677 #
DOE/ER-13150/T3 ..... N90-21380 #
DOE/ER-13333/6 ..... N90-21304 #
DOE/ER-13495/T3 ..... N90-21516 #
DOE/ER-45076/T1 ..... N90-21614 #
DOE/ER-45327/2 ..... N90-21176 #
DOE/ER-45366/2 ..... N90-21200 #
DOE/ER-53205/4 ..... N90-21632 #
DOE/ER-53291/150 ..... N90-21631 #

DOE/ET-32043/T31-VOL-1 ..... N90-21107 #
DOE/ET-32043/T31-VOL-2-BK-1 ..... N90-21103 #
DOE/ET-32043/T31-VOL-2-BK-2 ..... N90-21104 #
DOE/ET-53088/408 ..... N90-21639 #
DOE/ET-53088/414 ..... N90-21312 #
DOE/ET-53088/417 ..... N90-21641 #
DOE/ET-53088/418 ..... N90-21643 #
DOE/ET-53088/425 ..... N90-21640 #

DOE/FE-0106P ..... N90-21471 #
DOE/FE-0164 ..... N90-21483 #

DOE/NBB-0088P ..... N90-21487 #

DOE/PC-90961/T9 ..... N90-21311 #

DOT/FAA/CT-TN89/56 ..... N90-20968 #
DOT/FAA/CT-TN89/62 ..... N90-21500 #
DOT/FAA/CT-TN89/65 ..... N90-20967 #
DOT/FAA/CT-TN89/67 ..... N90-21508 #
DOT/FAA/CT-TN89/68 ..... N90-21256 #
DOT/FAA/CT-TN89/70 ..... N90-21042 #
DOT/FAA/CT-TN89/71 ..... N90-21248 #

DOT/FAA/CT-88/33 ..... N90-21247 #
DOT/FAA/CT-89/30 ..... N90-21008 #

DOT/FAA/DS-89/18 ..... N90-21045 #
DOT/FAA/DS-89/19 ..... N90-21509 #
DOT/FAA/DS-89/32 ..... N90-21049 #
DOT/FAA/DS-89/37 ..... N90-21003 #
DOT/FAA/DS-90/2 ..... N90-21249 #

DP-MS-88-225 ..... N90-21174 #
DP-MS-89-1 ..... N90-21366 #

E-2429 ..... N90-20942* #
E-3786 ..... N90-21351* #
E-4789 ..... N90-21037* #
E-4987 ..... N90-21250* #
E-4991 ..... N90-21038* #
E-5090 ..... N90-21123* #
E-5139 ..... N90-21602* #
E-5156 ..... N90-21138* #
E-5181 ..... N90-21210* #
E-5214 ..... N90-21124* #
E-5217 ..... N90-21564* #
E-5218 ..... N90-21361* #
E-5219 ..... N90-21300* #
E-5243 ..... N90-21420* #
E-5251 ..... N90-21274* #
E-5260 ..... N90-21036* #
E-5264 ..... N90-21263* #
E-5271 ..... N90-21360* #
E-5273 ..... N90-21137* #
E-5298 ..... N90-21402* #
E-5301 ..... N90-21182* #
E-5320 ..... N90-21570* #
E-5327 ..... N90-21273* #
E-5330 ..... N90-21261* #
E-5332 ..... N90-21181* #
E-5335 ..... N90-21296* #
E-5336 ..... N90-21291* #
E-5343 ..... N90-21278* #
E-5347 ..... N90-21600* #
E-5350 ..... N90-21567* #
E-5351 ..... N90-21399* #
E-5358 ..... N90-21271* #
E-5359 ..... N90-21272* #
E-5365 ..... N90-21275* #
E-5366 ..... N90-21303* #
E-5367 ..... N90-21306* #
E-5368 ..... N90-21307* #

E-5373 N90-21282* #
E-5375 N90-21110* #
E-5376 N90-21277* #
E-5379 N90-21143* #
E-5383 N90-21133* #
E-5389 N90-21131* #
E-5396 N90-21295* #
E-5402 N90-21283* #
E-5403 N90-21401* #
E-5406 N90-21192* #
E-5410 N90-21132* #
E-5411 N90-21469* #
E-5450 N90-21114* #
E-5453 N90-21287* #
E-5457 N90-21116* #
E-5469 N90-21394* #

EA-10559.04 N90-21482 #

EOARD-LR-89-068 N90-21720 #
EOARD-LR-89-069 N90-21046 #
EOARD-LR-90-001 N90-21001 #

EPA/600/D-89/195 N90-21481 #
EPA/600/D-89/263 N90-21504 #

F-603 N90-21721* #

FC-2094 N90-21388 #

FNAL-TM-1587 N90-21367 #
FNAL-TM-1615 N90-21217 #
FNAL-TM-1641 N90-21285 #

GA-A-19923 N90-21635 #
GA-A-19924 N90-21636 #

GEOPHYSICAL-PUBL-10 N90-21499 #

GL-TR-88-0291 N90-21490 #
GL-TR-89-0137 N90-21619 #
GL-TR-89-0278 N90-21052 #

GRI-89/0159 N90-21146 #
GRI-89/0161 N90-21467 #

IASSNS-HEP-89/48 N90-21613 #
IASSNS-HEP-89/51 N90-21679 #
IASSNS-HEP-90/19 N90-21678 #

IC-89/176 N90-21264 #
IC-89/218 N90-21707 #
IC-89/231 N90-21579 #
IC-89/233 N90-21265 #
IC-89/234 N90-21708 #
IC-89/235 N90-21581 #
IC-89/236 N90-21149 #
IC-89/245 N90-21166 #
IC-89/249 N90-21150 #
IC-89/256 N90-21194 #
IC-89/272 N90-21572 #
IC-89/273 N90-21573 #
IC-89/278 N90-21362 #
IC-89/283 N90-21650 #
IC-89/286 N90-21671 #
IC-89/287 N90-21582 #
IC-89/295 N90-21670 #
IC-89/296 N90-21580 #
IC-89/298 N90-21674 #
IC-89/304 N90-21574 #
IC-89/314 N90-21594 #
IC-89/315 N90-21651 #
IC-89/316 N90-21583 #
IC-89/326 N90-21575 #
IC-89/328 N90-21672 #
IC-89/331 N90-21606 #
IC-89/333 N90-21652 #
IC-89/348 N90-21675 #
IC-89/358 N90-21629 #
IC-89/360 N90-21627 #
IC-89/368 N90-21576 #
IC-89/370 N90-21647 #

ICASE-90-1 N90-21289* #
ICASE-90-19 N90-21290* #
ICASE-90-21 N90-21556* #
ICASE-90-23 N90-21566* #

ICOMP-89-32 N90-21036* #
ICOMP-90-09 N90-21291* #
ICOMP-90-10 N90-21567* #
ICOMP-90-11 N90-21131* #
ICOMP-90-12 N90-21570* #

IFSR-408 N90-21639 #
IFSR-414 N90-21312 #
IFSR-417 N90-21641 #
IFSR-418 N90-21643 #
IFSR-425 N90-21640 #

INIS-BR-1780 N90-21673 #
INIS-BR-1796 N90-21626 #
INIS-BR-1801 N90-21147 #

INIS-MF-11580 N90-21376 #
INIS-MF-11589 N90-21048 #

INPE-4704-TDL/343 N90-21628 #
INPE-4753-PRE/1425 N90-21093 #
INPE-4755-PRE/1427 N90-21094 #
INPE-4797-PRE/1451 N90-21436* #
INPE-4844-PRE/1473 N90-21689 #
INPE-4870-PRE/1481 N90-21437 #
INPE-4878-NTE/290 N90-21435 #
INPE-4892-PRE/1493 N90-21486 #
INPE-4899-PRE/1500 N90-21458 #
INPE-4902-PRE/1503 N90-21446 #
INPE-4904-PRE/1505 N90-21450 #
INPE-4905-PRE/1506 N90-21449 #
INPE-4906-PRE/1507 N90-21463 #
INPE-4907-PRE/1508 N90-21459 #
INPE-4909-PRE/1510 N90-21454 #
INPE-4911-PRE/1512 N90-21445 #
INPE-4918-PRE/1417 N90-21453 #
INPE-4919-RPE/594 N90-21141 #
INPE-4922-PRE/1519 N90-21465 #
INPE-4935-PRE/1425 N90-21438 #
INPE-4952-RPE/601 N90-21115 #
INPE-4956-PRE/1533 N90-21448 #
INPE-4961-TDL/390 N90-21713 #
INPE-4968-PRE/1537 N90-21462 #
INPE-4970-PRE/1538 N90-21452 #
INPE-4974-PRE/1539 N90-21447 #
INPE-4975-PRE/1540 N90-21484 #
INPE-4979-PRE/1544 N90-21457 #
INPE-4982-PRE/1542 N90-21442 #
INPE-4985-PRE/1547 N90-21714 #
INPE-4988-PRE/1550 N90-21105 #
INPE-4990-PRE/1555 N90-21444 #
INPE-4991-PRE/1556 N90-21054 #
INPE-4993-PRE/1555 N90-21451 #
INPE-4994-PRE/1556 N90-21460 #
INPE-4999-PRE/1561 N90-21494 #
INPE-5005-PRE/1562 N90-21268 #
INPE-5006-PRE/1563 N90-21461 #
INPE-5016-RPE/610 N90-21441 #
INPE-5017-RPE/611 N90-21439 #
INPE-5019-RPE/613 N90-21455 #
INPE-5023-RPE/616 N90-21456 #
INPE-5024-RPE/617 N90-21595 #
INPE-5026-PRE/1565 N90-21440 #
INPE-5032-MD/042 N90-21443 #

INS-T-490 N90-21528 #

IPPCZ-291 N90-21710 #

IR-186 N90-21682 #

ISBN-0-643-05070-1 N90-21496 #
ISBN-0-643-05086-8 N90-21495 #
ISBN-0-86776-323-X N90-21308 #
ISBN-0-86776-336-1 N90-21426 #
ISBN-91-7848-179-1 N90-21599 #
ISBN-92-835-0530-1 N90-21223 #
ISBN-92-835-0542-5 N90-20976 #
ISBN-92-835-0544-1 N90-21009 #
ISBN-851-754-933-4 N90-21589 #
ISBN-951-22-0027-9 N90-21270 #
ISBN-951-22-0040-6 N90-20963 #
ISBN-951-697-300-0 N90-21478 #
ISBN-951-697-304-3 N90-21499 #
ISBN-951-754-930-X N90-21253 #
ISBN-951-754-951-2 N90-21041 #
ISBN-951-754-969-5 N90-21163 #
ISBN-951-754-982-2 N90-21269 #
ISBN-951-754-995-4 N90-21588 #
ISBN-951-754-997-0 N90-21428 #

ISCR-1989-01 N90-21585 #

ISSN-0147-5711 N90-21683 #
ISSN-0284-5172 N90-21599 #
ISSN-0358-2620 N90-20963 #
ISSN-0735-2867 N90-21553* #
ISSN-0782-6087 N90-21499 #
ISSN-0782-6095 N90-21478 #
ISSN-0783-9375 N90-21428 #
ISSN-0784-848X N90-21269 #
ISSN-0784-848X N90-21270 #
ISSN-0784-3143 N90-21426 #
ISSN-0784-3143 N90-21588 #
ISSN-0784-3143 N90-21589 #
ISSN-0785-9732 N90-21253 #
ISSN-1045-2338 N90-21684 #

IYAF-88-144 N90-21623 #
IYAF-88-163 N90-21624 #

IZF-1989-25 N90-21518 #

JAERI-M-89-137 N90-21561 #
JAERI-M-89-151 N90-21195 #
JAERI-M-89-157 N90-21630 #
JAERI-M-89-191 N90-21562 #

JCP-4406 N90-21568* #

JINR-E-13-88-892 N90-21615 #

JINR-R-2-88-748 N90-21668 #
JINR-R-2-88-838 N90-21669 #
JINR-R-2-88-843 N90-21592 #
JINR-R-2-88-862 N90-21577 #
JINR-R-2-88-863 N90-21578 #
JINR-R-10-88-870 N90-21546 #
JINR-R-11-88-918 N90-21547 #

JINR-13-88-855 N90-21356 #
JINR-18-88-815 N90-21148 #

JPL-PUBL-87-4 N90-21479* #
JPL-PUBL-87-4 N90-21480* #

JPRS-UEE-90-002 N90-21284 #

JPRS-UES-88-004 N90-21431 #
JPRS-UES-89-002 N90-21432 #
JPRS-UES-90-005 N90-21433 #

JPRS-ULS-90-002 N90-21434 #

JPRS-UPM-90-002 N90-21593 #

K/DSRD-276 N90-21685 #

KBQ-FR-1 N90-21165* #

KCP-613-4074 N90-21152 #
KCP-613-4266 N90-21151 #

L-16586 N90-20946* #
L-16602 N90-21082* #
L-16652 N90-21004* #
L-16727 N90-21524* #
L-16736 N90-20974* #
L-16738 N90-21715* #
L-16740 N90-20921* #

LA-UR-90-378 N90-21515 #
LA-UR-90-515 N90-21558 #
LA-UR-90-590 N90-21667 #
LA-UR-90-768 N90-21377 #
LA-UR-90-782 N90-21466 #
LA-UR-90-839 N90-21196 #
LA-UR-90-870 N90-21694* #
LA-UR-90-874 N90-21691 #
LA-UR-90-875 N90-21693 #
LA-UR-90-876 N90-21692 #
LA-UR-90-897 N90-21587 #
LA-UR-90-898 N90-21206 #
LA-UR-90-955 N90-21586 #
LA-UR-90-1000 N90-21633 #
LA-UR-90-1014 N90-21612 #
LA-UR-90-1035 N90-21610 #
LA-UR-90-1037 N90-21712 #

LA-11558-T N90-21144 #
LA-11757-MS N90-21638 #
LA-11778-MS N90-21357 #

LBL-91-REV-9/89 N90-21607 #
LBL-26274 N90-21656 #
LBL-27360 N90-21655 #
LBL-27503 N90-21657 #
LBL-27814 N90-21476 #
LBL-28103 N90-21686 #
LBL-28483 N90-21379 #
LBL-28485 N90-21403 #

LC-89-600754 N90-21530 #
LC-89-600758 N90-21526 #

LMSC-D678511 N90-21410* #

LNCC-006/89 N90-21423 #

LR-563 N90-21425 #

LR-566 ..... N90-21427 #
LR-567 ..... N90-21310 #
LR-570 ..... N90-21369 #
LR-571 ..... N90-21429 #
LR-573 ..... N90-20964 #
LR-575-PT-8 ..... N90-21309 #
LR-589 ..... N90-21142 #

MCR-89-575 ..... N90-21058* #

MP-89-224 ..... N90-21155 #

MRL-RR-9-89 ..... N90-21128 #

MRL-TN-558 ..... N90-21510 #
MRL-TN-559 ..... N90-21222 #
MRL-TN-562 ..... N90-21120 #
MRL-TN-563 ..... N90-21202 #
MRL-TN-568 ..... N90-21044 #

MRL-TR-89-32 ..... N90-21201 #
MRL-TR-89-44 ..... N90-21203 #
MRL-TR-89-45 ..... N90-21204 #

MSU-ENGR-90-006 ..... N90-21301* #

MTI-88TR39 ..... N90-21395* #

MTL-TR-90-2 ..... N90-21183 #

NADC-89084-60 ..... N90-21523 #

NAL-TM-SE-8901 ..... N90-21043 #

NAPC-PE-188 ..... N90-21008 #

NAS 1.15:4182 ..... N90-21715* #
NAS 1.15:4183 ..... N90-20974* #
NAS 1.15:4185 ..... N90-21187* #
NAS 1.15:4192 ..... N90-21207* #
NAS 1.15:100387 ..... N90-21095* #
NAS 1.15:100391 ..... N90-21125* #
NAS 1.15:100393 ..... N90-21414* #
NAS 1.15:100394 ..... N90-21191* #
NAS 1.15:101454 ..... N90-21250* #
NAS 1.15:101675 ..... N90-21424* #
NAS 1.15:101680 ..... N90-21279* #
NAS 1.15:101797 ..... N90-21681* #
NAS 1.15:102160 ..... N90-21098* #
NAS 1.15:102161 ..... N90-21721* #
NAS 1.15:102209 ..... N90-21313* #
NAS 1.15:102220 ..... N90-21294* #
NAS 1.15:102304 ..... N90-21038* #
NAS 1.15:102371 ..... N90-21123* #
NAS 1.15:102404 ..... N90-21138* #
NAS 1.15:102442 ..... N90-21361* #
NAS 1.15:102472 ..... N90-21036* #
NAS 1.15:102477 ..... N90-21263* #
NAS 1.15:102481 ..... N90-21360* #
NAS 1.15:102484 ..... N90-21137* #
NAS 1.15:102485 ..... N90-21274* #
NAS 1.15:102496 ..... N90-21300* #
NAS 1.15:102501 ..... N90-21402* #
NAS 1.15:102517 ..... N90-21124* #
NAS 1.15:102522 ..... N90-21273* #
NAS 1.15:102523 ..... N90-21261* #
NAS 1.15:102527 ..... N90-21296* #
NAS 1.15:102534 ..... N90-21278* #
NAS 1.15:102538 ..... N90-21291* #
NAS 1.15:102539 ..... N90-21567* #
NAS 1.15:102540 ..... N90-21401* #
NAS 1.15:102541 ..... N90-21399* #
NAS 1.15:102545 ..... N90-21182* #
NAS 1.15:102546 ..... N90-21181* #
NAS 1.15:102547 ..... N90-21271* #
NAS 1.15:102548 ..... N90-21272* #
NAS 1.15:102550 ..... N90-21275* #
NAS 1.15:102551 ..... N90-21303* #
NAS 1.15:102552 ..... N90-21306* #
NAS 1.15:102553 ..... N90-21307* #
NAS 1.15:102557 ..... N90-21110* #
NAS 1.15:102559 ..... N90-21143* #
NAS 1.15:102562 ..... N90-21277* #
NAS 1.15:102563 ..... N90-21133* #
NAS 1.15:102565 ..... N90-21131* #
NAS 1.15:102568 ..... N90-21570* #
NAS 1.15:102572 ..... N90-21295* #
NAS 1.15:102574 ..... N90-21283* #
NAS 1.15:102576 ..... N90-21192* #
NAS 1.15:102579 ..... N90-21132* #
NAS 1.15:102580 ..... N90-21469* #
NAS 1.15:102587 ..... N90-21005* #
NAS 1.15:102591 ..... N90-21126* #
NAS 1.15:102594 ..... N90-21409* #
NAS 1.15:102599 ..... N90-21122* #
NAS 1.15:102602 ..... N90-21297* #
NAS 1.15:102605 ..... N90-21096* #
NAS 1.15:102615 ..... N90-21412* #
NAS 1.15:102633 ..... N90-21140* #
NAS 1.15:102636 ..... N90-21130* #
NAS 1.15:102637 ..... N90-21422* #
NAS 1.15:102646 ..... N90-21164* #
NAS 1.15:102651 ..... N90-21047* #
NAS 1.15:102653 ..... N90-21603* #
NAS 1.15:102900 ..... N90-21050* #
NAS 1.15:102939 ..... N90-21436* #
NAS 1.15:102991 ..... N90-21680* #
NAS 1.15:103117 ..... N90-21564* #
NAS 1.15:103122 ..... N90-21114* #
NAS 1.15:103125 ..... N90-21287* #
NAS 1.15:103127 ..... N90-21116* #
NAS 1.15:103132 ..... N90-21394* #
NAS 1.15:103304 ..... N90-21545* #
NAS 1.15:103305 ..... N90-21544* #
NAS 1.15:103306 ..... N90-21543* #
NAS 1.15:103307 ..... N90-21542* #
NAS 1.15:103308 ..... N90-21541* #
NAS 1.15:103309 ..... N90-21540* #
NAS 1.15:103310 ..... N90-21539* #
NAS 1.15:103311 ..... N90-21538* #
NAS 1.15:103312 ..... N90-21537* #
NAS 1.15:103313 ..... N90-21536* #
NAS 1.26:4264 ..... N90-21602* #
NAS 1.26:4267 ..... N90-20969* #
NAS 1.26:4282 ..... N90-21411* #
NAS 1.26:4285 ..... N90-20949* #
NAS 1.26:177541 ..... N90-21097* #
NAS 1.26:180498 ..... N90-21694* #
NAS 1.26:181728 ..... N90-21410* #
NAS 1.26:181899 ..... N90-21129* #
NAS 1.26:181925 ..... N90-21598* #
NAS 1.26:181966 ..... N90-21413* #
NAS 1.26:181967 ..... N90-20952* #
NAS 1.26:181989 ..... N90-21262* #
NAS 1.26:181992 ..... N90-21099* #
NAS 1.26:181994 ..... N90-21289* #
NAS 1.26:182003 ..... N90-21290* #
NAS 1.26:182008 ..... N90-20953* #
NAS 1.26:182010 ..... N90-21556* #
NAS 1.26:182012 ..... N90-21566* #
NAS 1.26:182014 ..... N90-21058* #
NAS 1.26:182018 ..... N90-21421* #
NAS 1.26:182027 ..... N90-21605* #
NAS 1.26:182855 ..... N90-21555* #
NAS 1.26:183930 ..... N90-21060* #
NAS 1.26:183932 ..... N90-21117* #
NAS 1.26:183942 ..... N90-21395* #
NAS 1.26:184982 ..... N90-21529* #
NAS 1.26:185129 ..... N90-20943* #
NAS 1.26:185148 ..... N90-21387* #
NAS 1.26:185159 ..... N90-21600* #
NAS 1.26:185185 ..... N90-21108* #
NAS 1.26:185186 ..... N90-21420* #
NAS 1.26:185203 ..... N90-21165* #
NAS 1.26:185215 ..... N90-21282* #
NAS 1.26:185225 ..... N90-21006* #
NAS 1.26:185231 ..... N90-21552* #
NAS 1.26:185607 ..... N90-21521* #
NAS 1.26:185611 ..... N90-21059* #
NAS 1.26:186059 ..... N90-21405* #
NAS 1.26:186165 ..... N90-21051* #
NAS 1.26:186227 ..... N90-20971* #
NAS 1.26:186408 ..... N90-21501* #
NAS 1.26:186448 ..... N90-21480* #
NAS 1.26:186449 ..... N90-21479* #
NAS 1.26:186450 ..... N90-21180* #
NAS 1.26:186451 ..... N90-20950* #
NAS 1.26:186455 ..... N90-21531* #
NAS 1.26:186457 ..... N90-21532* #
NAS 1.26:186465 ..... N90-21109* #
NAS 1.26:186477 ..... N90-21568* #
NAS 1.26:186494 ..... N90-21292* #
NAS 1.26:186495 ..... N90-21533* #
NAS 1.26:186499 ..... N90-21502* #
NAS 1.26:186501 ..... N90-21606* #
NAS 1.26:186510 ..... N90-21557* #
NAS 1.26:186513 ..... N90-21208* #
NAS 1.26:186515 ..... N90-21535* #
NAS 1.26:186529 ..... N90-21301* #
NAS 1.26:186531 ..... N90-21113* #
NAS 1.26:186533 ..... N90-21571* #
NAS 1.26:186539 ..... N90-21719* #
NAS 1.26:186540 ..... N90-21711* #
NAS 1.26:186541 ..... N90-21493* #
NAS 1.26:186561 ..... N90-21171* #
NAS 1.26:186562 ..... N90-21553* #
NAS 1.26:186576 ..... N90-20965* #
NAS 1.26:186577 ..... N90-21604* #
NAS 1.26:186583 ..... N90-21554* #
NAS 1.26:392231 ..... N90-21513* #
NAS 1.55:3041 ..... N90-21062* #
NAS 1.55:3063 ..... N90-20921* #
NAS 1.60:2462 ..... N90-20942* #
NAS 1.60:2980 ..... N90-21004* #
NAS 1.60:2989 ..... N90-20945* #
NAS 1.60:2994 ..... N90-21210* #
NAS 1.60:2998 ..... N90-21524* #
NAS 1.60:3013 ..... N90-21219* #
NAS 1.61:1222 ..... N90-21351* #
NAS 1.61:1235 ..... N90-21037* #

NAS-SR-1361 ..... N90-21249 #

NASA-CASE-ARC-11649-2-SB N90-21177*

NASA-CASE-LAR-13448-1 ..... N90-21198*
NASA-CASE-LAR-13817-1 ..... N90-21170*
NASA-CASE-LAR-13901-1-NP N90-21519*
NASA-CASE-LAR-13965-1-CU N90-21118*
NASA-CASE-LAR-14050-1 ..... N90-21216*

NASA-CASE-MFS-26047-1 ..... N90-21209*

NASA-CASE-MSC-21436-1 ..... N90-21390*

NASA-CASE-NPO-16859-1-CU N90-21527*
NASA-CASE-NPO-17205-1-CU N90-21525*
NASA-CASE-NPO-17235-1-CO N90-21358*
NASA-CASE-NPO-17278-1-CU N90-21215*
NASA-CASE-NPO-17280-1-CU N90-21061*

NASA-CP-3041 ..... N90-21062* #
NASA-CP-3063 ..... N90-20921* #

NASA-CR-4264 ..... N90-21602* #
NASA-CR-4267 ..... N90-20969* #
NASA-CR-4282 ..... N90-21411* #
NASA-CR-4285 ..... N90-20949* #
NASA-CR-177541 ..... N90-21097* #
NASA-CR-180498 ..... N90-21694* #
NASA-CR-181728 ..... N90-21410* #
NASA-CR-181899 ..... N90-21129* #
NASA-CR-181925 ..... N90-21598* #
NASA-CR-181966 ..... N90-21413* #
NASA-CR-181967 ..... N90-20952* #
NASA-CR-181989 ..... N90-21262* #
NASA-CR-181992 ..... N90-21099* #
NASA-CR-181994 ..... N90-21289* #
NASA-CR-182003 ..... N90-21290* #
NASA-CR-182008 ..... N90-20953* #
NASA-CR-182010 ..... N90-21556* #
NASA-CR-182012 ..... N90-21566* #
NASA-CR-182014 ..... N90-21058* #
NASA-CR-182018 ..... N90-21421* #
NASA-CR-182027 ..... N90-21605* #
NASA-CR-182855 ..... N90-21555* #
NASA-CR-183930 ..... N90-21060* #
NASA-CR-183932 ..... N90-21117* #
NASA-CR-183942 ..... N90-21395* #
NASA-CR-184982 ..... N90-21529* #
NASA-CR-185129 ..... N90-20943* #
NASA-CR-185148 ..... N90-21387* #
NASA-CR-185159 ..... N90-21600* #
NASA-CR-185185 ..... N90-21108* #
NASA-CR-185188 ..... N90-21420* #
NASA-CR-185203 ..... N90-21165* #
NASA-CR-185215 ..... N90-21282* #
NASA-CR-185225 ..... N90-21006* #
NASA-CR-185231 ..... N90-21552* #
NASA-CR-185607 ..... N90-21521* #
NASA-CR-185611 ..... N90-21059* #
NASA-CR-186059 ..... N90-21405* #
NASA-CR-186165 ..... N90-21051* #
NASA-CR-186227 ..... N90-20971* #
NASA-CR-186408 ..... N90-21501* #
NASA-CR-186448 ..... N90-21480* #
NASA-CR-186449 ..... N90-21479* #
NASA-CR-186450 ..... N90-21180* #
NASA-CR-186451 ..... N90-20950* #
NASA-CR-186455 ..... N90-21531* #
NASA-CR-186457 ..... N90-21532* #
NASA-CR-186465 ..... N90-21109* #
NASA-CR-186477 ..... N90-21568* #
NASA-CR-186494 ..... N90-21292* #
NASA-CR-186495 ..... N90-21533* #
NASA-CR-186499 ..... N90-21502* #
NASA-CR-186501 ..... N90-21606* #
NASA-CR-186510 ..... N90-21557* #
NASA-CR-186513 ..... N90-21208* #
NASA-CR-186515 ..... N90-21535* #
NASA-CR-186529 ..... N90-21301* #
NASA-CR-186531 ..... N90-21113* #
NASA-CR-186533 ..... N90-21571* #
NASA-CR-186539 ..... N90-21719* #
NASA-CR-186540 ..... N90-21711* #
NASA-CR-186541 ..... N90-21493* #
NASA-CR-186561 ..... N90-21171* #
NASA-CR-186562 ..... N90-21553* #

NASA-CR-166576 ..... N90-20965* #
NASA-CR-166577 ..... N90-21604* #
NASA-CR-166583 ..... N90-21554* #
NASA-CR-392231 ..... N90-21513* #

NASA-RP-1222 ..... N90-21351* #
NASA-RP-1235 ..... N90-21037* #

NASA-TM-4182 ..... N90-21715* #
NASA-TM-4183 ..... N90-20974* #
NASA-TM-4185 ..... N90-21187* #
NASA-TM-4192 ..... N90-21207* #
NASA-TM-100387 ..... N90-21095* #
NASA-TM-100391 ..... N90-21125* #
NASA-TM-100393 ..... N90-21414* #
NASA-TM-100394 ..... N90-21191* #
NASA-TM-101454 ..... N90-21250* #
NASA-TM-101675 ..... N90-21424* #
NASA-TM-101680 ..... N90-21279* #
NASA-TM-101797 ..... N90-21681* #
NASA-TM-102160 ..... N90-21098* #
NASA-TM-102161 ..... N90-21721* #
NASA-TM-102209 ..... N90-21313* #
NASA-TM-102220 ..... N90-21294* #
NASA-TM-102304 ..... N90-21038* #
NASA-TM-102371 ..... N90-21123* #
NASA-TM-102404 ..... N90-21138* #
NASA-TM-102442 ..... N90-21361* #
NASA-TM-102472 ..... N90-21036* #
NASA-TM-102477 ..... N90-21263* #
NASA-TM-102481 ..... N90-21360* #
NASA-TM-102484 ..... N90-21137* #
NASA-TM-102485 ..... N90-21274* #
NASA-TM-102496 ..... N90-21300* #
NASA-TM-102501 ..... N90-21402* #
NASA-TM-102517 ..... N90-21124* #
NASA-TM-102522 ..... N90-21273* #
NASA-TM-102523 ..... N90-21261* #
NASA-TM-102527 ..... N90-21296* #
NASA-TM-102534 ..... N90-21278* #
NASA-TM-102538 ..... N90-21291* #
NASA-TM-102539 ..... N90-21567* #
NASA-TM-102540 ..... N90-21401* #
NASA-TM-102541 ..... N90-21399* #
NASA-TM-102545 ..... N90-21182* #
NASA-TM-102546 ..... N90-21181* #
NASA-TM-102547 ..... N90-21271* #
NASA-TM-102548 ..... N90-21272* #
NASA-TM-102550 ..... N90-21275* #
NASA-TM-102551 ..... N90-21303* #
NASA-TM-102552 ..... N90-21306* #
NASA-TM-102553 ..... N90-21307* #
NASA-TM-102557 ..... N90-21110* #
NASA-TM-102559 ..... N90-21143* #
NASA-TM-102562 ..... N90-21277* #
NASA-TM-102563 ..... N90-21133* #
NASA-TM-102565 ..... N90-21131* #
NASA-TM-102568 ..... N90-21570* #
NASA-TM-102572 ..... N90-21295* #
NASA-TM-102574 ..... N90-21283* #
NASA-TM-102576 ..... N90-21192* #
NASA-TM-102579 ..... N90-21132* #
NASA-TM-102580 ..... N90-21469* #
NASA-TM-102587 ..... N90-21005* #
NASA-TM-102591 ..... N90-21126* #
NASA-TM-102594 ..... N90-21409* #
NASA-TM-102599 ..... N90-21122* #
NASA-TM-102602 ..... N90-21297* #
NASA-TM-102605 ..... N90-21096* #
NASA-TM-102615 ..... N90-21412* #
NASA-TM-102633 ..... N90-21140* #
NASA-TM-102636 ..... N90-21130* #
NASA-TM-102637 ..... N90-21422* #
NASA-TM-102646 ..... N90-21164* #
NASA-TM-102651 ..... N90-21047* #
NASA-TM-102653 ..... N90-21603* #
NASA-TM-102900 ..... N90-21050* #
NASA-TM-102939 ..... N90-21436* #
NASA-TM-102991 ..... N90-21680* #
NASA-TM-103117 ..... N90-21564* #
NASA-TM-103122 ..... N90-21114* #
NASA-TM-103125 ..... N90-21287* #
NASA-TM-103127 ..... N90-21116* #
NASA-TM-103132 ..... N90-21394* #
NASA-TM-103304 ..... N90-21545* #
NASA-TM-103305 ..... N90-21544* #
NASA-TM-103306 ..... N90-21543* #
NASA-TM-103307 ..... N90-21542* #
NASA-TM-103308 ..... N90-21541* #
NASA-TM-103309 ..... N90-21540* #
NASA-TM-103310 ..... N90-21539* #
NASA-TM-103311 ..... N90-21538* #
NASA-TM-103312 ..... N90-21537* #
NASA-TM-103313 ..... N90-21536* #

NASA-TP-2462 ..... N90-20942* #
NASA-TP-2980 ..... N90-21004* #
NASA-TP-2989 ..... N90-20946* #
NASA-TP-2994 ..... N90-21210* #
NASA-TP-2998 ..... N90-21524* #
NASA-TP-3013 ..... N90-21219* #

NCAR/TN-344-1A ..... N90-21497 #

NIST/SP-500/165 ..... N90-21530 #

NIST/TN-1332 ..... N90-21276 #

NISTIR-89/4173 ..... N90-21162 #
NISTIR-89/4184 ..... N90-21591 #

NLM/MED-90/01 ..... N90-21683 #
NLM/MED-90/03 ..... N90-21684 #

NOAA-TM-NESDIS-29 ..... N90-21498 #

NOAA-TR-ERL-438-WPL-62 ..... N90-21503 #

NOAA-TR-NESDIS-46 ..... N90-21477 #

NOSC/TD-1712 ..... N90-21259 #

NTSB/ARG-89/01 ..... N90-20966 #

NTSB/SIR-90/01 ..... N90-21000 #

NUS-5249-EXEC-SUMM ..... N90-21106 #
NUS-5250-VOL-3-BK-1 ..... N90-21101 #
NUS-5250-VOL-3-BK-2 ..... N90-21102 #

NWRA-CR-89-R039 ..... N90-21489 #

ORNL/FTR-3555 ..... N90-21511 #
ORNL/FTR-3566 ..... N90-21169 #
ORNL/FTR-3572 ..... N90-21197 #

ORNL/M-1117 ..... N90-21305 #

ORNL/TM-11435 ..... N90-21397 #

OTA-BP-CIT-59 ..... N90-21526 #

PB90-100009 ..... N90-21683 #
PB90-100025 ..... N90-21684 #
PB90-111691 ..... N90-21530 #
PB90-120296 ..... N90-20920 #
PB90-124348 ..... N90-21695 #
PB90-124728 ..... N90-21682 #
PB90-128976 ..... N90-21599 #
PB90-130147 ..... N90-21503 #
PB90-131111 ..... N90-21481 #
PB90-131152 ..... N90-21162 #
PB90-131228 ..... N90-21526 #
PB90-131285 ..... N90-21146 #
PB90-131293 ..... N90-21467 #
PB90-132432 ..... N90-21504 #
PB90-133158 ..... N90-21591 #
PB90-138066 ..... N90-20966 #
PB90-138413 ..... N90-21253 #
PB90-138421 ..... N90-21163 #
PB90-145160 ..... N90-21276 #
PB90-145533 ..... N90-21252 #
PB90-164757 ..... N90-21426 #
PB90-164781 ..... N90-21308 #
PB90-165614 ..... N90-21588 #
PB90-165622 ..... N90-21589 #
PB90-165630 ..... N90-21428 #
PB90-165671 ..... N90-21269 #
PB90-165689 ..... N90-21270 #
PB90-165754 ..... N90-21286 #
PB90-166000 ..... N90-21497 #
PB90-166588 ..... N90-21142 #
PB90-166778 ..... N90-20963 #
PB90-166786 ..... N90-21041 #
PB90-166802 ..... N90-21368 #
PB90-167024 ..... N90-21425 #
PB90-167032 ..... N90-21427 #
PB90-167040 ..... N90-21310 #
PB90-167065 ..... N90-21369 #
PB90-167073 ..... N90-21429 #
PB90-167131 ..... N90-20964 #
PB90-167149 ..... N90-21309 #
PB90-917004 ..... N90-21000 #

PD-CF-8942 ..... N90-20951 #
PD-CF-9003 ..... N90-21522 #
PD-CF-9004 ..... N90-20975 #

PD-FC-9001 ..... N90-20970 #

PML-1988-C159 ..... N90-21310 #

PNL-SA-16902 ..... N90-21468 #
PNL-SA-17321 ..... N90-21514 #
PNL-SA-17601 ..... N90-21167 #
PNL-SA-17792 ..... N90-21474 #

POLY-WRI-1567-89 ..... N90-21352 #

PROG-8860710 ..... N90-21467 #

PUBL-AIR-QUALITY-5 ..... N90-21478 #

R/D-6178-CH-02 ..... N90-21145 #

RAE-TM-MAT-STR-1138 ..... N90-20973 #

RAE-TM-MS-1129 ..... N90-20972 #

RAE-TRANS-2165 ..... N90-21381 #

REPT-9 ..... N90-21428 #
REPT-51 ..... N90-21269 #
REPT-52 ..... N90-21270 #
REPT-89/25 ..... N90-21695 #
REPT-90RR-13 ..... N90-21049 #

RFP-4256 ..... N90-21396 #

RPT/D0406-54 ..... N90-21165* #

RR-A267 ..... N90-21589 #
RR-A268 ..... N90-21588 #

RR-CE100 ..... N90-21308 #
RR-CE101 ..... N90-21426 #

R8928 ..... N90-21490 #

S-602 ..... N90-21098* #

SAND-87-8215B ..... N90-21676 #
SAND-88-3188 ..... N90-21220 #
SAND-89-0855 ..... N90-21363 #
SAND-89-1089 ..... N90-21370 #
SAND-89-1576C ..... N90-21173 #
SAND-89-2580C ..... N90-21205 #
SAND-89-2685C ..... N90-21548 #
SAND-89-2872C ..... N90-21560 #
SAND-89-2987C ..... N90-21475 #
SAND-89-7028 ..... N90-21470 #
SAND-90-0242C ..... N90-21267 #
SAND-90-0482C ..... N90-21549 #
SAND-90-0653C ..... N90-21186 #
SAND-90-0737C ..... N90-21364 #
SAND-90-0782C ..... N90-21175 #
SAND-90-0871C ..... N90-21687 #
SAND-90-1080C ..... N90-21430 #

SBIR-87-2 ..... N90-21681* #
SBIR-88-LUB-1 ..... N90-21389 #
SBIR-88-2 ..... N90-21680* #

SEL-82-806 ..... N90-21536* #
SEL-88-001 ..... N90-21541* #
SEL-88-002 ..... N90-21540* #
SEL-88-003 ..... N90-21542* #
SEL-89-001 ..... N90-21545* #
SEL-89-002 ..... N90-21544* #
SEL-89-003 ..... N90-21543* #
SEL-89-004 ..... N90-21539* #
SEL-89-005 ..... N90-21538* #
SEL-89-006 ..... N90-21537* #

SER-B-89-B16 ..... N90-21041 #
SER-B-89-B18 ..... N90-20963 #

SERI/TP-211-3656 ..... N90-21472 #
SERI/TP-211-3666 ..... N90-21660 #
SERI/TP-211-3667 ..... N90-21473 #

SFCC/PUB-54 ..... N90-21310 #

SP-RAPP-1989:28 ..... N90-21599 #

SU-SOL-90-7 ..... N90-21590 #

TDCK-89-1055 ..... N90-21518 #

TDL-343 ..... N90-21628 #

TELAC-88-14 ..... N90-21127 #

TKK-IGE-A12 ..... N90-21253 #

TKK-V-B46 ..... N90-21163 #

TL-89-JETS-GLM-1 ..... N90-21598* #

TR-1 ..... N90-21534 #
TR-425 ..... N90-21565 #

TSF1-R-014 ..... N90-21301* #

TWR-17849 ..... N90-21117* #
TWR-18782 ..... N90-21060* #

UAH-RR-804 ..... N90-21529* #

UCID-21791-3 ..... N90-21618 #
UCID-21936 ..... N90-21266 #
UCID-21941 ..... N90-21661 #
UCID-21955 ..... N90-21139 #
UCID-21964 ..... N90-21585 #

UCRL--101932 ..... N90-21057 #

UCRL-CR-103295 ..... N90-21155 #

UCRL-ID-103119 ..... N90-21637 #
UCRL-ID-103318 ..... N90-21404 #
UCRL-ID-103333 ..... N90-21617 #

UCRL-JC-103212 ..... N90-21663 #
UCRL-JC-103223 ..... N90-21153 #
UCRL-JC-103276 ..... N90-21659 #
UCRL-JC-103340 ..... N90-21658 #

UCRL-53918 ..... N90-21564 #
UCRL-53947 ..... N90-21172 #
UCRL-98567 ..... N90-21709 #
UCRL-100498-REV-1 ..... N90-21371 #
UCRL-101106 ..... N90-21156 #
UCRL-102016 ..... N90-21662 #
UCRL-102248 ..... N90-21666 #
UCRL-102862 ..... N90-21512 #
UCRL-102937 ..... N90-21365 #

UILU-ENG-89-2242 ..... N90-21557* #
UILU-ENG-90-2001 ..... N90-21553* #

ULS-FSAR-001-EXEC-SUMM ..... N90-21106 #
ULS-FSAR-002-VOL-1 ..... N90-21107 #
ULS-FSAR-003 ..... N90-21103 #
ULS-FSAR-004 ..... N90-21104 #
ULS-FSAR-005 ..... N90-21101 #
ULS-FSAR-006 ..... N90-21102 #

UM-P-89/13 ..... N90-21193 #
UM-P-89/29 ..... N90-21648 #
UM-P-89/36 ..... N90-21654 #
UM-P-89/38 ..... N90-21609 #
UM-P-89/41 ..... N90-21649 #

UMIACS-TR-89-48 ..... N90-21531* #
UMIACS-TR-89-75 ..... N90-21532* #

US-PATENT-APPL-SN-067846 ..... N90-21216*
US-PATENT-APPL-SN-113956 ..... N90-21527*
US-PATENT-APPL-SN-116811 ..... N90-21358*
US-PATENT-APPL-SN-118993 ..... N90-21519*
US-PATENT-APPL-SN-143434 ..... N90-21525*
US-PATENT-APPL-SN-172100 ..... N90-21215*
US-PATENT-APPL-SN-184217 ..... N90-21354
US-PATENT-APPL-SN-195226 ..... N90-21061*
US-PATENT-APPL-SN-196705 ..... N90-21620
US-PATENT-APPL-SN-210486 ..... N90-21170*
US-PATENT-APPL-SN-221386 ..... N90-21118*
US-PATENT-APPL-SN-231027 ..... N90-21177*
US-PATENT-APPL-SN-237657 ..... N90-21216*
US-PATENT-APPL-SN-244389 ..... N90-21209*
US-PATENT-APPL-SN-280056 ..... N90-21384
US-PATENT-APPL-SN-313839 ..... N90-21390*
US-PATENT-APPL-SN-331200 ..... N90-21189
US-PATENT-APPL-SN-354559 ..... N90-21355 #
US-PATENT-APPL-SN-397549 ..... N90-21386 #
US-PATENT-APPL-SN-414499 ..... N90-21375 #
US-PATENT-APPL-SN-429959 ..... N90-21190 #
US-PATENT-APPL-SN-442085 ..... N90-21184 #
US-PATENT-APPL-SN-442961 ..... N90-21185 #
US-PATENT-APPL-SN-444350 ..... N90-21385 #
US-PATENT-APPL-SN-450754 ..... N90-21293 #
US-PATENT-APPL-SN-456899 ..... N90-21281 #
US-PATENT-APPL-SN-459629 ..... N90-21211 #
US-PATENT-APPL-SN-461943 ..... N90-21251 #
US-PATENT-APPL-SN-466142 ..... N90-21055 #
US-PATENT-APPL-SN-501667 ..... N90-21002
US-PATENT-APPL-SN-546755 ..... N90-21260
US-PATENT-APPL-SN-838654 ..... N90-21198*
US-PATENT-APPL-SN-929869 ..... N90-21519*
US-PATENT-APPL-SN-938314 ..... N90-21353
US-PATENT-APPL-SN-938922 ..... N90-21111

US-PATENT-CLASS-62-467 ..... N90-21215*
US-PATENT-CLASS-89-1.14 ..... N90-21390*
US-PATENT-CLASS-89-1.57 ..... N90-21390*
US-PATENT-CLASS-073-801 ..... N90-21170*
US-PATENT-CLASS-102-267 ..... N90-21111
US-PATENT-CLASS-102-378 ..... N90-21390*
US-PATENT-CLASS-128-661.03 ..... N90-21519*
US-PATENT-CLASS-164-113 ..... N90-21216*
US-PATENT-CLASS-164-284 ..... N90-21216*
US-PATENT-CLASS-181-0.5 ..... N90-21215*
US-PATENT-CLASS-194-82.26 ..... N90-21390*
US-PATENT-CLASS-194-82.29 ..... N90-21390*
US-PATENT-CLASS-210-94 ..... N90-21209*
US-PATENT-CLASS-210-95 ..... N90-21209*
US-PATENT-CLASS-210-205 ..... N90-21209*
US-PATENT-CLASS-210-247 ..... N90-21209*
US-PATENT-CLASS-210-257.1 ..... N90-21209*
US-PATENT-CLASS-210-321.6 ..... N90-21209*
US-PATENT-CLASS-210-340 ..... N90-21209*
US-PATENT-CLASS-244-135 ..... N90-21002
US-PATENT-CLASS-249-127 ..... N90-21216*
US-PATENT-CLASS-264-022 ..... N90-21198*
US-PATENT-CLASS-324-209 ..... N90-21170*
US-PATENT-CLASS-324-226 ..... N90-21170*
US-PATENT-CLASS-324-227 ..... N90-21170*
US-PATENT-CLASS-324-235 ..... N90-21170*
US-PATENT-CLASS-324-239 ..... N90-21170*
US-PATENT-CLASS-350-3.69 ..... N90-21353
US-PATENT-CLASS-356-345 ..... N90-21620
US-PATENT-CLASS-357-4 ..... N90-21358*
US-PATENT-CLASS-357-29 ..... N90-21358*
US-PATENT-CLASS-357-30 ..... N90-21358*
US-PATENT-CLASS-357-58 ..... N90-21358*
US-PATENT-CLASS-357-90 ..... N90-21358*
US-PATENT-CLASS-361-383 ..... N90-21215*
US-PATENT-CLASS-361-384 ..... N90-21215*
US-PATENT-CLASS-361-385 ..... N90-21215*
US-PATENT-CLASS-364-229.4 ..... N90-21527*
US-PATENT-CLASS-364-267.9 ..... N90-21527*
US-PATENT-CLASS-364-940.67 ..... N90-21527*
US-PATENT-CLASS-364-942.51 ..... N90-21527*
US-PATENT-CLASS-364-944 ..... N90-21527*
US-PATENT-CLASS-364-975.5 ..... N90-21527*
US-PATENT-CLASS-371-11.3 ..... N90-21527*
US-PATENT-CLASS-371-37.4 ..... N90-21061*
US-PATENT-CLASS-371-38.1 ..... N90-21061*
US-PATENT-CLASS-371-041 ..... N90-21061*
US-PATENT-CLASS-371-043 ..... N90-21061*
US-PATENT-CLASS-377-69 ..... N90-21525*
US-PATENT-CLASS-377-79 ..... N90-21525*
US-PATENT-CLASS-377-111 ..... N90-21525*
US-PATENT-CLASS-377-114 ..... N90-21525*
US-PATENT-CLASS-377-116 ..... N90-21525*
US-PATENT-CLASS-377-123 ..... N90-21525*
US-PATENT-CLASS-377-126 ..... N90-21525*
US-PATENT-CLASS-382-17 ..... N90-21260
US-PATENT-CLASS-501-88 ..... N90-21177*
US-PATENT-CLASS-501-91 ..... N90-21177*
US-PATENT-CLASS-501-92 ..... N90-21177*
US-PATENT-CLASS-522-162 ..... N90-21198*
US-PATENT-CLASS-522-165 ..... N90-21198*
US-PATENT-CLASS-524-204 ..... N90-21189
US-PATENT-CLASS-526-262 ..... N90-21118*
US-PATENT-CLASS-528-4 ..... N90-21177*
US-PATENT-CLASS-528-10 ..... N90-21177*
US-PATENT-CLASS-528-30 ..... N90-21177*
US-PATENT-CLASS-528-176 ..... N90-21198*
US-PATENT-CLASS-528-308 ..... N90-21198*
US-PATENT-CLASS-528-322 ..... N90-21118*
US-PATENT-CLASS-548-400 ..... N90-21118*
US-PATENT-CLASS-548-524 ..... N90-21118*
US-PATENT-CLASS-556-402 ..... N90-21177*

US-PATENT-4,729,317 ..... N90-21111
US-PATENT-4,845,728 ..... N90-21525*
US-PATENT-4,851,491 ..... N90-21177*
US-PATENT-4,851,544 ..... N90-21118*
US-PATENT-4,852,578 ..... N90-21519*
US-PATENT-4,858,717 ..... N90-21215*
US-PATENT-4,860,074 ..... N90-21358*
US-PATENT-4,864,910 ..... N90-21390*
US-PATENT-4,865,114 ..... N90-21216*
US-PATENT-4,866,818 ..... N90-21527*
US-PATENT-4,878,296 ..... N90-21354
US-PATENT-4,878,695 ..... N90-21384
US-PATENT-4,878,718 ..... N90-21353
US-PATENT-4,881,270 ..... N90-21260
US-PATENT-4,881,813 ..... N90-21620
US-PATENT-4,907,233 ..... N90-21061*
US-PATENT-4,909,933 ..... N90-21209*
US-PATENT-4,910,233 ..... N90-21198*
US-PATENT-4,912,411 ..... N90-21170*

WIS-PH-89/01 ..... N90-21653 #

WRDC-TR-89-2149 ..... N90-21389 #

WRDC-20 ..... N90-21188 #

Y/DX-916 ..... N90-21688 #

Appendix—About STAR

Scientific and Technical Aerospace Reports (STAR) is a major component of a comprehensive National Aeronautics and Space Administration information system covering aeronautics, space, and supporting disciplines. *STAR* is issued on the 8th and 23rd of each month and announces current publications of the following types:

- NASA, NASA contractor, and NASA grantee reports
- Reports issued by other U.S. Government agencies, domestic and foreign institutions, universities, and private firms
- Translations in report form
- NASA-owned patents and patent applications
- Other U.S. Government agency and foreign patents and patent applications
- Domestic and foreign dissertations and theses

Journal, book, and conference literature, cover-to-cover journal translations, and certain foreign dissertations are announced in a companion journal, *International Aerospace Abstracts (IAA),* available on subscription from the American Institute of Aeronautics and Astronautics, Technical Information Service, 555 West 57th Street, 12th Floor, New York, NY 10019.

SUBJECT SCOPE

The subject scope of *STAR* and *IAA* includes all aspects of aeronautics and space research and development, supporting basic and applied research, and applications. Aerospace aspects of earth resources, energy development, conservation, oceanography, environmental protection, urban transportation, and other topics of high national priority are also covered.

OTHER NASA PUBLICATIONS

Other NASA publications and information services are described in the publication, *The NASA Scientific and Technical Information System ... and How to Use It,* available without charge from the NASA Scientific and Technical Information Facility, P.O. Box 8757, BWI Airport, MD 21240.

HOW TO USE *STAR* SUBJECT CATEGORIES

STAR is categorized by 10 major subject divisions broken down further into 76 specific subject categories and one general division/category. The major subject divisions are listed on page ii in the Table of Contents, together with a note for each that defines its scope and provides any cross-references. For example:

AERONAUTICS

Includes aeronautics (general); aerodynamics; air transportation and safety; aircraft communications and navigation; aircraft design, testing and performance; aircraft instrumentation; aircraft propulsion and power; aircraft stability and control; and research and support facilities (air).

For related information see also *Astronautics.*

Each major division is further divided into as many as nine specific categories, which are identified by category numbers.

Abstracts in *STAR* are grouped by subject category, the categories appearing in sequential order. Category breaks in the abstract section are identified by the category number and title, and a scope note. Cross-references to other categories are provided as appropriate. For example:

02 AERODYNAMICS

Includes aerodynamics of bodies, combinations, wings, rotors, and control surfaces; and internal flow in ducts and turbomachinery.

For related information see also *34 Fluid Mechanics and Heat Transfer.*

CROSS-REFERENCES

Individual *STAR* abstracts are not ordinarily cross-referenced, except for certain conference reports or book translations that have had separate abstracts written for their component papers or chapters. Citations and abstracts of the components follow immediately after those of the parent document. When the subject content of a component differs sufficiently from the general content of the parent, a cross-reference citation also is printed at the end of the category to which it normally would have been assigned if it were independent.

DOCUMENTS ON MICROFICHE

Documents on microfiche(1) are designated by a pound sign (#) following the accession number. The pound sign is used without regard to the source or quality of the microfiche.

LIMITED REPRODUCIBILITY

A Note of Limited Reproducibility appears in the citation, if one or a combination of the following factors affect the reproducibility of more than 20% of the document. These factors include: faint or broken type, color photographs, black and white photographs, foldouts, dot matrix print, charts/graphs with script notation, non-Roman alphabet, or some other factor that limits the reproducibility of that document. This notation also appears on the microfiche header, with the specific causing factor checked off on a list visible in the second frame.

COLOR COPIES

An increasing number of NASA scientific and technical reports are being produced with color graphs, charts, illustrations, and photographs. A message indicating that a document has color pages follows the Sales and Pricing (SAP) information in the *STAR* citation.

Registered users of the NASA Scientific and Technical Information System will receive ordered documents with color at no *additional* cost, as long as stock copies of that document are available. Otherwise, an additional fee of $2.00 per color page, over and above the standard document price will be charged. The NASA STI Facility staff will work with registered users over the telephone to inform and meet each individual's ordering needs.

AVAILABILITIES

One or more sources from which a document announced in *STAR* is available to the public is given in each citation. The most commonly indicated sources and their acronyms or abbreviations are listed below. If the publication is available from a source other than those listed, the publisher and his address will be displayed on the availability line or in combination with the corporate source line.

Avail: NTIS. Sold by the National Technical Information Service. Prices for hard copy (HC) and microfiche (MF) are indicated by a price code following the letters HC or MF in the *STAR* citation. Current values for the price codes are given in the tables on page A-7.

(1) A microfiche is a transparent sheet of film, 105 by 148 mm in size, containing as many as 60 to 98 pages of information reduced to micro images (not to exceed 26:1 reduction).

Initially distributed microfiche under the NTIS SRIM (Selected Research in Microfiche) is available at greatly reduced unit prices. For this service and for information concerning subscription to NASA printed reports, consult the NTIS Subscription Section, Springfield, VA 22161.

NOTE ON ORDERING DOCUMENTS: When ordering NASA publications (those followed by the * symbol), use the N accession number. NASA patent applications (only the specifications are offered) should be ordered by the US-Patent-Appl-SN number. Non-NASA publications (no asterisk) should be ordered by the AD, PB, or other *report number* shown on the last line of the citation, not by the N accession number. It is also advisable to cite the title and other bibliographic identification.

Avail: SOD (or GPO). Sold by the Superintendent of Documents, U.S. Government Printing Office, in hard copy. The current price and order number are given following the availability line. (NTIS will fill microfiche requests, as indicated above, for those documents identified by a # symbol.)

Avail: BLL (formerly NLL): British Library Lending Division, Boston Spa, Wetherby, Yorkshire, England. Photocopies available from this organization at the price shown. (If none is given, address inquiry to the BLL.)

Avail: DOE Depository Libraries. Organizations in U.S. cities and abroad that maintain collections of Department of Energy reports, usually in microfiche form, are listed in *Energy Research Abstracts*. Services available from the DOE and its depositories are described in a booklet, *DOE Technical Information Center - Its Functions and Services* (TID-4660), which may be obtained without charge from the DOE Technical Information Center.

Avail: ESDU. Pricing information on specific data, computer programs, and details on Engineering Sciences Data Unit (ESDU) topic categories can be obtained from ESDU International Ltd. Requesters in North America should use the Virginia address while all other requesters should use the London address, both of which are on page A-6.

Avail: Fachinformationszentrum, Karlsruhe. Sold by the Fachinformationszentrum Energie, Physik, Mathematik GMBH, Eggenstein Leopoldshafen, Federal Republic of Germany, at the price shown in deutschmarks (DM).

Avail: HMSO. Publications of Her Majesty's Stationery Office are sold in the U.S. by Pendragon House, Inc. (PHI), Redwood City, CA. The U.S. price (including a service and mailing charge) is given, or a conversion table may be obtained from PHI.

Avail: NASA Public Document Rooms. Documents so indicated may be examined at or purchased from the National Aeronautics and Space Administration, Public Documents Room (Room 126), 600 Independence Ave., S.W., Washington, DC 20546, or public document rooms located at NASA installations, and the NASA Pasadena Office at the Jet Propulsion Laboratory.

Avail: Univ. Microfilms. Documents so indicated are dissertations selected from *Dissertation Abstracts* and are sold by University Microfilms as xerographic copy (HC) and microfilm. All requests should cite the author and the Order Number as they appear in the citation.

Avail: US Patent and Trademark Office. Sold by Commissioner of Patents and Trademarks, U.S. Patent and Trademark Office, at the standard price of

$1.50 each, postage free. (See discussion of NASA patents and patent applications below.)

Avail: (US Sales Only). These foreign documents are available to users within the United States from the National Technical Information Service (NTIS). They are available to users outside the United States through the International Nuclear Information Service (INIS) representative in their country, or by applying directly to the issuing organization.

Avail: USGS. Originals of many reports from the U.S. Geological Survey, which may contain color illustrations, or otherwise may not have the quality of illustrations preserved in the microfiche or facsimile reproduction, may be examined by the public at the libraries of the USGS field offices whose addresses are listed in this Introduction. The libraries may be queried concerning the availability of specific documents and the possible utilization of local copying services, such as color reproduction.

Avail: Issuing Activity, or Corporate Author, or no indication of availability. Inquiries as to the availability of these documents should be addressed to the organization shown in the citation as the corporate author of the document.

NASA PATENTS AND PATENT APPLICATIONS

Patents and patent applications owned by NASA are announced in *STAR* under appropriate subject categories and are referenced in the *STAR* indexes. In the Report/Accession Number Index, patents are indexed by the NASA Case Number (which appears in lieu of the report number in other indexes), the U.S. Patent Number, the U.S. Patent Application Serial Number, and the U.S. Patent Class. Patent applications for which patents have not yet been issued are indexed by the NASA Case Number and the U.S. Patent Application Serial Number.

NASA *patent application specifications* are sold in paper copy and microfiche by the National Technical Information Service (NTIS). The US-Patent-Appl-SN- number should be used in ordering either paper copy or microfiche from NTIS. Printed copies of *patents* (which are not microfiched) are available for purchase from:

Commissioner of Patents and Trademarks
U.S. Patent and Trademark Office
Washington, DC 20231

When ordering patents, the U.S. Patent Number should be used, and payment must be remitted in advance, by money order or check payable to the Commissioner of Patents and Trademarks. Prepaid purchase coupons for ordering are also available from the Patent and Trademark Office. The patents and patent applications announced in *STAR* are owned by NASA and are available for royalty-free licensing. Requests for licensing terms and further information should be addressed to:

Associate General Counsel for Intellectual Property/Code GP
National Aeronautics and Space Administration
Washington, DC 20546

ELIGIBILITY AND REGISTRATION FOR NASA INFORMATION PRODUCTS AND SERVICES

A variety of services is available to organizations of the following types that have registered with NASA to receive specific services or products:

1. NASA offices and installations, contractors, subcontractors, grantees, and consultants;
2. Other U.S. Government agencies and their contractors;
3. Libraries in the United States that have arrangements with NASA to maintain collections of NASA documents for public reference;
4. Other organizations in the United States having a need for NASA documents in work related to aeronautics and space research;
5. Organizations abroad that have established reciprocal document exchange arrangements with NASA.

Only the central service points or central points of document acquisition and control within qualified organizations are eligible to register for NASA products and services. Domestic organizations that may be eligible to receive various classes of NASA publications and services should address their requests for registration or for further information to:

NASA Scientific and Technical Information Facility
ATTN: Registration Services
P.O. Box 8757
BWI Airport, MD 21240
301-621-0153

Organizations abroad should direct requests to Manager, International STI Activities, NTT, NASA Headquarters, Washington, DC 20546.

AVAILABILITY OF *STAR* ABSTRACTS ON MICROFICHE

Microfiche of the abstract sections of this issue and other issues of *STAR* are available on annual subscription from NTIS as PB90-911300, Attn: Subscriptions, 5285 Port Royal Road, Springfield, VA 22161. Annual subscription rates are $75.50 North America; $151.00 foreign. Abstract sections for previous years retroactive to 1964 are available at the current rates. Microfiche for individual *STAR* issue abstract sections are not available.

PUBLIC COLLECTIONS OF NASA DOCUMENTS

DOMESTIC: NASA and NASA-sponsored documents and a large number of aerospace publications are available to the public for reference purposes at the library maintained by the American Institute of Aeronautics and Astronautics, Technical Information Service, 555 West 57th Street, 12th Floor, New York, NY 10019

EUROPEAN: An extensive collection of NASA and NASA-sponsored publications is maintained by the British Library Lending Division, Boston Spa, Wetherby, Yorkshire, England, for public access. The British Library Lending Division also has available many of the non-NASA publications cited in *STAR*. European requesters may purchase facsimile copy or microfiche of NASA and NASA-sponsored documents, those identified by both the symbols # and * from ESA - Information Retrieval Service, European Space Agency, 8-10 rue Mario-Nikis, 75738 Paris CEDEX 15, France.

FEDERAL DEPOSITORY LIBRARY PROGRAM

In order to provide the general public with greater access to U.S. Government publications, Congress established the Federal Depository Library Program under the Government Printing Office (GPO), with 51 regional depositories responsible for permanent retention of material, inter-library loan, and reference services. At least one copy of nearly every NASA and NASA-sponsored publication, either in printed or microfiche format, is received and retained by the 51 regional depositories. A list of the regional GPO libraries, arranged alphabetically by state, appears on the inside back cover. These libraries are *not* sales outlets. A local library can contact a Regional Depository to help locate specific reports, or direct contact may be made by an individual.

FEDERAL REGIONAL DEPOSITORY LIBRARIES

ALABAMA

AUBURN UNIV. AT MONTGOMERY LIBRARY
Documents Department
Montgomery, AL 36193
(205) 279-9110 ext.253

UNIV. OF ALABAMA LIBRARY
Reference Department/Documents
Box S
Tuscaloosa, AL 35486
(205) 348-6046

ARIZONA

DEPT. OF LIBRARY, ARCHIVES, AND PUBLIC RECORDS
Third Floor State Capitol
1700 West Washington
Phoenix, AZ 85007
(602) 255-4121

ARKANSAS

ARKANSAS STATE LIBRARY
Documents Service Section
One Capitol Mall
Little Rock, AR 72201
(501) 371-2090

CALIFORNIA

CALIFORNIA STATE LIBRARY
Govt. Publications Section
914 Capitol Mall
Sacramento, CA 95814
(916) 322-4572

COLORADO

UNIV. OF COLORADO
Norlin Library
Government Publications Division
Campus Box 184
Boulder, CO 80309
(303) 492-8834

DENVER PUBLIC LIBRARY
Govt. Pub. Department
1357 Broadway
Denver, CO 80203
(303) 571-2346

CONNECTICUT

CONNECTICUT STATE LIBRARY
231 Capitol Avenue
Hartford, CT 06106
(203) 566-4971

FLORIDA

UNIV. OF FLORIDA LIBRARIES
Documents Department
Library West
Gainesville, FL 32611
(904) 392-0367

GEORGIA

UNIV. OF GEORGIA LIBRARIES
Government Documents Dept.
Athens, GA 30602
(404) 542-8949

HAWAII

UNIV. OF HAWAII
Hamilton Library
Government Documents Collection
2550 The Mall
Honolulu, HI 96822
(808) 948-8230

IDAHO

UNIV. OF IDAHO LIBRARY
Documents Section
Moscow, ID 83843
(208) 885-6344

ILLINOIS

ILLINOIS STATE LIBRARY
Federal Documents
Centennial Building
Springfield, IL 62756
(217) 782-5012

INDIANA

INDIANA STATE LIBRARY
Serials Section
140 North Senate Avenue
Indianapolis, IN 46204
(317) 232-3686

IOWA

UNIV. OF IOWA LIBRARIES
Government Publications Dept.
Iowa City, IA 52242
(319) 335-5926

KANSAS

UNIVERSITY OF KANSAS
Spencer Research Library
Government Documents
Lawrence, KS 66045
(913) 864-4662

KENTUCKY

UNIV. OF KENTUCKY LIBRARIES
Government Publications/Maps Dept.
Lexington, KY 40506
(606) 257-8400

LOUISIANA

LOUISIANA STATE UNIVERSITY
Middleton Library
Government Documents Dept.
Baton Rouge, LA 70803
(504) 388-2570

LOUISIANA TECHNICAL UNIV.
Prescott Memorial Library
Government Documents Dept.
Ruston, LA 71272
(318) 257-4962

MAINE

UNIVERSITY OF MAINE
Raymond H. Fogler Library
Govt. Documents & Microforms Dept.
Orono, ME 04469
(207) 581-1680

MARYLAND

UNIVERSITY OF MARYLAND
McKeldin Library
Documents/Maps Room
College Park, MD 20742
(301) 454-3034

MASSACHUSETTS

BOSTON PUBLIC LIBRARY
Government Documents Dept.
666 Boylston Street
Boston, MA 02117
(617) 536-5400 ext.226

MICHIGAN

DETROIT PUBLIC LIBRARY
5201 Woodward Avenue
Detroit, MI 48202
(313) 833-1409

LIBRARY OF MICHIGAN
Government Documents
P.O. Box 30007
735 E. Michigan Avenue
Lansing, MI 48909
(517) 373-1593

MINNESOTA

UNIVERSITY OF MINNESOTA
Wilson Library
Government Publications
309 Nineteenth Avenue South
Minneapolis, MN 55455
(612) 373-7813

MISSISSIPPI

UNIV. OF MISSISSIPPI LIB.
Government Documents Dept.
106 Old Gym Bldg.
University, MS 38677
(601) 232-5857

MISSOURI

University of Missouri at Columbia Library
Government Documents
Columbia, MO 65201
(314) 882-6733

MONTANA

UNIV. OF MONTANA
Mansfield Library
Documents Division
Missoula, MT 59812
(406) 243-6700

NEBRASKA

UNIVERSITY OF NEBRASKA - LINCOLN
Love Memorial Library
Documents Department
Lincoln, NE 68588
(402) 472-2562

NEVADA

UNIV. OF NEVADA-RENO LIB.
Govt. Pub. Department
Reno, NV 89557
(702) 784-6579

NEW JERSEY

NEWARK PUBLIC LIBRARY
U.S. Documents Division
5 Washington Street
P.O. Box 630
Newark, NJ 07101
(201) 733-7812

NEW MEXICO

UNIVERSITY OF NEW MEXICO
General Library
Government Publications/Maps Dept.
Albuquerque, NM 87131
(505) 277-5441

NEW MEXICO STATE LIBRARY
325 Don Gaspar Avenue
Santa Fe, NM 87501
(505) 827-3826

NEW YORK

NEW YORK STATE LIBRARY
Documents Sect. Cultural Educ. Ctr.
Empire State Plaza
Albany, NY 12230
(518) 474-5563

NORTH CAROLINA

UNIVERSITY OF NORTH CAROLINA AT CHAPEL HILL
Davis Library 080A
BA/SS Department Documents
Chapel Hill, NC 27514
(919) 962-1151

NORTH DAKOTA

NORTH DAKOTA STATE UNIVERSITY LIBRARY
Government Documents Dept.
Fargo, ND 58105
(701) 237-8352
In cooperation with Univ. of North Dakota, Chester Fritz Library
Grand Forks

OHIO

STATE LIBRARY OF OHIO
Documents Section
65 South Front Street
Columbus, OH 43266
(614) 644-7051

OKLAHOMA

OKLAHOMA DEPT. OF LIBRARIES
Government Documents
200 NE 18th Street
Oklahoma City, OK 73105
(405) 521-2502, ext. 252

OKLAHOMA STATE UNIV. LIB.
Documents Department
Stillwater, OK 74078
(405) 624-0489

OREGON

PORTLAND STATE UNIV.
Millar Library
934 SW Harrison - P.O. Box 1151
Portland, OR 97207
(503) 229-3673

PENNSYLVANIA

STATE LIBRARY OF PENN.
Government Publications Section
Box 1601
Walnut St. & Commonwealth Ave.
Harrisburg, PA 17105
(717) 787-3752

SOUTH CAROLINA

CLEMSON UNIV. COOPER LIB.
Documents Department
Clemson, SC 29634
(803) 656-5174
In cooperation with Univ. of South Carolina, Thomas Cooper Library, Columbia

TEXAS

TEXAS STATE LIBRARY
Public Services Department
P.O. Box 12927 - 1201 Brazos
Austin, TX 78711
(512) 463-5455

TEXAS TECH. UNIV. LIBRARY
Documents Department
Lubbock, TX 79409
(806) 742-2268

UTAH

UTAH STATE UNIVERSITY
Merrill Library & Learning Resources Center, UMC-30
Documents Department
Logan, UT 84322
(801) 750-2682

VIRGINIA

UNIVERSITY OF VIRGINIA
Alderman Library
Government Documents
Charlottesville, VA 22903
(804) 924-3133

WASHINGTON

WASHINGTON STATE LIBRARY
Document Section
Olympia, WA 98504
(206) 753-4027

WEST VIRGINIA

WEST VIRGINIA UNIV. LIB.
Government Documents Section
P.O. Box 6069
Morgantown, WV 26506
(304) 293-3640

WISCONSIN

ST. HIST SOC. OF WISCONSIN LIB.
Government Pub. Section
816 State Street
Madison, WI 53706
(608) 262-2781
In cooperation with Univ. of Wisconsin-Madison, Memorial Library

MILWAUKEE PUBLIC LIBRARY
Documents Division
814 West Wisconsin Avenue
Milwaukee, WI 53233
(414) 278-3065

WYOMING

WYOMING STATE LIBRARY
Supreme Court & Library Bldg.
Cheyenne, WY 82002
(307) 777-5919

National Aeronautics and
Space Administration
Code NTT
Washington, D.C.
20546
Official Business
Penalty for Private Use, $300

SPECIAL FOURTH-CLASS RATE
POSTAGE & FEES PAID
NASA
PERMIT No. G27

POSTMASTER: If Undeliverable (Section 158
Postal Manual) Do Not Return